

NIST GCR 10-917-9

Applicability of Nonlinear Multiple-Degree-of-Freedom Modeling for Design

Supporting Documentation

NEHRP Consultants Joint Venture
*A Partnership of the Applied Technology Council and the
Consortium of Universities for Research in Earthquake Engineering*



NIST
National Institute of
Standards and Technology
U.S. Department of Commerce

Disclaimers

This report was prepared for the Building and Fire Research Laboratory of the National Institute of Standards and Technology under contract number SB134107CQ0019, Task Order 68241. The statements and conclusions contained herein are those of the authors, and do not imply recommendations or endorsements by the National Institute of Standards and Technology.

This report was produced under contract to NIST by the NEHRP Consultants Joint Venture, a joint venture of the Applied Technology Council (ATC) and the Consortium of Universities for Research in Earthquake Engineering (CUREE). While endeavoring to provide practical and accurate information, the NEHRP Consultants Joint Venture, the authors, and the reviewers assume no liability for, nor make any expressed or implied warranty with regard to, the information contained in this report. Users of information contained in this report assume all liability arising from such use.

The policy of the National Institute of Standards and Technology is to use the International System of Units (metric units) in all of its publications. However, in North America in the construction and building materials industry, certain non-SI units are so widely used instead of SI units that it is more practical and less confusing to include measurement values for customary units only.

NIST GCR 10-917-9

Applicability of Nonlinear Multiple-Degree-of-Freedom Modeling for Design

Supporting Documentation

Prepared for
*U.S. Department of Commerce
Building and Fire Research Laboratory
National Institute of Standards and Technology
Gaithersburg, Maryland*

By
NEHRP Consultants Joint Venture
A partnership of the Applied Technology Council and the
Consortium of Universities for Research in Earthquake Engineering

September 2010



U.S. Department of Commerce
Gary Locke, Secretary

National Institute of Standards and Technology
Patrick D. Gallagher, Director

Participants

National Institute of Standards and Technology

John (Jack) R. Hayes, Director – National Earthquake Hazards Reduction Program
Kevin K. F. Wong, Technical Monitor

NEHRP Consultants Joint Venture

Applied Technology Council
201 Redwood Shores Parkway, Suite 240
Redwood City, California 94065
www.ATCouncil.org

Consortium of Universities for
Research in Earthquake Engineering
1301 S. 46th Street, Building 420
Richmond, California 94804
www.CUREE.org

Joint Venture Management Committee

James R. Harris
Robert Reitherman
Christopher Rojahn
Andrew Whittaker

Joint Venture Program Committee

Jon A. Heintz (Program Manager)
Michael Constantinou
C.B. Crouse
James R. Harris
William T. Holmes
Jack P. Moehle
Andrew Whittaker

Project Technical Committee

Michael Valley (Project Director)
Mark Aschheim
Craig Comartin
William T. Holmes
Helmut Krawinkler
Mark Sinclair

Project Review Panel

Michael Constantinou
Jerome F. Hajjar
Joseph Maffei
Jack P. Moehle
Farzad Naeim
Michael Willford

Working Group Members

Michalis Fragiadakis
Dimitrios Lignos
Chris Putman
Dimitrios Vamvatsikos

Preface - Supporting Documentation

The NEHRP Consultants Joint Venture is a partnership between the Applied Technology Council (ATC) and the Consortium of Universities for Research in Earthquake Engineering (CUREE). In 2007, the National Institute of Standards and Technology (NIST) awarded the NEHRP Consultants Joint Venture a National Earthquake Hazards Reduction Program (NEHRP) “Earthquake Structural and Engineering Research” task order contract (SB1341-07-CQ-0019) to conduct a variety of tasks. In 2008, NIST initiated Task Order 68241 entitled “Improved Nonlinear Static Seismic Analysis Procedures – Multiple-Degree-of-Freedom Modeling.” The purpose of this project was to conduct further studies on multiple-degree-of-freedom effects as outlined in the Federal Emergency Management Agency (FEMA) report, FEMA 440, *Improvement of Nonlinear Static Seismic Analysis Procedures* (FEMA, 2005).

The FEMA 440 Report concluded that current nonlinear static analysis procedures, which are based on single-degree-of-freedom (SDOF) models, are limited in their ability to capture the complex behavior of structures that experience multiple-degree-of-freedom (MDOF) response, and that improved nonlinear analysis techniques to more reliably address MDOF effects were needed. In response to this need, work on this project included a detailed review of recent research on nonlinear MDOF modeling and the conduct of focused analytical studies to fill gaps in available information. The objective of this work was to improve nonlinear MDOF modeling for structural design practice by providing guidance on: (1) the minimum level of MDOF model sophistication necessary to make performance-based engineering decisions; (2) selection of appropriate nonlinear analysis methods; and (3) possible new analytical approaches. Summary findings, conclusions, and recommendations from this work are contained in the main volume report, *Applicability of Nonlinear Multiple-Degree-of-Freedom Modeling for Design*. This volume, *Supporting Documentation*, contains appendices that provide detailed reporting on the focused analytical studies, ancillary studies, and literature review activities that formed the basis of the findings.

The NEHRP Consultants Joint Venture is indebted to the leadership of Mike Valley, Project Director, and to the members of the Project Technical Committee, consisting of Mark Aschheim, Craig Comartin, William Holmes, Helmut Krawinkler, and Mark Sinclair, for their significant contributions in the development of this report and the

resulting recommendations. Focused analytical studies were led by Mark Aschheim and Helmut Krawinkler and conducted by Michalis Fragiadakis, Dimitrios Lignos, Chris Putman, and Dimitrios Vamvatsikos. Technical review and comment at key developmental stages on the project were provided by the Project Review Panel consisting of Michael Constantinou, Jerry Hajjar, Joe Maffei, Jack Moehle, Farzad Naeim, and Michael Willford. The names and affiliations of all who contributed to this project are included in the list of Project Participants at the end of this report.

NEHRP Consultants Joint Venture also gratefully acknowledges Jack Hayes (Director, NEHRP) and Kevin Wong (NIST Technical Monitor) for their input and guidance in the preparation of this report and Ayse Hortacsu and Peter N. Mork for ATC report production services.

Jon A. Heintz
Program Manager

Table of Contents - Supporting Documentation

Preface	iii
List of Figures	xi
List of Tables.....	xvii
Introduction	1-1
Appendix A: Detailed Steel Moment Frame Studies	A-1
A.1 Introduction.....	A-1
A.2 Structures Utilized in Evaluation	A-2
A.3 Nonlinear Response History Analysis	A-3
A.3.1 Component Model and Analysis Platforms	A-3
A.3.2 Analysis Model Simplification	A-4
A.3.3 Results for 2-, 4-, and 8-Story Steel Moment Frames	A-13
A.3.4 Dispersion in Seismic Input and Engineering Demand Parameters.....	A-23
A.3.5 Results for Residual Drifts.....	A-26
A.3.6 Synthesis of Nonlinear Response History Analysis Results.....	A-29
A.4 Single Mode Nonlinear Static Procedure.....	A-30
A.4.1 Nonlinear Static Analysis Options Explored	A-31
A.4.2 Results for 2-, 4-, 8-Story Steel Special Moment Frames in Pre-Capping Region.....	A-33
A.4.3 Response Predictions in Negative Tangent Stiffness Region.....	A-46
A.4.4 Synthesis of Nonlinear Static Procedure Predictions.....	A-49
A.5 Multi Mode Nonlinear Static Procedure	A-54
A.5.1 Summary Description of Procedure.....	A-54
A.5.2 Results for 4- and 8-Story Steel Moment Frames.....	A-55
A.5.3 Synthesis of Modal Pushover Analysis Predictions.....	A-61
A.6 Assessment of Elastic Response Spectrum Analysis	A-62
A.7 Load Pattern Sensitivity and Response Prediction for a Frame Structure with Severe Strength Irregularity	A-64
A.7.1 Load Pattern Sensitivity	A-64
A.7.2 Response of a 4-Story Building with Strength Irregularity ...	A-65
A.8 Incorporation of Gravity System in Analysis Model.....	A-77
A.8.1 Potential importance of Incorporating Gravity System in Analysis Model.....	A-77
A.8.2 Case Study – 4-Story Steel Moment Frame Structure	A-77

Appendix B: Detailed Reinforced Concrete Moment Frame

Studies	B-1
B.1 Ground Motions.....	B-1
B.2 Structural Systems	B-2
B.3 Nonlinear Static Procedures.....	B-4
B.3.1 ASCE/SEI 41-06 Displacement Coefficient Method	B-4
B.3.2 N2/EC8 Method.....	B-15
B.3.3 Modal Pushover Analysis	B-16
B.3.4 Consecutive Modal Pushover	B-24
B.3.5 Modal Response Spectrum Analysis	B-31
B.4 Summary and Comparison of the Analysis Methods	B-38
B.5 Correlation between Intermediate-Level and Component-Level Demand Parameters	B-48

Appendix C: Detailed Reinforced Concrete Shear Wall Studies

C-1	C-1
C.1 Introduction.....	C-1
C.2 Structures Utilized in Evaluation.....	C-1
C.3 Nonlinear Response History Analysis	C-3
C.3.1 Component Models.....	C-3
C.3.2 Results for 2-, 4-, and 8-Story Reinforced Concrete Shear Wall Structure with Fiber Model.....	C-6
C.3.3 NRHA Results for 4-story Reinforced Concrete Shear Wall Structure with Simplified Spring Model.....	C-17
C.3.4 Synthesis of Nonlinear Response History Analysis Results	C-22
C.4 Single Mode Nonlinear Static Procedure.....	C-23
C.4.1 Nonlinear Static Analysis Options Explored	C-23
C.4.2 Results for 2- and 8-Story Reinforced Concrete Shear Wall Structures Utilizing FM-ASCE41.....	C-25
C.4.3 Results for 4-Story Reinforced Concrete Shear Wall Structure Utilizing Alternative Nonlinear Static Procedures	C-31
C.4.4 Synthesis of Nonlinear Static Procedure Predictions	C-38
C.5 Multi-Mode Nonlinear Static Procedure.....	C-42
C.5.1 Results for 4- and 8-Story Reinforced Concrete Shear Wall Structures	C-42
C.6 Importance of Failure Mode	C-47

Appendix D: Effect of Ground Motion Selection and Scaling on Engineering

Demand Parameter Dispersion	D-1
D.1 Effect of Intensity Measure on EDP Dispersion	D-1
D.1.1 Observations on Dispersion	D-5
D.1.2 Observations on Bias	D-15
D.2 Use of Record Subsets to Characterize EDP Distributions.....	D-26
D.2.1 Subset Selection Methods used for Estimating Median EDP Values.....	D-26
D.2.2 Subset Selection Methods used for Estimating 84% EDP Values	D-28
D.2.3 Subset Selection based on FEMA P-695 scaling.....	D-29
D.2.4 Subset Selection on S_{di} Scaling.....	D-46
D.2.5 Random Subset Selection on S_{di} Scaling.....	D-55

D.2.6	Subset Selection on S_{di} Scaling	D-57
D.2.7	Random Subset Selection on S_{di} Scaling	D-68
D.3	Characterization of Distributions of Response Quantities	D-71
D.3.1	Distribution of EDPs Obtained with S_a Scaling	D-72
D.3.2	Distribution of EDPs Obtained with S_{di} Scaling	D-81
D.4	Alternative Estimation of Dispersion Using Higher Intensity Levels	D-89
Appendix E: Direct Determination of Target Displacement		E-1
E.1	Introduction	E-1
E.2	Direct Computation of Equivalent Single-Degree-of-Freedom Response	E-1
E.3	The SPO2IDA Tool	E-6
E.4	Summary	E-10
Appendix F: Practical Implementation of Analysis Methods		F-1
F.1	Approach	F-1
F.2	General Modeling Assumptions	F-2
F.2.1	Ground Motions	F-2
F.3	Structures and Models	F-4
F.3.1	Building A	F-4
F.3.2	Building B	F-9
F.4	Analysis Methods	F-14
F.4.1	Nonlinear Response History Analysis	F-14
F.4.2	Response Spectrum Analysis	F-15
F.4.3	Nonlinear Static Procedure	F-15
F.4.4	Nonlinear Static Procedure with Elastic Higher Modes	F-16
F.4.5	Modal Pushover Analysis	F-16
F.4.6	Consecutive Modal Pushover Analysis	F-16
F.4.7	Extended Consecutive Modal Pushover Analysis	F-16
F.5	Results	F-18
F.5.1	Building A Results	F-18
F.5.2	Building B Results	F-30
F.6	Summary of Observations	F-71
F.6.1	Building A	F-71
F.6.2	Building B	F-78
F.6.3	Accuracy of Estimates of Demand Parameters	F-83
F.7	Conclusions	F-91
F.7.1	Modeling and Analysis Conclusions	F-91
F.7.2	Analysis Techniques Conclusions	F-92
F.7.3	Extended Consecutive Modal Pushover Conclusion	F-93
F.7.4	Assumptions and Limitations	F-93
Appendix G: Expanded Summaries of Relevant Codes, Standards, and Guidelines		G-1
G.1	ASCE/SEI 31-03 Seismic Evaluation of Existing Buildings	G-1
G.1.1	Scope of Application	G-1
G.1.2	Applicability of Analysis Procedures	G-2
G.1.3	Other Evaluation Requirements	G-3
G.1.4	Other Modeling Direction Provided	G-5

	G.1.5	Ground Motion Characteristics.....	G-6
	G.1.6	Discussion.....	G-6
G.2		ASCE/SEI 41-06 Seismic Rehabilitation of Existing Buildings (with Supplement No.1).....	G-6
	G.2.1	Scope of Application	G-6
	G.2.2	Applicability of Analysis Procedures	G-7
	G.2.3	Other Modeling Direction Provided	G-10
	G.2.4	Additional Analysis Requirements	G-11
	G.2.5	Ground Motion Characterization	G-12
	G.2.6	Discussion.....	G-12
G.3		ATC-40 Seismic Evaluation and Retrofit of Concrete Buildings.....	G-13
	G.3.1	Scope of Application	G-13
	G.3.2	Applicability of Analysis Procedures	G-14
	G.3.3	Other Modeling Direction Provided	G-16
	G.3.4	Additional Analysis Requirements	G-17
	G.3.5	Ground Motion Characterization	G-17
	G.3.6	Discussion.....	G-19
G.4		FEMA 440 Improvement of Nonlinear Static Seismic Analysis Procedures.....	G-20
	G.4.1	Scope of Application	G-20
	G.4.2	Applicability of Analysis Procedures	G-20
	G.4.3	Other Modeling Direction Provided	G-24
G.5		FEMA P-440A, Effects of Strength and Stiffness Degradation on Seismic Response	G-25
	G.5.1	Scope of Application	G-25
	G.5.2	Applicability of Analysis Procedures	G-26
G.6		FEMA 351 Recommended Seismic Evaluation and Upgrade Criteria and FEMA 352 Recommended Post-Earthquake Evaluation and Repair Criteria for Welded Steel Moment-Frame Buildings.....	G-27
	G.6.1	Scope of Application	G-27
	G.6.2	Applicability of Analysis Procedures	G-27
	G.6.3	Other Modeling Direction Provided	G-28
	G.6.4	Additional Analysis Requirements	G-30
	G.6.5	Ground Motion Characterization	G-31
	G.6.6	Discussion.....	G-32
G.7		ASCE/SEI 7-05 Minimum Design Loads for Buildings and Other Structures	G-32
	G.7.1	Scope of Application	G-32
	G.7.2	Applicability of Analysis Procedures	G-33
	G.7.3	Other Modeling Direction Provided	G-34
	G.7.4	Additional Analysis Requirements	G-35
	G.7.5	Ground Motion Characterization	G-36
G.8		NEHRP Recommended Seismic Provisions for New Buildings and Other Structures	G-36
	G.8.1	Scope of Application	G-36
	G.8.2	Applicability of Analysis Procedures	G-37
	G.8.3	Other Modeling Direction Provided	G-37
	G.8.4	Additional Analysis Requirements	G-38

G.9	PEER/ATC-72-1 Modeling and Acceptance Criteria for Seismic Design and Analysis of Tall Buildings	G-40
G.9.1	Scope of Application	G-40
G.9.2	Applicability of Analysis Procedures	G-40
G.9.3	Other Modeling Direction Provided	G-49

Appendix H: Bibliography of Recent Multiple-Degree-of-Freedom Modeling

Research	H-1
H.1 Pushover Methods of Analysis	H-1
H.1.1 General Features/Observations	H-1
H.1.2 Target Displacement	H-3
H.1.3 Load Vectors and Approaches	H-6
H.1.4 P-delta Effects	H-31
H.1.5 Modeling Choices	H-32
H.1.6 Efficacy and Limitations	H-44
H.2 Dynamic Approaches	H-75
H.2.1 Incremental Dynamic Analysis and Approximations	H-75
H.2.2 Simplified Dynamic Analysis	H-82
H.2.3 Collapse Prediction	H-89
H.2.4 Sensitivity of Response to Modeling	H-91
H.2.5 Efficacy and Limitations Relative to Empirical Results	H-95
H.3 Special Configurations and Typologies	H-95
H.3.1 Torsional or Plan Irregularities	H-95
H.3.2 Weak Stories	H-118
H.3.3 Vertical Irregularities	H-119
H.3.4 Diaphragm Flexibility	H-123
H.3.5 Base-Isolated Buildings	H-126
H.3.6 Systems with High Viscous Damping	H-130
H.4 Engineering Demand Parameters	H-137
H.4.1 Estimation of EDPs Using Different Analysis Methods and Simplified Structural Models	H-137
H.4.2 Complexity of Response and Effect of Configuration on Accuracy of Estimation of EDPs	H-145
H.5 Probabilistic Treatments	H-147
H.6 Design Methods	H-154
H.7 Applications	H-166
H.7.1 Masonry	H-166
H.7.2 Wood	H-169
H.7.3 Reinforced Concrete	H-172
H.7.4 Steel Braced Frames	H-176
H.7.5 Moment Frames	H-177
References	I-1
Project Participants	J-1

List of Figures - Supporting Documentation

Figure A-1	Plan view of buildings used for archetype selection	A-1
Figure A-2	Backbone curve for component model Analyt.M1	A-4
Figure A-3	Simplified model of moment-resisting frame structure	A-5
Figure A-4	Comparison of global pushover curves ($V_f/W - \theta_r$) of 1- and 3-bay steel SMF analytical models, 2-, 4-, and 8-story steel SMFs.....	A-7
Figure A-5	Comparison of response history results for 4-story steel SMF, using Drain-2DX 3-bay and OpenSees 1-bay models.....	A-8
Figure A-6	Comparison of θ_{si} , $V_{I+P-\Delta}$, and $OTM_{I+P-\Delta}$ obtained from NRHA of 3-bay model (left) and simplified 1-bay model (right), 4-story steel SMF, SF = 2.0.....	A-10
Figure A-7	Comparison of θ_{si} , $V_{I+P-\Delta}$, and $OTM_{I+P-\Delta}$ obtained from NRHA of 3-bay model (left) and simplified 1-bay model (right), 8-story steel SMF, SF = 2.0.....	A-11
Figure A-8	Comparison of story level EDPs (left side) with local EDPs (right side), 4-story steel SMF, SF = 2.0	A-12
Figure A-9	Peak absolute floor accelerations for 3-bay model for ground motion scale factors SF = 0.5, 1.0, and 2.0; 4-story steel SMF	A-13
Figure A-10	System information, 2-story steel SMF	A-17
Figure A-11	NRHA Peak story drift ratios, story shears, and story overturning moments, 2-story steel SMF	A-18
Figure A-12	System information, 4-story steel SMF	A-19
Figure A-13	NRHA Peak story drift ratios, story shears, and story overturning moments, 4-story steel SMF	A-20
Figure A-14	System information, 8-story steel SMF	A-21
Figure A-15	NRHA Peak story drift ratios, story shears, and story overturning moments, 8-story steel SMF	A-22
Figure A-16	Median and dispersion of 5% damped acceleration spectra of ground motion sets with (a) 44 records and (b) 17 records	A-23
Figure A-17	NRHA peak story drift ratios, story shears, and story overturning moments, 4-story steel SMF, SF = 1.0 and 2.0, 17 records.....	A-25
Figure A-18	NRHA median and 16 th percentile and NSP prediction (Analyt.M1-ASCE41) of 4-story steel SMF, SF = 3.0, 17 records.....	A-26
Figure A-19	NRHA residual story drift ratios, 2-, 4- and 8-story steel SMFs, SF = 1.0 and 2.0.....	A-28
Figure A-20.	Modified ASCE/SEI 41-06 component model from PEER/ATC-72-1 Report.....	A-31
Figure A-21	NSP information, 2-story steel SMF.....	A-36

Figure A-22	NSP to NRHA comparison, 2-story steel SMF, SF = 1.0 and 2.0	A-37
Figure A-23	NSP information, 4-story steel SMF	A-38
Figure A-24	NSP to NRHA comparison, 4-story steel SMF, SF = 1.0 and 2.0	A-39
Figure A-25	Component models and global pushover curves for Analyt.M1 and Analyt.M3	A-40
Figure A-26	NSP to NRHA comparison, 4-story steel SMF, SF=2, pushover based on Analyt.M3	A-40
Figure A-27	NSP information, 8-story steel SMF	A-41
Figure A-28	NSP to NRHA comparison, 8-story steel SMF, SF = 1.0 and 2.0	A-42
Figure A-29	NSP information, 4-story-steel SMF with $T_1 = 0.40$ sec	A-44
Figure A-30	NSP to NRHA comparison, 4-story steel SMF with $T_1 = 0.40$ sec	A-45
Figure A-31	NRHA roof drift statistics and median and NSP target displacement (ASCE41) of 4-story steel SMF, for SF = 3.0	A-48
Figure A-32	NSP to NRHA comparison, 4-story steel SMF, for SF = 3.0	A-49
Figure A-33	Ratio of NSP predictions to median NRHA result for story EDPs, using Analyt.M1-ASCE41 NSP option, SF = 1.0 and 2.0 -- target roof drift not in negative tangent stiffness region	A-53
Figure A-34	First and second mode pushovers and equivalent SDOF systems, 4-story steel SMF	A-56
Figure A-35	MPA to NRHA comparison, 4-story steel SMF, SF = 1.0 and 2.0	A-57
Figure A-36	MPA to NRHA comparison, 4-story steel SMF with $T_1 = 0.40$ sec., SF = 1.0 and 2.0	A-58
Figure A-37	First and second mode pushovers and equivalent SDOF systems, 8-story steel SMF	A-59
Figure A-38	MPA to NRHA comparison, 8-story steel SMF, SF = 1.0 and 2.0	A-60
Figure A-39	Elastic RSA to NRHA comparison, 4-story steel SMF, SF = 0.5 and 2.0	A-63
Figure A-40	Sensitivity of pushover deflected shape to load pattern	A-65
Figure A-41	NSP to NRHA comparison, 2-story shear building with two slightly different story shear capacities	A-65
Figure A-42	Illustration of strength irregularity created in the case study	A-66
Figure A-43	System information, 4-story shear building, regular base case	A-68
Figure A-44	System information for NSP and MPA, 4-story shear building, regular base case	A-69
Figure A-45	NSP to NRHA comparison of story level EDPs, 4-story shear building, regular base case, SF = 1.0 and 2.0	A-70
Figure A-46	MPA to NRHA comparison of story level EDPs, 4-story shear building, regular base case, SF = 0.5 and 1.0	A-71
Figure A-47.	System information, 4-story shear building with strength irregularity	A-72
Figure A-48	System information for NSP and MPA, 4-story shear building with strength irregularity	A-73
Figure A-49	NSP to NRHA comparison of story level EDPs, 4-story shear building with strength irregularity, SF = 0.5 and 1.0	A-74

Figure A-50	MPA to NRHA comparison of story level EDPs, 4-story shear building with strength irregularity, SF = 0.5 and 1.0.....	A-75
Figure A-51	Moment-rotation relationship for a shear tab connection with slab....	A-78
Figure A-52	Pushover curves (a) V_I and V_{I+P-A} vs. roof drift for 4-story steel SMF with gravity system included, (b) comparison of V_I vs. roof drift pushovers without and with gravity system.....	A-79
Figure A-53	comparison of NRHA and NSP predictions between models without (left) and with gravity system 4-story steel SMF, SF = 2	A-80
Figure A-54	comparison of NRHA and NSP predictions between models without (left) and with gravity system, 4-story steel SMF, SF = 3	A-81
Figure B-1	5%-damped unscaled mean and median response spectra	B-1
Figure B-2	Capacity curves of the nonlinear static procedures. The target displacements according to the ASCE/SEI 41-06 displacement coefficient method and the N2/EC8 method (section B.1.4) are shown. (a) 2-story RCMF, (b) 4-story RCMF, (c) 8-story RCMF.....	B-5
Figure B-3	2-story RCMF: NRHA versus ASCE/SEI 41-06 displacement coefficient method, peak story displacement.....	B-9
Figure B-4	2-story RCMF: NRHA versus ASCE/SEI 41-06 displacement coefficient method, peak story drift ratio.....	B-10
Figure B-5	2-story RCMF: NRHA versus ASCE/SEI 41-06 displacement coefficient method, peak story shears.....	B-10
Figure B-6	2-story RCMF: NRHA versus ASCE/SEI 41-06 displacement coefficient method, peak overturning moments.....	B-11
Figure B-7	4-story RCMF: NRHA versus ASCE/SEI 41-06 displacement coefficient method, peak story displacement.....	B-11
Figure B-8	4-story RCMF: NRHA versus ASCE/SEI 41-06 displacement coefficient method, peak story drift ratio.....	B-12
Figure B-9	4-story RCMF: NRHA versus ASCE/SEI 41-06 displacement coefficient method, peak story shears.....	B-12
Figure B-10	4-story RCMF: NRHA versus ASCE/SEI 41-06 displacement coefficient method, peak overturning moments.....	B-13
Figure B-11	8-story RCMF: NRHA versus ASCE/SEI 41-06 displacement coefficient method, peak story displacements	B-13
Figure B-12	8-story RCMF: NRHA versus ASCE/SEI 41-06 displacement coefficient method, peak story drift ratio.....	B-14
Figure B-13	8-story RCMF: NRHA versus ASCE/SEI 41-06 displacement coefficient method, peak story shears.....	B-14
Figure B-14	8-story RCMF: NRHA versus ASCE/SEI 41-06 displacement coefficient method, peak overturning moments.....	B-15
Figure B-15	2-story RCMF: (a) Peak roof displacements of the ASCE/SEI 41-06 method, (b) multi-linear approximation.....	B-17
Figure B-16	4-story RCMF: (a) Peak roof displacements of the ASCE/SEI 41-06 method, (b) multi-linear approximation.....	B-17

Figure B-17	8-story RCMF: (a) Peak roof displacements of the ASCE/SEI 41-06 method, (b) multi-linear approximation.....	B-18
Figure B-18	2-story RCMF: NRHA versus MPA, peak story displacement	B-19
Figure B-19	2-story RCMF: NRHA versus MPA, peak story drift ratio	B-19
Figure B-20	2-story RCMF: NRHA versus MPA, peak story shears	B-20
Figure B-21	2-story RCMF: NRHA versus MPA, peak overturning moments	B-20
Figure B-22	4-story RCMF: NRHA versus MPA, peak story displacement.	B-21
Figure B-23	4-story RCMF: NRHA versus MPA, peak story drift ratio	B-21
Figure B-24	4-story RCMF: NRHA versus MPA, peak story shears	B-22
Figure B-25	4-story RCMF: NRHA versus MPA, peak overturning moments	B-22
Figure B-26	8-story RCMF: NRHA versus MPA, peak story displacement	B-23
Figure B-27	8-story RCMF: NRHA versus MPA, peak story drift ratio	B-23
Figure B-28	8-story RCMF: NRHA versus MPA, peak story shears	B-24
Figure B-29	8-story RCMF: NRHA versus MPA, peak overturning moments	B-24
Figure B-30	2-story RCMF: NRHA versus CMP, peak story displacement	B-26
Figure B-31	2-story RCMF: NRHA versus CMP, peak story drift ratio	B-26
Figure B-32	2-story RCMF: NRHA versus CMP, peak story shears	B-27
Figure B-33	2-story RCMF: NRHA versus CMP, peak overturning moments	B-27
Figure B-34	4-story RCMF: NRHA versus CMP, peak story displacement	B-28
Figure B-35	4-story RCMF: NRHA versus CMP, peak story drift ratio	B-28
Figure B-36	4-story RCMF: NRHA versus CMP, peak story shears	B-29
Figure B-37	4-story RCMF: NRHA versus CMP, peak overturning moment.....	B-29
Figure B-38	8-story RCMF: NRHA versus CMP, peak story displacement	B-30
Figure B-39	8-story RCMF: NRHA versus CMP, peak story drift ratio	B-30
Figure B-40	8-story RCMF: NRHA versus CMP, peak story shears	B-31
Figure B-41	8-story RCMF: NRHA versus CMP, peak overturning moment.....	B-31
Figure B-42	2-story RCMF: NRHA versus MRSA, peak story displacement.....	B-32
Figure B-43	2-story RCMF: NRHA versus MRSA, peak story drift ratio	B-33
Figure B-44	2-story RCMF: NRHA versus MRSA, peak story shears.....	B-33
Figure B-45	2-story RCMF: NRHA versus MRSA, peak overturning moments ...	B-34
Figure B-46	4-story RCMF: NRHA versus MRSA, peak story displacement.....	B-34
Figure B-47	4-story RCMF: NRHA versus MRSA, peak story drift ratio	B-35
Figure B-48	4-story RCMF: NRHA versus MRSA, peak story shears.....	B-35
Figure B-49	4-story RCMF: NRHA versus MRSA, peak overturning moments ...	B-36
Figure B-50	8-story RCMF: NRHA versus MRSA, peak story displacement.....	B-36
Figure B-51	8-story RCMF: NRHA versus MRSA, peak story drift ratio	B-37
Figure B-52	8-story RCMF: NRHA versus MRSA, peak story shears.....	B-37
Figure B-53	8-story RCMF: NRHA versus MRSA, peak overturning moments ...	B-38
Figure B-54	2-story RCMF: ratio of estimate to NRHA median, peak story displacements.....	B-39

Figure B-55	2-story RCMF: ratio of estimate to NRHA median, peak story drift ratio	B-39
Figure B-56	2-story RCMF: ratio of Estimate to NRHA median, peak story shears	B-40
Figure B-57	2-story RCMF: ratio of estimate to NRHA median, peak overturning moments	B-40
Figure B-58	4-story RCMF: ratio of estimate to NRHA median, peak story displacements	B-41
Figure B-59	4-story RCMF: ratio of estimate to NRHA median, peak story drift ratio	B-41
Figure B-60	4-story RCMF: ratio of estimate to NRHA median, peak story shear	B-42
Figure B-61	4-story RCMF: ratio of estimate to NRHA median, peak overturning moments	B-42
Figure B-62	8-story RCMF: ratio of estimate to NRHA median, peak story displacements	B-43
Figure B-63	8-story RCMF: ratio of estimate to NRHA median, peak story drift ratio	B-43
Figure B-64	8-story RCMF: ratio of estimate to NRHA median, peak story shears	B-44
Figure B-65	8-story RCMF: ratio of estimate to NRHA median, peak overturning moments	B-44
Figure B-66	2-story RCMF: Correlation of peak story drift versus peak beam moment for the exterior beam of the 1 st (left) and the 2 nd story (right).....	B-49
Figure B-67	2-story RCMF: Correlation of peak overturning moment versus the peak column axial force of the exterior column of the 1 st (left) and the 2 nd story (right).....	B-50
Figure B-68	2-story RCMF: Correlation of peak story drift versus peak column moment for the exterior column of the 1 st (left) and the 2 nd story (right).....	B-50
Figure B-69	2-story RCMF: Correlation of peak story shear versus peak column shear for the exterior column of the 1 st (left) and the 2 nd story (right).....	B-50
Figure B-70	4-story RCMF: Correlation of peak story drift versus peak beam moment for the exterior beam of the 1 st (left) and the 2 nd story (right).....	B-51
Figure B-71	4-story RCMF: Correlation of peak overturning moment versus the peak column axial force of the exterior column of the 1 st (left) and the 2 nd story (right).....	B-51
Figure B-72	4-story RCMF: Correlation of peak story drift versus peak column moment for the exterior column of the 1 st (left) and the 2 nd story (right).....	B-51
Figure B-73	4-story RCMF: Correlation of peak story shear versus peak column shear for the exterior column of the 1 st (left) and the 2 nd story (right).....	B-52

Figure B-74	8-story RCMF: Correlation of peak story drift versus peak beam moment for the exterior column of the 1 st (left) and the 2 nd story (right)	B-52
Figure B-75	8-story RCMF: Correlation peak overturning moment versus the peak column axial force of the exterior column of the 1 st (left) and the 2 nd story (right).....	B-52
Figure B-76	8-story RCMF: Correlation of peak story drift versus peak column moment for the exterior column of the 1 st (left) and the 2 nd story (right)	B-53
Figure B-77	8-story RCMF: Correlation of peak story shear versus peak column shear for the exterior column of the 1 st (left) and the 2 nd story (right)	B-53
Figure B-78	2-story RCMF: Correlation of peak story drift versus peak beam moment	B-54
Figure B-79	2-story RCMF: Correlation of peak overturning moment versus peak column axial force	B-54
Figure B-80	2-story RCMF: Correlation of peak story drift versus peak column moment	B-55
Figure B-81	2-story RCMF: Correlation of peak story shear versus peak column shear	B-55
Figure B-82	4-story RCMF: Correlation of peak story drift versus beam moment	B-56
Figure B-83	4-story RCMF: Correlation of peak overturning moment versus peak column axial force	B-56
Figure B-84	4-story RCMF: Correlation of peak story drift versus peak column moment	B-57
Figure B-85	4-story RCMF: Correlation of peak story shear versus peak column shear	B-57
Figure B-86	8-story RCMF: Correlation of peak story drift versus peak beam moment.....	B-58
Figure B-87	8-story RCMF: Correlation of peak overturning moment versus peak column axial force	B-58
Figure B-88	8-story RCMF: Correlation of peak story drift versus peak column moment	B-59
Figure B-89	8-story RCMF: Correlation of peak story shear versus peak column shear	B-59
Figure C-1	Archetype configuration for reinforced concrete shear wall structures.....	C-1
Figure C-2	Moment-curvature relationship at base of story 1 of 4-story RCSW, FM mode	C-4
Figure C-3	Shear force – deformation models (a) if shear strength is expected to limit wall behavior, and (b) if bending strength is expected to limit wall behavior	C-5
Figure C-4	Modeling of flexural behavior with simplified plastic hinge springs and elastic elements.....	C-6
Figure C-5	System information, 2-story RCSW, FM Model	C-10

Figure C-6	NRHA Peak story drift ratios, story shears, and floor overturning moments, 2-story RCSW, FM Model, SF = 1.0 and 2.0.....	C-11
Figure C-7	System information, 4-story RCSW, FM Model	C-12
Figure C-8	NRHA Peak story drift ratios, story shears, and floor overturning moments, 4-story RCSW, FM Model, SF = 0.5 and 1.0.....	C-13
Figure C-9	NRHA Peak story drift ratios, story shears, and floor overturning moments, 4-story RCSW, FM Model, SF = 2.0 and 3.0.....	C-14
Figure C-10	System information, 8-story RCSW, FM Model	C-15
Figure C-11	NRHA Peak story drift ratios, story shears, and floor overturning moments, 8-story RCSW, FM Model, SF = 1.0 and 2.0.....	C-16
Figure C-12	OpenSees hysteresis model with pinching, “Pinching4.....	C-17
Figure C-13	System information, 4-story RCSW, SM Model	C-19
Figure C-14	NRHA Peak story drift ratios, story shears, and floor overturning moments, 4-story RCSW, SM Model, SF = 1.0 and 2.0.....	C-20
Figure C-15	NRHA Peak story drift ratios, story shears, and floor overturning moments, 4-story RCSW, FM Model (left), SM Model (right), SF = 3.0.....	C-21
Figure C-16	NSP Information, 2-story RCSW, FM-ASCE41	C-27
Figure C-17	NSP to NRHA comparison, 2-story RCSW, FM-ASCE41, SF = 1.0 and 2.0	C-28
Figure C-18	NSP Information, 8-story RCSW, FM-ASCE41	C-29
Figure C-19	NSP to NRHA comparison, 8-story RCSW, FM-ASCE41, SF = 1.0 and 2.0.....	C-30
Figure C-20	M-P interaction diagram for 4-story RCSW	C-32
Figure C-21	Tabulated NSP information, 4-story RCSW.....	C-34
Figure C-22	NSP pushover curves and equivalent SDOF systems, 4-story RCSW, FM-ASCE41, FM-Eq.SDOF, ASCE41-ASCE41	C-35
Figure C-23	NSP to NRHA comparison, 4-story RCSW, three different NSP options, SF = 0.5 and 1.0	C-36
Figure C-24	NSP to NRHA comparison, 4-story RCSW, three different NSP options, SF = 2.0 and 3.0	C-37
Figure C-25	Ratios of NSP prediction over median NRHA result for story EDPs, using FM-ASCE41 option, SF = 1.0 and 2.0.....	C-40
Figure C-26	Ratios of NSP prediction over median NRHA result for story EDPs, using FM-Eq.SDOF option, SF = 1.0 and 2.0	C-41
Figure C-27	First and second mode pushovers and equivalent SDOF systems, 4-story RCSW-, FM model.....	C-43
Figure C-28	MPA to NRHA comparison, 4-story RCSW, FM model, SF = 0.5 and 1.0	C-44
Figure C-29	MPA to NRHA comparison, 4-story RCSW, FM model, SF = 2.0 and 3.0.....	C-45
Figure C-30	First and second mode pushovers and equivalent SDOF systems, 8-story RCSW, FM model.	C-46
Figure C-31	MPA to NRHA comparison, 8-story RCSW, FM model, SF = 1.0 and 2.0.....	C-47

Figure C-32	System information, 4-story RCSW designed to fail in bending.....	C-50
Figure C-33	NSP to NRHA comparison, 4-story RCSW designed to fail in bending	C-51
Figure D-1	The bilinear fit of the capacity boundary (pushover curve), used to derive the ESDOF capacity curve for the 2-story RCMF, as used for S _{di} scaling.....	D-2
Figure D-2	The bilinear fit of the capacity boundary (pushover curve), used to derive the ESDOF capacity curve for the 4-story RCMF, as used for S _{di} scaling	D-3
Figure D-3	The bilinear fit of the capacity boundary (pushover curve), used to derive the ESDOF capacity curve for the 8-story RCMF, as used for S _{di} scaling.....	D-3
Figure D-4	Conceptual distributions of data for arbitrary EDPs given FEMA P-695 scaling (with scale factors of 0.5, 1.0, and 2.0) for an intensity measure (IM) other than PGVPEER used in FEMA P-695 scaling	D-5
Figure D-5	Dispersions of the local and maximum story drift ratios along the height of the 2-story RCMF for three different intensity levels.	D-6
Figure D-6	Dispersions of the local and maximum peak floor accelerations along the height of the 2-story RCMF for three different intensity levels.	D-6
Figure D-7	Dispersions of the maximum beam plastic hinge rotation for each story along the height of the 2-story RCMF for three different intensity levels.	D-7
Figure D-8	Dispersions of the maximum column plastic hinge rotation for each story along the height of the 2-story RCMF for three different intensity levels	D-7
Figure D-9	Dispersions of story shear for each story along the height of the 2-story RCMF for three different intensity levels	D-8
Figure D-10	Dispersions of the overturning moment for each story along the height of the 2-story RCMF for three different intensity levels	D-8
Figure D-11	Dispersions of the local and maximum story drift ratios along the height of the 4-story RCMF for three different intensity levels	D-9
Figure D-12	Dispersions of the local and maximum peak floor accelerations along the height of the 4-story RCMF for three different intensity levels	D-9
Figure D-13	Dispersions of the maximum beam plastic hinge rotation for each story along the height of the 4-story RCMF for three different intensity levels	D-10
Figure D-14	Dispersions of the maximum column plastic hinge rotation for each story along the height of the 4-story RCMF for three different intensity levels	D-10
Figure D-15	Dispersions of story shear for each story along the height of the 4-story RCMF for three different intensity levels	D-11
Figure D-16	Dispersions of the overturning moment for each story along the height of the 4-story RCMF for three different intensity levels	D-11

Figure D-17	Dispersions of the local and maximum story drift ratios along the height of the 8-story RCMF for three different intensity levels	D12
Figure D-18	Dispersions of the local and maximum peak floor accelerations along the height of the 8-story RCMF for three different intensity levels	D-12
Figure D-19	Dispersions of the maximum beam plastic hinge rotation for each story along the height of the 8-story RCMF for three different intensity levels.	D-13
Figure D-20	Dispersions of the maximum column plastic hinge rotation for each story along the height of the 8-story RCMF for three different intensity levels	D-13
Figure D-21	Dispersions of story shear for each story along the height of the 8-story RCMF for three different intensity levels.....	D-14
Figure D-22	Dispersions of the overturning moment for each story along the height of the 8-story RCMF for three different intensity levels.	D-14
Figure D-23	Bias of the local and maximum story drift ratios along the height of the 2-story RCMF for three different intensity levels	D-17
Figure D-24	Bias of the local and maximum peak floor accelerations along the height of the 2-story RCMF for three different intensity levels	D-17
Figure D-25	Bias of the maximum beam plastic hinge rotation for each story along the height of the 2-story RCMF for three different intensity levels	D-18
Figure D-26	Bias of the maximum column plastic hinge rotation for each story along the height of the 2-story RCMF for three different intensity levels	D-18
Figure D-27	Bias of the story shear for each story along the height of the 2-story RCMF for three different intensity levels.....	D-19
Figure D-28	Bias of the overturning moment for each story along the height of the 2-story RCMF for three different intensity levels.....	D-19
Figure D-29	Bias of the local and maximum story drift ratios along the height of the 4-story RCMF for three different intensity levels	D-20
Figure D-30	Bias of the local and maximum peak floor accelerations along the height of the 4-story RCMF for three different intensity levels	D-20
Figure D-31	Bias of the maximum beam plastic hinge rotation for each story along the height of the 4-story RCMF for three different intensity levels	D-21
Figure D-32	Bias of the maximum column plastic hinge rotation for each story along the height of the 4-story RCMF for three different intensity levels	D-22
Figure D-33	Bias of the story shear for each story along the height of the 4-story RCMF for three different intensity levels.....	D-22
Figure D-34	Bias of the overturning moment for each story along the height of the 4-story RCMF for three different intensity levels.....	D-22
Figure D-35	Bias of the local and maximum story drift ratios along the height of the 8-story RCMF for three different intensity levels.....	D-23

Figure D-36	Bias of the local and maximum peak floor accelerations along the height of the 8-story RCMF for three different intensity levels	D-23
Figure D-37	Bias of the maximum beam plastic hinge rotation for each story along the height of the 8-story RCMF for three different intensity levels.	D-24
Figure D-38	Bias of the maximum column plastic hinge rotation for each story along the height of the 8-story RCMF for three different intensity levels	D-24
Figure D-39	Bias of the story shear for each story along the height of the 8-story RCMF for three different intensity levels	D-25
Figure D-40	Bias of the overturning moment for each story along the height of the 8-story RCMF for three different intensity levels.....	D-26
Figure D-41	Mean and maximum absolute relative error for different EDP types over all 3 scale factors when selecting subsets within a FEMA P-695 stripe by matching globally the mean and median S_a values to estimate the 50% response (Method A).....	D-31
Figure D-42	Mean and maximum absolute σ -normalized error for different EDP types over all 3 scale factors when selecting subsets within a FEMA P-695 stripe by matching globally the mean and median S_a values to estimate the 50% response (Method A)	D-32
Figure D-43	Mean and maximum absolute relative error for different EDP types over all 3 scale factors when selecting subsets within a FEMA P-695 stripe by matching 50% local S_a values to estimate the 50% response (Method B).	D-36
Figure D-44	Mean and maximum absolute σ -normalized error for different EDP types over all 3 scale factors when selecting subsets within a FEMA P-695 stripe by matching 50% local S_a values to estimate the 50% response (Method B)	D-37
Figure D-45	Mean and maximum absolute relative error for different EDP types over all 3 scale factors when selecting subsets within a FEMA P-695 stripe by matching 84% local S_a values to estimate the 84% response (Method B)	D-41
Figure D-46	Mean and maximum absolute σ -normalized error for different EDP types over all 3 scale factors when selecting subsets within a FEMA P-695 stripe by matching 84% local S_a values to estimate the 84% response (Method B)	D-42
Figure D-47	The $S_a(T)$ individual spectra and their 16/50/84 summaries for the 44 ground motion records scaled to the median $S_a(T_I)$ value of the FEMA P-695 normalized clouds for the 2- and 8-story RCMFs. The shapes shown are invariant with changes in scale factor.....	D-47
Figure D-48	Mean and maximum absolute relative error for different EDP types over all 3 scale factors when selecting subsets within an S_a stripe by matching 50% local S_a values to estimate the 50% response.....	D-48
Figure D-49	Mean and maximum absolute relative error for different EDP types over all 3 scale factors when selecting subsets within an S_a stripe by matching 84% local S_a values to estimate the 84% response	D-49

Figure D-50	Mean and maximum absolute relative error for different EDP types over all 3 scale factors when randomly selecting subsets within an S_a stripe to estimate the 50% response (Trial 1).....	D-56
Figure D-51	Mean and maximum absolute relative error for different EDP types over all 3 scale factors when randomly selecting subsets within an S_a stripe to estimate the 50% response (Trial 2).....	D-57
Figure D-52	The $S_a(T)$ individual spectra and their 16/50/84 summaries for the 44 ground motion records scaled to the median S_{di} value of the FEMA P-695 normalized clouds for the 2- and 8-story RCMFs. The presence of a “pinch-point” at the first-mode period for low scale-factors shows when the structure remains elastic and S_{di} becomes perfectly correlated with S_a	D-60
Figure D-53	Mean and maximum absolute relative error for different EDP types over all 3 scale factors when selecting subsets within an S_{di} stripe by matching 50% local S_a values to estimate the 50% response.....	D-61
Figure D-54	Mean and maximum absolute relative error for different EDP types over all 3 scale factors when selecting subsets within an S_{di} stripe by matching 84% local S_a values to estimate the 84% response	D-62
Figure D-55	Mean and maximum absolute relative error for different EDP types over all 3 scale factors when randomly selecting subsets within an S_{di} stripe to estimate the 50% response (Trial 1).....	D-69
Figure D-56	Mean and maximum absolute relative error for different EDP types over all 3 scale factors when randomly selecting subsets within an S_{di} stripe to estimate the 50% response (Trial 2).....	D-70
Figure D-57	Normal probability plots to test for normality (N) and lognormality (LN) of maximum story drift (DR_{max}) and maximum floor acceleration (FA_{max}) over all stories given S_a -scaling for the 2-story RCMF	D-77
Figure D-58	Normal probability plots to test for normality (N) and lognormality (LN) of maximum story drift (DR_{max}) and maximum floor acceleration (FA_{max}) over all stories given S_a -scaling for the 4-story RCMF	D-78
Figure D-59	Normal probability plots to test for normality (N) and lognormality (LN) of maximum story drift (DR_{max}) and maximum floor acceleration (FA_{max}) over all stories given S_a -scaling for the 8-story RCMF	D-79
Figure D-60	Normal probability plots to test for normality (N) and lognormality (LN) of the 4 th floor maximum beam plastic hinge rotation given S_a -scaling for the 4-story RCMF at SF=2. The near-zero values make both distributions inadequate	D-80
Figure D-1	Testing the same data as in the above Figure D-60 after trimming values lower than 0.00038 rad. The lognormal fit is now acceptable, having similar dispersion but higher mean than before	D-80
Figure D-2	Normal probability plots to test for normality (N) and lognormality (LN) of maximum story drift (DR_{max}) and maximum floor acceleration (FA_{max}) over all stories given S_{di} -scaling for the 2-story RCMF	D-86
Figure D-3	Normal probability plots to test for normality (N) and lognormality (LN) of maximum story drift (DR_{max}) and maximum floor acceleration (FA_{max}) over all stories given S_{di} -scaling for the 4-story RCMF	D-87

Figure D-4	Normal probability plots to test for normality (N) and lognormality (LN) of maximum story drift (DR_{max}) and maximum floor acceleration (FA_{max}) over all stories given S_{di} -scaling for the 8-story RCMF	D-88
Figure E-1	comparison of peak roof displacement estimates with actual values for 2-story RCMF	E-3
Figure E-2	comparison of peak roof displacement estimates with actual values for 4-story RCMF	E-3
Figure E-3	comparison of peak roof displacement estimates with actual values for 8-story RCMF	E-4
Figure E-4	Ratio of peak roof displacement estimate obtained using an ESDOF system and the peak roof displacement obtained by NRHA for 2-story RCMR	E-4
Figure E-5	Ratio of peak roof displacement estimate obtained using an ESDOF system and the peak roof displacement obtained by NRHA for 4-story RCMF	E-5
Figure E-6	Ratio of peak roof displacement estimate obtained using an ESDOF system and the peak roof displacement obtained by NRHA for 8-story RCMF	E-5
Figure E-7	The normalized SPO2IDA backbone and its controlling parameters ...	E-7
Figure E-8	(a) The SPO curve of a nine-story steel structure and it's a pproximation with a trilinear and a quadrilinear model, (b) SPO curve versus the corresponding SPO2IDA capacity curves	E-7
Figure E-9	2-story RCMF, 1 st mode: ESDOF peak roof displacement estimation.....	E-9
Figure E-10	4-story RCMF, 1 st mode: ESDOF peak roof displacement estimation.....	E-9
Figure E-11	8-story RCMF, 1 st mode: ESDOF peak roof displacement estimation.....	E-10
Figure E-12	comparison of ESDOF and SPO2IDA estimates of roof displacement with results from 44 NRHAs and ASCE/SEI 41-06 estimates for the 2-story RCMF	E-11
Figure E-13	comparison of ESDOF and SPO2IDA estimates of roof displacement with results from 44 NRHAs and ASCE/SEI 41-06 estimates for the 4-story RCMF	E-11
Figure E-14	comparison of ESDOF and SPO2IDA estimates of roof displacement with results from 44 NRHAs and ASCE/SEI 41-06 estimates for the 8-story RCMF	E-12
Figure F-1	Average spectra.....	F-3
Figure F-2	Typical floor plan with moment frame layout	F-5
Figure F-3	Building A 3D SAP 2000 model	F-6
Figure F-4	transverse frame elevation of building A SAP model.....	F-6
Figure F-5	Typical nonlinear beam flexural plastic rotation hinge	F-7
Figure F-6	Typical nonlinear column flexural plastic rotation hinge	F-8
Figure F-7	Typical floor plan with concentric braced frame layout.....	F-10
Figure F-8	Building B PERFORM model	F-11

Figure F-9	Typical nonlinear HSS brace axial hinge.....	F-12
Figure F-10	Typical nonlinear beam flexural plastic rotation hinge	F-12
Figure F-11	Typical nonlinear infill shear pane	F-13
Figure F-12	Typical nonlinear column axial-dependent flexural plastic rotation hinge	F-13
Figure F-13	Building A pushover results	F-21
Figure F-14	Building A consecutive modal pushover results.....	F-21
Figure F-15	Building A NRHA peak story drift ratios	F-22
Figure F-16	Building A NRHA peak displacements, shears and OTMs	F-24
Figure F-17	Building A comparison of peak story displacement	F-24
Figure F-18	Building A comparison of peak story displacement	F-24
Figure F-19	Building A comparison of peak story drift	F-25
Figure F-20	Building A comparison of peak story drift	F-25
Figure F-21	Building A comparison of peak story shear.....	F-26
Figure F-22	Building A comparison of peak story shear.....	F-26
Figure F-23	Building A comparison of peak story overturning moment	F-27
Figure F-24	Building A comparison of peak story overturning moment	F-27
Figure F-25	Building A comparison of CMP extended peak displacement and story drift ratio	F-28
Figure F-26	Building A comparison of CMP extended peak shear and overturning moment.....	F-28
Figure F-27	Building A 2-stage CMP Deflected Shapes.....	F-29
Figure F-28	Building A 3-stage CMP Deflected Shapes.....	F-29
Figure F-29	Building B longitudinal (H1) pushover results.....	F-31
Figure F-30	Building B transverse (H2) pushover results	F-32
Figure F-31	Building B NRHA results in longitudinal direction (H1) for Scale Factor = 0.5	F-35
Figure F-32	Building B NRHA results in transverse direction (H2) for Scale Factor = 0.5	F-36
Figure F-33	Building B NRHA results in longitudinal direction (H1) for Scale Factor = 1.0	F-37
Figure F-34	Building B NRHA results in transverse direction (H2) for Scale Factor = 1.0.....	F-39
Figure F-35	Building B NRHA results in longitudinal direction (H1) for Scale Factor = 2.0	F-39
Figure F-36	Building B NRHA results in transverse direction (H2) for Scale Factor = 2.0.....	F-40
Figure F-37	Building B comparison of peak story drift ratio in longitudinal direction (H1).....	F-41
Figure F-38	Building B comparison of peak story drift Ratio in longitudinal direction (H1).....	F-42
Figure F-39	Building B comparison of peak story drift Ratio (reduced scale) in longitudinal direction (H1)	F-43

Figure F-40	Building B comparison of peak story drift Ratio (reduced scale) in longitudinal direction (H1)	F-44
Figure F-41	Building B comparison of peak story displacement in longitudinal direction (H1).....	F-45
Figure F-42	Building B comparison of peak story displacement in longitudinal direction (H1).....	F-46
Figure F-43	Building B comparison of peak story shear in longitudinal direction (H1).....	F-47
Figure F-44	Building B comparison of peak story shear in longitudinal direction (H1).....	F-48
Figure F-45	Building B comparison of peak story Overturning Moment in longitudinal direction (H1)	F-49
Figure F-46	Building B comparison of peak story Overturning Moment in longitudinal direction (H1)	F-50
Figure F-47	Building B comparison of peak story Drift Ratio in transverse direction (H2).....	F-51
Figure F-48	Building B comparison of peak story Drift Ratio in transverse direction (H2).....	F-52
Figure F-49	Building B comparison of peak story Drift Ratio (reduced scale) in transverse direction (H2)	F-53
Figure F-50	Building B comparison of peak story Drift Ratio (reduced scale) in transverse direction (H2)	F-54
Figure F-51	Building B comparison of peak story displacement in transverse direction (H2).....	F-55
Figure F-52	Building B comparison of peak story displacement in transverse direction (H2).....	F-56
Figure F-53	Building B comparison of peak story shear in transverse direction (H2).....	F-57
Figure F-54	Building B comparison of peak story shear in transverse direction (H2).....	F-58
Figure F-55	Building B comparison of peak story Overturning Moment in transverse direction (H2)	F-59
Figure F-56	Building B comparison of peak story Overturning Moment in transverse direction (H2)	F-60
Figure F-57	Building B comparison of CMP and NRHA peak story Drift Ratio in longitudinal direction (H1)	F-61
Figure F-58	Building B comparison of CMP and NRHA peak story Drift Ratio (reduced scale) in longitudinal direction (H1)	F-62
Figure F-59	Building B comparison of CMP and NRHA peak story displacement in longitudinal direction (H1)	F-63
Figure F-60	Building B comparison of CMP and NRHA peak story shear in longitudinal direction (H1)	F-64
Figure F-61	Building B comparison of CMP and NRHA peak story Overturning Moment in longitudinal direction (H1)	F-65

Figure F-62	Building B comparison of CMP and NRHA peak story Drift Ratio in transverse direction (H2)	F-66
Figure F-63	Building B comparison of CMP and NRHA peak story Drift Ratio (reduced scale) in transverse direction (H2)	F-67
Figure F-64	Building B comparison of CMP and NRHA peak story displacement in transverse direction (H2)	F-68
Figure F-65	Building B comparison of CMP and NRHA peak story shear in transverse direction (H2).....	F-69
Figure F-66	Building B comparison of CMP and NRHA peak story Overturning Moment in transverse direction (H2)	F-70
Figure F-67	Modified component model adapted from ASCE/SEI 41-06	F-72
Figure F-68	Building A ratio of peak story drift and story shear to NRHA baseline	F-87
Figure F-69	Building B ratio of peak story drift ratio (reduced scale) and story shear in longitudinal direction (H1 at Top) and transverse direction (H2 at bottom) to NRHA baseline	F-88
Figure F-70	Building A ratio of peak story drift and story shear to NRHA baseline	F-89
Figure F-71	Building B ratio of peak story drift ratio in longitudinal direction (H1 – At Top) and transverse direction (H2 – At bottom) to NRHA baseline	F-90
Figure G-1	Degradation of the force-displacement capacity boundary.....	G-26
Figure G-2	Relationship between IDA curves and the features of a typical force-displacement capacity boundary	G-27
Figure G-3	Comparison of nonlinear component model types.	G-41
Figure G-4	Individual deterioration modes for Ibarra-Krawinkler Model illustrated on a peak-oriented model.....	G-44
Figure G-5	Parameters of the initial backbone curve of the Ibarra-Krawinkler model	G-45
Figure G-6	Illustration of implementation of the four options for analytical component modeling.....	G-47

List of Tables - Supporting Documentation

Table A-1	Member Sizes of Steel SMFs Used in this Study	A-3
Table B-1	Modal Properties for the 2-story RCMF	B-2
Table B-2	Modal Properties for the 4-story RCMF	B-3
Table B-3	Modal Properties for the 8-story RCMF	B-3
Table B-4	Eigenmodes of the 2-Story RCMF	B-3
Table B-5	Eigenmodes of the 4-Story RCMF	B-3
Table B-6	Eigenmodes of the 8-Story RCMF	B-3
Table B-7	$R-C_1-T$ Calculations for the 2-Story RCMF	B-6
Table B-8	$R-C_1-T$ Calculations for the 4-Story RCMF	B-7
Table B-9	$R-C_1-T$ Calculations for the 8-Story RCMF	B-8
Table B-10	2-Story RCMRF: Summary of Analysis Methods Showing the Estimate/Median NRHA Ratio	B-45
Table B-11	4-Story RCMRF: Summary of Analysis Methods Showing the Estimate/Median NRHA Ratio	B-46
Table B-12	8-Story RCMRF: Summary of Analysis Methods Showing the Estimate/Median NRHA Ratio	B-47
Table C-1	Properties of RCSW Archetypes Used in This Study (from NIST, 2010)	C-3
Table D-1	Subset Estimation Errors for the 50% EDP Response of the 2-Story RCMF Using Selection Method A on FEMA-P695 Stripes	D-33
Table D-2	Subset Estimation Errors for the 50% EDP Response of the 4-Story RCMF Using Selection Method A on FEMA-P695	D-34
Table D-3	Subset Estimation Errors for the 50% EDP Response of the 2-Story RCMF Using Selection Method B on FEMA-P695 Stripes	D-38
Table D-4	Subset Estimation Errors for the 50% EDP Response of the 4-Story RCMF Using Selection Method B on FEMA-P695 Stripes	D-39
Table D-5	Subset Estimation Errors for the 84% EDP Response of the 2-Story RCMF Using Selection Method B on FEMA-P695 Stripes	D-43
Table D-6	Subset Estimation Errors for the 84% EDP Response of the 4-Story RCMF Using Selection Method B on FEMA-P695 Stripes	D-44
Table D-7	Subset Estimation Errors for the 50% EDP Response of the 2-Story RCMF Using Selection Method B on S_a Stripes	D-50
Table D-8	Subset Estimation Errors for the 84% EDP Response of the 2-Story RCMF Using Selection Method B on S_a Stripes	D-51
Table D-9	Subset Estimation Errors for the 50% EDP Response of the 4-Story RCMF Using Selection Method B on S_a Stripes	D-52

Table D-10	Subset Estimation Errors for the 84% EDP Response of the 4-Story RCMF Using Selection Method B on S_a Stripes	D-54
Table D-11	Subset Estimation Errors for the 50% EDP Response of the 2-Story RCMF Using Selection Method B on S_{di} Stripes.....	D-63
Table D-12	Subset Estimation Errors for the 84% EDP Response of the 2-Story RCMF Using Selection Method B on S_{di} Stripes.....	D-64
Table D-13	Subset Estimation Errors for the 50% EDP Response of the 4-Story RCMF Using Selection Method B on S_{di} Stripes.....	D-65
Table D-14	Subset Estimation Errors for the 84% EDP Response of the 4-Story RCMF Using Selection Method B on S_{di} Stripes.....	D-67
Table D-15	Acceptance Values for Testing the Distribution for S_a -Scaling at Levels Corresponding to Normalized Scale Factors of 0.5, 1.0, and 2.0 for the 2-story RCMF.....	D-73
Table D-16	Acceptance Values for Testing the Distribution for S_a -Scaling at Levels Corresponding to Normalized Scale Factors of 0.5, 1.0, and 2.0 for the 4-story RCMF.....	D-74
Table D-17	Acceptance Values for Testing the Distribution for S_a -Scaling at Levels Corresponding to Normalized Scale Factors of 0.5, 1.0, and 2.0 for the 8-story RCMF.....	D-75
Table D-18	Acceptance Values for Testing the Distribution for S_{di} -Scaling at Levels Corresponding to Normalized Scale Factors of 0.5, 1.0, and 2.0 for the 2-story RCMF.....	D-82
Table D-19	Acceptance Values for Testing the Distribution for S_{di} -Scaling at Levels Corresponding to Normalized Scale Factors of 0.5, 1.0, and 2.0 for the 4-story RCMF.....	D-83
Table D-20	Acceptance Values for Testing the EDP Distribution for S_{di} -Scaling at Levels Corresponding to Normalized Scale Factors of 0.5, 1.0, and 2.0 for the 8-story RCMF.....	D-84
Table D-21	Actual and Approximate Values of Dispersion (Standard Deviation of Natural Logs) at FEMA P-695 Intensity Levels as Estimated Using the Medians Obtained for Two Different S_{di} Intensity Levels.....	D-90
Table D-22	Actual and Approximate Values of Dispersion (Standard Deviation of Natural Logs) at $S_a(T_I)$ Intensity Levels as Estimated Using the Medians Obtained for Two Different S_{di} Intensity Levels.....	D-90
Table E-1	Mean ratios (ESDOF Estimate of Peak Roof Displacement/NRHA Value) for Each Frame and Scale Factor	E-6
Table F-1	Application Direction of Selected Ground Motions	F-3
Table F-2	Modal Properties for Building A – Original 3D Model.....	F-8
Table F-3	Eigenmodes of Building A – Original 3D Model.....	F-9
Table F-4	Modal Properties for Building A – 2D Model Analyzed.....	F-9
Table F-5	Eigenmodes of Building A – 2D Model Analyzed.....	F-9
Table F-6	Modal Properties for Building B	F-14
Table F-7	Eigenmodes of Building B (at Center of Mass).....	F-14
Table F-8	$R-C_1-T$ Calculations for Building A.....	F-20

Table F-9	<i>R-C₁-T</i> Calculations for Building B.....	F-33
Table F-10	CMP Target Roof Displacements of Building B (SF = 0.5).....	F-34
Table F-11	CMP Target Roof Displacements of Building B (SF = 1.0).....	F-34
Table F-12	CMP Target Roof Displacements of Building B (SF = 2.0).....	F-34
Table F-13	Accuracy of Response Quantity Estimates for Building A.....	F-84
Table F-14	Predicted Level of Performance (Based on ASCE 41 Acceptance Criteria) for Building A	F-84
Table F-15	Accuracy of Response Quantity Estimates for Building B – H1 Direction	F-85
Table F-16	Accuracy of Response Quantity Estimates for Building B – H2 Direction	F-86
Table G-1	Engineering Demand Parameters ¹ That May be Addressed Using These Analysis Procedures	G-4
Table G-2	Engineering Demand Parameters ¹ That May be Addressed Using These Analysis Procedures	G-9
Table G-3	Engineering Demand Parameters ¹ That May be Addressed Using These Analysis Procedures	G-15
Table G-4	Engineering Demand Parameters ¹ That May be Addressed Using These Analysis Procedures	G-28
Table G-5	Engineering Demand Parameters ¹ That May be Addressed Using These Analysis Procedures	G-34
Table G-6	Engineering Demand Parameters ¹ That May be Addressed Using These Analysis Procedures	G-39
Table G-7	Summary of Structural Elements Affecting the Backstay Effect for a Concrete Core Wall Building, and the Recommended Range of Stiffness Assumptions	G-53
Table G-8	Notes on Tall Building Structural Elements not Covered in Table G-7	G-55

Introduction - Supporting Documentation

1.1 Organization and Content

This report presents findings, conclusions, and recommendations resulting from a review of available research and practice regarding nonlinear multiple-degree-of-freedom (MDOF) effects, and focused analytical studies targeted to investigate selected issues related to MDOF modeling and response characteristics. The report is organized into two parts: (1) a main volume of summary information and conclusions; and (2) supporting documentation.

This volume, *Supporting Documentation*, contains appendices that provide detailed reporting on the focused analytical studies, ancillary studies, and literature review activities that formed the basis of the findings.

Appendix A presents focused studies on nonlinear response of steel moment frame structures. Nonlinear response history analysis is performed using the FEMA P-695 far-field ground motion set, and various options of single-mode nonlinear static analysis and modal pushover analysis procedures are explored and evaluated. In most cases, 2-, 4-, and 8-story archetypes are utilized. Peak values of story drift ratio, story shear force, and floor overturning moment are evaluated.

Appendix B presents focused studies on nonlinear response of reinforced concrete moment frame structures. Nonlinear response history analysis is performed using the FEMA P-695 far-field ground motion set, and various single-mode and multiple-mode nonlinear static analysis procedures are evaluated. Various 2-, 4-, and 8-story reinforced concrete moment frame archetypes are utilized. Peak values of floor displacement, story drift ratio, story shear force, and floor overturning moment are evaluated.

Appendix C presents focused studies on nonlinear response of reinforced concrete shear wall structures. Nonlinear response history analysis is performed using the FEMA P-695 far-field ground motion set, and various options of single-mode nonlinear static analysis and modal pushover analysis procedures are evaluated. In most cases, 2-, 4-, and 8-story archetypes are utilized. Peak values of story drift ratio, story shear force, and floor overturning moment are evaluated.

Appendix D presents an ancillary study undertaken to investigate the relationships between demand parameter dispersion (and bias), ground motion scaling method, and

size of the ground motion data set. The purpose of this study is to find more economical approaches for performing nonlinear response history analysis in practice.

Appendix E presents an ancillary study undertaken to test the practicality of direct determination of target displacement for nonlinear static analyses.

Appendix F presents an ancillary study undertaken to apply the methods tested in primary focused studies (with some extensions) to models of two special-case buildings encountered in practice using production software in common use by practitioners. The objective of this study was to further test the methods and identify practical challenges to their implementation.

Appendix G provides summaries of codes, standards, and guidelines that are relevant to nonlinear multiple-degree-of-freedom modeling in current engineering practice. Summaries include the scope of application, applicability of analysis procedures, other modeling direction provided, additional analysis requirements listed, as well as the ground motion characterization. These summaries also include a list of response quantities (i.e., demand parameters) that can be evaluated using the analysis procedures outlined in the respective documents.

Appendix H provides a bibliography of recent research that is of particular relevance to nonlinear multiple-degree-of-freedom modeling. The citations are organized topically and chronologically, and cover relevant research published since 2002.

Detailed Steel Moment Frame Studies

This appendix presents results of problem-focused studies on nonlinear response of steel moment frame structures. Nonlinear response history analysis is performed using the FEMA P-695 far-field ground motion set, and various options of single mode nonlinear static analysis and modal pushover analysis procedures are explored and evaluated. In most cases, 2-, 4-, and 8-story archetypes are utilized. Peak values of story drift ratio, story shear force, and floor overturning moment are evaluated.

A.1 Introduction

The purpose of this study is to evaluate important engineering demand parameters (EDPs) from results obtained from “best estimate” nonlinear response history analysis (NRHA), using 2-dimensional representations of 2-, 4- and 8-story steel special moment frame (steel SMF) structures. The EDP values obtained from such NRHA serve as benchmark values for assessing predictions by means of simplified methods.

This study focuses on the following three EDPs: maximum story drift ratio, maximum story shear force, and maximum floor overturning moment.

The quality of EDP predictions is assessed for the following simplified methods:

- Standard nonlinear static procedure (NSP) outlined in ASCE/SEI 41-06, *Seismic Rehabilitation of Existing Buildings* (ASCE, 2007)
- Variations to the ASCE/SEI 41-06 NSP
- Alternative pushover procedures with a focus on modal pushover analysis (MPA)
- Utilization of a simplified model of the structure.

Attention is devoted also to (a) the sensitivity of NSP predictions to the applied load pattern and the quality of NSP predictions for frame structures with a significant strength irregularity, and (b) a simple method for incorporating the gravity system in the analytical model and the potential importance of the gravity system on EDP predictions.

A.2 Structures Utilized in Evaluation

This study utilizes a subset of the steel special moment frame (SMF) archetypes designed and analyzed in the NIST GCR 10-917-8 report, *Evaluation of the FEMA P-695 Methodology for Quantification of Building Seismic Performance Factors* (NIST, 2010). The subset consists of three structures designed by means of response spectrum analysis (RSA) for seismic design category D_{\max} ($S_{DS} = 1.0g$ and $S_{DI} = 0.60g$), designated here as:

- 2-story steel SMF (Archetype ID 2- D_{\max} -RSA)
- 4-story steel SMF (Archetype ID 4- D_{\max} -RSA)
- 8-story steel SMF (Archetype ID 8- D_{\max} -RSA)

The structures consist of three-bay moment-resisting frames with the plan view shown in Figure A-1. In the structural systems as designed, the frames resist all seismic design forces and receive tributary gravity loads as indicated in the shaded portion of the figure.

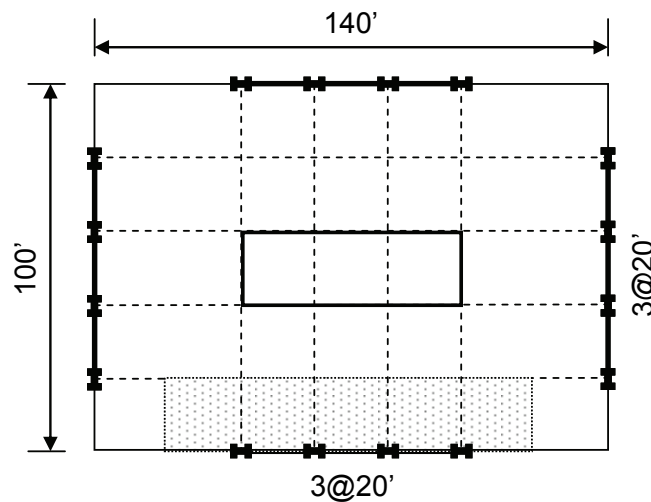


Figure A-1 Plan view of buildings used for archetype selection (from NIST, 2010).

The bay width, i.e., the centerline dimension between columns of each frame is 20'. The height of the first story is 15' (to top of steel beam), and the height of all other stories is 13'. The dead load is 90 psf uniformly distributed over each floor, and the cladding load is applied as a perimeter load of 25 psf. Unreduced life load is 50 psf on all floors and 20 psf on the roof. All beams are reduced-beam section (RBS) and designed in accordance with AISC 358, *Prequalified Connections for Special and Intermediate Steel Moment Frames for Seismic Applications* (AISC, 2005), using $a = 0.625b_f$, $b = 0.75d_b$, and $c = 0.250b_f$. Member sizes of the moment frames are summarized in Table A-1.

Table A-1 Member Sizes of Steel SMFs Used in this Study

Story Floor	Elevation (inches)	Beam	Exterior Columns	Interior columns	Doubler Plate (ext. col.)	Doubler Plate (int.col)
<i>2-Dmax-RSA (PG-IRSA)</i>						
1	164.65	W30X132	W24X131	W24X162	1/16	1 3/16'
2	320.65	W16X31	W24X131	W24X162	0	0
<i>4-Dmax-RSA (PG-2RSA)</i>						
1	66.55	W21X73	W24X103	W24X103	0	5/16
2	322.55	W21X73	W24X103	W24X103	0	5/16
3	478.55	W21X57	W24X62	W24X62	0	5/16
4	634.55	W21X57	W24X62	W24X62	0	5/16
<i>8-Dmax-RSA (PG-2RSA)</i>						
1	166.55	W30X108	W24X131	W24X162	1/16	9/16
2	322.55	W30X116	W24X131	W24X162	1/16	6/16
3	478.55	W30X116	W24X131	W24X162	1/16	11/16
4	634.55	W27X94	W24X131	W24X162	0	11/16
5	790.55	W27X94	W24X131	W24X131	0	6/16
6	946.55	W27X84	W24X131	W24X131	0	7/16
7	1102.55	W27X84	W27X94	W27X94	0	9/16
8	1258.55	W21X68	W27X94	W27X94	0	5/16

A.3 Nonlinear Response History Analysis

The analytical model of steel SMF building structural systems is based on the bare frame, i.e., no credit is given to the floor slab and, except for the gravity system case discussed in Section A.8, no credit is given to the contributions of gravity columns and simple connections to strength and stiffness of the structure. A leaning column is used for representation of P-Delta effects caused by gravity loads not directly tributary to the steel SMF. This representation is discussed in Section 7.2.4.

The record set used for nonlinear response history analysis (NRHA) is the set of 44 far-field ground motions employed in FEMA P-695 (FEMA, 2009).

A.3.1 Component Model and Analysis Platforms

The bare frame structure is analyzed with the latest version of either the Drain-2DX program (Prakash et al., 1993) or the Open System for Earthquake Engineering Simulation (OpenSees) platform (<http://opensees.berkeley.edu>, McKenna, 1997), utilizing recently developed component moment-rotation models. The models for flexural behavior of steel components, which are identical in the Drain-2DX and OpenSees versions used in this study, are based on the point hinge concept and utilize a backbone curve of the type shown in Figure A-2, a bilinear hysteretic model,

and cyclic deterioration parameters discussed in detail in the PEER/ATC-72-1 Report, *Modeling and Acceptance Criteria for Seismic Design and Analysis of Tall Buildings* (PEER/ATC, 2010), and Lignos and Krawinkler (2009, 2010). The deterioration parameters are based on regression equations derived from experimental results and provide different values for different steel W-sections as a function of geometric section properties and material properties that control deterioration in strength and stiffness due to local and lateral torsional buckling. This component model is referred to as the “modified IK model,” and analyses performed based on this component model are referred to as Analyt.M1. Results obtained with Analyt.M1 account for cyclic deterioration in NRHA (referred to as analysis option 1 in the PEER/ATC-72-1 report), but they do not account for cyclic deterioration in a pushover analysis, which is based on the initial (monotonic) backbone curve.

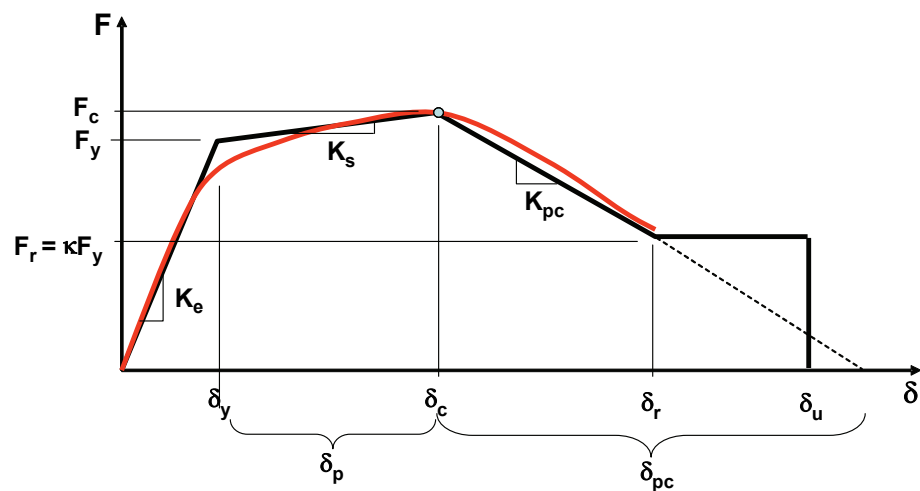


Figure A-2 Backbone curve for component model Analyt.M1 (PEER/ATC, 2010).

This study is concerned only with 2-dimensional modeling of structures. Thus, the assumption is that torsional and biaxial loading effects are negligible. The issue of torsion is discussed in Section 7.2. In all analyses Rayleigh damping of 2.5% is assigned at the first mode period T_1 and at $T = 0.2T_1$.

A.3.2 Analysis Model Simplification

As discussed in Section 7.1, a 2-dimensional model of a moment-resisting frame structure should represent, at least, the moment-frame(s) as well as all P-Delta effects tributary to the moment frame(s). If several moment-resisting frames exist, they may be placed in parallel, presuming that the assumption of a rigid diaphragm is reasonable. Thus, a 2-D model consists of moment-resisting frames, a P-Delta column, and, if presumed to be important, may incorporate a representation of the gravity system. In the context discussed here, which has a focus on global and story level EDPs such as story drifts and shears, it is often acceptable to represent all moment-resisting frames by a single bay frame, resulting in the simplified model illustrated in Figure A-3. Such a model reduces the computational effort and often

facilitates interpretation of global results. But the simplified model may not be adequate to extract local demands such as plastic hinge rotations in individual components and axial and shear forces in columns. Thus, its primary purpose is to assess global and story level EDPs and to detect weaknesses that may become the subject of a more detailed evaluation.

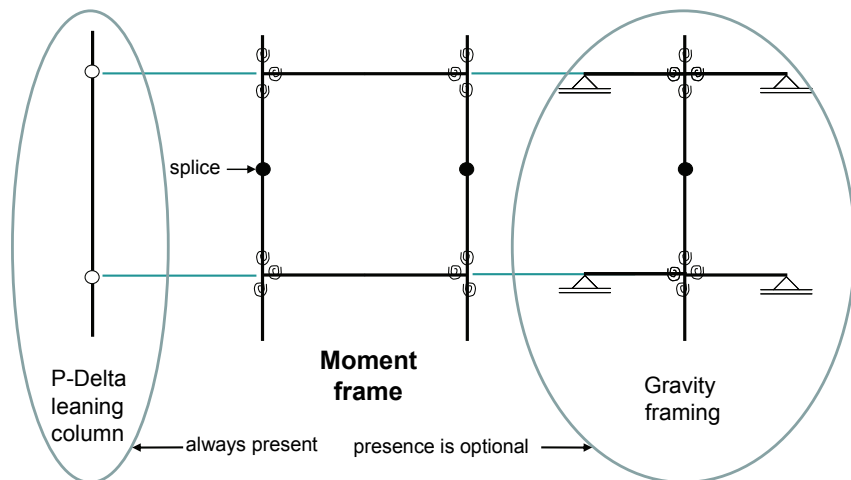


Figure A-3 Simplified model of moment-resisting frame structure.

Lumping together multi-bay frames into a single bay frame can be accomplished by setting $\sum EI_i/L_i$ and $\sum M_p$ of all beams equal to EI/L and M_p of the single bay beam, respectively, and setting $\sum EI_i$ and $\sum M_{pc}$ of all columns equal to $2EI$ and $2M_{pc}$ of the single bay columns, respectively. For taller frames in which overturning moment and axial deformations in columns are important, these effects can be approximated by setting L of the single bay frame equal to the distance between end columns of the multi-bay frame, and setting the area of the single bay column equal to the area of the end column of the multi-bay frame. This simplification is based on the assumption that overturning effects are resisted mostly by the two end columns. The approximations summarized in this paragraph are reasonable if all bays of the SMF are of about equal width, and become more approximate when spans of the SMF vary considerably.

As additional approximations, it is assumed that beams and columns can be represented by centerline dimensions and panel zone shear deformations can be ignored. For frames in which panel zones are sufficiently strong to develop the bending strength of the beams framing into the joint, the errors involved in making these two approximations often compensate each other. On the other hand, frames with weak panel zones should not be approximated in this manner. In essence, the resulting single bay frame is similar to the fishbone model used extensively in Japan (e.g., Luco et al., 2003), with the added advantage that overturning moments and column axial deformation effects are represented in the model.

The fishbone model can be used to represent the strength and stiffness properties of the gravity framing that is not part of the moment-resisting frame, as will be

discussed in Section A.8, and as is shown in the right portion of Figure A-3. If the gravity framing is included in the analytical model (not done here except for the case discussed in Section A.8), then the column of the fishbone can be used also to represent P-Delta effects not directly attributed to the moment-resisting frame. Otherwise, the need exists to provide a P-Delta (leaning) column as shown on the left of Figure A-3 and as discussed in Section 7.1

Single bay simplification has been tested for the aforementioned steel SMF structures. Comparisons of results obtained from the 3-bay Drain-2DX model and the single-bay OpenSees model (both incorporate a P-Delta column) can be made from the graphs presented in Figures A-4 to A-7.

Throughout this Appendix, the emphasis is on presenting of global pushover curves and results obtained for the following story-level EDPs:

- Peak story drift ratio, θ_{si}
- Peak story shear force $V_{I+P-\Delta}$, normalized by the seismically effective weight W (see Section 7.1 for definition of this EDP and why it should be the primary story force parameter)
- Peak floor overturning moments $OTM_{I+P-\Delta}$, normalized by WH , with W being the seismically effective weight tributary to the 2-D frame model and H being the height of the structure (see Section 7.1 for definition of this EDP)

Figure A-4 compares pushover curves for the 3- and 1-bay models of the 2-, 4-, and 8-story structures, in these cases using V_I as the load parameter. The graphs show clearly that the simplified 1-bay model captures accurately the global characteristics of the three-bay structure. They also demonstrate the following behavior patterns that are characteristic for steel SMFs:

- A large range of elastic behavior terminated by global yielding in one or several stories, usually triggered by beam plastic hinging or column plastic hinging at the base.
- A range of close to constant post-yield stiffness terminated by capping, which is defined as attainment of peak bending strength in beams and/or columns in one or several stories. The post yield tangent stiffness may be positive or negative, depending on the relative importance of strain hardening in the moment-rotation characteristics of individual components versus P-delta effects. In these examples, strain hardening is defined by the ratio of capping strength to yield strength of plastic hinges (M_c/M_y), which is taken as 1.1 for all plastic hinge regions. P-delta effects are often approximated by the stability coefficient $\theta = P\Delta/(Vh)$ in each story, although it must be emphasized that this approximation, which is based on elastic behavior, often is inadequate to represent P-delta effects in the inelastic range. Because of the increasing importance of P-delta effects for taller frame structures, the post-yield tangent stiffness decreases as the number of

stories increases, and becomes slightly negative already for the 4-story steel SMF structure.

- A range of post-capping behavior, characterized by a negative tangent stiffness whose magnitude is determined by the combined contributions of P-delta effects and post-capping deterioration characteristics of steel structural components. The larger the number of stories, the larger is usually the ratio of absolute value of post-capping stiffness to elastic stiffness. The range of negative post-capping tangent stiffness is of major concern in predicting EDPs, and dynamic instability (collapse) becomes an important issue in this range of behavior.

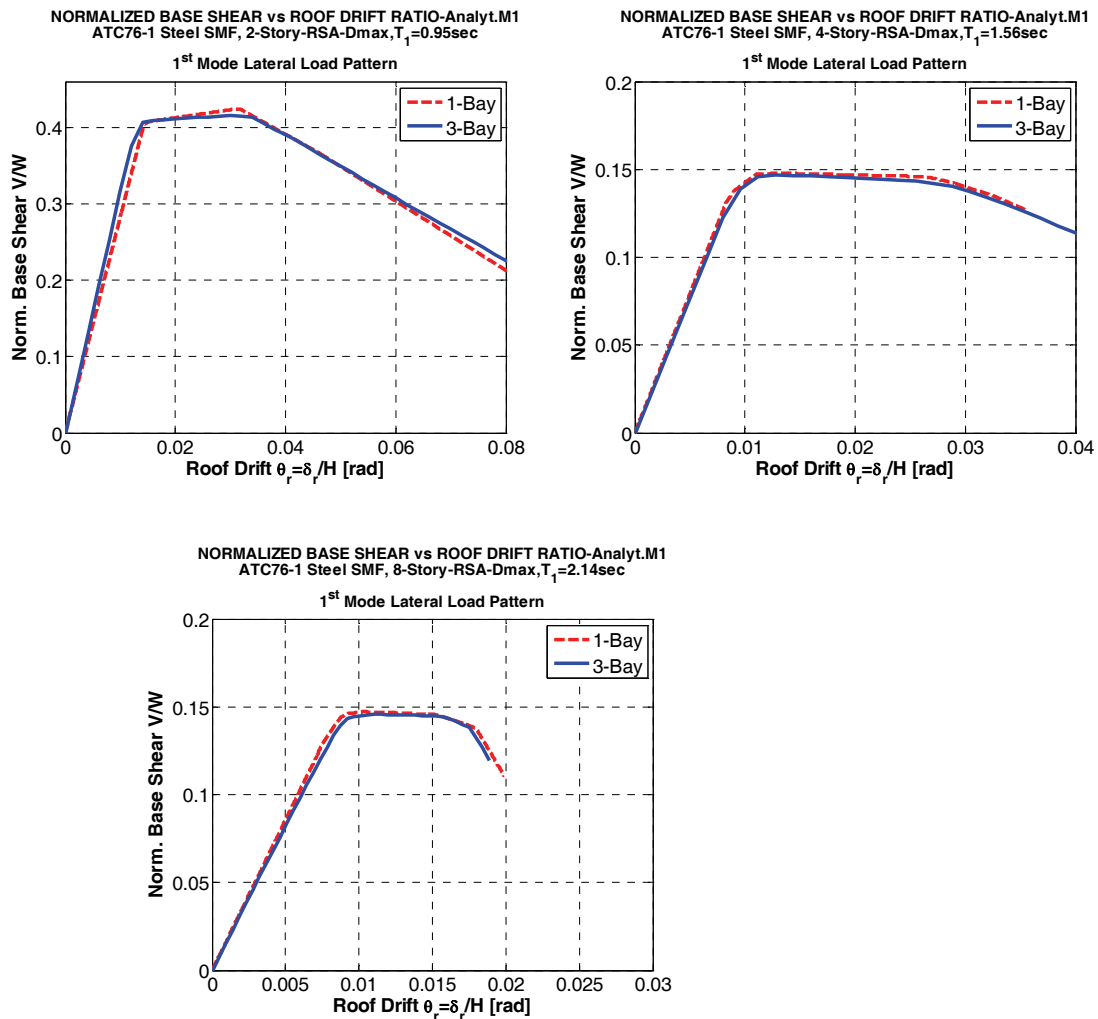


Figure A-4 Comparison of global pushover curves ($V_r/W - \theta_r$) of 1- and 3-bay steel SMF analytical models, 2-, 4-, and 8-story steel SMFs.

Nonlinear response history analysis predictions for a specific ground motion, obtained from the Drain-2DX 3-bay model (referred to here as ATCW (3-Bay)) and the OpenSees 1-bay model of the 4-story steel SMF, are compared in Figure A-5. The roof displacement history responses and the base shear history responses are

almost identical, providing confidence in the two analysis platforms and in the ability to represent the response of the 3-bay frame in a simplified 1-bay model.

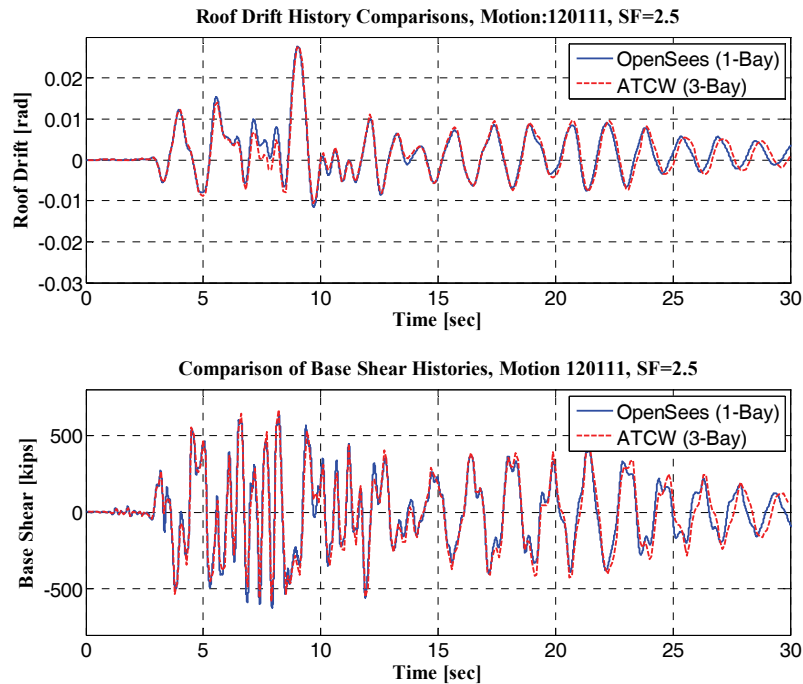


Figure A-5 Comparison of response history results for 4-story steel SMF, using Drain-2DX 3-bay and OpenSees 1-bay models.

A comparison of EDP predictions obtained from NRHA of the two analysis models is presented in Figures A-6 and A-7 for the 4- and 8- story steel SMFs. The suite of 44 far field ground motions used in the FEMA P-695 Report, *Quantification of Building Performance Factors* (FEMA, 2009b), with a scale factor (SF) of 2.0 has been used as input to the analytical models. Results are presented for story drift ratios, normalized story shear forces, $V_{I+P-\Delta}$, and normalized floor overturning moments, $OTM_{I+P-\Delta}$. Here and elsewhere in this Appendix, peak values are presented for individual ground motions (connected by light gray lines) and for median values (connected by bold solid line) as well as 16th and 84th percentile values (connected by bold dashed lines). Again, the results between the two models are similar for individual ground motions and are almost identical for statistical values.

A few general observations, common to most of the NRHA results in this appendix, are summarized here:

- The dispersion in response is largest for story drift ratios, smaller for story shears, and smallest for story overturning moments. This is discussed in Section A.3.4 in more detail.
- Story drift demands are not distributed uniformly over the height (particularly for the 8-story steel SMF) even though the design of all structures was drift controlled and a uniform distribution of drift exists under the code design loads.

- Story shear demands do not at all follow the lateral load patterns for which the structures have been designed. Based on code design criteria the shear in story 4 should be about 0.45 times the base shear, but it is about 0.75 times the base shear in the median. The reason is dynamic redistribution enforced by the fact that no weak story is detected in this structure.
- Floor overturning moment demands also do not follow a distribution based on the design load pattern. They are larger than anticipated, particularly in the upper stories, as will be shown later when pushover predictions are compared with NRHA results.

Figure A-8 presents a comparison of story EDPs and local EDPs, using NRHA results from the 4-story steel SMF for a ground motion scale factor 2.0. The left half of the figure shows EDP results for story drifts, story shear forces, and floor overturning moments. The right half shows results for plastic hinge rotation at RBS location closest to the exterior column, shear force V_{G+E} in an interior column, and axial force P_{G+E} in one of the two exterior columns. The patterns of story and local EDPs are similar but not identical since the relationships between local and story EDPs change from story to story and from component to component. Moreover, the column peak force quantities contain also gravity load effects, which are not reflected in the story force quantities shown on the left. The graphs are presented to illustrate that local EDPs are an essential part of the analysis effort needed to predict seismic performance. In this study the focus is on assessment of analysis procedures (NRHA versus static procedures), and in this context an evaluation of story level EDPs is more relevant because it provides clearer patterns of behavior that are not obscured by spurious behavior of individual components.

Examples of other salient results from NRHA of the 4-story 3-bay model are presented in Figure A-9 for absolute floor accelerations. Data on this important parameter have been computed for all structures in this project but are not presented for other cases because no comparison can be made with results from a static pushover analysis. It is a shortcoming of the nonlinear static procedure (NSP) that it does not provide any estimation of this EDP (and neither of residual drift), considering the increasing importance of floor acceleration (and residual drift) in loss assessment of structures (damage in nonstructural acceleration sensitive components), and its importance in estimating diaphragm forces. It is noteworthy that the maximum absolute floor acceleration does not vary radically over the height of this 4-story structure, and that it is distributed almost uniformly over the height for a ground motion scale factor of 2.0 at which the structure responds in the highly inelastic range.

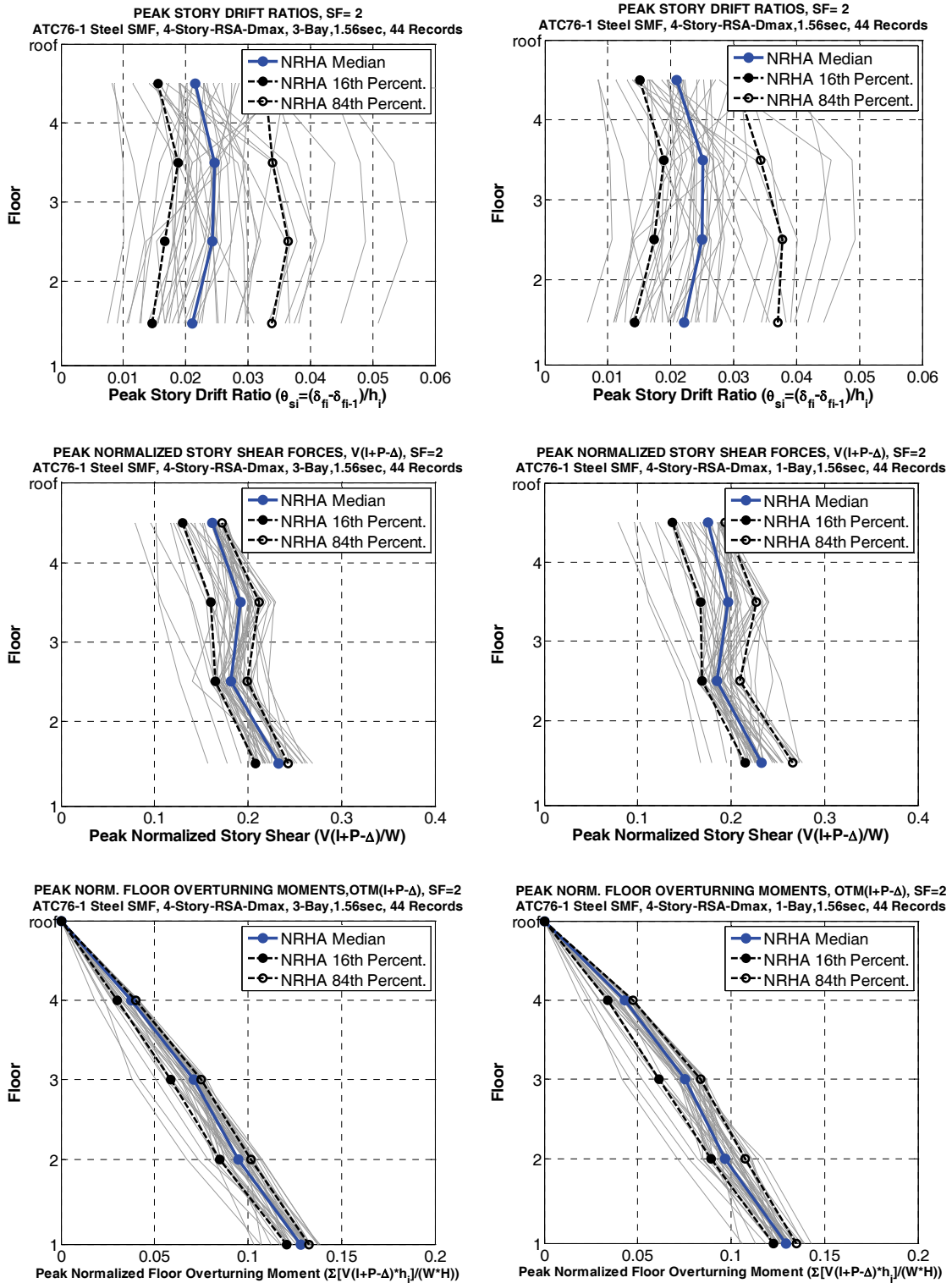


Figure A-6 Comparison of θ_{si} , $V_{I+P-\Delta}$, and $OTM_{I+P-\Delta}$ obtained from NRHA of 3-bay model (left) and simplified 1-bay model (right), 4-story steel SMF, SF = 2.0.

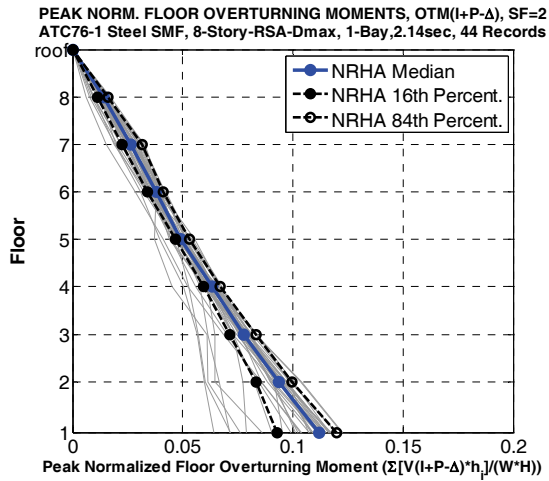
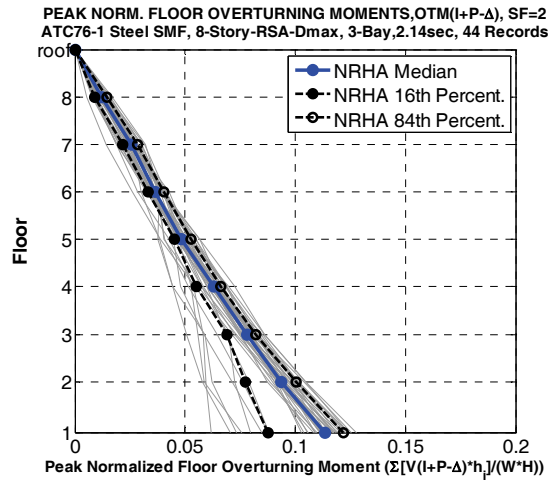
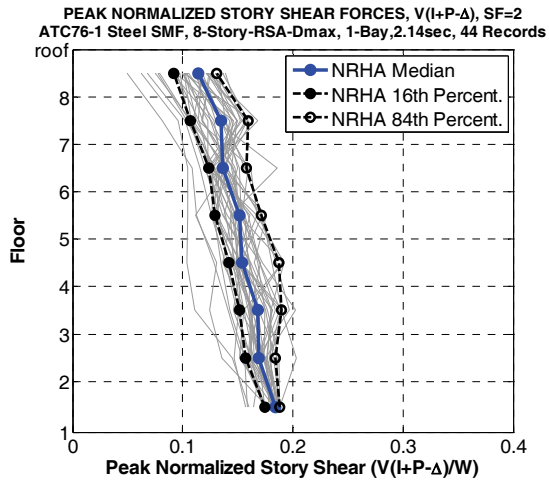
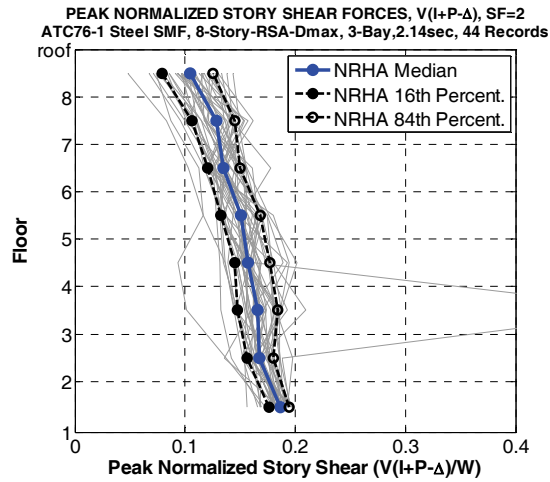
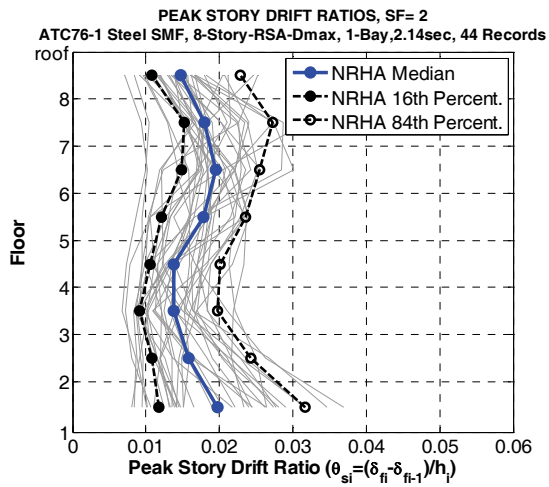
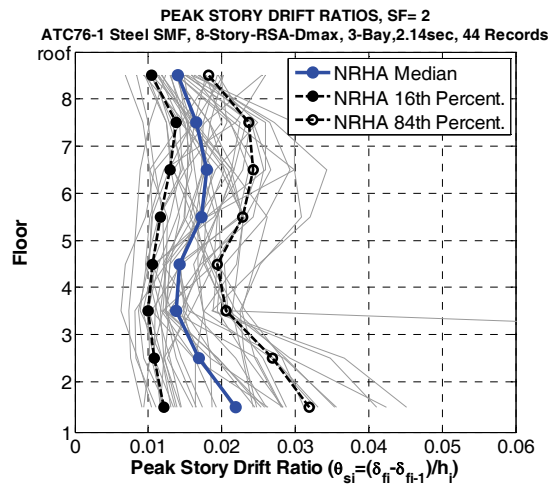


Figure A-7 Comparison of θ_{si} , $V_{I+P-\Delta}$, and $OTM_{I+P-\Delta}$ obtained from NRHA of 3-bay model (left) and simplified 1-bay model (right), 8-story steel SMF, SF = 2.0.

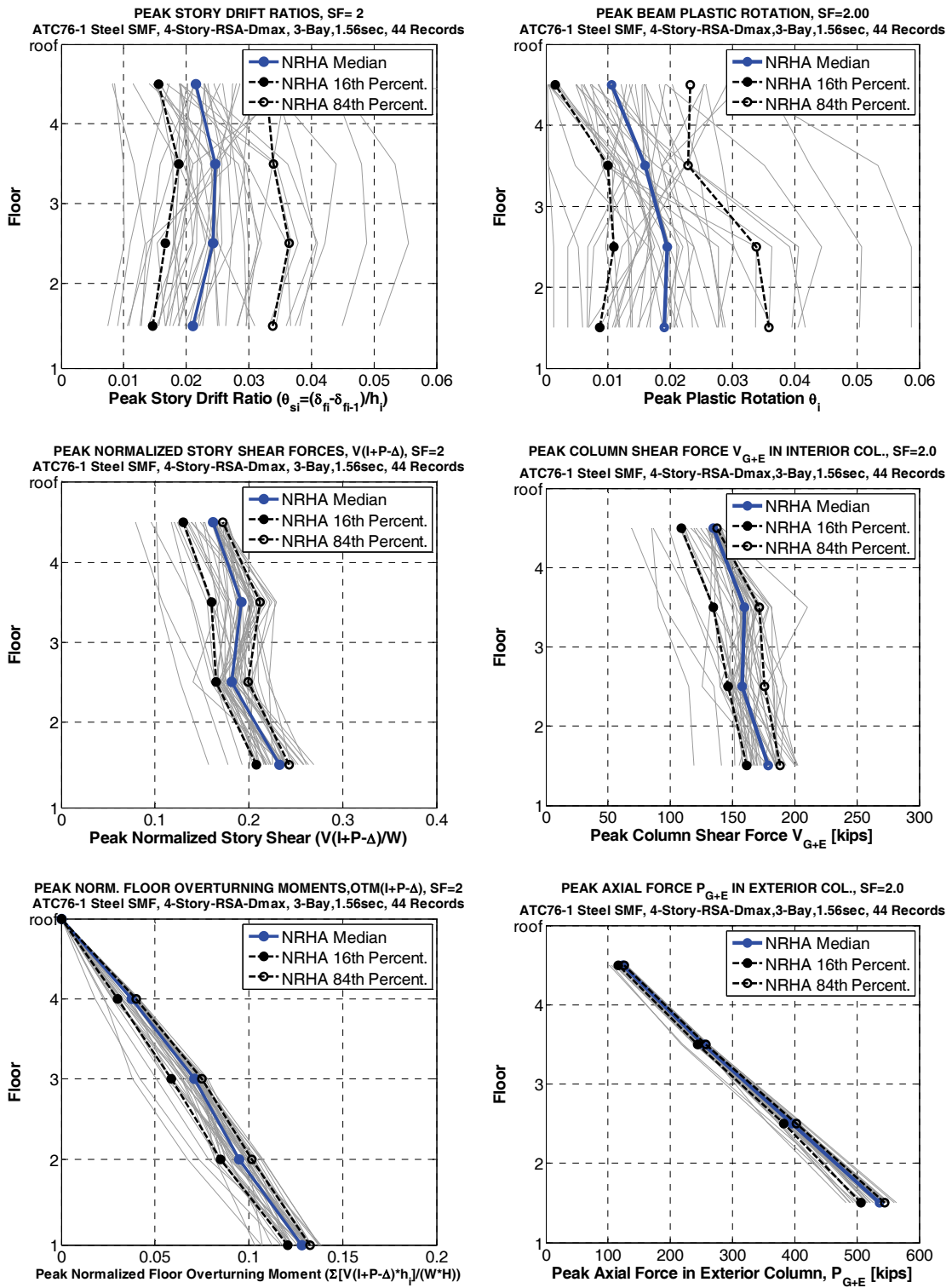


Figure A-8 Comparison of story level EDPs (left side) with local EDPs (right side), 4-story steel SMF, SF = 2.0.

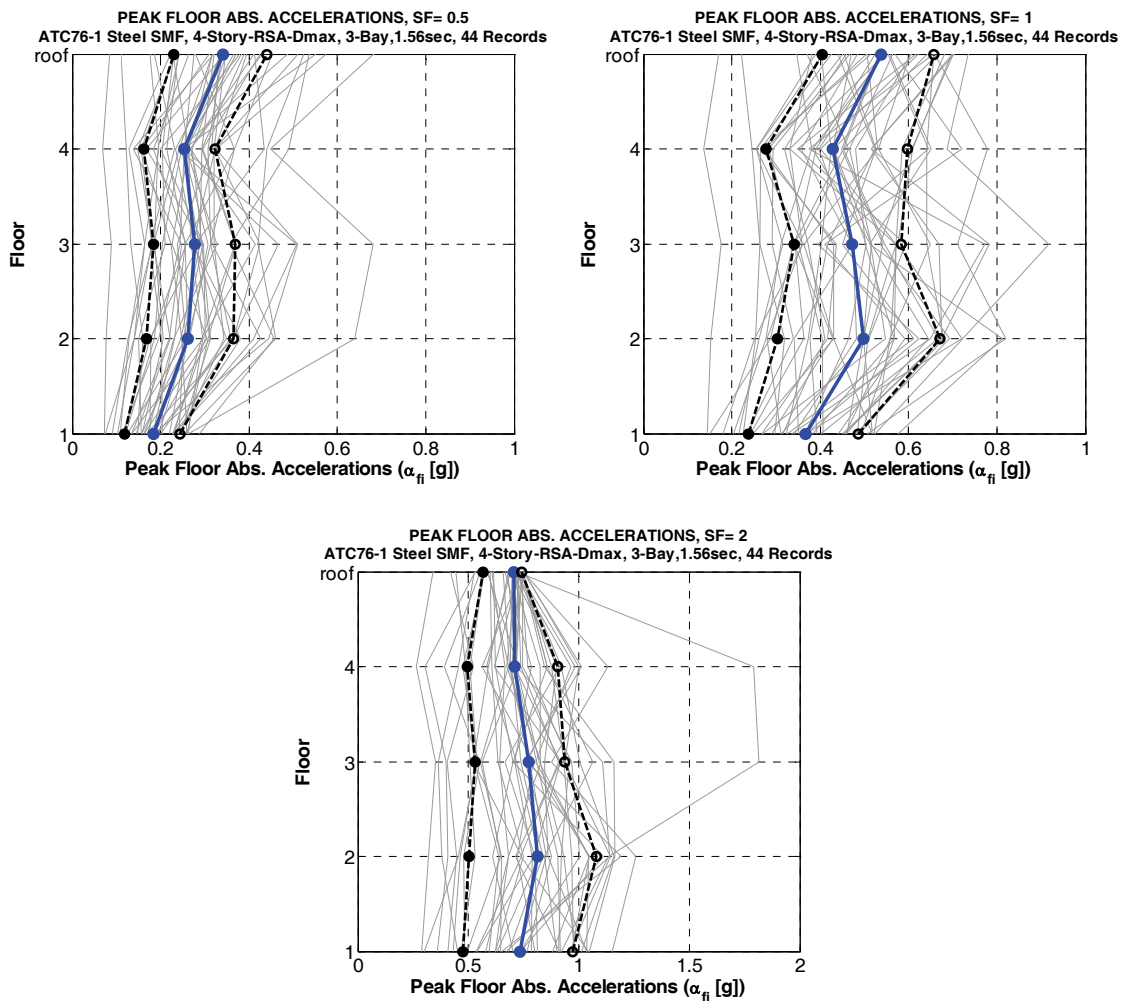


Figure A-9 Peak absolute floor accelerations for 3-bay model for ground motion scale factors SF = 0.5, 1.0, and 2.0; 4-story steel SMF.

Because of the good match between results obtained from the 1-bay and 3-bay models, from here on only results from analysis with the simplified 1-bay model are reported. It is noteworthy, and comforting, that the use of two independent analysis platforms (Drain-2DX and OpenSees) led to almost identical results in pushover analysis and NRHA far into the inelastic range. This leads to confidence that presently available computational methods and tools provide good response predictions, provided that component models have credible and compatible characteristics. In all cases analysis is based on the bare frame model.

A.3.3 Results for 2-, 4-, and 8-Story Steel Moment Frames

Presented in this section are two figures each for the 2-, 4-, and 8-story steel SMFs analyzed in this study. The first figure (Figures A-10, A-12, and A-14, respectively) presents system information and statistics of roof drift ratios, δ_r/H obtained from the NRHA for ground motion scale factors, SF, of 0.5, 1.0, and 2.0, a global pushover

curve, and deflection profiles from the pushover at the median value of roof drift ratios obtained from the NRHA for SF = 0.5, 1.0, and 2.0. The table of elastic dynamic properties lists also the median spectral acceleration of the FEMA P-695 ground motion suite for SF = 1.0. The listed S_a values are for 5% critical damping, even though the NRHA was performed with the assumption of 2.5% damping, which implies effective spectral accelerations that are about 25% larger than the tabulated ones.

The global pushover curves are presented for both V_I and $V_{I+P-\Delta}$. The difference between the two curves quantifies the importance of P-delta effects. For strength design of members affected by story shears or overturning moments (e.g., column axial forces), the quantities associated with inertia forces plus P-delta effects ($I+P-\Delta$) are the relevant ones. The first mode load pattern is applied in all pushover analyses.

Roof drift mean and standard deviation values in the second table exist only if all 44 data points are available; they are not reported if the structure collapses under one or more of the ground motions. Collapse implies that dynamic instability occurs due to the combination of deterioration and P-delta effects.

The pushover curves serve as an essential tool in understanding structural behavior. They illustrate post-yield and post-capping behavior, and indicate the roof drifts at which global yielding and capping (loss in strength due to deterioration) can be expected. The deflection profiles illustrate relative importance of individual story drifts and their changes as the structure gets pushed further into the inelastic range.

The second figure for each structure (Figures A-11, A-13, and A-15, respectively) presents NRHA results for the three story level EDPs, i.e., peak story drift ratios, story shears, and floor overturning moments. For the reason quoted in preceding paragraphs, $V_{I+P-\Delta}$ and $OTM_{I+P-\Delta}$ are used as the relevant story/floor force quantities. The peak floor overturning moment is obtained as the maximum of the sum of $V_{I+P-\Delta}h$ of all the stories above the floor. Figures A-11, A-13, and A-15 show EDP medians and dispersions obtained from NRHA using the full suite of ground motions. In each plot peak values are presented for individual ground motions (connected by light gray lines), and median values (connected by bold solid lines) as well as 16th and 84th percentile values (connected by black dashed lines). All statistical values are obtained by “counting” data points, i.e., no distribution has been fit to the data points. Results are presented for ground motion scale factors SF = 1.0 and 2.0. Results for SF = 0.5 offer little additional insight because the patterns are very similar to those observed for SF = 1.0.

When interpreting the NRHA results it needs to be considered that all steel SMF structural models are based on the bare frame and, therefore, the first mode period of each structure is rather long (0.95 sec., 1.56 sec., and 2.16 sec. for the 2-, 4- and

8-story structure, respectively). None of the structures have a first mode period that is in the short period range.

Summary of Observations for the 2-story steel SMF:

- The pushover curve exhibits a clearly positive post-yield stiffness even for the $V_I - \theta_r$ relationship. Capping occurs at a roof drift ratio larger than 0.03.
- The median roof drift ratio for SF = 1.0 (0.014) is around the global yield level, and roof drift ratio for SF = 2.0 (0.0274) is in the post-yield pre-capping range of the pushover.
- The deflection profile does not change considerably for the different SFs.
- NRHA story drift patterns are compatible with the deflection profiles, indicating that story drifts should be well predicted by means of a simple NSP for this structure.
- Base shears are compatible with pushover values, indicating little shear force amplification even at a SF of 2.0.
- The dispersion of story shears and overturning moments is small at SF = 2.0, indicating saturation of shear forces in both stories.

Summary of Observations for the 4-story steel SMF:

- The pushover curve exhibits a slightly negative post-yield tangent stiffness for the $V_I - \theta_r$ relationship, indicating increasing importance of P-delta. Capping occurs at a roof drift ratio around 0.03.
- The median roof drift ratio for SF = 1.0 (0.011) is around the global yield level, and roof drift ratio for SF = 2.0 (0.020) is in the post-yield pre-capping range of the pushover.
- The deflection profile does not change for the different SFs.
- NRHA story drifts are rather uniform over the height, indicating desirable behavior demonstrated by sharing of inelastic deformations between all stories.
- Base shears at SF = 2.0 are clearly higher than pushover values, indicating significant shear force amplification at the base.
- The story shear force distribution over the height is very different from a design shear force pattern or the standard first mode load pattern utilized in the nonlinear static procedure (NSP) of ASCE/SEI 41-06, *Seismic Rehabilitation of Existing Buildings* (ASCE, 2007). Story shear forces in the upper stories are greatly amplified compared to the load pattern used in design or pushover analysis.
- The distribution of overturning moments over the height is convex rather than concave as expected from code design and first mode load patterns.

Summary of Observations for the 8-story steel SMF:

- The pushover exhibits a slightly negative post-yield tangent stiffness for the $V_I - \theta_r$ relationship, indicating increasing importance of P-delta. Capping occurs at a roof drift ratio around 0.016.
- The median roof drift ratio for SF = 1.0 (0.0079) is below the global yield level, and roof drift ratio for SF = 2.0 (0.0128) is in the post-yield pre-capping range of the pushover.
- For a SF = 2.0, five collapses are observed (5 out of 44), indicating significant collapse potential even though the median roof drift is safely below the capping drift of 0.016.
- The deflection profile changes greatly between SF = 1.0 and 2.0, indicating concentration of inelastic deformations in the lower stories of the structure.
- NRHA story drifts do not exhibit the same pattern as the slope of the deflection profile, indicating important higher mode contributions.
- The story shear force distribution over the height is very different from a design shear force pattern or the standard first mode load pattern utilized in the ASCE/SEI 41-06 NSP. Story shear forces in the upper stories are greatly amplified compared to the load pattern used in design or pushover analysis.
- The distribution of overturning moments over the height is almost linear as if it were obtained from a constant story shear force diagram.

Seismically effective weight per frame: $W = 1383k$

($w_1 = 714k, w_2 = 669k$)

Elastic Dynamic Properties (SSMF-2-1-0.95-44)

	Mode 1	Mode 2
T_i [sec]	0.95	0.25
Γ_i	1.149	-0.131
Eff. Modal Mass	0.965	0.0249
$S_a(T_i, 5\% SF=1.0)$	0.379g	0.792g

Roof Drift Ratios from NRHA (H = 321 inches)

	SF=0.5	SF=1.0	SF=2.0
Median [%]	0.0070	0.0140	0.0274
16th [%]	0.0047	0.0095	0.0192
84th [%]	0.0099	0.0179	0.0357
Mean μ [%]	0.0075	NA	NA
σ [%]	0.0028	NA	NA
CoV	0.38	NA	NA
Collapses	0	1	1

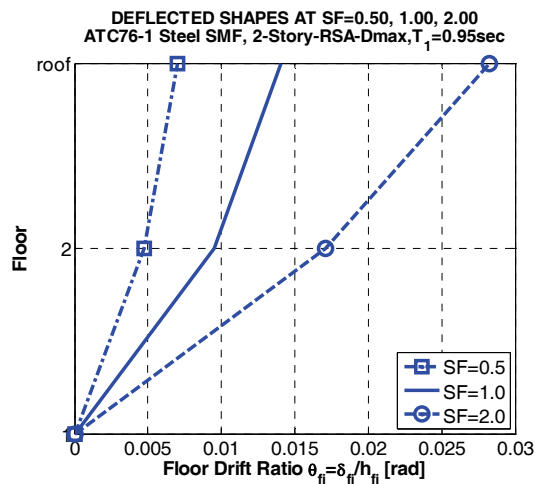
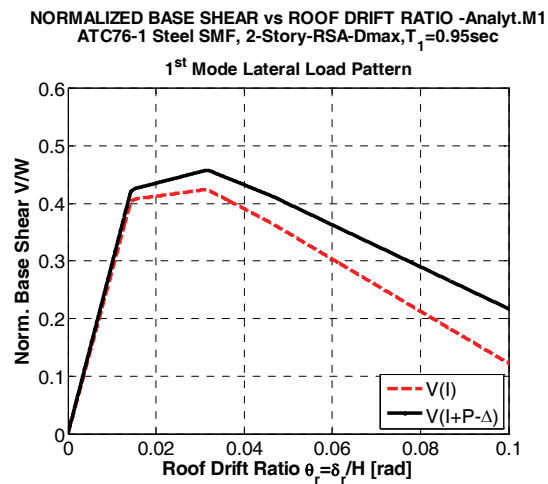


Figure A-10 System information, 2-story steel SMF.

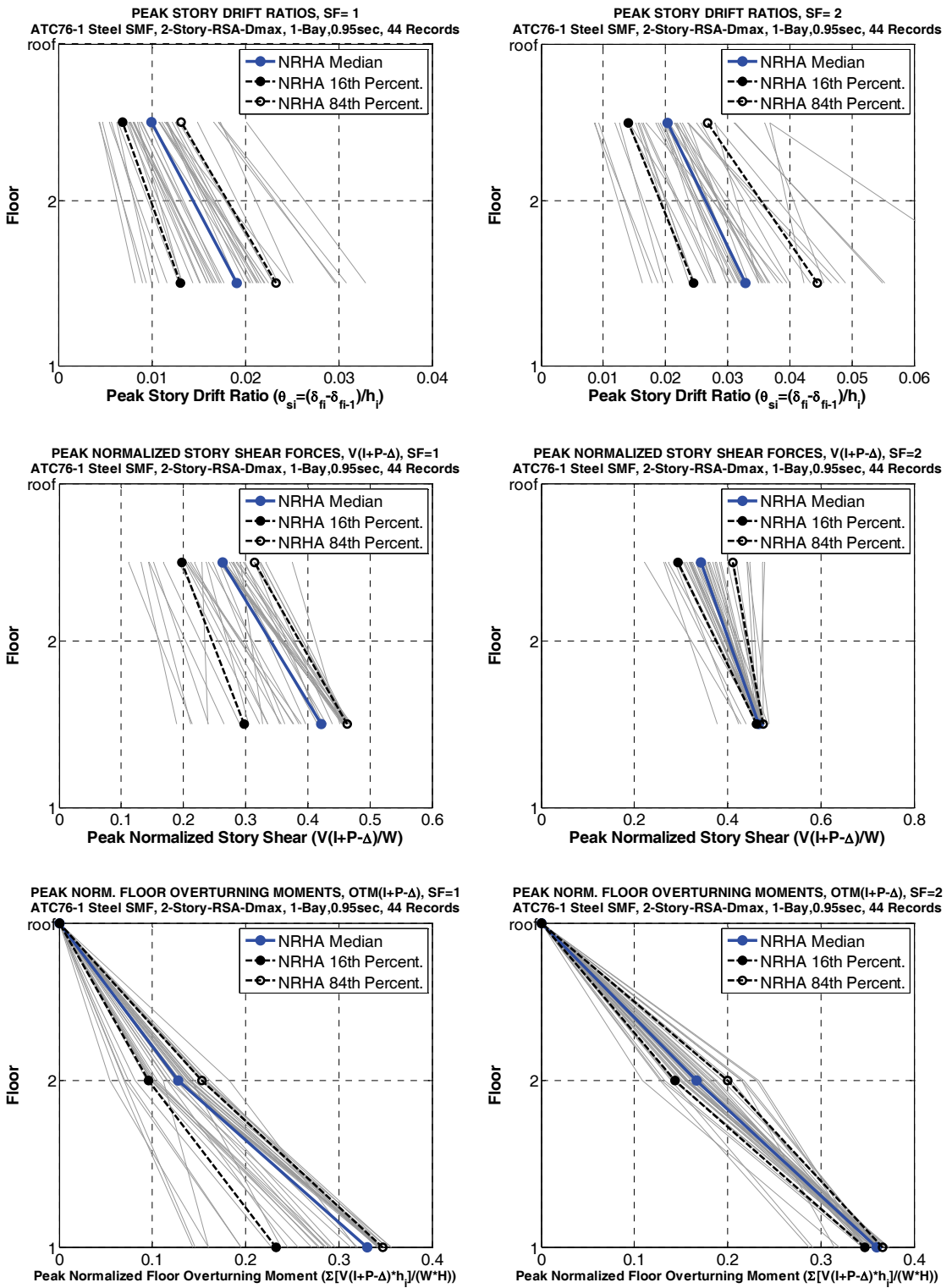


Figure A-11 NRHA Peak story drift ratios, story shears, and story overturning moments, 2-story steel SMF.

Seismically effective weight per frame: $W = 2,799k$

($w_1 = 714k$, $w_2 = w_3 = 708k$, $w_r = 669k$)

Elastic Dynamic Properties (SSMF-4-1-1.56-44)

	Mode 1	Mode 2	Mode 3	Mode 4
T_i [sec]	1.560	0.502	0.274	0.172
Γ_i	1.298	-0.403	0.159	-0.026
Eff. Modal Mass	0.815	0.107	0.049	0.017
$S_a(T_i, 5\% SF=1.0)$	0.208g	0.804g	0.792g	0.736g

Roof Drift Ratios from NRHA (H = 635 inches)

	SF=0.5	SF=1.0	SF=2.0
Median [%]	0.0058	0.011	0.020
16th [%]	0.0042	0.008	0.014
84th [%]	0.0095	0.015	0.029
Mean μ [%]	0.0068	N/A	N/A
σ [%]	0.0029	N/A	N/A
CoV	0.4262	N/A	N/A
Collapses	0	1	2

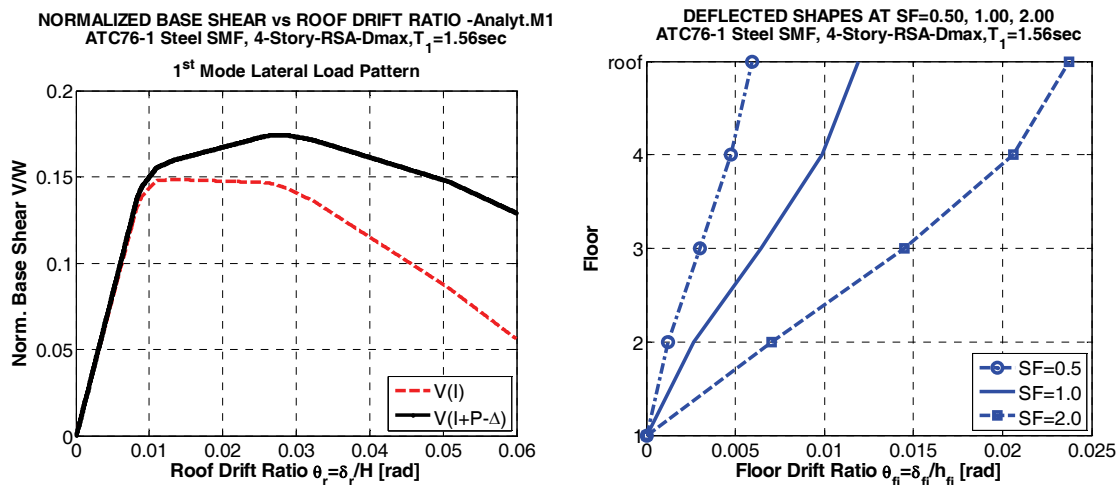


Figure A-12 System information, 4-story steel SMF.

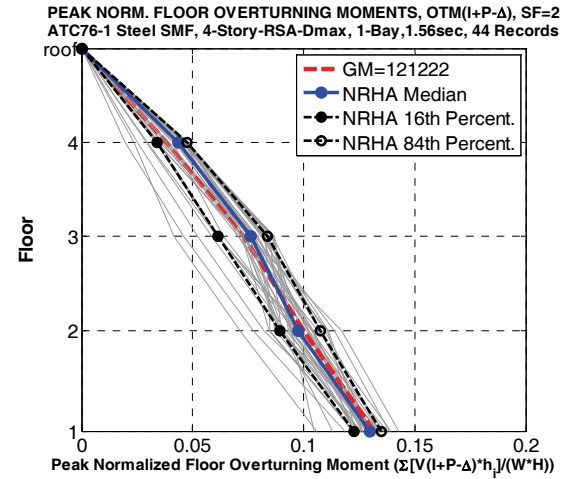
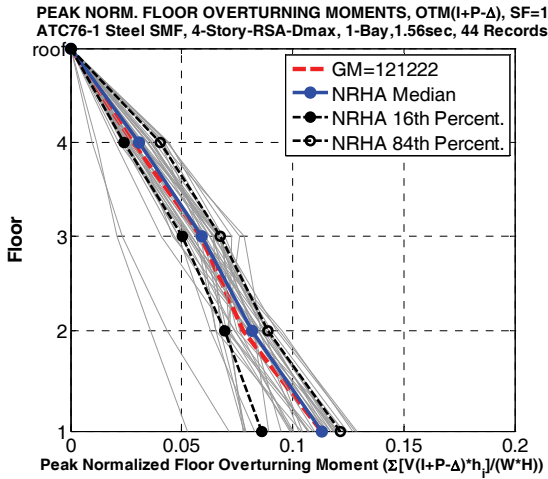
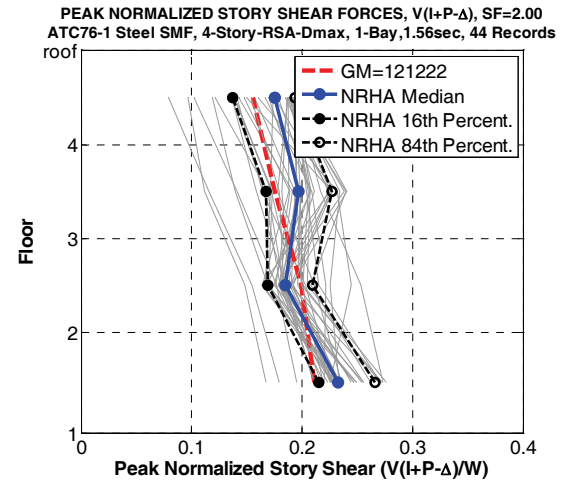
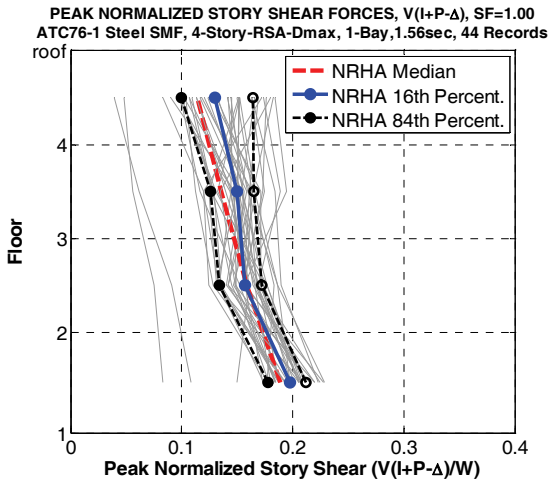
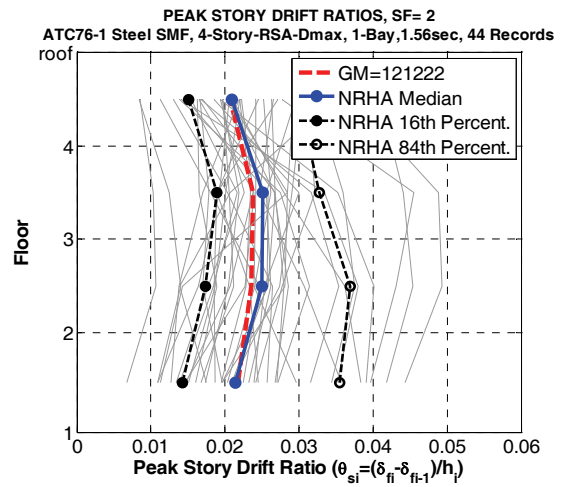
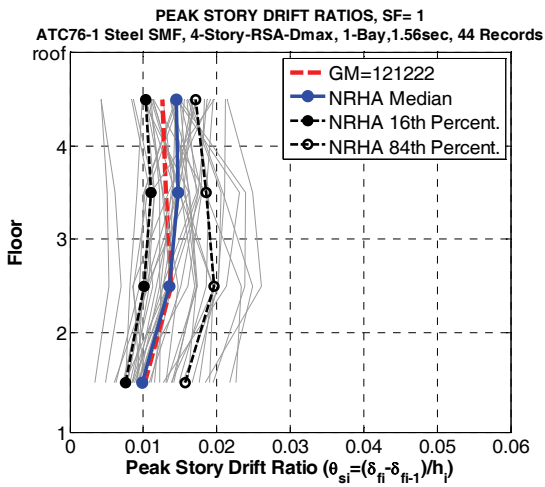


Figure A-13 NRHA Peak story drift ratios, story shears, and story overturning moments, 4-story steel SMF.

Seismically effective weight per frame: $W = 1383k$

($w_1 = 714k$, w_2 to $w_7 = 708k$, $w_r = 5,631k$)

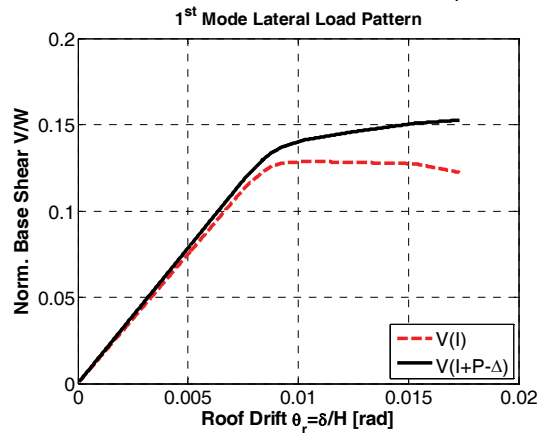
Elastic Dynamic Properties (SSMF-8-1-2.14-44)

	Mode 1	Mode 2	Mode 3	Mode 4	Mode 5	Mode 6	Mode 7	Mode 8
T_i [sec]	2.14	0.75	0.43	0.28	0.21	0.16	0.13	0.12
Γ_i	1.356	-0.513	0.283	-0.148	0.086	-0.033	0.012	-0.002
Eff. Modal Mass	0.784	0.119	0.044	0.017	0.014	0.006	0.004	0.001
$S_a(T_i, 5\% SF=1.0)$	0.174g	0.600g	0.929g	1.008g	1.043g	0.938g	0.834g	0.736g

Roof Drift Ratios from NRHA (H = 1259inches)

	SF=0.5	SF=1.0	SF=2.0
Median [%]	0.0045	0.0079	0.0128
16th [%]	0.0025	0.0045	0.0085
84th [%]	0.0065	0.0101	0.0161
Mean μ [%]	0.0045	0.0078	NA
σ [%]	0.0018	0.0028	NA
CoV	0.41	0.34	NA
Collapses	0	0	5

NORMALIZED BASE SHEAR vs ROOF DRIFT RATIO –Analyt.M1
ATC76-1 Steel SMF, 8-Story-RSA-Dmax,1-bay, $T_1=2.14$ sec



DEFLECTED SHAPES AT SF=0.50, 1.00, 2.00
ATC76-1 Steel SMF, 8-Story-RSA-Dmax, $T_1=2.14$ sec

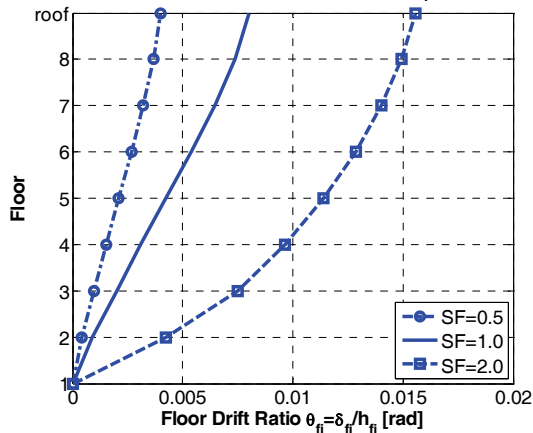


Figure A-14 System information, 8-story steel SMF.

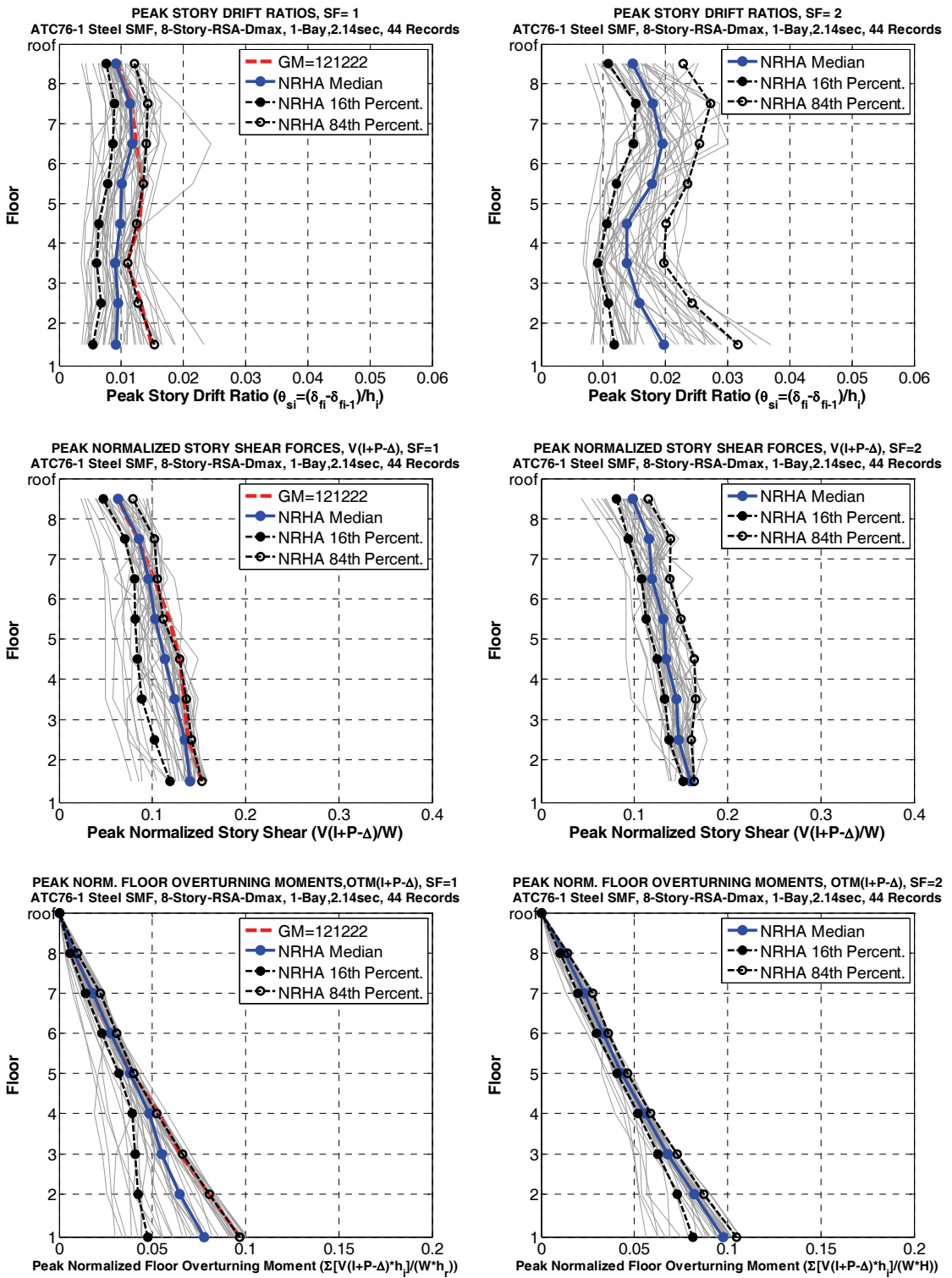


Figure A-15 NRHA Peak story drift ratios, story shears, and story overturning moments, 8-story steel SMF.

A.3.4 Dispersion in Seismic Input and Engineering Demand Parameters

All EDPs have a dispersion, which depends on the characteristics of the ground motions used to predict EDPs and on the uncertainties inherent in modeling strength and stiffness characteristics of structures. The latter is not addressed here, i.e., the following discussion is concerned only with dispersion due to ground motion characteristics. The structural model used in all the analyses is deterministic.

Dispersion in Seismic Input (Spectral Accelerations)

The two graphs in Figure A-16 show, for a SF of 1.0, the spectra of the suite of 44 ground motions from FEMA P-695 as well as the spectra for a subset of 17 records that best match the median spectrum. Both graphs also show median and the 16th and 84th percentile of the spectral values, and the spectrum of record 121222, which is the best individual match to the median spectrum of the 44 records. All spectra are for 5% damping, even though 2.5% damping was used in all analyses.

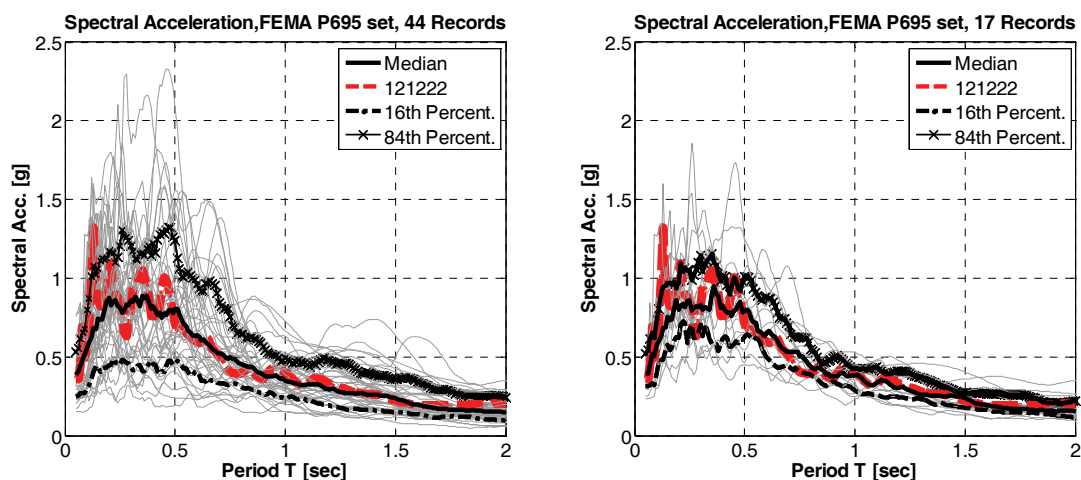


Figure A-16 Median and dispersion of 5% damped acceleration spectra of ground motion sets with (a) 44 records and (b) 17 records.

Estimates of the coefficient of variation (assumed equal to the standard deviation of the log of the data) of spectral accelerations are presented in Table A-2. Figure A-16 as well as Table A-2 show that the dispersion decreases significantly for the smaller set of records, whereas the median changes very little. The question is how much of this decrease in dispersion is reflected in the EDP estimates obtained from NRHA.

Table A-2 Estimates of Coefficient of Variation of Spectral Accelerations

Record Set (from FEMA P-695)	CoV of Spectral Acceleration (5% damping)			
	$T = 0.5 \text{ sec.}$	$T = 1.0 \text{ sec.}$	$T = 1.5 \text{ sec.}$	$T = 2.0 \text{ sec.}$
44 records	0.47	0.35	0.45	0.43
17 records	0.30	0.22	0.30	0.39

Dispersion in EDPs Based on Full Set of 44 Records and Subset of 17 Records

Figures A-11, A-13, and A-15 show EDP medians and dispersions obtained from NRHA using the full suite of 44 ground motions from FEMA P-695. For this set the dispersion in drifts is similar to the dispersion of the first mode S_a , indicating that higher mode effects and period elongation (for inelastic structures) add little to the dispersion from first mode spectral acceleration. The dispersion in story shears and overturning moments is much smaller in the inelastic range because of saturation of story shear demands due to attainment of bending strength in beam plastic hinge regions.

Comparable results for the subset of 17 records are presented in Figure A-17, using the 4-story steel SMF as an example. A comparison between Figures A-13 and C17 shows that the median EDPs change very little, but that the dispersion of EDPs for the subset of 17 records becomes smaller. The dispersion becomes clearly smaller for story drifts, and slightly smaller for story shears and overturning moments. If median values of EDPs are of primary interest, the use of a subset of records that better matches the target spectrum might be a good choice. If quantification of dispersion is of interest, the choice of the larger set of records is appropriate.

This assessment changes somewhat when severe ground motions are applied that drive the structure into the negative tangent stiffness range and bring it close to collapse. This happens when a ground motion scale factor of 3.0 is selected for the 4-story steel SMF structure. Results for the 44 record set are presented later in Figure A-32, and results for the 17 record set are presented in Figure A-18. For the 44 record set the structure collapses in 22 of the 44 analyses, whereas it collapses only in 5 of the 17 analyses performed with the 17 record subset. The reason is that records considered “outliers” in spectral acceleration demands get eliminated when the record set is narrowed down to those 17 records that provide the best match with the median record of the full set. The consequence is that now the median drift demands obtained from the 44 record set and the 17 record set vary by a considerable amount (e.g., 0.062 versus 0.032 for the 44 and 17 record set, respectively). This brings into question the appropriateness of selection of a record subset.

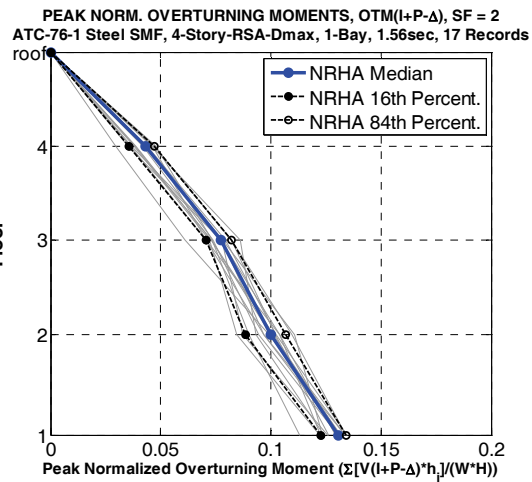
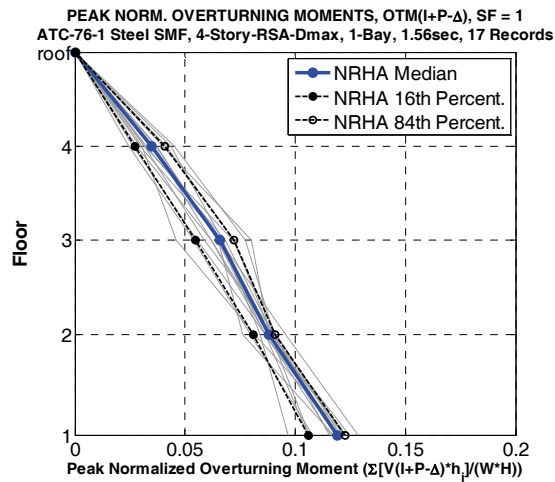
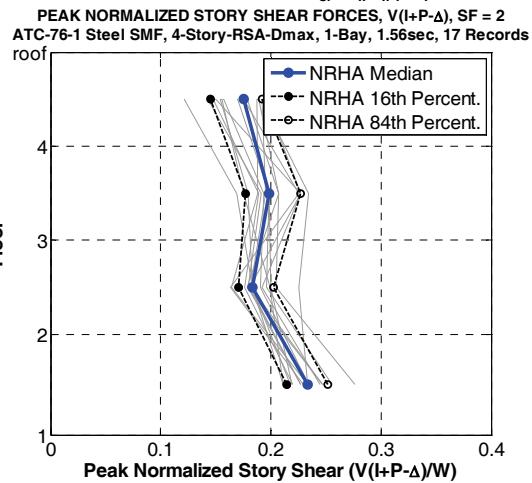
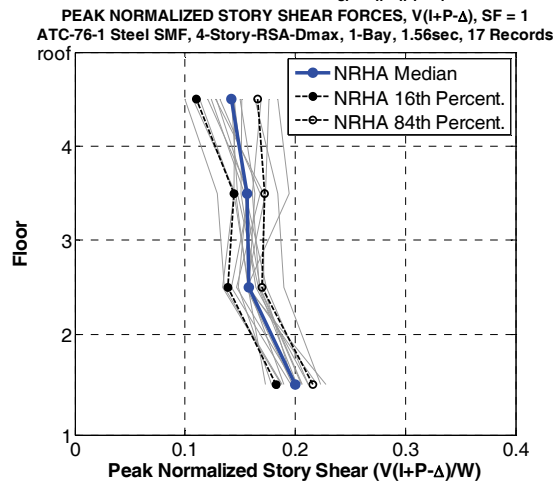
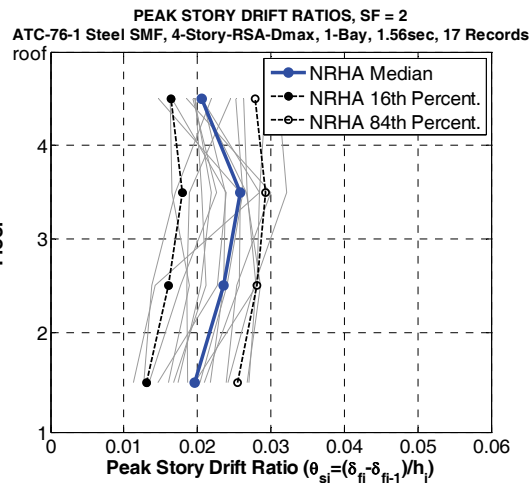
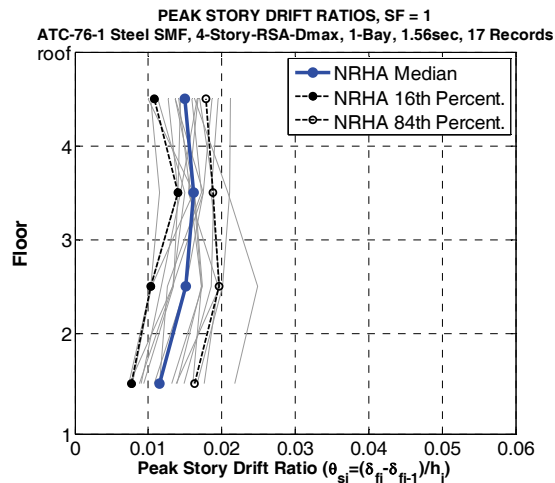


Figure A-17 NRHA peak story drift ratios, story shears, and story overturning moments, 4-story steel SMF, SF = 1.0 and 2.0, 17 records.

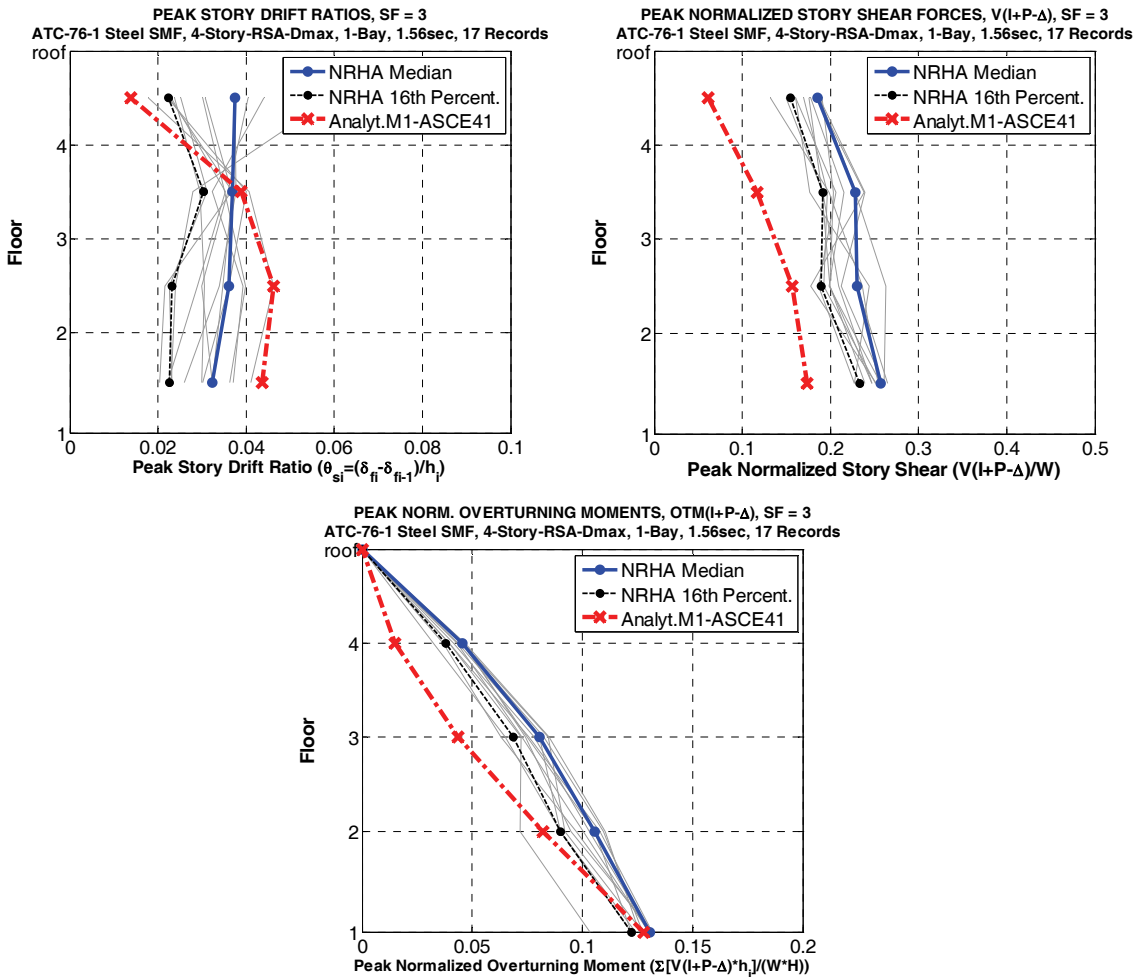


Figure A-18 NRHA median and 16th percentile and NSP prediction (Analyt.M1-ASCE41) of 4-story steel SMF, SF = 3.0, 17 records.

Use of a Single Record

Highlighted with a dashed bold line in Figure A-16 is the spectrum of the individual record that matches best to the median spectrum (record 121222). EDP results from NRHA analysis with this record are also highlighted (with a dashed line) in Figures A-13 and A-32, using the 4-story steel SMF structure as an example. Figure A-13 leads one to believe that EDPs obtained from this single record are very close to the median EDPs of all 44 records. However, Figure A-32 shows that for a large scale factor of 3.0 the difference in drift demands between the median of the 44 records and the individual record is very large. The indication is that a single record that matches closely with the target spectrum will not necessarily predict EDPs that match well with the median NRHA results.

A.3.5 Results for Residual Drifts

For completeness, selected results are presented in Figure A-19 for residual story drift, a quantity that cannot be estimated from a nonlinear static procedure. The dispersion of the residual drift is very large, as expected. On the other hand, the ratio of median residual story drift to median peak story drift (from Figs. A-11, A-13, and

A-15) is rather stable for an SF of 2.0 and is on the order of 1:3. There is no evidence that these ratios can be applied to other structural configurations or systems. And this ratio will depend strongly on the extent of inelasticity in the structure. Only NRHA will provide a reasonable estimate of this quantity. In the context of performance-based earthquake engineering, residual drift is becoming more important as it is used often as a measure of severe structural damage and as a tool in decision making on demolition of a structure.

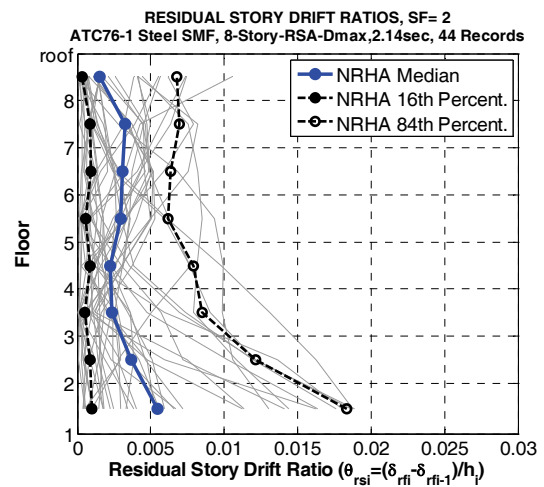
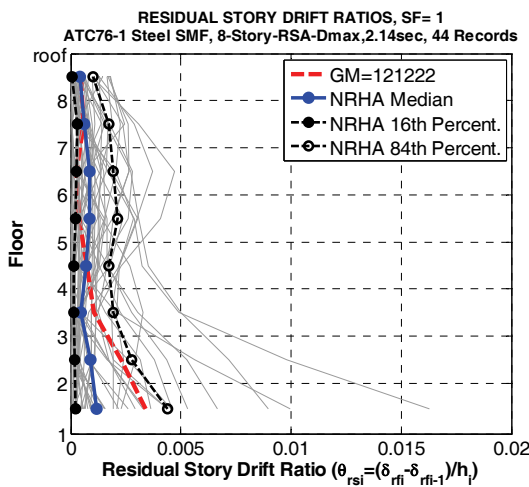
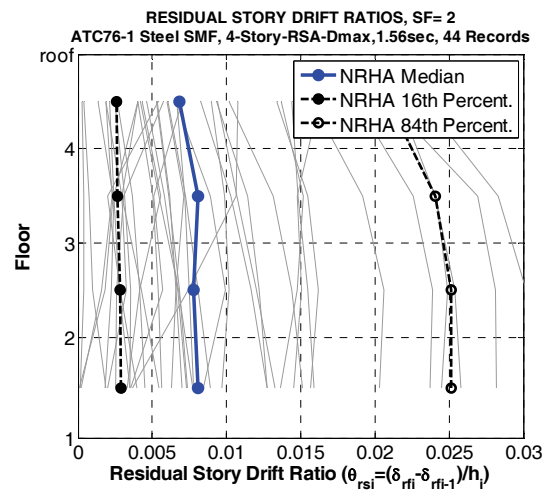
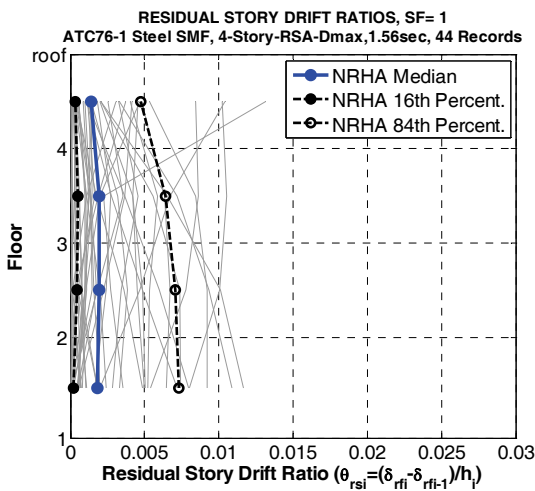
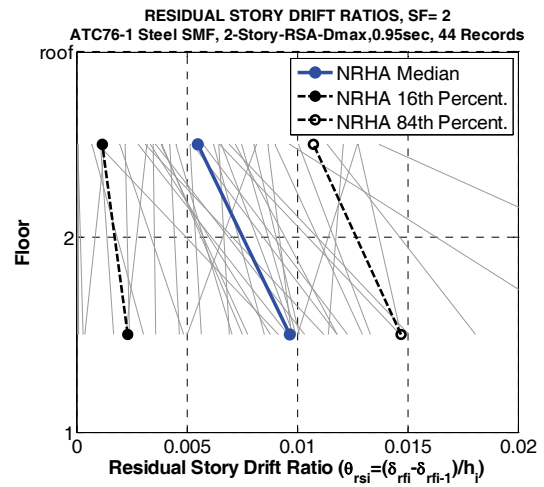
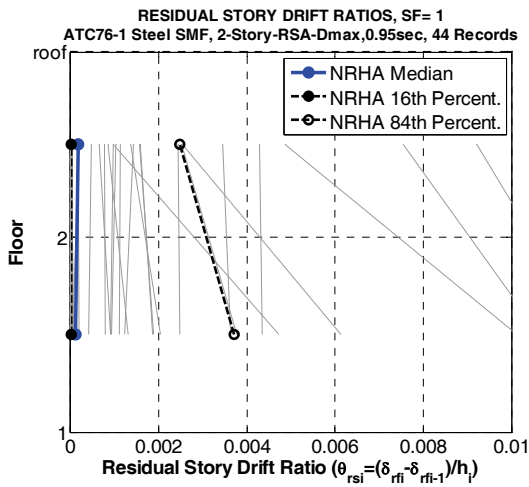


Figure A-19 NRHA residual story drift ratios, 2-, 4- and 8-story steel SMFs, SF = 1.0 and 2.0.

A.3.6 Synthesis of Nonlinear Response History Analysis Results

The study of NRHA of steel SMFs led to the following general observations and conclusions on modeling for NRHA and story-level EDPs.

- Two independent analysis platforms, Drain-2DX and OpenSees, produce almost identical results, provided the same component models are used in both platforms.
- A simplified single bay centerline representation of a multi-bay configuration is feasible provided that all bays of the SMF are of about equal width and stiffness, and provided that joint panel zones are not the components dominating strength characteristics of the frame structure (strong panel zones).
- A leaning column is an essential part of the analytical model if P-delta effects are transferred to the moment-resisting frames through the floor diaphragm.
- The gravity system, which is not part of the steel SMF, can be modeled approximately with a fishbone model placed in parallel with the moment frame. If the effect of axial loads on bending strength of the column is incorporated in the input properties for the fishbone column, then the column of the fishbone can also be utilized as the leaning column for P-delta effect modeling.
- The global pushover curve of regular steel SMFs is essentially trilinear, consisting of a large elastic range, a range of almost constant post-yield stiffness (this stiffness for the $V_I - \theta_r$ curve may have a small positive or a negative slope, depending on the importance of P-delta effects), and a post-capping stiffness that leads to relatively rapid deterioration in strength. The slope of the post-capping stiffness is determined by the combination of P-delta effects and deterioration effects in individual structural components.
- The taller the structure and the larger the extent of inelastic deformations, the more non-uniform will be the distribution of NRHA peak story drifts over the height. Important reasons for this phenomenon are higher mode effects and concentration of inelastic deformations in specific regions of the structure due to P-delta effects.
- The dispersion of peak story drift demands is similar to the dispersion of spectral acceleration at the first mode period of the structure. This conclusion is specific for the selected set of 44 ground motion records. When the dispersion of S_a at T_1 is reduced by selecting record subsets that provide a better match to the median spectra, the dispersion of the peak story drift is reduced correspondingly. The median of the peak story drift is not much affected by the subset selection, provided the response is in the “stable” range of performance, i.e., the roof drift ratio is smaller than the roof drift ratio associated with capping of the global pushover curve. This conclusion is invalidated when the structure is pushed into the post-capping range of behavior, in which case the median from the subset

may be much smaller than the median from the full set of records. The same pattern applies if the single record is used that provides a “best” match to the median spectrum.

- Peak story shear demands do not at all follow the lateral load pattern for which the structure has been designed or the first mode load pattern applied in a standard pushover analysis. Higher mode effects and inelastic dynamic redistribution may cause large shear force amplifications in specific stories, resulting in a peak shear force distribution over the height that is much more uniform than anticipated from design or pushover load patterns. The NRHA base shear might be clearly higher than the value obtained from a pushover analysis. These effects increase with the number of stories.
- Peak floor overturning moment demands follow the same patterns as story shear demands. As a consequence, the peak overturning moment profile over the height might be close to linear (implying constant story shear over the height) or even slightly convex rather than concave as expected from design considerations or obtained from a first mode pushover analysis.
- The dispersion in story shears and floor overturning moment demands is much smaller in the inelastic range than the elastic one because of saturation of story shear demands due to attainment of bending strength in beam (or column) plastic hinge regions.

A.4 Single Mode Nonlinear Static Procedure

This work focuses on evaluating the feasibility and limitations of the standard single mode nonlinear static procedure (NSP) of ASCE/SEI 41-06. The objective here is to follow the ASCE/SEI 41-06 procedure rigorously, explore simple alternatives, and provide a quantitative assessment of NSP predictions of relevant EDPs in comparison to the NRHA results discussed in the previous section. Three archetypes from the NIST funded ATC 76-1 Project, namely 2-, 4-, and 8-story steel SMF structures are employed for this purpose.

The all-important issue of lateral load pattern is not explored here. Previous work (FEMA 440) has addressed this issue and came to the conclusion that variations in invariant lateral load patterns do not improve the accuracy of EDP predictions. The load pattern applied in all cases discussed here is the pattern structured after the elastic first mode deflected shape, as recommended in ASCE/SEI 41-06. The emphasis is on methods of pushover analysis, ways to compute the target displacement at which the pushover data are to be evaluated, and evaluation of NSP results with a focus on the previously discussed story EDPs peak story drift, peak story shear force ($V_{I+P-\Delta}$), and floor overturning moments ($OTM_{I+P-\Delta}$).

A.4.1 Nonlinear Static Analysis Options Explored

Given a prescribed lateral load pattern, there are options for modeling the structure for pushover analysis and for selecting the method for target displacement prediction. In general, the latter is based on predicting the displacement demand for an equivalent single-degree-of-freedom (SDOF) system that represents the first mode characteristics of the multiple-degree-of-freedom (MDOF) structure and mapping this demand back to the global pushover curve to find the point at which the structure should be evaluated (sometimes referred to as performance point). In the ASCE/SEI 41-06 coefficient method this process is greatly simplified and the equivalent SDOF system does not become an explicit part of the target displacement estimation.

Pushover Analysis Options

In this study the following three options are explored for models of structural components, which then are assembled in the OpenSees analysis platform

- **ASCE41:** ASCE/SEI 41-06 component models are used, but assuming a post-capping stiffness obtained by linearly connecting peak point C and point E of the generic ASCE/SEI 41-06 model. This modification, illustrated in Figure A-20, is made in order to avoid numerical analysis stability problems and to conform better to data and analysis models developed over the last decade.

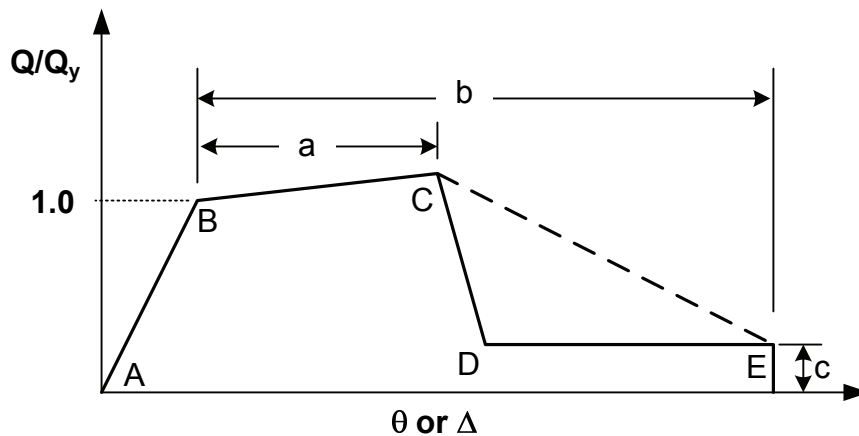


Figure A-20. Modified component model adapted from ASCE/SEI 41-06 (PEER/ATC, 2010).

- **Analyt.M1:** Modified IK component model with monotonic backbone curve is used (Figure A-2), i.e., PEER/ATC-72-1 analysis option 1; cyclic deterioration is not reflected in pushover analysis.
- **Analyt.M3:** Modified IK component model with modified backbone curve is used to account for cyclic deterioration in pushover analysis, i.e., PEER/ATC-72-1 analysis option 3.

The first two options were executed for all three steel SMFs, the third option was explored only for the 4-story steel SMF.

Target Displacement Options

- **ASCE41:** Target displacement obtained from ASCE/SEI 41-06 coefficient method.
- **EqSDOF:** Target displacement based on median displacement obtained from a first mode equivalent SDOF system and NRHA using the 44 ground motions of the FEMA P-695 set and the analysis tool IIDAP (Lignos, 2009). Equivalent SDOF properties are obtained from the base shear V_I – roof displacement pushover curve (not the $V_{I+P-\Delta}$ – roof displacement pushover curve), which implies that P-delta effects are accounted for approximately in the development of the equivalent SDOF system.

IIDAP is an SDOF analysis program that computes displacements of SDOF systems from NRHA, using the backbone curve and hysteresis rules of the modified IK component model (Figure A-2), with or without cyclic deterioration.

Single Mode NSP Options

The NSP may consist of any combination of the aforementioned pushover analysis options and target displacement options, i.e.,

- ASCE41-ASCE41
 - Pushover analysis option: ASCE/SEI 41-06 component models
 - Target displacement option: ASCE/SEI 41-06 coefficient method
- ASCE41-EqSDOF
 - Pushover analysis option: ASCE/SEI 41-06 component models
 - Target displacement option: Median target drift obtained from equivalent SDOF analysis with IIDAP, without cyclic deterioration (cyclic deterioration is considered in ASCE/SEI 41-06 component models)
- Analyt.M1-ASCE41
 - Pushover analysis option: modified IK component model, PEER/ATC-72-1 analysis option 1 (based on monotonic backbone curve)
 - Target displacement option: ASCE/SEI 41-06 coefficient method
- Analyt.M1-EqSDOF
 - Pushover analysis option: modified IK component model, PEER/ATC-72-1 analysis option 1 (based on monotonic backbone curves)
 - Target displacement option: Median target drift from equivalent SDOF analysis with IIDAP, incorporating cyclic deterioration (because pushover option based on monotonic backbone curve of modified IK component model). The cyclic deterioration parameter λ from PEER/ATC-72-1 is set to the median value for steel beams, which is equal to 50.

- Analyt.M3-ASCE41
 - Pushover analysis option: modified IK component model, PEER/ATC-72-1 analysis option 3 (based on modified backbone curves that account for cyclic deterioration (NIST, 2010))
 - Target displacement option: ASCE/SEI 41-06 coefficient method
- Analyt.M3-EqSDOF
 - Pushover analysis option: modified IK component model, PEER/ATC-72-1 analysis option 3 (based on modified backbone curves that accounts for cyclic deterioration (NIST, 2010))
 - Target displacement option: Median target drift from equivalent SDOF analysis with IIIDAP, without cyclic deterioration (because cyclic deterioration is considered in pushover analysis option)

The first four options have been evaluated for all three steel SMFs, and the last two options only for the 4-story steel SMF.

A.4.2 Results for 2-, 4-, and 8-story Steel Special Moment Frames in Pre-capping Region

Steel SMF Archetypes

For each archetype a pair of figures is presented in this section. The first figure shows ASCE41 and Analyt.M1 pushover curves and the associated equivalent SDOF systems, as well as target drift ratios obtained from the following four NSP options: ASCE41-ASCE41, ASCE41-EqSDOF, Analyt.M1-ASCE41, and Analyt.M1-EqSDOF.

The second figure presents a NSP to NRHA comparison, with the NSP results for the aforementioned four NSP options superimposed on the previously discussed NRHA results. Results are presented for SF = 1.0 and 2.0; results for SF = 0.5 are similar to those for SF = 1.0 and add little additional insight.

Common to all cases presented here is the observation that the target displacement demands are safely below the roof drifts associated with global capping. The implication is that the post-capping negative stiffness region is not a critical consideration in the NSP predictions.

Summary of Observations for 2-story Steel SMF (Figures A-21 and A-22):

- The ASCE41 and Analyt.M1 pushover curves have similar roof drifts at the corner points, but quite different post-elastic stiffnesses. The slightly negative post-yield tangent stiffness of the ASSCE41 pushover is caused by the ASCE/SEI 41-06 criterion that post yield component behavior is determined by the assumption of 3% strain hardening in $M-\theta$, and P-delta effects exceed this strain hardening effect. In the Analyt.M1 component model the post-yield

stiffness is caused by a 10% increase in M_y regardless of the amount of pre-capping plastic hinge rotation capacity.

- The ASCE/SEI 41-06 criteria for post-capping behavior (see Figure A-20) result in a steep post-capping tangent stiffness leading to rapid deterioration. This does not correspond to statistical data from component tests on which the Analyt.M1 model is based (Lignos and Krawinkler, 2009, 2010).
- The ASCE/SEI 41-06 coefficient method pays no attention to the aforementioned differences, i.e., it results in the same target displacement prediction for both the ASCE41 and Analyt.M1 pushovers.
- All target displacement predictions are within 10% of the median roof drift obtained from NRHA.
- NSP results compare well with NRHA results, except for the story drift predictions for SF = 2.0 based on the ASCE/SEI 41-06 pushover. The reason is the negative tangent stiffness in the post-yield range of the ASCE41 pushover.

Summary of Observations for 4-story Steel SMF (Figures A-23 to A-26):

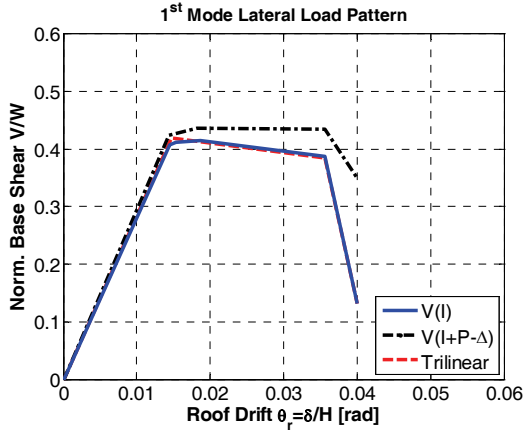
- In this structure the ASCE/SEI 41-06 pushover underestimates post-yield strength and deformation capacities of structures compared to the Analyt.M1 model. The latter model is based on expected values of component properties, whereas more conservative (low) values have been selected intentionally in the ASCE/SEI 41-06 modeling criteria. The consequences on target displacement predictions are not necessarily large (see table in Figure A-23) unless the ground motion demands are very high (see Section A.4.3)
- The use of the low estimate ASCE/SEI 41-06 pushover model together with an equivalent SDOF model for target displacement prediction (ASCE41-EqSDOF) may provide estimates of performance that are lower than might be justifiable. For SF = 2.0 the EqSDOF leads to 33 collapses, which are a direct consequences of the relatively short yield plateau obtained in the ASCE/SEI 41-06 pushover.
- In a side study in which the Analyt.M3 model (option 3 of the analysis options discussed in Section 2.2.5 of NIST, 2010) was used to predict the pushover curve, it was found that the Analyt.M3 pushover curve is close to the ASCE/SEI 41-06 pushover curve, and that the NSP predictions based on ASCE41 and Analyt.M3 pushover curves are similar, see Figures. A-25 and A-26. This provides confidence that the ASCE/SEI 41-06 modeling parameters for steel SMFs are reasonable, albeit much lower than median values.
- For all options, NSP story drift predictions show a significant deviation from median NRHA values (Figure A-24). In the inelastic range (SF = 2.0) drifts in the lower stories are overestimated and drifts in the upper stories are underestimated.

- NSP story shear predictions for the 4-story steel SMF are not good representations of NRHA results in the inelastic range ($SF = 2.0$). Story shears are consistently underestimated, particularly in the upper stories. But also the maximum NSP base shear, which corresponds to the peak of the $V_{I+P-\Delta}$ pushover curves in Figure A-23, is about 25% below the NRHA median base shear. The reason is dynamic redistribution, which amplifies story shear forces compared to those obtained from a predetermined lateral load pattern. If story shears are an important performance consideration, then the validity of quantitative values obtained from a pushover analysis diminished for this 4-story steel SMF.
- Similar observations apply to floor overturning moments, which control axial forces in columns of frame structures. In the upper stories the NSP predictions are less than half those obtained from NRHA. The situation is better at the base, because maximum shear forces in individual stories occur at different times.
- The outcome is that even for this relatively low-rise steel SMF structure NSP predictions may provide misleading quantitative information, particularly for force quantities.

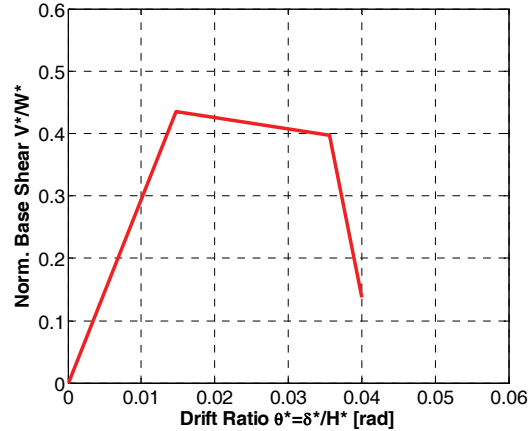
Summary of Observations for 8-story Steel SMF (Figs. A-27 and A-28):

- The observations made for the 4-story steel SMF are valid also for the 8-story steel SMF structure.

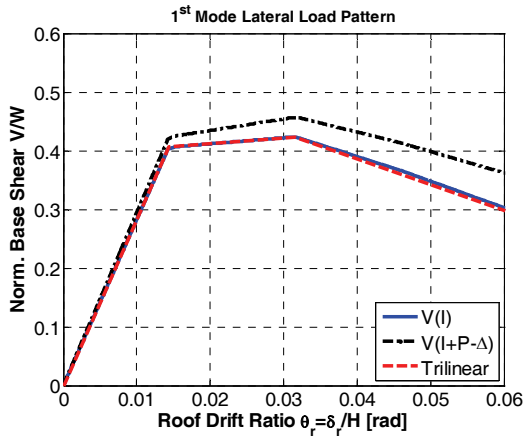
NORMALIZED BASE SHEAR vs ROOF DRIFT RATIO –ASCE41
 ATC76-1 Steel SMF, 2-Story-RSA-Dmax,1-bay, $T_1=0.95\text{sec}$



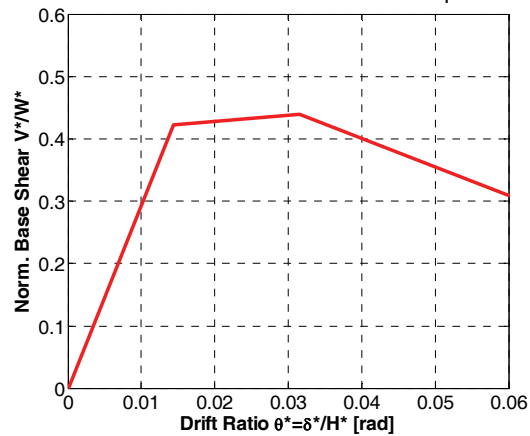
EQUIVALENT SDOF SYSTEM-ASCE41
 ATC76-1 Steel SMF, 2-Story-RSA-Dmax,1-bay, $T_1=0.95\text{sec}$



NORMALIZED BASE SHEAR vs ROOF DRIFT RATIO –Analyt.M1
 ATC76-1 Steel SMF, 2-Story-RSA-Dmax,1-bay, $T_1=0.95\text{sec}$



EQUIVALENT SDOF SYSTEM-Analyt.M1
 ATC76-1 Steel SMF, 2-Story-RSA-Dmax,1-bay, $T_1=0.95\text{sec}$



Properties of Equivalent SDOF System

<i>Model</i>	V_y^*/W^*	T_e [sec]	α_s	θ_p/θ_y	θ_{pc}/θ_y
ASCE41	0.42	0.95	-0.202	2.33	0.447
Analyt.M1	0.42	0.95	0.039	2.19	6.69

NRHA Median and Target Roof Drift Ratios (H = 321 inches)

	NRHA Median	ASCE41-ASCE41	ASCE41-Eq.SDOF	Analyt.M1-ASCE41	Analyt.M1-Eq.SDOF
SF = 0.5	0.0070	0.0070	0.0073	0.0070	0.0070
SF = 1.0	0.0140	0.0140	0.0138	0.0140	0.0130
SF = 2.0	0.0274	0.0280	0.0276	0.0280	0.0250

Figure A-21 NSP information, 2-story steel SMF.

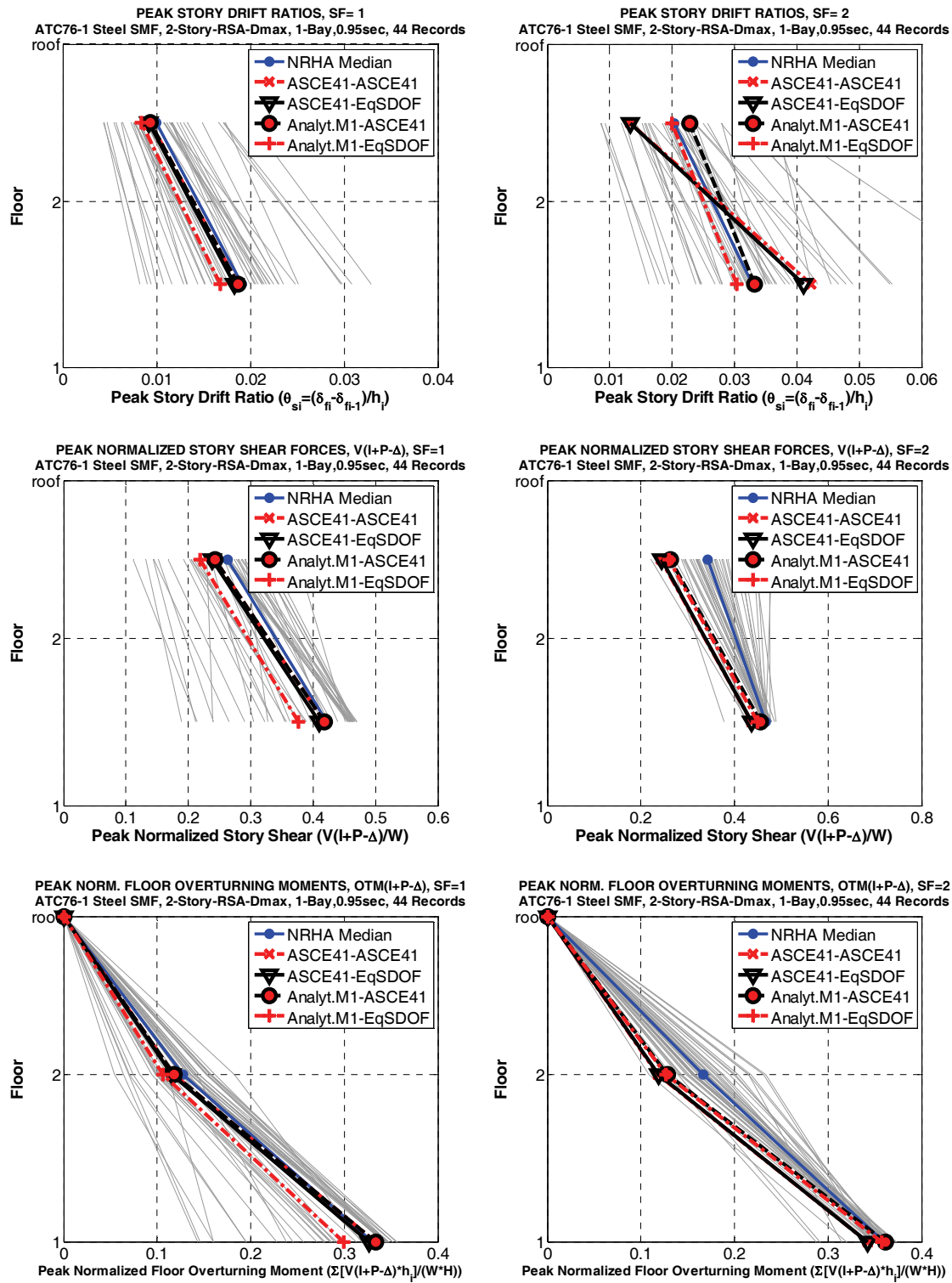
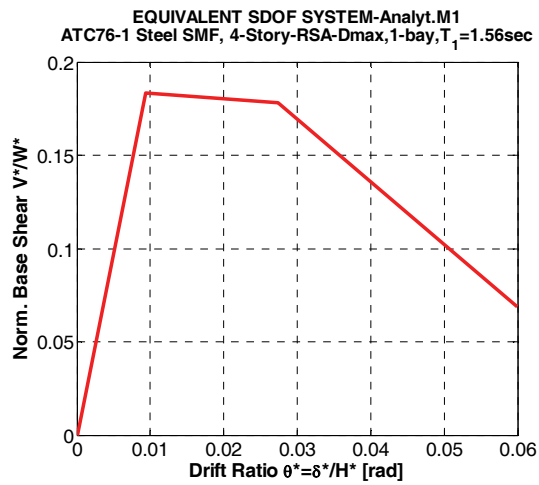
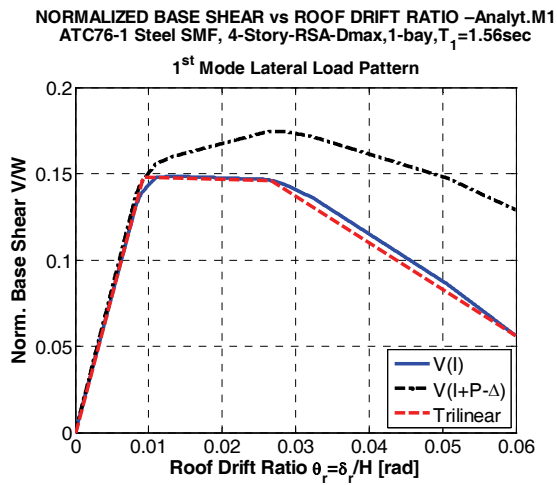
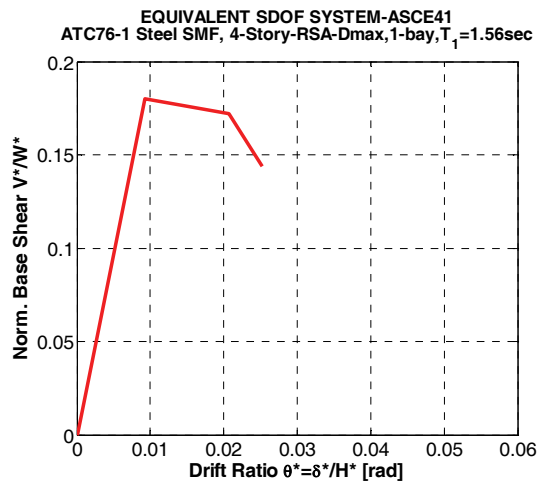
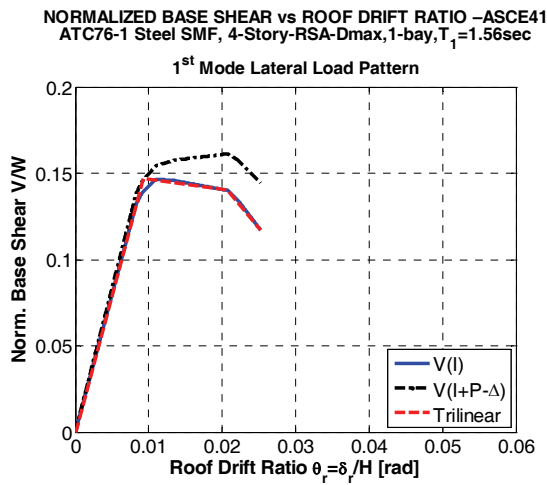


Figure A-22 NSP to NRHA comparison, 2-story steel SMF, SF = 1.0 and 2.0.



Properties of Equivalent SDOF systems

Model	V_y^*/W^*	T_e [sec]	α_s	θ_p/θ_y	θ_{pc}/θ_y
ASCE41	0.183	1.56	-0.0603	1.27	2.90
Analyt.M1	0.183	1.56	-0.0158	2.00	5.59

NRHA Median and Target Roof Drift Ratios (H = 635 inches)

	NRHA Median	ASCE41-ASCE41	ASCE41-Eq.SDOF	Analyt.M1-ASCE41	Analyt.M1-Eq.SDOF
SF = 0.5	0.0058	0.0059	0.0061	0.0059	0.0060
SF = 1.0	0.0110	0.0119	0.0112 (6 collapses)	0.0119	0.0113
SF = 2.0	0.0200	0.0238	N/A (33 collapses)	0.0238	0.0225

Figure A-23 NSP information, 4-story steel SMF.

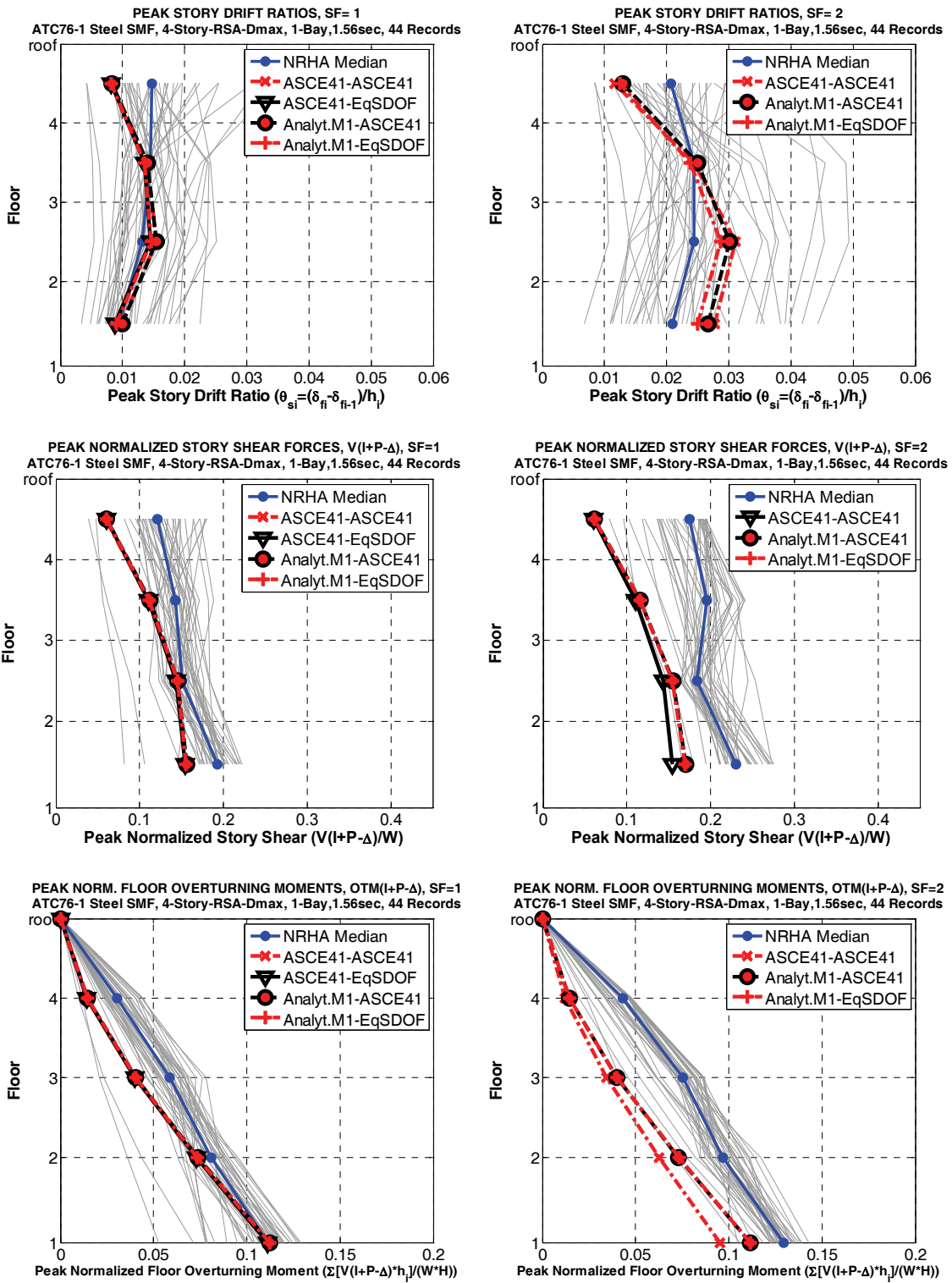


Figure A-24 NSP to NRHA comparison, 4-story steel SMF, SF = 1.0 and 2.0.

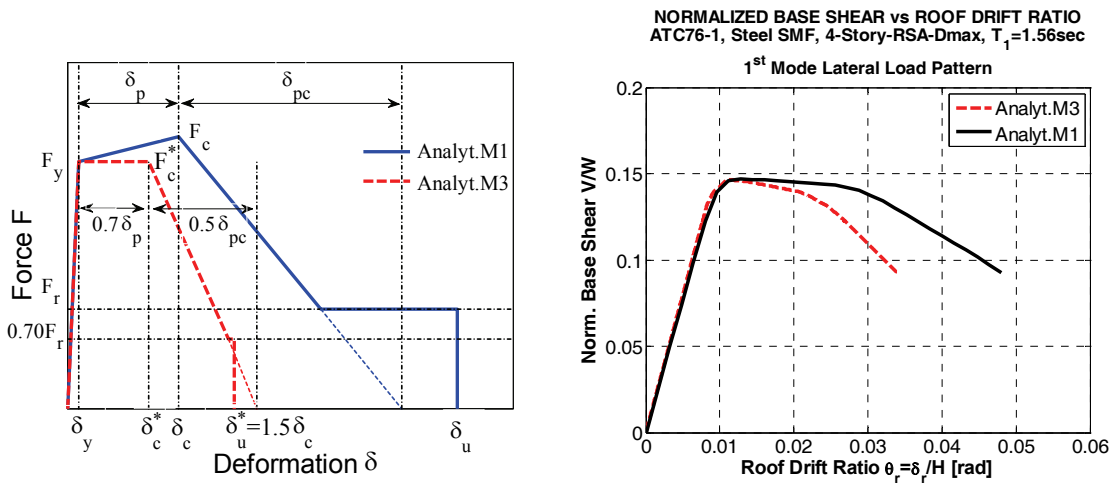


Figure A-25 Component models and global pushover curves for Analyt.M1 and Analyt.M3.

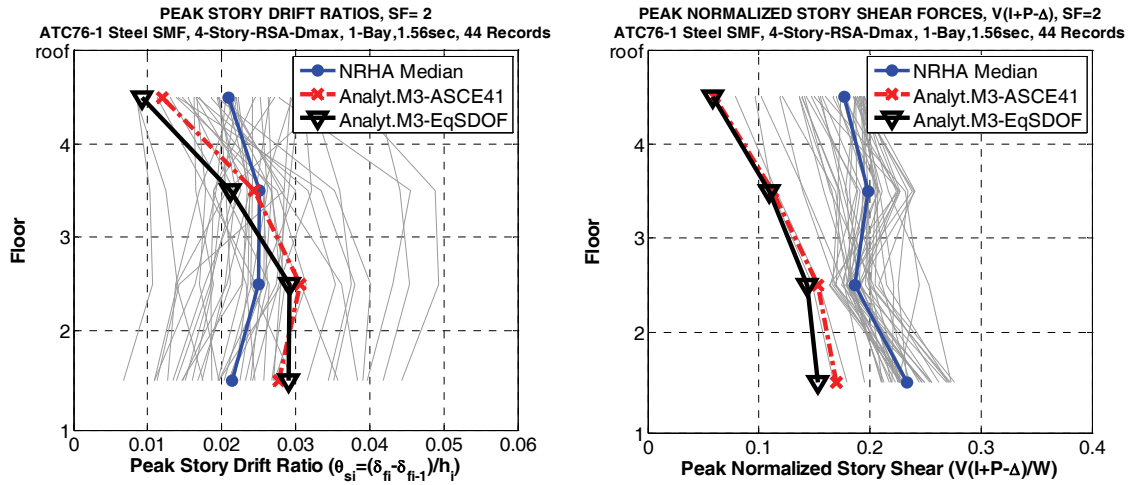
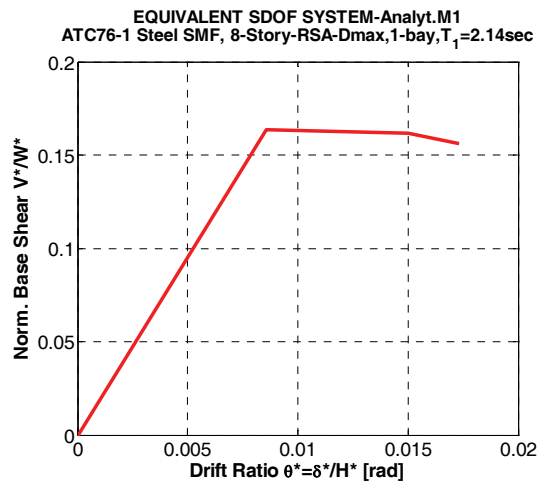
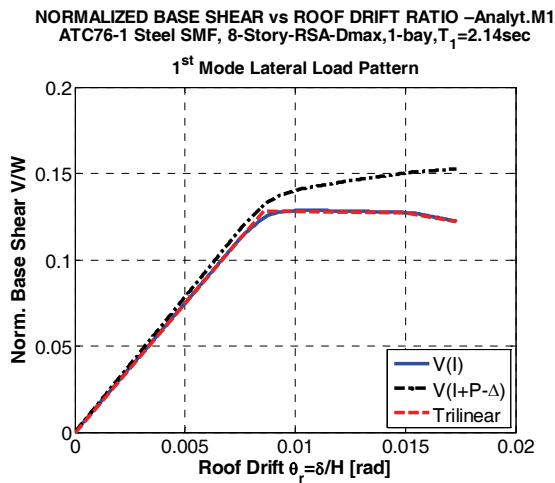
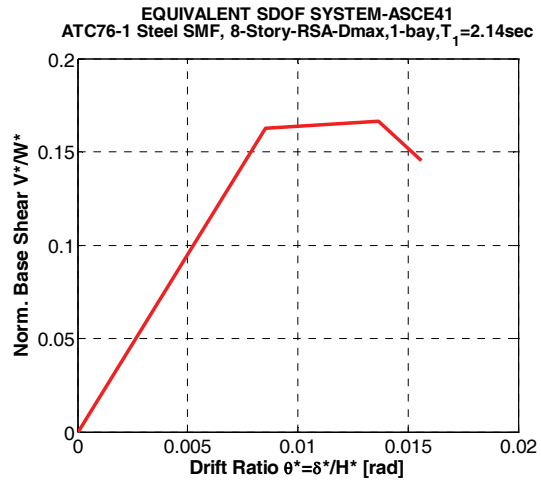
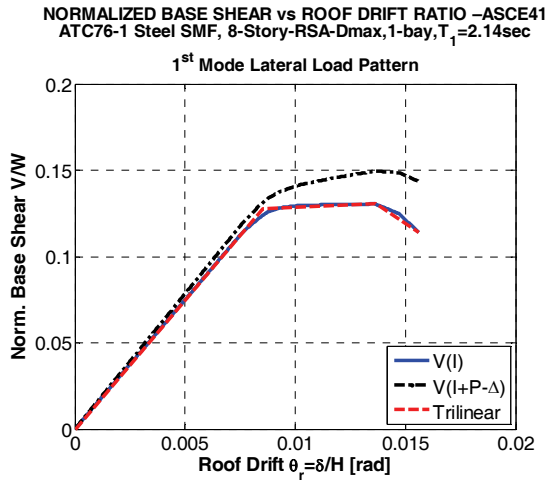


Figure A-26 NSP to NRHA comparison, 4-story steel SMF, SF=2, pushover based on Analyt.M3.



Properties of Equivalent SDOF systems

Model	V_y^*/W^*	T_c [sec]	α_s	θ_p/θ_y	θ_{pc}/θ_y
ASCE41	0.163	2.14	0.0063	0.60	1.79
Analyt.M1	0.168	2.14	-0.0175	0.75	7.36

NRHA Median and Target Roof Drift Ratios (H = 1258 inches)

	NRHA Median	ASCE41-ASCE41	ASCE41-Eq.SDOF	AnalM1-ASCE41	AnalM1-Eq.SDOF
SF = 0.5	0.0045	0.0040	0.0039	0.0039	0.0041
SF = 1.0	0.0079	0.0080	0.0078	0.0079	0.0073
SF = 2.0	0.0128	0.0160	0.0132	0.0159	0.0134

Figure A-27 NSP information, 8-story steel SMF.

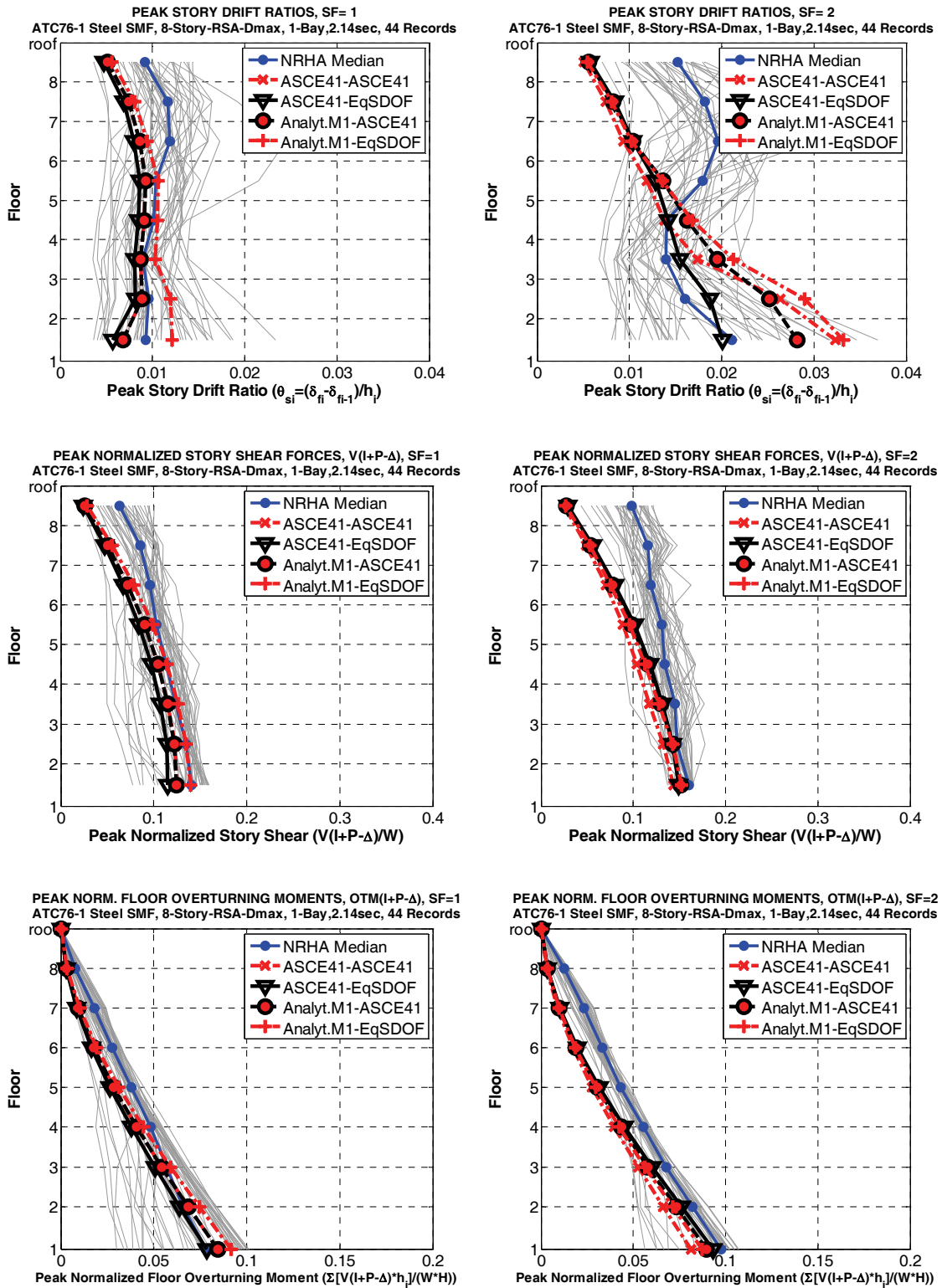


Figure A-28 NSP to NRHA comparison, 8-story steel SMF, SF = 1.0 and 2.0.

4-Story Steel SMF with $T_1 = 0.4$ sec.

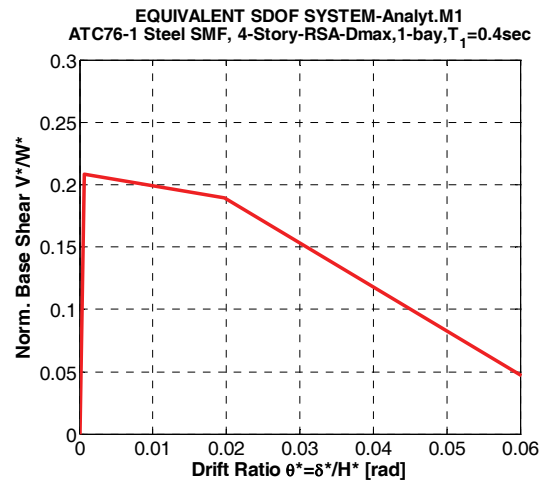
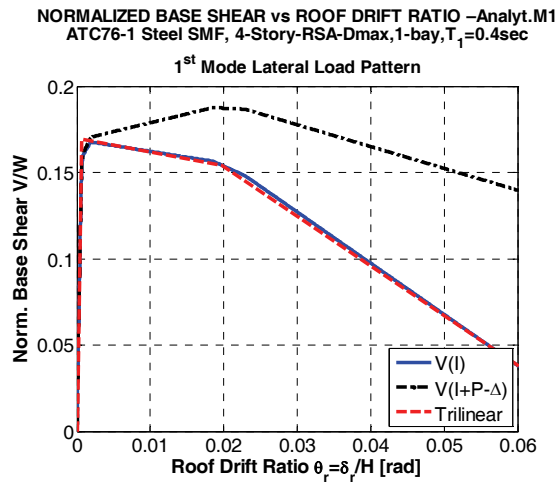
In order to assess the importance of higher mode effects on NSP predictions, the 4-story steel SMF was “re-designed” by modifying the stiffness properties of the original design by a factor that changes the first mode period from 1.56 sec. to 0.4 sec. ($T = 0.1N$). The strength of the components was not changed. For the original structure the ratio of elastic spectral acceleration at second mode to first mode is $0.804/0.208 = 3.9$. For the redesigned structure the ratio is $0.683/0.819 = 0.8$. This was expected to considerably reduce the higher mode effects and maybe lead to better NSP predictions. Only the Analyt.M1-ASCE41 NSP option was evaluated.

System properties of the redesigned structure, pushover curves, and median NRHA as well as target roof ratios are summarized in Figure A-29. These drift ratios are small, but are associated with large inelastic deformations because of the very small yield drift. For ground motion scale factors of 1.0 and 2.0 the targets and NRHA roof drifts match reasonably well. NSP to NRHA comparisons are shown in Figure A-30. The story drift NSP predictions match rather well, but the story shear force and floor overturning moment predictions are as poor as for the steel SMF with $T_1 = 1.56$ sec. The lesson is that better story drift NSP predictions can be achieved if the structure is stiff and elastic higher mode effects are reduced. But this does not help for story based forces such as shear forces and overturning moment. These force quantities may experience large dynamic amplifications in the inelastic range, which cannot be predicted by a single mode NSP based on an invariant load pattern. Focusing on base shear, the maximum base shear from the pushover is V_{I+P-A}/W is 0.19, whereas the corresponding median NRHA value for SF = 2.0 is 0.33.

What has changed, somewhat, is the shear force distribution over the height, which in the short period structure follows more closely the applied first mode lateral load pattern. This, and a corresponding change in overturning moment distribution are the only major differences in force EDPs between the $T_1 = 1.56$ and $T_1 = 0.4$ sec. structures.

Elastic Dynamic Properties (SSMF-4-1-0.40-44)

	Mode 1	Mode 2	Mode 3	Mode 4
T_i [sec]	0.40	0.128	0.069	0.043
Γ_i	1.301	-0.407	0.158	-0.025
Eff. Modal Mass	0.811	0.109	0.051	0.016
$S_a(T_i, 5\% SF=1.0)$	0.819g	0.683g	0.442g	0.389g



Properties of Equivalent SDOF systems

Model	V_y^*/W^*	T_e [sec]	α_s	θ_p/θ_y	θ_{pc}/θ_y
Analyt.M1	0.209	0.40	-0.0036	28.19	78.86

NRHA Median and Target Roof Drift Ratios (H = 635 inches)

	NRHA Median	Analyt.M1-ASCE41
SF = 0.5	0.00120	0.00195
SF = 1.0	0.00300	0.00389
SF = 2.0	0.00820	0.00779

Figure A-29 NSP information, 4-story-steel SMF with $T_1 = 0.40$ sec.

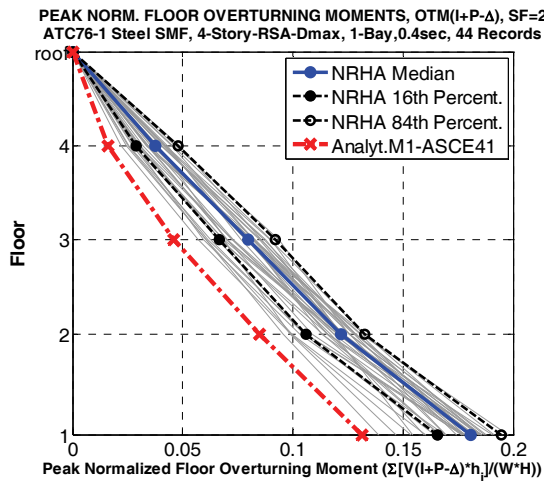
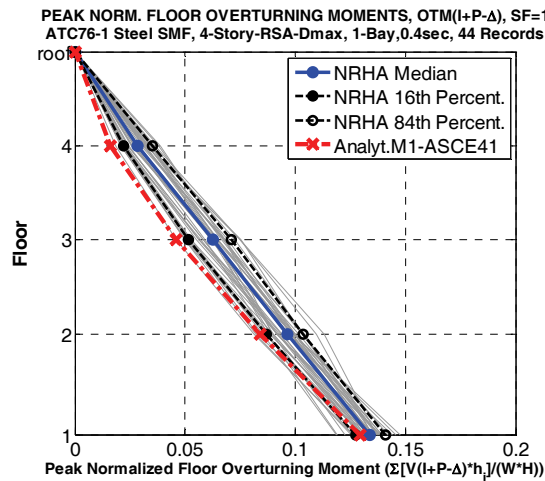
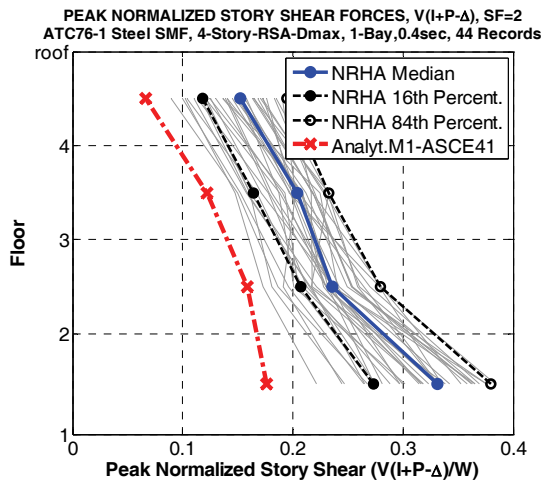
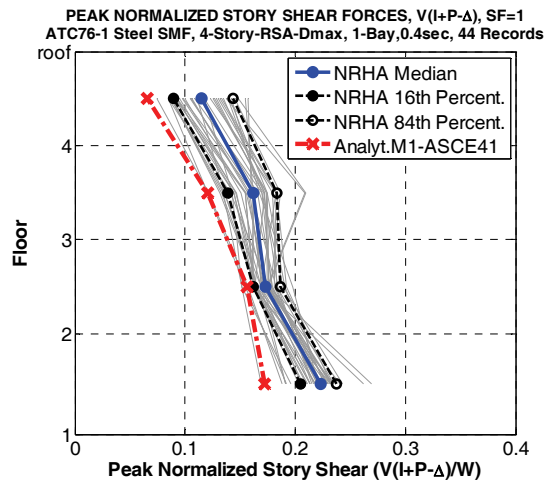
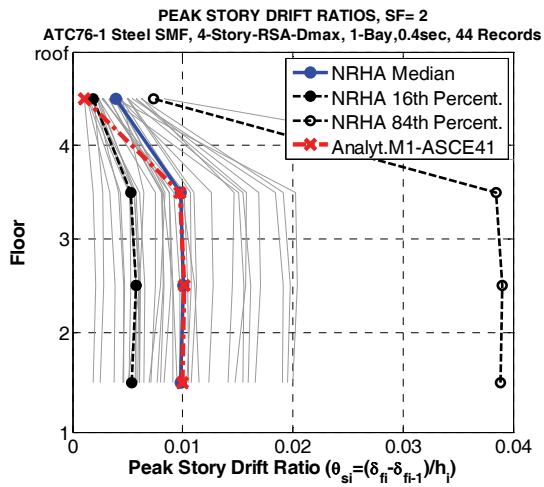
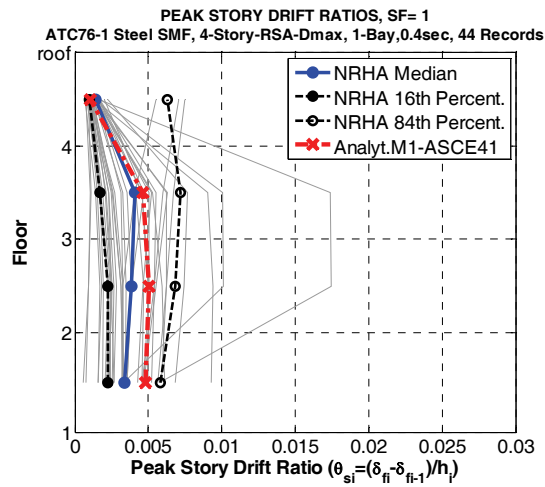


Figure A-30 NSP to NRHA comparison, 4-story steel SMF with $T_1 = 0.40$ sec.

A.4.3 Response Predictions in Negative Tangent Stiffness Region

For all cases discussed so far, the roof drift demands were confined mostly to values smaller than the capping drift for NRHA, and were always smaller than the capping drift for the target roof drift value. In all cases it was found that target displacement predictions are not very sensitive to the NSP options employed, i.e., the ASCE/SEI 41-06 coefficient method as well as alternatives based directly on an equivalent SDOF are adequate to predict the target roof drift.

It has been pointed out that the target displacement is much more difficult to predict when its value in the global pushover curve is associated with a clearly negative tangent stiffness, which exists when the structure enters the post-capping region of component behavior (Krawinkler and Zareian, 2009). One test case is explored here, using the 4-story SMF and a ground motion scaling factor of 3.0. NSP predictions based on a pushover curve obtained from ASCE/SEI 41-06 component models are not feasible because for this pushover curve the collapse potential based on tests of R_{di} (FEMA P-440A, *Effects of Strength and Stiffness Degradation on Seismic Response* (FEMA, 2009a)) is found to be unacceptable. But the pushover curve obtained from Anayt.M1 model did pass the R_{di} criterion of FEMA P-440A ($R = 5.0 < R_{di} = 5.8$). Therefore, Analyt.M1-ASCE41 and Analyt.M1-EqSDOF NSP options could be explored—the former predicting the target displacement from the ASCE coefficient method, and the latter predicting the target displacement from the equivalent SDOF system using NRHA. The latter approach did predict an unacceptable collapse potential because 38 collapses were observed when the Eq. SDOF system obtained from the Analyt.M1 pushover curve was subjected to the 44 ground motions from FEMA P-695 (even though $R = 5.0 < R_{di} = 5.8$). Thus, the only approach that provided results was the Analyt.M1-ASCE41 option, in which the ASCE/SEI 41-06 coefficient method was applied to the Analyt.M1 pushover curve to obtain the target roof drift.

Roof drifts from NRHA and from the ASCE/SEI 41-06 coefficient method are listed in Figure A-31. The NRHA median is in question because 22 collapses occurred in the NRHA, and the median is assumed to be associated with the largest roof drift of the surviving ground motions. Both the NRHA median and the ASCE/SEI 41-06 target drift are marked on the pushover curve shown in Figure A-31, illustrating that both drift values are in the range of negative tangent stiffness caused by P-delta and deterioration. NSP to NRHA comparisons are shown in Figure A-32. The NSP predictions for all three story-based EDPs are worse than for the SF = 2.0 case shown in Figure A-24.

The conclusions to be drawn from this case study are

- The ASCE coefficient method is likely to provide a poor prediction of target roof drift if this drift is in the post-capping region of the pushover curve.

- The process of assessing collapse potential by means of R_{di} is not necessarily conservative. The Analyt.M1 pushover curve passed the R_{di} test even though the NRHA with the equivalent SDOF system did lead to a great majority of collapses (38 of 44) when the FEMA P-695 ground motion suite is used as input.
- A feasible and likely conservative approach to predict collapse potential and target drift from the equivalent SDOF system is to use an SDOF NRHA tool such as IIDAP. Several tools of this type exist, and they become essential when the target drift is in the negative tangent stiffness region of the pushover curve.

Median Roof Drift Ratio (H = 635inches)

	SF=3.0
Median [%]	0.049
16th [%]	0.026
84th [%]	N/A
Mean μ [%]	N/A
σ [%]	N/A
CoV	N/A
Collapses	22

NRHA Median and Target Roof Drift Ratios (H = 635 inches)

	NRHA Median	ASCE41- ASCE41	ASCE41- Eq.SDOF	Analyt.M1- ASCE41	Analyt.M1- Eq.SDOF
SF = 3.0	0.049 22 collapses	N/A	N/A	0.0356	N/A 38 collapses

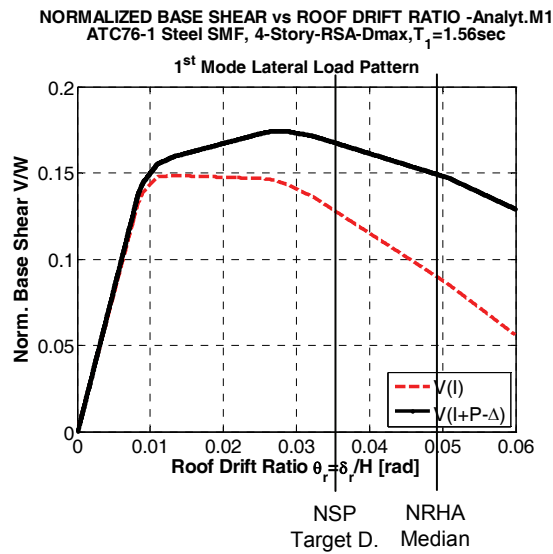


Figure A-31 NRHA roof drift statistics and median and NSP target displacement (ASCE41) of 4-story steel SMF, for SF = 3.0.

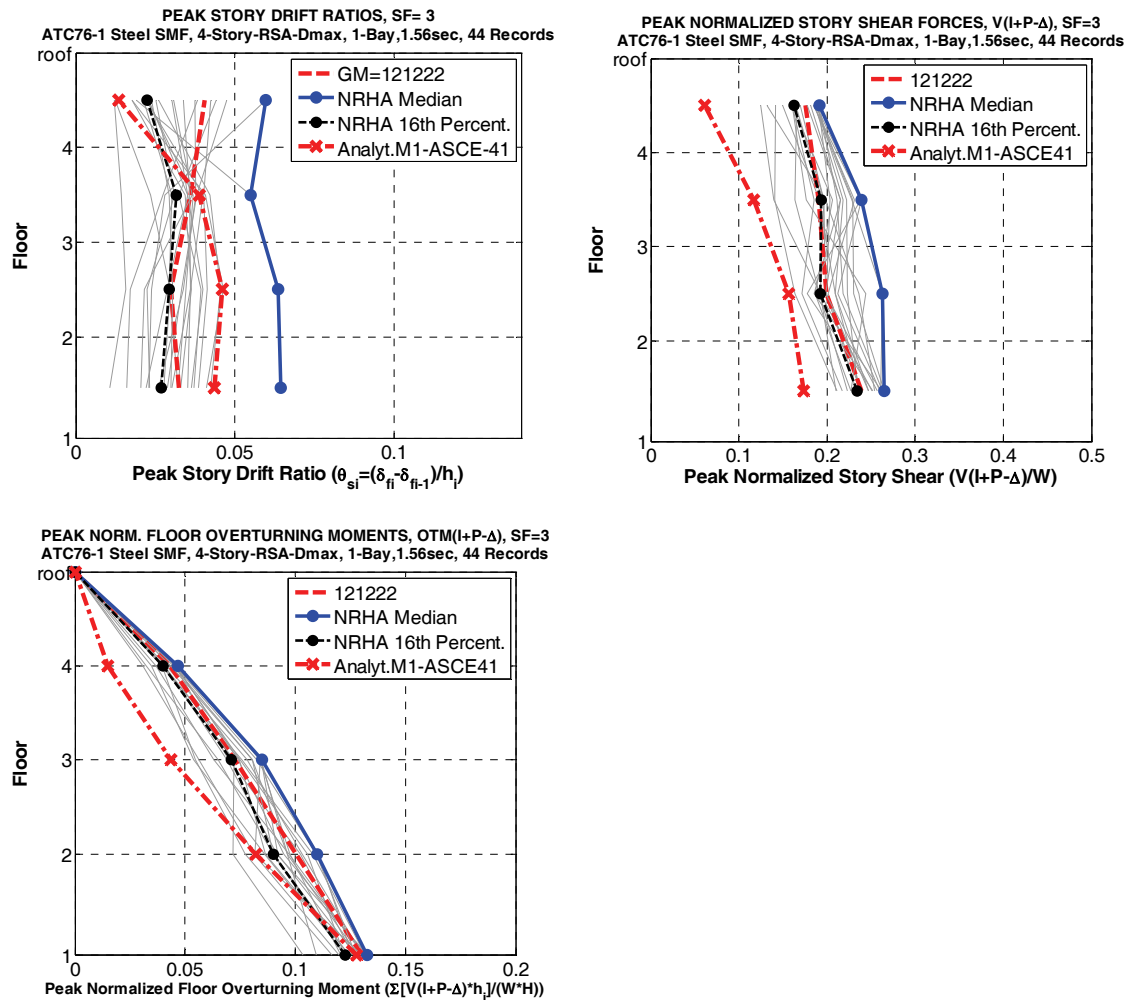


Figure A-32 NSP to NRHA comparison, 4-story steel SMF, for SF = 3.0.

A.4.4 Synthesis of Nonlinear Static Procedure Predictions

Plots summarizing the ratio of NSP predictions over median NRHA results for peak story drifts, peak story shear forces, and peak floor overturning moments are presented in Figure A-33, using the Analyt.M1-ASCE41 NSP option and SF = 1.0 and 2.0. For these ground motion scale factors the target drift is safely below the global capping point, i.e., it is not in the negative tangent stiffness region of the pushover response. A ratio smaller than 1.0 implies that the NSP under-predicts the median demands computed by NRHA. The medians of NRHA results obtained from OpenSees analysis with the modified IK component model are used as benchmark values. They may not represent the absolute truth, but they represent the relative truth in the context of NSP to NRHA comparison since in both the static and dynamic analysis procedures compatible analytical models are used. The NRHA results for steel SMFs are based on a bilinear hysteresis model of moment-rotation relationships that incorporates deterioration in strength and stiffness.

The ratios presented in Figure A-33 are insufficient to pass judgment, and the reader is referred to previous figures that show absolute values of NRHA and NSP predictions. For instance, if an EDP is very small (e.g., overturning moment in story 4 of a 4-story structure), the NSP prediction might be off by a factor of 2 but this might have no consequence because two times very small is still small.

Under the condition that the target drift demand is safely below the capping drift, the following summary observations and conclusions on NSP predictions for regular steel SMFs are made. These observations and conclusions apply only for steel SMFs, which are characterized by (a) a clear elastic stiffness that is maintained until story or global yielding occurs and causes a rapid decrease in stiffness, and (b) a relatively long first mode period. The latter is important because it keeps first mode response out of the short period region, and consequently emphasizes an inelastic response in which roof displacement is not very sensitive to the extent of inelastic deformations (equal displacement rule for nonlinear SDOF systems).

- The quality of NSP predictions does not depend strongly on the method used to predict the target displacement. Results are very similar for the ASCE/SEI 41-06 coefficient method and a more refined equivalent SDOF option. The main reason is that the various target displacement options resulted in about the same roof drift, which is close to the median roof drift obtained from NRHA. But this conclusion cannot be extended beyond the range of the steel SMF archetypes used in this study (first mode periods between 0.95 and 2.14 sec.), and may not apply for short period structures in which the roof drift can be very sensitive to the extent of inelastic deformations.
- The quality of NSP predictions does not depend strongly on the component model used to perform the pushover analysis (presuming the component model is reasonable). Results are similar whether the analysis is based on the ASCE/SEI 41-06 component model or the more refined modified IK component model (Analyt.M1). There are exceptions, such as in cases in which differences in component models lead to either a positive or slightly negative post-yield tangent stiffness. An example is the story drift in the second story of the 2-story steel SMF.
- All combinations of pushover analysis models and target displacement prediction models evaluated here provided similar EDP predictions, with exceptions as noted in item 2. Again, this conclusion cannot be extended beyond the range of structures evaluated here (essentially trilinear pushover curve, and relatively long first mode period).
- The ASCE/SEI 41-06 pushover method usually underestimates post-yield strength and deformation capacities of structures compared to the Analyt.M1 model. The latter model is based on expected values of component properties, whereas more conservative (low) values have been selected intentionally in the

ASCE/SEI 41-06 modeling criteria. The consequences on target displacement predictions are not necessarily large, unless the ground motion demands are very high.

- The use of the low capacity ASCE41 pushover model together with an equivalent SDOF model for target displacement prediction (ASCE41-EqSDOF) may provide estimates of performance that are lower than might be intended. For SF = 2.0 the ASCE41-EqSDOF combination leads to 33 collapses, which is a direct consequence of the relatively short yield plateau obtained in the ASCE/SEI 41-06 pushover.
- Except perhaps for the 2-story SMF, the quality of NSP predictions depends strongly on the lateral load pattern used in the pushover analysis. Utilization of the elastic first mode load pattern locks in the relative magnitude of story shears in the individual stories and does not permit consideration of dynamic redistribution. This makes NSP predictions questionable for steel SMFs with more than 2 stories, and very inaccurate for structures with 4 or more stories. In general, for structures with 4 or more stories, NSP predictions underestimate story EDP demands. This holds true particularly for story shear and overturning moment demands, and much more so for the demands in upper stories than lower stories.
- Even in the first story, the NRHA story shear demands can be much higher than predicted by NSP methods. The reason is dynamic amplification due to redistribution of inelastic deformations to adjacent stories, which cannot be accounted for in a first mode invariant load pattern. An example is the first story shear demand in the 4-story steel SMF for a SF of 2.0, which is about 50% higher than predicted by the various NSP methods.
- If story shears are an important performance consideration, then the validity of quantitative values obtained from an invariant load pattern NSP is in question for a 4-story steel SMF. The same cannot be said for reinforced concrete shear walls (see Appendix C).
- Similar observations apply to floor overturning moments, which control axial forces in columns of frame structures. In the upper stories the NSP predictions are often less than half those obtained from NRHA. The situation is better at the base, because maximum shear forces in individual stories occur at different times.
- Making the structure stiffer (e.g., the 4-story 0.4 sec. case) may improve story drift predictions but not story shear force predictions.

Different conclusions are drawn if the target drift exceeds the capping drift, i.e., it is in the negative tangent stiffness region.

- The ASCE coefficient method is likely to provide a poor prediction of target roof drift if this drift is in the post-capping region of the pushover curve.
- The process of assessing collapse potential by means of R_{di} is not necessarily conservative. The Analyt.M1 pushover curve passed the R_{di} test even though the NRHA with the equivalent SDOF system did lead to 38 collapses when the FEMA P-695 set of 44 ground motions is employed. The NRHA of the MDOF system did lead to 22 collapses.
- Perhaps the only feasible and likely conservative approach is to predict collapse potential and target drift from the equivalent SDOF system using an SDOF NRHA tool such as IIDAP. Many such tools exist, and they become essential when the target drift is in the negative tangent stiffness region of the pushover curve.

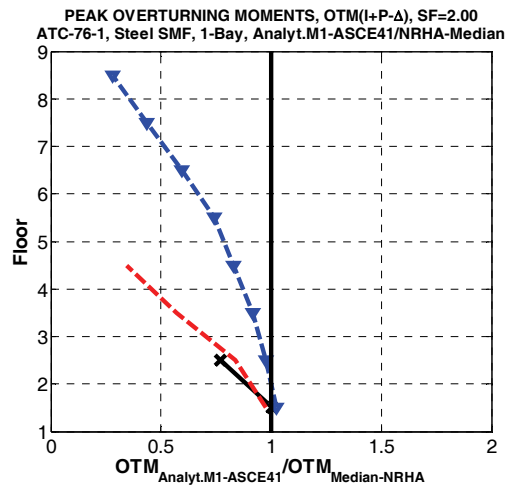
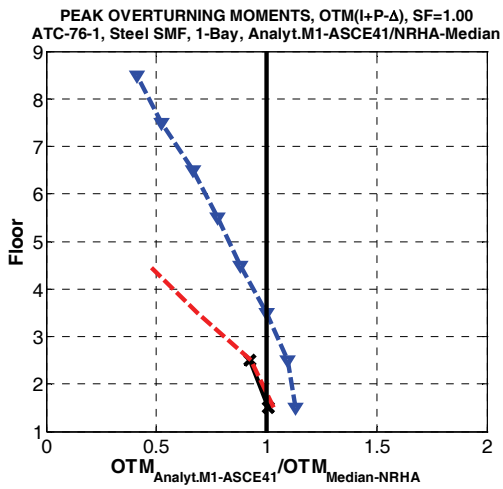
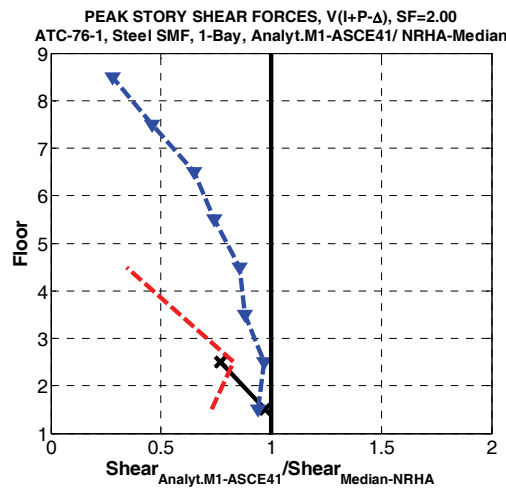
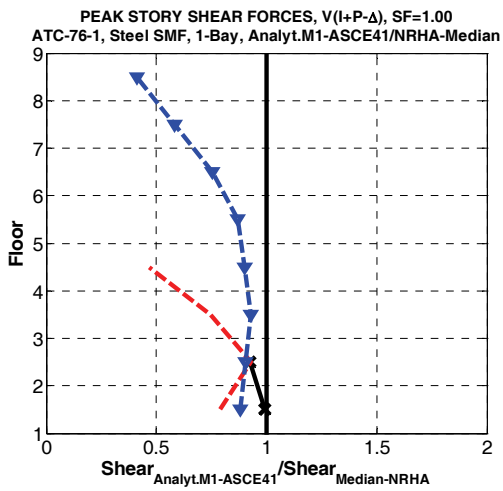
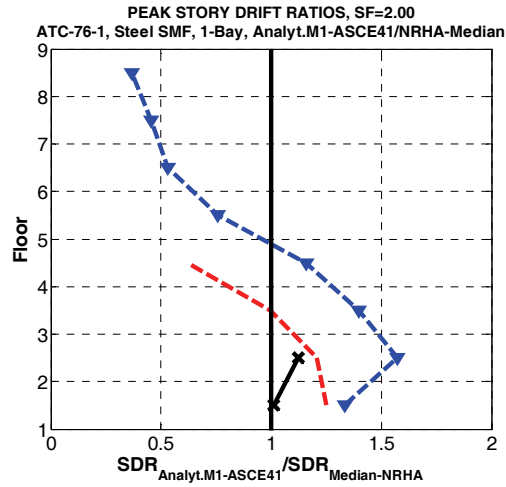
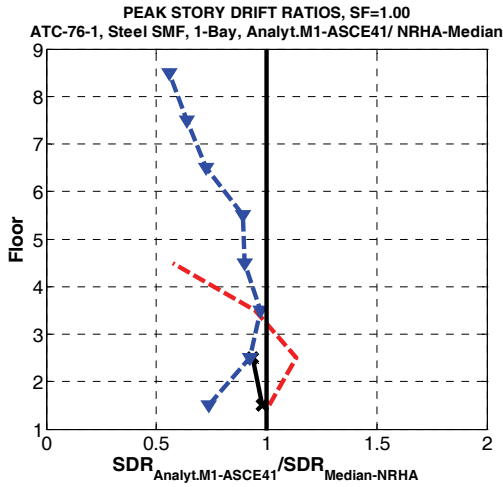


Figure A-33 Ratio of NSP predictions to median NRHA result for story EDPs, using Analyt.M1-ASCE41 NSP option, SF = 1.0 and 2.0 -- target roof drift not in negative tangent stiffness region.

A.5 Multi Mode Nonlinear Static Procedure

The multi-mode nonlinear static procedure tested in this study was the modal pushover analysis, often referred to as MPA (Chopra and Goel, 2002). This is not to say that other methods cannot deliver results of similar quality, but the emphasis here is on simple methods of general use to practicing engineers. Increasing the complexity of the analysis method is a deterrent to its use by the engineering profession. Moreover, this study is concerned only with the evaluation of analysis methods for relatively low-rise building structures.

A.5.1 Summary Description of Procedure

For background to the MPA the reader is referred to the literature (e.g., Chopra and Goel, 2002 and Chopra, 2007). Summarized here are basic implementation steps for seismic evaluation of the peak response r_{no} of structural systems using MPA. The 4-story steel SMF is used to illustrate the outcome of the steps.

1. Compute the elastic mode shapes ϕ_n and natural periods T_n of the structural system based on eigenvalue analysis.
2. Develop the base shear V_{bn} versus roof displacement u_{rn} pushover curve using the n th-“mode” lateral load distribution s_n^* , which is given by $s_n^* = m\phi_n$, in which m is the mass matrix of the structural system. Figure A34 shows the pushover curves of the 4-story steel SMF using the first and second mode lateral load distributions. The y- and x-axis is normalized with respect to the seismic weight and the total height of the steel SMF, respectively.
3. Idealize the pushover curve as a multi-linear (in this case trilinear) curve (see Figure A-34). The post-yield range up to capping is fitted using the ASCE/SEI 41-06 procedure (equal area procedure). From the capping point to the end point of the curve the same fitting method is employed.
4. Develop the base shear V_{bn}^* versus displacement δ^* of the n th-“mode” equivalent SDOF system. This step requires the computation of the effective modal mass, $M_n^* = L_n \Gamma_n$, in which,

$$L_n = \phi_n^T m l \text{ and } \Gamma_n = \phi_n^T m l / \phi_n^T m \phi_n \quad (\text{A-1})$$

- a. The vertical axis of the n th-“mode” equivalent SDOF system (see right part of Figure A-34) is created after scaling the base shear V_{bn} of the MDOF system with M_n^* to obtain $V_{bn}^* = V_{bn} / M_n^*$.
- b. The horizontal axis of the equivalent SDOF system is created after scaling the roof displacement of the MDOF system with $\Gamma_n \phi_{rn}$ to obtain $\delta^* = \delta / \Gamma_n \phi_{rn}$, in which ϕ_{rn} is the contribution of the n th-“mode” at the roof of the MDOF system.

- c. The vibration period T_n of the n th-“mode” SDOF system is given by,

$$T_n = 2\pi (M_n^* \delta_n^* / V_{bn})^{1/2} \quad (\text{A-2})$$

It should be noted that T_n may differ by a small amount from the value of the corresponding linear MDOF system. This issue is more evident in shear wall and concrete structural systems since their lateral stiffness before and after initial cracking is not the same.

5. Compute the displacement history $\delta_n^*(t)$ of the n th-“mode” inelastic SDOF system with force-deformation relationship of the type shown in Figure A-34 (right), and mass proportional damping ζ_n equal to the value that is assigned to the n th-“mode” of the MDOF system. In this study, nonlinear response history analysis is employed to compute the maximum displacement response of the n th-“mode” equivalent SDOF systems for a set of ground motions. Using the median of absolute maximum displacements, $\delta_{n,max}^*$, of the equivalent modal SDOF system, we can calculate the target roof displacement δ_{rno} for the n th mode pushover in the MDOF domain from the following relationship:

$$\delta_{rno} = \Gamma_n \phi_{rn} \delta_{n,max}^* \quad (\text{A-3})$$

6. Determine the total response of the MDOF system by combining the “modal” responses r_{n+g} (internal forces and deformations due to combined gravity and lateral forces) using a modal combination rule. In this study the Square Root of Sum of the Squares (SRSS) was used since the natural periods of the examples used are well separated. The total response r is given by,

$$r = \max[r_g \pm (\sum r_n^2)^{1/2}] \quad (\text{A-4})$$

In the results presented in this section, the Analyt.M1 model was employed for modal pushover analysis, and the IIIDAP program was used to compute median displacements for the equivalent modal SDOF systems, using the 44 ground motions from FEMA P-695. In Goel and Chopra, (2005) and Chopra, (2007) an improved estimate of plastic hinge rotations and member forces using MPA in the inelastic range is obtained by computing plastic hinge rotations from the total story drifts (see also Gupta and Krawinkler, 1999). This does require an additional nonlinear static analysis. This approach was not applied in the results presented in this section.

A.5.2 Results for 4- and 8-story Steel Moment Frames

Results are presented here for the 4- and 8-story steel SMFs as well as for the 4-story SMF with $T_l = 0.4$ sec. The latter one is evaluated because second mode effects should be of less importance because $S_a(T_2)/S_a(T_1)$ is 0.8 as compared to 3.9 for the $T_l = 1.56$ sec. 4-story frame. Figures A-34 and A-37 present curves from first and second mode pushovers and the corresponding equivalent SDOF systems. Figures A-35, A-36, and A-38 present MPA to NRHA comparisons for story drifts, story shear forces, and floor overturning moments.

Nonlinear analysis should be used for first and higher mode pushovers, resulting in diagrams of the type shown in the lower portion of Figures A-34 and A-37. But in many cases, particularly for low-rise regular structure, the higher mode target displacement obtained from the equivalent SDOF system is less than the yield displacement, which implies that the higher mode contribution is elastic. If this is the case, all deformations and forces obtained from the MPA are modal combinations of inelastic first mode contributions and elastic higher mode contributions. In general, this is a preferred procedure compared to the elastic response spectrum analysis (RSA) in which all modal contributions are assumed to be elastic up front.

The results presented in this section are for cases of regular steel SMFs in which the target displacement is smaller than the capping displacement, i.e., the response has not entered the negative tangent stiffness region. The effect of severe strength irregularities on MPA predictions is discussed in Section A.7.

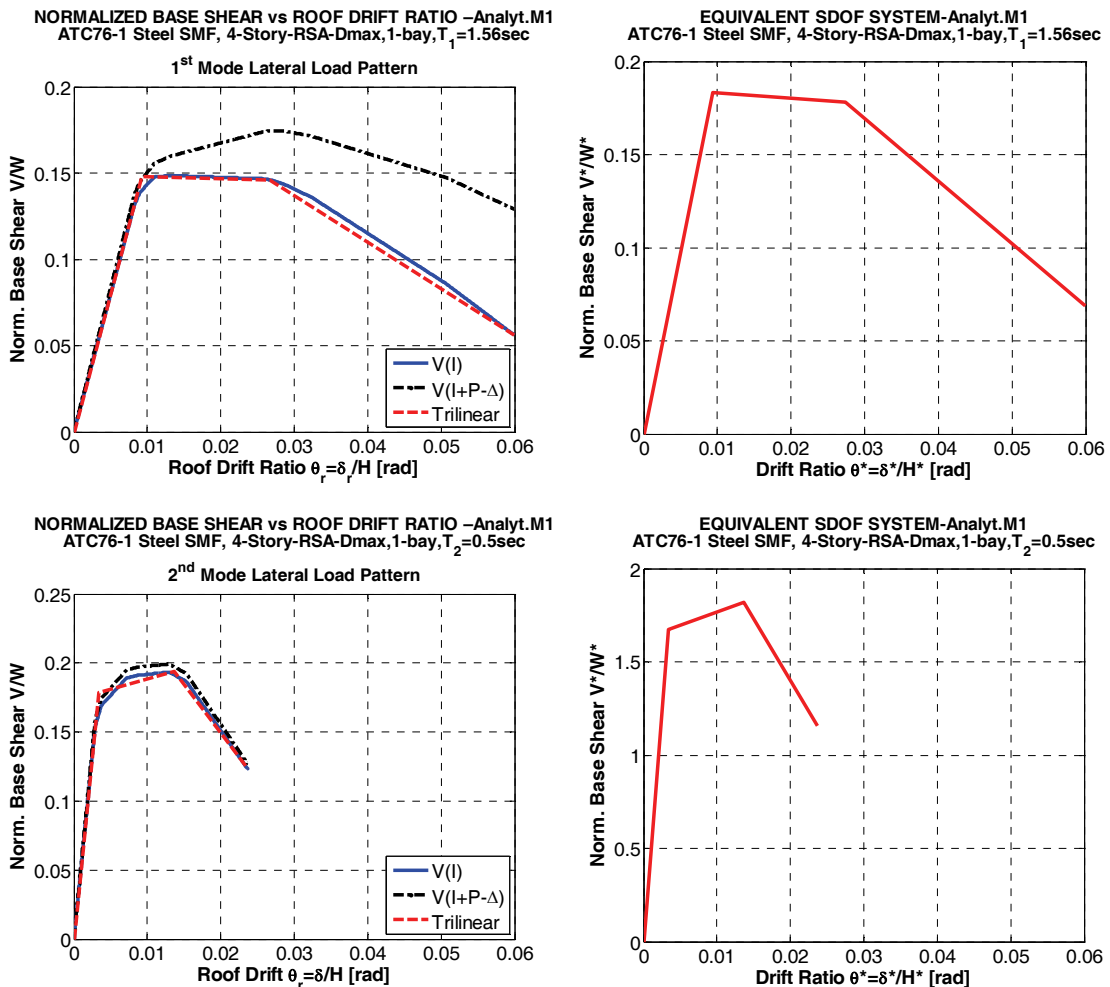


Figure A-34 First and second mode pushovers and equivalent SDOF systems, 4-story steel SMF.

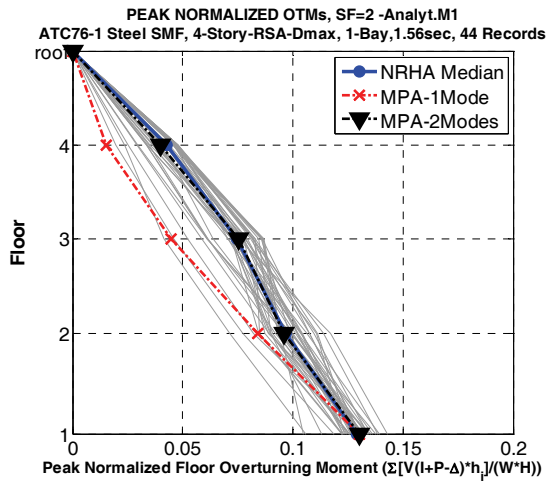
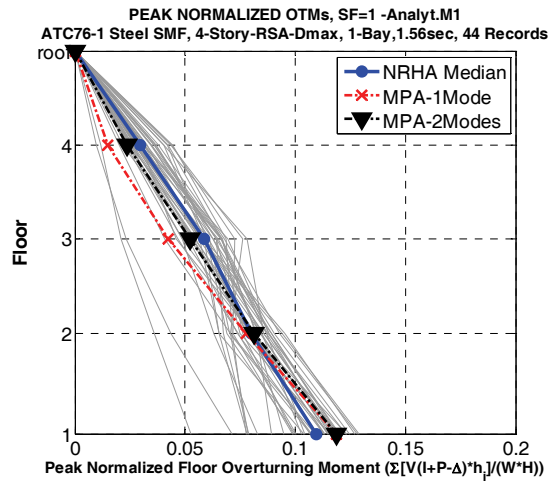
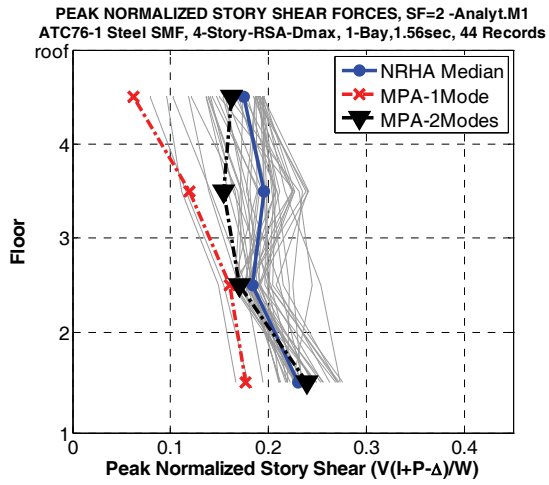
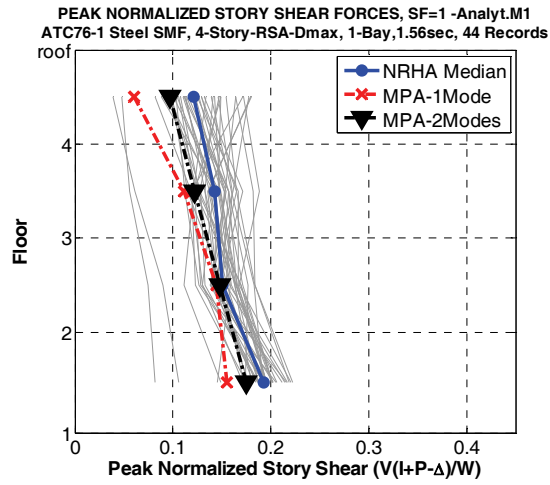
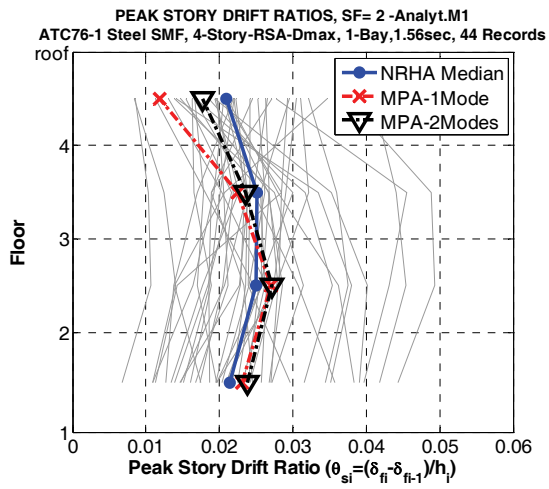
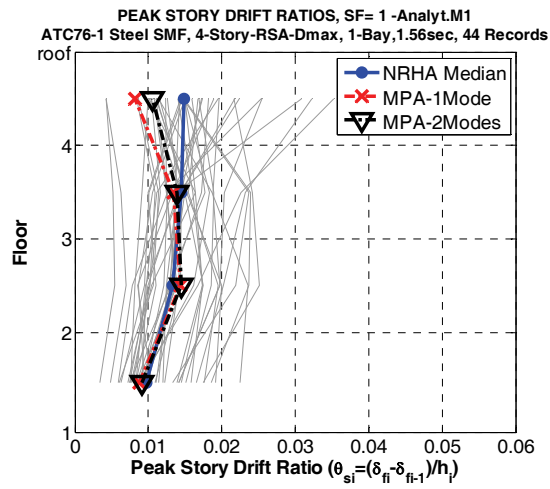


Figure A-35 MPA to NRHA Comparison, 4-story steel SMF, SF = 1.0 and 2.0.

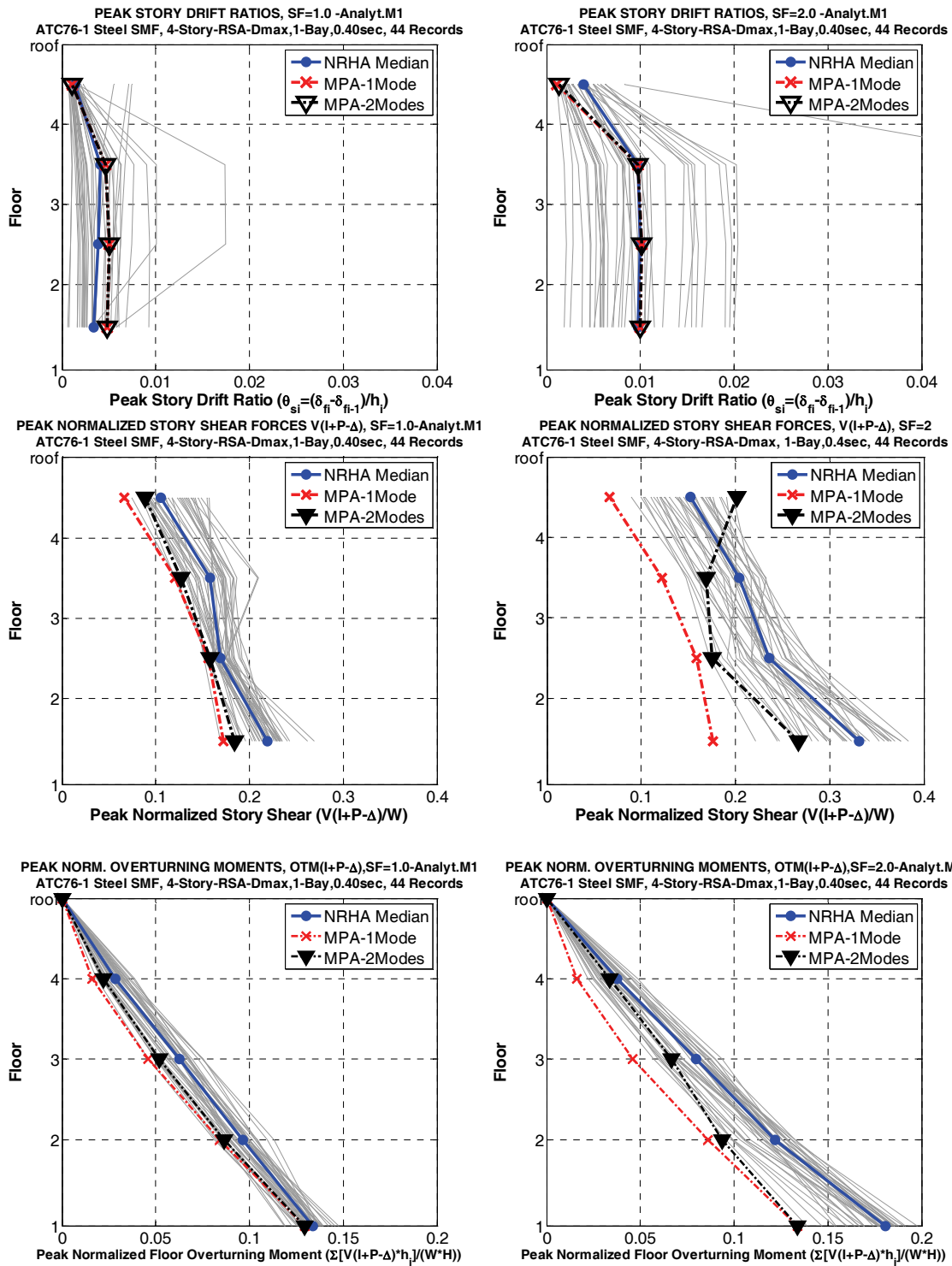


Figure A-36 MPA to NRHA Comparison, 4-story steel SMF with $T_1 = 0.40$ sec., SF = 1.0 and 2.0.

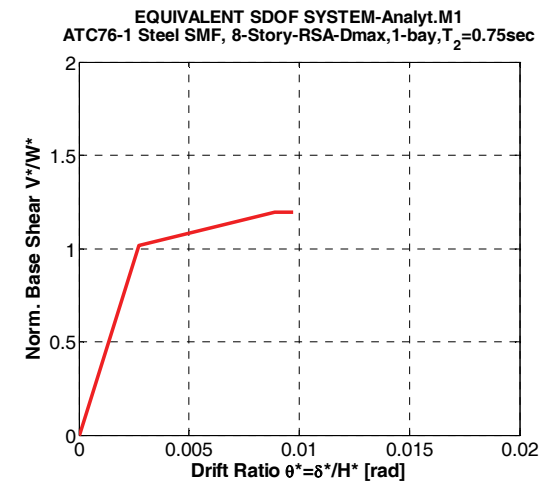
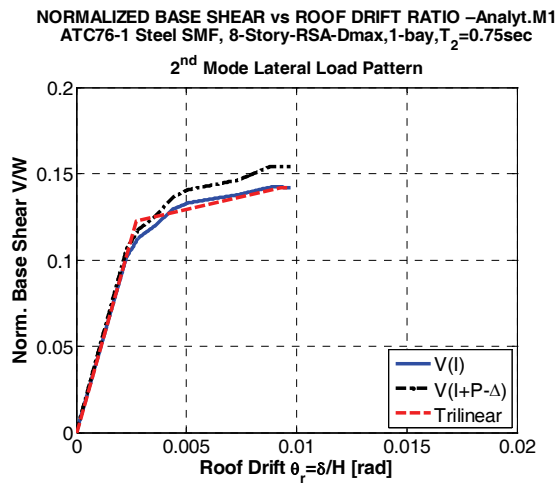
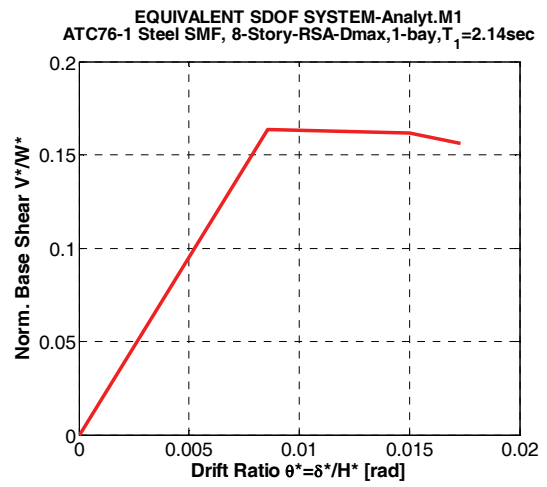
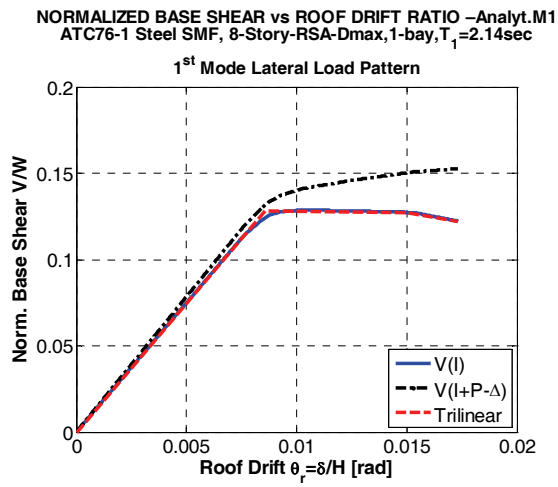


Figure A-37 First and second mode pushovers and equivalent SDOF systems, 8-story steel SMF.

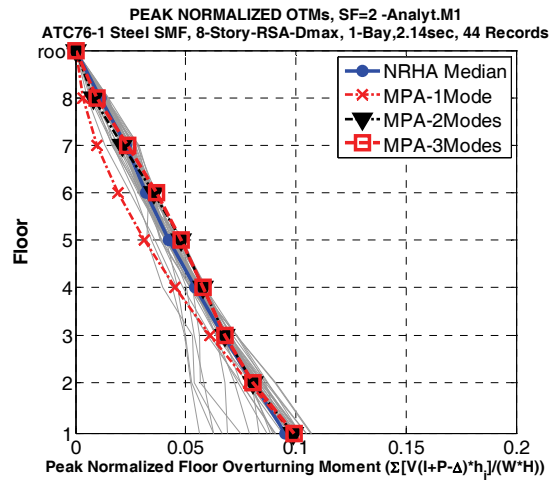
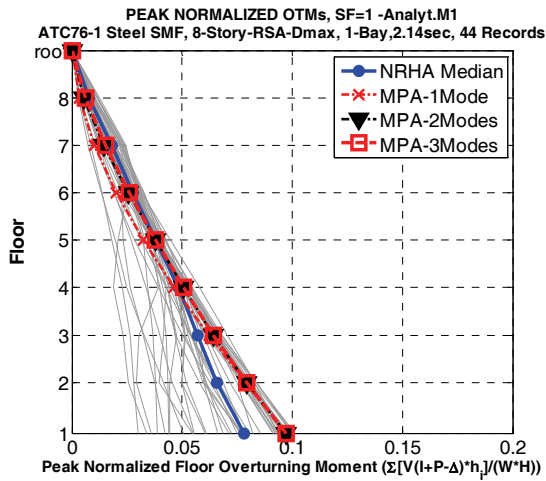
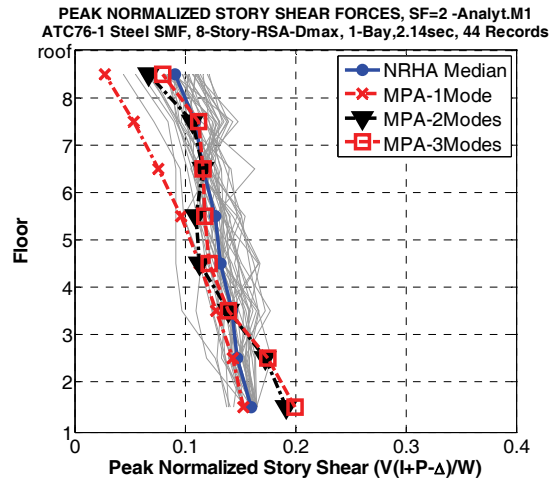
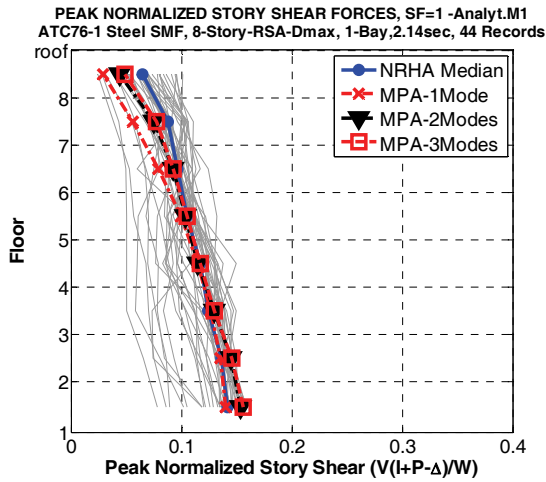
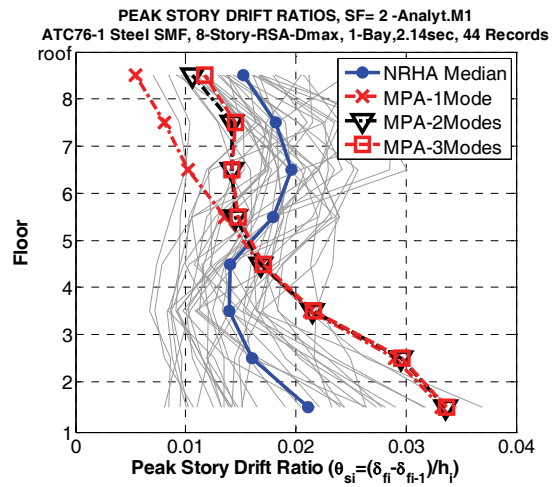
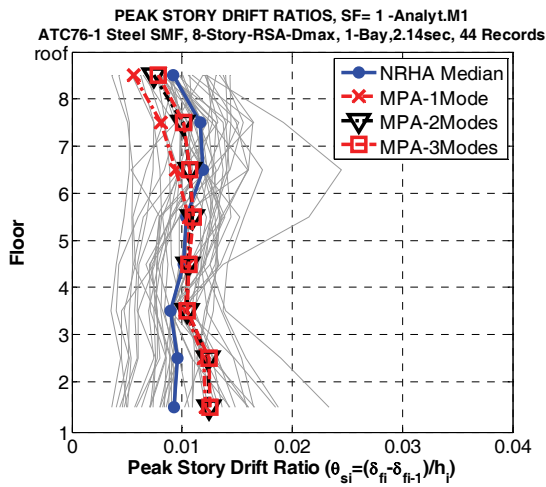


Figure A-38 MPA to NRHA Comparison, 8-story steel SMF, SF = 1.0 and 2.0.

A.5.3 Synthesis of Modal Pushover Analysis Predictions

Based on the small study with 4- and 8-story regular steel SMF structures, supplemented by MPA evaluation of the 4-story shear beams discussed in Section A.7, the following summary observations and conclusions are made on the benefits of MPA predictions for steel SMFs compared to NSP predictions.

- In all cases investigated the MPA led to improved EDP predictions compared to the single mode NSP options. The MPA employed here is based on the component model used in the NRHA, i.e., Analyt.M1, and on predicting modal target displacements from NRHA of equivalent modal SDOF systems.
- Incorporation of the second mode led to considerable improvement in EDP predictions. Consideration of the third mode did not change the results my much even for the 8-story steel SMF.
- In the case of the 4-story regular steel SMF with $T_1 = 1.56$ sec., the improvement of all story-based EDP predictions compared to NSP predictions is remarkable. For the 4-story regular structure with $T_1 = 0.4$ sec. the contribution due to second mode participation brings the MPA/NRHA_{median} base shear ratio to 0.85 compared to 0.57 for the NSP for a SF=2.0.
- In the 8-story steel SMF the MPA significantly improved drift, shear force, and overturning moment predictions in the upper stories, compared to NSP. But it predicted drifts in the lower stories that are more than 50% larger than those obtained from NRHA for a ground motion scale factor of 2.0. The reason is that for this scale factor the first mode pushover shows large amplification of story drifts in the lower stories (bottom right graph in Figure A-14), which are not present in the NRHA. This shows the sensitivity to load patterns, which is present in the MPA as it is in a single mode NSP that uses an invariant load pattern.
- Load pattern sensitivity is also an issue if a structure can develop plastic mechanisms in individual stories, as in the example illustrated later in Section A-7.
- In the regular steel SMF structures investigated here the second mode contribution is elastic, which simplifies the modal combination and avoids ambiguities that might be caused by displacement reversals sometimes observed in inelastic higher mode pushover analyses.
- If a displacement reversal occurs, it indicates sensitivity to the selected load patterns and the use of the MPA is not recommended.

A.6 Assessment of Elastic Response Spectrum Analysis

This section summarizes a test case for predicting story level EDPs from elastic response spectrum analysis (RSA) as an alternative to inelastic static procedures. The median acceleration spectrum for 2.5% damping obtained from the 44 ground motions from FEMA P-695 was used for this purpose. The test structure is the 4-story steel SMF. Results for the story drifts, story shears, and floor overturning moments are shown in Figure A-39 for ground motion scale factors $SF = 0.5$ and 2.0 .

As expected, EDP predictions by means of RSA are very good for the ground motion intensity associated with $SF = 0.5$. In this case the median NRHA results are in the elastic range, i.e., this case is a test of the accuracy of predictions of elastic dynamic response from RSA. If the ground motion intensity is quadrupled ($SF = 2.0$), the NRHA response is highly inelastic, as judged from the graph in the right upper corner of Fig. A-39 and considering that yield story drift ratio for all four stories is slightly less than 1%. The RSA predictions of story drifts are reasonable for this case of inelastic response, because this structure does not have noticeable irregularities. But the RSA predictions for force quantities are way off, to no surprise.

Summary of Observations on the use of RSA

- RSA is a very useful tool for predicting deformation and force EDPs provided the structure is in the elastic range or close to it.
- If no severe strength or stiffness irregularities exist, the RSA might provide good drift predictions even in the inelastic range of behavior, but it will not provide good information on force quantities.
- The RSA is prone to provide misleading information if a strength discontinuity exists
- Because of its limitations in capturing inelastic response characteristics, the RSA is not recommended as a general tool for EDP predictions, unless it can be established that the response is elastic or close to it.

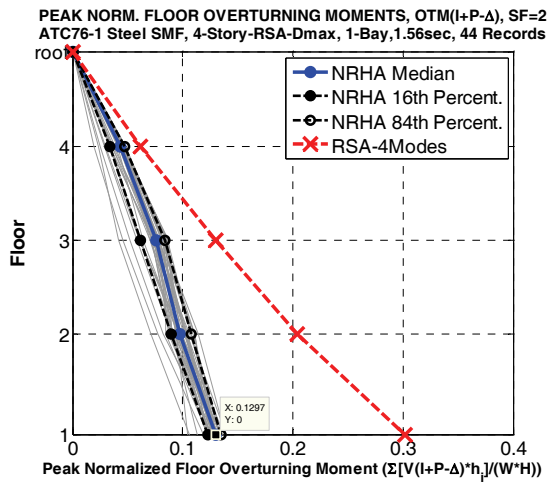
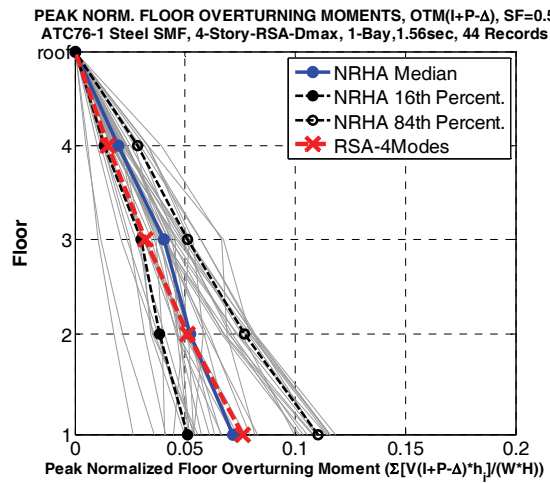
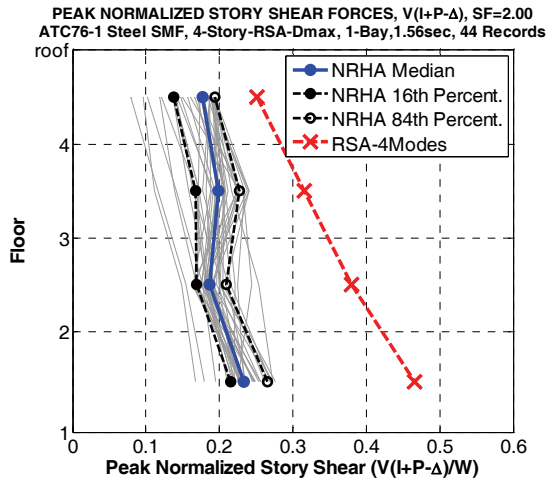
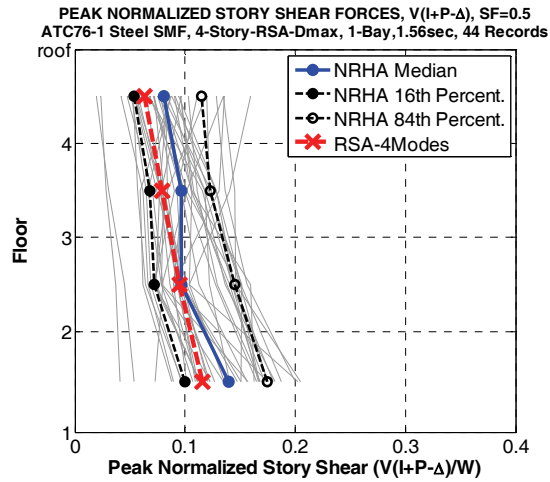
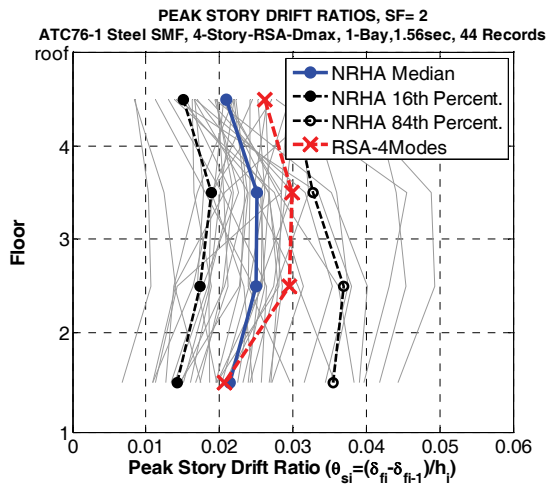
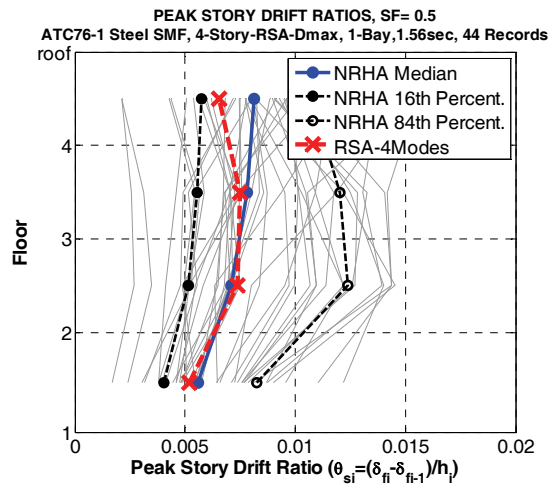


Figure A-39 Elastic RSA to NRHA Comparison, 4-story steel SMF, SF = 0.5 and 2.0.

A.7 Load Pattern Sensitivity and Response Prediction for a Frame Structure with Severe Strength Irregularity

In this section single bay shear building models are used to illustrate important points that need consideration when the nonlinear dynamic response is predicted by means of static procedures that rely on an invariant lateral load pattern. Shear buildings imply that only columns contribute to lateral strength and stiffness and beams are considered to be rigid and of infinite strength. Thus, lateral frame stiffness is equal to $2 \cdot 12EI/L^3$, and the story shear – drift relationship becomes a unique diagram determined by the moment rotation relationship of plastic hinges at the column ends. A simple bilinear diagram is assumed in the shear building models used here.

It is acknowledged that such simple structures rarely exist and that certain shortcomings of NSP procedures are amplified by these simplifications. But the following case studies serve to illustrate potential problems in an unambiguous manner.

A.7.1 Load Pattern Sensitivity

A 2-story shear building with the following properties is used here for illustration.

$$T_l = 0.5 \text{ sec}$$

$$I_{\text{col}} = 5000 \text{ in}^4 \text{ per column in each story}$$

$$\text{Story height} = 12 \text{ ft each story}$$

$$\text{Gravity Load} = 1000 \text{ kips per story}$$

$$V_y \text{ in story 2} = 320 \text{ kip}$$

$$V_y \text{ in story 1} = 460 \text{ kip (case A in Figure A-40)}$$

$$V_y \text{ in story 1} = 500 \text{ kip (case B in Figure A-40)}$$

Elastic - perfectly plastic moment-rotation relationship at all plastic hinge locations in columns

Triangular lateral load distribution for pushover analysis

Pushover curves for cases A and B are elastic-plastic and almost identical, with the only difference being that maximum base shear for case A is 460k whereas it is 480k for case B. However, the pushover deflected shapes for the two cases are very different, as shown in the right portion of Figure A-40. For the same target displacement, δ_b , the story drift for case A in story 1 is a multiple of that in story 2, and vice versa for case B. Thus, an NSP prediction of story drift will produce very different results for the two cases, as shown in bold dashed lines in Figure A-41. However, nonlinear response history analysis produces almost identical story drifts for the two cases, as indicated by the median story drifts shown in bold solid lines. This is a simple illustration of how wrong NSP predictions of story drifts can be if an

invariant load pattern is used and the deflected shape of the structure is sensitive to the applied load pattern. The pushover gives a clear indication of a strength irregularity, which in reality does not exist.

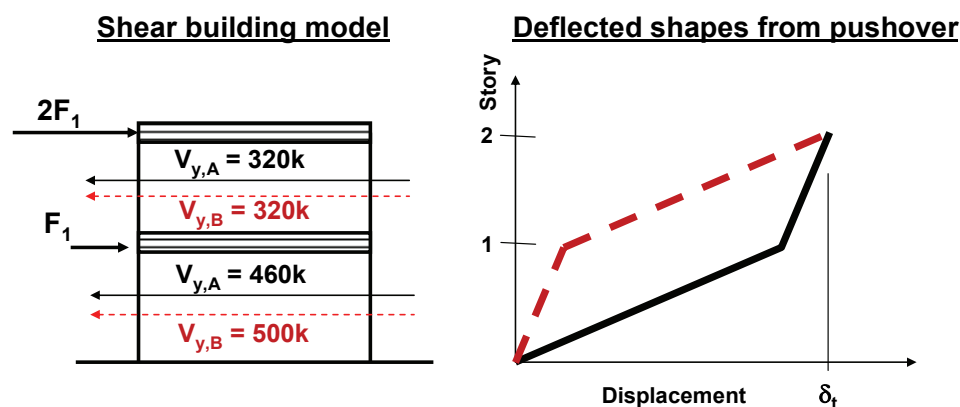


Figure A-40 Sensitivity of pushover deflected shape to load pattern.

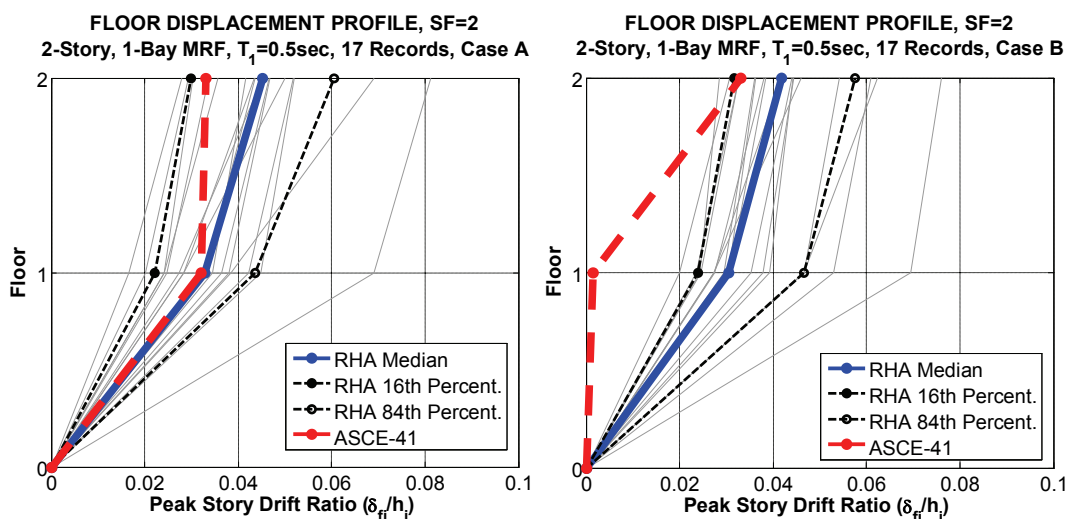


Figure A-41 NSP to NRHA comparison, 2-story shear building with two slightly different story shear capacities.

A.7.2 Response of a 4-Story Building with Strength Irregularity

Strength irregularities are well defined in ASCE/SEI 41-06. Section 2.4.1.1.3 states that a “weak story irregularity shall be considered to exist in any direction of the building if the ratio of the average shear demand capacity ratio (DCR) of any story to that of an adjacent story in the same direction exceeds 125%”. The following case study is performed in order to assess the potential of nonlinear static procedures for predicting EDPs of structures with a strength irregularity.

The case study is concerned with a 4-story shear building that has the same story masses as the previously discussed 4-story steel SMF and whose column stiffnesses are tuned so that the structure has the same period as the 4-story steel SMF, i.e.,

1.56 sec. The column yield strength was determined by the seismic load criteria employed in the design of the previously discussed 4-story steel SMF, but using a constant overstrength factor of 2.0 in each story. Column peak (capping) strength was assumed to be equal to 1.1 times the yield strength. The resulting structure has a distribution of shear strength over the height that follows the code shear force pattern used for design of the previously discussed 4-story steel SMF. This regular structure served as base case for design of an irregular structure and for comparing EDP predictions for regular and irregular structures.

Strength irregularity for the case study structure was created by increasing the story shear strength in all stories above the first one by the amount needed to create a shear strength in story 2 that is 50% higher than the shear strength of story 1, see Figure A-42. The stiffness of the individual stories was not changed in order to maintain the same first mode period of 1.56 sec.

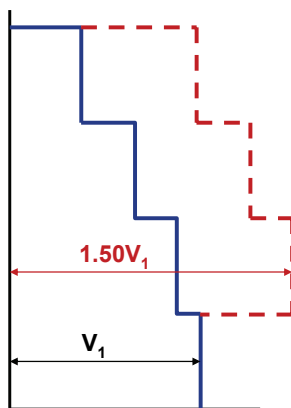


Figure A-42 Illustration of strength irregularity created in the case study.

In this manner a pair of structures was generated; one having a smooth code-type variation of strength over the height (referred to as “regular base case”), and the other having a severe strength irregularity. Nonlinear response history analysis (NRHA), two single mode nonlinear static procedures (Analyt.M1-ASCE41 and Analyt.M1-EqSDOF), and the MPA have been employed for EDP prediction.

System information for the regular base case structure is presented in Figures A-43 and A-44. The deflection profiles in the left lower portion of Figure A-43 show that the first mode pushover leads to a concentration of inelastic drifts in the first story. This is a misrepresentation caused by the invariant load pattern that forces most of the inelastic deformations into the one story that yields first. In this case it is the first story, but for a slightly different load pattern it could be any of the other stories.

First mode and second mode pushovers and corresponding equivalent SDOF systems are shown in Figure A-44. NSP target roof drift predictions are close to the median drift of the NRHA. 38 collapses are observed for a ground motion scale factor $SF = 2.0$ if the target displacement is predicted from NRHA of the equivalent SDOF, whereas the NRHA of the MDOF structure caused only 14 collapses. This confirms

the observation made elsewhere that NRHA with the equivalent SDOF leads to a conservative (high) prediction of collapse incidences.

Nonlinear response history analysis (NRHA) results for the regular base case are shown together with NSP predictions in Figure A-45, and together with MPA predictions in Figure A-46. Story force (shear forces and overturning moments) predictions are rather accurate, but story drift predictions are far off in the first story in which the pushover shows concentration of inelastic deformations. The NRHA results do not confirm this concentration of inelastic deformations.

System information for the shear building with strength irregularity is presented in Figures A-47 and A-48. The pushover curves and deflection profiles are almost identical to those for the regular base case structure even though the strength of all but the first story has been increased by a large amount. For this case very similar pushover curves and deflection profiles would be obtained even if a different load pattern had been applied. For this case the pushover did expose a real strength irregularity and not the fictitious irregularity it indicated for the regular base case.

The effect of the strength irregularity is evident in the NRHA results shown in Figures A-49 and A-50. The median drift in the first story is large compared to that in other stories, as expected from the strength irregularity and quite different from the regular base case. Both the NSP and MPA capture rather well the effect of this strength irregularity on the first story drift. But both do not fully capture the dynamic amplification effect that increases the story shears in the upper stories, with the MPA giving a somewhat better prediction. The large drift amplification in the first story did lead to 28 collapses for a ground motion scale factor $SF = 2.0$, which is the reason why no results are presented for this scale factor.

Seismically effective weight per frame: $W = 2,799k$

($w_1 = 714k$, $w_2 = w_3 = 708k$, $w_r = 669k$)

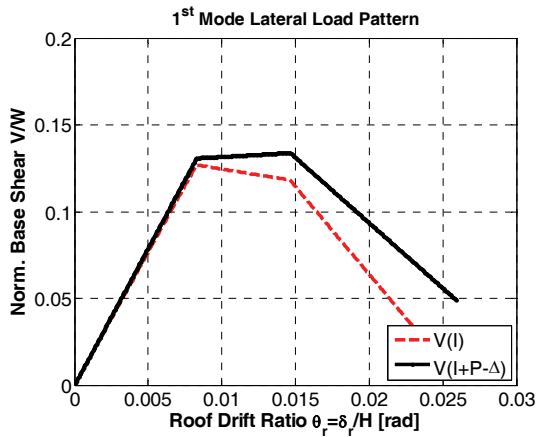
Story Shear Strength (Overstrength Factor = 2.0)

Story	Vy (kip)
4	155
3	271
2	343
1	375

Roof Drift Ratios from NRHA (H = 635 inches)

	SF=0.5	SF=1.0	SF=2.0
Median [%]	0.0072	0.0133	0.0239
16th [%]	0.0047	0.0085	0.0158
84th [%]	0.0107	0.0232	N/A
Mean μ [%]	0.0075	N/A	N/A
σ [%]	0.0030	N/A	N/A
CoV	0.4006	N/A	N/A
Collapses	0	4	14

NORMALIZED BASE SHEAR vs ROOF DRIFT RATIO -Analyt.M1
Steel SMF, 4-Story Shear-Beam, Base-Case, $T_1=1.56$, 44 records



FLOOR DISPLACEMENT PROFILE
Steel SMF, 4-Story Shear Beam, Base Case, $T_1=1.56$, 44 Records

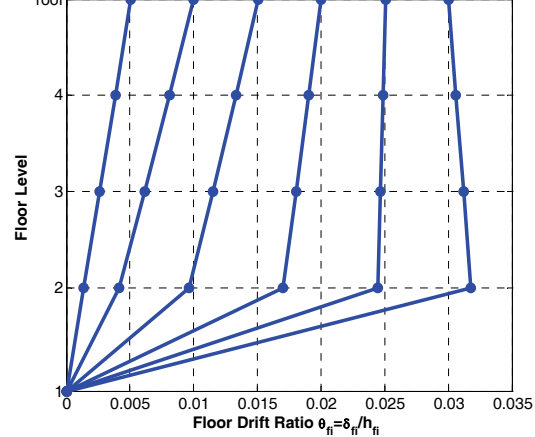
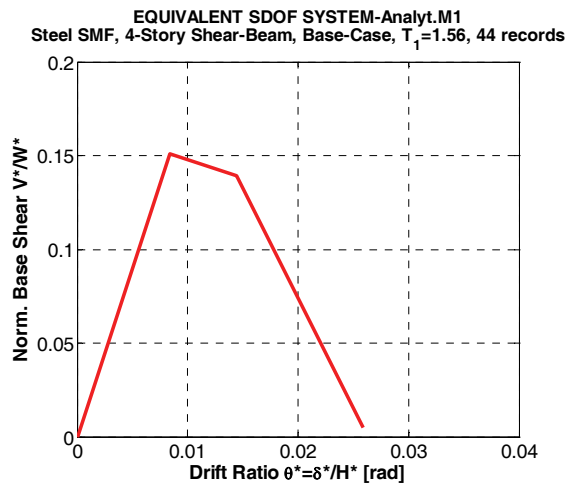
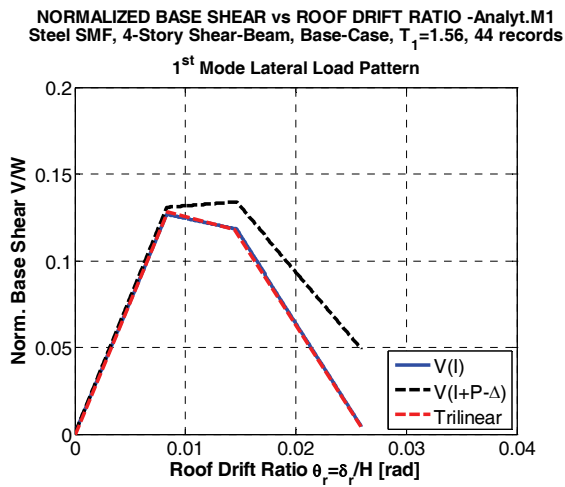


Figure A-43 System information, 4-story shear building, regular base case.



Properties of Equivalent SDOF system

Model	V_y^*/W^*	T_e [sec]	α_s	θ_p/θ_y	θ_{pc}/θ_y
Analyt.M1	0.151	1.56	-0.1513	0.724	1.429

NRHA Median and Target Roof Drift Ratios (H = 635 inches)

	NRHA Median	Analyt.M1-ASCE41	Analyt.M1-Eq.SDOF
SF = 0.5	0.0072	0.0061	0.0061 (2 collapses)
SF = 1.0	0.0133	0.0121	0.0120 (11 collapses)
SF = 2.0	0.0239	0.0242	N/A (38 collapses)

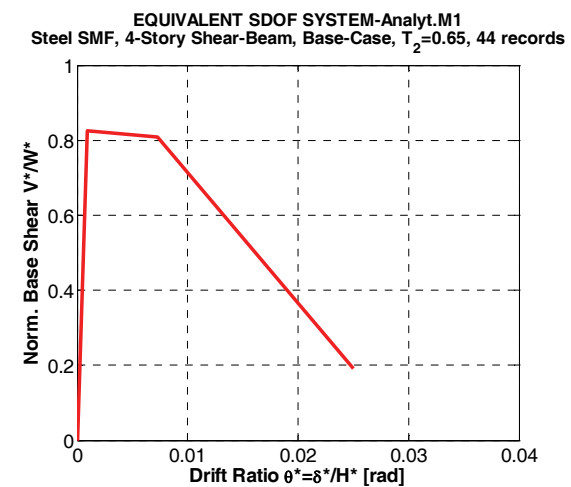
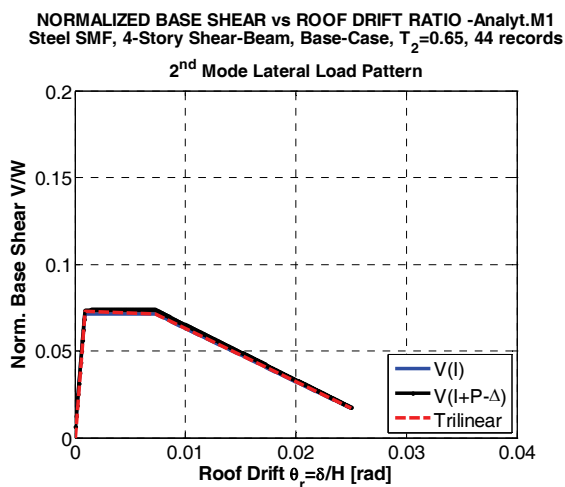


Figure A-44 System information for NSP and MPA, 4-story shear building, regular base case.

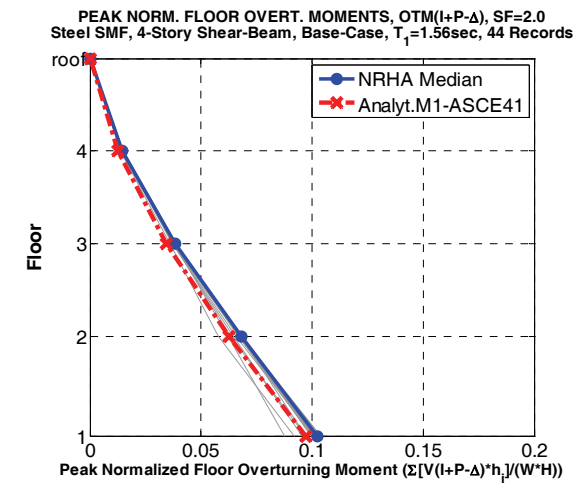
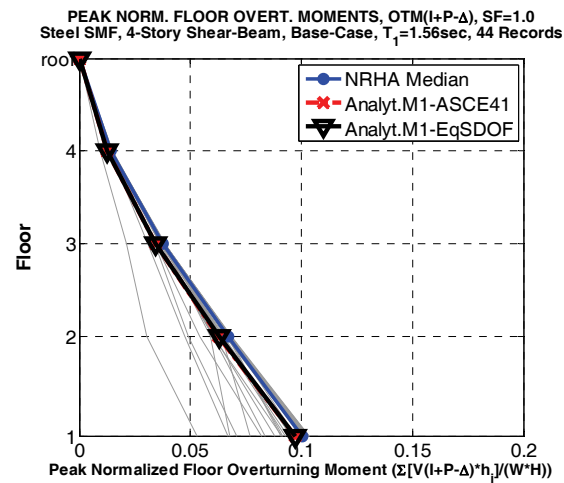
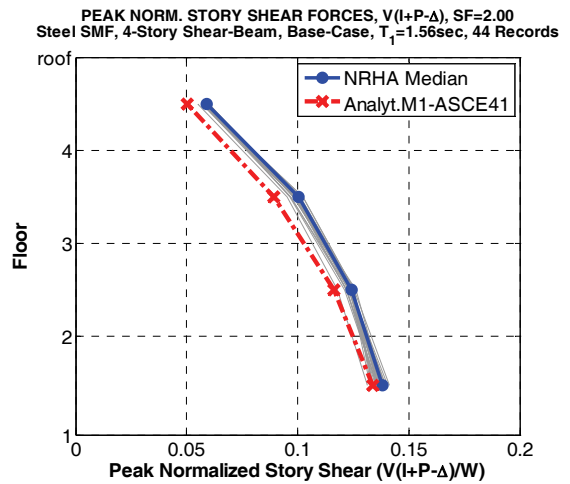
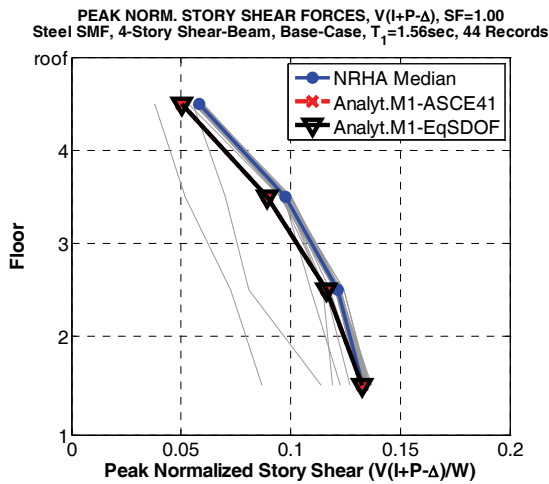
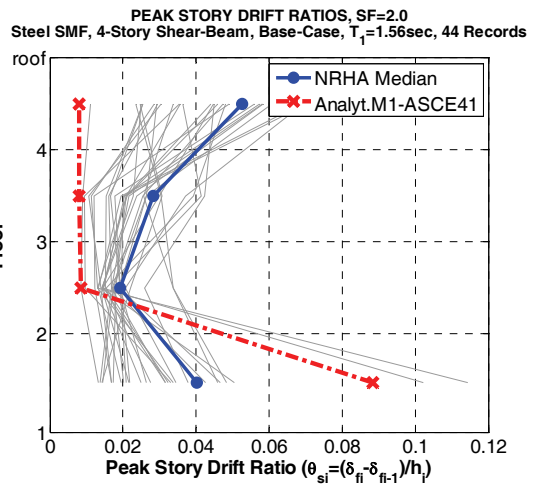
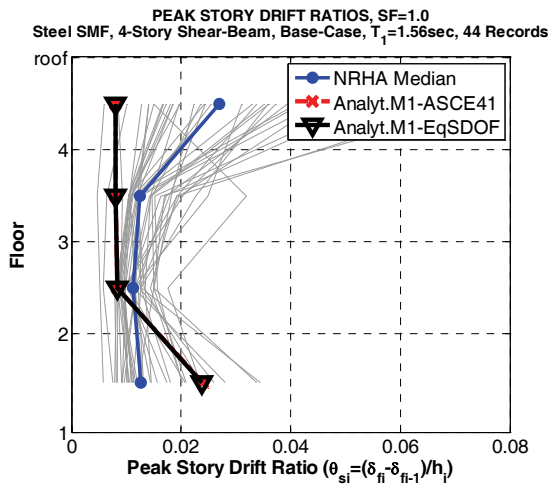


Figure A-45 NSP to NRHA comparison of story level EDPs, 4-story shear building, regular base case, SF = 1.0 and 2.0.

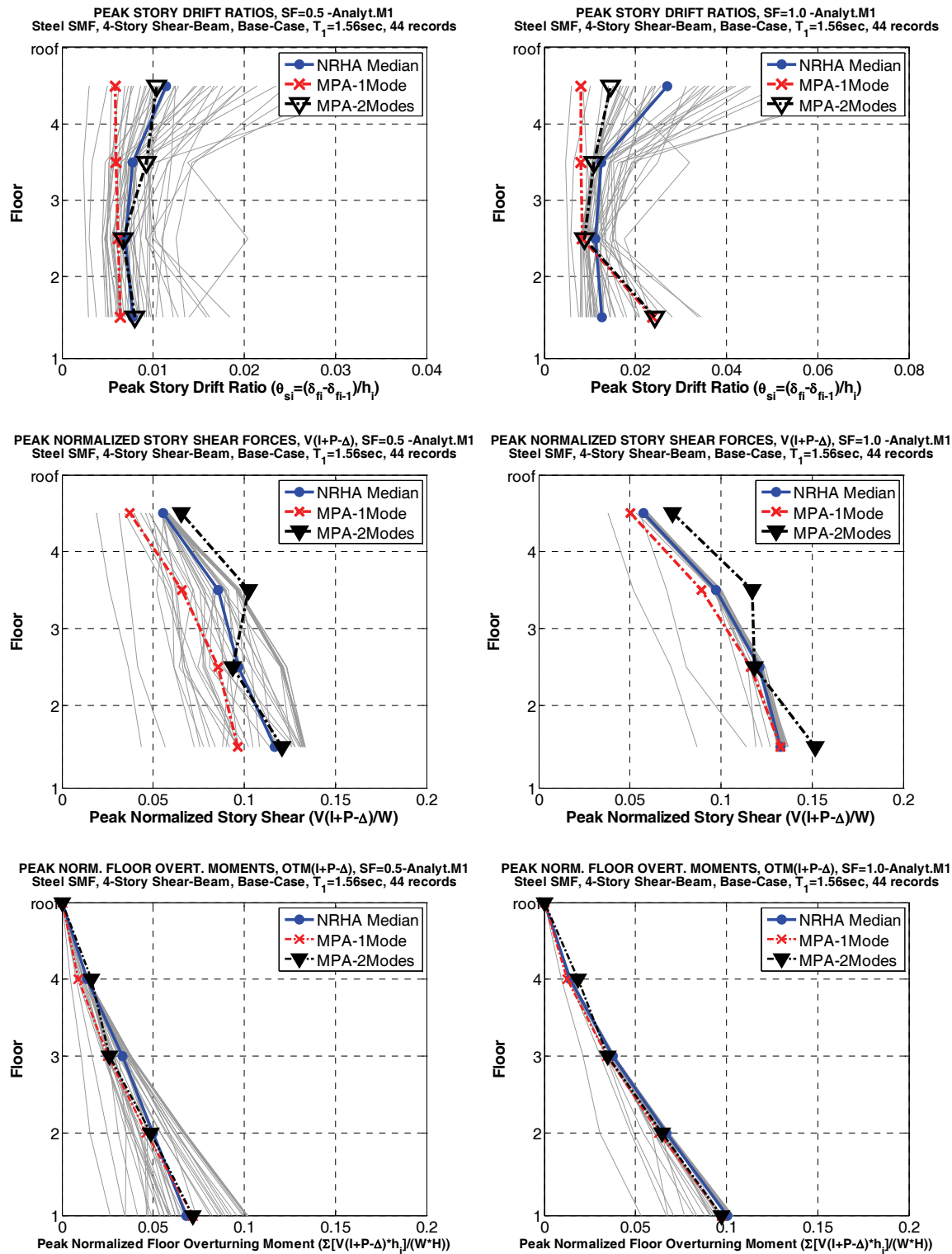


Figure A-46 MPA to NRHA comparison of story level EDPs, 4-story shear building, regular base case, SF = 0.5 and 1.0.

Seismically effective weight per frame: $W = 2,799k$

($w_1 = 714k$, $w_2 = w_3 = 708k$, $w_r = 669k$)

Story Shear Strength (Overstrength Factor in Story 1 = 2.0)

Story	V _y (kip)
4	343
3	459
2	563
1	375

Roof Drift Ratios from NRHA (H = 635 inches)

	SF=0.5	SF=1.0	SF=2.0
Median [%]	0.0066	0.0117	N/A
16th [%]	0.0047	0.0086	-
84th [%]	0.0098	0.0165	N/A
Mean μ [%]	N/A	N/A	N/A
σ [%]	N/A	N/A	N/A
CoV	N/A	N/A	N/A
Collapses	1	4	28

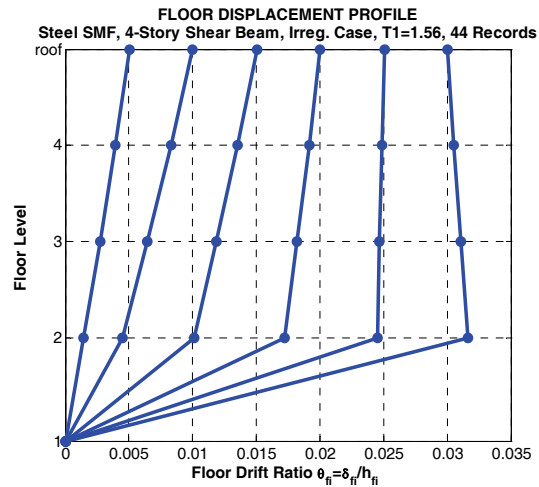
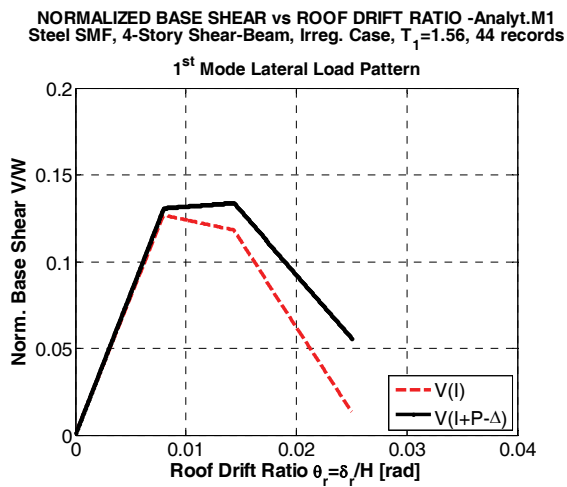
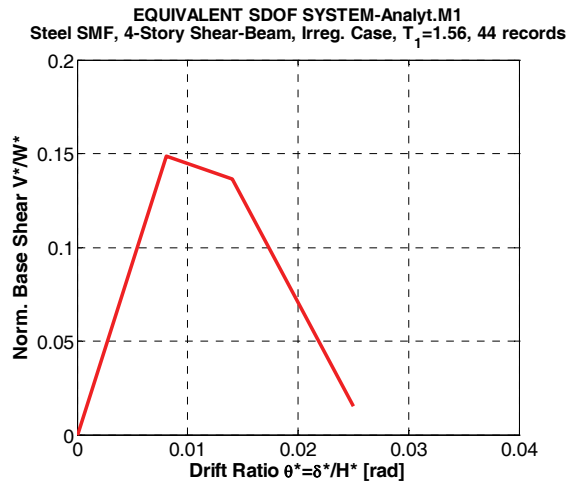
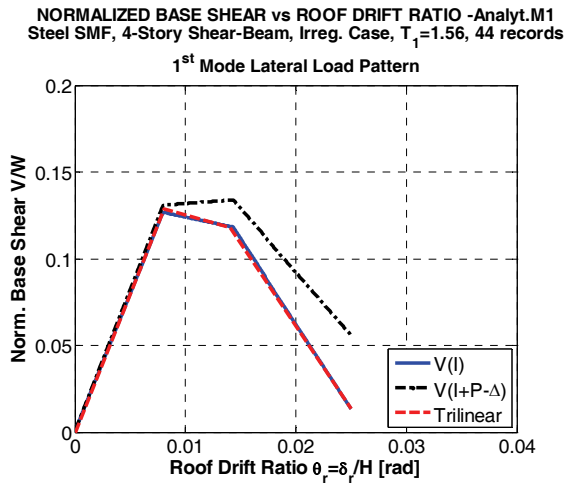


Figure A-47. System information, 4-story shear building with strength irregularity.



Properties of Equivalent SDOF system

Model	V_y^*/W^*	T_e [sec]	α_s	θ_p/θ_y	θ_{pc}/θ_y
Analyt.M1	0.149	1.56	-0.1555	0.74	1.539

NRHA Median and Target Roof Drift Ratios (H = 635 inches)

	NRHA Median	Analyt.M1-ASCE41	Analyt.M1-Eq.SDOF
SF = 0.5	0.0066	0.0060	0.0060 (2 collapses)
SF = 1.0	0.0047	0.0120	0.0120 (12 collapses)
SF = 2.0	N/A	0.0220	N/A 39 collapses

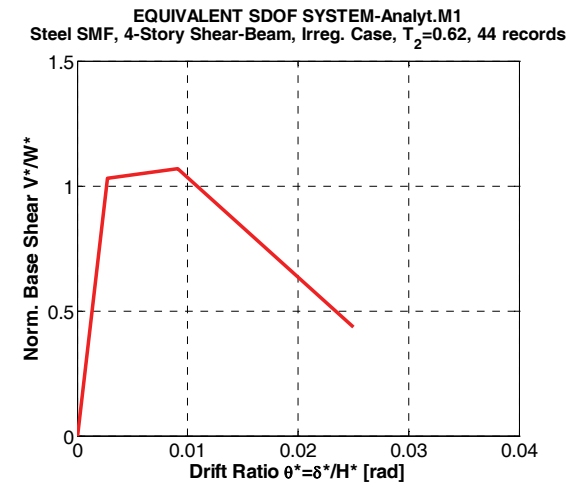
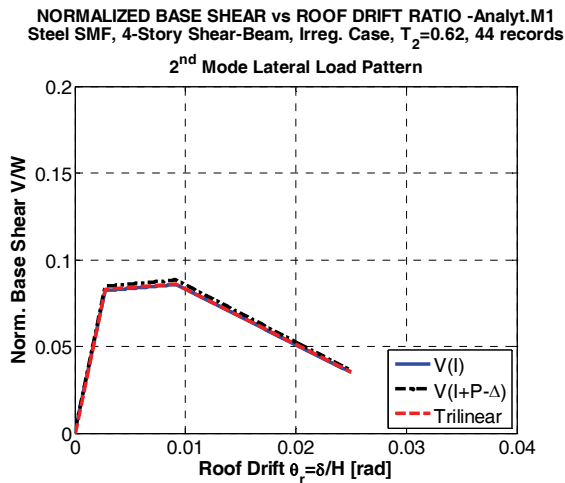


Figure A-48 System information for NSP and MPA, 4-story shear building with strength irregularity.

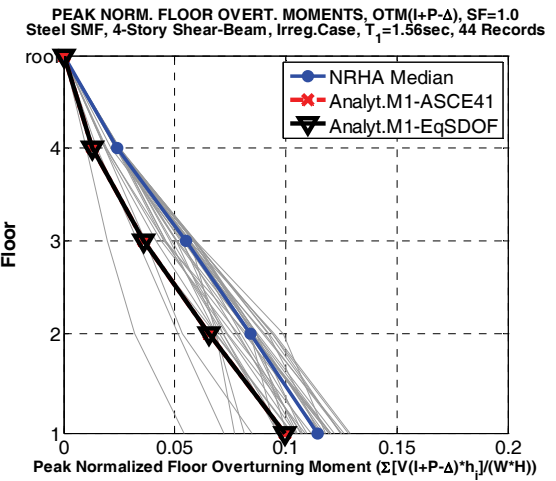
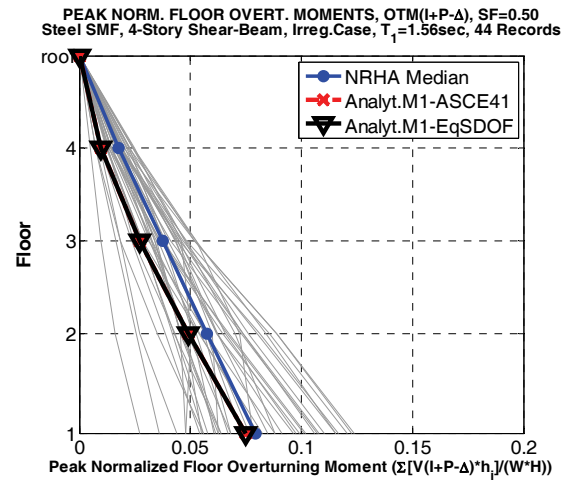
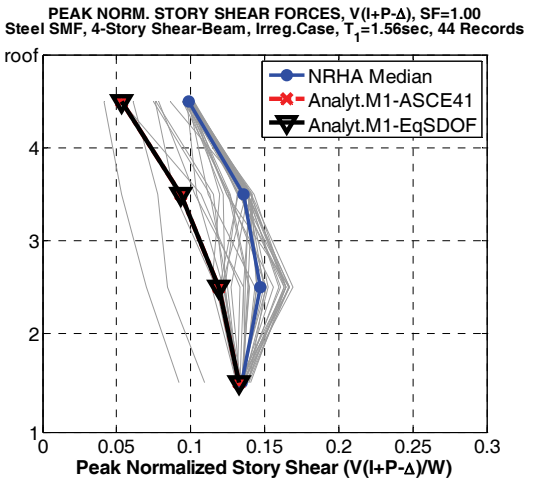
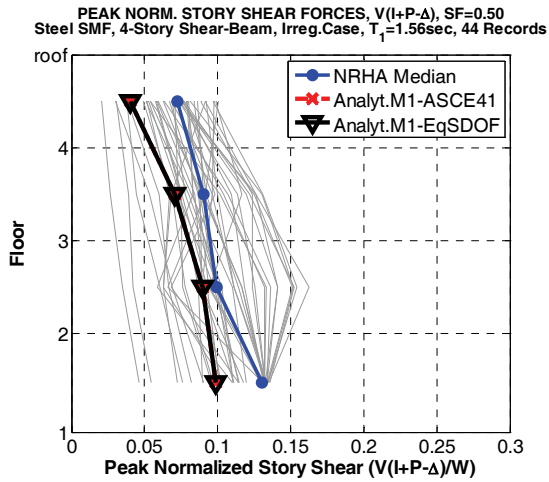
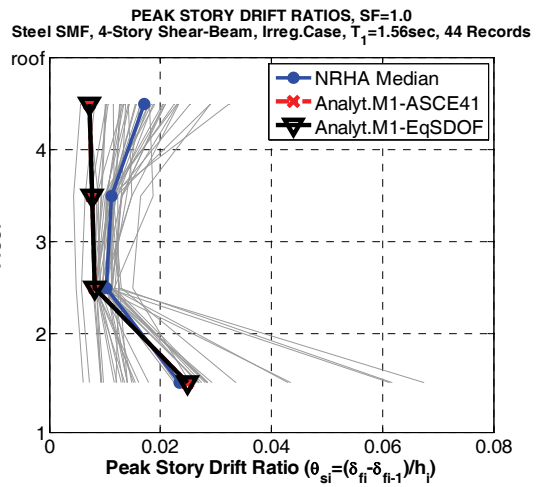
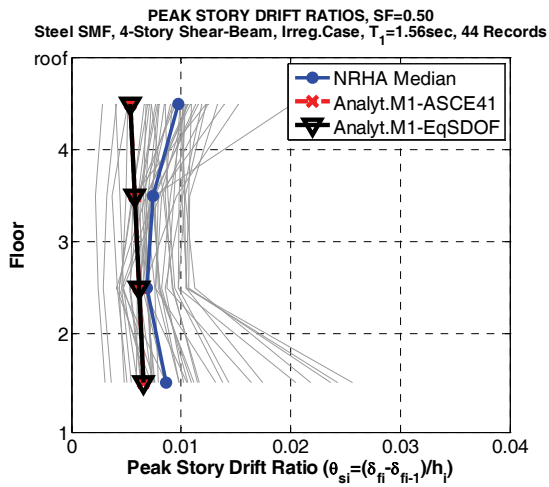


Figure A-49 NSP to NRHA comparison of story level EDPs, 4-story shear building with strength irregularity, SF = 0.5 and 1.0.

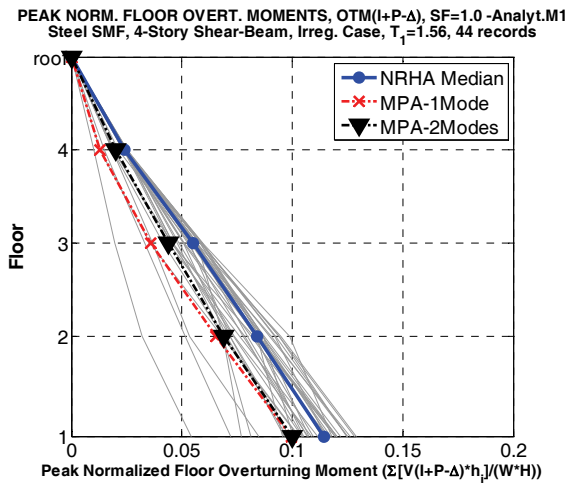
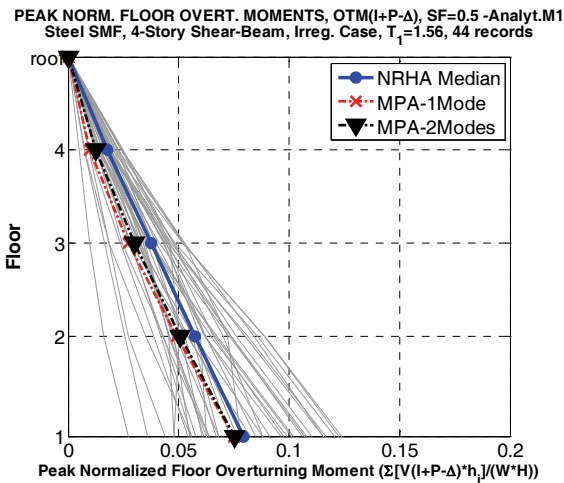
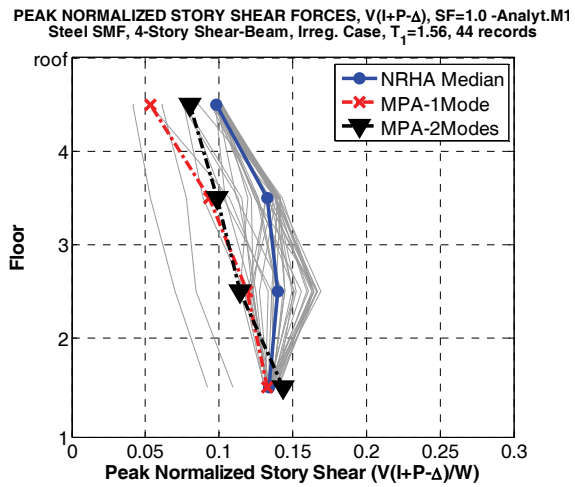
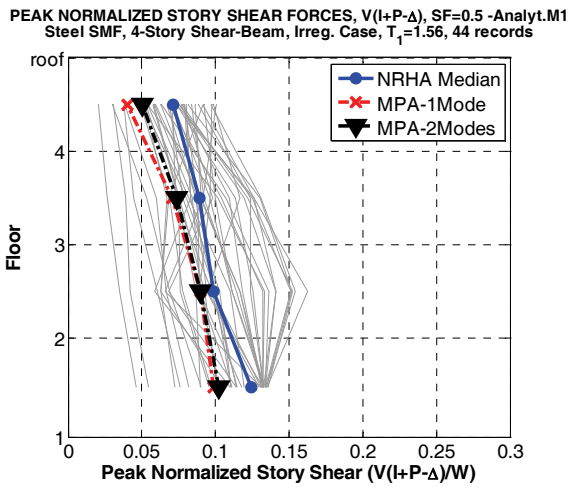
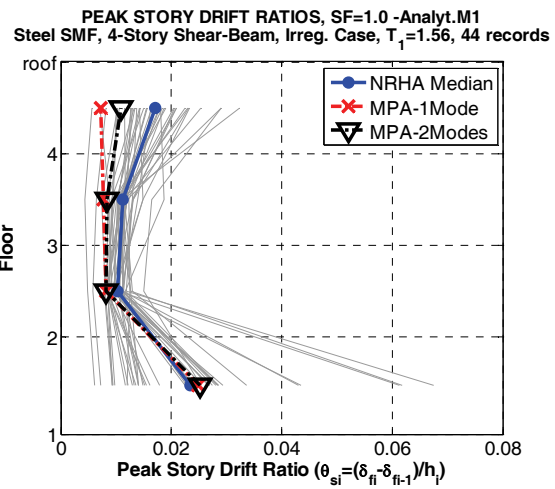
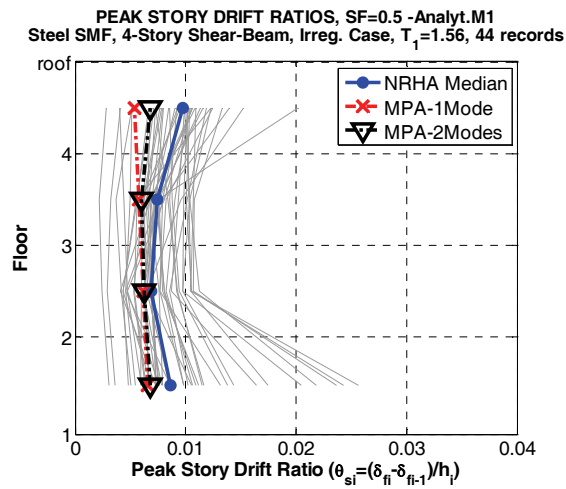


Figure A-50 MPA to NRHA comparison of story level EDPs, 4-story shear building with strength irregularity, SF = 0.5 and 1.0

Summary Observations and Conclusions on Load Pattern Sensitivity and Strength Irregularities:

- Pushover behavior of regular structures in which little or no redistribution of inelastic deformations takes place from one story to another is very sensitive to the selected load pattern. Any invariant load pattern, such as a first mode load pattern, is likely to produce misleading results. The selected static load pattern will dictate where the pushover will “detect a weak story,” whether or not such a weakness exists in reality.
- Structures of this type have story strength and stiffness properties that can be determined rather accurately from code equations or from engineering mechanics principles. If the pushover analysis indicates an irregularity that concentrates drifts in a single story, such code equations or mechanics principles should be employed to assess whether an irregularity indeed exists or whether the perception of an irregularity is created by the application of an invariant load pattern.
- If a standard pushover analysis indicates an irregularity, but this irregularity is not confirmed by a story strength and stiffness analysis, then the standard pushover should be abandoned because it has created an “artificial” irregularity caused by the selected invariant load pattern. Again, NRHA or the use of advanced adaptive pushover methods are feasible alternative.
- If an irregularity exists and it is concentrated in a single story, then the single mode nonlinear static procedure should be capable of detecting this irregularity. The story drift predictions obtained from a single mode nonlinear static analysis are expected to be reasonable for the weak story, but might be considerably off in other stories. The same observations apply to story shear and floor overturning moment.
- If irregularities exist in more than one story, then an invariant single mode static load pattern will hardly be able to detect more than the first irregularity, and therefore might lead to misleading results.
- If irregularities exist in more than one story, it is recommended to either rectify the irregularities or perform NRHA or to use advanced adaptive pushover methods that are capable of capturing these irregularity effects.
- Most of the reservations expressed here on the use of NSP apply also to the use of the MPA method.

A.8 Incorporation of Gravity System in Analysis Model

A.8.1 Potential Importance of Incorporating Gravity System in Analysis Model

Components of the gravity system must have sufficient strength and deformation capacity to resist tributary gravity loads at the maximum drifts computed for the lateral load resisting system. But it usually is left up to the engineer whether or not to include contributions of the gravity system to lateral stiffness and strength, i.e., whether or not to incorporate the gravity system in the analysis model. The general recommendation is to incorporate the gravity system because the analysis might expose weaknesses that are not evident from inspection. An incentive for incorporating the gravity system is its potential benefit in decreasing drift demands and collapse capacity. This might be particularly attractive if the pushover curve exhibits an early negative tangent stiffness that may lead to large displacement amplification or even collapse. The negative stiffness will be reduced potentially by incorporating the gravity system or might even turn into a positive stiffness.

If strength and deformation capacity of individual components of the gravity system are not of concern, a simple way to incorporate the gravity framing is by means of a fishbone arrangement of the type shown in the right part of Figure A-3. An arrangement with two half-beams is preferred because it prevents accumulation of a large axial force in the spine (column) of the fishbone. In this arrangement all beams are lumped into a single beam (I/L of beam = $\sum EI_i/L_i$ of all beams), all columns are lumped into a single column (I of column = $\sum I_j$ of all columns), and all gravity connections are lumped into two connections represented by rotational springs.

Beams can be represented usually by elastic elements, provided the connections of beams to columns are weaker than the beams. Column bending strength should include the effects of tributary axial forces due to gravity loads. Column splice locations should be represented by additional nodes if the bending strength at these locations is a potential weakness. Post-yield properties of the columns should be based on average plastic hinge properties of the column sections. Modeling of connection strength and stiffness is often a challenge, and should be done conservatively as illustrated in the example discussed in the next section.

A.8.2 Case Study - 4-Story Steel Moment Frame Structure

A preliminary design of the gravity beams and columns for this structure was performed using tributary areas deduced from the plan view shown in Figure A-1, and strength and stiffness properties of these elements was estimated as discussed in the previous section. Since only half of the structure is modeled, the spine (column) of the fishbone represents 6 gravity columns and four moment frame columns bending about the weak axis. The beam represents 7 gravity beams.

Connection properties were estimated from procedures and tests summarized in Liu and Astaneh-Asl (2004). Behavior of a typical steel shear tab connection is shown in Figure A-51. Because of the complex behavior of these connections, greatly simplified and generally conservative models need to be employed. In the case illustrated the simple elastic-perfectly plastic spring model superimposed on the experimental results is used. The yield rotation for this spring is 0.008, which is about the same as the yield rotations of the beams of the moment frame. Pre-capping plastic rotation θ_p is 0.10 and post-capping θ_{pc} is assumed as 0.15. The yield strength is a compromise between positive and negative strength values that can be sustained at very large inelastic rotations. This model ignores the additional strength at relatively small rotations. This example is only for illustration, and no specific recommendations for modeling of shear tab connections are made here.

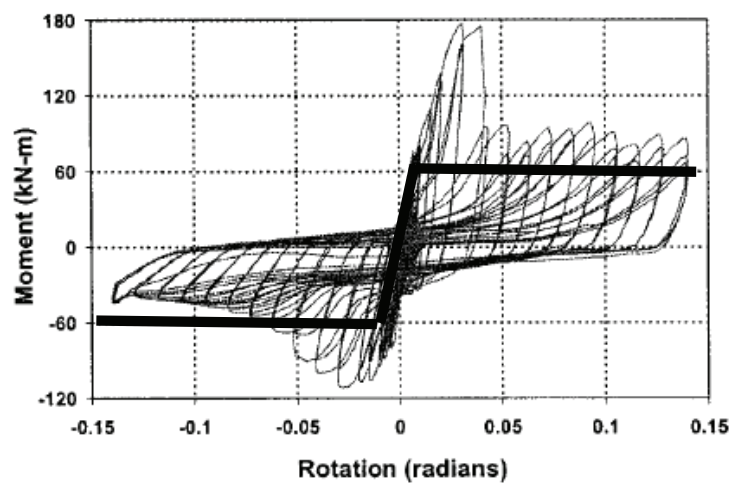


Figure A-51 Moment-rotation relationship for a shear tab connection with slab (Liu and Astaneh-Asl, 2004).

Pushover diagrams for the structure with gravity system included, and a comparison of pushovers without and with gravity system are presented in Figure A-52. As the right graph shows, in this example not much is gained in the pushover strength and deformation capacity by incorporating the gravity system in the analysis model.

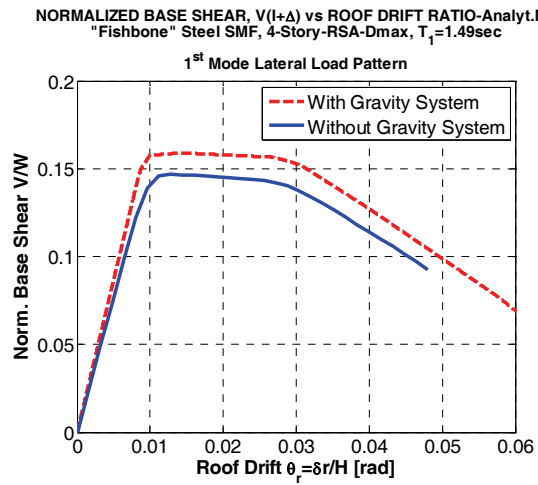
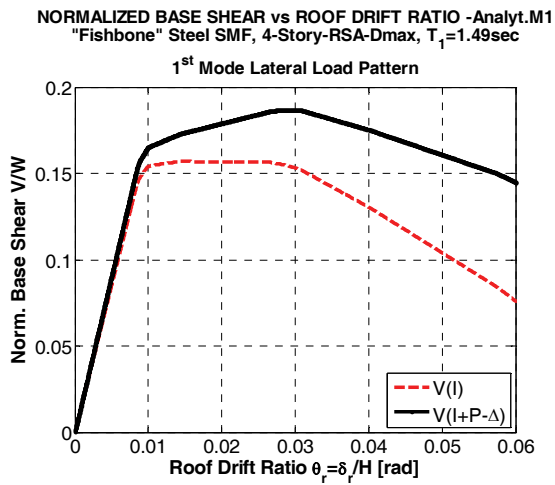


Figure A-52 Pushover curves (a) V_I and $V_{I+P-\Delta}$ vs. roof drift for 4-story steel SMF with gravity system included, (b) comparison of V_I vs. roof drift pushovers without and with gravity system.

The small gain when incorporating the gravity system in this example is seen also in Figures A-53 and A-54, which show NRHA and NSP results for ground motion scale factors $SF = 2.0$ and 3.0 . The gain is inconsequential for $SF = 2.0$. For $SF = 3.0$ maximum response is mostly in the negative tangent stiffness region. In this case incorporation of the gravity system reduces the median roof drift from 0.049 to 0.034 , and reduces the number of collapses from 22 to 11 .

The observations made here are specific to the single structure evaluated. The benefit gained from incorporating the gravity system may depend strongly on the structural configuration. The example presented here serves only as illustration of the process.

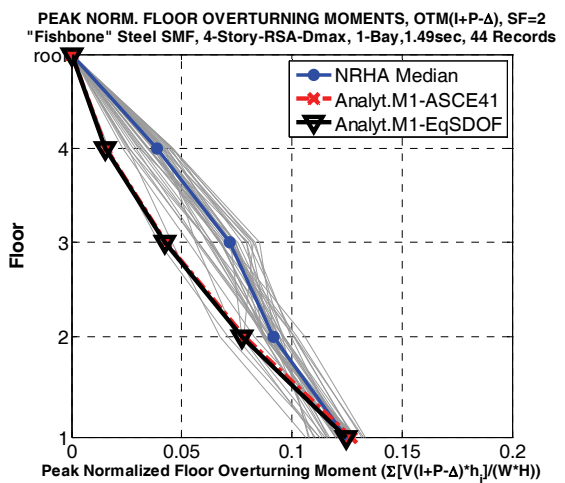
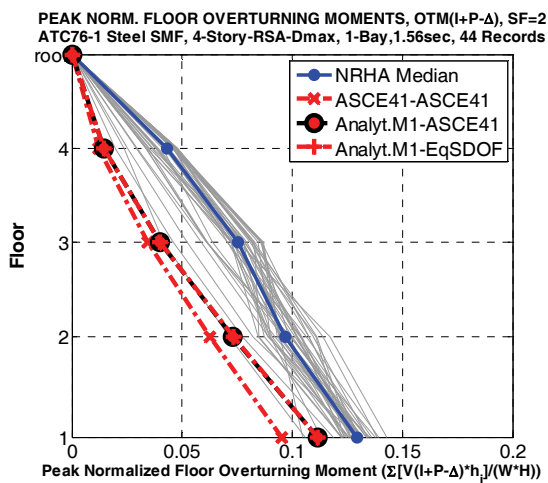
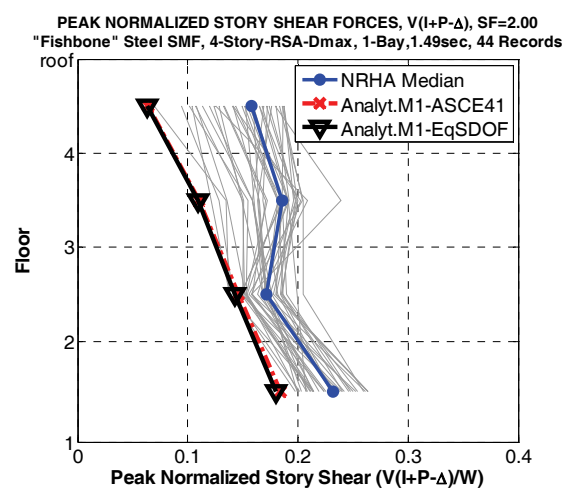
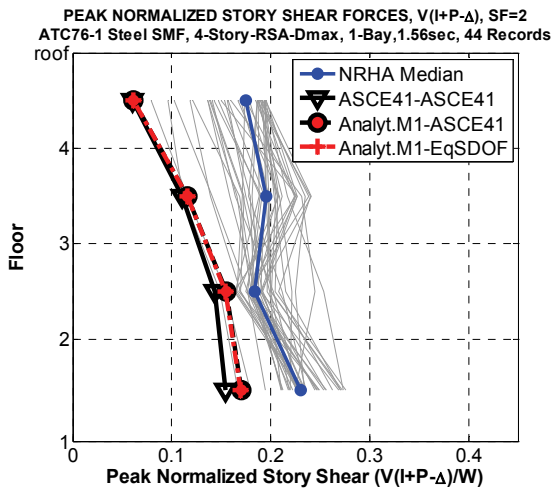
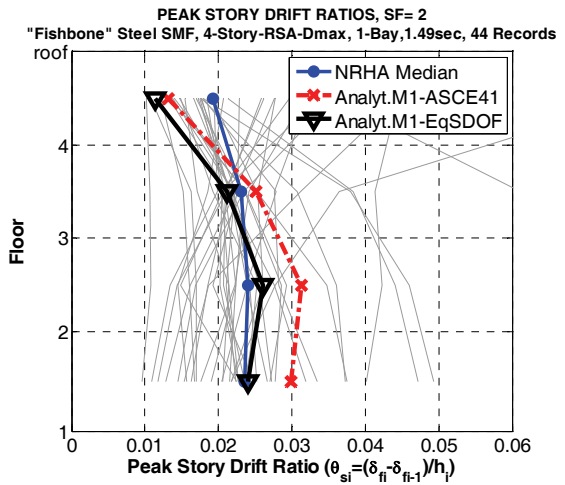
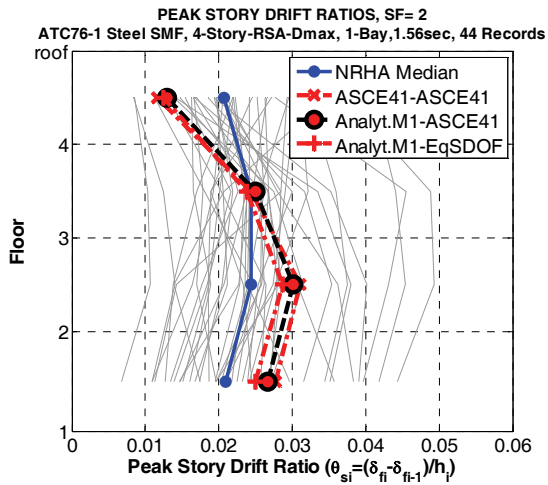


Figure A-53 Comparison of NRHA and NSP predictions between models without (left) and with gravity system 4-story steel SMF, SF = 2.

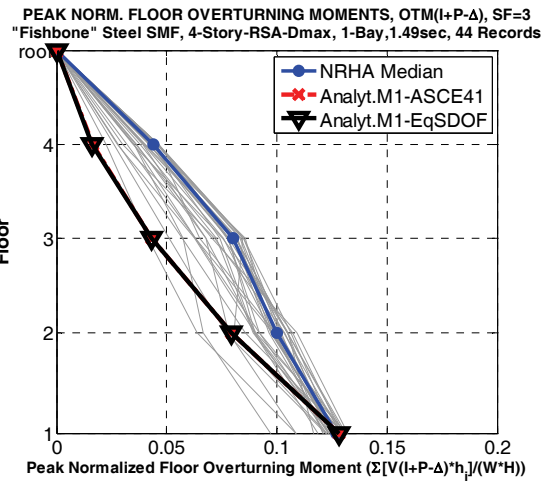
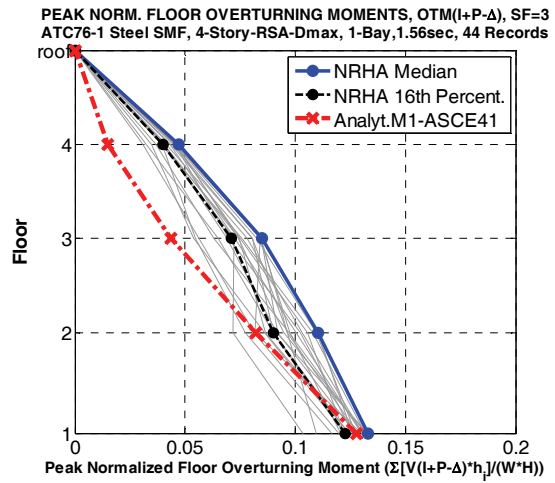
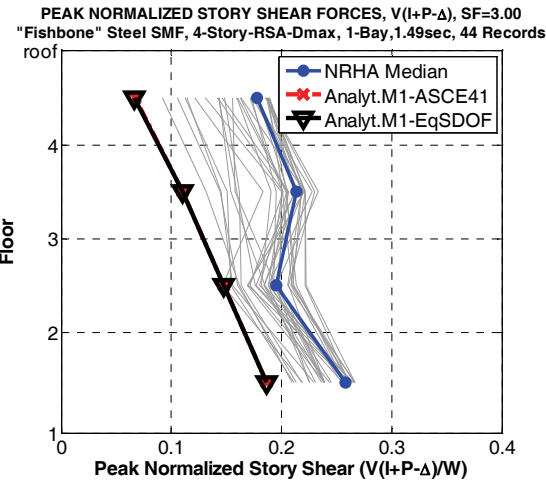
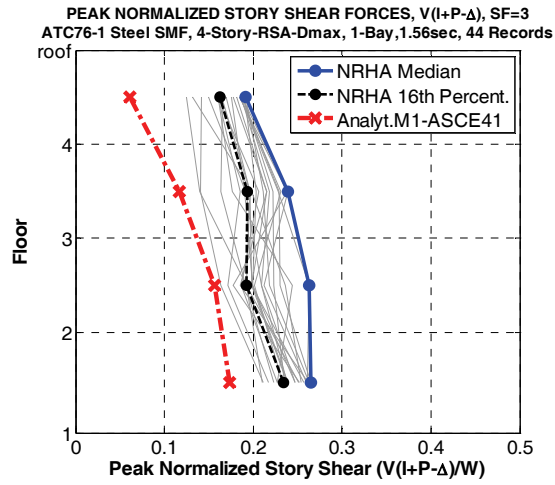
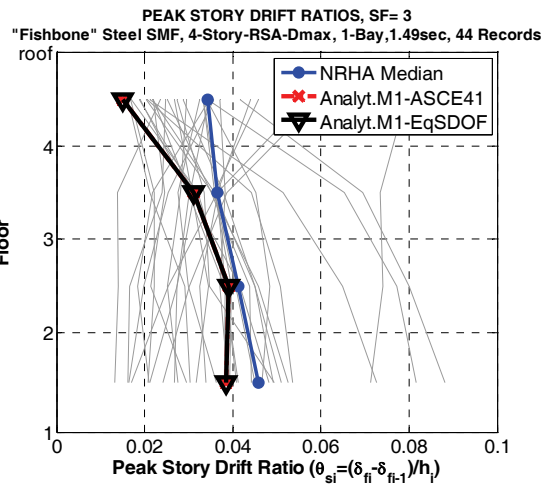
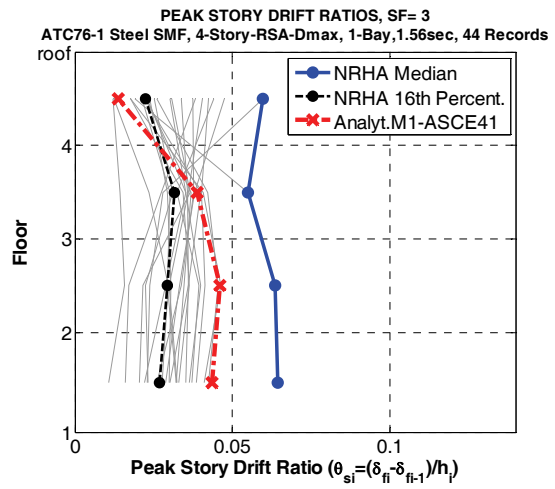


Figure A-54 Comparison of NRHA and NSP predictions between models without (left) and with gravity system, 4-story steel SMF, SF = 3.

Detailed Reinforced Concrete Moment Frame Studies

This appendix presents results of problem-focused studies on nonlinear response of reinforced concrete moment frame structures. Nonlinear response history analysis is performed using the FEMA P-695 far-field ground motion set, and various single-mode and multiple-mode nonlinear static analysis procedures are evaluated. Various 2-, 4-, and 8-story reinforced concrete moment-resisting frame archetypes are utilized. Peak values of floor displacement, story drift ratio, story shear force, and floor overturning moment are evaluated.

B.1 Ground Motions

Nonlinear Response History Analysis (NRHA) was performed using the suite of 44 ground motion records utilized in the FEMA P-695, *Quantification of Seismic Performance Factors* (FEMA, 2009b), far-field data set. The ground motions were normalized on the basis of the elastic design spectrum as discussed in FEMA P-695 with scale factors (SF) equal to 0.5, 1.0 and 2.0 applied subsequently. For Nonlinear Static Procedures (NSP) the mean 5%-damped response spectrum of the NRHA scaled record set was used.

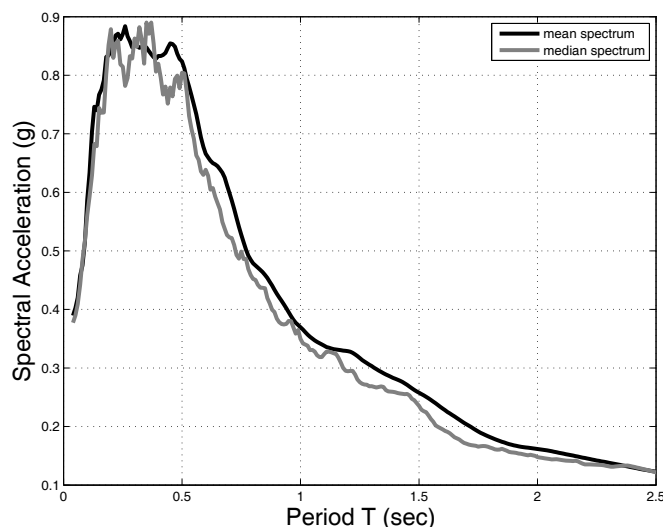


Figure B-1 5%-damped unscaled mean and median response spectra.

B.2 Structural Systems

The structural systems considered are a two-story, three-bay (2-story RCMF), a four-story, three-bay (4-story RCMF) and an eight-story, three-bay (8-story RCMF) reinforced concrete moment frame building. The archetype models have ID numbers 1001, 1010, 1012 according to FEMA P-695 notation, where their detailed description can be found. In brief, the buildings considered are special reinforced concrete moment frames, designed according to the 2003 International Building Code (ICC, 2003). The member sizes have been determined by minimum size requirements and column-beam compatibility, in addition to joint shear requirements. The column strengths were determined on the basis of the strong-column-weak-beam (SCWB) philosophy. The selection of the beam stirrups was controlled by shear capacity design, while for the columns the transverse reinforcement was chosen to ensure capacity design and satisfy confinement requirements.

The models incorporate one-dimensional line-type elements. Component models are used to simulate the nonlinear degrading response of beams, columns and joints. The component models are discussed in FEMA P-695 and Ibarra et al. (2005). The models do not take into consideration shear failure, meaning that the shear capacities are not represented in the structural models. The flexural strengths of the component models were established based on the expected axial load ratio of each column according to the $1.05(\text{Dead Load}) + 0.25(\text{Live Load})$ loading case and remained constant throughout the loading history. An additional leaning column element is also used to capture P-delta effects caused by the gravity load on the internal gravity frames. Rayleigh damping is defined for all beams and all columns, but not for the joints. To compensate for the reduction in damping in the joints, the stiffness proportional damping coefficients were increased by 10%.

The modal properties of the three RCMF frame models are listed in the tables that follow (Table B-1, B-2 and B-3). Figure B-1 shows the modes of the buildings.

Table B-1 Modal Properties for the 2-story RCMF

	Mode 1	Mode 2
T_1	0.625 (sec)	0.182 (sec)
L_n	0.958	-0.328
Γ_n	1.177	-0.1610
M_n	0.814	2.033
M_n^*	1.128	0.0527
M_n^*/Weight	94.04%	4.39%
Height (H)	336 (in)	
Story mass (constant)	0.60 (k-s-s/in)	
Total Weight	463.68 (k)	

Table B-2 Modal Properties for the 4-story RCMF

	Mode 1	Mode 2	Mode 3
T_1	0.855 (s)	0.27 (s)	0.146 (s)
L_n	3.81	-1.23	0.84
Γ_n	1.25	-0.328	0.13
M_n	3.03	3.766	6.40
M_n^*	4.77	0.41	0.11
$M_n^*/Weight$	89.06 %	7.56%	2.08%
Height (H)		648 (in)	
Story mass (constant)		1.34 (k-s-s/in)	
Total Weight		2071.1 (k)	

Table B-3 Modal Properties for the 8-story RCMF

	Mode 1	Mode 2	Mode 3
T_1	1.80 (s)	0.60 (s)	0.34 (s)
L_n	3.23	-1.07	0.65
Γ_n	1.27	-0.40	0.22
M_n	2.53	2.68	2.99
M_n^*	4.12	0.43	0.14
$M_n^*/Weight$	85.75%	8.9%	2.92%
Height (H)		1272 (in)	
Story mass (constant)		0.60 (k-s-s/in)	
Total Weight		1854.7 (k)	

Table B-4 Eigenmodes of the 2-Story RCMF

1st mode	0.5978, 1.0000
2nd mode	-1.5453, 1.0000

Table B-5 Eigenmodes of the 4-Story RCMF

1st mode	0.3443, 0.6316, 0.8646, 1.0000
2nd mode	-0.9486, -0.954, -0.0192, 1.0000
3rd mode	1.3662, -0.4185, -1.3175, 1.0000

Table B-6 Eigenmodes of the 8-Story RCMF

1st mode	0.193, 0.3628, 0.520, 0.6612, 0.7886, 0.8910, 0.9617, 1.0000
2nd mode	-0.5591, -0.9090, -1.0045, -0.8175, -0.3756, 0.1845, 0.6890, 1.0000
3rd mode	0.8791, 1.0090, 0.3770, -0.5415, -1.0740, -0.7508, 0.1800, 1.0000

B.3 Nonlinear Static Procedures

B.3.1 ASCE/SEI 41-06 Displacement Coefficient Method

The target displacement is calculated as:

$$\delta_t = C_0 C_1 C_2 S_a \frac{T_e^2}{4\pi^2} \quad (\text{B-1})$$

where C_0 is considered as in ASCE/SEI 41-06 Section 3.3.3.2 and is here taken equal to the modal participation factor of the equivalent SDOF system. The C_1 coefficient is obtained with the relationship:

$$C_1 = 1 + \frac{R-1}{aT_e^2} \quad (\text{B-2})$$

where R has been taken as:

$$R = C_m S_a \left(\frac{W/g}{F_y} \right) \geq 1 \quad (\text{B-3})$$

In Equation B-2, we assume: $a = 130$ for site class B (FEMA 440: $a = 130, 90, 60$ for site class B, C, D, respectively).

If $T < 0.2\text{s}$, $C_1 = 0.2$.

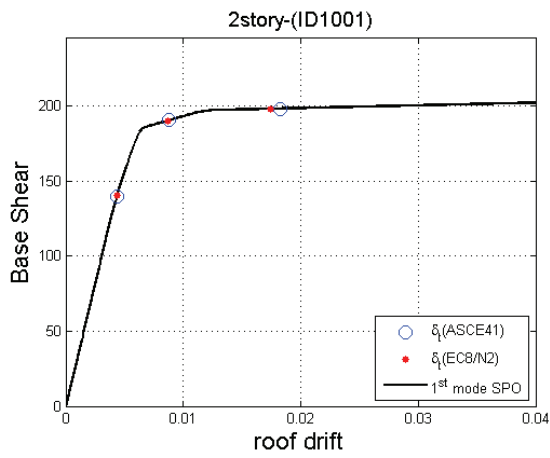
C_m of Equation B-3 is considered equal to the modal mass participation ratio M_n^*/W .

The coefficient C_2 is calculated with the formula in ASCE/SEI 41-06:

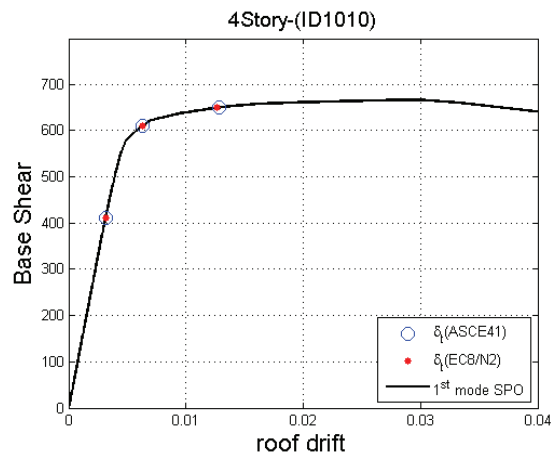
$$C_2 = 1 + \frac{1}{800} \left(\frac{R-1}{T_e} \right)^2 \quad (\text{B-4})$$

If $T < 0.2\text{s}$, $C_2 = 0.2$, and $C_2 = 1$ for $T > 0.7\text{s}$.

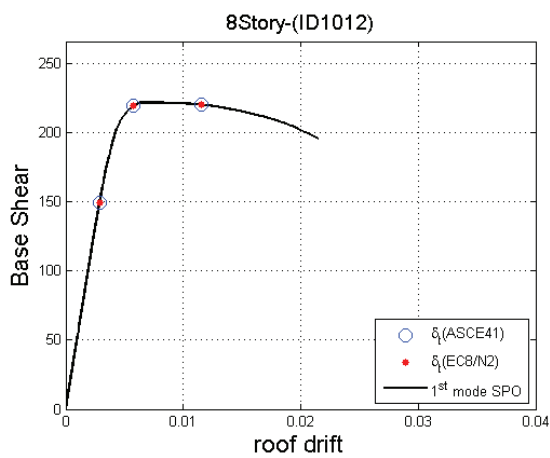
The buildings are pushed with a first-mode lateral load pattern according to ASCE/SEI 41-06. Table B-7, Table B-8, and Table B-9 show the calculations of the displacement coefficient method (Equations B-1 through B-4) for the three buildings. The calculations for higher modes for the three intensity levels are also shown, since they are required for the multi-modal nonlinear static methods and the direct determination of the target displacements with ESDOF systems (Appendix E). According to the tables and the figures that follow, all three buildings remain linear elastic for the first intensity level (SF = 0.5), are about at yield for the second level (SF = 1.0) and are well in the inelastic range for the third level (SF = 2.0).



(a)



(b)



(c)

Figure B-2 Capacity curves of the nonlinear static procedures. The target displacements according to the ASCE/SEI 41-06 displacement coefficient method and the N2/EC8 method (section B.1.4) are shown. (a) 2-story RCMF, (b) 4-story RCMF, (c) 8-story RCMF.

Table B-7 R-C₁-T Calculations for the 2-Story RCMF

Scale Factor=0.5	Mode 1	Mode 2
D _y / H	0.0058	0.0018
F _y (kip)	195.7	114.7
T _e (s)	0.625	0.182
S _a (g)	0.32	0.416
C ₀	1.177	abs(-0.161)
C _m	0.94	0.0439
R	max(0.72,1)=1	max(0.074,1)=1
C ₁	1	1
C ₂	1	1
C ₃	1	1
(T ² /4π ²) S _a (in)	1.24	0.134
δ _t (in)	1.4668	0.0217
V _t (kip)	142.89	4.88
Scale Factor=1	Mode 1	Mode 2
D _y / H	0.0058	0.0018
F _y (kip)	195.7	114.7
T _e (s)	0.625	0.182
S _a (g)	0.65	0.8318
C ₀	1.177	abs(-0.161)
C _m	0.94	0.0439
R	1.450	max(0.15, 1)=1
C ₁	1.01	1
C ₂	1.0007	1
C ₃	1	1
(T ² /4π ²) S _a (in)	2.49	0.269
δ _t (in)	2.9616	0.0433
V _t (kip)	190.74	9.77
Scale Factor=2	Mode 1	Mode 2
D _y / H	0.0058	0.0018
F _y (kip)	195.7	114.7
T _e (s)	0.625	0.182
S _a (g)	1.30	1.66
C ₀	1.177	abs(-0.161)
C _m	0.94	0.0439
R	2.904	max(0.3, 1) =1
C ₁	1.037	1
C ₂	1.0116	1
C ₃	1	1
(T ² /4π ²) S _a (in)	4.98	0.538
δ _t (in)	6.1580	0.0867
V _t (kip)	198.23	21.98

Table B-8 R-C₁-T Calculations for the 4-Story RCMF

Scale Factor=0.5	Mode 1	Mode 2	Mode 3
D _y / H	0.0046	0.0013	0.0008
F _y (kip)	629.12	441.68	310.06
T _e (s)	0.85	0.27	0.146
S _a (g)	0.23	0.432	0.378
C ₀	1.254	abs(-0.328)	0.132
C _m	0.89	0.0756	0.0208
R	max(1, 0.66)=1	max(1, 0.153)=1	max(1, 0.053)=1
C ₁	1	1	1
C ₂	1	1	1
C ₃	1	1	1
(T ² /4π ²) S _a (in)	1.632	0.315	0.0794
δ _t (in)	2.0469	0.1034	0.0105
V _t (kip)	420.6500	54.40	7.68
Scale Factor=1	Mode 1	Mode 2	Mode 3
D _y / H	0.0046	0.0013	0.0008
F _y (kip)	629.12	441.68	310.06
T _e (s)	0.85	0.27	0.146
S _a (g)	0.45	0.864	0.757
C ₀	1.254	abs(-0.328)	0.132
C _m	0.89	0.0756	0.0208
R	1.338	max(0.306,1)=1	max(0.105,1)=1
C ₁	1.0036	1	1
C ₂	1	1	1
C ₃	1	1	1
(T ² /4π ²) S _a (in)	3.264	0.63	0.158
δ _t (in)	4.108	0.207	0.0209
V _t (kip)	611.7360	114.24	15.36
Scale Factor=2	Mode 1	Mode 2	Mode 3
D _y / H	0.0046	0.0013	0.0008
F _y (kip)	629.12	441.68	310.06
T _e (s)	0.85	0.27	0.146
S _a (g)	0.91	1.73	1.514
C ₀	1.254	abs(-0.328)	0.132
C _m	0.89	0.0756	0.0208
R	2.66	max(0.612,1)=1	max(0.21,1)=1
C ₁	1.0177	1	1
C ₂	1	1	1
C ₃	1	1	1
(T ² /4π ²) S _a (in)	6.53	1.261	0.317
δ _t (in)	8.33	0.4137	0.0419
V _t (kip)	649.7600	221.48	30.72

Table B-9 R-C₁-T Calculations for the 8-Story RCMF

Scale Factor=0.5	Mode 1	Mode 2	Mode 3
D _y / H	0.0040	0.0013	0.0004
F_y (kip)	214.59	197.86	99.41
T _e (s)	1.80	0.60	0.34
S _a (g)	0.09	0.33	0.42
C ₀	1.27	abs(-0.40)	0.21
C _m	0.85	0.09	0.03
R	1	max(1, 0.28)=1	max(1,0.23)=1
C ₁	1	1	1
C ₂	1	1	1
C ₃	1	1	1
(T ² /4π ²) S _a (in)	2.88	1.167	0.48
δ _t (in)	3.67	0.46	0.105
V _t (kip)	149.46	54.51	20.44
Scale Factor=1	Mode 1	Mode 2	Mode 3
D _y / H	0.0040	0.0013	0.0004
F _y (kip)	214.59	197.86	99.41
T _e (s)	1.80	0.60	0.34
S _a (g)	0.18	0.67	0.85
C ₀	1.27	abs(-0.40)	0.21
C _m	0.85	0.09	0.03
R	1.35	max(0.56,1)=1	max(0.46,1)=1
C ₁	1	1	1
C ₂	1	1	1
C ₃	1	1	1
(T ² /4π ²) S _a (in)	5.76	2.33	0.965
δ _t (in)	7.35	0.93	0.209
V _t (kip)	219.28	100.69	40.87
Scale Factor=2	Mode 1	Mode 2	Mode 3
D _y / H	0.0040	0.0013	0.0004
F _y (kip)	214.59	197.86	99.41
T _e (s)	1.80	0.60	0.34
S _a (g)	0.36	1.34	1.70
C ₀	1.27	abs(-0.40)	0.21
C _m	0.85	0.09	0.03
R	2.35	1.13	max(0.92,1)=1
C ₁	1	1.003	1
C ₂	1	1.0001	1
C ₃	1	1	1
(T ² /4π ²) S _a (in)	11.52	4.67	1.93
δ _t (in)	14.7	1.88	0.418
V _t (kip)	220.13	146.52	79.89

Comparative results of the ASCE/SEI 41-06 approach versus the results of NRHA are shown in the figures that follow. The comparison is performed with respect to the following Engineering Demand Parameters (EDP):

- peak story displacements,
- peak story drift,
- peak story shears,
- peak story overturning moments.

Summary of Observations:

For the 2- and the 4-story buildings close estimates for the peak story displacements and the peak story drifts are obtained. The story drift is slightly underestimated for the top story of the 4-story RCMF. For the 8-story frame, the story drift estimates are accurate for the lower stories, where the maximum drift values occur, but the drifts at the top stories are underestimated. For SF = 2, the drift estimate is erroneous even for the low stories.

Regarding story shears, for elastic, nearly-elastic limit-states (SF = 0.5 and 1) good estimates are obtained for the lower stories, while story shears are consistently underestimated for the top stories. When the buildings deform in the inelastic range (SF = 2), loss of accuracy is observed also in the lower stories.

The dispersion of peak story overturning moments is decreased as the intensity level increases and is practically very small for SF = 2. A small loss of accuracy is observed for SF = 2, possibly related to inaccuracies in the estimate of story shears.

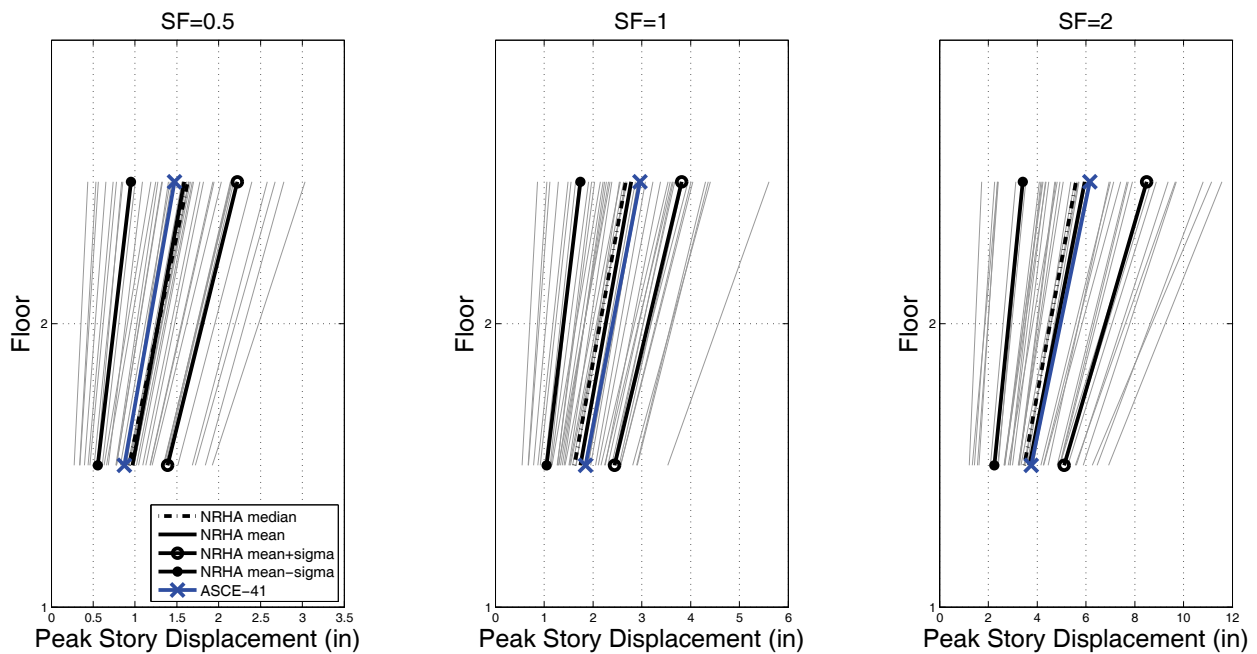


Figure B-3 2-story RCMF: NRHA versus ASCE/SEI 41-06 displacement coefficient method, peak story displacement.

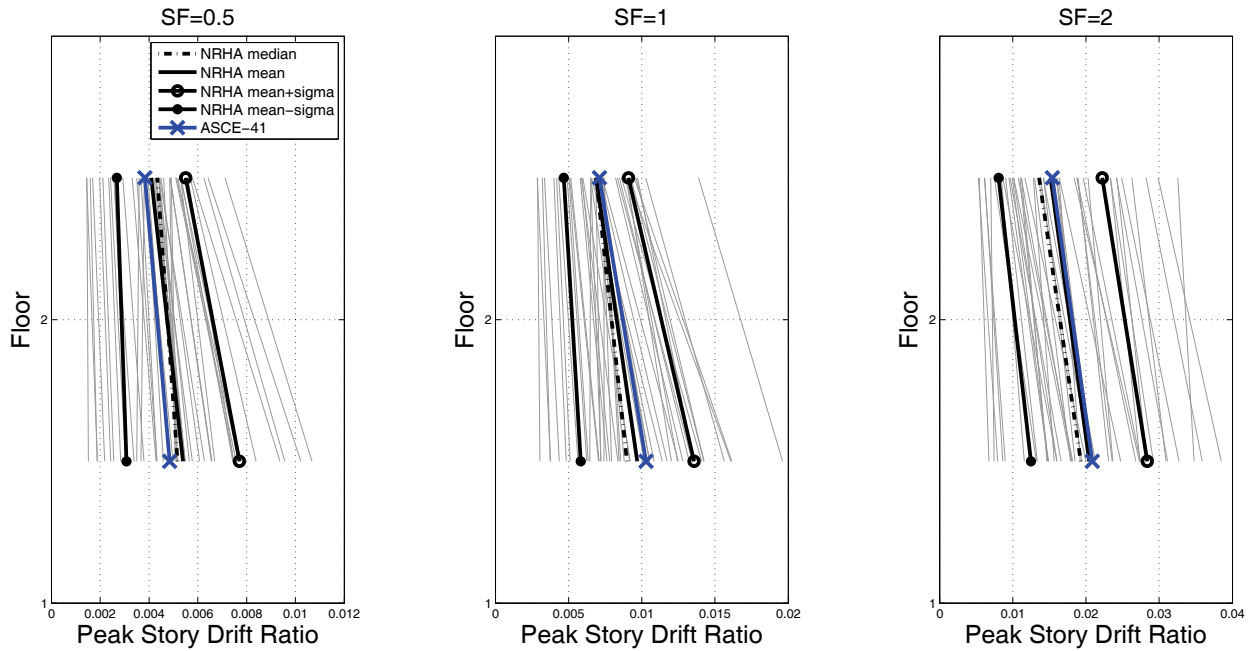


Figure B-4 2-story RCMF: NRHA versus ASCE/SEI 41-06 displacement coefficient method, peak story drift ratio.

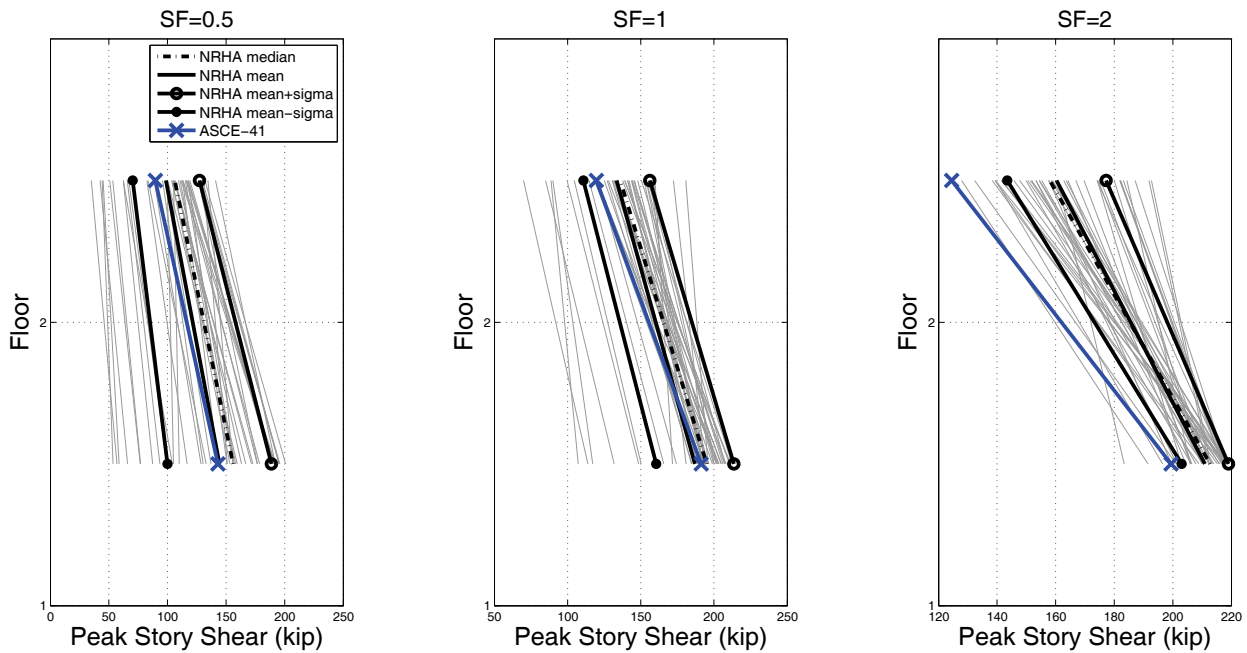


Figure B-5 2-story RCMF: NRHA versus ASCE/SEI 41-06 displacement coefficient method, peak story shears.

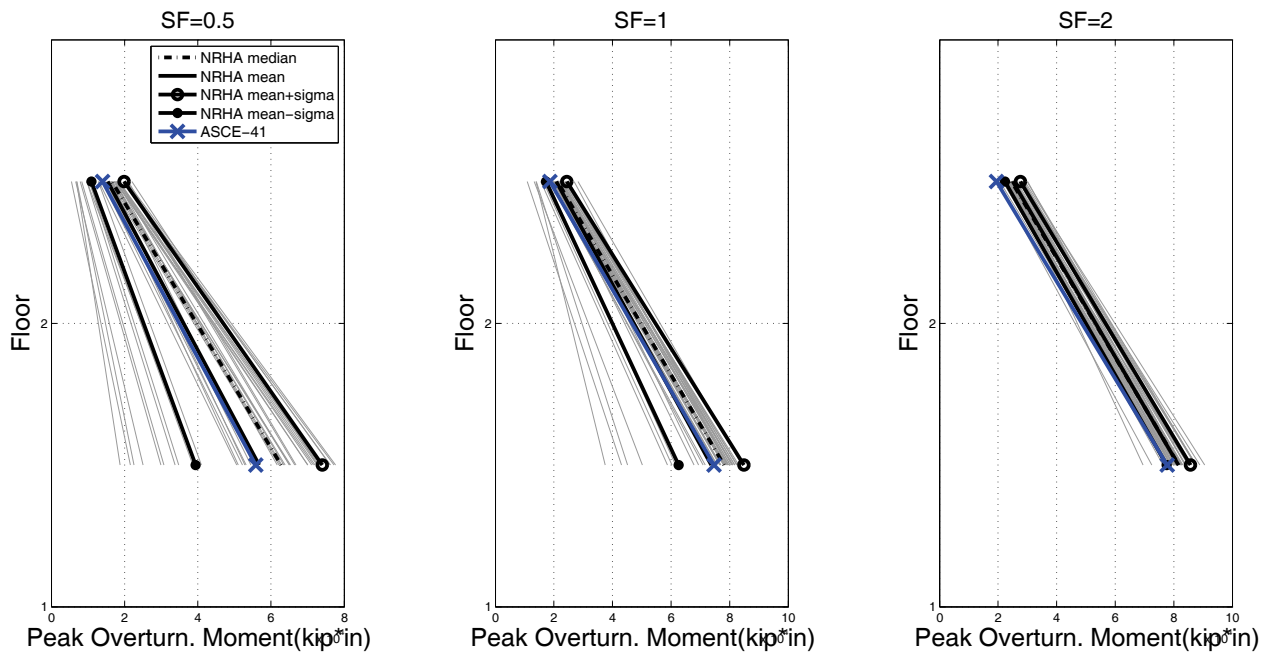


Figure B-6 2-story RCMF: NRHA versus ASCE/SEI 41-06 displacement coefficient method, peak overturning moments.

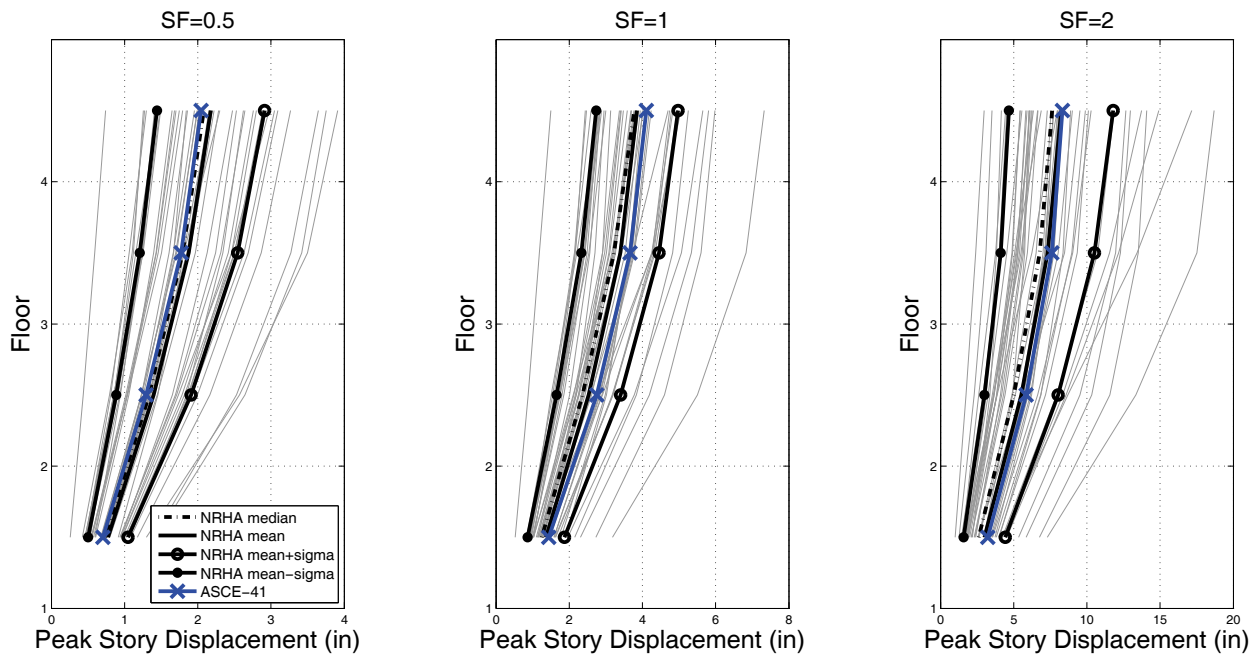


Figure B-7 4-story RCMF: NRHA versus ASCE/SEI 41-06 displacement coefficient method, peak story displacement.

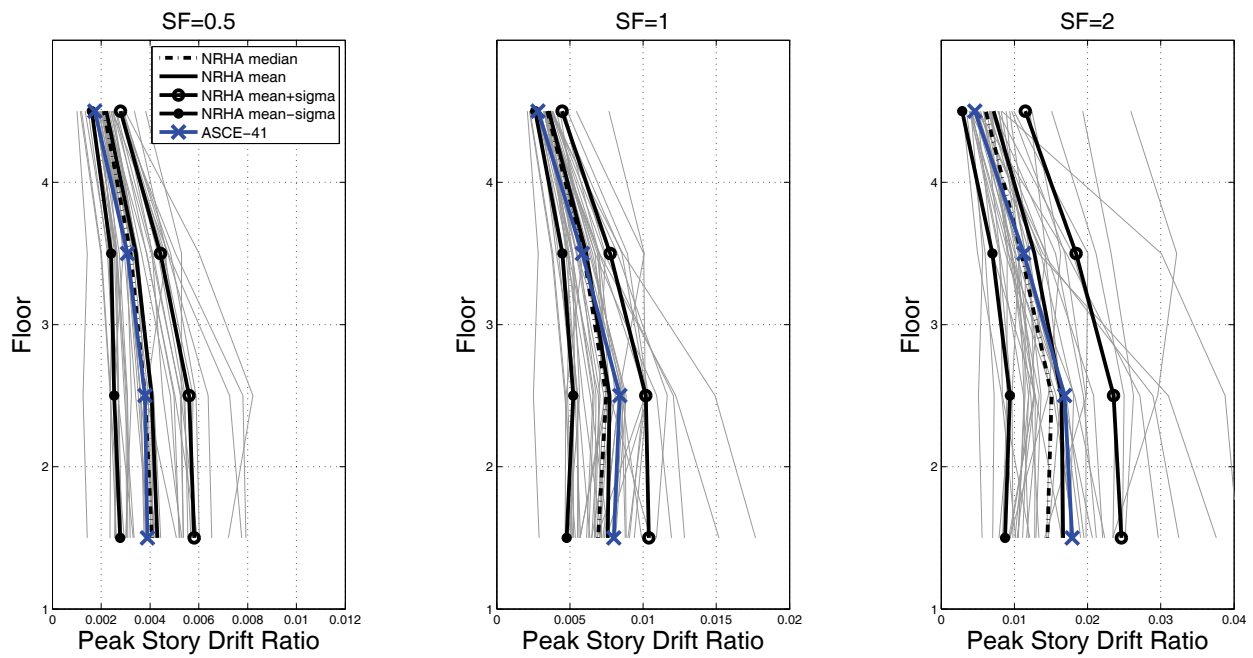


Figure B-8 4-story RCMF: NRHA versus ASCE/SEI 41-06 displacement coefficient method, peak story drift ratio.

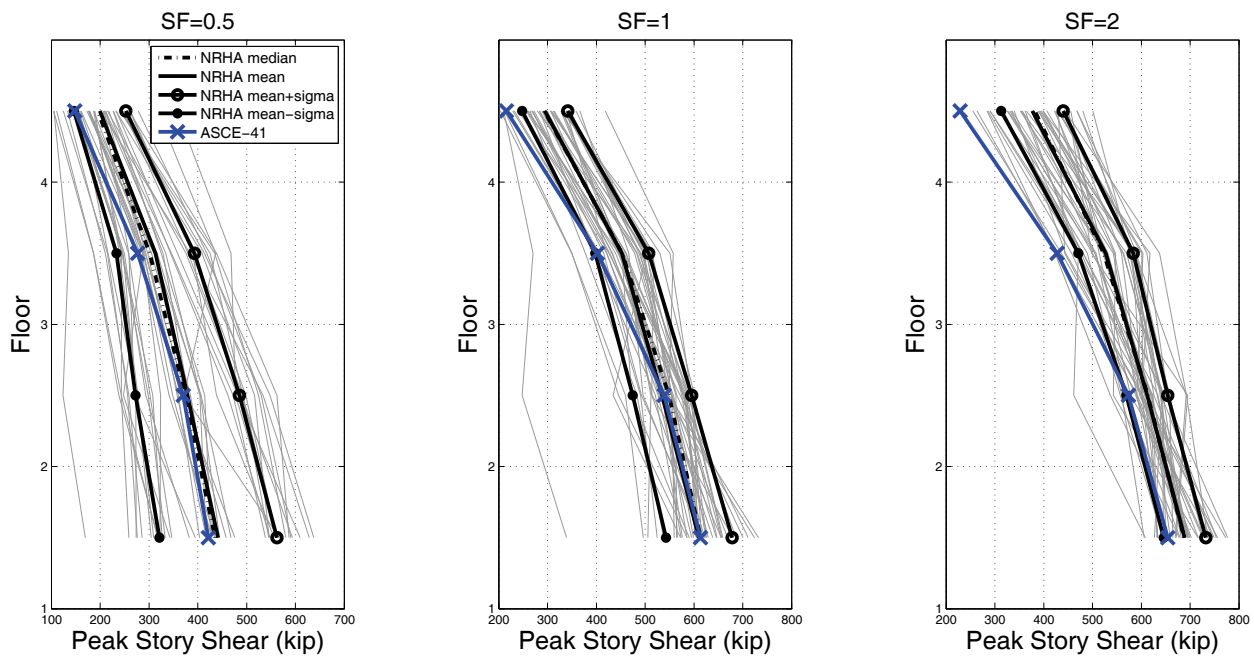


Figure B-9 4-story RCMF: NRHA versus ASCE/SEI 41-06 displacement coefficient method, peak story shears.

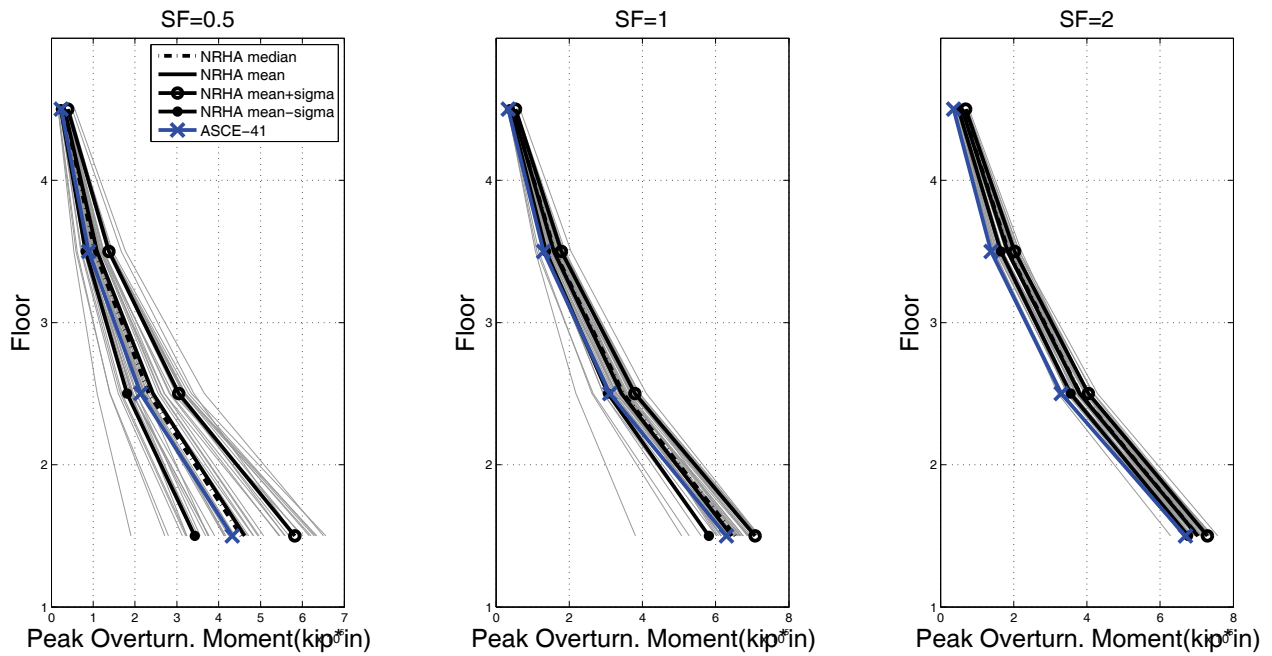


Figure B-10 4-story RCMF: NRHA versus ASCE/SEI 41-06 displacement coefficient method, peak overturning moments.

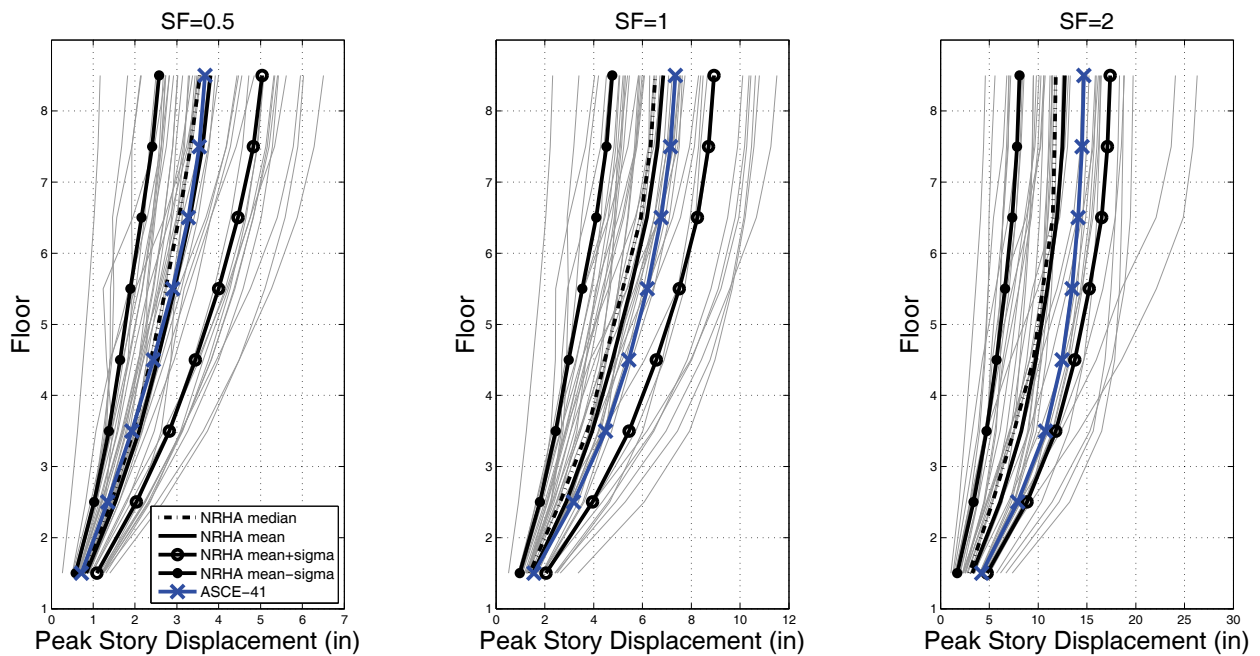


Figure B-11 8-story RCMF: NRHA versus ASCE/SEI 41-06 displacement coefficient method, peak story displacements.

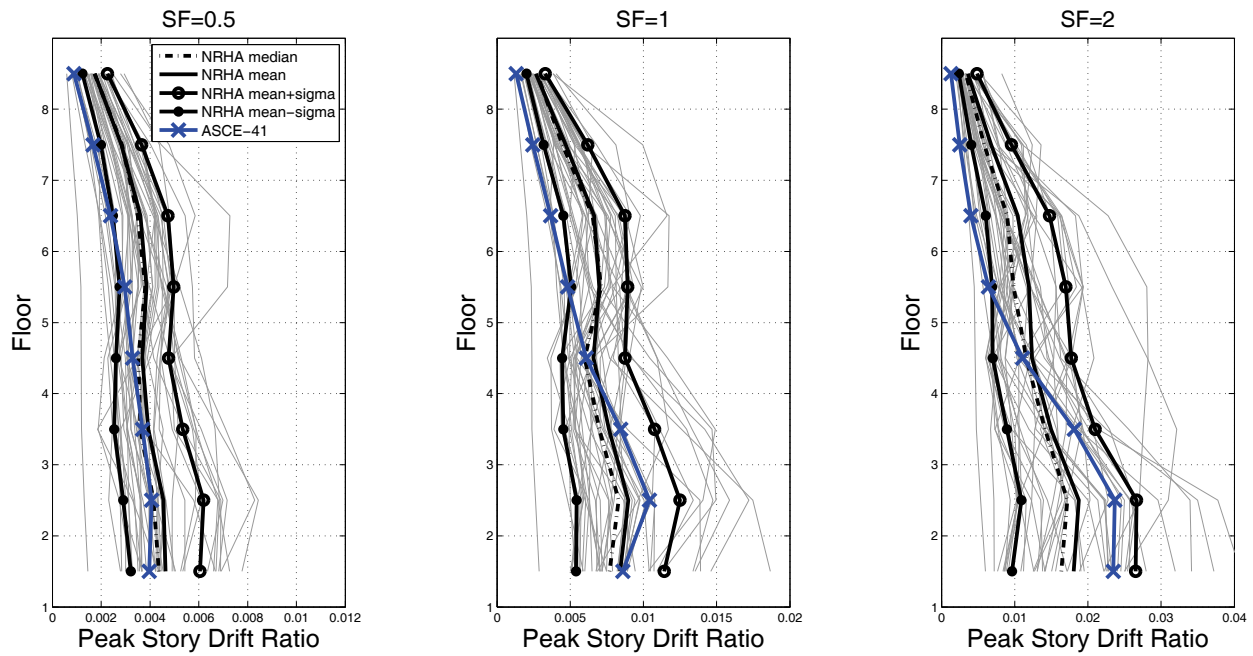


Figure B-12 8-story RCMF: NRHA versus ASCE/SEI 41-06 displacement coefficient method, peak story drift ratio

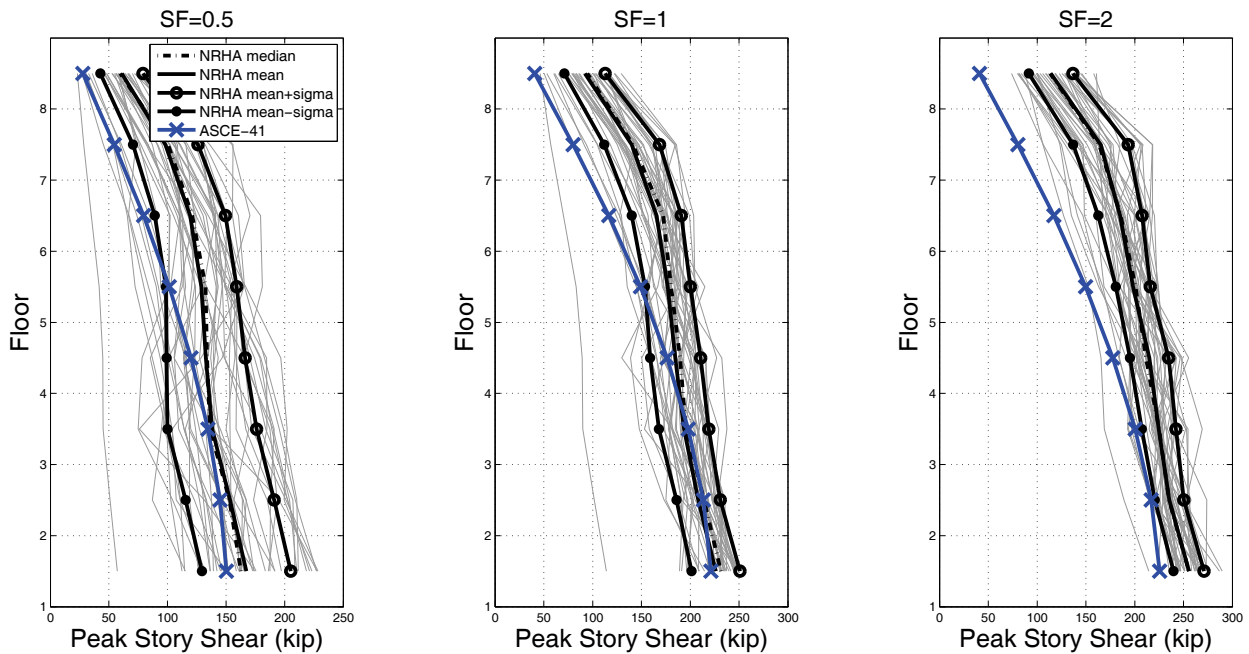


Figure B-13 8-story RCMF: NRHA versus ASCE/SEI 41-06 displacement coefficient method, peak story shears

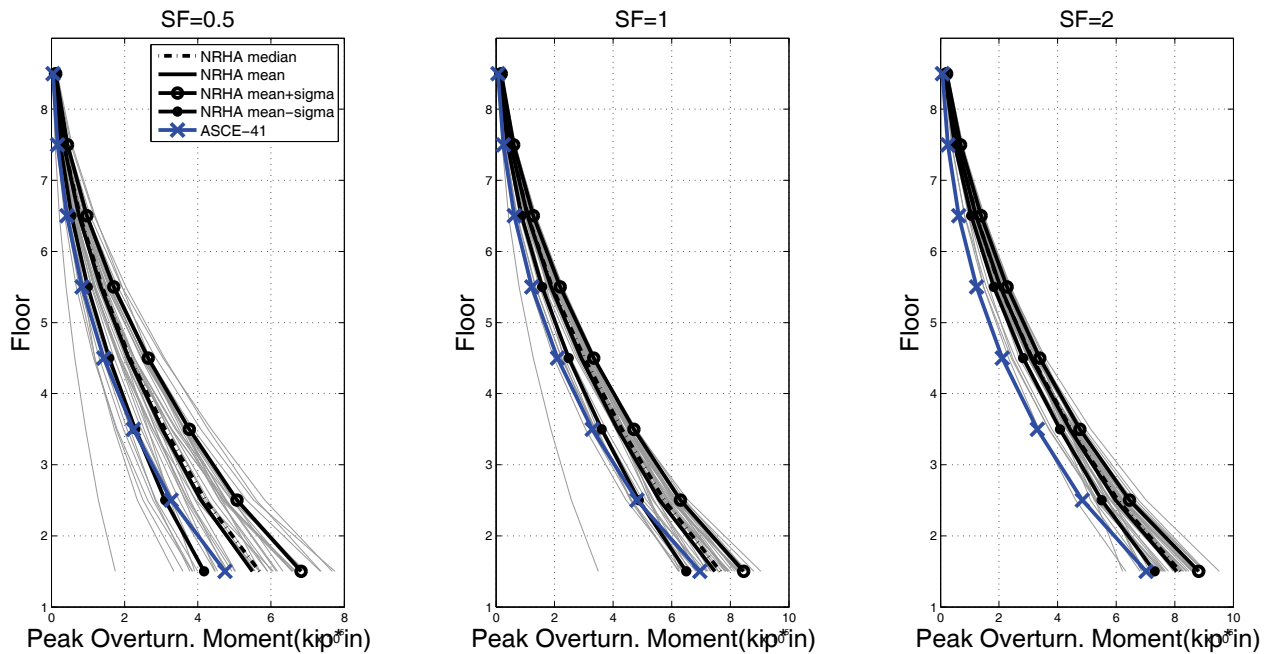


Figure B-14 8-story RCMF: NRHA versus ASCE/SEI 41-06 displacement coefficient method, peak overturning moments.

B.3.2 N2/EC8 Method

Soil type B is assumed, resulting in $T_c = 0.5$. The target displacement of a structure with period T_e and unlimited elastic capacity is:

$$d_{et} = S_a(T_e) \left(\frac{T_e}{2\pi} \right)^2 \quad (B-5)$$

The target displacement of the MDOF system is δ_t and the displacement of the corresponding SDOF is d_t^* where $d_t = \Gamma_n d_t^* = C_0 d_t^*$. Different expressions are used for structures in the short-period range and in the medium and long period range:

$T_e < T_c$ (short period range): If $(F_y / C_0) / M^* \geq S_a(T_e)$, the response is elastic and thus $d_t^* = d_{et}$, otherwise the response is nonlinear and the target displacement is calculated as:

$$d_t^* = \frac{d_{et}}{q_u} \left(1 + (q_u - 1) \frac{T_c}{T_e} \right) \geq d_{et} \quad (B-6)$$

where $q_u = S_a(T_e) M^* / F_y$.

$T_e \geq T_c$ (medium and long period range): The target displacement of the inelastic system is equal to that of an elastic structure, thus $d_t^* = d_{et}$.

2-story RCMF:

Since $T_1 = 0.62 \text{ sec} \geq T_c$ the building is in the medium to long period range. Therefore:

$$d_{et} = [0.33g \quad 0.65g \quad 1.30g] \left(\frac{0.625}{2\pi} \right)^2 = [1.25 \quad 2.49 \quad 4.98](in) \quad (B-7)$$

$$\delta_t = C_0 d_{et} = 1.18 \cdot d_{et} = [1.467 \quad 2.93 \quad 5.87](in) \quad (B-8)$$

4-story RCMF:

Since $T_1 = 0.855 \text{ sec} \geq T_c$ the building is in the medium to long period range.

$$d_{et} = [0.23g \quad 0.46g \quad 0.91g] \left(\frac{0.855}{2\pi} \right)^2 = [1.63 \quad 3.26 \quad 6.53](in) \quad (B-9)$$

$$\delta_t = C_0 d_{et} = 1.25 \cdot d_{et} = [2.05 \quad 4.01 \quad 8.19](in) \quad (B-10)$$

8-story RCMF:

Since $T_1 = 1.80 \text{ sec} \geq T_C$ the building is in the medium to long period range. Therefore, for the first mode:

$$d_{et} = [0.09g \quad 0.18g \quad 0.36g] \left(\frac{1.80}{2\pi} \right)^2 = [2.9 \quad 5.76 \quad 11.53](in) \quad (B-11)$$

$$\delta_t = C_0 d_{et} = 1.27 \cdot d_{et} = [3.68 \quad 7.35 \quad 14.70](in) \quad (B-12)$$

The values above are very close to those of the ASCE/SEI 41-06 displacement coefficient method and the same applies to higher modes of vibration where the structures remain elastic. Thus, emphasis is given to the ASCE/SEI 41-06 approach and no further results are shown for the N2/EC8 method.

B.3.3 Modal Pushover Analysis

The steps of the Modal Pushover Analysis (MPA) method (Chopra and Goel, 2002), are summarized below:

1. Calculate the natural frequencies, the mode shapes and the lateral load patterns $\mathbf{s}_n^* = \mathbf{m}\boldsymbol{\phi}_n$.
2. For the n^{th} mode, develop the base shear-roof displacement curve, $V_{bn}-u_m$, for the \mathbf{s}_n^* distribution of forces.
3. Idealize the pushover curve as a bilinear curve and compute the target displacements δ_t for every mode using the ASCE/SEI 41-06 $R-C_1-T$ relationship.
4. From the pushover database (Step 2), extract values of desired responses r_{n+g} due to the combined effects of gravity and lateral loads at roof displacement equal to $u_m + u_{rg}$.
5. Repeat steps 2–4 for as many modes as required for sufficient accuracy, thus 2 modes for the 2-story RCMF and 3 for the 4-story and the 8-story RCMF.

6. Compute the dynamic response due to the n^{th} mode: $r_n = r_{n+g} - r_g$, where r_g is the contribution of gravity loads alone. Determine the total response (demand) by combining gravity response and the peak modal responses using the SRSS rule: $r \approx \max[r_g \pm (\sum r_n^2)^{1/2}]$.

A fitting algorithm is applied to obtain the yield point from the capacity curves obtained with the lateral load patterns proportional to each mode of vibration. The target displacements were obtained with the ASCE/SEI 41-06 $R-C_1-T$ relationship, as summarized in Tables B-7, B-8 and B-9. The following figures show that the higher modes of vibration remain linear elastic for all three buildings.

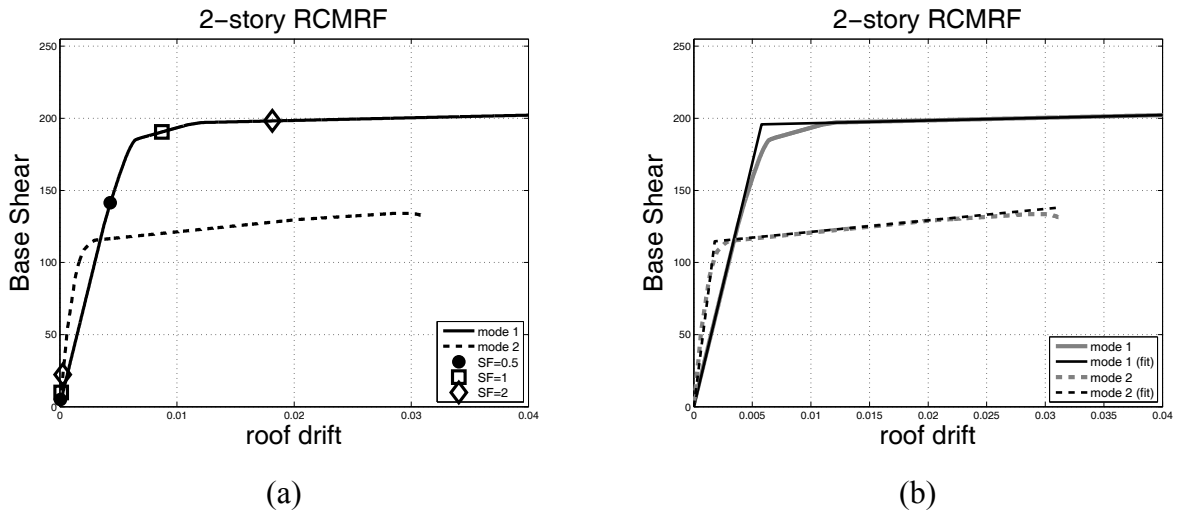


Figure B-15 2-story RCMF: (a) Peak roof displacements of the ASCE/SEI 41-06 method, (b) multi-linear approximation

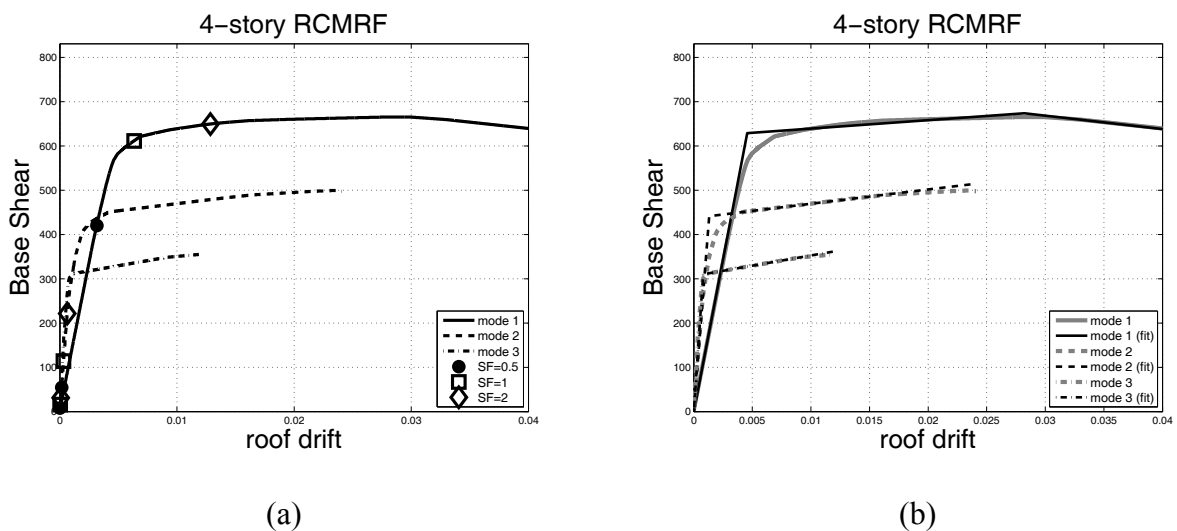


Figure B-16 4-story RCMF: (a) Peak roof displacements of the ASCE/SEI 41-06 method, (b) multi-linear approximation

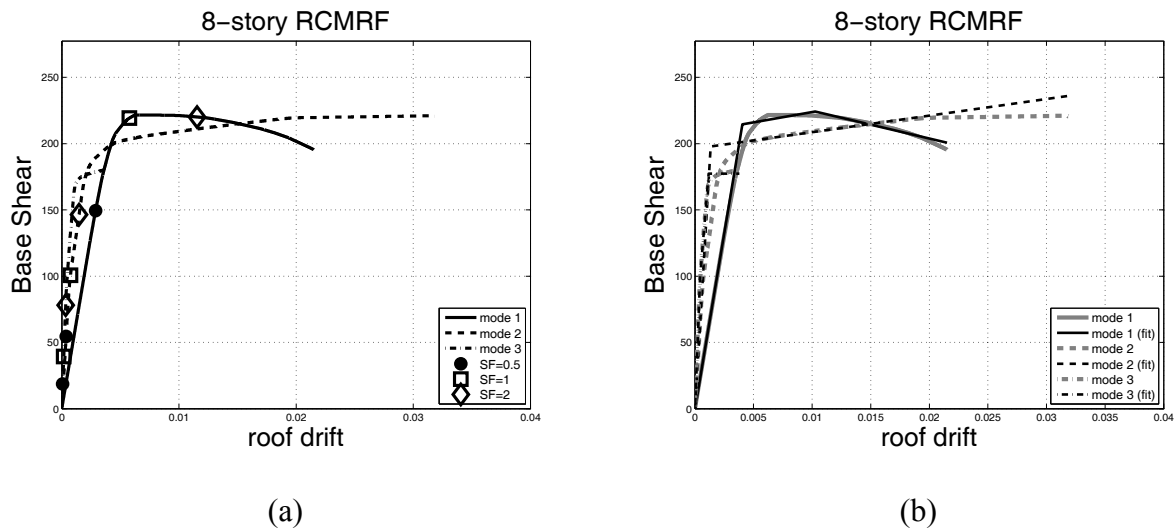


Figure B-17 8-story RCMF: (a) Peak roof displacements of the ASCE/SEI 41-06 method, (b) multi-linear approximation

In the figures that follow the comparison between the NRHA results and the results of the MPA method are summarized with respect to the three intensity levels and the EDPs considered.

Summary of Observations:

For the 2- and the 4-story buildings, the higher modes have negligible effects on the estimate of displacements and drifts. Thus, for these buildings, the results of the MPA method are nearly identical to those of ASCE/SEI 41-06 for drifts and displacements. However, for the 8-story frame, inclusion of higher mode contributions provides some improvement in the drift profile estimates at the top stories; no improvement in displacement estimates is apparent. Drift estimates at the lower stories, where the maximum values occur, are not improved.

Story shear estimates are generally improved by the inclusion of higher modes in the MPA procedure, particularly for the 4- and 8-story frames. Bias in the story shears is observed for the top stories, for the 4-story RCMF the bias is considerably reduced when higher modes of vibration are included, especially for SF = 2. For the 8-story RCMF, even the 3rd mode affects the story shear results, resulting in small overestimates at the top stories.

The accuracy of peak overturning moment estimates follows the trend for the story shear estimates. Inclusion of higher modes results in improved estimates for the 4-story RCMF at SF = 2 and also for the 8-story RCMF. For the latter building, a loss of accuracy is observed for SF = 2.

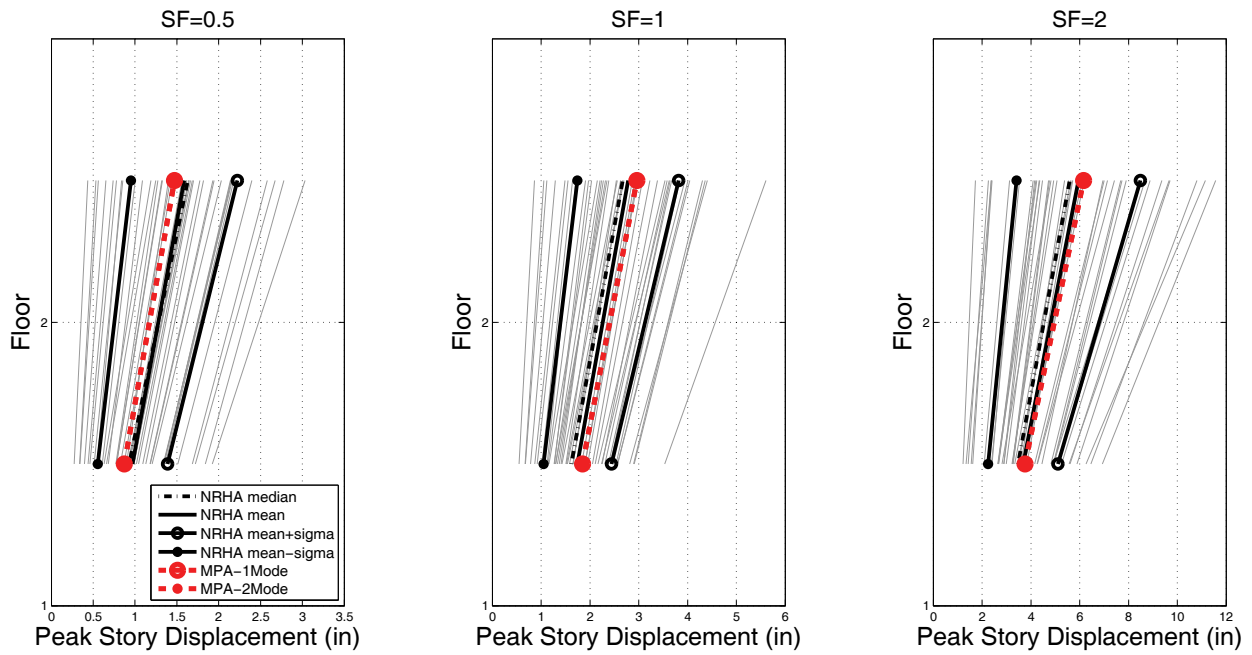


Figure B-18 2-story RCMF: NRHA versus MPA, peak story displacement.

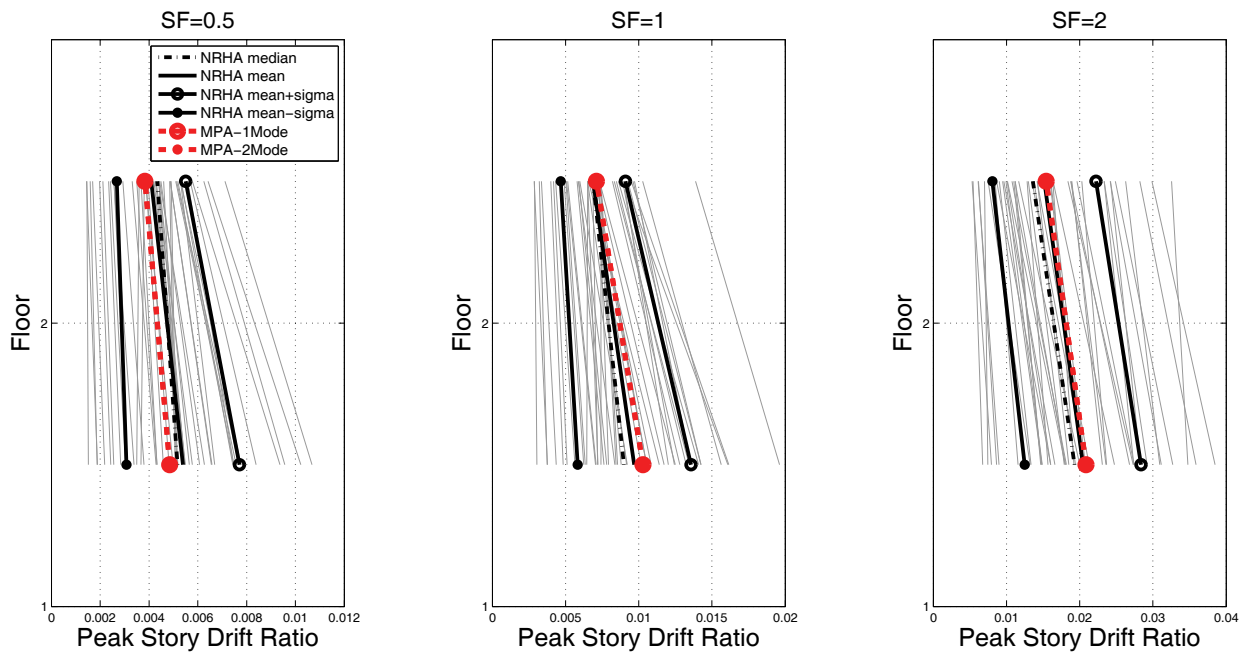


Figure B-19 2-story RCMF: NRHA versus MPA, peak story drift ratio.

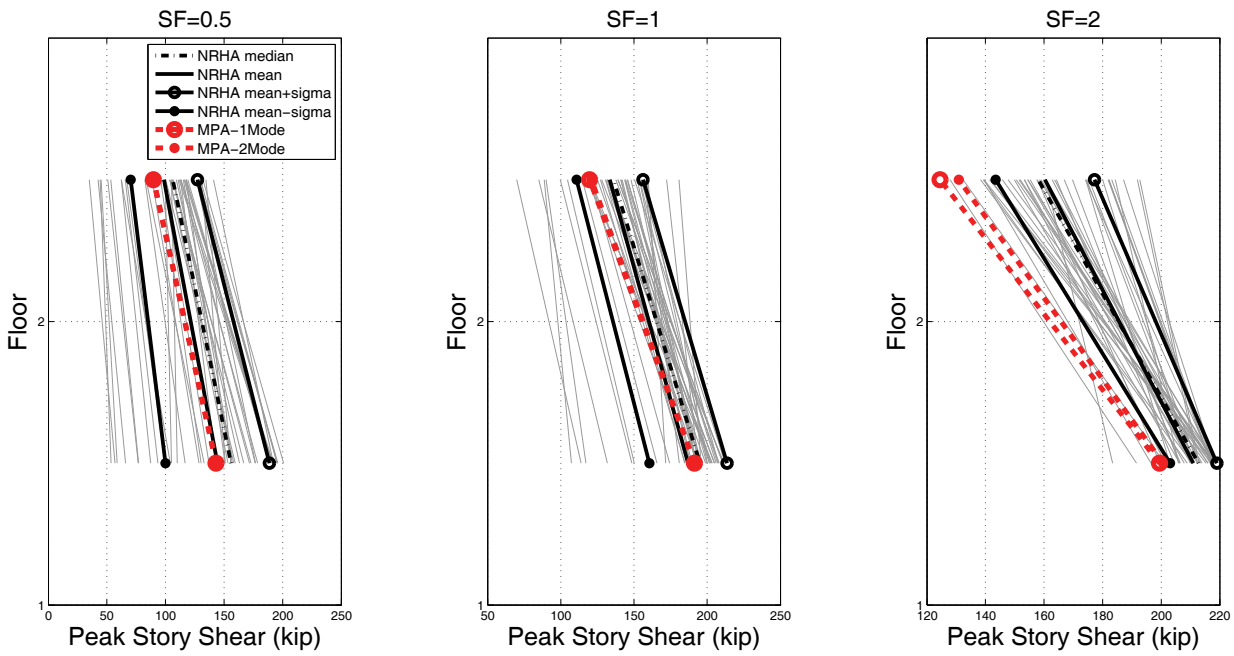


Figure B-20 2-story RCMF: NRHA versus MPA, peak story shears.

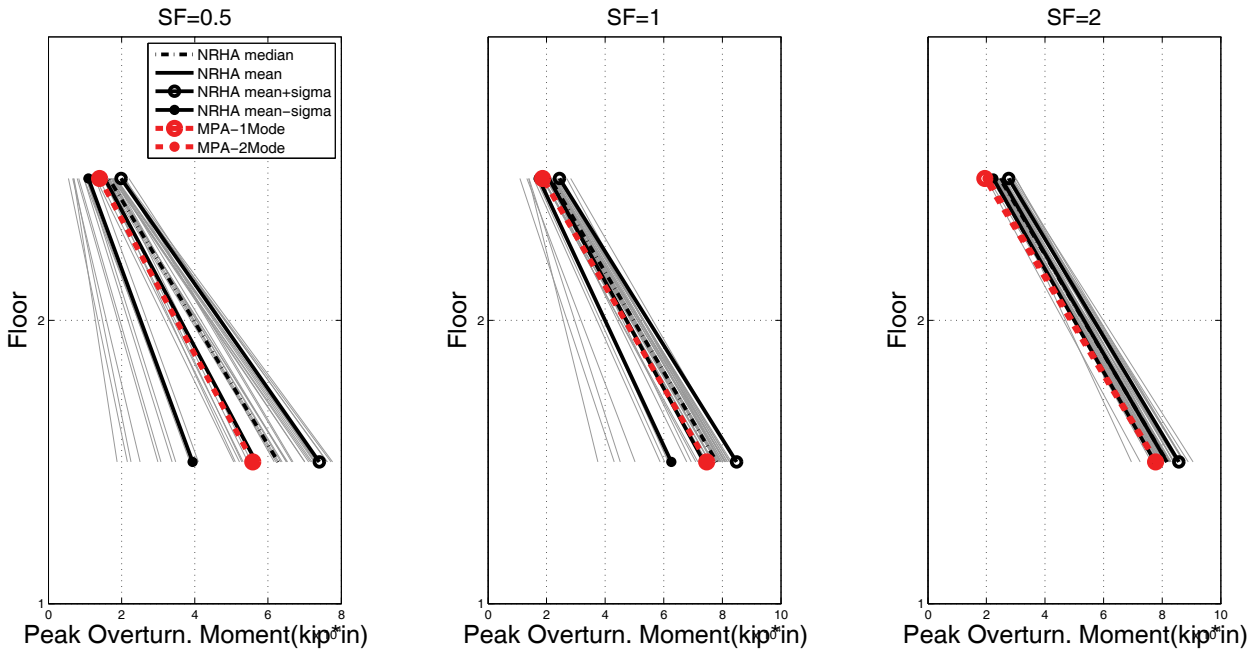


Figure B-21 2-story RCMF: NRHA versus MPA, peak overturning moments.

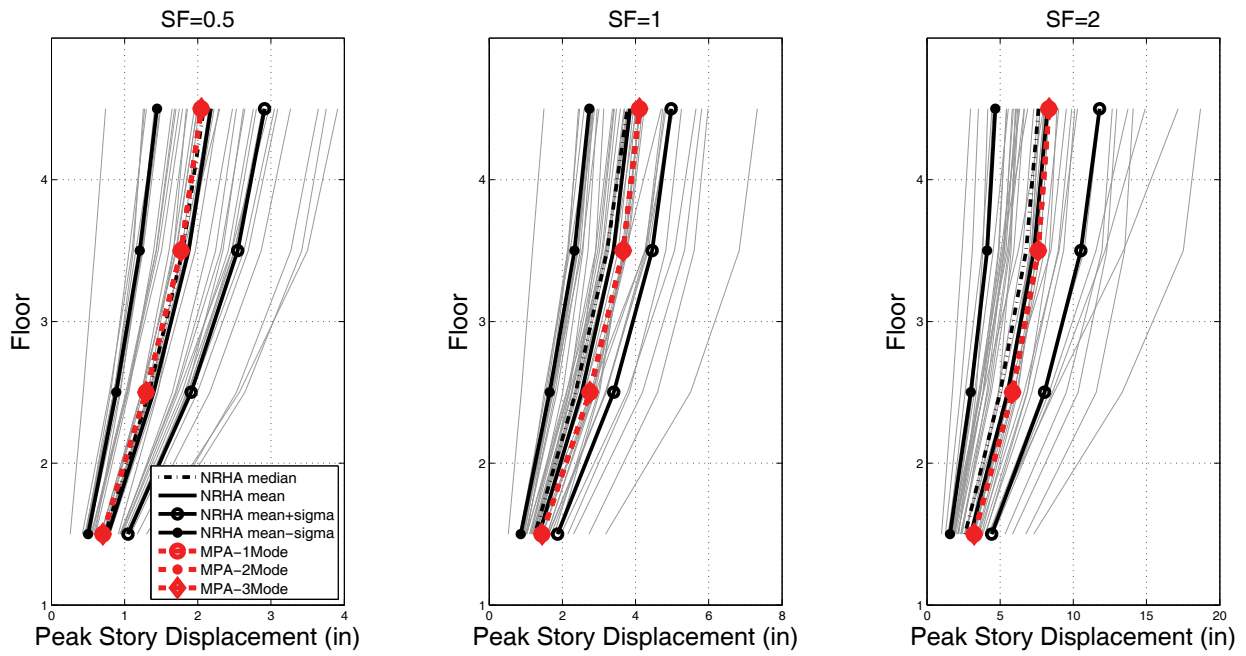


Figure B-22 4-story RCMF: NRHA versus MPA, peak story displacement.

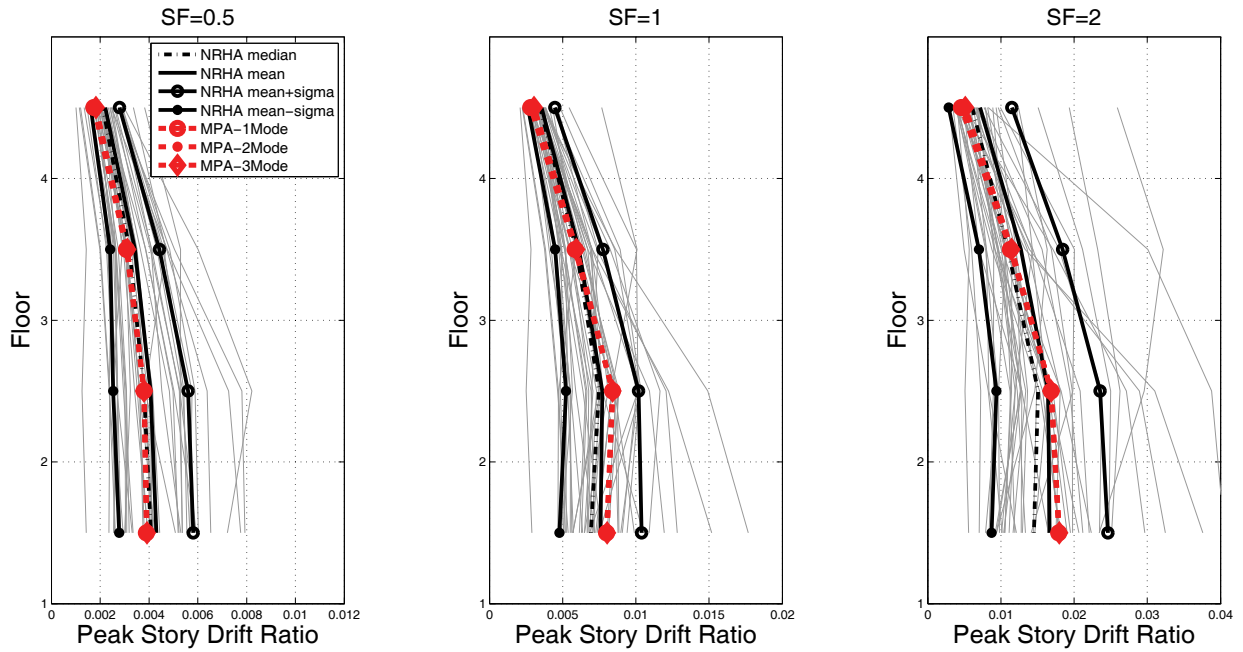


Figure B-23 4-story RCMF: NRHA versus MPA, peak story drift ratio.

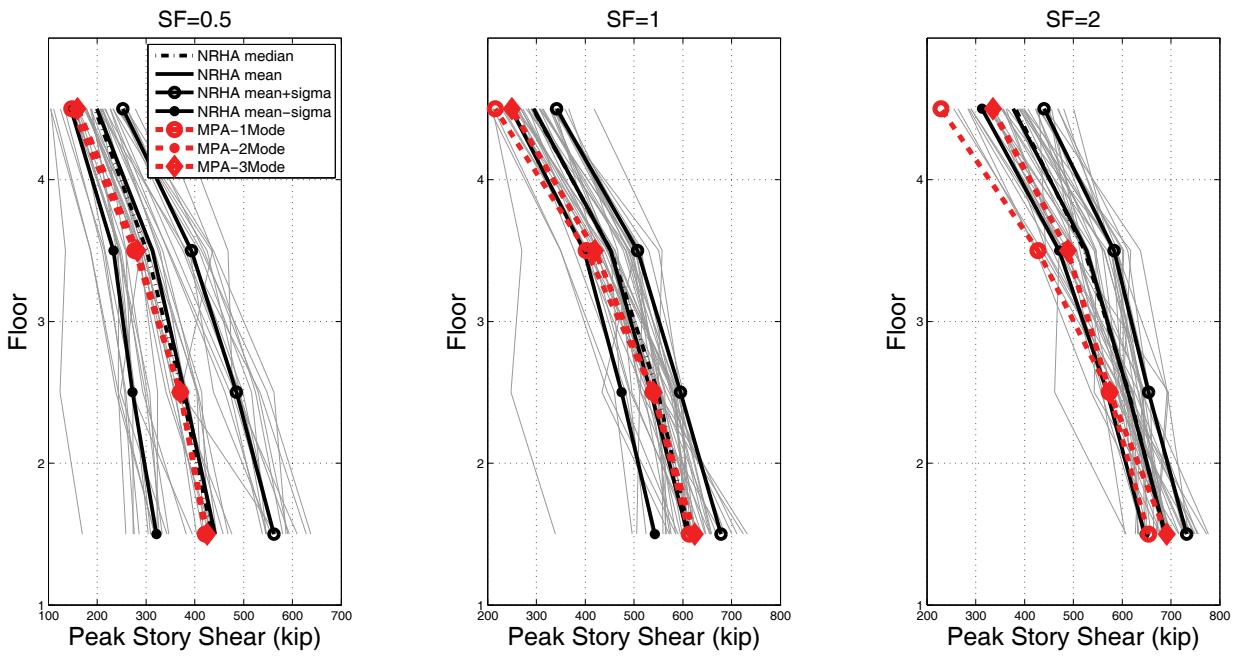


Figure B-24 4-story RCMF: NRHA versus MPA, peak story shears.

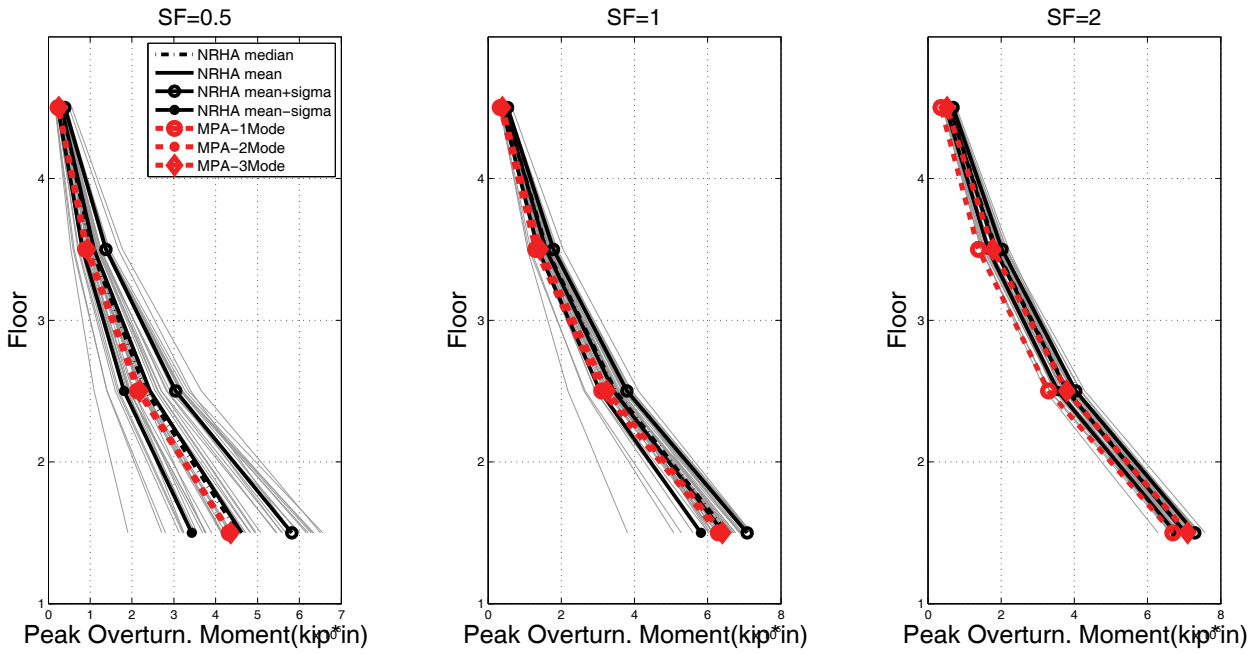


Figure B-25 4-story RCMF: NRHA versus MPA, peak overturning moments.

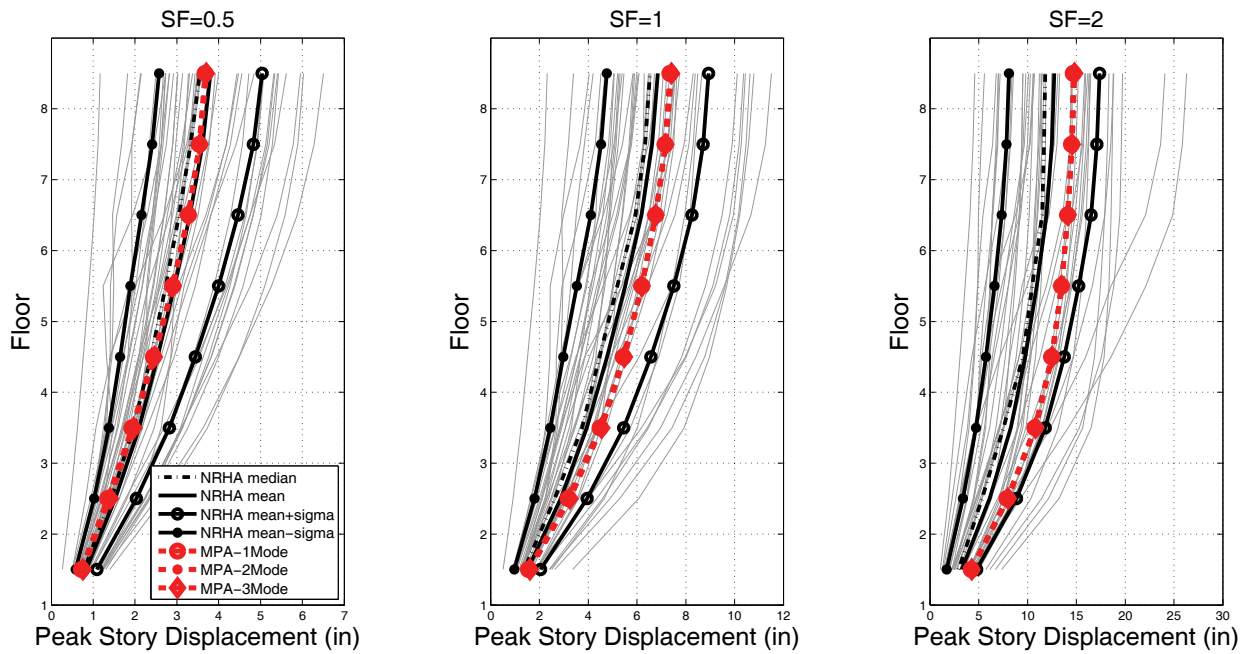


Figure B-26 8-story RCMF: NRHA versus MPA, peak story displacement.

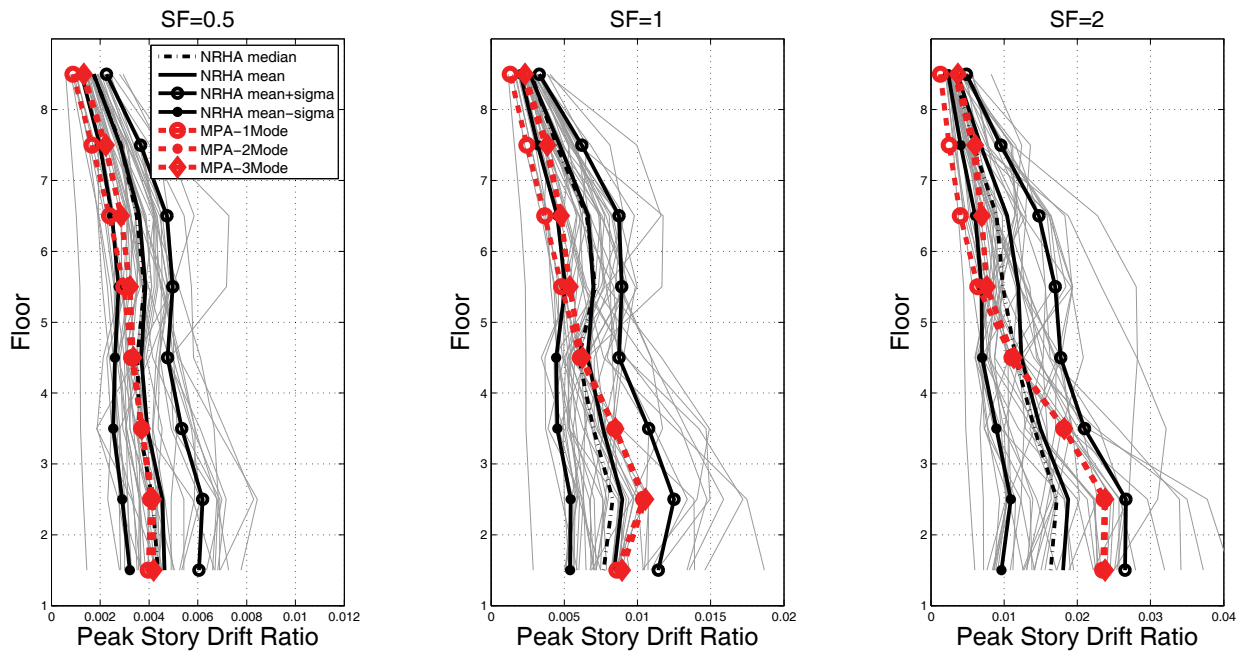


Figure B-27 8-story RCMF: NRHA versus MPA, peak story drift ratio.

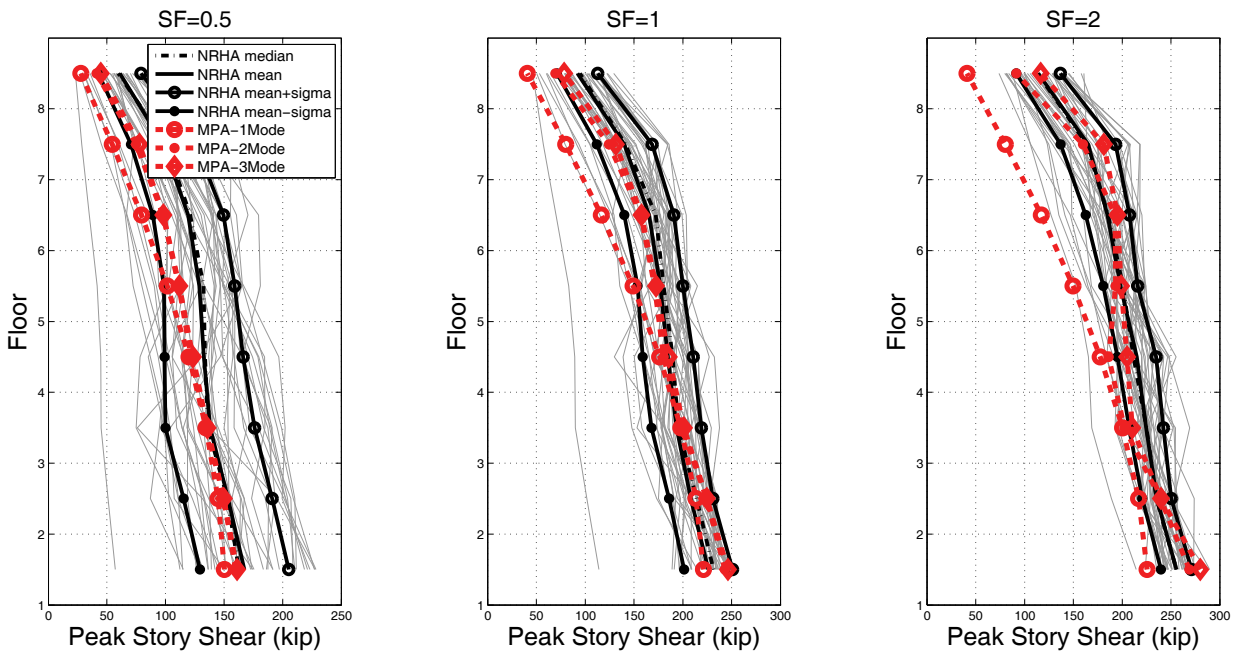


Figure B-28 8-story RCMF: NRHA versus MPA, peak story shears.

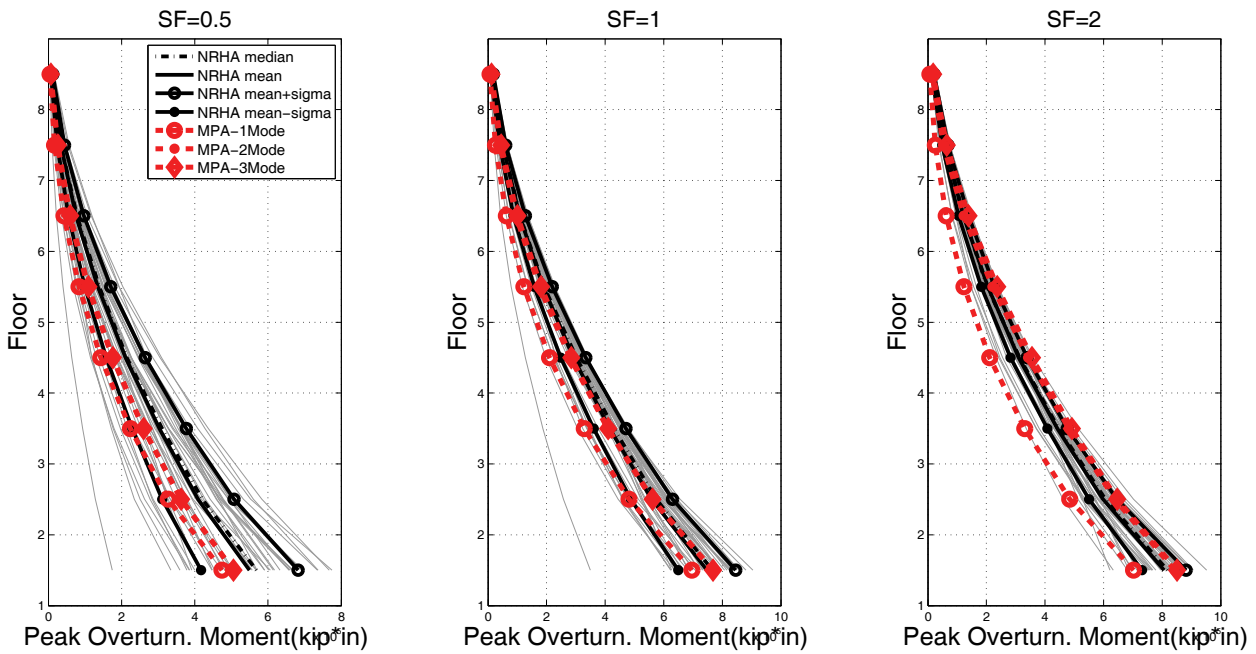


Figure B-29 8-story RCMF: NRHA versus MPA, peak overturning moments.

B.3.4 Consecutive Modal Pushover

The steps of the Consecutive Modal Pushover (CMP) method (Poursha et al. 2009) are summarized below:

1. Calculate the natural frequencies, the modal-shapes and the lateral load patterns $\mathbf{s}_n^* = \mathbf{m}\boldsymbol{\phi}_n$.
2. Compute the total target displacement δ_t using the ASCE/SEI 41-06 $R-C_1-T$ relationship.
3. The CMP procedure consists of single-stage and multi-stage pushover analyses. For the buildings considered, a two-stage CMP is applicable. The steps of the method are:
 - a. Develop the base shear-roof displacement, $V_{bn}-u_{rn}$, pushover curve using an inverted triangular (or 1st mode based) lateral load pattern for medium-rise buildings and a uniform force distribution for high-rise buildings, until the target displacement, δ_t . The first stage is effectively identical to that obtained in a first-mode pushover analysis according to ASCE/SEI 41-06.
 - b. The second pushover analysis is a two-stage pushover analysis. In the first stage, the lateral forces are proportional to the first mode, $\mathbf{s}_1^* = \mathbf{m}\boldsymbol{\phi}_1$, until the displacement increment at the roof reaches $u_{r1} = \alpha_1\delta_t$, where α_1 is the first mode mass participation factor. Then, the second stage is implemented with incremental lateral forces proportional to the second mode, $\mathbf{s}_2^* = \mathbf{m}\boldsymbol{\phi}_2$, until the displacement increment at the roof equals $u_{r2} = (1-\alpha_1)\delta_t$. The initial condition of the second stage is that of the last increment of the first stage.
 - c. For buildings with $T_1 \geq 2.2$ s an additional third consecutive pushover/stage should be performed.
4. Calculate the peak values of the EDPs resulting from the one- and the two-stage pushover analyses, denoted as r_1 and r_2 , respectively.
5. Calculate the envelope, r , of the peak EDP values as: $r = \max\{r_1, r_2\}$.

In the figures that follow, the CMP estimates are compared with the NRHA results with respect to the three intensity levels and the EDPs considered.

Summary of Observations:

Regarding displacements and drifts it is difficult to identify whether there is improvement for the low-rise buildings (2- and 4-stories). For the 8-story RCMF, the method gives reasonable estimates, but it still underestimates the top story drifts, as most methods do.

For story shears, it is also difficult to identify clear trends. Improved estimates are obtained for SF = 1 and some smaller improvement for SF = 2 (4-story RCMF). Error is present for the linear elastic case for the low-rise buildings (SF = 0.5). This error refers mostly to estimates of the story shear demand of the top stories. For the 8-story RCMF, the forces at the top stories are considerably underestimated, while the corresponding displacements are overestimated.

The overturning moments again follow the trends of the story shears. A small improvement is observed for SF = 1 and SF = 2, while the second stage produces error in the prediction of the first story for SF = 0.5.

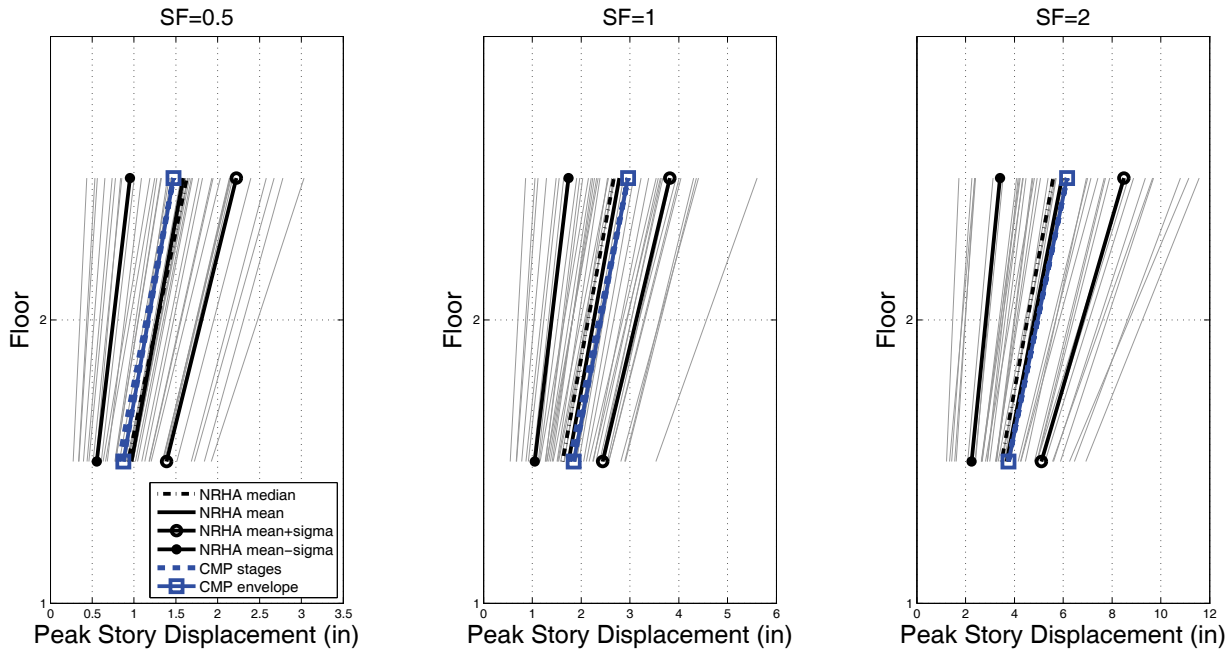


Figure B-30 2-story RCMF: NRHA versus CMP, peak story displacement.

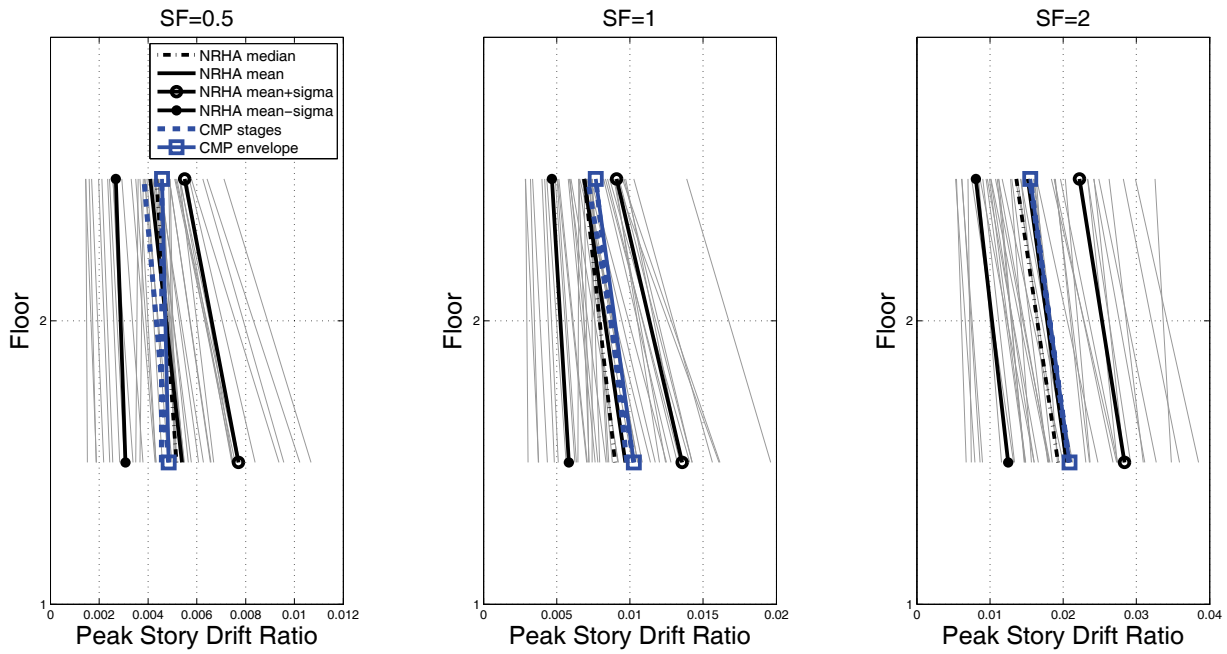


Figure B-31 2-story RCMF: NRHA versus CMP, peak story drift ratio.

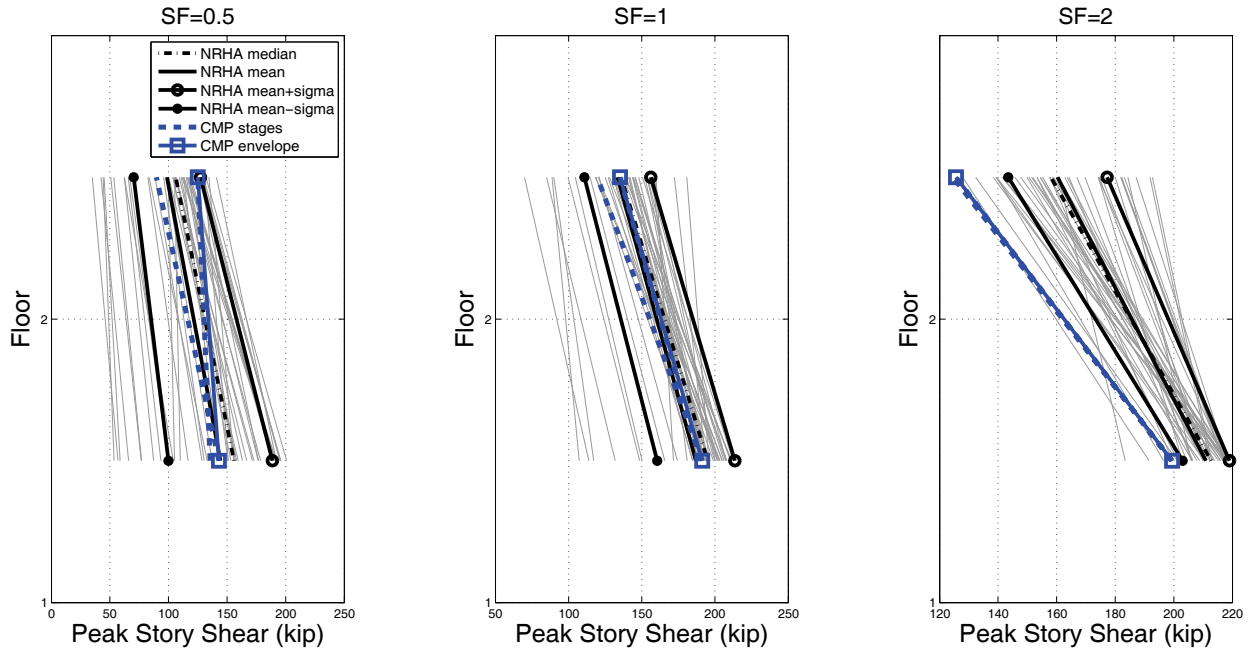


Figure B-32 2-story RCMF: NRHA versus CMP, peak story shears.

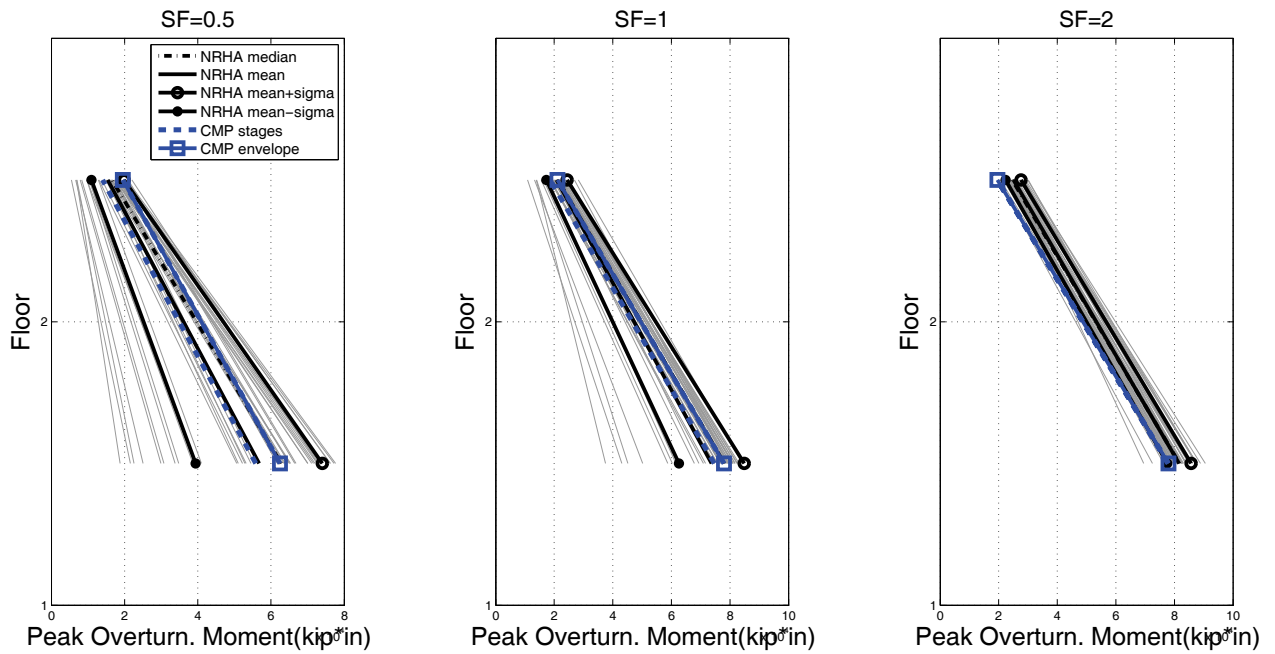


Figure B-33 2-story RCMF: NRHA versus CMP, peak overturning moments.

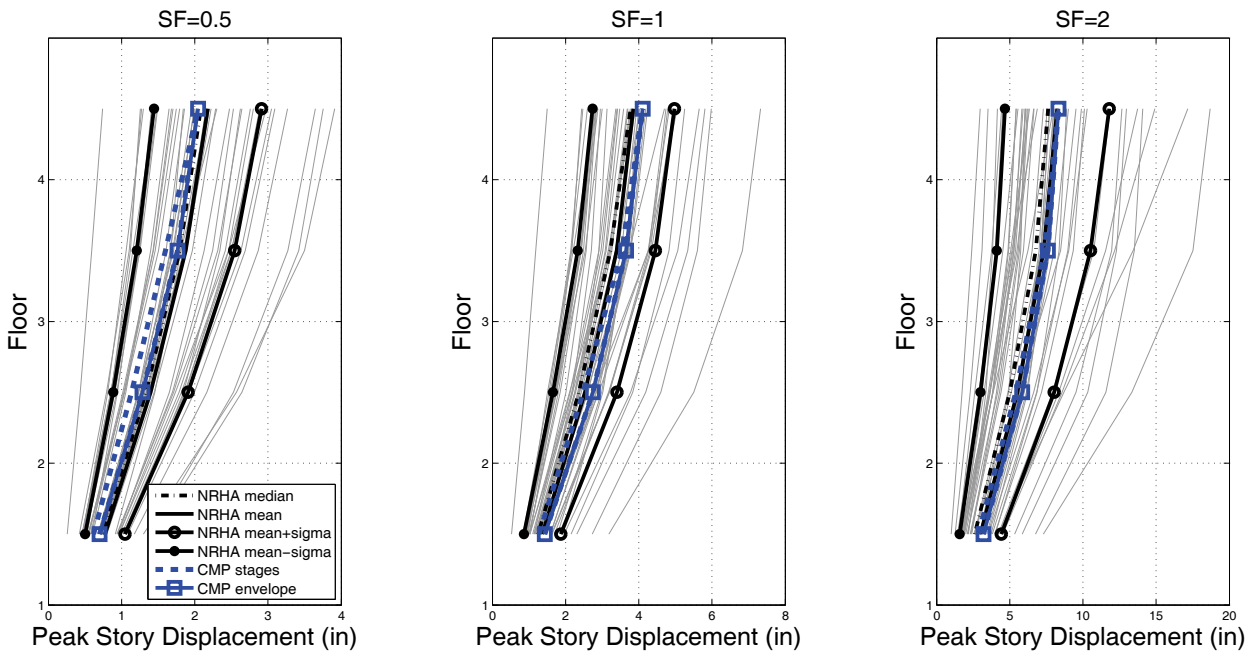


Figure B-34 4-story RCMF: NRHA versus CMP, peak story displacement.

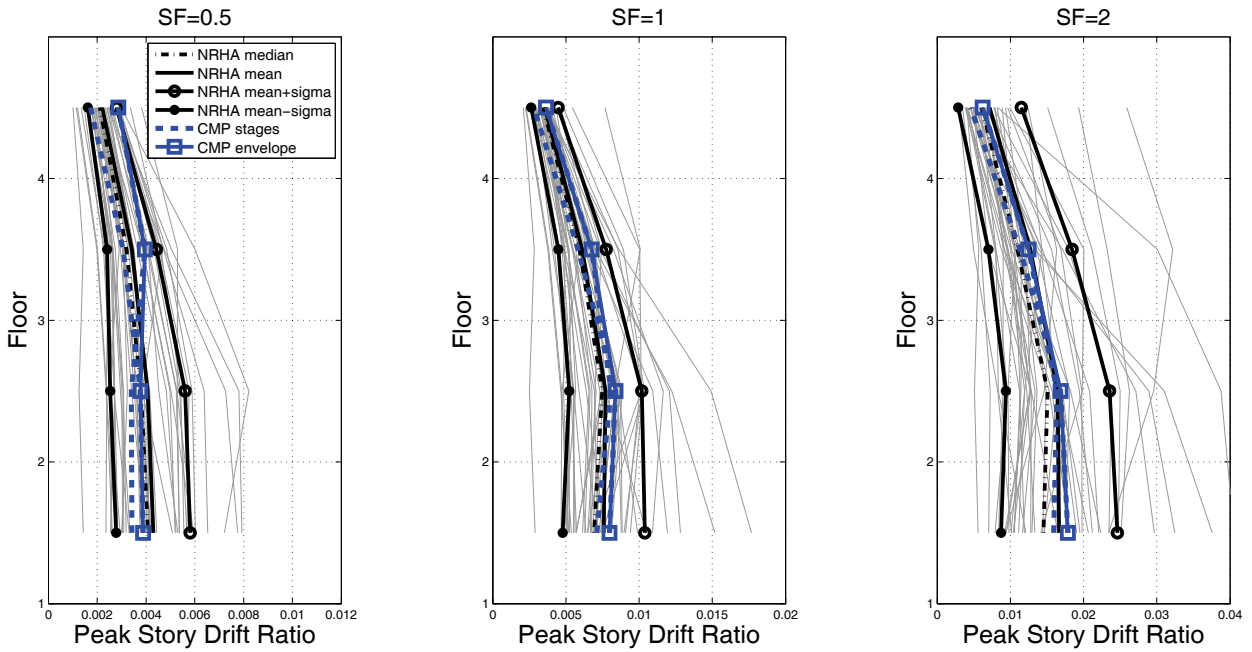


Figure B-35 4-story RCMF: NRHA versus CMP, peak story drift ratio.

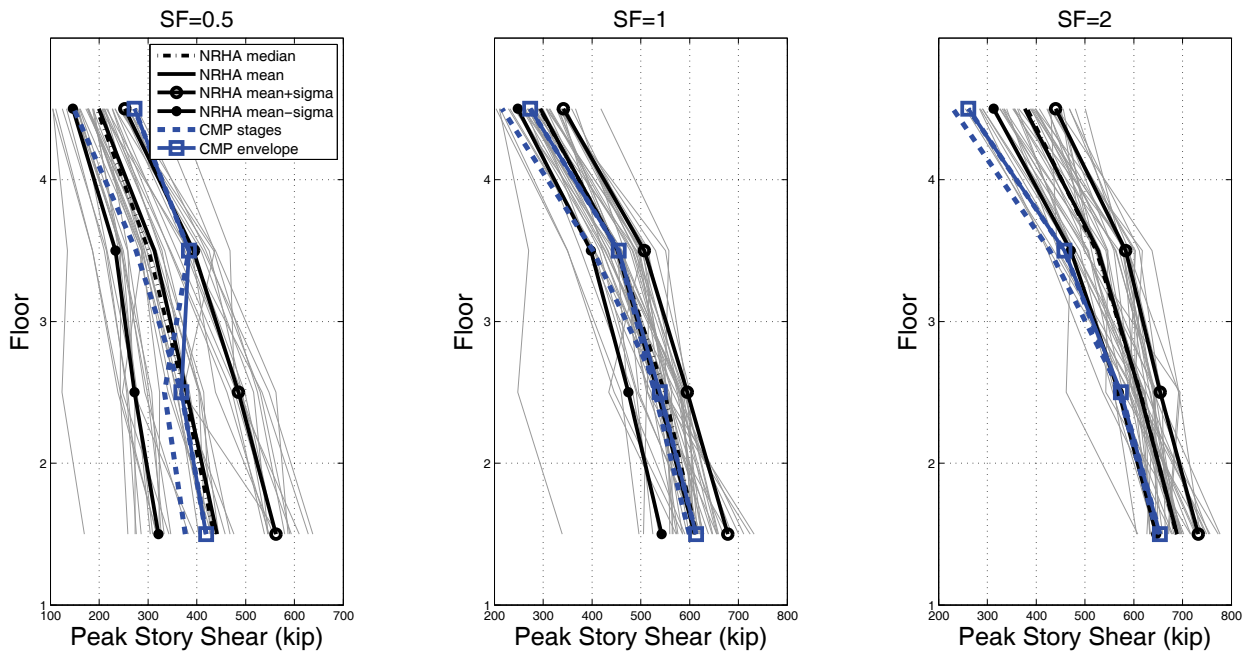


Figure B-36 4-story RCMF: NRHA versus CMP, peak story shears.

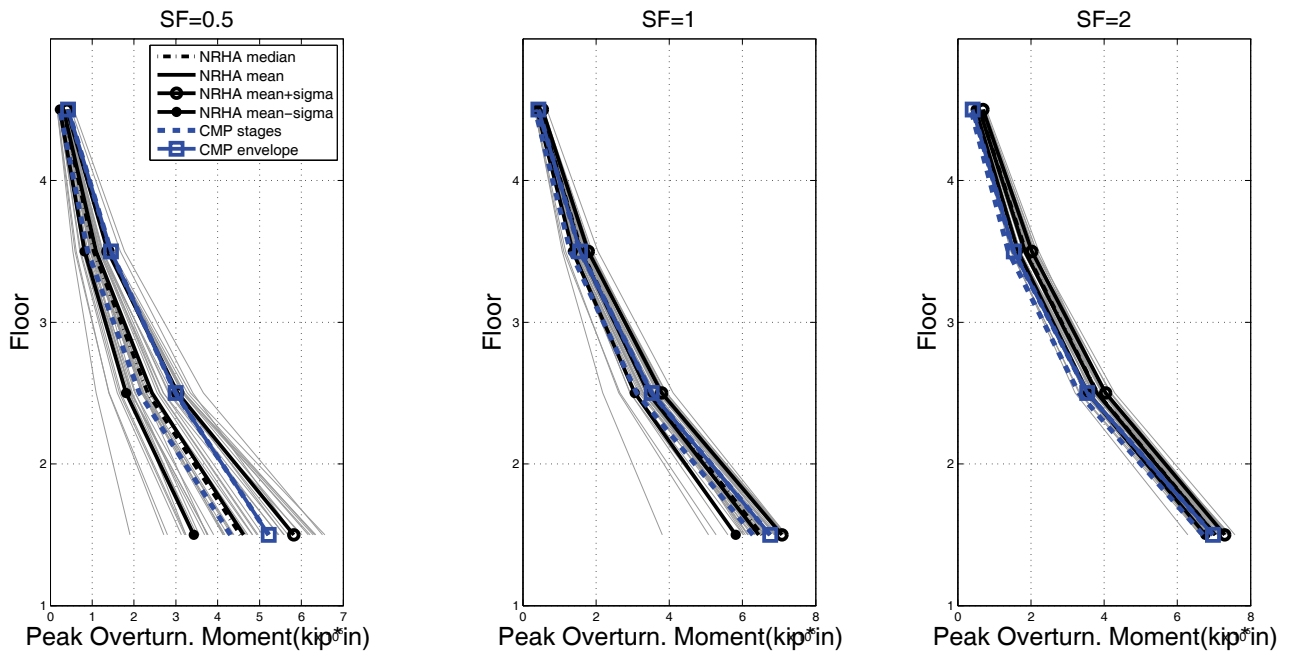


Figure B-37 4-story RCMF: NRHA versus CMP, peak overturning moment.

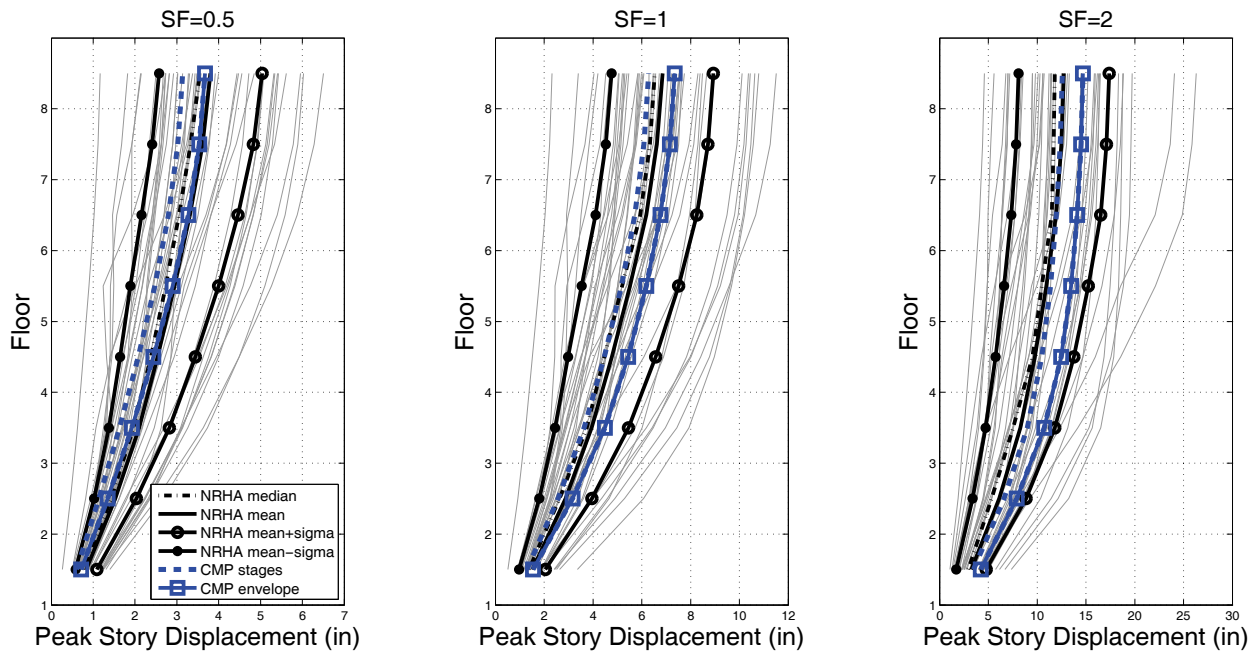


Figure B-38 8-story RCMF: NRHA versus CMP, peak story displacement.

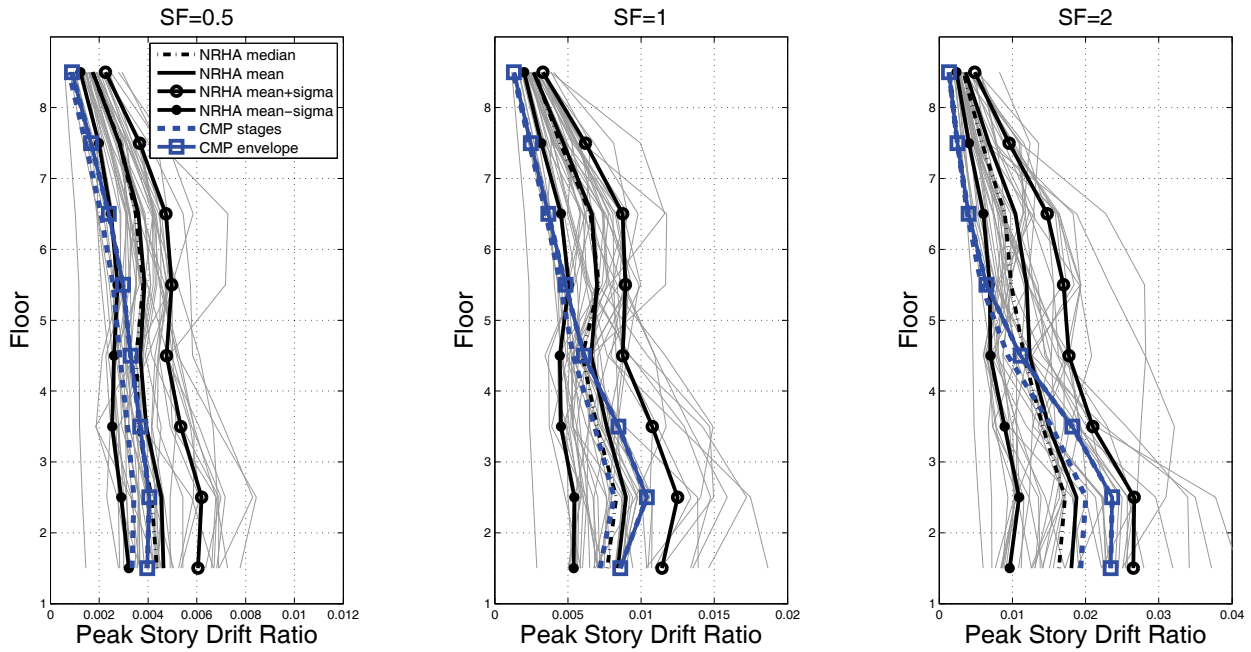


Figure B-39 8-story RCMF: NRHA versus CMP, peak story drift ratio.

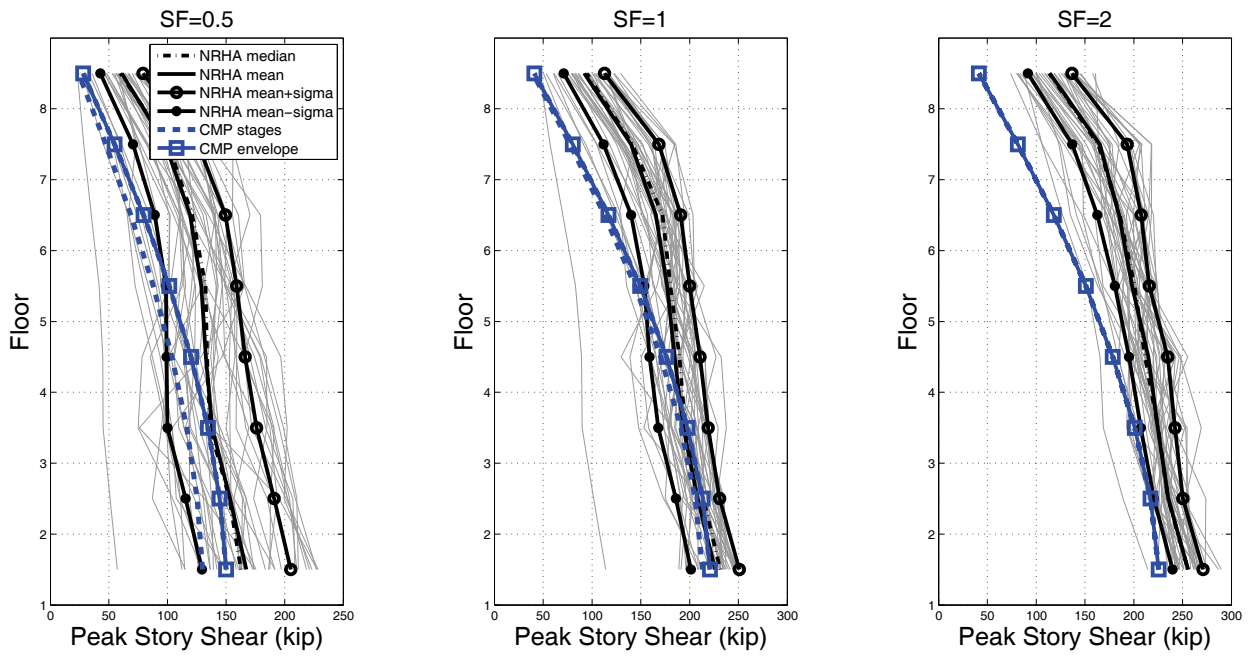


Figure B-40 8-story RCMF: NRHA versus CMP, peak story shears.

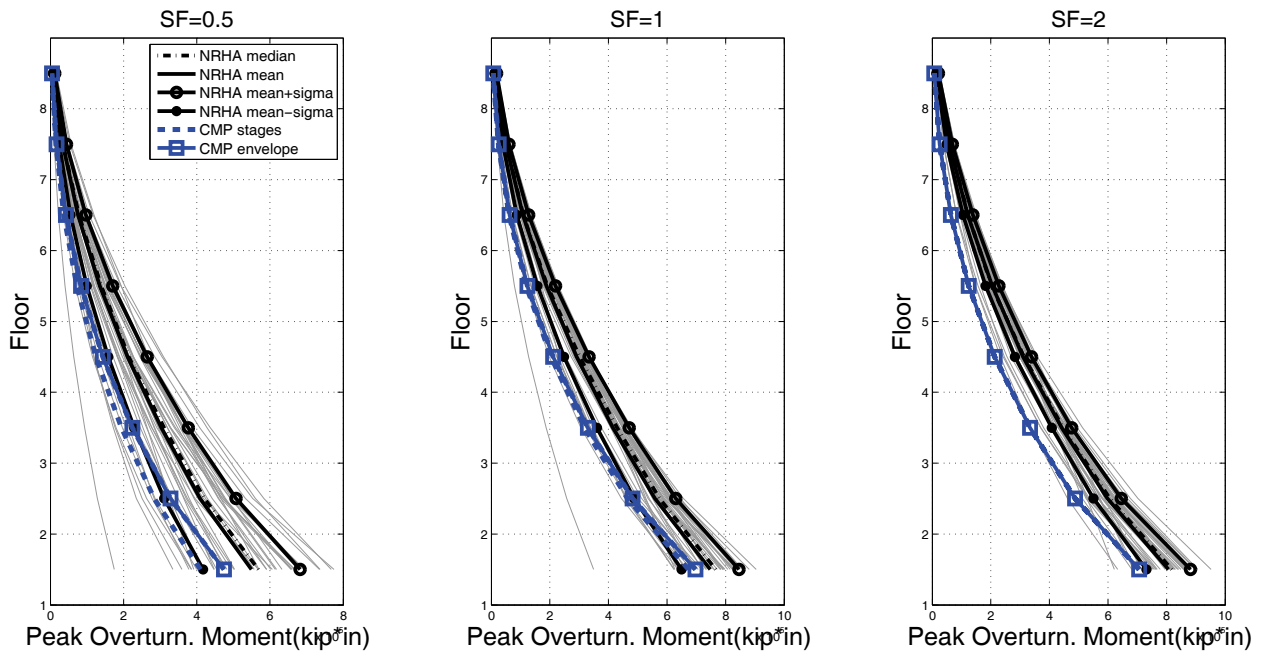


Figure B-41 8-story RCMF: NRHA versus CMP, peak overturning moment.

B.3.5 Modal Response Spectrum Analysis

When applied to structures in the nonlinear range of response, Modal Response Spectrum Analysis (MRSA) relies on simple extrapolations of linear behavior and thus approximately represents the equal displacement rule for deformation-related

quantities. The demands are calculated performing linear-elastic analysis using lateral load patterns proportional to the modes of vibration; the load patterns match those used in the MPA procedure. Target displacements are calculated using the C_1 and C_2 relationships of ASCE/SEI 41-06. The EDP values obtained using every mode-proportional lateral load pattern are then combined with the SRSS rule to obtain the final response estimate.

The figures that follow compare results obtained by MRSA and NRHA with respect to the three intensity levels and the EDPs considered.

Summary of Observations:

For the low-rise buildings (2- and 4-story RCMF), close estimates for both buildings are obtained for peak story drifts and peak story displacements regardless of the level of nonlinearity. This also applies to the 8-story frame. The second mode improves the estimates for the 8-story frame. For the $SF = 0.5$ level, the response coincides with that of the ASCE/SEI 41-06 method. Since the target displacement of the MPA and the MRSA methods are the same, for the $SF = 1$ and $SF = 2$ intensity levels, the two methods differ only slightly in the displacement and drift estimates for the lower stories.

As expected, significant errors in the MRSA story shears and overturning moments develop as the level of nonlinearity increases. For $SF = 0.5$, where both buildings are linear elastic, accurate estimates of force-related EDPs are obtained, although the benefit of including higher modes is apparent only for the 8-story building.

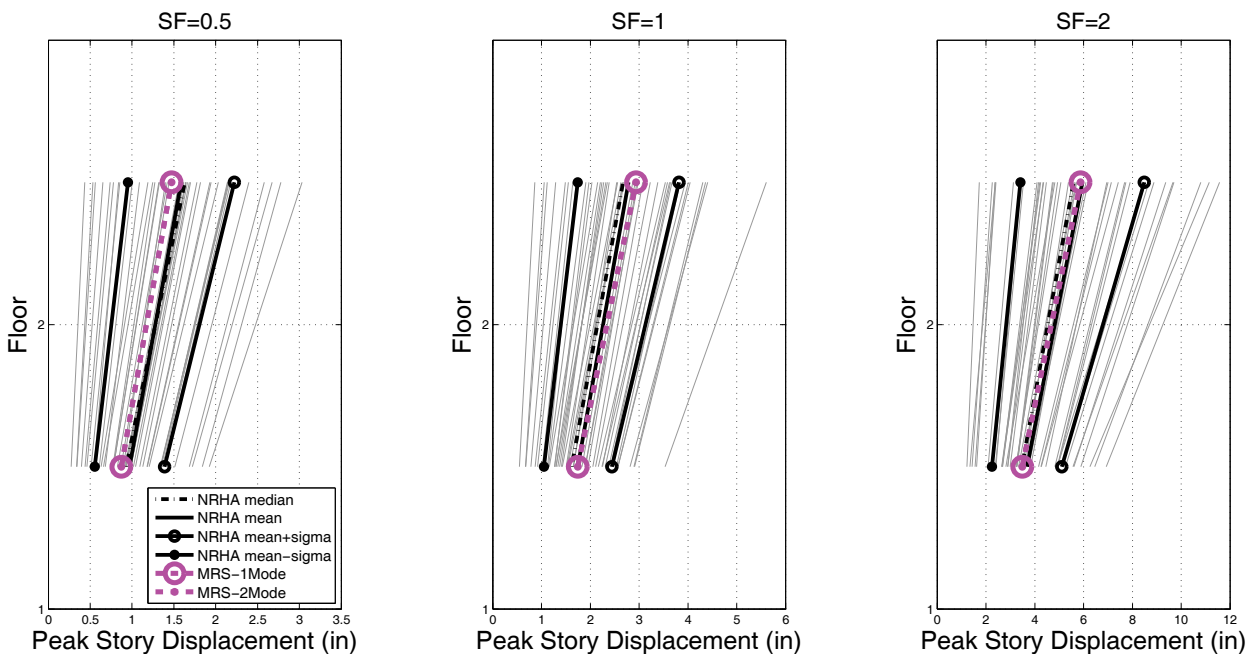


Figure B-42 2-story RCMF: NRHA versus MRSA, peak story displacement.

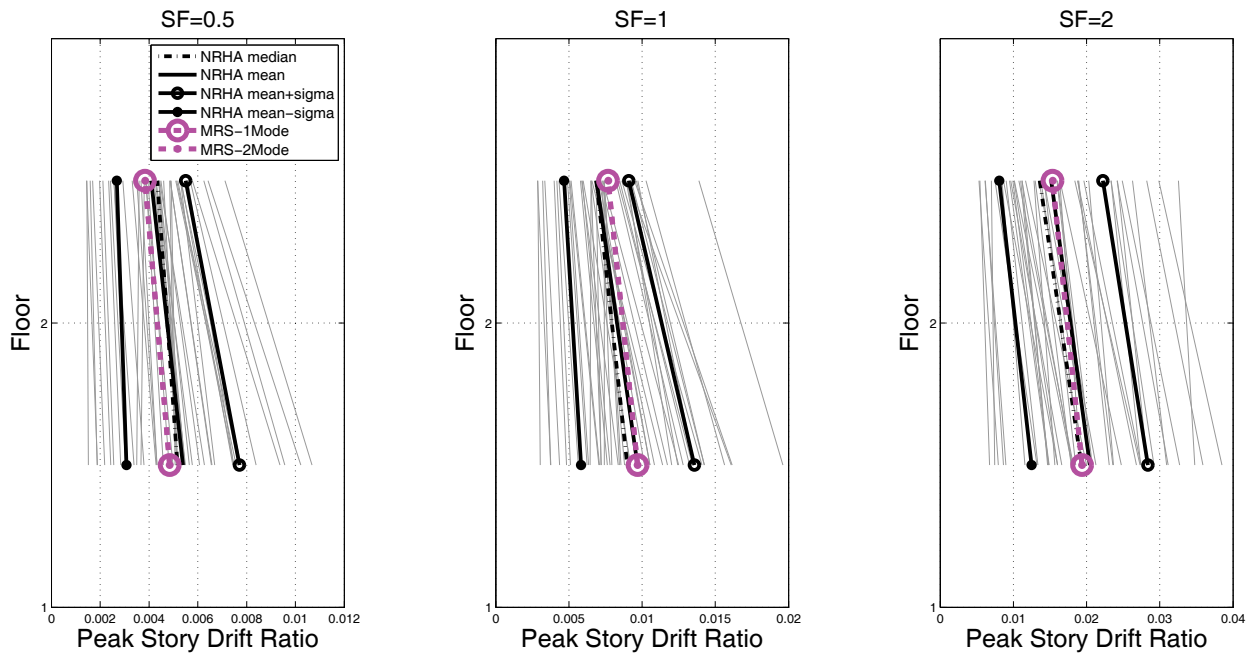


Figure B-43 2-story RCMF: NRHA versus MRSa, peak story drift ratio.

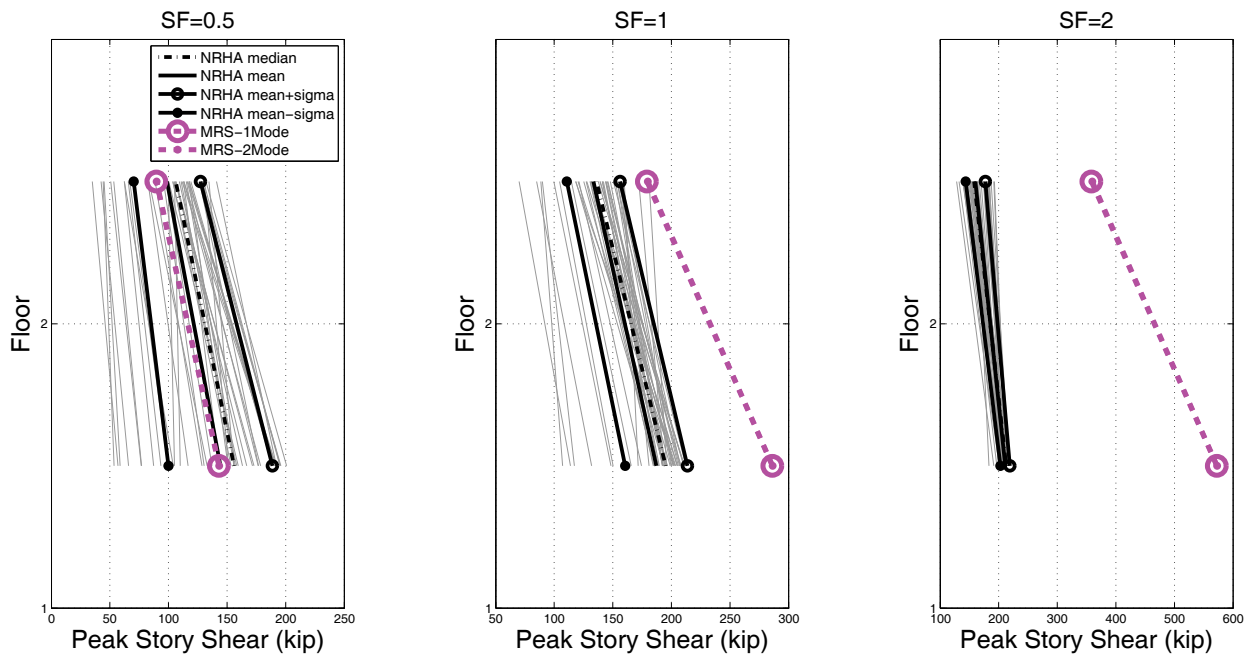


Figure B-44 2-story RCMF: NRHA versus MRSa, peak story shears.

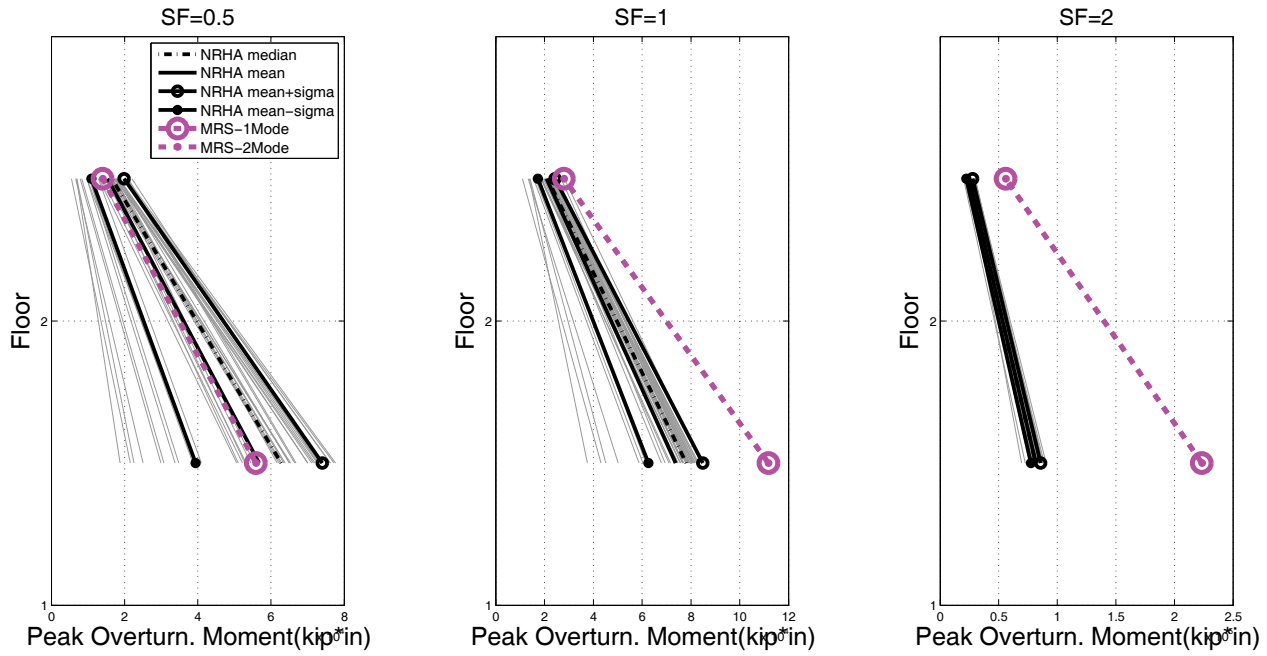


Figure B-45 2-story RCMF: NRHA versus MRS, peak overturning moments.

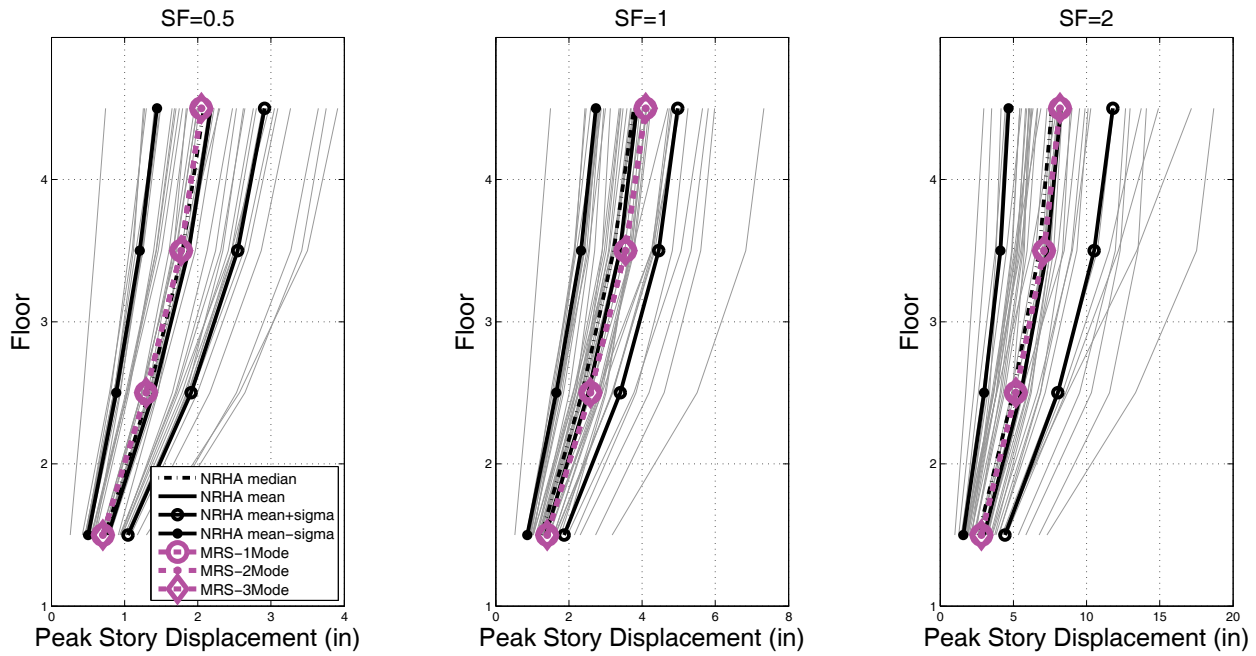


Figure B-46 4-story RCMF: NRHA versus MRS, peak story displacement.

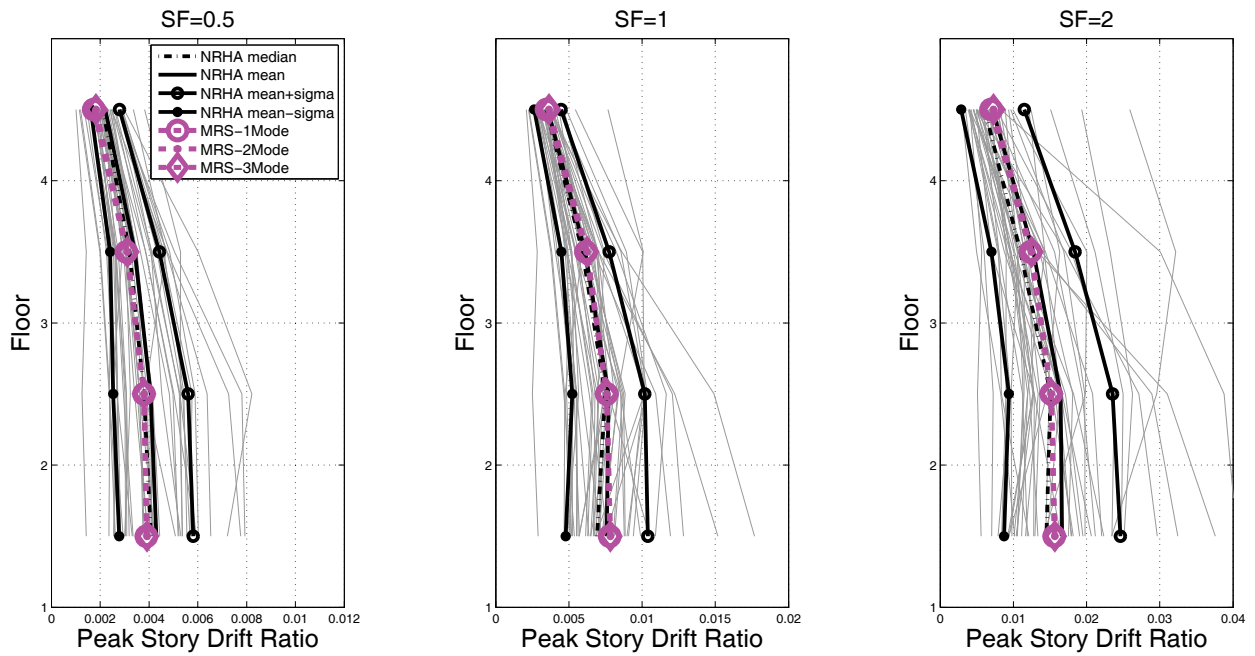


Figure B-47 4-story RCMF: NRHA versus MRSa, peak story drift ratio.

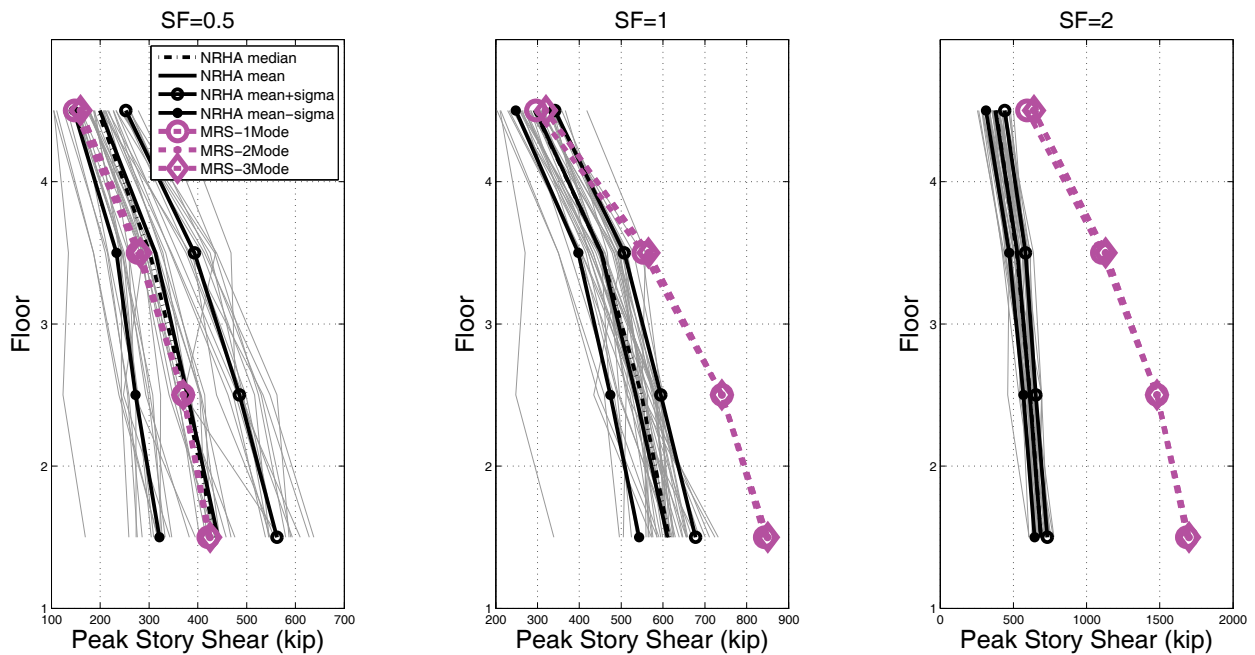


Figure B-48 4-story RCMF: NRHA versus MRSa, peak story shears.

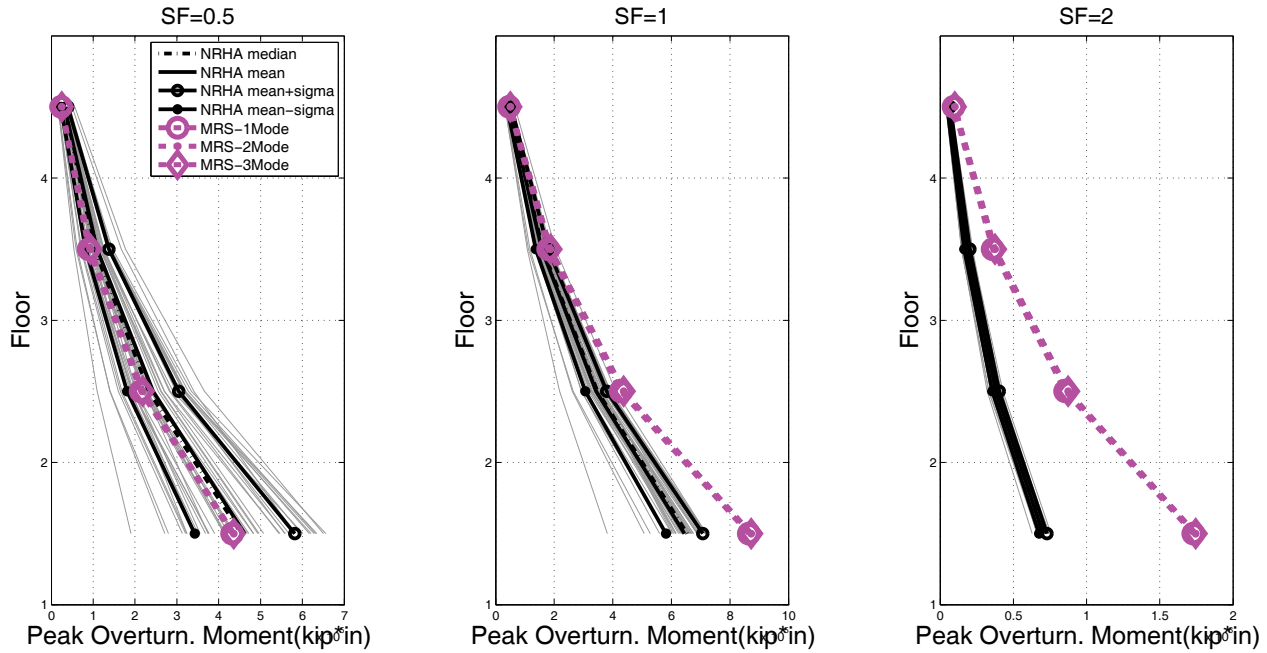


Figure B-49 4-story RCMF: NRHA versus MRSA, peak overturning moments.

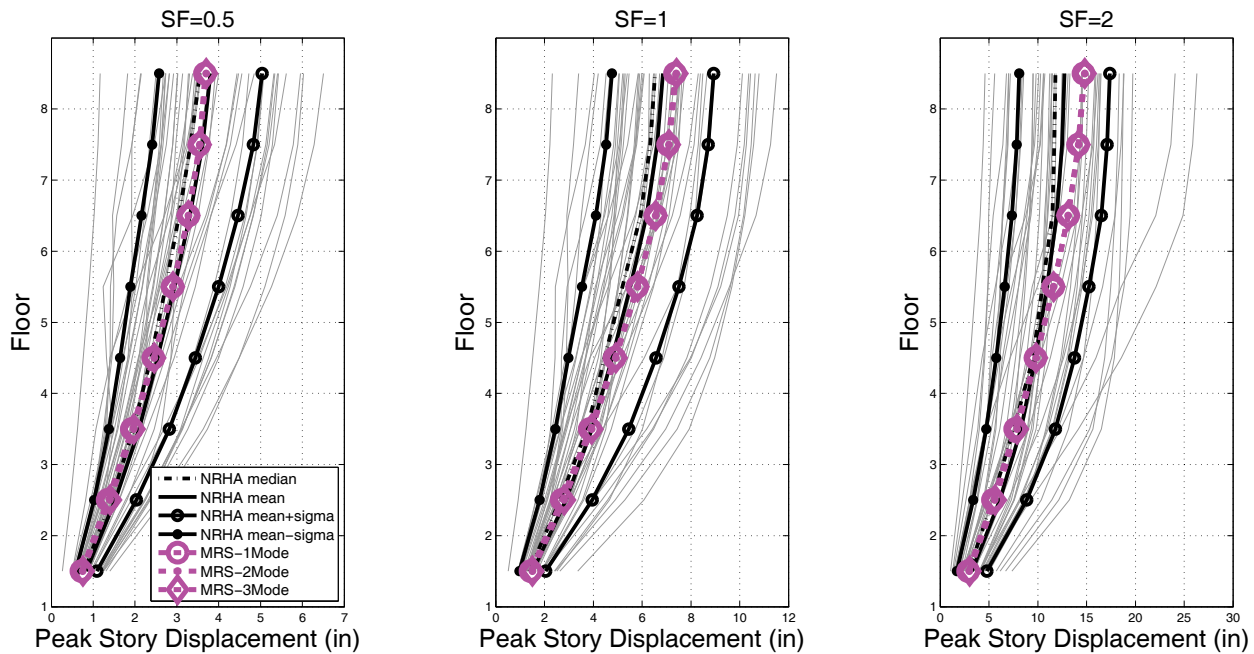


Figure B-50 8-story RCMF: NRHA versus MRSA, peak story displacement.

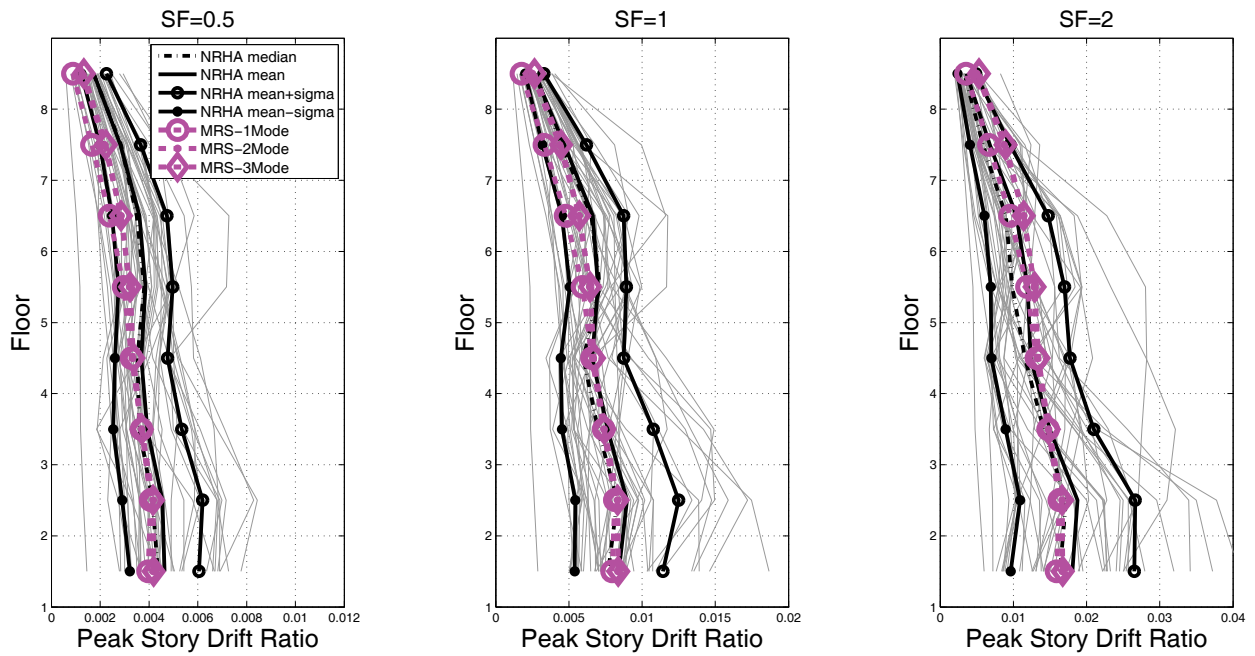


Figure B-51 8-story RCMF: NRHA versus MRS, peak story drift ratio.

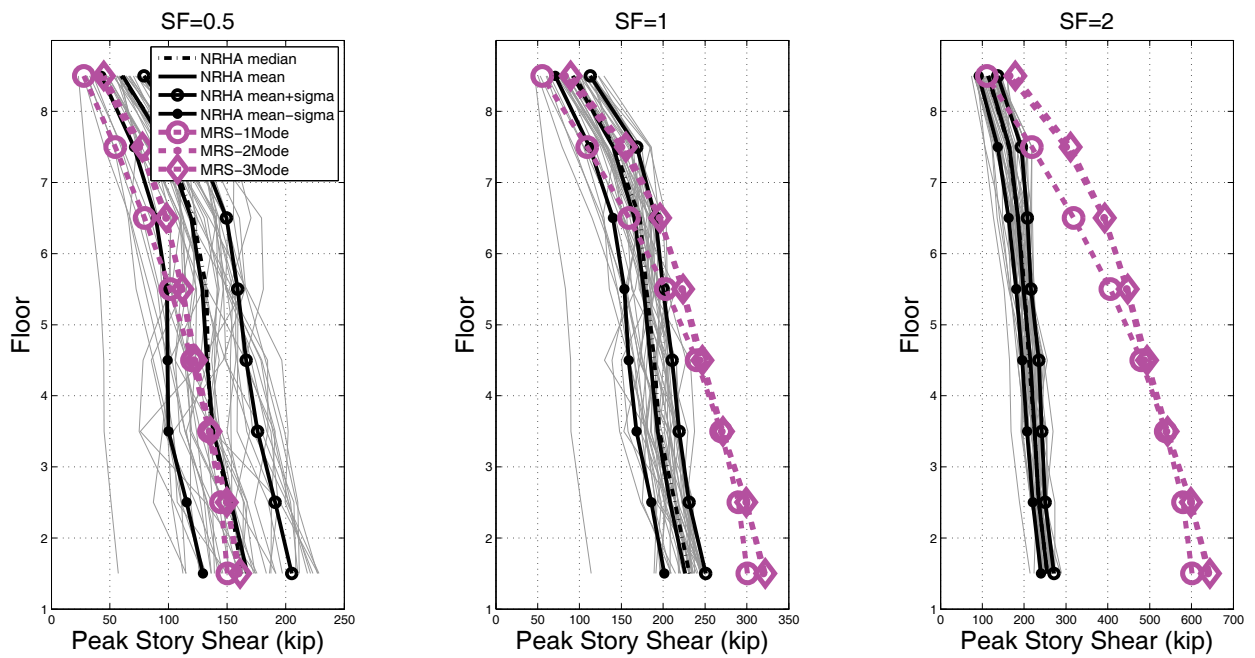


Figure B-52 8-story RCMF: NRHA versus MRS, peak story shears.

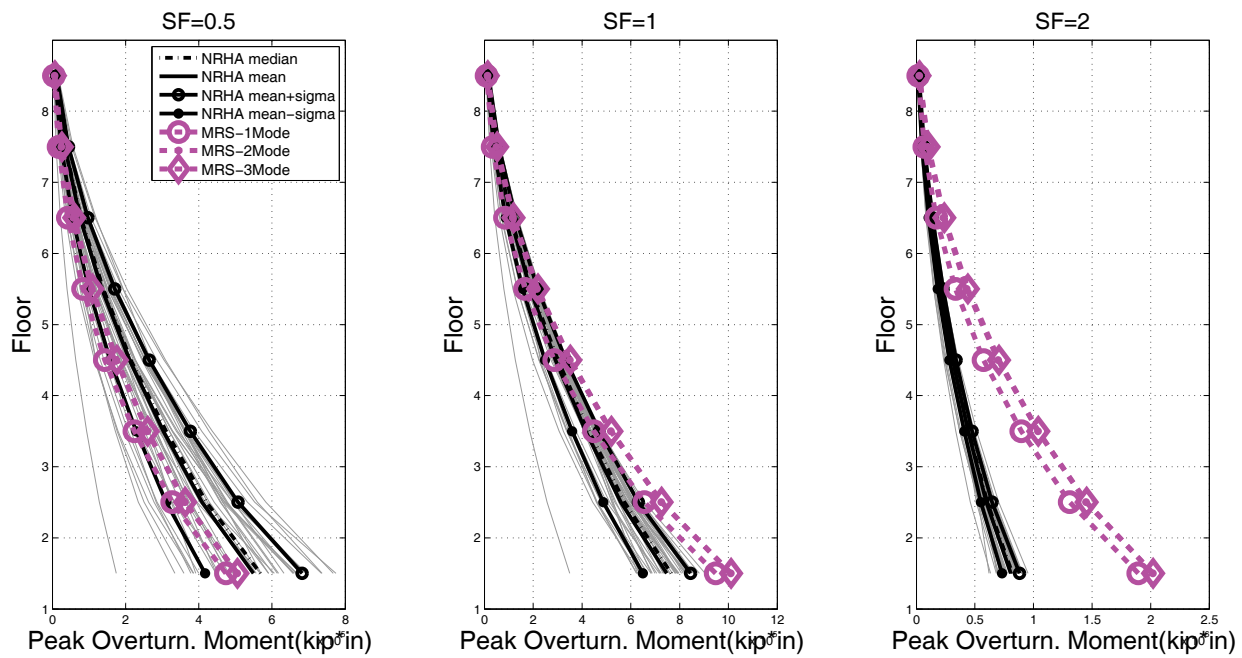


Figure B-53 8-story RCMF: NRHA versus MRS, peak overturning moments.

B.4 Summary and Comparison of the Analysis Methods

The following figures and tables present ratios of response quantity estimates using various methods to median values obtained from nonlinear response history analysis.

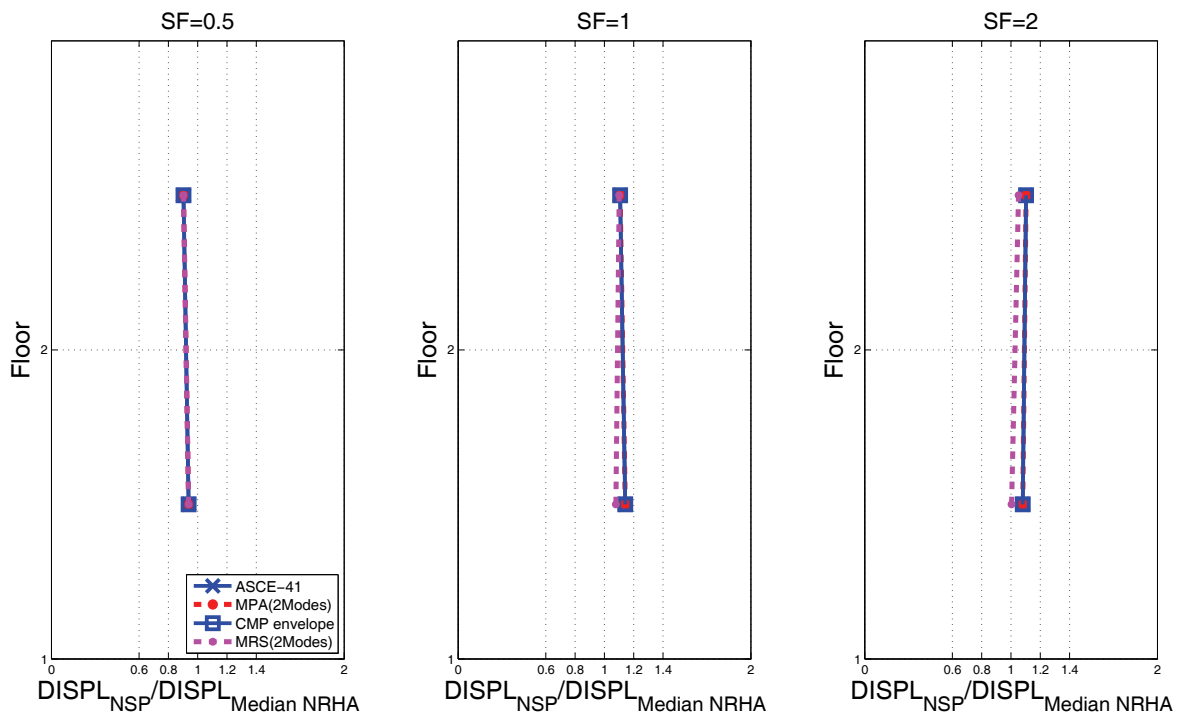


Figure B-54 2-story RCMF: ratio of estimate to NRHA median, peak story displacements.

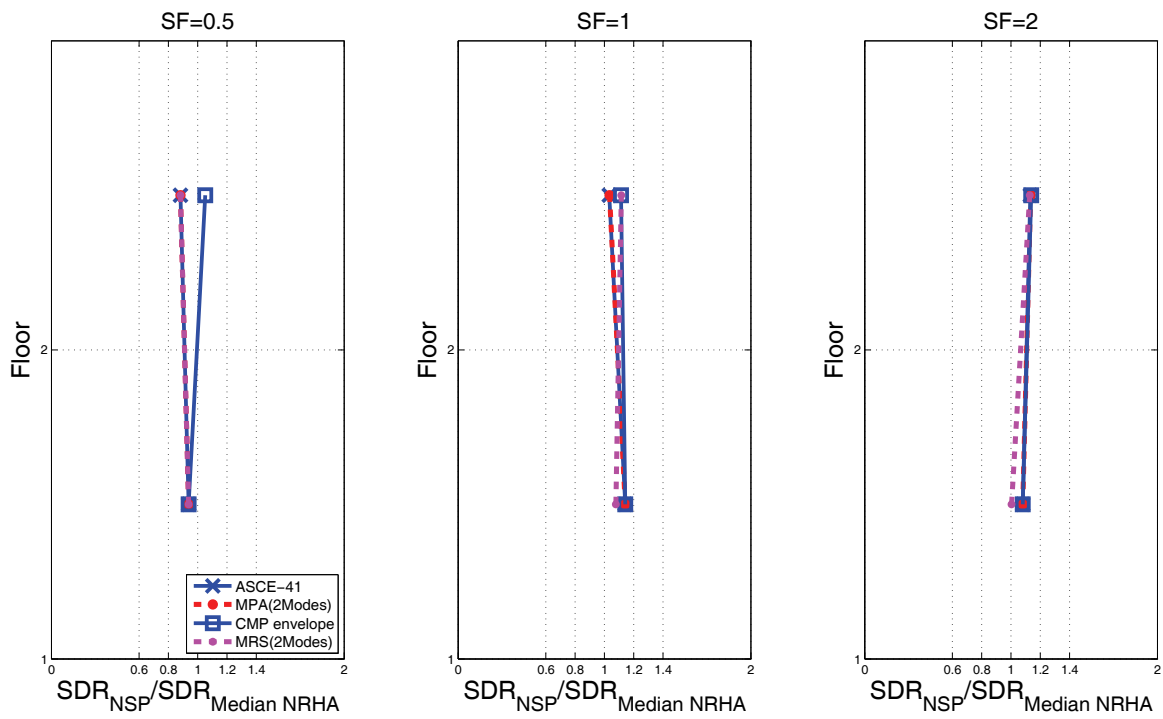


Figure B-55 2-story RCMF: ratio of estimate to NRHA median, peak story drift ratio.

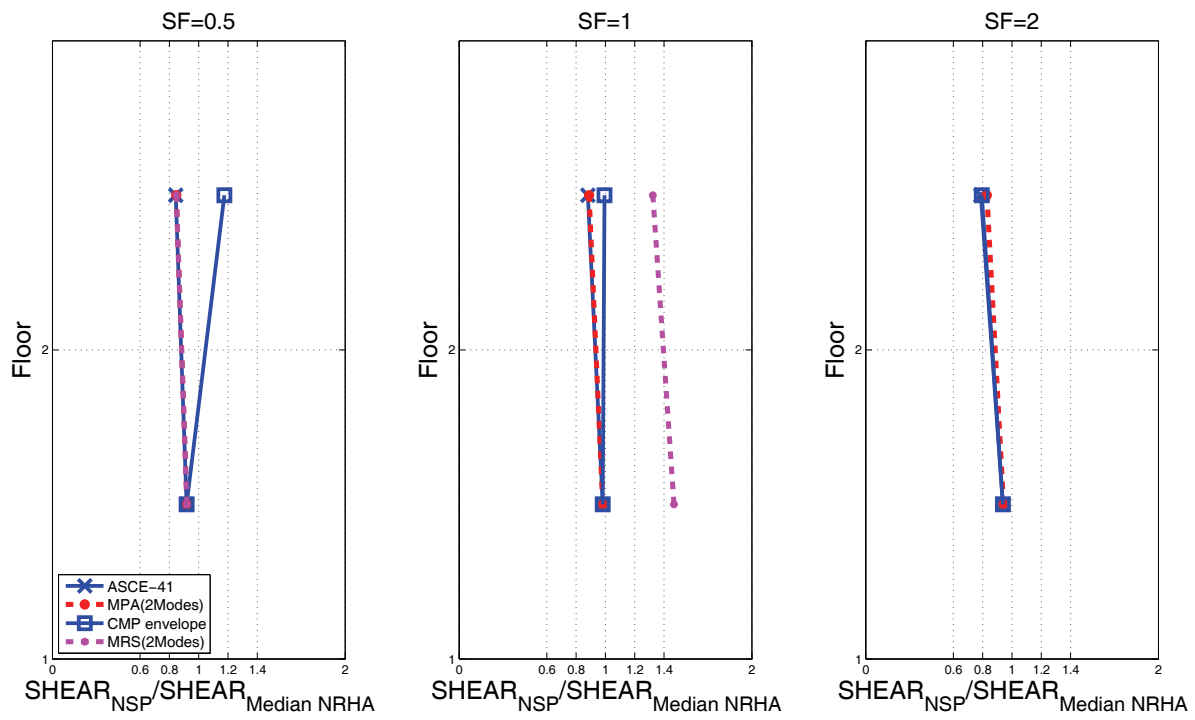


Figure B-56 2-story RCMF: ratio of Estimate to NRHA median, peak story shears.

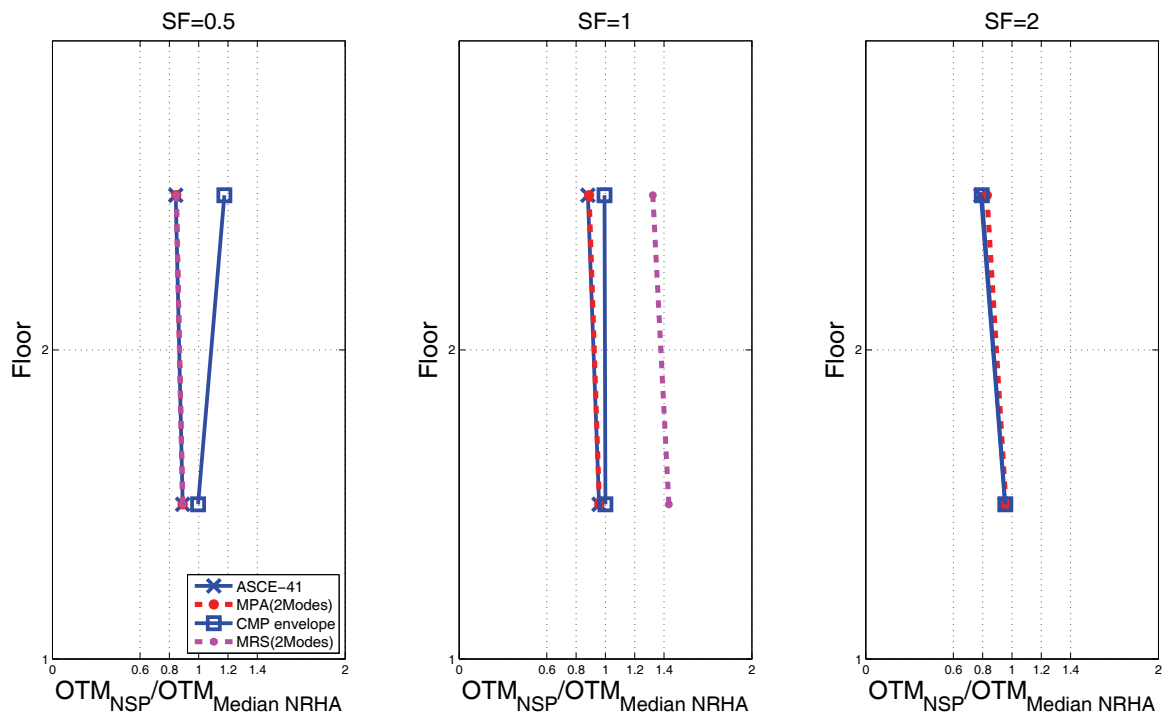


Figure B-57 2-story RCMF: ratio of estimate to NRHA median, peak overturning moments.

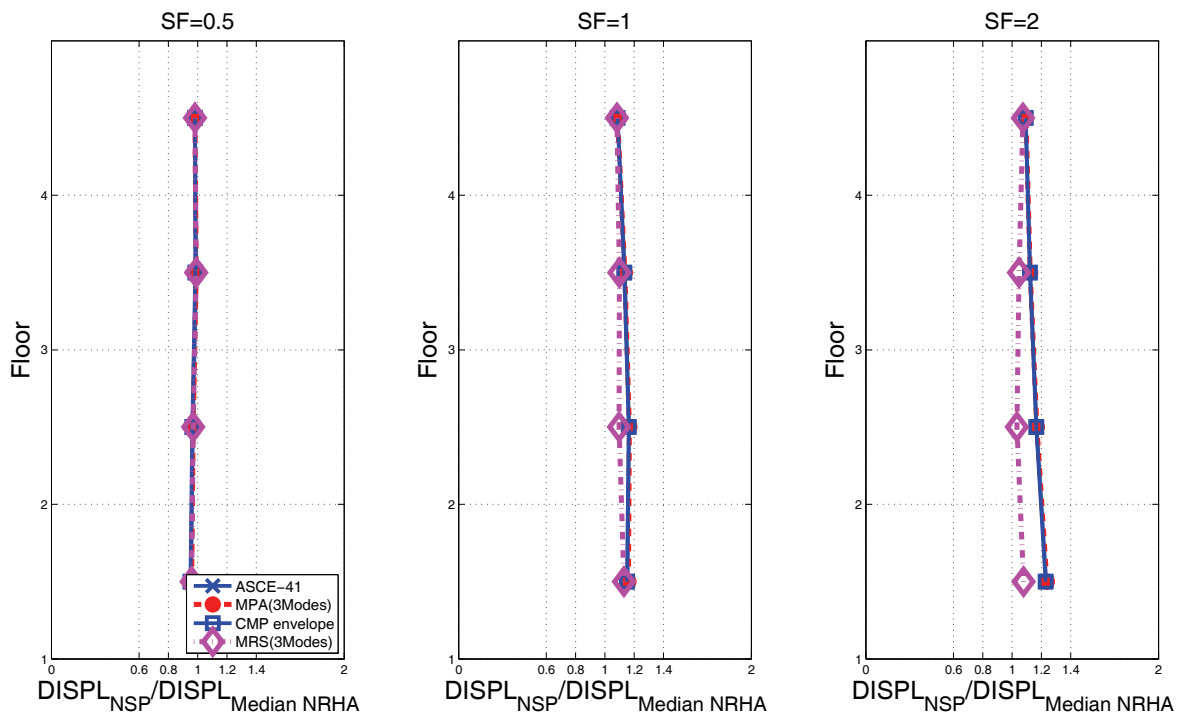


Figure B-58 4-story RCMF: ratio of estimate to NRHA median, peak story displacements.

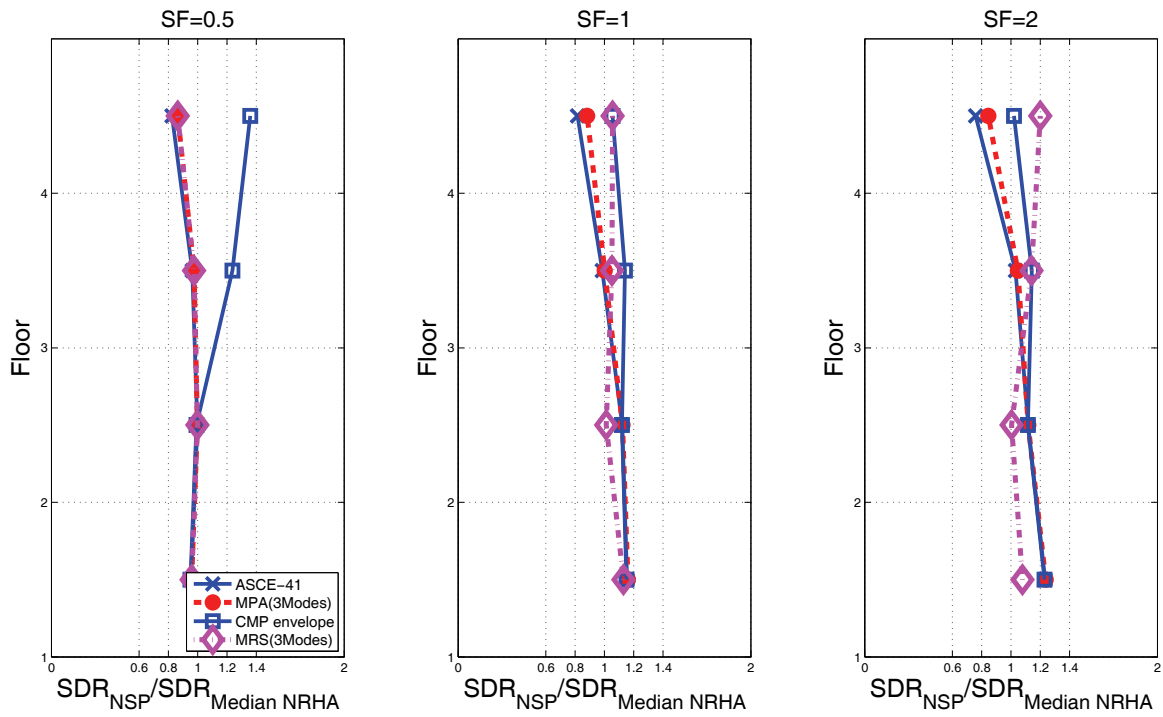


Figure B-59 4-story RCMF: ratio of estimate to NRHA median, peak story drift ratio.

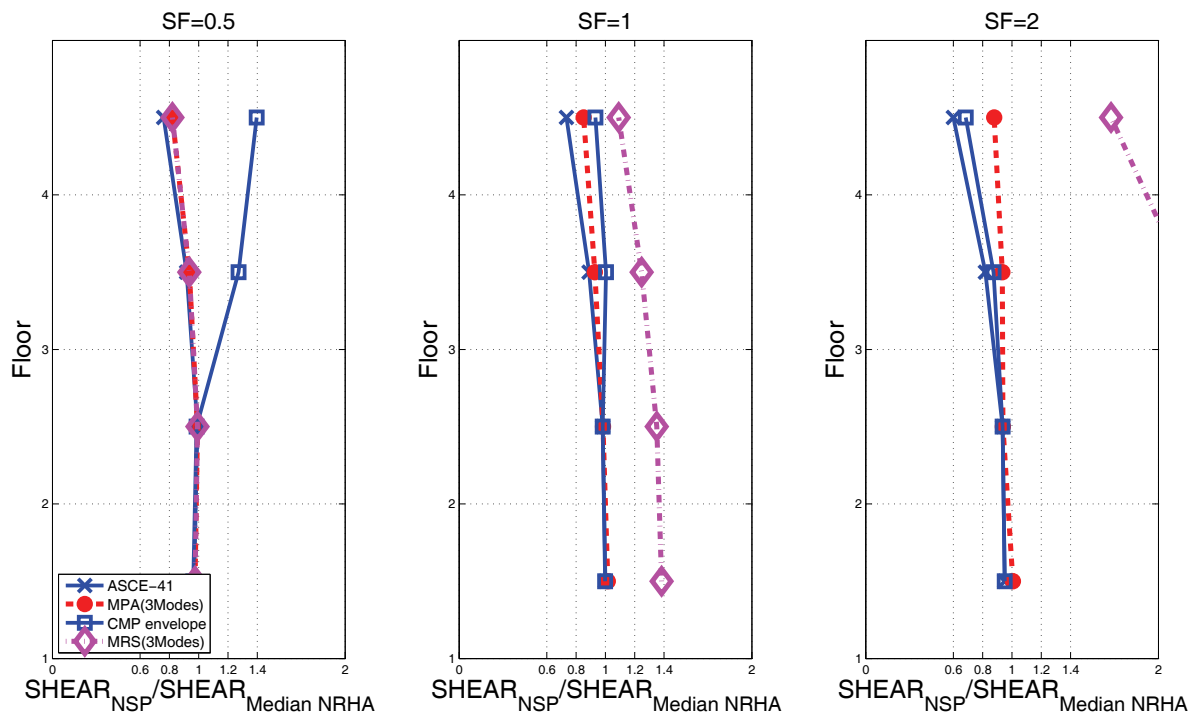


Figure B-60 4-story RCMF: ratio of estimate to NRHA median, peak story shears.

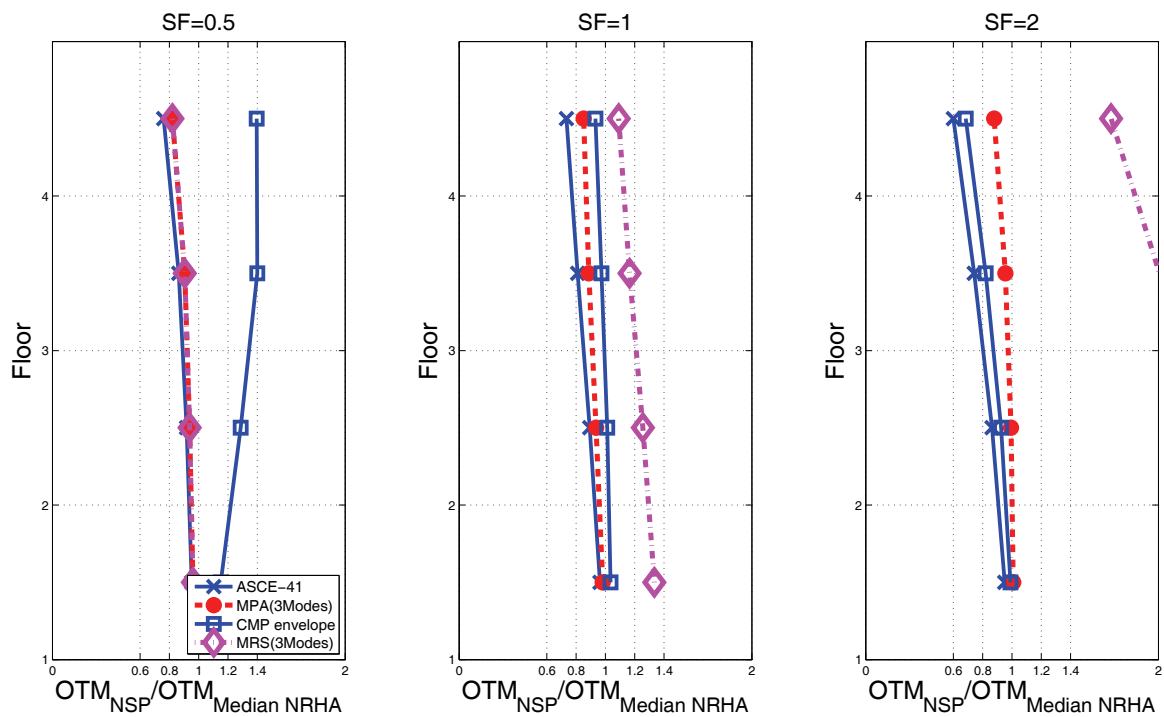


Figure B-61 4-story RCMF: ratio of estimate to NRHA median, peak overturning moments.

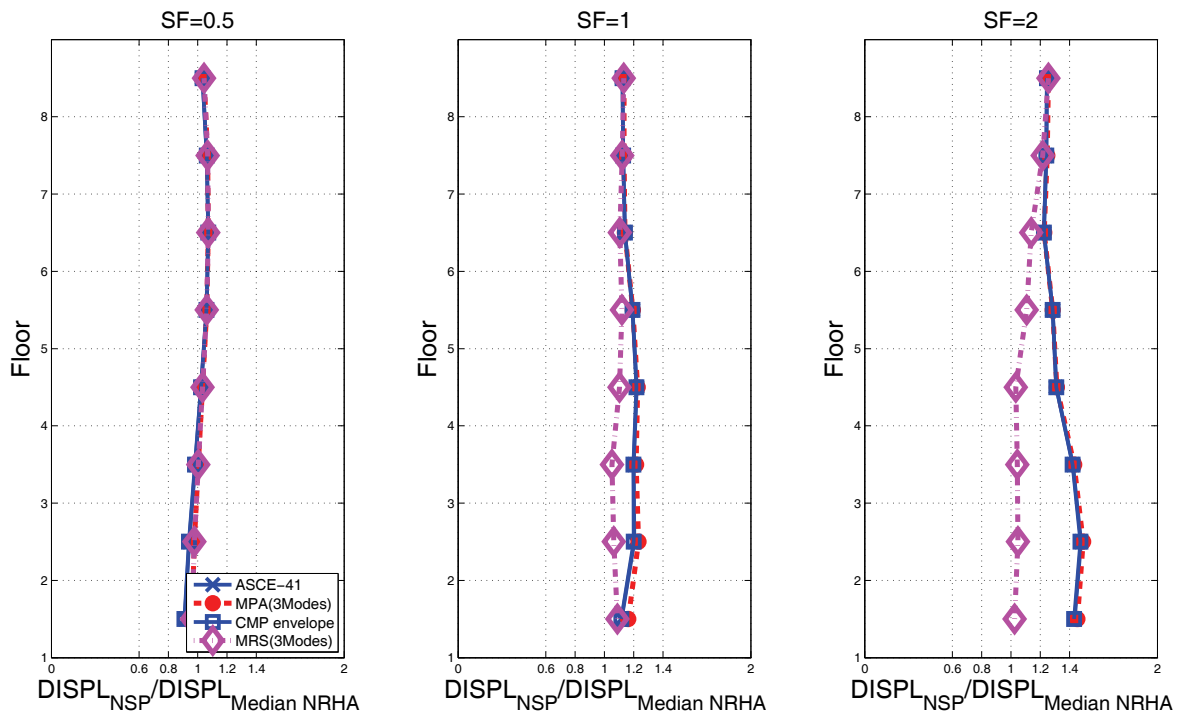


Figure B-62 8-story RCMF: ratio of estimate to NRHA median, peak story displacements.

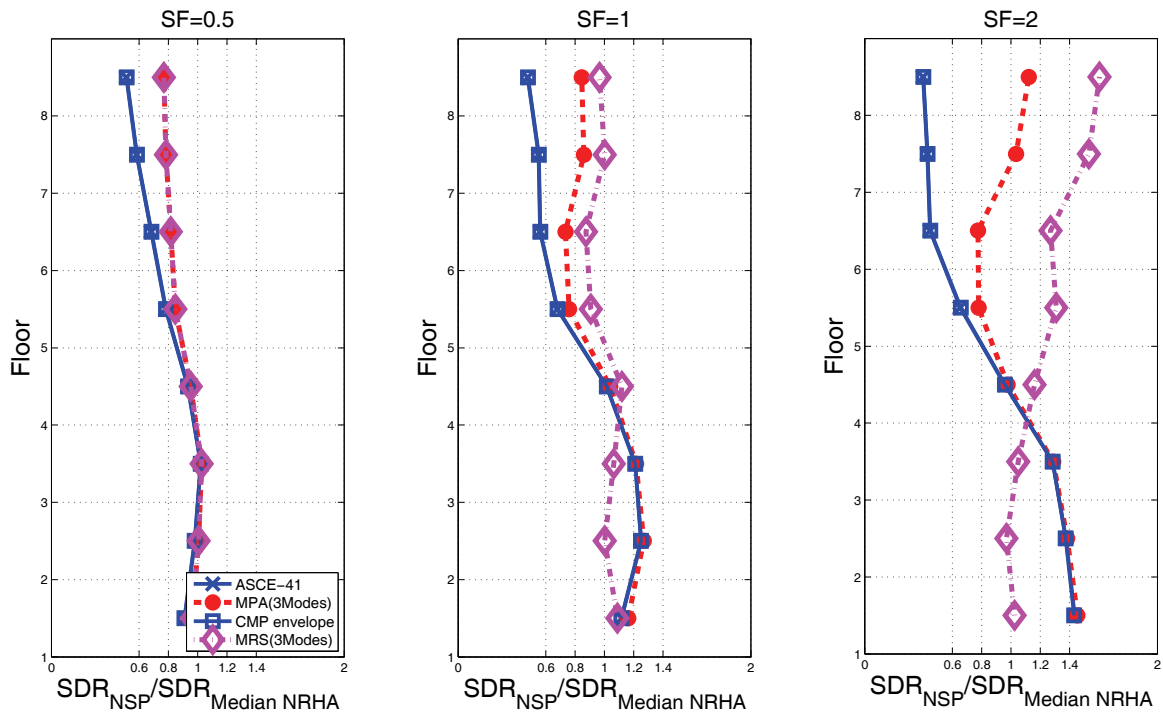


Figure B-63 8-story RCMF: ratio of estimate to NRHA median, peak story drift ratio.

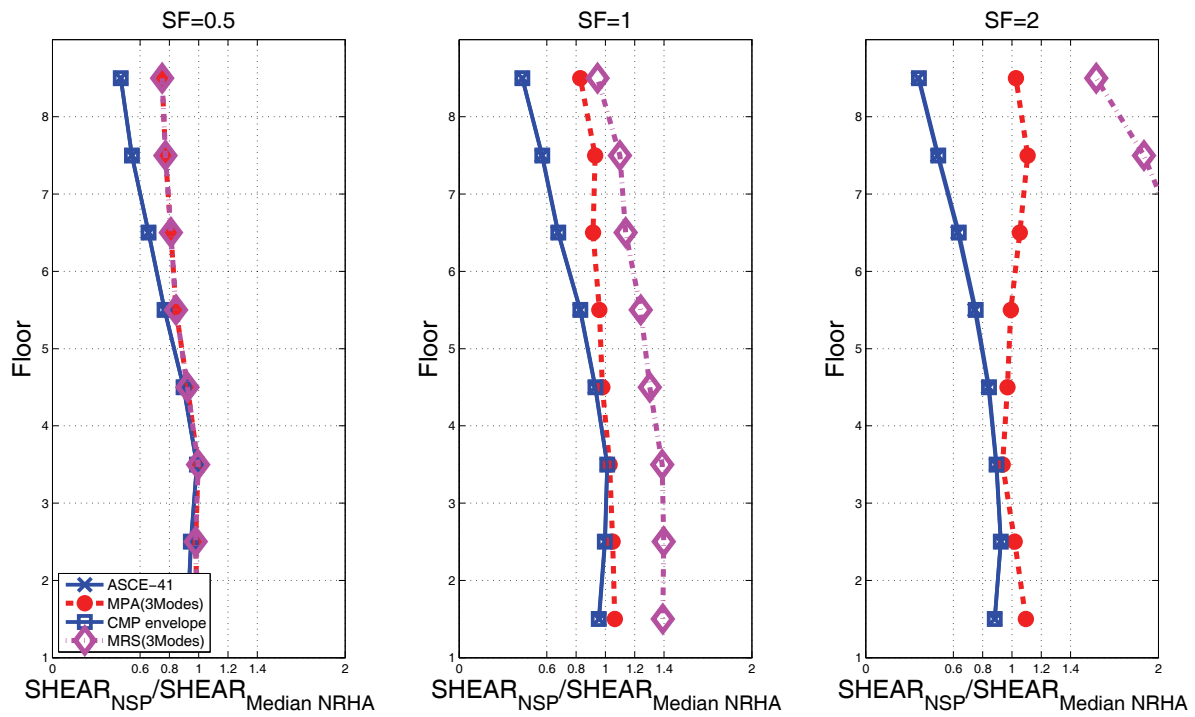


Figure B-64 8-story RCMF: ratio of estimate to NRHA median, peak story shears.

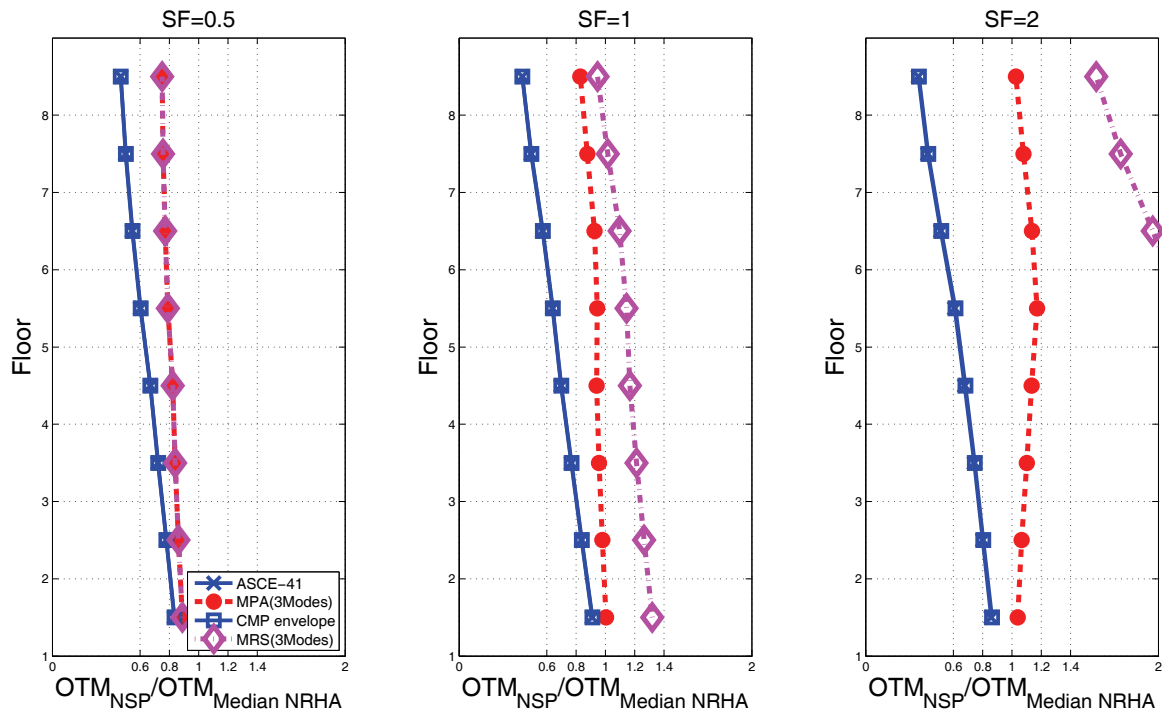


Figure B-65 8-story RCMF: ratio of estimate to NRHA median, peak overturning moments.

Table B-10 2-Story RCMF: Summary of Analysis Methods Showing the Estimate/Median NRHA Ratio

Story	Analysis method											
	First mode Static Pushover			Multi mode Pushover Analysis			Concecutive Modal Pushover Analysis			Elastic Modal Response Spectrum Analysis		
	SF = 0.5	SF = 1	SF = 2	SF = 0.5	SF = 1	SF = 2	SF = 0.5	SF = 1	SF = 2	SF = 0.5	SF = 1	SF = 2
Peak story displacements												
1	0.94	1.14	1.08	0.94	1.14	1.08	0.94	1.14	1.08	0.94	1.08	1.00
2	0.90	1.11	1.10	0.90	1.11	1.10	0.90	1.11	1.10	0.90	1.10	1.05
Min	0.90	1.11	1.08	0.90	1.11	1.08	0.90	1.11	1.08	0.90	1.08	1.00
Max	0.94	1.14	1.10	0.94	1.14	1.10	0.94	1.14	1.10	0.94	1.10	1.05
Peak story drift												
1	0.94	1.14	1.08	0.94	1.14	1.08	0.94	1.14	1.08	0.94	1.08	1.00
2	0.88	1.03	1.13	0.88	1.04	1.13	1.05	1.11	1.14	0.88	1.12	1.13
Min	0.88	1.03	1.08	0.88	1.04	1.08	0.94	1.11	1.08	0.88	1.08	1.00
Max	0.94	1.14	1.13	0.94	1.14	1.13	1.05	1.14	1.14	0.94	1.12	1.13
Peak story shears												
1	0.92	0.98	0.94	0.92	0.98	0.94	0.92	0.98	0.94	0.92	1.47	2.69
2	0.84	0.88	0.79	0.85	0.89	0.83	1.18	0.99	0.79	0.85	1.32	2.28
Min	0.84	0.88	0.79	0.85	0.89	0.83	0.92	0.98	0.79	0.85	1.32	2.28
Max	0.92	0.98	0.94	0.92	0.98	0.94	1.18	0.99	0.94	0.92	1.47	2.69
Peak overturning moments												
1	0.89	0.96	0.95	0.89	0.96	0.96	1.00	1.00	0.95	0.89	1.43	2.74
2	0.84	0.88	0.79	0.85	0.89	0.83	1.18	0.99	0.79	0.85	1.32	2.28
Min	0.84	0.88	0.79	0.85	0.89	0.83	1.00	0.99	0.79	0.85	1.32	2.28
Max	0.89	0.96	0.95	0.89	0.96	0.96	1.18	1.00	0.95	0.89	1.43	2.74

Table B-11 4-Story RCMF: Summary of Analysis Methods Showing the Estimate/Median NRHA Ratio

Story	Analysis method											
	First mode Static Pushover			Multi mode Pushover Analysis			Concecutive Modal Pushover Analysis			Elastic Modal Response Spectrum Analysis		
	SF = 0.5	SF = 1	SF = 2	SF = 0.5	SF = 1	SF = 2	SF = 0.5	SF = 1	SF = 2	SF = 0.5	SF = 1	SF = 2
	Peak story displacements											
1	0.96	1.15	1.23	0.96	1.16	1.24	0.95	1.15	1.23	0.96	1.13	1.08
2	0.97	1.17	1.17	0.97	1.17	1.17	0.96	1.16	1.17	0.97	1.10	1.03
3	0.99	1.14	1.12	0.99	1.14	1.12	0.98	1.13	1.12	0.99	1.10	1.05
4	0.98	1.09	1.09	0.98	1.09	1.09	0.98	1.09	1.09	0.98	1.08	1.07
min	0.96	1.09	1.09	0.96	1.09	1.09	0.95	1.09	1.09	0.96	1.08	1.03
max	0.99	1.17	1.23	0.99	1.17	1.24	0.98	1.16	1.23	0.99	1.13	1.08
Peak story drift												
1	0.96	1.15	1.23	0.96	1.16	1.24	0.95	1.15	1.23	0.96	1.13	1.08
2	1.00	1.12	1.12	1.00	1.12	1.12	0.99	1.12	1.12	1.00	1.01	1.01
3	0.96	0.99	1.03	0.98	1.00	1.05	1.24	1.14	1.14	0.98	1.05	1.14
4	0.82	0.82	0.76	0.86	0.88	0.84	1.36	1.05	1.02	0.86	1.06	1.20
min	0.82	0.82	0.76	0.86	0.88	0.84	0.95	1.05	1.02	0.86	1.01	1.01
max	1.00	1.15	1.23	1.00	1.16	1.24	1.36	1.15	1.23	1.00	1.13	1.20
Peak story shears												
1	0.97	1.00	0.95	0.98	1.02	1.01	0.96	1.00	0.95	0.98	1.38	2.47
2	0.99	0.98	0.94	0.99	0.98	0.94	0.99	0.98	0.94	0.99	1.35	2.42
3	0.92	0.89	0.82	0.94	0.93	0.93	1.27	1.00	0.88	0.94	1.25	2.16
4	0.76	0.73	0.60	0.82	0.85	0.88	1.40	0.93	0.68	0.82	1.09	1.68
min	0.76	0.73	0.60	0.82	0.85	0.88	0.96	0.93	0.68	0.82	1.09	1.68
max	0.99	1.00	0.95	0.99	1.02	1.01	1.40	1.00	0.95	0.99	1.38	2.47
Peak overturning moments												
1	0.95	0.96	0.95	0.96	0.98	1.01	1.15	1.03	0.99	0.96	1.34	2.48
2	0.92	0.89	0.86	0.94	0.94	0.99	1.29	1.01	0.93	0.94	1.26	2.29
3	0.86	0.81	0.74	0.90	0.89	0.96	1.40	0.97	0.82	0.90	1.17	2.01
4	0.76	0.73	0.60	0.82	0.85	0.88	1.40	0.93	0.68	0.82	1.09	1.68
min	0.76	0.73	0.60	0.82	0.85	0.88	1.15	0.93	0.68	0.82	1.09	1.68
max	0.95	0.96	0.95	0.96	0.98	1.01	1.40	1.03	0.99	0.96	1.34	2.48

Table B-12 8-Story RCMF: Summary of Analysis Methods Showing the Estimate/Median NRHA Ratio

Story	Analysis method											
	First mode Static Pushover			Multi mode Pushover Analysis			Concecutive Modal Pushover Analysis			Elastic Modal Response Spectrum Analysis		
	SF = 0.5	SF = 1	SF = 2	SF = 0.5	SF = 1	SF = 2	SF = 0.5	SF = 1	SF = 2	SF = 0.5	SF = 1	SF = 2
	Peak story displacements											
1	0.91	1.12	1.44	0.96	1.16	1.45	0.91	1.12	1.43	0.96	1.09	1.02
2	0.94	1.20	1.48	0.98	1.23	1.49	0.94	1.20	1.48	0.98	1.06	1.05
3	0.98	1.20	1.42	1.00	1.22	1.43	0.98	1.20	1.42	1.00	1.05	1.04
4	1.02	1.22	1.31	1.03	1.23	1.31	1.02	1.22	1.31	1.03	1.10	1.03
5	1.06	1.19	1.29	1.06	1.19	1.29	1.06	1.19	1.28	1.06	1.12	1.11
6	1.07	1.14	1.23	1.07	1.14	1.23	1.07	1.14	1.23	1.07	1.10	1.14
7	1.06	1.13	1.24	1.07	1.13	1.25	1.06	1.13	1.24	1.07	1.12	1.22
8	1.03	1.12	1.25	1.04	1.13	1.26	1.03	1.12	1.25	1.04	1.13	1.26
Min	0.91	1.12	1.23	0.96	1.13	1.23	0.91	1.12	1.23	0.96	1.05	1.02
Max	1.07	1.22	1.48	1.07	1.23	1.49	1.07	1.22	1.48	1.07	1.13	1.26
	Peak story drift											
1	0.91	1.12	1.44	0.96	1.16	1.45	0.91	1.12	1.43	0.96	1.09	1.02
2	0.98	1.25	1.38	1.01	1.27	1.38	0.98	1.25	1.37	1.01	1.00	0.97
3	1.02	1.21	1.29	1.03	1.22	1.29	1.02	1.21	1.29	1.03	1.06	1.05
4	0.93	1.02	0.96	0.95	1.04	0.98	0.93	1.02	0.96	0.95	1.12	1.16
5	0.78	0.68	0.65	0.85	0.76	0.78	0.78	0.68	0.66	0.85	0.91	1.31
6	0.68	0.56	0.45	0.82	0.73	0.78	0.68	0.56	0.45	0.82	0.87	1.27
7	0.58	0.55	0.43	0.78	0.86	1.03	0.58	0.55	0.43	0.78	1.00	1.53
8	0.51	0.48	0.40	0.77	0.84	1.12	0.51	0.48	0.40	0.77	0.97	1.61
Min	0.51	0.48	0.40	0.77	0.73	0.78	0.51	0.48	0.40	0.77	0.87	0.97
Max	1.02	1.25	1.44	1.03	1.27	1.45	1.02	1.25	1.43	1.03	1.12	1.61
	Peak story shears											
1	0.92	0.96	0.88	0.99	1.06	1.10	0.92	0.96	0.88	0.99	1.39	2.52
2	0.95	1.00	0.92	0.98	1.05	1.02	0.95	1.00	0.92	0.98	1.40	2.55
3	0.99	1.01	0.89	1.00	1.03	0.94	0.99	1.01	0.89	1.00	1.39	2.41
4	0.90	0.93	0.84	0.92	0.98	0.97	0.90	0.93	0.84	0.92	1.30	2.34
5	0.77	0.83	0.75	0.84	0.96	0.99	0.77	0.83	0.75	0.84	1.24	2.23
6	0.66	0.68	0.63	0.81	0.92	1.05	0.66	0.68	0.64	0.81	1.14	2.11
7	0.54	0.57	0.49	0.77	0.93	1.11	0.54	0.57	0.50	0.77	1.10	1.90
8	0.47	0.43	0.36	0.75	0.83	1.03	0.47	0.43	0.36	0.75	0.95	1.57
Min	0.47	0.43	0.36	0.75	0.83	0.94	0.47	0.43	0.36	0.75	0.95	1.57
Max	0.99	1.01	0.92	1.00	1.06	1.11	0.99	1.01	0.92	1.00	1.40	2.55

Table B-12 8-Story RCMF: Summary of Analysis Methods Showing the Estimate/Median NRHA Ratio (continued)

Story	Analysis method											
	First mode Static Pushover			Multi mode Pushover Analysis			Concecutive Modal Pushover Analysis			Elastic Modal Response Spectrum Analysis		
	SF = 0.5	SF = 1	SF = 2	SF = 0.5	SF = 1	SF = 2	SF = 0.5	SF = 1	SF = 2	SF = 0.5	SF = 1	SF = 2
Peak overturning moments												
1	0.83	0.91	0.86	0.89	1.00	1.04	0.83	0.91	0.86	0.89	1.32	2.47
2	0.78	0.84	0.80	0.86	0.98	1.07	0.78	0.84	0.80	0.86	1.26	2.40
3	0.72	0.77	0.74	0.84	0.96	1.10	0.72	0.77	0.75	0.84	1.21	2.33
4	0.67	0.70	0.68	0.82	0.94	1.13	0.67	0.70	0.68	0.82	1.17	2.25
5	0.60	0.64	0.61	0.79	0.94	1.17	0.60	0.64	0.61	0.79	1.14	2.17
6	0.55	0.57	0.51	0.77	0.93	1.14	0.55	0.57	0.52	0.77	1.10	1.96
7	0.50	0.49	0.42	0.76	0.88	1.08	0.50	0.50	0.43	0.76	1.02	1.74
8	0.47	0.43	0.36	0.75	0.83	1.03	0.47	0.43	0.36	0.75	0.95	1.57
<i>min</i>	0.47	0.43	0.36	0.75	0.83	1.03	0.47	0.43	0.36	0.75	0.95	1.57
<i>max</i>	0.83	0.91	0.86	0.89	1.00	1.17	0.83	0.91	0.86	0.89	1.32	2.47

B.5 Correlation Between Intermediate-Level and Component-Level Engineering Demand Parameters

Design codes and standards focus practicing engineers' attention on component-level engineering demand parameters (EDPs), while intermediate level EDPs such as floor displacements, story drifts, story shears, and floor overturning moments, as well as global (system) level EDPs have been emphasized in much of this document.

Generally, accurate estimates of intermediate level EDPs are necessary if a method has the potential to accurately estimate a local level EDP. The figures that follow demonstrate the correlation of local and intermediate level EDP values obtained by NRHA. Four pairs of component and intermediate level EDPs are shown, as follows:

- column axial load and story overturning moment,
- column shear force and story shear,
- beam end rotation and story drift,
- column end rotation and story drift.

Results are presented in two sets of figures. On the abscissa, the component level EDP is plotted, while on the ordinate, the corresponding intermediate-level EDP is shown. The first set of figures presents the EDP values for a specific section of a beam (or a column) as obtained after the 132 (3×44) NRHA analyses, along with

lines representing correlations obtained by principal components analysis. The second set of Figures shows the corresponding median values for every column and beam of the building.

Summary of Observations:

The first set of figures (Figure B-67 to B-78) presents the correlation in terms of “clouds” of data points, with the correlation coefficient provided for every scale factor in the legend. According to the correlation coefficient values shown, the correlation varies with the intensity level and with the pair of component and intermediate level EDPs evaluated. In almost every case, good correlation is obtained for SF = 0.5 and SF = 1 (usually of the order of 0.9 and 0.7, respectively). In some cases, relatively low values are obtained for SF = 2.

For the second set of Figures (Figure B-79 to B-90), in general, good correlation is observed for all four combinations and every frame building. The best correlation appears for the column shear force vs. story shear and the column axial load vs. story overturning moment pairs, while column end rotation and story drift have a somewhat worse correlation. The linear regression lines indicate the degree to which the plotted values are linearly correlated. Although conclusions cannot be drawn for the 2-story building, the 4-story and the 8-story regression lines have small error relative to the median data.

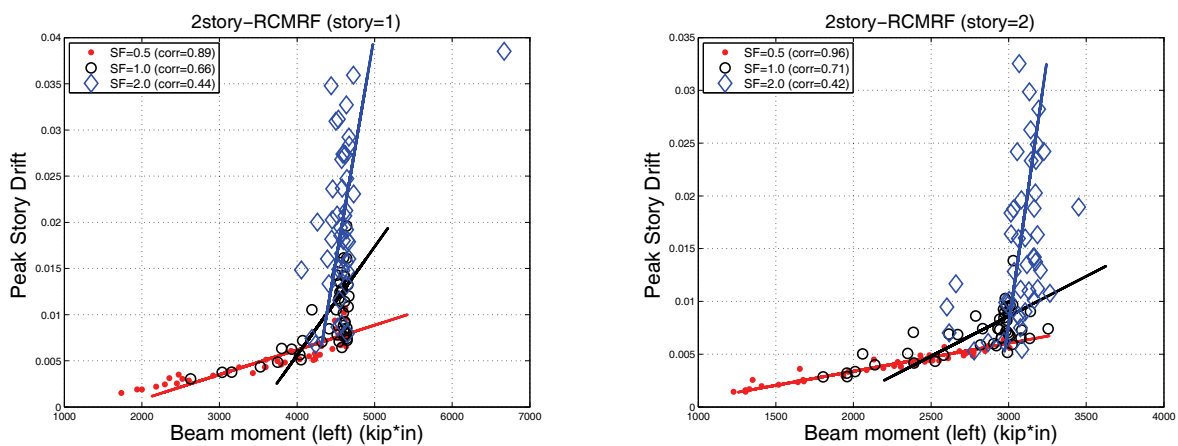


Figure B-66 2-story RCMF: Correlation of peak story drift versus peak beam moment for the exterior beam of the 1st (left) and the 2nd story (right)

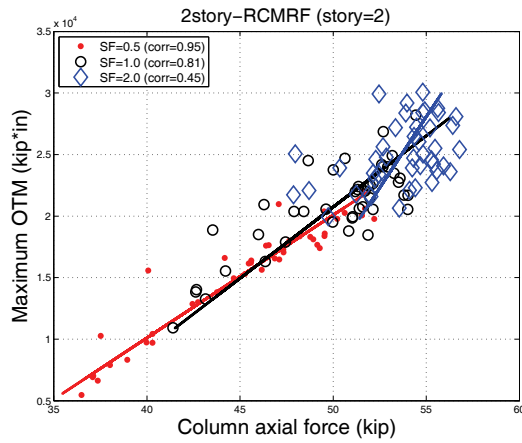
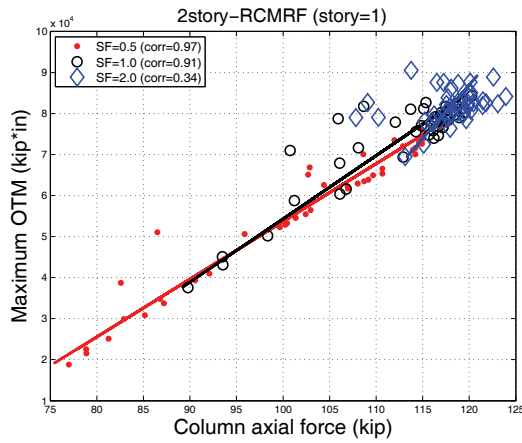


Figure B-67 2-story RCMF: Correlation of peak overturning moment versus the peak column axial force of the exterior column of the 1st (left) and the 2nd story (right)

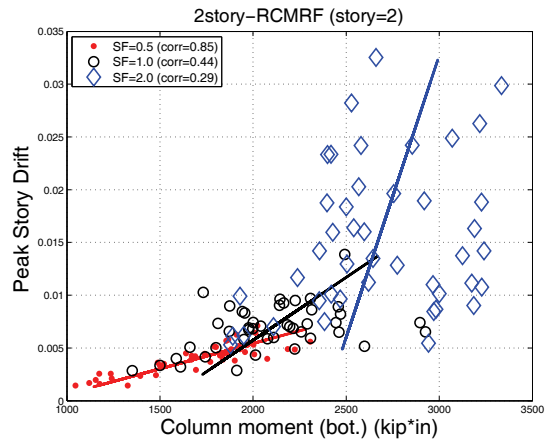
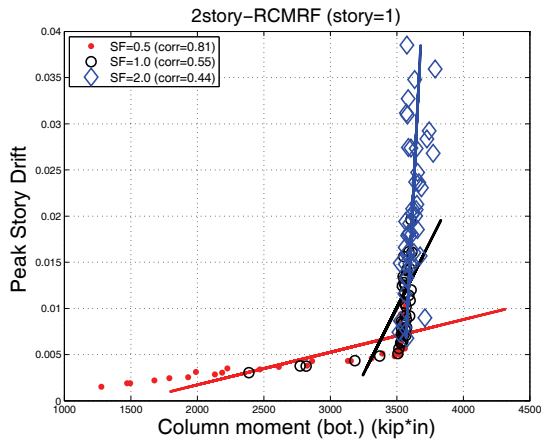


Figure B-68 2-story RCMF: Correlation of peak story drift versus peak column moment for the exterior column of the 1st (left) and the 2nd story (right)

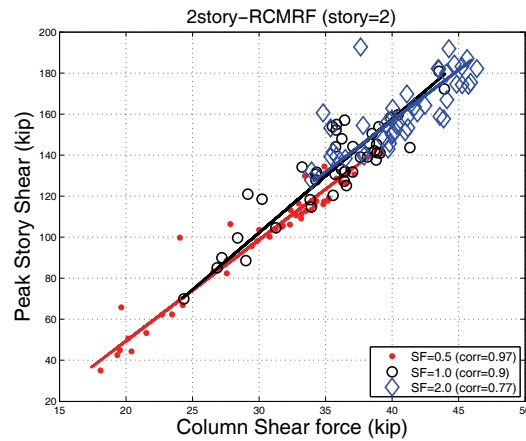
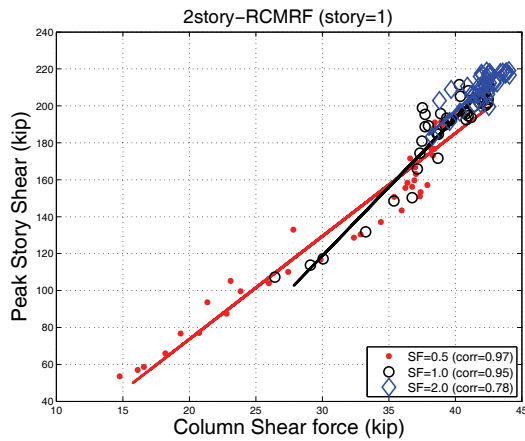


Figure B-69 2-story RCMF: Correlation of peak story shear versus peak column shear for the exterior column of the 1st (left) and the 2nd story (right)

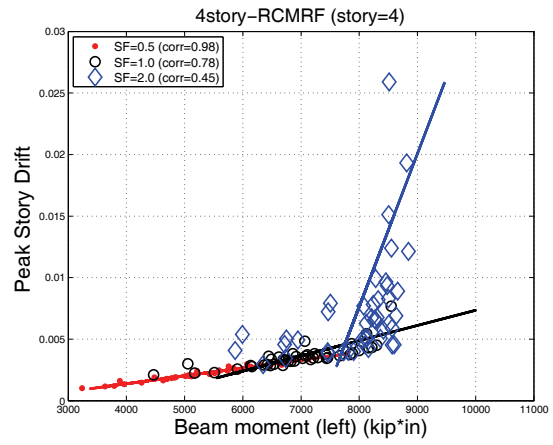
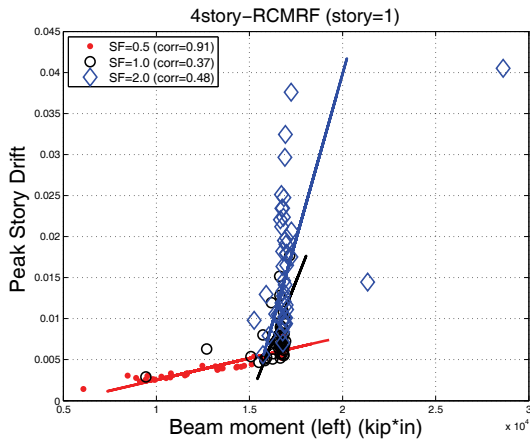


Figure B-70 4-story RCMF: Correlation of peak story drift versus peak beam moment for the exterior beam of the 1st (left) and the 2nd story (right)

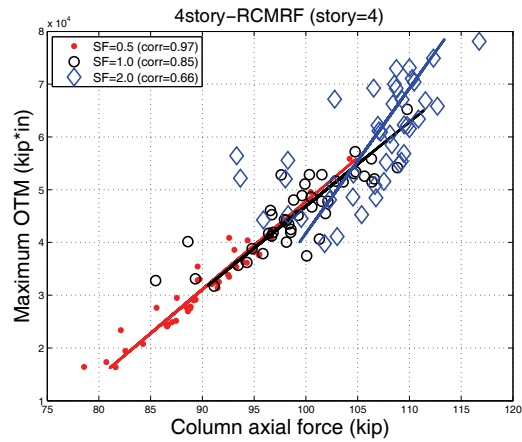
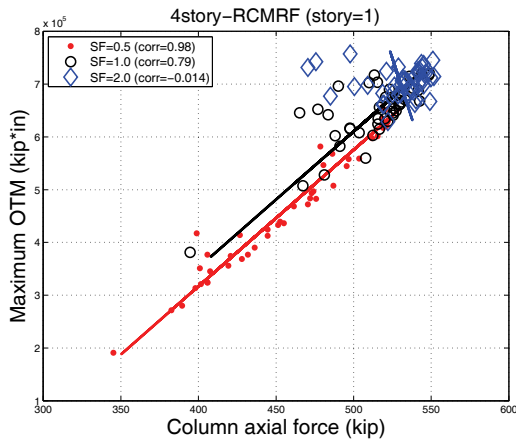


Figure B-71 4-story RCMF: Correlation of peak overturning moment versus the peak column axial force of the exterior column of the 1st (left) and the 2nd story (right)

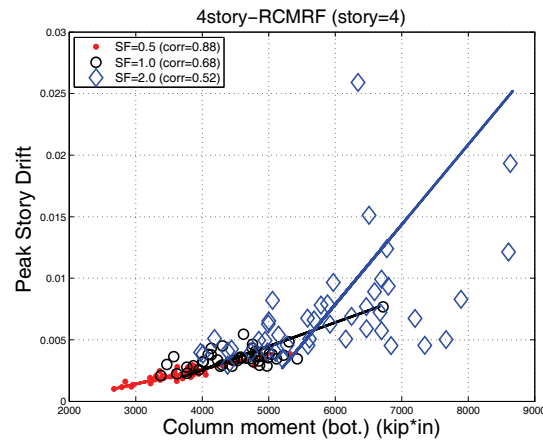
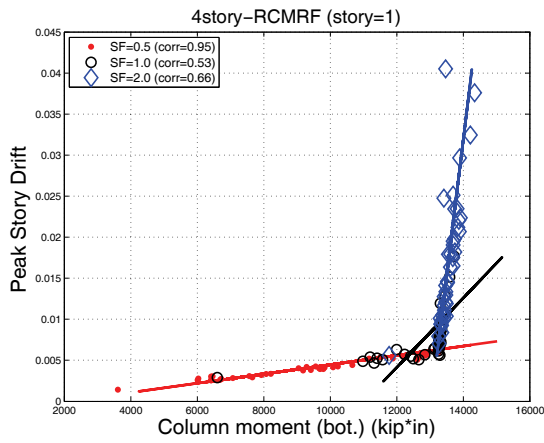


Figure B-72 4-story RCMF: Correlation of peak story drift versus peak column moment for the exterior column of the 1st (left) and the 2nd story (right).

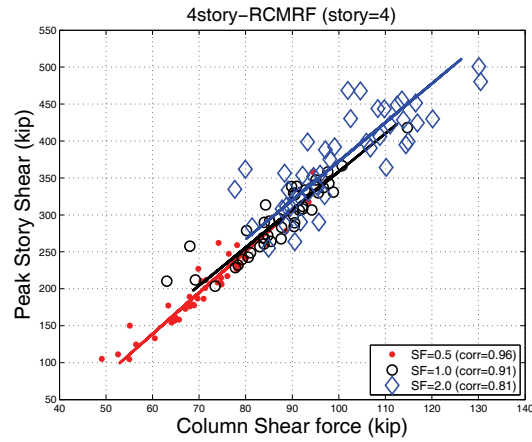
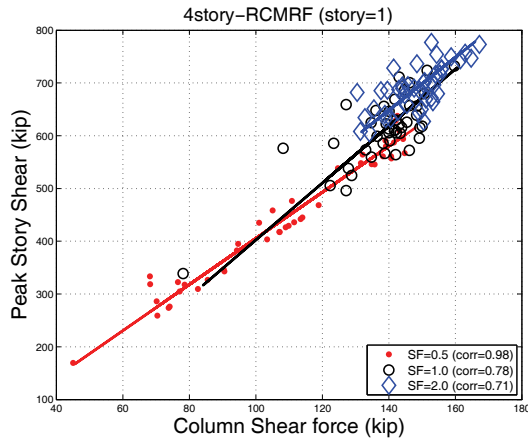


Figure B-73 4-story RCMF: Correlation of peak story shear versus peak column shear for the exterior column of the 1st (left) and the 2nd story (right).

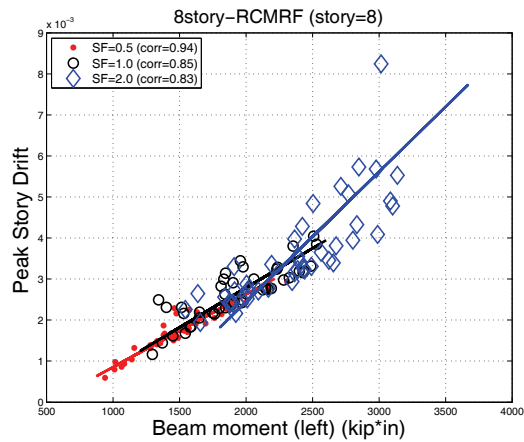
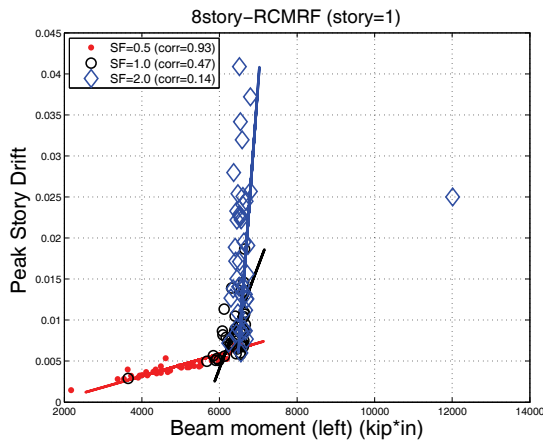


Figure B-74 8-story RCMF: Correlation of peak story drift versus peak beam moment for the exterior column of the 1st (left) and the 2nd story (right).

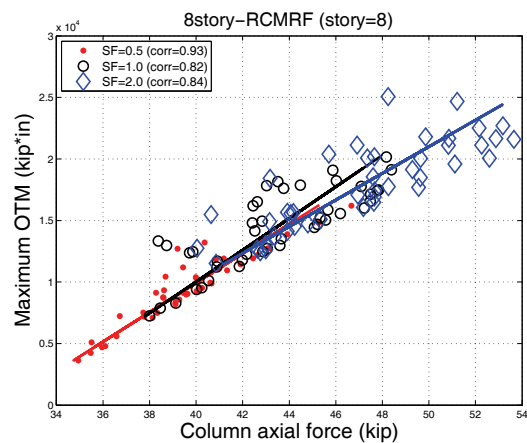
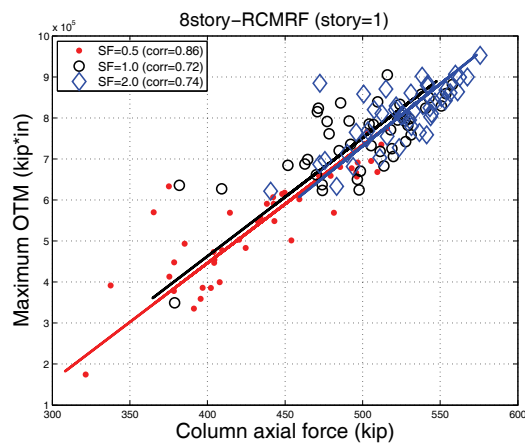


Figure B-75 8-story RCMF: Correlation peak overturning moment versus the peak column axial force of the exterior column of the 1st (left) and the 2nd story (right).

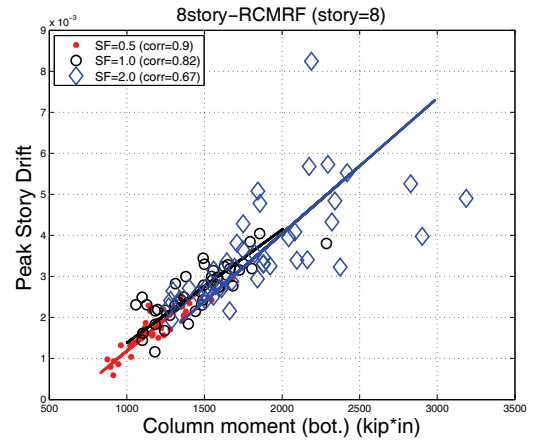
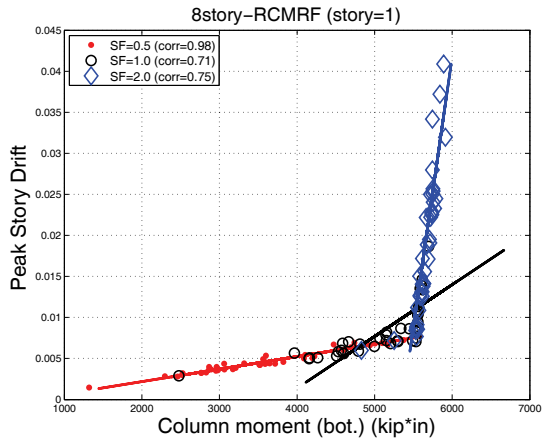


Figure B-76 8-story RCMRF: Correlation of peak story drift versus peak column moment for the exterior column of the 1st (left) and the 2nd story (right).

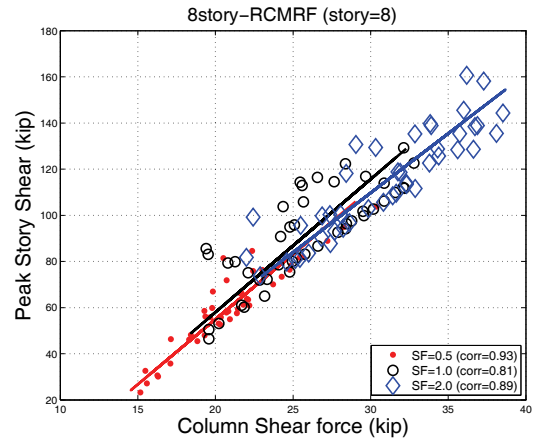
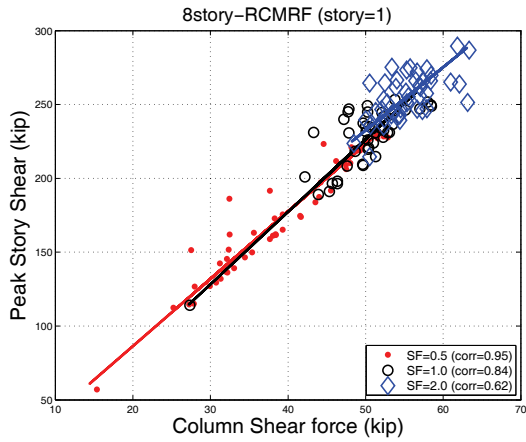


Figure B-77 8-story RCMRF: Correlation of peak story shear versus peak column shear for the exterior column of the 1st (left) and the 2nd story (right).

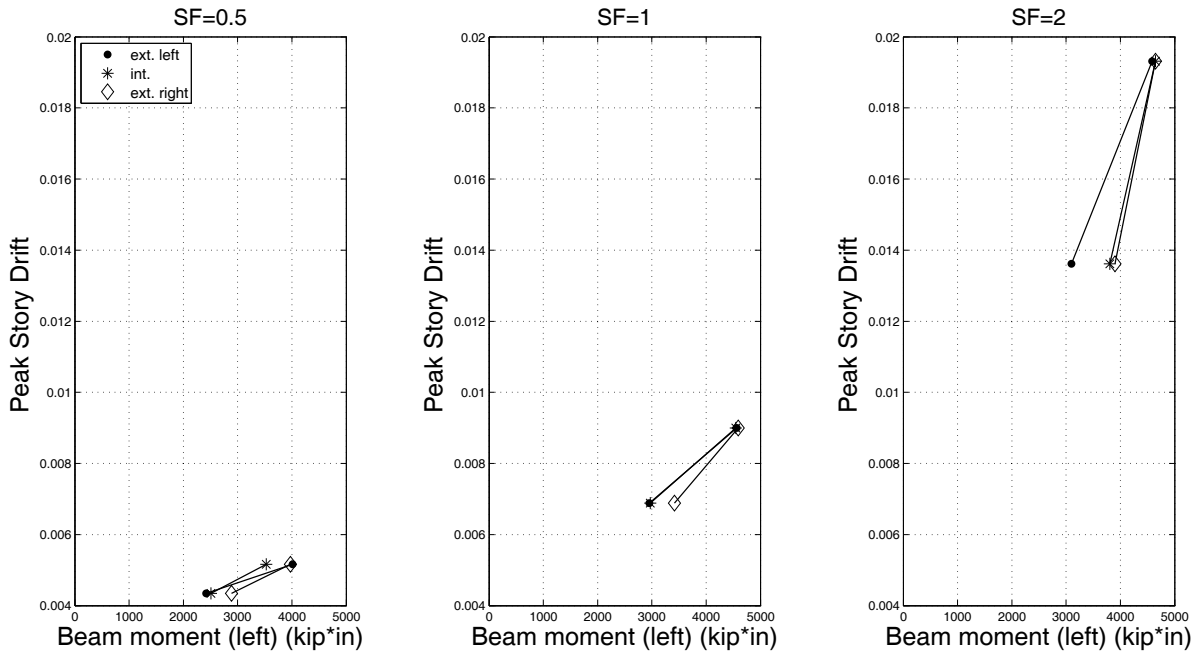


Figure B-78 2-story RCMF: Correlation of peak story drift versus peak beam moment

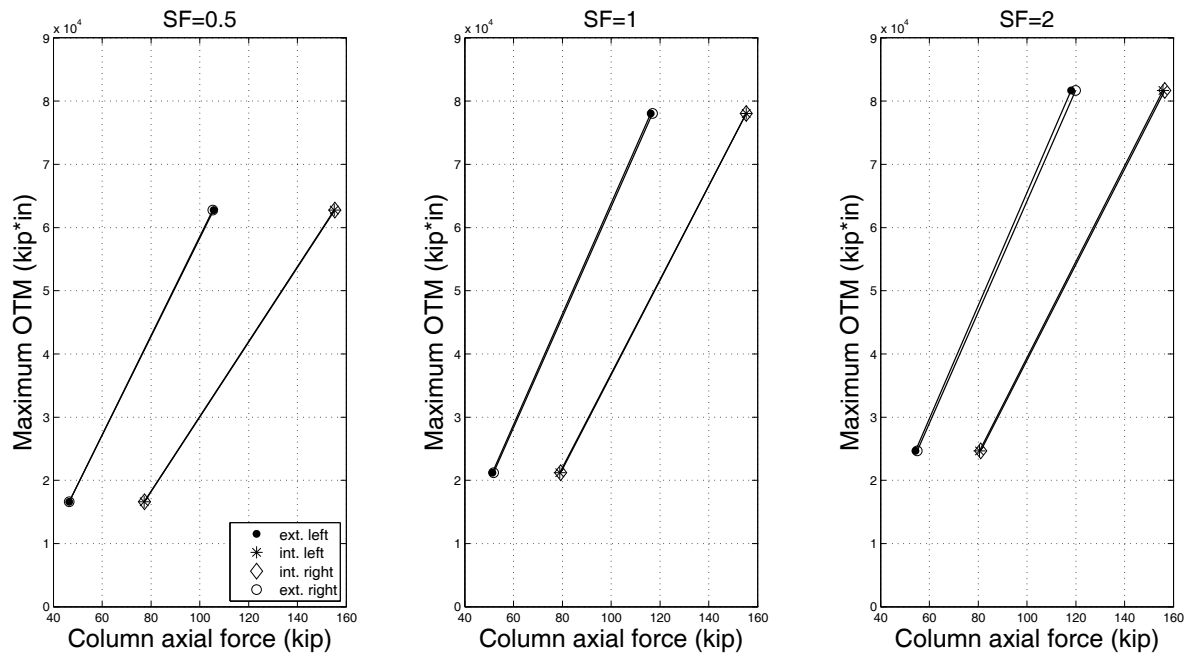


Figure B-79 2-story RCMF: Correlation of peak overturning moment versus peak column axial force.

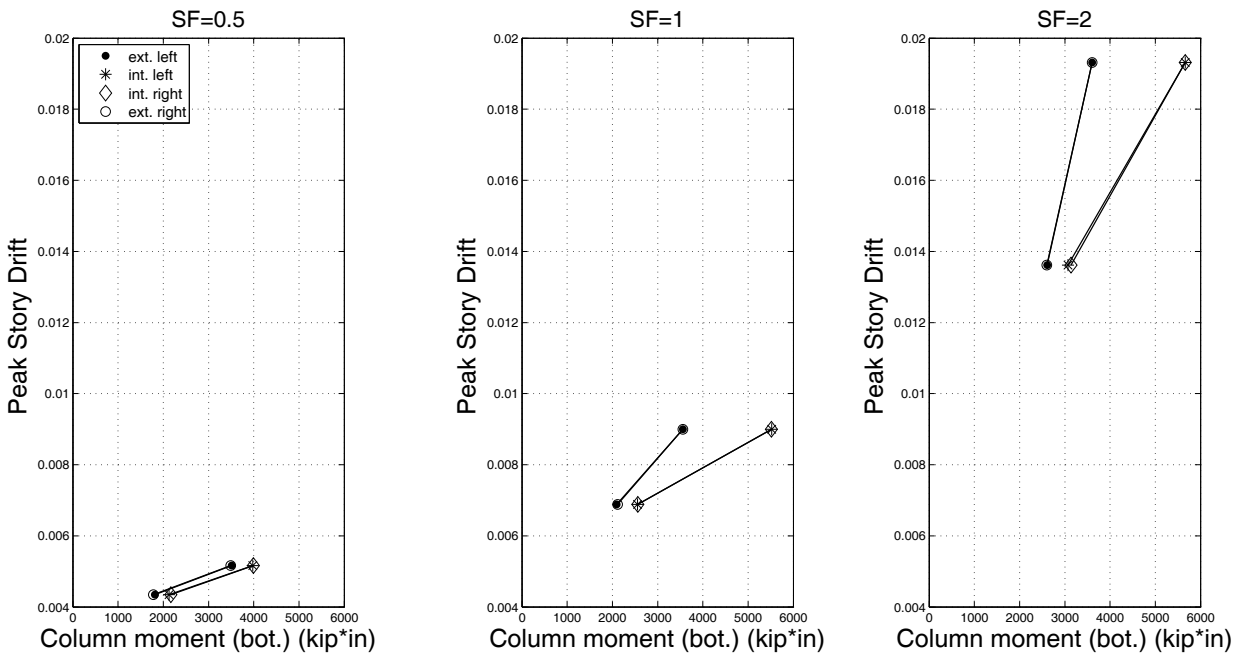


Figure B-80 2-story RCMF: Correlation of peak story drift versus peak column moment.

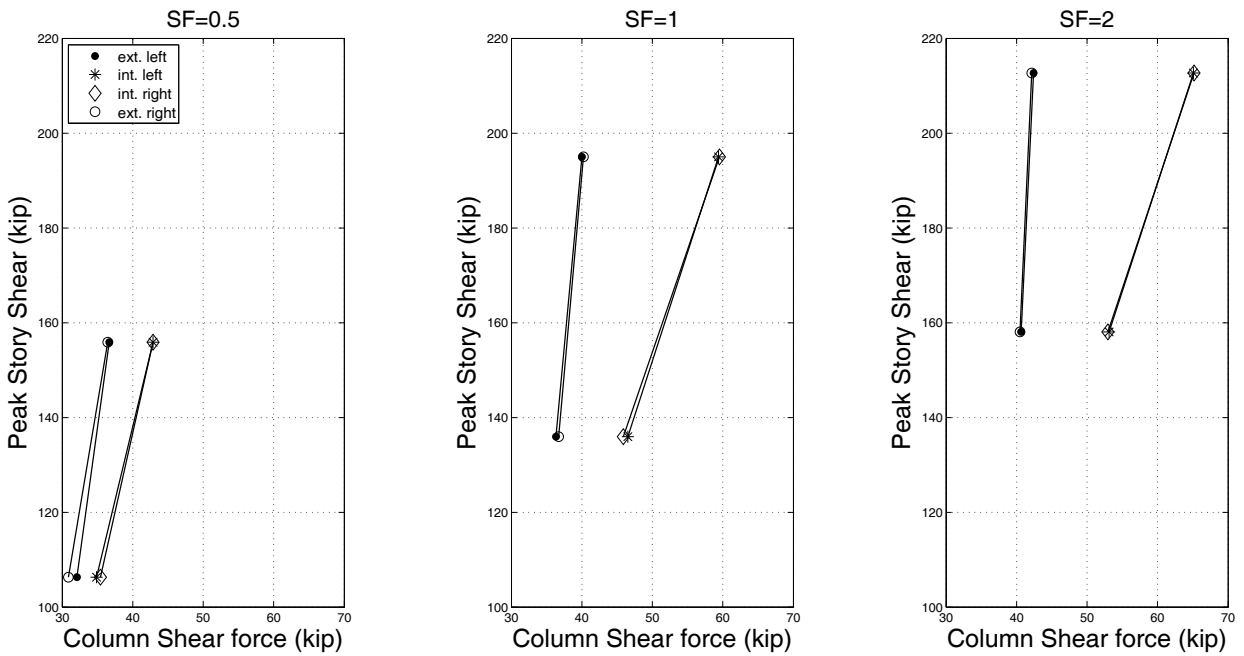


Figure B-81 2-story RCMF: Correlation of peak story shear versus peak column shear.

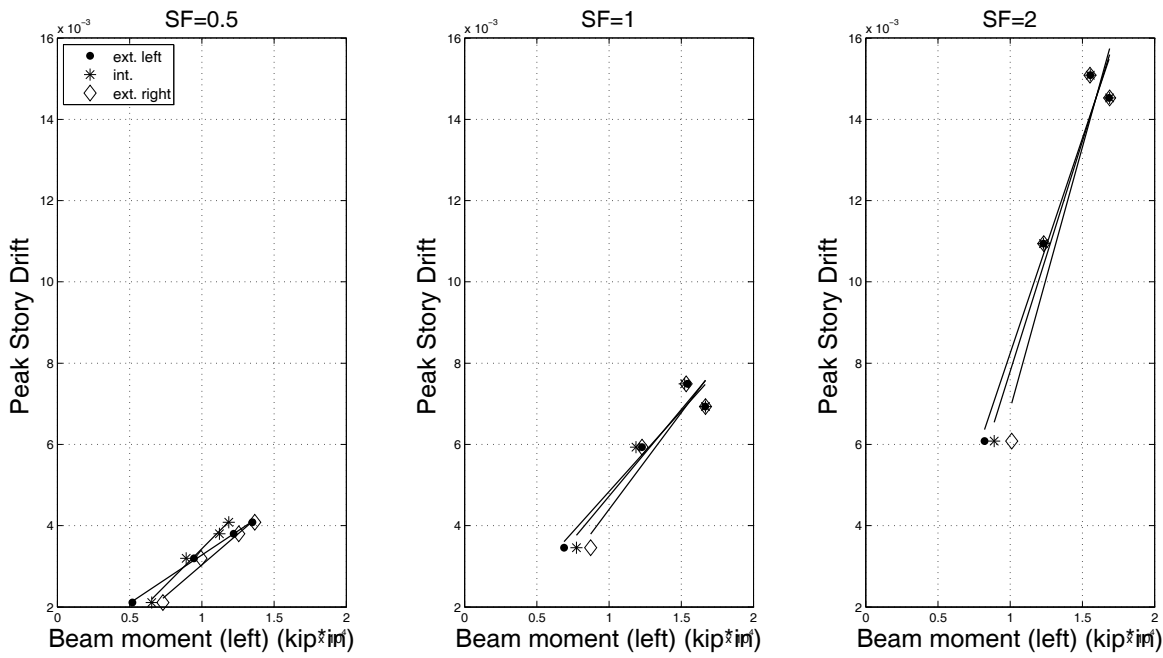


Figure B-82 4-story RCMF: Correlation of peak story drift versus beam moment.

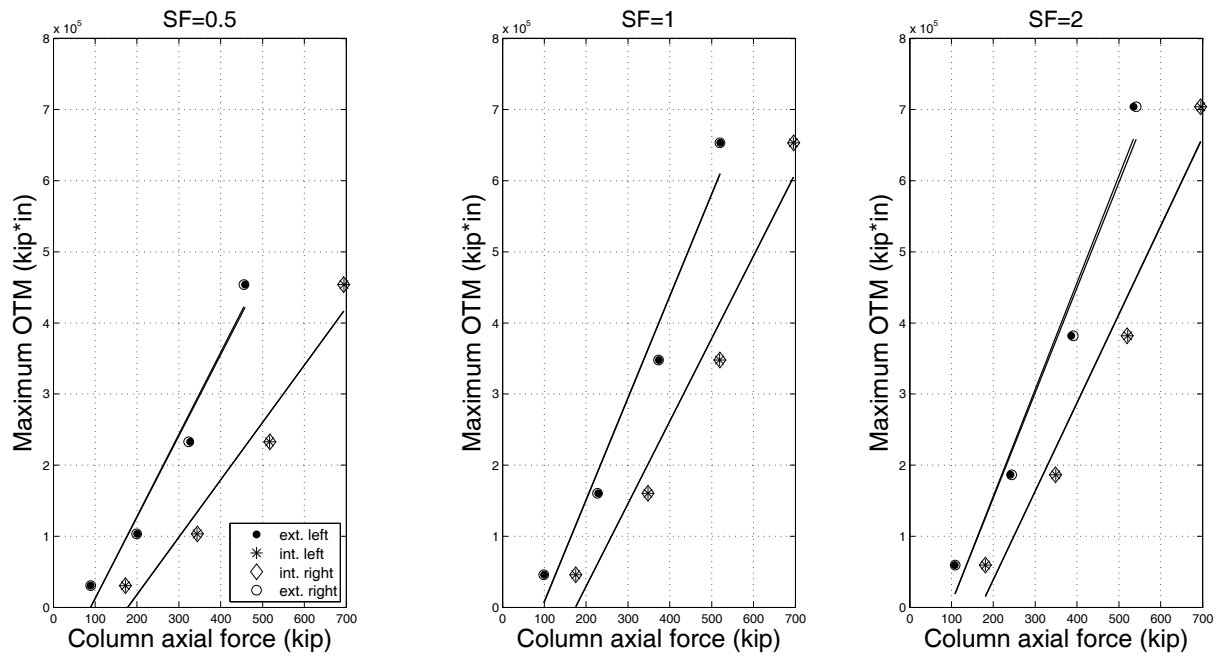


Figure B-83 4-story RCMF: Correlation of peak overturning moment versus peak column axial force.

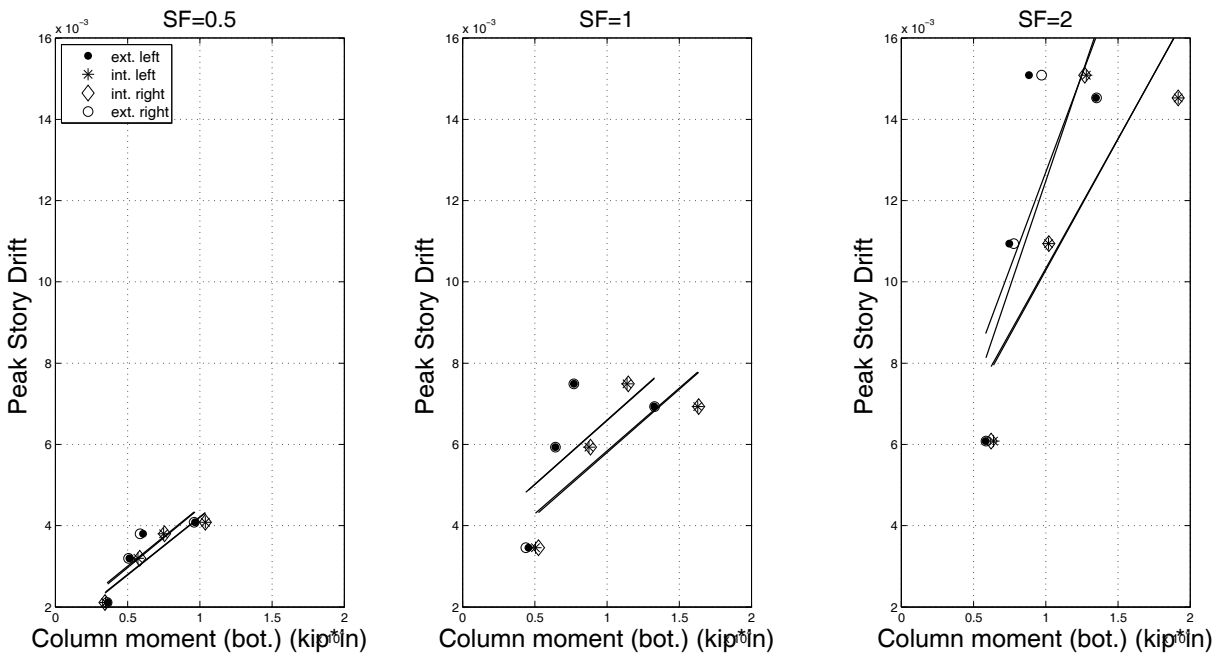


Figure B-84 4-story RCMF: Correlation of peak story drift versus peak column moment

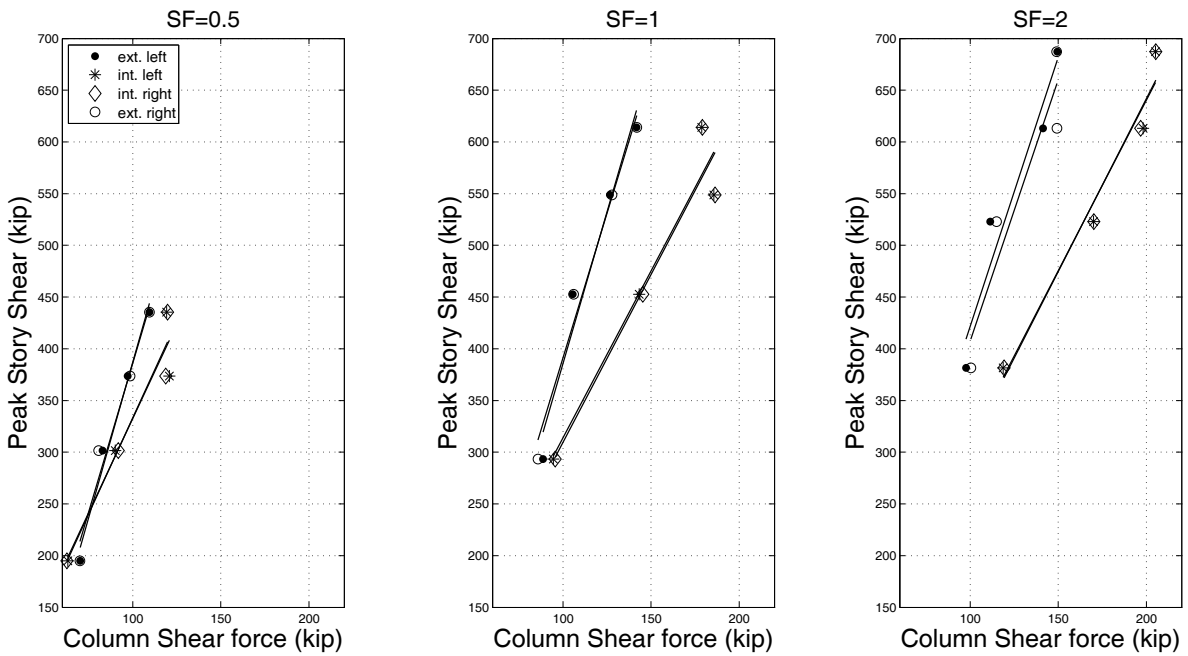


Figure B-85 4-story RCMF: Correlation of peak story shear versus peak column shear.

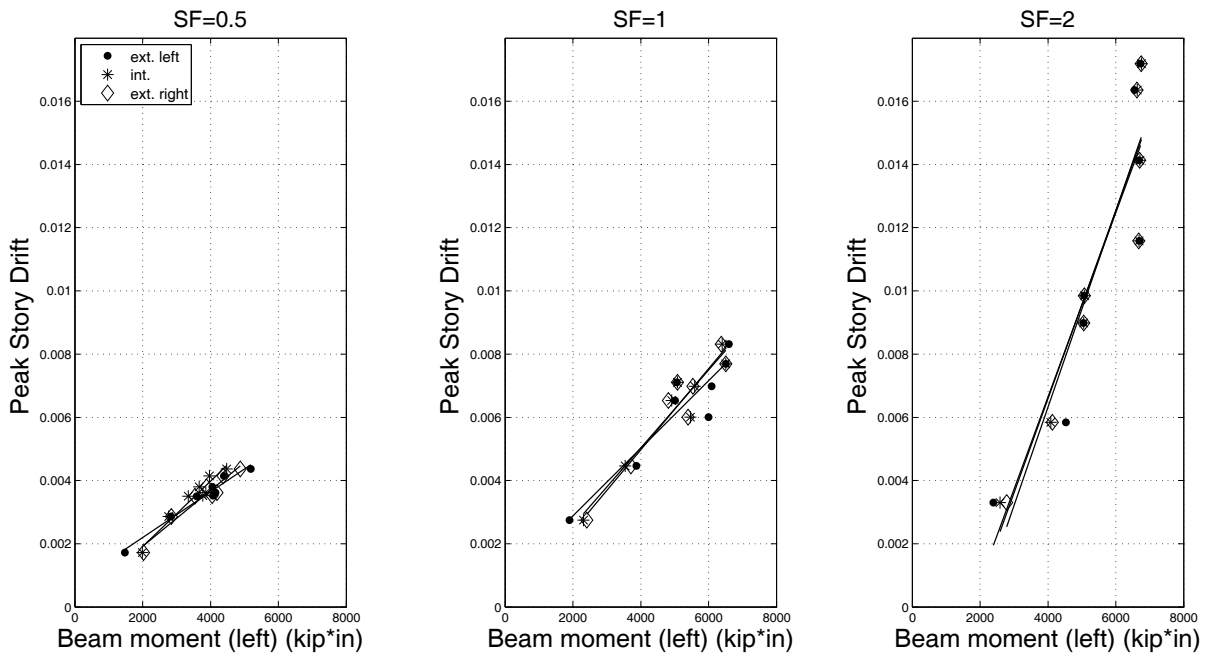


Figure B-86 8-story RCMF: Correlation of peak story drift versus peak beam moment

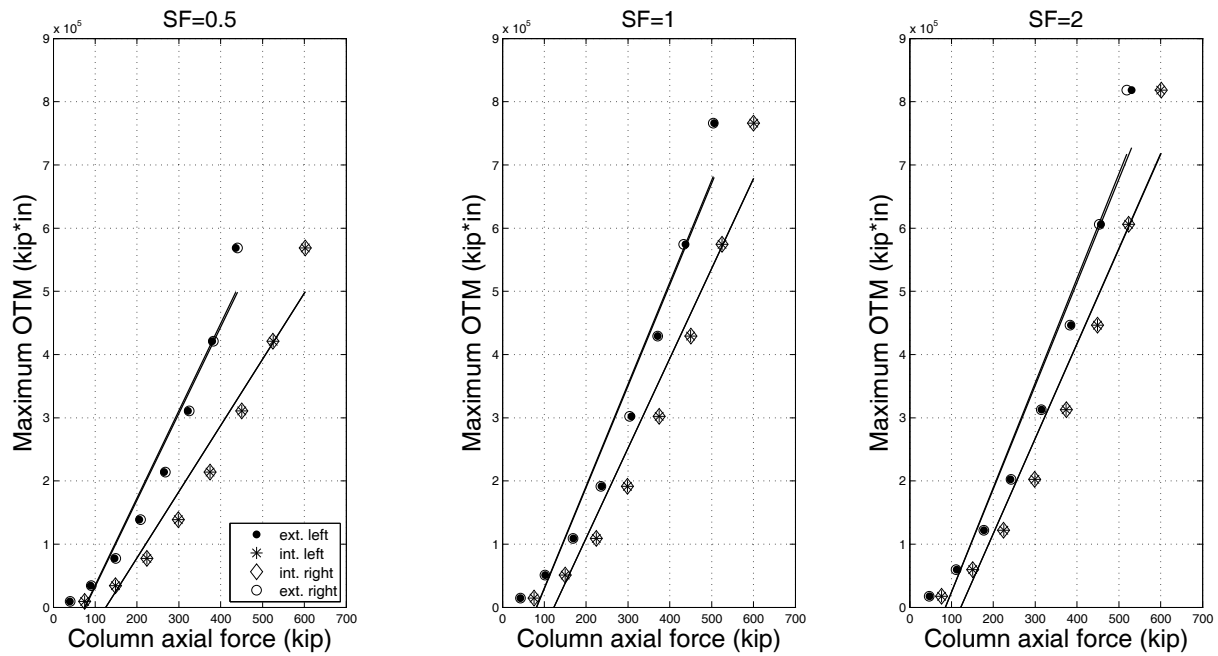


Figure B-87 8-story RCMF: Correlation of peak overturning moment versus peak column axial force.

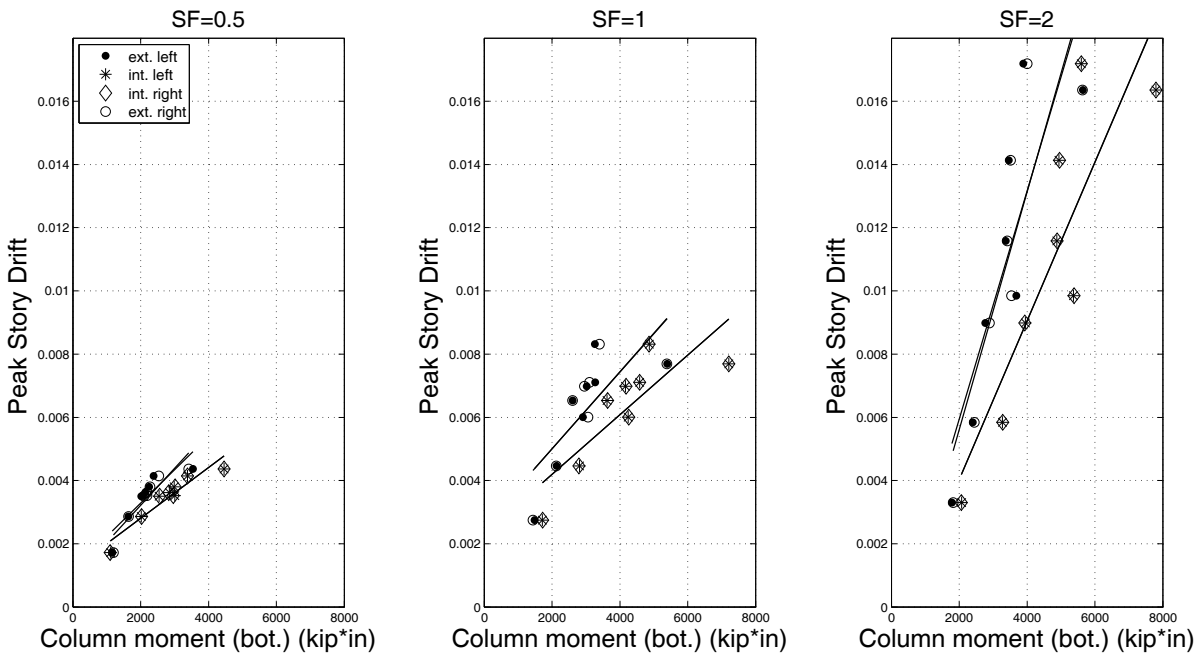


Figure B-88 8-story RCMF: Correlation of peak story drift versus peak column moment.

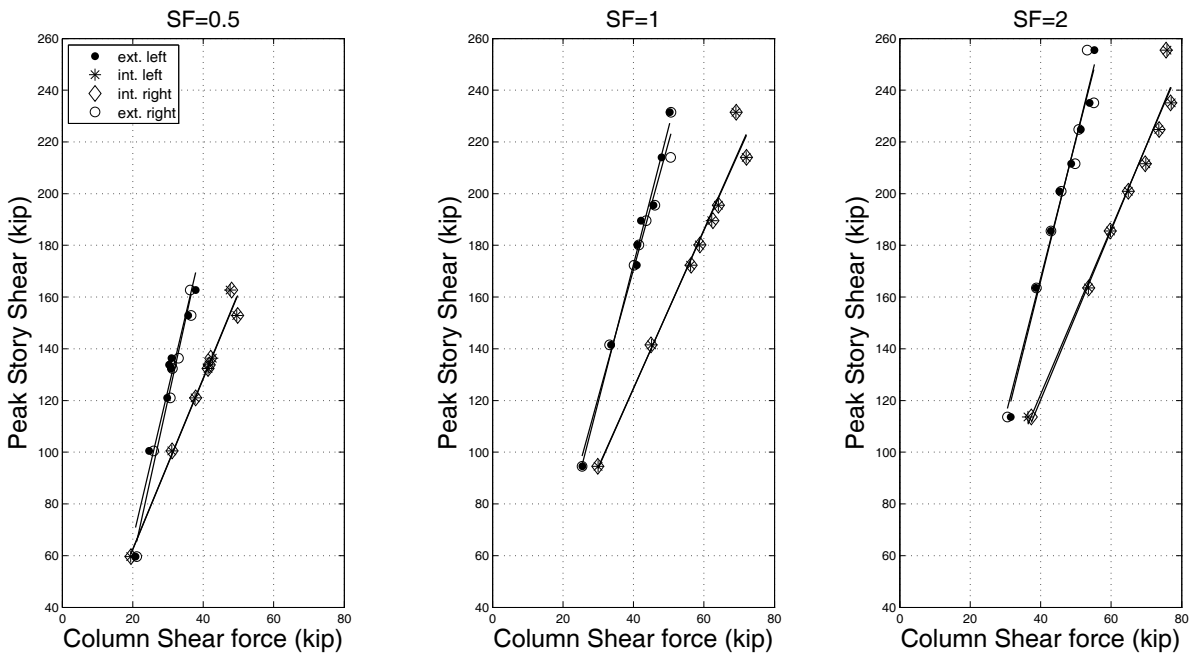


Figure B-89 8-story RCMF: Correlation of peak story shear versus peak column shear.

Detailed Reinforced Concrete Shear Wall Studies

This appendix presents results of problem-focused studies on nonlinear response of reinforced concrete shear wall structures. Nonlinear response history analysis is performed using the FEMA P-695 far-field ground motion set, and various options of single mode nonlinear static analysis and modal pushover analysis procedures are evaluated. In most cases 2-, 4-, and 8-story archetypes are utilized. Only rectangular walls without openings have been included in this study. Peak values of story drift ratio, story shear force, and floor overturning moment are evaluated.

C.1 Introduction

The purpose of this study is to evaluate important engineering demand parameters (EDPs) from results obtained from “best estimate” nonlinear response history analysis (NRHA), using 2-dimensional representations of 2-, 4- and 8-story reinforced concrete shear wall (RCSW) structures. The EDP values obtained from such NRHA serve as benchmark values for assessing predictions by means of simplified methods.

This study focuses on the following three EDPs: peak story drift ratio, peak story shear force, and peak floor overturning moment. Because the structural system of the case study buildings consists of identical solid shear walls on the four sides of the building, the story level EDPs are also EDPs of the individual shear walls.

The quality of EDP predictions is assessed for the following simplified methods:

- First mode nonlinear static procedure (NSP) outlined in ASCE/SEI 41-06
- Variations to the ASCE/SEI 41-06 NSP
- Alternative pushover procedures with a focus on modal pushover analysis (MPA)
- Simplified spring model of the shear walls.

C.2 Structures Utilized in Evaluation

This study utilizes mostly a subset of reinforced concrete shear wall (RCSW) archetypes designed and analyzed as part of the NIST-funded ATC-76-1 Project concerned with evaluation of the FEMA P-695 Methodology for Quantification of Building Seismic Performance Factors. The final report of this project (NIST, 2010)

describes the shear wall structures in detail. Salient features of the subset utilized in this study are summarized below.

The subset consists of three structures, designated here as

- 2-story RCSW (Archetype ID 12)
- 4-story RCSW (Archetype ID 13)
- 8-story RCSW (Archetype ID 14)

Figure C-1 shows the floor plan of the three archetypes. The story heights are 13 feet for the first story and 12 feet for all other stories above. Table C-1 lists basic properties of the three archetypes. For more detailed information about the archetypes, please refer to NIST GCR 10-917-8.

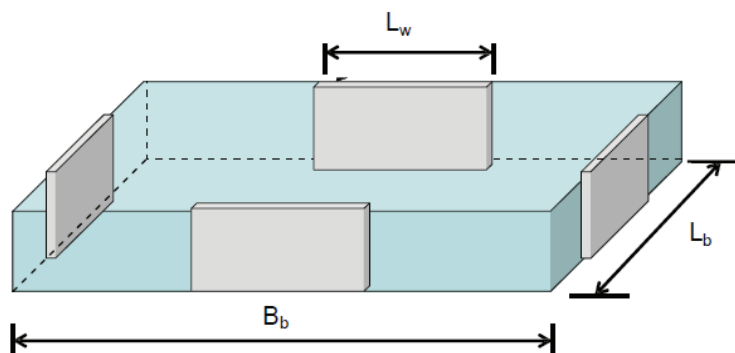


Figure C-1 Archetype configuration for reinforced concrete shear wall structures (from NIST, 2010).

The structures have been designed for seismic design category D_{\max} ($S_{DS} = 1.0g$ and $S_{DI} = 0.60g$) with a low ($0.075A_g f'_c$) axial stress level.

For the 2-story archetype, the wall thickness was selected to produce the maximum shear stress allowed per ACI 318 ($8\sqrt{f'_c}$). Over the wall height, the quantity of boundary longitudinal and web reinforcement was reduced at every two floors to account for the lower demands. Therefore, the ratios of M_u/M_n and V_u/V_n , remain relatively constant over the wall height.

Table C-1 Properties of RCSW Archetypes Used in This Study (from NIST, 2010)

Archetype ID: 12	$P = 0.075Agf_c$	$L_w = 25 \text{ ft}$	$tw = 10 \text{ in}$
plan: 280' x 240'	Atrib.: 60' x 45'	$v_{wall} = 7.9\sqrt{f_c}$	$\Phi V_n/V_u = 1.17$
<i>Story</i>	<i>Boundary reinforcement</i>	<i>Web reinforcement</i>	<i>Special boundary elements</i>
1-2	14#11	#4@10"	YES
Archetype ID: 13	$P = 0.075Agf_c$	$L_w = 24 \text{ ft}$	$tw = 12 \text{ in}$
plan: 150' x 140'	Atributory: 50' x 30'	$v_{wall} = 4.3\sqrt{f_c}$	$\Phi V_n/V_u = 1.1$
<i>Story</i>	<i>Boundary reinforcement</i>	<i>Web reinforcement</i>	<i>Special boundary elements</i>
1-2	14#11	#5@10"	YES
3-4	--	#5@18"	NO
Archetype ID: 14	$P = 0.075Agf_c$	$L_w = 32 \text{ ft}$	$tw = 14 \text{ in}$
plan: 110' x 100'	Atributory: 30' x 30'	$v_{wall} = 2.0\sqrt{f_c}$	$\Phi V_n/V_u = 1.65$
<i>Story</i>	<i>Boundary reinforcement</i>	<i>Web reinforcement</i>	<i>Special boundary elements</i>
-2	14#11	#4@10"	YES
3-4	8#11	#4@10"	YES
5-6	--	#4@10"	NO
7-8	--	#4@10"	NO

C.3 Nonlinear Response History Analysis

The analytical model is based on the bare wall, i.e., no credit is given to the contributions of the gravity system. P-Delta effects tributary to the gravity system are considered by adding a P-Delta column in parallel to the wall. This study is concerned only with 2-dimensional modeling of structures. Thus, the assumption is that torsional effects are negligible. The issue of torsion is discussed in Section 7.2. In all analyses Rayleigh damping of 2.5% is assigned at the first mode period T_1 and at $T = 0.2T_1$. All nonlinear response history analyses (NRHAs) and pushover analyses are performed with the OpenSees platform (<http://opensees.berkeley.edu>). The FEMA P-695 set of 44 ground motions is used in NRHA.

C.3.1 Component Models

Fiber Model (FM Model)

Displacement based beam-column elements together with translational shear springs were used to model wall elements for all archetypes.

The OpenSees C02 model was used for modeling both confined and unconfined concrete. Peak strength, f_{pc} , for unconfined concrete was selected to be 6.1 ksi to

represent the actual strength for a specified strength of 5 ksi, and strain at peak strength, e_{psc0} , was selected to be 0.0027, which yields an initial modulus ($E_0 = 2f_{pc}/e_{psc0}$) of approximately 4500 ksi. Stress and strain values used to define the post-peak descending branch of the unconfined stress–strain relation (f_{pcU} and e_{psU}) were selected to be 1.4 ksi and 0.01. Concrete crushing was taken as the point where the post-peak linear descending branch reaches the residual concrete stress (defined as 20% of the peak confined concrete stress). Confined concrete model parameters were varied over the wall height at locations where transverse reinforcement changed.

Concrete tensile strength (f_t), concrete tensile modulus (E_t), and unloading parameter (λ), which defines the unloading slope in terms of the initial concrete modulus (unloading slope = λE_0), were selected to be 0.586 ksi, 410 ksi, and 0.1, based on the information provided by Orakcal and Wallace (2006).

Reinforcement was modeled as a “hysteretic material” in OpenSees. Expected values of yield and ultimate strength of reinforcement were taken as 68 ksi and 100 ksi, respectively. A tensile strain value of 0.05 was selected to correspond to failure associated with rebar buckling and subsequently rebar fracture. After reaching a strain of 0.05, the stress capacity of the reinforcing bar drops to near zero. Use of a more complex model, where the strain value associated with rebar buckling/fracture is varied was not justified given the uncertainty associated with existing test results and models, and given that the equation used in ACI 318-08, Equation (21-5), to calculate the quantity of transverse reinforcement required at wall boundaries (fairly uniform quantity of transverse reinforcement).

Modeling flexural behavior. Flexural behavior was modeled by 6”×6” fiber elements, which is a denser mesh than was used in the NIST-funded ATC-76-1 Project, but otherwise adopting the model and OpenSees input file used. A typical moment-curvature result obtained from this model is shown in Figure C-2.

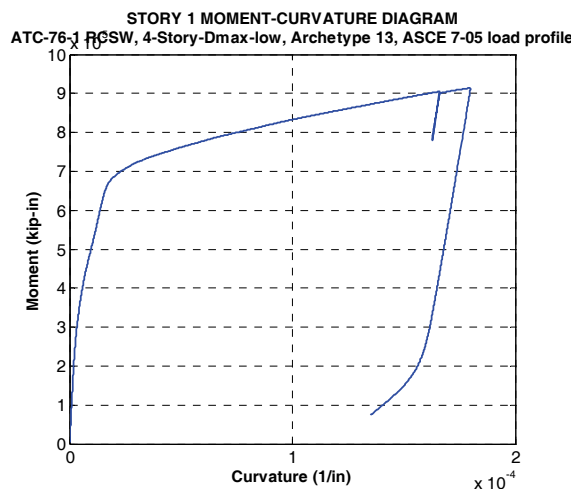


Figure C-2 Moment-curvature relationship at base of story 1 of 4-story RCSW, FM model.

Modeling of shear behavior. Shear behavior was modeled by adopting the rules and analysis model used in the NIST-funded ATC-76-1 Project. A translational shear spring was employed to model shear force-deformation relationship in every story. The model shown in Figure C-3(a) was employed for walls whose behavior was expected to be controlled by shear, and the model shown in Figure C-3(b) was adopted for walls in which flexural yielding was expected to limit the wall shear demands. It was assumed that the latter mode would control the 4- and 8-story RCSWs. In the model shown in Figure C-3(b) no yield strength was assigned to the shear spring, i.e., it was assumed that yielding in shear will never occur.

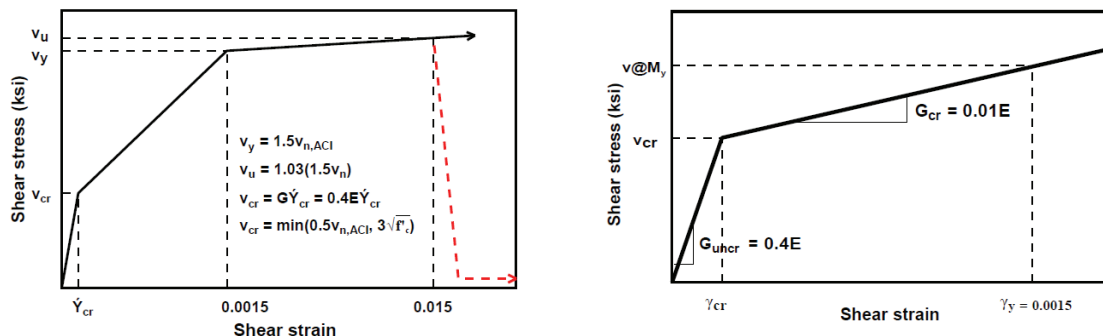


Figure C-3 Shear force – deformation models (a) if shear strength is expected to limit wall behavior, and (b) if bending strength is expected to limit wall behavior (from NIST, 2010).

Simplified Spring Model (SM Model)

A simplified flexural spring model was developed since fiber models result in behavior modes that are believed to account for localized failure modes such as concrete crushing and steel buckling and fracture, but are difficult to visualize and judge by methods employed in codes and in standard engineering models. There are well established problems with using simplified spring models, such as difficulties in accounting for movement of neutral axis, rocking, interaction with frames due to rocking, and moment gradient effects (Vulcano and Bertero, 1987, Orakcal et al., 2006). Moreover, reliable data does not exist for quantifying rotation capacity and post-capping behavior of reinforced concrete walls. For these reasons the simplified spring model was tuned to provide a good match of the global pushover curve obtained from the fiber model.

Using a simplified spring model of the type shown in Figure C-4 permits explicit modeling of post-yield and post-capping behavior, using the same model parameters as have been employed in the SSMF study summarized in Appendix A.

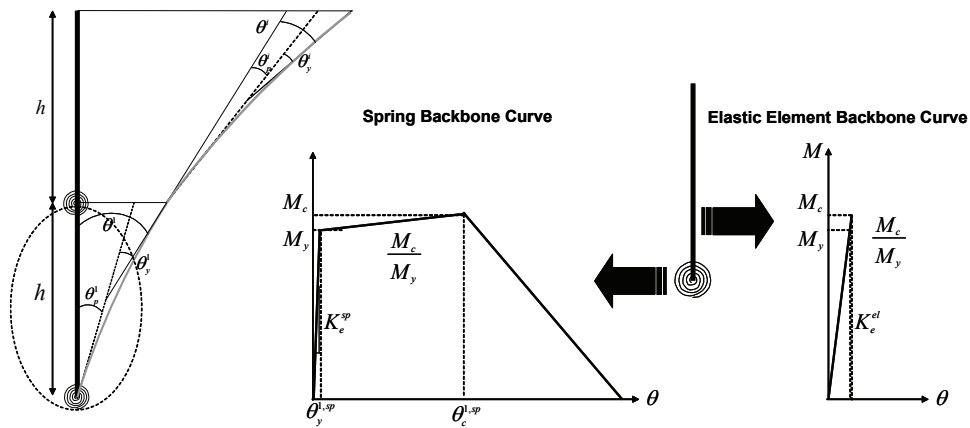


Figure C-4 Modeling of flexural behavior with simplified plastic hinge springs and elastic elements (Zareian and Krawinkler, 2009).

C.3.2 Results for 2-, 4-, and 8-Story Reinforced Concrete Shear Wall Structures with Fiber Model

Presented here are two figures each for the 2-, 4-, and 8-story RCSWs modeled with the fiber model (FM model). The first figure presents system information and statistics of roof drift ratios (δ_r/H) obtained from the NRHA for ground motion scale factors, SF, of 0.5, 1.0, and 2.0, the global pushover curves (without and with P-Delta shears) and deflection profiles from the pushover at the median value of roof drift ratios obtained from the NRHA for SF = 0.5, 1.0, and 2.0. The table of elastic dynamic properties lists also the median spectral acceleration of the FEMA P-695 ground motion set for SF = 1.0. The S_a values are for 5% critical damping, even though the NRHA was performed with the assumption of 2.5% damping, which implies effective spectral accelerations that are about 25% larger than the tabulated ones. For the 4-story structure, information is presented also for SF = 3.0, because the NRHA median roof drift ratio for SF = 2.0 barely exceeds the yield drift.

The global pushover curves shows both V_I and $V_{I+P-\Delta}$. The difference between the two curves quantifies the importance of P-delta effects. The first mode load pattern is applied in all pushover analyses.

Mean and standard deviation values in the second table exist only if all 44 data points are available; they are not reported if the structure “collapses” under one or more of the ground motions. “Collapse” implies that numerical instability occurred even if a very small integration step size was used. The complexities of a fiber model make it difficult to trace the events that lead to numerical instability, which was the main reason to perform NRHA also with a simplified spring (SM) model.

The pushover curve serves as an essential tool in understanding structural behavior. It illustrates post-yield and post-capping behavior, and indicates the roof drifts at which global yielding and capping (loss in strength due to deterioration) can be expected. The deflection profiles illustrate relative importance of individual story drifts and their changes as the structure gets pushed further into the inelastic range.

But the results may be strongly dependent on the lateral load pattern used in the pushover analysis.

The second figure for each structure presents NRHA results for the three story level EDPs, i.e., peak story drift ratios, story shears, and floor overturning moments. The EDPs $V_{I+P-\Delta}$ and $OTM_{I+P-\Delta}$ are used as the relevant story/floor force quantities because they identify the maximum force demands in the shear wall. The peak floor overturning moment $OTM_{I+P-\Delta}$ is obtained as the maximum of the sum of $V_{I+P-\Delta} \times h$ of all the stories above the floor. In each plot peak values are presented for individual ground motions (connected by light gray lines), and median values (connected by bold solid lines) as well as 16th and 84th percentile values (connected by black dashed lines). All statistical values are obtained by “counting” data points, i.e., no distribution has been fitted to the data points. Results are presented for ground motion scale factors SF = 1.0 and 2.0, except for the 4-story RCSW for which results are presented for SF = 0.5, 1.0, 2.0, and 3.0.

The following general observations are common to the NRHA results for all three structures investigated:

- All pushover curves exhibit a clear kink around the load level at which significant cracking occurs in either shear or bending. A realistic multi-linear representation of the pushover curve requires at least three lines before capping.
- Significant shear deformations were observed in the inelastic pushover and dynamic response of all three walls, but the strength of the structures was limited by flexural yielding, even for the 2-story wall.
- All FM pushover curves exhibit a rapid deterioration in strength after the peak strength has been attained. This is very different from the behavior observed for steel SMFs (Appendix A). It is believed that the reason for it lays in the formulation of the fiber model for bending behavior. This rapid deterioration in strength needs to be further explored, but this was not within the scope of this study.
- The dispersion in NRHA response is largest for story drift ratios, smaller for story shears, and smallest for story overturning moments. The smaller dispersion in story shears and floor OTMs comes from “saturation” of strength capacities (in either bending or shear) as the structure responds inelastically to ground motions. But it is noted that there is dispersion in these EDPs even at large inelastic deformations at which the global pushover curve indicates full saturation of force quantities. The reason is dynamic redistribution once plastification occurs in bending at a specific location in the wall.
- Maximum NRHA story shear demands are much more in line with design and pushover shear force patterns than was observed for steel SMF structures (Appendix A). The same observation applies to floor overturning moments.

- The increase in NRHA shear demands for the 4-story RCSW, compared to the peak strength obtained in the pushover analysis, is surprisingly large. It is not known whether this increase is due to dynamic amplification or due to modeling issues in the FM models.

Summary of Observations for the 2-story RCSW:

- The post-cracking region of the pushover exhibits a small stiffness, which is attributed to large shear deformations prior to yielding in bending. The large shear deformations are evident also in the deflected shapes at the bottom of Figure C-5. But the strength of this wall with a low aspect ratio of $h/L = 25/25$ is limited by flexural yielding.

Summary of Observations for the 4-story RCSW:

- Even though bending strength controlled behavior at large inelastic deformations, the lateral stiffness in the early response (before global yielding in pushover) was controlled by shear deformations. This caused the “shear type” deflected shapes shown in Figure C-7 and probably is responsible for the NRHA drift distribution over the height (Figure C-8), which again indicates a shear mode rather than bending mode of deformations (except for $SF = 3.0$).
- The NRHA analysis for $SF = 2$ leads to a small median roof drift of only 0.0129, which in the pushover curve corresponds to about global yielding. This drift is only about 25% of the drift at capping. Nevertheless, 8 “collapses” (cases of numerical instability) did occur in the analysis.
- The NRHA analysis for $SF = 3$ did lead to a larger median roof drift (0.0191), but it did not produce any “collapses” (cases of numerical instability) even though the same time step and convergence criteria were used as in the $SF = 2$ analysis.
- The NRHA story drift pattern changes drastically when the ground motion scale factor is increased from 2 to 3. The pattern for $SF = 3$ is more in line with expectations for RCSWs failing in bending. For $SF = 3$ the first story drift decreases greatly compared to $SF = 2$, whereas for all other stories the story drift increases greatly. This indicates a transition from shear controlled to bending controlled behavior.
- The median base shear at $SF = 3$ is 1.75 times as large as that for $SF = 2$, and it is 50% larger than the peak pushover base shear. It is also 20% larger than the shear capacity, which in Figure C-3(a) is defined as $1.03(1.5V_n)$. These observations cannot be explained without a more in-depth evaluation, which could not be performed as part of this study. It appears that no capping was employed for the shear spring, i.e., the shear strength increases regardless of the shear attracted by the spring.

- The median base overturning moment for $SF = 3$ is about 25% larger than the maximum overturning moment from the pushover, even though the pushover strength is controlled by bending behavior.
- The latter two observations are difficult to justify, and for this reason a simplified spring model was developed for this shear wall structure in order to assist in result interpretation. Results from this simplified model are summarized in Section C.3.3.

Summary of Observations for 8-story RCSW:

- The demands on this shear wall are very low, even for $SF = 2.0$. This helps to explain the unusual story drift and shear force pattern seen in the HRHA results (Figure C-11). Story drifts decrease in upper stories of this relatively tall and slender shear wall ($h/d = 3$), which is due to the small shear stiffness compared to flexural stiffness. Shear deformations dominate the response up to global flexural yielding.
- Story shear force patterns are the opposite of what was observed for steel SMF structures (Appendix A). They resemble a pattern caused by uniform lateral story loads, whereas the steel SMF shear force pattern resembled one caused by a concentrated load at the top. Neither load pattern came close to resembling a first mode load pattern.

Seismically effective weight per wall: $W = 10,080k$

($w_1 = 5,040k$, $w_2 = 5,040k$)

Elastic Dynamic Properties (RCSW-2-FM)

	Mode 1	Mode 2
T_i [sec]	0.500	0.087
Γ_i	1.200	-0.200
Eff.Mod.Mass	0.901	0.099
$S_a(T_i, 5\% SF=1.0)$	0.804g	0.517g

Roof Drift Ratios from NRHA (H = 300 inches)

	SF=0.5	SF=1.0	SF=2.0
Median [%]	0.0036	0.0087	0.0186
16th [%]	0.0023	0.0057	0.0134
84th [%]	0.0053	0.0121	0.0271
Mean μ [%]	0.0038	0.0088	0.0198
σ [%]	0.0016	0.0033	0.0070
CoV	0.4109	0.3801	0.3516
Collapses	0	0	0

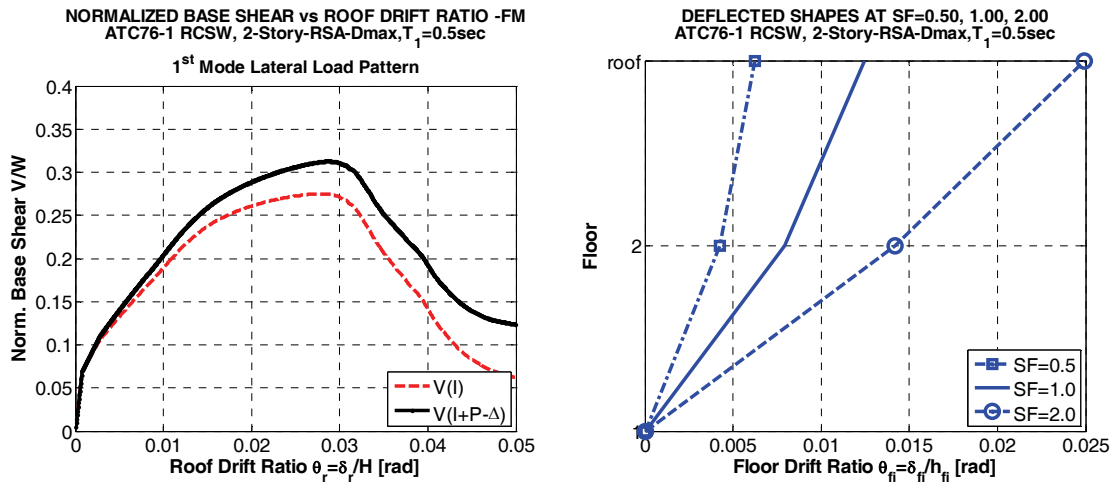


Figure C-5 System information, 2-story RCSW, FM Model.

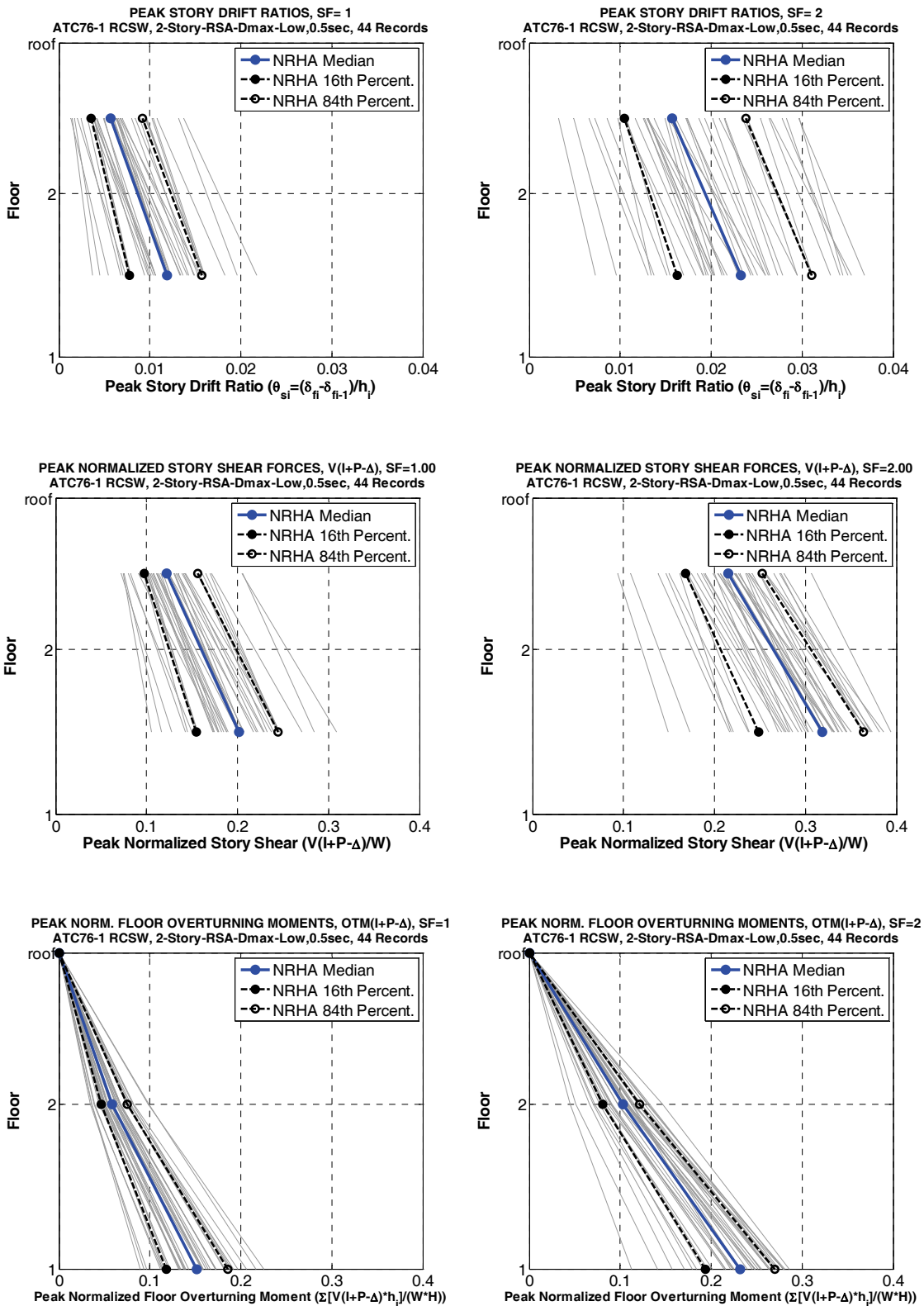


Figure C-6 NRHA Peak story drift ratios, story shears, and floor overturning moments, 2-story RCSW, FM Model, SF = 1.0 and 2.0.

Seismically effective weight per frame: $W = 6,300k$

($w_i = 1575k$)

Elastic Dynamic Properties (RCSW-4-FM)

	Mode 1	Mode 2	Mode 3	Mode 4
T_i [sec]	0.660	0.120	0.063	0.015
Γ_i	1.339	-0.425	0.109	-0.024
Ef.Mod.Mass	0.811	0.162	0.023	0.004
$S_a(T_i, 5\% SF=1.0)$	0.571g	0.629g	0.409g	0.423g

Roof Drift Ratios from NRHA (H = 588 inches)

	SF=0.5	SF=1.0	SF=2.0	SF=3.0
Median [%]	0.0025	0.0053	0.0129	0.0191
16th [%]	0.0018	0.0037	0.0088	0.0140
84th [%]	0.0035	0.0081	N/A	0.0290
Mean μ [%]	0.0026	0.0059	N/A	0.0210
σ [%]	0.0009	0.0024	N/A	0.0074
CoV	0.3321	0.4026	N/A	0.3517
Collapses	0	0	8	0

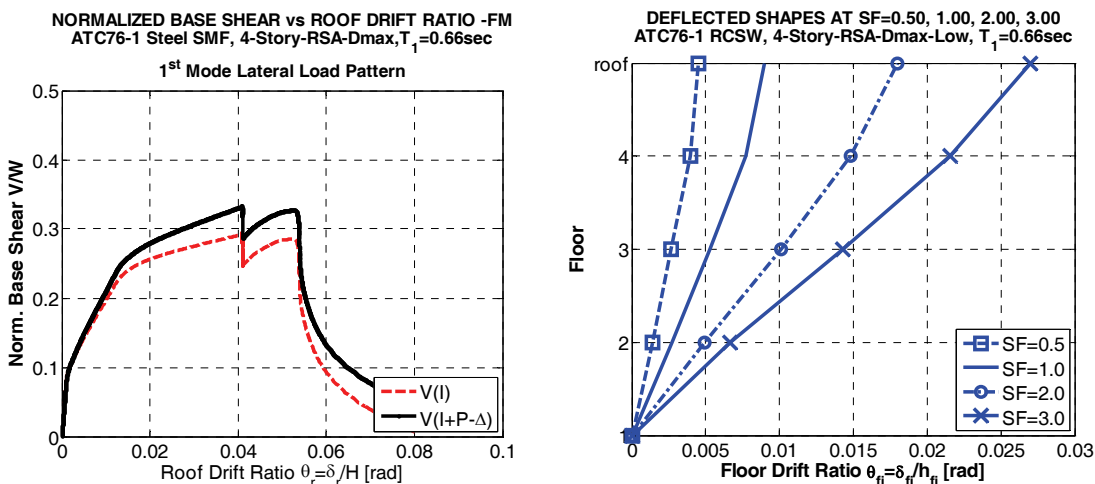


Figure C-7 System information, 4-story RCSW, FM Model.

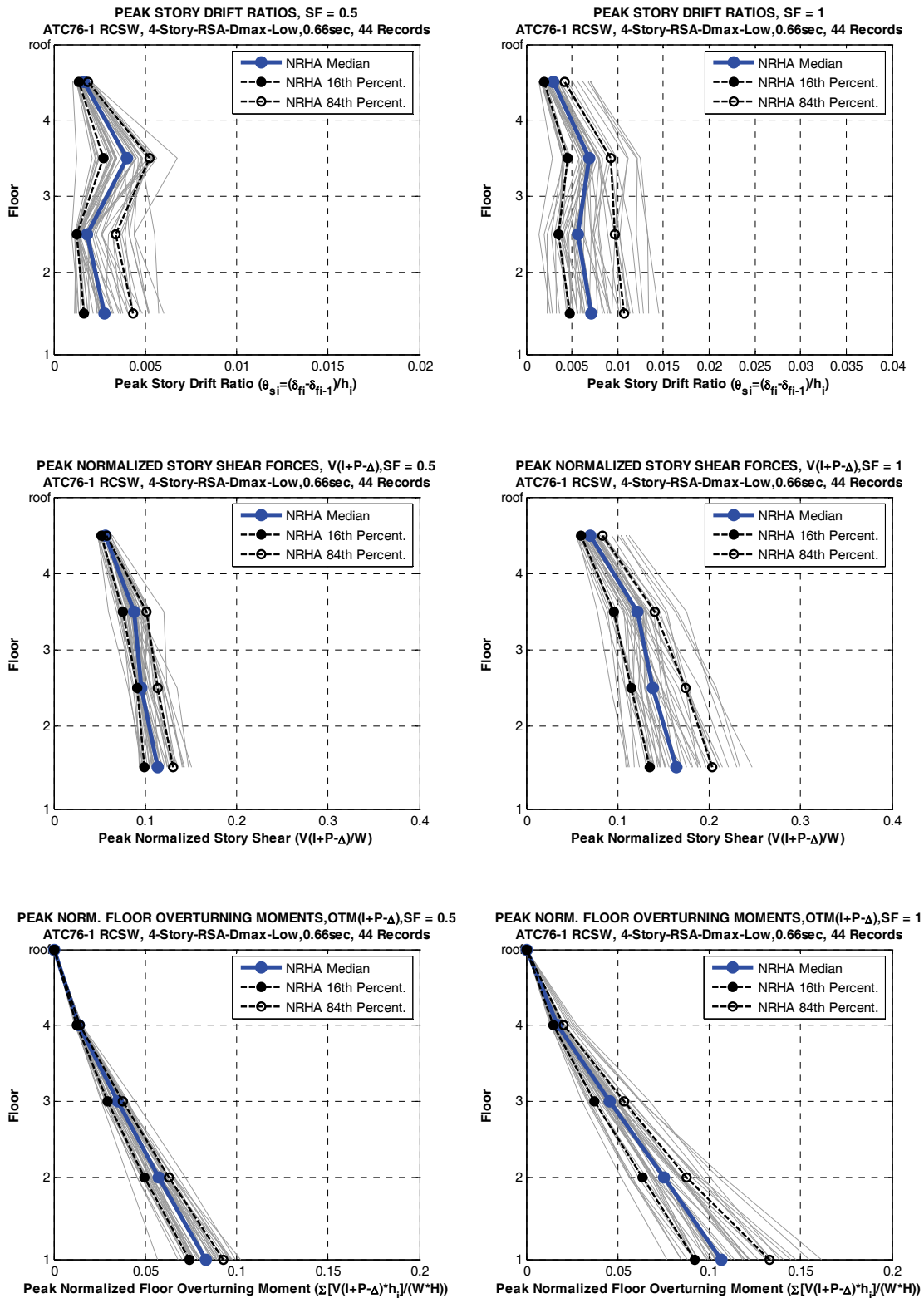


Figure C-8 NRHA Peak story drift ratios, story shears, and floor overturning moments, 4-story RCSW, FM Model, SF = 0.5 and 1.0.

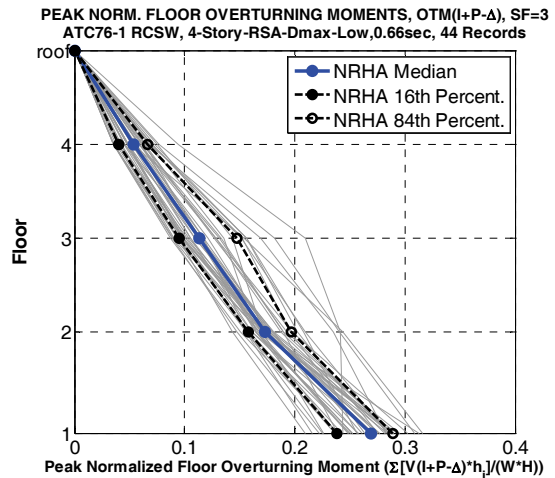
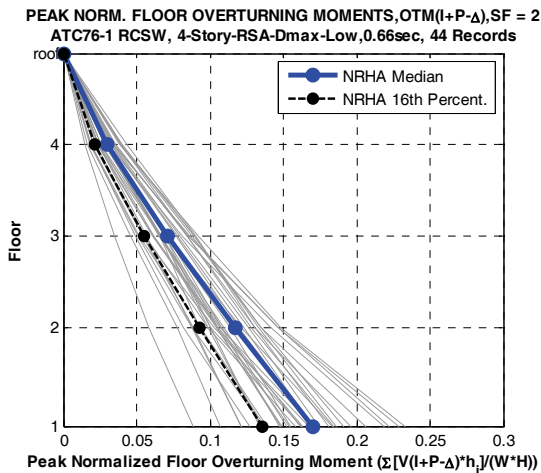
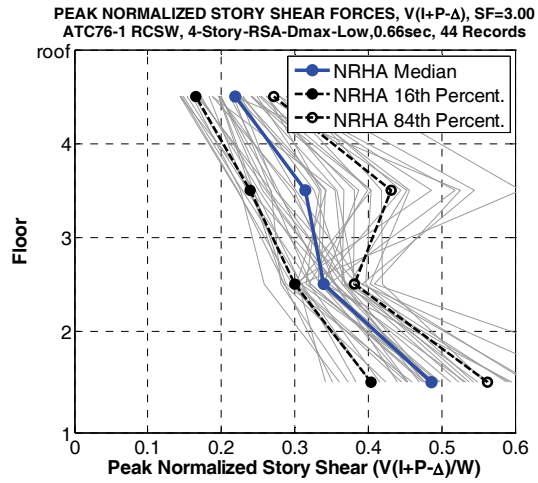
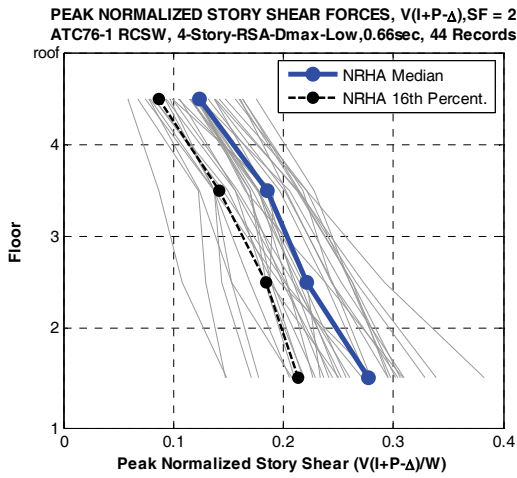
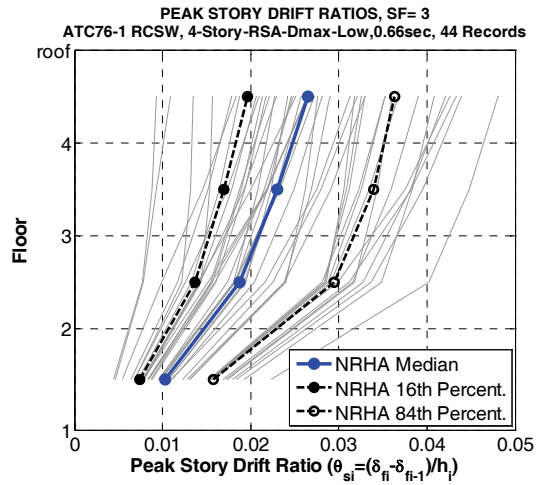
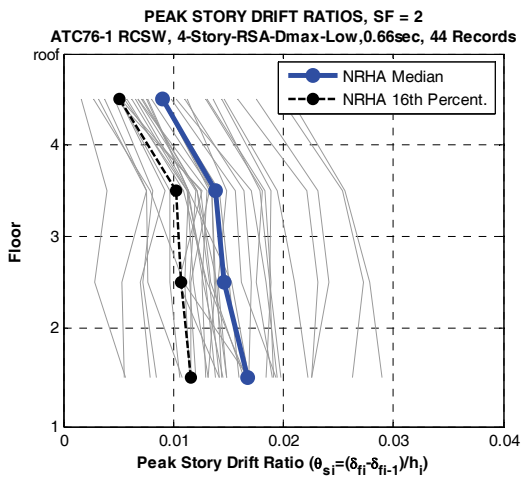


Figure C-9 NRHA Peak story drift ratios, story shears, and floor overturning moments, 4-story RCSW, FM Model, SF = 2.0 and 3.0.

Seismically effective weight per frame: $W = 6,600k$

($w_i = 825k$)

Elastic Dynamic Properties (RCSW-8-FM)

	Mode 1	Mode 2	Mode 3	Mode 4	Mode 5	Mode 6	Mode 7	Mode 8
T_i [sec]	0.760	0.200	0.113	0.101	0.086	0.049	0.038	0.035
Γ_i	1.356	-0.513	0.283	0.148	-0.086	-0.033	0.012	-0.002
Ef.Mod.Mass	0.784	0.119	0.044	0.017	0.014	0.006	0.004	0.001
$S_a(T_i, 5\% SF=1.0)$	0.477g	0.878g	0.588g	0.552g	0.482g	0.384g	0.320g	0.310g

Roof Drift Ratios from NRHA (H = 1164 inches)

	SF=0.5	SF=1.0	SF=2.0
Median [%]	0.0014	0.0029	0.0059
16th [%]	0.0010	0.0020	0.0047
84th [%]	0.0019	0.0045	0.0075
Mean μ [%]	0.0015	0.0032	0.0060
σ [%]	0.0005	0.0011	0.0016
CoV	0.3254	0.3540	0.2689
Collapses	0	0	0

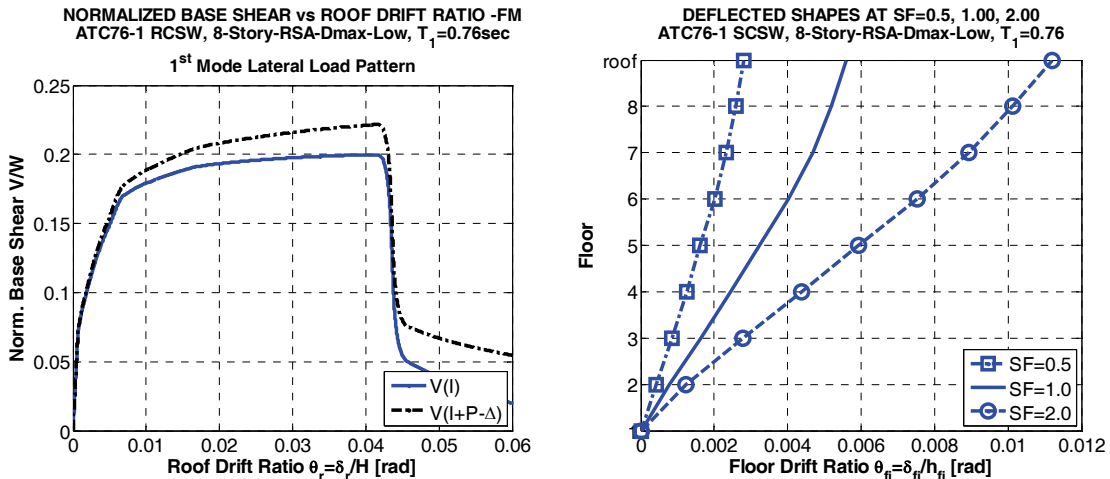


Figure C-10 System information, 8-story RCSW, FM Model.

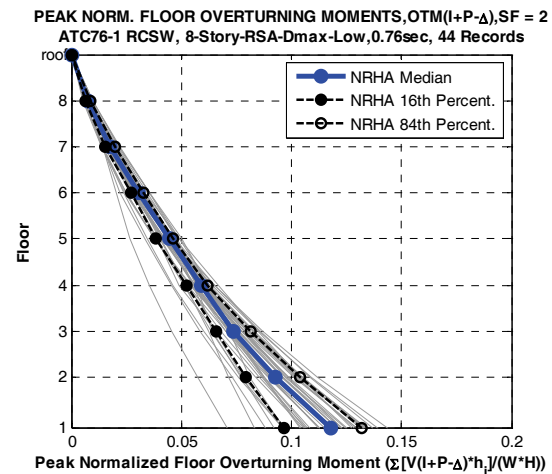
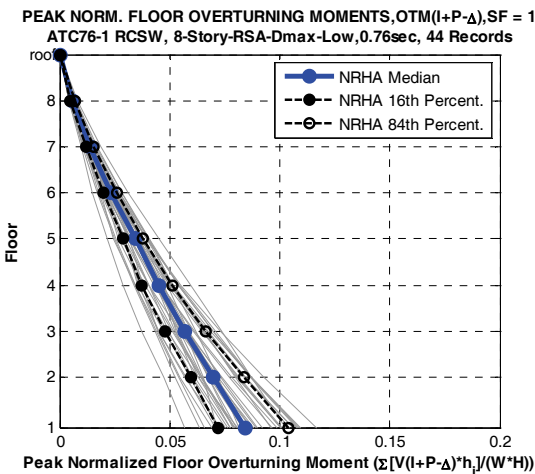
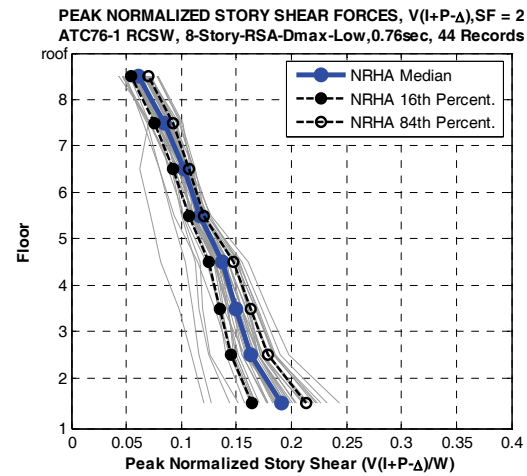
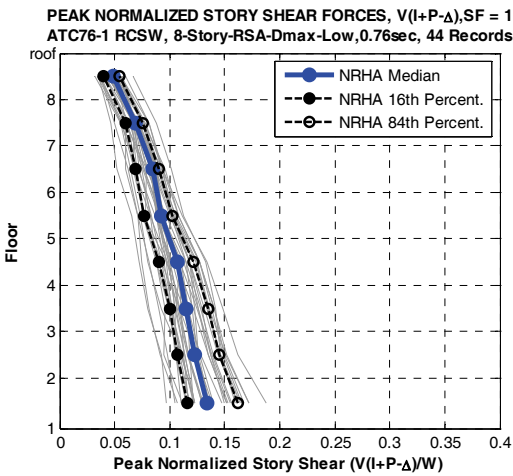
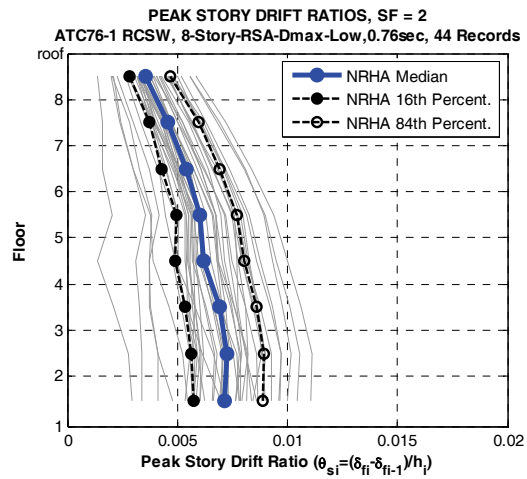
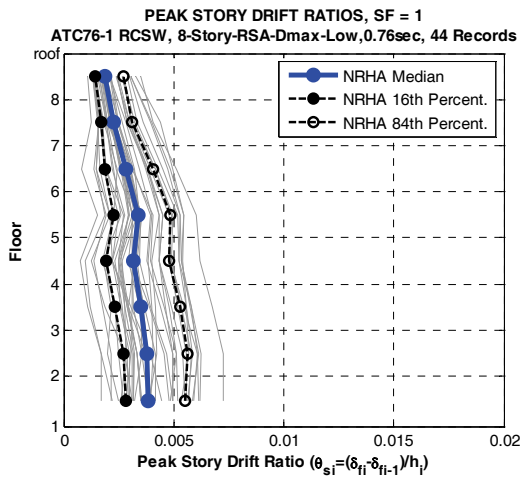


Figure C-11 NRHA Peak story drift ratios, story shears, and floor overturning moments, 8-story RCSW, FM Model, SF = 1.0 and 2.0.

C.3.3 Results for 4-Story Reinforced Concrete Shear Wall Structure with Simplified Spring Model

Considering the challenges with physical interpretation of fiber model results, an attempt was made to develop a simplified spring model (SM model) for the 4-story RCSW whose properties resemble those of the FM model. This model consists of translational story shear springs and rotational flexural springs at the floor levels, see Figure C-4.

Stiffness properties and cracking and yield strengths of the shear springs are identical to those employed in the FM model. The major difference to the FM model is that in the SM model the shear spring “caps” (loses strength) at the shear value of $1.03(1.5V_n)$, see Figure C-3(a). Shear hysteresis behavior is represented by the OpenSees Pinching4 model (Figure C-12). The ratio of deformation at which reloading occurs to the maximum hysteretic deformation demand is set to 0.5. The ratio of the force at which reloading begins to the force corresponding to the maximum hysteretic deformation demand is also set to 0.5.

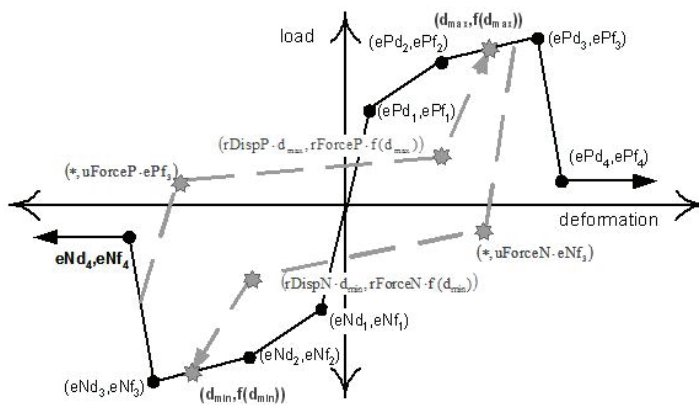


Figure C-12 OpenSees hysteresis model with pinching, “Pinching4.”

Flexural behavior is modeled by elastic elements between plastic hinges at the floor levels. It is recognized that this will not result in an accurate representation of flexural behavior of shear walls (e.g., Orakcal et al., 2006), but it is believed adequate for the purpose intended, which is trying to understand the NRHA response of this structure in terms of quantities familiar to the profession.

The elastic stiffness of the elements between floor levels was assigned a value of $0.35I_g$, even though Table 6-5 in ASCE/SEI 41-06 recommends $0.5I_g$. The 0.35 coefficient was obtained by matching rotation and floor deflections to the results of the FM model. Similarly, strength and rotation capacities of the plastic hinge springs were based on matching to results of the FM model.

Figure C-13 shows the force and deformation properties of the shear and flexural springs, the median roof drift demands obtained from NRHA, and two pushover

diagrams. The left diagram compares the global pushover curve of the FM and SM models, and the right one shows the V_I and $V_{I+P-\Delta}$ pushover curves of the SM model. The NRHA median roof drifts can be compared to those listed for the FM model in Figure C-7.

Results obtained from the NRHA for SF = 1.0 and 2.0 are presented in Figure C-14. The results can be compared directly with those presented in Figures C-8 and C-9 for the FM model. The SM model results compare rather well with the FM model results for these two ground motion scale factors. All EDPs (median roof drift, story drift, story shear, and floor overturning moment) are about 10% to 20% larger for the SM model, but the patterns are the same for both models. This provides confidence that, given comparable component strength and deformation properties, both models predict consistent seismic demands – for ground motion intensities that do not drive the structure far into the inelastic range. But it needs to be said that the component properties of the SM model were intentionally matched to those of the FM model, without an attempt to compute strength properties from established engineering principles and to take deformation properties from established sources such as ASCE/SEI 7, *Minimum Design Loads for Buildings and Other Structures* (ASCE, 2010). This will be attempted in the ASCE41-ASCE41 option discussed in Section C.4.3.

There is one important difference between FM and SM results for SF = 2.0. The FM analysis resulted in 8 “collapses” (cases of numerical instability), but the SM analysis did not cause any “collapses.” The latter is more in line with expectations considering that the median roof drift is a rather small fraction of the roof drift at capping (peak strength).

In Figure C-15 a direct comparison is presented between FM and SM analysis results for a ground motion scale factor SF = 3.0. Significant differences for all EDPs are observed. Median story drifts in the SM model do not exhibit the drastic change in pattern observed in the FM model. Story shears in the SM model are more in line with expectations, i.e., the median base shear for SF = 3 is only about 30% larger than for SF = 2 and is smaller than or at most equal to the base shear capacity. The median base overturning moment capacity is close to the overturning moment capacity obtained from the pushover analysis. Thus, the conflicting observations made for the FM model seem to be rectified in the SM model.

Moment – Rotation Capacities

Story	My (k-in)	Mc (k-in)	Mr (k-in)	θ_p (rad)	θ_{pc} (rad)
1	720000	950000	0	0.025	0.025
2	720000	950000	0	0.025	0.025
3	320000	370000	0	0.02	0.02
4	320000	370000	0	0.02	0.02

Shear Force - Deformation Capacities

Story	Vcr (k)	Vy (k)	Vc (k)	Vr (k)	γ_{cr} (in)	γ_y (in)	γ_c (in)	γ_r (in)
1	572	1145	2631	0	0.00018	0.00727	0.0255	0.0285
2	572	1145	2631	0	0.00018	0.00727	0.0255	0.0285
3	354	708	2044	0	0.00011	0.00466	0.0218	0.0285
4	354	708	2044	0	0.00011	0.00466	0.0218	0.0285

Roof Drift Ratios from NRHA (H = 588 inches)

	SF=0.5	SF=1.0	SF=2.0	SF = 3.0
Median [%]	0.0036	0.0077	0.0171	0.0346
16th [%]	0.0022	0.0050	0.0124	0.0204
84th [%]	0.0048	0.0100	0.0244	---
Mean μ [%]	0.0036	0.0079	0.0187	---
σ [%]	0.0012	0.0029	0.0088	---
CoV	0.334	0.367	0.473	---
Collapses	0	0	0	16

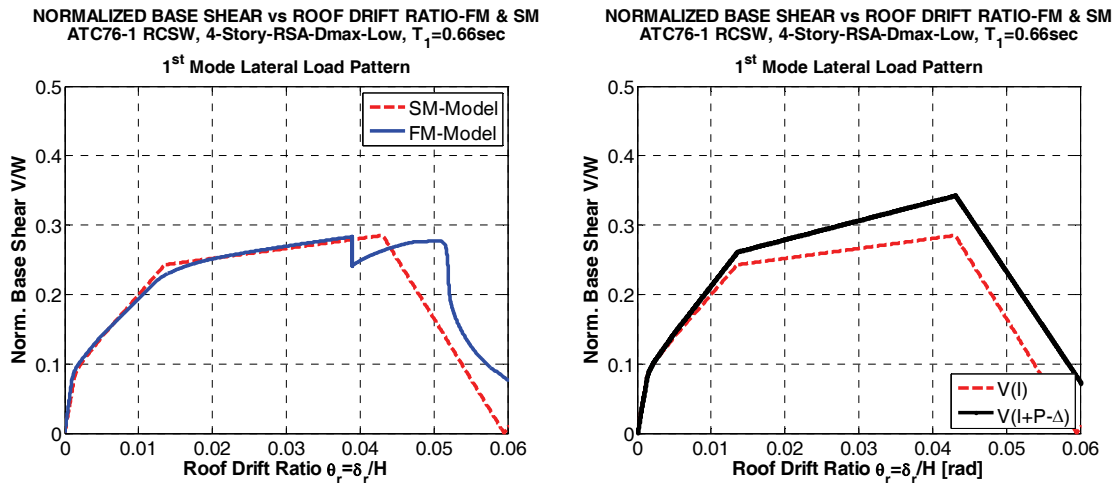


Figure C-13 System information, 4-story RCSW, SM Model.

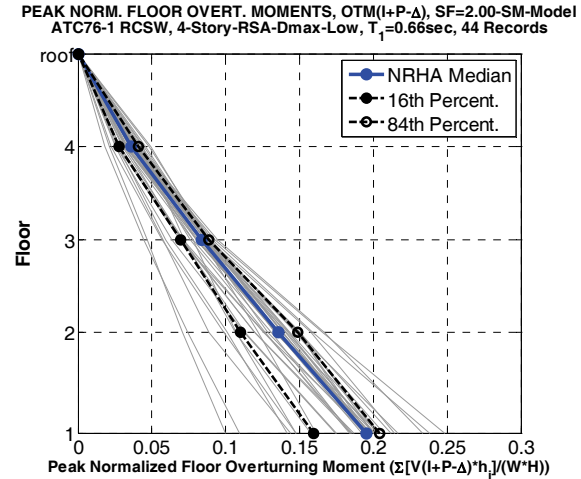
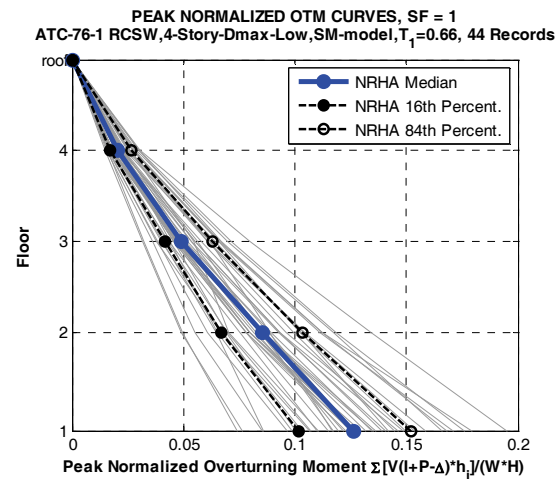
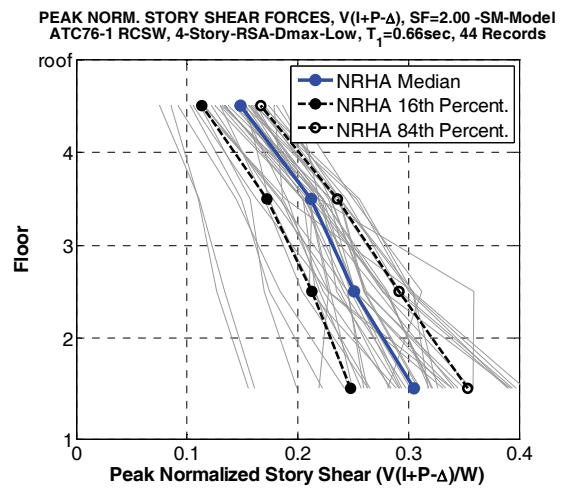
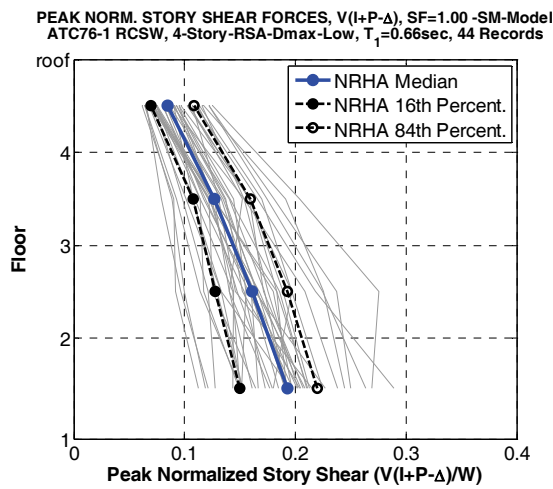
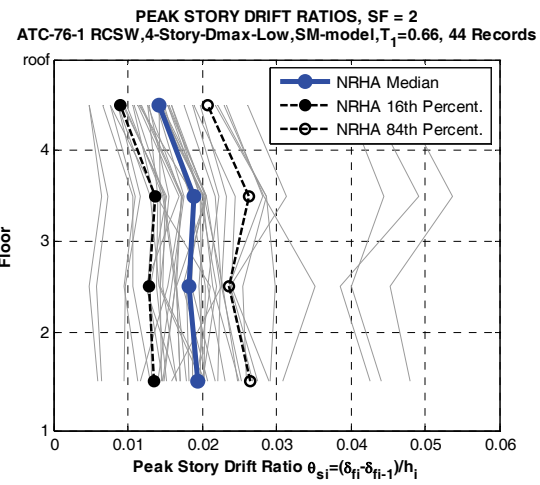
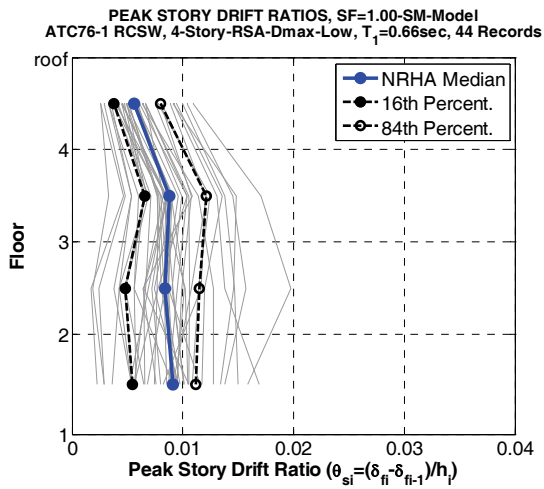


Figure C-14 NRHA Peak story drift ratios, story shears, and floor overturning moments, 4-story RCSW, SM Model, SF = 1.0 and 2.0.

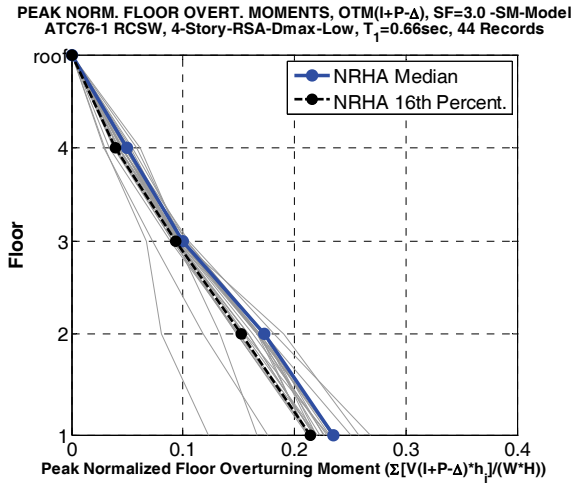
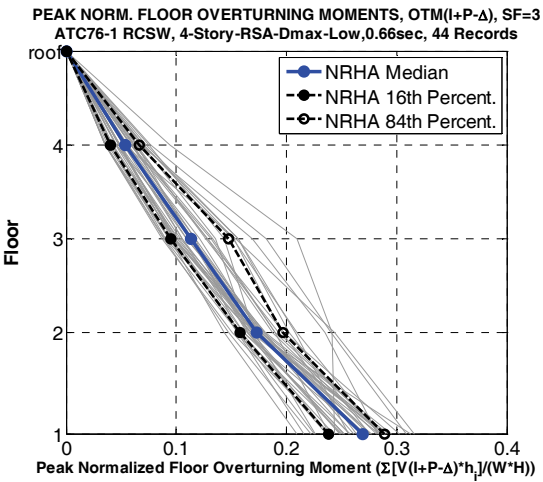
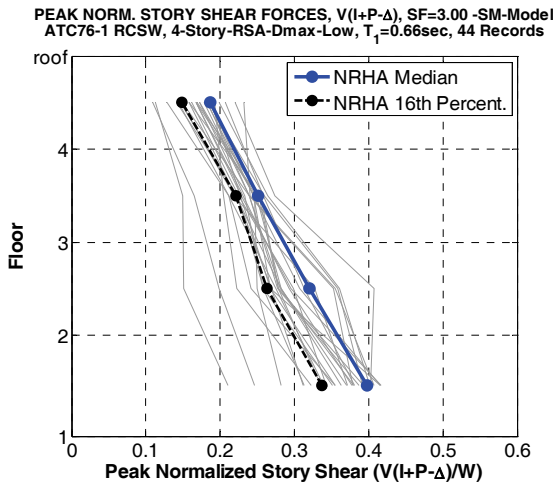
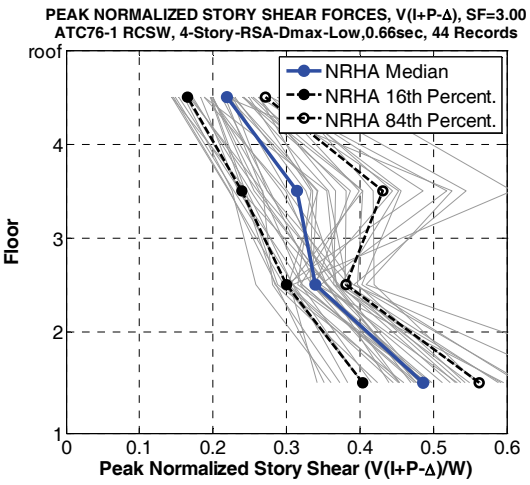
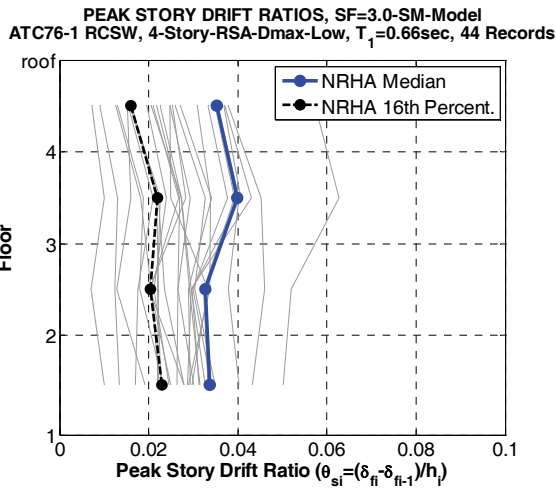
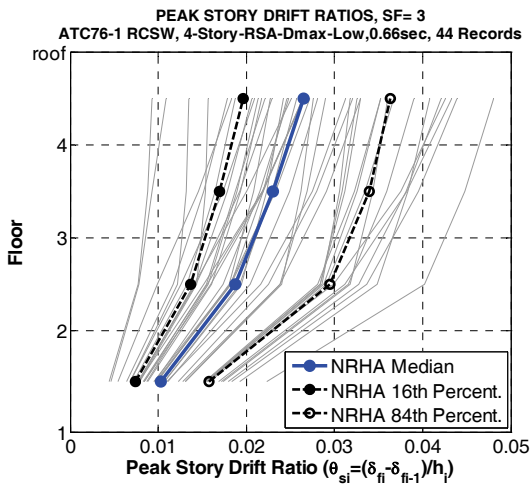


Figure C-15 NRHA Peak story drift ratios, story shears, and floor overturning moments, 4-story RCSW, FM Model (left), SM Model (right), SF = 3.0.

C.3.4 Synthesis of Nonlinear Response History Analysis Results

This portion of the study, concerned with NRHA of reinforced concrete shear wall structures (RCSWs), led to the following general conclusions on analytical modeling for the purpose of estimating strength demands in walls and story drift demands. Only solid rectangular walls have been used in this study.

1. Fiber models have great potential and provide information that cannot be obtained from simplified spring models, but at this time it is difficult to evaluate their reliability and to see how an engineer can use judgment to assess the soundness of results obtained from fiber model analysis.
2. Simple models consisting of elastic elements and flexural as well as shear springs may be adequate to capture important behavior modes for regular shear walls without openings, conditioned that consequences of previously pointed out shortcomings of these models can be evaluated. Stiffness and strength properties up to yielding can be captured adequately with spring models. More effort needs to be devoted to quantification of deformation capacities, particularly the very important plastic deformation before strength decrease (capping point), and the post-capping negative tangent stiffness. These are the quantities that control acceptable performance of structures. Systematic collection and evaluation of experimental data, which are the primary source to quantify these quantities, is much needed.
3. All FM pushover curves exhibit a rapid deterioration in strength after the peak strength has been attained. This is very different from the behavior observed for steel SMFs (Appendix A). The reason for it lays in the formulation of the fiber model for bending behavior. This rapid deterioration in strength needs to be further explored. It is doubtful that this rapid loss in strength is equally present in the NRHA in which responses of fiber models are difficult to trace. An indication that this rapid loss in strength does not occur in NRHA is the observation that the 4-story FM model survived all 44 records with a SF = 3.0 without dynamic instability (collapse) and with shear and overturning moment capacities that greatly exceed those indicated by the global pushover curve.
4. All pushover curves have a large initial stiffness, but this stiffness degrades rapidly at relatively low load levels. In the 4- and 8-story structures, modeling of post-cracking shear behavior in the translational shear springs was mostly responsible for this stiffness deterioration. After this “kink” the lateral stiffness remains reasonably constant until it decreases rapidly due to flexural yielding. After “yielding” the stiffness remains close to constant until it drops rapidly due to flexural failure as defined by the material parameters used in the fiber model. This behavior indicates simplified representation of pushover curves requires a multi-linear diagram.

5. The increase in NRHA shear demands for the low-rise 2- and 4-story RCSWs, compared to the peak strength values obtained in the pushover analysis, is surprisingly large. It is not known whether this increase is due to dynamic amplification or due to modeling issues in the FM models.
6. NRHA story shear demands are much more in line with design and pushover shear force patterns than was observed for steel SMF structures (Appendix A). The same observation applies to floor overturning moments.

C.4 Single Mode Nonlinear Static Procedure

This work focuses on evaluating the feasibility and limitations of the standard single mode nonlinear static procedure (NSP) of ASCE/SEI 41-06. The objective here is to follow the ASCE/SEI 41-06 procedure rigorously, explore simple alternatives, and provide a quantitative assessment of NSP predictions of relevant EDPs in comparison to the NRHA results discussed in the previous section. The structures were introduced in Section C.2.

The all-important issue of lateral load pattern is not explored here. Previous work (FEMA 440) has addressed this issue and came to the conclusion that variations in invariant lateral load patterns do not improve the accuracy of EDP predictions. The load pattern applied in all cases discussed here is the pattern structured after the elastic first mode deflected shape, as recommended in ASCE/SEI 41-06. The emphasis is on methods of pushover analysis, ways to compute the target displacement at which the pushover data are to be evaluated, and evaluation of NSP results with a focus on the previously discussed story EDPs peak story drift, peak story shear force (V_{I+P-A}), and floor overturning moments (OTM_{I+P-A}). For the archetype shear wall structures the peak story shear force and floor overturning demands are equal to the local shear force and moment demands for the wall.

C.4.1 Nonlinear Static Analysis Options Explored

Given a prescribed lateral load pattern, there are many options for modeling the structure for pushover analysis and for selecting the method for target displacement prediction. In general, the latter is based on predicting the displacement demand for an equivalent SDOF system that represents the first mode characteristics of the MDOF structure and mapping this demand back to the global pushover curve to find the point at which the structure should be evaluated (often referred to as performance point). In the ASCE/SEI 41-06 coefficient method this process is greatly simplified and the equivalent SDOF system does not become an explicit part of the target displacement estimation.

Pushover Analysis Options

In this study the following options are explored for models of structural components, which then are assembled in the OpenSees analysis platform:

- **ASCE41:** ASCE/SEI 41-06 component models are used, but assuming a post-capping stiffness obtained by linearly connecting peak point C and point E of the generic ASCE/SEI 41-06 model.
- **FM:** Fiber model used in the NIST funded ATC 76-1 Project is utilized to represent flexural behavior, and a story shear spring is used to represent shear behavior.

The FM analysis option was executed for all three RCSWs, whereas the ASCE41 option was explored only for the 4-story RCSW.

Target Displacement Options

- **ASCE41:** Target displacement is obtained from ASCE/SEI 41-06 coefficient method, using the idealized trilinear force-displacement curve recommended in ASCE/SEI 41-06, where effective elastic stiffness is obtained by placing a line through the displacement at $0.6V_y$.
- **Eq.SDOF:** Target displacement is based on median displacement obtained from an equivalent SDOF system and NRHA with the 44 FEMA P-695 ground motions, using a nonlinear SDOF analysis program (in this study the program IIDAP was employed). Equivalent SDOF properties are obtained from the base shear V_I – roof displacement pushover curve (not the $V_{I+P-\Delta}$ – roof displacement pushover curve). In the case of shear wall structures in which the global pushover curve shows a clear kink around cracking, the idealized force-displacement curve is better represented by a multi-linear curve that has at least 4 stiffnesses (pre-cracking, post-cracking, post-yielding, and post-capping).

Single Mode NSP Options

The NSP may consist of any combination of the aforementioned pushover analysis options and target displacement options, i.e.:

- ASCE41-ASCE41
 - Pushover analysis option: ASCE/SEI 41-06 component models
 - Target displacement option: ASCE/SEI 41-06 coefficient method (trilinear diagram)
- FM-ASCE41
 - Pushover analysis option: fiber model used for RCSWs in the NIST funded ATC 76-1 Project
 - Target displacement option: ASCE/SEI 41-06 coefficient method (trilinear diagram)

- FM-Eq.SDOF
 - Pushover analysis option: fiber model utilized for RCSWs in the NIST funded ATC 76-1 Project
 - Target displacement option: Median target drift from obtained Equivalent SDOF analysis with IIDAP, utilizing a multi-linear force-displacement relationship. Cyclic deterioration is not incorporated explicitly because it is not considered in FM analysis executed in the NIST funded ATC 76-1 Project.

C.4.2 Results for 2- and 8-Story Reinforced Concrete Shear Wall Structures Utilizing FM-ASCE41

For the 2- and 8-story RCSWs structures only the FM-ASCE41 option is explored. For each structure a pair of figures is presented. The first figure shows FM pushover curves with the idealized ASCE/SEI 41-06 force-displacement curve superimposed, and the associated equivalent SDOF systems, as well as target drift ratios obtained from this NSP options.

The second figure presents a NSP to NRHA comparison, with the NSP results superimposed on the previously discussed NRHA results. Results are presented for SF = 1.0 and 2.0; results for SF = 0.5 are similar to those for SF = 1.0 and add little new insight.

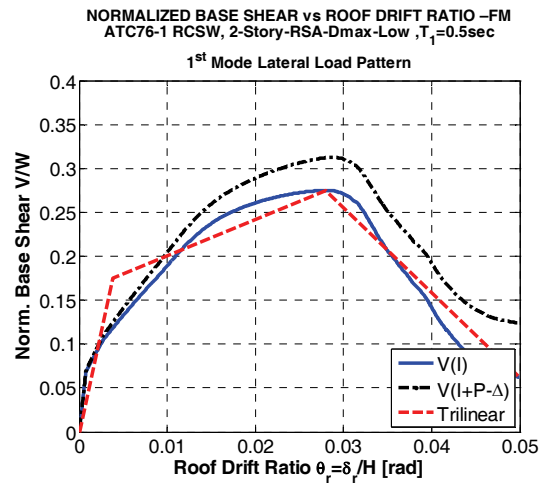
Summary of Observations for 2-story RCSW (Figures C-16 and C-17):

- The target displacements and NSP story drifts are 20% to 60% larger than the NRHA median roof drifts and story drifts. Much of the difference can be attributed to the use of the simplified trilinear pushover curve on which the ASCE/SEI 41-06 coefficient method is based.
- Shear force and OTM demands are predicted rather accurately by the FM-ASCE41 nonlinear static procedure.

Summary of Observations for 8-story RCSW (Figures C-18 and C-19):

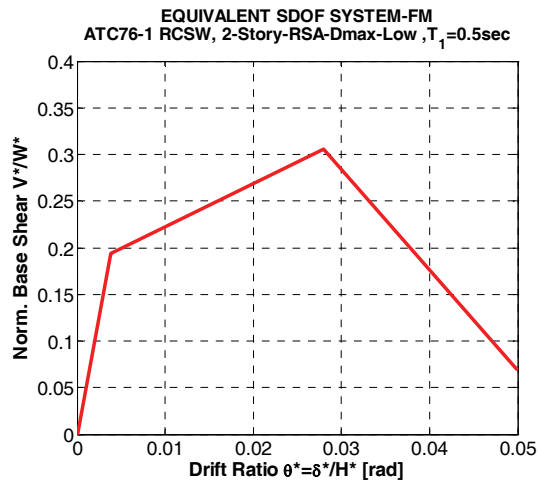
- The pushover curves show that the NRHA drift demands imposed on this structure are rather low and barely reach global yielding for SF = 2.0.
- The target roof drifts obtained from the ASCE/SEI 41-06 coefficient method compare poorly with the median NRHA drifts. In this example, and in the 4-story examples discussed in Section C.4.3, the simplification made when representing the pushover curve with a trilinear curve that intersects the pushover curve at the drift associated with $0.6V_y$ was found to be the main reason for the poor target displacement predictions. The importance of this simplification diminishes as the structure gets pushed further into the inelastic range, but it certainly has a clear effect at the target drift levels of this 8-story structure.

- Because of the poor prediction of target roof drifts, the prediction of story drifts is equally poor. It is poor not only in magnitude but also in distribution over the height. Again, much of this is believed to be caused by the use of a trilinear pushover representation.
- Story shear and floor overturning moment predictions from the FM-ASCE41 NSP provide a good match with the median NRHA values.



Properties of Equivalent SDOF systems

Model	V_y^*/W^*	T_e [sec]	ξ	θ_p/θ_y	θ_{pc}/θ_y
FM-ASCE41	0.198	0.70	0.083	6.3	7.9



NRHA Median and Target Roof Drift Ratios (H = 300 inches)

	NRHA Median	FM-ASCE41
SF = 0.5	0.0036	0.0062
SF = 1.0	0.0087	0.012
SF = 2.0	0.0186	0.0249

Figure C-16 NSP Information, 2-story RCSW, FM-ASCE41.

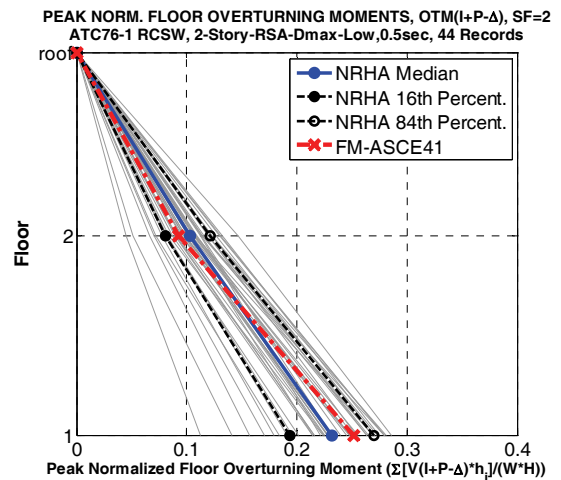
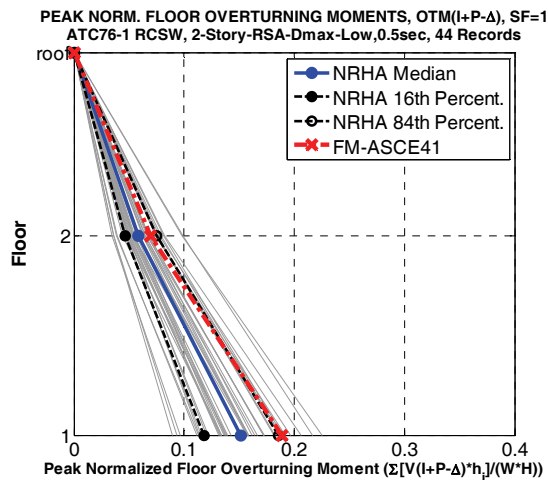
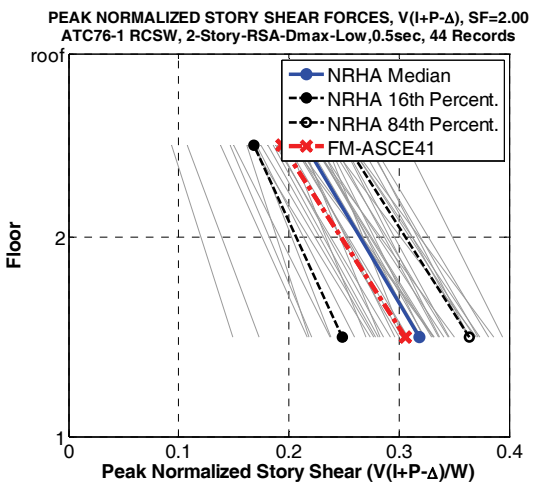
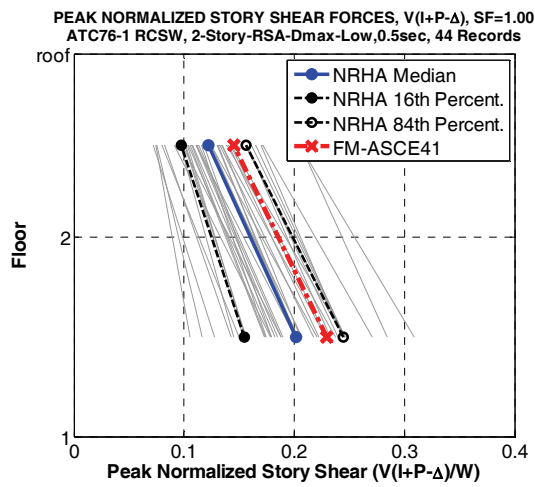
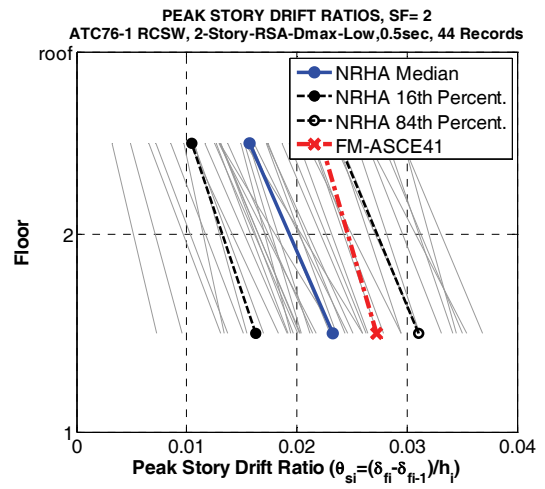
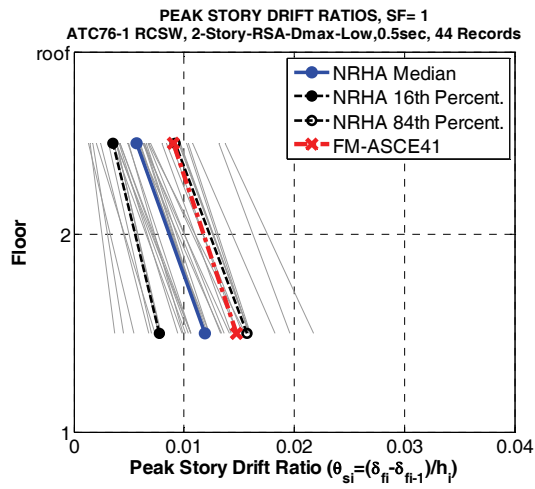
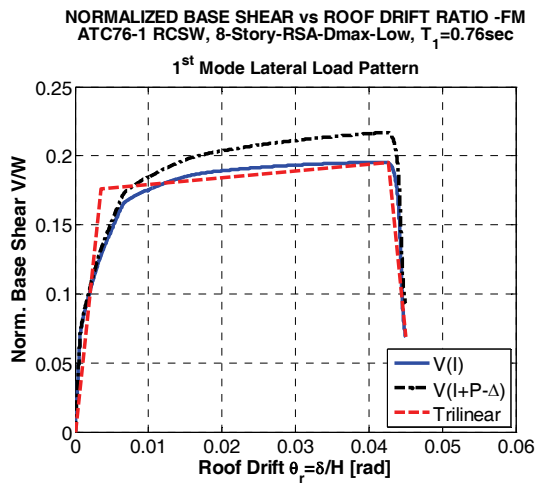
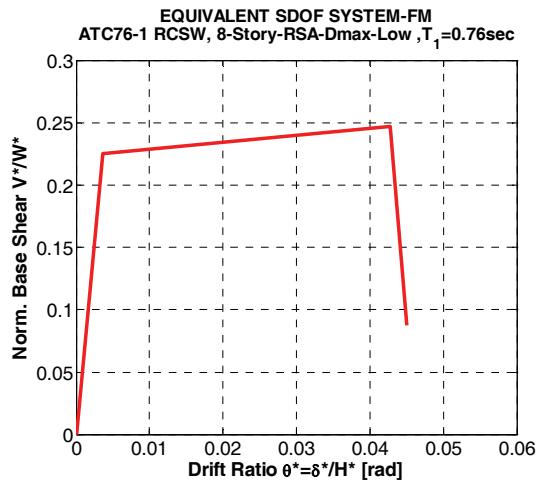


Figure C-17 NSP to NRHA comparison, 2-story RCSW, FM-ASCE41, SF = 1.0 and 2.0.



Properties of Equivalent SDOF systems

<i>Model</i>	V_y^*/W^*	T_e [sec]	α_s	θ_p/θ_y	θ_{pc}/θ_y
FM-ASCE41	0.22	1.09	0.01	10.94	1.035



NRHA Median and Target Roof Drift Ratios (H = 1164.00inches)

	NRHA Median	FM-ASCE41
SF = 0.5	0.0014	0.0028
SF = 1.0	0.0029	0.0056
SF = 2.0	0.0059	0.0112

Figure C-18 NSP Information, 8-story RCSW, FM-ASCE41.

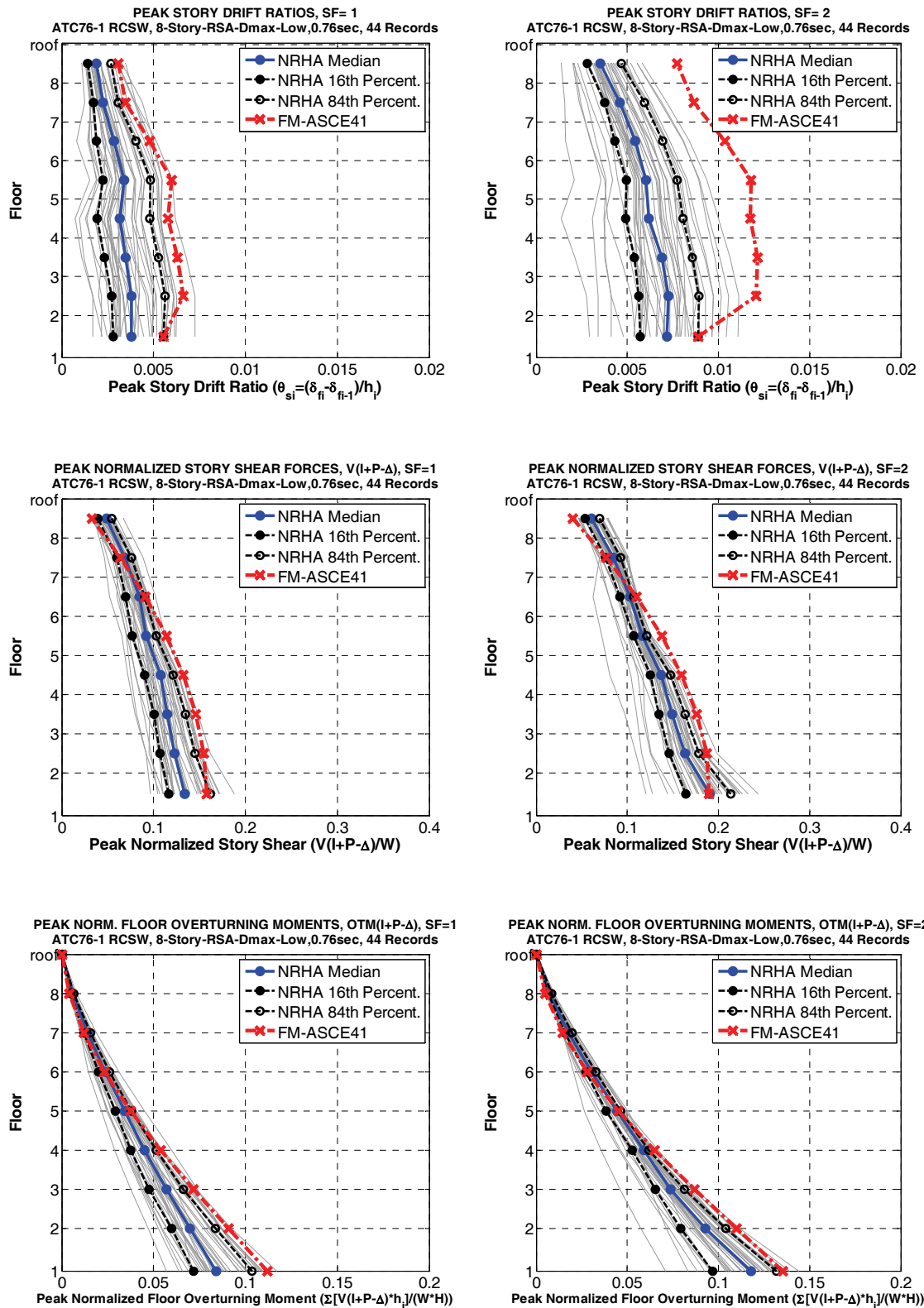


Figure C-19 NSP to NRHA comparison, 8-story RCSW, FM-ASCE41, SF = 1.0 and 2.0.

C.4.3 Results for 4-Story Reinforced Concrete Shear Wall Structure Utilizing Alternative Nonlinear Static Procedures

Results from exploration of alternative NSPs are documented in Figures C-21 to C-24. Figure C-21 presents basic data for the ASCE41-ASCE41 NSP option discussed below, properties of the equivalent SDOF system, and NRHA median roof drifts and target roof drifts from three NSP options. Figure C-22 presents pushover curves and equivalent SDOF systems for the three NSP options explored here. Figures C-23 and C-24 present NSP to NRHA comparisons.

For all RCSW structures (2, 4, and 8 stories) the FM-ASCE41 NSP option (as recommended presently in ASCE/SEI 41-06) leads to rather poor predictions of story drifts, see Figure C-23 for the 4-story RCSW. Therefore, emphasis was placed on a better representation of the global pushover curve in the equivalent SDOF system in order to obtain a better estimate of the target displacement. For this purpose the global pushover curve was represented in a multi-linear manner rather than the trilinear manner recommended in ASCE/SEI 41-06. A multi-linear (quadrilinear) representation was selected that accounts for the large difference in pre- and post-cracking stiffness, see second row of graphs presented in Figure C-22. The target displacement of the corresponding equivalent SDOF system was predicted with the program IIDAP, by subjecting the equivalent SDOF system to the set of 44 ground motions from FEMA P-695 and computing the median displacement, which was then mapped back to the MDOF domain. This mapped value was used as target displacement to predict the EDPs from the global pushover. The EDP predictions obtained in this manner (denoted as FM-Eq.SDOF) show a large improvement over the predictions obtained from use of the trilinear ASCE/SEI 41-06 equivalent SDOF system (see Figures C-23 and C-24) – except for SF = 3, which imposes high demands on the FM model and yields the debatable results discussed in Section C.3.2.

As an alternative, EDP predictions for the 4-story RCSW were obtained also from using ASCE/SEI 41-06 component models to perform the pushover analysis together with the ASCE/SEI 41-06 target displacement procedure (ASCE41-ASCE41 option). The challenge here was to determine moment and shear strength properties based on ASCE/SEI 41-06 recommendations. The values for bending strength obtained from the FM model and computed from ACI criteria together with ASCE/SEI 41-06 criteria for expected material properties differ a significant amount. Since exploration of the use of ASCE/SEI 41-06 component models is central to this study, it was pursued further with the following assumptions in order to permit comparison with the NRHA results, which are based on the FM model. The moment and shear capacity values presented in Figure C-21 are based on ASCE/SEI 41-06 criteria for M_y and V_y , and on the information provided in the report on the NIST funded ATC 76-1 Project for M_c and V_c . The latter implies that in the third story only the reinforcement in the outer 25% of the cross section is used to compute M_y , because

there are no confined boundary zones in that story. Where employing ASCE/SEI 41-06 criteria for V_y implies that V_y and V_c should take on the same value (Section 6.7.2.3 of ASCE/SEI 41-06), computing M_c and V_c means that the design information on M_n and V_n provided in NIST GCR 10-917-8 is used to compute M_c and V_c . For M_c a multiplier of 1.25 is used to account for the difference between expected and nominal material properties, but this multiplier was not used for V_c in accordance with ASCE-41. This was done to achieve a reasonable match in strength between the ASCE pushover and the FM pushover, in order to permit comparison of results.

The estimated strength values M_c are significantly larger than would be calculated from basic engineering models and using the reinforcement layout provided in NIST GCR 10-917-8. The FM peak moment value M_c can be obtained only with a much larger axial force that was used in design of this structure. As Figure C-20 shows, the bending capacity of the wall is very sensitive to the axial force in the wall. A small difference in axial force changes the bending capacity by a large amount, and consequently the failure mode in the wall may change from bending to shear or vice versa. And nonlinear dynamic response in a wall that deforms primarily in shear may be very different from that deforming primarily in bending.

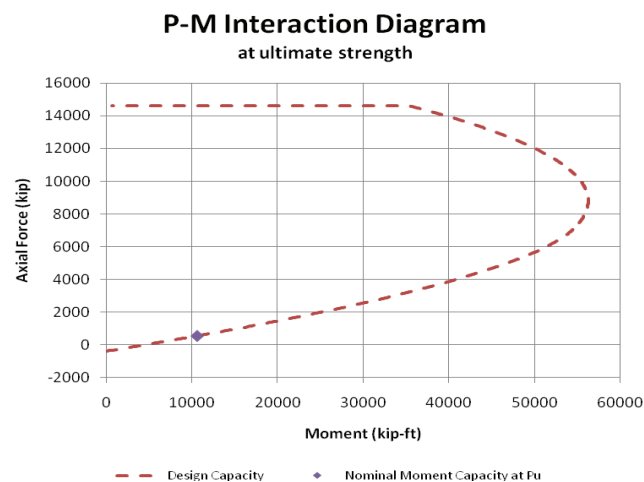


Figure C-20 M-P interaction diagram for 4-story RCSW.

The pushover curve obtained from the ASCE/SEI 41-06 approach is very different from that obtained from the FM model, see Figure C-22. This brings up the challenging question of shear versus flexural failure and its consequences. Because of the relatively high moment capacity M_c this shear wall, when subjected to the first mode load pattern, fails in shear. And in shear the ASCE/SEI 41-06 document assigns very small deformation capacity to this wall. As a consequence, the pushover curve of the wall according to ASCE/SEI 41-06 criteria is very different from that obtained from the FM model. The pushovers are not that different in strength (because of the aforementioned adjustment of bending strength) but they are radically different in deformation capacity. This difference led to very different NSP

predictions (ASCE41-ASCE41) compared to those obtained from FM-ASCE41 and FM-Eq.SDOF, see Figure C-23. ASCE41-ASCE41 predictions were possible only for SF = 0.5 and 1.0, because for larger ground motion scale factors the predicted roof drift exceeded the deformation capacity indicated by the ASCE/SEI 41-06 pushover.

The advantage is that there is a large discrepancy between EDP predictions obtained from a fiber model pushover analysis and an ASCE/SEI 41-06 pushover analysis. This study can only point out this discrepancy but cannot attempt to solve it. The discrepancy is evident in the pushover curves and in the NSP predictions. The ASCE41 pushover predicts unacceptable performance (represented by intolerable roof drift in the ASCE/SEI 41-06 pushover and by collapses in NRHA with the FM model) at ground motion intensities (represented by the scale factor SF) less than one third of that predicted by the FM model. These observations do not imply that the ASCE/SEI 41-06 component models are incorrect; they merely imply that there are huge differences between a pushover curve obtained from ASCE/SEI 41-06 and a pushover curve obtained from the FM model.

Given that the FM model is the proper model to predict EDPs by means of NRHA, it is important to note that the FM-Eq.SDOF NSP approach provides a very good match with NRHA median results for all three story EDPs (drift, shear force, and OTM) – up to a ground motion scale factor of 2.0. The improvement is the multi-linear representation of the pushover curve for formation of the equivalent SDOF system, as compared to the FM-ASCE41 approach in which the pushover curve is represented by a trilinear diagram. The latter does not lead to good EDP predictions in most cases.

For a ground motion scale factor SF = 3.0 all NSP predictions do not compare well with the median NRHA values. At this time it is not known whether this is due to problems with the NSP approaches or problems inherent in the FM model.

**Strength and Deformation Properties per ASCE/SEI 41-06, Supplemented by
(NIST, 2010) Data**

Story	My (k-in)	Mc (k-in)	Mr (k-in)	θ_y (rad)	θ_p (rad)	θ_{pc} (rad)
1	558050	833333	334118	0.001542	0.01284	0.005
2	526177	833333	394633	0.001465	0.01500	0.005
3	128338	305555	68972	0.000332	0.00800	0.007
4	91490	305555	46941	0.000229	0.00800	0.007

Story	Vy (k)	Vc (k)	Vr (k)	γ_y (in)	γ_p (in)	γ_{pc} (in)
1	1227	1227	491	0.0015	0.006	0.0125
2	1227	1227	491	0.0015	0.006	0.0125
3	933	933	373	0.0015	0.006	0.0125
4	933	933	373	0.0015	0.006	0.0125

Properties of Equivalent SDOF systems

<i>Model</i>	V_{cr}^*/W^*	V_y^*/W^*	T_e [sec]	α_s	θ_p/θ_y	θ_{pc}/θ_y
FM-ASCE41		0.28	0.95	0.030	8.2	4.59
FM-Eq.SDOF	0.095	0.28	0.66	---	3.4	1.5
ASCE41-ASCE41	---	0.20	0.73	0.227	2.5	---

NRHA Median and Target Roof Drift Ratios (H = 588 inches)

	NRHA Median	FM-ASCE41	FM-Eq.SDOF	ASCE41-ASCE41
SF = 0.5	0.0025	0.0045	0.0024	0.0038
SF = 1.0	0.0053	0.0090	0.0048	0.0072
SF = 2.0	0.0129	0.0181	0.011	---
SF = 3.0	0.0191	0.0218	0.0214	---

Figure C-21 Tabulated NSP information, 4-story RCSW.

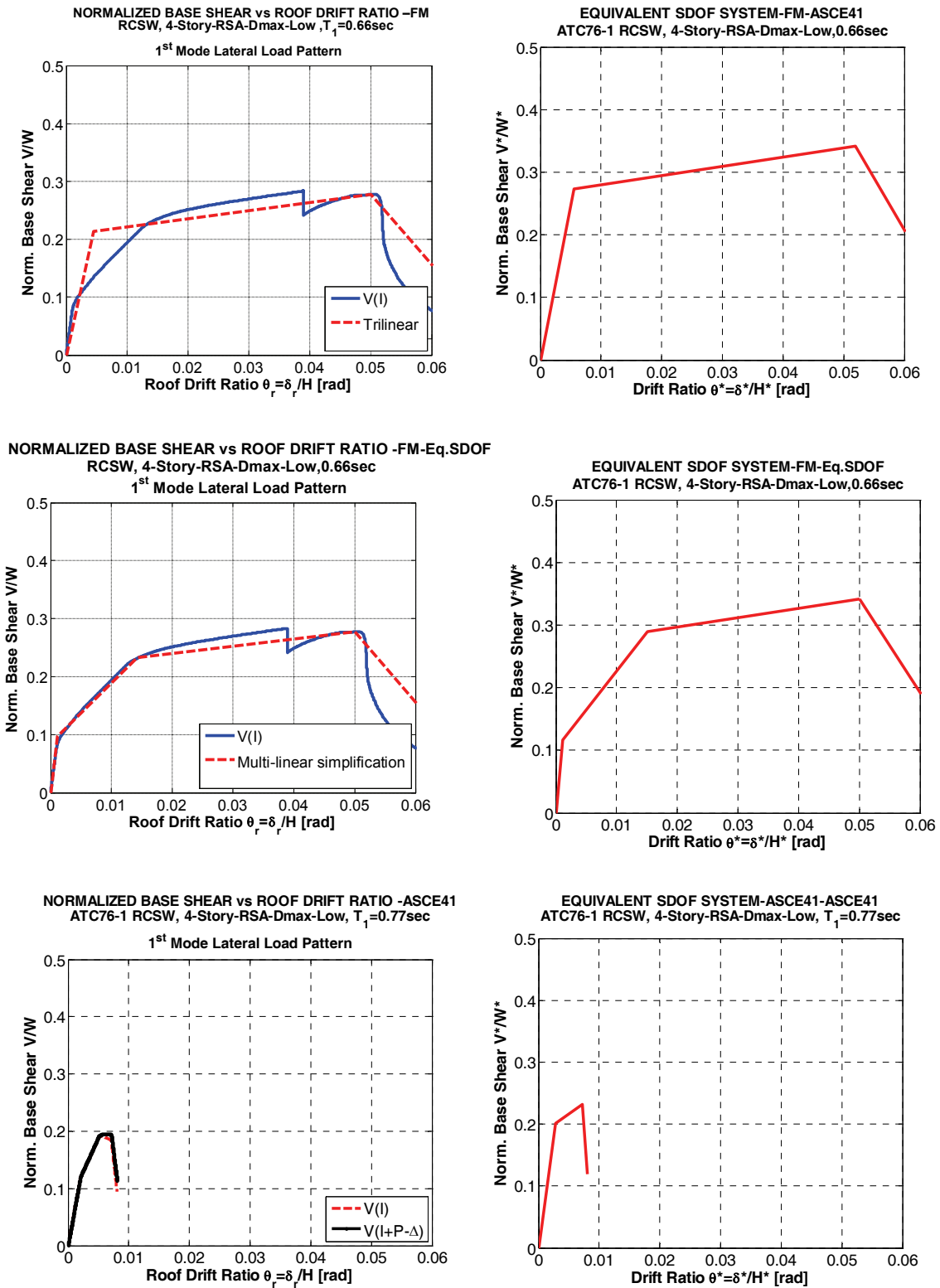


Figure C-22 NSP pushover curves and equivalent SDOF systems, 4-story RCSW, FM-ASCE41, FM-Eq.SDOF, ASCE41-ASCE41.

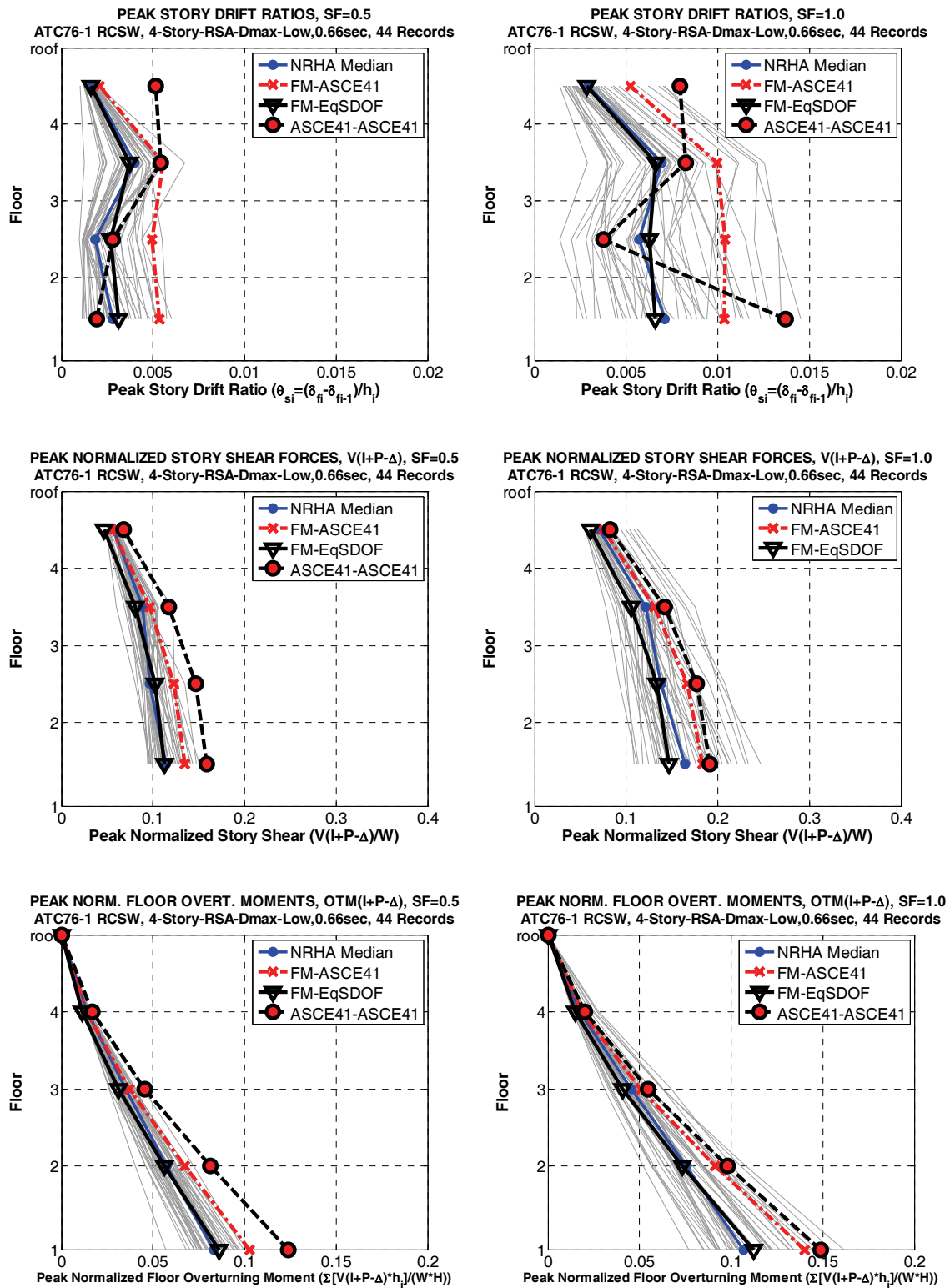


Figure C-23 NSP to NRHA comparison, 4-story RCSW, three different NSP options, SF = 0.5 and 1.0.

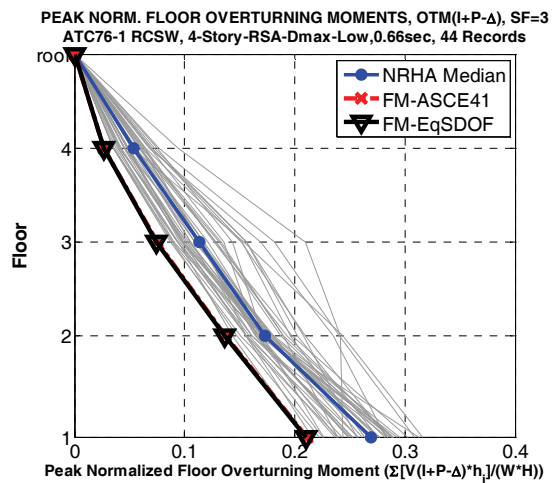
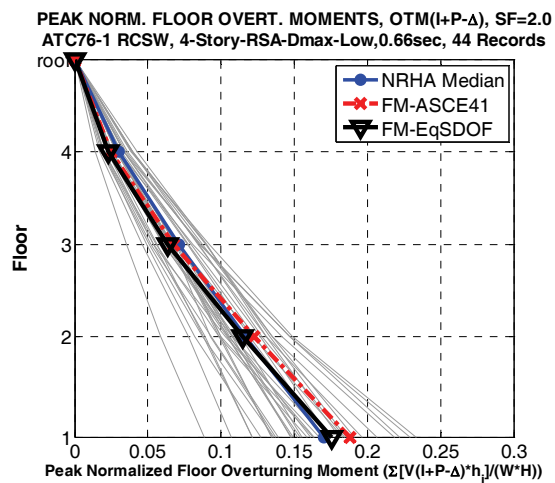
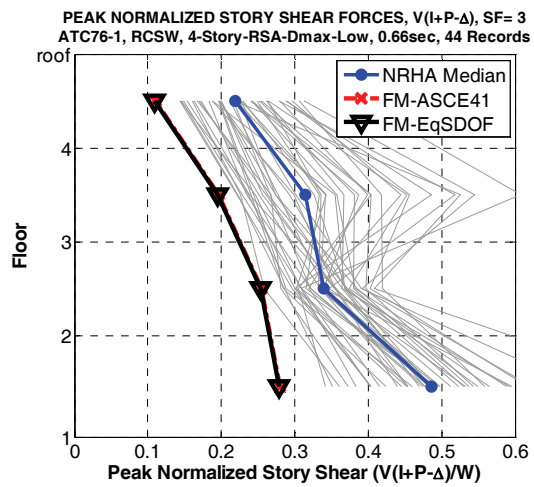
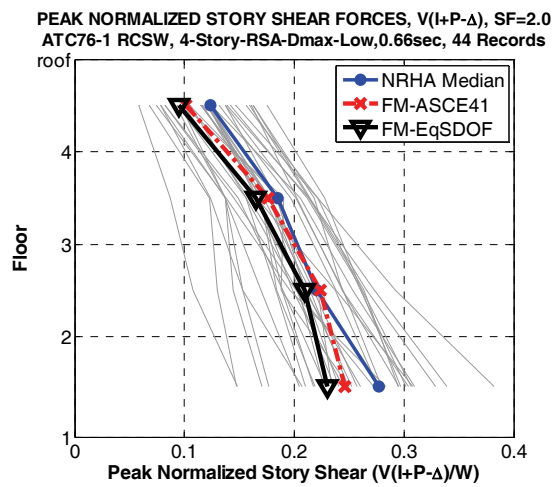
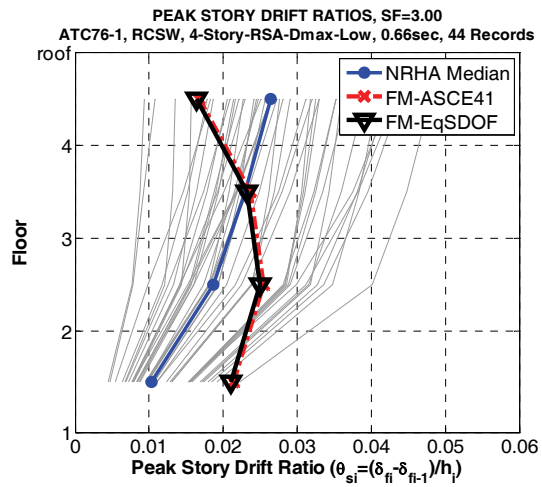
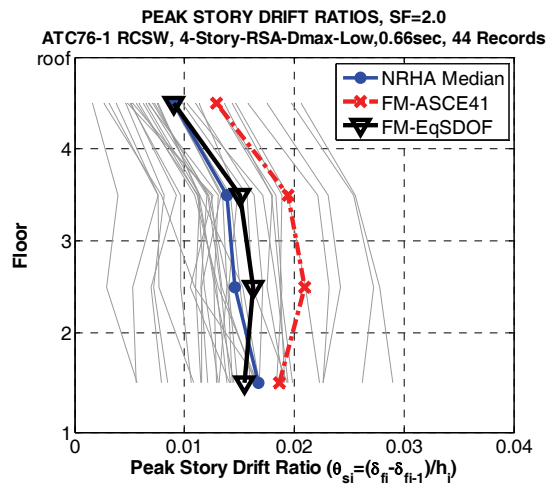


Figure C-24 NSP to NRHA comparison, 4-story RCSW, three different NSP options, SF = 2.0 and 3.0.

C.4.4 Synthesis of Nonlinear Static Procedure Predictions

Plots summarizing the ratio of NSP predictions over median NRHA results for peak story drifts, peak story shear forces, and peak floor overturning moments are presented in Figure C-25, using the FM-ASCE41 nonlinear static procedure (NSP) option and ground motion scale factors $SF = 1.0$ and 2.0 . For these ground motion scale factors the target roof drift is below the global capping point, i.e., issues of post-capping behavior do not enter. A ratio smaller than 1.0 implies that the NSP under-predicts the median demands computed by NRHA. The medians of NRHA results obtained from the fiber model (FM model) are used as benchmark values. They may not represent the absolute truth, but they represent the best estimate in the context of NSP to NRHA comparison since in both the static and dynamic analysis procedures compatible analytical models are used. Issues associated with the debatable results of the FM NRHA for $SF = 3.0$ are avoided by not presenting results for this scale factor.

Figure C-26 presents the $NSP/NRHA_{med}$ ratios for the FM-Eq.SDOF option, using the 4-story RCSW for illustration. In this option the target displacement was obtained by using a multi-linear simplification of the global pushover curve that considers pre- and post-cracking stiffness, and by subjecting the corresponding equivalent SDOF system to the FEMA P-695 ground motion set to obtain a median displacement estimate.

This study focused on a small set of shear wall structures. These structures are considered to be representative of regular low-rise shear wall structures. They do not incorporate significant irregularities in strength or stiffness. Thus, the observations made here are specific for the cases investigated, and extrapolation to other cases has to be done with caution.

1. The simplification made when representing the pushover curve with a trilinear diagram that intersects the pushover curve at the drift associated with $0.6V_y$, as is recommended in ASCE/SEI 41-06, was found to lead to poor target displacement predictions, particularly when the NRHA predicts roof drifts that are not much larger than those associated with global yielding. This is the main reason why many of the ratios shown in Figure C-25 deviate considerable from 1.0 . The importance of this simplification diminishes as the structure gets pushed further into the inelastic range.
2. The use of a multi-linear equivalent SDOF system for prediction of target displacement does lead to a considerable improvement in target displacement and EDP predictions from a nonlinear static procedure. This approach should be employed for structures in which the pushover exhibits a clear stiffness discontinuity due to pre- and post-cracking behavior. Utilization of the approach requires the prediction of SDOF displacement demands for a set of representative ground motions. Tools for performing such an SDOF analysis are available, but

implementation requires also the availability of representative sets of ground motions.

3. Utilizing the approach summarized in item 2, very good EDP predictions were obtained for the 4-story RCSW, see Figure C-26. It is not known to what extent this improvement can be extrapolated to the 8-story RCSW.
4. NSP predictions in the post-capping range could not be explored because of the very rapid decrease in strength exhibited by the FM model pushovers. It appears that none of the selected wall structures did have a predictable post-capping range.
 - In general, NSP predictions for wall structures provide a better match to NRHA results than for steel moment frame structures (Appendix A) because story shear and bending strengths for walls are well defined and less redistribution of strength occurs between adjacent stories.
 - In the three RCSW structures investigated, the yielding mode in the pushover analysis was the same as the yielding mode that dominated in the NRHA (except for the 4-story RCSW and ground motion scale factor $SF = 3.0$). In general, bending was the dominant mode of failure. If the failure mode is different in NSP and HRHA, then none of the above observations might apply. This issue is addressed in Section C-6.

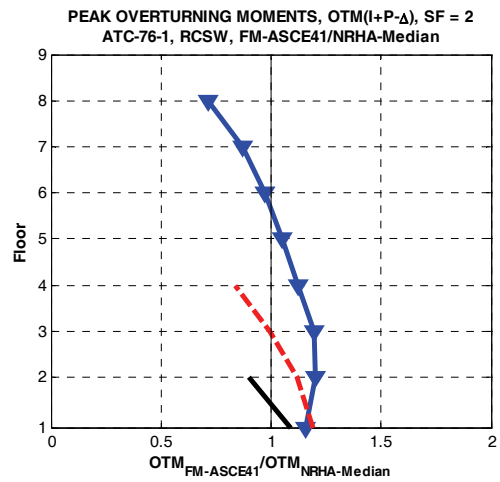
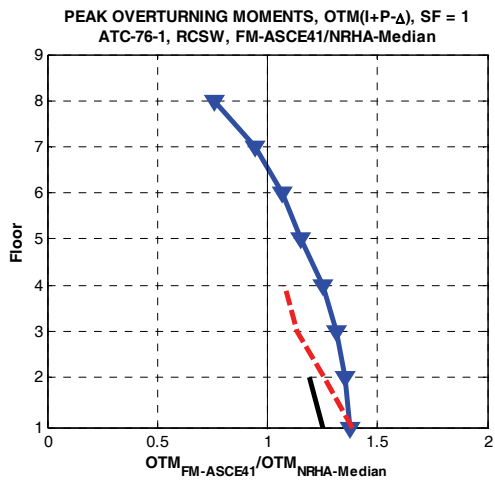
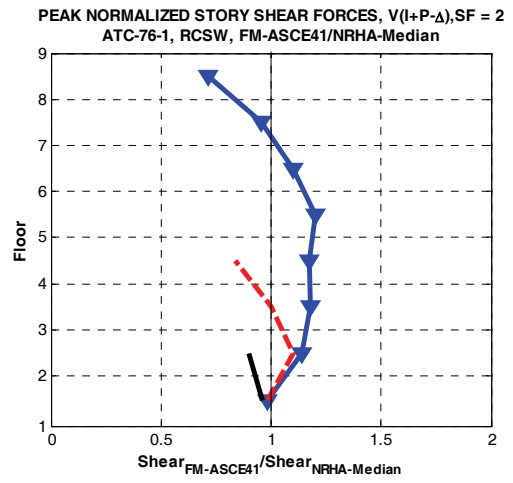
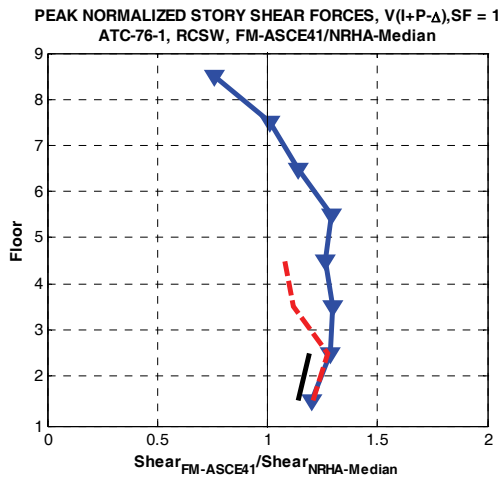
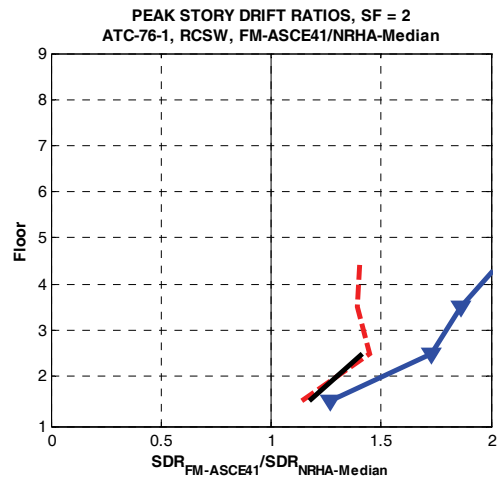
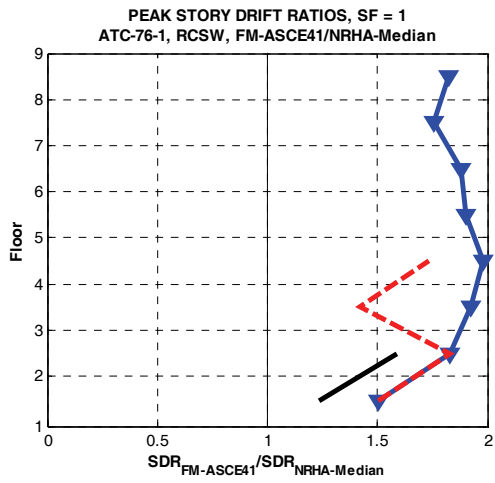


Figure C-25 Ratios of NSP prediction over median NRHA result for story EDPs, using FM-ASCE41 option, SF = 1.0 and 2.0.

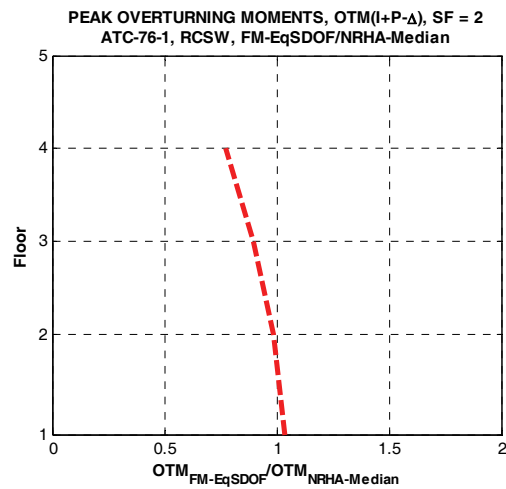
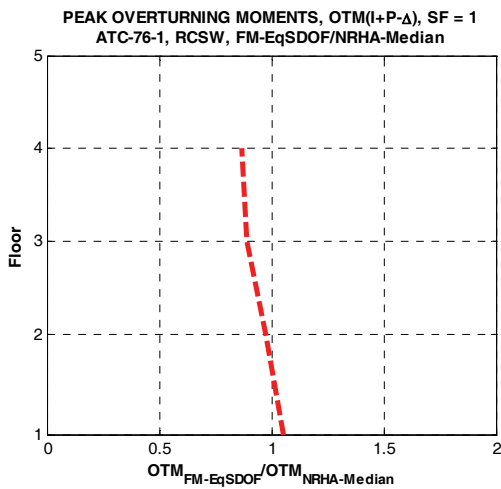
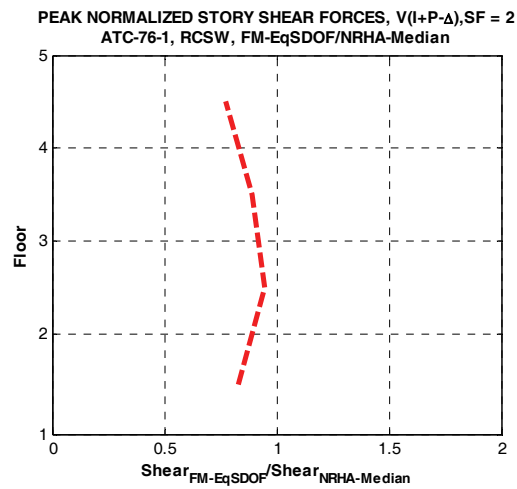
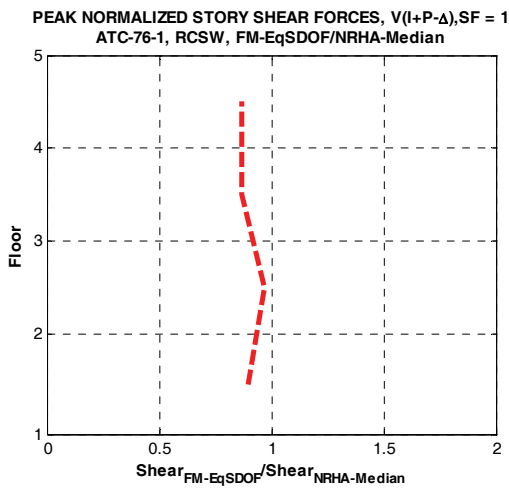
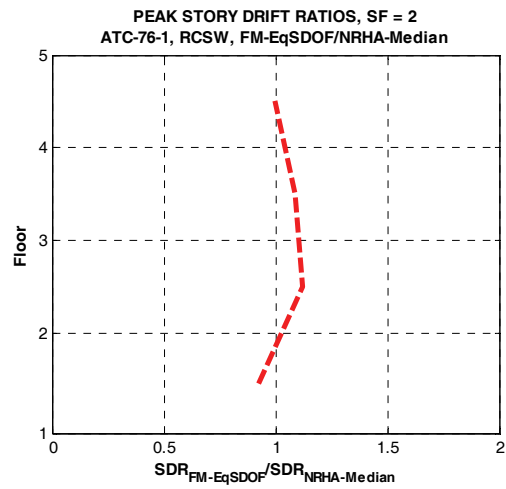
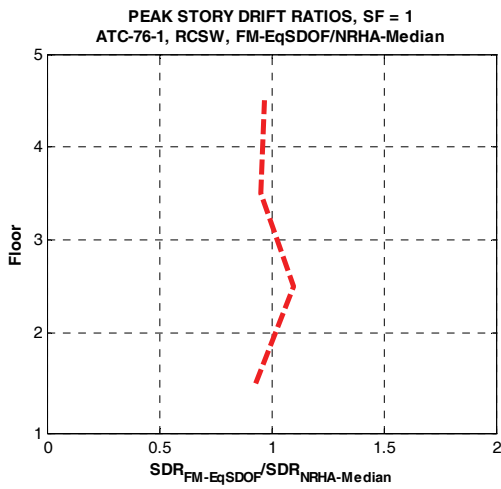


Figure C-26 Ratios of NSP prediction over median NRHA result for story EDPs, using FM-Eq.SDOF option, SF = 1.0 and 2.0.

C.5 Multi-Mode Nonlinear Static Procedure

The only multi-mode nonlinear static procedure tested in this study was the modal pushover analysis, often referred to as MPA (Chopra and Goel, 2001, 2002). This is not to say that other methods cannot deliver results of similar quality, but the emphasis here is on simple models for general use to practicing engineers. Increasing the complexity of the analysis method is a deterrent to its use by the engineering profession. Moreover, this study is concerned only with the evaluation of analysis methods for relatively low-rise building structures.

A summary description of the MPA is provided in Section A.5.1 of Appendix A. When employing the MPA it is essential to start with a good idealization of modal pushovers for estimation of target displacements. For systems in which pushovers exhibit multi-linear characteristics due to pre-and post-cracking behavior, like shear walls, it is recommended to use a multi-linear idealization rather than the trilinear ASCE/SEI 41-06 idealization with an effective elastic stiffness.

C.5.1 Results for 4- and 8-Story Reinforced Concrete Shear Wall Structures

Results are presented here for the 4- and 8-story RCSWs, using the FM model for NRHA and pushover analysis. Figures C-27 and C-30 present pushover curves from first and second mode lateral load patterns and the corresponding equivalent SDOF systems, using discrete pre- and post-cracking stiffnesses. MPA modal properties are based on elastic pre-cracking properties. Figures C-28, C-29, and C-31 present MPA to NRHA comparisons for story drifts, story (wall) shear forces, and floor (wall) overturning moments.

The results presented in this section are for specific cases of RCSWs in which the target roof displacement varies from pre-yielding to significant inelastic behavior for a very high intensity ground motion set ($SF = 3$ for 4-story RCSW). The MPA predictions are very good for low level responses, but the quality of predictions decreases as the extent of inelastic deformations increases. For the 4-story RCSW the addition of second mode response is somewhat detrimental rather than beneficial to reproducing some of the median NRHA EDPs for a ground motion scale factor of 2.0. But in general the modal pushover overestimates response quantities. On the other hand, adding second mode contributions improved considerably the predictions of story shear forces and overturning moments for the 8-story shear wall structure. Judgment on the quality of predictions for the 4-story RCSW for a scale factor of 3.0 is withheld because of previously expressed doubts about the accuracy of the nonlinear response history analysis results for this large scale factor.

Judging from the results obtained for the 4- and 8-story structures, the modal pushover analysis produces close or conservative (high) predictions of demand parameters for the range of regular shear wall structures evaluated here. Caution

must be exercised if the response is sensitive to the yielding mode of the shear wall (see Section C.6) as it is not clear whether the modal pushover will capture such a change in yielding mode.

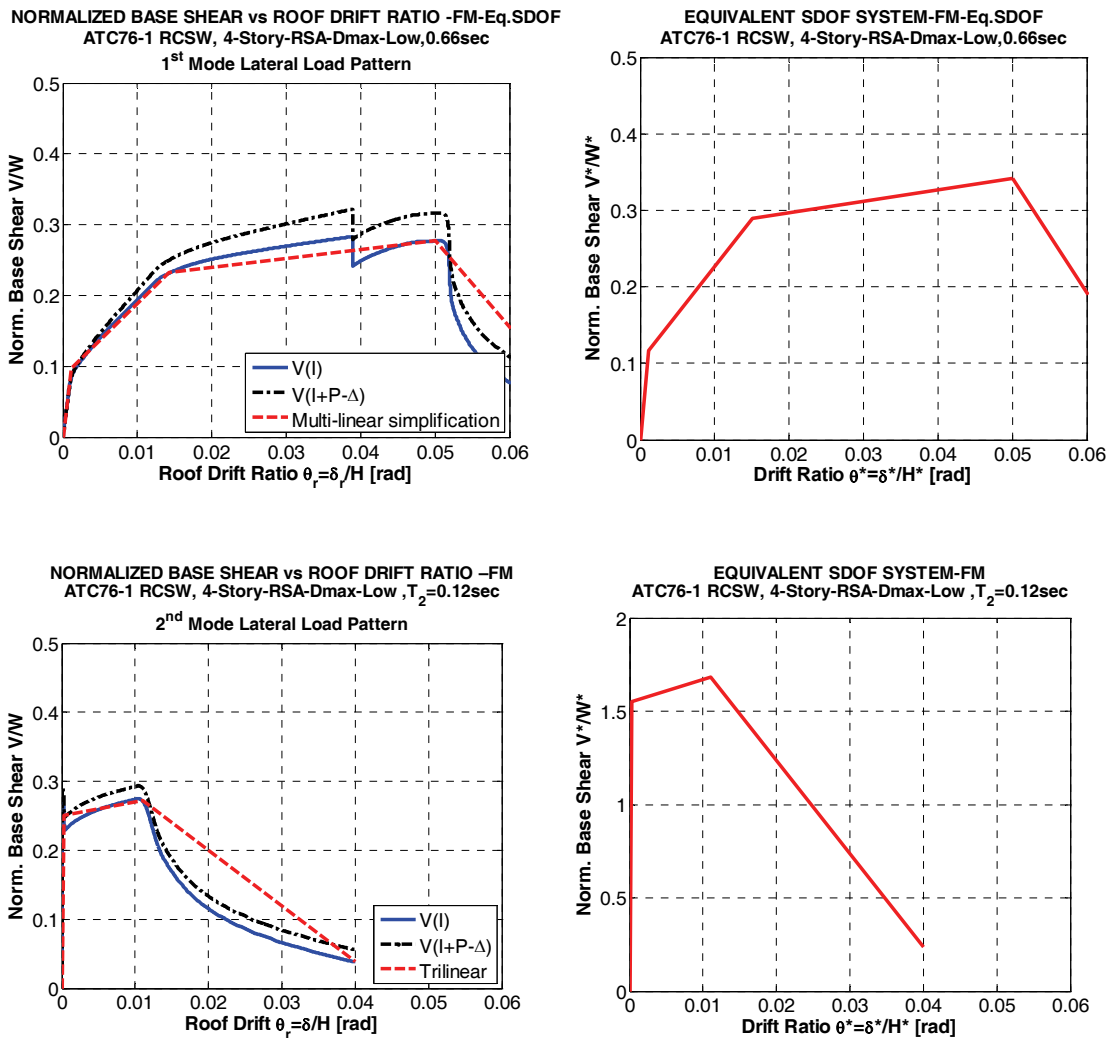


Figure C-27 First and second mode pushovers and equivalent SDOF systems, 4-story RCSW-, FM model.

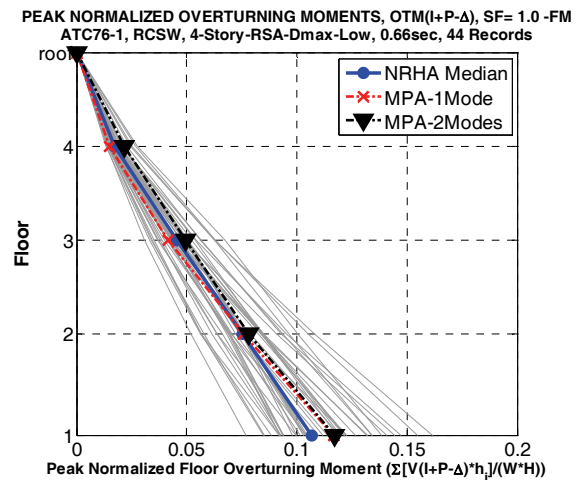
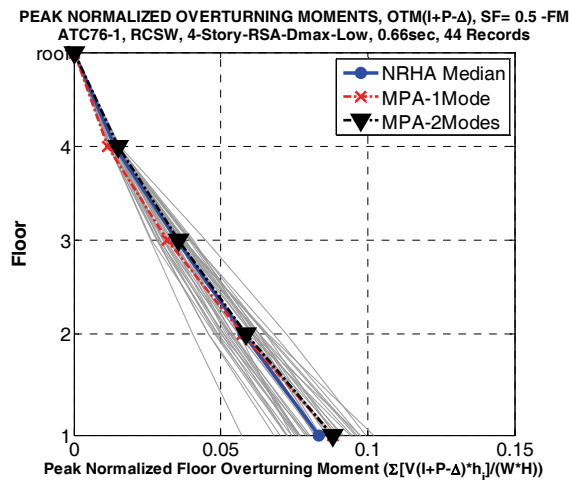
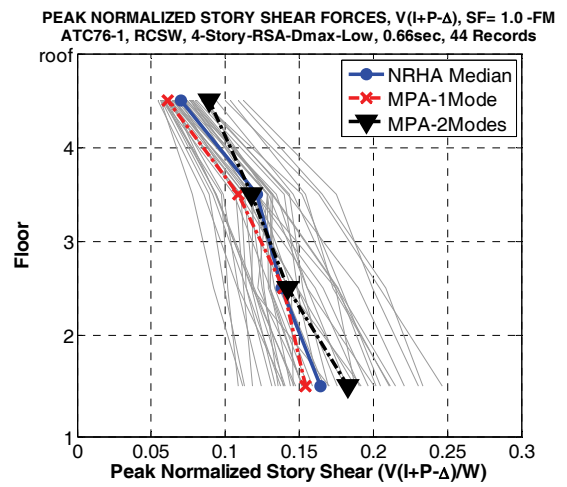
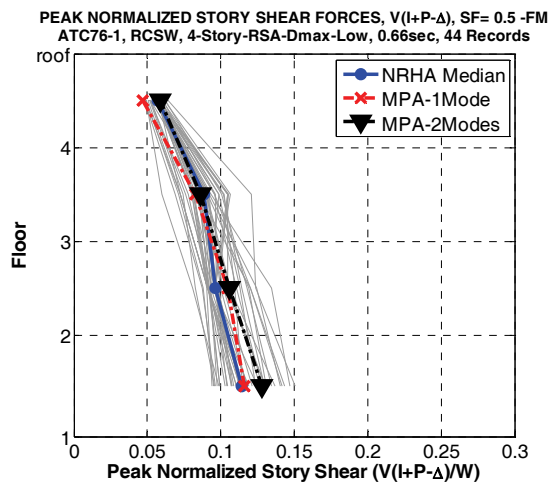
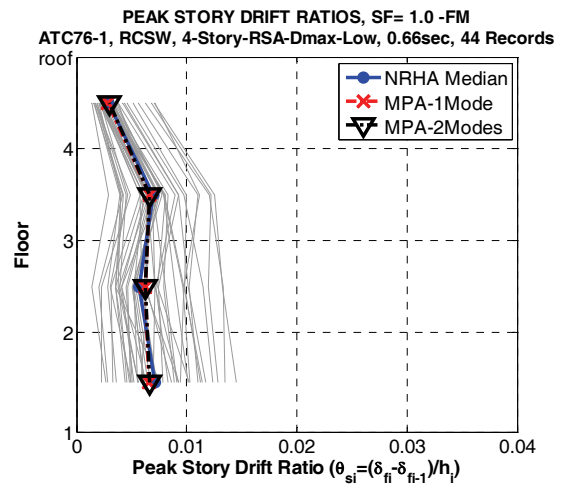
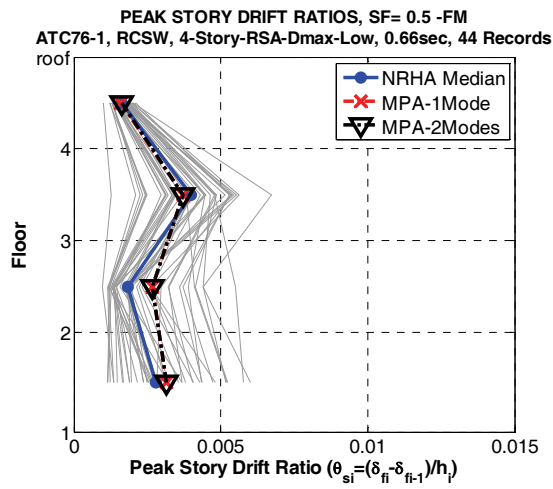


Figure C-28 MPA to NRHA comparison, 4-story RCSW, FM model, SF = 0.5 and 1.0.

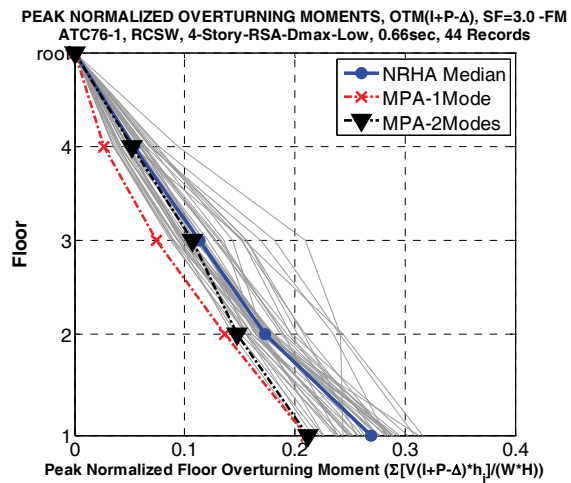
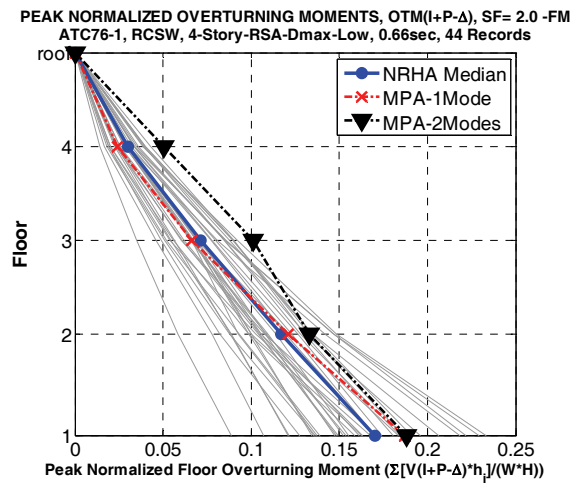
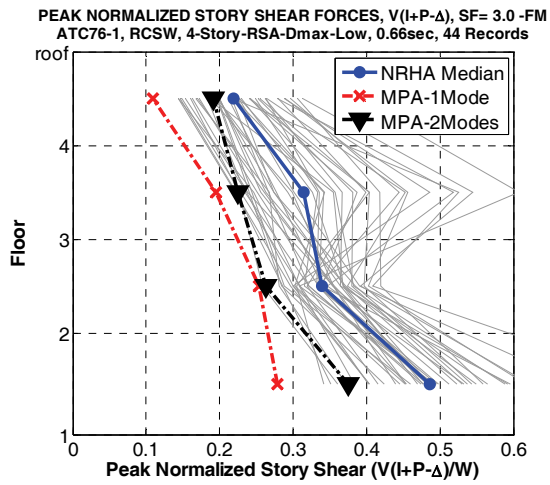
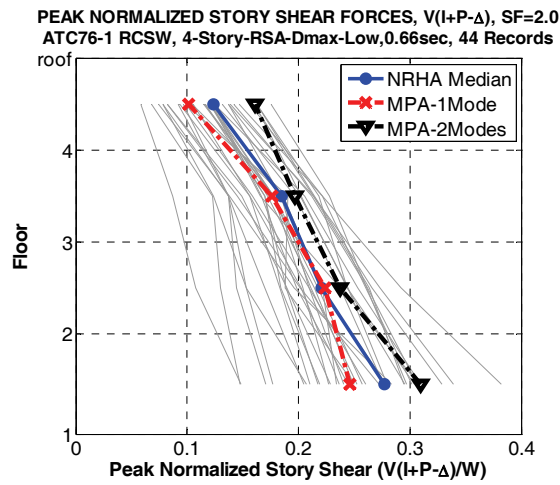
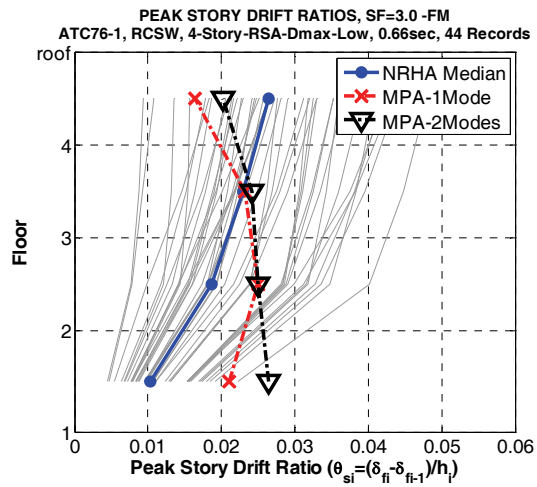
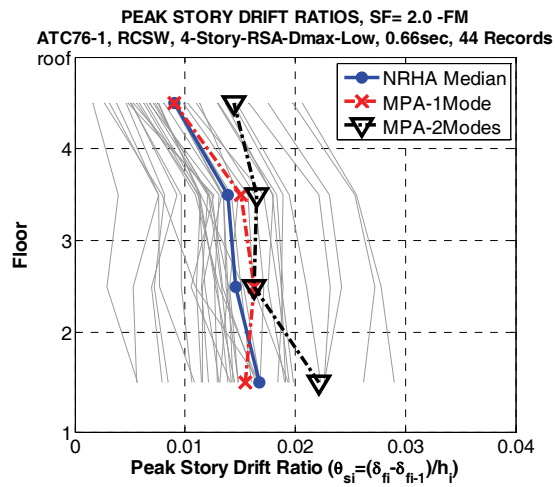
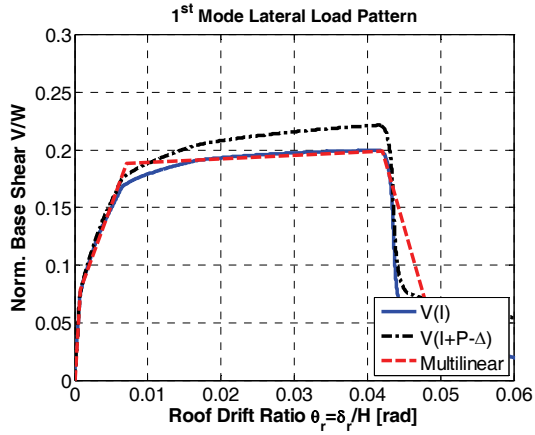
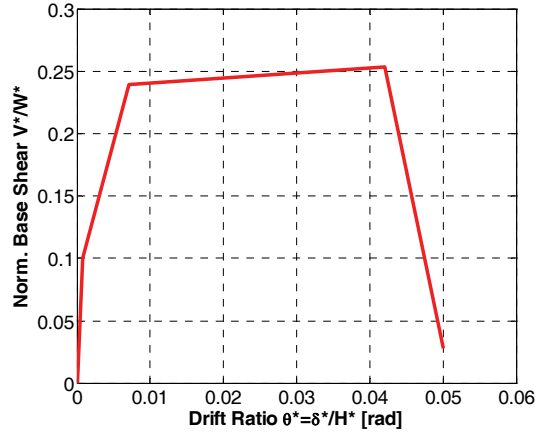


Figure C-29 MPA to NRHA comparison, 4-story RCSW, FM model, SF = 2.0 and 3.0.

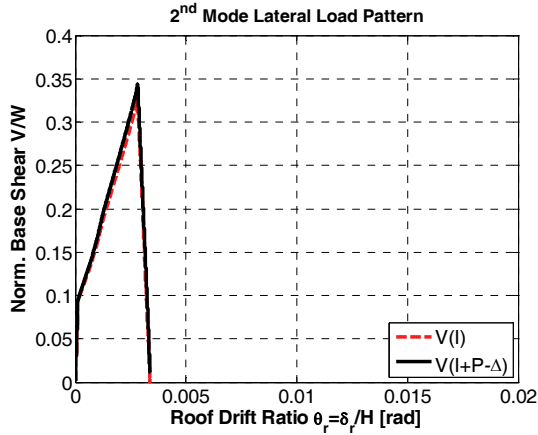
NORMALIZED BASE SHEAR vs ROOF DRIFT RATIO -FM-Eq.SDOF
 ATC76-1 RCSW, 8-Story-RSA-Dmax-Low, $T_1=0.76\text{sec}$



EQUIVALENT SDOF SYSTEM-FM-Eq.SDOF
 ATC76-1 RCSW, 8-Story-RSA-Dmax-Low, $T_1=0.76\text{sec}$



NORMALIZED BASE SHEAR vs ROOF DRIFT RATIO -FM-Eq.SDOF
 ATC76-1 RCSW, 8-Story-RSA-Dmax-Low, $T_2=0.20\text{sec}$



EQUIVALENT SDOF SYSTEM-FM-Eq.SDOF
 ATC76-1 RCSW, 8-Story-RSA-Dmax-Low, $T_2=0.20\text{sec}$

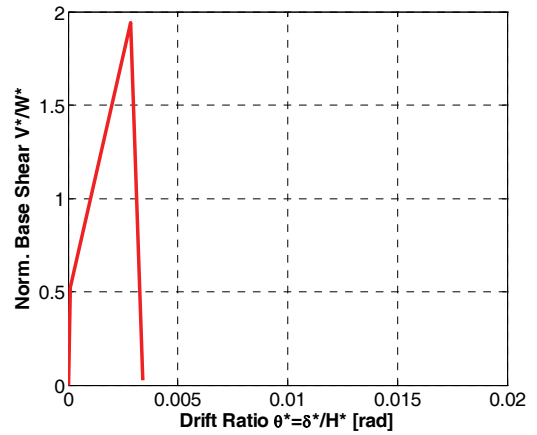


Figure C-30 First and second mode pushovers and equivalent SDOF systems, 8-story RCSW, FM model.

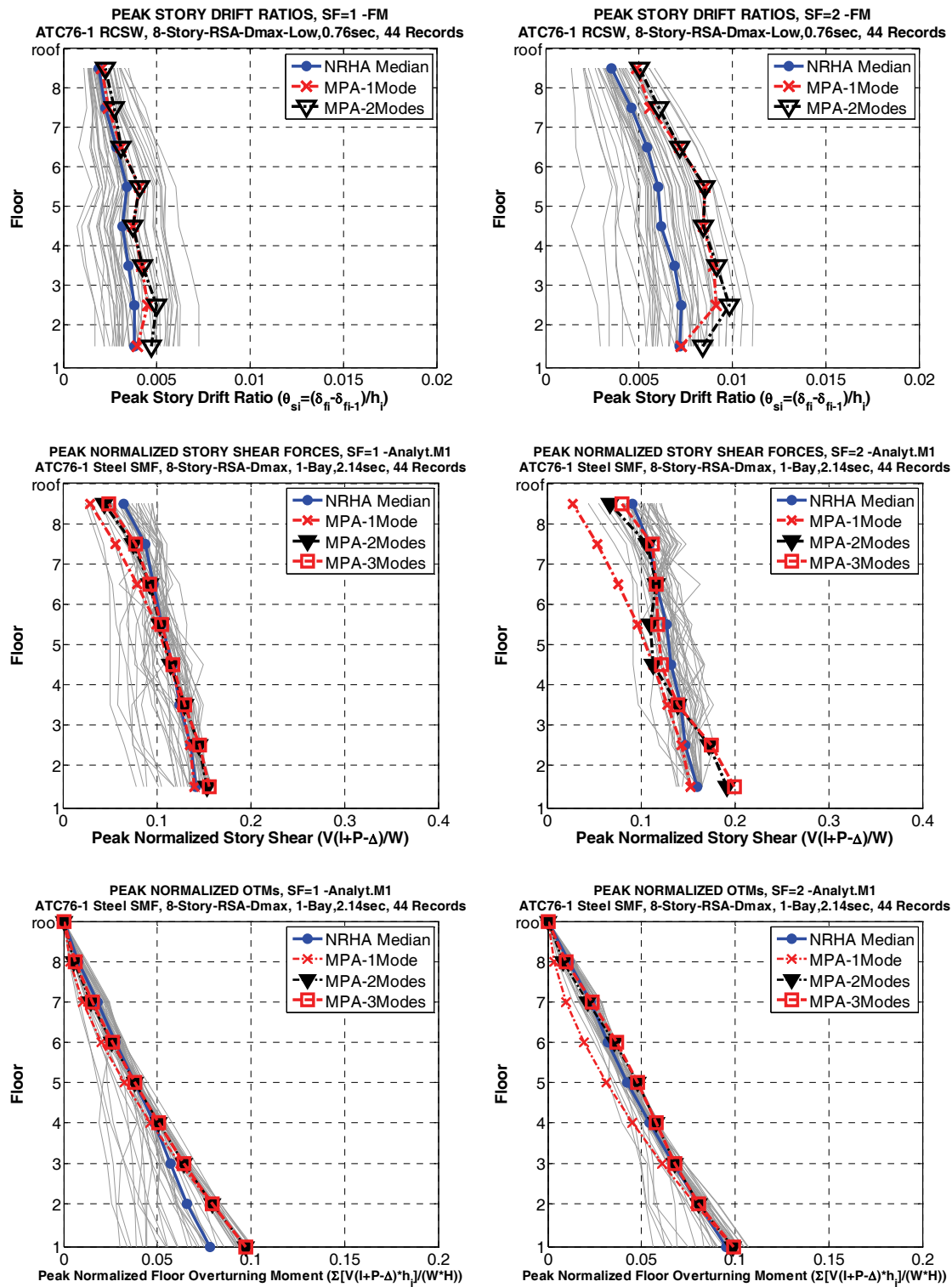


Figure C-31 MPA to NRHA comparison, 8-story RCSW, FM model, SF = 1.0 and 2.0.

C.6 Importance of Failure Mode

Shear wall performance depends strongly on the type of failure mode. It is generally accepted that a shear failure mode is much less desirable (less ductile) than a flexural failure mode, provided that the shear wall is adequately confined to develop ductility

in bending. In design, and in a single mode pushover analysis with an invariant load pattern, the relative magnitude of bending moment to shear force are locked to specific values in every story. Many NRHA studies have shown that the relative magnitude of bending moment to shear force (M/V ratio) may vary considerably during the elastic and more so the inelastic response (e.g., Krawinkler and Zareian 2009). For instance, if a shear wall develops a bending plastic hinge at the base under an invariant lateral load pattern, the pushover base shear force can increase only by the amount of hinge strain hardening, which usually is small. In a NRHA the base shear force might increase by a large amount (for taller buildings easily exceeding a factor of 2) due to dynamic amplification. This increase cannot be captured in a pushover analysis with an invariant lateral load pattern. But this increase might alter the failure mode from a flexural mode to a shear mode, which may have severe consequences on seismic performance.

In order to illustrate the importance of the failure mode concept, the 4-story RCSW building was redesigned according to the following criteria:

- Design quantities M_u and V_u for stories 1 and 3 as provided in NIST GCR 10-917-8.
- Overstrength of 2.0 in stories 1 and 3.
- Strength of story 2 equal to strength of story 1, and strength of story 4 equal to strength of story 3.

The properties of the analytical model, which is a simplified spring model (flexural plastic hinge spring at every floor and translational shear spring in every story), are given as:

- $M_y = 2.0 \times 1.1 M_u / 0.9$
- $V_y = 2.0 \times 1.1 V_u / 0.75$
- $M_c / M_y = 1.1$
- $V_c / V_y = 1.05$
- $I = 0.35 I_g$

These properties, as well as deformation capacities assumed in the analysis, are shown in Figure C-32. They are kept constant in stories 1 and 2, and stories 3 and 4. The hysteresis model with pinching shown in Figure C-12 is employed for shear spring modeling, and a simple bilinear hysteresis model is employed for modeling of flexural plastic hinging.

Based on these criteria, the RCSW fails in a bending mode in the pushover analysis, because of the difference in ϕ -factors between bending and shear (0.9 versus 0.75). The pushover and deflection profiles are shown in Figure C-32. NRHA analysis was performed for a SF of 2.0, resulting in the roof drift statistical values shown at the

bottom of Figure C-32. The median of 0.0152 seems to indicate that the drift demands are not excessive, but the observation that 11 collapses occurred demonstrates that the structure has a large collapse potential at the ground motion level associated with a SF of 2.0. All collapses occurred because of shear failure in the first story. This would not at all be disclosed by a NSP, which, based on the target roof drift of 0.0152 and an inspection of the global pushover curve indicated benign performance problems.

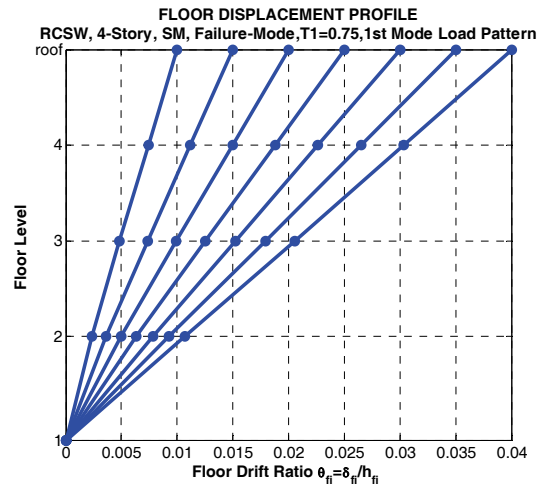
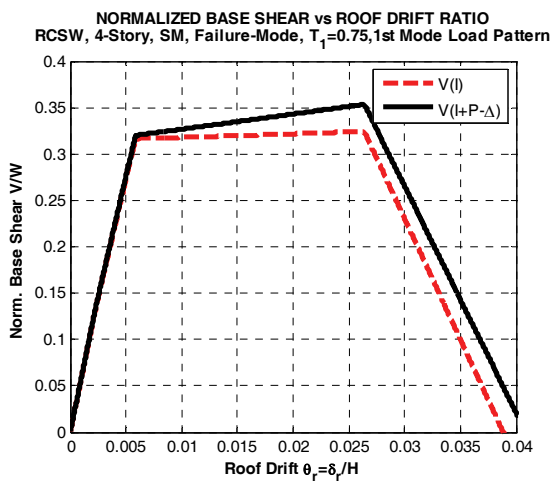
Figure C-33 shows that NSP provides reasonable predictions of story drifts, except in the first story, but mediocre predictions of story shear demands because of dynamic shear force amplification that is not disclosed in the pushover analysis. The fact that there is almost no dispersion in the NRHA results for the base shear shows clearly that almost all structures attained shear strength rather than bending strength in the first story, which is the opposite of what would be concluded from the pushover analysis. The primary concern about pushover based performance evaluation in this case is not necessarily the mediocre prediction of story shear, it is the misleading feeling of comfort of sufficient collapse safety. The main reason why there were not more collapses in the NRHA is that a rather large deformation capacity ($\gamma_c = 0.01$) was assigned to the shear mode of behavior in this example.

This section points out a potentially severe problem that would not be detected by a pushover analysis that is based on invariant load patterns. Applying an amplification factor to wall shear is one way to mitigate this problem. Another one is to perform nonlinear response history analysis.

Strength and Deformation Properties (RCSW-4-SM-Failure-Mode)

Story	My (kip-in)	Mc (kip-in)	θ_p (rad)	θ_{pc} (rad)
1	953333	1048667	0.02	0.02
2	953333	1048667	0.02	0.02
3	476667	524333	0.02	0.02
4	476667	524333	0.02	0.02

Story	Vcr (k)	Vy (k)	Vc (kip)	Vr (k)	γ_{cr} (rad)	γ_y (rad)	γ_c (rad)	γ_{pc} (rad)
1	810	2567	2695	0	0.00018	0.0015	0.01	0.01
2	810	2567	2695	0	0.00018	0.0015	0.01	0.01
3	560	1775	1863	0	0.00018	0.0015	0.01	0.01
4	560	1775	1863	0	0.00018	0.0015	0.01	0.01



Roof Drift Ratio from NRHA (H = 588 inches)

	SF=2.0
Median [%]	0.0152
16th [%]	0.0080
84th [%]	N/A
Mean μ [%]	N/A
σ [%]	N/A
CoV	N/A
Collapses	11

Figure C-32 System information, 4-story RCSW designed to fail in bending.

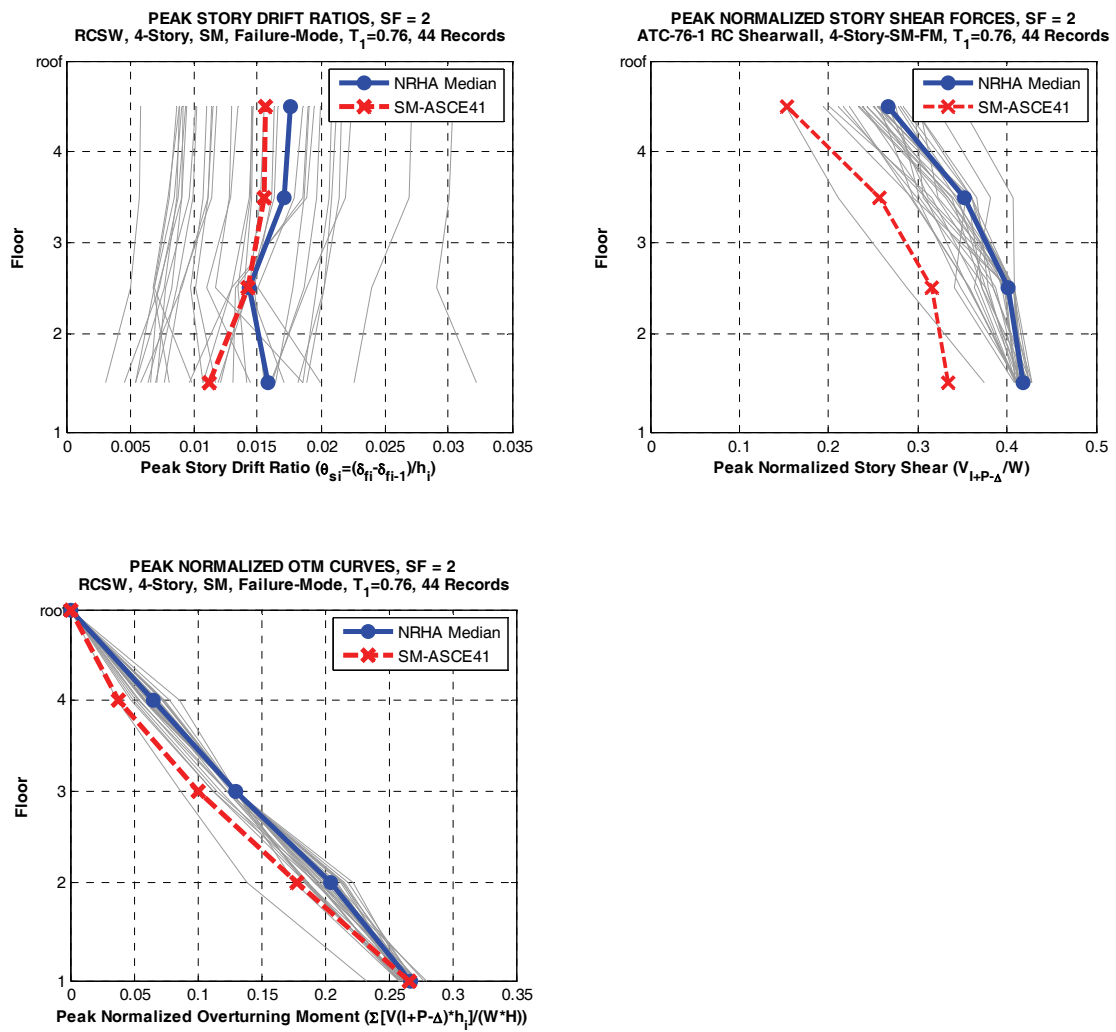


Figure C-33 NSP to NRHA comparison, 4-story RCSW designed to fail in bending.

Effect of Ground Motion Selection and Scaling on Engineering Demand Parameter Dispersion

This appendix presents results from an ancillary study undertaken to investigate the relationships between demand parameter dispersion (and bias), ground motion scaling method, and size of the ground motion data set. The purpose of this study is to find more economical approaches for performing nonlinear response history analysis in practice.

D.1 Effect of Intensity Measure on EDF Dispersion

A major issue in the estimation of structural response is the selection of the intensity measure (IM). This has been well documented in many recent studies, mainly dealing with the important points of efficiency to produce low engineering demand parameter (EDP) dispersion for a given IM level, and sufficiency of any candidate IM with respect to the typical parameters of the probabilistic seismic hazard analysis (PSHA), such as distance, R , and magnitude, M (Luco and Cornell, 2007). Nevertheless, the goals of efficiency and sufficiency are linked (Vamvatsikos and Cornell, 2005), as a more efficient IM will always improve upon sufficiency as well.

In this section, the efficiency of different IMs was evaluated using a sample of three reinforced-concrete moment resisting frames (RCMFs) developed for the FEMA P-695 report, *Quantification of Seismic Performance Factors* (FEMA, 2009b). The 2-, 4-, and 8-story frames were also used for evaluating the accuracy of nonlinear static procedures in Appendix B. The efficiency of the following four IMs (or scaling methods) was investigated:

1. FEMA P-695 scaling. This method uses ground motion records that have already been normalized to have the same value of PGV_{PEER} , modified by uniformly applied scale factors of 0.5, 1.0, or 2.0. PGV_{PEER} is the geometric mean of the Peak Ground Velocity (PGV) of the two horizontal components of the ground motion, averaged over different orientations. Thus, FEMA-P695 scaling is effectively equivalent to using PGV_{PEER} as the IM, and practically it can be thought of as PGV-scaling. While this approach to scaling was never intended to minimize dispersion, it may work best for buildings having moderate periods.

2. Standard $S_a(T_1)$ scaling. This has been shown to be quite good for first-mode dominated buildings but is known to lack efficiency and sufficiency as higher modes become important (e.g., Luco and Cornell 2007).
3. Improved $S_a(T_a, T_b)$ scaling, where $S_a(T_a, T_b) = S_a(T_a)^{0.5} S_a(T_b)^{0.5}$ is the geometric mean of two elastic spectral values. Originally suggested by Cordova et al. (2000) with $T_a=T_1$ and $T_b=2T_1$, it has been extensively tested by Vamvatsikos and Cornell (2005), who suggested that using different periods T_a, T_b for different intensity levels provides high efficiency and sufficiency. For reasons of simplicity, both periods are kept the same for all intensity levels for each structural model in this study, equal to $T_a=T_1$ and $T_b=T_2$.
4. The inelastic spectral displacement $S_{di}(T_1)$ of an equivalent SDOF (ESDOF) system. The ESDOF system has the same period as the structure and an elastoplastic backbone matched to have the same maximum base shear (Figures D-1 to D-3). A version of this was suggested by Luco and Cornell and was further developed by Tothong and Cornell (2008), who show its efficiency and sufficiency, at least with respect to displacement-based EDPs such as the maximum story drift over the height of the building.

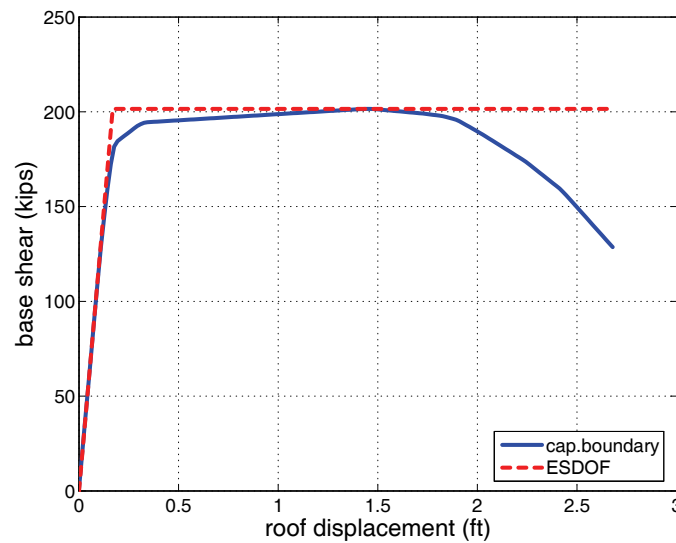


Figure D-1 The bilinear fit of the capacity boundary (pushover curve), used to derive the ESDOF capacity curve for the 2-story RCMF, as used for S_{di} scaling.

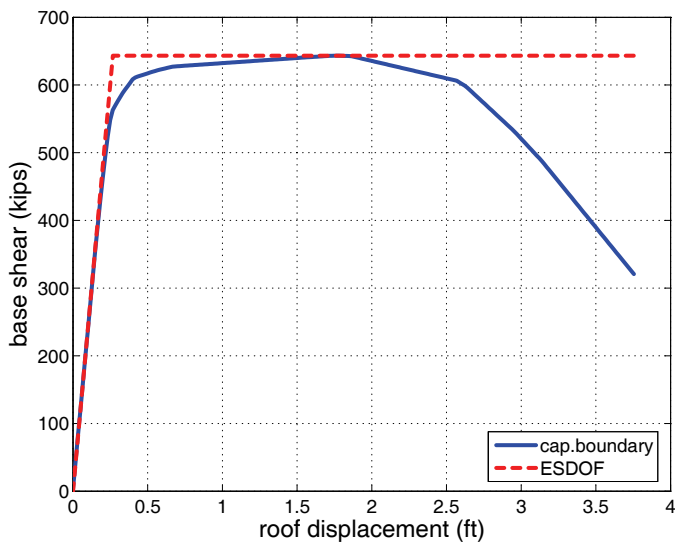


Figure D-2 The bilinear fit of the capacity boundary (pushover curve), used to derive the ESDOF capacity curve for the 4-story RCMF, as used for S_{di} scaling.

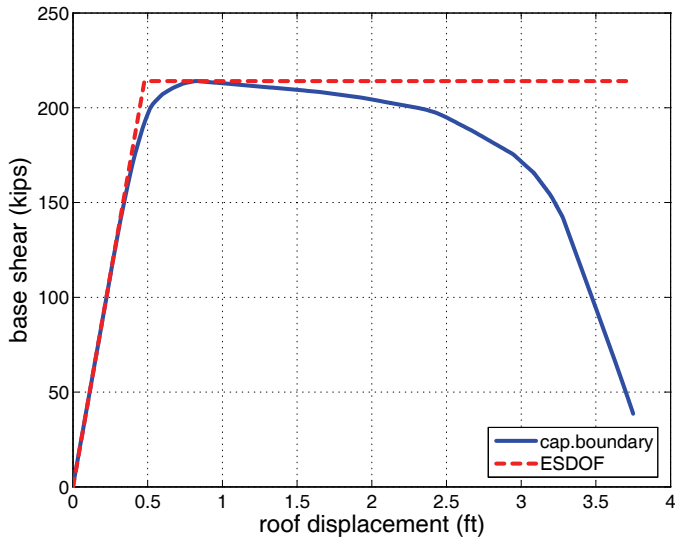


Figure D-3 The bilinear fit of the capacity boundary (pushover curve), used to derive the ESDOF capacity curve for the 8-story RCMF, as used for S_{di} scaling.

To limit the scope of the investigation, three scaling levels that are of practical engineering significance were used. Scale factors of 0.5, 1.0, and 2.0 were applied to the ground motions as scaled in FEMA P-695, roughly corresponding to nearly elastic, mildly inelastic and mostly inelastic behavior. Even at the highest scale factor, few cases of global dynamic instability occurred, as may be expected for a well-designed building.

The four scaling methods (or intensity measures) differ in that the first three IMs have a linear relationship to the scale factors of the individual records. On the other

hand, $S_{di}(T_i)$ is a nonlinear IM that has a complex relationship with the scale factor and must be evaluated separately at every scale factor level.

To compare EDP dispersions at similar intensity levels, given these differences, the median value of IM of interest was determined for the ground motions scaled by 0.5, 1.0, and 2.0, and the ground motion records were rescaled to each have the median IM level for purposes of determining EDP dispersions. This process is illustrated conceptually in Figure D-4, where one of the IMs (other than PGV_{PEER}) is plotted for the motions scaled to the FEMA P-695 intensity level. Regardless of the EDP, the projection on the IM axis remains the same. The median of this projection establishes the intensity level for any of the IMs other than PGV_{PEER} . Although this is quite simple for the first three IMs, it requires an elaborate post-processing maneuver for S_{di} due to its nonlinearity. In all cases this is accomplished using advanced parametric spline interpolation based on a centripetal scheme to allow accurate mapping of IMs to EDPs for any possible combination of IM and EDP (Vamvatsikos and Cornell, 2004). The EDP values corresponding to the given IM level were computed for each ground motion record using this interpolation method based on results previously obtained at multiple intensities.

For each building and each scale factor the dispersion in the estimates is compared and the bias in the estimates is reported. The dispersion normally is estimated as the standard deviation of the logarithm of the data, but due to the presence of collapses, the dispersion is estimated as $0.5 \cdot (\ln EDP_{84} - \ln EDP_{16})$ —that is, one-half the difference between the 84% and 16% quantiles. The bias is estimated vis-à-vis the FEMA P-695 scaling results, simply as $(EDP_{50}^{IM} - EDP_{50}^{P695}) / EDP_{50}^{P695}$, where EDP_{50}^{P695} refers to the median of the FEMA P-695 scaled responses. The reported bias may be attributed to using slightly different hazard levels for each intensity measure rather than being an attribute of a scaling method. The reported bias can be treated as an indication of the differences in the EDP results that may occur when using different IMs.

Results are obtained for a variety of EDPs, including global responses, as indicated by the maximum story drift ratio over the height of the structure (DR_{max}) and the maximum peak floor acceleration (FA_{max}) over the height of the structure, and peak intermediate and local responses of engineering significance: individual story drifts (DR_i), floor accelerations (FA_i), story shears (SS_i), story overturning moments (OTM_i), story maximum beam plastic hinge rotations (BPR_i), and story maximum column plastic hinge rotations (CPR_i).

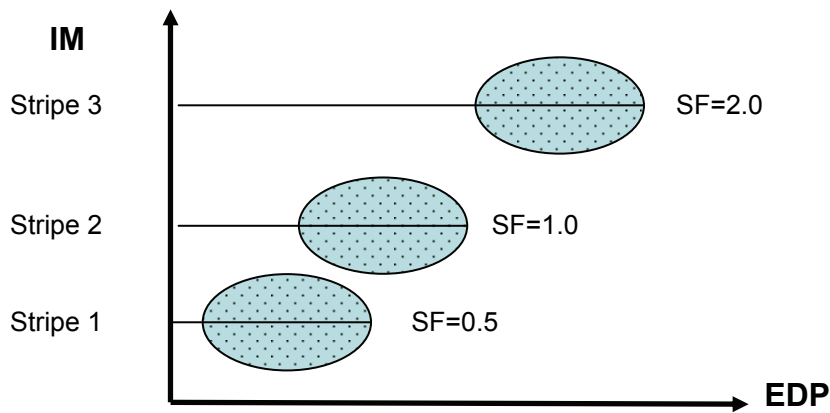


Figure D-4 Conceptual distributions of data for arbitrary EDPs given FEMA P-695 scaling (with scale factors of 0.5, 1.0, and 2.0) for an intensity measure (IM) other than PGV_{PEER} used in FEMA P-695 scaling.

D.1.1 Observations on Dispersion

Dispersion results for peak story drift, peak floor acceleration, story shear, overturning moment and maximum plastic hinge rotation over all beams and columns of each story are plotted in Figures D-5 through D-22, over the height of each building, with dispersion in the peak value over the height of the building plotted above the roof level, where applicable. Peak values were obtained for each of $N = 44$ ground motion records. Peak values over the height are used as a reflection of how well the most severe behavior of the entire system is represented, as a surrogate for system response. Peak plastic hinge rotations are the maximum values tributary to a floor or story, and are indicative of local damage.

Peak story drifts and accelerations show in all cases dispersions on the order of 30-60%. Story shears and overturning moments tend to have dispersions that increase with height, starting at 10% at the 1st floor and increasing up to 20% or 30% at the top floor, for all four IMs. This pattern is most clear for the taller buildings at higher intensity levels, and may be associated with saturation of story shears due to plastic hinge formation. Dispersions of beam and column plastic hinge rotations are much higher than those of other response quantities investigated, often exceeding 100% at higher scale factors. This is attributed to (1) as the member begins to develop inelastic response, chord rotations have begun to have an increasingly large effect on plastic hinge rotations (there is no effect during elastic response) and (2) different mechanisms involving different stories may be activated by different ground motion records (see Haselton and Deielein, 2007). Plastic hinge rotation values can easily range from near-zero to more than 0.02 rad for a given scale factor.

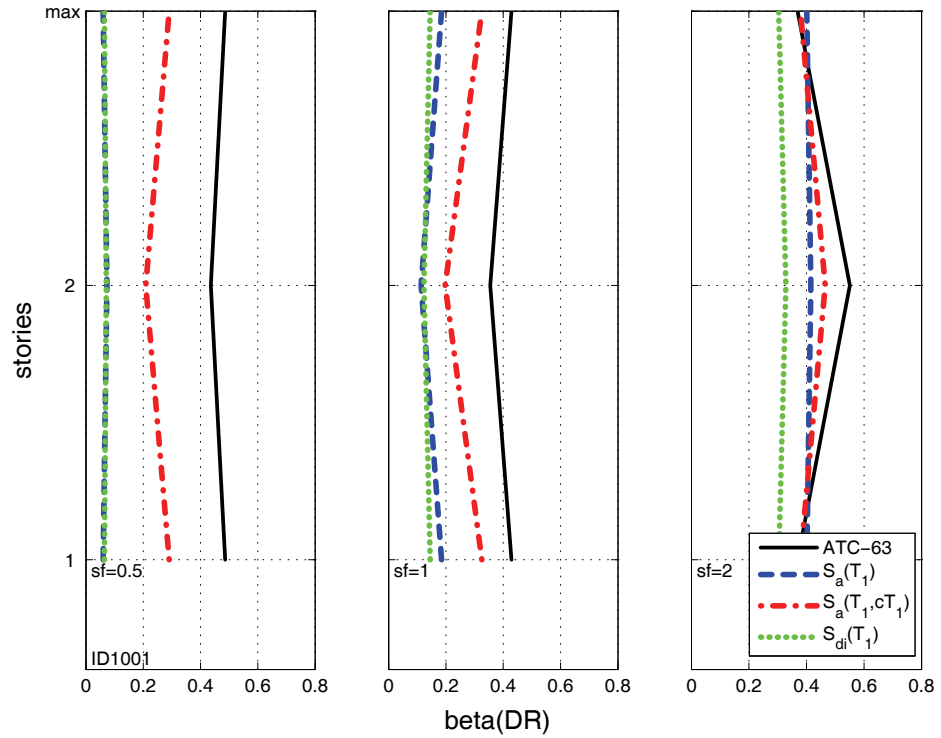


Figure D-5 Dispersions of the local and maximum story drift ratios along the height of the 2-story RCMF for three different intensity levels.

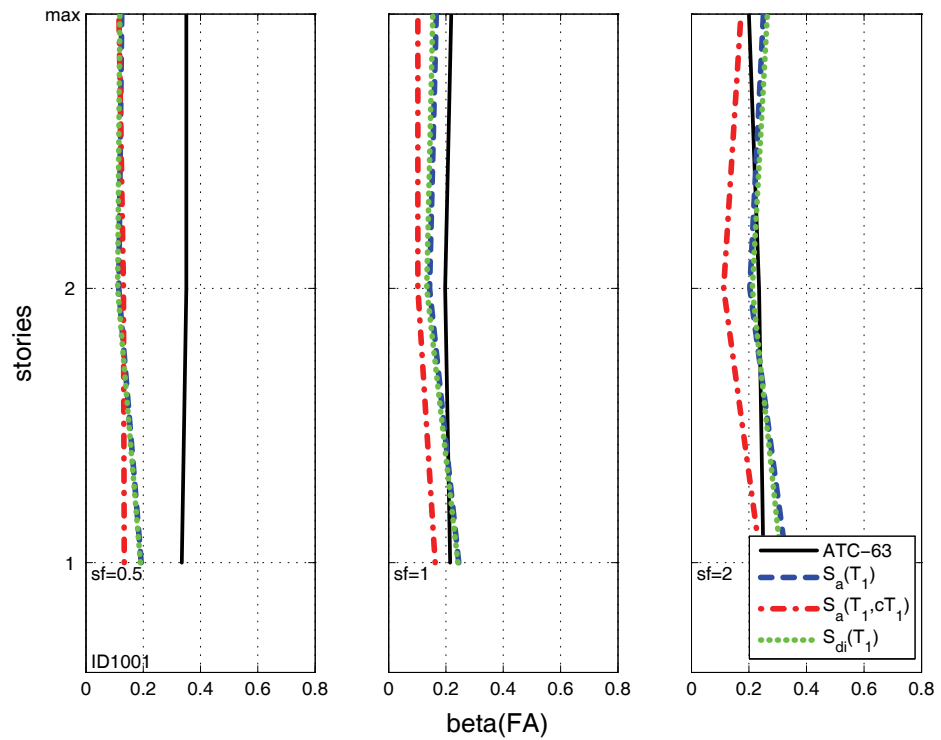


Figure D-6 Dispersions of the local and maximum peak floor accelerations along the height of the 2-story RCMF for three different intensity levels.

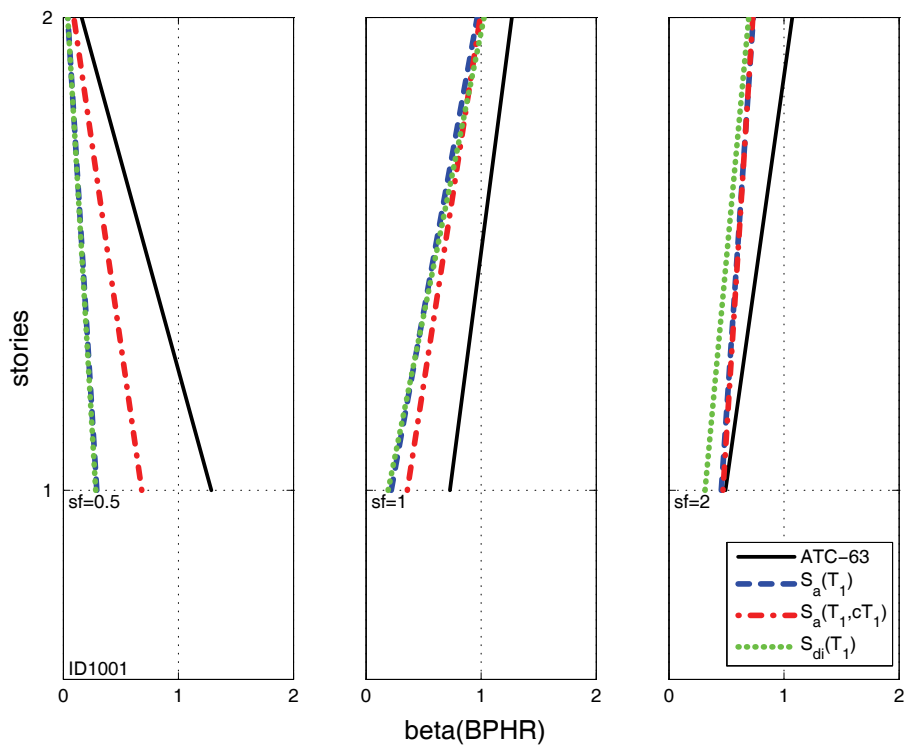


Figure D-7 Dispersions of the maximum beam plastic hinge rotation for each story along the height of the 2-story RCMF for three different intensity levels.

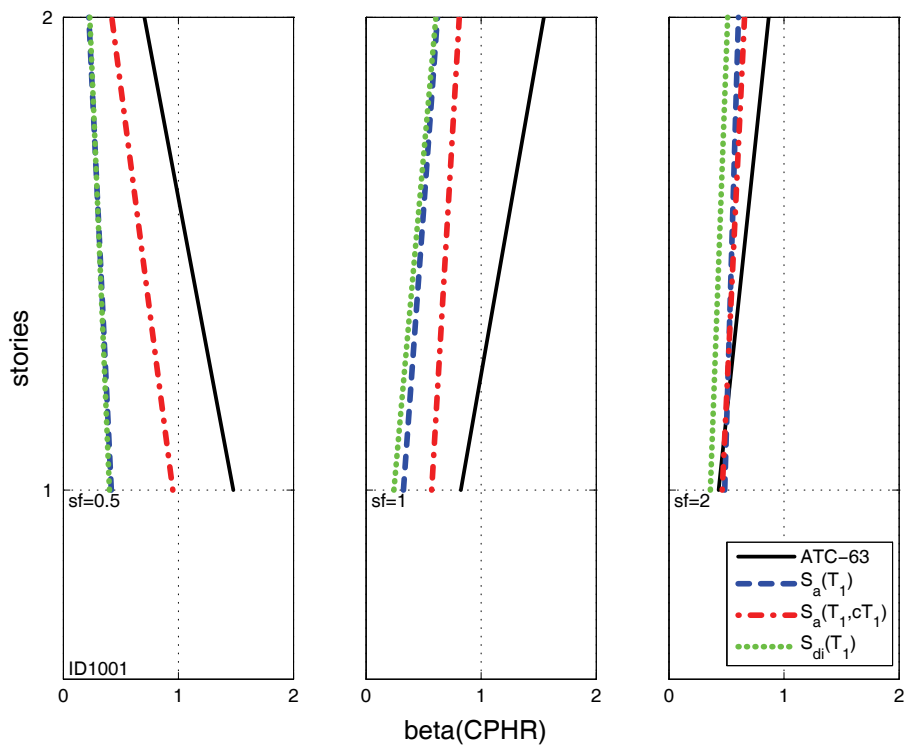


Figure D-8 Dispersions of the maximum column plastic hinge rotation for each story along the height of the 2-story RCMF for three different intensity levels.

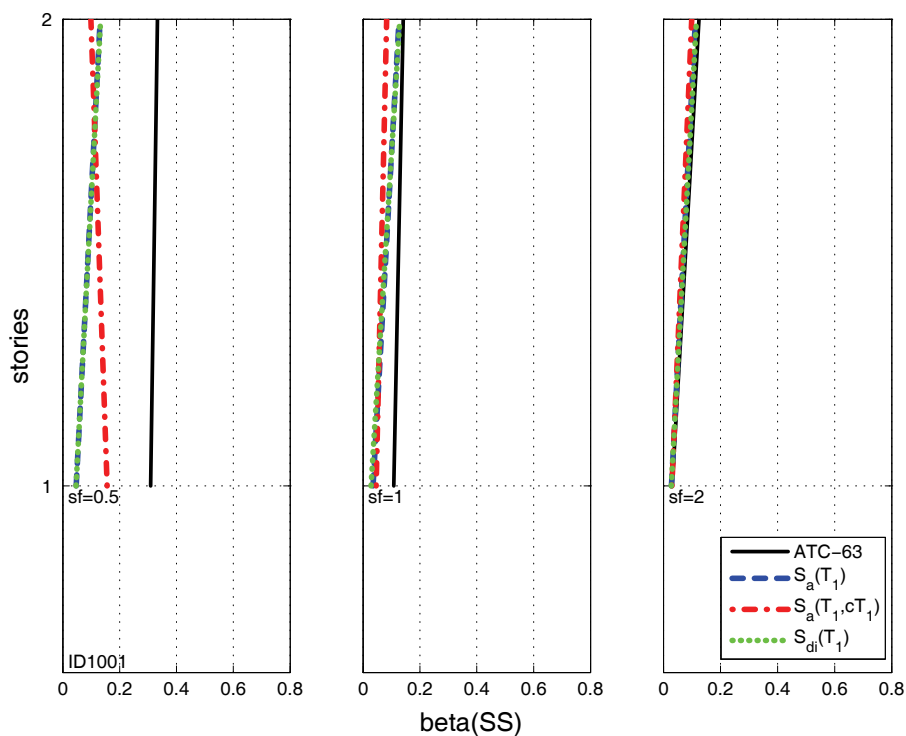


Figure D-9 Dispersions of story shear for each story along the height of the 2-story RCMF for three different intensity levels.

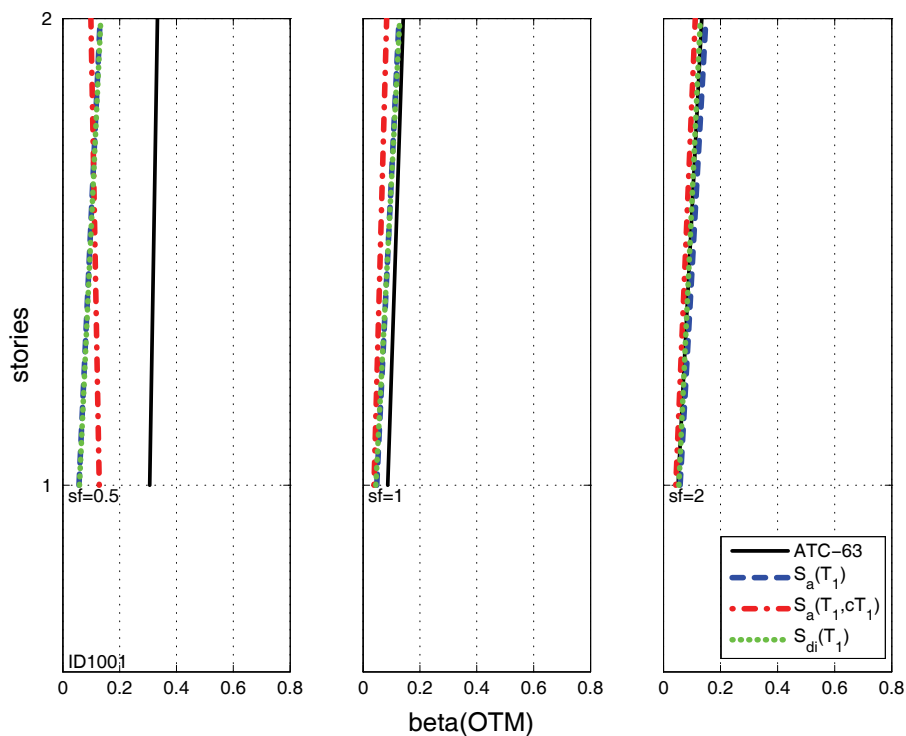


Figure D-10 Dispersions of the overturning moment for each story along the height of the 2-story RCMF for three different intensity levels.

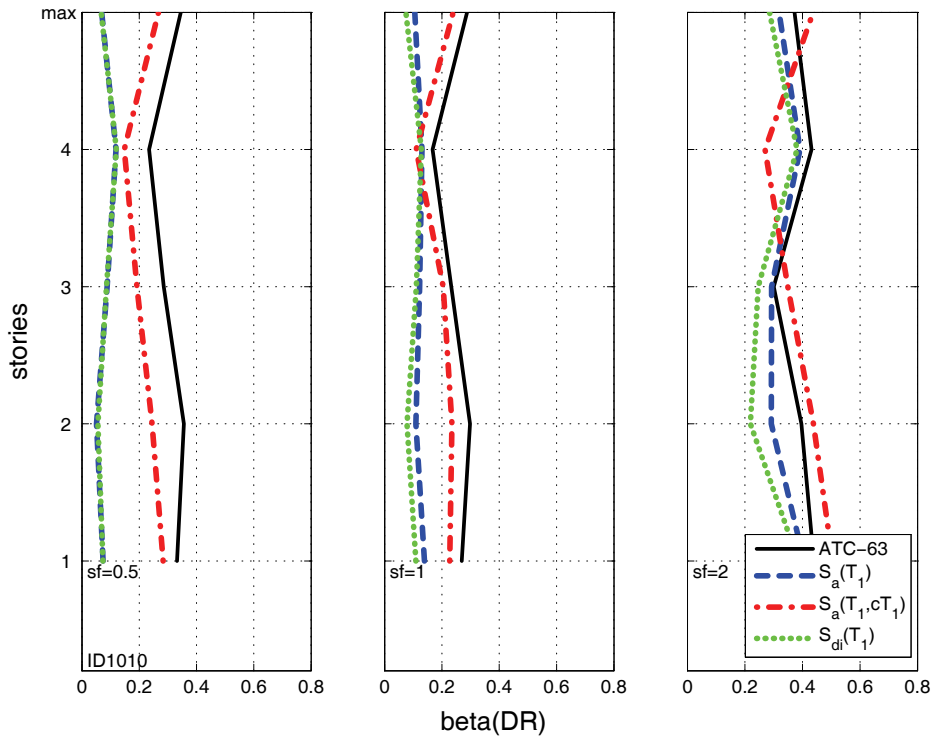


Figure D-11 Dispersions of the local and maximum story drift ratios along the height of the 4-story RCMF for three different intensity levels.

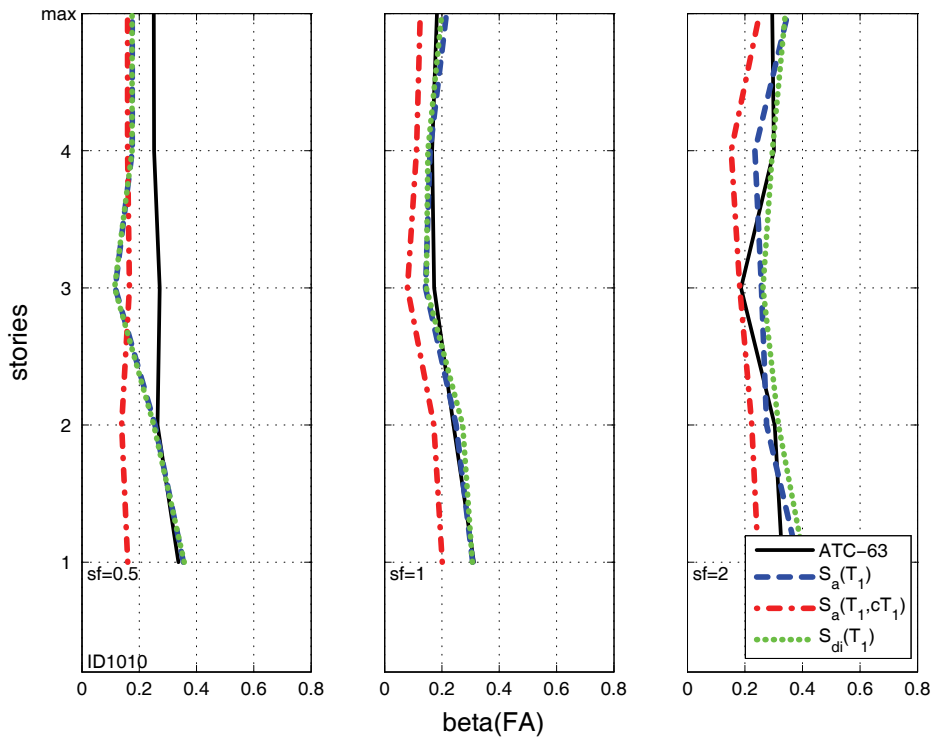


Figure D-12 Dispersions of the local and maximum peak floor accelerations along the height of the 4-story RCMF for three different intensity levels.

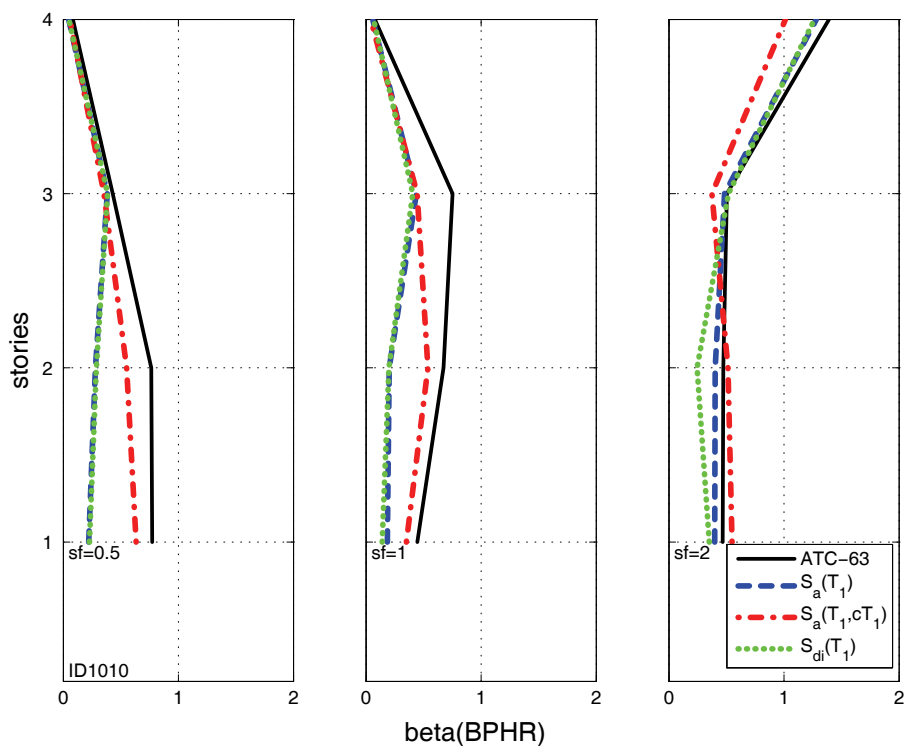


Figure D-13 Dispersions of the maximum beam plastic hinge rotation for each story along the height of the 4-story RCMF for three different intensity levels.

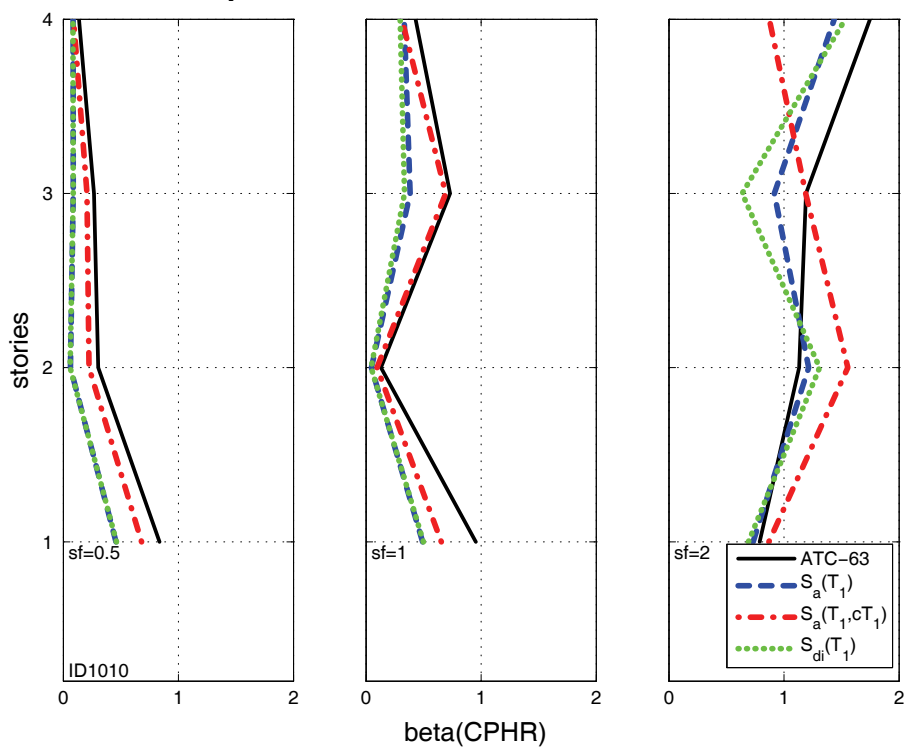


Figure D-14 Dispersions of the maximum column plastic hinge rotation for each story along the height of the 4-story RCMF for three different intensity levels.

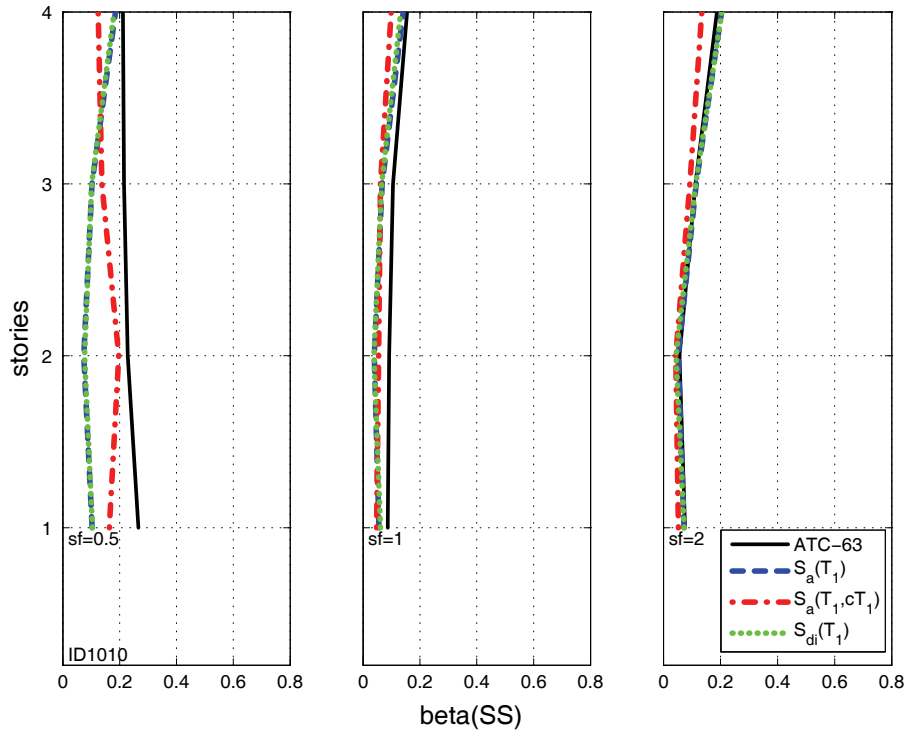


Figure D-15 Dispersions of story shear for each story along the height of the 4-story RCMF for three different intensity levels.

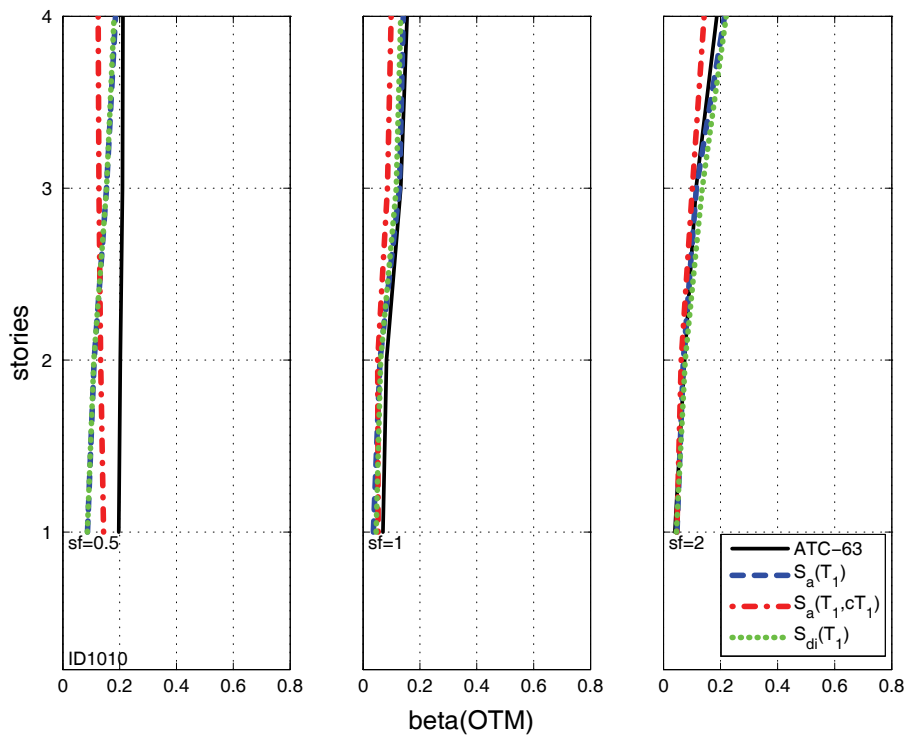


Figure D-16 Dispersions of the overturning moment for each story along the height of the 4-story RCMF for three different intensity levels.

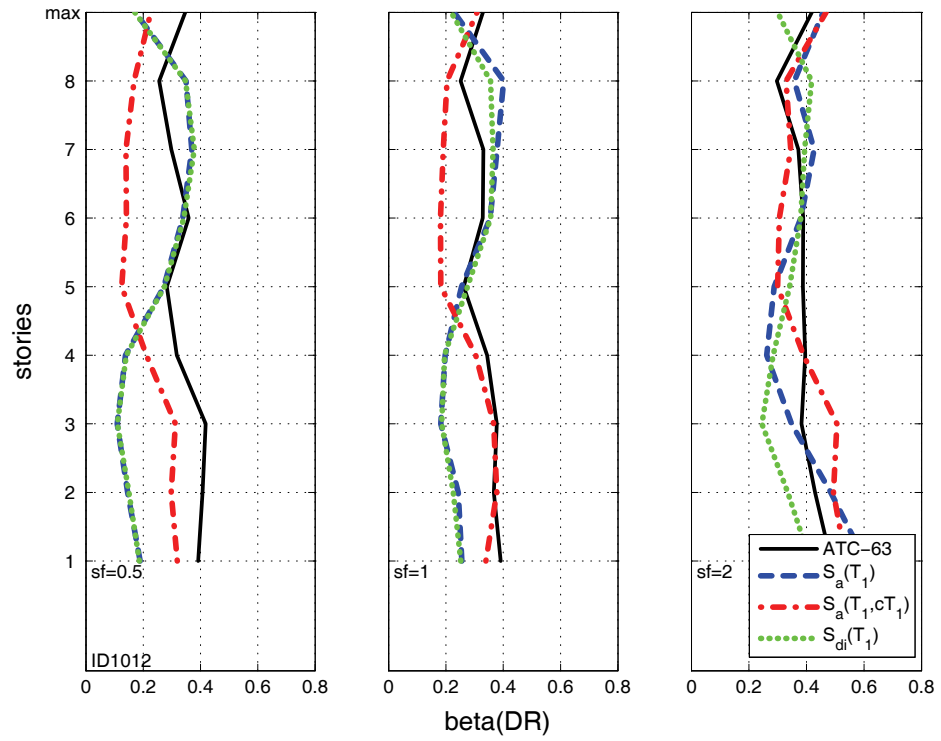


Figure D-17 Dispersions of the local and maximum story drift ratios along the height of the 8-story RCMF for three different intensity levels.

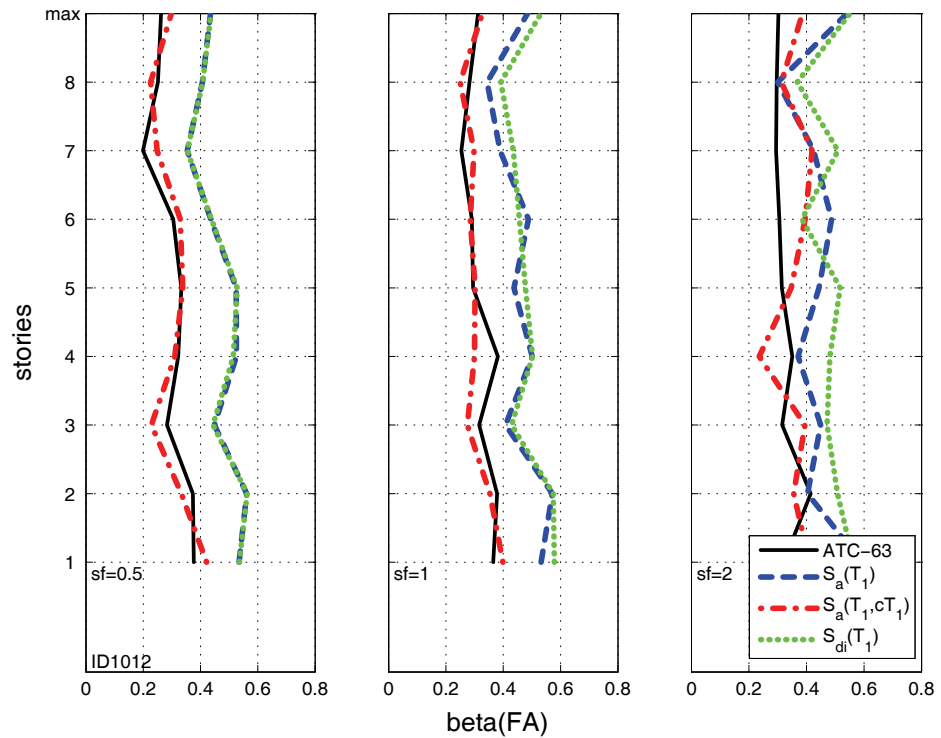


Figure D-18 Dispersions of the local and maximum peak floor accelerations along the height of the 8-story RCMF for three different intensity levels.

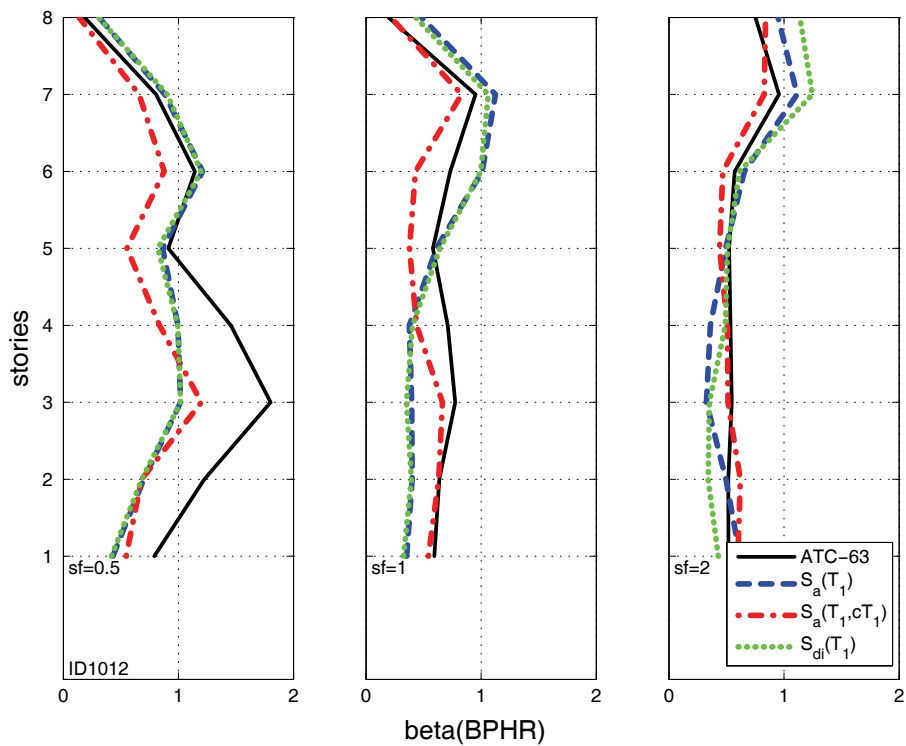


Figure D-19 Dispersions of the maximum beam plastic hinge rotation for each story along the height of the 8-story RCMF for three different intensity levels.

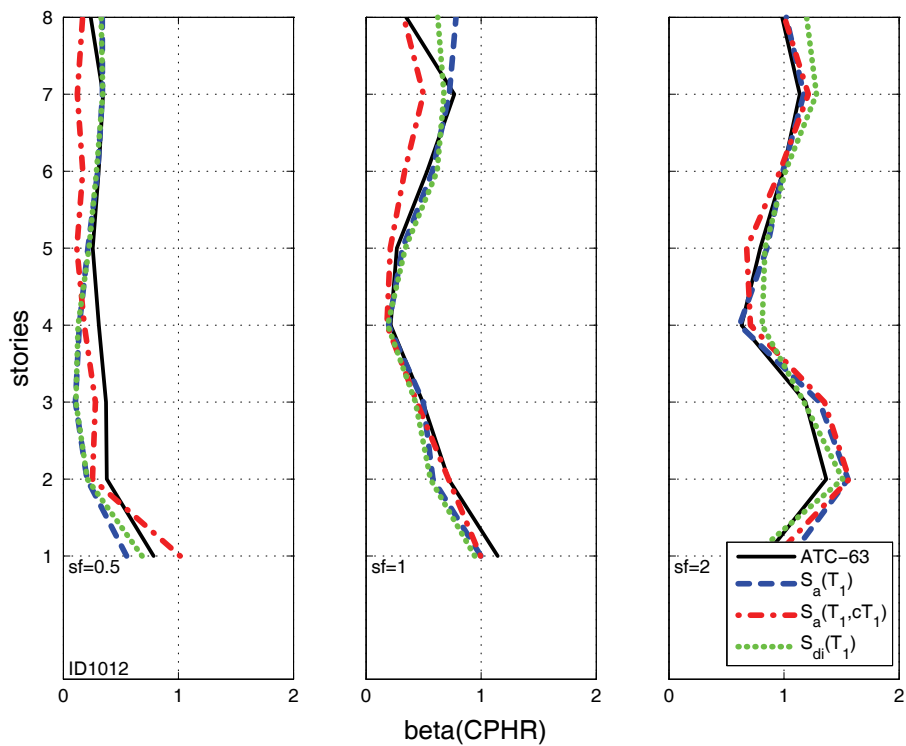


Figure D-20 Dispersions of the maximum column plastic hinge rotation for each story along the height of the 8-story RCMF for three different intensity levels.

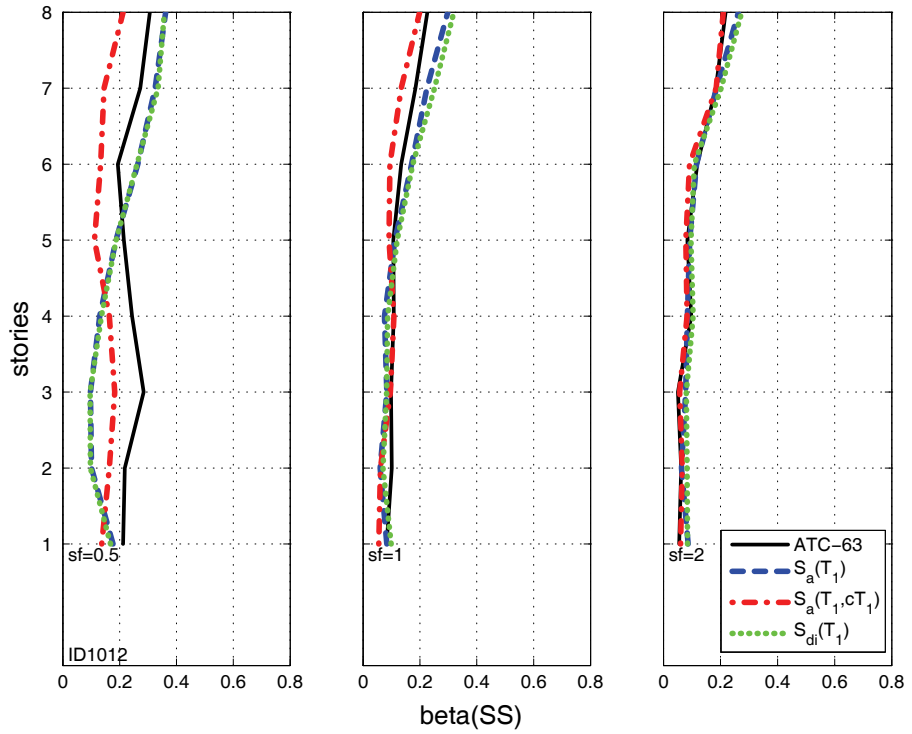


Figure D-21 Dispersions of story shear for each story along the height of the 8-story RCMF for three different intensity levels.

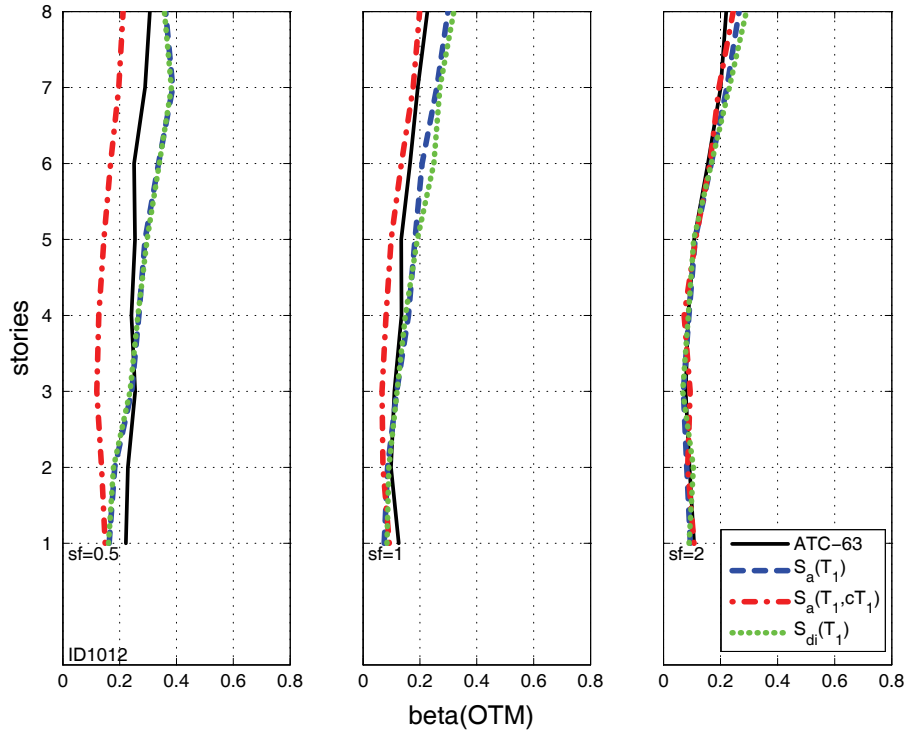


Figure D-22 Dispersions of the overturning moment for each story along the height of the 8-story RCMF for three different intensity levels.

Regarding the efficiency of the different intensity measures, it is important to note that for low intensities (SF = 0.5 and 1), dispersions obtained with $S_a(T_1)$ and $S_{di}(T_1)$ scaling are nearly indistinguishable. This is to be expected, as these structures remain elastic or nearly so at these scale factors. For higher intensities, S_{di} seems to offer a small advantage over $S_a(T_1)$ in dispersion reduction, reaching an improvement of almost 25%; this advantage is expected to increase with an increase in the intensity of inelastic response.

Interestingly, for the tallest structure, both the FEMA P-695 and the $S_a(T_1, T_2)$ methods provide relatively low dispersion, especially for floor accelerations. For the $S_a(T_1, T_2)$ method, where T_2 is set close to either the 2nd or the 3rd mode period, this remarkable improvement persists, needing no precise selection to bear results. For drift ratio response, $S_a(T_1, T_2)$ is of similar significance as $S_a(T_1)$ and $S_{di}(T_1)$. $S_a(T_1, T_2)$ does not offer much advantage for shorter structures, especially at lower intensities. Nevertheless, a different choice in the second period that would capture period elongation (as suggested by Cordova et al., 2000) has been shown to work very well for drift ratios. In all cases, $S_a(T_1, T_2)$ results in relatively low dispersion for floor accelerations, clearly performing as well as or better than any of the other three IMs for any combination of period and scale factor presented above.

In general, the FEMA P-695 scaling method is on par with the best IMs for the 4-story building, where PGV can be a good predictor. Apart from its good performance for FAs for the 8-story building, the FEMA P-695 scaling method is not as useful for other period ranges. As expected, away from the moderate period range its performance worsens. In addition, it is a poor predictor of drift ratio responses at lower intensity levels, at least as compared to the S_a and S_{di} methods, which are more efficient for the drift-related structural EDPs.

In summary, no one IM could be identified that results in the smallest dispersion in EDPs at all scale factors and for all EDPs considered. The $S_a(T_1)$ and $S_{di}(T_1)$ methods offer a definite advantage at lower intensities and practically at all intensities for the drift-related quantities, while the FEMA P-695 and $S_a(T_1, T_2)$ methods offer unparalleled performance for acceleration-related quantities.

D.1.2 Observations on Bias

Estimates of bias using the different scaling methods (or intensity measures) are plotted in Figures D-23 through D-40 below. The median response at each median IM level is compared to the median response obtained for the motions scaled according to the FEMA P-695 approach to estimate the bias. In all cases, the bias is less than 20% for peak floor accelerations and story drifts and at most 10% for story shear and overturning moments, while it exceeded 20% and sometimes even 40% for plastic hinge rotations in some cases. These results are consistent with the magnitude of the dispersions observed for each response parameter. For example, the higher dispersions observed for plastic hinge rotations earlier naturally give rise to a higher

apparent bias. In general, floor accelerations for the $S_a(T_1)$ and $S_{di}(T_1)$ methods are biased slightly lower than those from the FEMA P-695 method. Story shears and overturning moments have negligible bias. Story drift bias is inconsistent. In most cases, slightly higher bias is observed for scale factors of 0.5 and 2.0 among the different scaling methods relative to that obtained with a scale factor of 1.0, with the exception of plastic hinge rotations, which often have higher bias at higher intensities.

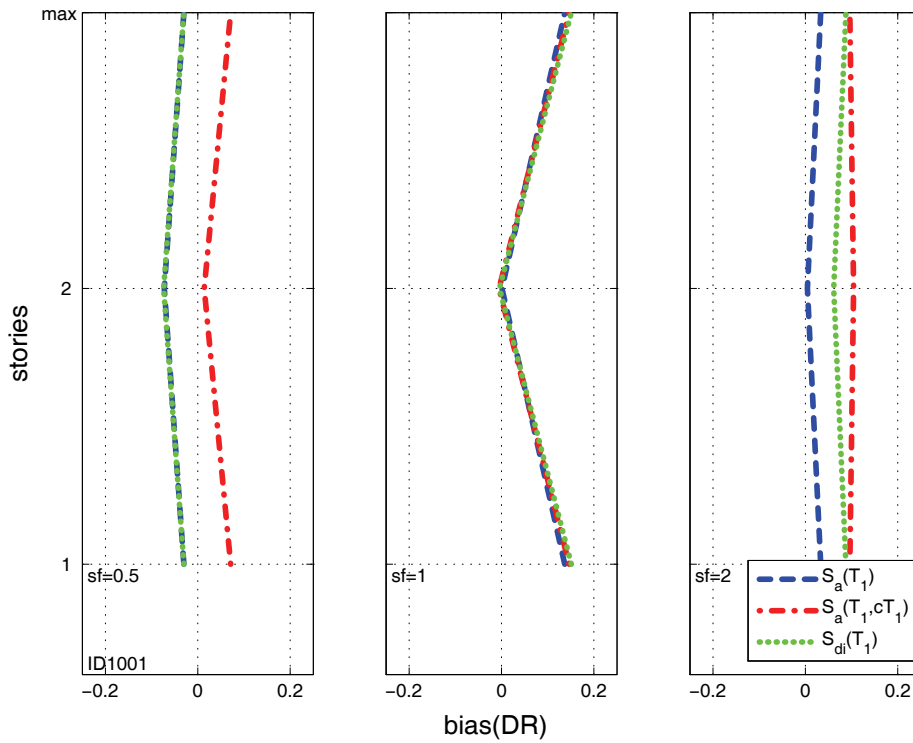


Figure D-23 Bias of the local and maximum story drift ratios along the height of the 2-story RCMF for three different intensity levels.

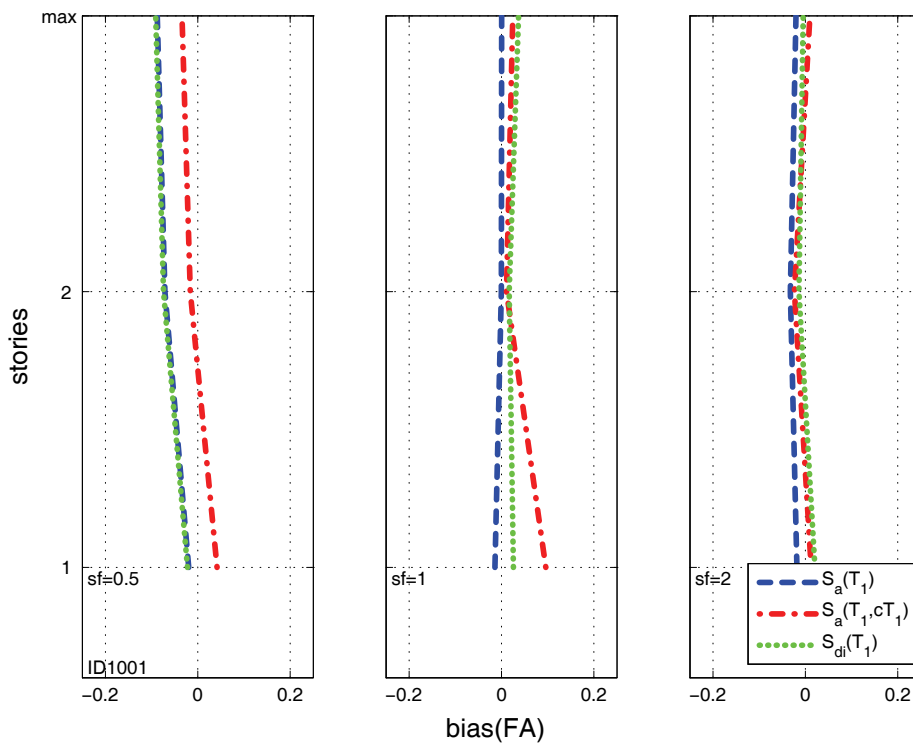


Figure D-24 Bias of the local and maximum peak floor accelerations along the height of the 2-story RCMF for three different intensity levels.

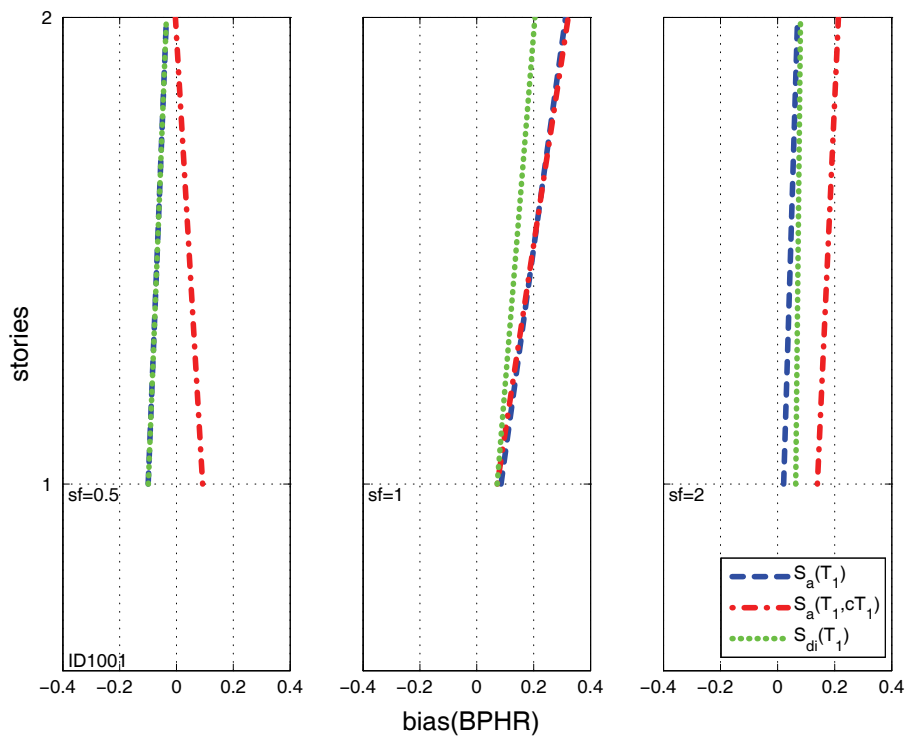


Figure D-25 Bias of the maximum beam plastic hinge rotation for each story along the height of the 2-story RCMF for three different intensity levels.

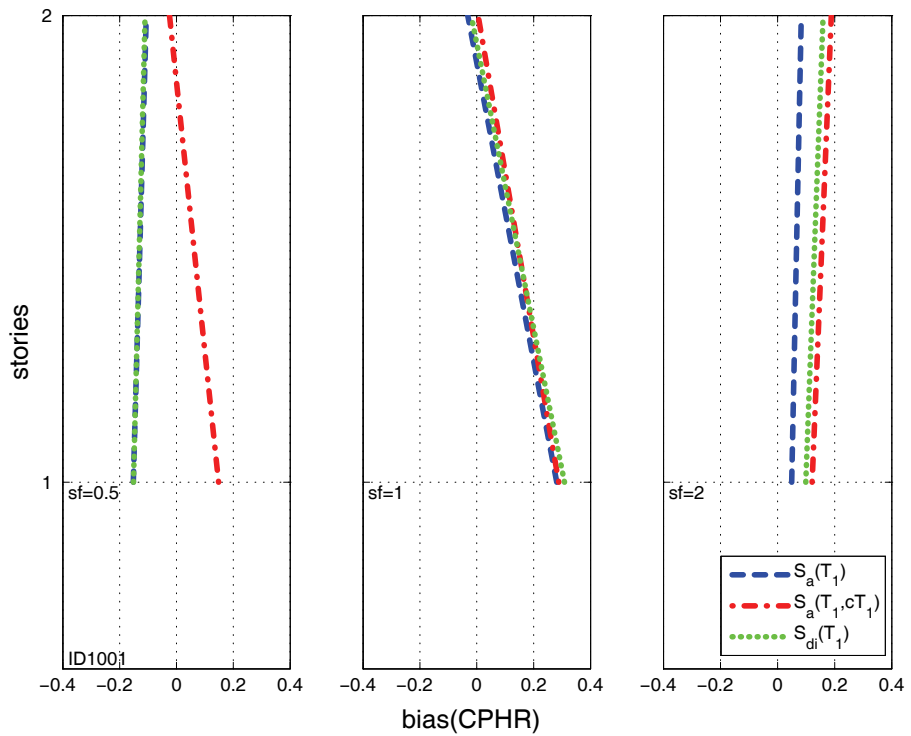


Figure D-26 Bias of the maximum column plastic hinge rotation for each story along the height of the 2-story RCMF for three different intensity levels.

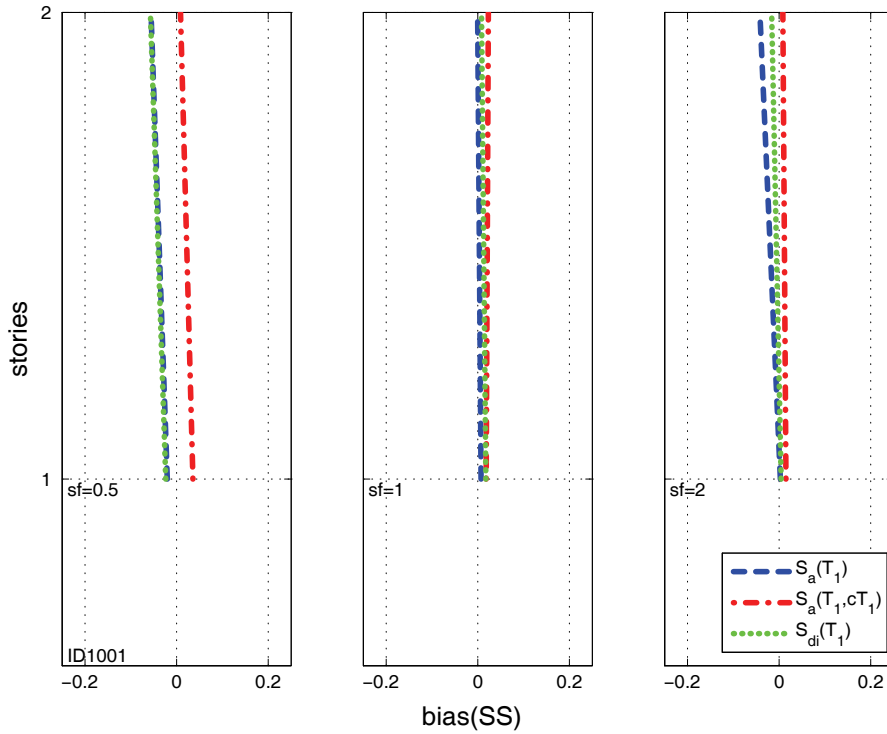


Figure D-27 Bias of the story shear for each story along the height of the 2-story RCMF for three different intensity levels.

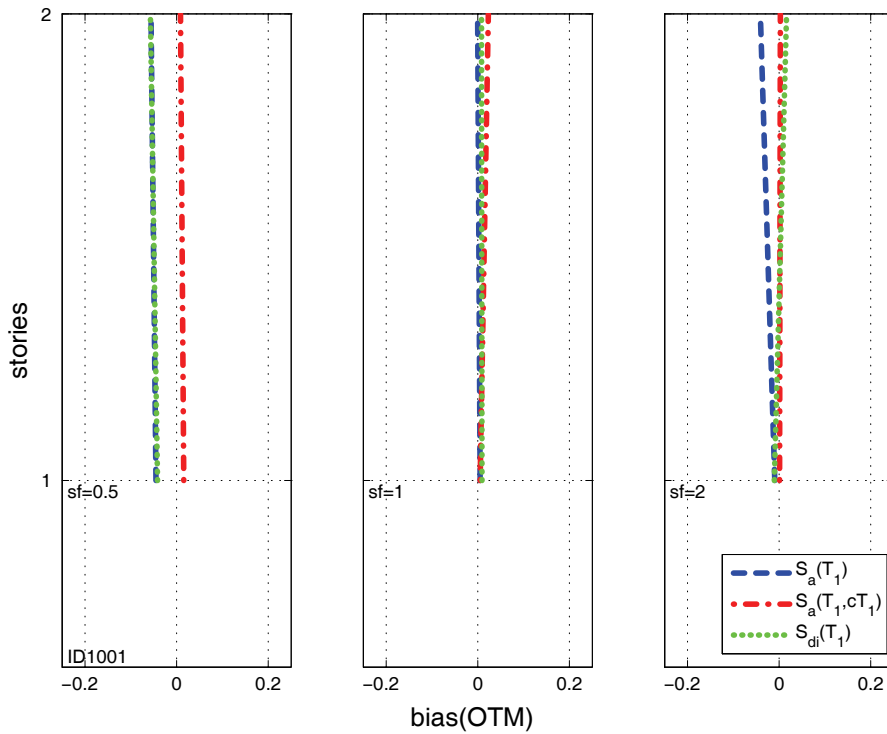


Figure D-28 Bias of the overturning moment for each story along the height of the 2-story RCMF for three different intensity levels.

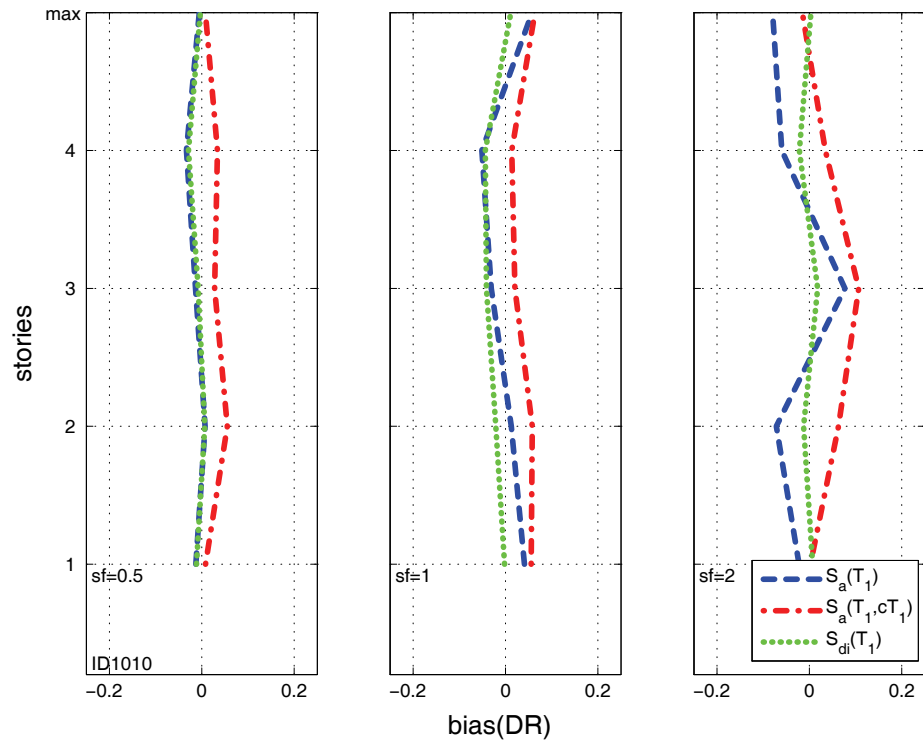


Figure D-29 Bias of the local and maximum story drift ratios along the height of the 4-story RCMF for three different intensity levels.

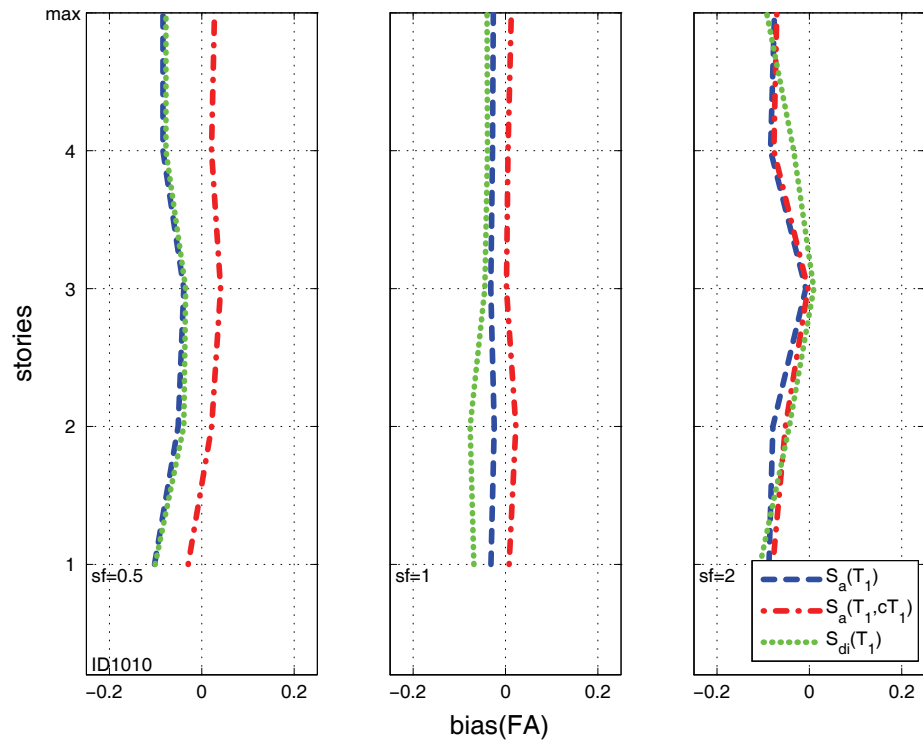


Figure D-30 Bias of the local and maximum peak floor accelerations along the height of the 4-story RCMF for three different intensity levels.

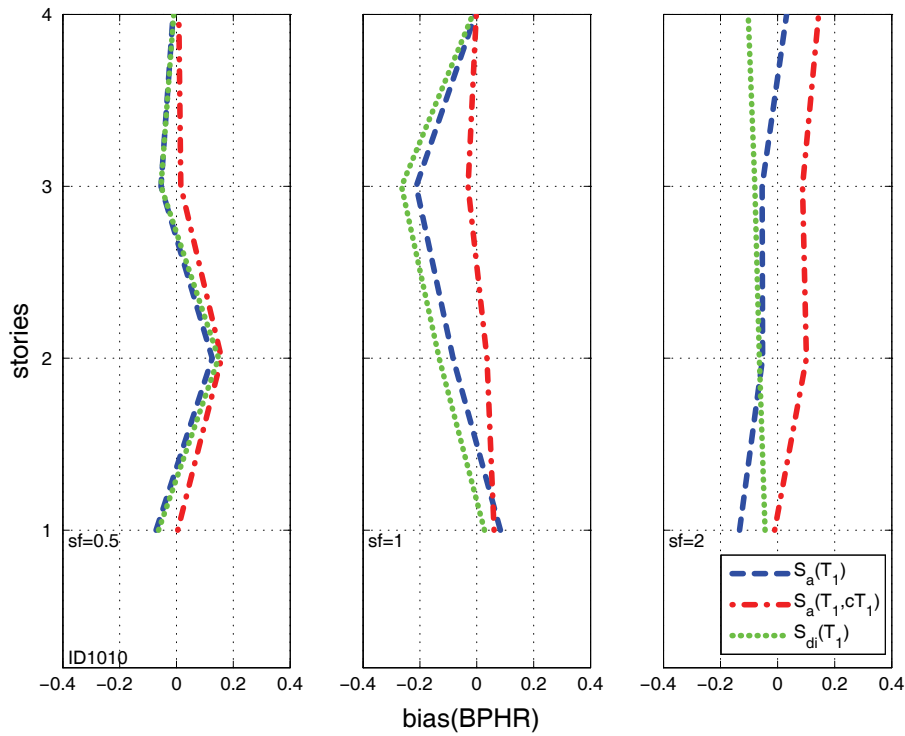


Figure D-31 Bias of the maximum beam plastic hinge rotation for each story along the height of the 4-story RCMF for three different intensity levels.

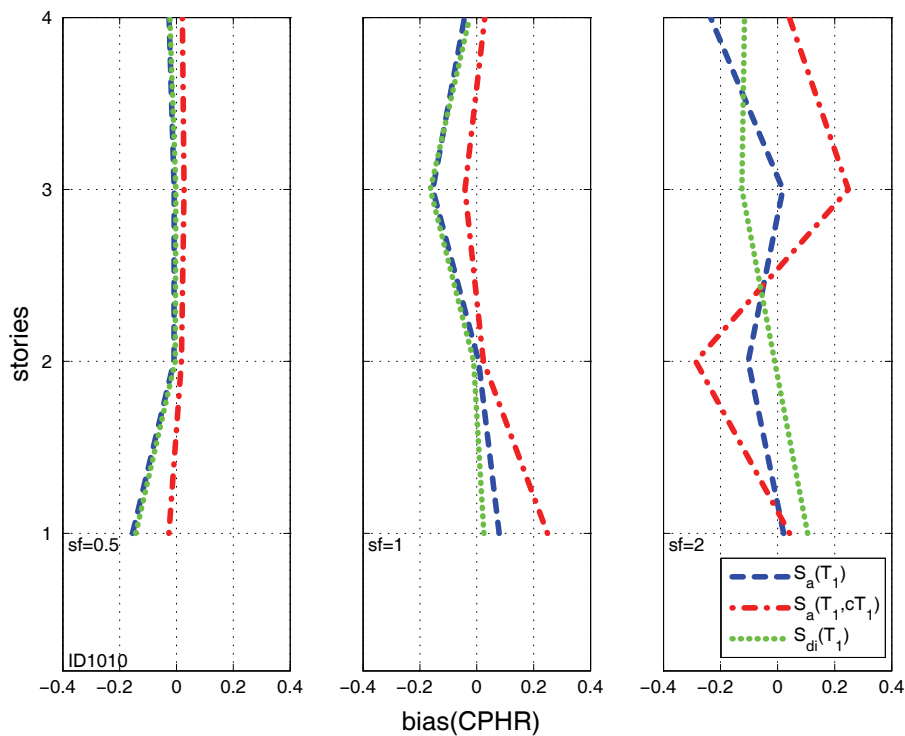


Figure D-32 Bias of the maximum column plastic hinge rotation for each story along the height of the 4-story RCMF for three different intensity levels.

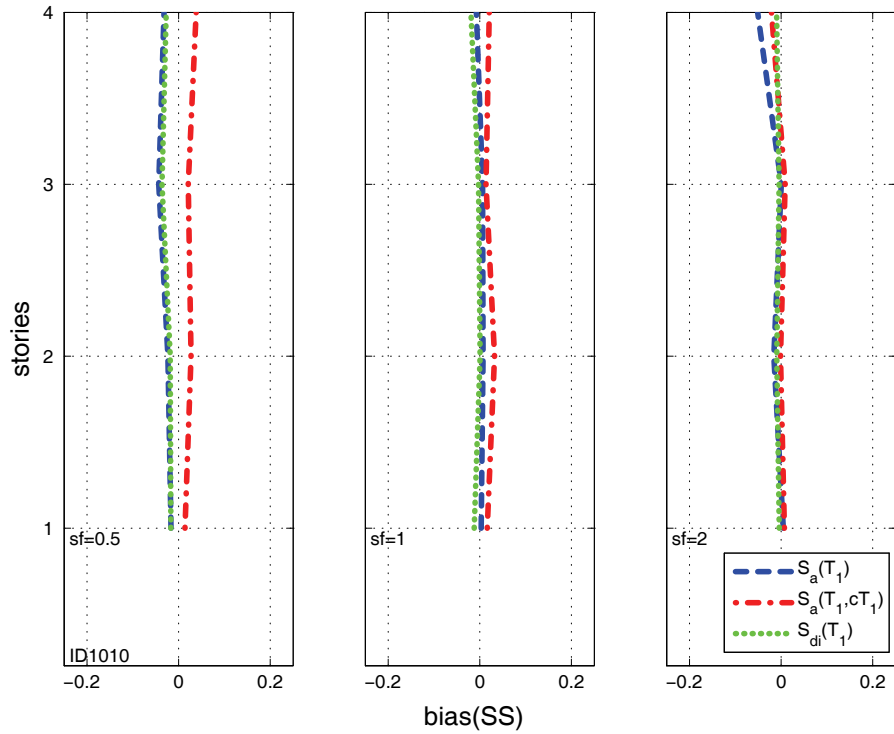


Figure D-33 Bias of the story shear for each story along the height of the 4-story RCMF for three different intensity levels.

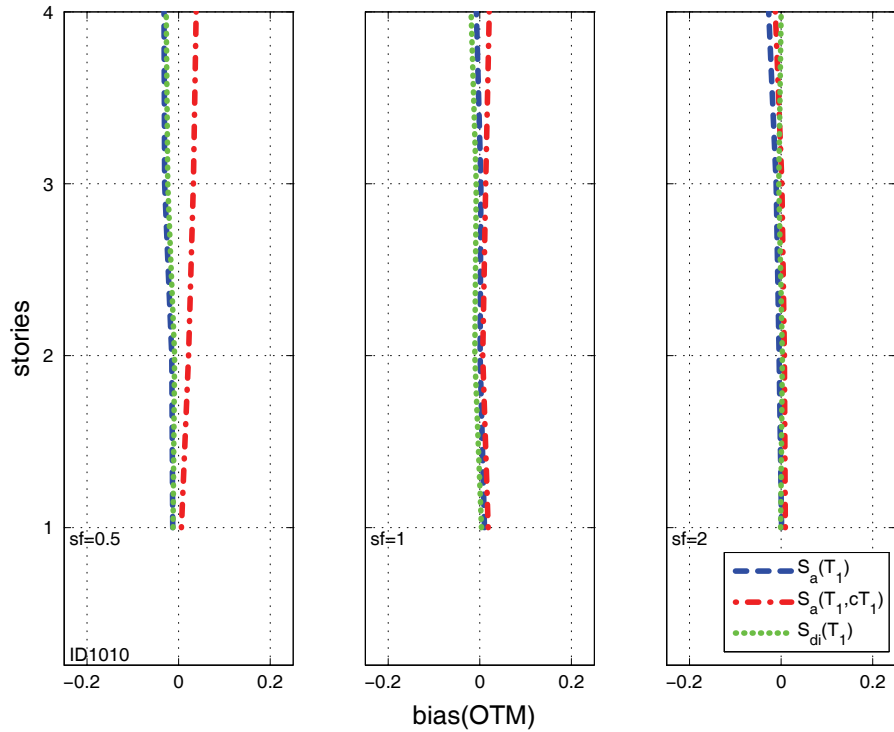


Figure D-34 Bias of the overturning moment for each story along the height of the 4-story RCMF for three different intensity levels.

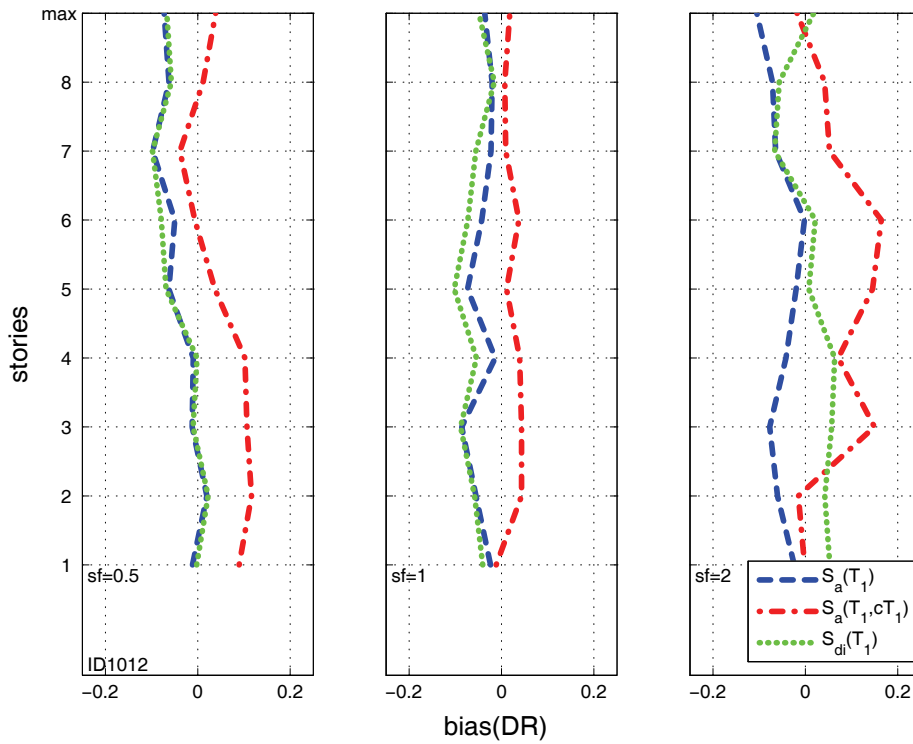


Figure D-35 Bias of the local and maximum story drift ratios along the height of the 8-story RCMF for three different intensity levels.

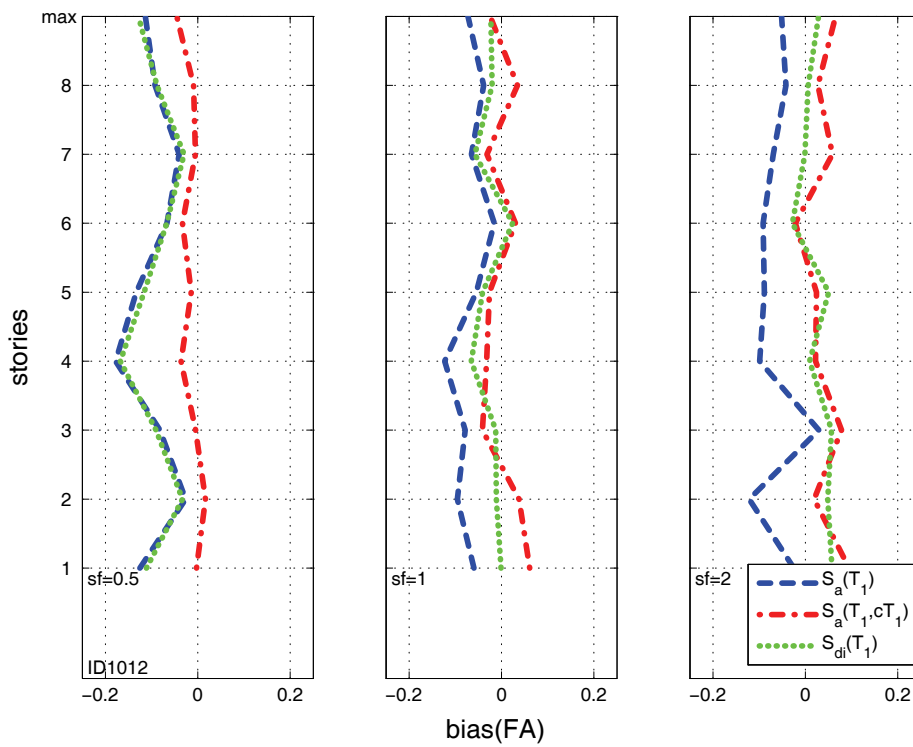


Figure D-36 Bias of the local and maximum peak floor accelerations along the height of the 8-story RCMF for three different intensity levels.

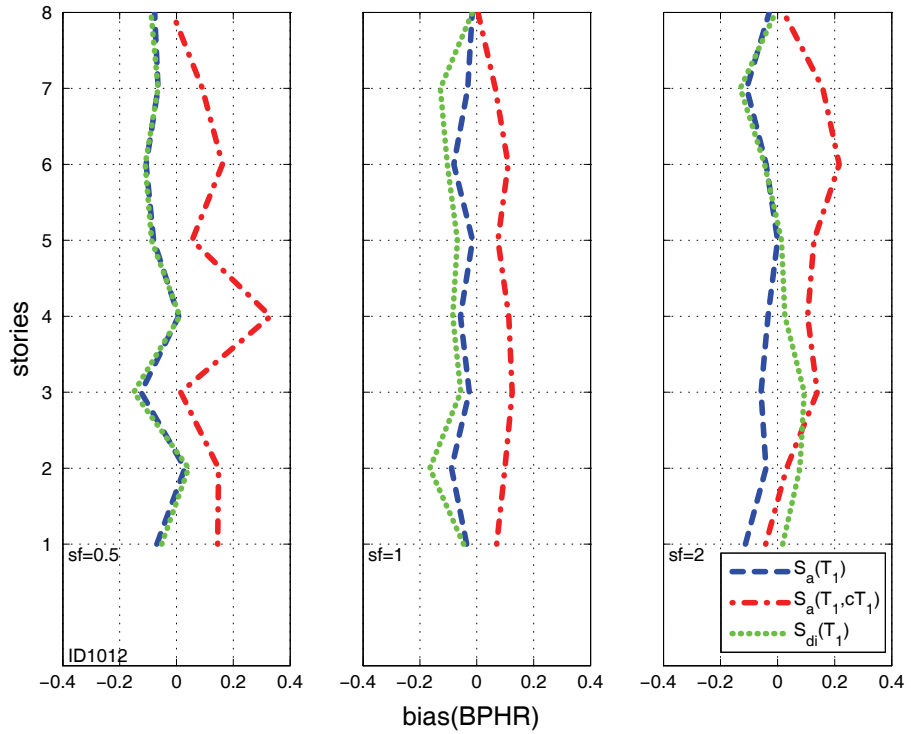


Figure D-37 Bias of the maximum beam plastic hinge rotation for each story along the height of the 8-story RCMF for three different intensity levels.

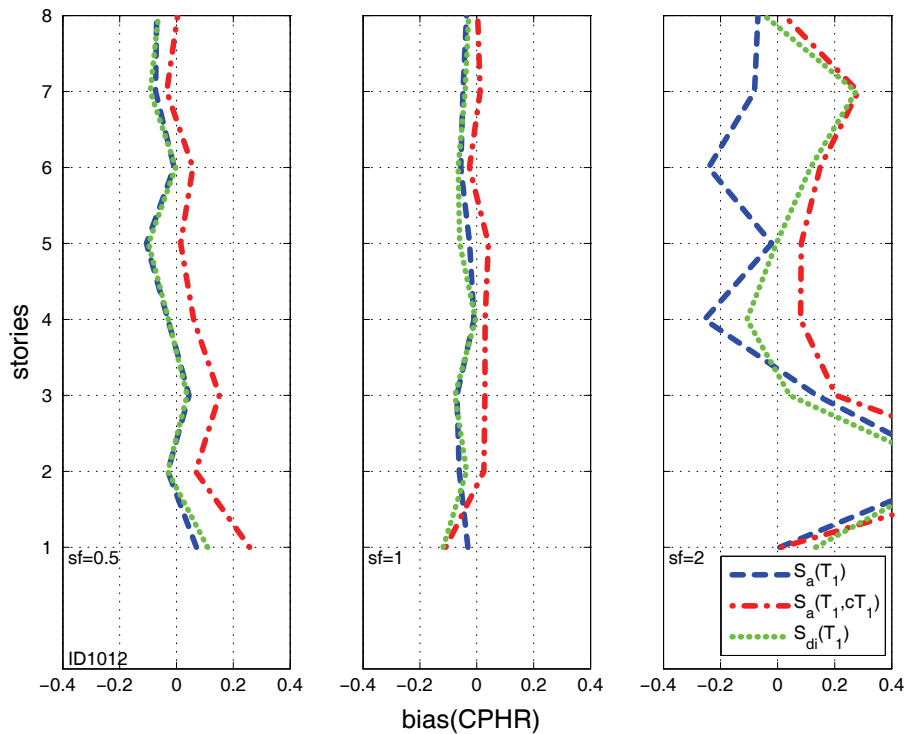


Figure D-38 Bias of the maximum column plastic hinge rotation for each story along the height of the 8-story RCMF for three different intensity levels.

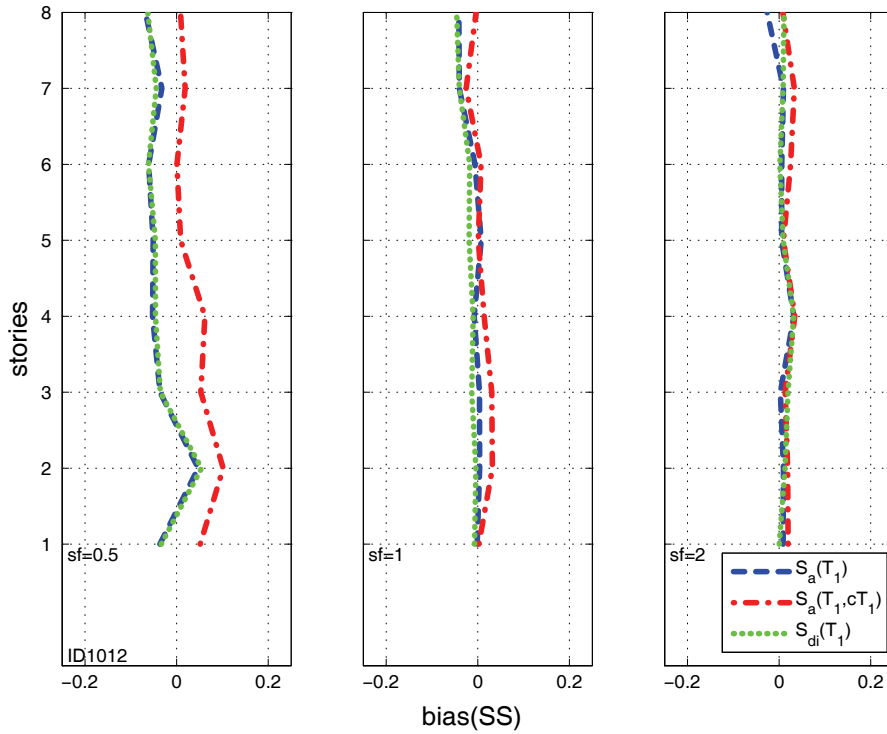


Figure D-39 Bias of the story shear for each story along the height of the 8-story RCMF for three different intensity levels.

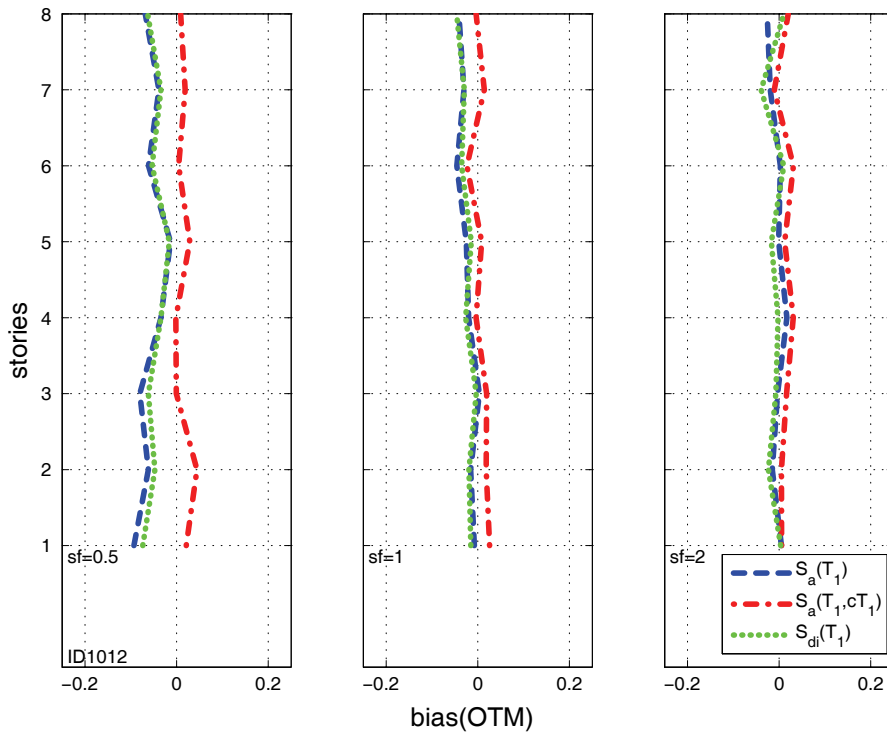


Figure D-40 Bias of the overturning moment for each story along the height of the 8-story RCMF for three different intensity levels.

D.2 Use of Record Subsets to Characterize EDP Distributions

Different IMs can provide different degrees of efficiency in response estimation; the greater the efficiency of the IM, the smaller the number of records needed to achieve a desired confidence in estimating the distribution (central value and dispersion) of a response quantity. There is evidence in the literature, such as Azarbakht and Dolsek (2007, 2010), for methods to select targeted subsets of records that can estimate just the mean/median or the 84-percentile of maximum story drift response using a reduced number of nonlinear dynamic analyses. This is a result that has great significance for implementation of design or analysis methods in practice that rely on response history analysis.

This section further develops this idea, exploring the possibility of using carefully selected subsets of records to estimate median and 84% EDP values. Different methods for scaling ground motions (using different intensity measures) and selecting subsets are investigated. In essence, these methods aim to pick subsets that match median or 84% elastic spectra; estimates of median or 84% EDP values are determined as the median of the EDP values obtained with the respective subsets. The median and 84% EDP values can be used to approximately characterize the distribution of the EDP response. Errors in the estimates are evaluated relative to the median and 84% EDP values determined for the full set of 44 records scaled according to the same intensity measure.

The following subsections discuss subset selection methods on the basis of the FEMA P-695, $S_a(T_i)$, and S_{di} scaling methods, employing different optimization criteria to identify the “optimal” subset for our purposes.

D.2.1 Subset Selection Methods Used for Estimating Median EDP Values

Two candidate methods were tried to select motions that comprised a subset. To properly define them, the following symbols are introduced: The operator $[\cdot]_{A,x\%}$ denotes the x percentile of dataset A , $E_A[\cdot]$ is its mean, and “sub” and “all” are used to distinguish the subset and the full set.

Selection Method A:

- Minimize the average of the sums of squared differences from (a) the mean and (b) median of the elastic spectrum of the ground motion suite within the range $[0.04s, 2s]$. Formally:

$$\text{minimize } \frac{1}{2} \int_{0.04s}^{2s} \left\{ \begin{aligned} & (E_{sub}[S_a(T)] - E_{all}[S_a(T)])^2 + \\ & ([S_a(T)]_{sub,50\%} - [S_a(T)]_{all,50\%})^2 \end{aligned} \right\} dT \quad (D-1)$$

The “optimal” subsets were selected using the following procedure:

1. Select the best single record.

2. Select the two additional records that form the next optimal subset by searching through all possible combinations of the remaining records.
3. Repeat Step 2 until the desired subset size is obtained.

Selection Method B:

- Minimize the sum of the absolute *relative* differences from the median of the elastic spectrum of the ground motion suite within the period range $R_T \equiv [0.8T_i, 1.2T_2] \cup [0.8T_1, 1.5T_1]$, designed to capture both the higher mode effects and the expected lengthening of the “first-mode” after yielding. The lower period is T_i determined as a function of the number of stories N_{st} :

$$i = \text{ceil}(\sqrt{N_{st}})$$
where “ceil” is a function that rounds up to the nearest highest integer.

Formally:

$$\text{minimize } \int_{R_T} \left| \frac{[S_a(T)]_{sub,50\%} - [S_a(T)]_{all,50\%}}{[S_a(T)]_{all,50\%}} \right| dT \quad (D-2)$$

To select the “optimal” subsets one could use the same procedure as method A, but the following simpler method was preferred:

1. Estimate the “signed” and “unsigned” objective values S^i and U^i for each i -th record by adapting Equation D-2 with and without the absolute value, respectively:

$$S^i = \int_{R_T} \frac{S_a^i(T) - [S_a(T)]_{all,50\%}}{[S_a(T)]_{all,50\%}} dT \quad (D-3)$$

$$U^i = \int_{R_T} \left| \frac{S_a^i(T) - [S_a(T)]_{all,50\%}}{[S_a(T)]_{all,50\%}} \right| dT \quad (D-4)$$

2. Separate the records into two lists: A “negative” and a “positive” list according to the sign of the “signed” objective value.
3. Merge the two lists by selecting records alternatively from each. Start from the “positive” list and pick the record with the lowest “unsigned” value, then similarly proceed with the “negative” list to pick the second record. Remove them from the lists.
4. Continue until the desired subset size is reached.

For both selection methods, a proper optimization to select the true optimal subsets in each case would be cumbersome, involving a difficult combinatorial optimization problem. In its place, the simplified selection procedures described above were introduced. The approach used for Method B can be easily implemented, e.g., in a spreadsheet.

Method B mainly differs in its structure-dependent fitting range and its use of a much simpler selection algorithm exploiting the relative robustness of the percentile estimators to run more efficiently. It also employs an integral over relative differences rather than plain differences. Since higher differences generally appear at the lower end of the spectrum, Method A will tend to weigh lower periods more heavily than Method B, which strives for more equal weighting. Of course, it is conceivable that the degree of nonlinearity in the structure itself should influence the relative weighting of different areas in the spectrum, favoring, for example, the periods above T_1 when deep in the post-yield range of response versus periods around, e.g., T_2 when close to linear elastic behavior. This points to the expectation that, for the sake of simplicity, the proposed selection methods may not be equally efficient at all intensity levels.

As described in subsequent sections, estimates of median EDP values were determined from NRHA as the medians obtained using record subsets that were identified using Methods A and B. Specifically, given a selected subset A of N_A records, the median (50%) value of an EDP response determined using the full set of records was estimated as the median of the N_A EDP values determined using the subset records. For median estimates:

$$EDP_{50} \cong [EDP_i]_{A,50\%} \quad (D-5)$$

D.2.2 Subset Selection Methods used for Estimating 84% EDP Values

With slight modification, the above selection methods can be used to estimate the 84% EDP values. To do so, record subsets are selected whose median approximately matches the 84% spectra obtained for the full set of motions. Selection Method A is not such a viable candidate though as it requires use of the mean which is not easy to generalize to different fractiles. On the other hand, Selection Method B can be easily adapted by replacing the median of the entire subset with its 84% value. Thus, the equations to estimate the signed and unsigned objective values now become:

$$S^i = \int_{R_T} \frac{S_a^i(T) - [S_a(T)]_{all,84\%}}{[S_a(T)]_{all,84\%}} dT \quad (D-6)$$

$$U^i = \int_{R_T} \left| \frac{S_a^i(T) - [S_a(T)]_{all,84\%}}{[S_a(T)]_{all,84\%}} \right| dT \quad (D-7)$$

However, the estimation of the 84% needs more care, as the errors can be much higher than occur with estimates of the median. Consider that for a given scale factor (or intensity level) record subsets A and B have been selected in accordance with the median and 84% spectra of the full set, having sizes N_A and N_B , respectively. Then, a relatively conservative estimate of the 84% can be made by taking the maximum of three distinct values:

1. The median of EDP values obtained using subset B
2. The median of the largest N_B peak EDP values from subsets A and B together
3. The 84% of the EDP values from subsets A and B together.

Care should be exercised though: the 3rd estimate is intended to be useful only for large samples, as it can become too conservative for small subset sizes (e.g., N_B less than about 9 relative to a full set size of 44). On the other hand, it has to be used for larger subsets as the use of medians in the first two estimates will tend to underestimate the 84%. Therefore, the combined, multi-part estimate of the 84% EDP is:

$$EDP_{84} \cong \begin{cases} \max\left([EDP_i]_{B,50\%}, [EDP_i]_{\max(A,B),50\%}\right), & \text{if } N_B < 9 \\ \max\left([EDP_i]_{B,50\%}, [EDP_i]_{\max(A,B),50\%}, [EDP_i]_{A+B,84\%}\right), & \text{if } N_B \geq 9 \end{cases} \quad (D-8)$$

where the cutoff value of N_B would be about 20% of the full set size, more generally, for other full set sizes. Based on the foregoing estimates of EDP_{50} and EDP_{84} , a lognormal distribution of the EDP would be characterized by mean EDP_{50} and dispersion $\ln(EDP_{84}) - \ln(EDP_{50})$.

D.2.3 Subset Selection based on FEMA P-695 scaling

The suite of ground motion records established in FEMA P-695 was scaled by factors of 0.5, 1.0, and 2.0. Progressively larger subsets of size 1,3,5,...,17 records were selected to attempt an economical estimation of the median (or mean) response quantity obtained using the full set of 44 ground motion records. A second record subset was used to attempt estimation of the 84% response quantity obtained using the full set of 44 ground motion records.

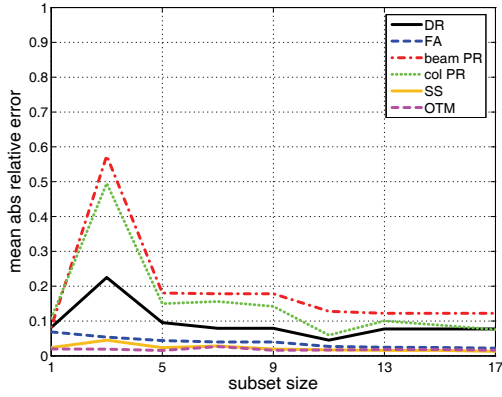
Selection Methods A and B were applied to each of the three buildings and for each of the three scale factor levels to estimate median response using subsets up to size 17. The detailed results of the relative absolute error in each estimate of the median responses are presented in Figure D-41 for all three buildings and the three scale factors, appropriately summarized into their mean and maximum values for each category of EDP (e.g., story drifts, floor accelerations, etc.). The same results appear for each individual story in Table D-1. An ideal method for subset selection would be characterized by (a) a low magnitude of error for each EDP type and (b) a consistent trend in the error of the procedure, where a monotonic reduction in error with increasing subset size is desirable.

None of the above criteria is perfectly satisfied for Method A. The error trend could be said to be globally decreasing with subset size, but some local non-monotonic trends are present, indicating cases where increasing the subset size results in slightly worse estimates. In addition, the mean relative errors are low with the exception of

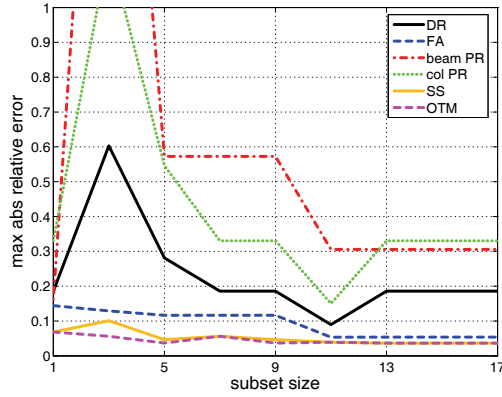
the beam and column plastic hinge rotations. These EDPs have the highest estimation errors, with relative errors sometimes exceeding 100%. This observation needs to be understood in the context of the large dispersion associated with these EDPs. Therefore, Figure D-42 shows the corresponding σ -normalized error, i.e., the difference normalized by the standard deviation of the EDP (evaluated using the full set of 44 records), for each building and EDP type. Therein it becomes apparent that, given the dispersion magnitude of each EDP, the relative errors are not that different among the different response types. As well, the nature of plastic hinge rotations, which may range between near-zero values for some records to quite large for others, is a challenge for any simplified approach to characterize. This issue is further discussed in Section D.3.1, where it is shown how trimming such near-zero values can stabilize the distribution and thus the estimates of plastic hinge rotations.

The results of Selection Method B are summarized in Figures D-43 and D-44 for the 50% response and are presented in detail in Tables D-3 and D-4. While the magnitude of the errors is very similar to that of Method A, the global trends are somewhat smoother and closer to monotonic. The more narrowly targeted period range seems to benefit Method B. Combined with the simpler selection algorithm used, this gives a small but distinct advantage to Method B. Therefore, Method B is used for the remainder of this section.

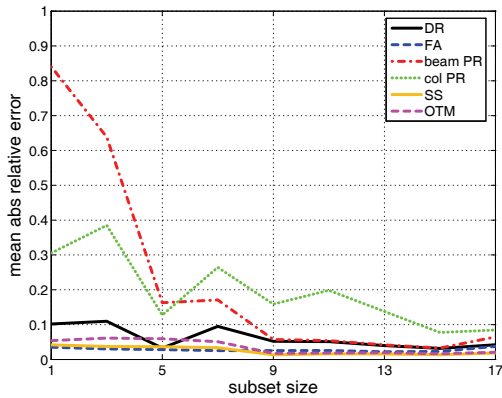
To further investigate the applicability of Method B, the 84% estimation results were determined and are presented in Figures D-45 and D-46 and Tables D-5 and D-6, for the 2- and 4-story frames, respectively. In all cases, mean errors are very well behaved, even though errors in the 84% values are naturally larger than those for median estimates. Still, there are some localized cases where the errors rise out of proportion, inflating the maximum relative error in many EDP categories, most notably for plastic hinge rotations. Nevertheless, the multi-part estimation methodology used for the 84% response helps to drive such estimates to the high side, generally resulting in a conservative estimate.



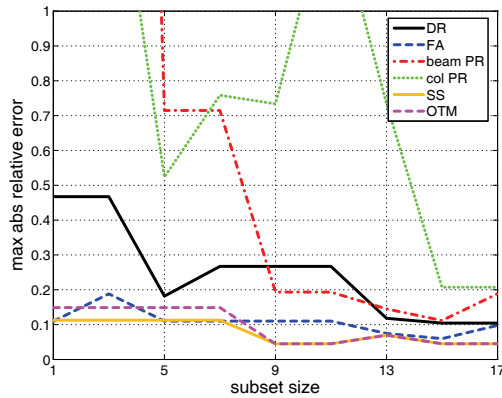
(a) 2-story, mean error



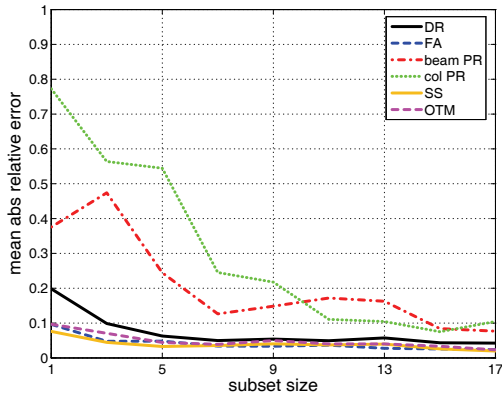
(b) 2-story, max error



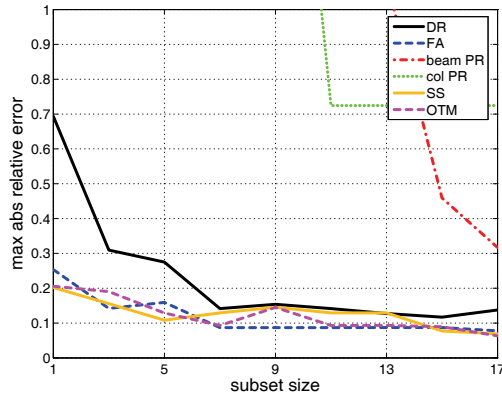
(c) 4-story, mean error



(d) 4-story, max error

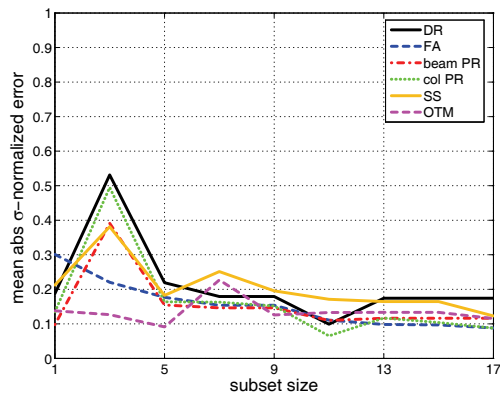


(e) 8-story, mean error

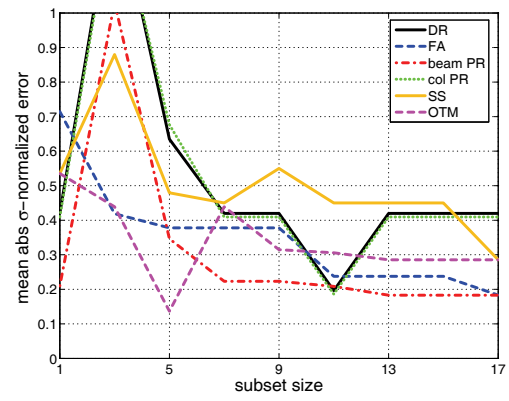


(f) 8-story, max error

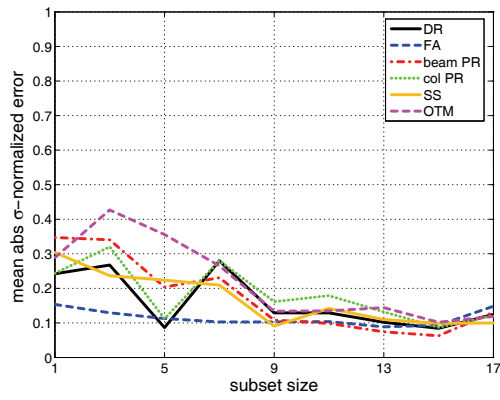
Figure D-41 Mean and maximum absolute relative error for different EDP types over all 3 scale factors when selecting subsets within a FEMA P-695 stripe by matching globally the mean and median S_a values to estimate the 50% response (Method A).



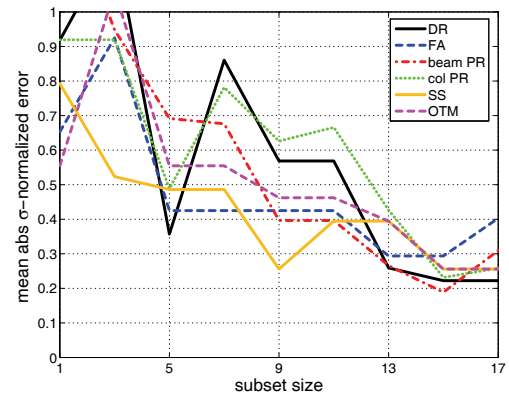
(a) 2-story, mean error



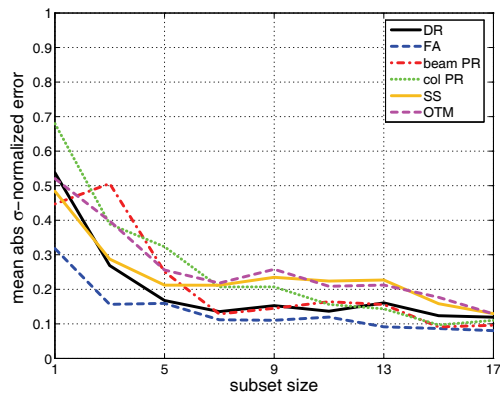
(b) 2-story, max error



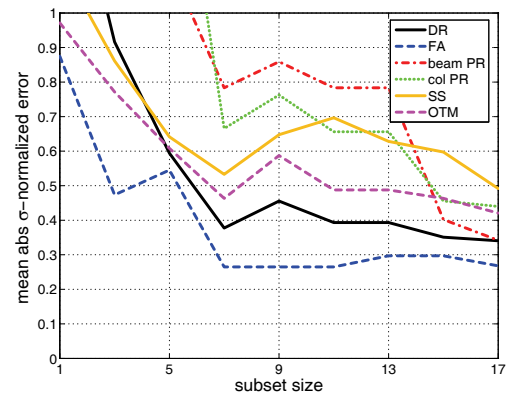
(c) 4-story, mean error



(d) 4-story, max error



(e) 8-story, mean error



(f) 8-story, max error

Figure D-42 Mean and maximum absolute σ -normalized error for different EDP types over all 3 scale factors when selecting subsets within a FEMA P-695 stripe by matching globally the mean and median S_a values to estimate the 50% response (Method A).

Table D-1 Subset Estimation Errors for the 50% EDP Response of the 2-Story RCMF Using Selection Method A on FEMA-P695 Stripes

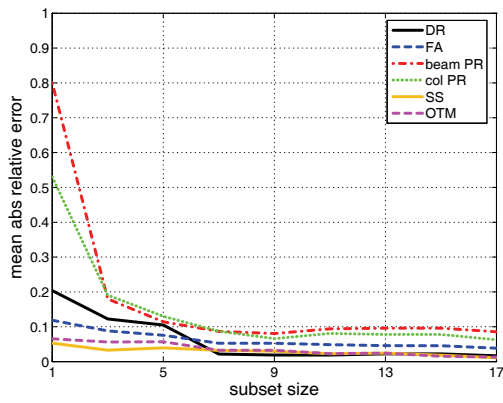
EDP	SF	50% EDP Relative Error								
		Subset Size								
		1	3	5	7	9	11	13	15	17
DR1	0.5	9%	22%	9%	9%	9%	9%	9%	9%	9%
	1	19%	60%	28%	19%	19%	-3%	19%	19%	19%
	2	-6%	1%	1%	1%	1%	-1%	1%	1%	1%
DR2	0.5	4%	6%	5%	5%	5%	4%	5%	5%	5%
	1	1%	30%	4%	4%	4%	3%	3%	3%	3%
	2	-1%	-1%	-1%	-6%	-6%	-9%	-6%	-6%	-6%
DRmax	0.5	9%	22%	9%	9%	9%	9%	9%	9%	9%
	1	19%	60%	28%	19%	19%	-3%	19%	19%	19%
	2	-6%	1%	1%	1%	1%	-1%	1%	1%	1%
FA1	0.5	-11%	13%	12%	12%	12%	-1%	-1%	-1%	-1%
	1	1%	3%	3%	5%	5%	5%	5%	5%	3%
	2	5%	5%	3%	-4%	-4%	-4%	-4%	3%	3%
FA2	0.5	6%	6%	5%	5%	5%	5%	5%	5%	5%
	1	-5%	-3%	-3%	-2%	-2%	-2%	1%	1%	1%
	2	14%	4%	4%	2%	2%	-1%	-1%	2%	2%
FMax	0.5	4%	4%	3%	3%	3%	3%	3%	3%	3%
	1	-5%	-3%	-3%	-2%	-2%	-2%	1%	1%	1%
	2	11%	7%	2%	-1%	-1%	-1%	-1%	1%	1%
BPR1	0.5	16%	24%	22%	22%	22%	16%	16%	16%	16%
	1	13%	63%	21%	13%	13%	1%	11%	11%	11%
	2	1%	1%	1%	-3%	-3%	-4%	-3%	-3%	-3%
BPR2	0.5	1%	1%	1%	1%	1%	1%	1%	1%	1%
	1	-7%	249%	57%	57%	57%	31%	31%	31%	31%
	2	-11%	6%	6%	-11%	-11%	-23%	-11%	-11%	-11%
CPR1	0.5	2%	46%	3%	3%	3%	2%	2%	2%	2%
	1	33%	108%	55%	33%	33%	-15%	33%	33%	33%
	2	-10%	1%	1%	1%	2%	1%	2%	2%	1%
CPR2	0.5	-1%	25%	-1%	25%	16%	-1%	14%	7%	1%
	1	-17%	117%	30%	30%	29%	6%	6%	6%	6%
	2	-2%	0%	0%	-2%	-2%	-10%	-2%	-2%	-2%
SS1	0.5	2%	10%	5%	5%	5%	2%	2%	2%	2%
	1	0%	8%	4%	3%	3%	0%	0%	0%	0%
	2	-2%	2%	1%	2%	2%	2%	2%	2%	1%
SS2	0.5	-3%	0%	3%	0%	0%	-1%	0%	0%	0%
	1	-1%	-1%	-1%	2%	2%	2%	2%	2%	-1%
	2	7%	-6%	0%	-6%	0%	-4%	-4%	-4%	-4%
OTM1	0.5	0%	4%	4%	4%	4%	2%	4%	4%	4%
	1	1%	1%	1%	3%	3%	1%	1%	1%	0%
	2	0%	0%	-1%	-1%	-1%	-1%	-1%	-1%	-1%
OTM2	0.5	-3%	0%	3%	0%	0%	-1%	0%	0%	0%
	1	-1%	-1%	-1%	2%	2%	2%	2%	2%	-1%
	2	7%	-6%	0%	-6%	0%	-4%	-4%	-4%	-4%

Table D-2 Subset Estimation Errors for the 50% EDP Response of the 4-Story RCMF Using Selection Method A on FEMA-P695

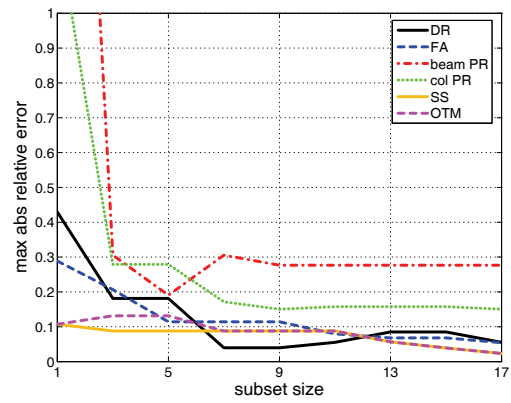
EDP	SF	50% EDP relative error								
		subset size								
		1	3	5	7	9	11	13	15	17
<i>DR1</i>	0.5	1%	1%	1%	1%	1%	1%	-3%	-3%	-3%
	1	2%	2%	2%	23%	2%	2%	2%	2%	-3%
	2	-27%	27%	1%	27%	27%	27%	12%	10%	10%
<i>DR2</i>	0.5	-1%	-1%	-1%	1%	1%	-1%	-1%	-1%	-5%
	1	-4%	-1%	-1%	14%	-1%	-4%	-1%	-1%	-4%
	2	-26%	23%	-2%	11%	11%	11%	11%	8%	8%
<i>DR3</i>	0.5	-1%	-1%	-1%	0%	0%	0%	0%	-1%	-4%
	1	-4%	-2%	-2%	9%	-2%	-2%	-2%	-2%	-3%
	2	8%	41%	8%	8%	6%	-6%	6%	6%	-1%
<i>DR4</i>	0.5	1%	1%	1%	1%	-1%	-1%	-1%	-2%	-5%
	1	0%	0%	0%	0%	0%	0%	0%	0%	-2%
	2	47%	47%	18%	11%	9%	5%	9%	9%	9%
<i>DRmax</i>	0.5	-1%	-1%	-1%	-1%	-1%	-1%	-1%	-1%	-5%
	1	-2%	-2%	-2%	21%	-2%	-2%	-1%	-1%	-2%
	2	-29%	15%	-9%	15%	15%	15%	10%	0%	0%
<i>FA1</i>	0.5	2%	2%	3%	3%	3%	3%	3%	3%	2%
	1	0%	0%	0%	0%	0%	0%	0%	0%	-2%
	2	-5%	-3%	-3%	-3%	-3%	-3%	-3%	-3%	-3%
<i>FA2</i>	0.5	-1%	-1%	11%	11%	11%	11%	-1%	-4%	-4%
	1	4%	4%	4%	4%	4%	5%	4%	4%	4%
	2	-7%	1%	1%	1%	1%	1%	-7%	1%	-7%
<i>FA3</i>	0.5	-5%	-5%	-5%	-1%	-1%	-1%	-1%	-1%	-5%
	1	-11%	1%	1%	1%	1%	1%	1%	1%	-1%
	2	6%	19%	6%	6%	6%	6%	6%	6%	6%
<i>FA4</i>	0.5	0%	0%	0%	0%	0%	0%	0%	-4%	-10%
	1	-2%	-1%	0%	0%	0%	0%	0%	0%	0%
	2	2%	5%	2%	2%	2%	-1%	-2%	-1%	-1%
<i>FAmx</i>	0.5	0%	0%	0%	0%	0%	0%	0%	-4%	-10%
	1	-2%	-1%	1%	1%	1%	1%	1%	0%	0%
	2	-6%	-3%	-3%	-3%	-3%	-3%	-3%	-1%	-1%
<i>BPR1</i>	0.5	1%	1%	1%	1%	-1%	-1%	-1%	-1%	-12%
	1	8%	8%	8%	29%	8%	0%	0%	0%	-1%
	2	-29%	19%	13%	19%	19%	19%	13%	9%	9%
<i>BPR2</i>	0.5	-2%	12%	12%	12%	-2%	-2%	-2%	-2%	-10%
	1	-15%	-11%	-11%	9%	-11%	-11%	-11%	-11%	-12%
	2	-23%	27%	18%	18%	-5%	-5%	0%	0%	0%
<i>BPR3</i>	0.5	-9%	32%	19%	19%	15%	15%	15%	6%	-5%
	1	-2%	-2%	-2%	1%	-2%	-2%	-2%	-2%	-19%
	2	54%	54%	40%	25%	2%	-6%	2%	2%	2%
<i>BPR4</i>	0.5	1%	1%	1%	1%	0%	0%	0%	-1%	-3%
	1	0%	0%	0%	0%	0%	0%	0%	0%	-1%
	2	865%	600%	71%	71%	4%	-4%	4%	4%	4%

Table D-2 Subset Estimation Errors for the 50% EDP Response of the 4-Story RCMF Using Selection Method A on FEMA-P695 (continued)

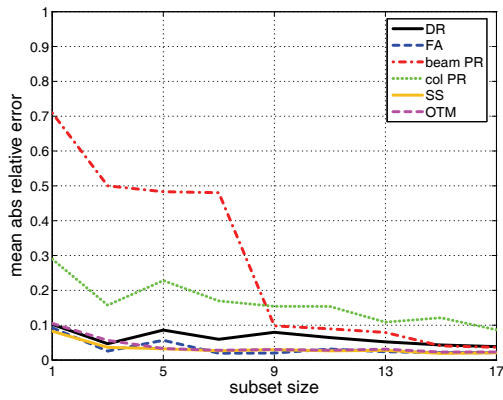
EDP	SF	50% EDP relative error								
		subset size								
		1	3	5	7	9	11	13	15	17
<i>CPR1</i>	0.5	-5%	16%	16%	16%	5%	10%	5%	5%	-5%
	1	-1%	14%	14%	76%	14%	14%	1%	1%	-1%
	2	-41%	51%	1%	51%	51%	51%	34%	19%	19%
<i>CPR2</i>	0.5	1%	1%	1%	1%	1%	1%	1%	0%	-8%
	1	-3%	0%	0%	0%	-3%	-2%	-2%	-2%	-3%
	2	-52%	-27%	-19%	73%	73%	134%	73%	-19%	-19%
<i>CPR3</i>	0.5	-1%	-1%	-1%	20%	3%	3%	3%	0%	-1%
	1	-24%	52%	52%	52%	-18%	-18%	-16%	-16%	-18%
	2	-74%	120%	0%	0%	0%	0%	4%	4%	4%
<i>CPR4</i>	0.5	0%	0%	0%	0%	-1%	-1%	-1%	-2%	-3%
	1	-6%	21%	5%	1%	1%	5%	5%	5%	1%
	2	159%	159%	44%	27%	21%	1%	21%	21%	21%
<i>SS1</i>	0.5	2%	2%	2%	2%	0%	0%	0%	0%	-1%
	1	4%	4%	3%	3%	2%	2%	2%	2%	1%
	2	0%	0%	1%	1%	0%	1%	0%	0%	0%
<i>SS2</i>	0.5	2%	2%	2%	2%	2%	-1%	-1%	-1%	-4%
	1	-2%	1%	1%	2%	1%	-2%	1%	1%	0%
	2	-4%	1%	0%	0%	0%	-2%	0%	1%	0%
<i>SS3</i>	0.5	9%	9%	9%	9%	1%	1%	1%	-1%	-3%
	1	2%	2%	2%	2%	0%	0%	0%	0%	0%
	2	4%	4%	4%	4%	2%	2%	2%	2%	2%
<i>SS4</i>	0.5	11%	11%	11%	11%	-3%	-3%	-3%	-4%	-4%
	1	-3%	-1%	5%	1%	1%	2%	2%	1%	-1%
	2	-8%	-8%	-5%	-5%	-5%	-5%	-7%	-5%	-5%
<i>OTM1</i>	0.5	9%	9%	9%	9%	3%	3%	3%	-3%	-5%
	1	0%	3%	3%	0%	0%	0%	1%	0%	0%
	2	1%	4%	1%	1%	1%	-1%	1%	1%	1%
<i>OTM2</i>	0.5	12%	12%	12%	12%	1%	1%	1%	-2%	-4%
	1	0%	2%	2%	1%	0%	0%	0%	0%	0%
	2	4%	3%	1%	0%	0%	0%	1%	1%	1%
<i>OTM3</i>	0.5	15%	15%	15%	15%	0%	0%	0%	-2%	-3%
	1	-1%	-1%	3%	2%	2%	2%	2%	1%	-1%
	2	-1%	-4%	-4%	-4%	-4%	-4%	-1%	-1%	-1%
<i>OTM4</i>	0.5	11%	11%	11%	11%	-3%	-3%	-3%	-4%	-4%
	1	-3%	-1%	5%	1%	1%	2%	2%	1%	-1%
	2	-8%	-8%	-5%	-5%	-5%	-5%	-7%	-5%	-5%



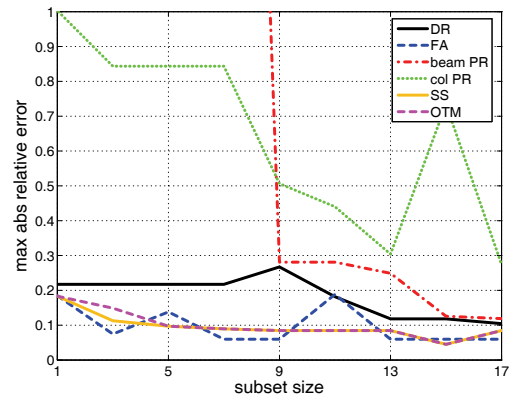
(a) 2-story, mean error



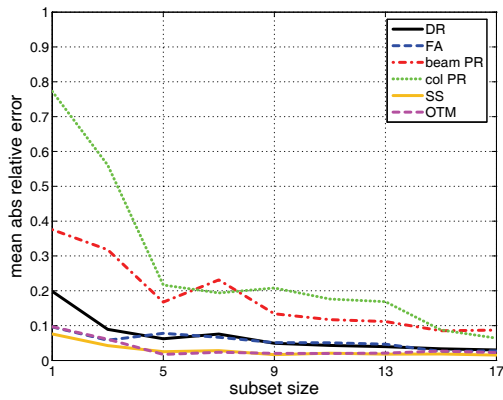
(b) 2-story, max error



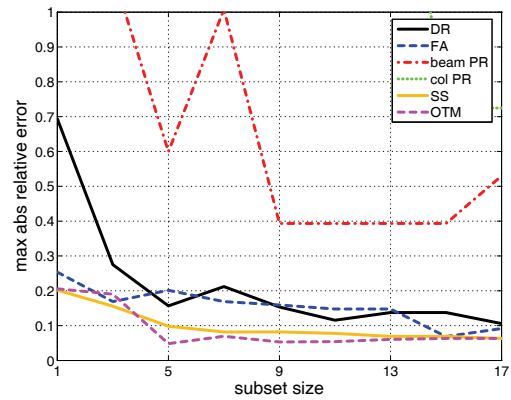
(c) 4-story, mean error



(d) 4-story, max error

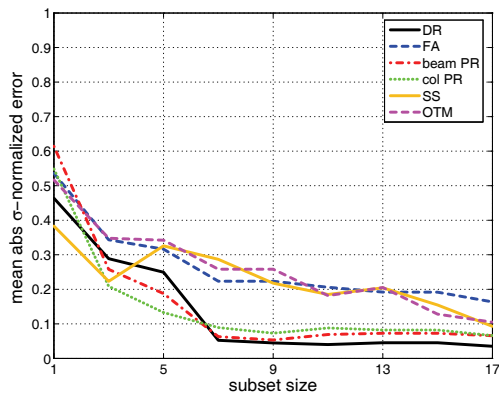


(e) 8-story, mean error

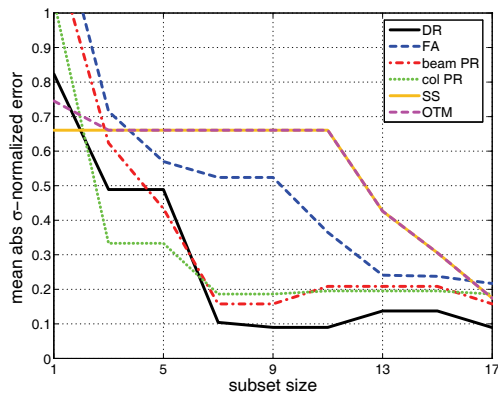


(f) 8-story, max error

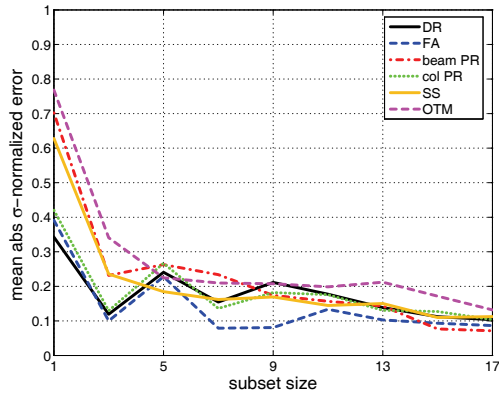
Figure D-43 Mean and maximum absolute relative error for different EDP types over all 3 scale factors when selecting subsets within a FEMA P-695 stripe by matching 50% local S_a values to estimate the 50% response (Method B).



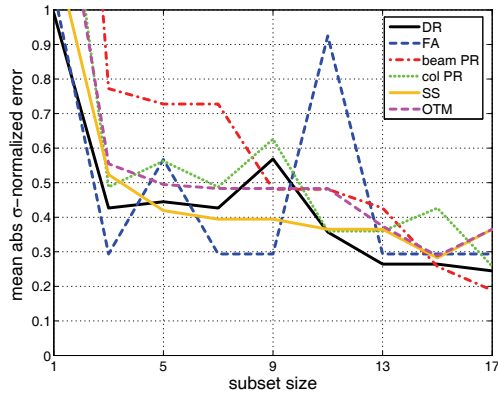
(a) 2-story, mean error



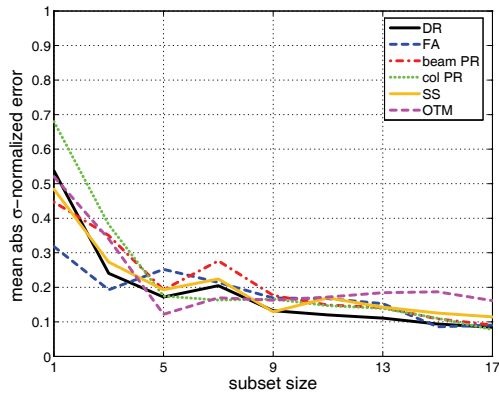
(b) 2-story, max error



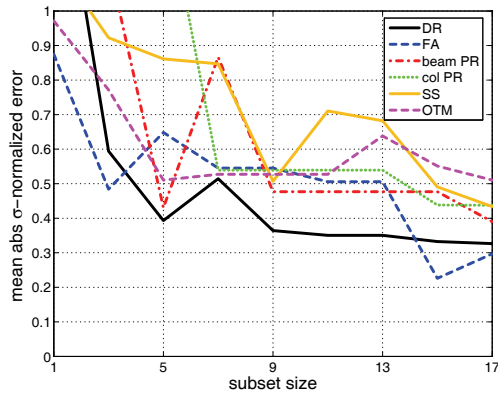
(c) 4-story, mean error



(d) 4-story, max error



(e) 8-story, mean error



(f) 8-story, max error

Figure D-44 Mean and maximum absolute σ -normalized error for different EDP types over all 3 scale factors when selecting subsets within a FEMA P-695 stripe by matching 50% local S_a values to estimate the 50% response (Method B).

Table D-3 Subset Estimation Errors for the 50% EDP Response of the 2-Story RCMF Using Selection Method B on FEMA-P695 Stripes

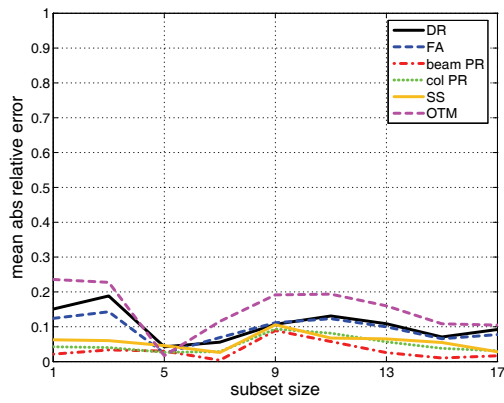
EDP	SF	50% EDP Relative Error								
		Subset Size								
		1	3	5	7	9	11	13	15	17
<i>DR1</i>	0.5	2%	-17%	-17%	0%	0%	0%	0%	0%	0%
	1	34%	-14%	-14%	-4%	-4%	-4%	-4%	-4%	-3%
	2	18%	8%	3%	3%	3%	-1%	-1%	-1%	-1%
<i>DR2</i>	0.5	5%	-18%	-18%	4%	1%	1%	1%	1%	1%
	1	28%	-7%	-7%	1%	1%	1%	1%	1%	1%
	2	43%	-6%	-1%	-1%	-1%	-6%	-9%	-9%	-6%
<i>DRmax</i>	0.5	2%	-17%	-17%	0%	0%	0%	0%	0%	0%
	1	34%	-14%	-14%	-4%	-4%	-4%	-4%	-4%	-3%
	2	18%	8%	3%	3%	3%	-1%	-1%	-1%	-1%
<i>FA1</i>	0.5	-7%	-7%	-11%	-7%	-7%	-7%	-7%	-7%	-5%
	1	29%	11%	11%	11%	11%	8%	5%	5%	3%
	2	8%	8%	8%	5%	5%	5%	5%	5%	3%
<i>FA2</i>	0.5	7%	-19%	-7%	5%	5%	5%	5%	5%	5%
	1	8%	4%	4%	4%	4%	4%	4%	4%	4%
	2	19%	2%	4%	4%	4%	4%	4%	4%	4%
<i>FAMAX</i>	0.5	5%	-21%	-9%	3%	3%	3%	3%	3%	3%
	1	10%	3%	3%	3%	3%	3%	3%	3%	3%
	2	14%	4%	11%	4%	4%	4%	4%	4%	4%
<i>BPR1</i>	0.5	-1%	-17%	-17%	-1%	-1%	-1%	-1%	-1%	-1%
	1	42%	-19%	-19%	-1%	-1%	-1%	-1%	-1%	0%
	2	35%	-3%	1%	1%	1%	-3%	-4%	-4%	-4%
<i>BPR2</i>	0.5	8%	-9%	-6%	1%	0%	0%	0%	0%	1%
	1	324%	31%	-7%	31%	28%	28%	28%	28%	28%
	2	71%	-29%	-17%	-17%	-17%	-23%	-23%	-23%	-17%
<i>CPR1</i>	0.5	-28%	-28%	-28%	-15%	-15%	-15%	-15%	-15%	-15%
	1	58%	-27%	-27%	-15%	-15%	-16%	-16%	-16%	-15%
	2	16%	9%	3%	3%	3%	2%	1%	-1%	-1%
<i>CPR2</i>	0.5	22%	22%	-1%	-1%	-5%	-5%	-5%	-5%	-1%
	1	125%	-18%	-18%	-17%	0%	0%	0%	0%	0%
	2	68%	-10%	-2%	-2%	-2%	-10%	-10%	-10%	-6%
<i>SS1</i>	0.5	-3%	-3%	-3%	-2%	-2%	-2%	-2%	-2%	0%
	1	0%	-1%	-1%	0%	0%	-1%	-1%	-1%	-1%
	2	-2%	0%	-2%	-2%	0%	1%	1%	1%	0%
<i>SS2</i>	0.5	11%	-2%	-2%	-1%	-1%	-1%	-1%	-1%	-1%
	1	9%	9%	9%	9%	9%	9%	6%	2%	2%
	2	6%	-4%	6%	6%	6%	0%	-4%	-4%	-2%
<i>OTM1</i>	0.5	4%	-13%	-13%	0%	0%	0%	0%	0%	1%
	1	7%	6%	3%	3%	3%	3%	3%	1%	1%
	2	3%	0%	0%	0%	0%	0%	-1%	-1%	-1%
<i>OTM2</i>	0.5	11%	-2%	-2%	-1%	-1%	-1%	-1%	-1%	-1%
	1	9%	9%	9%	9%	9%	9%	6%	2%	2%
	2	6%	-4%	6%	6%	6%	0%	-4%	-4%	-2%

Table D-4 Subset Estimation Errors for the 50% EDP Response of the 4-Story RCMF Using Selection Method B on FEMA-P695 Stripes

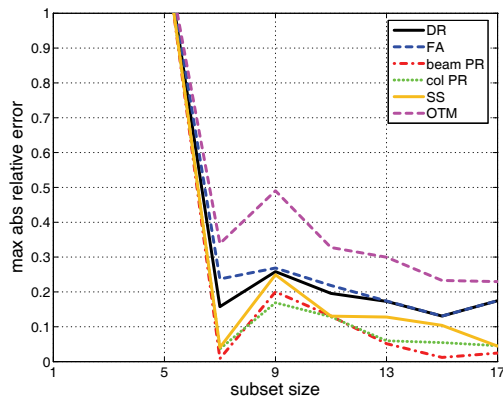
EDP	SF	50% EDP Relative Error								
		Subset Size								
		1	3	5	7	9	11	13	15	17
<i>DR1</i>	0.5	-3%	-3%	-9%	-3%	-3%	-3%	-3%	-3%	-3%
	1	-3%	2%	-3%	1%	1%	-1%	-1%	-1%	-1%
	2	-9%	-9%	12%	12%	27%	12%	12%	12%	10%
<i>DR2</i>	0.5	14%	-1%	-7%	-1%	-7%	-7%	-7%	-5%	-5%
	1	4%	-1%	-1%	0%	-1%	-1%	0%	0%	0%
	2	-4%	-4%	19%	19%	15%	12%	12%	12%	8%
<i>DR3</i>	0.5	17%	-1%	-7%	-1%	-7%	-7%	-1%	0%	-1%
	1	14%	-2%	-3%	-2%	-3%	-3%	-2%	0%	0%
	2	11%	11%	11%	11%	8%	8%	8%	8%	8%
<i>DR4</i>	0.5	16%	1%	-11%	-4%	-5%	-5%	-4%	-2%	-4%
	1	16%	0%	-2%	-2%	-2%	-2%	0%	0%	0%
	2	22%	22%	22%	22%	18%	18%	11%	5%	9%
<i>DRmax</i>	0.5	6%	-1%	-10%	-1%	-5%	-5%	-5%	-5%	-5%
	1	3%	-2%	-2%	0%	-1%	-1%	-1%	-1%	-1%
	2	-11%	-11%	10%	10%	15%	10%	10%	10%	0%
<i>FA1</i>	0.5	8%	2%	-14%	2%	2%	2%	2%	2%	1%
	1	7%	0%	0%	2%	2%	2%	2%	2%	2%
	2	7%	-3%	-3%	1%	1%	3%	1%	1%	1%
<i>FA2</i>	0.5	-4%	-4%	-5%	-4%	-4%	-4%	-4%	-4%	-4%
	1	-3%	4%	2%	4%	4%	5%	4%	4%	4%
	2	-15%	-7%	-7%	1%	1%	2%	1%	1%	1%
<i>FA3</i>	0.5	10%	-5%	-7%	-5%	-5%	-5%	-5%	-1%	-1%
	1	-1%	-1%	-7%	-1%	-1%	-1%	-1%	-1%	-1%
	2	0%	6%	0%	6%	6%	19%	6%	6%	6%
<i>FA4</i>	0.5	18%	0%	-14%	0%	0%	0%	0%	0%	-4%
	1	18%	-1%	-2%	-1%	-1%	-1%	3%	3%	0%
	2	-5%	2%	-5%	2%	2%	2%	1%	-2%	1%
<i>FAmx</i>	0.5	18%	0%	-14%	0%	0%	0%	0%	0%	-4%
	1	18%	-1%	-2%	-1%	-1%	-1%	3%	3%	0%
	2	6%	-3%	-3%	-1%	-1%	1%	-1%	-1%	1%
<i>BPR1</i>	0.5	5%	1%	-22%	1%	-12%	-12%	-12%	-12%	-12%
	1	0%	0%	-1%	0%	0%	0%	0%	0%	0%
	2	-12%	-12%	9%	9%	19%	9%	13%	13%	9%
<i>BPR2</i>	0.5	77%	12%	-2%	12%	-2%	-2%	2%	2%	2%
	1	6%	-11%	-12%	-11%	-12%	-12%	-11%	-3%	-3%
	2	0%	0%	2%	2%	2%	2%	2%	2%	2%
<i>BPR3</i>	0.5	159%	32%	-9%	20%	-9%	-9%	-6%	6%	-5%
	1	58%	-2%	-19%	-19%	-28%	-28%	-19%	-2%	-2%
	2	28%	40%	40%	40%	28%	28%	25%	2%	3%
<i>BPR4</i>	0.5	7%	1%	-3%	-1%	-1%	-1%	-1%	-1%	-1%
	1	9%	0%	-1%	0%	0%	0%	0%	0%	0%
	2	488%	488%	460%	460%	-4%	-4%	-4%	-5%	-4%

Table D-4 Subset Estimation Errors for the 50% EDP Response of the 4-Story RCMF Using Selection Method B on FEMA-P695 Stripes (continued)

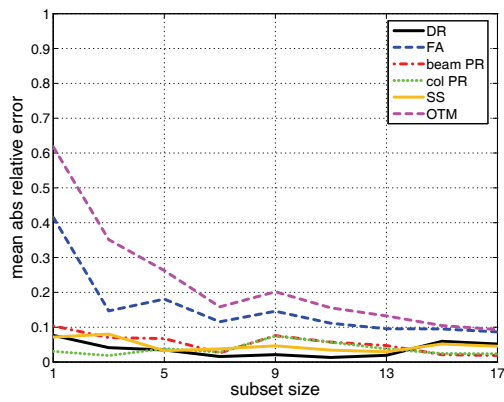
EDP	SF	50% EDP Relative Error								
		Subset Size								
		1	3	5	7	9	11	13	15	17
CPR1	0.5	-48%	-5%	-48%	-5%	-5%	-30%	-30%	-5%	-5%
	1	-13%	-1%	-1%	-1%	-1%	-13%	-3%	-3%	-3%
	2	-14%	-14%	19%	19%	51%	19%	19%	34%	19%
CPR2	0.5	2%	1%	-10%	0%	-8%	-8%	-8%	-8%	-8%
	1	3%	0%	-3%	0%	0%	0%	0%	0%	0%
	2	-42%	-42%	-42%	-42%	-27%	-42%	-27%	73%	-27%
CPR3	0.5	10%	-1%	-8%	-1%	-8%	-8%	-2%	-1%	-1%
	1	2%	2%	26%	26%	16%	2%	2%	2%	2%
	2	16%	16%	23%	23%	16%	10%	10%	10%	10%
CPR4	0.5	14%	0%	-5%	-2%	-2%	-2%	-2%	-2%	-2%
	1	100%	24%	-6%	-1%	7%	7%	7%	7%	7%
	2	84%	84%	84%	84%	44%	44%	21%	1%	21%
SS1	0.5	-2%	-1%	-2%	-2%	-2%	-2%	-2%	-2%	-2%
	1	7%	4%	3%	3%	3%	-1%	-1%	-1%	-1%
	2	0%	0%	0%	0%	0%	0%	0%	0%	0%
SS2	0.5	11%	2%	-7%	2%	-7%	-7%	-7%	-4%	-4%
	1	8%	1%	1%	1%	1%	0%	1%	1%	1%
	2	5%	1%	1%	1%	1%	1%	1%	1%	1%
SS3	0.5	8%	8%	-4%	5%	-4%	-4%	-4%	-1%	-3%
	1	8%	2%	0%	0%	-1%	-1%	0%	0%	0%
	2	9%	4%	1%	1%	0%	0%	0%	0%	1%
SS4	0.5	16%	11%	-10%	-9%	-8%	-8%	-8%	-4%	-8%
	1	18%	-1%	-3%	-1%	2%	2%	4%	4%	2%
	2	-7%	-8%	-7%	-7%	-7%	-5%	-5%	-5%	-2%
OTM1	0.5	10%	9%	-5%	4%	-5%	-5%	-5%	-3%	-5%
	1	10%	3%	1%	2%	1%	1%	2%	2%	1%
	2	1%	1%	1%	1%	1%	1%	1%	1%	0%
OTM2	0.5	13%	12%	-4%	3%	-4%	-4%	-4%	-2%	-4%
	1	12%	2%	0%	1%	0%	0%	1%	1%	0%
	2	6%	4%	3%	3%	3%	3%	1%	1%	1%
OTM3	0.5	17%	15%	-3%	-1%	-3%	-3%	-3%	-1%	-3%
	1	15%	-1%	-1%	-1%	1%	1%	2%	2%	1%
	2	0%	-1%	0%	0%	0%	0%	-1%	-1%	0%
OTM4	0.5	16%	11%	-10%	-9%	-8%	-8%	-8%	-4%	-8%
	1	18%	-1%	-3%	-1%	2%	2%	4%	4%	2%
	2	-7%	-8%	-7%	-7%	-7%	-5%	-5%	-5%	-2%



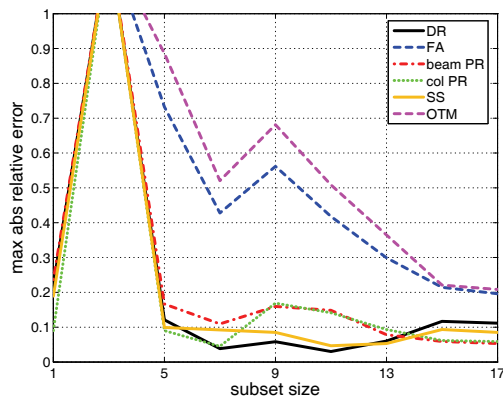
(a) 2-story, mean error



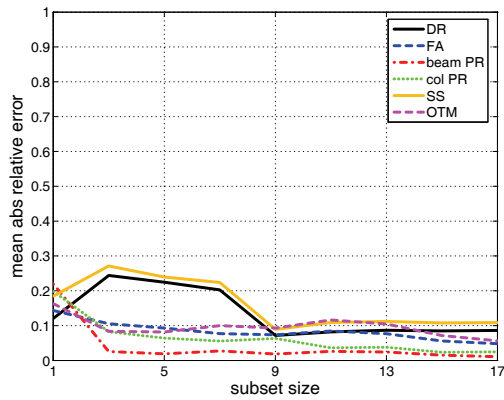
(b) 2-story, max error



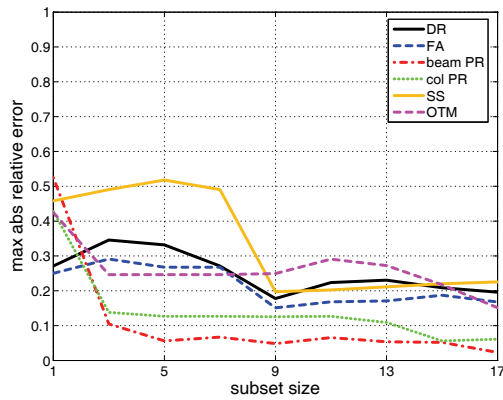
(c) 4-story, mean error



(d) 4-story, max error

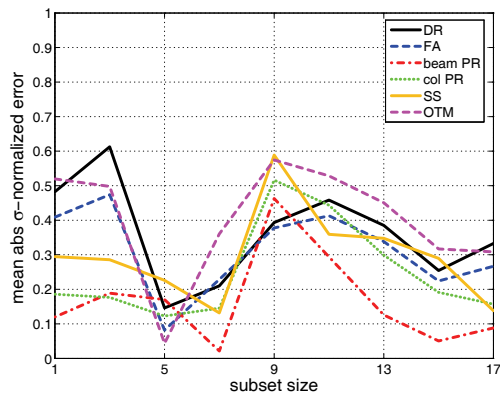


(e) 8-story, mean error

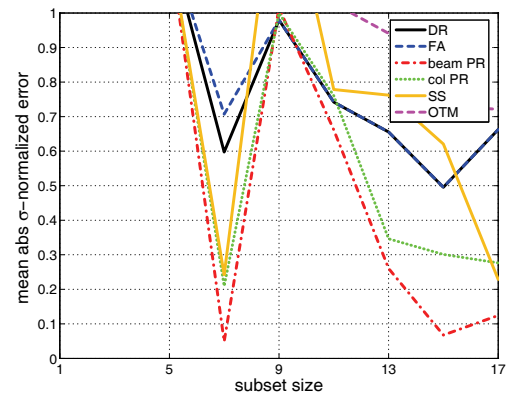


(f) 8-story, max error

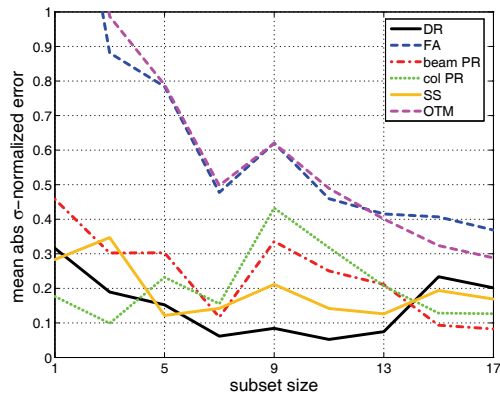
Figure D-45 Mean and maximum absolute relative error for different EDP types over all 3 scale factors when selecting subsets within a FEMA P-695 stripe by matching 84% local S_a values to estimate the 84% response (Method B).



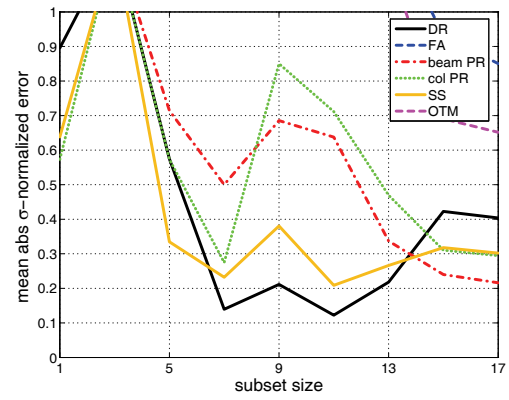
(a) 2-story, mean error



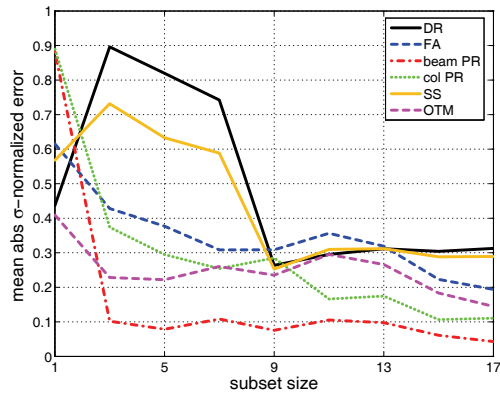
(b) 2-story, max error



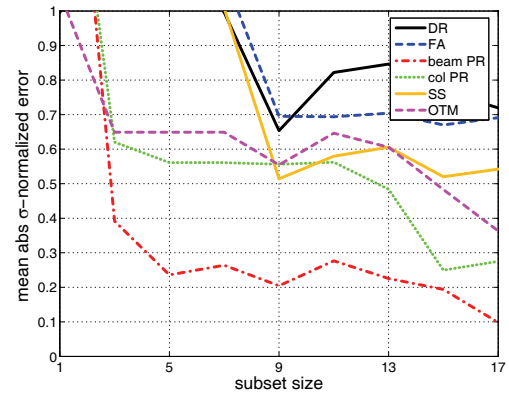
(c) 4-story, mean error



(d) 4-story, max error



(e) 8-story, mean error



(f) 8-story, max error

Figure D-46 Mean and maximum absolute σ -normalized error for different EDP types over all 3 scale factors when selecting subsets within a FEMA P-695 stripe by matching 84% local S_a values to estimate the 84% response (Method B).

Table D-5 Subset Estimation Errors for the 84% EDP Response of the 2-Story RCMF Using Selection Method B on FEMA-P695 Stripes

EDP	SF	84% EDP relative error								
		subset size								
		1	3	5	7	9	11	13	15	17
<i>DR1</i>	0.5	30%	30%	-1%	-1%	6%	18%	12%	5%	7%
	1	0%	-8%	-8%	0%	0%	1%	4%	3%	4%
	2				16%	26%	20%	17%	13%	17%
<i>DR2</i>	0.5	19%	19%	1%	1%	6%	10%	7%	4%	2%
	1	0%	0%	0%	0%	2%	3%	3%	3%	3%
	2				24%	27%	22%	17%	12%	13%
<i>DRmax</i>	0.5	30%	30%	-1%	-1%	6%	18%	12%	5%	7%
	1	0%	-8%	-8%	0%	0%	1%	4%	3%	4%
	2				16%	26%	20%	17%	13%	17%
<i>FA1</i>	0.5	0%	0%	0%	0%	0%	1%	2%	1%	0%
	1	4%	-7%	-6%	-1%	6%	3%	1%	-1%	-2%
	2				0%	20%	13%	5%	-1%	-2%
<i>FA2</i>	0.5	7%	6%	4%	4%	6%	6%	6%	5%	4%
	1	-2%	-2%	-2%	-1%	5%	5%	5%	5%	5%
	2				-4%	17%	13%	6%	1%	0%
<i>FAMAX</i>	0.5	7%	6%	4%	4%	6%	6%	6%	5%	4%
	1	-6%	-6%	-5%	0%	1%	1%	1%	1%	0%
	2				-4%	25%	13%	13%	10%	4%
<i>BPR1</i>	0.5	42%	42%	0%	0%	8%	23%	13%	5%	4%
	1	5%	-3%	-3%	0%	1%	2%	5%	4%	5%
	2				34%	49%	33%	30%	23%	23%
<i>BPR2</i>	0.5	2%	2%	2%	2%	2%	3%	2%	1%	1%
	1	-1%	-1%	-1%	-1%	0%	2%	7%	2%	7%
	2				49%	50%	42%	26%	12%	14%
<i>CPR1</i>	0.5	68%	68%	-2%	-2%	14%	42%	26%	10%	14%
	1	0%	-11%	-11%	0%	1%	3%	5%	4%	5%
	2				14%	36%	22%	17%	12%	17%
<i>CPR2</i>	0.5	84%	84%	6%	6%	36%	71%	39%	16%	18%
	1	-1%	-1%	-1%	-1%	6%	6%	6%	6%	6%
	2				47%	52%	41%	28%	15%	18%
<i>SS1</i>	0.5	5%	2%	0%	0%	1%	2%	1%	0%	0%
	1	1%	-2%	-2%	0%	0%	0%	1%	1%	1%
	2	-5%	-3%	-1%	-1%	0%	0%	0%	0%	0%
<i>SS2</i>	0.5	4%	0%	-6%	0%	1%	1%	0%	0%	1%
	1	-4%	-4%	-4%	-1%	1%	0%	0%	0%	0%
	2	1%	-1%	-4%	-4%	0%	0%	0%	0%	-1%
<i>OTM1</i>	0.5	7%	6%	1%	1%	2%	4%	2%	1%	1%
	1	3%	2%	0%	0%	1%	1%	0%	0%	0%
	2	3%	3%	3%	-1%	3%	2%	1%	1%	0%
<i>OTM2</i>	0.5	4%	0%	-6%	0%	1%	1%	0%	0%	1%
	1	-4%	-4%	-4%	-1%	1%	0%	0%	0%	0%
	2	1%	-1%	-4%	-4%	0%	0%	0%	0%	-1%

*Empty cells show where the estimated EDP is indeterminate (global collapse).

Table D-6 Subset Estimation Errors for the 84% EDP Response of the 4-Story RCMF Using Selection Method B on FEMA-P695 Stripes

EDP	SF	84% EDP relative error								
		subset size								
		1	3	5	7	9	11	13	15	17
<i>DR1</i>	0.5	-3%	-3%	-3%	-3%	-3%	-3%	-3%	7%	5%
	1	-19%	-12%	-12%	-1%	3%	-1%	-1%	7%	6%
	2	0%		0%	0%	1%	0%	1%	8%	7%
<i>DR2</i>	0.5	-1%	1%	-1%	-1%	0%	0%	0%	1%	1%
	1	1%	1%	1%	0%	0%	0%	0%	1%	1%
	2	22%		4%	4%	6%	3%	6%	12%	11%
<i>DR3</i>	0.5	4%	11%	4%	-1%	1%	-1%	-2%	4%	3%
	1	28%	28%	19%	11%	15%	10%	5%	11%	9%
	2	95%		40%	37%	38%	37%	29%	21%	20%
<i>DR4</i>	0.5	-1%	3%	0%	3%	3%	3%	3%	4%	4%
	1	43%	43%	19%	2%	10%	2%	9%	2%	2%
	2	172%		73%	43%	56%	42%	30%	18%	18%
<i>DRmax</i>	0.5	-4%	-2%	-4%	-4%	-2%	-2%	-2%	4%	3%
	1	0%	0%	0%	0%	1%	0%	-1%	3%	3%
	2	28%		3%	3%	5%	3%	5%	17%	16%
<i>FA1</i>	0.5	-10%	2%	2%	2%	8%	6%	6%	6%	5%
	1	24%	24%	17%	1%	16%	15%	8%	1%	1%
	2	1%		1%	1%	2%	1%	0%	0%	1%
<i>FA2</i>	0.5	-8%	-2%	-8%	0%	1%	-1%	6%	4%	3%
	1	0%	0%	-1%	0%	4%	2%	1%	0%	0%
	2	-19%		-11%	-11%	15%	10%	6%	2%	1%
<i>FA3</i>	0.5	-3%	2%	-3%	-3%	-1%	-3%	1%	2%	2%
	1	-1%	-1%	-1%	1%	6%	2%	1%	1%	1%
	2	9%		9%	-4%	12%	9%	5%	1%	1%
<i>FA4</i>	0.5	-1%	4%	-1%	4%	5%	4%	5%	6%	6%
	1	0%	0%	-5%	0%	4%	2%	1%	0%	-1%
	2	5%		5%	5%	17%	14%	9%	5%	4%
<i>FAmix</i>	0.5	-1%	4%	-1%	4%	5%	4%	5%	6%	6%
	1	9%	9%	3%	3%	6%	3%	3%	3%	2%
	2	-1%		-1%	-1%	8%	3%	1%	-1%	1%
<i>BPR1</i>	0.5	-4%	-4%	-4%	-9%	-3%	-5%	-3%	9%	8%
	1	-19%	-14%	-10%	-4%	-3%	-4%	-2%	3%	2%
	2	9%		-1%	-1%	3%	-1%	3%	9%	9%
<i>BPR2</i>	0.5	4%	10%	4%	-1%	1%	-1%	-1%	4%	3%
	1	10%	7%	7%	-1%	3%	-1%	-3%	4%	3%
	2	67%		26%	26%	27%	26%	15%	14%	13%
<i>BPR3</i>	0.5	37%	37%	0%	-8%	-4%	-9%	6%	12%	10%
	1	86%	86%	31%	7%	18%	7%	19%	7%	6%
	2	167%		89%	52%	68%	51%	36%	22%	21%
<i>BPR4</i>	0.5	0%	1%	0%	1%	1%	1%	1%	1%	1%
	1	185%	185%	5%	2%	3%	2%	3%	2%	1%
	2	292%		172%	77%	119%	76%	63%	51%	49%

Table D-6 Subset Estimation Errors for the 84% EDP Response of the 4-Story RCMF Using Selection Method B on FEMA-P695 Stripes (continued)

EDP	SF	84% EDP relative error								
		subset size								
		1	3	5	7	9	11	13	15	17
CPR1	0.5	-30%	-31%	-30%	-30%	-15%	-22%	-14%	0%	-1%
	1	-54%	-25%	-25%	-6%	7%	-7%	-11%	23%	19%
	2	-9%		0%	0%	1%	0%	1%	10%	9%
CPR2	0.5	0%	0%	-1%	-4%	0%	-1%	0%	2%	2%
	1	0%	0%	-1%	-1%	1%	0%	1%	3%	3%
	2	-14%		-14%	-14%	23%	-3%	36%	72%	69%
CPR3	0.5	0%	5%	0%	-4%	-2%	-4%	-6%	5%	4%
	1	9%	-33%	9%	9%	10%	8%	-13%	11%	11%
	2	1%		1%	0%	0%	-1%	0%	13%	11%
CPR4	0.5	-3%	0%	-3%	0%	1%	0%	1%	2%	1%
	1	390%	390%	162%	12%	78%	12%	18%	12%	10%
	2	245%		118%	66%	89%	65%	48%	32%	32%
SS1	0.5	-1%	-1%	-1%	-1%	0%	-1%	1%	3%	3%
	1	0%	0%	0%	0%	3%	1%	1%	4%	4%
	2	-1%	-1%	-1%	-1%	-1%	-1%	1%	2%	2%
SS2	0.5	0%	0%	0%	0%	0%	0%	0%	1%	1%
	1	2%	2%	2%	1%	2%	1%	1%	1%	1%
	2	2%	0%	2%	2%	5%	2%	2%	2%	1%
SS3	0.5	4%	6%	4%	2%	3%	2%	3%	4%	4%
	1	10%	10%	6%	2%	4%	2%	3%	2%	2%
	2	4%	-2%	0%	0%	0%	0%	0%	0%	0%
SS4	0.5	-2%	-1%	-1%	6%	7%	6%	7%	6%	6%
	1	3%	3%	0%	0%	0%	0%	0%	0%	0%
	2	5%	5%	0%	2%	5%	5%	3%	2%	1%
OTM1	0.5	2%	5%	2%	2%	3%	2%	1%	2%	2%
	1	3%	3%	3%	3%	3%	2%	3%	3%	2%
	2	4%	0%	0%	0%	1%	1%	0%	0%	0%
OTM2	0.5	2%	4%	2%	1%	1%	1%	1%	2%	2%
	1	4%	4%	3%	1%	2%	1%	2%	1%	1%
	2	6%	0%	0%	0%	0%	0%	0%	0%	0%
OTM3	0.5	0%	0%	0%	0%	0%	0%	0%	0%	0%
	1	3%	3%	0%	0%	1%	0%	1%	0%	0%
	2	7%	7%	-1%	-2%	2%	1%	0%	-1%	-1%
OTM4	0.5	-2%	-1%	-1%	6%	7%	6%	7%	6%	6%
	1	3%	3%	0%	0%	0%	0%	0%	0%	0%
	2	5%	5%	0%	2%	5%	5%	3%	2%	1%

*Empty cells show where the estimated EDP is indeterminate (global collapse).

D.2.4 Subset Selection on S_a Scaling

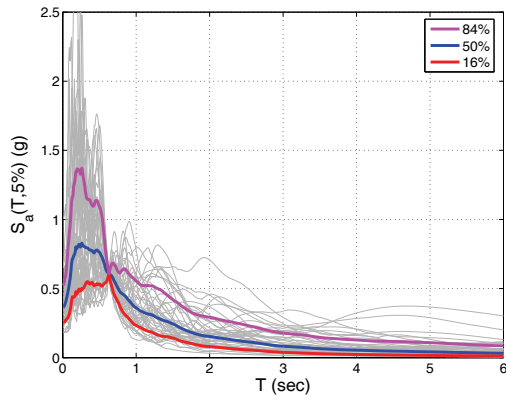
Selection Method B was also used to select ground motion records scaled to common values of pseudo-spectral acceleration (also termed S_a scaling). As with FEMA P-

695 scaling, “optimal” record subsets were sought that allow accurate estimation of the 50% or the 84% EDP response of the entire set of 44 records at a prescribed S_a level.

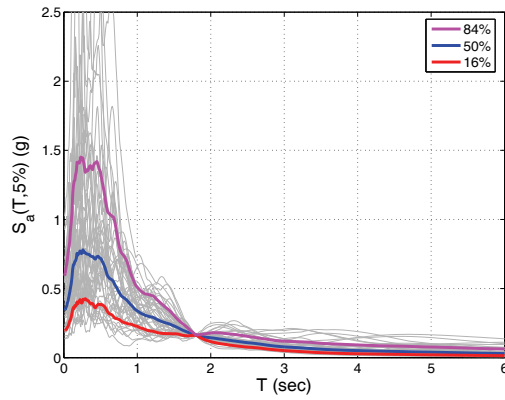
To further aid in understanding this technique, Figure D-47 shows the shape of the elastic spectra after scaling to a common S_a value, as well as the 16, 50, and 84% spectra. The common value of pseudo-spectral acceleration was determined as the median value of $S_a(T_1)$ obtained using the FEMA P-695 ground motions after scaling by scale factors of 0.5, 1.0, and 2.0 (as indicated in Figure D-1).

Figures D-48 and D-49 and Tables D-7 through D-10 present the relative absolute errors in the estimation of the 50% and 84% EDP response. In all cases, there is a very satisfying monotonic trend in the errors with subset size increase, while the mean errors are quite low for almost all EDPs. The maxima show again some isolated cases of bad performance, nevertheless the overall verdict is positive and marks quite an improvement over the FEMA P-695 scaling results presented earlier. In most cases, the results are better for the shorter buildings, especially for the 2-story.

Surprisingly, the median estimate of the beam and column plastic hinge rotations often shows higher mean and maximum errors than their 84% estimate. This goes contrary to intuition but can be attributed to the effect of the multiple near-zero response values (see also Section D.3.1). In essence, these near-zero values influence the median a lot more than they influence the 84%, partly due to the second component involved in the multipart estimation formula (Equation D-8) that effectively removes most of these near-zero values. This protective effect can be extended partly to the median as well if plastic hinge rotations lower than, say, 0.0004 rad (practically of no engineering significance), are removed from the sample when any significantly higher values (e.g., 10 times larger) are present. This may lead to an overestimation of the median at lower intensities but will generally provide a conservative estimate.

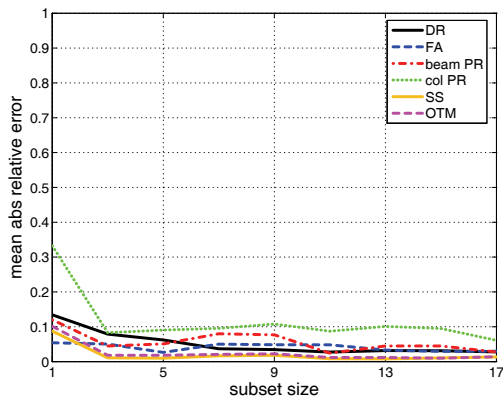


(e) SF=1.0, 2-story

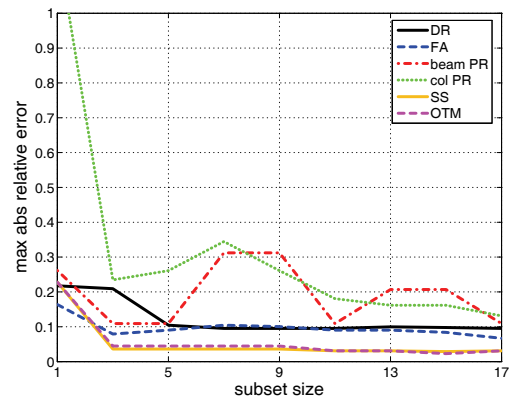


(f) SF=1.0, 8-story

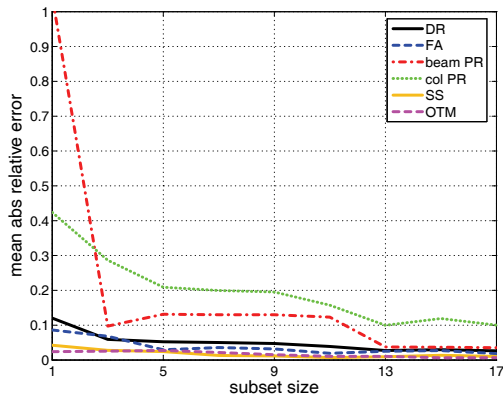
Figure D-47 The $S_a(T)$ individual spectra and their 16/50/84 summaries for the 44 ground motion records scaled to the median $S_a(T_1)$ value of the FEMA P-695 normalized clouds for the 2- and 8-story RCMFs. The shapes shown are invariant with changes in scale factor.



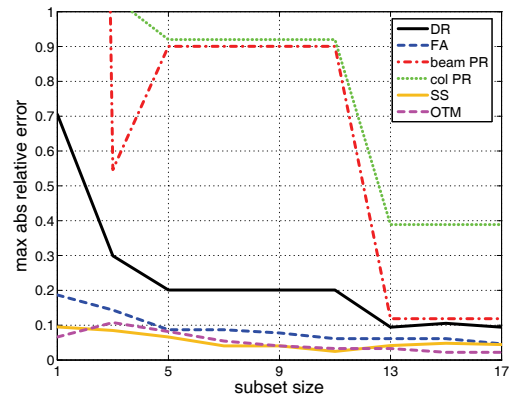
(a) 2-story, mean error



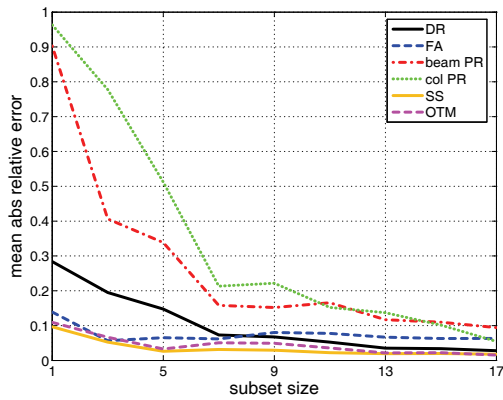
(b) 2-story, max error



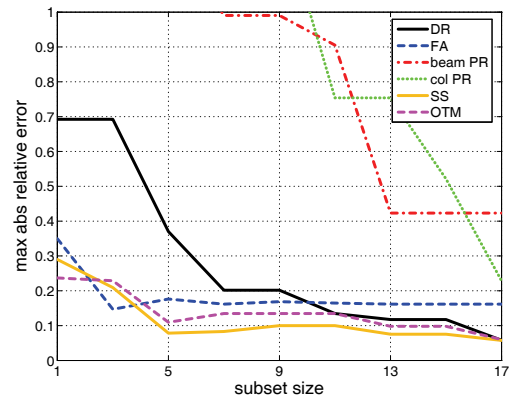
(c) 4-story, mean error



(d) 4-story, max error

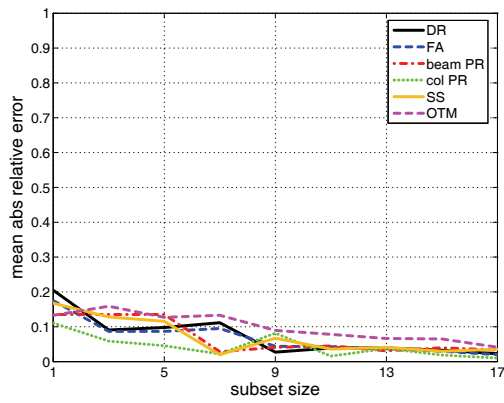


(e) 8-story, mean error

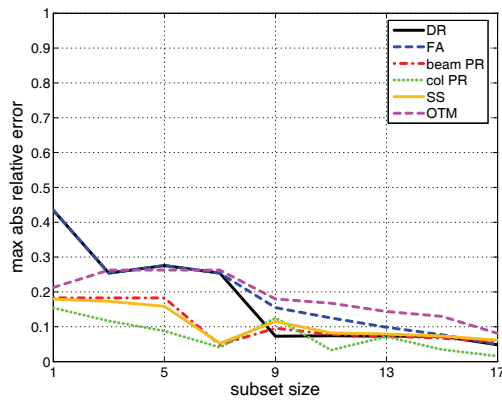


(f) 8-story, max error

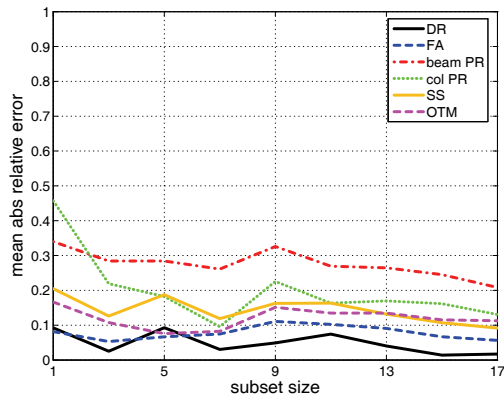
Figure D-48 Mean and maximum absolute relative error for different EDP types over all 3 scale factors when selecting subsets within an S_a stripe by matching 50% local S_a values to estimate the 50% response.



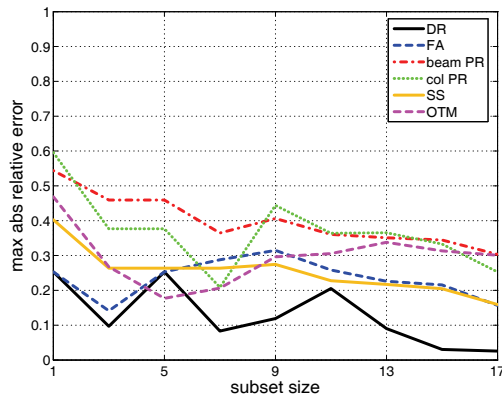
(a) 2-story, mean error



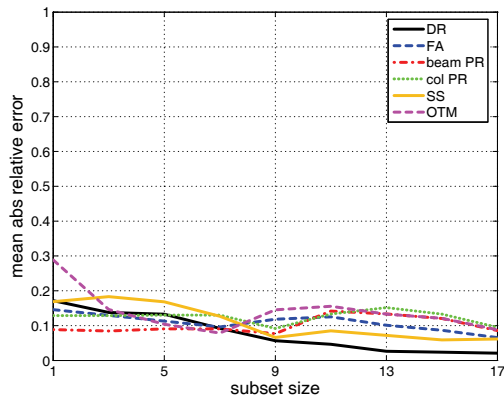
(b) 2-story, max error



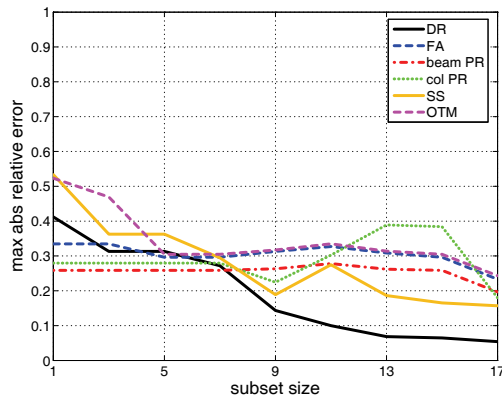
(c) 4-story, mean error



(d) 4-story, max error



(e) 8-story, mean error



(f) 8-story, max error

Figure D-49 Mean and maximum absolute relative error for different EDP types over all 3 scale factors when selecting subsets within an S_a stripe by matching 84% local S_a values to estimate the 84% response.

Table D-7 Subset Estimation Errors for the 50% EDP Response of the 2-Story RCMF Using Selection Method B on S_a Stripes

EDP	SF	50% EDP Relative Error								
		Subset Size								
		1	3	5	7	9	11	13	15	17
<i>DR1</i>	0.5	-9%	-6%	-4%	-2%	0%	0%	0%	0%	0%
	1	-22%	2%	6%	4%	4%	2%	-2%	-2%	2%
	2	21%	21%	10%	-10%	-10%	-10%	-10%	-10%	-10%
<i>DR2</i>	0.5	-6%	-6%	-5%	-2%	-2%	0%	0%	0%	-1%
	1	-4%	-1%	3%	-1%	-1%	-1%	-1%	-1%	-1%
	2	7%	7%	7%	-1%	-1%	-1%	-4%	-4%	-1%
<i>DRmax</i>	0.5	-9%	-6%	-4%	-2%	0%	0%	0%	0%	0%
	1	-22%	2%	6%	4%	4%	2%	-2%	-2%	2%
	2	21%	21%	10%	-10%	-10%	-10%	-10%	-10%	-10%
<i>FA1</i>	0.5	3%	-6%	-9%	-10%	-10%	-9%	-9%	-8%	-6%
	1	16%	1%	1%	-2%	-2%	-5%	-2%	-2%	-2%
	2	-3%	-3%	-3%	-8%	-8%	-8%	-3%	-3%	-3%
<i>FA2</i>	0.5	-8%	-8%	0%	-2%	-4%	-2%	-2%	-2%	-2%
	1	-1%	-5%	-1%	-5%	-3%	-3%	-1%	-1%	-1%
	2	6%	6%	6%	-3%	-3%	-3%	-3%	-2%	-3%
<i>FAMAX</i>	0.5	-8%	-8%	0%	-2%	-4%	-2%	-2%	-2%	-2%
	1	-1%	-6%	-1%	-6%	-4%	-4%	-1%	-1%	-1%
	2	2%	2%	2%	-7%	-7%	-7%	-7%	-5%	-7%
<i>BPR1</i>	0.5	5%	5%	0%	-31%	-31%	0%	0%	0%	-1%
	1	-21%	1%	6%	2%	1%	1%	-1%	-1%	1%
	2	7%	7%	7%	-1%	-1%	-2%	-4%	-4%	-2%
<i>BPR2</i>	0.5	-3%	-3%	-3%	-1%	-1%	0%	0%	0%	-1%
	1	26%	-1%	4%	-1%	-1%	-1%	-1%	-1%	1%
	2	-11%	-11%	-11%	-11%	-11%	-11%	-21%	-21%	-11%
<i>CPR1</i>	0.5	15%	15%	-26%	-34%	-26%	-18%	-11%	-11%	-11%
	1	-38%	-1%	10%	7%	7%	-1%	-4%	-4%	-1%
	2	23%	23%	7%	-13%	-13%	-13%	-15%	-14%	-13%
<i>CPR2</i>	0.5	120%	9%	8%	0%	0%	3%	3%	0%	0%
	1	2%	0%	2%	0%	-16%	-16%	-16%	-16%	-10%
	2	2%	2%	2%	2%	2%	-2%	-12%	-12%	-2%
<i>SS1</i>	0.5	7%	2%	-1%	-2%	-2%	-1%	1%	-1%	-1%
	1	0%	0%	0%	1%	1%	0%	0%	0%	0%
	2	2%	-1%	-1%	-1%	-1%	0%	0%	0%	1%
<i>SS2</i>	0.5	23%	0%	0%	-2%	-3%	-3%	-3%	-2%	-3%
	1	16%	0%	0%	0%	0%	0%	0%	0%	0%
	2	-4%	-4%	-4%	-4%	-4%	0%	0%	-3%	-3%
<i>OTM1</i>	0.5	9%	3%	3%	-3%	-3%	0%	0%	0%	-1%
	1	6%	1%	1%	0%	0%	0%	0%	0%	0%
	2	-3%	-2%	-2%	-3%	-3%	-2%	-2%	-2%	-2%
<i>OTM2</i>	0.5	23%	0%	0%	-2%	-3%	-3%	-3%	-2%	-3%
	1	16%	0%	0%	0%	0%	0%	0%	0%	0%
	2	-4%	-4%	-4%	-4%	-4%	-1%	-1%	-1%	-2%

Table D-8 Subset Estimation Errors for the 84% EDP Response of the 2-Story RCMF Using Selection Method B on S_a Stripes

EDP	SF	84% EDP Relative Error								
		Subset Size								
		1	3	5	7	9	11	13	15	17
<i>DR1</i>	0.5	-7%	0%	0%	-6%	1%	2%	0%	0%	-1%
	1	11%	-2%	-2%	-2%	0%	-2%	-4%	-2%	-1%
	2	43%	-25%	-28%	-25%	-7%	-7%	-7%	-7%	-5%
<i>DR2</i>	0.5	-10%	-1%	0%	-1%	-1%	-1%	0%	0%	0%
	1	-1%	-1%	0%	0%	2%	0%	0%	0%	0%
	2	33%	-22%	-23%	-23%	-15%	-13%	-10%	-8%	-5%
<i>DRmax</i>	0.5	-7%	0%	0%	-6%	1%	2%	0%	0%	-1%
	1	11%	-2%	-2%	-2%	0%	-2%	-4%	-2%	-1%
	2	43%	-25%	-28%	-25%	-7%	-7%	-7%	-7%	-5%
<i>FA1</i>	0.5	-10%	-10%	-10%	-2%	-1%	-4%	-2%	-3%	-2%
	1	-13%	-13%	-13%	-1%	1%	-2%	0%	-2%	-3%
	2	-18%	-18%	-18%	5%	10%	8%	7%	7%	6%
<i>FA2</i>	0.5	-15%	-4%	-4%	2%	2%	1%	2%	2%	1%
	1	-13%	-12%	-9%	4%	13%	3%	7%	3%	2%
	2	-4%	-2%	-1%	0%	10%	-1%	2%	-1%	1%
<i>FAMAX</i>	0.5	-17%	-6%	-6%	0%	0%	-1%	0%	0%	-1%
	1	-15%	-15%	-13%	-1%	9%	-1%	4%	-1%	-3%
	2	-18%	-17%	-16%	5%	12%	8%	8%	7%	6%
<i>BPR1</i>	0.5	-12%	-12%	-12%	-13%	-7%	-7%	-5%	-7%	-4%
	1	7%	-10%	0%	0%	2%	0%	0%	0%	0%
	2	21%	-26%	-26%	-26%	-18%	-17%	-14%	-13%	-8%
<i>BPR2</i>	0.5	-5%	-1%	0%	-1%	-1%	-1%	0%	0%	0%
	1	-52%	-44%	-5%	-5%	14%	-2%	0%	-2%	-3%
	2	34%	-24%	-27%	-27%	-19%	-16%	-13%	-9%	-5%
<i>CPR1</i>	0.5	-5%	-5%	-5%	-22%	-8%	-6%	-5%	-6%	-7%
	1	18%	-3%	-3%	-3%	0%	-3%	-5%	-3%	-2%
	2	47%	-29%	-30%	-29%	-10%	-10%	-10%	-9%	-6%
<i>CPR2</i>	0.5	51%	42%	-2%	-21%	-16%	-22%	-18%	-22%	-14%
	1	-25%	-25%	13%	13%	15%	10%	8%	6%	2%
	2	36%	-23%	-25%	-25%	-17%	-13%	-9%	-4%	-2%
<i>SS1</i>	0.5	4%	4%	4%	2%	3%	2%	2%	2%	1%
	1	5%	5%	0%	0%	1%	0%	-1%	0%	0%
	2	0%	0%	0%	0%	0%	0%	0%	0%	0%
<i>SS2</i>	0.5	3%	3%	3%	-2%	-1%	-2%	3%	2%	3%
	1	0%	0%	0%	0%	0%	0%	0%	1%	2%
	2	-16%	-5%	-5%	-5%	-1%	-1%	-1%	0%	0%
<i>OTM1</i>	0.5	1%	-5%	0%	0%	0%	-1%	0%	0%	0%
	1	1%	1%	1%	1%	1%	0%	1%	3%	1%
	2	-8%	-8%	-5%	-5%	-2%	-3%	-3%	-1%	-2%
<i>OTM2</i>	0.5	3%	3%	3%	-2%	-1%	-2%	3%	2%	3%
	1	0%	0%	0%	0%	0%	0%	0%	1%	2%
	2	-22%	-12%	-12%	-8%	-7%	-7%	-7%	-6%	-7%

Table D-9 Subset Estimation Errors for the 50% EDP Response of the 4-Story RCMF Using Selection Method B on S_a Stripes

EDP	SF	50% EDP Relative Error								
		Subset Size								
		1	3	5	7	9	11	13	15	17
<i>DR1</i>	0.5	6%	6%	-2%	-3%	-3%	-3%	-6%	-3%	-3%
	1	1%	1%	0%	0%	0%	-2%	-2%	-2%	-1%
	2	-24%	2%	-11%	-11%	-11%	-11%	0%	-11%	0%
<i>DR2</i>	0.5	3%	2%	3%	2%	2%	2%	1%	1%	0%
	1	0%	0%	-1%	-1%	-2%	-2%	-2%	-1%	0%
	2	-19%	-13%	-13%	-13%	-12%	1%	1%	1%	4%
<i>DR3</i>	0.5	3%	-4%	3%	2%	2%	2%	2%	1%	1%
	1	4%	4%	4%	4%	-4%	-4%	4%	4%	4%
	2	7%	7%	-2%	-2%	-2%	-2%	-2%	-2%	7%
<i>DR4</i>	0.5	8%	-5%	4%	4%	4%	0%	0%	0%	0%
	1	9%	5%	5%	-1%	0%	0%	0%	0%	0%
	2	71%	30%	20%	20%	20%	20%	9%	9%	9%
<i>DRmax</i>	0.5	4%	4%	1%	-2%	-2%	-2%	-5%	-4%	-4%
	1	-4%	-4%	-4%	-4%	-4%	-5%	-4%	-4%	-4%
	2	-18%	-2%	-6%	-6%	-3%	-2%	-2%	-2%	0%
<i>FA1</i>	0.5	19%	5%	5%	5%	5%	5%	5%	5%	5%
	1	5%	-7%	1%	1%	5%	1%	4%	4%	1%
	2	9%	9%	9%	9%	8%	6%	6%	6%	2%
<i>FA2</i>	0.5	9%	7%	2%	2%	2%	-2%	-2%	-2%	-2%
	1	10%	8%	4%	4%	4%	1%	1%	1%	1%
	2	5%	11%	5%	5%	5%	5%	5%	6%	5%
<i>FA3</i>	0.5	2%	-1%	2%	2%	1%	-1%	1%	1%	1%
	1	-6%	-6%	2%	2%	2%	-1%	2%	2%	2%
	2	12%	12%	-2%	-1%	0%	0%	0%	0%	0%
<i>FA4</i>	0.5	13%	-4%	0%	2%	2%	0%	2%	2%	2%
	1	3%	3%	3%	3%	0%	-2%	0%	0%	0%
	2	14%	14%	1%	8%	4%	1%	-1%	1%	1%
<i>FAmix</i>	0.5	13%	-4%	0%	2%	2%	0%	2%	2%	2%
	1	3%	3%	3%	3%	3%	-2%	3%	3%	1%
	2	6%	6%	6%	6%	5%	3%	3%	5%	3%
<i>BPR1</i>	0.5	18%	15%	2%	-4%	-4%	-4%	-6%	-4%	-4%
	1	6%	6%	-5%	-5%	-5%	-5%	-5%	-3%	0%
	2	-17%	-1%	-3%	-3%	-3%	-3%	-1%	-3%	-1%
<i>BPR2</i>	0.5	-6%	2%	2%	2%	0%	2%	2%	4%	2%
	1	2%	2%	2%	2%	-8%	-8%	-4%	2%	2%
	2	-13%	-13%	-13%	-13%	-13%	2%	2%	2%	6%
<i>BPR3</i>	0.5	-1%	-1%	6%	-1%	3%	6%	3%	3%	3%
	1	43%	10%	10%	10%	-3%	-3%	-3%	-3%	5%
	2	80%	55%	26%	26%	26%	26%	7%	7%	7%
<i>BPR4</i>	0.5	3%	-1%	0%	0%	0%	0%	0%	-1%	-1%
	1	2%	0%	0%	0%	0%	0%	0%	0%	0%
	2	1061%	11%	90%	90%	90%	90%	12%	12%	12%

Table D-9 Subset Estimation Errors for the 50% EDP Response of the 4-Story RCMF Using Selection Method B on S_a Stripes (continued)

EDP	SF	50% EDP Relative Error								
		Subset Size								
		1	3	5	7	9	11	13	15	17
<i>CPR1</i>	0.5	20%	42%	20%	1%	1%	-1%	-4%	-1%	-1%
	1	2%	15%	2%	2%	2%	-12%	-12%	-12%	-10%
	2	-40%	10%	-22%	-22%	-22%	-22%	5%	-22%	5%
<i>CPR2</i>	0.5	5%	4%	3%	1%	1%	1%	0%	-2%	-2%
	1	-2%	0%	0%	0%	0%	0%	0%	0%	0%
	2	-47%	90%	-35%	-44%	-44%	-44%	-35%	-39%	-35%
<i>CPR3</i>	0.5	3%	0%	3%	3%	3%	3%	3%	3%	3%
	1	-7%	-7%	-7%	-7%	-7%	-7%	17%	18%	18%
	2	-70%	-63%	-63%	-63%	-57%	2%	2%	2%	2%
<i>CPR4</i>	0.5	5%	-2%	1%	1%	1%	0%	0%	-1%	-1%
	1	-5%	-5%	-1%	-1%	2%	2%	-1%	2%	2%
	2	302%	104%	92%	92%	92%	92%	39%	39%	39%
<i>SS1</i>	0.5	6%	6%	0%	0%	0%	0%	-4%	-4%	-4%
	1	3%	3%	2%	1%	1%	1%	-1%	-1%	-1%
	2	-3%	1%	1%	1%	1%	0%	1%	0%	0%
<i>SS2</i>	0.5	9%	3%	3%	4%	3%	-1%	-1%	-1%	-1%
	1	-5%	-4%	-4%	0%	0%	0%	0%	1%	1%
	2	-3%	-3%	-3%	2%	2%	2%	2%	2%	2%
<i>SS3</i>	0.5	0%	-1%	-1%	0%	0%	0%	0%	0%	0%
	1	2%	0%	0%	0%	0%	0%	0%	0%	0%
	2	5%	1%	1%	1%	2%	2%	1%	1%	0%
<i>SS4</i>	0.5	7%	4%	7%	4%	4%	1%	1%	-1%	-1%
	1	3%	0%	3%	2%	0%	-1%	-1%	-1%	-1%
	2	5%	-8%	-6%	-1%	0%	0%	0%	5%	0%
<i>OTM1</i>	0.5	0%	0%	0%	3%	3%	1%	1%	1%	1%
	1	1%	1%	1%	1%	0%	0%	0%	0%	0%
	2	0%	0%	0%	0%	0%	0%	0%	0%	0%
<i>OTM2</i>	0.5	2%	2%	2%	2%	2%	1%	1%	0%	0%
	1	1%	1%	1%	-1%	-1%	-1%	-1%	-1%	-1%
	2	5%	0%	0%	0%	0%	0%	0%	0%	0%
<i>OTM3</i>	0.5	4%	4%	6%	4%	4%	3%	3%	-1%	-1%
	1	0%	0%	0%	0%	0%	0%	0%	0%	0%
	2	4%	-8%	-5%	-5%	-1%	-1%	-1%	0%	0%
<i>OTM4</i>	0.5	7%	4%	7%	4%	4%	1%	1%	-1%	-1%
	1	3%	0%	3%	2%	0%	-1%	-1%	-1%	-1%
	2	3%	-11%	-8%	-3%	-3%	-3%	-3%	2%	2%

*Empty cells show where the estimated EDP is indeterminate (global collapse).

Table D-10 Subset Estimation Errors for the 84% EDP Response of the 4-Story RCMF Using Selection Method B on S_a Stripes

EDP	SF	84% EDP Relative Error								
		Subset Size								
		1	3	5	7	9	11	13	15	17
DR1	0.5	-1%	-1%	-7%	-8%	-2%	-4%	-3%	-1%	-2%
	1	6%	0%	0%	1%	2%	3%	2%	1%	3%
	2	25%	1%	25%	1%	12%	21%	9%	1%	1%
DR2	0.5	-2%	-3%	-2%	-3%	-2%	-2%	-2%	-2%	-2%
	1	-3%	-10%	-3%	-1%	-1%	0%	1%	0%	1%
	2	19%	0%	19%	3%	10%	16%	8%	3%	3%
DR3	0.5	-8%	-6%	0%	0%	4%	3%	4%	3%	3%
	1	-9%	0%	-1%	0%	2%	1%	5%	4%	3%
	2	-16%	3%	3%	22%	23%	24%	23%	22%	16%
DR4	0.5	9%	9%	9%	6%	14%	9%	13%	9%	8%
	1	0%	9%	1%	1%	5%	2%	4%	2%	2%
	2	-1%	14%	14%	29%	31%	26%	19%	14%	12%
DRmax	0.5	-1%	-1%	-2%	-4%	-1%	-2%	-1%	-1%	-1%
	1	4%	4%	4%	4%	6%	5%	4%	4%	5%
	2	25%	1%	25%	1%	12%	21%	9%	1%	1%
FA1	0.5	31%	31%	31%	27%	36%	30%	28%	27%	20%
	1	54%	46%	46%	36%	41%	36%	35%	34%	30%
	2	34%	34%	34%	34%	35%	30%	29%	27%	23%
FA2	0.5	21%	16%	16%	16%	24%	20%	18%	16%	16%
	1	31%	27%	27%	27%	37%	31%	28%	27%	23%
	2	31%	16%	16%	16%	22%	14%	20%	16%	13%
FA3	0.5	41%	38%	38%	21%	28%	19%	22%	21%	17%
	1	57%	15%	15%	11%	14%	13%	12%	12%	11%
	2	60%	8%	8%	8%	44%	36%	37%	33%	25%
FA4	0.5	24%	24%	22%	8%	22%	19%	20%	18%	15%
	1	57%	22%	-2%	10%	15%	11%	10%	10%	7%
	2	37%	25%	25%	0%	11%	0%	1%	3%	2%
Famax	0.5	24%	24%	24%	9%	24%	21%	20%	18%	15%
	1	40%	22%	22%	22%	24%	22%	21%	20%	14%
	2	26%	26%	26%	26%	27%	23%	22%	20%	16%
BPR1	0.5	3%	0%	-12%	-12%	-10%	-9%	-7%	-3%	-5%
	1	4%	-3%	-2%	-2%	1%	3%	1%	0%	3%
	2	26%	0%	26%	0%	11%	21%	8%	3%	2%
BPR2	0.5	-22%	-4%	-4%	-4%	0%	4%	3%	5%	4%
	1	-14%	-14%	-6%	0%	4%	2%	5%	3%	7%
	2	-8%	-2%	0%	3%	6%	9%	5%	3%	2%
BPR3	0.5	-47%	9%	9%	9%	29%	31%	34%	31%	30%
	1	-9%	27%	18%	13%	22%	17%	21%	18%	16%
	2	0%	10%	10%	21%	30%	18%	13%	10%	8%
BPR4	0.5	4%	4%	4%	3%	6%	4%	5%	4%	4%
	1	3%	7%	3%	2%	5%	3%	4%	3%	3%
	2	10%	43%	43%	43%	64%	42%	38%	36%	28%
CPR1	0.5	-24%	-10%	-24%	-24%	-8%	-12%	-15%	-10%	-7%
	1	22%	2%	2%	2%	15%	19%	13%	9%	18%
	2	36%	2%	36%	2%	17%	29%	13%	2%	1%

Table D-10 Subset Estimation Errors for the 84% EDP Response of the 4-Story RCMF Using Selection Method B on S_a Stripes (continued)

EDP	SF	84% EDP Relative Error								
		Subset Size								
		1	3	5	7	9	11	13	15	17
CPR2	0.5	0%	-1%	-2%	-4%	-2%	-3%	-1%	-1%	-1%
	1	-4%	-2%	-2%	-2%	0%	1%	0%	2%	1%
	2	223%	-15%	172%	-15%	99%	146%	84%	42%	33%
CPR3	0.5	-7%	-7%	-6%	-6%	2%	1%	2%	1%	3%
	1	-49%	-38%	-32%	17%	23%	16%	21%	17%	26%
	2	-30%	-9%	2%	2%	4%	5%	3%	2%	5%
CPR4	0.5	4%	4%	4%	4%	8%	4%	7%	4%	4%
	1	-38%	174%	4%	4%	87%	17%	28%	20%	15%
	2	-2%	22%	22%	39%	49%	36%	28%	22%	16%
SS1	0.5	-2%	-2%	-7%	-6%	-2%	-3%	-2%	-2%	-2%
	1	2%	0%	0%	0%	3%	2%	1%	1%	1%
	2	1%	1%	1%	1%	1%	1%	1%	1%	1%
SS2	0.5	0%	-6%	-6%	-3%	-2%	-4%	-5%	-4%	-5%
	1	3%	-2%	0%	0%	1%	1%	2%	2%	2%
	2	-7%	-3%	-3%	0%	1%	0%	1%	1%	1%
SS3	0.5	-12%	7%	5%	5%	7%	7%	7%	7%	6%
	1	-5%	5%	0%	0%	4%	2%	4%	3%	2%
	2	-3%	-3%	-3%	-1%	6%	10%	5%	1%	1%
SS4	0.5	-4%	18%	14%	14%	14%	14%	14%	14%	14%
	1	7%	16%	7%	7%	15%	13%	9%	7%	6%
	2	-8%	4%	4%	4%	8%	7%	8%	7%	6%
OTM1	0.5	-7%	6%	6%	3%	4%	2%	3%	3%	2%
	1	-3%	3%	3%	2%	2%	1%	3%	3%	3%
	2	0%	0%	0%	0%	0%	0%	0%	0%	0%
OTM2	0.5	-7%	9%	7%	7%	8%	7%	8%	7%	7%
	1	0%	8%	4%	4%	4%	4%	4%	4%	4%
	2	0%	3%	3%	0%	1%	2%	1%	0%	0%
OTM3	0.5	-10%	14%	8%	8%	10%	7%	10%	8%	7%
	1	0%	8%	0%	0%	4%	1%	1%	1%	1%
	2	-5%	4%	4%	-2%	5%	3%	5%	4%	3%
OTM4	0.5	-4%	18%	14%	14%	14%	14%	14%	14%	14%
	1	7%	16%	7%	7%	15%	13%	9%	7%	6%
	2	-10%	1%	1%	1%	6%	4%	6%	5%	6%

D.2.5 Random Subset Selection based on S_a Scaling

To test further the actual potential of the subset selection technique based on S_a scaling, a number of trials with random selection of record subsets at the given S_a level were performed. The general idea is to understand whether the observed influence of subset size on accuracy of EDP estimates is an outcome of the selection process, or if it should be attributed to the improvement generally expected with increasing subset size. The results of two representative trials to estimate the median EDP response appear in Figures D-50 and D-51. Therein it is apparent that there may indeed exist cases where the random selection will provide errors similar to those

obtained with the median-oriented subset selection method described previously. Still, it is unlikely that a small random subset of records will be able to match the performance of Selection Method B, even for estimation of the median. In other words, the S_a scaling/subset selection method offers superior performance to that of random selection, offering substantial robustness and a relative assurance of error reduction with larger sample sizes.

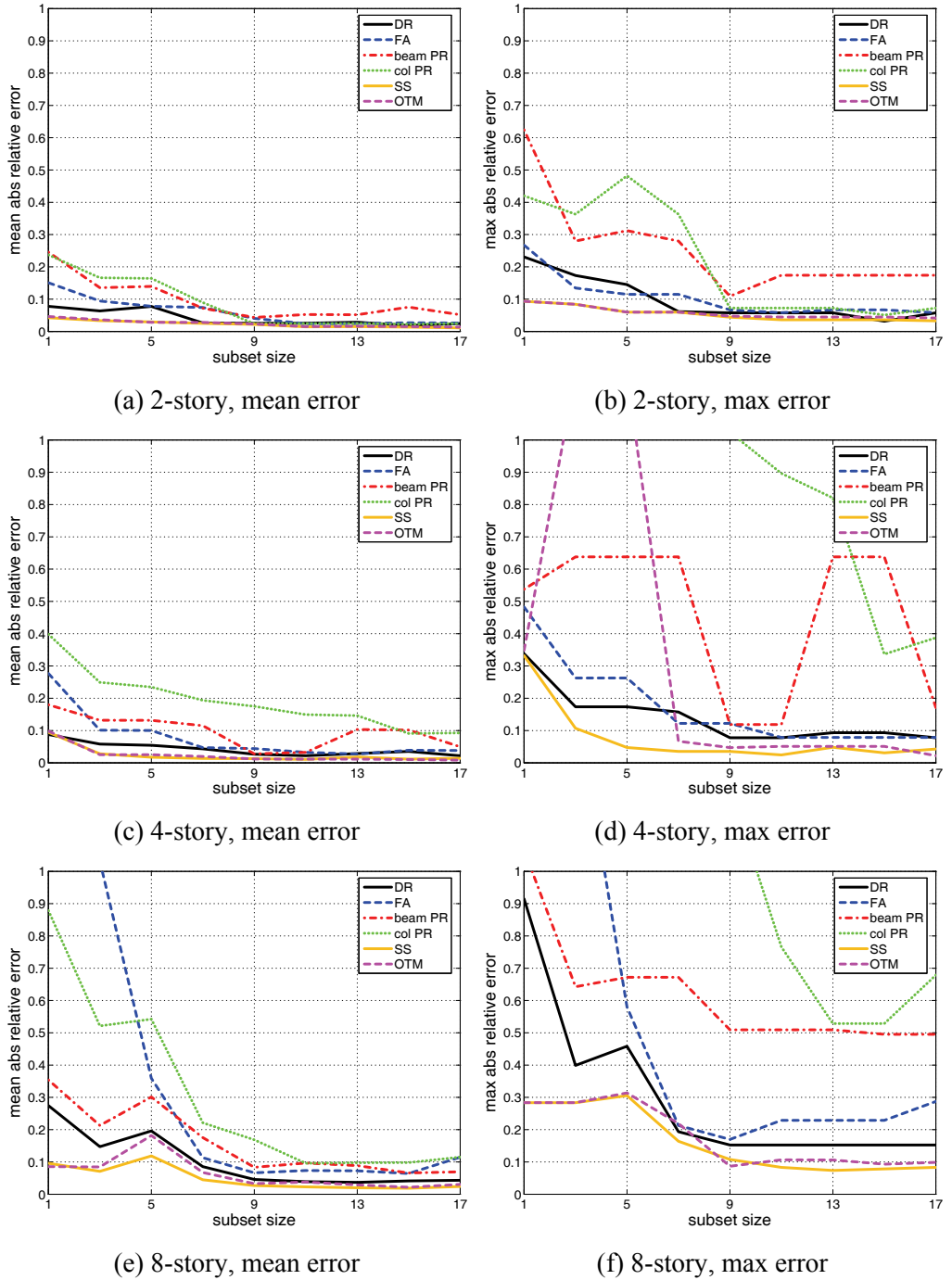


Figure D-50 Mean and maximum absolute relative error for different EDP types over all 3 scale factors when randomly selecting subsets within an S_a stripe to estimate the 50% response (Trial 1).

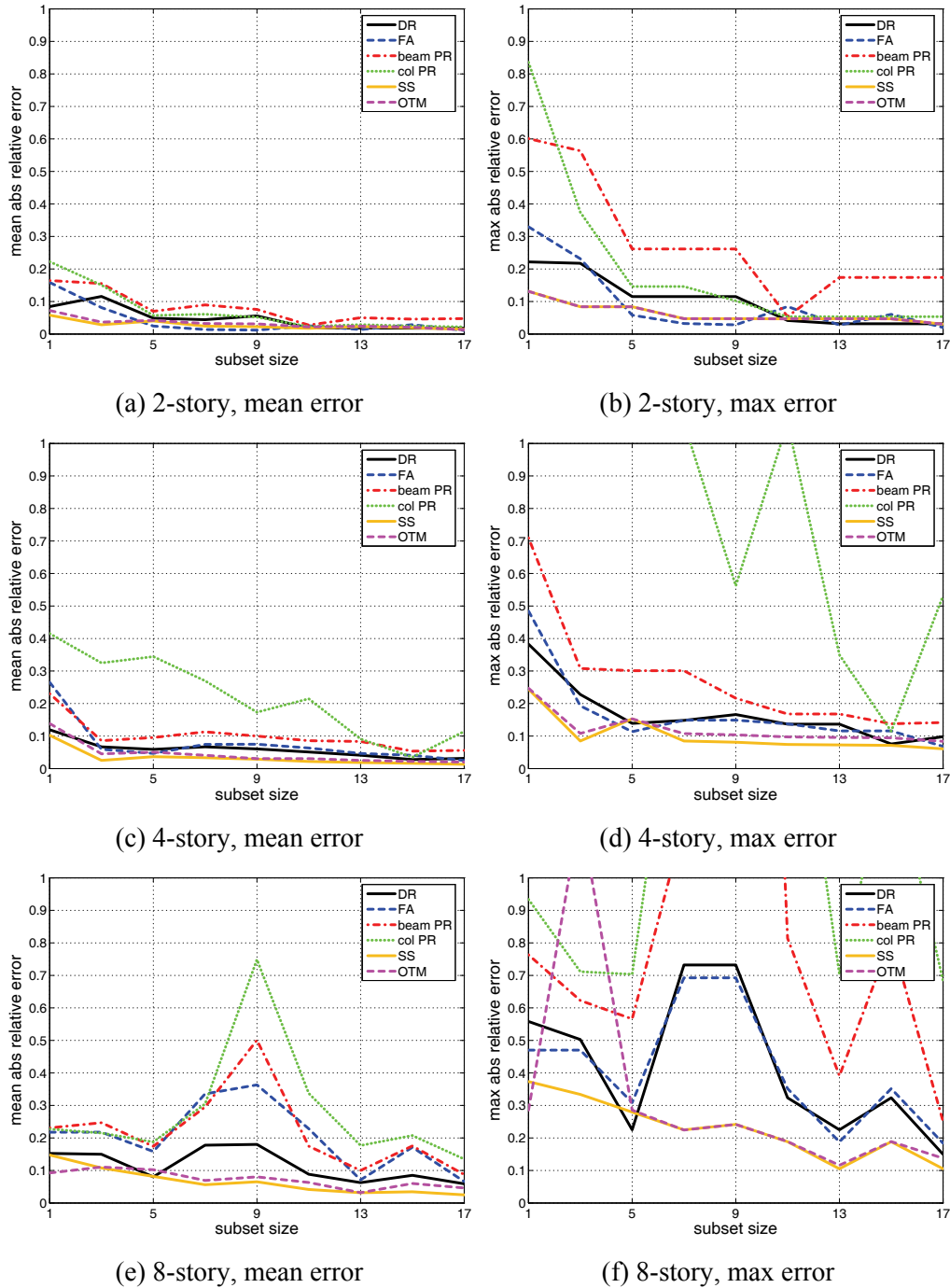


Figure D-51 Mean and maximum absolute relative error for different EDP types over all 3 scale factors when randomly selecting subsets within an S_a stripe to estimate the 50% response (Trial 2).

D.2.6 Subset Selection on S_{di} Scaling

S_{di} scaling was tested as an alternative to S_a and FEMA P-695 scaling. In this case “optimal” record subsets at a common S_{di} intensity level were sought that would

allow accurate estimation of the 50% or the 84% EDP response obtained for the entire set of 44 records. After scaling to achieve the common S_{di} value, equal to the median of the S_{di} values obtained for each scale factor, for each structure, elastic spectra were plotted for the full suite of 44 motions, from which median and 84% spectra were determined. Record subsets were identified based on matching the median elastic spectra of the subset to either the median or 84% spectra of the full suite over a specified period range.

Due to the different nature of S_{di} it is not appropriate to use the same range of period for record selection as was used for the other two scaling methods. The lengthening of the “first-mode period” in the post-yield range can be adequately captured by S_{di} itself, therefore only the higher mode region should be considered for subset selection. Therefore, the range over which the record subsets are selected was chosen to be $[0.8T_i, 1.2T_2]$. The lower period was T_i determined as a function of the number of stories N_{st} :

$$i = \text{ceil}\left(\sqrt{N_{st}}\right) \quad (\text{D-9})$$

where “ceil” is the function that rounds up to the nearest highest integer.

To further aid in understanding this technique, Figure D-52 shows the shape of the elastic spectra scaled to the S_{di} stripes that correspond to the median response of the equivalent oscillator subject to the FEMA P-695 cloud (a technique exemplified in Figure D-1). For scale factors of 0.5 and 1 the oscillator is essentially elastic, making S_{di} scaling practically the same as $S_a(T_1)$ scaling in this region; that is why there is a “pinch point” in the scaled spectra at T_1 . The true power in S_{di} scaling should be judged mainly from the results corresponding to a scale factor of 2.

Results for maximum and mean absolute relative error are summarized in Figures D-53 and D-54 while detailed results appear in Tables D-11 through D-14 both for the 50% and the 84% response. In general, median estimates, show a monotonic reduction in error as the number of records increases. Using at least 5 records produces a mean error that is always less than 10% and a maximum error that is almost always less than 30%, for all response quantities investigated except plastic hinge rotations, related to the same issues discussed previously for S_a scaling.

These results are on par with the results for Selection Method B using either FEMA P-695 or S_a scaling showing that all approaches to subset selection offer similar advantages, albeit with some distinguishing characteristics. Interestingly, S_a scaling appears to perform somewhat better than S_{di} scaling for estimates of median EDPs, while S_{di} scaling appears to be somewhat better than S_a scaling for estimates of 84% EDPs. These distinctions appear even though S_a and S_{di} scaling are indistinguishable for elastic response, mainly due to the different period-matching ranges involved in the record selection: The problem of properly weighting the higher modes relative to the fundamental mode may hinder S_a scaling but does not enter into S_{di} scaling.

Examination of the results suggests that observations regarding the efficiency of each scaling method (Section D.1) are relevant here. For example, FEMA P-695 scaling seems to perform better for acceleration-related quantities while, excluding plastic hinge rotations, the maximum error is mainly driven by the drift-related EDPs at high scale factors. On the other hand, some of the local floor accelerations are poorly estimated using subsets selected on the basis of S_{di} scaling. While the generality of these observations may be limited by the sample of three buildings, they provide some evidence that the subset selection method reflects some of the same strengths and weaknesses of the intensity measure used as its basis.

Regarding estimates of the 84% quantile (Figure D-54), results obtained with S_{di} scaling/subset selection generally are better (having less error) than the 50% estimates at the same S_{di} intensity level; this may be an attribute of S_{di} scaling, since the multipart estimation formula (Equation D-8) was used for all three scaling methods. For all EDP types investigated, the estimates are at most within 20% of the actual value, except in the case of the 8-story frame where some localized plastic hinge rotation errors can reach up to 40%. Similar to the case of S_a scaling, this improved performance for the 84% estimates of plastic hinge rotations can be extended to the 50% results with minor postprocessing of the plastic hinge rotation values to eliminate the troublesome near-zero values.

In summary, the numerical experiments described herein suggest the possibility of selecting record subsets to be used for nonlinear response history analysis, as described in Chapter 9. The period ranges reported in this section are preliminary, resulting from various trials for the sample of three moment frame buildings; further study may lead to refinements that are better suited to a larger variety of buildings.

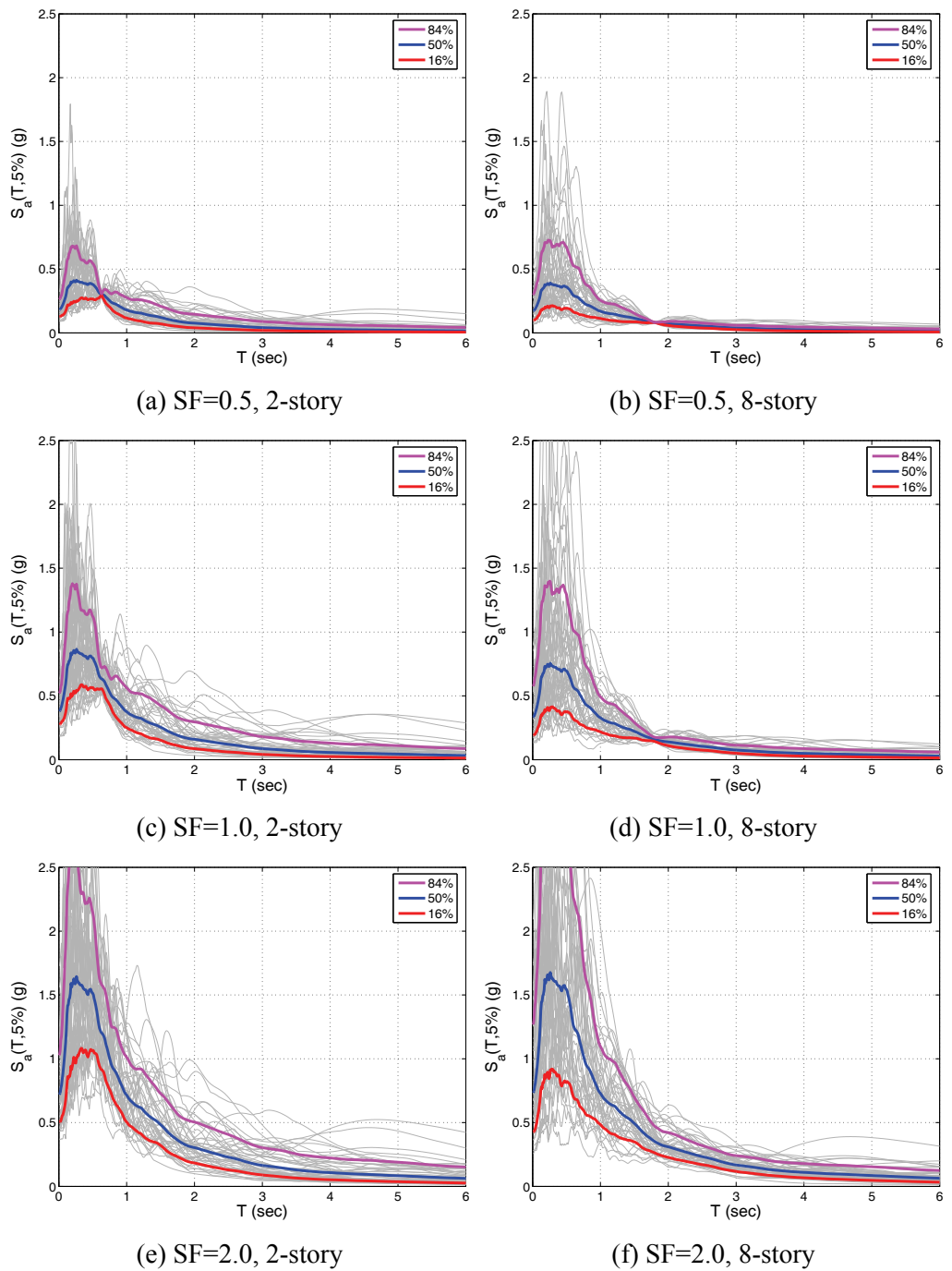
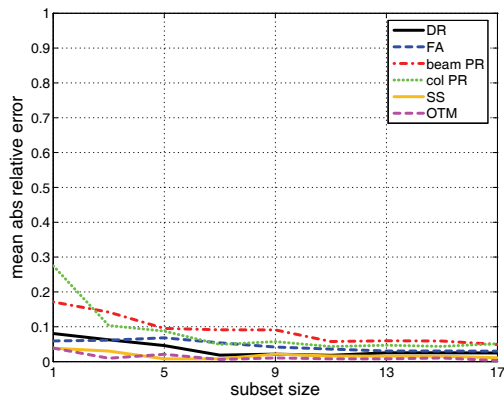
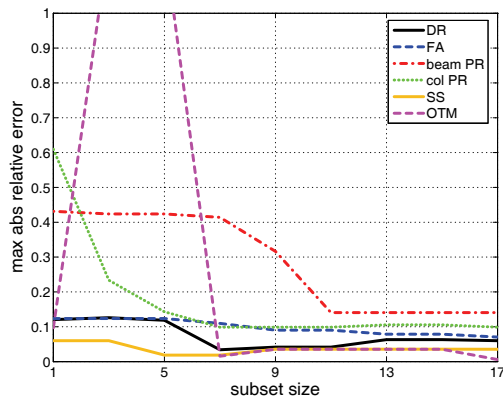


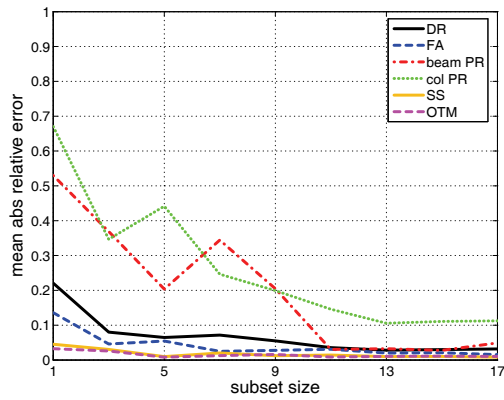
Figure D-52 The $S_a(T)$ individual spectra and their 16/50/84 summaries for the 44 ground motion records scaled to the median S_{di} value of the FEMA P-695 normalized clouds for the 2- and 8-story RCMFs. The presence of a “pinch-point” at the first-mode period for low scale-factors shows when the structure remains elastic and S_{di} becomes perfectly correlated with S_a .



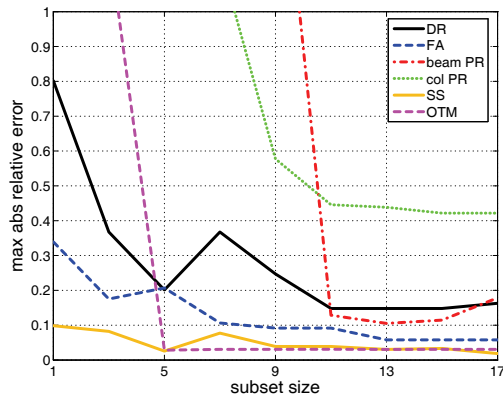
(a) 2-story, mean error



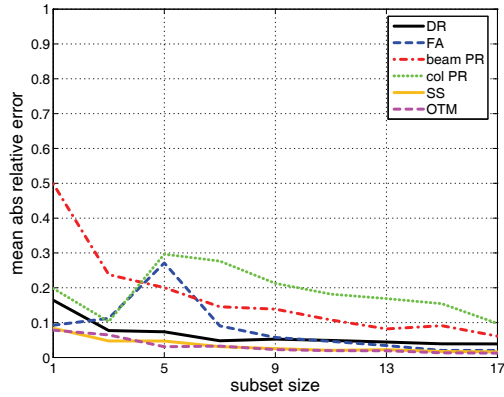
(b) 2-story, max error



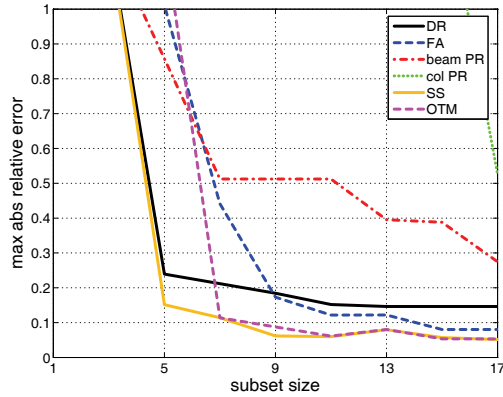
(c) 4-story, mean error



(d) 4-story, max error

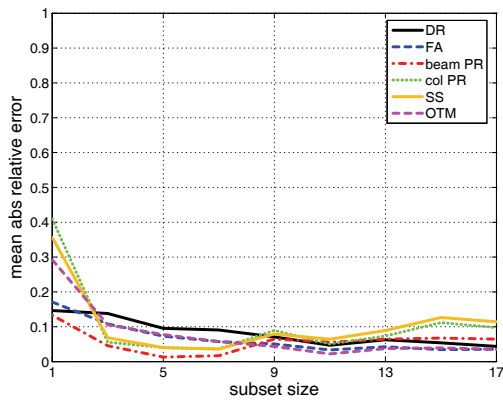


(e) 8-story, mean error

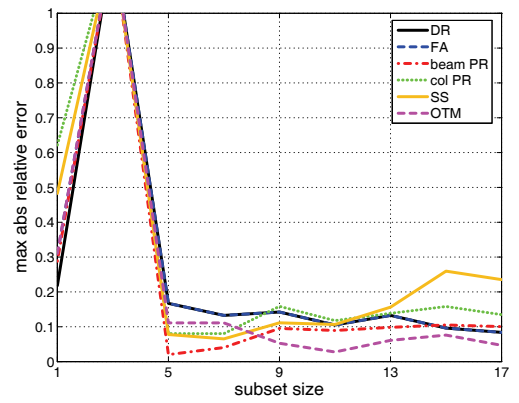


(f) 8-story, max error

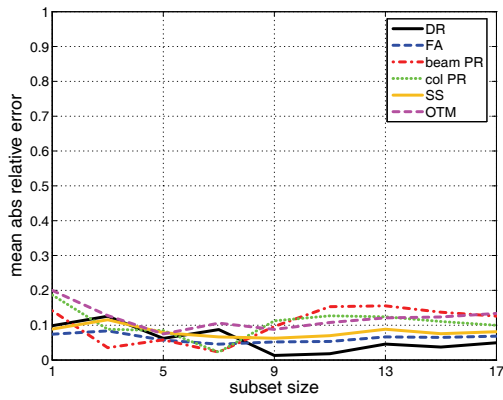
Figure D-53 Mean and maximum absolute relative error for different EDP types over all 3 scale factors when selecting subsets within an S_{di} stripe by matching 50% local S_a values to estimate the 50% response.



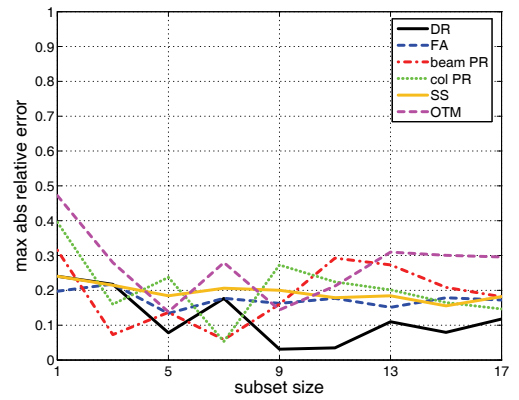
(a) 2-story, mean error



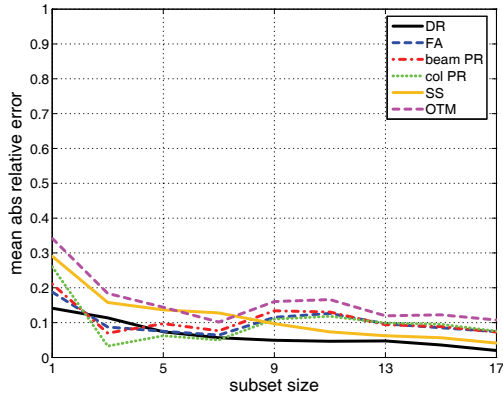
(b) 2-story, max error



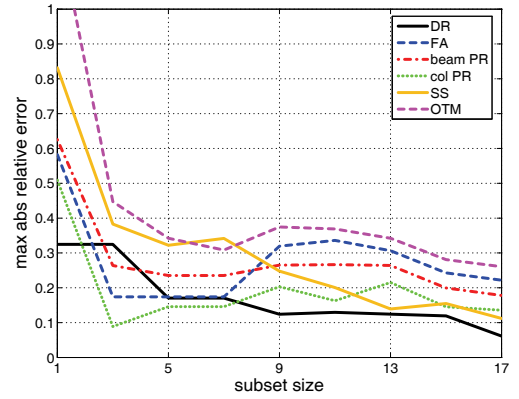
(c) 4-story, mean error



(d) 4-story, max error



(e) 8-story, mean error



(f) 8-story, max error

Figure D-54 Mean and maximum absolute relative error for different EDP types over all 3 scale factors when selecting subsets within an S_{di} stripe by matching 84% local S_a values to estimate the 84% response.

Table D-11 Subset Estimation Errors for the 50% EDP Response of the 2-Story RCMF Using Selection Method B on S_{di} Stripes

EDP	SF	50% EDP Relative Error								
		Subset Size								
		1	3	5	7	9	11	13	15	17
DR1	0.5	-7%	-3%	-3%	-1%	0%	0%	0%	0%	0%
	1	-12%	-12%	-4%	2%	4%	2%	0%	0%	2%
	2	12%	-6%	12%	-3%	-3%	-3%	-6%	-6%	-6%
DR2	0.5	-1%	-1%	-1%	-1%	0%	0%	0%	0%	0%
	1	-9%	1%	1%	1%	4%	4%	4%	4%	4%
	2	-1%	-13%	-1%	-1%	-1%	-1%	-6%	-6%	-2%
DRmax	0.5	-7%	-3%	-3%	-1%	0%	0%	0%	0%	0%
	1	-12%	-12%	-4%	2%	4%	2%	0%	0%	2%
	2	12%	-6%	12%	-3%	-3%	-3%	-6%	-6%	-6%
FA1	0.5	-12%	-12%	-12%	-9%	-9%	-9%	-8%	-8%	-6%
	1	-8%	-8%	-8%	-11%	-8%	-8%	-8%	-8%	-6%
	2	-7%	-7%	-7%	-7%	-7%	-3%	-3%	-3%	-7%
FA2	0.5	2%	-1%	-4%	-4%	-2%	-1%	-1%	-1%	-1%
	1	-8%	-8%	-8%	-1%	2%	2%	2%	2%	2%
	2	4%	6%	6%	6%	6%	6%	4%	4%	3%
FMax	0.5	2%	-1%	-4%	-4%	-2%	-1%	-1%	-1%	-1%
	1	-10%	-10%	-10%	-3%	0%	0%	0%	0%	0%
	2	1%	2%	2%	2%	2%	2%	1%	1%	-1%
BPR1	0.5	-29%	12%	6%	0%	0%	4%	1%	0%	1%
	1	-14%	-6%	-5%	1%	11%	10%	1%	1%	1%
	2	0%	-9%	0%	0%	0%	0%	-9%	-9%	-7%
BPR2	0.5	0%	0%	-1%	-1%	0%	0%	0%	0%	0%
	1	-43%	-42%	-42%	-41%	-32%	-14%	-14%	-14%	-14%
	2	-16%	-16%	2%	-11%	-11%	-6%	-11%	-11%	-6%
CPR1	0.5	-61%	14%	14%	3%	-8%	3%	3%	3%	7%
	1	-23%	-23%	-8%	5%	5%	1%	0%	0%	1%
	2	14%	-7%	14%	-4%	-4%	-4%	-7%	-7%	-7%
CPR2	0.5	3%	3%	3%	3%	3%	3%	3%	-1%	3%
	1	-55%	-4%	-4%	-4%	4%	4%	4%	4%	4%
	2	-8%	-11%	-8%	-10%	-10%	-10%	-11%	-11%	-10%
SS1	0.5	-6%	-6%	-2%	-2%	-2%	0%	0%	0%	0%
	1	-4%	-4%	1%	1%	-2%	1%	0%	0%	1%
	2	2%	2%	-1%	-1%	-1%	-1%	-1%	-1%	-2%
SS2	0.5	0%	0%	0%	0%	0%	0%	0%	0%	0%
	1	-5%	0%	0%	0%	4%	4%	4%	4%	0%
	2	-6%	-6%	-1%	-1%	4%	4%	4%	4%	4%
OTM1	0.5	-3%	-3%	-3%	-2%	-2%	0%	0%	-1%	0%
	1	-2%	0%	0%	0%	0%	0%	0%	0%	0%
	2	-3%			-1%	0%	0%	0%	0%	0%
OTM2	0.5	0%	0%	0%	0%	0%	0%	0%	0%	0%
	1	-5%	0%	0%	0%	4%	4%	4%	4%	0%
	2	-10%		7%	-1%	1%	1%	1%	1%	1%

*Empty cells show where the estimated EDP is indeterminate (global collapse).

Table D-12 Subset Estimation Errors for the 84% EDP Response of the 2-Story RCMF Using Selection Method B on S_{di} Stripes

EDP	SF	84% EDP Relative Error								
		Subset Size								
		1	3	5	7	9	11	13	15	17
<i>DR1</i>	0.5	-9%	-9%	-8%	-7%	-4%	-1%	-2%	-2%	-2%
	1	-22%	-19%	-4%	-7%	-3%	-3%	-4%	-4%	-3%
	2	-13%		17%	13%	14%	11%	13%	10%	8%
<i>DR2</i>	0.5	6%	4%	4%	0%	4%	4%	4%	3%	3%
	1	-22%	-11%	-1%	-4%	0%	0%	0%	0%	0%
	2	-31%		10%	3%	5%	2%	3%	1%	5%
<i>DRmax</i>	0.5	-9%	-9%	-8%	-7%	-4%	-1%	-2%	-2%	-2%
	1	-22%	-19%	-4%	-7%	-3%	-3%	-4%	-4%	-3%
	2	-13%		17%	13%	14%	11%	13%	10%	8%
<i>FA1</i>	0.5	29%	1%	1%	0%	7%	1%	1%	1%	1%
	1	-10%	-8%	-2%	-4%	3%	7%	9%	11%	10%
	2	1%		1%	1%	10%	9%	10%	9%	8%
<i>FA2</i>	0.5	47%	9%	0%	0%	3%	1%	2%	7%	6%
	1	-14%	-2%	4%	-2%	8%	3%	6%	16%	13%
	2	62%		8%	8%	16%	12%	14%	11%	10%
<i>FAmix</i>	0.5	45%	7%	3%	0%	4%	2%	3%	6%	5%
	1	-14%	-7%	-1%	-7%	8%	11%	16%	26%	24%
	2	48%		8%	4%	11%	6%	8%	6%	5%
<i>BPR1</i>	0.5	-26%	-3%	-3%	-4%	-4%	3%	-3%	-3%	-3%
	1	-31%	-18%	-11%	-11%	-5%	-3%	-6%	-8%	-2%
	2	-30%		9%	2%	4%	1%	2%	1%	5%
<i>BPR2</i>	0.5	5%	3%	3%	0%	3%	2%	1%	3%	2%
	1	-83%	-42%	-30%	-30%	-12%	-3%	1%	-2%	4%
	2	-47%		3%	1%	2%	1%	1%	1%	1%
<i>CPR1</i>	0.5	-58%	-4%	-3%	-4%	-4%	-3%	-3%	-3%	-3%
	1	-36%	-31%	-4%	-12%	-5%	-4%	-5%	-6%	-4%
	2	-14%		16%	15%	15%	12%	15%	11%	10%
<i>CPR2</i>	0.5	43%	43%	43%	-22%	11%	-4%	-1%	6%	4%
	1	-62%	-33%	-10%	-22%	-1%	1%	0%	-1%	2%
	2	-42%		5%	3%	4%	2%	3%	2%	4%
<i>SS1</i>	0.5	-9%	0%	0%	0%	0%	1%	0%	1%	1%
	1	-4%	-4%	0%	0%	0%	1%	0%	2%	2%
	2	1%		1%	0%	1%	0%	0%	0%	0%
<i>SS2</i>	0.5	4%	5%	4%	3%	3%	3%	4%	5%	5%
	1	6%	2%	2%	-3%	0%	1%	2%	4%	3%
	2	-5%		5%	3%	6%	6%	5%	4%	4%
<i>OTM1</i>	0.5	0%	0%	1%	0%	0%	1%	2%	2%	1%
	1	-3%	-1%	-1%	-1%	0%	3%	3%	3%	2%
	2	-7%		0%	-3%	-3%	1%	1%	3%	2%
<i>OTM2</i>	0.5	4%	5%	4%	3%	3%	3%	4%	5%	5%
	1	6%	2%	2%	-3%	0%	1%	2%	4%	3%
	2	-9%		2%	2%	2%	3%	2%	3%	3%

*Empty cells show where the estimated EDP is indeterminate (global collapse).

Table D-13 Subset Estimation Errors for the 50% EDP Response of the 4-Story RCMF Using Selection Method B on S_{di} Stripes

EDP	SF	50% EDP Relative Error								
		Subset Size								
		1	3	5	7	9	11	13	15	17
<i>DR1</i>	0.5	7%	-6%	-6%	-3%	-3%	-3%	-2%	-3%	-3%
	1	-1%	-2%	-1%	-1%	0%	0%	0%	0%	0%
	2	80%	-14%	20%	-14%	-14%	-14%	10%	10%	10%
<i>DR2</i>	0.5	3%	-1%	-1%	-1%	2%	0%	2%	2%	2%
	1	9%	-2%	6%	6%	6%	2%	0%	0%	0%
	2	59%	6%	6%	5%	5%	5%	5%	5%	5%
<i>DR3</i>	0.5	3%	2%	-5%	1%	2%	1%	-2%	-1%	0%
	1	1%	-2%	1%	1%	1%	-2%	-2%	-2%	-2%
	2	46%	31%	15%	25%	25%	15%	15%	15%	16%
<i>DR4</i>	0.5	8%	-2%	-2%	-2%	-1%	-1%	-1%	-1%	-1%
	1	-1%	0%	0%	0%	0%	0%	0%	0%	0%
	2	38%	37%	15%	37%	15%	2%	0%	0%	2%
<i>DRmax</i>	0.5	4%	-7%	-7%	-5%	-2%	-2%	-1%	-2%	-2%
	1	6%	-5%	2%	2%	3%	2%	-1%	-1%	-1%
	2	64%	-4%	9%	-4%	-4%	-4%	0%	2%	2%
<i>FA1</i>	0.5	19%	-18%	-18%	-7%	-1%	-1%	-1%	-1%	1%
	1	32%	-11%	-21%	-11%	-9%	-4%	-5%	-5%	-4%
	2	-2%	-2%	-2%	0%	3%	9%	3%	5%	3%
<i>FA2</i>	0.5	8%	1%	-3%	-3%	-3%	1%	1%	0%	1%
	1	34%	11%	-4%	-4%	6%	8%	6%	6%	6%
	2	-4%	5%	5%	3%	5%	5%	3%	3%	2%
<i>FA3</i>	0.5	2%	1%	-2%	1%	1%	0%	0%	0%	0%
	1	16%	4%	4%	4%	0%	3%	0%	0%	0%
	2	1%	0%	0%	0%	1%	1%	0%	0%	0%
<i>FA4</i>	0.5	13%	2%	-5%	0%	0%	0%	-1%	-1%	0%
	1	25%	1%	1%	1%	1%	1%	1%	1%	1%
	2	-7%	2%	2%	2%	2%	2%	2%	2%	2%
<i>FAmx</i>	0.5	13%	2%	-5%	0%	0%	0%	-1%	-1%	0%
	1	25%	1%	1%	1%	1%	1%	1%	1%	1%
	2	-5%	9%	9%	-1%	9%	9%	5%	5%	1%
<i>BPR1</i>	0.5	19%	-7%	-4%	-4%	2%	2%	3%	2%	0%
	1	4%	-9%	-3%	-3%	4%	-3%	-3%	-3%	-3%
	2	77%	-15%	15%	-13%	-13%	-13%	5%	5%	6%
<i>BPR2</i>	0.5	-7%	-6%	1%	1%	1%	-6%	0%	1%	1%
	1	13%	-6%	8%	8%	8%	2%	-5%	-5%	-5%
	2	59%	25%	11%	11%	11%	5%	11%	11%	18%
<i>BPR3</i>	0.5	-1%	-1%	-1%	6%	6%	-1%	-3%	-1%	-1%
	1	-22%	-6%	0%	0%	0%	0%	-6%	-1%	0%
	2	62%	48%	34%	48%	34%	2%	2%	2%	11%
<i>BPR4</i>	0.5	3%	0%	-1%	-1%	0%	0%	0%	0%	0%
	1	1%	1%	0%	0%	0%	0%	0%	0%	0%
	2	367%	319%	167%	319%	167%	2%	2%	2%	14%
<i>CPR1</i>	0.5	19%	19%	27%	20%	20%	19%	19%	11%	1%
	1	-27%	-27%	-2%	-2%	3%	3%	3%	3%	3%
	2	124%	-30%	32%	-30%	-30%	-30%	13%	13%	16%

Table D-13 Subset Estimation Errors for the 50% EDP Response of the 4-Story RCMF Using Selection Method B on S_{di} Stripes (Continued)

EDP	SF	50% EDP Relative Error								
		Subset Size								
		1	3	5	7	9	11	13	15	17
CPR2	0.5	5%	0%	-6%	-2%	-2%	0%	1%	0%	0%
	1	3%	0%	0%	0%	1%	0%	0%	0%	1%
	2	252%	-32%	191%	-32%	-32%	-32%	-4%	42%	36%
CPR3	0.5	3%	3%	-6%	-1%	2%	-1%	0%	0%	0%
	1	20%	20%	46%	46%	45%	45%	44%	20%	19%
	2	230%	169%	159%	42%	42%	29%	42%	42%	42%
CPR4	0.5	5%	0%	-2%	-1%	0%	0%	0%	0%	0%
	1	0%	0%	0%	4%	4%	3%	0%	0%	3%
	2	115%	115%	58%	115%	58%	14%	-1%	1%	14%
SS1	0.5	7%	0%	0%	-4%	-4%	-4%	0%	0%	0%
	1	-3%	-3%	-3%	-2%	-1%	-1%	-1%	-1%	0%
	2	3%	-2%	0%	-2%	-1%	-1%	-1%	0%	0%
SS2	0.5	9%	3%	2%	1%	1%	1%	1%	-1%	-1%
	1	7%	2%	2%	1%	1%	1%	1%	0%	1%
	2	1%	8%	1%	4%	4%	4%	1%	3%	1%
SS3	0.5	0%	0%	0%	0%	0%	0%	0%	0%	0%
	1	-4%	-1%	-1%	-1%	-1%	-1%	-1%	-1%	2%
	2	1%	8%	1%	8%	1%	-1%	-1%	-1%	-1%
SS4	0.5	6%	3%	0%	0%	0%	0%	-3%	-3%	-2%
	1	10%	3%	0%	0%	-1%	-1%	-1%	0%	0%
	2	-4%	1%	-1%	1%	1%	4%	1%	1%	1%
OTM1	0.5	0%	3%	1%	1%	1%	0%	0%	0%	1%
	1	3%	3%	0%	1%	0%	0%	0%	0%	0%
	2			1%	3%	3%	3%	3%	3%	3%
OTM2	0.5	1%	5%	2%	1%	1%	0%	0%	0%	0%
	1	1%	2%	1%	2%	2%	1%	0%	0%	0%
	2	3%	0%	0%	3%	3%	1%	0%	1%	1%
OTM3	0.5	3%	3%	3%	3%	3%	0%	-1%	-1%	-1%
	1	2%	1%	0%	0%	0%	0%	-1%	-1%	-1%
	2	3%	1%	1%	1%	3%	1%	0%	1%	1%
OTM4	0.5	6%	3%	0%	0%	0%	0%	-3%	-3%	-2%
	1	10%	3%	0%	0%	-1%	-1%	-1%	0%	0%
	2			0%	0%	3%	3%	3%	3%	2%

*Empty cells show where the estimated EDP is indeterminate (global collapse).

Table D-14 Subset Estimation Errors for the 84% EDP Response of the 4-Story RCMF Using Selection Method B on S_{di} Stripes

EDP	SF	84% EDP relative error								
		subset size								
		1	3	5	7	9	11	13	15	17
<i>DR1</i>	0.5	0%	-12%	-7%	-6%	1%	-1%	2%	1%	1%
	1	-11%	-11%	-7%	-7%	0%	2%	4%	3%	3%
	2	20%	-22%	-6%	-18%	3%	-2%	11%	8%	11%
<i>DR2</i>	0.5	-3%	-7%	-7%	-4%	-3%	-3%	-2%	-2%	-3%
	1	0%	-10%	-3%	-3%	-1%	-1%	-1%	-1%	-1%
	2	24%	-15%	-8%	-15%	0%	-1%	8%	7%	12%
<i>DR3</i>	0.5	-8%	-8%	-6%	-6%	2%	2%	4%	3%	3%
	1	0%	-1%	-1%	-1%	2%	3%	4%	4%	3%
	2	8%	4%	-2%	-1%	5%	7%	4%	7%	11%
<i>DR4</i>	0.5	9%	-2%	9%	-1%	13%	8%	9%	8%	7%
	1	7%	-2%	-2%	-2%	2%	4%	7%	6%	5%
	2	-13%	-13%	-13%	6%	16%	18%	15%	18%	17%
<i>DRmax</i>	0.5	0%	-11%	-7%	-2%	0%	-1%	2%	1%	1%
	1	-1%	-11%	-5%	-4%	2%	3%	4%	4%	3%
	2	20%	-22%	-6%	-18%	3%	-2%	11%	8%	11%
<i>FA1</i>	0.5	32%	2%	2%	2%	14%	20%	27%	21%	18%
	1	15%	-7%	-1%	-1%	16%	29%	20%	19%	18%
	2	0%	0%	7%	0%	2%	4%	7%	6%	5%
<i>FA2</i>	0.5	21%	4%	14%	4%	14%	15%	16%	15%	15%
	1	7%	-6%	-6%	-6%	10%	19%	18%	17%	15%
	2	10%	-2%	5%	0%	1%	4%	5%	5%	5%
<i>FA3</i>	0.5	40%	-10%	24%	5%	27%	22%	20%	16%	15%
	1	-3%	-3%	-1%	-1%	2%	8%	6%	5%	4%
	2	-16%	-16%	3%	-1%	0%	3%	3%	5%	4%
<i>FA4</i>	0.5	24%	-10%	18%	1%	19%	15%	18%	15%	13%
	1	4%	4%	4%	4%	8%	18%	16%	14%	13%
	2	-25%	-10%	-1%	-1%	10%	11%	11%	11%	10%
<i>FAmix</i>	0.5	24%	-10%	18%	1%	20%	15%	18%	16%	14%
	1	-1%	-1%	-1%	-1%	7%	18%	11%	11%	10%
	2	-1%	-1%	5%	4%	4%	5%	5%	5%	4%
<i>BPR1</i>	0.5	2%	-20%	-12%	-7%	0%	-1%	0%	-1%	-1%
	1	-4%	-16%	-6%	-6%	1%	1%	1%	1%	1%
	2	22%	-21%	-5%	-21%	5%	-2%	17%	13%	18%
<i>BPR2</i>	0.5	-22%	-15%	-14%	-14%	-4%	-4%	1%	0%	-1%
	1	-5%	-8%	-5%	-5%	-2%	-5%	-5%	-5%	-5%
	2	19%	-6%	-6%	-7%	-5%	-2%	7%	5%	13%
<i>BPR3</i>	0.5	-47%	-28%	-1%	-28%	14%	21%	31%	30%	30%
	1	17%	-9%	-9%	-9%	13%	15%	17%	16%	15%
	2	-9%	-9%	-9%	0%	14%	17%	12%	18%	16%
<i>BPR4</i>	0.5	4%	-1%	4%	-1%	6%	3%	4%	3%	3%
	1	4%	-1%	0%	0%	2%	3%	1%	1%	1%
	2	-58%	-58%	-58%	6%	43%	59%	32%	60%	54%
<i>CPR1</i>	0.5	-24%	-24%	-18%	-18%	-5%	-8%	-6%	-6%	-7%
	1	-54%	-38%	-32%	-33%	0%	11%	6%	5%	4%
	2	23%	-30%	-8%	-20%	5%	-1%	11%	8%	11%
<i>CPR2</i>	0.5	0%	-4%	-4%	-3%	-1%	-1%	-1%	-1%	-1%
	1	-2%	-4%	-3%	-4%	-1%	2%	2%	2%	1%
	2	-47%	-75%	-47%	-47%	29%	7%	23%	38%	35%
<i>CPR3</i>	0.5	-7%	-8%	-7%	-7%	-2%	2%	1%	1%	0%
	1	-28%	-28%	-12%	-12%	0%	0%	0%	-2%	-4%
	2	37%	12%	8%	-36%	9%	5%	2%	2%	5%

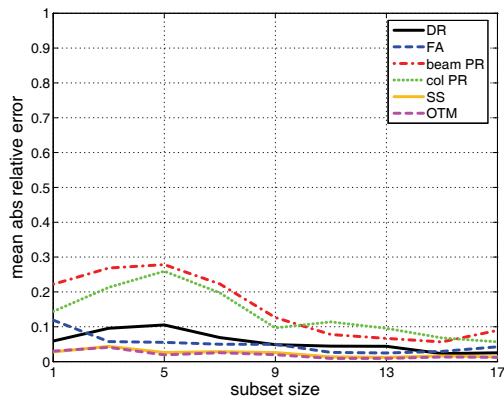
Table D-14 Subset Estimation Errors for the 84% EDP Response of the 4-Story RCMF Using Selection Method B on S_{di} Stripes (continued)

EDP	SF		84% EDP relative error									
			subset size									
			1	3	5	7	9	11	13	15	17	1
CPR4	0.5	4%	-2%	4%	-2%	7%	4%	4%	4%	4%	4%	4%
	1	139%	51%	51%	51%	66%	85%	51%	44%	38%	38%	
SS1	2	-34%	-29%	-29%	17%	24%	33%	17%	34%	30%	30%	
	0.5	-3%	-8%	-3%	-3%	0%	-1%	2%	1%	1%	1%	
SS2	1	-7%	-5%	0%	-1%	1%	2%	2%	1%	1%	1%	
	2	2%	2%	1%	1%	2%	2%	2%	1%	1%	1%	
SS3	0.5	-1%	-6%	-7%	-8%	-5%	-5%	-4%	-4%	-3%	-3%	
	1	3%	0%	0%	0%	0%	0%	0%	0%	0%	0%	
SS4	2	0%	3%	3%	0%	4%	3%	3%	2%	2%	2%	
	0.5	-12%	-5%	5%	-5%	5%	6%	8%	7%	6%	6%	
OTM1	1	5%	-1%	-1%	-1%	6%	5%	4%	4%	3%	3%	
	2	3%	-1%	-1%	1%	1%	1%	1%	2%	2%	2%	
OTM2	0.5	-4%	-4%	14%	-4%	15%	14%	14%	14%	14%	14%	
	1	18%	0%	4%	4%	8%	11%	7%	7%	7%	7%	
OTM3	2	-7%	-4%	-3%	-3%	6%	7%	7%	6%	6%	6%	
	0.5	-7%	0%	0%	0%	5%	4%	3%	2%	2%	2%	
OTM4	1	1%	0%	0%	0%	0%	1%	0%	0%	0%	0%	
	2	-5%	-5%	0%	0%	0%	0%	0%	0%	1%	1%	
OTM5	0.5	-7%	-3%	7%	-3%	8%	9%	7%	7%	7%	7%	
	1	7%	0%	0%	0%	3%	4%	3%	2%	2%	2%	
OTM6	2	-3%	-3%	-1%	-1%	0%	0%	1%	1%	1%	1%	
	0.5	-10%	-10%	8%	-10%	9%	12%	8%	7%	7%	7%	
OTM7	1	11%	-1%	0%	0%	4%	4%	4%	4%	4%	4%	
	2	-10%	-5%	-5%	-5%	-3%	-2%	0%	1%	2%	2%	
OTM8	0.5	-4%	-4%	14%	-4%	15%	14%	14%	14%	14%	14%	
	1	18%	0%	4%	4%	8%	11%	7%	7%	7%	7%	
OTM9	2	-10%	-7%	1%	1%	6%	6%	6%	5%	5%	5%	

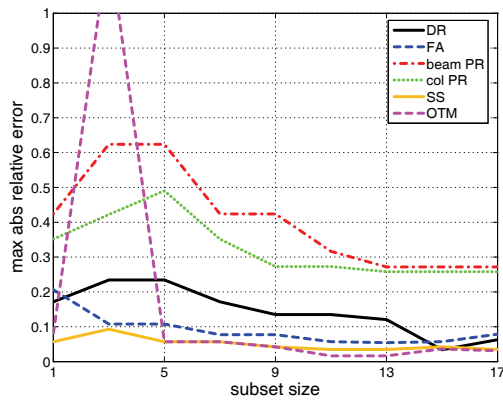
D.2.7 Random Subset Selection on S_{di} Scaling

To test further the actual potential of the subset selection technique based on S_{di} scaling, a number of trials with random selection of record subsets for the given S_{di} stripe were performed. As with the random S_a -based subset selection (Section D.2.5), the general idea is to understand whether the reduction in error with increasing subset size is the outcome of the selection process or if it should be attributed simply to the improvement expected with increasing subset size.

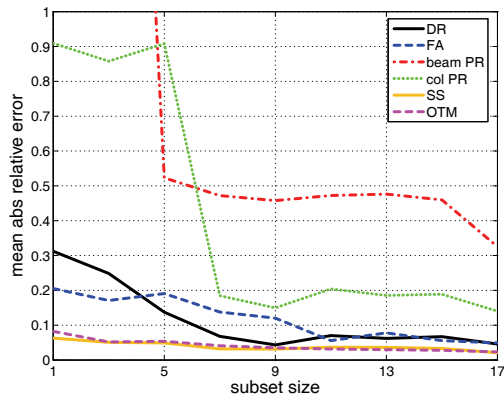
Figures D-55 and D-56 show results obtained for two of these randomized selection trials for the estimation of the 50% response. There are cases where the random selection may outperform the careful selection schemes, providing lower maximum and mean errors. Nevertheless, there are also many cases where the mean and maximum absolute errors are significantly larger and where the behavior is erratic, with the error sometimes increasing considerably with increasing subset size. It is apparent that the S_{di} scaling method offers superior performance to that of random selection, offering substantial robustness and a relative assurance of error reduction with larger sample sizes.



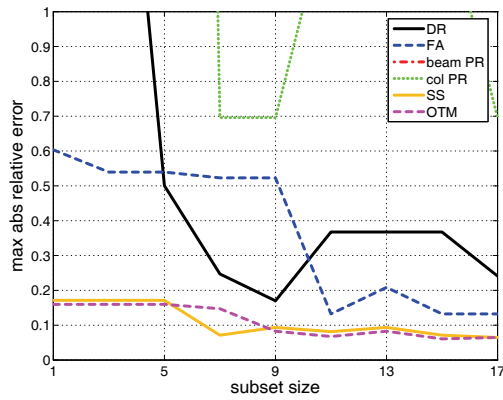
(a) 2-story, mean error



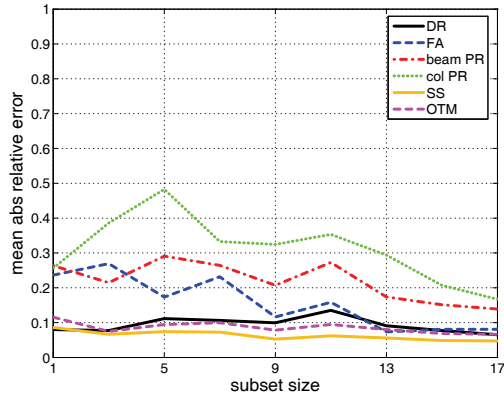
(b) 2-story, max error



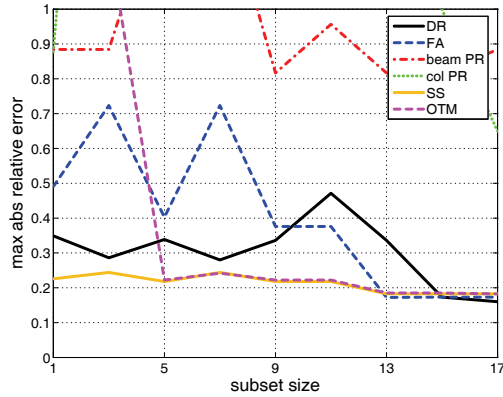
(c) 4-story, mean error



(d) 4-story, max error

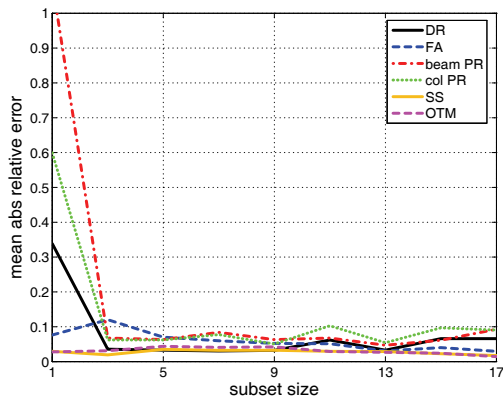


(e) 8-story, mean error

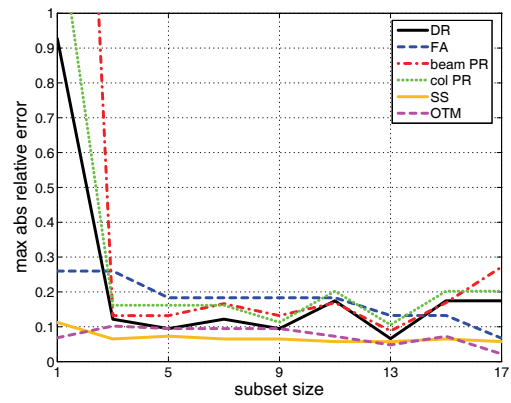


(f) 8-story, max error

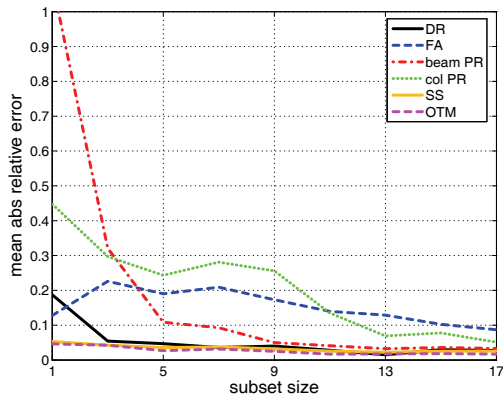
Figure D-55 Mean and maximum absolute relative error for different EDP types over all 3 scale factors when randomly selecting subsets within an S_{di} stripe to estimate the 50% response (Trial 1).



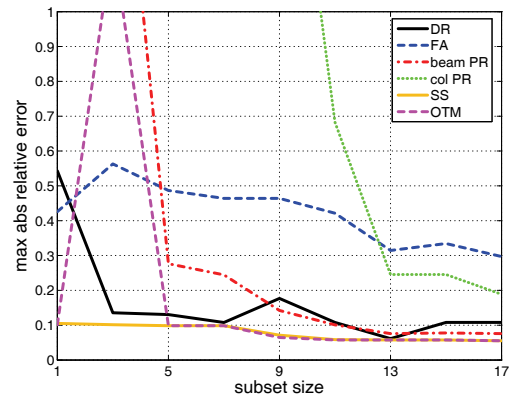
(a) 2-story, mean error



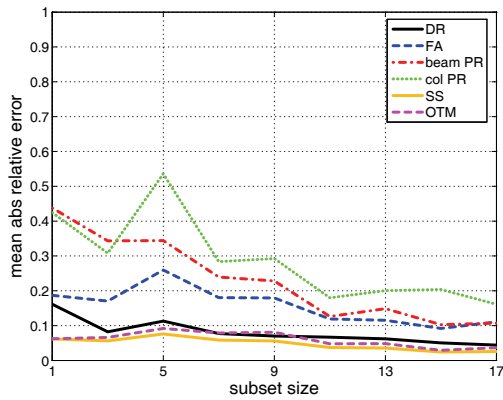
(b) 2-story, max error



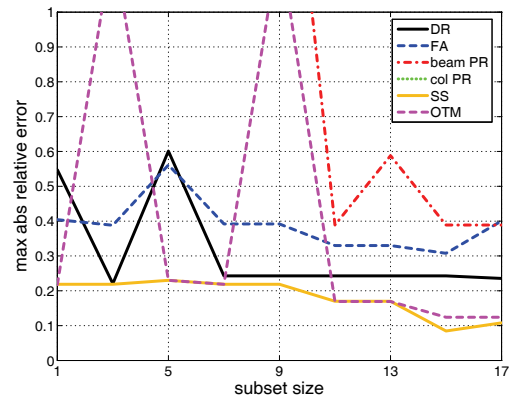
(c) 4-story, mean error



(d) 4-story, max error



(e) 8-story, mean error



(f) 8-story, max error

Figure D-56 Mean and maximum absolute relative error for different EDP types over all 3 scale factors when randomly selecting subsets within an S_{di} stripe to estimate the 50% response (Trial 2).

D.3 Characterization of Distributions of Response Quantities

There is adequate work in the literature to suggest that PGA and $S_a(T_I)$ scaling result in approximately lognormal distributions of the resulting EDP responses.

Nevertheless, this has only been tested for global EDP responses, such as roof displacement and maximum story drift. There is reason enough to suggest that the PGV scaling that corresponds to the FEMA P-695 scheme should have similar qualities. Still, little has been done to test the effect of $S_{di}(T_I)$ scaling on the resulting distributions. It is plausible that the nonlinear scaling effect introduced by $S_{di}(T_I)$ scaling may remove some of the extreme responses that make the lognormal distribution so attractive, especially as the intensity increases, perhaps opening the way to consider a normal distribution assumption. Therefore, in the following pages the normality or log-normality of the distributions of various EDPs is tested for both $S_a(T_I)$ and $S_{di}(T_I)$ scaling.

Robust or non-robust measures may be used to define the distribution against which to test. For example, for the lognormal, defining the parameters of the distribution by using the mean and the standard deviation of the natural log of the data is a non-robust measure as it is vulnerable to extremely low or high values, i.e., outliers. On the other hand, estimating the log-mean by the median of the log-data and the dispersion by one half the difference of the 16% and 84% quantiles of the log-data is more robust and generally will yield much better results for lognormal distributions. For the normal distribution, robust estimators may sometimes work well and sometimes not as well. Nevertheless, since the results described herein generally support the assumption of a lognormal distribution, use of robust estimators as described above is preferable. Thus, for N samples of EDP response, namely EDP_1 to EDP_N , and using the operator $[\cdot]_{x\%}$ (e.g., $[EDP]_{x\%}$) to denote the calculation of the $x\%$ fractile of a sample, the preferred estimators for the parameters of a lognormal distribution are as follows:

$$m = [\ln EDP]_{50\%}$$

$$\beta \cong \frac{1}{2} ([\ln EDP]_{84\%} - [\ln EDP]_{16\%}) \cong [\ln EDP]_{84\%} - [\ln EDP]_{50\%} \quad (D-10)$$

where m = log-mean and β = dispersion of a lognormal distribution. Of the two alternative formulations presented above for the dispersion β , the first one is more accurate as it uses symmetric fractile values on both sides of the median; this form is used for the following results. The second expression might become preferable as it involves use of the higher fractiles only. Thus, it places heavier weight on the higher demands which are of engineering interest, producing in general more conservative results when using probabilistic approaches as discussed in Chapter 9.

The distributions of EDP responses obtained using ground motions scaled to common values of S_a or S_{di} were tested for normality and lognormality using the standard Kolmogorov-Smirnoff goodness-of-fit test for normality (or, with equivalent results,

the Lilliefors version). The resulting acceptance p-values are tabulated in the following sections. When such a value is higher than a specific p-value, such as 5%, it means that any departure from the assumed distribution is (with the probability of the p-value) an artifact of the sample, rather than an “irrefutable” statistical fact.

D.3.1 Distribution of EDPs obtained with S_a Scaling

The distribution of the responses was checked against normal and lognormal assumptions for the 2-, 4-, and 8-story RCMFs, for S_a levels centered at the three scaling levels.

Results are shown in graphical format as Q-Q (quantile-quantile) plots in Figures D-57 to D-59 for the peak floor accelerations and story drifts for both normal and lognormal distributions; any significant deviation of the data from the straight lines plotted in Figures D-57 to D-59 would indicate an inadequate fit. Results from Kolmogorov-Smirnoff (K-S) goodness-of-fit tests appear in Tables D-15 to D-17 for all EDPs. The normal distribution provides a good fit for several EDPs, performing well for story shears and overturning moments, but fails to represent many story drifts, floor accelerations, and plastic hinge rotations well. The lognormal distribution generally provides a better fit to the EDPs than a normal distribution, and the lognormal distribution assumption cannot be rejected except for several cases involving the beam and column plastic hinge rotations (PHRs). Even for the lognormal fits, the lower and upper tails of the distributions of EDP values often are higher than would be expected based on a lognormal distribution, indicated by values that plot to the right of the line on the Q-Q plots. These plots also indicate that lognormal distributions, although adequate, may sometimes offer lower acceptance values for floor accelerations compared to other EDPs.

With regard to the plastic hinge rotations, in several cases, the acceptance p-values are nearly zero, indicating it is very unlikely that the underlying (true) distributions of plastic hinge rotations are normal or lognormal. This may be attributed to the nature of plastic hinge rotations, which (1) depend on the formation of particular inelastic mechanisms and (2) remain zero for deformations below the yield rotation, and then increase in proportion to the imposed deformation. Thus, as explained earlier when discussing dispersions, there are many near-zero values at each intensity level that distort the results.

To improve understanding of this issue it is useful to observe what happens for an isolated case, e.g., the 4th story beam plastic hinge rotations for the 4-story RCMF that appear for a scale factor of SF=2 in Figure D-60. The abundance of the near-zero plastic hinge rotations, typically below 0.0004, is apparent. Since values of engineering interest are mainly the higher values of demands, it becomes advantageous to trim all near-zero values and then fit a distribution to the remaining values. Thus, if all values less than 0.00038 are removed, a robust fit to the trimmed sample produces a dispersion $\beta = 1.17$ (close to the value of 1.25 determined for the

complete sample), while the mean increases to 0.0017 rad, from a value of 0.00039 rad obtained for the untrimmed sample. As seen in Figure D-61, the new fit is much improved and would be accepted by the goodness-of-fit test, having a p-value of 0.51. It could be argued that the resulting distribution no longer describes the full sample of response, nevertheless it constitutes an accurate description of the range of higher values and provides the means for a conservative assessment.

Table D-15 Acceptance Values for Testing the Distribution for S_a -Scaling at Levels Corresponding to Normalized Scale Factors of 0.5, 1.0, and 2.0 for the 2-story RCMF

EDP	Normal Assumption			Lognormal Assumption		
	0.5	1	2	0.5	1	2
DR1	92%	85%	5%	96%	73%	44%
DR2	67%	83%	7%	76%	88%	27%
DRmax	92%	85%	5%	96%	73%	44%
FA1	28%	1%	14%	55%	10%	66%
FA2	7%	54%	73%	14%	65%	77%
FAmix	3%	18%	34%	7%	42%	86%
BPR1	24%	79%	2%	17%	69%	32%
BPR2	58%	0%	12%	66%	39%	99%
CPR1	45%	80%	8%	10%	57%	74%
CPR2	0%	72%	16%	0%	70%	63%
SS1	66%	79%	31%	63%	85%	27%
SS2	6%	40%	11%	12%	62%	19%
OTM1	55%	83%	7%	62%	82%	9%
OTM2	6%	40%	12%	12%	62%	20%
collapses	0	0	0	0	0	0
misfit	2	2	3	1	0	0

*The highlighted cells show where the acceptance value is lower than or equal to 5%, signaling a probable misfit at the 95% confidence level.

Table D-16 Acceptance Values for Testing the Distribution for S_a -Scaling at Levels Corresponding to Normalized Scale Factors of 0.5, 1.0, and 2.0 for the 4-story RCMF

EDP	Normal Assumption			Lognormal Assumption		
	0.5	1	2	0.5	1	2
DR1	48%	91%	32%	43%	88%	99%
DR2	98%	91%	13%	99%	95%	35%
DR3	33%	85%	77%	46%	84%	70%
DR4	47%	60%	3%	51%	67%	29%
DRmax	53%	73%	24%	49%	68%	37%
FA1	52%	40%	46%	89%	76%	55%
FA2	32%	26%	28%	77%	54%	88%
FA3	31%	54%	51%	52%	76%	52%
FA4	26%	41%	29%	45%	74%	90%
PFAmax	26%	3%	40%	45%	14%	59%
BPR1	77%	51%	12%	55%	26%	52%
BPR2	48%	99%	20%	38%	94%	81%
BPR3	0%	75%	58%	0%	96%	93%
BPR4	40%	97%	0%	47%	98%	0%
CPR1	18%	76%	38%	11%	100%	99%
CPR2	64%	92%	0%	54%	90%	0%
CPR3	24%	0%	8%	31%	0%	35%
CPR4	14%	0%	0%	23%	0%	94%
SS1	61%	79%	90%	60%	89%	81%
SS2	63%	98%	95%	70%	97%	97%
SS3	34%	99%	66%	39%	99%	57%
SS4	20%	41%	71%	44%	49%	81%
OTM1	72%	97%	76%	71%	96%	69%
OTM2	75%	95%	41%	72%	98%	32%
OTM3	17%	36%	59%	41%	34%	49%
OTM4	21%	41%	82%	44%	49%	91%
collapses	0	0	1	0	0	1
misfit	1	3	4	1	2	2

*The highlighted cells show where the acceptance value is lower than or equal to 5%.

Table D-17 Acceptance Values for Testing the Distribution for S_a -Scaling at Levels Corresponding to Normalized Scale Factors of 0.5, 1.0, and 2.0 for the 8-story RCMF

EDP	Normal Assumption			Lognormal Assumption		
	0.5	1	2	0.5	1	2
DR1	56%	84%	4%	84%	100%	87%
DR2	68%	36%	18%	81%	42%	77%
DR3	23%	41%	34%	32%	42%	41%
DR4	100%	81%	90%	99%	80%	97%
DR5	89%	48%	76%	99%	71%	88%
DR6	88%	55%	72%	95%	99%	95%
DR7	97%	25%	3%	93%	90%	29%
DR8	78%	65%	18%	86%	86%	61%
DRmax	24%	42%	3%	53%	50%	26%
FA1	26%	32%	9%	94%	92%	78%
FA2	38%	23%	10%	94%	99%	21%
FA3	75%	63%	75%	100%	85%	97%
FA4	12%	9%	11%	85%	74%	92%
FA5	5%	15%	15%	74%	43%	42%
FA6	19%	5%	4%	90%	44%	51%
FA7	74%	28%	7%	97%	85%	40%
FA8	41%	45%	37%	98%	81%	53%
FAmax	26%	28%	10%	88%	84%	66%
BPR1	57%	35%	4%	63%	58%	71%
BPR2	81%	71%	52%	54%	95%	95%
BPR3	28%	77%	69%	59%	89%	91%
BPR4	41%	55%	93%	43%	90%	82%
BPR5	5%	54%	94%	100%	56%	84%
BPR6	0%	13%	18%	78%	72%	67%
BPR7	0%	0%	1%	3%	22%	93%
BPR8	88%	0%	0%	73%	0%	0%
CPR1	22%	35%	5%	51%	22%	58%
CPR2	89%	0%	0%	96%	0%	9%
CPR3	35%	0%	0%	31%	0%	7%
CPR4	91%	4%	0%	97%	12%	1%
CPR5	58%	1%	0%	61%	6%	0%
CPR6	74%	0%	0%	98%	5%	0%

Table D-17 Acceptance Values for Testing the Distribution for S_a -Scaling at Levels Corresponding to Normalized Scale Factors of 0.5, 1.0, and 2.0 for the 8-story RCMF (continued)

EDP	Normal Assumption			Lognormal Assumption		
	0.5	1	2	0.5	1	2
CPR7	90%	0%	0%	83%	2%	0%
CPR8	54%	0%	0%	62%	1%	0%
SS1	77%	19%	36%	77%	20%	33%
SS2	92%	80%	64%	89%	86%	60%
SS3	58%	98%	41%	74%	98%	52%
SS4	82%	80%	83%	97%	89%	74%
SS5	69%	31%	83%	49%	27%	82%
SS6	91%	66%	70%	86%	43%	78%
SS7	99%	93%	86%	88%	98%	86%
SS8	59%	98%	84%	77%	99%	73%
OTM1	11%	85%	85%	13%	80%	68%
OTM2	37%	89%	93%	52%	78%	95%
OTM3	38%	39%	84%	44%	22%	80%
OTM4	99%	59%	77%	87%	33%	60%
OTM5	89%	75%	41%	88%	76%	34%
OTM6	99%	90%	48%	96%	95%	38%
OTM7	64%	96%	56%	100%	100%	44%
OTM8	60%	98%	70%	77%	99%	80%
collapses	0	1	1	0	1	1
Misfit	3	10	14	1	5	6

*The highlighted cells show where the acceptance value is lower than or equal to 5%.

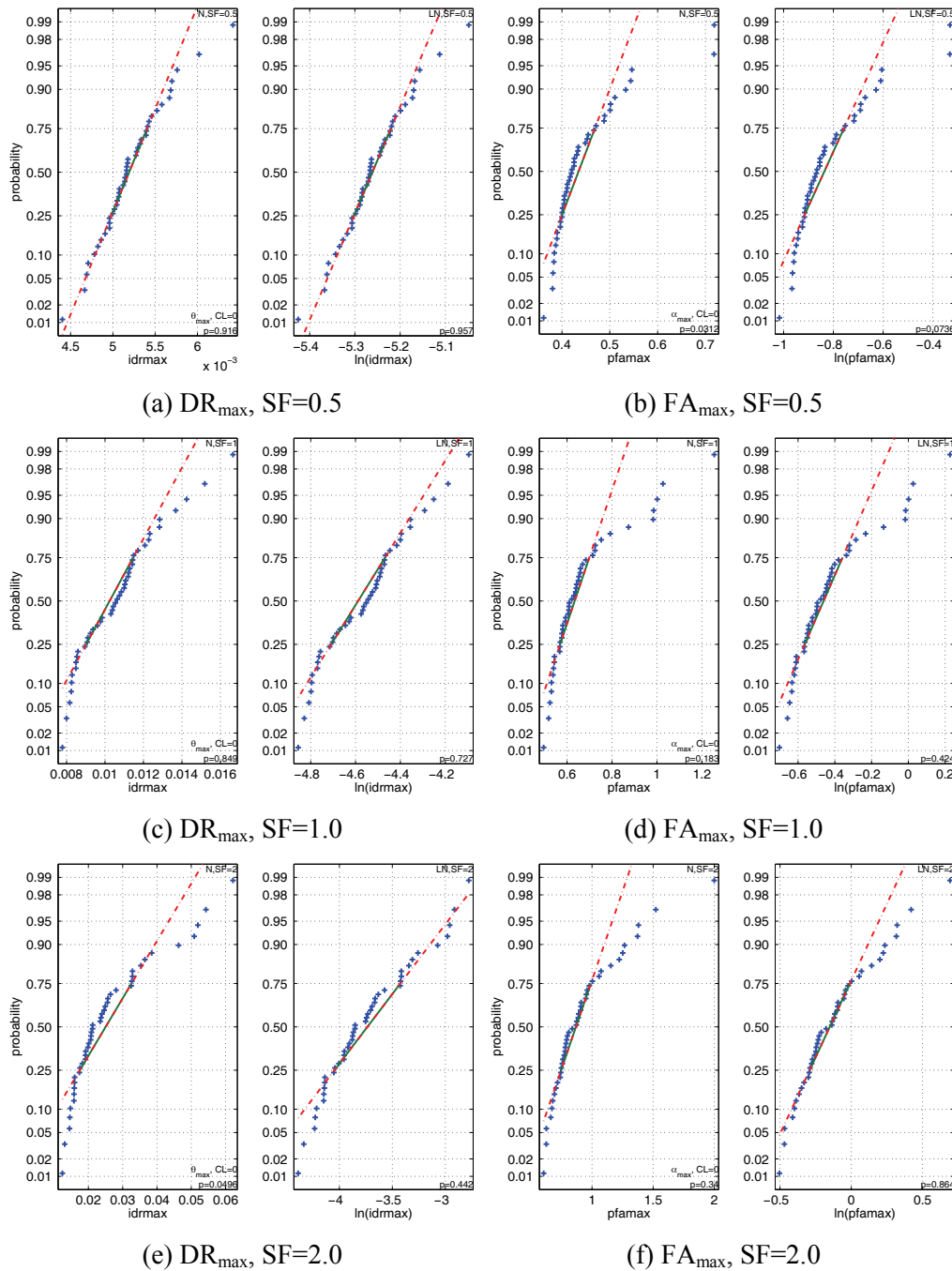


Figure D-57 Normal probability plots to test for normality (N) and lognormality (LN) of maximum story drift (DR_{max}) and maximum floor acceleration (FA_{max}) over all stories given S_a -scaling for the 2-story RCMF.

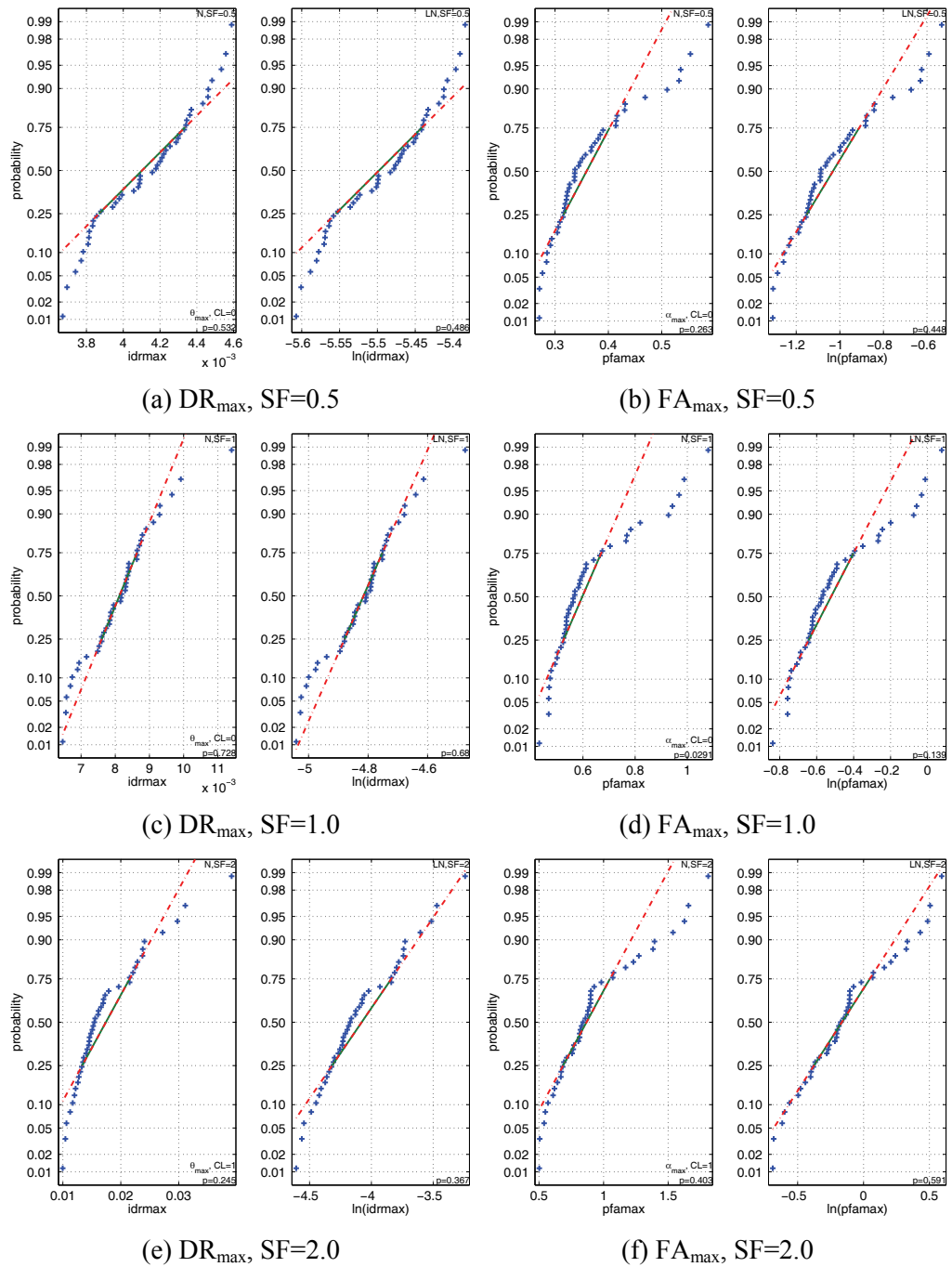


Figure D-58 Normal probability plots to test for normality (N) and lognormality (LN) of maximum story drift (DR_{max}) and maximum floor acceleration (FA_{max}) over all stories given S_a -scaling for the 4-story RCMF.

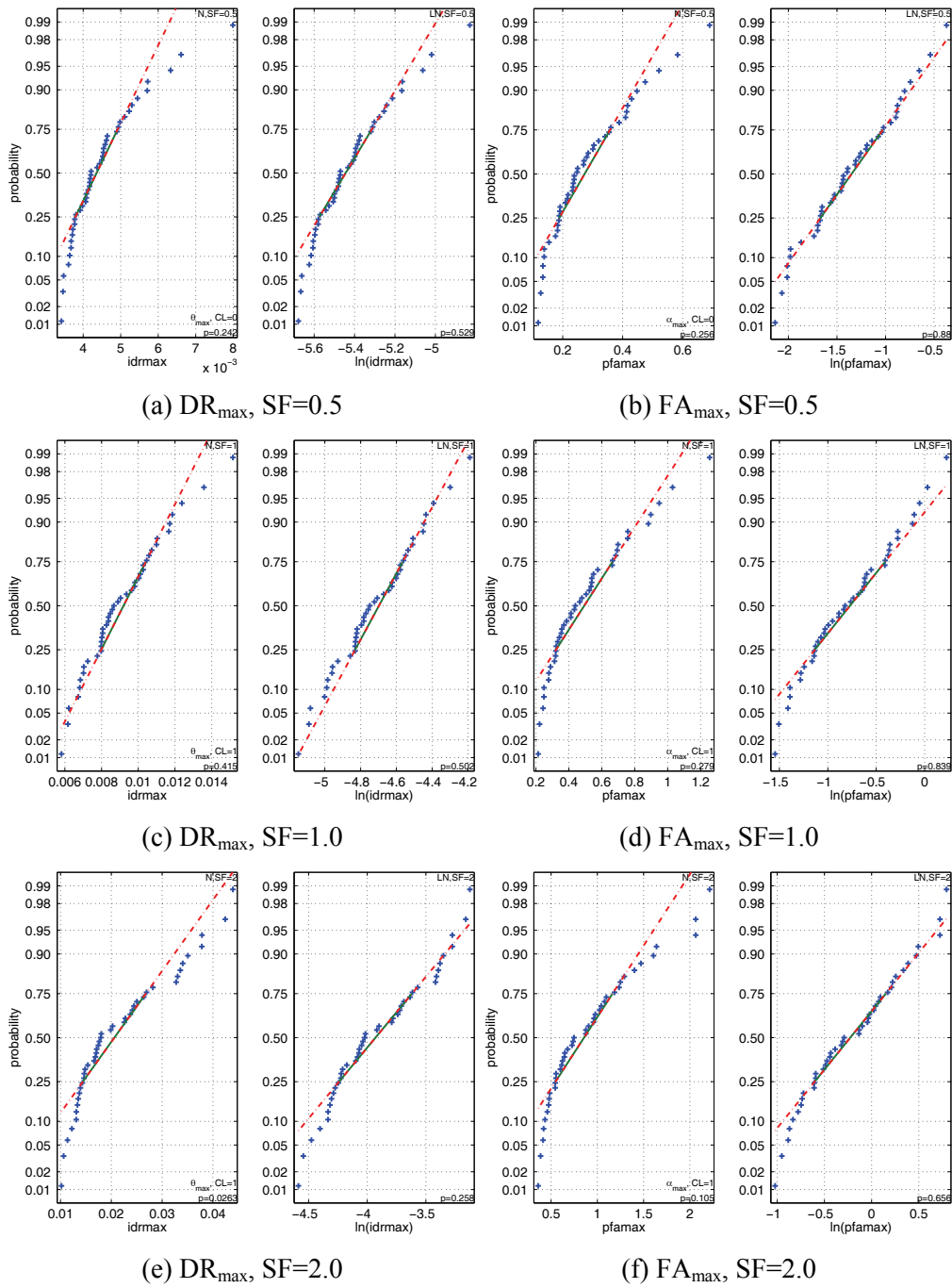


Figure D-59 Normal probability plots to test for normality (N) and lognormality (LN) of maximum story drift (DR_{max}) and maximum floor acceleration (FA_{max}) over all stories given S_a -scaling for the 8-story RCMF.

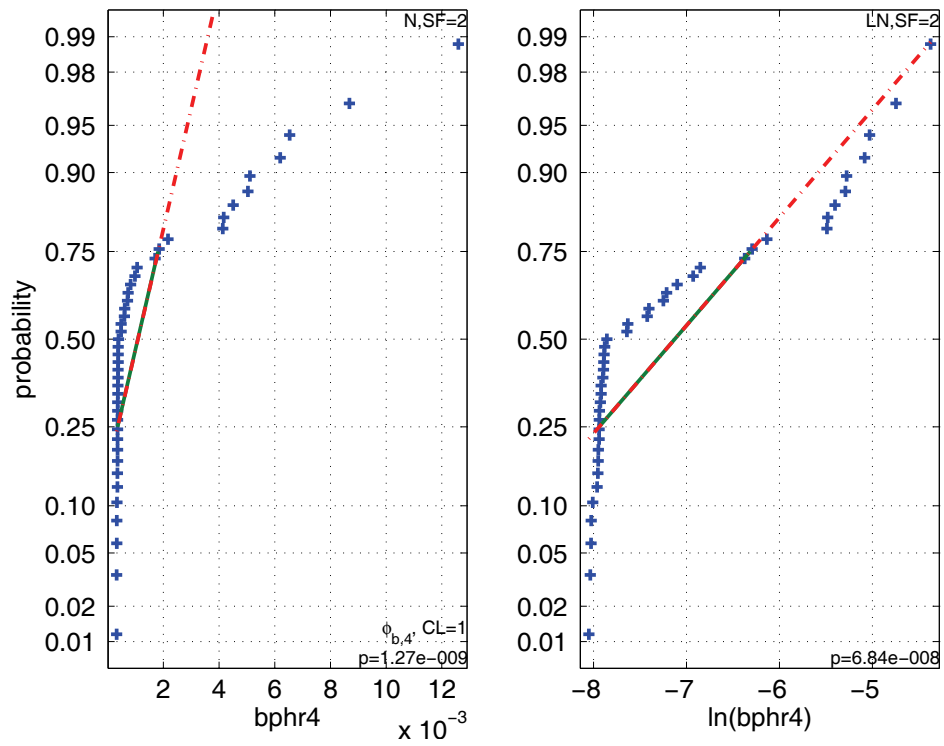


Figure D-60 Normal probability plots to test for normality (N) and lognormality (LN) of the 4th floor maximum beam plastic hinge rotation given S_a -scaling for the 4-story RCMF at SF=2. The near-zero values make both distributions inadequate.

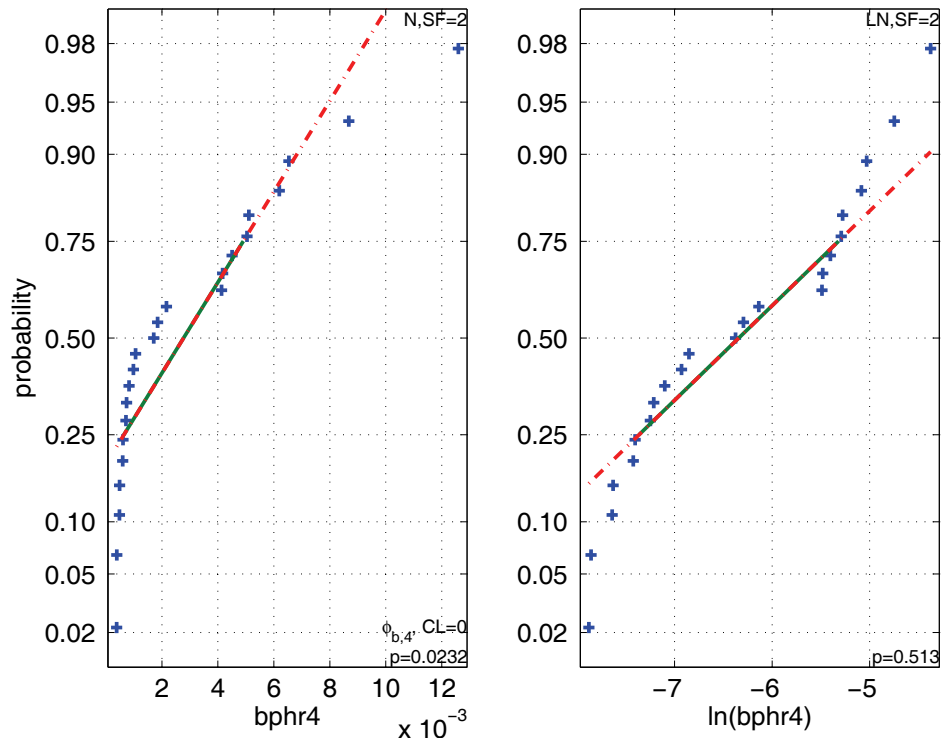


Figure D-61 Testing the same data as in the above Figure D-60 after trimming values lower than 0.00038 rad. The lognormal fit is now acceptable, having similar dispersion but higher mean than before.

D.3.2 Distribution of EDPs Obtained with S_{di} Scaling

Just as for S_a scaling (Section D.3.1), distributions of EDPs were determined at each of three S_{di} intensity levels, which correspond to median values of S_{di} obtained for the FEMA P-695 motions scaled by factors of 0.5, 1.0, and 2.0, and the distribution of EDP responses were tested for normality and lognormality. Just as for S_a scaling, robust measures were used to determine the parameters of the lognormal distribution (Equation D-10).

The resulting acceptance p-values appear in Tables D-18 through 20. The results indicate that the normal distribution is a good option for drift-related quantities, while in several cases it is inadequate for acceleration and force-based quantities. This fact represents a partial reversal of the observations made for the normal distribution for S_a scaling, where it was found improper for several drift and some acceleration EDPs but not for story shears or overturning moments. On the other hand, the lognormal achieves good results for practically all buildings, scale factors, and EDPs considered, with the exception of some beam and column plastic rotations due to the presence of near-zero values, a problem that also occurs with the normal distribution.

To understand better the reasons for these results, Figures D-62 through D-64 plot the the Q-Q (quantile-quantile) or normal/lognormal probability plots for maximum drift ratio over the height (DR_{\max}) and maximum floor acceleration over the height (FA_{\max}) for each of the three buildings. There are some significant outliers in the right tail, indicating large response values that cannot be accounted for by the normal distribution. In some isolated cases, even the lognormal is inadequate to describe such large departures from the mean. This happens mostly for beam and column plastic hinge rotations due to the presence of large numbers of near-zero values. In such cases, trimming the lower values, which are not of engineering interest, allows satisfactory lognormal fits, as discussed in the previous section.

Table D-18 Acceptance Values for Testing the Distribution for S_{dr} -Scaling at Levels Corresponding to Normalized Scale Factors of 0.5, 1.0, and 2.0 for the 2-story RCMF

EDP	Normal Assumption			Lognormal Assumption		
	0.5	1	2	0.5	1	2
DR1	94%	67%	62%	96%	57%	81%
DR2	62%	10%	54%	64%	22%	99%
DRmax	94%	67%	62%	96%	57%	81%
FA1	34%	3%	80%	64%	14%	100%
FA2	13%	62%	64%	24%	68%	93%
FAmx	8%	49%	49%	16%	62%	93%
PHR1	32%	72%	71%	26%	85%	98%
BPR2	76%	0%	25%	82%	31%	99%
CPR1	34%	72%	65%	7%	62%	58%
CPR2	0%	7%	55%	0%	74%	90%
SS1	46%	78%	27%	45%	78%	23%
SS2	4%	14%	6%	10%	28%	13%
OTM1	74%	68%	13%	79%	67%	16%
OTM2	4%	14%	33%	10%	28%	40%
collapses	0	0	1	0	0	1
misfit	3	2	0	1	0	0

*The bold values show where the acceptance value is lower than or equal to 5%, signaling a probable misfit at the 95% level.

Table D-19 Acceptance Values for Testing the Distribution for S_{dl} -Scaling at Levels Corresponding to Normalized Scale Factors of 0.5, 1.0, and 2.0 for the 4-story RCMF

EDP	Normal Assumption			Lognormal Assumption		
	0.5	1	2	0.5	1	2
DR1	43%	89%	26%	38%	89%	90%
DR2	80%	76%	81%	90%	84%	87%
DR3	30%	96%	48%	43%	95%	71%
DR4	27%	57%	22%	35%	57%	87%
DRmax	46%	94%	69%	45%	89%	98%
FA1	48%	59%	48%	95%	91%	81%
FA2	41%	3%	15%	72%	13%	34%
FA3	29%	37%	24%	52%	61%	55%
FA4	26%	67%	38%	38%	76%	72%
FAmix	26%	10%	8%	38%	27%	16%
BPR1	65%	57%	57%	52%	45%	96%
BPR2	43%	99%	73%	35%	99%	90%
BPR3	0%	43%	28%	0%	55%	88%
BPR4	44%	71%	0%	52%	84%	0%
CPR1	21%	77%	22%	10%	72%	54%
CPR2	87%	66%	0%	77%	71%	0%
CPR3	35%	0%	3%	37%	2%	46%
CPR4	20%	0%	0%	32%	0%	84%
SS1	83%	62%	90%	83%	67%	97%
SS2	72%	99%	79%	78%	99%	77%
SS3	46%	99%	53%	52%	99%	46%
SS4	17%	66%	83%	37%	69%	74%
OTM1	70%	83%	82%	69%	82%	76%
OTM2	68%	76%	37%	65%	83%	29%
OTM3	23%	79%	90%	51%	79%	90%
OTM4	17%	67%	63%	37%	69%	56%
collapses	0	0	0	0	0	0
misfit	1	3	4	1	2	2

*The bold values show where the acceptance value is lower than or equal to 5%.

Table D-20 Acceptance Values for Testing the EDP Distribution for S_{dr} -Scaling at Levels Corresponding to Normalized Scale Factors of 0.5, 1.0, and 2.0 for the 8-story RCMF

EDP	Normal Assumption			Lognormal Assumption		
	0.5	1	2	0.5	1	2
DR1	81%	39%	65%	75%	38%	71%
DR2	70%	93%	94%	88%	91%	56%
DR3	20%	86%	47%	26%	98%	35%
DR4	68%	48%	98%	60%	51%	98%
DR5	87%	55%	57%	100%	75%	96%
DR6	74%	84%	63%	92%	97%	80%
DR7	80%	47%	7%	77%	88%	22%
DR8	78%	94%	8%	80%	79%	52%
DRmax	15%	69%	89%	35%	63%	93%
FA1	29%	69%	59%	81%	35%	92%
FA2	35%	54%	85%	96%	66%	87%
FA3	70%	89%	43%	97%	79%	100%
FA4	16%	44%	83%	94%	96%	99%
FA5	6%	28%	65%	76%	68%	65%
FA6	18%	55%	3%	86%	78%	73%
FA7	81%	25%	5%	92%	96%	80%
FA8	39%	71%	19%	96%	78%	73%
FAmix	17%	52%	60%	79%	45%	100%
BPR1	59%	42%	83%	72%	26%	63%
BPR2	89%	49%	35%	66%	98%	16%
BPR3	10%	93%	70%	73%	89%	43%
BPR4	40%	77%	64%	45%	97%	98%
BPR5	6%	71%	66%	99%	31%	70%
BPR6	0%	25%	10%	79%	52%	45%
BPR7	0%	0%	1%	2%	40%	74%
BPR8	97%	0%	0%	91%	3%	0%
CPR1	28%	30%	91%	62%	43%	14%
CPR2	89%	0%	0%	98%	0%	7%
CPR3	81%	0%	0%	77%	1%	17%
CPR4	96%	66%	1%	96%	88%	22%
CPR5	81%	3%	0%	87%	24%	0%
CPR6	72%	0%	0%	95%	13%	13%

Table D-20 Acceptance Values for Testing the EDP Distribution for S_{dir} Scaling at Levels Corresponding to Normalized Scale Factors of 0.5, 1.0, and 2.0 for the 8-story RCMF (continued)

EDP	Normal Assumption			Lognormal Assumption		
	0.5	1	2	0.5	1	2
CPR7	78%	0%	0%	76%	7%	1%
CPR8	72%	0%	0%	74%	5%	0%
SS1	88%	48%	44%	88%	31%	51%
SS2	90%	90%	52%	85%	89%	67%
SS3	62%	93%	78%	76%	94%	81%
SS4	88%	43%	42%	99%	40%	54%
SS5	60%	25%	98%	42%	24%	96%
SS6	89%	57%	90%	84%	41%	90%
SS7	93%	87%	84%	99%	97%	99%
SS8	62%	98%	75%	81%	86%	73%
OTM1	26%	86%	56%	30%	81%	51%
OTM2	33%	52%	97%	48%	45%	91%
OTM3	87%	29%	27%	95%	15%	24%
OTM4	100%	57%	63%	87%	32%	64%
OTM5	100%	85%	75%	77%	45%	82%
OTM6	98%	88%	88%	97%	71%	64%
OTM7	66%	98%	43%	100%	97%	37%
OTM8	58%	98%	56%	77%	87%	80%
collapses	0	1	2	0	1	2
misfit	2	8	11	1	4	4

*The bold values show where the acceptance value is lower than or equal to 5%.

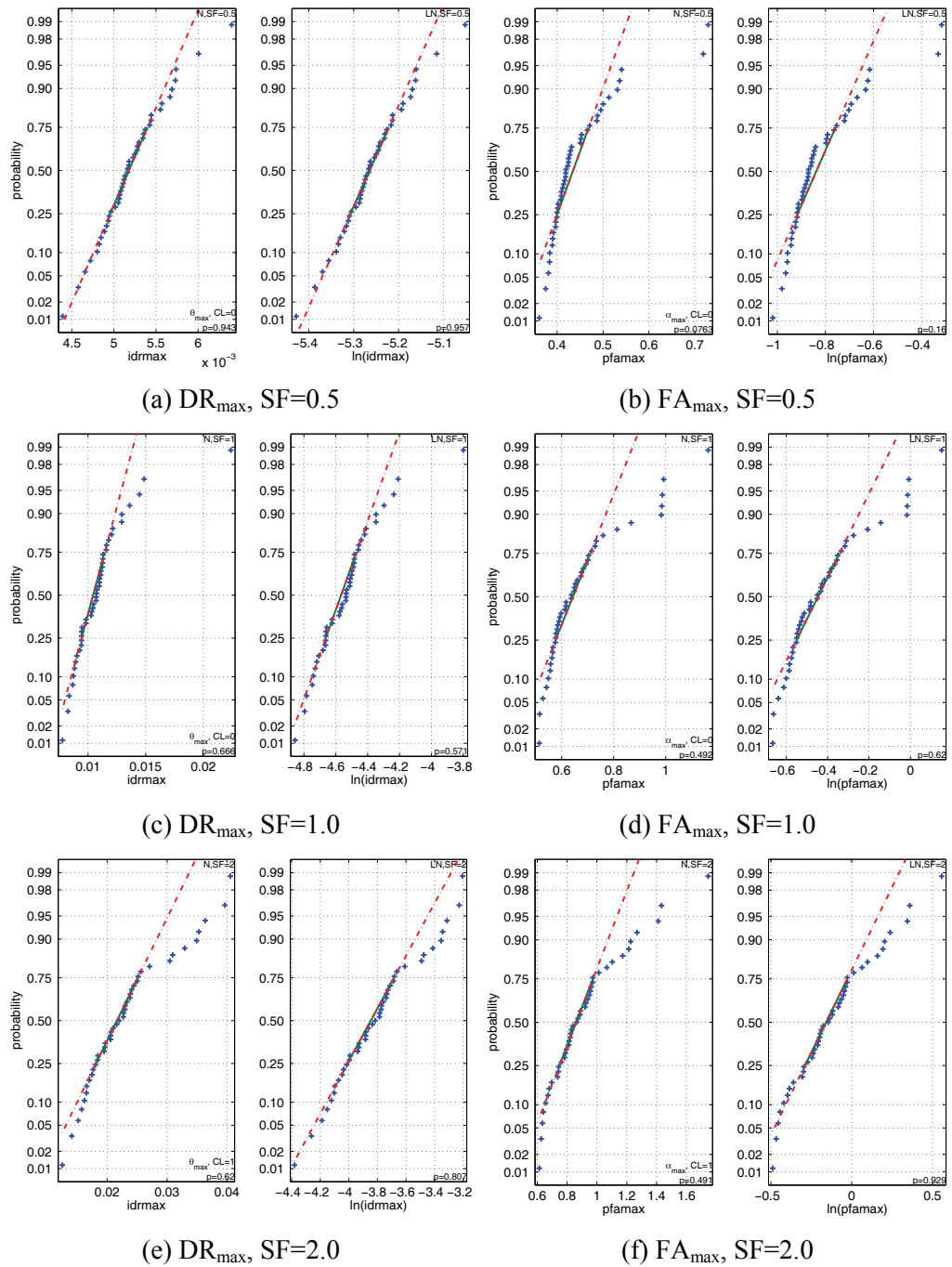


Figure D-62 Normal probability plots to test for normality (N) and lognormality (LN) of maximum story drift (DR_{max}) and maximum floor acceleration (FA_{max}) over all stories given S_{dr} -scaling for the 2-story RCMF.

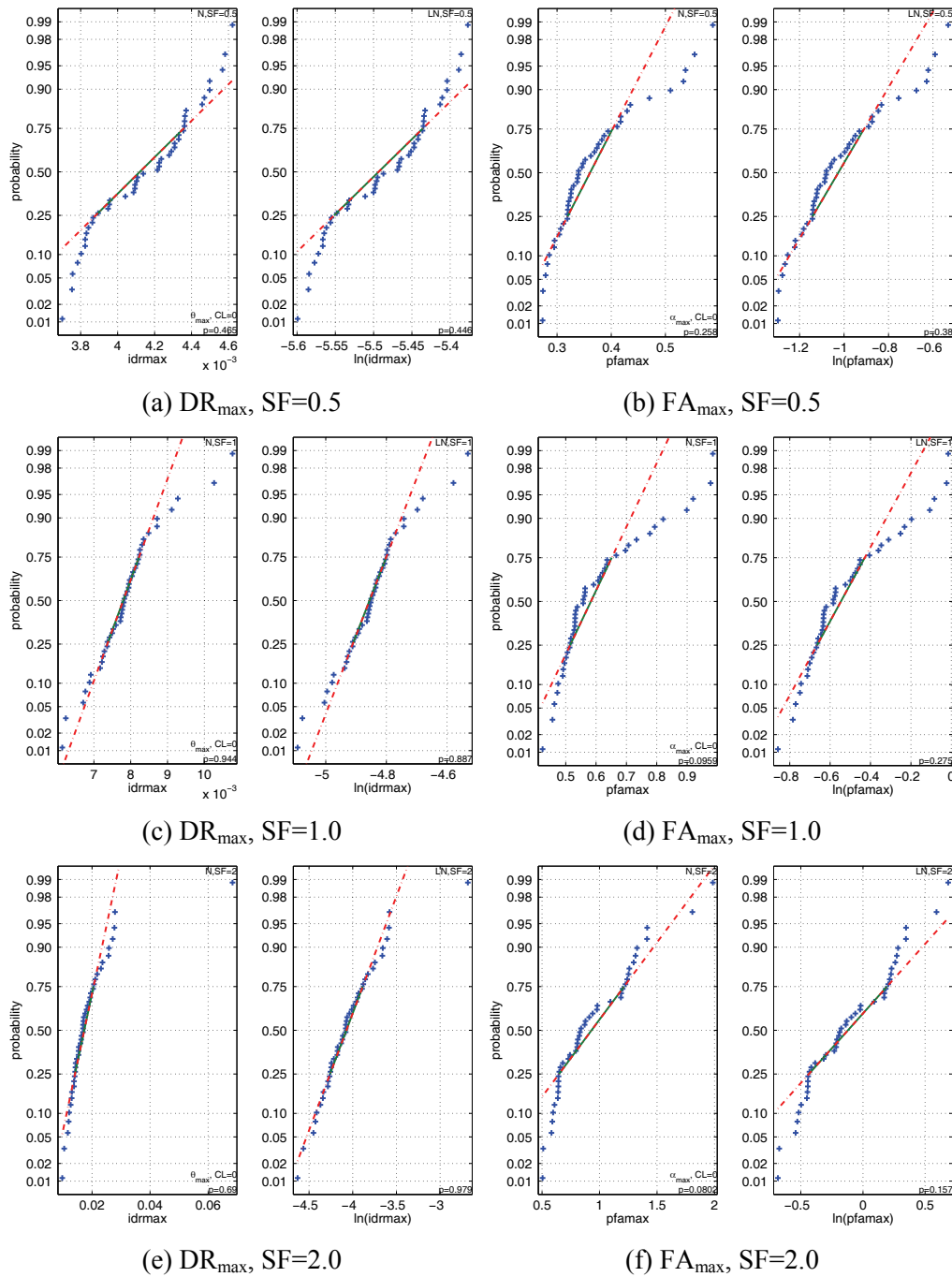


Figure D-63 Normal probability plots to test for normality (N) and lognormality (LN) of maximum story drift (DR_{max}) and maximum floor acceleration (FA_{max}) over all stories given S_d-scaling for the 4-story RCMF.

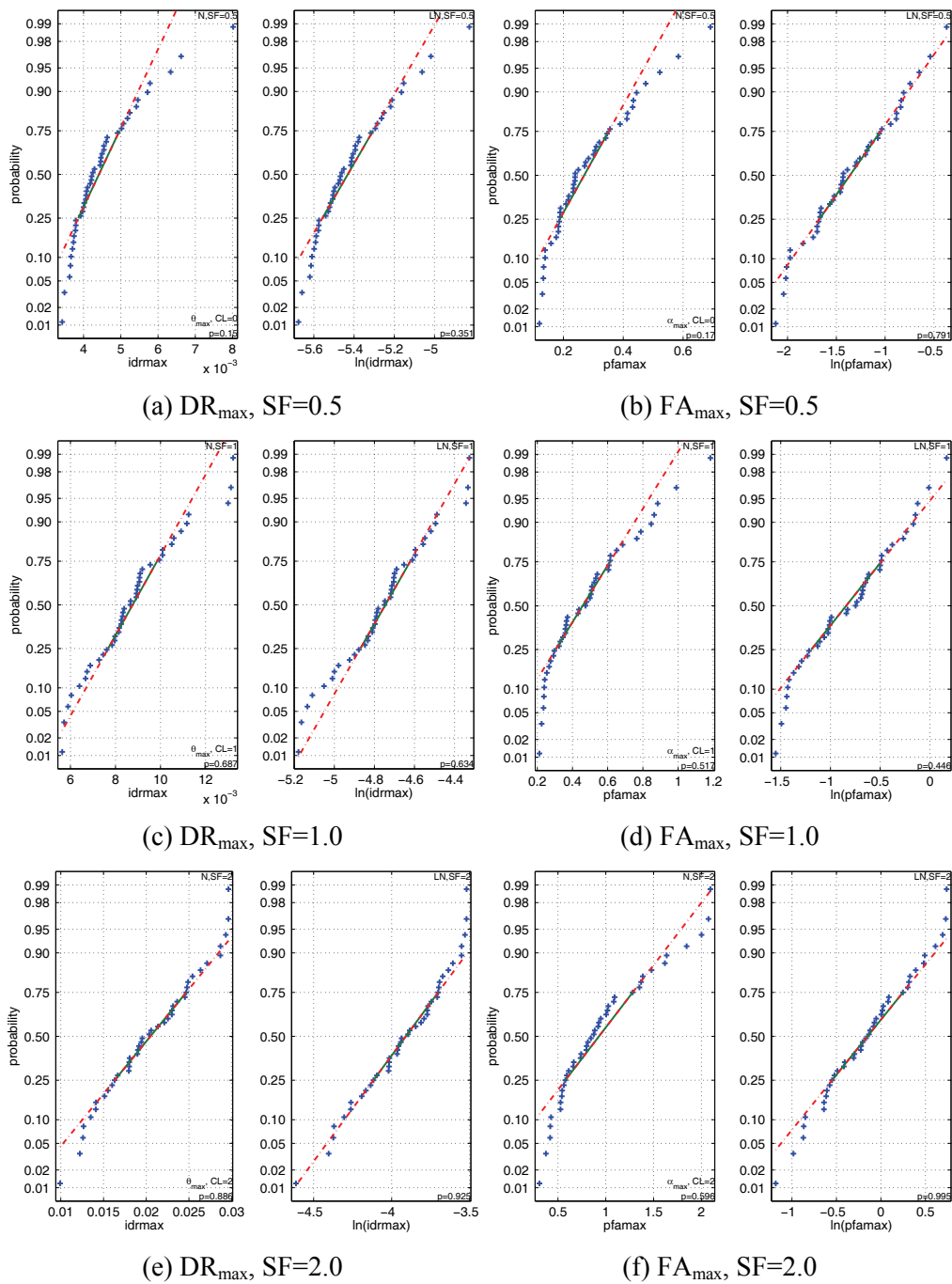


Figure D-64 Normal probability plots to test for normality (N) and lognormality (LN) of maximum story drift (DR_{max}) and maximum floor acceleration (FA_{max}) over all stories given S_{dI} -scaling for the 8-story RCMF.

D.4 Alternative Estimation of Dispersion Using Higher Intensity Levels

As expected, the estimation of EDP distributions with small subsets is prone to error. Since estimation of median values generally is simpler than characterization of dispersion, an alternative approach to estimating dispersion is investigated in this section: using the median response at a higher IM level to estimate the 84% EDP value obtained at a lower IM level.

While there are several theoretical arguments against such a proposition, there is evidence to suggest that, when away from the region of dynamic instability and well within the equal displacement rule, such a scheme may work. In this case, S_{di} was used as the IM and the following approach was used:

1. For a given PGV or $S_a(T_I)$ intensity level (established using scale factors of 0.5, 1.0, and 2.0), estimate the 50% and 84% S_{di} response of the equivalent oscillator. These are the Base (B) and the High (H) intensity levels, respectively.
2. Using ground motions scaled to the two S_{di} intensity levels, B and H, corresponding to the 50% and 84% response, perform response history analyses of the MDOF structure to estimate median EDPs using either the full set of records or a properly selected subset.
3. Estimate the dispersion of the EDP at the base level as $(EDP_{50\%}^H - EDP_{50\%}^B) / EDP_{50\%}^B$.

This estimation is attempted only for the maximum story drift response, which according to our earlier results should be one the EDPs that are easy to estimate, and at scale factors of 0.5, 1.0, and 2.0 using both FEMA P-695 (i.e., PGV) and $S_a(T_I)$ intensity levels as the basis. The results appear in Tables D-21 and D-22 respectively. The method performs better for the FEMA P-695 stripes than for the S_a stripes, where an obvious weakness of the design of the numerical experiment appears: The equivalent SDOF system has no dispersion at all for S_a stripes that correspond to intensities below the oscillator “yield point”. On the other hand, the MDOF system does indeed have at least some dispersion there due to the higher mode effects. In other words, the high efficiency of the $S_a(T_I)$ measure in the elastic region hurts this scheme, resulting in errors that reach almost 100%. It may be that a better equivalent SDOF system or some inclusion of higher mode effects in S_{di} (e.g., in the way of Luco and Cornell, 2007) could improve this substantially, at least when not using FEMA P-695 scaling. However, it should be noted that use of any assumed uniform value of beta between 0.29 and 0.58 outperforms the method tested here for FEMA P-695 intensity levels. Where the assumed value is less than 0.43, dispersion is underestimated, and where it is greater than 0.43, dispersion is overestimated, for these particular buildings.

Table D-21 Actual and Approximate Values of Dispersion (Standard Deviation of Natural Logs) at FEMA P-695 Intensity Levels as Estimated Using the Medians Obtained for Two Different S_{df} Intensity Levels

		scale factor	0.5	1.0	2.0
2-story	real		0.46	0.53	0.51
	approx		0.52	0.54	0.40
	Error		13%	0%	-21%
4-story	real		0.39	0.32	0.49
	approx		0.45	0.48	0.69
	error		17%	49%	39%
8-story	real		0.46	0.44	0.38
	approx		0.64	0.77	0.56
	error		39%	73%	48%
All	avg abs error		23%	41%	36%

Table D-22 Actual and Approximate Values of Dispersion (Standard Deviation of Natural Logs) at $S_a(T_1)$ Intensity Levels as Estimated Using the Medians Obtained for Two Different S_{df} Intensity Levels

		scale factor	0.5	1.0	2.0
2-story	real		0.07	0.16	0.67
	approx		0.01	0.01	0.25
	error		-90%	-93%	-62%
4-story	real		0.05	0.08	0.53
	approx		0.00	0.03	0.43
	error		-96%	-65%	-19%
8-story	real		0.24	0.27	0.87
	approx		0.00	0.04	0.17
	error		-99%	-85%	-80%
All	avg abs error		95%	81%	54%

Direct Determination of Target Displacement

This appendix presents results from an ancillary study undertaken to test the practicality of direct determination of target displacement for nonlinear static analyses.

E.1 Introduction

The displacement coefficient method and equivalent linearization have often been used to determine the target displacement to be used in nonlinear static (pushover) analysis. Two alternatives to these approaches are described in this appendix: (1) direct computation of the response of equivalent SDOF (ESDOF) oscillators to a suite of ground motion records, and (2) the use of a computational tool known as SPO2IDA. The first approach has the latitude to allow arbitrary hysteretic characteristics and specific ground motion records that may be considered characteristic of a particular site (e.g., magnitude, distance, and type of fault mechanism) to be incorporated directly in the estimate. The second approach makes use of a large database of results for SDOF systems having relatively complex capacity boundaries. Both approaches provide information on both central tendency (mean or median) and dispersion in target displacement. The approaches are described and illustrated with examples in this Appendix.

E.2 Direct Computation of Equivalent Single-Degree-of-Freedom Response

In this approach the response of an ESDOF oscillator is determined by nonlinear response history analysis to a suite of ground motions. The capacity curves obtained by nonlinear static analysis are approximated with a piecewise-linear curve (Appendix B, Figures B-15b, B-16b, B-17b). Based on the piecewise-linear approximation, the properties of the equivalent SDOF for the n^{th} mode are obtained as:

$$F_{y,n}^{ESDOF} = F_{y,n}^{MDOF} / M^* \quad (\text{E-1})$$

$$D_{y,n}^{ESDOF} = D_{y,n}^{MDOF} / \Gamma_n \quad (\text{E-2})$$

where M^* and Γ_n are listed in Tables B-1, B-2, B-3. The period of the corresponding ESDOF system is equal to:

$$T_n = 2\pi \left(L_n D_{y,n}^{ESDOF} / F_{y,n}^{ESDOF} \right)^{0.5} \quad (\text{E-3})$$

The damping of the MDOF reinforced concrete moment frames was equal to 5% of critical damping in the first and the third modes. For ESDOF systems for other modes (i.e., the second mode), viscous damping is calculated as:

$$\zeta_n = \frac{\alpha_0}{2} \frac{1}{\omega_n} + \frac{\alpha_1}{2} \omega_n \quad (\text{E-4})$$

where α_0 and α_1 are the Rayleigh damping coefficients used for the MDOF structures, and ω_n is the circular frequency of mode n . The damping coefficient ζ_2 was found equal to 2.28, 3.66 and 3.79 for the 2-, 4- and 8-story building, respectively.

Having established the properties of the ESDOF systems, nonlinear dynamic analyses are run for each ground motion of interest. Peak displacements in each analysis are multiplied by the modal participation factor to determine the corresponding peak displacement estimate for the MDOF system:

$$\delta_t^{MDOF} = \Gamma_n \delta_t^{ESDOF} \quad (\text{E-5})$$

Figures E-1 through E-3 compare ESDOF estimates of peak roof displacement with the actual peak roof displacements determined for the MDOF system responding to each ground motion record. The comparisons were done for scale factors of 0.5, 1.0, and 2.0 applied to the FEMA P-695 (FEMA, 2009b) far-field ground motion record set. The linear correlation coefficients are also provided in the legend. For all three buildings, almost perfect correlation is achieved for scaling factor equal to 0.5 where the buildings remain elastic. The correlations are on the order of 90% for the second level of intensity, while a reduction in correlation is evident for a scale factor of 2.0. In the latter case, the correlation coefficient is on the order of 80% for the lower, first-mode dominated buildings (2-story and 4-story RCMRF), while it decreases to 74% for the 8-story RCMRF.

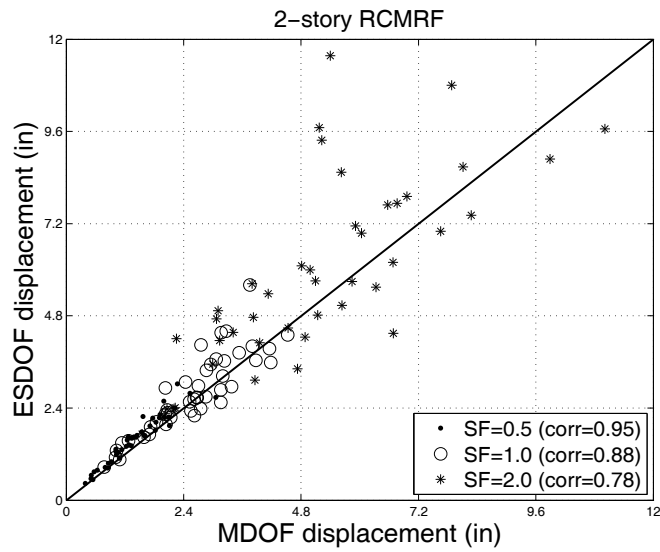


Figure E-1 Comparison of peak roof displacement estimates with actual values for 2-story RCMRF.

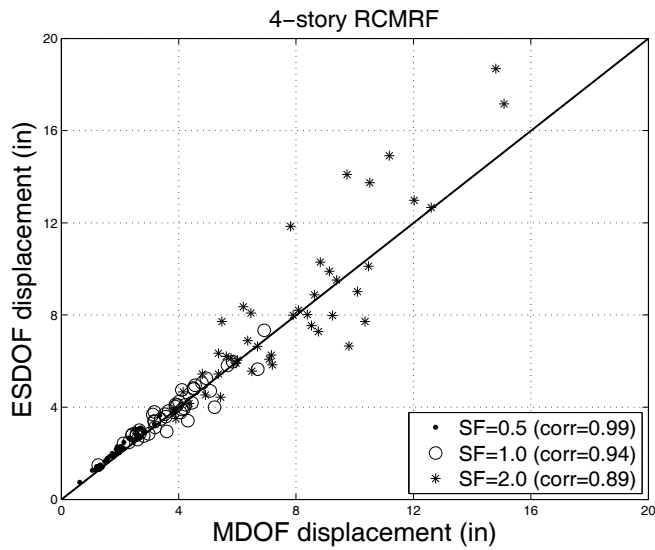


Figure E-2 Comparison of peak roof displacement estimates with actual values for 4-story RCMRF.

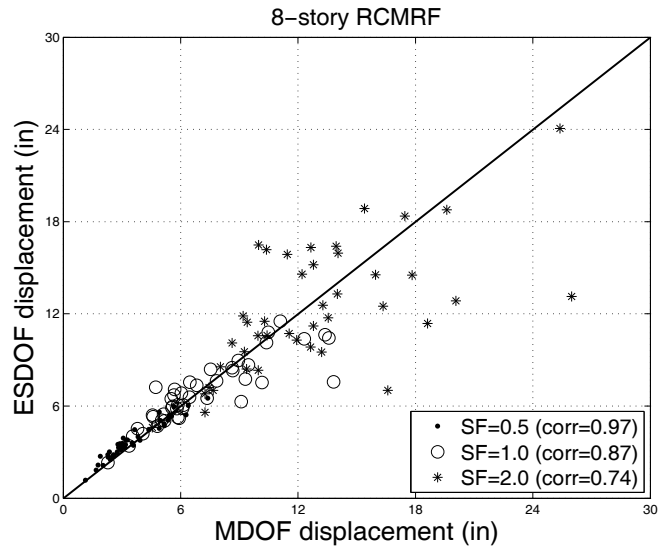


Figure E-3 Comparison of peak roof displacement estimates with actual values for 8-story RCMRF.

Figures E-4 through E-6 plot the ratio of the ESDOF estimate peak roof displacement and the value determined by NRHA, as a function of a measure of the degree of inelastic response given by the peak roof displacement obtained by NRHA normalized by the yield displacement. Yield displacements were estimated on the basis of first mode pushover analysis to be 0.65, 0.5, and 0.45% of the building height for the 2-, 4-, and 8-story moment frames, respectively.

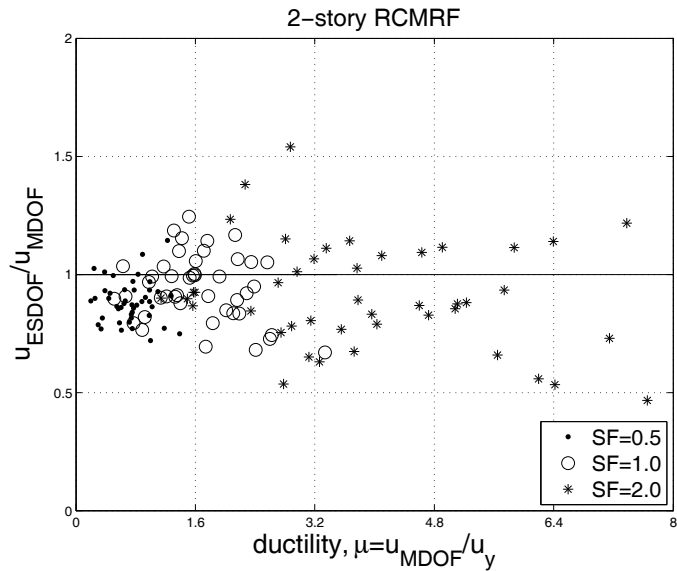


Figure E-4 Ratio of peak roof displacement estimate obtained using an ESDOF system and the peak roof displacement obtained by NRHA for 2-story RCMRF.

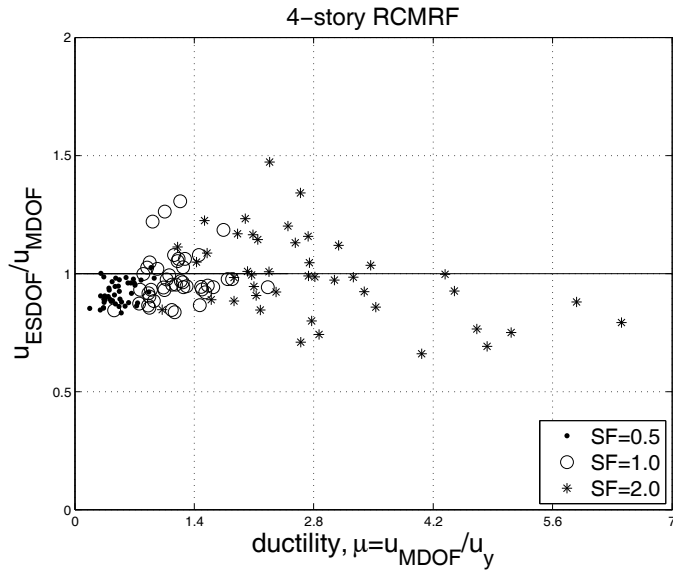


Figure E-5 Ratio of peak roof displacement estimate obtained using an ESDOF system and the peak roof displacement obtained by NRHA for 4-story RCMRF.

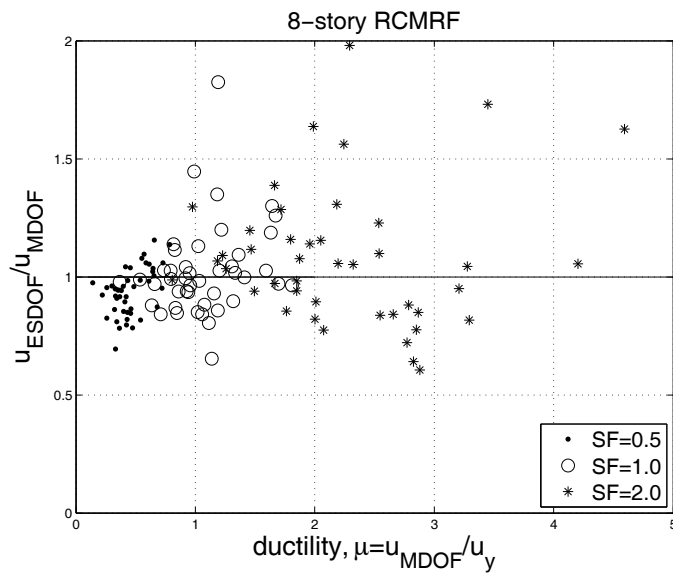


Figure E-6 Ratio of peak roof displacement estimate obtained using an ESDOF system and the peak roof displacement obtained by NRHA for 8-story RCMRF.

Finally, Table E-1 summarizes averages of the ratios (ESDOF estimate/NRHA value) over the 44 ground motions at each scale factor, for the 2-, 4-, and 8-story reinforced concrete moment-resistant frames. It is apparent that peak displacements are estimated with relatively good accuracy overall, with a tendency towards lower values for the fewest stories and lowest scale factors and higher values for the largest number of stories and highest scale factors.

Table E-1 Mean Ratios (ESDOF Estimate of Peak Roof Displacement/NRHA Value) for Each Frame and Scale Factor

Scale Factor	2-story RCMRF	4-story RCMRF	8-story RCMRF
0.5	0.88	0.92	0.94
1.0	0.94	0.98	1.02
2.0	0.91	0.98	1.11

E.3 The SPO2IDA Tool

A large database of results has been developed for SDOF oscillators having varied capacity boundaries. Fairly sophisticated interpolation routines have been developed that allow the target displacement to be estimated. The tool functions much like an $R-C_1-T$ (or $R-\mu-T$) relationship and is available in the form of an Excel spreadsheet and as a Matlab function. The tool is known as SPO2IDA because it takes as input Static Pushover data and produces as output Incremental Dynamic Analysis data, in the form of peak displacement estimates (Vamvatsikos and Cornell, 2006). The application of the tool to MDOF systems is discussed in detail in Fragiadakis and Vamvatsikos (2010); a summary is provided here.

The SPO2IDA tool utilizes information from the static pushover force-deformation curve to generate summary Incremental Dynamic Analysis (IDA) curves representing 16th, 50th and 84th percentile estimates of peak displacement. The tool relies on elaborate techniques to fit equations (Vamvatsikos & Cornell, 2006) to the pre-determined responses of SDOF systems having varied periods, moderately pinching hysteresis, and 5% viscous damping. A large range of piecewise linear static pushover curves is considered, spanning from simple bilinear to complex quadrilinear with elastic, hardening, and negative-stiffness segments followed by a final residual plateau that terminates with a drop to zero strength, as shown in Figure E-7. Incremental dynamic analyses of the oscillators were performed and the resulting 16th, 50th, and 84th percentile IDA curves were established; these in turn were fitted by parametric equations. The statistical IDAs are recreated in normalized coordinates of $R = S_a(T, 5\%) / S_{ay}(T, 5\%)$ versus ductility μ , where $S_{ay}(T, 5\%)$ is the $S_a(T, 5\%)$ value to cause first yield.

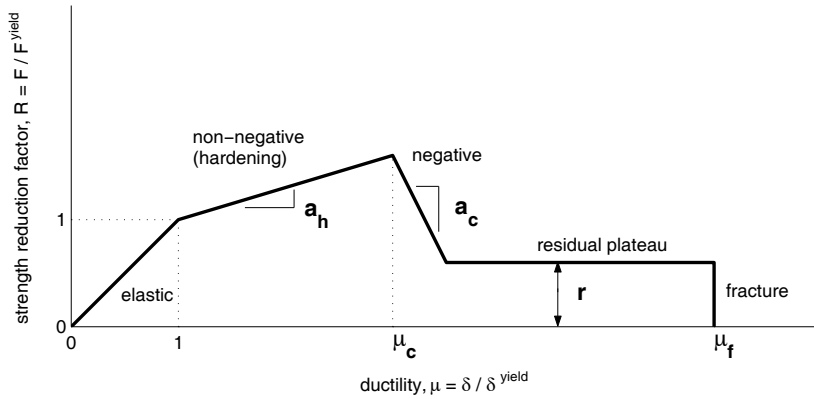


Figure E-7 The normalized SPO2IDA backbone and its controlling parameters (Vamvatsikos and Cornell, 2006).

SPO2IDA receives as input a trilinear or quadrilinear approximation of the static pushover curve, as shown in Figure E-8. For a trilinear approximation, the extracted parameters are: F_y , a_h , μ_h , a_c , while r is set equal to zero and μ_f is defined as the intersection of the horizontal axis with the descending branch of the trilinear model. When a quadrilinear model is chosen, the parameters of Figure E-7 are extracted from the NSP curve.

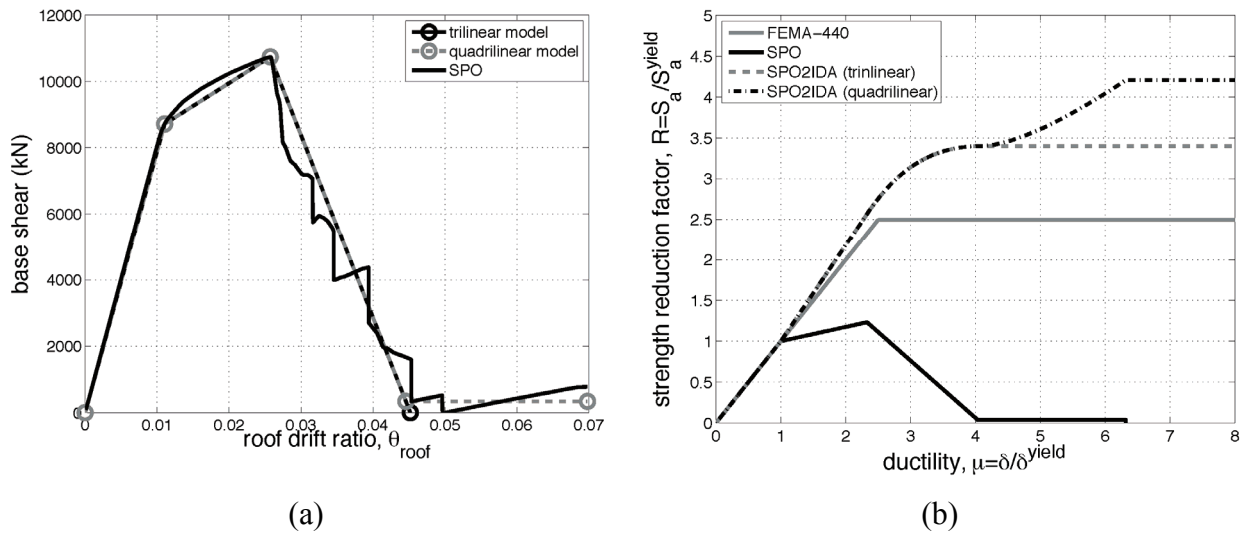


Figure E-8 (a) The SPO curve of a nine-story steel structure and its approximation with a trilinear and a quadrilinear model, (b) SPO curve versus the corresponding SPO2IDA capacity curves (Fragiadakis and Vamvatsikos, 2010).

Figure E-8 (b) shows in $R-\mu$ coordinates the SPO2IDA-produced capacities together with the corresponding NSP curve for a nine-story steel moment frame. The difference between the trilinear and the quadrilinear approximation is the truncation of the tail of the NSP (Figure E-8(a)), which results in a slight underestimation of the R capacity when the trilinear model is adopted. Figure E-8(b) also shows the capacity predicted with a simpler code-prescribed $R-\mu-T$ relationship, such as that of the

ASCE/SEI 41-06 guidelines. For medium to long periods (typically $T > 1$), almost every such relationship follows the equal-displacement rule and thus the ratio of R and μ is equal to one. ASCE/SEI 41-06 also sets an upper limit on the maximum R -value, R_{\max} , also shown in Figure E-8(b).

To apply SPO2IDA to the reinforced concrete moment frames here considered, the NSP curves have already been approximated with a trilinear model. Thus the parameters that describe the capacity curves are known (Appendix B). Also, the demand, expressed as R -values, is given in Section D.4.1. Thus, the corresponding ductility μ values are readily available and the inelastic displacement ratio C_1 is obtained as $C_1 = \mu/R$. In addition to providing central (median or 50th percentile) values, SPO2IDA also provides a measure of the dispersion, expressed as the 16th and 84th percentiles of the C_1 value. The final target roof displacements are calculated using Equation (1) of Appendix B, with $C_1 = \mu/R$ and $C_2 = C_3 = 1$. When $R = 1$, the prediction of the SPO2IDA tool is similar to that of ASCE/SEI 41-06. For $R = 1$, the 16th, 50th, 84th percentiles of the demand coincide.

Figures E-9, E-10 and E-11, compare estimates of peak roof displacement made using the ASCE/SEI 41-06 displacement coefficient approach and the SPO2IDA tool with results obtained for the 1st mode ESDOF oscillators. Mean and mean ± 1 standard deviation of the response are shown for the 1st mode ESDOF oscillators since the ASCE/SEI 41-06 relationship provides an estimate of the mean. For the SPO2IDA estimates, 16th and 84th percentiles are provided to characterize the dispersion, since this is the only measure of dispersion that the underlying equations provide. Both the ASCE/SEI 41-06 and SPO2IDA relations are based on ground motion suites that differ from the suite used to determine the ESDOF responses. The complete list of ground motions used to develop the SPO2IDA estimates is provided in Vamvatsikos and Cornell (2006).

For every building and regardless of the scaling factor, the mean or median peak displacement is closely estimated using the ASCE/SEI 41-06 and SPO2IDA relationships. There are cases, where the average values practically coincide (e.g., 8-story RCMRF, scale factor = 1.0). The figures clearly indicate that individual ground motions can produce peak values that deviate considerably from the mean. The width of the intervals of mean ± 1 standard deviation and 16th–84th percentiles provides a measure of dispersion. It is apparent that the dispersion estimate provided by SPO2IDA is close to that determined with the ESDOF systems, although the limiting values of the intervals differ.

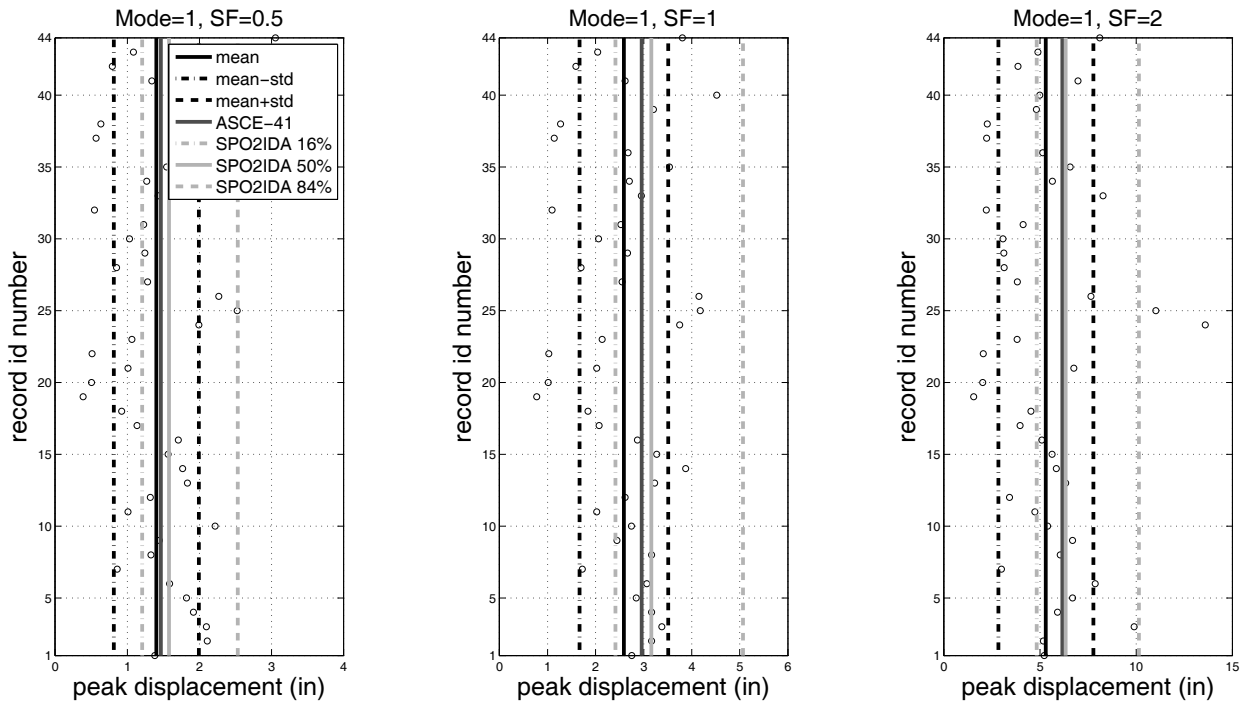


Figure E-9 2-story RCMRF, 1st mode: ESDOF peak roof displacement estimation.

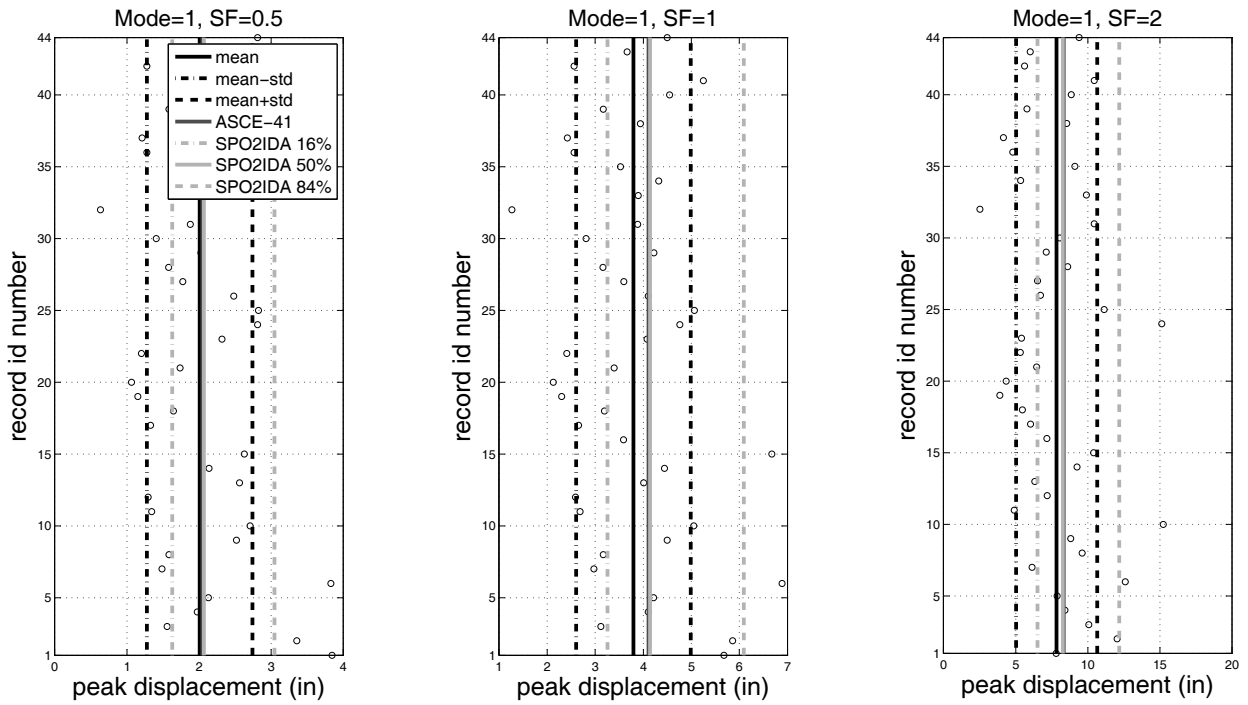


Figure E-10 4-story RCMRF, 1st mode: ESDOF peak roof displacement estimation.

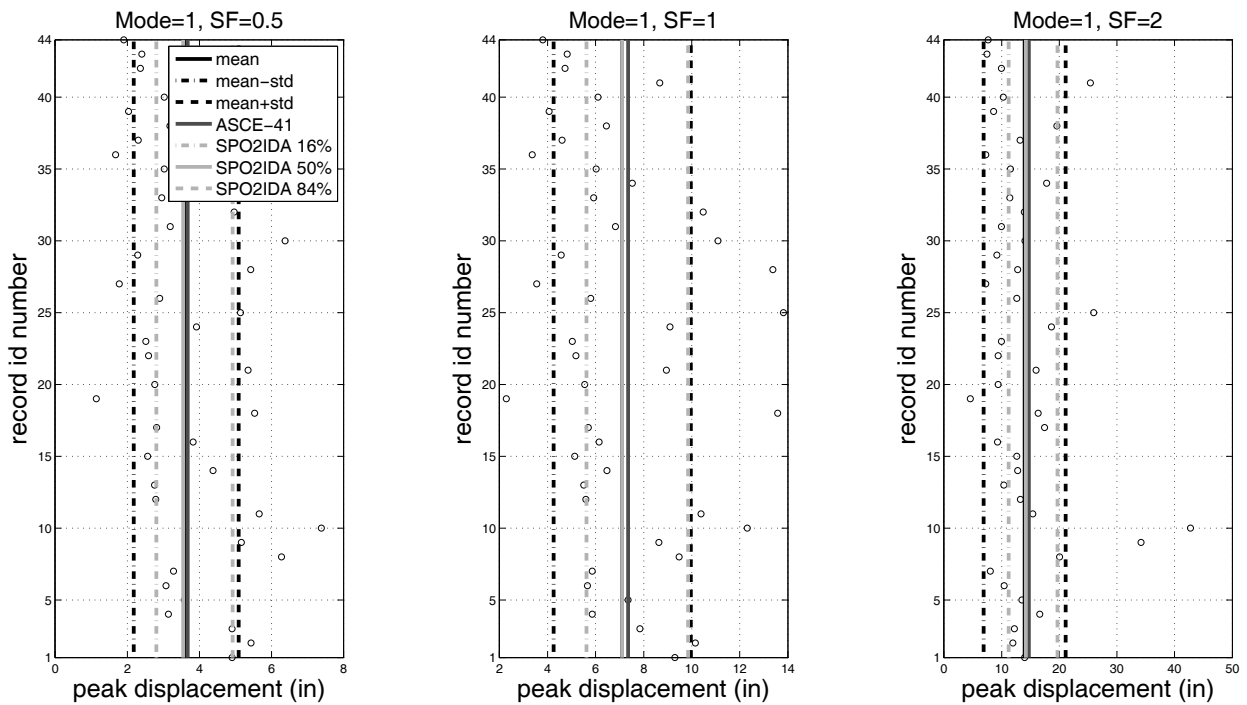


Figure E-11 8-story RCMRF, 1st mode: ESDOF peak roof displacement estimation.

E.4 Summary

Data presented in Sections E.2 and E.3 are summarized in Figures E-12 through E-14. The plots indicate mean \pm 1 standard deviation values given for the NRHAs of the MDOF system as well as for the ESDOF system, and 16, 50, and 84 percentile results determined using SPO2IDA. It is apparent that all approaches give fairly similar estimates of peak displacement, particularly given the range of values that occur at each scale factor.

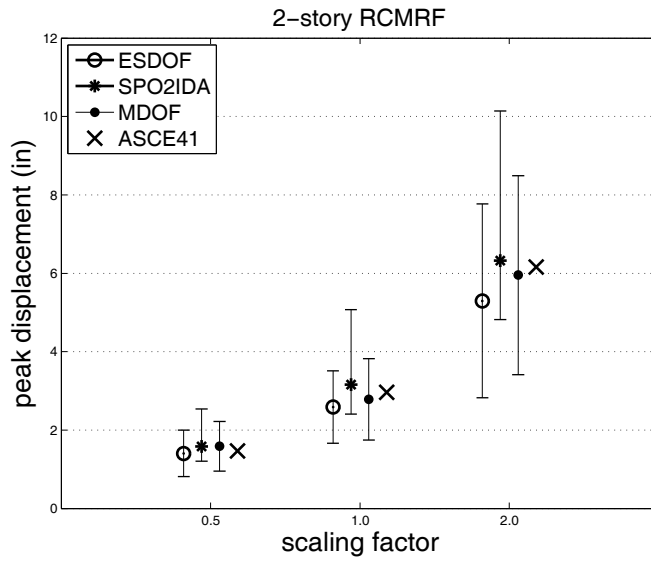


Figure E-12 Comparison of ESDOF and SPO2IDA estimates of roof displacement with results from 44 NRHAs and ASCE/SEI 41-06 estimates for the 2-story RCMRF.

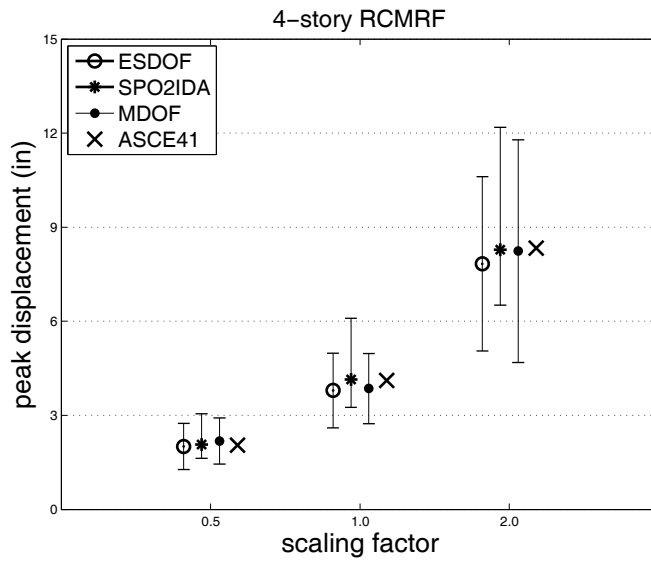


Figure E-13 Comparison of ESDOF and SPO2IDA estimates of roof displacement with results from 44 NRHAs and ASCE/SEI 41-06 estimates for the 4-story RCMRF.

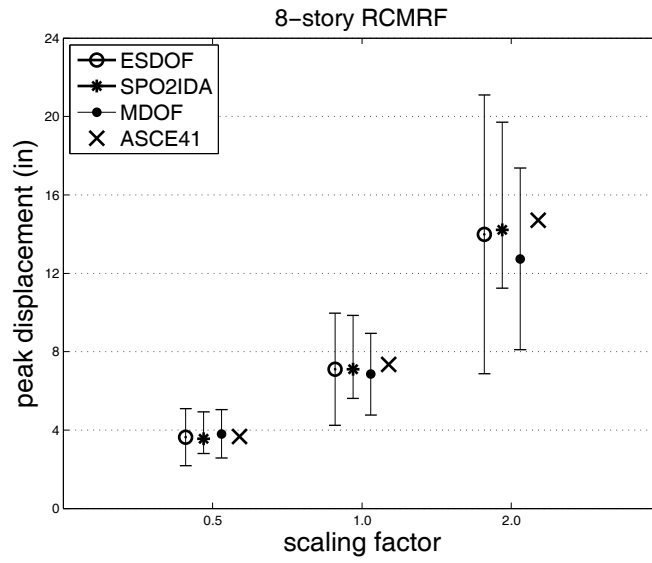


Figure E-14 Comparison of ESDOF and SPO2IDA estimates of roof displacement with results from 44 NRHAs and ASCE/SEI 41-06 estimates for the 8-story RCMRF.

Practical Implementation of Analysis Methods

This appendix presents results from an ancillary study undertaken to apply the methods tested in primary focused studies (with some extensions) to models of two special-case buildings encountered in practice using production software in common use by practitioners. The objective of this study was to further test the methods and identify practical challenges to their implementation.

F.1 Approach

This appendix examines potential procedures for assessing higher mode response using some real buildings as well as procedures and software typically available to the practicing design professional. The primary reference document for the modeling and assessment is ASCE/SEI 41-06, *Seismic Rehabilitation of Existing Buildings* (ASCE, 2007), with revisions noted below.

The first objective of this study was to identify challenges and potential issues for the practicing design professional in performing nonlinear response history analysis (NHRA). This includes testing the hypothesis that all that is required to do nonlinear response history analysis is simply to get some records and run the models since practitioners are already building nonlinear models for pushover analysis.

The second objective was to evaluate various analysis techniques for their ability to capture the higher mode response of the structures. Two buildings, Building A and Building B, were selected and modeled that they do not meet the requirements of ASCE/SEI 41-06 for nonlinear static analysis, at least for the higher input demands. Each is based on a real building for which previous three-dimensional computer models have been built. These original models were altered and simplified to some degree.

Building A is a six story steel moment frame structure and Building B is a three story braced frame structure with a flexible roof diaphragm. The following analysis methods were used to analyze each structure:

- Nonlinear static pushover analysis per ASCE/SEI 41-06, designated ASCE 41 or NSP (Section F.4.3)
- Single and multiple mode response spectrum analysis, designated RSA-1 mode and RSA-all modes (Section F.4.2)

- Nonlinear pushover analysis plus elastic higher modes, designated ASCE 41+RSA higher modes (Section F.4.4)
- Modal pushover analysis, designated MPA (Section F.4.5)
- Consecutive modal pushover, designated CMP (Section F.4.6)
- Extended consecutive modal pushover, designated CMP-extended or ECMP (Section F.4.7)

A brief summary of each method is included together with a summary and comparison of key results. The engineering demand parameters used in the comparison of the various procedures were story displacements, story drift ratios, story shears, and story overturning moments.

These were compared to results taken from a suite of nonlinear response history analyses (NHRA) scaled to the same input demand. No attempt was made to compute or compare the ASCE/SEI 41-06 building component limit states for each analysis type. In addition to a comparison of the results, a discussion of the use of the different techniques is also included.

F.2 General Modeling Assumptions

Since the focus of the study involves how a practicing professional would analyze a real building, the modeling assumptions made were consistent with typical assumptions made in a nonlinear analysis. Where necessary, simplifications have been made to accommodate software limitations in order to perform the baseline nonlinear response history analyses.

Each building was initially modeled in three dimensions. The intent of a three-dimensional structure is to capture bi-directional effects of the input ground motions and torsional response of the structure. The final study was limited to unidirectional loading only; bi-directional and torsional effects are recommended for further study.

F.2.1 Ground Motions

When bi-directional and torsional effects are considered in a three-dimensional analysis the ground motions are used as pairs, not as individual ground motions. Since the initial intent was to capture these effects the ground motions used in the study were paired together as orthogonal components. The FEMA P-695, *Quantification of Seismic Performance Factors* (FEMA, 2009b), far-field data set, was used in this study and has 22 pairs (44 individual) of ground motions records. From these 22 pairs, analyses were conducted using eight pairs of ground motions, a number of records more typical of current structural engineering practice.

To select the eight ground motion pairs, first a square-root-sum-of-the-squares (SRSS) spectrum of each ground motion pair was constructed using the orthogonal components of each pair. From the original 22 pairs, eight ground motions pairs

were chosen such that the average spectrum of their SRSS spectra was roughly equivalent to the average SRSS spectrum of the 22 pairs (see Figure F-1). Depending on what was considered to be the target spectrum, this approach varies from the ASCE/SEI 41-06 provisions for ground motion scaling but is consistent with the more recent provisions in ASCE 7-10, *Minimum Design Loads for Buildings and Other Structures* (ASCE, 2010).

From these eight pairs, the ground motion components from each pair were oriented along the principal axes as shown in Table F-1, such that the average spectrum of the ground motions in the X-direction was roughly equivalent to the average spectrum of the ground motions in the Y-direction. Figure F-1 presents the average spectra.

Table F-1 Application Direction of Selected Ground Motions

GM Pair	1	2
12012	X	Y
12052	Y	X
12062	Y	X
12072	X	Y
12092	X	Y
12121	X	Y
12122	X	Y
12132	X	Y

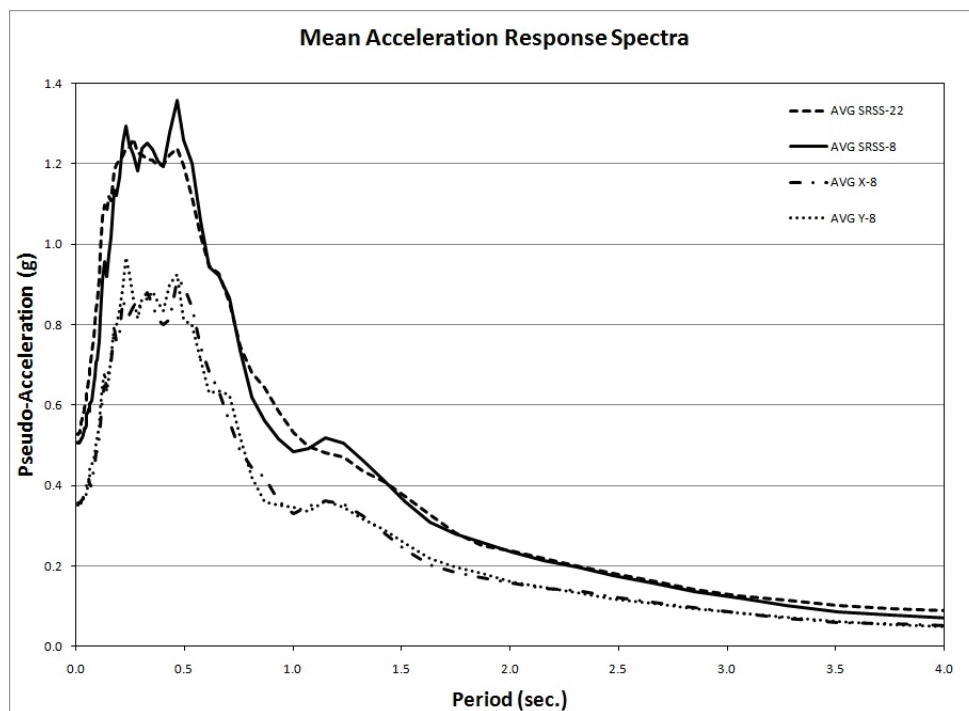


Figure F-1 Average Spectra

The spectrum determined from the average of the eight ground motion components in each primary direction was then used as the input spectrum for all other analysis procedures.

For each analysis method the input demands were applied at scale factors of 0.5, 1.0, and 2.0, except as noted below.

F.3 Structures and Models

F.3.1 Building A

Building Description

Building A is a 6-story steel framed structure with a moment resisting frame lateral system. The building is 111 feet by 260 feet in plan, with an overall building height of 82 feet. The typical story height is approximately 13 feet and the first story is 15 feet 9 inches. Longitudinal bay widths are 20 feet, and transverse bay widths are 37 feet.

The moment frames are located along exterior longitudinal frame lines and each transverse frame line. A typical floor plan with moment frame layout is shown in Figure F-2. All columns are W14×342 wide flange shapes and all beams are W30 wide flange shapes ranging from 99 to 116 pounds per foot. Columns within the frames generally are oriented with their strong axis in the direction of the moment frames, except at the columns that are shared between the transverse frames and longitudinal frames along the exterior; these are oriented with their strong axis in the direction of the longitudinal frames.

From a seismic retrofit, two buckling restrained braced (BRB) frames are located within the longitudinal exterior frames, and three are located within the transverse frames. Core sizes of the BRB frames range from approximately four square inches to thirty square inches. Diaphragms are concrete fill over metal deck.

3D Nonlinear Model

The original 3D analysis model (see Figure F-3) for Building A was developed to reflect the dimensions, members, and materials of the building. SAP 2000 software, developed by Computers and Structures, Inc, was used for modeling. The 3D analysis model had been used for pushover analysis of the existing structure and strengthening scheme that included the additional buckling-restrained braced frames. An attempt was made to run NRHA on this original 3D model, but the analyses failed to complete successfully.

A series of progressive simplifications and alterations were made to the model as outlined below to develop a model that would successfully complete NRHA for the selected ground motions in a reasonable time frame. After each major revision the NRHA was reattempted.

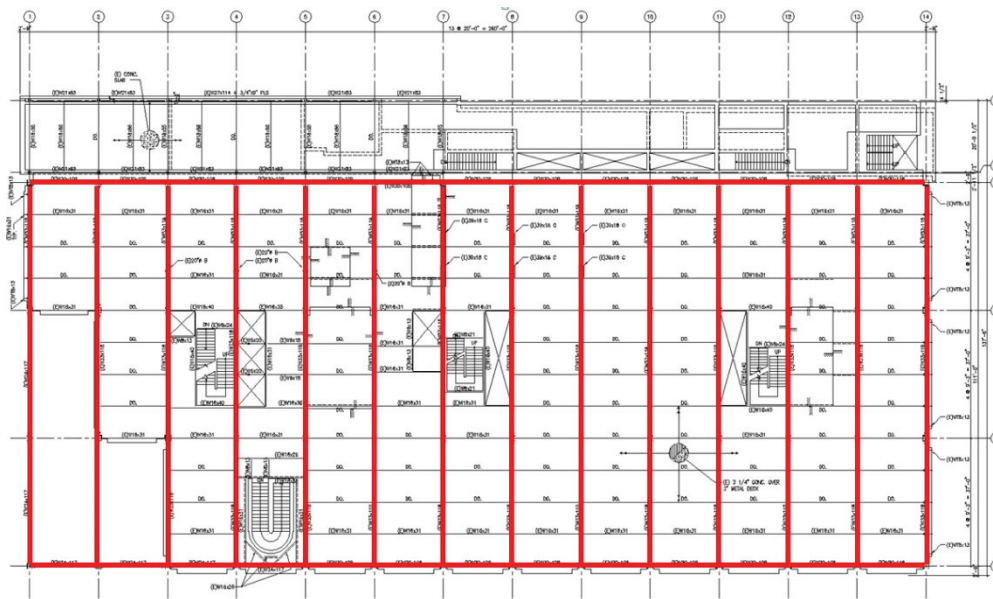


Figure F-2 Typical floor plan with moment frame layout.

The following is a summary of the required revisions:

- Braced frames removed, effectively returning the building to the pre-retrofit condition.
- Box columns sections removed from corners, framing for all transverse frames made equal. Added frame hinge overrides.
- All horizontal and vertical foundation springs for pile elements and existing elements removed, including uplift elements. Column bases were fixed.
- All column PMM hinges removed, replaced with M3 and M2 flexural hinges with backbone set for constant axial load. The hinges did not include axial strength degradation, or rapid strength loss.
- Moment connection hinges, converted all from rapid strength loss “pre-Northridge” hinges to ductile hinges, properties per Figure F-5. (Model runs NRHA at this point but too slow to complete suite in a reasonable time-frame).
- Simplified 3D model to single 2D model in transverse direction.

The following additional revisions were made to the frame to make the behavior more relevant to the study goals:

- Revised steel frame sizes to reduce tendency to form a soft story mechanism in the lower levels.
- Increased the tributary mass to the 2D frame to increase nonlinear demands.
- Dropped the 0.5 scale factor assessment as the conclusions were similar to the 1.0 scale factor.

The final model used in this evaluation was the 2D frame shown in Figure F-4 below.

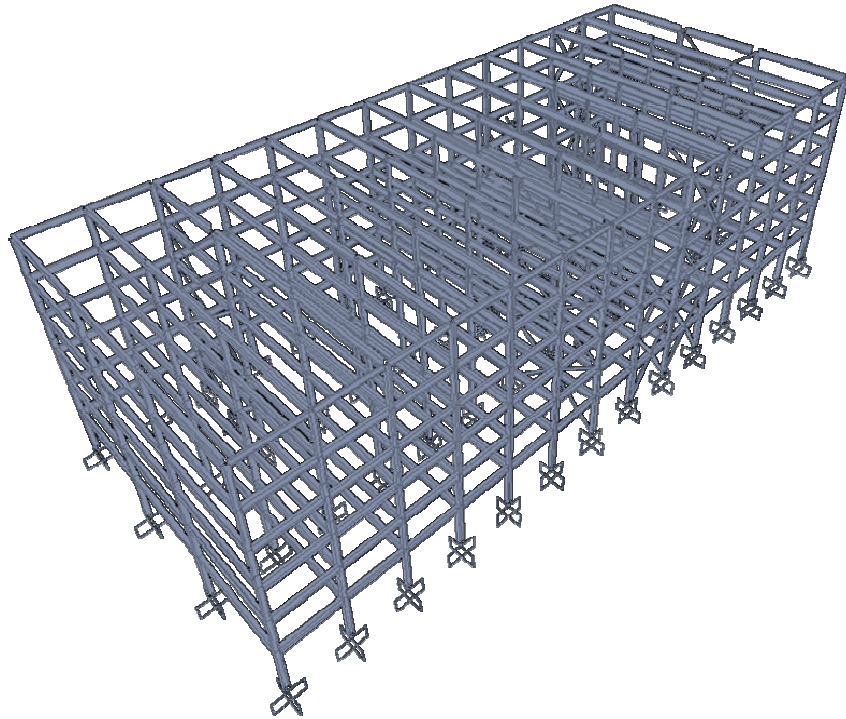


Figure F-3 Building A 3D SAP 2000 Model.

2D Nonlinear Model

From the simplification procedure described above, the final two-dimensional model used in the analysis methods is shown below in Figure F-4.

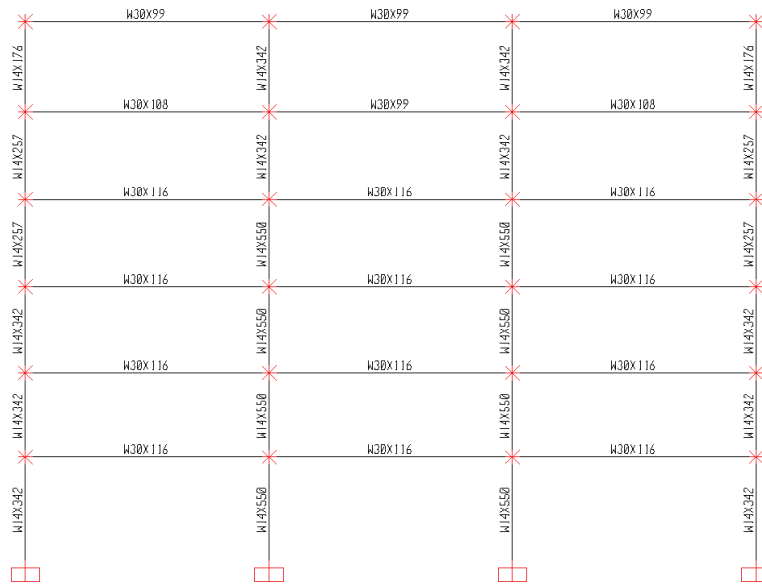


Figure F-4 Transverse frame elevation of Building A SAP model.

Nonlinear behavior was included in the structural elements per the requirements of ASCE/SEI 41-06. Nonlinear flexural hinges were modeled in all the moment frame beam members at beam-column connections. A representative backbone curve for the beam-column connection hinge is shown in Figure F-5, including the typical beam elastic flexibility. The analysis failed to converge once the hinges began to degrade.

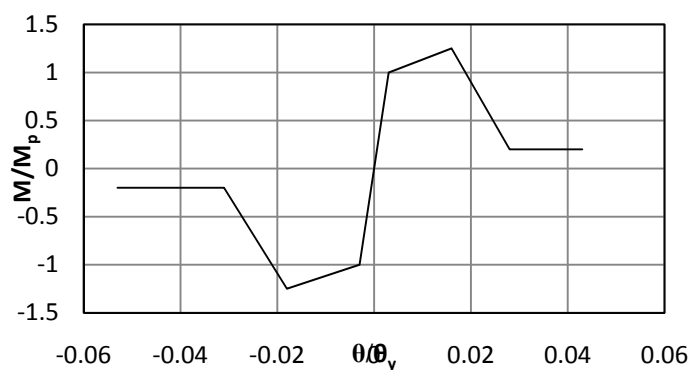


Figure F-5 Typical nonlinear beam flexural plastic rotation hinge.

The moment frame members were sized to exhibit strong column-weak beam behavior; however, nonlinearity can occur in the columns, particularly at the base, roof, and during formation of collapse mechanisms.

Flexural column hinges were included at the base and top of all columns. To simplify the model, the flexural strength and rotational capacity of the hinges were developed neglecting the effect of axial load. Typical nonlinear column flexural plastic rotation hinge properties are shown in Figure F-6.

Comparing the reported story drifts for the various analysis methods to the rotations in Figures F-5 and F-6 provides a qualitative means to assess the consequence of the reported drift variation. Figures F-5 and F-6 suggest that the hinges might reasonably have shifted from the “yielded” portion of the backbone curve to the “degraded” portion. Typically this would correspond to a change in the ASCE/SEI 41-06 performance level prediction from life safety to collapse prevention. If, on the other hand, a pushover technique produced story drifts that are substantially less than those from the reference response history analysis, the severity of performance could be underestimated.

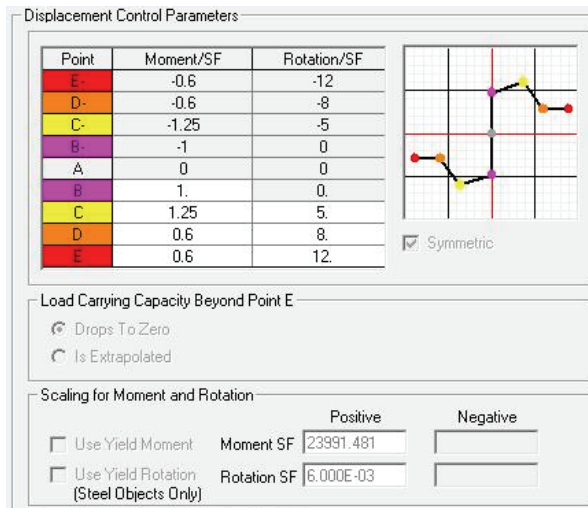


Figure F-6 Typical nonlinear column flexural plastic rotation hinge

Modal Properties

Tables F-2 and F-3 summarize the modal properties for the full 3D Building A, and Tables F-4 and F-5 provide the modal properties for the simplified transverse 2D frame analyzed as part of this study.

Note that the increased fundamental period for the 2D model compared with the corresponding transverse mode for the 3D model is due to a significant increase in mass for the 2D model. Initial analysis of the 2D model indicated essentially elastic response, even for records with a scale factor equal to 2.0. In order to increase the level of nonlinear response, the mass tributary to the 2D frame was increased.

Table F-2 Modal Properties for Building A – Original 3D Model

		Transverse		Longitudinal	
		Mode 2	Mode 5	Mode 1	Mode 4
	T₁ (s)	1.33	0.47	1.55	0.79
	M_n*	54.0	7.10	52.6	7.79
	M_n*/Weight	84.1%	11.1%	82.0%	12.1%
	Height, H (in)			985	
Story mass (k-s²/in)	Roof			12.2	
	4th, 5th			10.1	
	1st, 2nd, 3rd			10.6	
	Total Weight (k)			24,800	

Table F-3 Eigenmodes of Building A – Original 3D Model

		1st Floor	2nd Floor	3rd Floor	4th Floor	5th Floor	Roof
Transverse	Mode 2	0.220	0.393	0.565	0.736	0.890	1.00
	Mode 5	-0.608	-0.918	-0.910	-0.496	0.245	1.00
Longitudinal	Mode 1	0.185	0.352	0.523	0.693	0.855	1.00
	Mode 3	-0.514	-0.832	-0.887	-0.571	0.097	1.00

Note: Values are at the center of mass, normalized to roof level.

Table F-4 Modal Properties for Building A – 2D Model Analyzed

		Mode 1	Mode 2	Mode 3
T_1 (s)		3.68	1.18	0.63
M_n^*		37.88	5.2	1.49
M_n^*/Weight		85.3%	11.7%	3.3%
Height, H (in)		985		
Story mass ($k\text{-s}^2/\text{in}$)	Roof	6.8		
	3 rd , 4 th , 5 th	8		
		1 st , 2 nd		
Total Weight (k)		17,138		

Table F-5 Eigenmodes of Building A – 2D Model Analyzed

	1 st Floor	2 nd Floor	3 rd Floor	4 th Floor	5 th Floor	Roof
Mode 1	0.20	0.40	0.59	0.77	0.91	1.00
Mode 2	-2.01	-0.63	0.79	1.58	1.61	1.00
Mode 3	0.95	0.95	-0.01	-0.99	-0.63	1.00

Note: Values are at the center of mass, normalized to roof level.

F.3.2 Building B

Building Description

Building B is a three-story steel braced framed structure. The building is 168 feet by 210 feet in plan, with an overall building height of 46 feet. The first two stories are 15 feet tall, and the upper story is 16 feet tall. The longitudinal and transverse bay widths are 21 feet. The 3D model was prepared with the PERFORM 3D software, developed by Computers and Structures, Inc.

In the longitudinal direction there are two braced frames along each exterior frame line. Each braced frame consists of two bays of braces in a chevron configuration extending to the roof level. In the transverse direction there are three braced frames--two exterior, and one interior. The exterior braced frames consist of five braced bays extending to the roof level. The interior braced frame is two bays wide and extends only two stories. A typical floor plan with braced frame layout is shown in Figure F-7. Braces are either HSS6×6 or HSS8×8. Columns are W10 or W12 sections.

Grade beams connect the footings of all perimeter columns as well as the footing of the interior braced frame. The first two diaphragms are concrete fill over metal deck, and the roof diaphragm is bare metal deck.

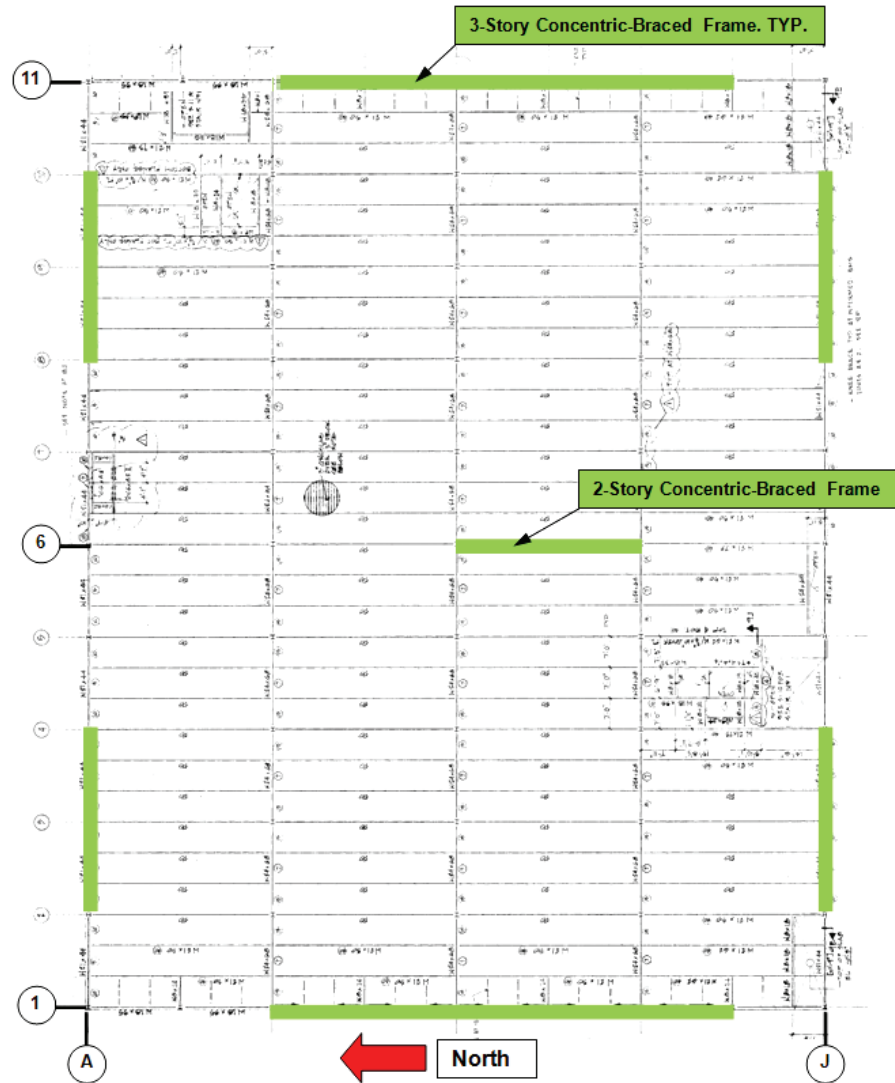
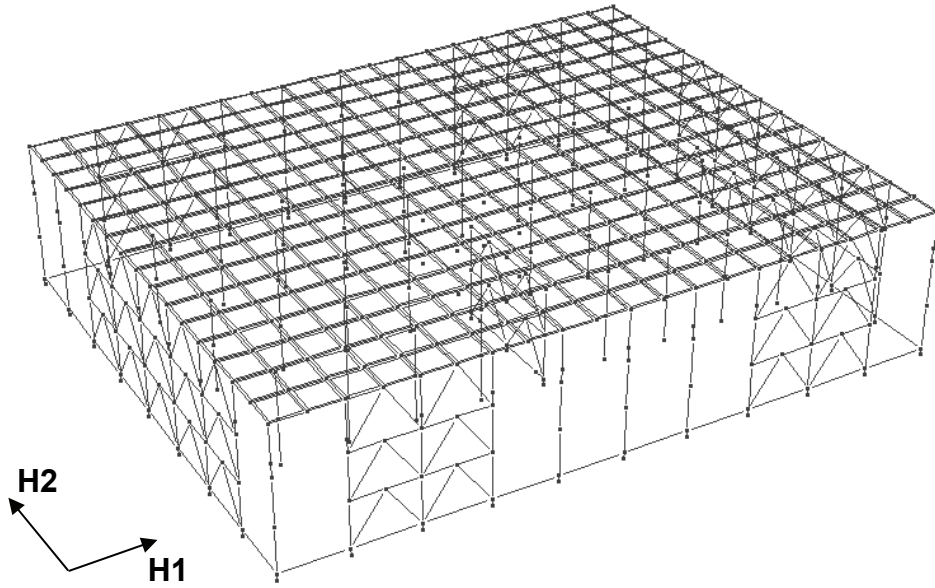


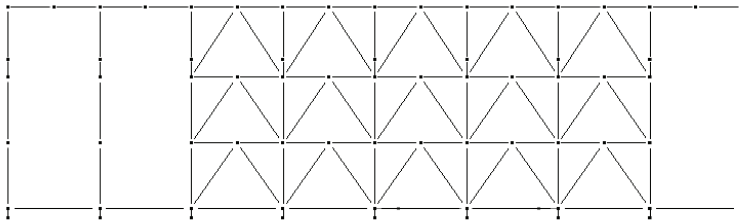
Figure F-7 Typical floor plan with concentric braced frame layout.

Nonlinear Modeling

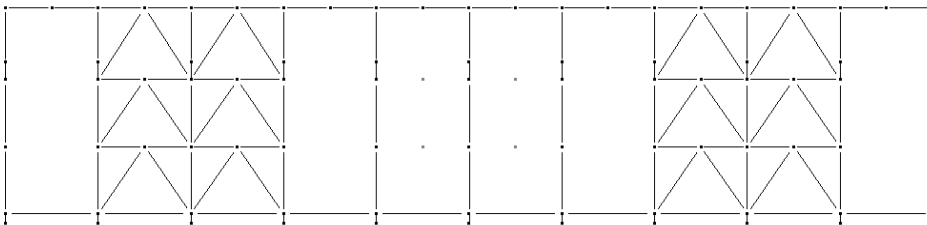
The model was developed to reflect the dimensions, members, and materials of the building. Figure F-8 shows an overall 3D view of the model and elevation views of typical longitudinal and transverse frame lines.



(a) Three-Dimensional View



(b) Transverse Frame Elevation (H2)



(c) Longitudinal Frame Elevation (H1)

Figure F-8 Building B PERFORM model.

Nonlinear behavior was included in the structural elements per the requirements of ASCE/SEI 41-06. Braces were modeled as nonlinear axial struts, which incorporate the asymmetric brace behavior (see Figure F-9). In compression the brace was controlled by its buckling strength, but in tension the brace strength was controlled by the tensile strength of the brace or brace connection.

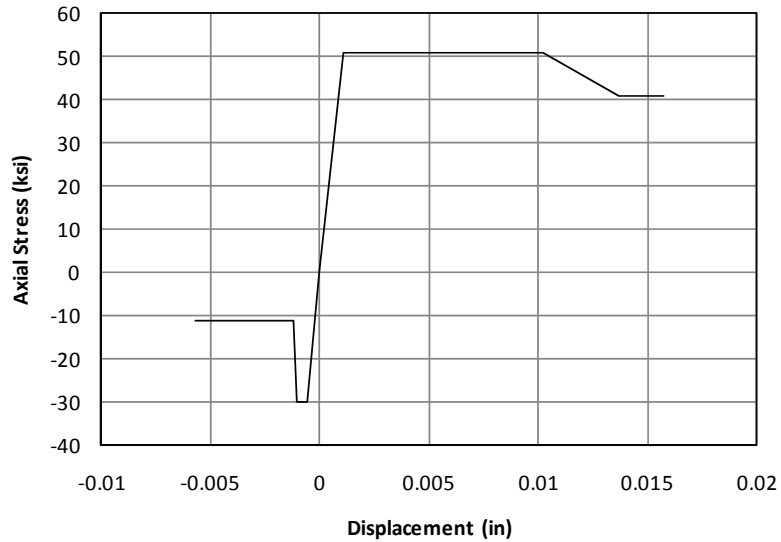


Figure F-9 Typical nonlinear HSS brace axial hinge.

The asymmetric post-yield behavior of the braces can produce large unbalanced load at midspan of the beams to which they connect, so nonlinear flexural hinges were included in the beams. A typical beam hinge backbone is shown in Figure F-10.

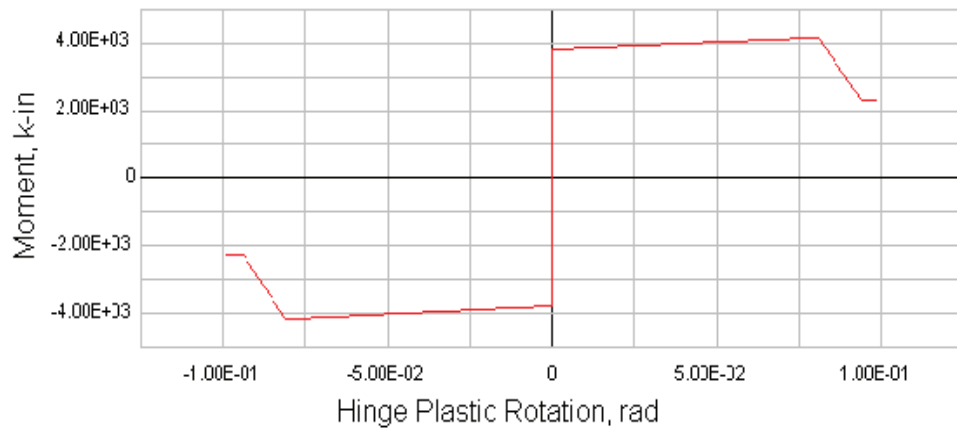


Figure F-10 Typical nonlinear beam flexural plastic rotation hinge.

Grade beams were assumed to provide fixity at the base of the columns, so nonlinear flexural hinges were included in grade beams.

Shear elements of the roof diaphragm were modeled as nonlinear to capture the yielding and buckling of the bare metal deck. An example of the roof diaphragm infill shear panel backbone is shown in Figure F-11.

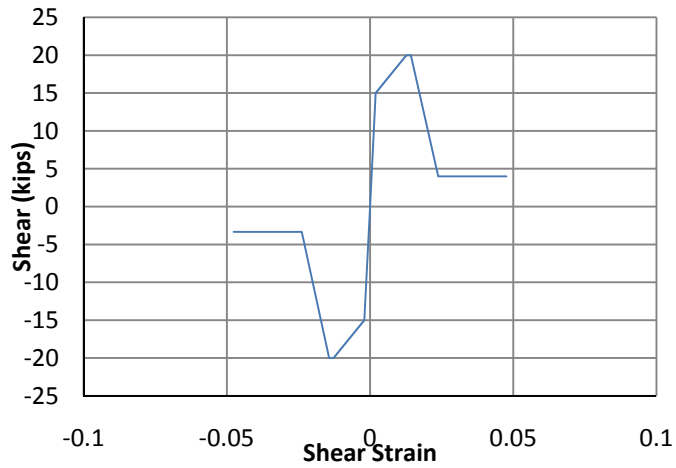


Figure F-11 Typical nonlinear infill shear panel.

Nonlinear elements were provided at the base of each column to model expected axial load moment interaction. Backbone curves were defined for two levels of axial load (see Figure F-12) and the analysis program interpolated between the two axial load levels.

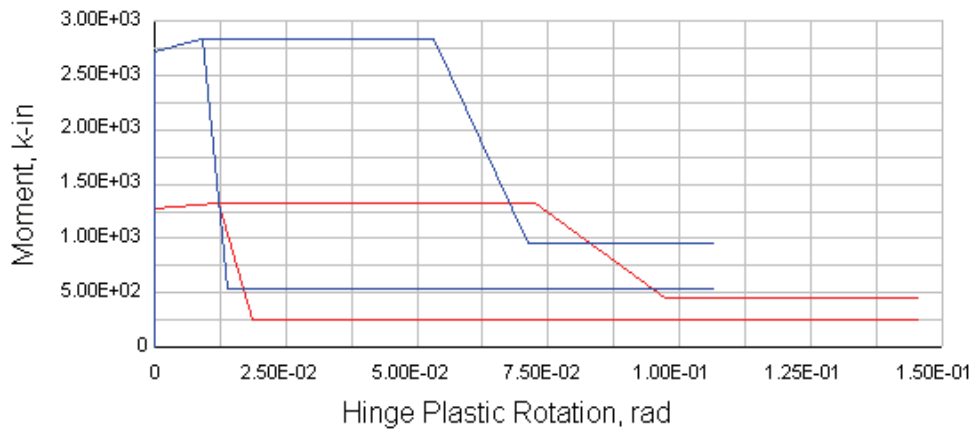


Figure F-12 Typical nonlinear column axial-dependent flexural plastic rotation hinge.

Modal Properties

Tables F-6 and F-7 summarize the modal properties for Building B. The flexible bare metal deck roof diaphragm had a significant impact on observed modal properties.

Table F-6 Modal Properties for Building B

	Transverse (H2)		Longitudinal (H1)	
	Mode 2	Mode 5	Mode 1	Mode 3
T_1 (s)	0.539	0.295	0.549	0.318
Γ_n	1.40	0.48	1.72	0.76
M_n^*	6.17	11.51	12.17	5.62
M_n^*/Weight	31.6%	58.9%	62.3%	28.8%
Height, H (in)	552			
Story mass	Roof		2.92	
(k-s ² /in)	1 st , 2 nd		8.31	
Total Weight (k)	7,550			

Table F-7 Eigenmodes of Building B (at center of mass)

		1 st Floor	2 nd Floor	Roof	Roof Adjusted*
Transverse (H2)	Mode 2	0.045	0.103	1.00	0.90
	Mode 5	-0.429	-0.768	0.972	0.37
Longitudinal (H1)	Mode 1	0.131	0.294	0.999	0.85
	Mode 3	-0.257	-0.419	0.998	0.55

*Values adjusted to represent average response of flexible roof diaphragm

F.4 Analysis Methods

A brief summary of each analysis procedure examined as part of this assessment is provided below. The procedure abbreviations shown in the title are used throughout the presented results.

In each analysis, vertical gravity loads were considered in addition to the lateral loadings, and correspond to the expected dead load plus one-quarter live load.

F.4.1 Nonlinear Response History Analysis

The results from the nonlinear response history analyses are taken as the baseline for comparison. Ground motion scale factors of 0.5, 1.0, and 2.0 were considered. For some analyses only the larger scale factors were considered where the structure was essentially elastic for both the 0.5 and 1.0 scale factors.

Damping was assumed to be 5% in all analysis types. Rayleigh-only damping was used in the Building A model and a mixture of Rayleigh and modal damping was used in the Building B model. An inherent damping value of 5% is higher than would typically be used for these building types; a value of 2% would be more

appropriate. This means that the response history deformation results could be 20% to 25% lower than would otherwise be expected. Force demands would also be higher, depending on the degree of nonlinearity in the analysis.

The drifts presented in Figure F-16 for Building A show a variety of deformation patterns with peak story drifts occurring in upper levels in some records and in lower levels for other records. This variability illustrates the challenge of developing a single pushover analysis protocol that captures both type of behavior.

Building B shows nonlinear response occurring in the braced frames in both directions in some records (Figure F-36 and F-38) indicating the formation of a soft story mechanism at the 1st story. In the same figures the effect of rocking in the H1 direction is visible in both the drift and displacement plots with lower demands below the roof level than in the H2 direction.

F.4.2 Response Spectrum Analysis

Typically in a three-dimensional model the spectrum would be analyzed using 100% of the spectrum in one direction and 30% of the spectrum in the orthogonal direction. However, since bi-directional effects were not included in this assessment, the response spectrum analysis was performed using 100% of the spectrum in each direction separately.

Results are shown for single and multimode analyses. Although the single mode analysis results do not include the ASCE/SEI 41-06 C_1 , C_2 , and C_m factors, they are still indicative of the results of static analysis.

The input spectrum was the average of the spectra from the time-history components applied in each building direction. This provides an apples-to-apples comparison with the other procedures (i.e., same input demand). It also ignores such issues as C_d/R in ASCE/SEI 7, and that the design spectrum would actually be the average SRSS of the components and not the average of the individual components. The results should be increased by a factor of approximately 1.4 for this comparison. As mentioned above, no bi-directional or torsional response was considered.

F.4.3 Nonlinear Static Procedure

For this method, uniaxial loading using the fundamental mode in each direction was applied separately to the target displacement computed using the average time-history spectrum for that direction.

The building was analyzed in both directions and the target displacement was calculated from the idealized pushover curves. Deformations were evaluated as those at the target displacement and forces are evaluated as the envelope of results up to and including those at the target displacement.

F.4.4 Nonlinear Static Procedure with Elastic Higher Modes

One postulated analysis procedure was to combine the higher mode response spectrum results with the primary mode pushover results. When the pushover analysis is in the elastic range, these results match the response spectrum results, which is typically the case for the smaller scale factors. The procedure is the same as modal pushover analysis when the higher modes are elastic.

F.4.5 Modal Pushover Analysis

In this type of analysis, the results of multiple pushover analyses are combined. Each pushover used has a loading pattern based on a unique building mode in the direction under consideration. Sufficient modal pushovers are run to capture the modes with significant mass participation. For each modal pushover, a target displacement is calculated per the requirements of ASCE/SEI 41-06. Then at each target displacement, the engineering demand parameters of interest (drift, displacement, member forces, hinge rotation, etc.) are determined. The load due to gravity is subtracted from the parameter of interest value from each modal pushover. The values of the modified pushover results are then combined by the square root of the sum of the squares (SRSS) method. As a final step, the load due to gravity is added back to achieve the final value for the parameter of interest.

F.4.6 Consecutive Modal Pushover Analysis

CMP is similar to the NSP method, but instead of a single pushover analysis the results of multiple single stage and multi-stage pushover analyses are enveloped to determine parameters of interest. Initially natural frequencies and mode shapes are calculated and the pushover target displacement is calculated per the requirements of ASCE/SEI 41-06. The single stage pushover is similar to ASCE/SEI 41-06 procedures. This initial single-stage pushover is followed by a two stage consecutive pushover analysis. The target displacement for the first mode pushover is equal to the first mode target displacement multiplied by the first mode participating mass ratio. This first mode push is followed by a second mode push beginning with the structural state from the end of the first mode pushover.

The CMP procedure sets the target displacement for the second mode in a two-mode pushover based on the first mode target displacement multiplied by (one minus the first mode participating mass ratio), i.e., the first mode is only pushed to the target times the mass participation factor. For buildings with a fundamental period of 2.2 seconds or more, a three-stage pushover analysis is also completed. Then the parameter of interest (drift, displacement, member forces, hinge rotation, etc.) is determined based on an envelope of single- and multi-stage pushover analyses.

F.4.7 Extended Consecutive Modal Pushover Analysis

The consecutive model pushover technique was modified based on observations from the previous analyses. The effect of sign (direction) of the modes was considered by

altering the sign of the applied higher modes. This has the effect of generating different loading deformation patterns in the structure, similar to that which occurs in the nonlinear response history analyses for different earthquake records.

It was further observed that the deformation pattern observed in the building was more significantly altered if the high mode pushover was applied before the fundamental mode pushover. This suggested the idea of running a series of consecutive pushover analyses with modes of different signs and in different sequences. The objective of this was to develop the range of deformation patterns that might occur in the building. Since each analysis is comparable to a different earthquake the results could be either enveloped or averaged as desired for the particular engineering demand parameter under consideration.

Slightly different approaches were adopted for Buildings A and B, due to the experimental nature of the work. For Building A, the CMP procedure required three modes due to the relatively long first mode period. This means there was a potentially large number of consecutive modal pushover combinations. To limit the number of analyses, the assessment focused on consecutive combinations in which the higher mode pushovers were performed first since these tended to produce more variation in the observed mechanism that formed in the frame. A total of seven consecutive modal pushover sequences were examined, as follows:

- +M1 (same as ASCE 41, one single mode pushover)
- +M2+M1 and +M2–M1 (two × 2-mode pushovers)
- +M3+M2+M1, +M3+M2–M1, –M3+M2+M1, –M3+M2–M1 (four × 3-mode pushovers)

The CMP procedure sets the target displacement of the second mode in a two-stage pushover based on the first mode target displacement multiplied by (one minus the first mode participating mass ratio)—that is, the first mode is only pushed to the target times the mass participation factor. When the second mode was applied first, it became apparent that the higher mode response was being overestimated as the computed target displacements substantially exceeded the target displacements computed for the modal pushover analysis (MPA) for the higher mode alone.

For the three stage analyses, a slight variation from the original CMP procedure was adopted to better balance the contribution of the two higher modes. The total higher mode contribution of both mode 2 and mode 3 was based on one minus the first mode mass participation. This was converted to a spectral displacement which was then apportioned to each mode in proportion to its own computed spectral displacement, and the values converted back to roof displacement.

For Building B, the CMP approach required only two modes for the assessment as the structure is relatively stiff. Consequently, all of the potential consecutive modal combinations were examined, as follows:

- +M1 (same as ASCE 41, one single mode pushover)
- +M1+M2, +M1–M2, +M2+M1 and +M2–M1 (four × 2-mode pushovers)

Due to the flexible roof diaphragm, the first mode mass participation ratio in the building is relatively low, particularly in the H2 direction (~30%). This means that the computed target displacement for the second mode is unrealistically high – much higher than the target computed for the modal pushover analysis procedure (MPA). As a result, the +M2+/-M1 cases for scale factor 2.0 failed to reach the initial M2 target displacement due to numerical instability, indicating probable local structural collapse. The M2 target displacement for the scale factor 2.0 analyses in the H2 direction was therefore adjusted downward as follows:

1. Compute the M1 and M2 spectral displacement targets and SRSS value separately, as performed for the MPA procedure.
2. Determined the ratio of the M2 target to the total, and increase this ratio slightly to account for the missing mass in modes 3 and above.
3. Set the M2 pushover target as the above ratio times the originally computed roof target displacement.

Alternate approaches for computing the target displacements are discussed in the following sections.

F.5 Results

F.5.1 Building A Results

The two dimensional model was analyzed and results are presented in the y-direction. Bi-directional or torsional loading was not considered.

The scale factor 0.5 results were omitted because the conclusions are similar to those for scale factor 1.0. For the CMP extended analyses, only scale factor 2.0 analyses were performed.

For the nonlinear response history analysis with scale factor 2.0, only six of the eight analyses ran to completion, so median results are presented, taken as the average of the 4th and 5th ranked result of the completed analyses.

Section F.6.1 provides a summary of observations based on the results presented in this section. The following results are presented for Building A:

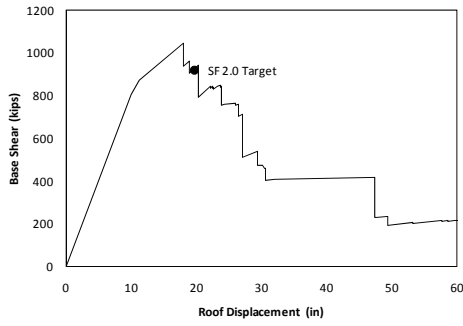
- *R-C₁-T* Calculations – Table F-8
- Pushover Curves for Modes 1 through 3 – Figure F-13

- Consecutive Modal Pushover Curves – Figure F-14
- NRHA Peak Story Drift Ratio Plots – Figure F-15
- NRHA Peak Story Displacement, Shear, and OTM Plots – Figure F-16
- ASCE 41 Type Methods Peak Story Displacement Plots – Figure F-17
Modal Type Methods Peak Story Displacement Plots – Figure F-18
- ASCE 41 Type Methods Peak Story Drift Ratio Plots – Figure F-19
Modal Type Methods Peak Story Drift Ratio Plots – Figure F-20
- ASCE 41 Type Methods Peak Story Shear Plots – Figure F-21
Modal Type Methods Peak Story Shear Plots – Figure F-22
- ASCE 41 Type Methods Peak Story Overturning Moment Plots – Figure F-23
Modal Type Methods Peak Story Overturning Moment Plots – Figure F-24
- CMP Extended Peak Story Displacement and Drift Plots – Figure F-25
CMP Extended Peak Story Shear and Overturning Moment Plots – Figure F-26
- 2-Stage CMP Deflected Shapes – Figure F-27
3-Stage CMP Deflected Shapes – Figure F-28

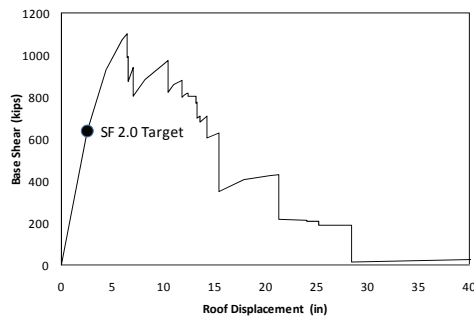
Table F-8 R-C₁-T Calculations for Building A

Scale Factor = 1.0	Mode 1	Mode 2	Mode 3*
F_y (kip)	900	650	N/A
T_e (s)	3.68	1.18	0.63
S_a (g)	.057	0.356	N/A
C_0	1.3	0.25	0.22
C_m	0.85	0.12	0.03
R	0.93	8.01	
C_1	1	1	
C_2	1	1	
$(T^2/4\pi^2) S_a$ (in)	2373	1521	N/A
δ_t (in)	9.86	1.32	
V_t (kip)	797	337	
Scale Factor = 2.0	Mode 1	Mode 2	Mode 3
F_y (kip)	850	620	N/A
T_e (s)	3.68	1.18	0.63
S_a (g)	0.11	0.71	N/A
C_0	1.3	0.25	0.22
C_m	0.85	0.12	0.03
R	1.96	2.36	
C_1	1	1	
C_2	1	1	
$(T^2/4\pi^2) S_a$ (in)	4747	3042	N/A
δ_t (in)	19.73	2.43	
V_t (kip)	941	621	

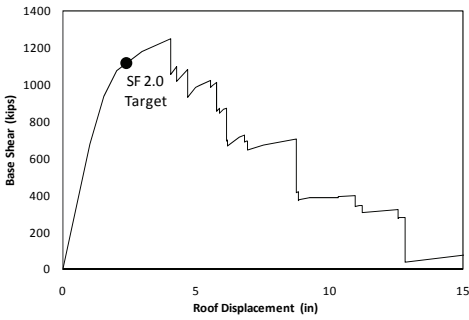
*Mode 3 target displacement not required by analysis methods used and therefore associated parameters not calculated.



(a) Mode 1



(b) Mode 2



(c) Mode 3

Figure F-13 Building A pushover results.

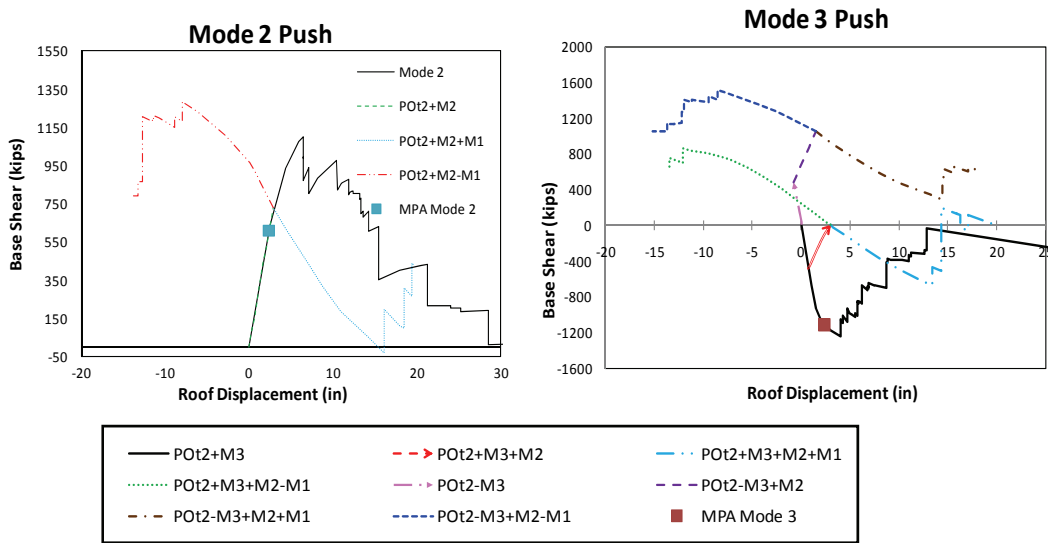


Figure F-14 Building A consecutive modal pushover results.

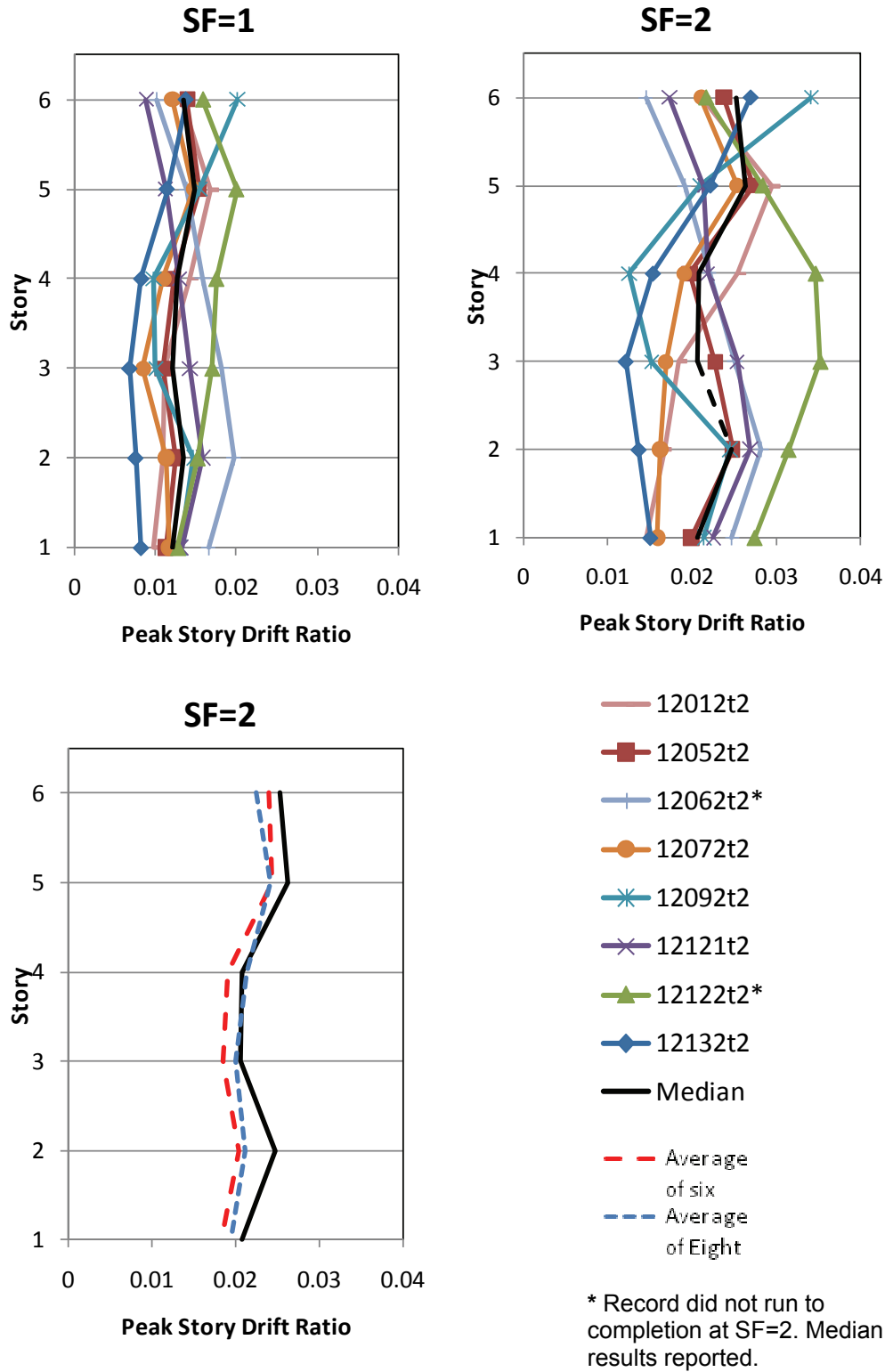


Figure F-15 Building A NRHA peak story drift ratios.

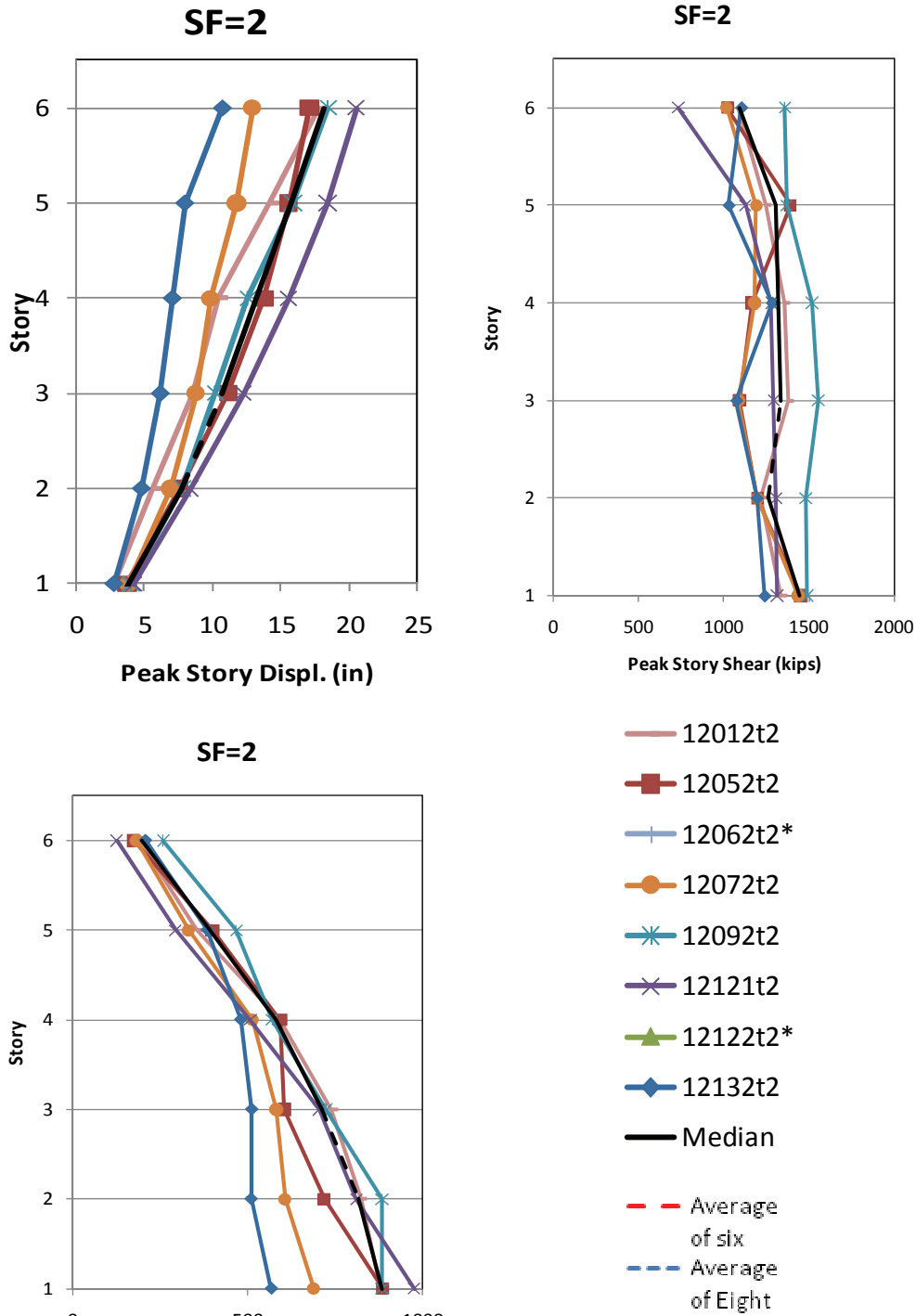


Figure F-16 Building A NRHA peak displacements, shears and OTMs.

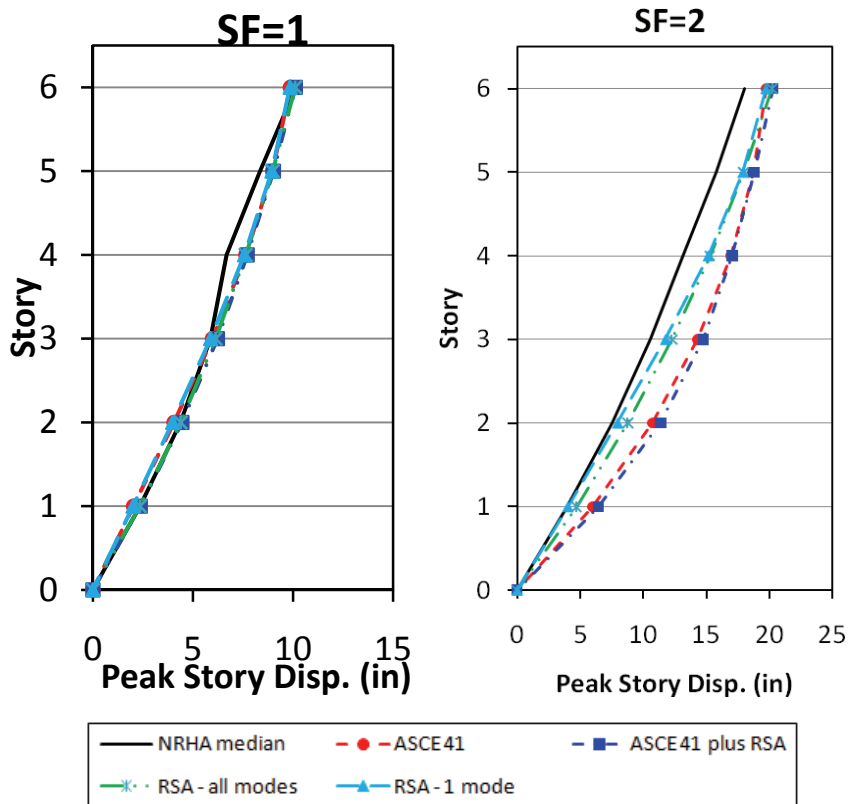


Figure F-17 Building A Comparison of Peak Story Displacement.

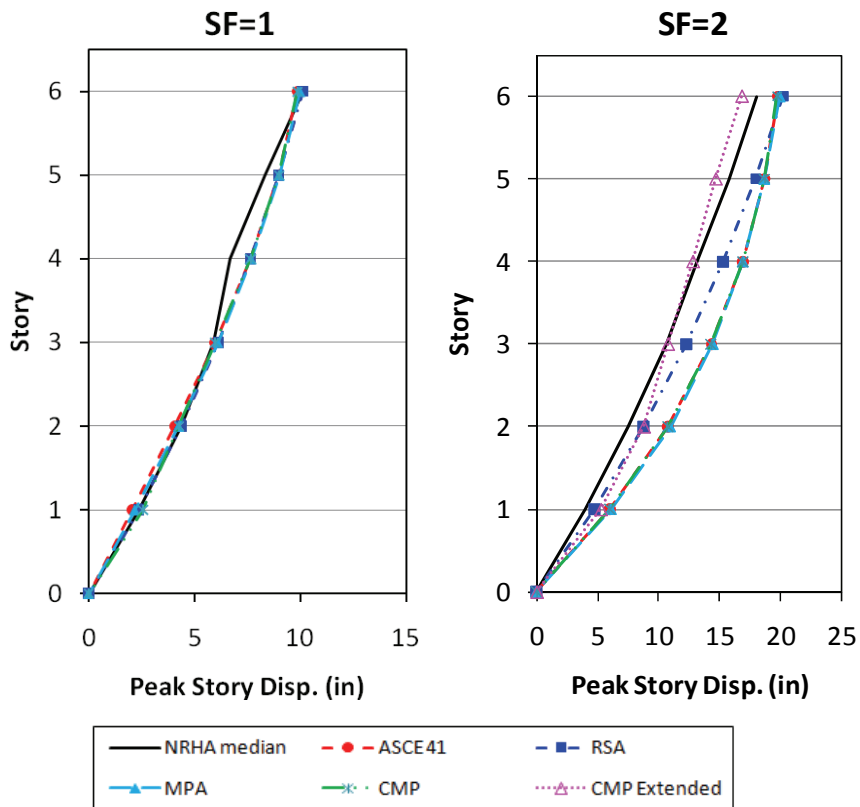


Figure F-18 Building A comparison of peak story displacement.

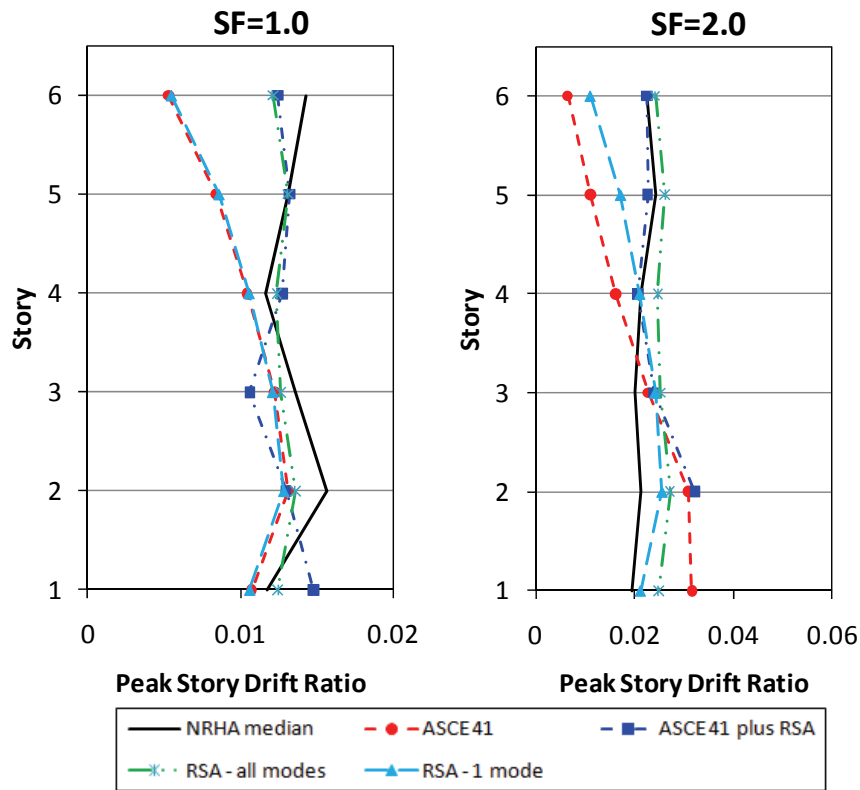


Figure F-19 Building A comparison of peak story drift.

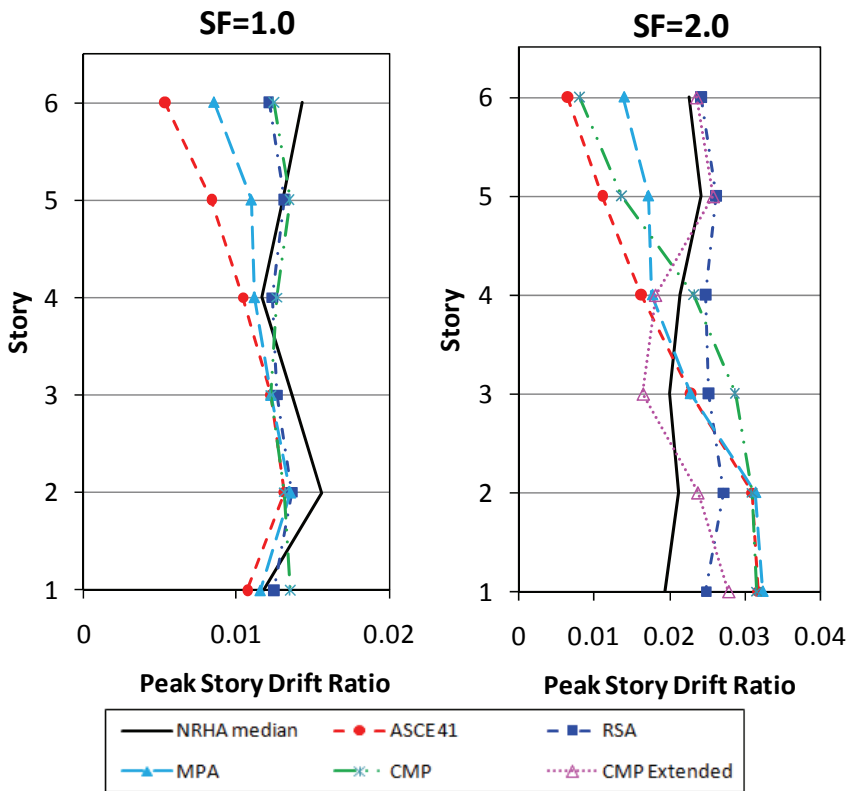


Figure F-20 Building A comparison of peak story drift.

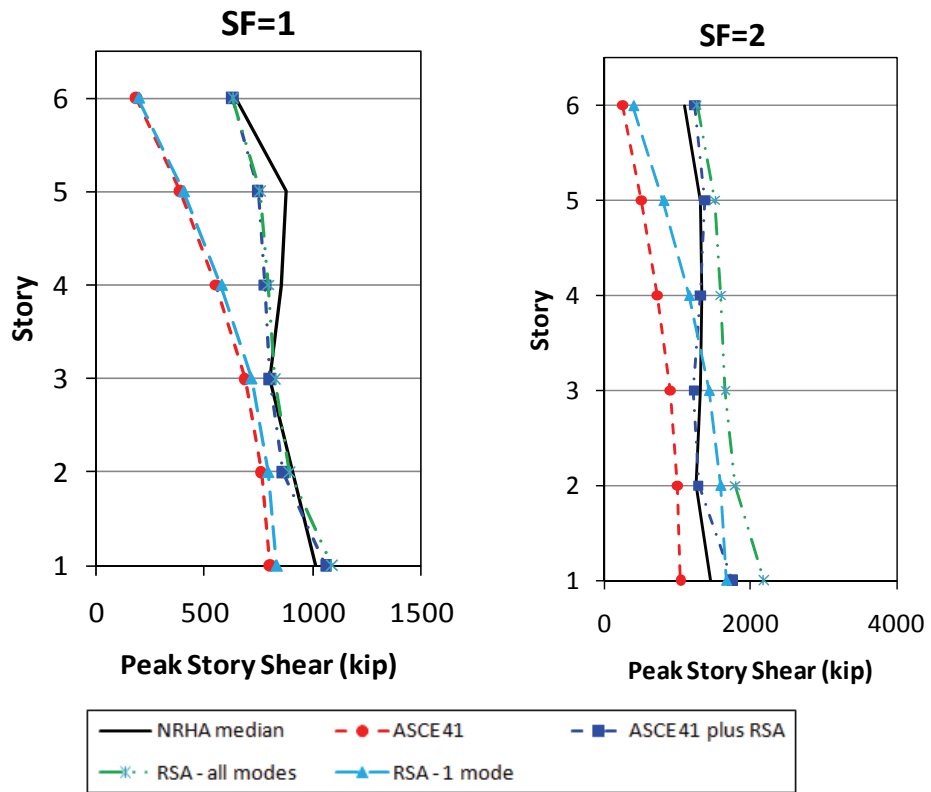


Figure F-21 Building A comparison of peak story shear.

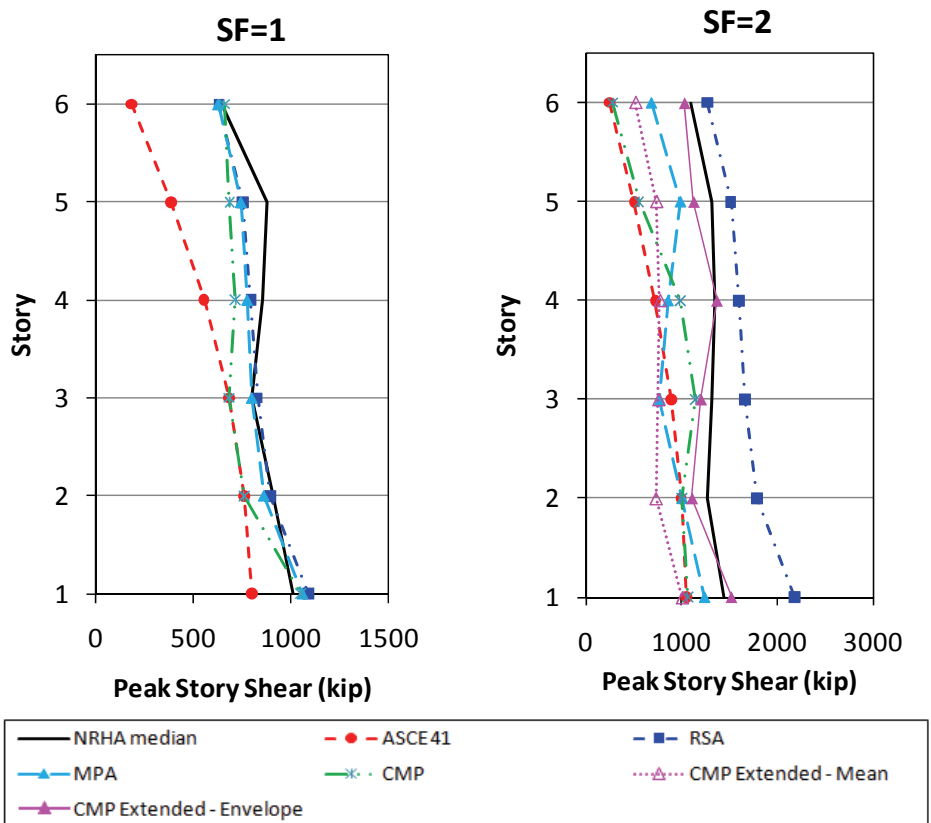


Figure F-22 Building A comparison of peak story shear.

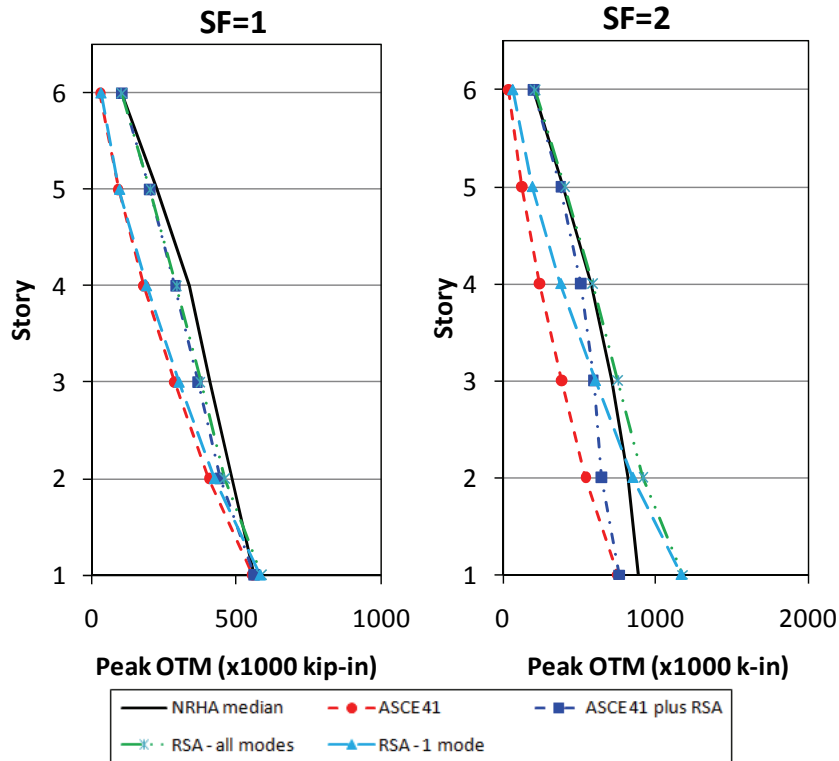


Figure F-23 Building A comparison of peak story overturning moment.

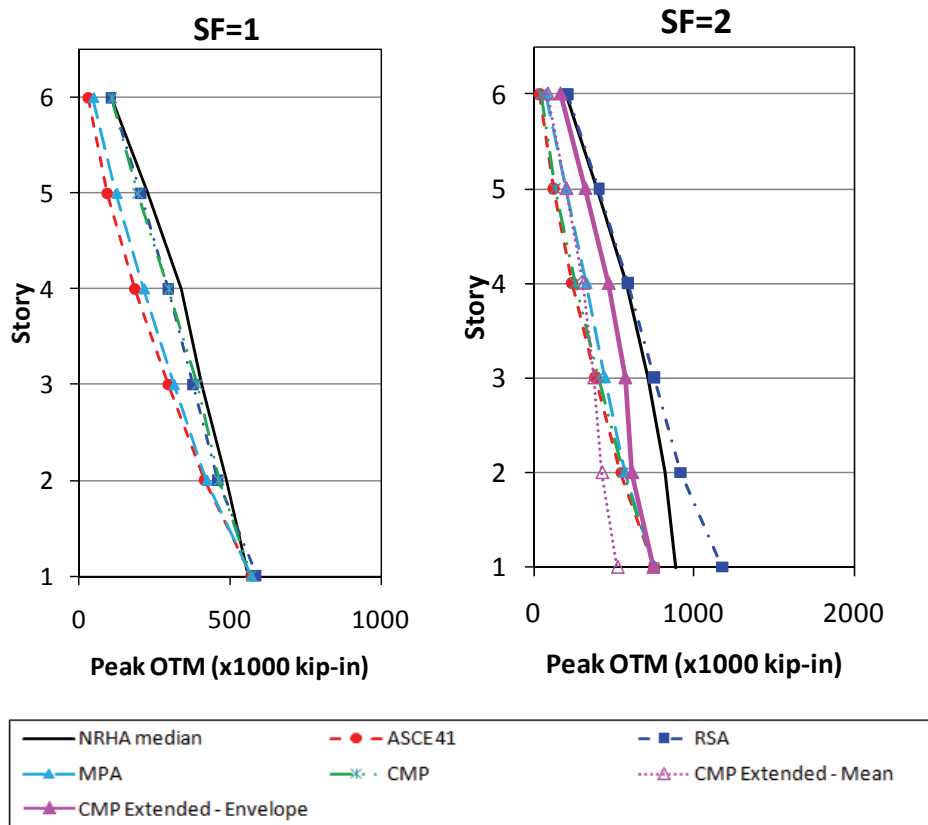


Figure F-24 Building A comparison of peak story overturning moment.

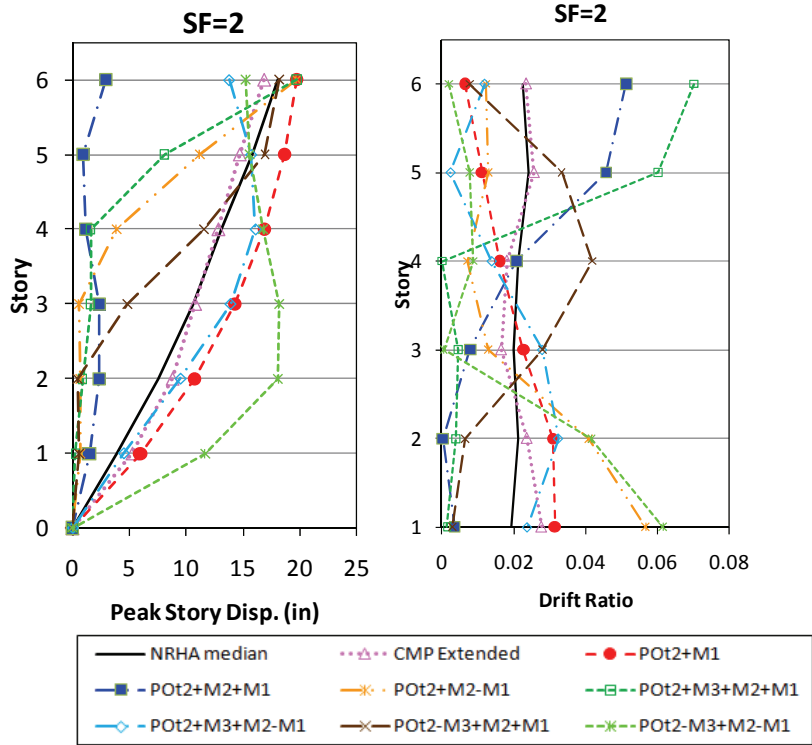


Figure F-25 Building A Comparison of CMP Extended peak displacement and story drift ratio.

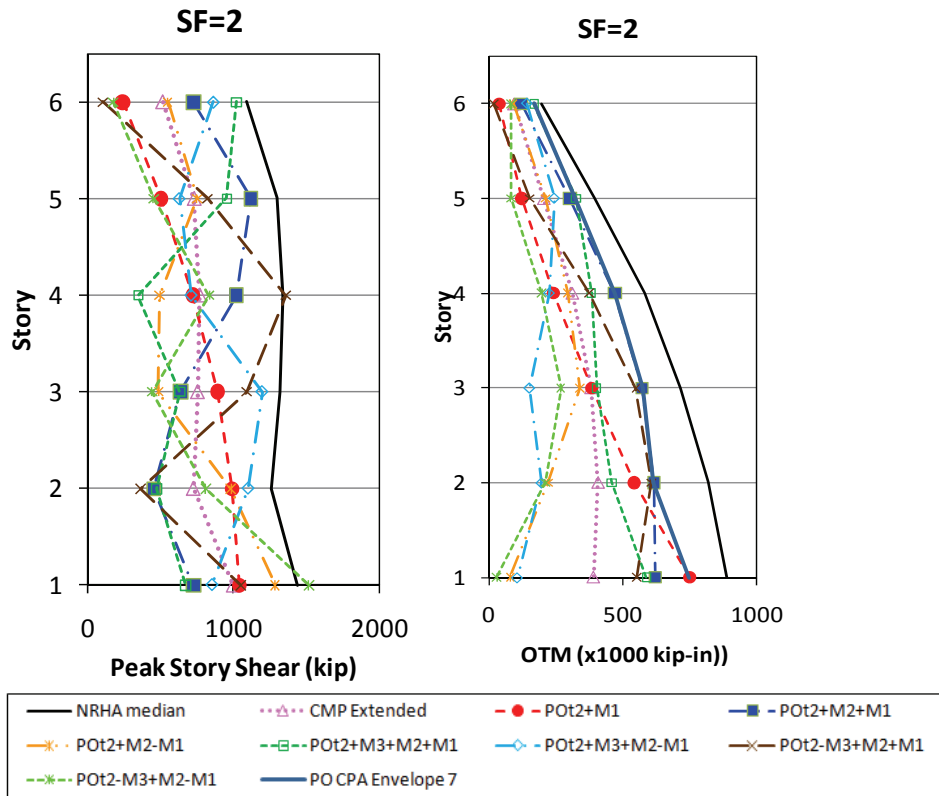


Figure F-26 Building A Comparison of CMP Extended peak shear and overturning moment.

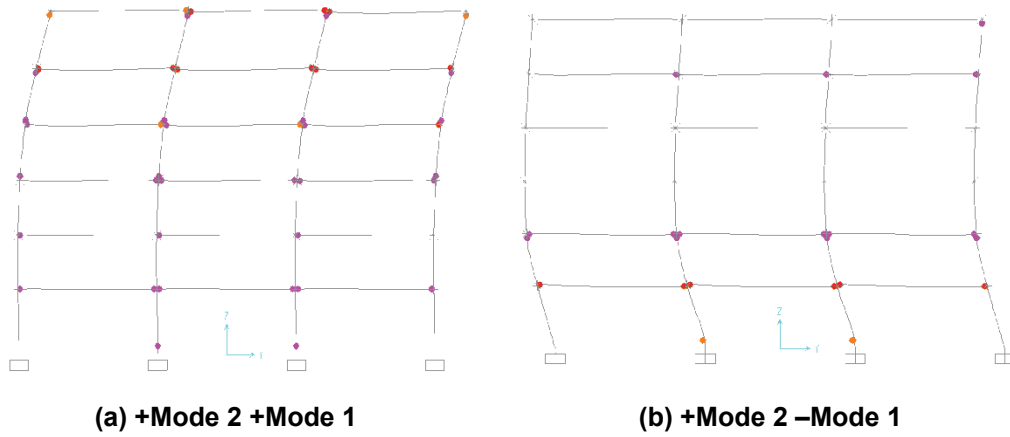


Figure F-28 Building A 2-stage CMP deflected shapes

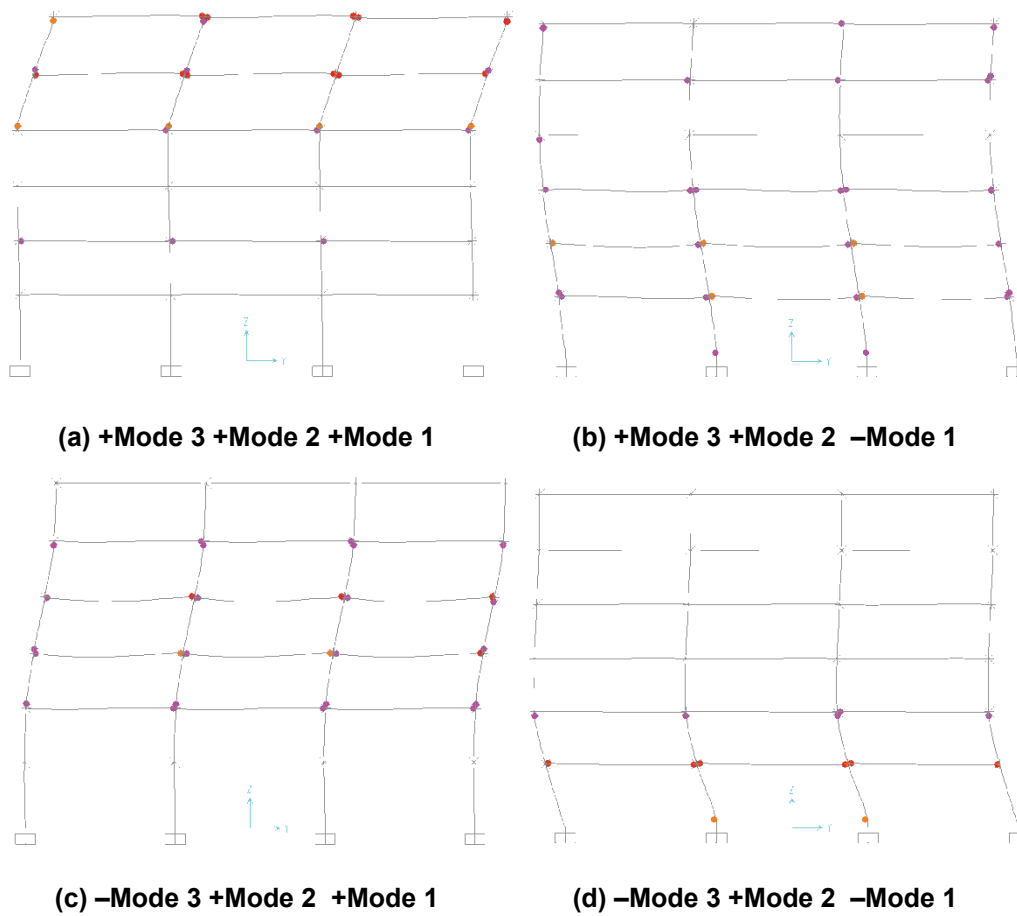


Figure F-28 Building A 3-stage CMP deflected shapes.

F.5.2 Building B Results

The three dimensional model was analyzed separately in each direction and results are presented separately in the H1 (X-direction) and H2 (Y-direction). Bi-directional or torsional loading was not considered. The overall structural response in the two directions is quite different. In the H1 direction, the structure tends to “rock” on the relatively short braced frames, while in the H2 direction the longer braced frames resist overturning more effectively which forces lateral deformations into the framing members. The two sets of analyses can effectively be considered studies of different structures and so are presented separately.

The flexible roof diaphragm means that third floor drifts are considerably higher at the center of the diaphragm than at the edge. Roof displacements and third floor drifts are therefore shown at both locations. Some of the displacement and drift results are duplicated at two different horizontal scales as the high values at the center of the roof location make assessment of results difficult.

For each of the H1 and H2 directions, the response history results are presented first, with one page of results showing all demand parameters for a specified direction and scale factor. The remaining results are divided into two sets of charts, one for the procedures currently in ASCE 41, and the second for procedures not currently included in ASCE 41. The last set of results show more detailed results for the CMP Extended analyses and a series of figures that display the state of the model at the end of each pushover analysis.

Section F.6.2 provides a summary of observations based on the results presented in this section. The following results are presented for Building B:

- *R-C₁-T* Calculations – Table F-9
- CMP Target Roof Displacement (SF = 0.5, 1.0, 2.0) – Table F-10, F-11 & F-12
- Pushover Curves in H1 and H2 Direction – Figures F-29 (H1) and F-30 (H2)
- NRHA Results in H1 and H2 Direction for SF = 0.5 – Figures 31 (H1) and 32 (H2)
NRHA Results in H1 and H2 Direction for SF = 1.0 – Figures 33 (H1) and 34 (H2)
NRHA Results in H1 and H2 Direction for SF = 2.0 – Figures 35 (H1) and 36 (H2)
- ASCE 41 Type Methods Peak Story Drift Ratio Plots (H1) – Figure F-37
Modal Type Methods Peak Story Drift Ratio Plots (H1) – Figure F-38
- ASCE 41 Type Methods Peak SDR (reduced scale) Plots (H1) – Figure F-39
Modal Type Methods Peak SDR (reduced scale) Plots (H1) – Figure F-40

- ASCE 41 Type Methods Peak Story Displacement Plots (H1) – Figure F-41
Modal Type Methods Peak Story Displacement Plots (H1) – Figure F-42
- ASCE 41 Type Methods Peak Story Shear Plots (H1) – Figure F-43
Modal Type Methods Peak Story Shear Plots (H1) – Figure F-44
- ASCE 41 Type Methods Peak Story OTM Plots (H1) – Figure F-45
Modal Type Methods Peak Story OTM Plots (H1) – Figure F-46
- ASCE 41 Type Methods Peak Story Drift Ratio Plots (H2) – Figure F-47
Modal Type Methods Peak Story Drift Ratio Plots (H2) – Figure F-48
- ASCE 41 Type Methods Peak SDR (reduced scale) Plots (H2) – Figure F-49
Modal Type Methods Peak SDR (reduced scale) Plots (H2) – Figure F-50
- ASCE 41 Type Methods Peak Story Displacement Plots (H2) – Figure F-51
Modal Type Methods Peak Story Displacement Plots (H2) – Figure F-52
- ASCE 41 Type Methods Peak Story Shear Plots (H2) – Figure F-53
Modal Type Methods Peak Story Shear Plots (H2) – Figure F-54
- ASCE 41 Type Methods Peak Story OTM Plots (H2) – Figure F-55
Modal Type Methods Peak Story OTM Plots (H2) – Figure F-56
- CMP Extended Peak Story Drift Plots, Drift (reduced scale) Plots, Displacement Plots, Shear Plots, Overturning Moment Plots (H1) – Figures F-57 to F-61
- CMP Extended Peak Story Drift Plots, Drift (reduced scale) Plots, Displacement Plots, Shear Plots, Overturning Moment Plots (H2) – Figures F-62 to F-66

Pushover Analyses

Results of the pushovers used for the ASCE 41, MPA and CMP procedures are shown below. Due to the relatively flexible roof diaphragm, the second mode in the H1 and H2 direction is not mode 4 and 5 as would typically be the case.

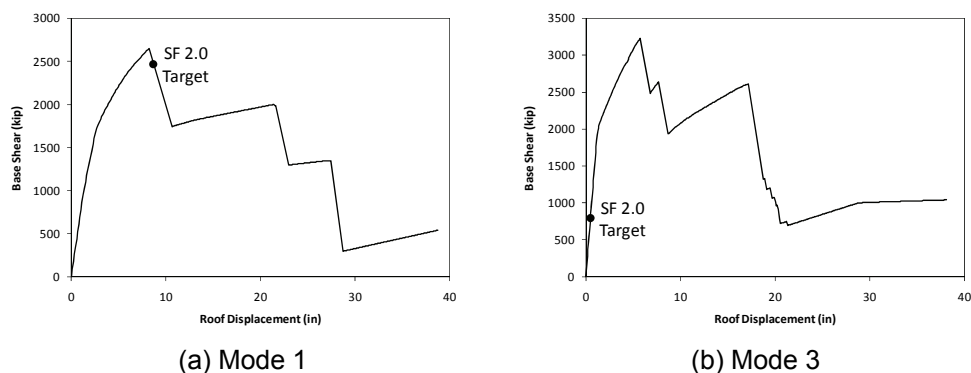
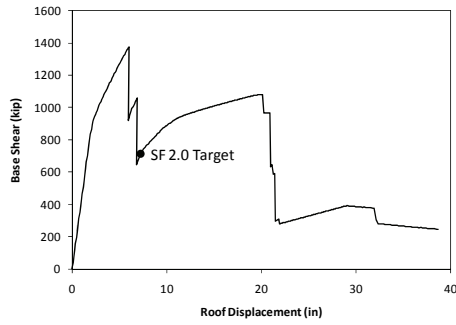
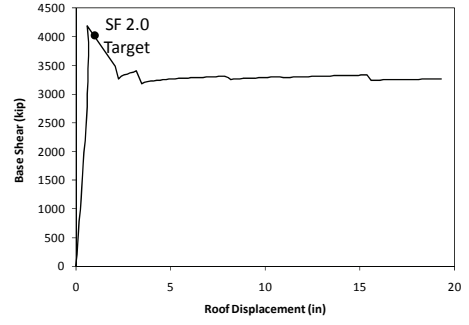


Figure F-29 Building B longitudinal (H1) pushover results.



(a) Mode 2



(b) Mode 5

Figure F-30 Building B Transverse (H2) pushover results.

Table F-9 R-C₁-T Calculations for Building B

Scale Factor =	Transverse (H2)		Longitudinal (H1)	
	Mode 2	Mode 5	Mode 1	Mode 3
0.5				
D _y /H	0.0040	0.0015	0.0049	0.0042
F _y (kip)	950	4050	1950	1725
T _e (s)	0.538	0.295	0.561	0.318
S _a (g)	0.39	0.42	0.38	0.43
C ₀	1.40	0.48	1.72	0.76
C _m	0.32	0.59	0.62	0.29
R	1	1	1	1
C ₁	1	1	1	1
C ₂	1	1	1	1
(T ² /4π ²) S _a (in)	1.12	0.36	1.13	0.43
δ _t (in)	1.57	0.17 [0.27]	1.94 [1.97]	0.33 [0.26]
V _t (kip)	678	741 [1145]	1338 [1359]	248 [198]
1.0				
D _y /H	0.0040	0.0015	0.0049	0.0042
F _y (kip)	950	4050	1950	1725
T _e (s)	0.538	0.295	0.561	0.318
S _a (g)	0.79	0.84	0.76	0.86
C ₀	1.40	0.48	1.72	0.76
C _m	0.32	0.59	0.62	0.29
R	1.93	1	1.78	1
C ₁	1.05	1	1.04	1
C ₂	1	1	1	1
(T ² /4π ²) S _a (in)	2.23	0.72	2.27	0.86
δ _t (in)	3.32 [3.21]	0.35 [0.52]	4.08 [4.15]	0.66 [0.52]
V _t (kip)	1071 [1059]	1506 [2420]	2039 [2054]	495 [395]
2.0				
D _y /H	0.0040	0.0015	0.0049	0.0042
F _y (kip)	950	4050	1950	1725
T _e (s)	0.538	0.295	0.561	0.318
S _a (g)	1.57	1.68	1.52	1.73
C ₀	1.40	0.48	1.72	0.76
C _m	0.32	0.59	0.62	0.29
R	3.85	1	3.56	1
C ₁	1.16	1	1.14	1
C ₂	1.04	1	1.03	1
(T ² /4π ²) S _a (in)	4.46	1.43	4.54	1.71
δ _t (in)	7.56 [7.26]	0.82 [0.94]	9.10 [8.69]	1.31 [1.05]
V _t (kip)	744 [712]	4050 [4027]	2320 [2470]	984 [791]

Note: Alternate values shown in [] are values that were revised based on an adjustment to the bilinear idealization. The revised values were used to calculate the pushover targets for the CMP Extended procedure shown in the following tables.

Table F-10 CMP Target Roof Displacements of Building B (SF = 0.5)

		1 st Push (in)	2 nd Push (in)	Total (in)
Transverse (H2)	Case 1 (M1)	1.57	NA	1.57
	Case 2 (M1+M2)	0.50	1.07	1.57
	Case A* (M1-M2)	0.50	-1.07	-0.57
	Case 3 (M2+M1)	1.07	0.50	1.57
	Case 4 (-M2+M1)	-1.07	0.50	-0.57
Longit. (H1)	Case 1 (M1)	1.97	NA	1.97
	Case 2 (M1+M2)	1.22	0.75	1.97
	Case A* (M1-M2)	1.22	-0.75	0.47
	Case 3 (M2+M1)	0.75	1.22	1.97
	Case 4 (-M2+M1)	-0.75	1.22	0.47

*Case A did not complete due to numerical stability

Table F-11 CMP Target Roof Displacements of Building B (SF = 1.0)

		1 st Push (in)	2 nd Push (in)	Total (in)
Transverse (H2)	Case 1 (M1)	3.21	NA	3.21
	Case 2 (M1+M2)	1.03	2.18	3.21
	Case A* (M1-M2)	1.03	-2.18	-1.16
	Case 3 (M2+M1)	2.18	1.03	3.21
	Case 4 (-M2+M1)	-2.18	1.03	-1.16
Longit. (H1)	Case 1 (M1)	4.15	NA	4.15
	Case 2 (M1+M2)	2.57	1.58	4.15
	Case A* (M1-M2)	2.57	-1.58	0.99
	Case 3 (M2+M1)	1.58	2.57	4.15
	Case 4 (-M2+M1)	-1.58	2.57	0.99

*Case A did not complete due to numerical stability

Table F-12 CMP Target Roof Displacements of Building B (SF = 2.0)

		1 st Push (in)	2 nd Push (in)	Total (in)
Transverse (H2)	Case 1 (M1)	7.26	NA	7.26
	Case 2 (M1+M2)	2.32	4.94	7.26
	Case A* (M1-M2)	2.32	-4.94	-2.61
	Case B* (M2+M1)	4.94	2.32	7.26
	Case C* (-M2+M1)	-4.94	2.32	-2.61
	Case 3+ (M2+M1)	2.49	4.77	7.26
	Case 4+ (-M2+M1)	-2.49	4.77	-2.28
Longit. (H1)	Case 1 (M1)	8.69	NA	8.69
	Case 2 (M1+M2)	5.39	3.30	8.69
	Case A* (M1-M2)	5.39	-3.30	2.09
	Case 3 (M2+M1)	3.30	5.39	8.69
	Case 4 (-M2+M1)	-3.30	5.39	2.09

*Cases A, B, and C did not complete due to numerical stability

*Cases 3 and 4 modified to reduce Mode 2 target displacement

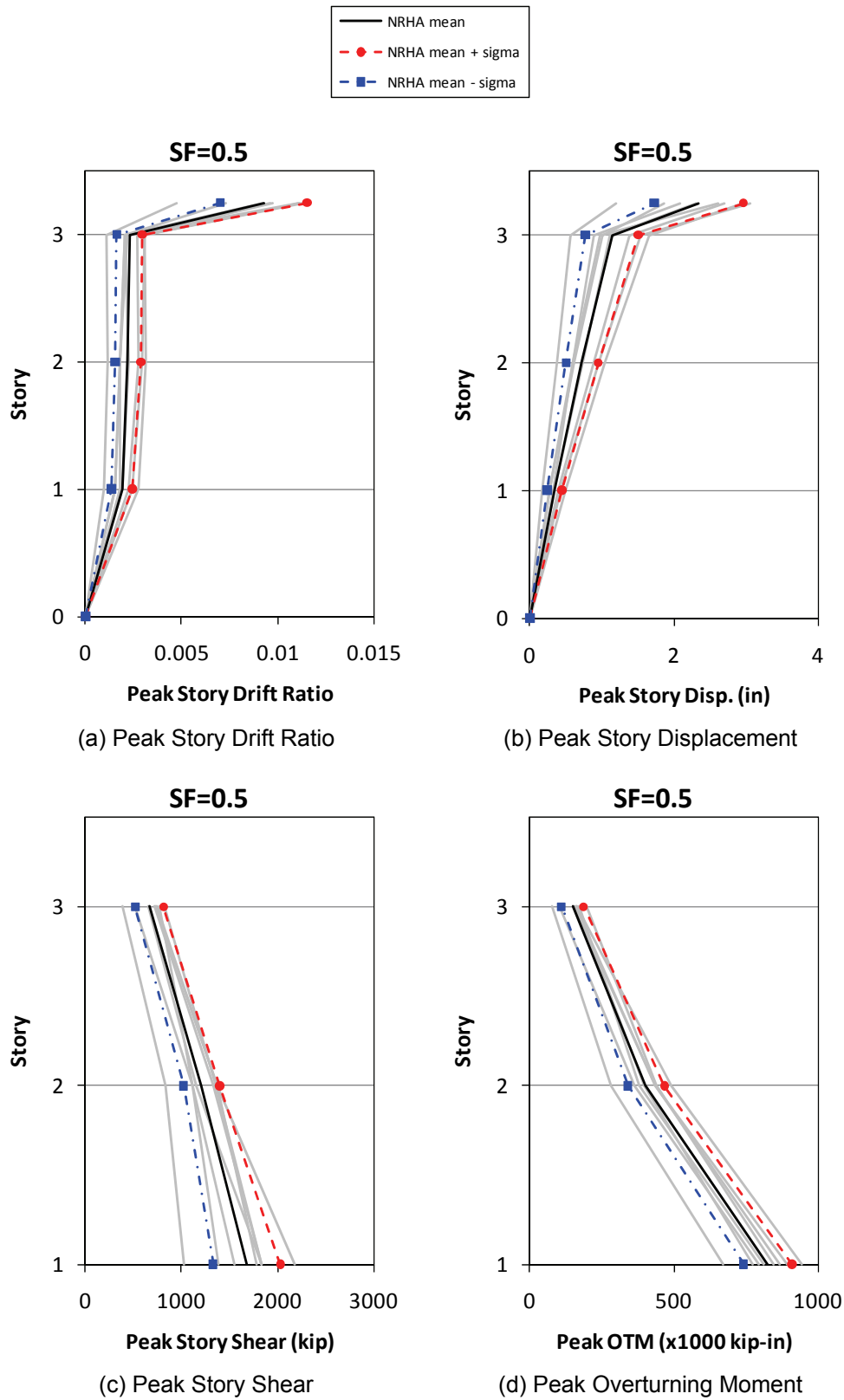


Figure F-31 Building B NRHA results in longitudinal direction (H1) for Scale Factor = 0.5.

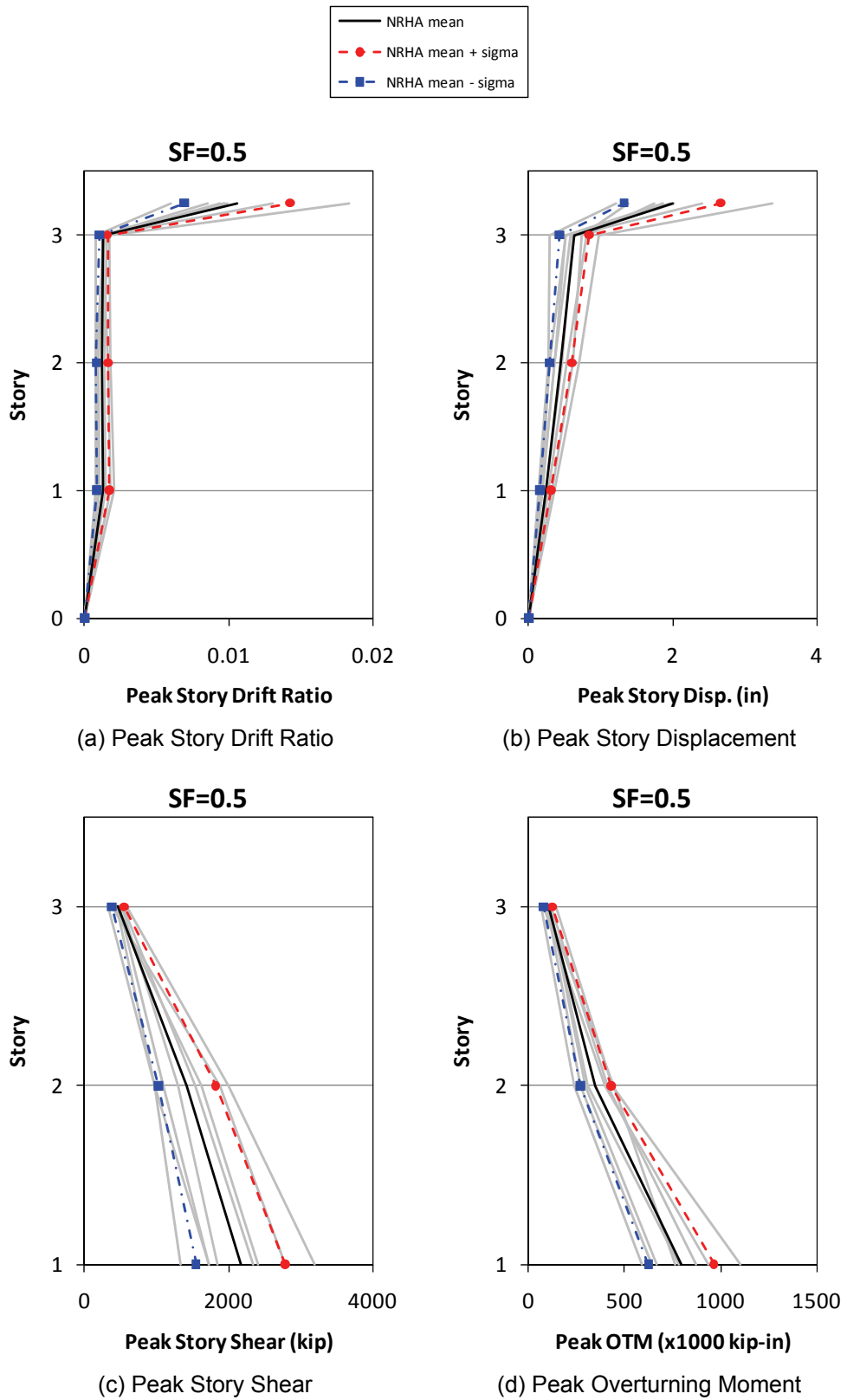


Figure F-32 Building B NRHA results in transverse direction (H2) for Scale Factor = 0.5.

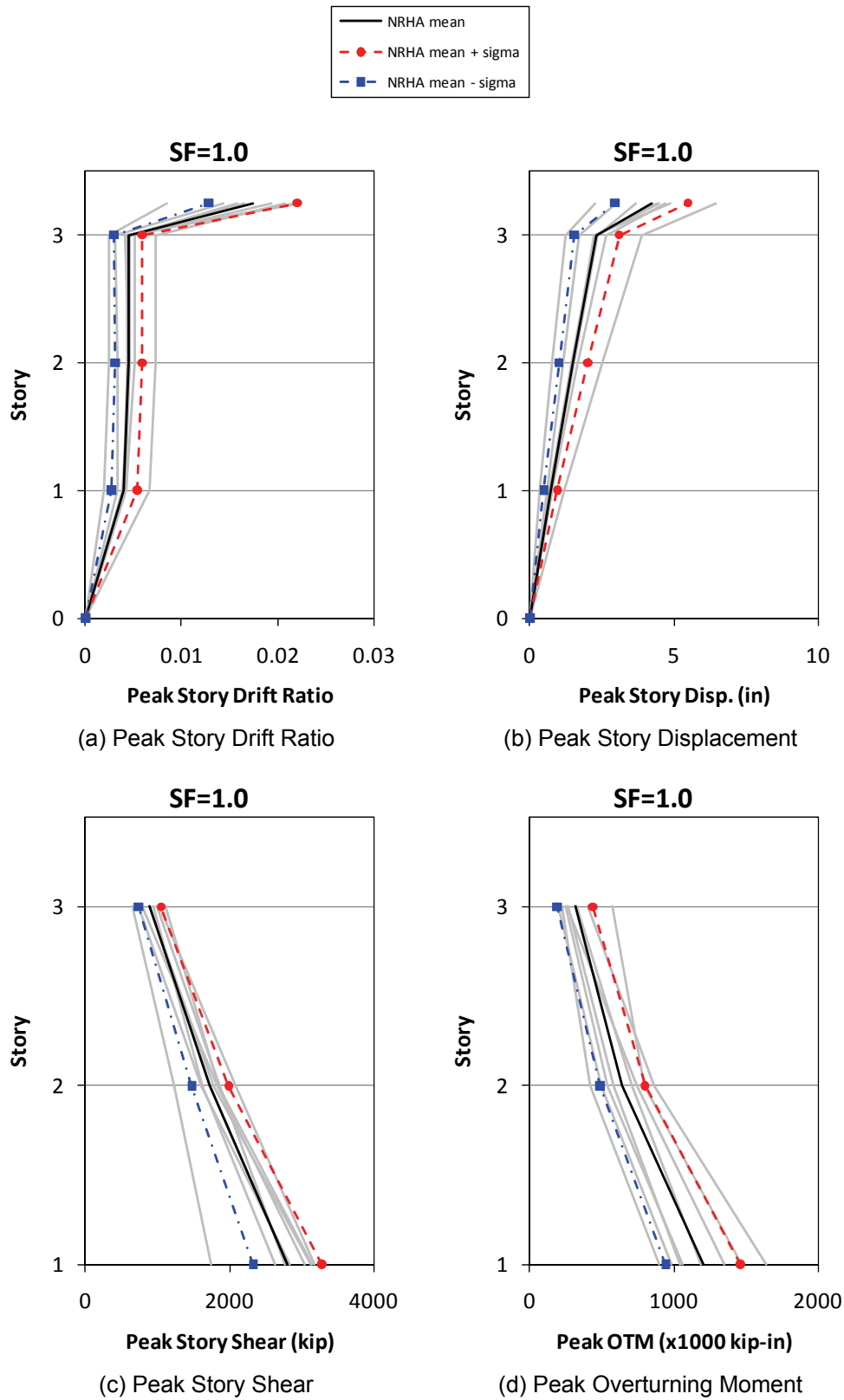


Figure F-33 Building B NRHA results in longitudinal direction (H1) for Scale Factor = 1.0.

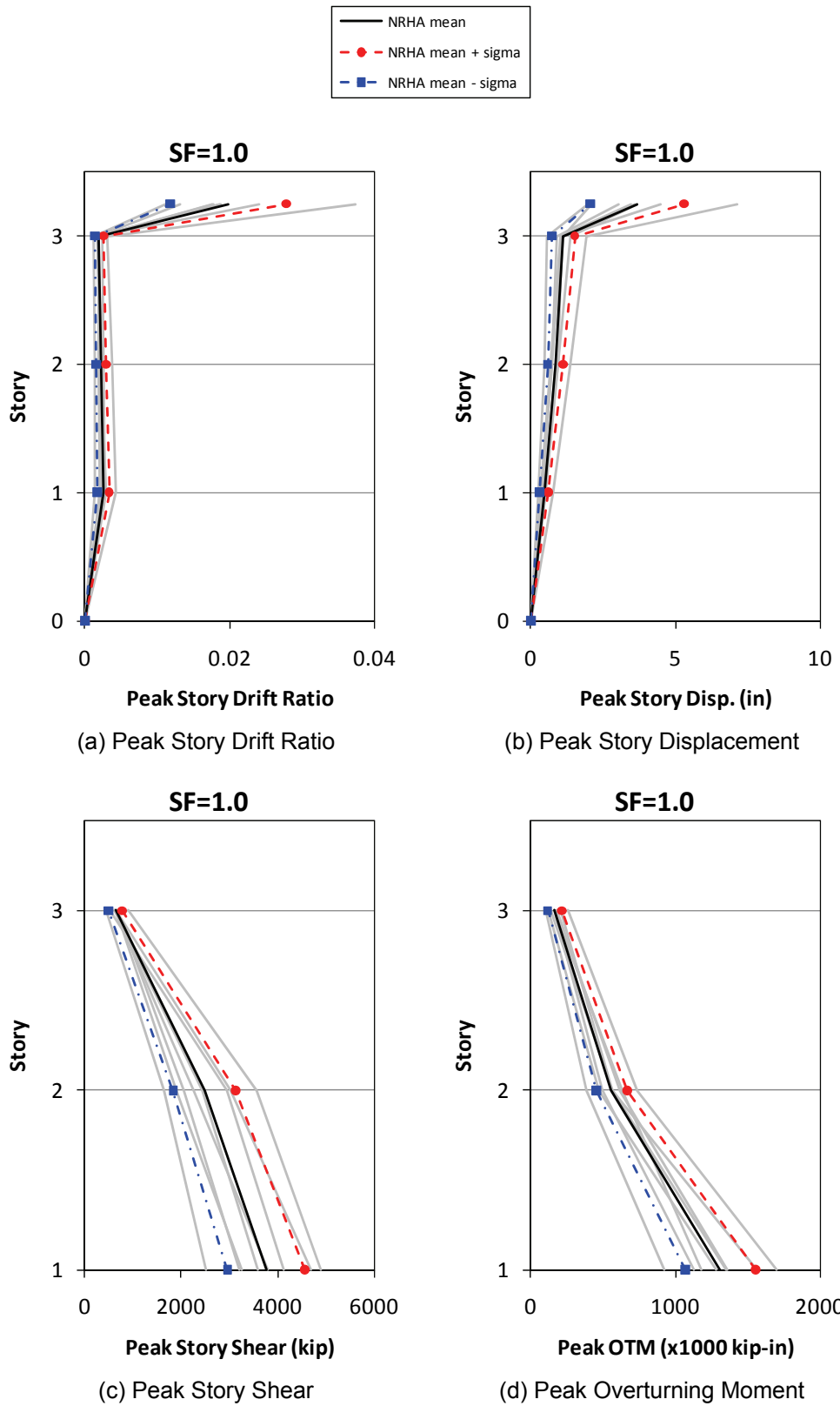


Figure F-34 Building B NRHA results in transverse direction (H2) for Scale Factor = 1.0.

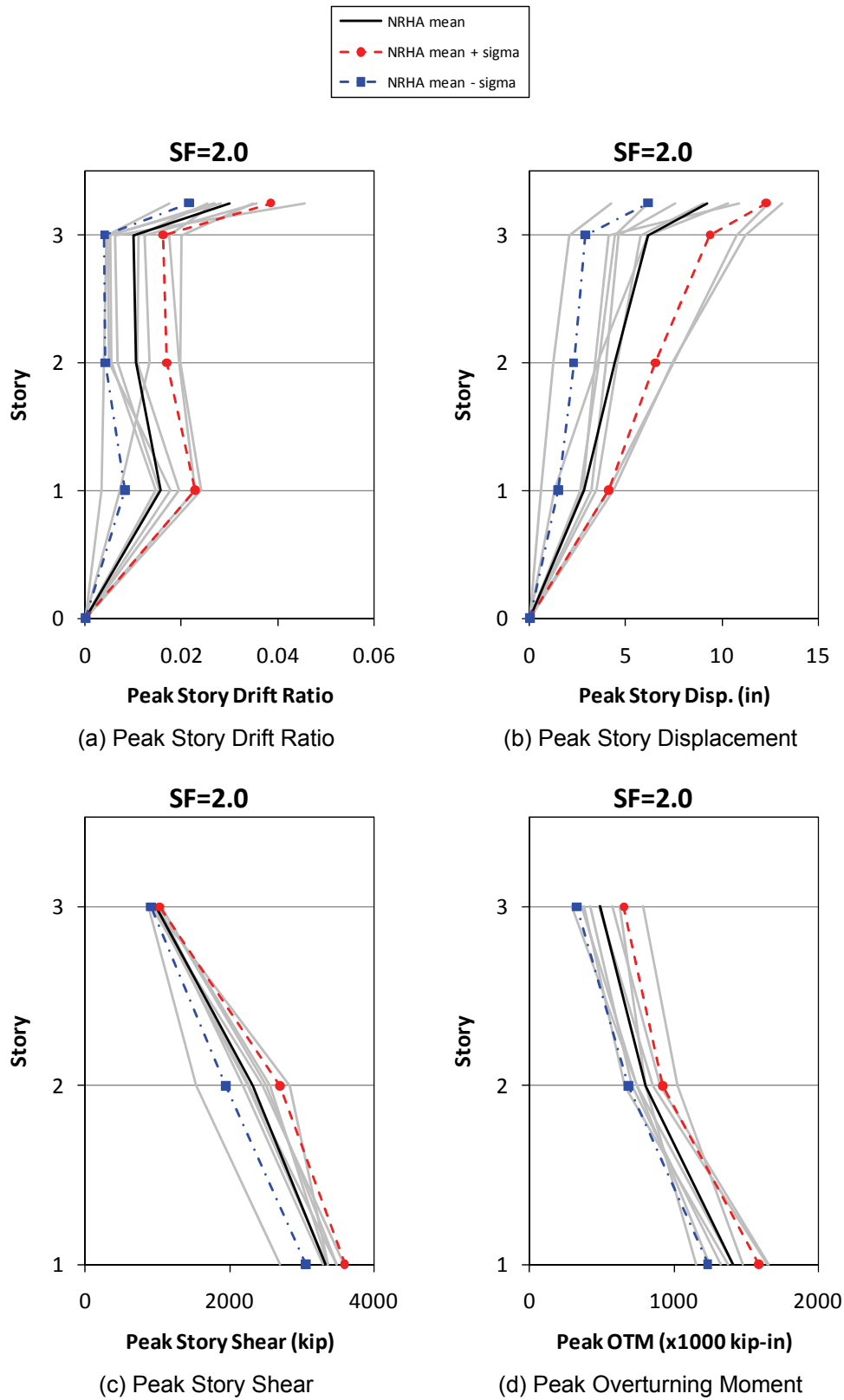


Figure F-35 Building B NRHA results in longitudinal direction (H1) for Scale Factor = 2.0.

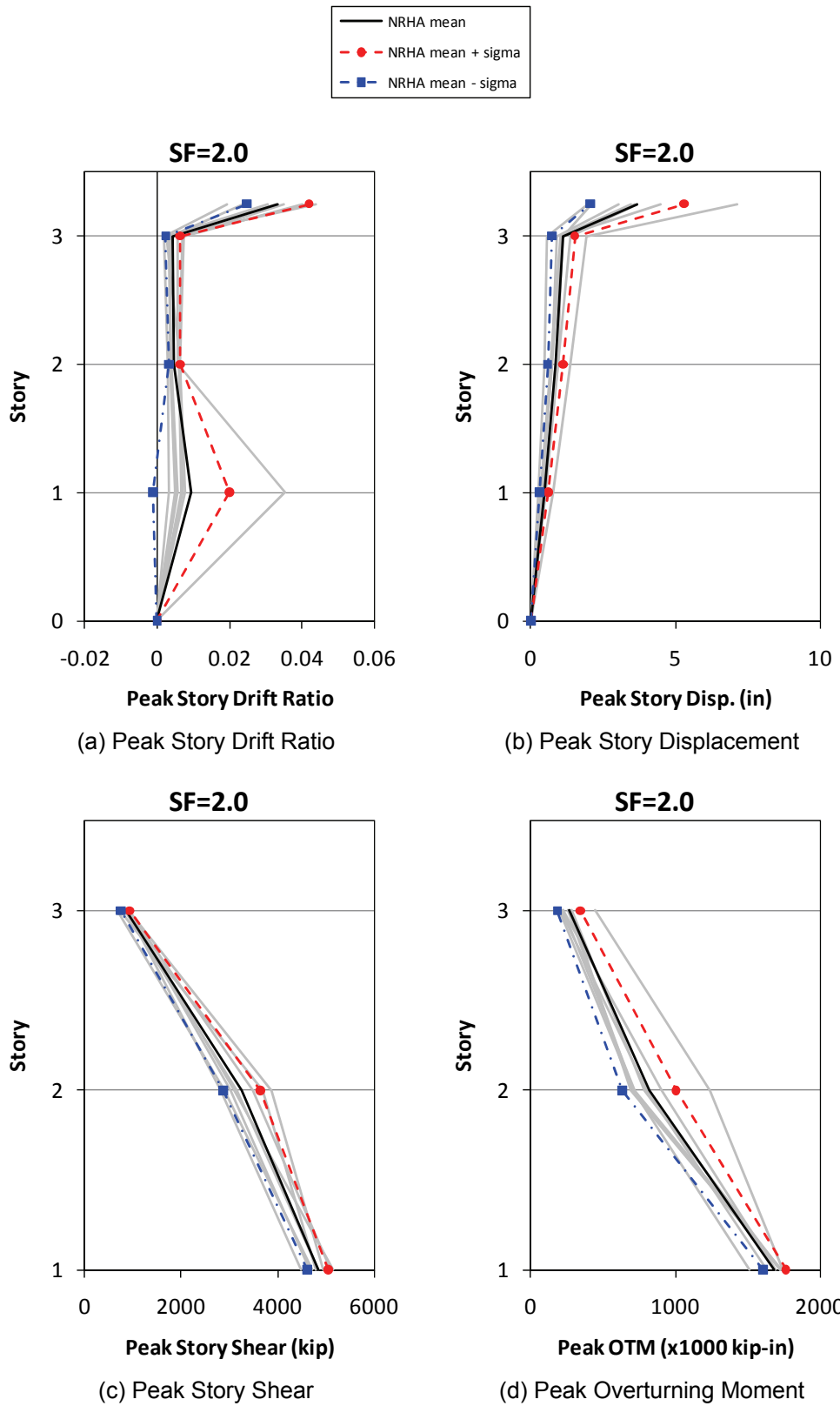


Figure F-36 Building B NRHA results in transverse direction (H2) for Scale Factor = 2.0.

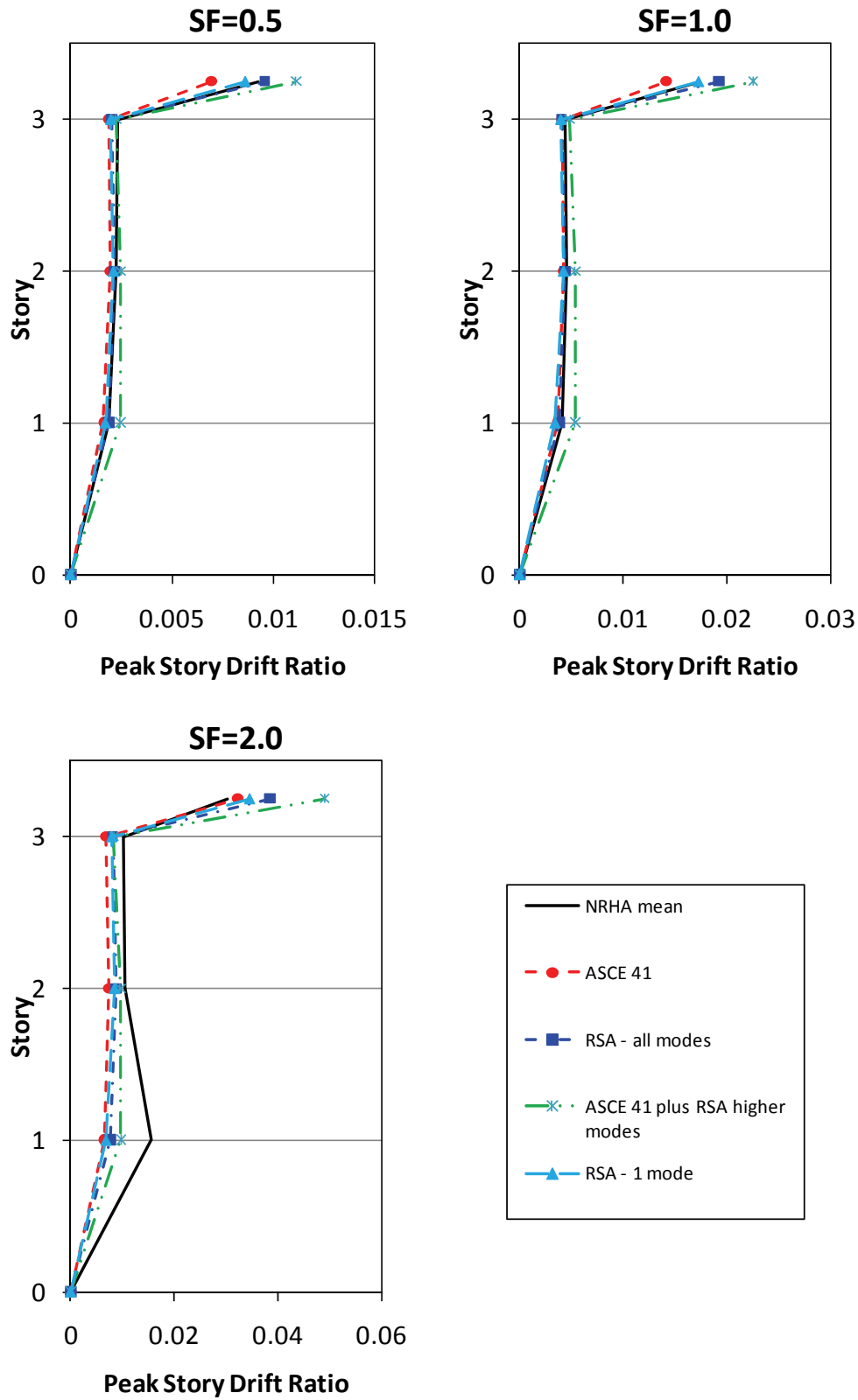


Figure F-37 Building B comparison of peak story drift ratio in longitudinal direction (H1).

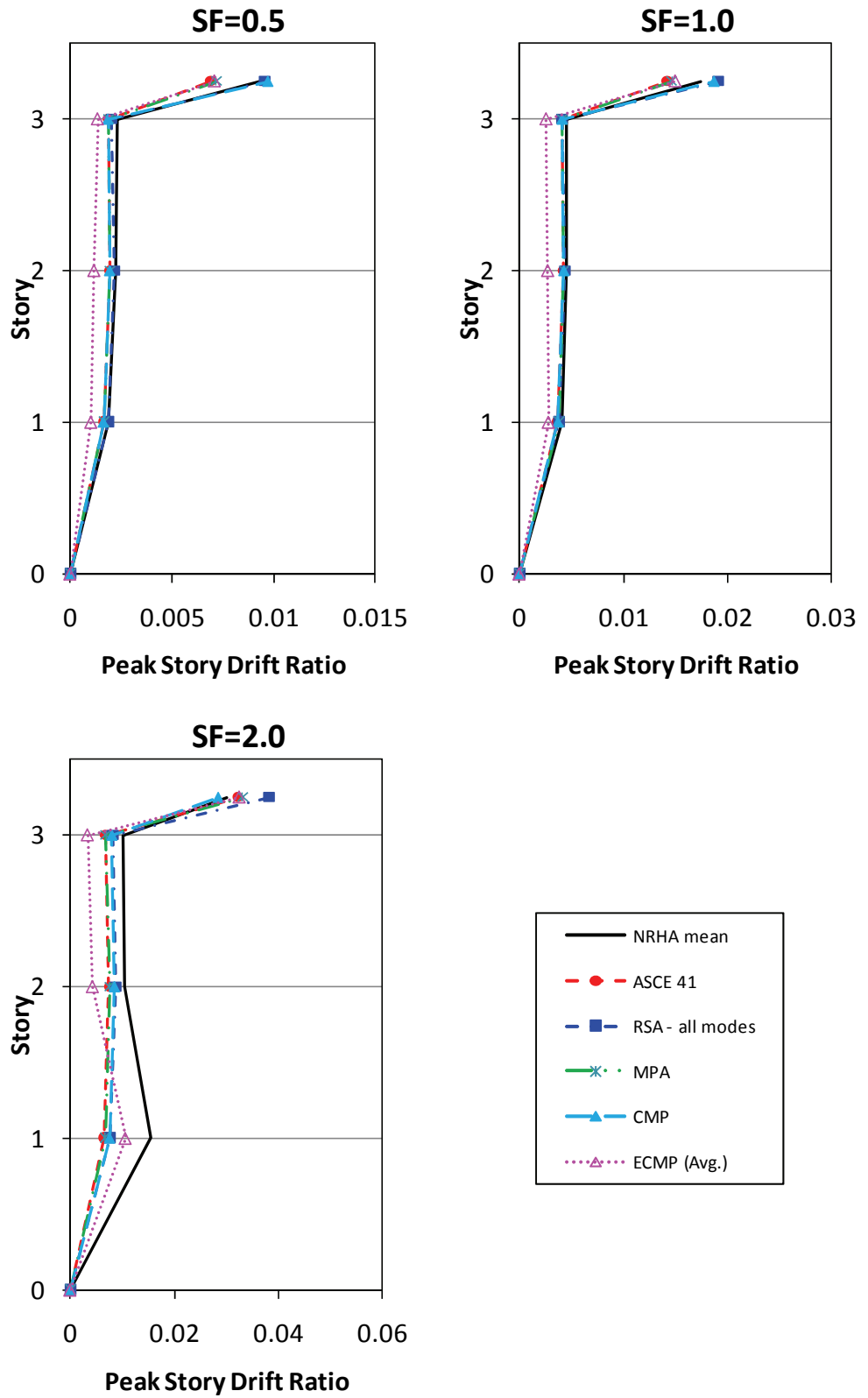


Figure F-38 Building B comparison of peak story drift ratio in longitudinal direction (H1).

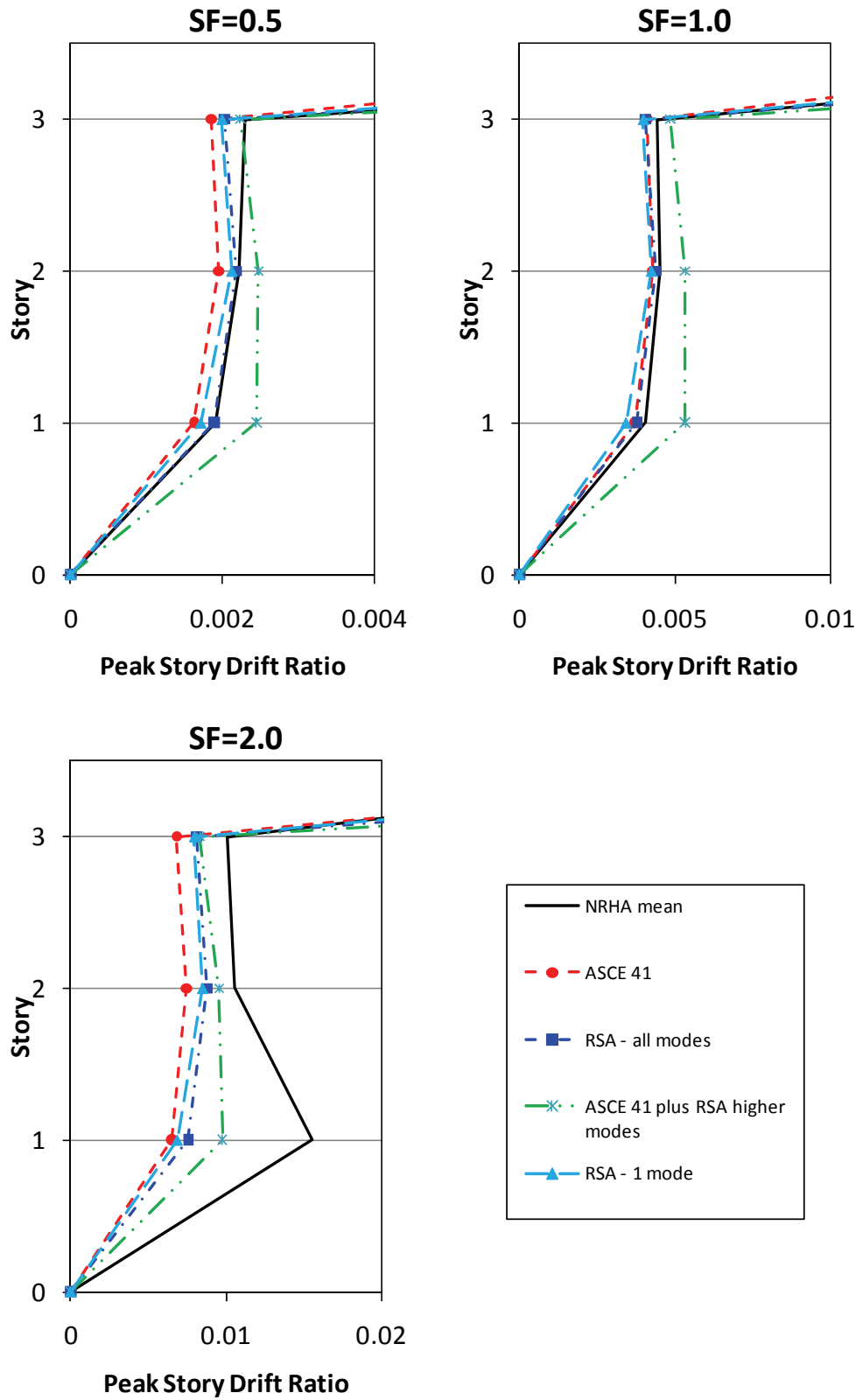


Figure F-39 Building B comparison of peak story drift ratio (reduced scale) in longitudinal direction (H1).

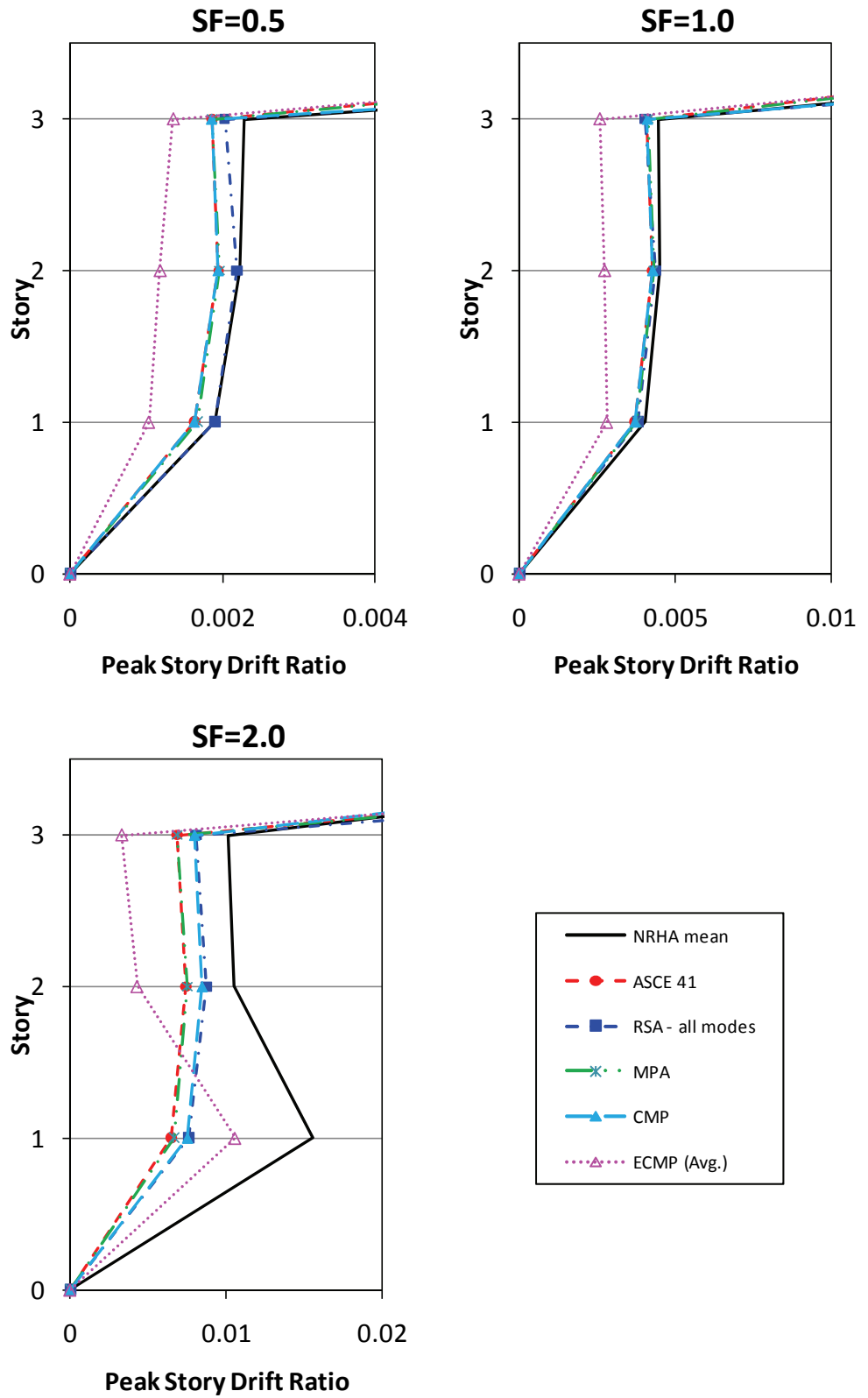


Figure F-40 Building B comparison of peak story drift ratio (reduced scale) in longitudinal direction (H1).

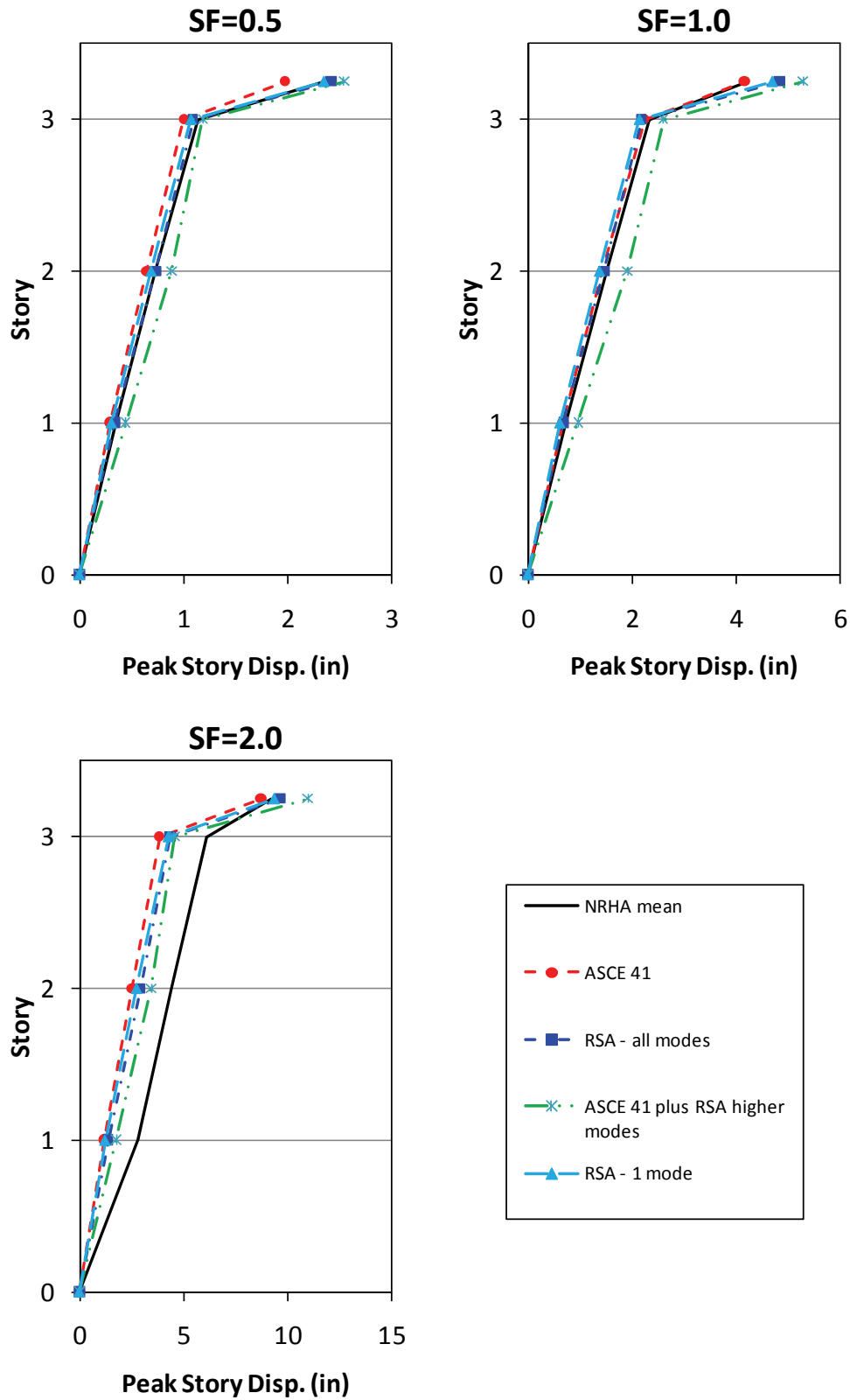


Figure F-41 Building B comparison of peak story displacement in longitudinal direction (H1).

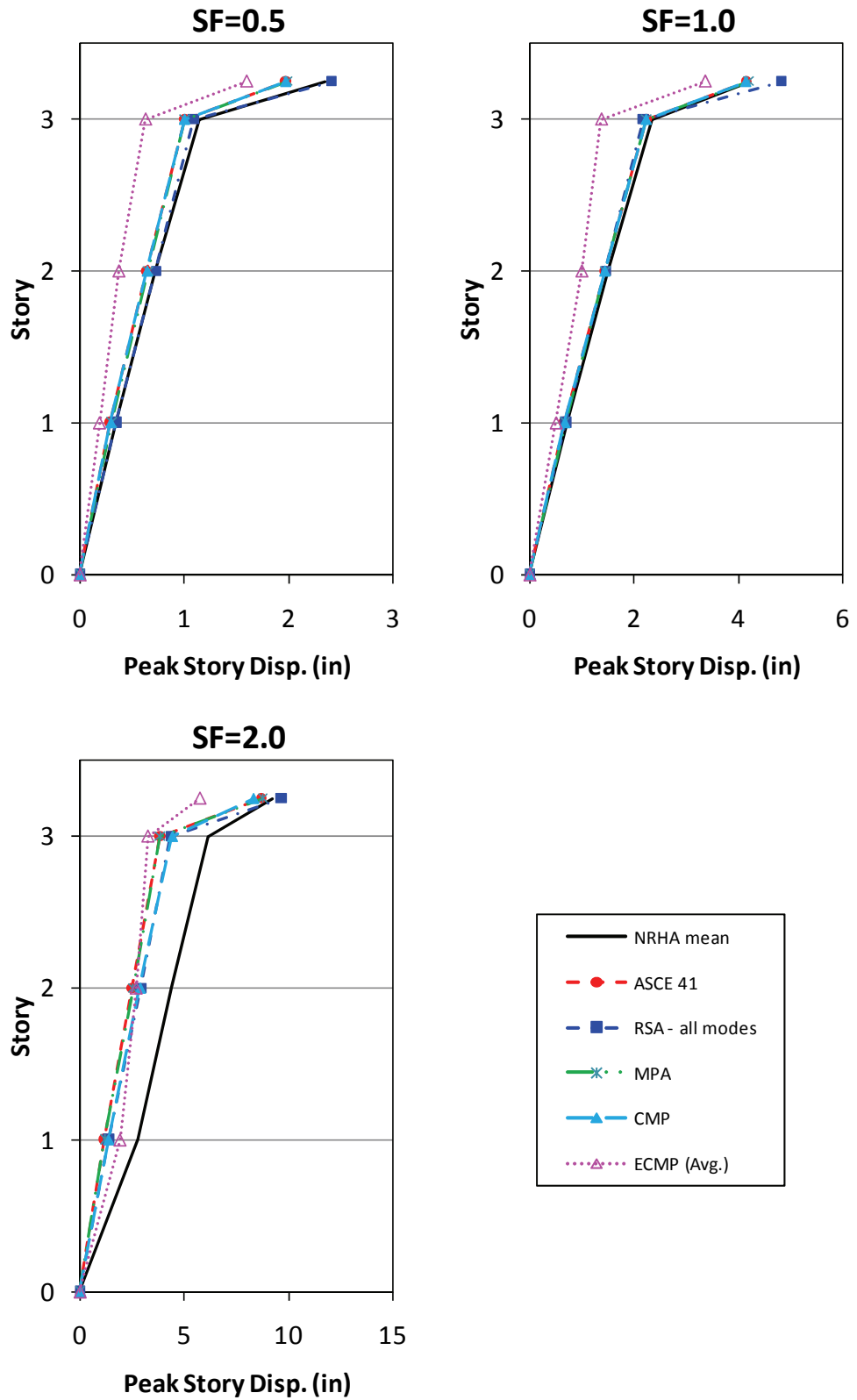


Figure F-42 Building B comparison of peak story displacement in longitudinal direction (H1).

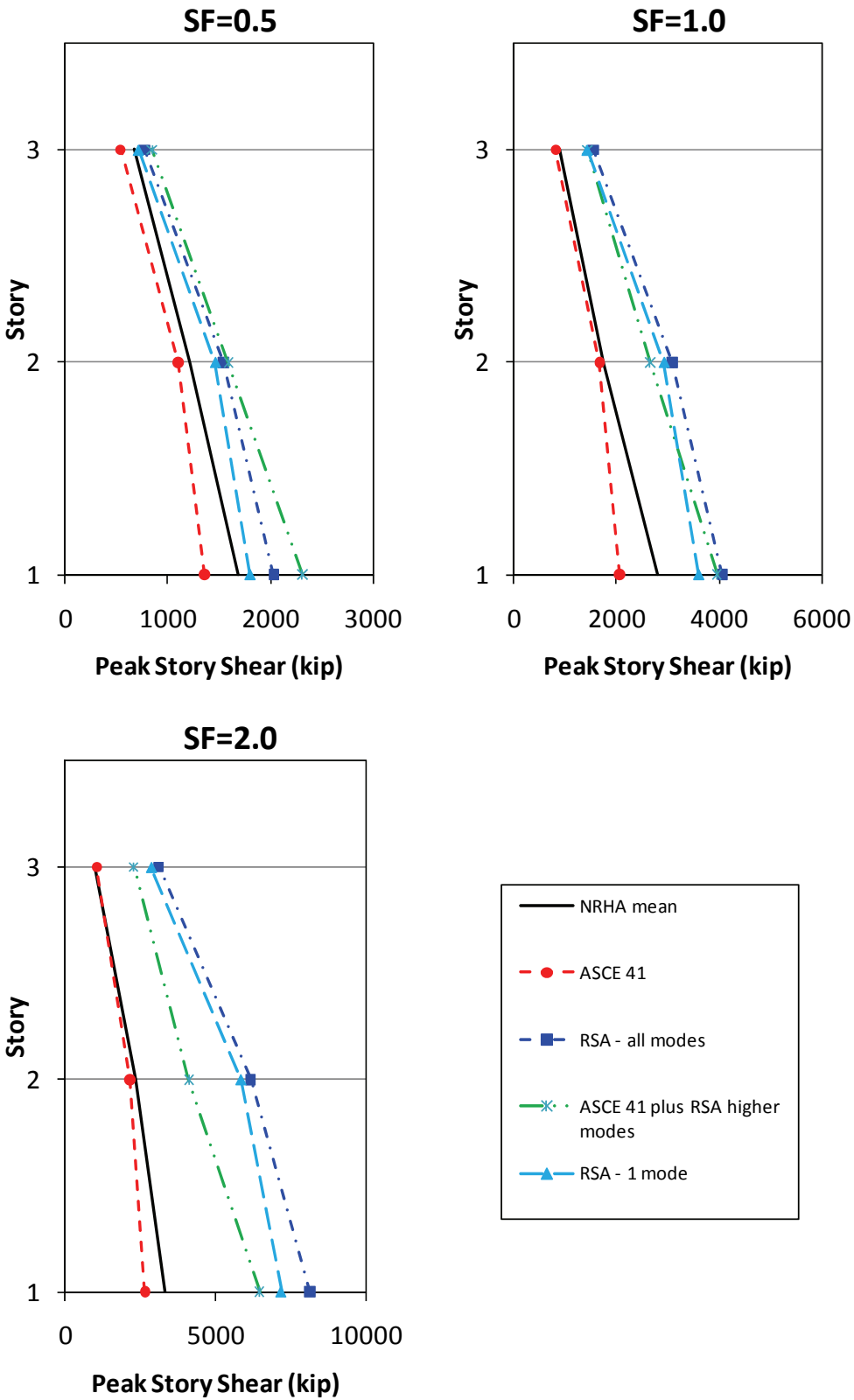


Figure F-43 Building B comparison of peak story shear in longitudinal direction (H1).

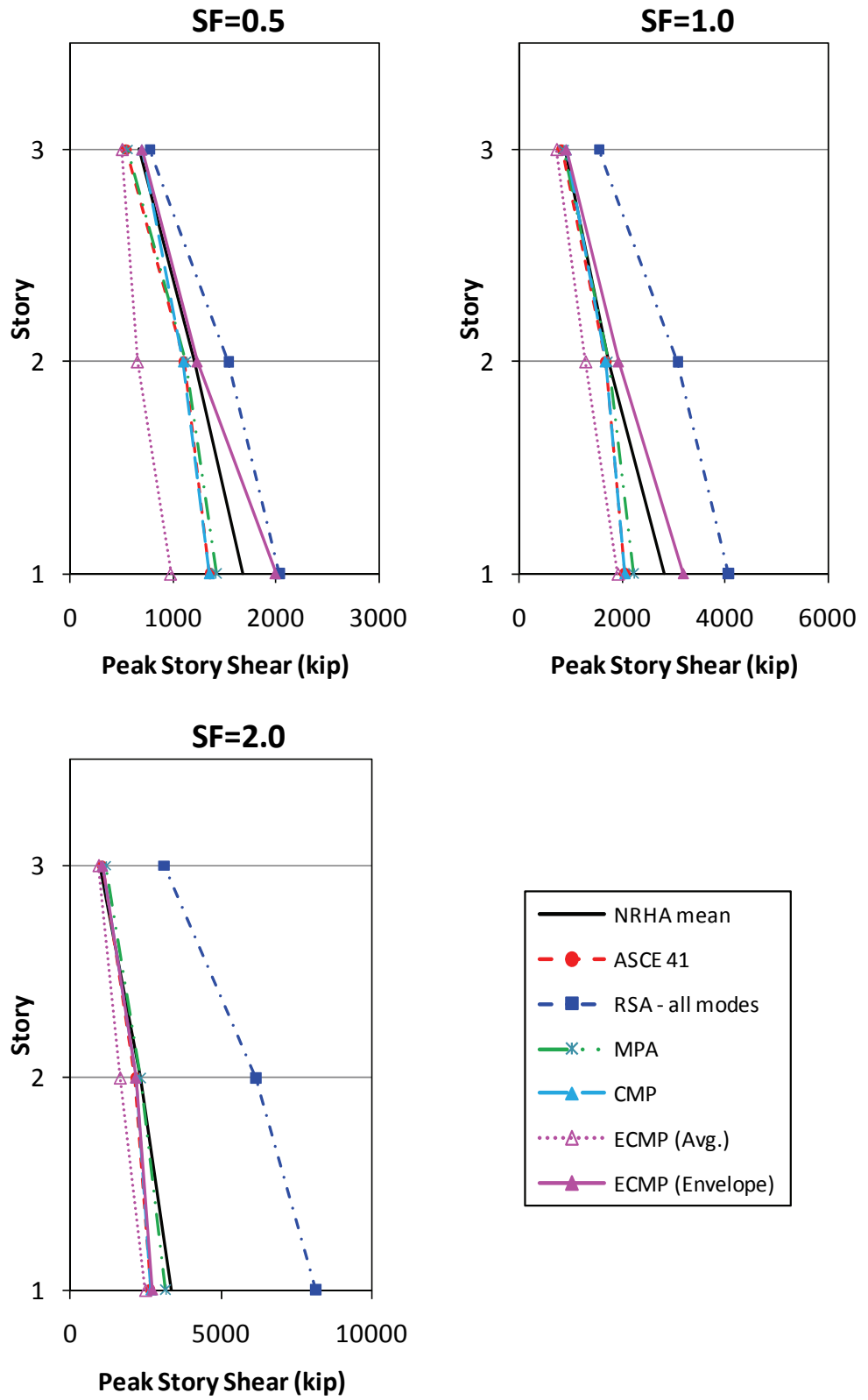


Figure F-44 Building B comparison of peak story shear in longitudinal direction (H1).

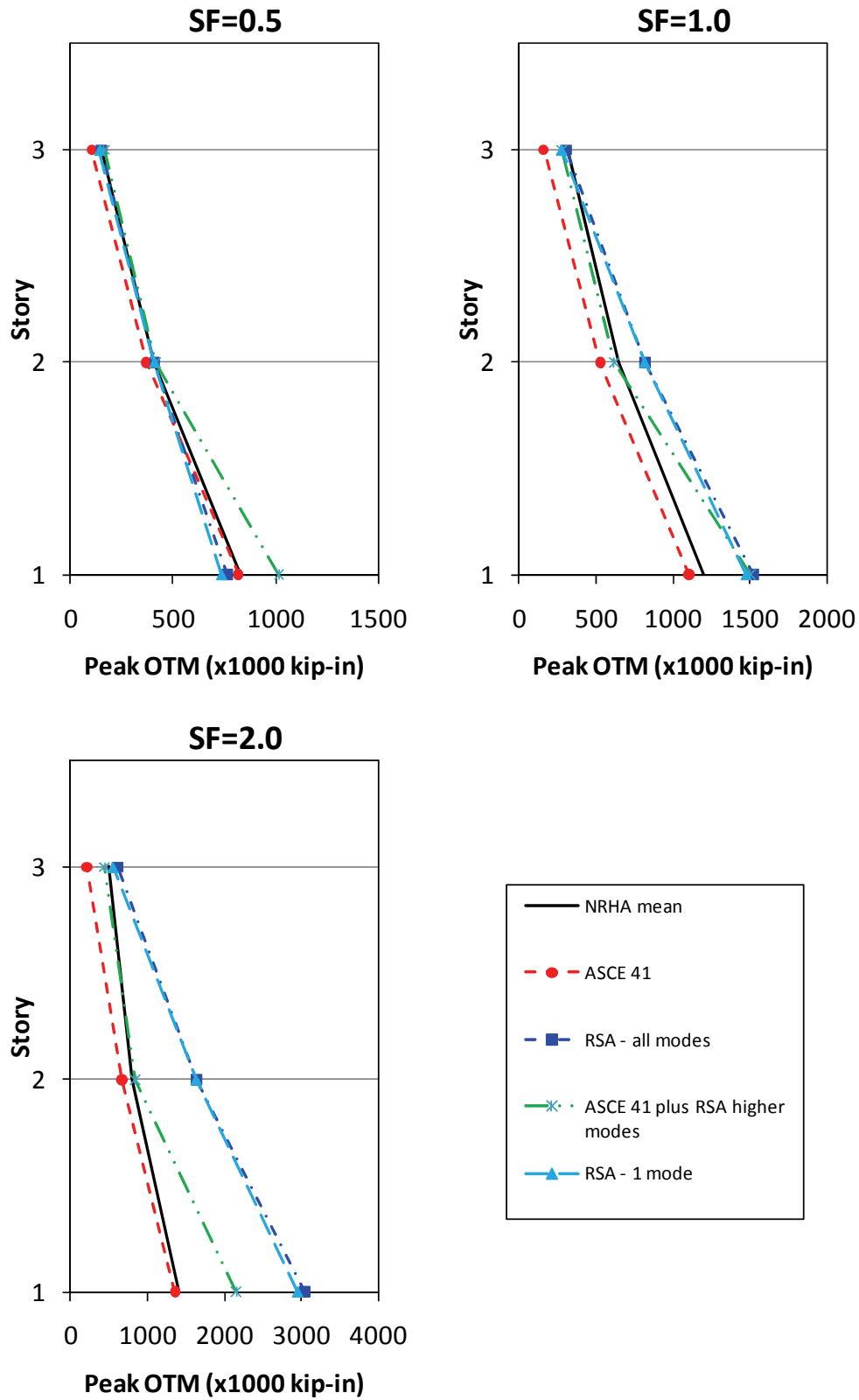


Figure F-45 Building B comparison of peak story overturning moment in longitudinal direction (H1).

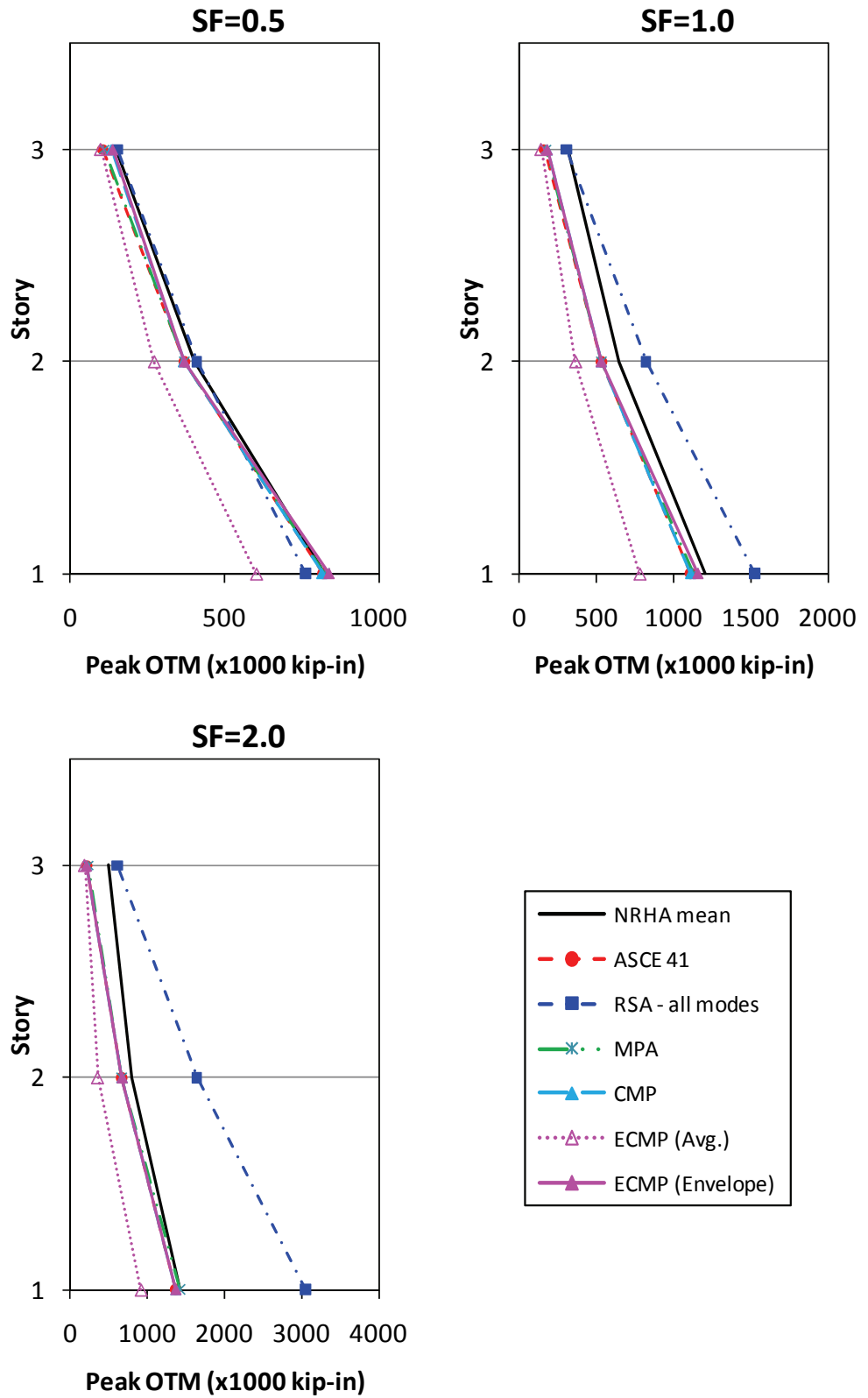


Figure F-46 Building B comparison of peak story overturning moment in longitudinal direction (H1).

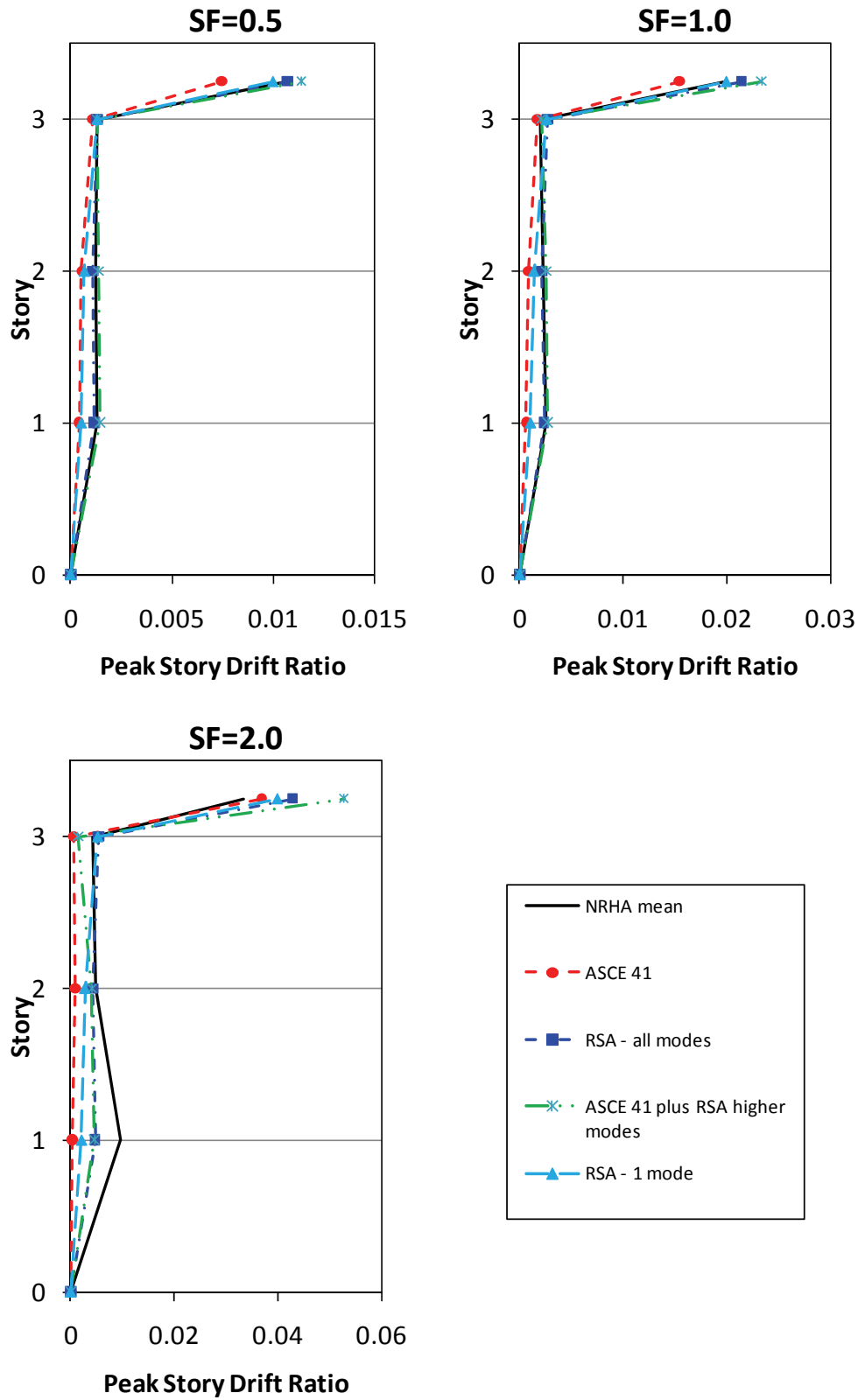


Figure F-47 Building B comparison of peak story drift ratio in transverse direction (H2).

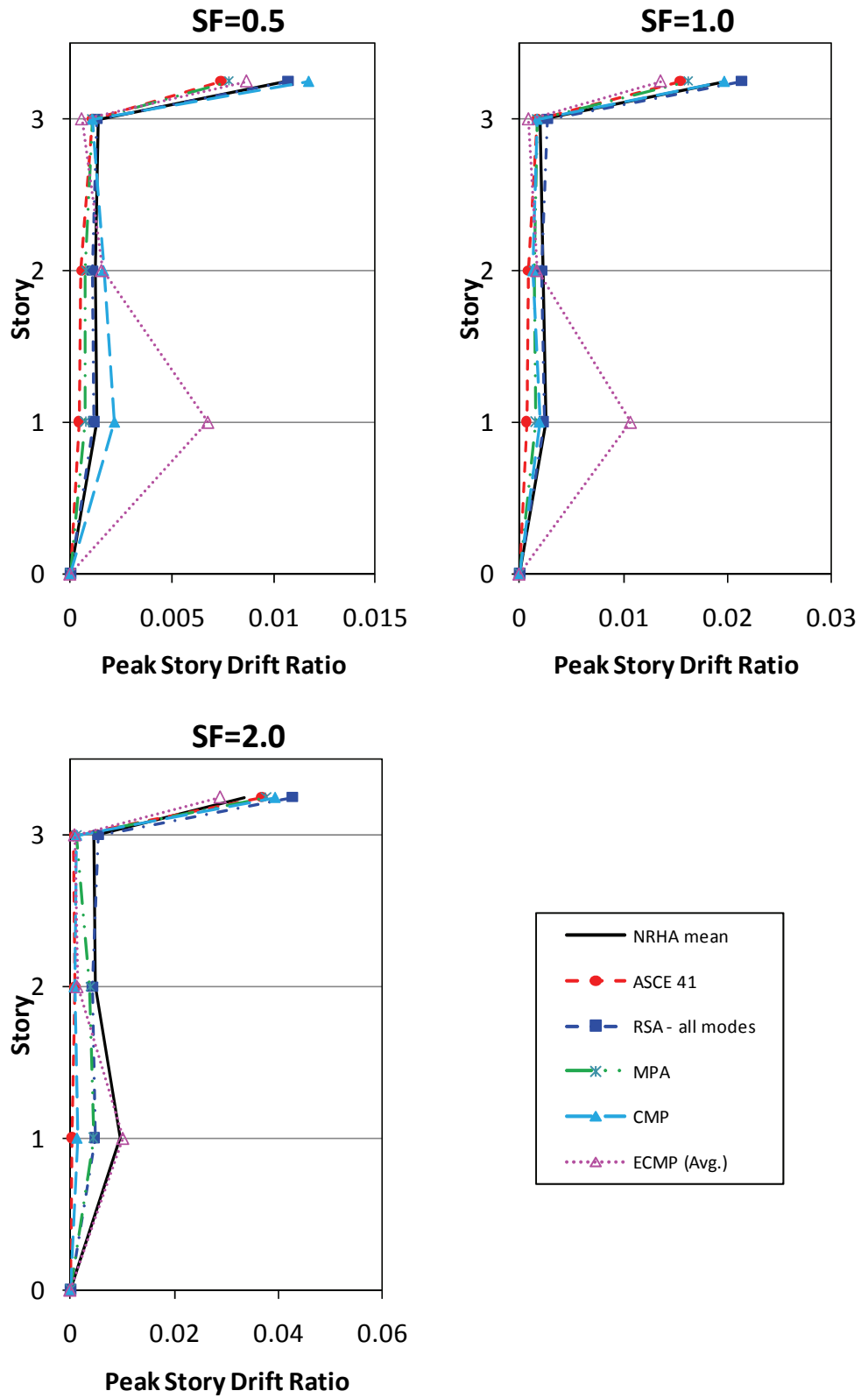


Figure F-48 Building B comparison of peak story drift ratio in transverse direction (H2).

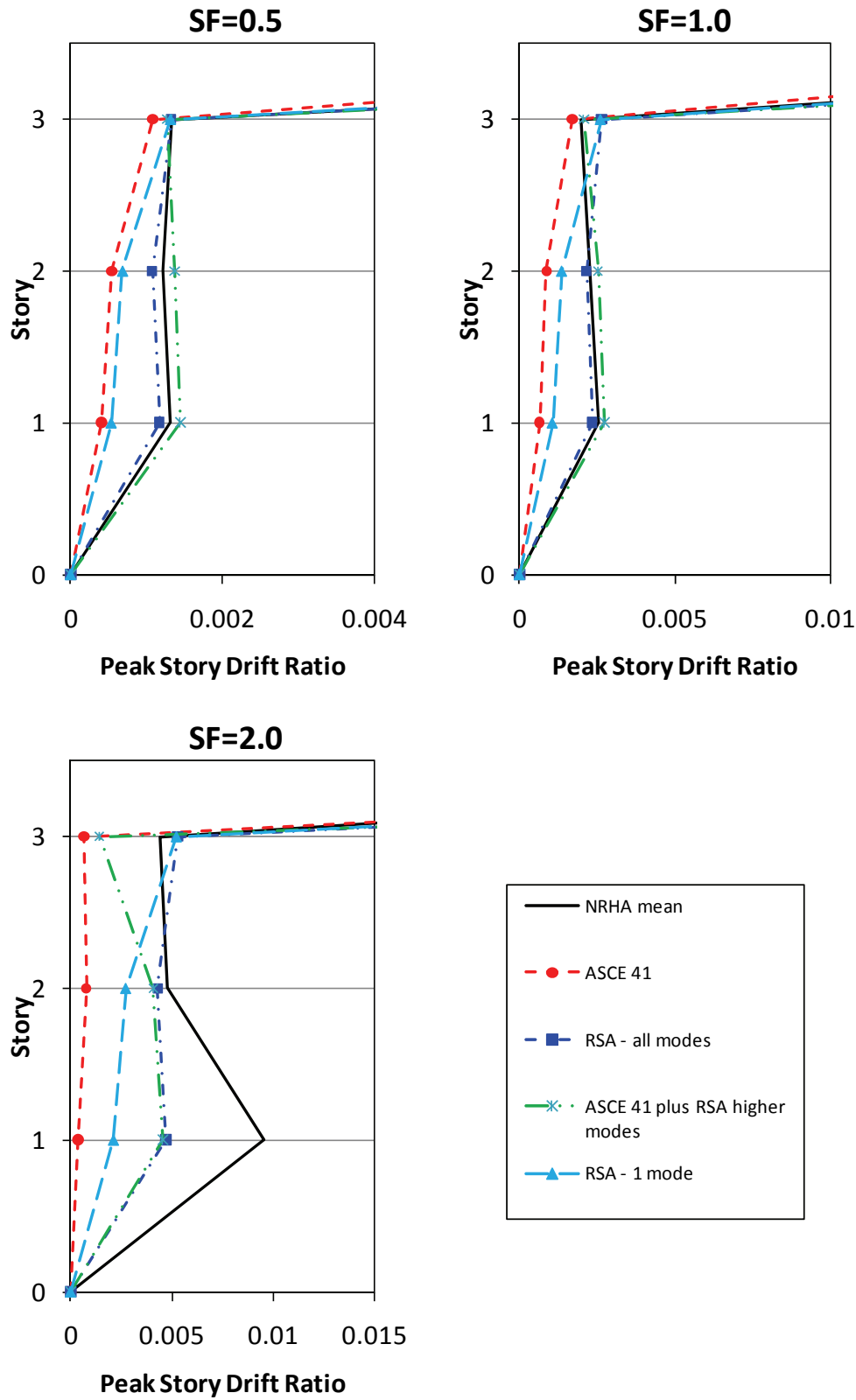


Figure F-49 Building B comparison of peak story drift ratio (reduced scale) in transverse direction (H2).

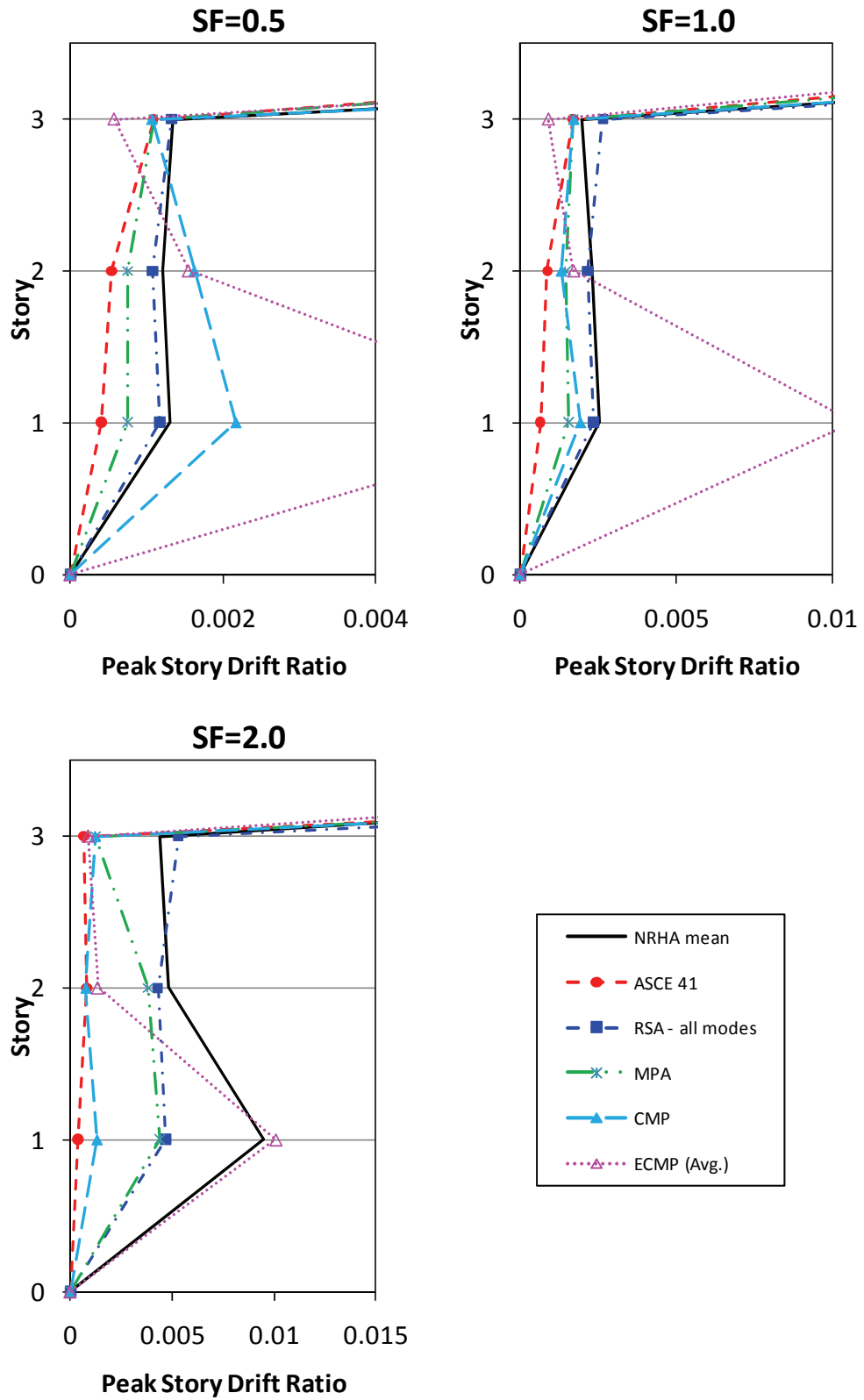


Figure F-50 Building B comparison of peak story drift ratio (reduced scale) in transverse direction (H2).

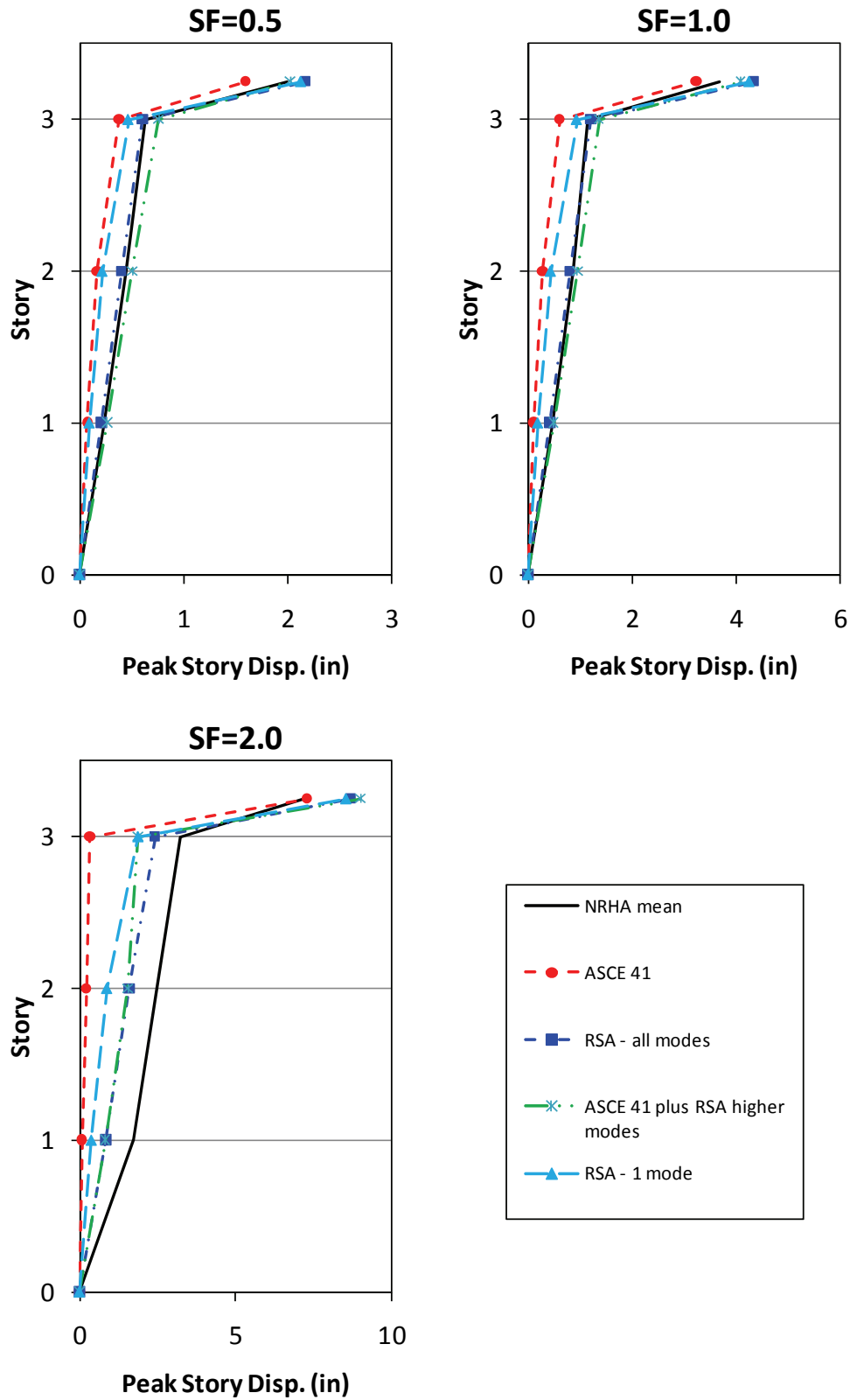


Figure F-51 Building B comparison of peak story displacement in transverse direction (H2).

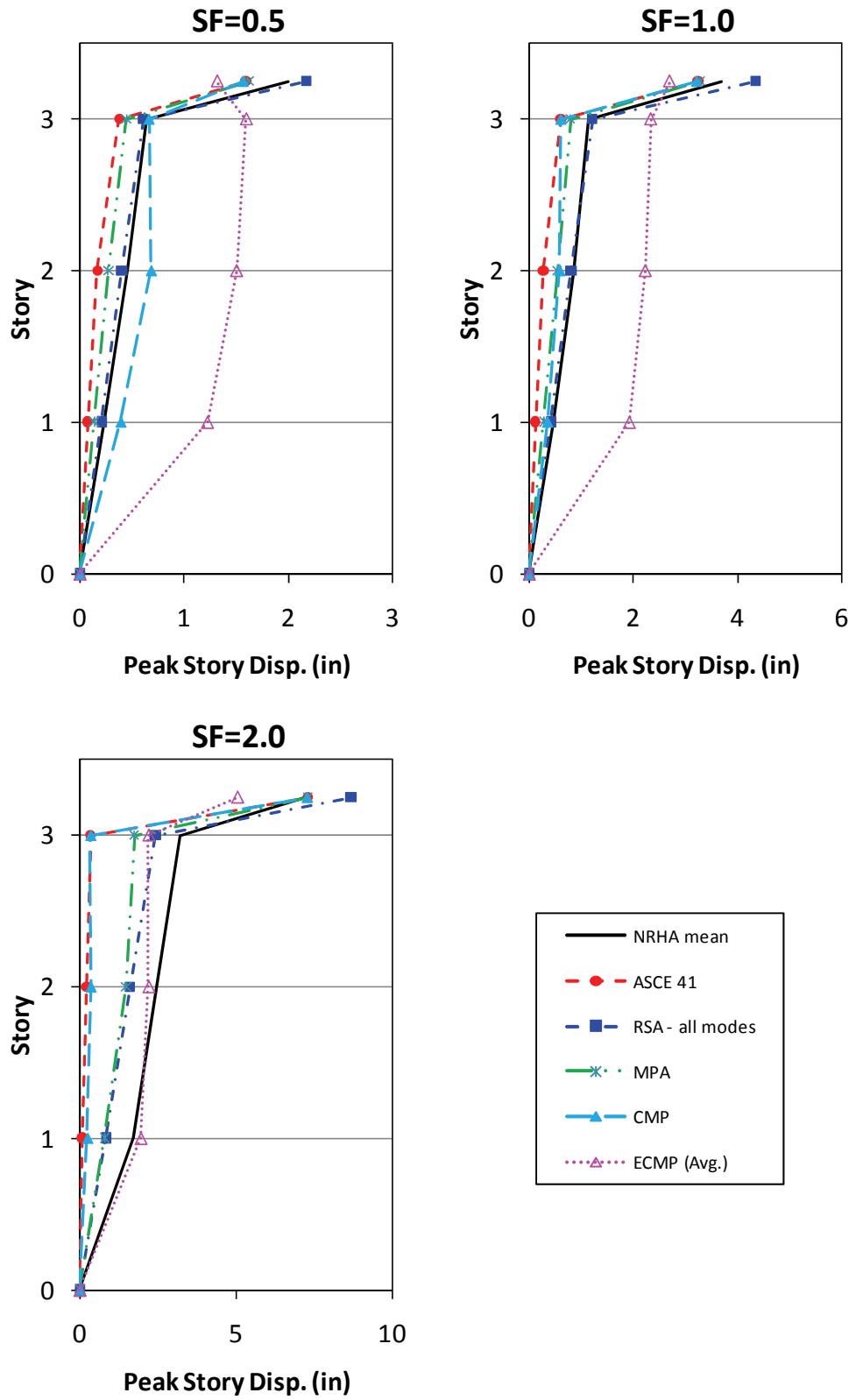


Figure F-52 Building B comparison of peak story displacement in transverse direction (H2).

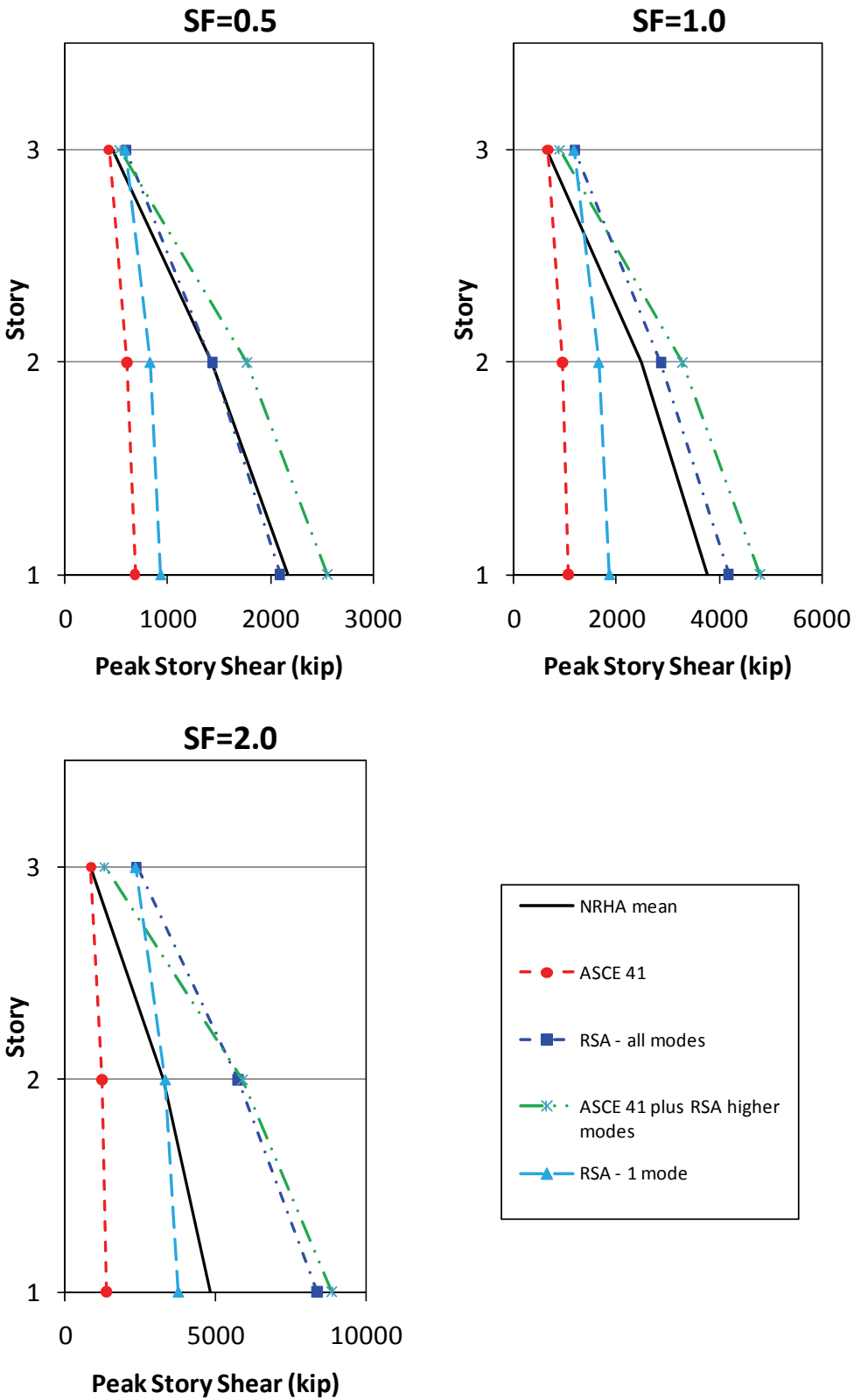


Figure F-53 Building B comparison of peak story shear in transverse direction (H2).

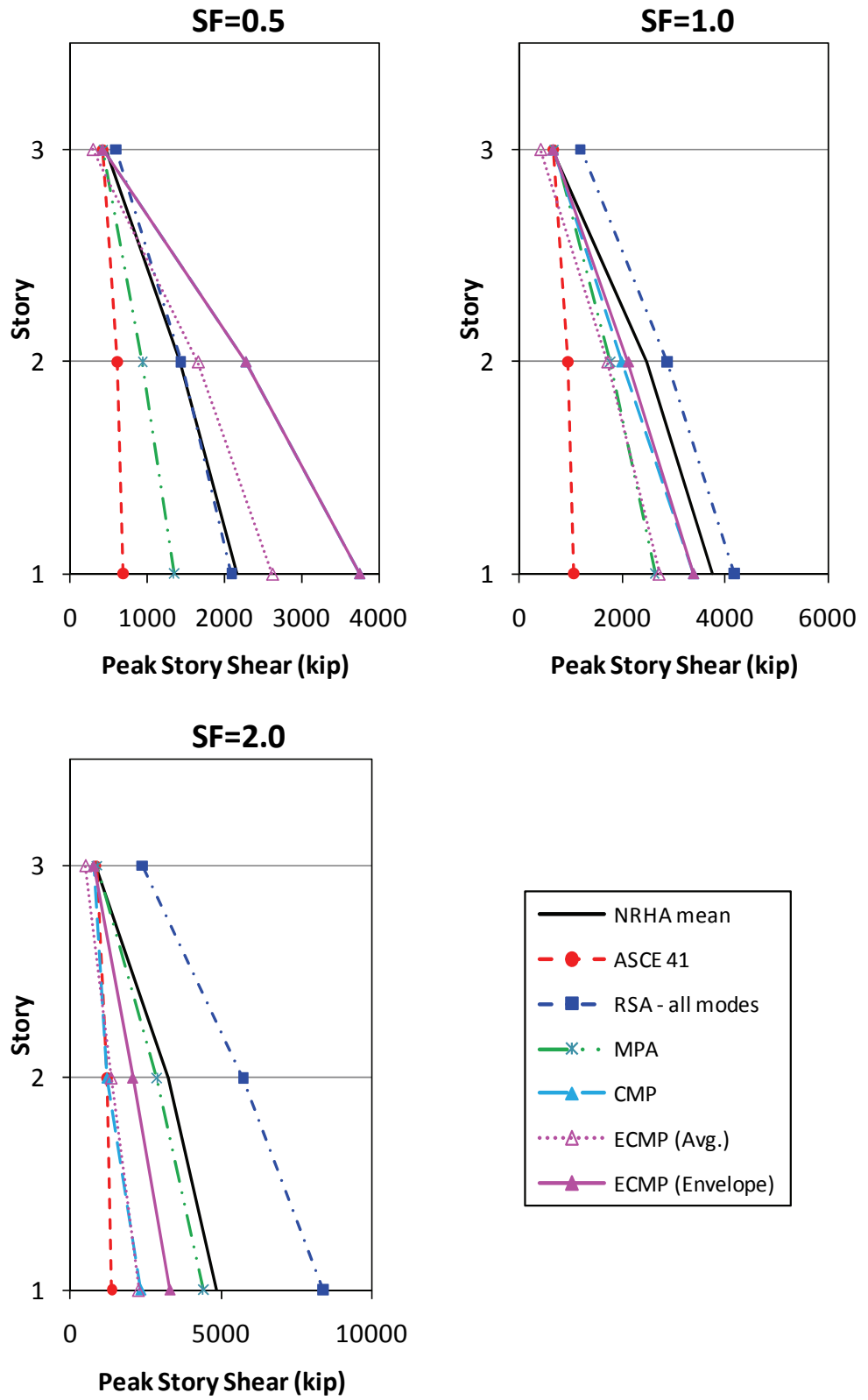


Figure F-54 Building B comparison of peak story shear in transverse direction (H2).

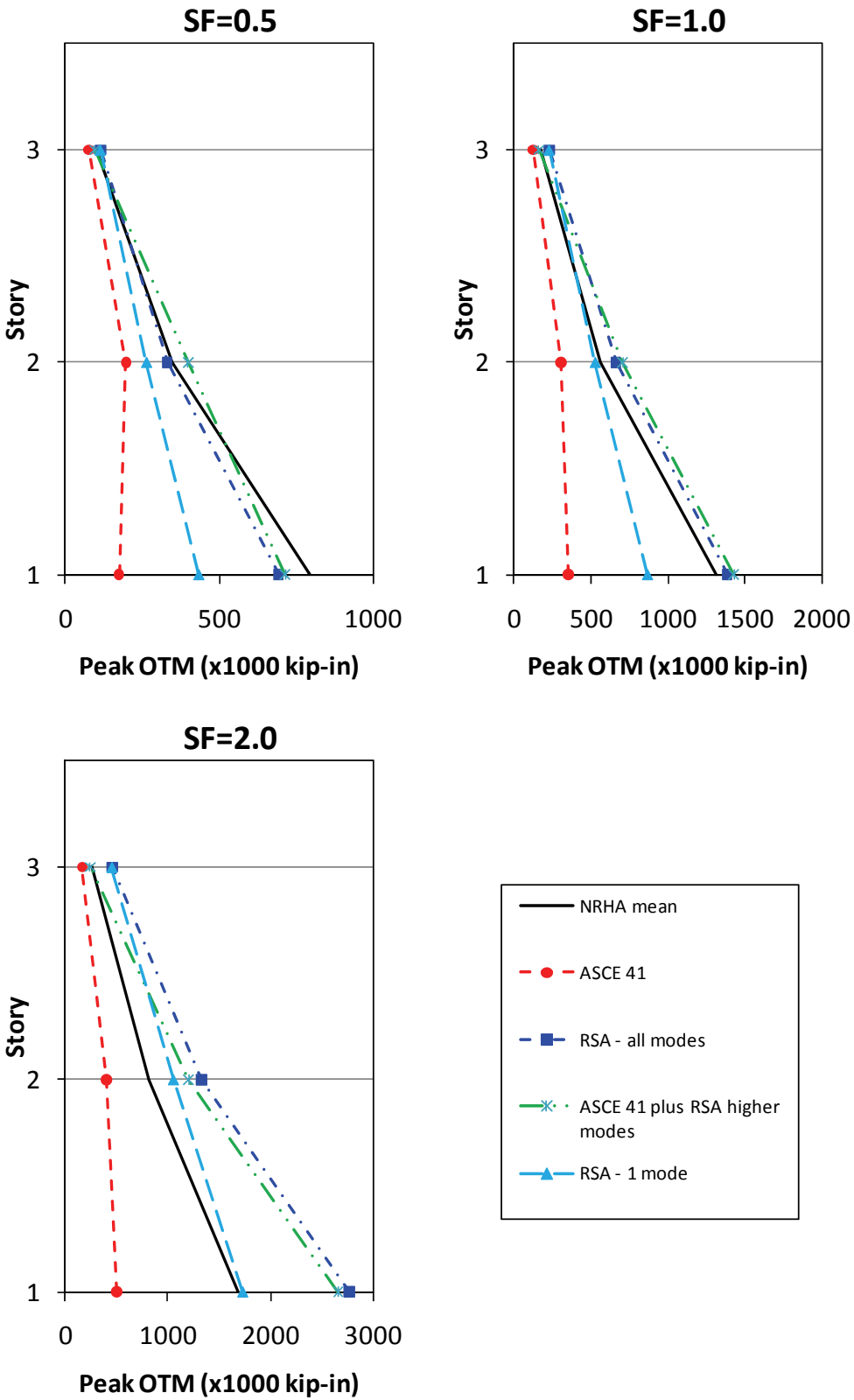


Figure F-55 Building B comparison of peak story overturning moment in transverse direction (H2).

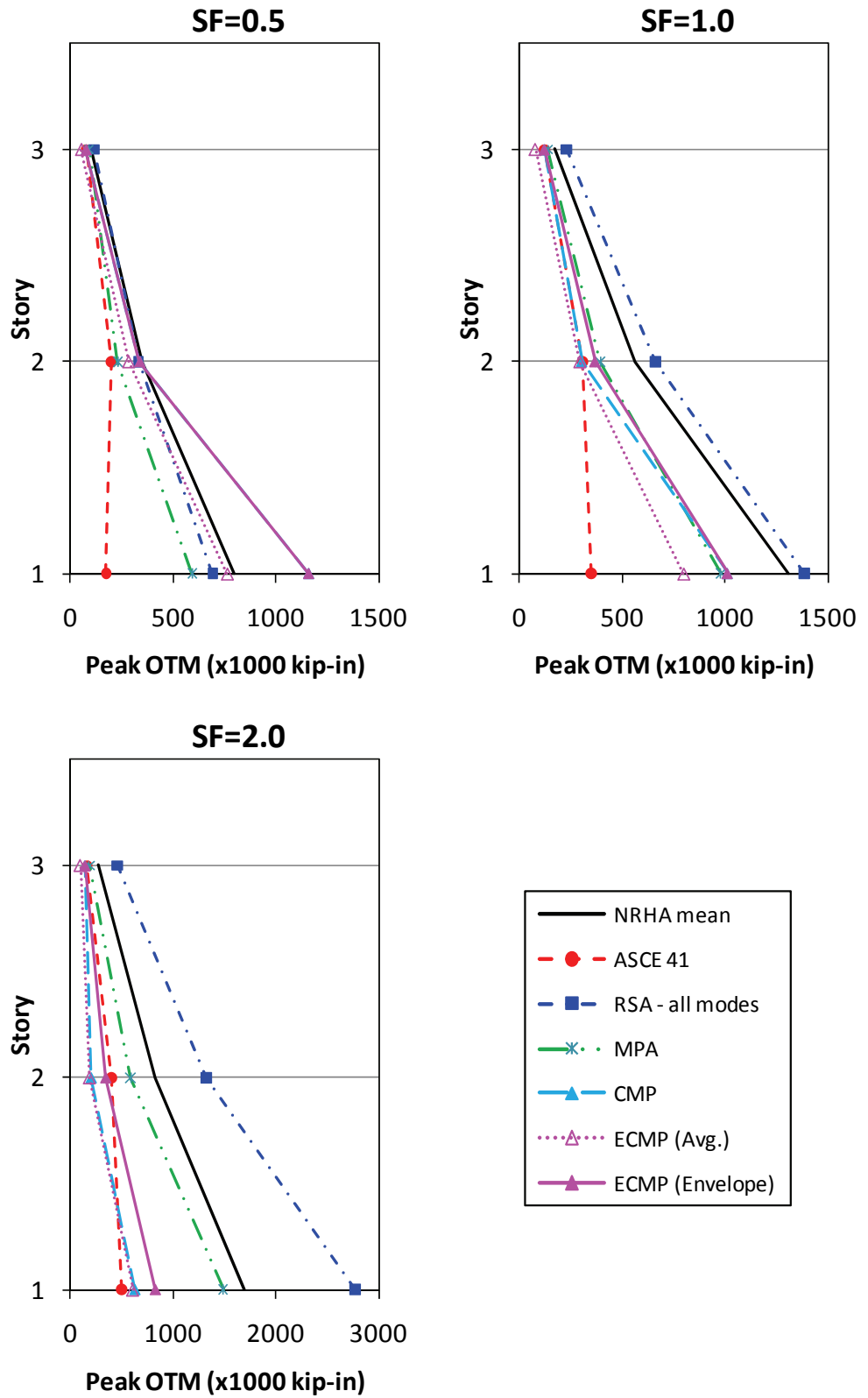


Figure F-56 Building B comparison of peak story overturning moment in transverse direction (H2).

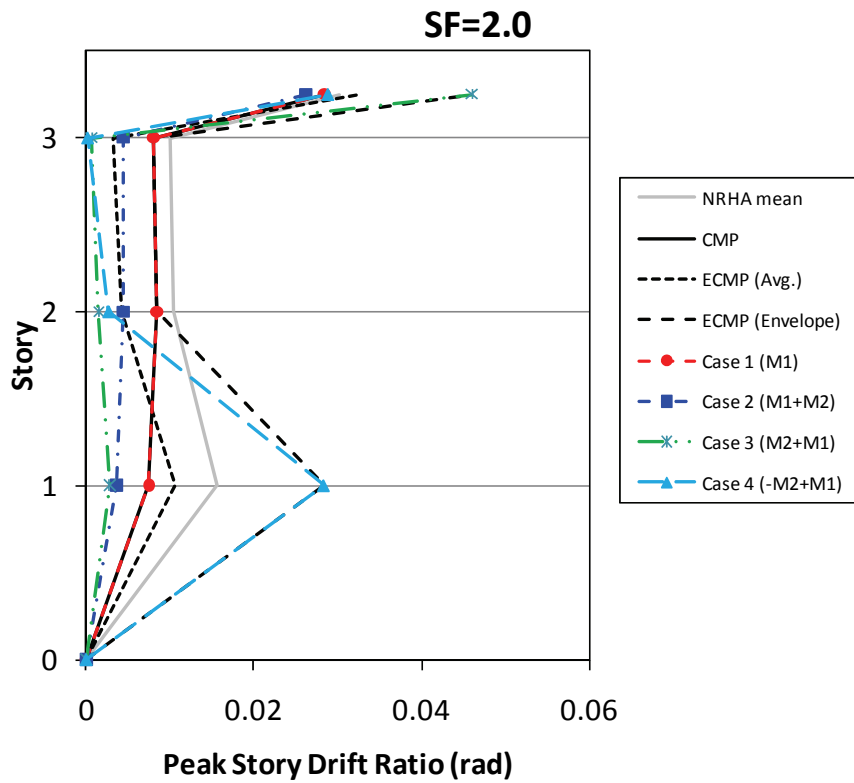
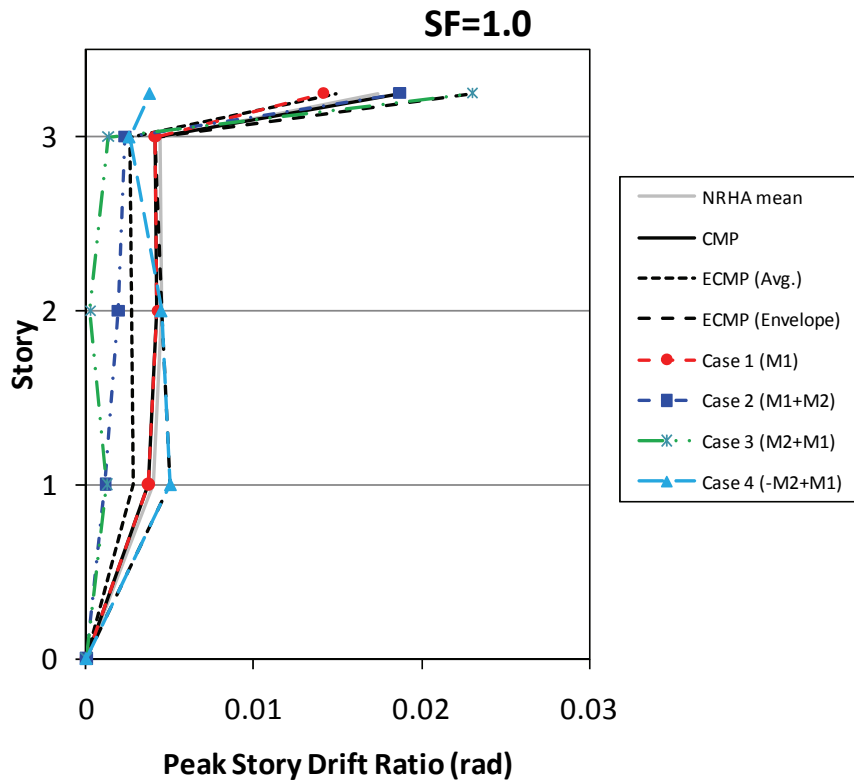


Figure F-57 Building B comparison of CMP and NRHA peak story drift ratio in longitudinal direction (H1).

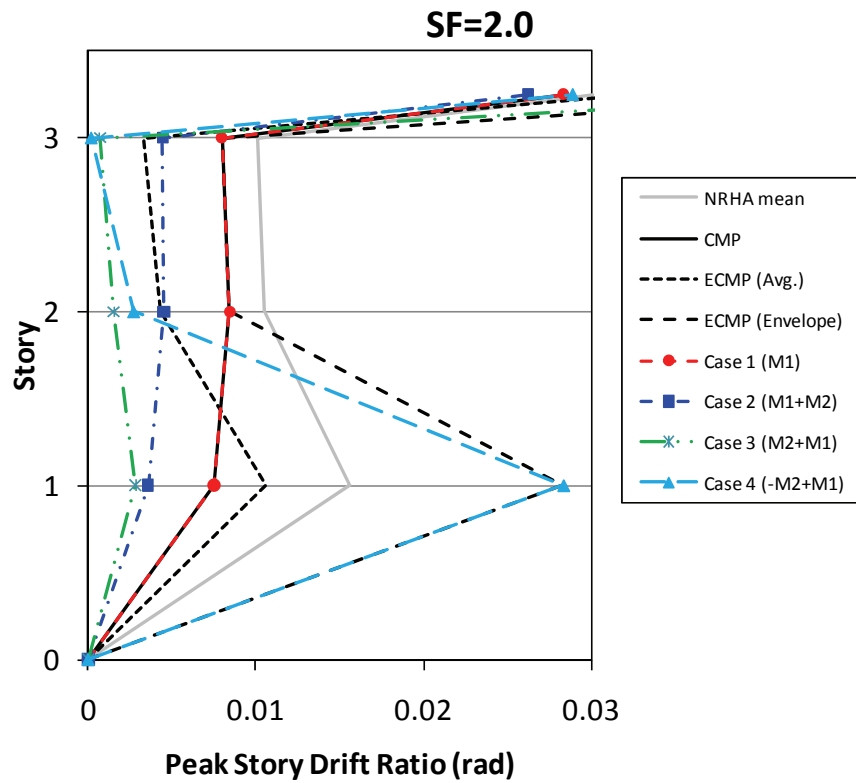
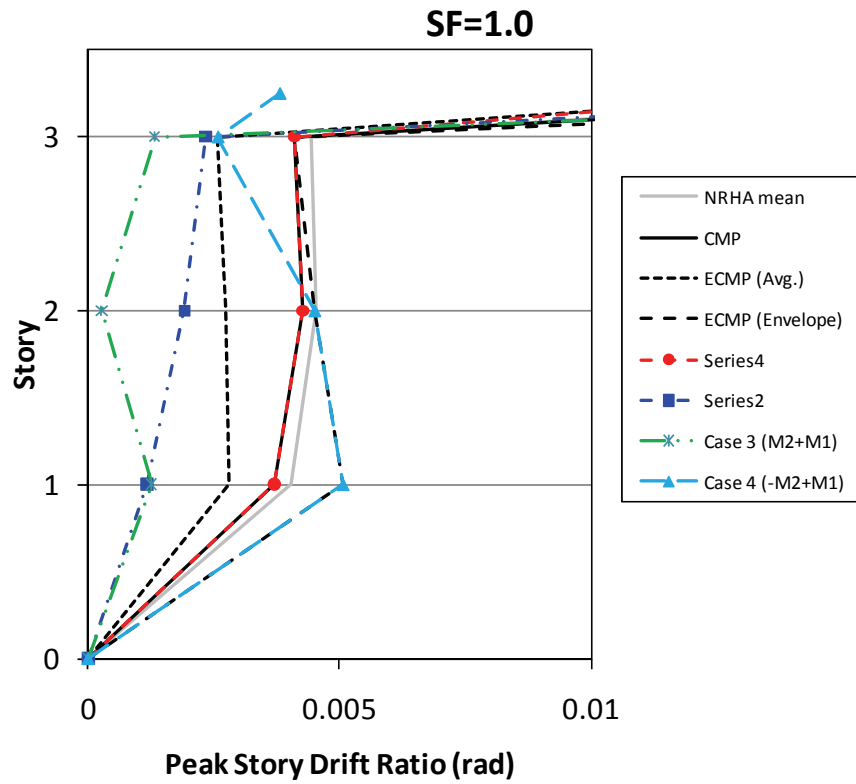


Figure F-58 Building B comparison of CMP and NRHA peak story drift ratio (reduced scale) in longitudinal direction (H1).

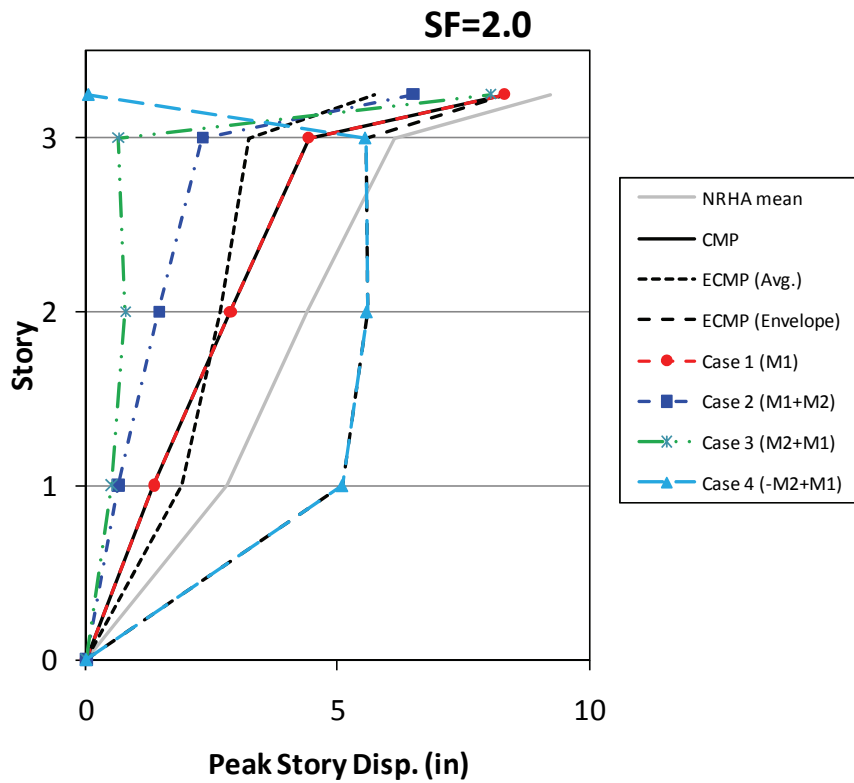
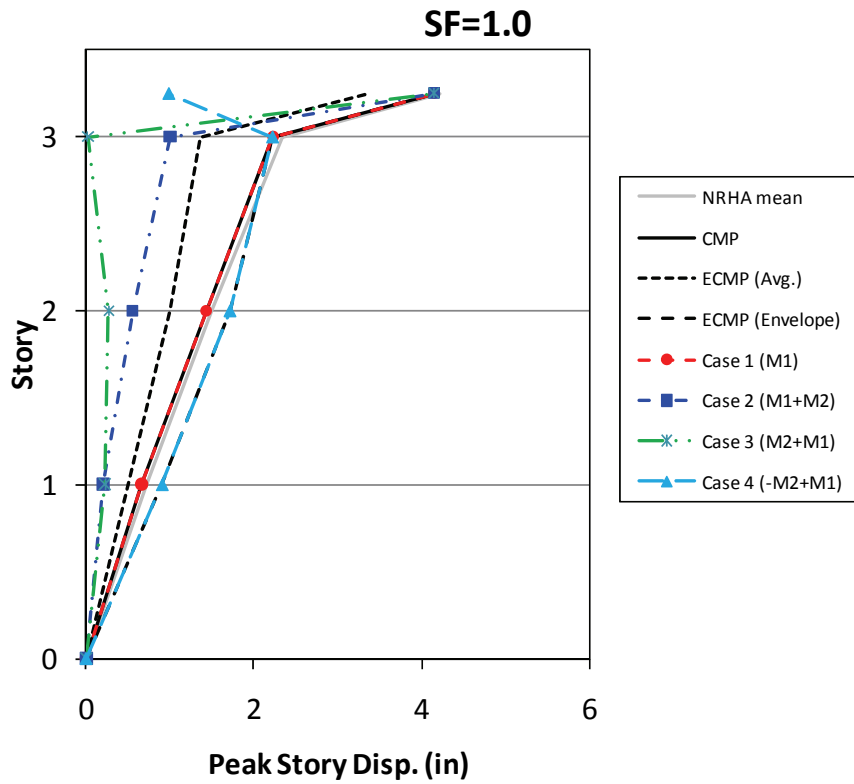


Figure F-59 Building B comparison of CMP and NRHA peak story displacement in longitudinal direction (H1).

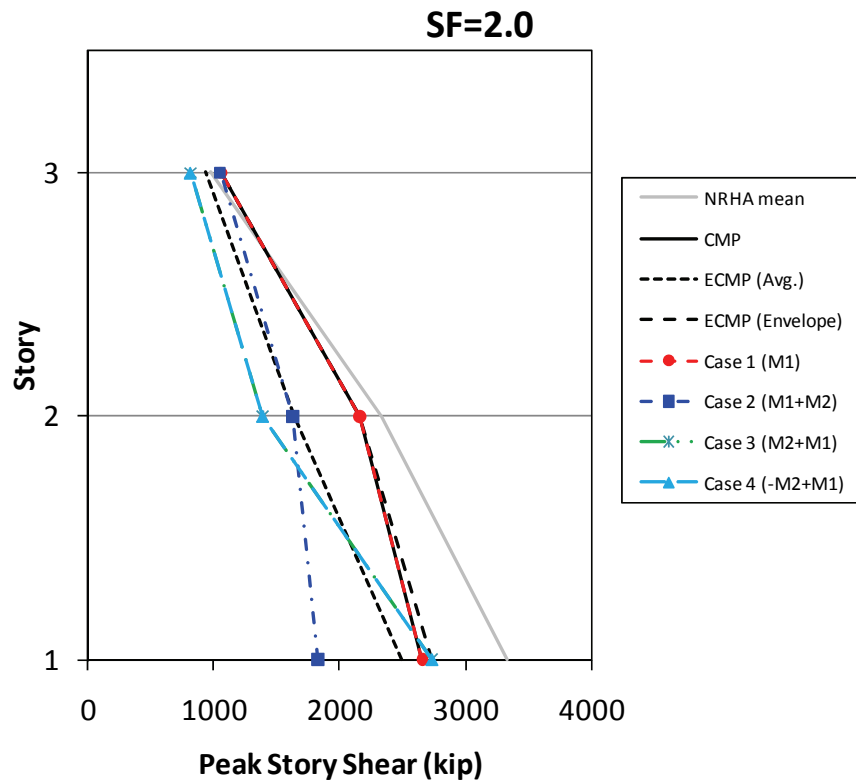
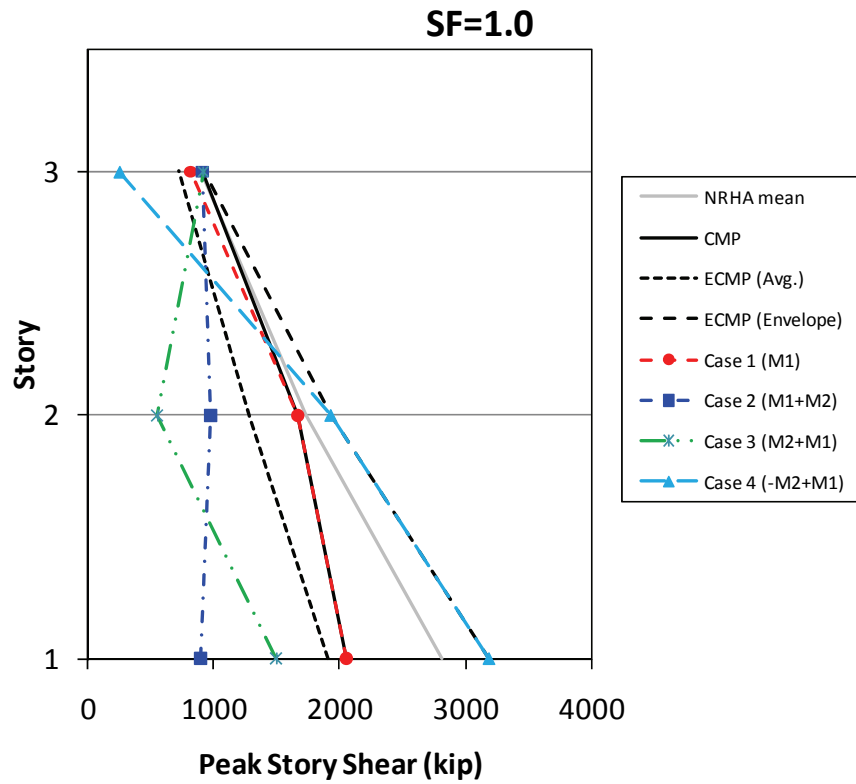


Figure F-60 Building B comparison of CMP and NRHA peak story shear in longitudinal direction (H1).

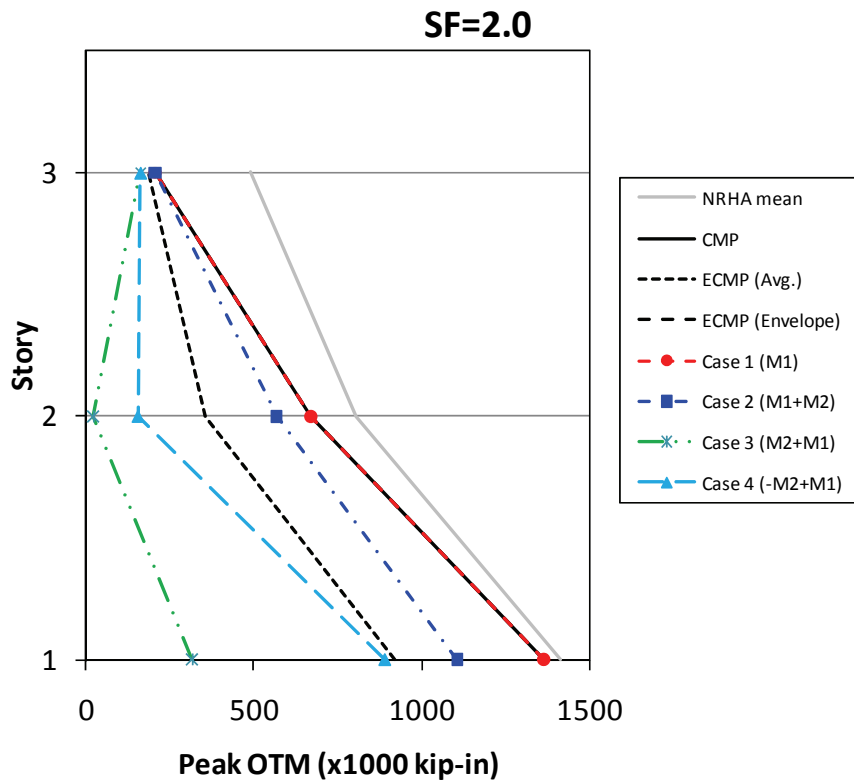
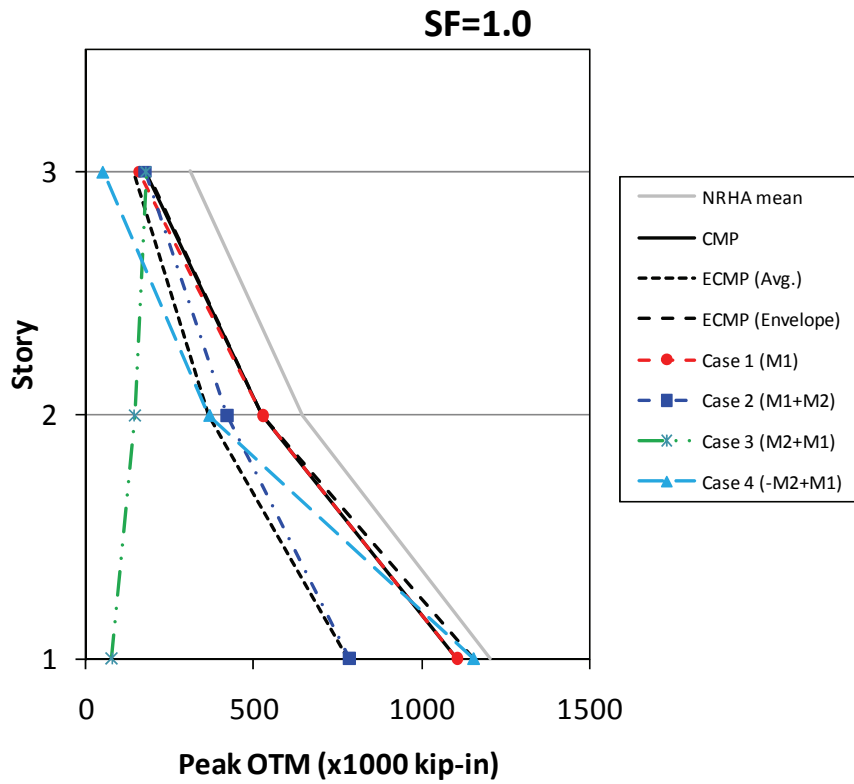


Figure F-61 Building B comparison of CMP and NRHA peak story overturning moment in longitudinal direction (H1).

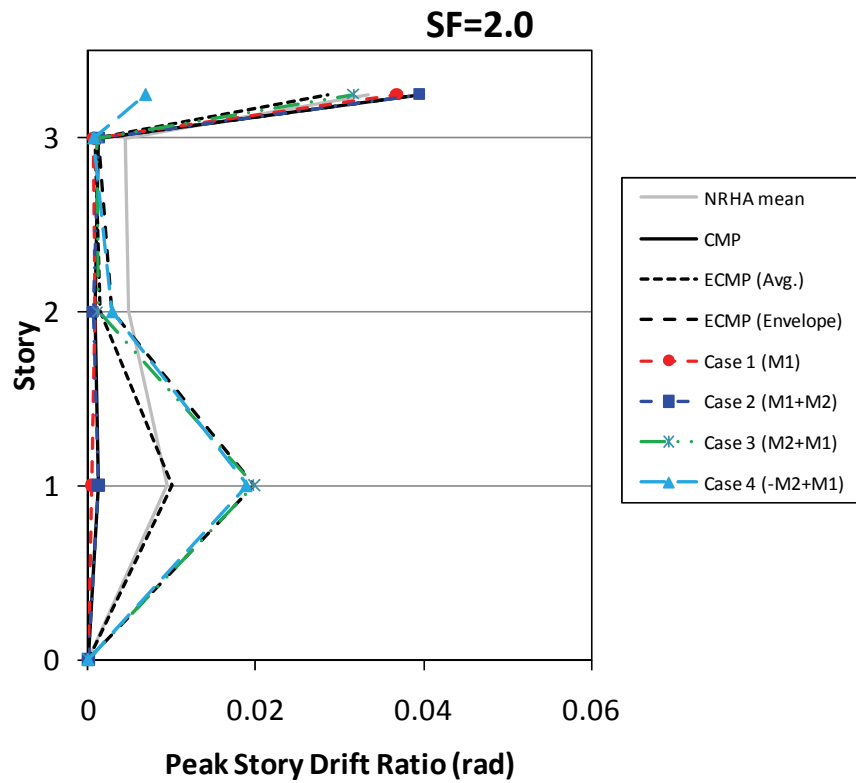
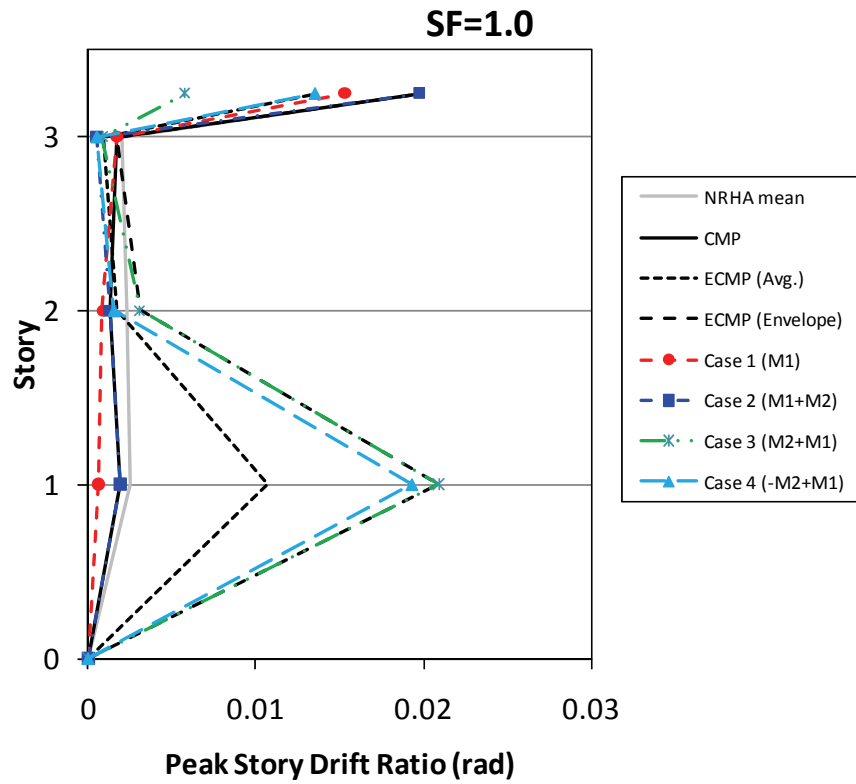


Figure F-62 Building B comparison of CMP and NRHA peak story drift ratio in transverse direction (H2).

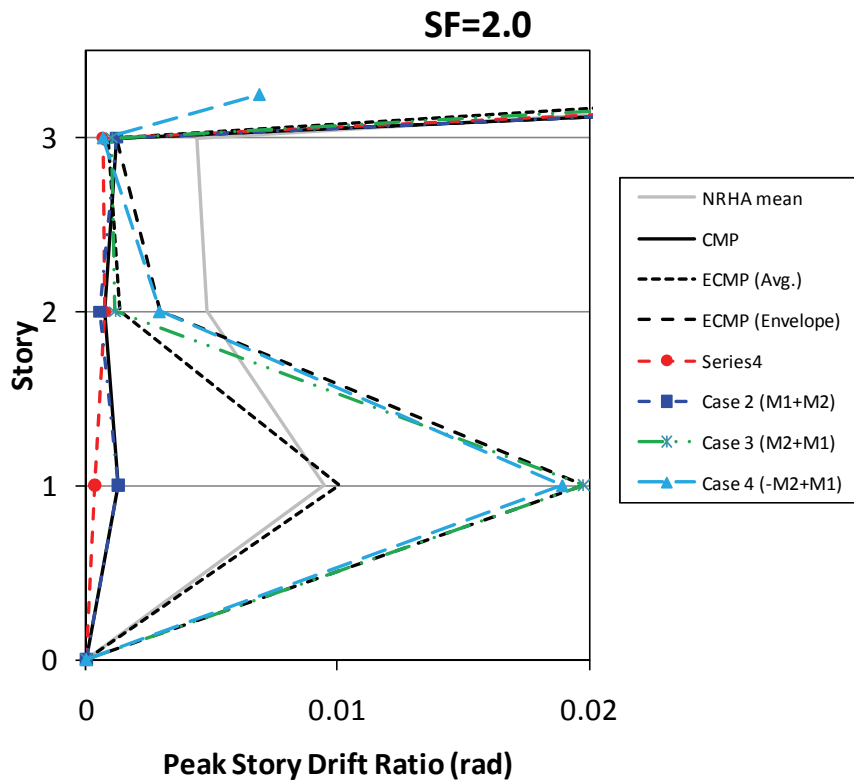
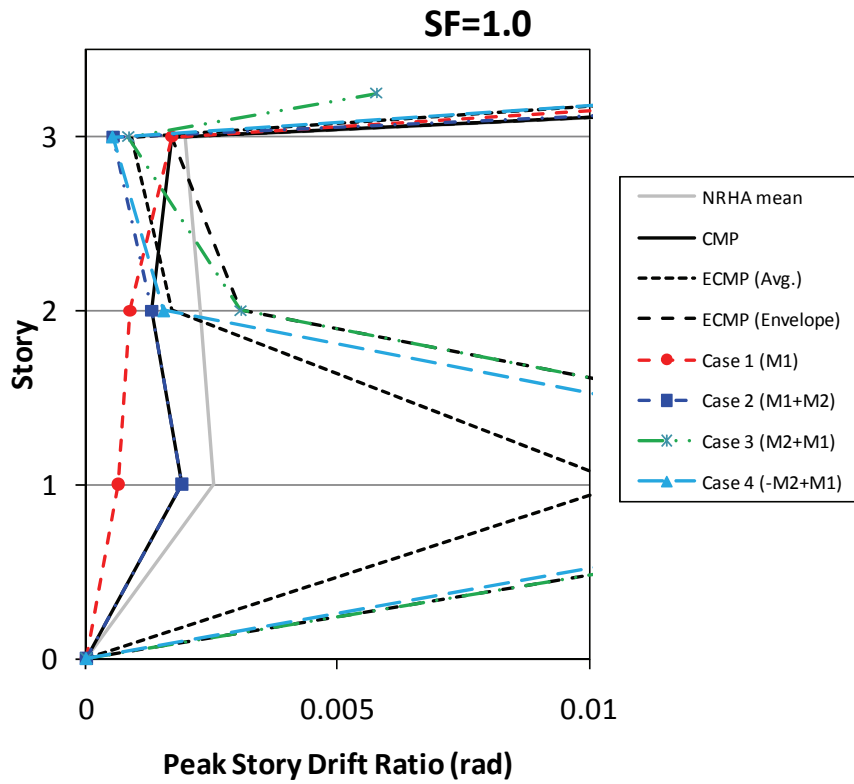


Figure F-63 Building B comparison of CMP and NRHA peak story drift ratio (reduced scale) in transverse direction (H2).

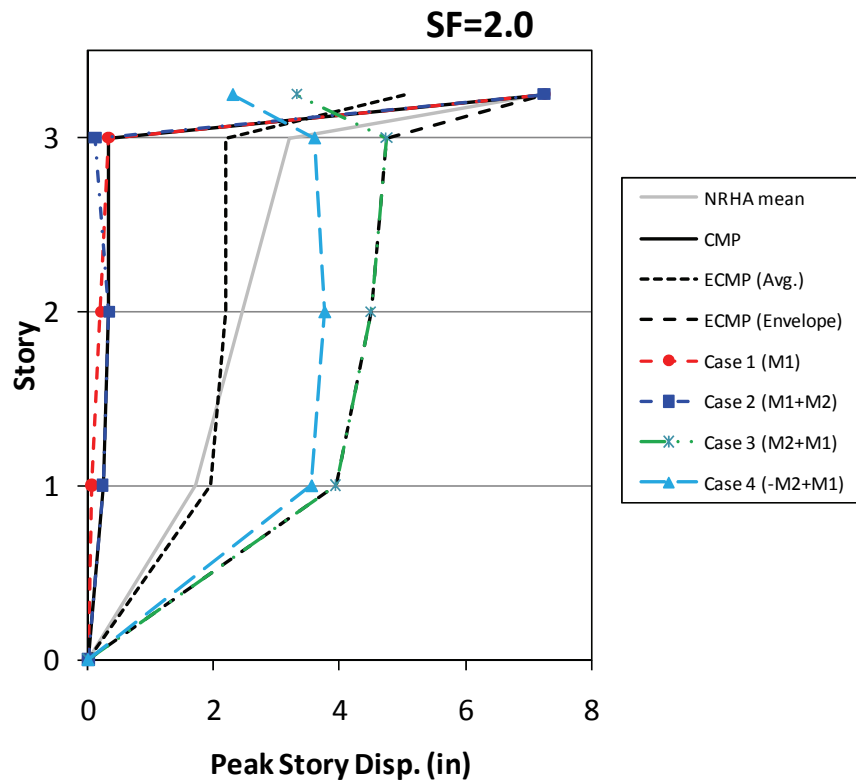
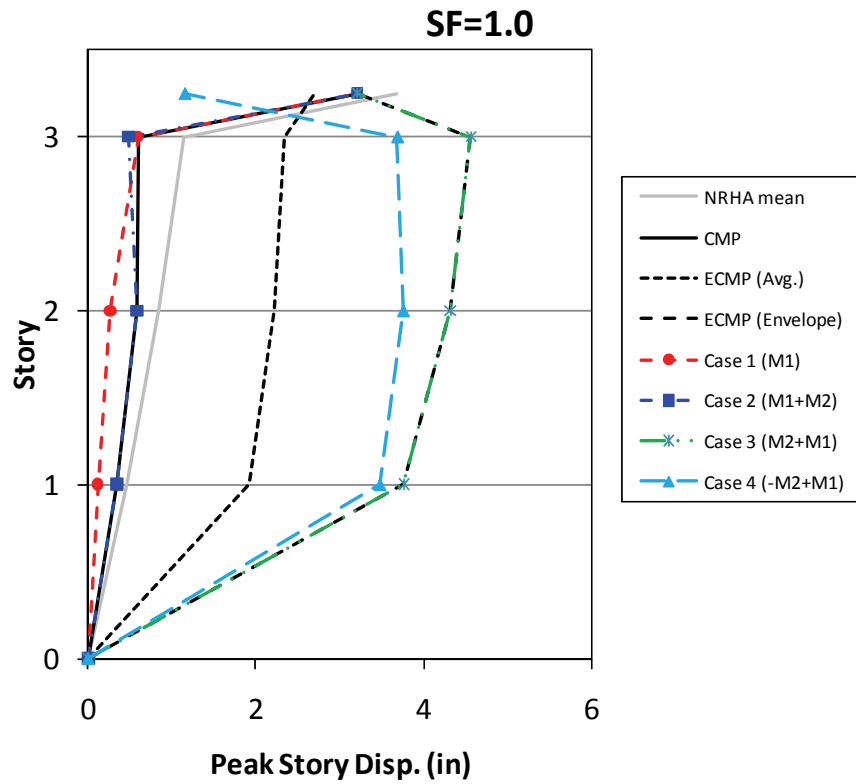


Figure F-64 Building B comparison of CMP and NRHA peak story displacement in transverse direction (H2).

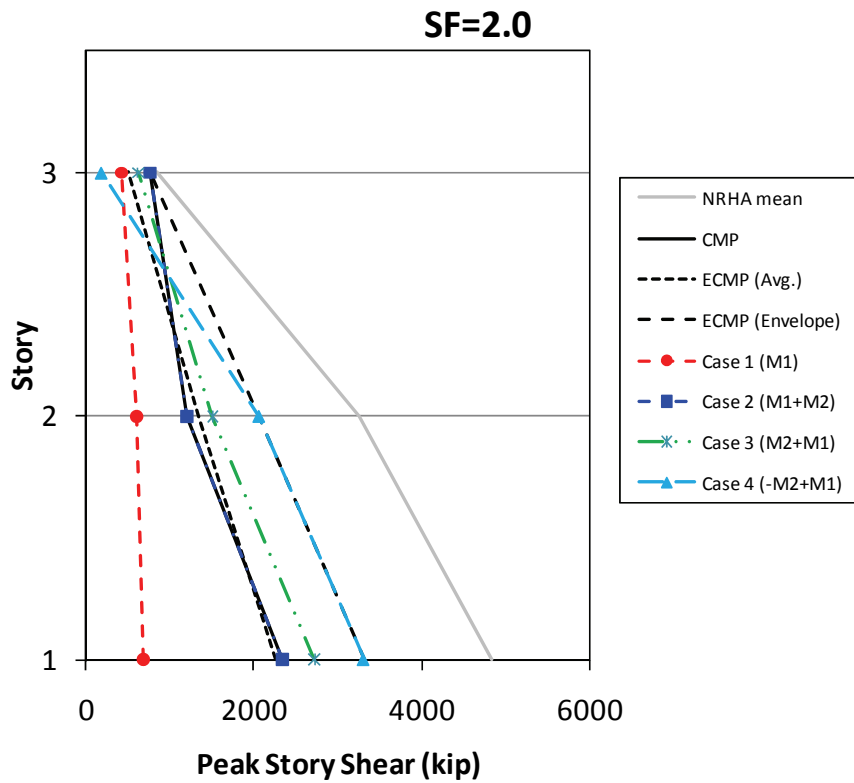
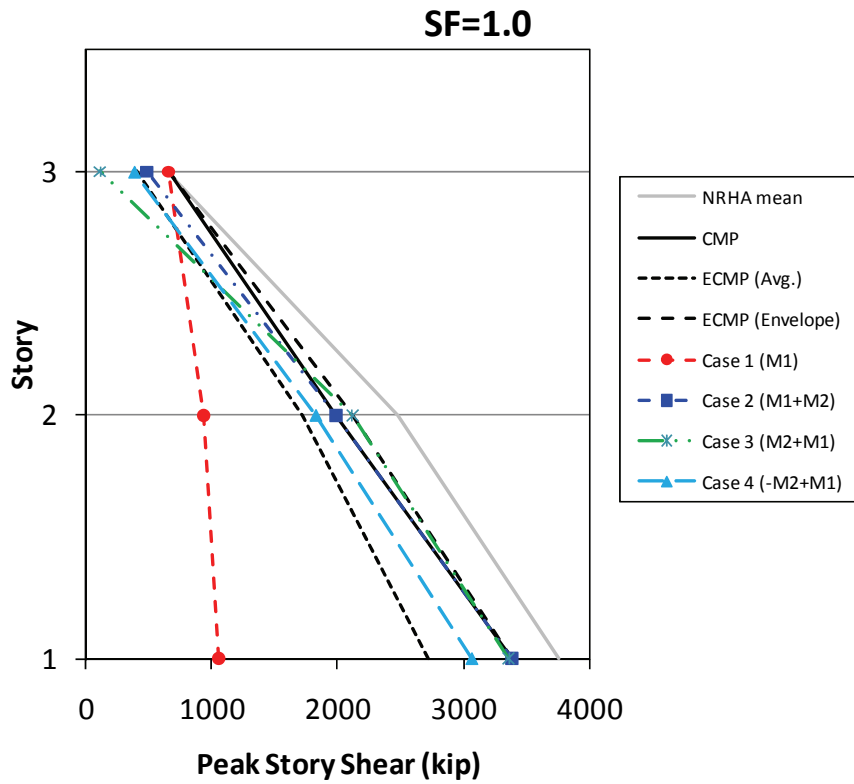


Figure F-65 Building B comparison of CMP and NRHA peak story shear in transverse direction (H2).

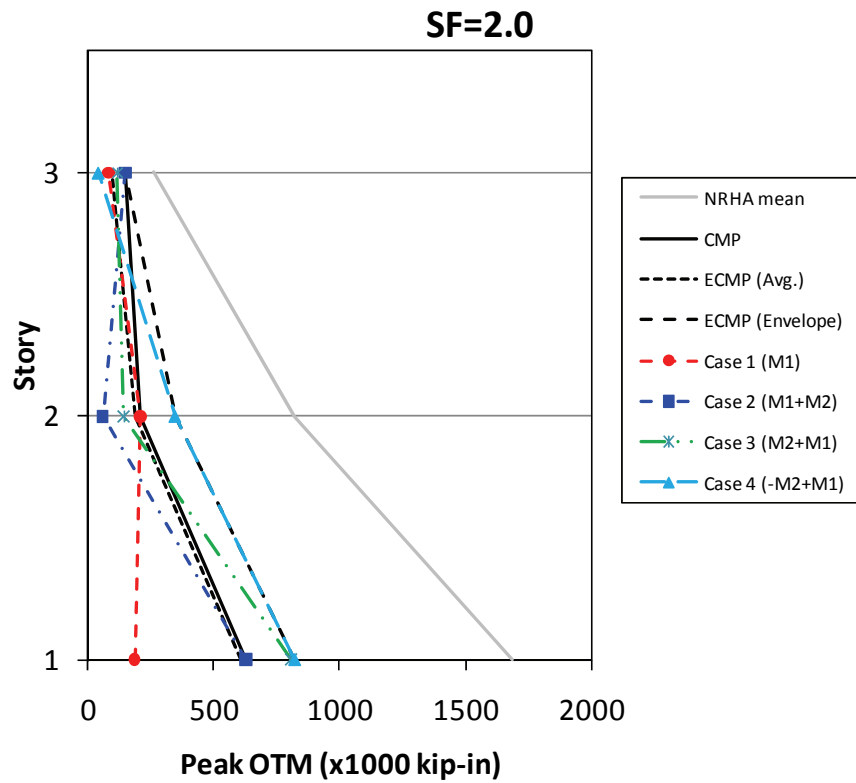
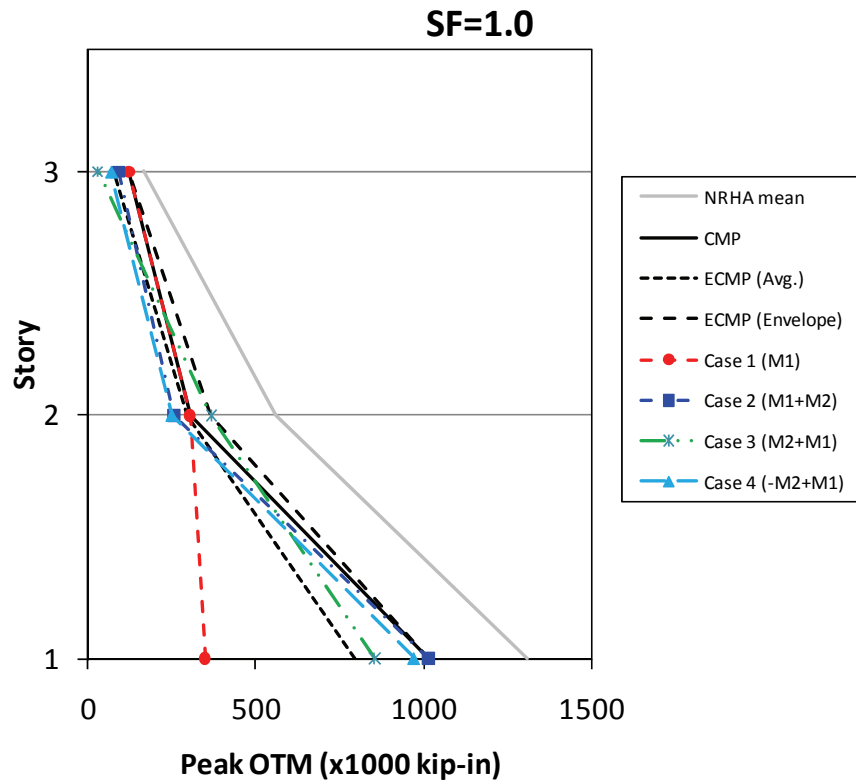


Figure F-66 Building B comparison of CMP and NRHA peak story overturning moment in transverse direction (H2).

F.6 Summary of Observations

Observations are presented for each building separately. They are broken into sections, described as follows.

The first section provides observations regarding the global building response and explains why some results were not included. The second provides observations on modeling and analysis in the chosen software. This is followed by a section briefly describing the nonlinear response history analyses results and model behavior, which are the baseline for comparison of the other analysis techniques.

The next section summarizes the results of the four techniques that are currently included in ASCE/SEI 41-06, or are closely related thereto. This includes all traces on the first of each pair of charts: Nonlinear Response History Analysis (NRHA), Pushover Analysis (ASCE 41), and the three Response Spectrum Analysis techniques (RSA-all modes, RSA-1mode, and ASCE 41+RSA higher modes).

Separate sections then follow for the techniques not currently included in ASCE/SEI 41-06: Modal Pushover Analysis (MPA), Consecutive Modal Pushover (CMP), and the extended Consecutive Modal Pushover (ECMP).

F.6.1 Building A

Overall Building Behavior

During the simplification from a three-dimensional to a two-dimensional model, additional modifications were made to increase the seismic demands in the frame, which initially was elastic even for the scale factor 2.0 analyses. The tributary mass was increased—increasing the fundamental period of the structure from 1.3 seconds to a relatively long 3.7 seconds. Column sizes were increased to reduce rotation demands in the PMM hinges which otherwise prevented the analyses from running to completion. The PMM hinges were eventually replaced with flexural only hinges.

The average response spectrum from the ground motion accelerations drops off quite rapidly at long periods, which partially offsets the impact of increasing the mass. Consequently the deformation demands in the moment connection hinges typically did not exceed the bi-linear portion of the response. Use of a larger scale factor of 4.0 was investigated but abandoned after it was determined that analyses would stop any time a hinge entered the degraded portion of the backbone curve.

The mass participation in the first mode is 85% indicating the effect of higher modes should be relatively modest. This is considered a typical higher modes problem, since the higher modes are a consequence of increased building height.

Modeling and Analysis

SAP 2000 has a graphical user interface that facilitates rapid model construction and relatively easy editing of structural geometry or properties. While the interface was easy to use, some difficulties were encountered during portions of the various analyses.

The original 3D pushover model was developed and modified over time adding progressively greater complexity as various behaviors were investigated. The final model was relatively complex and would take several hours to run. Story drifts in the pushover analyses beyond 3% typically were not achieved as the analyses would not converge, and were beyond the range of interest of the project.

The beam-column hinges originally were defined to drop flexural strength significantly and suddenly, as defined in ASCE/SEI 41-06 for pre-Northridge connections. This behavior along with the overall model complexity required use of the “restart-using secant” analysis option as other techniques would not converge.

Consequently the nonlinear behavior of the hinges was simplified and the default hinges were required to have a “shallower” unloading slope. The nonlinear hinges were assigned such that ASCE/SEI 41-06 point C (see Figure F-67) was connected directly to point E, and typically extended E by 50% to 100%.

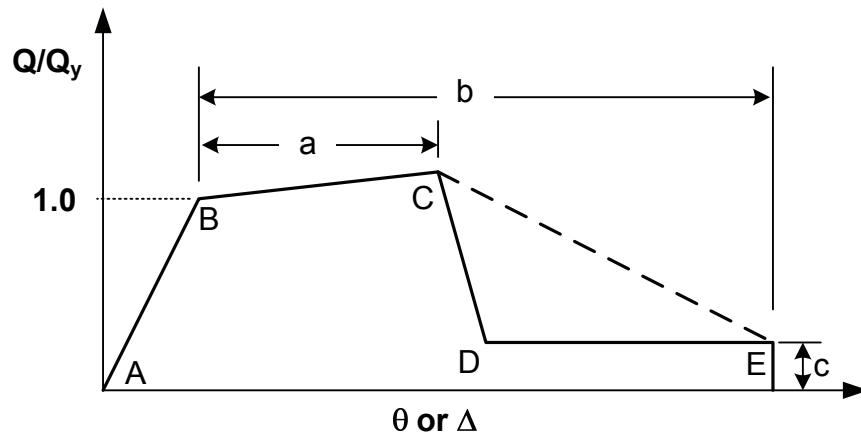


Figure F-67 Modified component model adapted from ASCE/SEI 41-06 (PEER/ATC, 2010).

The original 3D model was never intended to be used for NHRA. Had it been built with that purpose in mind, with progressively more complexity added after verification of the previous results, this effort may have been more successful. However, given the limited NHRA success that was achieved with only a very simple model; it seems very unlikely that NHRA could be performed on a model with anything resembling the same degree of complexity as the original 3D model.

Difficulties were also encountered in running the consecutive modal pushover analyses. Typically the initial pushover ran to completion, but subsequent pushovers

often did not converge. The pushover analysis control parameters were varied to obtain convergence, with no one set of values providing convergence across all cases. The analysis control output is limited and so selection of successful parameters is mostly a matter of trial and error.

Ignoring P-Delta effects significantly increased the analysis speed and the likelihood of convergence for both pushover and NHRA.

Nonlinear Response History Analysis

As the demand level increases, either in pushover analysis or NHRA, the initial deformation mechanism in the building is beam hinge yielding with column hinging occurring at the base of the columns and immediately below the roof level.

Hinging at other column locations, particularly in the exterior weak-direction columns, was observed in some of the CMP-Extended pushover analyses, as can be seen in Figures F-27 and F-28.

A comparison of the NHRA drift results presented in Figure F-15 illustrates the increased dispersion resulting from increasing the scale factor from 1.0 to 2.0. As discussed previously the Building A structure is essentially linear at scale factor 1.0.

Pushover and Response Spectrum Analysis

This includes Pushover Analysis (ASCE 41) and Response Spectrum Analysis techniques (RSA-all modes, RSA-1mode). The Nonlinear Response History Analysis (NRHA) results form the basis of comparison. The results presented in Figures F-17, F-19, F-21 and F-23 compare the story drift, story displacement, story shear and story overturning moment (OTM).

The pushover target displacements are summarized for each mode in Table F-8 and the pushover curves for each mode are shown in Figure F-13. The actual pushover analyses successfully reached very large roof displacements compared to the Table F-8 target values. For all analyses except the mode-1 pushover analysis at scale factor 2.0, the structure is elastic.

At scale factor 1.0, the structure is essentially elastic and so the RSA-1mode results match the ASCE 41 results. The three RSA-based techniques also produce results that are very similar to each other and also close to the nonlinear response history results.

The frame has no irregularities so linear analysis would be permitted per ASCE 41 Section 2.4.1.2. A response spectrum or linear dynamic analysis would be required because of the relatively long period of the frame.

There is a threefold increase observed in the sixth story shear between the ASCE 41 pushover and the RSA demands. This is well in excess of the 1.3 factor that would trigger consideration of higher mode response. This means that the combined

procedure of Section 2.4.2.1 would be required, whereby a supplemental response spectrum analysis would be required in addition to the pushover analysis. The computed value of R for this assessment is below R_{max} indicating that NRHA would not be required even at scale factor 2.0.

At scale factor 2.0, the linear and nonlinear methods start to diverge, at least for the reported story shears and OTMs. This is most clearly visible in Figure F-21. Notice the divergence between the ASCE 41 and RSA-1mode cases, and also between the ASCE 41+RSA higher modes and the RSA-all modes case – when going from scale 1.0 to 2.0.

The basic RSA case does a relatively good job of matching drifts, but overestimates shears as the scale factor increases. RSA can be used either standalone or as a supplement to the ASCE 41 NSP to account for higher mode response as required in Section 2.4.2.1. This process works because results from the two analysis techniques are never combined.

The m -factors for the supplemental response spectrum analysis are permitted to be increased by 1.33, presumably to avoid having the analysis excessively limit the performance conclusions as the component ductility implied in the nonlinear deformation limits often exceeds the m -factor for the corresponding performance level.

Specific frame demands were not examined; however, for the representative moment connections considered in this evaluation, a comparison can be drawn as follows:

- Moment Frame Connection Plastic Rotation limits (Figure F-5)
 - Immediate Occupancy ~ 0.009 radians
 - Secondary Life-Safety ~ 0.018 radians
- Corresponding m -factors
 - Immediate Occupancy ~ 1.8, or 2.4 including the permitted 1.33 increase.
 - Secondary Life-Safety ~ 2.8, or 3.7 including the permitted 1.33 increase.
- Beam yield rotation ~ 0.004 radians, frame effective yield ~ 1.1% drift (from Figure F-14). Say 1.0% drift for beam yield.
- Range of reported drifts for scale factor 2.0:
 - ASCE 41 Pushover Analysis: 0.7% to 3.2%.
 - Median Response History: 1.9% to 2.3%.
 - Response Spectrum Analysis: 2.4% to 2.7% (all modes)
1.1% to 2.6% (1-mode)
 - ASCE 41+RSA Higher modes: 2.1% to 3.4%.

Assuming that drift can be taken as a reasonable proxy for plastic rotation, the following performance limits can be estimated for the scale factor 2.0 results:

- ASCE 41 Pushover Analysis: $3.2\% - 1.0\% = 2.2\%$ “plastic drift/rotation”
 $0.022 \text{ rad.} > 0.018 \text{ rad.}$, Collapse Prevention
- Median Response History: $2.3\% - 1.0\% = 1.3\%$ “plastic drift/rotation”
 $0.013 \text{ rad.} < 0.018 \text{ rad.}$, Life Safety
- RSA-All Modes: $2.7\% / 1.0\% = 2.7$ “ductility demand”
 $2.7 < m=2.8$, i.e. Life Safety
- RSA-1mode: $2.6\% / 1.0\% = 2.6$ “ductility demand”
 $2.6 < m=2.8$, i.e. Life Safety
- ASCE 41+RSA Higher Modes: $3.4\% / 1.0\% = 3.4$ “ductility demand”
 $3.4 > m=2.8$, i.e. Collapse Prevention
- Combined Procedure: Collapse Prevention, governed by Pushover
(ASCE 41 Section 2.4.2.1)

The method used above is approximate, but it demonstrates that variations in response quantities may lead to a corresponding change in the conclusions regarding building performance level. In this case, the controlling response quantities from the simplified analysis methods were more conservative than those from nonlinear response history analysis. If the estimated response quantities had been less conservative than those from nonlinear response history analysis, the severity of response would have been underestimated. The results are summarized in Table F-14.

Modal Pushover Analysis (MPA)

Modal Pushover Analysis (MPA) results are presented in Figures F-18 through F-24, which compare results to the other two nonlinear modal techniques, CMP and extended version of CMP, and to the response history analysis results. Results from the ASCE 41 pushover analysis and the response spectrum analysis (RSA) are included for comparison.

Results are also presented for a special case of MPA – taking the SRSS of the results of the ASCE 41 pushover analysis with the higher mode response from the linear response spectrum analysis. Higher mode response was determined from a RSA with a modified spectrum where the first modes in each direction were removed.

If results are combined across multiple pushover analyses there is an inherent conflict because forces in the deformation controlled components can exceed the member capacities. This implies that a yield or some type of model event should have occurred earlier in the analysis than was indicated by the NSP alone. The presence of

the higher mode forces may also change the mechanism that develops in the frame, as can be seen from the CMP Extended results.

While MPA does introduce alternate deformation patterns into the analysis it does not consider interaction between the modal demands as can be achieved using CMP. For example, performing the M2 pushover before or after the M1 pushover does not affect the results of an MPA assessment. If a CMP Extended analysis were performed instead, then two unique deformation patterns would have been developed.

The MPA technique improved the match to the NRHA results for all demand parameters, and at both scale factors, where it was performed. The degree of overall improvement was similar to that achieved using the CMP technique.

MPA also has an advantage over the CMP in that fewer pushover runs are required to meet the procedure requirements.

For the MPA procedure the following ASCE 41 performance level is inferred for the scale factor 2.0 results:

- Range of reported drifts: 1.4% to 3.2%.
- Performance Level: $3.2\% - 1.0\% = 2.2\%$ “plastic drift/rotation”
0.022 rad. > 0.018 rad., Collapse Prevention
Note: $0.022 / 0.004 = 5.5$, also CP.

Consecutive Modal Pushover (CMP) and CMP Extended

The CMP method only considered a positive mode 2 push after mode 1 and so the observed improvement was relatively modest. This illustrates the importance of considering both positive and negative signs of the modes in this procedure.

The CMP Extended pushover curves are shown in Figure F-14. The base shear versus roof displacement trace can be followed for the various modal combinations considered. The pushover curve intersections indicate the transition points from one mode to another.

For the two-mode CMP Extended cases, the transition displacement from M2 and M1 is a reasonable match to the MPA target displacement. A similar degree of nonlinearity is indicated at the end of the subsequent M1 pushovers. However, a review of the analysis results in Figures F-25 and F-26 shows that quite different deformation patterns have developed in the two pushover curves (gold and blue traces). This is confirmed in Figure F-27, which shows the deformed frame elevations at the end of the two pushover cases.

For the three-mode CMP Extended analyses, the situation is now more complex as four different consecutive analyses were performed. Reviewing the analysis results

in Figures F-25 and F-26 and the deformed frame elevations in Figure F-28 shows that each analysis produced peak response in a different part of the structure.

By comparing the extended consecutive modal pushover deformation and drift results in Figure F-16 with the NRHA results in Figure F-15, many insights were discovered. The extended consecutive modal pushover results are generally more variable than the response history analysis results. However, the average of the seven extended consecutive modal pushover analyses is a good match to the median response history analysis result. This is consistent with the concept that each extended consecutive modal pushover analysis is a different “earthquake event,” and therefore the average response of the seven analyses is meaningful.

The extended consecutive modal pushover analysis story shears are shown in Figure F-22. The mean extended consecutive modal pushover values are significantly lower than the median response history analysis values. However, examining the corresponding response history analysis results reveals that the results are reasonably tightly grouped so that median and maximum results are relatively close together – presumably due to plastic mechanisms capping the demand.

The tight grouping of the results suggests an alternate method to compare the two sets of results - by comparing enveloped values instead of mean. This concept has some basis in the ASCE/SEI 7 code provisions for response history analysis. In ASCE/SEI 7, the capacity of force-controlled or “omega-level” components is calculated the same way: such that the demands are increased by considering the maximum response from the suite of records instead of the mean.

In ASCE/SEI 41-06, the same concept applies – the force-controlled component is intended to have some margin of strength above the expected capacity of the deformation-controlled components, but the implementation is handled slightly differently. The demands for both force-controlled and deformation-controlled components are taken as the mean from the NHRA, and the force-controlled components are assigned a lower component strength.

Examining Figure F-22, it is apparent that the extended consecutive modal pushover method is providing an improved match to the maximum demands relative to the other techniques.

Four additional analysis combinations could have been generated by doing variations on $\pm M2 \pm M3 \pm M1$ and two more by doing $+M1 \pm M2$. One of that latter pair forms the basis for the original consecutive modal pushover techniques.

The MPA target displacements are also shown on the curves indicating that at scale factor 2.0 both the M2 and M3 responses are elastic. As discussed in Section 4, the method of estimating the M3 and M2 target displacements was varied from the original CMP, otherwise the deformation in M3 would have been excessive.

For the CMP procedure the following ASCE 41 performance level is inferred for the scale factor 2.0 results:

- Range of reported drifts: 0.8% to 3.2%.
- Performance Level: 3.2%–1.0% = 2.2% “plastic drift/rotation”
0.022 rad. > 0.018 rad., Collapse Prevention
Note: $0.022 / 0.004 = 5.5$, also CP.

For the extended CMP procedure the following ASCE 41 performance level is inferred for the scale factor 2.0 results:

- Range of reported drifts: 1.7% to 2.8%.
- Performance Level: 2.8%–1.0% = 1.8% “plastic drift/rotation”
0.018 rad. \leq 0.018 rad., Life Safety
Note: $0.018 / 0.004 = 4.5$, Collapse Prevention.

In this case the extended CMP assessment would rate the building as meeting the Life-Safety performance level (just), while the base CMP and MPA procedures rate the building as meeting the Collapse Prevention performance level.

F.6.2 Building B

Overall Building Behavior

Although the flexible diaphragm contributes heavily to the seismic response in both directions, the seismic response of the building is quite different in the H1 (X) and H2 (Y) directions. As the diaphragm deformation increases all the third floor columns are mobilized in bending as a secondary load path at this level.

The braced frames are arranged in a typical chevron configuration. When one brace buckles in compression the tension brace pulls the beam downward at mid-span forming a flexural hinge at the beam mid-point. Brace buckling typically initiates at the ground floor and initiates a soft-story response in the structure. Similar to the third floor, there is a secondary load path from bending on the ground floor columns with fixity provided by the intact second floor braced frames.

The braced frame bays are arranged in pairs in the H1 direction and are continuous in the H2 direction. This means that the H1 direction frames can rock on their bases with overturning resistance provided by their tributary dead load and from the continuous grade beams. The flexibility associated with the potential rocking motion increases the first longitudinal mode participating mass significantly (62% in H1 versus 32% in H2), despite the periods being approximately the same.

The H2 response of Building B presents a debatably more challenging and quite different higher mode response problem than that presented by Building A. The roof

diaphragm mechanism is entirely different from the soft story mechanism, yet both occur in the building during different earthquake records (Figure F-35).

Modeling and Analysis

While PERFORM-3D is a powerful nonlinear analysis tool, the graphical user interface is somewhat less intuitive than that provided in SAP2000. Nonetheless, with some experience, the user can construct models, run analyses, and view and extract results reasonably efficiently.

For the models used in this Appendix, PERFORM-3D ran the analyses quite quickly—pushover analyses complete in minutes, NRHA's complete in hours. Including P-Delta effects slows but does not stop the analysis.

In contrast with Building A, the Building B model was constructed with NRHA in mind, and so analyses were performed during the various stages of development. Pushover analyses were also performed during development of the model; however, these were primarily for validation purposes.

The pushover analyses were then successfully run on the completed model, with a few exceptions that were not related to convergence problems. However, it is understood that the same solution algorithms are used for both NRHA and pushover analyses, with the latter simply being a special case of the former. Had the Building B model been constructed first for pushover analysis, and then the NRHA been performed, it is believed that the analyses would have successfully converged once the necessary NRHA information had been added.

The program has limited analysis control parameters available to the user. Mostly this does not appear to matter as analyses generally converge provided no instability or other problem exists.

Some planning is required regarding what results will be needed from the analysis as certain types of output cannot be easily obtained after the analysis has been run (e.g., section cut forces).

Unlike SAP2000, PERFORM-3D does not include any automated design or checking of structural members. This is a reflection of its focus on nonlinear analysis – so much so that the linear analysis capabilities of the program are actually quite limited. In particular, for response spectrum analysis, there are limited results reported, only nodal displacement, drifts, and section cut forces. The results are reported only for a single RSA at a time, and no load combinations with RSA results are possible within the software.

In the modal analysis, translational quantities are reported but no rotational quantities. This makes identification of the important torsional building modes more difficult.

Nonlinear Response History Analysis

A comparison of the NHRA results presented in Figures F-31 through F-34 show that for scale factors of 0.5 and 1.0, the results of the individual ground motion analyses are fairly tightly grouped around the mean indicating a generally elastic response of the building at these demand levels. In both directions the structure is mostly elastic with the exception of the metal deck roof diaphragm which is relatively weak and flexible.

At scale factor 2.0, significant nonlinear response is observed in the braced frames in both directions, Figures F-35 and F-36. At this higher demand level, drift and displacement results indicate the initial formation of a soft story mechanism at the first story, and a comparison with the smaller scale factors show the increased dispersion of individual ground motions resulting from the inelastic response.

The effect of rocking in the H1 direction is visible in the drift and displacement plots with lower demands below the roof level than in the H2 direction.

Pushover and Response Spectrum Analysis

Results for the current analysis techniques used in ASCE/SEI 41-06 include all traces on the first of each pair of charts: Pushover Analysis (ASCE 41), and the Response Spectrum Analysis techniques (RSA-all modes and RSA-1mode). Results for the analysis using ASCE 41+RSA higher modes are included here for comparison because the method is closely related. The Nonlinear Response History Analysis (NRHA) results form the basis of comparison.

The ASCE 41 and MPA pushover target displacements are summarized for each mode in Table F-9 and the pushover curves for each mode are shown in Figure F-29 and F-30. The actual pushover analyses successfully reached large roof displacements compared to the Table F-9 target displacement values. The structure is essentially elastic for all except the scale factor 2.0 results for the fundamental mode in each direction.

The results for the story drift and displacement, story displacement, story shear and story OTM are compared across the five analysis techniques in Figures F-37, F-39, F-41, F-43, and F-45 for the longitudinal (H1) direction, and Figures F-47, F-49, F-51, F-53, and F-55 for the transverse (H2) direction.

In the H1 direction, the drift and displacement results are a relatively good match to the NHRA results for scale factors 0.5 and 1.0 (Figures F-37, F-39). At scale factor 2.0, all methods fail to pick up the soft story at level 1 and underestimate the response. In the H2 direction the single mode methods (ASCE 41 and RSA-1mode) markedly underestimate the NHRA results even at the lower scale factors due to the lower mass participation in the fundamental mode.

The story shear results in the H1 direction show clearly the effect of rocking on the response, Figure F-43. The ASCE 41 results are a relatively close match to the NHRA results at all scale factors. The linear methods show increasing overestimation as expected. In the H2 direction (Figure F-53) the single mode methods, ASCE 41 and RSA-1mode, underestimate the NHRA results even at low scale factors due the low participating mass. The two multimode methods (RSA and ASCE 41+RSA Higher Modes) show good agreement in the elastic range at low scale factors, but again overestimate at scale factor 2.0. The overturning moments show a similar trend.

In the H1 direction, the rocking deformation becomes increasingly better developed at higher scale factors. As the scale factor increases the proportion of the roof displacement occurring in the roof diaphragm decreases (Figure F-42). If the C_0 and C_m factors were recalculated using the displaced shape at the target displacement then presumably C_0 would reduce from 1.72, and C_m factor would increase from 0.62. The nonlinear rocking deformation decreased the importance of the higher modes to the overall response of the structure. The rocking mechanism may also be acting as a filter, preventing the higher modes from being excited. This would account for the good agreement between the ASCE 41 and NHRA story shears and OTMs, even at large scale factors.

In the H2 direction, nonlinearity is initially limited to the roof diaphragm and then occurs in the first story braced frames. There is no rocking mode to control the response which becomes increasing less “single mode” at the larger scale factors. The ASCE 41 pushover story shears and OTMs consequently underestimate the ASCE 41 results at all scale factors.

Modal Pushover Analysis (MPA)

The MPA results for the story drift, story displacement, story shear, and story OTM are compared to the results of the other two nonlinear modal techniques, CMP and extended version of CMP in Figures F-38, F-40, F-42, F-44, and F-46 for the longitudinal (H1) direction, and Figures F-48, F-50, F-52, F-54, and F-56 for the transverse (H2) direction. Results from the ASCE 41 and RSA analyses are included in these charts for comparison.

MPA improves the agreement with the NHRA results over the ASCE 41 pushover results for all demand parameters and scale factors. The improvement is most noticeable in the H2 direction (e.g. Figure F-50). However, the MPA technique failed to pick up the story mechanism that developed in the first floor as the target displacement for the second mode in each direction was lower than that required to cause buckling of the braces.

Consecutive Modal Pushover (CMP) and CMP Extended

In the H1 directions, the CMP results are nearly identical to the pushover and MPA results. In the H2 direction, the CMP method results produce inconsistent changes relative to the NHRA results, depending on scale factor. The difference is attributed to the CMP method only considering a positive direction second mode pushover applied after the first mode pushover. Since it was scaled to produce an increase in roof displacement, the second mode in each direction tends to reduce the mode story shears in the lower levels. This accounts for the comparatively low responses at the first and second floor for scale factor 2.0. This illustrates the importance of considering both positive and negative signs of the modes in this procedure.

The extended consecutive modal pushover procedure did not produce the same quality of match to the nonlinear response history analysis response prediction as observed for Building A. Some improvement was observed; however, several areas were identified where the method requires additional refinement.

The target displacements used for each leg of the CMP analyses are shown in Tables F-9, F-10 and F-11 for scale factors 0.5, 1.0 and 2.0, respectively. As noted in Section F.4.7, the method of computing the target displacements results in a relatively high value for the second mode, which becomes particularly apparent if the higher mode pushover analysis is performed first.

In the H2 direction for scale factor 2.0, the target roof displacement computed for the 2nd mode push was 4.9 inches (Table F-12), compared to a MPA target displacement of only 0.8 inches (Table F-9). This implies an unrealistic level of higher mode ductility demand which prevented these analyses from running to completion.

A revised method of computing the 2nd mode target displacement was quickly devised as described in Section F.4.7 and the value was reduced to 2.5 inches for the H2, scale factor 2.0 analyses for the $\pm M2+M1$ cases (Case 3 and Case 4). Target displacements for other scale factors and the H1 direction were not revised as those analyses ran to completion.

Results for one of the CMP Extended cases ($+M1-M2$) are not shown. It was not possible to get PERFORM 3D to run this case correctly. Regardless of how the second mode pushover was applied, the result was always $+M1+M2$. Omission of this case will also have some effect on the average and envelope results.

A problem was discovered in the results of the CMP analysis that was not possible to correct prior to publication. The story shear and OTM results are those at the last step of the analysis, rather than the maximum value over the whole pushover analysis. This will tend to reduce the reported values by an unknown amount. Displacement and drift results are correctly reported as last step values.

As a result of the above, the Building B CMP results should be viewed as a work in progress and used to guide future development of the technique. Some useful observations can still be made.

The results of the different CMP and CMP Extended pushovers are shown in Figures F-57 through F-66. Figure F-58 shows that one of the pushover cases ($-M2+M1$) successfully generated the soft story mechanism at the 1st story that was observed in some of the NRHA results.

As for Building A, the dispersion in CMP Extended results greatly exceeds those from NRHA. This is primarily due to the overestimation of the second mode response.

The average and envelope results of the CMP Extended method and the base CMP results are compared to the NRHA, MPA, and RSA results in odd-numbered Figures F-38 to F-56. Both over and under-estimation of the NRHA responses are present for the reasons outlined above.

F6.3 Accuracy of Estimates of Demand Parameters

The tables below summarize the accuracy of the estimates of the demand parameters for different analysis methods for the two buildings analyzed. The story shear and drift ratio information is provided graphically in Figures F-67 through F-70.

Table F-13 Accuracy of Response Quantity Estimates for Building A

Scale Factor	Analysis Procedure	Response Quantity*			
		Disp.	Story Drift	Story Shear	OTM
1.0	ASCE 41	0.9 to 1.0	0.4 to 0.9	0.4 to 0.8	0.3 to 1.0
	ASCE 41 plus RSA higher modes	1.0 to 1.0	0.9 to 1.3	1.0 to 1.0	1.0 to 1.0
	RSA - all modes	1.0 to 1.0	0.8 to 1.1	1.0 to 1.1	1.0 to 1.0
	RSA-1 mode	0.9 to 1.0	0.4 to 0.9	0.3 to 0.8	0.3 to 1.0
	MPA	0.9 to 1.0	0.6 to 1.0	1.0 to 1.0	0.4 to 1.0
	CMP	1.0 to 1.1	0.9 to 1.1	1.0 to 1.0	1.0 to 1.0
2.0	ASCE 41	1.1 to 1.5	0.3 to 1.6	0.2 to 0.7	0.2 to 0.8
	ASCE 41 plus RSA higher modes	1.1 to 1.6	1.0 to 1.8	1.1 to 1.2	0.9 to 1.0
	RSA - all modes	1.1 to 1.2	1.1 to 1.3	1.2 to 1.5	1.0 to 1.3
	RSA - 1 mode	1.0 to 1.1	0.5 to 1.1	0.4 to 1.2	0.3 to 1.3
	MPA	1.1 to 1.6	0.6 to 1.7	0.6 to 0.9	0.4 to 0.8
	CMP	1.1 to 1.5	0.4 to 1.6	0.3 to 0.7	0.2 to 0.8
	CMP Extended	0.9 to 1.3	1.0 to 1.4	0.5 to 0.7	0.4 to 0.6
	CMP Extended – Maximum	N/A	N/A	0.9 to 1.1	0.8 to 0.9

* Values are the minimum and maximum ratios of estimated response quantity to mean value from nonlinear response history analysis.

Table F-14 Predicted Level of Performance (based on ASCE 41 acceptance criteria) for Building A

Scale Factor	Analysis Procedure	Performance Level
2.0	Nonlinear Response History	Life Safety
	ASCE 41	Collapse Prevention
	ASCE 41 plus RSA higher modes	Collapse Prevention
	RSA - all modes	Life Safety
	RSA - 1 mode	Life Safety
	MPA	Collapse Prevention
	CMP	Collapse Prevention
	CMP Extended	Life Safety
	ASCE 41 Section 2.4.2.1 Combined *	Collapse Prevention

* Worse prediction from ASCE 41 nonlinear static procedure and RSA- all modes.

Table F-15 Accuracy of Response Quantity Estimates for Building B – H1 Direction

Scale Factor	Analysis Procedure	Response Quantity*			
		Disp.	Story Drift	Story Shear	OTM
0.5	ASCE 41	0.9 to 0.9	0.8 to 0.9	0.8 to 0.8	0.7 to 1.0
	RSA - all modes	1.0 to 1.0	0.9 to 1.0	1.2 to 1.2	0.9 to 1.0
	ASCE 41 plus RSA higher modes	1.0 to 1.3	1.0 to 1.3	1.3 to 1.4	1.1 to 1.2
	RSA - 1 mode	0.9 to 0.9	0.9 to 0.9	1.1 to 1.1	0.9 to 0.9
	MPA	0.9 to 0.9	0.9 to 0.9	0.8 to 0.8	0.7 to 1.0
	CMP	0.9 to 0.9	0.8 to 0.9	0.8 to 1.0	0.9 to 1.0
1.0	ASCE 41	0.9 to 1.0	0.9 to 0.9	0.7 to 0.9	0.5 to 0.9
	RSA - all modes	0.9 to 0.9	0.9 to 0.9	1.4 to 1.7	1.0 to 1.3
	ASCE 41 plus RSA higher modes	1.1 to 1.3	1.1 to 1.3	1.4 to 1.6	0.9 to 1.2
	RSA - 1 mode	0.8 to 0.9	0.8 to 0.9	1.3 to 1.6	0.9 to 1.2
	MPA	0.9 to 1.0	0.9 to 0.9	0.8 to 1.0	0.5 to 0.9
	CMP	0.9 to 1.0	0.9 to 0.9	0.7 to 1.0	0.6 to 0.9
2.0	ASCE 41	0.4 to 0.6	0.4 to 0.7	0.8 to 1.1	0.4 to 1.0
	RSA - all modes	0.5 to 0.7	0.5 to 0.8	2.4 to 3.2	1.2 to 2.2
	ASCE 41 plus RSA higher modes	0.6 to 0.7	0.6 to 0.8	1.9 to 2.3	0.9 to 1.5
	RSA - 1 mode	0.4 to 0.7	0.4 to 0.8	2.2 to 2.9	1.1 to 2.1
	MPA	0.4 to 0.6	0.4 to 0.7	0.9 to 1.2	0.5 to 1.0
	CMP	0.5 to 0.8	0.5 to 0.7	0.8 to 1.1	0.4 to 1.0

* Values are the minimum and maximum ratios of estimated response quantity to mean value from nonlinear response history analysis.

Table F-16 Accuracy of Response Quantity Estimates for Building B – H2 Direction

Scale Factor	Analysis Procedure	Response Quantity*			
		Disp.	Story Drift	Story Shear	OTM
0.5	ASCE 41	0.3 to 0.6	0.3 to 0.8	0.3 to 0.9	0.2 to 0.7
	RSA - all modes	0.9 to 1.0	0.9 to 1.0	1.0 to 1.3	0.9 to 1.1
	ASCE 41 plus RSA higher modes	1.1 to 1.2	1.0 to 1.1	1.2 to 1.2	0.9 to 0.9
	RSA - 1 mode	0.4 to 0.7	0.4 to 1.0	0.4 to 1.3	0.5 to 1.1
	MPA	0.6 to 0.7	0.6 to 0.8	0.6 to 0.9	0.7 to 0.9
	CMP	1.0 to 1.7	0.8 to 1.7	0.9 to 1.7	0.7 to 1.5
1.0	ASCE 41	0.3 to 0.5	0.3 to 0.9	0.3 to 1.0	0.3 to 0.7
	RSA - all modes	0.9 to 1.1	0.9 to 1.3	1.1 to 1.9	1.1 to 1.4
	ASCE 41 plus RSA higher modes	1.1 to 1.2	1.0 to 1.1	1.3 to 1.4	1.0 to 1.1
	RSA - 1 mode	0.4 to 0.8	0.4 to 1.3	0.5 to 1.8	0.7 to 1.3
	MPA	0.6 to 0.7	0.6 to 0.9	0.7 to 1.1	0.7 to 0.8
	CMP	0.5 to 0.7	0.7 to 0.9	0.9 to 1.0	0.7 to 0.8
2.0	ASCE 41	0.0 to 1.0	0.0 to 0.2	0.3 to 1.0	0.3 to 0.6
	RSA - all modes	0.2 to 1.2	0.5 to 1.2	1.7 to 2.8	1.6 to 1.7
	ASCE 41 plus RSA higher modes	0.5 to 1.3	0.3 to 0.5	1.6 to 1.8	0.9 to 1.6
	RSA - 1 mode	0.5 to 1.2	0.2 to 1.2	0.8 to 2.8	1.0 to 1.7
	MPA	0.5 to 1.0	0.3 to 0.5	0.9 to 1.1	0.7 to 0.9
	CMP	0.1 to 1.0	0.1 to 0.3	0.5 to 0.9	0.4 to 0.6

* Values are the minimum and maximum ratios of estimated response quantity to mean value from nonlinear response history analysis.

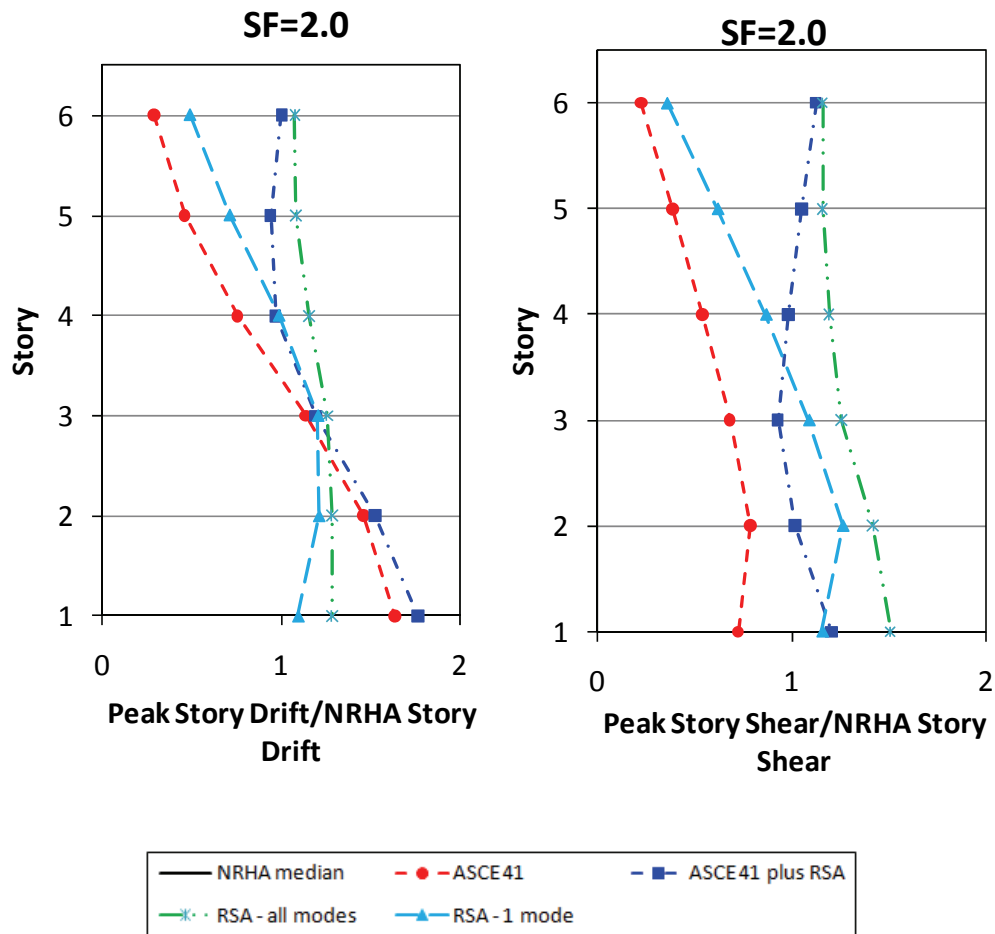


Figure F-68 Building A ratio of peak story drift and story shear to NRHA baseline.

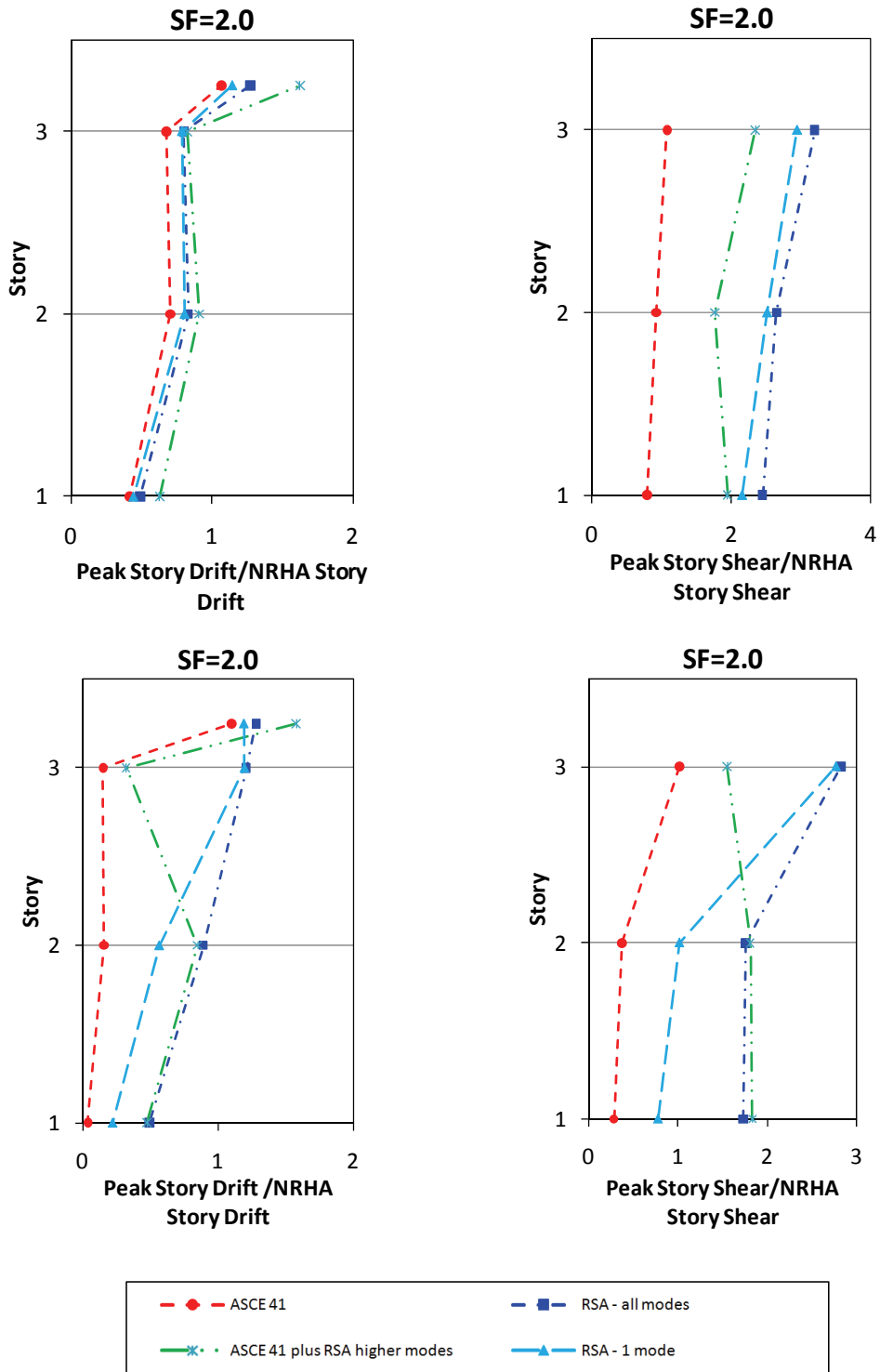


Figure F-69 Building B ratio of peak story drift ratio (reduced scale) and story shear in longitudinal direction (H1 at top) and transverse direction (H2 at bottom) to NRHA baseline.

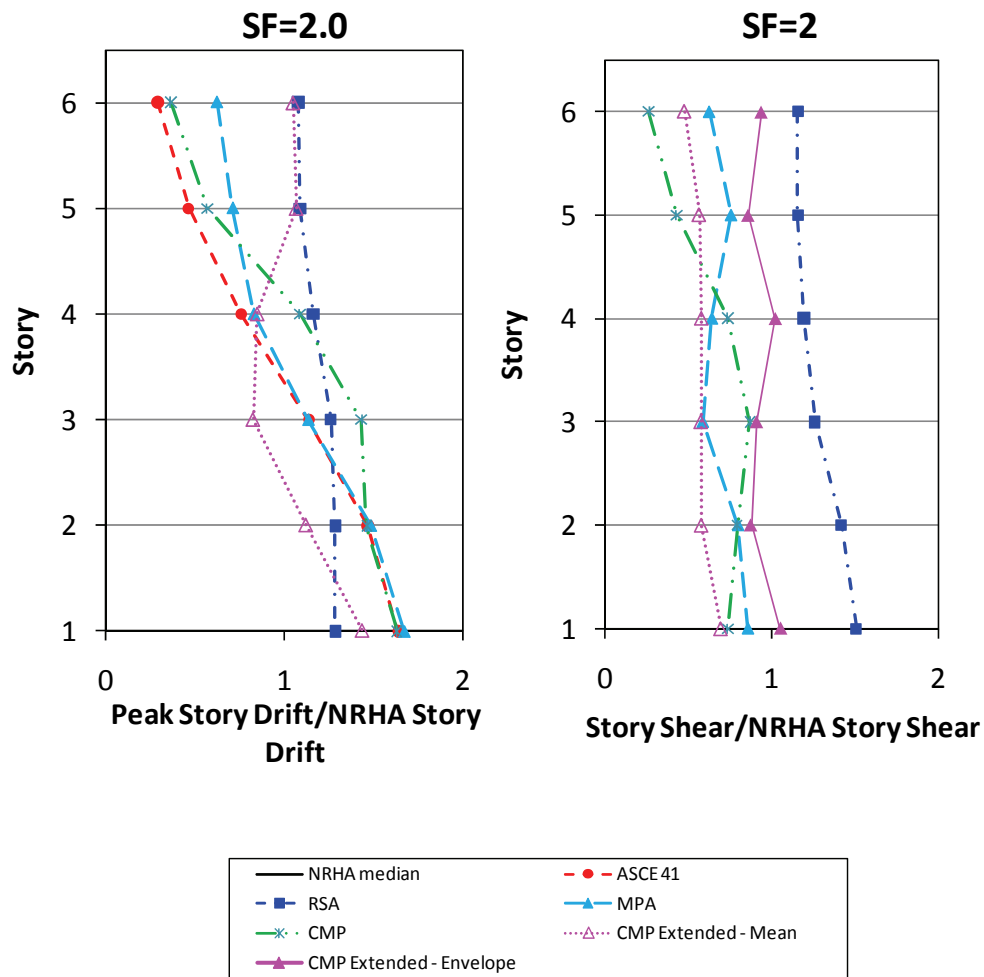


Figure F-70 Building A ratio of peak story drift and story shear to NRHA baseline.

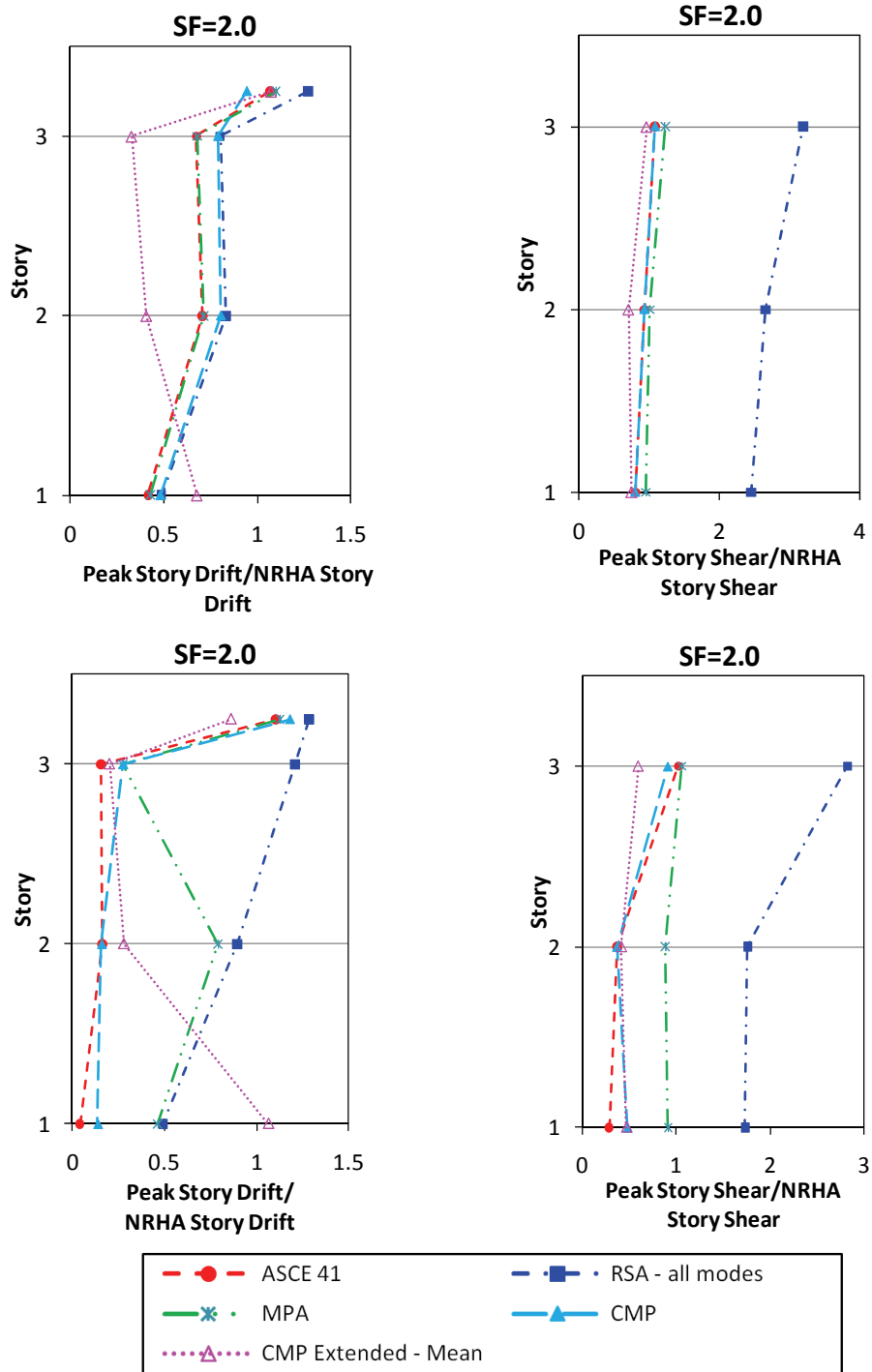


Figure F-71 Building B ratio of peak story drift ratio in longitudinal direction (H1 – at top) and transverse direction (H2 – at bottom) to NRHA baseline.

F.7 Conclusions

The conclusions have been divided into sections according to the study objectives, the first being to identify challenges and potential issues for the practicing design professional in performing nonlinear response history analysis (NHRA). This includes testing the hypothesis that since practitioners are already building nonlinear models for pushover analysis, all that is required to do nonlinear response-history analysis is simply to get some records and “run the models.”

The second objective was to evaluate the ability of the various techniques to capture higher mode response of the structures. A discussion of additional considerations for the use of the studied methods as well as areas of possible future research is also included.

F.7.1 Modeling and Analysis Conclusions

The following challenges and potential issues were identified for the practicing design professional in performing nonlinear response history analysis:

- More information is required for nonlinear response history analysis than for pushover analysis. Appropriate models must be selected and implemented for structural/ inherent damping and cyclic hysteretic behavior and ground acceleration records must be selected and appropriately applied to the model. There is at present no set of uniformly applicable guidelines that provide this type of information to the practitioner.
- A wide variety of structural analysis programs are in current use by practicing engineers. A limited subset is capable of nonlinear response history analysis. Many of these programs are less capable or suitable for traditional structural analysis and design tasks – e.g., say rapid model-building or gravity load design. This may necessitate development of an additional structural model.
- For a given evaluation or design project the complete set of response history analyses requires many more solution steps than for the corresponding set of pushover analyses. The maximum size and complexity of a response history model may therefore be lower than that of a pushover model.
- Although there are groups working to develop standard suite of recorded ground motion accelerations, there is at present no standard set of procedures for selection and scaling of records. Using a consultant this process may take weeks to months—a duration that may not be available.
- Some code documents and jurisdictions (e.g. ASCE/SEI 7 Section 16.2.5) require peer review of nonlinear response history analysis.

For the immediately-foreseeable future it appears that many practicing structural engineers still require a viable simplified method of nonlinear analysis that is less complex than nonlinear response history analysis.

An extensive body of work and many reference standards and guidelines (e.g., ASCE/SEI 41-06, ATC-40) have been developed around pushover analysis. It would be advantageous if a technique existed that appropriately accounted for higher mode effects, which was an extension of current pushover analysis, rather than an entirely new method.

F.7.2 Analysis Techniques Conclusions

Various techniques for capturing higher mode response were examined by comparing each set of analysis results to those from a reference suite of nonlinear response history analyses. Care must be taken in drawing conclusions from this study since only two buildings were examined, but the following observations are offered:

- Higher modes effects were found to be significant in the response of both structures. Pushover analysis was found to typically significantly underestimate story shear and overturning moment demands relative to nonlinear response history analysis. The impact of this variation on seismic performance conclusions (e.g. ASCE/SEI 41-06 performance level or required seismic strengthening) was not evaluated but is recommended for further study.
- A single pushover analysis could not capture the range of building deformation mechanisms that developed in different response history analyses.
- The linear response spectrum analysis method produced reasonably consistent results provided the overall building nonlinear deformation patterns that occurred in the response history analysis resembled those of the elastic structure – e.g., no story-mechanisms.
- Both buildings did not pass the check for significant higher mode behavior provided in ASCE/SEI 41-06 Section 2.4.2.1. The minimum permitted analysis method would be the dual-requirement method of both response spectrum and pushover; nonlinear response history analysis would not have been mandated. The dual-requirement method improves the enveloping of force demands, however, the pushover analysis failed to capture the story deformation mechanisms that developed in some of the response history analyses at higher input scale factors.
- The modal pushover analysis technique improved the match of results to those from nonlinear response history analysis, but similarly did not capture the formation of story mechanisms in the structures that formed at higher scale factors.
- Limitations were identified in the consecutive modal pushover technique related to the sequence and sign of the modal pushovers and the higher mode target

displacements. However, the technique appears promising as final component forces and deformation are always coincident with the backbone curve. This also occurs for pushover analysis, but not for the other techniques examined in this study.

F.7.3 Extended Consecutive Modal Pushover Conclusions

Preliminary work on a proposed extension to the consecutive modal pushover method concluded the following:

- By varying the sequence and sign of the consecutive modal pushover analyses different types of structural response and deformation mechanism are excited in the structure. For both buildings, the observed CMP deformation mechanisms included all those found to occur in the corresponding suite of response history analyses. It is proposed that each CMP analysis be treated as a separate “earthquake” and the results of the analyses be averaged for deformations and enveloped for forces.
- The proposed averaging of the responses for deformations and enveloping for forces is philosophically consistent with both new and existing building reference standards and with the principles of capacity design. ASCE/SEI 7 Section 16.2.4.1 requires “omega-level” components to be designed for the envelope of the forces from the response history analysis and ASCE/SEI 41-06 accomplishes the same result by requiring a lower capacity for force-controlled components.
- The proposed approach produced good agreement for one building but for the second building the results were inconsistent due to overestimation of the higher mode component of the CMP target displacement. Additional improvement to the method is required to make it a generally applicable procedure.

F.7.4 Assumptions and Limitations

When examining the results and conclusions presented in this study the following should be noted:

- Damping was set at 5% in all types of analysis (as near as possible). Response history analyses would likely have been performed using lower value which could have increased deformation demands by 25% or more.
- No attempt was made to consider bi-directional loading. This did not particularly affect the structures in the study, but could substantially complicate some of the analysis types examined here. For example, it is unclear how this would be deployed in consecutive modal pushover analysis. The issue can likely be resolved but requires further study.
- Bi-directional loading provisions vary by reference code and analysis type. Response spectrum analysis per ASCE/SEI 7 would require the use of 100% in the primary plus 30% in the orthogonal direction. Conflicting provisions exist

for linear static, nonlinear static, and response history analysis across both existing and new building. These differences should be considered when drawing any conclusions from the results presented here.

- No attempt was made to consider torsional response due to inherent or accidental mass eccentricity. Loads were applied either through the center of mass, or using mode shapes for the structure which was artificially made to be perfectly symmetric. Torsional effects are perhaps the single most important form of higher mode response that need be addressed in structural analysis. Similar to bi-directional loading, it is not immediately obvious how this would be implemented in consecutive modal pushover analysis, and the issue requires further study.
- The spectral input in each direction for all types of analysis was assumed to be the same. Specifically, the spectrum for the pushover and response spectra analyses was taken equal to the average of the earthquake components applied in that direction. This is inconsistent with the latest ground motion scaling requirements for three-dimensional analysis as prescribed in ASCE/SEI 7-10. For three-dimensional analysis at far-field sites these provisions would require the average SRSS response spectrum to exceed the target; as a result the input along each direction would be lower than assumed here.
- The study has focused around the provisions of ASCE/SEI 41-06. Other code documents such as ASCE-7 include provisions that use factors such as C_d and R that will result in smaller computed response spectrum analysis displacements. These differences should be considered when drawing any conclusions from the results presented here.
- This study has presented analysis results (displacement, drifts, shears, etc.) but has presented only limited conclusions from these analyses. That is:
 - What would have been the result of a more thorough examination of the structural performance level? - immediate-occupancy/life-safety/collapse prevention.
 - Which components would have been found to be deficient and why?
 - What would have been the recommended strengthening? (if any)

The preferred method for gauging the accuracy of the various procedures examined in this study should be a comparison of the conclusions and not simply a comparison of the analysis results. For example, in ASCE/SEI 41-06 the m -factors used for linear analysis frequently imply different permissible ductility demands than do the nonlinear component deformation limits for the same performance level. This should be considered in future research on this topic.

Expanded Summaries of Relevant Codes, Standards, and Guidelines

This appendix provides summaries of codes, standards, and guidelines that are relevant to nonlinear multiple-degree-of-freedom modeling in current engineering practice. Summaries include the scope of application, applicability of analysis procedures, other modeling direction provided, additional analysis requirements listed, as well as the ground motion characterization. These summaries also include a list of response quantities (i.e., demand parameters) that can be evaluated using the analysis procedures outlined in the respective documents.

G.1 ASCE/SEI 31-03 Seismic Evaluation of Existing Buildings

G.1.1 Scope of Application

ASCE/SEI 31-03, *Seismic Evaluation of Existing Buildings* (ASCE, 2003), provides a three-tiered process for the seismic evaluation of existing buildings. ASCE/SEI 41-06 is the companion document (see separate summary), which provides a process for the seismic rehabilitation of existing buildings. ASCE/SEI 31-03 includes Tier 1, Tier 2, and Tier 3 procedures, which use increasingly sophisticated methods of analysis.

The Tier 1 procedure is a quick, checklist-based approach. Checklists provided cover all major building types, both structural and nonstructural components, site and geologic hazards, varying degrees of site seismicity, and different performance levels (IO and LS). It is intended as a screening tool to isolate deficiencies for further investigation. The procedure consists of quick-checks that can be performed by hand if necessary.

The Tier 2 assessment can be a complete building evaluation, or can be targeted only at the deficiencies identified in the Tier 1 assessment. The analysis usually consists of a linear static or linear dynamic analysis, using m -factors, similar to ASCE/SEI 41-06. Tier 2 assessment may be required in some cases even if Tier 1 does not indicate any deficiencies. A special procedure (ABK, 1984) is provided for URMs.

The Tier 3 procedure is more complex, where the nonlinear response of the building is considered. For requirements, the user is referred to ASCE/SEI 41-06, which has provisions on the Nonlinear Static Procedure (NSP). Neither ASCE/SEI 31-03 nor ASCE/SEI 41-06 has detailed guidance for the Nonlinear Dynamic Procedure (NDP).

The flowchart in ASCE/SEI 31-03 Section 1.2 describes the evaluation process well.

An important difference between ASCE/SEI 31-03 and ASCE/SEI 41-06 is that since ASCE/SEI 31-03 is for evaluation of existing buildings and not strengthening design, the component m -factors are different in the two documents, being lower in ASCE/SEI 41-06. Where using ASCE/SEI 41-06 for a Tier 3 evaluation, the user is permitted to reduce the ground motion by 25 percent.

ASCE/SEI 31-03 also provides a table of benchmark buildings—that is, buildings that are assumed to meet a certain level of performance by virtue of being designed using a relatively recent edition of the building code. The edition varies by building type.

G.1.2 Applicability of Analysis Procedures

Tier 1: Screening Phase

- Benchmark buildings by year exempted from Tier 1 checklist (Section 3.2, Table 3-1).
- Complete required checklists determined by seismicity and level of performance (Table 3-2), indicating Compliant, Non-compliant, or N/A.
- Maximum height requirements for Tier 1 checklist (Section 3.4, Table 3-3). Beyond these values, must do a full Tier 2 or, in some cases, Tier 3, regardless of Tier 1 findings.

Tier 2: Evaluation Phase

LDP analysis required as follows:

- For buildings taller than 100 feet
- For buildings with mass, stiffness, geometric irregularities:
 - Soft story irregularity: stiffness of lateral force-resisting system is less than 70% of that of adjacent story or 80% of average of 3 stories above or below for IO/LS. (V1)
 - Geometry irregularity: change in horizontal dimension of the lateral force-resisting system of more than 30% in a story relative to adjacent stories for IO/LS. (V3)
 - Mass irregularity: change in effective mass with respect to adjacent story exceeds 50%. (V2)
- With exception of diaphragm actions and deformations, all actions and deformations calculated using the LDP must be multiplied by C (Table 3-4); for dynamic analyses using site-specific, 2%/50 year spectrum, multiply by 2/3.
- Additional processes for assessment:
- If structure has more specific procedures for evaluating each building component, including information on capacities, etc. These match the Tier 1

checklist checks; each Tier 1 check has a corresponding Tier 2 procedure for mitigation.

- Includes special procedure for URMs.

Tier 3: Detailed Evaluation Phase

- Permits multiplying demands by 0.75 where using rehabilitation documents (such as ASCE/SEI 41-06) for evaluation.
- LSP and LDP are permitted as Tier 3 procedures, but nonlinear response must be considered; use of m -factors qualifies. For instance, an ASCE/SEI 41-06 assessment, with demands multiplied by 0.75, can qualify as an ASCE/SEI 31-03 Tier 3 assessment.

LDP, NSP, or NDP is required for Tier 3 as follows (otherwise can use LSP):

- $T \geq 3.5T_s$.
- Story horizontal dimension exceed 1.4 times that of adjacent story (above or below).
- Torsional stiffness irregularity, corner-to-average drift ratio > 150%.
- Vertical stiffness irregularity, average story drift > 150% of that in adjacent level (above or below).
- Non-orthogonal lateral system.

Table G-1 below summarizes engineering demand parameters that may be addressed by the application of the analysis procedures covered in ASCE/SEI 31-03. The table identifies system-, intermediate-, and component level engineering demand parameters according to performance level, period limitations, regularity, and other limitations.

G.1.3 Other Evaluation Requirements

- Default conservative material properties are assumed unless otherwise noted. (Section 2.2).
- Default material properties may be used in all cases (unlike ASCE/SEI 41-06).
- Site/structure conditions must be determined.
- Determine level of performance (IO or LS), seismicity, and building type.

Table G-1 Engineering Demand Parameters¹ That May be Addressed Using These Analysis Procedures

Perf. level ²	Period (height)	Regularity ³	Other limitations	Analysis Procedures			
				LSP	LDP	Plastic	NSP or NDP
<i>Tier 1 Requirements</i>							
IO Low	1-4 stories	Not limited	Tier 1 OK for all bldg types except PC2A is full Tier 2	I1, C3, C4		C2, C4 ⁵	See ASCE/SEI 41-06 ⁸
IO Mod	1-4 stories	Not limited	Tier 1 OK for all bldg types except below Full Tier 2 for bldg types S1,S1A,S5,S5A,C1,C3,C3A,P C1,PC1A,PC2A,RM1, mixed	I1, C3, C4		C2, C4 ⁵	See ASCE/SEI 41-06 ⁸
			Tier 3 for bldg types URM, URMA				See ASCE/SEI 41-06 ⁸
IO High	1-4 stories	Not limited	Tier 1 OK for all bldg types except below Full Tier 2 for bldg types S1,S1A,S5,S5A,C1,C3,C3A,P C1,PC1A,PC2,PC2A,RM1, mixed	I1, C3, C4	See Tier 2 Procedures below	C2, C4 ⁵	See ASCE/SEI 41-06 ⁸
			Tier 3 for bldg types URM, URMA				
LS Low	No limit	Not limited	Tier 1 OK for all bldg types	I1, C3, C4		C2, C4 ⁵	See ASCE/SEI 41-06 ⁸
LS Mod and High	2-6 stories ⁷	Not limited	Tier 1 OK for all bldg types	I1, C3, C4		C2, C4 ⁵	See ASCE/SEI 41-06 ⁸
CP			Not considered			C2, C4 ⁵	See ASCE/SEI 41-06 ⁸
<i>Tier 2 Requirements</i>							
IO, LS	h < 100 ft	No V1,V2,V3	See Tier 1 limitations above	S2 ⁶ ,I1, C3, C4 ⁴	S2 ⁶ ,I1,I2 C3,C4 ⁴	C2, C4 ⁵	See ASCE/SEI 41-06 ⁸
	h < 100 ft	V1,V2,V3	See Tier 1 limitations above		S2 ⁷ ,I1,I2 C3,C4 ⁴	C2, C4 ⁵	See ASCE/SEI 41-06 ⁸
LS	< 6 stories		URM, flexible diaphragm, min 2 lines each direction except single story with open front on one side	S2,C3,C4		C2, C4 ⁵	See ASCE/SEI 41-06 ⁸
<i>Tier 3 Requirements</i>							
IO, LS				See ASCE/SEI 41-06 ⁸	See ASCE/SEI 41-06 ⁸	See ASCE/SEI 41-06 ⁸	See ASCE/SEI 41-06 ⁸

Table G-1 Engineering Demand Parameters¹ That May be Addressed Using These Analysis Procedures (continued)

Footnotes:

¹Engineering Demand Parameters addressed explicitly (or implicitly)

System EDPs	Intermediate EDPs	Component EDPs
S1: Identify global collapse	I1: Quantify story drift	C1: Identify local collapse
S2: Identify mechanism	I2: Quantify floor acceleration	C2: Identify mechanism
		C3: Quantify deformation
		C4: Quantify force

²Performance levels addressed explicitly (or implicitly)

IO: Immediate Occupancy; LS: Life Safety; CP: Collapse Prevention with corresponding hazard level, if indicated DE: Design Earthquake; MCE: Maximum Considered Earthquake, or Seismicity: Low, Mod-Moderate, or High

³Structural irregularities

Horizontal	Vertical
H1: Torsional stiffness	V1: Soft story
H2: Reentrant corner	V2: Mass
H3: Diaphragm discontinuity	V3: Setback
H4: Out-of-plane offset	V4: In-plane offset
H5: Non-orthogonal systems	V5: Weak story
H6: Torsional strength	

⁴Force-controlled component actions are permitted to be evaluated using the *J*-factor, as provided in Section 4.2.4.3.2.

⁵Where LSP is used, limit analysis can be used to determine component forces. For example Section 4.2.4.3.2 permits force-controlled actions to be calculated based on the capacity of deformation-controlled actions.

⁶The system mechanism can be evaluated to some degree by comparison of the relevant component DCRs.

⁷Table 3-3 appears to conflict with Section 4.2.6.1 which limits the Tier 2 special procedure to 6 stories or a Tier 3 must be performed.

⁸LSP is permitted as Tier 3 procedure where $T < 3.5T_s$, and none of irregularities V1, V3, H1, or H5 are present.

G.1.4 Other Modeling Direction Provided

Model for LSP/LDP (Section 4.2.3)

- Two-dimensional model for buildings with stiff diaphragms may be developed if torsional effects are negligible; otherwise three-dimensional model is required.
- Lateral force-resisting frames with flexible diaphragms may be modeled using either a two-dimensional assembly of components or a three-dimensional assembly with diaphragms modeled explicitly using flexible elements.
- Horizontal torsion modeled as eccentricity torsion plus accidental torsion (5% eccentricity), with the same amplification as in ASCE/SEI 41-06.
- All primary components (intended to resist seismic forces) must be modeled, and secondary components may be modeled. The total stiffness of all secondary components may not exceed 25 percent of the stiffness of primary components.
- Component action either force-controlled or deformation-controlled.
 - Deformation-controlled actions are divided by *m* (modifier for expected ductility).

G.1.5 Ground Motion Characteristics

- Spectral acceleration for computing pseudo lateral forces is based on S_S and S_I from ASCE 7-02 mapped values. These values represent an earthquake with 2% probability of exceedance in 50 years with deterministic-based maximum values near known fault sources.
- Site classification is based on the soil properties averaged over the top 100 ft of soil. If sufficient data to classify a soil profile is not available, assumed site class D.
- 10% probability of exceedance in 50 years may be used in lieu of 2/3 MCE values where appropriate.
- Site-specific response spectra must be mean spectra based on input ground motions at 2% probability of exceedance in 50 years. The site-specific response spectra need not exceed 150% of median deterministic spectra for the characteristic event on the controlling fault. Spectral amplitudes of the 5% damped site response spectra in the period range of greatest significance must not be less than 70% of the mapped spectral acceleration unless confirmed by an independent 3rd party.

G.1.6 Discussion

The material testing requirements in ASCE/SEI 31-03 are less onerous than those in ASCE/SEI 41-06. However, there are no specific requirements for the Tier 3 analysis, so the user will likely refer to ASCE/SEI 41-06, which may be unnecessarily demanding for evaluation (as opposed to strengthening).

For additional discussion, see the ASCE/SEI 41-06 summary.

G.2 ASCE/SEI 41-06 Seismic Rehabilitation of Existing Buildings (with Supplement No. 1)

G.2.1 Scope of Application

ASCE/SEI 41-06, *Seismic Rehabilitation of Existing Buildings* (ASCE, 2007), addresses the seismic rehabilitation of existing buildings. It is the companion document to ASCE/SEI 31-03 *Seismic Evaluation of Existing Buildings*. As the names indicate, it is intended that ASCE/SEI 31-03 be used for evaluating existing buildings, and strengthening, if required, be designed using ASCE/SEI 41-06.

ASCE/SEI 31-03 has three levels of assessment, Tiers 1, 2, and 3, which use increasingly sophisticated methods of analysis. The Tier 3, or nonlinear analysis procedures, are not described in ASCE/SEI 31-03. Typically ASCE/SEI 41-06 is used as the reference document for such assessments.

ASCE/SEI 31-03 describes specific building types (e.g., S2 – Steel Braced Frame with Rigid Diaphragm) and describes different evaluation procedures according to

each type of building and deficiency via the Tier 1 checklists. ASCE/SEI 41-06 is a more general-purpose document; it is divided into chapters on requirements, analysis procedures, and various building components according to type and material (e.g., foundations, steel moment frame connections, etc.).

Although the ASCE/SEI 41-06 provisions are intended for use with existing buildings they have become an important reference document for performance-based design of both new and existing buildings.

G.2.2 Applicability of Analysis Procedures

Restrictions on use of Linear Procedures (Section 2.4.1)

ASCE/SEI 41-06 provides four types of analysis, two linear (LSP, LDP) and two nonlinear (NSP, NDP). The two linear procedures are not permitted for buildings with one or more significant irregularities and one or more component DCRs > 2 . The significant irregularities are:

- In plane discontinuity, such as offset in braced frame bay. (V4)
- Out-of-plane discontinuity, such as setback shear wall. (H4)
- Weak story irregularity, where average DCR in a story exceeds 125 percent of that in an adjacent story. (V5)
- Torsional strength irregularity, where DCR of one side exceeds 1.5 times that of other side. (H6)

Additional Restrictions on use of Linear Static Procedure (Section 2.4.1.2)

ASCE/SEI 41-06 further restricts the use of linear analysis by limiting where the LSP can be used. To use LSP, all of the following requirements must be satisfied:

- $T < 3.5T_s$.
- Story horizontal dimension must not be more than 1.4 times that of adjacent story (above or below). (no V3)
- Torsional stiffness, corner-to-average drift ratio must not exceed 150%. (no H1)
- Vertical stiffness, average story drift must not exceed 150% of that in adjacent level (above or below). (no V1)
- Must have orthogonal lateral system. (no H5)

Linear Dynamic Procedure

There are no other restrictions on the use of the linear dynamic procedure beyond the restrictions on the use of linear procedures in general, and the limitations on the use of the linear static procedure. That is, provided a building meets the requirements for linear analysis, it can be analyzed using the LDP.

The LDP is also used to supplement an NSP where higher modes are judged to be significant; see NSP.

Restrictions on use of Nonlinear Procedures (Section 2.4.2)

Nonlinear procedures are permitted where linear are not. Where using nonlinear procedures, material testing is required, which is not necessarily the case for linear procedures.

Restrictions on use of Nonlinear Static Procedure (Section 2.4.2.1)

Both of the following requirements must be satisfied to use the NSP alone:

- The strength ratio $R < R_{max}$.
- Higher mode effects must be judged not to be significant; both of the following must be satisfied:
 - If higher modes are significant, model response spectrum analysis must be performed with enough modes to achieve 90% mass participation. Second response spectrum analysis of first-mode-only-response must be performed.
 - Higher modes are significant if shear in any story of multimode analysis exceeds 130% of that from single-mode analysis.

If R exceeds R_{max} , an NDP analysis is required.

If higher modes are significant, then the NSP can still be used provided it is supplemented with an LDP. The m -factors for the LDP may be increased by a factor of 1.33. The building is required to meet the acceptance criteria for both analyses.

Table G-2 below summarizes engineering demand parameters that may be addressed by the application of the analysis procedures covered in ASCE/SEI 41-06. The table identifies system-, intermediate-, and component level engineering demand parameters according to performance level, period limitations, regularity, and other limitations.

Table G-2 Engineering Demand Parameters¹ That May be Addressed Using These Analysis Procedures

Perf. level ²	Period (height)	Regularity ³	Other limitations	Analysis Procedures							
				LSP	LDP	Plastic	NSP	NDP			
All	$T \leq 3.5T_s$	No H1, H4, H5, H6, V1, V3, V4, V5	No DCR > 2	S2 ⁶ , I1, C3, C4 ⁴	S2 ⁷ , I1, I2, C3, C4 ⁴	C2, C4 ⁵	S2, I1, C1, C2, C3, C4	S1, S2, I1, I2, C1, C2, C3, C4			
	$T > 3.5T_s$	No H4, H6, V4, V5	No DCR > 2		S2 ⁷ , I1, I2, C3, C4 ⁴	C2, C4 ⁵	S2, I1, C1, C2, C3, C4	S1, S2, I1, I2, C1, C2, C3, C4			
All	<i>Implied period limit</i>	Not limited	$R < R_{max}$ ⁷	Either	Suppl. S2 ⁷ , I1, I2, C3, C4 ⁴	C2, C4 ⁵	S2, I1, C1, C2, C3, C4	S1, S2, I1, I2, C1, C2, C3, C4			
			$V_{(i=n)} < 1.3V_{(i=1)}$ ⁸								
			$R < R_{max}$ ⁷						Or	C2, C4 ⁵	S1, S2, I1, I2, C1, C2, C3, C4
			$V_{(i=n)} > 1.3V_{(i=1)}$ ⁸								
		$R > R_{max}$ ⁷		C2, C4 ⁵	S1, S2, I1, I2, C1, C2, C3, C4						

¹Engineering Demand Parameters addressed explicitly (or implicitly)

System EDPs

S1: Identify global collapse

S2: Identify mechanism

Intermediate EDPs

I1: Quantify story drift

I2: Quantify floor acceleration

Component EDPs

C1: Identify local collapse

C2: Identify mechanism

C3: Quantify deformation

C4: Quantify force

²Performance levels addressed explicitly (or implicitly)

IO: Immediate Occupancy; LS: Life Safety; CP: Collapse Prevention with corresponding hazard level, if indicated

DE: Design Earthquake; MCE: Maximum Considered Earthquake or Seismicity

Low, Mod-Moderate, or High

³Structural irregularities

Horizontal

H1: Torsional stiffness

H2: Reentrant corner

H3: Diaphragm discontinuity

H4: Out-of-plane offset

H5: Non-orthogonal systems

H6: Torsional strength

Vertical

V1: Soft story

V2: Mass

V3: Setback

V4: In-plane offset

V5: Weak story

⁴Force-controlled component actions are permitted to be evaluated using the *J*-factor, as provided in Section 3.4.2.1.2.

⁵Where LSP is used, limit analysis can be used to determine component forces. For example Section 6.4.2.4.1 permits forces such as joint actions to be determined using the capacities of the connected components.

⁶The system mechanism can be evaluated to some degree by comparison of the relevant component DCRs.

⁷The strength ratio *R* must be less than the maximum permitted value, R_{max} , or the NDP is required.

⁸If higher modes are significant then either the pushover analysis must be supplemented using the LDP, or an NDP performed.

G.2.3 Other Modeling Direction Provided

Basic Modeling Analysis Assumptions (Sections 3.2.2.1 and 3.2.2.2)

- In general, a building must be modeled in three dimensions, but two-dimensional modeling is permitted as follows:
 - Diaphragms are rigid and the horizontal displacement modifier does not exceed 1.5
 - LSP/LDP: forces and displacement amplified by a displacement modifier.
 - NSP: target displacement amplified by a displacement modifier.
 - NDP: ground motion amplified by a displacement modifier.
 - Or, diaphragms are flexible
- If 2D model used, 3D dimensional nature of components and elements must be considered when calculating stiffness and strength properties.
- For nonlinear procedures, a connection must be modeled if it is weaker or less ductile than the connected components, or if its flexibility results in a change to forces or deformations of more than 10%.
- Torsion includes 5% accidental mass eccentricity for rigid diaphragm structures, unless it is less than 25% of inherent torsion, or results in less than a 10 percent increase in response quantities at all levels.
- Torsional demands include an A_x amplifier for ratios above 1.2.

Primary and Secondary Components (Section 3.2.2.3)

- Primary components must be evaluated for earthquake-induced forces and deformations.
- Secondary components must be evaluated for earthquake-induced deformations.
- Linear models include stiffness and resistance of primary components only; if secondary component lateral stiffness exceeds 25%, some secondary components must be classified as primary components.
- Nonlinear procedures include resistance and stiffness of all components as well as strength and stiffness degradation
 - Nonstructural components must be classified as structural components if lateral stiffness exceeds 10% of total lateral stiffness of story.

P-Delta Effects (Section 3.2.5)

- For nonlinear procedures, static P-Delta effects must be incorporated in the analysis by including the nonlinear force-deformation relationship of all components subjected to axial forces.

Concurrent Seismic Effects (Section 3.2.7.1)

- For linear analysis, use 100% of forces and deformations in the main direction under consideration, and 30% in the perpendicular direction.
- For nonlinear analysis, use 100% of forces and deformations in the main direction under consideration, and 30% of the forces only in the perpendicular direction.

Structural Pounding (Section 2.6.10)

- For the LS and CP performance levels the required clearance need not be provided if diaphragms are at the same elevations and building heights differ by less than 50% of the height of the shorter building.

Vertical Seismic Effects (Section 2.6.11 & 3.2.7.2)

- Vertical effects must be considered for cantilevers, prestressed components, and where gravity load demands exceed 80% of nominal capacity. Vertical and horizontal seismic effects need not be combined.

Overturning (Section 3.2.10)

- Dead load alone may be used to resist reduced overturning forces, but the unreduced forces must be used for performance levels above life-safety.

G.2.4 Additional Analysis Requirements

For linear procedures diaphragm forces are developed in a manner similar to that required by new building codes. Diaphragm nonlinearity is addressed more explicitly by reference to the appropriate material chapters for permissible m -factors. The diaphragm design procedure for the NSP references the same provisions as for the LSP and LDP. Diaphragms may be designed for the actual forces from the analysis in the NDP.

ASCE/SEI 41-06 includes procedures for the evaluation of nonstructural components in Chapter 11. Different component types require evaluation for different combinations of performance level and seismicity level. The evaluation consists of reference to prescriptive codes or standards, or a force and/or displacement analysis procedure that is similar in approach to that used in new building codes (equation for F_p , etc.)

Specific guidance and acceptance criteria are provided for evaluation and rehabilitation of different nonstructural components, (such as glazing clearances, veneer, partitions, and parapets). In some cases reference is made to structural performance measures that may govern the evaluation (such as building drift for glazing or veneer).

ASCE/SEI 41-06 also includes a chapter on seismic isolation and energy dissipation systems. These provisions are based on new building code requirements, which have

been in steady development since the 1980s. Additional modeling guidance is provided for various device types and the provisions have been integrated to some degree with the Chapter 3 analysis procedures. Except for the NDP, the assessment uses an equivalent stiffness and damping approach that is conceptually different from the Chapter 3 provisions.

G.2.5 Ground Motion Characterization

Ground motion characterization in ASCE/SEI 41-06 is by definition of the BSE-1 and BSE-2 site response spectra. Damping is assumed to be 5% of critical except for bare (unclad) structures (2%), certain types of wood-frame structures (10%), and where other values are required for seismic isolation or energy dissipation system design.

Procedures are included to develop spectra for other hazard levels, and for generating damped and vertical spectra should these be required. If a site-specific spectrum is developed it must not fall below 70% of the corresponding ASCE/SEI 41-06 defined response spectrum.

If response history analysis is to be performed, either linear (LDP) or nonlinear (NDP), then at least three ground motion data sets must be developed. The selection and scaling provisions are similar to those used in new codes and elsewhere, with minor variations. The average SRSS of the spectral pairs must exceed 1.3 times the target spectrum over the period range $0.2T$ to $1.5T$. If three pairs are used then design is for the maximum response; if seven or more are used, design can be for the average response.

G.2.6 Discussion

The linear analysis provisions are quite restrictive. Component DCRs > 2 are likely to occur in typical buildings being evaluated. In addition, relatively few buildings will meet all the regularity provisions, so it is probable that these requirements are being ignored in practice. In addition, a new building could be designed using the linear analysis provisions of the current building code, using linear analysis and (aside from the benchmark building option), it would not meet the requirements for evaluation by linear analysis by a significant margin.

The provisions on restriction for the NSP appear to have been written with moment frame structures in mind (e.g., the LDP is triggered due to the height and number of stories). However, the LDP could also be triggered in relatively short, stiff structures due to conditions such as podium/setbacks, large plan areas, or where multiple diaphragms are present. The 130% threshold is not very high and could easily be exceeded in these conditions.

Where NSP is performed, use of the degrading or descending part of the pushover curve is likely. This implies potentially large element DCRs for some structural

components in a corresponding linear analysis (such as spandrels in a pier/spandrel system). The supplemental LDP could be triggered due to one of the aforementioned conditions, with little chance of meeting the requirements; the 1.33 multiplier on m -factors relatively small compared to the gain in effective “ m -factor” is achieved by going to NSP in the first place. For example, reinforced concrete spandrel beams could have secondary life-safety plastic rotation limits of 2% to 6%. In a linear analysis, the yield rotation could easily be less than 0.1-0.2%, implying effective m -factors of 20 to 60 at the target displacement. It would be difficult to get the LDP to work in these circumstances.

The NSP also permits use of the secondary limits for primary components. Since linear analysis models may include only primary components, it appears that use of 1.33 times secondary m -factors would not be permitted for the supplemental LDP check. Even if it were permitted, that would not offset the problem noted above.

One challenging provision is the use of R_{max} to trigger the jump to the NDP. Jumping to the NDP presents a substantial increase in effort relative to other techniques; ground motions must be obtained and the requirement for peer review is added.

Buildings are frequently evaluated using ASCE/SEI 41-06 where the results of ASCE/SEI 31-03 Tier 1 or Tier 2 evaluation are not favorable, or where the scope of strengthening is believed to be excessive. In the former case, the evaluating engineer will first check the existing building against 75% of the ground motion using, for example, an NSP analysis to determine whether strengthening is required to meet the target performance objective. Unfortunately, even a modest amount of strengthening means that the structure must be designed using 100% of the ground motion, presenting another substantial step function. It is also not clear whether R_{max} should be evaluated at the 75% or 100% level.

G.3 ATC-40 Seismic Evaluation and Retrofit of Concrete Buildings

G.3.1 Scope of Application

The ATC-40, *Seismic Evaluation and Retrofit of Concrete Buildings* (ATC, 1996), was intended to introduce a new technical procedure for nonlinear static analysis based on equivalent linearization known as the Capacity Spectrum Method. In addition, the State of California in funding the project wanted to illustrate the broader effort to evaluate and retrofit concrete buildings. Thus the document serves many purposes beyond the technical.

One chapter of the document is devoted to a summary of principles related to structural dynamics. Although the details of nonlinear seismic analysis are not included, the basic principles outlined in this chapter provide very helpful information to engineers who are less familiar with structural dynamics. The document foresees the possibility of multi-mode pushover analysis prior to its more

detailed development in later years; no guidance is provided on when and how this procedure would be implemented.

ATC-40 contains extensive guidance on inelastic modeling of component and elements of concrete buildings. This could apply to any type of nonlinear finite element analysis using response histories. It recommends that all concrete buildings include foundation modeling, and detailed information on modeling techniques (similar to that in ASCE/SEI 41-06) is included.

Of particular interest and importance to this report are the practical example building analyses included in the second volume of the document. Each of these buildings was analyzed using the capacity spectrum method. The results are compared to nonlinear response history analysis results. Although the results reflect a large degree of variability, in general, the nonlinear static procedure seems to predict overall displacements reasonably well. Story shear forces predicted by NSPs tend to be very low compared to NRHA. Overturning moments are also low but to a lesser degree indicating, perhaps, the effects of higher mode participation.

G.3.2 Applicability of Analysis Procedures

With respect to the limitations of NSPs, ATC-40 recommends that buildings with fundamental periods greater than one second be subject to nonlinear response history analysis. On the global level, the use of nonlinear static procedures is restricted to those structures that degrade no more than 20% in maximum strength. Otherwise nonlinear response history analysis including degradation effects is required.

However, the document notes that nonlinear response history analysis was not practical generally in 1997. That was particularly true concerning degradation effects. The guidelines also note that linear procedures are acceptable for simple structures.

Table G-3 below summarizes engineering demand parameters that may be addressed by the application of the analysis procedures covered in ATC-40. The table identifies system-, intermediate-, and component level engineering demand parameters according to performance level, period limitations, regularity, and other limitations.

Table G-3 Engineering Demand Parameters¹ That May be Addressed Using These Analysis Procedures

Perf. level ²	Period (height) ⁵	Regularity ³	Other limitations	Analysis Procedures				
				LSP	LDP	Plastic ⁴	NSP ⁷	NDP
IO		3D required in some cases. ⁸		Recommended for	Not		S2, I1, C1,	Required where capacity curve shows more than 20% degradation in strength
LS				"simple" structures	addressed		C2, C3, C4	
CP ⁶								

¹Engineering Demand Parameters addressed explicitly (or implicitly)

System EDPs

S1: Identify global collapse

S2: Identify mechanism

Intermediate EDPs

I1: Quantify story drift

I2: Quantify floor acceleration

Component EDPs

C1: Identify local collapse

C2: Identify mechanism

C3: Quantify deformation

C4: Quantify force

²Performance levels addressed explicitly (or implicitly)

IO: Immediate Occupancy; LS: Life Safety; CP: Collapse Prevention with corresponding hazard level, if indicated

DE: Design Earthquake; MCE: Maximum Considered Earthquake

³Structural irregularities

Horizontal

H1: Torsional stiffness

H2: Reentrant corner

H3: Diaphragm discontinuity

H4: Out-of-plane offset

H5: Non-orthogonal systems

H6: Torsional strength

Vertical

V1: Soft story

V2: Mass

V3: Setback

V4: In-plane offset

V5: Weak story

⁴Not addressed.

⁵There is a "soft" limitation of $T_1 \leq 1.0$ for NSPs.

⁶Called Structural Stability (SS) in ATC-40

⁷ Global strength degradation limited to 20% of peak strength

⁸ If the maximum displacement exceeds 120 percent of the displacement at the center of mass in a linear analysis, then three dimensional NSP analysis is required.

Selection of analysis procedure

The document notes that some buildings may be too complex to rely on the nonlinear static procedures. These cases may require time history analyses of the nonlinear behavior of structures during example earthquakes. The kinds of buildings that may require these specialized analyses are those that are highly irregular or complicated. Other examples of building systems that may necessitate more sophisticated analysis are energy dissipation or base isolation systems.

At the other end of the spectrum are simpler buildings for which use of nonlinear static analysis is not necessary. For those cases, use of simpler, linear elastic analysis procedures may be sufficient.

Although there are no hard and fast rules to identify them, buildings that possess one or more of the following characteristics could be considered candidates:

- Small size
- Low-rise (one or two stories)
- Uncomplicated (regular) structural systems
- Highly redundant lateral force resisting system
- Low occupancy

Another situation where use of simplified procedures is appropriate is where existing structural systems are so inadequate that complete new systems must be installed in any event.

G.3.3 Other Modeling Direction Provided

Multimode Considerations

The document notes that pushover analyses using the fundamental mode shape generally are valid for fundamental periods of vibration up to about one second. For structures with long fundamental periods, higher mode effects may be more critical on some components of the structure than the effects of the fundamental mode.

Multi-mode pushover analyses are described as follows: Force distributions are applied to deform the building into the second and the third translational mode shapes. Yield patterns will be substantially different from those obtained for the first mode shape. The V versus Δ_{roof} values for the higher modes are converted to S_a versus S_d curves using the higher mode participation factors and effective modal weights. These curves are plotted on the ADRS format and the demands on each of the modes can be determined. Each component of the structure is then evaluated for the different modes.

Torsional Considerations

For buildings that are non-symmetric about a vertical plane parallel to the design lateral forces, the effects of torsion should be included in the development of the pushover curve. If a three dimensional model is used to capture the torsional effects, then the static lateral forces should be applied at the center of mass of each floor, and the displacements plotted on the capacity curve should be at the center of mass of the roof. Two dimensional modeling and analysis may be used if the torsional effects are sufficiently small such that the maximum displacement at any point on the floor is less than 120 percent of the displacement at the corresponding center of mass. If the maximum displacement exceeds 120 percent of the displacement at the center of mass, then three dimensional analysis is required. For two dimensional analysis, an acceptable approach to considering the effects of torsion when developing the capacity curve is to identify the ratio of maximum displacements to the center of mass displacement at each floor level using linear static analysis or linear dynamic analysis of a three dimensional model, and then to increase the displacement at the center of mass of the roof, at each point on the capacity curve, by the maximum of these ratios.

G.3.4 Additional Analysis Requirements

Diaphragm acceptability should consider the strength of the diaphragm and its connections with adjacent elements. The assessment should consider at least the following:

- Shear strength of the slab and its connections with walls or other elements and components
- Adequacy of chords along the boundaries of the diaphragm, at reentrant corners, and at other irregularities in plan or elevation
- Strength of drag struts and collectors near concentrated loads and openings
- Tension due to out-of-plane anchorage of walls, wall panels, and other elements and components.

In general, inelastic response should not be permitted in diaphragms, except where it is demonstrated by analysis or tests that inelastic action can be tolerated considering the selected performance levels.

G.3.5 Ground Motion Characterization

Ground motion provisions generally are based on the ICBO 1996 code provisions.

The Design Earthquake and Maximum Earthquake hazard levels are based on UBC (and CBC) definitions of ground shaking. The document acknowledges other definitions of seismic criteria—namely, those developed for the 1997 *NEHRP Provisions* (BSSC 1996) for design of new buildings and those adopted in the FEMA

273 Guidelines (the predecessor of ASCE/SEI 41-06) for seismic rehabilitation of existing buildings.

Serviceability Earthquake

The Serviceability Earthquake (SE) is defined probabilistically as the level of ground shaking that has a 50 percent chance of being exceeded in a 50-year period. This level of earthquake ground shaking is typically about 0.5 times the level of ground shaking of the Design Earthquake.

Design Earthquake

The Design Earthquake (DE) is defined probabilistically as the level of ground shaking that has a 10 percent chance of being exceeded in a 50-year period.

Maximum Earthquake

The Maximum Earthquake (ME) is defined deterministically as the maximum level of earthquake ground shaking which may ever be expected at the building site within the known geologic framework.

- The criteria for each hazard level include the following:
- Site geology and soil characteristics
- Site seismicity characteristics
- Site response spectra

Site geology and soil characteristics and site seismicity characteristics are based directly on the requirements proposed by the SEAOC Seismology Committee (ICBO 1996) for the 1997 UBC. In all cases, elastic site response spectra are described by a standard (two domain) shape defined by the coefficients C_a and C_v . Elastic response spectra are described by a standard shape to simplify the application of these spectra to nonlinear static analysis procedures. The NSP analysis procedure begins with the 5% damped spectrum. The capacity spectrum method then modifies the spectrum to increase damping based on ductility demand to find a Performance Point (Target Displacement) that represents the displacement of the system for the selected hazard level.

Where required for analysis, not fewer than three pairs of horizontal time history components should be selected from earthquake ground motion records. A set of seven or more pairs of time history components is recommended and would be necessary for the design to be based on the average (rather than the maximum) value of the response quantity of interest. Recorded earthquakes should be selected to have a magnitude, source characteristics, and distance from source to site that is the same as (or consistent with) the magnitude, source characteristics and source-to-site distance of the event that dominates the ground shaking hazard at the building site. Recorded earthquakes should also be selected to have site conditions that are the

same as (or consistent with) the site conditions of the building. Where three appropriate recorded ground motion time history pairs are not available, appropriate simulated ground motion time history pairs may be used to make up the total number required. The intent of these requirements is that each pair of time history components have an appropriate duration, contain near-source pulses (for sites within 10 km of active faults) and include other time domain characteristics that represent the ground shaking expected at the building site. Each pair of horizontal ground motion components should be scaled in the time domain such that the average value of the spectra of all scaled time history components matches the site response spectrum over the period range of interest. The period range of interest includes, but is not limited to, periods at or near the effective period of the building associated with the performance point determined by the nonlinear static analysis procedure (Chapter 8). If higher mode effects are being considered, then the period range of interest should also include periods at or near each higher-mode period of interest. A ground motion expert should assist the structural engineer in the selection and scaling of appropriate time histories.

The document also provides earthquake ground motion records. Two sets of 10 earthquake records each are identified as suitable candidates for time history analysis. One set contains records at sites at least 10 km from fault rupture and the other set contains records at sites near fault rupture (e.g., sites within about 5 km of fault rupture).

The duration of ground shaking should be considered when selecting time histories and when determining an appropriate level of effective damping for the structural system. Two distinctly different earthquake scenarios should be considered when evaluating duration effects on potential structural degradation and reduction in damping capacity. The first earthquake scenario is important for sites near a seismic source (fault). The second earthquake scenario is important for sites far from fault rupture (far from the causative source). Sites located in seismic zone 4 (with a near-source factor of $N < 1.2$) should be assumed to have long-period ground shaking unless either the seismic source that governs ground shaking hazard at the site has a maximum moment magnitude of $M \leq 6.5$ and the site soil profile is rock or stiff soil; an important potential contributor to duration could be long-period resonance at soil sites due to basin effects. Long duration ground shaking should be assumed for soft soil sites unless a geotechnical study recommends otherwise.

G.3.6 Discussion

This document has been superseded by *FEMA 440* with respect to the details of nonlinear static analysis using the capacity spectrum method of equivalent linearization. Much valuable guidance, however, remains.

G.4 FEMA 440 Improvement of Nonlinear Static Seismic Analysis Procedures

G.4.1 Scope of Application

The purpose of this document, FEMA 440, *Improvement of Nonlinear Static Seismic Analysis Procedures* (FEMA, 2005), is to evaluate and improve both the Coefficient Method and the Capacity Spectrum Method of nonlinear static analysis. There is a detailed summary of the benefits and limitations of analysis procedures. It recognizes the possibility of using a SDOF oscillator in a simplified nonlinear dynamic analysis. This is considered useful to investigate the effects of dispersion attributable to ground motion variability. It also suggests the use of sticks and fishbones to develop simple MDOF models.

The document introduces a limit on the minimum strength of a building model to avoid lateral dynamic instability. If this limit is not met then NRHA including the effects of degradation is required. Detailed guidance on NRHA is not included.

As a part of the investigation, the various types of load vectors used for NSPs were evaluated by comparing the results of NSP analyses to NRHAs for a number of different building models. It was found that NSPs do a reasonable job of estimating global displacement demand using a vector proportional to the first mode shape. However, forces and component actions (such as drifts) are poorly estimated when compared with NRHA results. A key observation was that any single time history tended to produce better results than any of the load vectors assumed for NSP analysis. Based on this the document envisions a step-by-step hybrid procedure.

The document also report that the results of the MDOF studies indicate that the FEMA 356 requirement for supplementary linear dynamic analysis if higher mode effects are significant is not useful. Higher modes are considered significant if the SRSS of story shears from modes that incorporate at least 90% of the mass exceeds 130% of story shear from a first-mode response-spectrum analysis. All example buildings met this requirement and yet had significant higher mode effect as demonstrated by NRHA.

The results also indicate the multi-mode pushover analysis does somewhat better in predicting response than an SDOF pushover. However, the results were inconsistent and the effort required for MPA was considered by many to be worse than NRHA.

G.4.2 Applicability of Analysis Procedures

Various combinations of structural model types and characterizations of seismic ground motion define a number of options for inelastic analysis. The selection of one option over another depends on the purpose of the analysis, the anticipated performance objectives, the acceptable level of uncertainty, the availability of

resources, and the sufficiency of data. In some cases, applicable codes and standards may dictate the analysis procedure.

The primary decision is whether to choose inelastic procedures over more *conventional linear elastic analysis*. In general, linear procedures are applicable where the structure is expected to remain nearly elastic for the level of ground motion of interest or where the design results in nearly uniform distribution of nonlinear response throughout the structure. In these cases, the level of uncertainty associated with linear procedures is relatively low. As the performance objective of the structure implies greater inelastic demands, the uncertainty with linear procedures increases to a point that requires a high level of conservatism in demand assumptions and/or acceptability criteria to avoid unintended performance. Inelastic procedures facilitate a better understanding of actual performance. This can lead to a design that focuses upon the critical aspects of the building, leading to more reliable and efficient solutions.

Nonlinear dynamic analysis using the combination of ground motion records with a detailed structural model theoretically is capable of producing results with relatively low uncertainty. In nonlinear dynamic analyses, the detailed structural model subjected to a ground-motion record produces estimates of component deformations for each degree of freedom in the model. Intermediate- or system-level demands are computed directly from the basic component actions. There is still uncertainty with the detailed models, associated primarily with the lack of data on actual component behavior, particularly at high ductilities. In addition, the variability of ground motion results in significant dispersion in engineering demand parameters; dispersion increases with higher shaking intensity and with greater inelasticity.

Simplified nonlinear dynamic analysis with equivalent multi-degree-of-freedom models also uses ground motion records to characterize seismic demand. However, since component-level response is not modeled directly, these techniques produce engineering demand parameters at the intermediate- and system-levels only. For example, a “stick” model produces story displacements and drifts. The engineer may be able to estimate corresponding component actions using the assumptions that were originally the basis of the simplified model. Thus the uncertainty associated with the component actions in the simplified model is greater than that associated with the detailed model.

Simplified nonlinear dynamic analysis with equivalent single-degree-of-freedom (SDOF) models is a further simplification using ground motion records to characterize seismic shaking. The result of the analysis is an estimate of global displacement demand. It is important to recognize that the resulting lower-level engineering demands (such as story drifts and component actions) are calculated from the global displacement using the force-deformation relationship for the oscillator. In contrast to the use of the more detailed model, they are related directly

to the assumptions, and associated uncertainties, made to convert the detailed structural model to an equivalent SDOF model in the first place. This adds further to the overall uncertainty associated with the simplified nonlinear dynamic analysis. If the SDOF model is subjected to multiple time histories a statistical representation of response can be generated.

Nonlinear static procedures (NSPs) convert MDOF models to equivalent SDOF structural models and represent seismic ground motion with response spectra as opposed to ground-motion records. They produce estimates of the maximum global displacement demand. Story drifts and component actions are related subsequently to the global demand parameter by the pushover or capacity curve that was used to generate the equivalent SDOF model. This is similar to simplified nonlinear dynamic analyses using SDOF models. In contrast to the use of simplified dynamic analyses using multiple ground motion records, the use of nonlinear static procedures implies greater uncertainty due to the empirical procedures used to estimate the maximum displacement. This is true even if spectra representative of the multiple ground motion records are used in the nonlinear static analysis.

The relative uncertainty associated with each of the analysis options varies. The actual uncertainty inherent in any specific analysis depends on a number of considerations. Nonlinear dynamic analyses can be less uncertain than other techniques if the nonlinear inelastic properties of the components in the detailed structural model are accurate and reliable. If the component properties are poorly characterized, however, the results might not be an improvement over other alternatives. Some analysis options are better than others, depending on the parameter of interest. For example, with simplified dynamic analyses, a SDOF oscillator can be subjected to a relatively large number of ground motion records to provide a good representation of the uncertainty associated with global displacement demand due to the variability of the ground motion. On the other hand, if the engineer is comfortable with the estimate of maximum global displacement from a nonlinear static procedure, a multi-mode pushover analysis might provide improved estimates of story drift that may not be available from the simplified SDOF dynamic analyses.

Limitation of Simplified Procedures

Nonlinear static procedures appear to be reliable for the design and evaluation of low-rise buildings. However, MDOF effects associated with the presence of significant higher-mode response in relatively tall frame buildings, can cause story drift, story shear, overturning moment, and other response quantities to deviate significantly from estimates made on the basis of single-mode pushover analyses. Multimode pushover procedures appear capable of more reliable estimates than do single-mode procedures; however, they cannot be deemed completely reliable based on currently available data. The dividing line between buildings for which reliable results can be obtained using NSPs and those for which the results cannot be relied

upon is nebulous. The sufficiency of nonlinear static procedures and the need for nonlinear dynamic analysis depend on a number of related considerations.

- *Response quantity of interest.* As illustrated in the examples, current simplified procedures are often adequate for estimating displacements. They seem to produce reasonable estimates of story drift for low-rise frame buildings and wall buildings. However, for virtually all cases, the simplified procedures produce unreliable estimates of story shear and overturning moments. If required for evaluation or design, accurate estimates of these parameters require more detailed analyses.
- *Degree of inelasticity.* The example buildings indicate that the importance of MDOF effects increases with the amount of inelasticity in the structure. NSPs may be adequate for situations in which the performance goals for a structure are such that only slight or moderate levels of inelasticity are expected.
- *Periods of vibration of the fundamental and higher modes relative to the spectral demands at these periods.* Higher-mode contributions become more significant for structures with fundamental periods that fall in the constant-velocity portion of the response spectrum. It appears that accurate estimates of the distribution of story drift over the height of moment-resisting frames cannot be obtained with NSPs alone where the fundamental period of the structure exceeds approximately twice the characteristic site period, T_s . A significantly lower limit applies to the determination of story forces in both wall and frame structures, however.
- *Structural system type.* Shear walls and frames have different higher-mode periods relative to their fundamental mode periods. These systems have characteristically different percentages of mass participating in the first and higher modes and develop characteristically different types of mechanisms. As noted previously, NSPs do not predict story forces reliably, and more sophisticated analytical techniques may be required for systems sensitive to these parameters.
- *Post-elastic strength.* Both the studies on the response of SDOF oscillators (Chapter 3) and the SDOF examples (Appendix F) demonstrate that systems with a critical level of negative post-elastic strength degradation are prone to dynamic instability. This has been documented in other recent research as well. As discussed in Chapter 4, the critical post-elastic stiffness should be based on *P-delta* effects and other types of in-cycle degradation. Systems with strength values less than those specified in Chapter 4 require nonlinear response history analysis.
- *Inelastic mechanism.* Forces associated with response in other modes may influence the development of an inelastic mechanism, and thus, pushover analyses may not always identify the governing mechanism (Krawinkler and Seneviratna, 1998).

G.4.3 Other Modeling Direction Provided

Limitation on Strength for In-Cycle Strength Degradation Including P-delta Effects

FEMA 440 sets forth a limit on minimum strength (maximum value of R) required to avoid dynamic instability. It recommends that the R_{max} limit be applied to all NSPs. This recommended limit was adopted in ASCE/SEI 41-06.

FEMA 440 indicates that if this limitation is not satisfied, then a nonlinear dynamic analysis using representative ground motion records for the site should be implemented to investigate the potential for dynamic instability, and that the structural model must appropriately model the strength degradation characteristics of the structure and its components.

Multiple-Degree-of-Freedom Effects

FEMA 440 describes a severe limitation of NSPs with respect to MDOF effects. Engineering evaluation of performance and design of structures is based primarily on component forces and deformations, which are compared to some type of acceptance criteria. NSPs attempt to relate the intensity of component deformations and forces directly to a global displacement parameter (such as roof displacement or first-mode spectral displacement), but the SDOF model can approximate MDOF response only very crudely. FEMA 440 confirms earlier work that questions the adequacy of simplified procedures to address MDOF effects. Some of the practical observations are as follows:

- NSPs generally provide reliable estimates of maximum floor and roof displacements and, in some cases, may provide reasonable estimates of the largest story drifts that may occur at any location over the height.
- NSPs do not accurately predict maximum drifts at each story, particularly within tall, flexible structures.
- NSPs are very poor predictors of story forces, including shear forces and overturning moments in taller structures.
- Use of multiple load vectors does not produce more reliable results
- In some cases, multi-mode pushover analysis may improve estimates of story drifts, but such improvements are inconsistent, require a disproportionate increase in effort, and are not accompanied by improved estimates of component-level demands.

Incremental Response-Spectrum Analysis

FEMA 440 describes a successful application of a multi-modal incremental response-spectrum analysis method, in which contributions of multiple modes are considered in an incremental pushover analysis. The incremental nature of the analysis allows the effects of softening due to inelasticity in one mode to be reflected in the

properties of the other modes. An example was used to illustrate application of the method to a generic frame model of the nine-story SAC building (neglecting gravity loads and *P-delta* effects), comparing estimates based on four modes with those determined by nonlinear dynamic analysis. Very good agreement is shown for floor displacement, story drift, story shear, floor overturning moment, and beam plastic hinge rotation.

Nonlinear Dynamic Procedure Using Scaled Response Histories

A limited study, described in FEMA 440, resulted in two suggestions: 1) Use of a small subset of properly selected and scaled ground motion records (as few as one) could produce more meaningful results than NSP. 2) Scaling ground motions to achieve a consistent roof displacement may reduce the uncertainty of predictions.

Modification for SSI Effects

FEMA 440 adds simplified methods for including the kinematic effects of soil-structure interaction in nonlinear static analysis procedures. The approach for kinematic SSI is to reduce the free field ground motion (FFM) to account for base slab averaging and for embedment effects resulting in a representation of the foundation input motion (FIM). Both reductions are dependent upon geometric properties of the structure and vary with period. The reductions are greatest for low periods and tend to diminish as the period approach about 0.5 sec. The adjustment is essentially equivalent to adding a high-T pass filter to FFM. FEMA 440 includes a procedure to account for the additional inertial effect of SSI due to foundation (radiation) damping. The kinematic SSI procedures were later adopted by ASCE/SEI 41-06.

G.5 FEMA P-440A Effects of Strength and Stiffness Degradation on Seismic Response

G.5.1 Scope of Application

The FEMA P-440A report, *Effects of Strength and Stiffness Degradation on Seismic Response* (FEMA, 2009a), is a follow-up to FEMA 440 to further investigate the effects of strength and stiffness degradation on response. The work comprised extensive analyses of SDOF systems using Incremental Dynamic Analysis procedures to predict lateral dynamic instability. The work introduced the concept of a force-displacement capacity boundary in place of conventional load-dependent backbone curves for both component and global hysteretic behavior, which has important implications for both NSPs and NRHAs by eliminating a source of over-prediction of response.

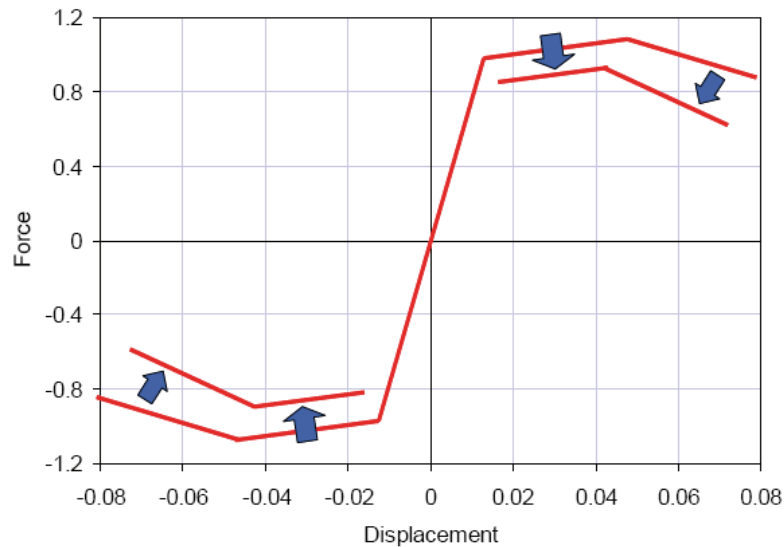


Figure G-1 Degradation of the force-displacement capacity boundary.

The document also proposes a revised equation for the minimum strength of a system determined from an NSP to avoid dynamic instability without having to perform a NRHA. The proposed new equation and the results of synthetic IDA using the SPO2IDA program were compared to the actual IDA results of MDOF models of several buildings. The results indicate that lateral dynamic instability of MDOF systems may be predicted fairly accurately by the simplified procedures. This may be due to the fact that the instability is due primarily to actual total displacement as opposed to component actions. The document does not address any other system-, intermediate-, or component-level EDPs.

G.5.2 Applicability of Analysis Procedures

Improved equation for evaluating lateral dynamic instability

An improved estimate for the median strength ratio (R_{di}) at which lateral dynamic instability occurs was developed based on nonlinear regression calibrated to the median response of the spring systems included in the investigation. The prediction of critical strength ratio depends on the shape of the capacity boundary and on the presence or absence of stiffness degradation.

Preliminary studies of six multi-story buildings ranging in height from 4 to 20 stories indicate that many of the findings for SDOF systems, such as the relationship between force-displacement capacity boundary and IDA curves and the equation for R_{di} may apply to MDOF systems.

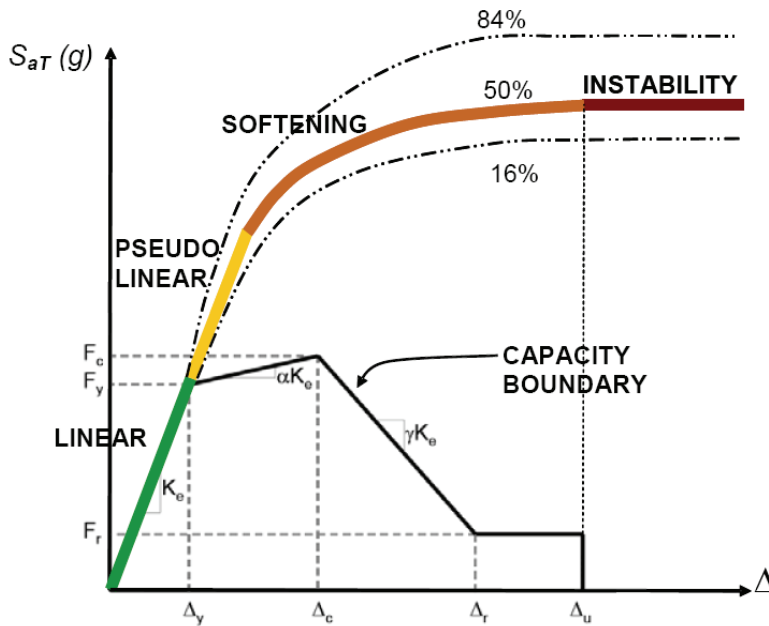


Figure G-2 Relationship between IDA curves and the features of a typical force-displacement capacity boundary.

G.6 FEMA 351 Recommended Seismic Evaluation and Upgrade Criteria and FEMA 352 Recommended Post-Earthquake Evaluation and Repair Criteria for Welded Steel Moment-Frame Buildings

G.6.1 Scope of Application

The documents, FEMA 351 Report, *Recommended Seismic Evaluation and Upgrade Criteria* (FEMA, 2000a) and FEMA 352 Report, *Recommended Post-Earthquake Evaluation and Repair Criteria for Welded Steel Moment-Frame Buildings* (FEMA, 2000b), are two of the SAC Joint Venture products developed to address steel moment frame buildings. They present a simplified analysis procedure that was apparently developed using NRHAs of prototype buildings that did not have any of the irregularities listed in FEMA 273. The procedure applies factors to demands and capacities to attempt to adjust for uncertainty and reliability. The engineer can choose analysis procedures based upon performance goal, fundamental period, irregularities, and relative beam and column strengths in accordance with a table in the document. Appendix A provides an alternative for irregular buildings that is based on NRHA.

G.6.2 Applicability of Analysis Procedures

Table G-4 below summarizes engineering demand parameters that may be addressed by the application of the analysis procedures covered in FEMA 351. The table identifies system-, intermediate-, and component level engineering demand parameters according to performance level, period limitations, regularity, and other limitations.

Table G-4 Engineering Demand Parameters¹ That May be Addressed Using These Analysis Procedures

Perf.	Period (height)	Regularity ³	Other limitations	Analysis Procedures				
				LSP	LDP	Plastic	NSP	NDP
IO	$T \leq 3.5T_s$	Not limited		I1	I1, C4 ⁴	C4 ⁵	I1, C4 ⁴	I1, C4 ⁴
	$T > 3.5T_s$	Not limited			I1, C4 ⁴			I1, C4 ⁴
CP	$T \leq 3.5T_s$	No H4, H6, V4, V5	Strong column	I1	I1, C4 ⁴	C4 ⁵	I1, C4 ⁴	I1, C4 ⁴
			Weak column				I1, C4 ⁴	I1, C4 ⁴
		H4, H6, V4, or V5					I1, C4 ⁴	I1, C4 ⁴
	$T > 3.5T_s$	No H4, H6, V4, V5	Strong column		I1, C4 ⁴			I1, C4 ⁴
		H4, H6, V4, or V5	Weak column					I1, C4 ⁴

¹Engineering Demand Parameters addressed explicitly (or implicitly)

System EDPs

- S1: Identify global collapse
- S2: Identify mechanism

Intermediate EDPs

- I1: Quantify story drift
- I2: Quantify floor acceleration

Component EDPs

- C1: Identify local collapse
- C2: Identify mechanism
- C3: Quantify deformation
- C4: Quantify force

²Performance levels addressed explicitly (or implicitly)

- IO: Immediate Occupancy; LS: Life Safety; CP: Collapse Prevention with corresponding hazard level, if indicated
- DE: Design Earthquake; MCE: Maximum Considered Earthquake

³Structural irregularities

Horizontal

- H1: Torsional stiffness
- H2: Reentrant corner
- H3: Diaphragm discontinuity
- H4: Out-of-plane offset
- H5: Non-orthogonal systems
- H6: Torsional strength

Vertical

- V1: Soft story
- V2: Mass
- V3: Setback
- V4: In-plane offset
- V5: Weak story

⁴Only column compression and column splice tension are addressed.

⁵Where LSP is used, column compression and column splice tension must be determined using plastic analysis.

G.6.3 Other Modeling Direction Provided

Two- or three-dimensional modeling

Two-dimensional models are often used to simulate three-dimensional response. Estimates of load distribution between the lateral load-resisting elements in the building are required, and the accuracy of the analysis depends upon the accuracy of distribution. Three-dimensional linearly elastic models may be used to estimate this

distribution; however, these models are unable to account for load redistribution occurring because of inelastic behavior. When many plastic hinges form nearly simultaneously, creating local frame mechanisms, the effects of torsional contributions may not be represented accurately. If a structure has significant torsional irregularity, three-dimensional models should be used.

The NSP is also limited with regard to evaluation of simultaneous response to ground shaking in different directions. Little research has been performed on appropriate methods of accounting for multi-directional response using this technique. Therefore, these criteria have adapted standard approaches used in linear analysis for this purpose.

Independent analysis along each principal axis of the three-dimensional mathematical model is permitted unless multidirectional evaluation is required by Section 3.2.7 in FEMA 273. Mathematical models describing the framing along each axis (axis 1 and axis 2) of the building should be developed for two-dimensional analysis. The effects of horizontal torsion should be considered as required by Section 3.2.2.2 of FEMA 273.

Although two-dimensional models may provide adequate response information for regular, symmetric structures and structures with flexible diaphragms, three-dimensional mathematical models should be used for analysis and design of buildings with plan irregularity as defined in FEMA 302. Two-dimensional modeling, analysis, and design of buildings with stiff or rigid diaphragms are acceptable, if torsional effects are sufficiently small to be ignored or are captured indirectly.

Multidirectional excitation effects may be accounted for by combining 100% of the response due to loading in direction A with 30% of the response due to loading in the direction B; and by combining 30% of the response in direction A with 100% of the response in direction B, where A and B are orthogonal directions of response for the building.

The effects of actual horizontal torsion must be considered. Accidental torsion should not be considered. Accidental torsion is an artificial device used by the building codes to account for actual torsion that can occur, but is not apparent in an evaluation of the center of rigidity and center of mass in an elastic stiffness evaluation. Inelastic torsion can develop during nonlinear response of the structure if yielding develops in an unsymmetrical manner in the structure. FEMA 351 indirectly accounts for the uncertainty related to these torsional effects in the calculation of demand and resistance factors.

G.6.4 Additional Analysis Requirements

Nonstructural

Although the performance of nonstructural components of buildings are critically important to the way in which buildings are used following an earthquake, treatment of this topic is beyond the scope of FEMA 351 and FEMA 352. FEMA 273 provides a more complete set of recommendations with regard to evaluating the performance of nonstructural components.

Global displacement demand

The document requires the continuation of the pushover analysis to displacements that are 150% of the target displacement to allow an understanding of the probable behavior of the building under somewhat larger loading than anticipated. If the pushover analysis should become unstable prior to reaching 150% of the target displacement, this does not indicate that a design is unacceptable, but does provide an indication of how much reserve remains in the structure at the design ground motion.

Frame geometry and panel zone modeling

It is permissible for the model to assume centerline-to-centerline dimensions for the purpose of calculating stiffness of beams and columns. Alternatively, more realistic assumptions that account for the flexibility of panel zones may be used. Regardless, calculation of moments and shears should be performed at the face of the column.

Diaphragms

Floor and roof diaphragms must be evaluated using the procedure outlined in FEMA 273 Section 3.3.1.3D. The lateral seismic load on each flexible diaphragm must be distributed along the span of that diaphragm, considering its displaced shape.

Foundation Modeling

In general, foundations may be modeled as unyielding. Assumptions with regard to the extent of fixity against rotation provided at the base of columns should realistically account for the relative rigidities of the frame and foundation system, including soil compliance effects, and the detailing of the column base connections. For purposes of determining building period and dynamic properties, soil-structure interaction may be modeled as permitted by the building code. Most steel moment frames can be adequately modeled by assuming that the foundation provides rigid support for vertical loads. However, the flexibility of foundation systems (and the attachment of columns to those systems) can significantly alter the flexural stiffness at the base of the frame. Where relevant, these factors should be considered in developing the analytical model.

P-delta Effects

P-delta effects, caused by gravity loads acting on the displaced configuration of the building, may be critical in the seismic performance of steel moment-frame buildings, which are usually flexible and may be subjected to large lateral displacements.

The structure should be investigated to ensure that lateral drifts induced by earthquake response do not result in a condition of instability under gravity loads. An approximate procedure is included in the document. For nonlinear procedures, second-order effects should be considered directly in the analysis. The geometric stiffness of all elements and components subjected to axial forces should be included in the mathematical model.

Uncertainty and reliability

Confidence level is determined through evaluation of a factored demand-to-capacity ratio. Demand and capacity are determined similarly to conventional strength design procedures. The approach is called the “Greek method” by some because Greek letters are used for the factors in the equations.

G.6.5 Ground Motion Characterization

The ground shaking hazard maps provided with the FEMA 302 *NEHRP Recommended Provisions* and the FEMA 273 *NEHRP Rehabilitation Guidelines* have been prepared based on hazard curves that have been developed by the United States Geological Survey for a grid-work of sites encompassing the United States and its territories. FEMA 302 defines two specific levels of hazard for consideration in design and specifies methods for developing response spectra for each of these levels. The two levels are:

- Maximum Considered Earthquake (MCE) ground shaking. This is the most severe level of ground shaking that is deemed appropriate for consideration in the design process for building structures, though not necessarily the most severe level of ground shaking that could ever be experienced at a site. In most regions, this ground shaking has a 2% probability of exceedance in 50 years, or roughly a 2,500 year mean recurrence interval. In regions of very high seismicity, near major active faults, the MCE ground shaking level is limited by a conservative, deterministic estimate of the ground shaking resulting from a maximum magnitude earthquake on the known active faults in the region. The probability that such deterministic ground shaking will be experienced at a site can vary considerably, depending on the activity rate of the individual fault
- Design Earthquake (DE) ground shaking. This is the ground shaking level upon which design lateral forces, used as the basis for analysis and design in FEMA 302, are based. It is defined as a spectrum that is 2/3 of the shaking intensity calculated for the MCE spectrum, at each period. The probability that DE ground

shaking will be experienced varies, depending on the regional (and in some cases, site) seismicity.

The procedures neglect uncertainties associated with the definition of the seismicity, that is, the intensity of ground shaking at various probabilities. Such uncertainties can be as large, and perhaps larger, than the uncertainties associated with structural performance estimation. Thus the confidence calculated in accordance with the procedures of this chapter is really a confidence associate with structural performance, given the presumed seismicity.

The earthquake shaking should be characterized by suites of ground motion acceleration.

G.6.6 Discussion

The performance evaluation procedures contained in FEMA 351 and FEMA 352 permit estimation of a level of confidence that a structure will be able to achieve a desired performance objective. In recognition of this, the documents adopt a reliability-based probabilistic approach to performance evaluation that acknowledges explicitly these inherent uncertainties. These uncertainties are expressed in terms of a confidence level. If an evaluation indicates a high level of confidence (for example, 90 or 95%) that a performance objective can be achieved, then this means it is very likely (but not guaranteed) that the building will be capable of meeting the desired performance. If lower confidence is calculated (for example, 50%) this is an indication that the building may not be capable of meeting the desired performance objective. If still lower confidence is calculated (for example, 30%) then this indicates the building likely will not be able to meet the desired performance objective.

G.7 ASCE/SEI 7-05 Minimum Design Loads for Buildings and Other Structures

G.7.1 Scope of Application

This standard, ASCE/SEI 7-05, *Minimum Design Loads for Buildings and Other Structures* (ASCE, 2006), covers all new building structures and certain nonbuilding structures except those exempted:

- Detached one and two family dwellings where $S_S < 0.4$ or where SDC is A, B, or C.
- Detached one and two family dwellings not included above but which comply with IRC
- Agricultural storage structures with only incidental human occupancy.
- Special structures not addressed in Chapter 15 covered by other seismic regulations such as bridges, hydraulic structures, and nuclear power plants.

As specified in Appendix 11B, existing structures where alterations have increased the seismic load to any element by more than 10% or reduced the capacity of any element by more than 10%. It is unclear how consistently Appendix 11B is enforced, how the appendix relates to Chapter 34 of the IBC, and how often local jurisdictions have adopted different regulations.

G.7.2 Applicability of Analysis Procedures

Selection of Analysis Procedure is covered in Section 12.6. Analysis Procedures include Equivalent Lateral Force Analysis, Modal Response Spectrum Analysis, and Seismic Response History Procedures. The applicability of Analysis Procedures is summarized in Table 12.6-1 which includes several variables:

- Seismic Design Category
- Occupancy Category
- Height measured both in stories (2 and 3 stories) and as implied by period ($\leq 3.5T_s$)
- Certain irregularities

Although Table 12.6-1 is obtuse, it can be deduced that:

- Equivalent Lateral Force Analysis can be used
 - for all structures assigned to SDC B and C,
 - for all light frame construction with SDC D, E, F, and
 - for all structures with $T < 3.5 T_s$ except those with horizontal torsional irregularity type 1a or 1b or with vertical irregularity type 1a, 1b, 2, or 3.
- Structures for which ELF is not allowed (structures with $T > 3.5T_s$ or other structures with irregularities listed above) must use either Modal Response Spectrum Analysis or Response History Analysis.

Table G-5 below summarizes engineering demand parameters that may be addressed by the application of the analysis procedures covered in ASCE 7. The table identifies system-, intermediate-, and component level engineering demand parameters according to performance level, period limitations, regularity, and other limitations.

Table G-5 Engineering Demand Parameters¹ That May be Addressed Using These Analysis Procedures

Perf. level ²	Period (height)	Regularity ³	Other limitations	Analysis Procedures				
				LSP	LDP	Plastic	NSP	NDP
IO ^{4,5}	any	Not limited	SDC B or C	I1,C4	I1, C4	C4 ⁶	--	I1, C3
LS	$T \leq 3.5T_s$	No H1, V1, V2, V3	SDC D, E, F	I1,C4	I1, C4	C4 ⁶	--	I1, C3
		H1, V1, V2, V3			I1, C4	C4 ⁶	--	I1, C3
		Not limited			I1, C4	C4 ⁶	--	I1, C3
NS ⁷	any	Must apply A_x		I1	I1, I2			(I1, I2) ⁸

¹Engineering Demand Parameters addressed explicitly (or implicitly)

System EDPs

S1: Identify global collapse

S2: Identify mechanism

Intermediate EDPs

I1: Quantify story drift

I2: Quantify floor acceleration

Component EDPs

C1: Identify local collapse

C2: Identify mechanism

C3: Quantify deformation

C4: Quantify force

²Performance levels addressed explicitly (or implicitly)

IO: Immediate Occupancy; LS: Life Safety; CP: Collapse Prevention
with corresponding hazard level, if indicated

DE: Design Earthquake; MCE: Maximum Considered Earthquake

³Structural irregularities

Horizontal

H1: Torsional stiffness

H2: Reentrant corner

H3: Diaphragm discontinuity

H4: Out-of-plane offset

H5: Non-orthogonal systems

H6: Torsional strength

Vertical

V1: Soft story

V2: Mass

V3: Setback

V4: In-plane offset

V5: Weak story

⁴ IO assumed to be associated with Occupancy Category IV, although some features (such as more stringent drift limits) are also associated with Occupancy Category III.

⁵ In one range of site seismicity, IO will change the seismic design category of a building from C to D, thereby invoking all the analysis controls associated with Seismic Design Categories D, E, and F.

⁶ Section 12.4.3.1 permits use of “rational, plastic mechanism analysis” to compute the “maximum force that can develop in” an element.

⁷ Nonstructural Components

⁸ Use of accelerations and story drifts from response history analysis for design of nonstructural components is not mentioned directly, but this interpretation is common.

G.7.3 Other Modeling Direction Provided

- Foundations may be assumed rigid. If assumed flexible, procedure specified.
- Soil structure interaction method included as an alternate.
- Model to include stiffness and strength of elements “significant” to the distribution of forces and deformations.

- Seismic mass defined.
- P-delta considered.
- If horizontal irregularity H1, H4, H5, must use three-dimensional model.
- Rules for assuming that diaphragms are rigid or flexible; where rules are not satisfied, explicit diaphragm modeling is required.
- Concrete cracked sections to be considered.
- Steel panel zone deformations to be considered.
- Restraining components not part of the lateral system must be assumed to be both active and inactive in the design (envelope).

G.7.4 Additional Analysis Requirements

- Simplified two-stage analysis provided for structures with flexible upper portion and rigid lower portion.
- Application of accidental torsion mandatory. Accidental torsion is amplified where H1 irregularity exists.
- Drift computed using C_d factors generally less than R .
- Separate rules for analysis procedures for seismically isolated structures. EDPs always limited to forces and displacements.
 - ELF is acceptable if 1) $S_I < 0.6$; 2) Site Class A, B, C, D; 3) ≤ 4 stories or 65 feet; 4) $T_{eff} \leq 3$ s; 5) $T_{eff} \leq 3$ times T of superstructure; 6) regular; 7) system not severely degrading, provides restoring force, and allows total maximum displacement.
 - Modal response spectrum is acceptable if meets item 2 and 7 above.
 - Otherwise use response history.
- Separate rules for analysis procedures for damped structures. EDPs limited to forces and displacements.
 - ELF is acceptable if $\beta \leq 35\%$, regular, $h \leq 100$ feet, 2 dampers per story configured to resist torsion, rigid diaphragms
 - Response spectrum is acceptable if 2 dampers per floor configured against torsion, and $\beta \leq 35\%$
 - Otherwise, nonlinear procedures of 18.3 required

G.7.5 Ground Motion Characterization

- Minimum base shear was reinserted as a Supplement after studies for the FEMA P-695 report showed that taller concrete frames were systematically failing the FEMA P-695 criteria for selection of R factors.
- 5% damped spectra specified except for damped or isolated structures. Spectra for damped and isolated chapters are modified for analysis with use of a Ω factor specific for each level of higher damping.
- 3 or 7 times histories (no consideration of uncertainty in response).
- ELF and Modal Response Spectrum Analysis section written assuming two-dimensional analysis with direction combination rules. (MRSA answers scaled by R/I). Site specific spectrum limited in proportion to “mapped” values.
- NDP: Regular structures with independent lateral system can be done in two dimensions with motions scaled to 1.0 times the target spectrum. Irregular structures must be done in three dimensions with the SRSS of the two components scaled to 1.3 times the target spectrum.
- Ground motion scaling for isolated and damped structures given independently in each chapter but all consistent with Chapter 16.

G.8 NEHRP Recommended Seismic Provisions for New Buildings and Other Structures

With the adoption of ASCE/SEI 7 as a reference document, FEMA P-750, *NEHRP Recommended Seismic Provisions for New Buildings and Other Structures: Part 1, Provisions* (FEMA, 2009c), is now more closely aligned with that document. Differences regarding analysis procedures are contained primarily in Part 3.

G.8.1 Scope of Application

All new building structures and certain non-building structures are covered except those exempted:

- Detached one and two family dwellings where $S_S < 0.4$ or where SDC is A, B, or C
- Detached one and two family dwellings not included above but which comply with IRC
- Agricultural storage structures with only incidental human occupancy
- Special structures not addressed in Chapter 15 covered by other seismic regulations such as bridges, hydraulic structures, and nuclear power plants

As specified in Appendix 11B, existing structures where alterations have increased the seismic load to any element by more than 10% or reduced the capacity of any element by more than 10%. It is unclear how consistently Appendix 11B is enforced,

how the appendix relates to Chapter 34 of the IBC, and how often local jurisdictions have adopted different regulations.

G.8.2 Applicability of Analysis Procedures

Selection of Analysis Procedure is covered in Section 12.6. Analysis Procedures include Equivalent Lateral Force Analysis, Modal Response Spectrum Analysis, and Seismic Response History Procedures. The applicability of Analysis Procedures is summarized in Table 12.6-1 which includes several variables:

- Seismic Design Category.
- Occupancy Category.
- Height measured in stories (2 and 3 stories), in feet (≤ 160 feet), and as implied by period ($\leq 3.5T_s$).
- Certain irregularities.

Although Table 12.6-1 is obtuse, it can be deduced that:

- Equivalent Lateral Force Analysis can be used
 - for all structures assigned to SDC B and C,
 - for all light frame construction with SDC D, E, F,
 - for all regular structures with $h \leq 160$ feet or $T < 3.5T_s$, and
 - for irregular structures with $h \leq 160$ feet except those with horizontal torsional irregularity type 1a or 1b or with vertical irregularity type 1a, 1b, 2, or 3.
- Structures for which ELF is not allowed (due to height, period, or irregularity as above) must use either Modal Response Spectrum Analysis or Response History Analysis.

Table G-6 below summarizes engineering demand parameters that may be addressed by the application of the analysis procedures covered in NEHRP Provisions. The table identifies system-, intermediate-, and component level engineering demand parameters according to performance level, period limitations, regularity, and other limitations.

G.8.3 Other Modeling Direction Provided

- Foundations may be assumed rigid. If assumed flexible, procedure specified.
- Soil structure interaction method included as an alternate.
- Model to include stiffness and strength of elements “significant” to the distribution of forces and deformations.
- Seismic mass defined.

- P-delta considered.
- If horizontal irregularity H1, H4, H5, must use three-dimensional model.
- Rules for assuming that diaphragms are rigid or flexible; where rules are not satisfied, explicit diaphragm modeling is required.
- Concrete cracked sections to be considered.
- Steel panel zone deformations to be considered.
- Restraining components not part of the lateral system must be assumed to be both active and inactive in the design (envelope).

G.8.4 Additional Analysis Requirements

- Simplified two-stage analysis provided for structures with flexible upper portion and rigid lower portion.
- Application of accidental torsion mandatory. Accidental torsion is amplified where H1 irregularity exists.
- Drift computed using C_d factors generally less than R .
- Separate rules for analysis procedures for seismically isolated structures. EDPs always limited to forces and displacements.
 - ELF is acceptable if 1) $S_I < 0.6$; 2) Site Class A, B, C, D; 3) ≤ 4 stories or 65 feet; 4) $T_{eff} \leq 3$ s; 5) $T_{eff} \leq 3$ times T of superstructure; 6) regular; 7) system not severely degrading, provides restoring force, and allows total maximum displacement.
 - Modal response spectrum is acceptable if meets item 2 and 7 above.
 - Otherwise use response history.
- Separate rules for analysis procedures for damped structures. EDPs limited to forces and displacements.
 - ELF is acceptable if $\beta \leq 35\%$, regular, $h \leq 100$ feet, 2 dampers per story configured to resist torsion, rigid diaphragms.
 - Response spectrum is acceptable if 2 dampers per floor configured against torsion, and $\beta \leq 35\%$.
 - Otherwise, nonlinear procedures of 18.3 required.

Table G-6 Engineering Demand Parameters¹ That May be Addressed Using These Analysis Procedures

Perf. level ²	Period (height)	Regularity ³	Other limitations	Analysis Procedures				
				LSP	LDP	Plastic	NSP	NDP
IO ^{4,5}	any	Not limited	SDC B or C	I1,C4	I1, C4	C4 ⁶	--	I1, C3
LS	$T \leq 3.5T_s$	No irregularities	SDC D, E, F	I1,C4	I1, C4	C4 ⁶	--	I1, C3
		$h \leq 160$ ft	No H1, V1, V2, V3	I1,C4	I1, C4	C4 ⁶	--	I1, C3
	else	H1, V1, V2, V3			I1, C4	C4 ⁶	--	I1, C3
		Not limited			I1, C4	C4 ⁶	--	I1, C3
NS ⁷	any	Must apply A_x		I1	I1, I2			(I1, I2) ⁸
LS ⁹	$h \leq 40$ ft ¹⁰	No irregularities	$R_d \leq R_{max}$				S3, C3, C4	
CP ¹¹	any	Not limited						S2 ¹² , I1, C3, C4
IO	any	Not limited						S2 ¹² , I1, C3, C4

¹Engineering Demand Parameters addressed explicitly (or implicitly)

System EDPs	Intermediate EDPs	Component EDPs
S1: Identify global collapse	I1: Quantify story drift	C1: Identify local collapse
S2: Identify mechanism	I2: Quantify floor acceleration	C2: Identify mechanism
S3 global strength		C3: Quantify deformation
		C4: Quantify force

²Performance levels addressed explicitly (or implicitly)

IO: Immediate Occupancy; LS: Life Safety; CP: Collapse Prevention with corresponding hazard level, if indicated
DE: Design Earthquake; MCE: Maximum Considered Earthquake

³Structural irregularities

Horizontal	Vertical
H1: Torsional stiffness	V1: Soft story
H2: Reentrant corner	V2: Mass
H3: Diaphragm discontinuity	V3: Setback
H4: Out-of-plane offset	V4: In-plane offset
H5: Non-orthogonal systems	V5: Weak story
H6: Torsional strength	

⁴ IO assumed to be associated with Occupancy Category IV, although some features (such as more stringent drift limits) are also associated with Occupancy Category III.

⁵ In one range of site seismicity, IO will change the seismic design category of a building from C to D, thereby invoking all the analysis controls associated with Seismic Design Categories D, E, and F.

⁶ Section 12.4.3.1 permits use of "rational, plastic mechanism analysis" to compute the "maximum force that can develop in" an element.

⁷ Nonstructural Components

⁸ Use of accelerations and story drifts from response history analysis for design of nonstructural components is not mentioned directly, but this interpretation is common.

⁹Nonlinear static procedure in Part 3 is limited to Occupancy Category I and II buildings. There is no mention of a two level acceptance check similar to the BSO of ASCE/SEI 41-06. Since system and detailing requirements of ASCE 7 apply, it is apparently assumed that a check of CP at MCE is not warranted.

¹⁰ No explicit limits on period but height is limited to 40 feet, so periods will be low.

¹¹ Nonlinear response history in Part 3; CP at MCE for Occupancy Category I and II; LS at MCE for Occupancy Category IV, and 80% of CP for Occupancy Category III. (Plus unspecified "serviceability" checks.)

¹² Required to show global stability

- ELF and Modal Response Spectrum Analysis section written assuming two-dimensional analysis with direction combination rules. (MRSA answers scaled by R/I). Site specific spectrum limited in proportion to “mapped” values.
- NDP: Regular structures with independent lateral system can be done in two dimensions with motions scaled to 1.0 times the target spectrum. Irregular structures must be done in three dimensions with the SRSS of the two components scaled to 1.0 times the target spectrum. This creates an inconsistency between two-dimensional analysis using ELF, MRSA, and Response History Analysis and three-dimensional Response History Analysis because both are scaled to 1.0. Due to orthogonal combination requirements, the two-dimensional analysis will result in effects larger than those associated with the mapped “maximum direction acceleration” (by approximately 1.3 to 1.4 times).

G.9 PEER/ATC-72-1 Modeling and Acceptance Criteria for Seismic Design and Analysis of Tall Buildings

G.9.1 Scope of Application

These guidelines in PEER/ATC-72-1, *Modeling Acceptance Criteria for Seismic Design and Analysis of Tall Buildings* (PEER/ATC, 2010) represent a compilation of the latest information on analytical simulation, system and component behavior, material properties, and recommendations specific to the seismic design of tall building structural systems. There is an implicit assumption that tall buildings will be subject to NRHAs and NSPs are not treated in the document. The information contained in the document is an impressive compendium of nonlinear modeling guidelines for many components. Of particular interest are techniques for dealing with diaphragms and podiums at the base of a tall building.

G.9.2 Applicability of Analysis Procedures

This document is directed at nonlinear response history analysis. It also addresses a two-stage design using MRSA for initial proportioning of designated yielding elements followed by NRHA to verify that other mechanisms and actions remain essentially elastic.

Modeling, simulation, and acceptance criteria

Current codes, although legally applicable to tall buildings, are based on, and emphasize design requirements for, low- to moderate-rise construction. As such, they fall short in conveying specific modeling, analysis, and acceptance criteria for very tall buildings because the dynamic and mechanical aspects of response that control the behavior of tall buildings are different from those of shorter buildings. Specialized engineering procedures, consensus-based and backed by research and experience, are needed. Criteria should address appropriately aspects of reliability of safety, capital preservation, re-occupancy, and functionality.

Types of Nonlinear Models

Inelastic structural component models generally can be distinguished by the degree of idealization in the model. For example, shown in G-3 is a comparison of three idealized model types for simulating the nonlinear response of a reinforced concrete beam-column

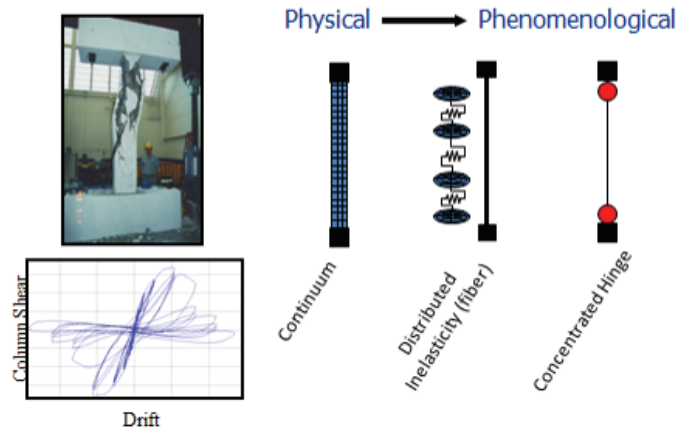


Figure G-3 Comparison of nonlinear component model types.

Inelastic Component Attributes

With the objective of accurately simulating the structural performance, nonlinear response history analysis models should be based on the expected properties of the materials and components, as opposed to the nominal or minimum specified properties that are otherwise used in design. These properties generally will include the stiffness, strength, and deformation characteristics of the components, and the term “expected” refers to properties that are defined based on the median values from a large population that represents the materials or components used in the structure. Use of expected structural properties is important in two regards. First, they will provide an accurate and unbiased measure of the expected response of the overall system. Second, and equally important, use of the expected values throughout the model will more accurately characterize the relative force and deformation demands between components of indeterminate structural systems. In this regard the goal is to avoid any systematic bias that may result from differences between nominal and expected properties for various components of the structure.

Energy Dissipation and Viscous Damping

Traditionally, viscous damping has been used as a convenient way to idealize energy dissipation in elastic dynamic response history analyses. For inelastic dynamic analyses, it is important to identify the sources of energy dissipation and determine how these effects are represented in the analysis model. For components that are modeled with nonlinear elements, most of the energy dissipation will be modeled explicitly through the hysteretic response. However, energy dissipation that is modeled at low deformations may vary significantly with the type of analysis model

used. For example, in reinforced concrete, continuum finite element models will tend to capture damping effects due to concrete cracking that is not captured in lumped plasticity spring models (see G-3). In tall buildings, the relative contribution of damping from certain components may be substantially different from values typically assumed in low-rise buildings. For example, measured data show that damping tends to be less in tall buildings, suggesting that there may be proportionally less damping due to soil-foundation interaction or due to special “isolation” detailing of nonstructural partitions and other components. Further information and specific suggestions regarding damping are covered in Section 2.4.

Gravity Load Effects in Nonlinear Analysis

Unlike linear analyses, nonlinear analyses are load path dependent, where the results depend on the combined gravity and lateral load effects. For seismic performance assessment by nonlinear analysis, the gravity load applied in the analysis should be equal to the expected gravity load, which is different from the factored loads assumed for standard design checks. Generally, the gravity load should be equal to the unfactored dead load and a fraction of the design live load. The dead load should include the structure self weight, architectural finishes (partitions, exterior wall, floor and ceiling finishes), and mechanical and electrical services and equipment. For overall system response of tall buildings, the live load should be reduced from the nominal design live load to reflect (a) the low probability of the nominal live load occurring throughout the building, and (b) the low probability of the nominal live load and earthquake occurring simultaneously. Generally, the first of these two effects can be considered by applying a live load reduction multiplier of 0.4 and the second by applying a load factor of 0.5 (such as is applied to evaluation of other extreme events). The net result is a load factor of 0.2 (0.4×0.5) that should be applied to the nominal live load. So, for example, in a residential occupancy with a nominal live load of 40 psf, the amount to be considered in nonlinear analysis would be equal to 8 psf (0.2×40 psf). For storage loads, only the 0.5 factor would apply. Accordingly, a general load factor equation for gravity loads (nominal dead load D and live load L) applied for nonlinear analysis is: $1.0D + 0.2L$ (except that the load factor for storage live loads and similar areas should be 0.5).

The expected gravity loads should be used as the basis for establishing the seismic mass and expected gravity loads to apply in the nonlinear analysis. The vertical gravity loads of the entire building should be included in the analysis so as to capture destabilizing P-delta effects stabilized by the seismic force-resisting system. So, for example, the nonlinear analysis of the lateral system should include the destabilizing P-delta effects on gravity columns (so-called leaning columns) that rely on the seismic force-resisting system for lateral stability.

Acceptance Criteria

Nonlinear response analysis is purposeful only if it is associated with a set of criteria for acceptable performance. The report on Task 2 of the Tall Building Initiative (TBI 2007) addresses performance objectives for tall buildings, which generally involves comparisons of force and deformation demands imposed by the earthquake to corresponding limit state capacities of the structural components and systems. The emphasis in this report is on defining capacities for two structural limit states, one associated with the onset of structural damage requiring repair and the other associated with the onset of significant degradation in structural components.

- **Onset of Structural Damage:**

In general, it is presumed that the onset of structural damage typically will occur at forces and deformations beyond the yield point with some permanent deformations associated with yielding of steel and cracking of concrete.

- **Onset of Significant Structural Degradation:**

The onset of significant strength and stiffness degradation of structural components is a prerequisite for deterioration of the overall structural response and collapse. Thus, while significant degradation of component response is not synonymous with collapse, it is an important indicator as to when the structural integrity is compromised sufficiently to raise concerns about structural collapse. The onset of significant component degradation is also an important indicator to gauge the accuracy of the structural analysis and the extent to which the nonlinear analysis captures accurately the strength and stiffness degradation that occurs at larger deformations.

Modes of Deterioration

1. **Basic strength deterioration:**

The strength deteriorates with the number and amplitude of cycles, even if the displacement associated with the strength cap has not been reached. This can be represented by a translation (and possibly rotation) of the pre-capping strength bound towards the origin (see Figure 2.2-10(a)).

2. **Post-capping strength deterioration:**

The strength deteriorates further when a negative tangent stiffness is attained. This can be represented by a translation (and possibly rotation) of the post-capping strength bound towards the origin (see Figure 2.2-10(b)).

3. **Unloading stiffness deterioration:**

The unloading stiffness deteriorates with the number and amplitude of cycles. This can be represented by a rotation of the unloading slope (see Figure 2.2-10(c)).

4. **Accelerated reloading stiffness deterioration:**

For a given deformation amplitude the second cycle indicates a smaller peak strength than the first cycle; however, the resistance increases and the strength

envelope is attained if the amplitude of the second cycle is increased (this mode is observed, for instance, in reinforced concrete beams subjected to a high shear force) If the strength envelope is attained upon increasing the deformation amplitude, then this type of deterioration should not be referred to as strength deterioration but as accelerated reloading stiffness deterioration. It can be represented by a movement of the point at which the strength envelope is reached away from the origin (see Figure G-4d).

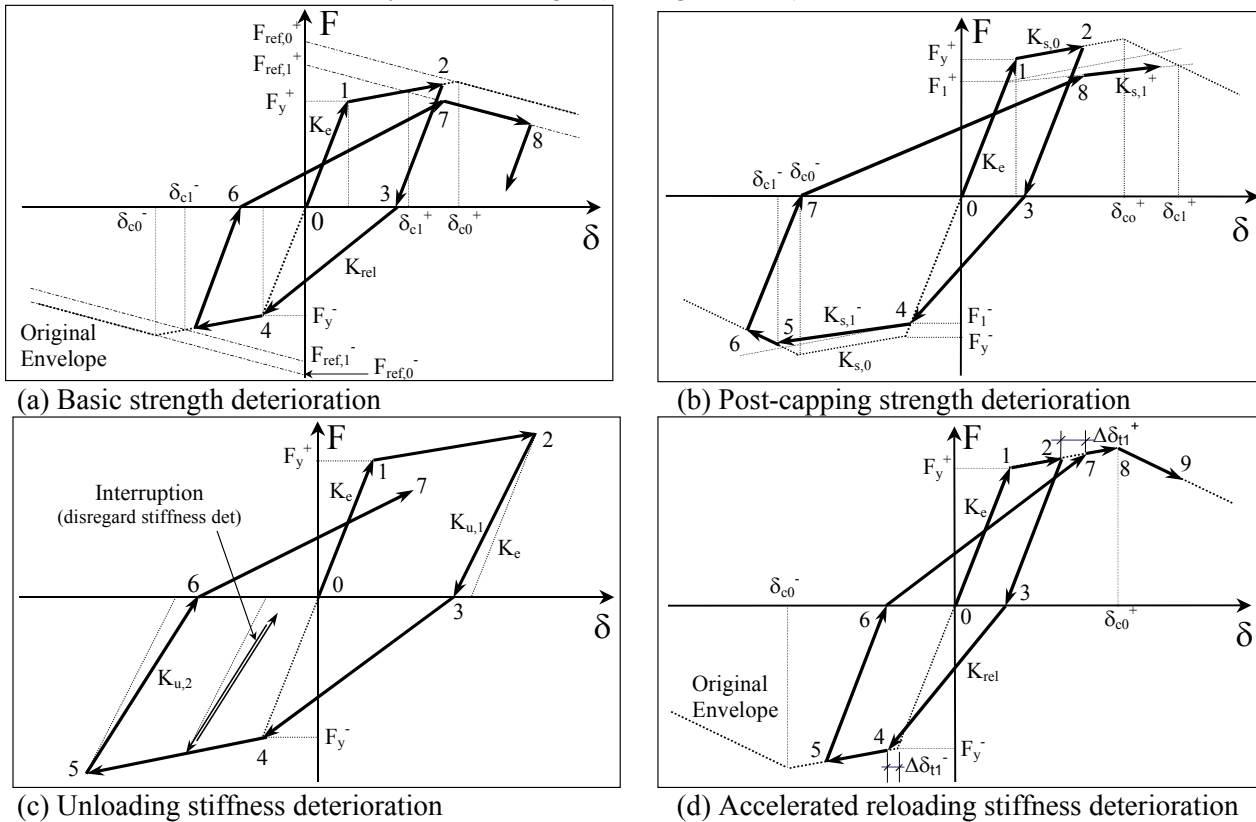


Figure G-4 Individual deterioration modes for Ibarra-Krawinkler Model illustrated on a peak-oriented model (Ibarra et al., 2005).

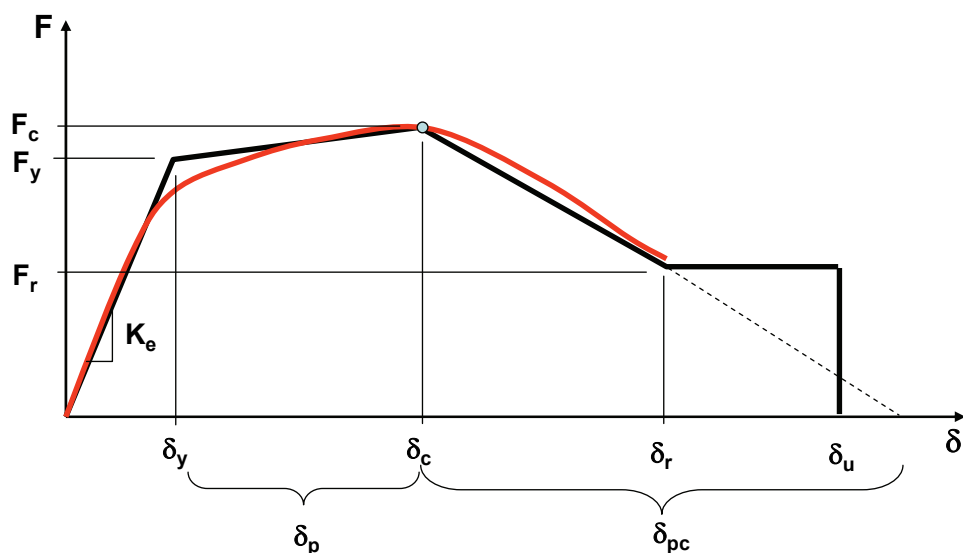
Backbone curve

The backbone curve is a reference force – deformation relationship that defines the bounds within which the hysteretic response of the component is confined. If no cyclic deterioration has occurred, the backbone curve is close to the monotonic loading curve, and is referred to as the initial backbone curve. Once cyclic deterioration sets in, the branches of the backbone curve move toward the origin and are continuously updated (they may translate and/or rotate). The instantaneous backbone curve may be referred to as a cyclic backbone curve, but it must be understood that this cyclic backbone curve is loading history dependent and changes continuously after each excursion that causes damage in the component.

The initial backbone curve is close to—but does not have to be identical to—the monotonic loading curve. It usually contains compromises that should be made in order to simplify response description. For instance, it might accounts for an average

effect of cyclic hardening (which likely is small for RC components but may be significant for steel components).

A typical initial backbone curve concept and necessary definitions are illustrated in Figure G-5. The quantities F and δ are generic force and deformation quantities. For flexural plastic hinge regions $F = M$ and $\delta = \theta$. Refinements (e.g., more accurate multi-linear descriptions) can be implemented as deemed necessary. It is important to note that the initial backbone curve incorporates monotonic strength deterioration for deformations exceeding the so-called capping point (point of maximum strength under monotonic loading).



- Effective yield strength and deformation (F_y and δ_y)
- Effective elastic stiffness, $K_e = F_y/\delta_y$
- Capping strength and associated deformation for monotonic loading (F_c and δ_c)
- Pre-capping plastic deformation for monotonic loading, δ_p
- Effective post-yield tangent stiffness, $K_p = (F_c - F_y)/\delta_p$
- Post-capping deformation range, δ_{pc}
- Effective post-capping tangent stiffness, $K_{pc} = F_c/\delta_{pc}$
- Residual strength, $F_r = \kappa F_y$
- Ultimate deformation, δ_u

Figure G-5 Parameters of the initial backbone curve of the Ibarra-Krawinkler model (PEER/ATC, 2010).

Analytical Modeling Options

- Option 1 – explicit incorporation of cyclic deterioration in analytical model:
Incorporate cyclic deterioration explicitly in the analytical model, using the initial backbone curve as a reference boundary surface that moves “inward” (toward the origin) as a function of the loading history.
- Option 2 – use of cyclic envelope (skeleton) curve as modified initial backbone curve; no cyclic deterioration of the backbone curve in analytical model:

If the cyclic envelope (skeleton) curve is known (e.g., from a cyclic test that follows a generally accepted loading protocol) then it should be acceptable to use this skeleton curve as the modified initial backbone curve for analytical modeling and ignore additional cyclic deterioration - provided that the bounds established by the cyclic envelope (skeleton) curve are not exceeded in the analysis, i.e., the ultimate deformation δ_u should be limited to the maximum deformation recorded in the cyclic test. When using this approximation, one must be sure to include the negative stiffness (deformation or strain softening) portion of the cyclic envelope (skeleton) curve as part of the modified initial backbone curve of the analytical model.

- Option 3 – use of factors for modification of initial backbone curve; no cyclic deterioration in analytical model:

If only the initial backbone curve is known (or predicted) and cyclic deterioration is not incorporated in the analytical model (i.e., the initial backbone curve remains a non-moving boundary for cyclic loading), then the shape of the backbone curve must be modified to account approximately for cyclic deterioration effects. Numerical values of the modification factors might depend on material and configuration of the structural component.

- Option 4 – no strength deterioration in analytical model:

If the post-capping (negative tangent stiffness) portion of the modified initial backbone curve of option 2 or 3 is not incorporated in the analytical model (i.e., a non-deteriorating model is employed), then the ultimate deformation of the component should be limited to the deformation associated with 80% of the capping strength on the descending branch of the modified initial backbone curve as obtained from option 2 or 3.

Figure G-6 illustrates the four options for a typical experimental cyclic loading history and a peak-oriented hysteresis model. The differences appear to be small, but primarily because the illustrations are for a symmetric and step-wise increasing loading history, which is typical for experimental studies. As intended, the larger the simplification the more the inelastic deformation capacity is being reduced. This is most evident in Figures G-6 (c) and (d), in which the attainment of the estimated δ_u limits the inelastic deformation capacity.

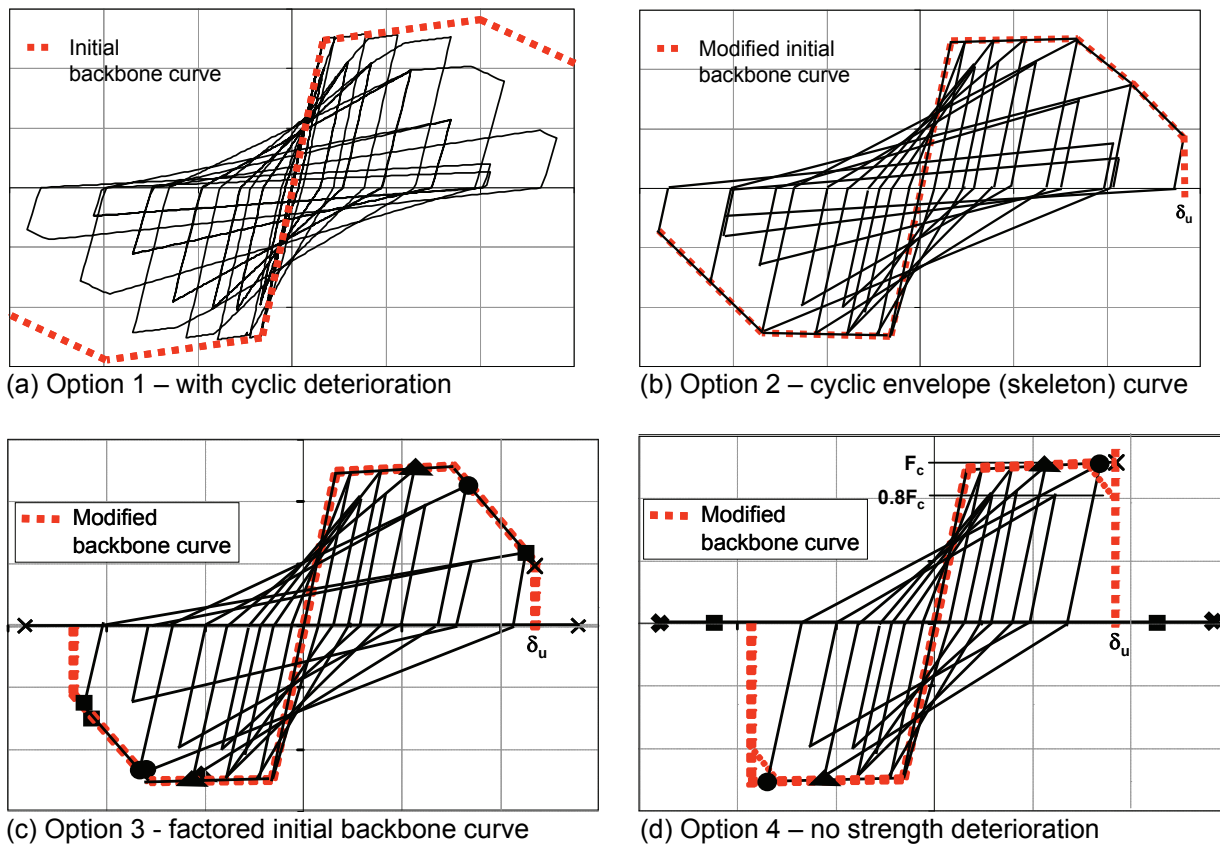


Figure G-6 Illustration of implementation of the four options for analytical component modeling (PEER/ATC, 2010).

The choice of an appropriate component modeling option and of the basic hysteresis model used to represent the cyclic response of structural components needs to be justified and becomes part of the analysis documentation.

P-Delta Effect Recommendations

- Every nonlinear response history analysis should incorporate structure P-Delta effects. A relatively small elastic story stability coefficient does not assure that the P-Delta effects are benign in the inelastic range.
- If there are “leaning columns” (columns that carry gravity loads but are not part of the lateral load-resisting system), then the P-Delta tributary to these columns must be represented in the analytical model.
- The length and slope of the strain hardening region (i.e., δ_p and M_c/M_y) and of the post-capping region (i.e., δ_{pc}) of the structural components may greatly affect the lateral drift under severe ground motions because of “ratcheting” of the response in individual stories (story drift amplification due to large P-delta effects). For this reason estimates of these parameters should be reasonable and conservative (low). The implication is that option 4 for analytical modeling of components should be used only if the post-capping portion of the nondeteriorating model is relatively small compared to the strain hardening portion.

- Any deformation mode that may lead to concentrations of inelastic deformations in a single story (or to partial mechanisms involving several stories) should be incorporated in the analytical model. This pertains particularly to possible plastic hinging in columns of moment frames, severe deterioration of bracing elements (or their connections) in a braced frame, and shear failure in walls.
- If the analytical model incorporates the strengthening and stiffening effects of components that are not explicitly part of the lateral load-resisting system (e.g., gravity columns, simple connections, slab effects), then it should be shown that these components maintain their effectiveness for the full range of deformation experienced by the structure.

Damping: Recommendations for Nonlinear Analysis and Design

For nonlinear analysis, damping (energy dissipation) effects are included through a combination of hysteretic and viscous damping. Generally, the damping effects in the structural components of the lateral force-resisting system are explicit in the nonlinear analysis through hysteretic response of the inelastic component models. Damping effects of other structural members (e.g., gravity framing), foundation-soil interaction, and nonstructural components that are not otherwise modeled in the analysis can be incorporated through equivalent viscous damping. The amount of viscous damping should be adjusted based on specific features of the building design and may be represented by either modal damping, explicit viscous damping elements, or a combination of stiffness and mass proportional damping (e.g., Rayleigh damping). Among the various alternatives, it is generally recommended to model viscous damping using modal damping, Rayleigh damping, or a combination of the two. Care should be taken when specifying stiffness-proportional damping components of Rayleigh damping to avoid over-damping in higher modes and/or due to high elastic stiffness in gap-type (including fiber concrete materials) or rigid-plastic materials and components.

Based on a review of the evidence described previously, the following are suggested as appropriate values of equivalent viscous damping for use in nonlinear analysis of typical buildings, where most of the hysteretic energy dissipation is accounted for in the nonlinear models for structural members of the lateral force resisting system:

$$D = \alpha/30 \text{ (for } N < 30) \tag{G-1}$$

$$D = \alpha/N \text{ (for } N > 30) \tag{G-2}$$

where D is the maximum percent critical damping, N is the number of stories (> 30), and α is a coefficient with a recommended range of $\alpha = 60$ to 120 . Referring to Figure 2.4-5 in PEER/ATC-72-1, as compared to the measured damping data reported previously (Figure 2.4-1), the resulting damping ranges between 2% to 4% for 30-story buildings and 1% to 2% for 70-story buildings. Damping values for

specific buildings should reflect the structural material and system, the foundation conditions, and the nonstructural partition walls. Generally, systems of structural steel framing would tend toward the lower range of damping ($\alpha = 60$) and systems of reinforced concrete would tend toward the upper range ($\alpha = 120$).

Expected Properties and Uncertainty

In general, all of the component model parameters should be defined based on their median properties, rather than some lower values (e.g., allowable, design or nominal strengths) that are used for elastic design.

Statistical Characterization of Modeling Uncertainties

In addition to the mean or average values, the variability in component response quantities should be assessed, taking into account the underlying sources of uncertainties. Variability is generally described through the standard deviation of the data.

Based on these observations, and recognizing the limited amount of test data to characterize the full-scale response of components in tall buildings, the following values of dispersion are suggested in the absence of other available information: 0.2 for dispersion in strength, 0.3 for dispersion in stiffness and yield deformation, and 0.5 for dispersion in capping and post capping deformation.

In the absence of a more complete evaluation of the sources of uncertainty present, it is suggested to use a composite uncertainty on analysis demand parameters of 0.5 for systems that are well defined and responding in the elastic range. For highly nonlinear response, it is suggested to use a composite uncertainty on demand parameters of 0.65. As such, these values could be applied to calculated displacement or component force demands to calculate various limit states (e.g., to calculate the probability that the calculated shear demand in a reinforced concrete wall is less than a critical limiting value).

G.9.3 Other Modeling Direction Provided

Podium and backstay effects

All structural elements related to podium and backstay effect need to be modeled in the analysis with suitable stiffness assumptions so that appropriate design forces are determined. Once the design forces are established, appropriate assumptions must be made in the design of each structural element.

The types of elements that must be modeled and designed include the following: Floor diaphragms and collectors, concrete walls, concrete moment frames, steel moment frames, steel braced frames, foundation mat slabs, pile caps, footings, and soil or pile spring stiffness.

Floor Diaphragms, Collectors, and Diaphragm Segments

In addition to supporting gravity loads, floor and roof structures act as structural diaphragms that connect to and provide lateral stability to vertical structural elements, and they distribute lateral forces to the vertical elements of the seismic force-resisting system (e.g., walls, moment frames, or braced frames). The lateral forces on floor and roof diaphragms are resisted by in-plane action of the diaphragm.

In the seismic analysis of a building, the structural diaphragms can be modeled in one of three ways: rigid, semi-rigid, or flexible. In reality, all floor and roof diaphragms are semi-rigid because they have a finite value of in-plane stiffness. However, for practical design purposes, an idealized rigid or flexible diaphragm is often used to simplify the analysis task. In some cases new building code requirements in ASCE 7-05 will require semi-rigid modeling, even though a rigid diaphragm model could provide an acceptable estimate of diaphragm actions.

Concrete, or concrete-on-steel-deck diaphragms common in tall buildings typically are modeled as rigid or semi-rigid. A rigid diaphragm model is usually appropriate for regular structures. Diaphragms carrying large force transfers should be modeled as semi-rigid. Backstay diaphragms certainly fall into this category. Other floors in tall buildings — those that do not carry significant force transfers — often can be modeled as rigid.

A semi-rigid diaphragm model is more accurate, particularly for more flexible or irregular configurations, because it explicitly considers the diaphragm stiffness properties. It also provides diaphragm shear and moment design forces more directly. The chief disadvantage of a semi-rigid diaphragm model is that it can add complication to the analytical work, including computer input and analysis run time.

In general, a rigid diaphragm assumption is appropriate if the distribution of forces in the vertical elements of the seismic force-resisting system would be similar to results using a semi-rigid assumption. Short of running both rigid and semi-rigid models and comparing results, the decision of which assumption is appropriate for a given building should be based on the considerations discussed in the sections that follow.

Design of Floor Diaphragms and Collectors: Diaphragm In-Plane Shear

For reinforced concrete diaphragms, the diaphragm nominal strength to resist seismic in-plane shear is defined by ACI 318-08 Section 21.12.8, as the effective area of the diaphragm multiplied by its nominal stress capacity. In accordance with ACI 318-08, Equation 21-10, the nominal shear strength for a floor or roof slab acting as a diaphragm is:

$$V_n = A_{cv} \left(2\sqrt{f'_c} + \rho_n f_y \right)$$

where A_{cv} is the net area of concrete section bounded by the slab thickness and length in the direction of shear force considered.

Strut-and-Tie Models

Potentially (with further development of requirements) methods using a strut-and-tie analogy could be used to design diaphragms for shear and flexure. The design of collectors and diaphragm segments could also be considered in the strut-and-tie model, if forces amplified by Ω_0 are used for the whole model. Code provisions for strut-and-tie models are given in Appendix A of ACI 318-08.

The method is more directly applicable to reinforced concrete floor diaphragm slabs, but could be applied to concrete-on-steel-deck floors, possibly with modifications to account for the strength contribution of the steel deck. Potentially, strut and tie methods could be a logical way of considering the contribution of steel floor beams to in-plane diaphragm strength.

Example applications (Reineck, 2002) show that strut-and-tie models for seismic forces can become complex. Because of differences in the specified force reduction factors (ϕ) designs for flexure and collector tension by the ACI appendix can require more reinforcement than the conventional design approaches for reinforced concrete. While strut-and-tie models can provide good design insight to the engineer¹, it seems that more development and calibration of code provisions is required before such models can be used as the basic design process for diaphragms and collectors.

Diaphragm In-Plane Flexure

Like a beam, a reinforced concrete diaphragm acts to resist in-plane flexure with a force couple of concrete in compression and reinforcement in tension. For reinforced concrete floor diaphragm slabs, the most appropriate way to calculate the flexural strength of a diaphragm is by the same procedure that is used for beams and walls, according to ACI 318-08 Section 21.12.9.1.

Diaphragms of concrete on steel deck can be designed for flexure using a similar approach, possibly with additional consideration of the strength provided by the steel deck in the direction parallel to its ribs, and by steel floor beams.

Distribution of Collector Forces

Collectors are designed for tension and compression based on a calculated or assumed distribution of axial forces along the collector line. Design practices that have been used in the past, such as assuming uniform shear along a collector line, can

¹ Strut-and-tie models are potentially most useful for the design of diaphragms with significant openings. An illustration of this applicability is an example given in Paulay and Priestley [1992] that uses strut-and-tie models for the seismic design of a wall with openings.

be inappropriate and impractical if applied to diaphragms with collector forces amplified by Ω_0 or taken from nonlinear response history analyses.

The design approach recommended in PEER/ATC-72-1 is that the engineer can choose a reasonable distribution of forces that satisfies equilibrium and does not exceed the capacities of the provided collectors and shear transfer mechanisms. Forces assumed should be consistent with those taken from the semi-rigid diaphragm model. The engineer must verify adequate resistance to the chosen force distribution at all critical sections in the seismic-force path.

Collectors are designed for forces amplified by Ω_0 because the design intention is that collectors should remain essentially elastic for a level of force that causes the building's walls or moment frames to yield and dissipate earthquake energy. The objective is to ensure that while some force redistribution may need to occur in the floor diaphragm, the diaphragm and its collectors should have the ultimate strength to resist the forces that correspond to nonlinear behavior of the walls or moment frames.

Recommended Stiffness Properties for Modeling of Podium and Backstay Effects

Considering the issues described above regarding backstay force paths and the behavior and properties of floor diaphragms and seismic-force-resisting elements, PEER/ATC-72-1 recommends element stiffness properties as shown in Table G-7. The table is based on the example of a concrete-core wall building, but is applicable to other types of non-perimeter seismic force-resisting systems.

Table G-7 Summary of Structural Elements Affecting the Backstay Effect for a Concrete Core Wall Building, and the Recommended Range of Stiffness Assumptions

Structural element or property	Assumption for upper bound of backstay effect	Assumption for lower bound of backstay effect	Notes
<i>Structural elements of the podium</i>			
Flexural stiffness EI for floor diaphragms and perimeter reinforced concrete walls (assumed to be elements with squat in-plane aspect ratios).	0.5 times gross section properties	0.2 times gross section properties, or fully cracked, transformed section properties. Consider reducing stiffness for strain penetration effects.	Using gross section properties for squat elements results in very small predicted deformations. Thus including sources of additional deformation, such as strain penetration, can result in stiffness properties that are a small fraction of gross properties.
Shear stiffness GA_v for floor diaphragms and perimeter reinforced concrete walls (assumed to be elements with squat in-plane aspect ratios).	0.5 times gross section properties	0.05 to 0.2 times gross section properties, or calculate per ratio of horizontal reinforcement per Powell [20xx]	The shear stiffness of a concrete wall or diaphragm can greatly reduce upon diagonal cracking of walls. Diagonal cracking can be assumed to occur where average shear stress exceeds $3\sqrt{f_c}$
Foundation stiffness for perimeter reinforced concrete walls (e.g., vertical springs under wall footings)	Upper-bound soil stiffness or fixed base assumption	Lower-bound soil stiffness	
Lateral stiffness for passive resistance of soil on the face of perimeter reinforced concrete walls (e.g., horizontal springs around the below-grade portion of the building)	Lower-bound soil stiffness or leave out soil springs. (Although upper-bound properties will increase overall backstay, they will also take force out of diaphragms and perimeter wall and thus may not govern design.)		Passive resistance of soil occurs under compression but not tension, and soil spring properties should be adjusted to account for this. The stiffness of passive resistance can be small compared to the stiffness of the perimeter walls, and thus can often be neglected.

Table G-7 Summary of Structural Elements Affecting the Backstay Effect for a Concrete Core Wall Building, and the Recommended Range of Stiffness Assumptions (continued)

Structural element or property	Assumption for upper bound of backstay effect	Assumption for lower bound of backstay effect	Notes
<i>Structural elements of the core wall and its foundation</i>			
Flexural stiffness EI for core wall	0.3 times gross section properties, or fully cracked, transformed section properties, or modeled with nonlinear fiber elements, possibly accounting for strain penetration [Maffei and Schotanus 2007].		In typical cases, this stiffness is not bracketed because it is less influential to backstay effects than the modeling of the podium structure and foundation stiffness.
Shear stiffness GA_v for core wall	0.3 times gross section properties, or smaller if shear cracking is expected, based on shear stress exceeding $3\sqrt{f'_c}$.		In typical cases, this stiffness is not bracketed because it is less influential to backstay effects than the modeling of the podium structure and foundation stiffness.
Flexural stiffness EI for mat slab or pile cap	0.3 times gross section properties, or fully cracked, transformed section properties.		In typical cases, this stiffness is not influential and not highly uncertain, and thus need not be bracketed.
Shear stiffness GA_v for mat slab or pile cap	0.3 times gross section properties, or smaller if shear cracking is expected, based on shear stress exceeding $3\sqrt{f'_c}$.		In typical cases, this stiffness is not influential, and thus need not be bracketed.
Foundation stiffness under concrete core wall (e.g., vertical springs under wall mat slab or representation of vertical pile stiffness)	Lower-bound soil or pile stiffness	Upper-bound soil or pile stiffness or fixed base assumption	

Table G-8 Notes on Tall Building Structural Elements not Covered in Table G-7

Structural Element	Notes on stiffness assumptions and design
Concrete-on-steel-deck floor diaphragms	In-plane shear and flexural stiffness properties are uncertain and should be bracketed in the analysis. For upper-bound stiffness properties, and for consideration of strength, the engineer should consider how the diaphragm properties are affected by the steel deck and the attached floor beams and girders.
Concrete moment frames	Stiffness properties can be taken from references such as Paulay and Priestley [1992]. The effects noted in Section ? for concrete elements should be accounted for. The bond slip and strain penetration of beam bars passing through beam-column joints can reduce stiffness.
Steel moment frames	Typically panel zone (beam-column joint) stiffness and the stiffness of column base conditions are the most uncertain items in the analysis. For deeper steel sections, beam and column shear deformations can reduce effective stiffness.
Steel braced frames: buckling-restrained braced frames, eccentric braced frames, concentric braced frames	For buckling-restrained braced frames, the frame contribution to stiffness usually is significant.

Input ground motions for tall buildings with subterranean levels

It is common practice to configure tall buildings with several levels below grade. Interaction between the soil, foundation, and structure is expected to affect significantly the character and intensity of the motion that is input to the superstructure. The issue is to define the input ground motions for tall buildings with subterranean levels considering this interaction.

Capacity design process

Tall buildings can be designed according to a two-stage process that follows the capacity-design approach and assesses seismic performance under severe earthquake ground motions. This is the design approach that has been used for non-prescriptive seismic designs of tall buildings [SEAONC 2007], and is recommended in this document for all tall buildings in high seismic zones.

The first stage of the process is to design the building to comply with all code provisions (except for identified exceptions such as the height limit). This means that the designated yielding elements of the building (e.g., flexural design of the core-wall hinge zone and the coupling beams) are designed for code-level demands including the code R factor. For tall buildings with long periods, this code-level demand typically is governed by minimum base shear requirements.

The second stage is to analyze the structure using a nonlinear response history analysis at the Maximum Considered Earthquake (MCE) level of ground motion. The

MCE level is currently defined in building codes to correspond to a 975-year return period in California and about a 2500-year return period elsewhere. The purpose of this analysis is to:

- Verify that the expected seismic behavior of the structure is governed by the intended mechanism, with nonlinear behavior occurring only in the designated structural elements
- Verify that all other potential mechanisms and actions remain essentially elastic. Where evaluating actions designed to remain elastic, the design should consider the dispersion of the analysis results, rather than just the average response. Record-to-record variability is often the largest source of dispersion in analysis results, but other assumptions that are uncertain and have a large effect on the resulting design should also be considered.

Bibliography of Recent Multiple-Degree-of-Freedom Modeling Research

This appendix provides a bibliography of recent research that is of particular relevance to the topic of multiple-degree-of-freedom modeling. The citations are organized topically and chronologically, and cover relevant research published since 2002.

The focus of the literature review was improvements to nonlinear static procedures, simplified dynamic analysis procedures, and applications to flexible diaphragm systems, high damping systems, and torsionally irregular systems. Earthquake engineering abstracts were searched for publications containing the phrases "pushover" or "NSP" or the combination "simpl*," "dynamic", and "analysis." This search yielded approximately 1800 unique abstracts. Each was reviewed, and approximately 1 in 6 was judged to be of possible relevance to the project. Additional references of interest known to the project team were also included.

H.1 Pushover Methods of Analysis

H.1.1 General Features/Observations

Title: Do we really need inelastic dynamic analysis?
Author: Elnashai, Amr S.
Source: Journal of Earthquake Engineering. Vol. 6, no. Special Issue 1, pp. 123-130. 2002
Descriptors Nonlinear static analysis; Nonlinear dynamic pushover analysis; Hyogoken-Nanbu earthquake; Kobe; Japan; Jan. 17; 1995; multistory reinforced concrete structures

Abstract: The paper examines the requirements for inelastic static and dynamic analysis applied to earthquake design and assessment. Conventional pushover, with various load distributions, as well as advanced adaptive concepts are examined and compared to incremental dynamic analysis. Regions of applicability of each are discussed and suggestions regarding which method is better suited under a given set of conditions are qualitatively made. It is concluded that there will always be a class of structure-input motion pairs where inelastic dynamic analysis is necessary. Future developments should aim at reducing the regions where dynamic analysis is needed, hence static analysis may be used with confidence in other cases.

Title: Structural analysis in earthquake engineering: a breakthrough of simplified non-linear methods
Author: Fajfar, P
Source: The Twelfth European Conference on Earthquake Engineering [Proceedings] [electronic resource] , pp. 20 pages. 2002
Descriptors: Mathematical models; Earthquake engineering; Displacement; Spectra; Structural analysis; Capacity; Similarity; Resources; Approximation; Seismic phenomena; Marketing; Asymmetry; Draft; Statics; Demand; Nonlinearity; Standards; Randomness; Equivalence

Abstract: Structural response to strong earthquake ground motion cannot be accurately predicted due to large uncertainties and the randomness of structural properties and ground motion parameters. Consequently, excessive sophistication in structural analysis is not warranted. For the time being, the most rational analysis and performance evaluation methods for practical applications seem to be simplified nonlinear procedures, which combine the nonlinear static (pushover) analysis of a relatively simple mathematical model and the response spectrum approach. In recent years, a breakthrough of these procedures has been observed. They have been implemented into modern guidelines and codes. This paper discusses such procedures. After a brief overview of the methods, the major attention is focused on the N2 method, which has been implemented into the recent draft of the Eurocode 8 standard. The theoretical background of the extended version of the method, which can be applied for asymmetric structures, is presented. The similarities and differences between different methods, the determination of target displacement in the capacity spectrum method, the problems related to the application of simplified methods to analysis of 3D models, the approximations and limitations of the simplified inelastic methods, and direct displacement-based design are discussed. Although different methods may yield in many cases similar results, they differ with respect to simplicity, transparency and clarity of theoretical background. The most important difference is related to the determination of displacement demand. The use of inelastic spectra is considered to be more appropriate than the use of highly damped equivalent elastic spectra.

Title: Advantages and limitations of adaptive and non-adaptive force-based pushover procedures
Author: Antoniou, S; Pinho, R
Source: Journal of Earthquake Engineering. Vol. 8, no. 4, pp. 497-522. July 2004
Descriptors: Seismic engineering; Buildings; Dynamic tests; Earthquake design; Reinforced concrete; Vibration; Stiffness

Abstract: The recent drive for use of performance-based methodologies in design and assessment of structures in seismic areas has significantly increased the demand for the development of reliable nonlinear inelastic static pushover analysis tools. As a result, the recent years have witnessed the introduction of the so-called adaptive pushover methods, which, unlike their conventional pushover counterparts, feature

the ability to account for the effect that higher modes of vibration and progressive stiffness degradation might have on the distribution of seismic storey forces. In this paper, the accuracy of these forcebased adaptive pushover methods in predicting the horizontal capacity of reinforced concrete buildings is explored, through comparison with results from a large number of nonlinear time-history dynamic analyses. It is concluded that, despite its apparent conceptual superiority, current force-based adaptive pushover features a relatively minor advantage over its traditional non-adaptive equivalent, particularly in what concerns the estimation of deformation patterns of buildings, which are poorly predicted by both types of analysis.

Title: Assessment of current nonlinear static procedures for seismic evaluation of buildings
Author: Kalkan, Erol; Kunnath, Sashi K
Affiliation: Department of Civil and Environmental Engineering, University of California, Davis, CA 95616, United States
Source: Engineering Structures. Vol. 29, no. 3, pp. 305-316. Mar. 2007

Abstract: An essential and critical component of evolving performance-based design methodologies is the accurate estimation of seismic demand parameters. Nonlinear static procedures (NSPs) are now widely used in engineering practice to predict seismic demands in building structures. While seismic demands using NSPs can be computed directly from a site-specific hazard spectrum, nonlinear time-history (NTH) analyses require an ensemble of ground motions and an associated probabilistic assessment to account for aleatoric variability in earthquake recordings. Despite this advantage, simplified versions of NSP based on invariant load patterns such as those recommended in ATC-40 and FEMA-356 have well-documented limitations in terms of their inability to account for higher mode effects and the modal variations resulting from inelastic behavior. Consequently, a number of enhanced pushover procedures that overcome many of these drawbacks have also been proposed. This paper investigates the effectiveness of several NSPs in predicting the salient response characteristics of typical steel and reinforced concrete (RC) buildings through comparison with benchmark responses obtained from a comprehensive set of NTH analyses. More importantly, to consider diverse ground motion characteristics, an array of time-series from ordinary far-fault records to near-fault motions having fling and forward directivity effects was employed. Results from the analytical study indicate that the Adaptive Modal Combination procedure predicted peak response measures such as inter-story drift and component plastic rotations more consistently than the other NSPs investigated in the study.

H.1.2 Target Displacement

Title: Statistics of single-degree-of-freedom estimate of displacement for pushover analysis of buildings
Author: Chopra, Anil K; Goel, Rakesh K; Chintanapakdee, Chatpan
Source: Journal of Structural Engineering. Vol. 129, no. 4, pp. 459-469. 2003

Descriptors: Displacement; Roofs; Buildings; Ductility; Marketing; Demand; Dispersion; Statistics; Frames; Deformation; Gravitation; Approximation; Expenses; Guidelines

Abstract: The basic premise that the roof displacement of a multistory building can be determined from the deformation of a single degree-of-freedom (SDF) system is investigated. The responses of both systems are determined rigorously by nonlinear response history analysis, without introducing any of the approximations underlying the simplified methods for estimating the deformation of a SDF system (see, e.g., FEMA 273 or ATC-40 guidelines). The statistics of the SDF system estimate of roof displacement are presented for a variety of generic frames and six SAC buildings subjected to ground motion ensembles. Data obtained for generic frames indicate that the first "mode" SDF system overestimates the median roof displacement for systems subjected to large ductility demand, but underestimates for small ductility demand. The bias and dispersion tend to increase for longer period systems for every value of ductility demand. Similar data for SAC buildings demonstrate that the bias and dispersion on the SDF estimate of roof displacement increases when P-delta effects (due to gravity loads) are included. The modal pushover analysis procedure has the advantage of reducing the dispersion in the roof displacement and the underestimation of the median roof displacement for elastic or nearly elastic cases at the expense of increasing slightly the overestimate of roof displacement of buildings responding far into the inelastic range.

Title: Inelastic spectra for infilled reinforced concrete frames

Author: Dolsek, Matjaz; Fajfar, Peter

Source: Earthquake Engineering & Structural Dynamics. Vol. 33, no. 15, pp. 1395-1416. Dec. 2004

Descriptors: Ductility; Frames; Reinforced concrete; Displacement; Dynamic structural analysis; Structural members; Earthquake engineering

Abstract: In two companion papers a simplified non-linear analysis procedure for infilled reinforced concrete frames is introduced. In this paper a simple relation between strength reduction factor, ductility and period (R- μ -T relation) is presented. It is intended to be used for the determination of inelastic displacement ratios and of inelastic spectra in conjunction with idealized elastic spectra. The R- μ -T relation was developed from results of an extensive parametric study employing a SDOF mathematical model composed of structural elements representing the frame and infill. The structural parameters, used in the proposed R- μ -T relation, in addition to the parameters used in a usual (e.g. elasto-plastic) system, are ductility at the beginning of strength degradation, and the reduction of strength after the failure of the infills. Formulae depend also on the corner periods of the elastic spectrum. The proposed equations were validated by comparing results in terms of the reduction factors, inelastic displacement ratios, and inelastic spectra in the acceleration-displacement format, with those obtained by non-linear dynamic analyses for three sets of recorded and semi-artificial ground motions. A new approach was used for

generating semi-artificial ground motions compatible with the target spectrum. This approach preserves the basic characteristics of individual ground motions, whereas the mean spectrum of the whole ground motion set fits the target spectrum excellently. In the parametric study, the R- μ -T relation was determined by assuming a constant reduction factor, while the corresponding ductility was calculated for different ground motions. The mean values proved to be noticeably different from the mean values determined based on a constant ductility approach, while the median values determined by the different procedures were between the two means. The approach employed in the study yields a R- μ -T relation which is conservative both for design and performance assessment (compared with a relation based on median values).

Title: Inelastic displacement ratios of degrading systems
Author: Chenouda, M; Ayoub, A
Source: Journal of Structural Engineering , no. 6, pp. 1030-1045. June 2008
Descriptors: Displacement; Seismic analysis; Degradation; Hysteresis; Nonlinear response; Inelasticity; Seismic phenomena; Seismic engineering; Earthquake design; Mathematical models; Dynamical systems; Dynamics; Collapse; Excitation; Design engineering; Nonlinearity; Dynamic structural analysis; Demand analysis; Performance evaluation

Abstract: Seismic code provisions in several countries have recently adopted the new concept of performance-based design. New analysis procedures have been developed to estimate seismic demands for performance evaluation. Most of these procedures are based on simple material models though, and do not take into account degradation effects, a major factor influencing structural behavior under earthquake excitations. More importantly, most of these models cannot predict collapse of structures under seismic loads. This study presents a newly developed model that incorporates degradation effects into seismic analysis of structures. A new energy-based approach is used to define several types of degradation effects. The model also permits collapse prediction of structures under seismic excitations. The model was used to conduct extensive statistical dynamic analysis of different structural systems subjected to a large ensemble of recent earthquake records. The results were used to propose approximate methods for estimating maximum inelastic displacements of degrading systems for use in performance-based seismic code provisions. The findings provide necessary information for the design evaluation phase of a performance-based earthquake design process, and could be used for evaluation and modification of existing seismic codes of practice.

Title: Enhanced displacement coefficient method for degrading multi-degree- of-freedom systems
Author: Emrah Erduran¹ and Sashi K. Kunnath
Source: Earthquake Spectra Volume 26, Issue 2, pp. 311-326 (May 2010)

Abstract: The displacement coefficient method proposed in FEMA 440 was evaluated using response statistics from a comprehensive set of nonlinear simulations of multi degree of freedom systems under both far-fault and near-fault ground motions. The study finds that it is practically difficult to achieve high relative strength factors (R values equal to or greater than 6.0) for very stiff systems thereby dictating the need to define R-dependent demand coefficients. The approximate expressions proposed in FEMA 440 for the C2 coefficient is shown to underestimate the displacement demand of stiffness-degrading short period systems. Additional nonlinear simulations were performed to investigate the combined effect of strength degradation and P-Delta effects on the displacement demands of MDOF systems. A new expression for the modification factor that reflect combined P-Delta and degrading effects for the estimation of displacement demands is proposed.

H.1.3 Load Vectors and Methods

Single vector (invariant) approaches

Title: A "new" multimode load pattern for pushover analysis: the effect of higher modes of vibration
Author: Almeida, R; Carneiro-Barros, R
Source: Earthquake Resistant Engineering Structures IV , pp. 3-13. 2003
Descriptors: Vibration; Seismic phenomena; Nonlinear dynamics; Earthquake engineering

Abstract: The effect of the higher modes of vibration on the total nonlinear dynamic response of a structure is a very important and unsolved problem. To simplify the process the static nonlinear pushover analysis was proposed associated with the capacity spectrum method, utilizing a load pattern proportional to the shape of the fundamental mode of vibration of the structure. The results of the pushover analysis, with this load pattern, are very accurate for structures that respond primarily in the fundamental mode. However, when the higher modes of vibration become important for the total response of the structure, this load pattern loses its accuracy. To minimize this problem a "new" multimode load pattern is proposed, based on the relative participation of each mode of vibration in the elastic response of a structure subjected to an earthquake ground motion.

Title: Application of the simplified nonlinear - N2 method for some common types of RC structures
Author: Fischinger, M; Isakovic, T; Kante, P
Source: Skopje Earthquake: 40 Years of European Earthquake Engineering, SE 40EEE [Proceedings] [electronic resource] , pp. 8 pages. 2003
Descriptors: Earthquake engineering; Reinforced concrete; Bridges (structures); Walls; Resources; Slovenia; Seismic phenomena; Statics; Buildings

Abstract: The nonlinear N2 method, which was developed by the Institute of Structural Engineering, Earthquake Engineering and Construction IT (IKPIR) at the

University of Ljubljana, Slovenia, was included in the latest version of Eurocode 8. The method, which combines the nonlinear static (pushover) analysis and the response spectrum approach, was successfully applied in the blind prediction of the response of a cantilever wall as well as in the parametric study of idealized buildings with structural walls. It has been also used for the nonlinear analysis of reinforced concrete bridges. The N2 method proved to be a very efficient tool for the analysis of the majority of the structures considered in this paper, except for some types of irregular bridges. However, N2, as well as all similar pushover-based procedures, should not be uncritically used. One should take into account specific problems regarding each specific type of structure and, if necessary, modify the method appropriately.

Title: Review of the development of the Capacity Spectrum Method
Author: Freeman, Sigmund A
Source: ISET Journal of Earthquake Technology. Vol. 41, no. 1, pp. 1-13. Mar. 2004
Descriptors: Buildings; Spectral lines; Stockpiling; Earthquake design; Seismic phenomena; Amplitudes; Viscous damping

Abstract: The Capacity Spectrum Method (CSM), a performance-based seismic analysis technique, can be used for a variety of purposes such as rapid evaluation of a large inventory of buildings, design verification for new construction of individual buildings, evaluation of an existing structure to identify damage states, and correlation of damage states of buildings to various amplitudes of ground motion. The procedure compares the capacity of the structure (in the form of a pushover curve) with the demands on the structure (in the form of response spectra). The graphical intersection of the two curves approximates the response of the structure. In order to account for non-linear inelastic behavior of the structural system, effective viscous damping values are applied to linear-elastic response spectra similar to inelastic response spectra. The paper summarizes the development of the CSM from the 1970s to the present and includes discussions on modifications presented by other researchers, as well as recommendations by the author.

Title: A Penultimate Proposal of Equivalent Damping Values for the Capacity Spectrum Method
Author: Freeman, Sigmund A
Source: 100th Anniversary Earthquake Conference. 2006
Descriptors: Hysteresis; Spectra; Earthquake dampers; Seismic phenomena; Damping capacity

Abstract: The Capacity Spectrum Method (CSM), by means of a graphical procedure, compares the capacity of the structure, represented by a nonlinear equivalent force-displacement curve sometimes referred to as a pushover curve, with the demands of earthquake ground motion, represented by response spectra. Whereas a 5 percent damped spectrum is generally used to represent linear-elastic response, higher percentages of damping are used to imitate inelastic response spectra. There

had been a school of thought that felt the surrogate damping values should be directly linked to hysteretic damping based on energy loss due to hysteretic cyclic behavior. When this method is used, the resulting inelastic reduction factors appear to most researchers to be too large. In order to compensate for this concern, adjustments were made and the results were presented in the Applied Technology Council (ATC) publication ATC-40. Since its publication, ATC-40 has created many ensuing interesting discussions and debates that led to substantial research and discussion on the merits of inelastic response spectra and equivalent (surrogate) damped spectra and on the appropriateness of using damped spectra to represent inelastic response, the latest being the ATC study published as FEMA 440. Although the conclusions of researchers do not appear to be wholly consistent with each other, a comparative study presented in this paper gives the hope that a consensus can be reached that can reasonably be accepted as a design and evaluation guideline.

Title: Evaluation of seismic performance of multistory building structures based on the equivalent responses
Author: Lee, Dong-Guen; Choi, Won-Ho; Cheong, Myung-Chae; Kim, Dae-Kon
Source: Engineering Structures. Vol. 28, no. 6, pp. 837-856. May 2006
Descriptors: Seismic phenomena; Seismic engineering; Earthquake construction; Seismic response; Earthquake design; Performance evaluation; Equivalence; Mathematical analysis; Seismic design; Displacement; Architecture; Coefficients

Abstract: The prediction of inelastic seismic responses and the evaluation of seismic performance of a building structure are very important subjects in performance-based seismic design. Currently, the inelastic time history analysis method and the pushover analysis method such as the displacement coefficient method (FEMA-273) and the capacity spectrum method (ATC-40) can be adapted to evaluate the seismic performance of a building structure. However, the pushover analysis methods have some drawbacks in estimating the accurate inelastic seismic responses. In this study, an improved analytical method based on the equivalent responses of multistory building structures is proposed to estimate the inelastic seismic responses efficiently and accurately. The proposed method can be used to accurately evaluate the seismic performance not only for the global inelastic behavior of a building but also for its local inelastic seismic responses. In order to demonstrate the accuracy and validity of the proposed method, inelastic seismic responses estimated by the proposed method are compared with those obtained from other existing methods. When the proposed method is applied in the pushover analysis more improved analytical results could be obtained than those from the conventional capacity spectrum method (CSM).

Title: A mathematical basis for the convergence of the capacity spectrum method by Y. Y. Lin et al., Earthquake Engineering and Structural Dynamics 2004; 33(9):1059-1066
Author: Yang, Dixiong; Li, Gang

Source: Earthquake Engineering & Structural Dynamics. Vol. 35, no. 8, pp. 1051-1052. 10 July 2006

Descriptors: Iterative methods; Seismic phenomena; Dynamic structural analysis; Earthquake engineering; Linearization

Abstract: The above-referenced paper established an iterative procedure of simplified capacity spectrum method (CSM) in ATC-40, and applied the fixed point concept to analyse the reason of convergent failure of iteration scheme derived from the equivalent linearization of inelastic SDOF system in the CSM. Nevertheless, the analysis only limited to the convergent and divergent solution, but neglected the periodic oscillation of solution in the other references. Furthermore, the identified criterion for the convergence of iterative map was used inappropriately.

Title: A lateral load pattern considering higher modes influence in push-over analysis.

Author: Sun, Guo-Hua; He, Ruo-Quan; Gao, Xiao-Ying

Source: Beijing Gongye Daxue Xuebao (Journal of Beijing University of Technology). Vol. 33, no. 6, pp. 587-591. June 2007

Descriptors: Mathematical models; Force distribution; Seismic phenomena; Fittings; Nonlinear dynamics; Architecture; Drift; Nonlinearity; Sun; Earthquake design; Dynamic tests; Civil engineering; Soil (material); Structural steels; Stiffness; Earthquake engineering; Frames; Lateral loads

Abstract: Push-over method couldn't reflect the higher modes' influence on high-rise structure. Based on some important factors, such as story weight, story stiffness, mode participation ratio, etc., this paper developed a simple fixed lateral force distribution model, which the effect of higher modes can be considered. In this paper, through fitting beta spectrum for the third soil site, ten earthquake records were selected, and four moment-resisting steel frames were designed to analyze the push-over procedure and dynamic nonlinear time history procedure. Moreover, according to the index of story drift ratio, an improved fixed lateral force distribution was demonstrated.

Title: On the design and evaluation of seismic response of RC buildings according to direct displacement-based design approach

Author: Benedetti, A; Landi, L; Malavolta, D

Source: 14th World Conference on Earthquake Engineering: Innovation Practice Safety. 2008

Descriptors: Reinforced concrete; Frames; Earthquake design; Seismic phenomena; Seismic response; Displacement; Seismic engineering; Buildings; Planes; Nonlinear dynamics; Methodology

Abstract: This paper describes a research work on the evaluation of seismic response of reinforced concrete frames designed according to Direct Displacement-Based Design (DDBD) approach. A group of plane RC frames, characterized by a variable number of storeys, was designed by means of this methodology. Then, seismic performance of designed frames was studied by carrying out pushover and non-linear

dynamic analyses. Results of analyses were compared with the seismic behavior expected from design. Some evaluations are also made on the differences between DDBD and more traditional force-based design procedures.

Title: An alternative pushover analysis procedure to estimate seismic displacement demands
Author: Kim, Sun-Pil; Kurama, Yahya C
Source: Engineering Structures. Vol. 30, no. 12, pp. 3793-3807. Dec. 2008
Descriptors: Seismic phenomena; Demand analysis; Marketing; Displacement; Estimates; Seismic engineering; Earthquake construction; Earthquake design; Roofs; Invariants; Seismic response; Nonlinear dynamics; Grounds; Nonlinearity; Frame structures; Design engineering; Structural steels; Force distribution; Benchmarking

Abstract: An alternative pushover analysis procedure is proposed to estimate the peak seismic lateral displacement demands for building structures responding in the nonlinear range. As compared with other pushover analysis procedures, the main advantage of the proposed procedure is that the effects of higher modes on the lateral displacement demands are lumped into a single invariant lateral force distribution that is proportional to the total seismic masses at the floor and roof levels. The applicability and validity of the proposed procedure, which is referred to as the Mass Proportional Pushover (MPP) procedure, are critically evaluated through comparisons with multi-degree-of-freedom nonlinear dynamic time-history analysis results for a set of benchmarked three-story, nine-story, and twenty-story steel moment resisting building frame structures. The estimated demands are also compared with results from a Modal Pushover Analysis (MPA) procedure. The comparisons demonstrate that the proposed Mass Proportional Pushover procedure provides, on average, better roof and floor lateral displacement demand estimates than the Modal Pushover Analysis procedure. The improvement from the proposed procedure is larger for the nine-story and twenty-story structures than the improvement for the three-story structure and is also larger for the Design Basis Earthquake (DBE) ground motion set than the Maximum Considered Earthquake (MCE) set.

Title: Non linear analysis of structures according to new European design code
Author: Mestrovic, D; Cizmar, D; Pende, M
Source: 14th World Conference on Earthquake Engineering: Innovation Practice Safety. 2008
Descriptors: Mathematical models; Seismic phenomena; Mathematical analysis; Earthquake design; Limit states; Seismic response; Spectrum analysis; Demand; Nonlinearity; Seismic engineering; Marketing; Design engineering; Earthquake engineering; Collapse; Oscillations; Computer simulation; Format; Degrees of freedom; Planes

Abstract: Structures designed in seismically active regions must comply with two basic demands: first, structure must be designed for loads during usage (ultimate limit

state and serviceability limit state) and second, structure must be sound enough to avoid collapse during earthquake (ultimate limit state). Except from linear-elastic calculations, very often are used non-linear methods. In this article simple plain frame concrete structure will be analyzed using N2 method from Eurocode 8 (EN 1998-1:2004). N2 is simple non-linear method used for calculation of structures during earthquakes. It combines multi degree pushover analysis with spectrum analysis of equivalent single degree of freedom (SDOF) system. It is formulated in acceleration-displacement format, which is very suitable for visual overview of basic variables that account for seismic response of the structure. N2 method can be considered as combination of pushover analysis and spectrum analysis. Inelastic demand spectrum is obtained from elastic spectrum. Results obtained are accurate enough if structure has dominant first mode of oscillation. For now, it is used only for plane structures. This paper will give numerical example of N2 method. It is concluded that inelastic structural response is crucial in earthquake engineering. Modern methods, supported with usage of computers and strict design codes ensure better understanding of structural response during earthquakes and at the same time seismic resistant structures.

Multimode (Invariant) Pushovers

Title: A modal pushover analysis procedure for estimating seismic demands for buildings
Author: Chopra, Anil K.; Goel, Rakesh K.
Source: Earthquake Engineering & Structural Dynamics. Vol. 31, no. 3, pp. 561-582. Mar. 2002
Descriptors: SAC Joint Venture; Los Angeles; Southern California; Multistory steel moment-resisting frames; modal pushover analysis; Nonlinear analysis; Story drift; Performance-based earthquake engineering

Abstract: This paper develops an improved pushover analysis procedure based on structural dynamics theory, which retains the conceptual simplicity and computational attractiveness of current procedures with invariant force distribution. In this modal pushover analysis (MPA), the seismic demand due to individual terms in the modal expansion of the effective earthquake forces is determined by a pushover analysis using the inertia force distribution for each mode. Combining these "modal" demands due to the first two or three terms of the expansion provides an estimate of the total seismic demand on inelastic systems. When applied to elastic systems, the MPA procedure is shown to be equivalent to standard response spectrum analysis (RSA). When the peak inelastic response of a 9-storey steel building determined by the approximate MPA procedure is compared with rigorous nonlinear response history analysis, it is demonstrated that MPA estimates the response of buildings responding well into the inelastic range to a similar degree of accuracy as RSA in estimating peak response of elastic systems. Thus, the MPA procedure is accurate enough for practical application in building evaluation and design.

Title: A pushover procedure for tall buildings
Author: A. S. Moghadam, W. K Tso
Source: *Proceedings of the 12th European Conference on Earthquake Engineering*, London, UK, Paper 395, 2002.

Abstract: Pushover analysis has been chosen as the preferred method for seismic evaluation of structures by most rehabilitation guidelines and codes. The method usually results in reasonable estimation of seismic responses for lowrise buildings. However, its application to tall buildings mostly leads to unsatisfactory results. Some methods in the literature have been proposed to resolve the problem. They may help to identify failure mechanisms in some cases; but, in general, they cannot provide an estimation of the seismic responses and their distribution in the building. To address the effects of higher modes in responses of tall buildings, a method is developed that estimates the maximum seismic responses by combining the results of pushover analyses. To demonstrate the application of the method, it is applied to a 20-story building. The results show that the proposed procedure is a promising method for extending the pushover procedure to tall buildings.

Title: Evaluation of a modified MPA procedure assuming higher modes as elastic to estimate seismic demands
Author: Chopra, Anil K; Goel, Rakesh K; Chintanapakdee, Chatpan
Source: *Earthquake Spectra*. Vol. 20, no. 3, pp. 757-778. Aug. 2004
Descriptors: Seismic phenomena; Computation; Vibration mode; Earthquake dampers; Spectra; Frames; Structural engineering

Abstract: The modal pushover analysis (MPA) procedure, which includes the contributions of all significant modes of vibration, estimates seismic demands much more accurately than current pushover procedures used in structural engineering practice. Outlined in this paper is a modified MPA (MMPA) procedure wherein the response contributions of higher vibration modes are computed by assuming the building to be linearly elastic, thus reducing the computational effort. After outlining such a modified procedure, its accuracy is evaluated for a variety of frame buildings and ground motion ensembles. Although it is not necessarily more accurate than the MPA procedure, the MMPA procedure is an attractive alternative for practical application because it leads to a larger estimate of seismic demands, improving the accuracy of the MPA results in some cases (relative to nonlinear response history analysis) and increasing their conservatism in others. However, such conservatism is unacceptably large for lightly damped systems, with damping significantly less than 5%. Thus the MMPA procedure is not recommended for such systems.

DOI:10.1193/1.1775237

Title: Method of modal combinations for pushover analysis of buildings
Author : Kalkan, Erol; Kunnath, Sashi K
Source: 13 WCEE: 13th World Conference on Earthquake Engineering Conference Proceedings. 2004

Descriptors: Seismic phenomena; Buildings; Earthquake construction; Force distribution; Dynamic characteristics

Abstract: Nonlinear static procedures (NSP) are finding widespread use in performance based seismic design since it provides practitioners a relatively simple approach to estimate inelastic structural response measures. However, conventional NSPs using lateral load patterns recommended in FEMA-356 do not adequately represent the effects of varying dynamic characteristics during the inelastic response or the influence of higher modes. To overcome these drawbacks, some improved procedures have recently been proposed by several researchers. A method of modal combinations (MMC) that implicitly accounts for higher mode effects is investigated in this paper. MMC is based on invariant force distributions formed from the factored combination of independent modal contributions. The validity of the procedure is validated by comparing response quantities such as inter-story drift and member ductility demands using other pushover methods and also the results of nonlinear time history analyses. The validation studies are based on evaluation of three existing steel moment frame buildings: two of these structures were instrumented during the Northridge earthquake thereby providing realistic support motions for the time-history predictions. Findings from the investigation indicate that the method of modal combinations provides a basis for estimating the potential contributions of higher modes when determining inter-story drift demands and local component demands in multistory frame buildings subjected to seismic loads.

Title: Identification of modal combination for nonlinear static analysis of building structures,
Author: S.K. Kunnath
Source: *Computer-Aided Civil and Infrastructure Engineering*, 19, 246-259, 2004.

Abstract: An essential requisite in performance-based seismic design is the estimation of inelastic deformation demands in structural members. An increasingly popular analytical method to establish these demand values is a "pushover" analysis in which a model of the building structure is subjected to an invariant distribution of lateral forces. Although such an approach takes into consideration the redistribution of forces following yielding of sections, it does not incorporate the effects of varying dynamic characteristics during the inelastic response. Simple modal combination schemes are investigated in this article to indirectly account for higher mode effects. Because the modes that contribute to deformations may be different from the modes that contribute to forces, it is necessary to identify unique modal combinations that provide reliable estimates of both force and deformation demands. The proposed procedure is applied to typical moment frame buildings to assess the effectiveness of the methodology. It is shown that the envelope of demands obtained from a series of nonlinear static analysis using the proposed modal-combination-based lateral load patterns results in better estimation of inter-story drift, a critical parameter in seismic evaluation and design.

Title: Extension of modal pushover analysis to compute member forces
Author: Goel, Rakesh K; Chopra, Anil K
Source: Earthquake Spectra. Vol. 21, no. 1, pp. 125-139. Feb. 2005
Descriptors: Seismic phenomena; Earthquake construction; Buildings; Error analysis; Computation; Force distribution; Spectrum analysis

Abstract: This paper extends the modal pushover analysis (MPA) procedure for estimating seismic deformation demands for buildings to compute member forces. Seismic demands are computed for six buildings, each analyzed for 20 ground motions. A comparison of seismic demands computed by the MPA and nonlinear response history analysis (RHA) demonstrates that the MPA procedure provides good estimates of the member forces. The bias (or error) in forces is generally less than that noted in earlier investigations of story drifts and is comparable to the error in the standard response spectrum analysis (RSA) for elastic buildings. The four FEMA-356 force distributions, on the other hand, provide estimates of member forces that may be one-half to one-fourth of the value from nonlinear RHA.

Title: Role of higher-"Mode" pushover analyses in seismic analysis of buildings
Author: Goel, Rakesh K; Chopra, Anil K
Source: Earthquake Spectra. Vol. 21, no. 4, pp. 1027-1041. Nov. 2005
Descriptors: Buildings; Seismic phenomena; Earthquake construction; Spectra

Abstract: The role of higher-"mode" pushover analyses in seismic analysis of buildings is examined in this paper. It is demonstrated that the higher-"mode" pushover curves reveal plastic hinge mechanisms that are not detected by the first-"mode" or other FEMA-356 force distributions, but these purely local mechanisms are not likely to develop during realistic ground motions in an otherwise regular building without a soft and/or weak story. Furthermore, the conditions necessary for "reversal" of a higher-"mode" pushover curve are examined. It is shown that "reversal" in a higher-"mode" pushover curve occurs after formation of a mechanism if the resultant force above the bottom of the mechanism is in the direction that moves the roof in a direction opposite to that prior to formation of the mechanism. Such "reversal" can occur only in higher-"mode" pushover analyses but not in the pushover analyses for the first-"mode" or other FEMA-356 force distributions. However, the "reversal" in higher-"mode" pushover curves was found to be very rare in several recent investigations that examined behavior of many moment-resisting frame buildings. Included are guidelines for implementing the Modal Pushover Analysis for buildings that display "reversal" in a higher-"mode" pushover curve.

Title: Studies on and improvements in modal pushover analysis.
Author: Mao, Jianmeng; Xie, Lili; Zhai, Changhai
Source: Dizhen Gongcheng yu Gongcheng Zhendong/Earthquake Engineering and Engineering Vibration. Vol. 26, no. 6, pp. 50-55. Nov.-Dec. 2006
Descriptors: Earthquake engineering; Seismic phenomena; Vibration; Inertia

Abstract : Because the traditional pushover analysis can not take the contributions of higher modes into account, it is difficult to apply this method to high-rise structures. To overcome this limitation, a modal pushover analysis procedure (MPA) is proposed by some researchers, which can involve the combination of multi-mode contributions to response. In this paper, much improvement on MPA procedure is made with consideration of the redistribution of inertia forces after structural yielding. The method is verified by one example. It is concluded that the method presented in this paper has higher accuracy than MPA procedure.

Title: Evaluation of the MPA procedure for estimating seismic demands: RC-SMRF buildings
Author: Bobadilla, Hugo; Chopra, Anil K
Source: Earthquake Spectra. Vol. 24, no. 4, pp. 827-845. Nov. 2008
Descriptors: Buildings; Seismic phenomena; Demand; Seismic engineering; Earthquake construction; Marketing; Estimating; Grounds; Hysteresis; Deformation; Seismic response; Nonlinearity; Excitation; Accuracy; Construction; Reinforced concrete; Deterioration; Computation; Stiffness

Abstract: The modal pushover analysis (MPA) procedure is extended for analysis of reinforced concrete special moment resisting frame (RC-SMRF) buildings, after demonstrating that the theory, assumptions, and approximations underlying this procedure are valid for such systems. The principal extension of the procedure is in the hysteretic model for modal SDF systems, chosen as the peak-oriented model to represent the global monotonic and cyclic behavior of such buildings, characterized by deterioration of stiffness and strength under cyclic deformation. The median seismic demands for 4-, 8-, 12-, and 20-story RC-SMRF buildings-designed to comply with current codes-due to an ensemble of 78 ground motions scaled to four intensity levels were computed by MPA and nonlinear RHA, and compared. It is demonstrated that, even for the most intense ground motions that deform the buildings far into the inelastic range, the MPA procedure demonstrates an adequate degree of accuracy that should make it useful for practical application in estimating seismic demands for RC-SMRF buildings. In contrast the FEMA-356 force distributions are inadequate in estimating seismic demands for the 8-, 12-, and 20-story buildings at all excitation intensities, from the weakest that causes response essentially within the linearly elastic range, to the strongest that drives the buildings far into the inelastic range.

Title: Approximate modal analysis of multistory symmetrical buildings with restricted inelasticity
Author: Georgoussis, George K
Source: Structural Design of Tall and Special Buildings. Vol. 17, no. 2, pp. 313-330. June 2008
Descriptors: Dynamical systems; Nonlinear dynamics; Cantilever beams; Nonlinearity; Mathematical models; Joining; Decomposition; Equivalence; Approximation; Seismic phenomena; Education;

Elastic constants; Buildings; Excitation; Planes; Dynamics;
Earthquake construction; Dynamic mechanical properties; Ductility

Abstract: Simplified capacity curves are presented for modal decomposition of multistory inelastic cantilever bents. These structural systems are uniform over the height and plasticity is assumed to be restricted into the beams, since significant rotation ductility factors may be attained in these members without loss of strength. The approximate method of modal decomposition of multistory inelastic bents is based on the concept that the total response may be obtained from the contributions of equivalent nonlinear single-degree-of-freedom (SDOF) modal systems, in combination with the technique of modal superposition. In particular, the contribution of the first mode equivalent inelastic SDOF system is examined, since its modal contribution is of higher importance. The response of such SDOF systems basically depends on their capacity curve, which may be formulated by using the dynamic properties (frequency, effective modal mass and mode shape) of the initially elastic bent, as well as the corresponding properties of the bent when the entire set of coupling beams is assumed to be yielded. The procedure is presented for plane cantilever bents, but it can be easily extended to symmetrical structural systems composed of different types of inelastic bents. Its application is illustrated by means of a 10-story inelastic coupled-wall bent subject to a strong earthquake motion, equal to 1*5X El Centro N-S ground excitation, and the results compare well with those obtained from a step-by-step nonlinear time history analysis of the discrete member model.

Title: A consecutive modal pushover procedure for estimating the seismic demands of tall buildings
Author: Poursha, Mehdi; Khoshnoudian, Faramarz; Moghadam, A S
Source: Engineering Structures. Vol. 31, no. 2, pp. 591-599. Feb. 2009
Descriptors: Seismic phenomena; Seismic engineering; Chemical-mechanical polishing; Tall buildings; Earthquake construction; Marketing; Demand; Nonlinearity; Earthquake design; Estimating; Vibration mode; Seismic response; Tools; Low rise buildings; Estimates; Demand analysis; Design engineering; Special steels; Frames

Abstract: 1 for use in practical applications for building evaluation and design verification. The NSP is, however, restricted to single-mode response. It is therefore valid for low-rise buildings where the behaviour is dominated by the fundamental vibration mode. It is well recognized that the seismic demands derived from the conventional NSP are greatly underestimated in the upper storeys of tall buildings, in which higher-mode contributions to the response are important. This paper presents a new pushover procedure which can take into account higher-mode effects. The procedure, which has been named the consecutive modal pushover (CMP) procedure, utilizes multi-stage and single-stage pushover analyses. The final structural responses are determined by enveloping the results of multi-stage and single-stage pushover analyses. The procedure is applied to four special steel moment-resisting frames with different heights. A comparison between estimates from the CMP procedure and the

exact values obtained by nonlinear response history analysis (NL-RHA), as well as predictions from modal pushover analysis (MPA), has been carried out. It is demonstrated that the CMP procedure is able to effectively overcome the limitations of traditional pushover analysis, and to accurately predict the seismic demands of tall buildings.

Single-Vector Adaptive Pushovers

Title: Development and verification of a displacement-based adaptive pushover procedure
Author: Antoniou, S; Pinho, R
Source: Journal of Earthquake Engineering. Vol. 8, no. 5, pp. 643-661. Sept. 2004
Descriptors: Displacement; Adaptive structures; Earthquake engineering; Deformation; Dynamic tests; Reinforced concrete; Buildings

Abstract: In this paper, an innovative displacement-based adaptive pushover procedure, whereby a set of laterally applied displacements, rather than forces, is monotonically applied to the structure, is presented. The integrity of the analysis algorithm is verified through an extensive comparative study involving static and dynamic nonlinear analysis of 12 reinforced concrete buildings subjected to four diverse acceleration records. It is shown that the new approach manages to provide much improved response predictions, throughout the entire deformation range, in comparison to those obtained by force-based methods. In addition, the proposed algorithm proved to be numerically stable, even in the highly inelastic region, whereas the additional modelling and computational effort, with respect to conventional pushover procedures, is negligible. This novel adaptive pushover method is therefore shown to constitute an appealing displacement-based tool for structural assessment, fully in line with the recently introduced deformation- and performance oriented trends in the field of earthquake engineering.

Title: A Displacement-based adaptive pushover for seismic assessment of steel and reinforced concrete buildings
Author: Pinho, R; Antoniou, S; Pietra, D
Source: 100th Anniversary Earthquake Conference. 2006
Descriptors: Seismic phenomena; Earthquake construction; Displacement; Adaptive structures; Buildings; Reinforced concrete; Damage accumulation

Abstract: A number of recent studies raised doubts on the effectiveness of conventional pushover methods, whereby a constant single-mode incremental force vector is applied to the structure, in estimating the seismic demand/capacity of framed buildings subjected to earthquake action. The latter motivated the recent development and introduction of the so-called Adaptive Pushover methods whereby the loading vector is updated at each analysis step, reflecting the progressive damage accumulation and resulting modification of the modal parameters, that characterise the structural response at increasing loading levels. Within such adaptive framework,

the application of a displacement, as opposed to force, incremental loading vector becomes not only feasible, since the latter is updated at each step of the analysis according to the current dynamic characteristics of the structure, but also very appealing, since inline with the present drive for development and code implementation of displacement or, more generally, deformation-based design and assessment methods. Further, such innovative displacement-based pushover algorithm seems to lead to superior response predictions, with little or no additional modelling and computational effort, with respect to conventional pushover procedures.

Title: Study on displacement-based pushover procedure.
Author: Wang, Mengfu; Wang, Rui
Source: Dizhen Gongcheng yu Gongcheng Zhendong (Earthquake Engineering and Engineering Vibration). Vol. 26, no. 5, pp. 73-80. Sept.-Oct. 2006
Descriptors: Displacement; Seismic phenomena; Shear; Walls; Adaptive structures; Deformation; Earthquake engineering; Frames; Algorithms; Assessments; Tools; Vibration; Nonlinear dynamics; Nonlinearity; Dynamic structural analysis; Civil engineering; Integrity; Trends

Abstract: In this paper, an innovative displacement-based adaptive pushover procedure, in which a set of laterally applied displacements, rather than forces, is monotonically applied to the structure, is presented. The integrity of the analysis algorithm is verified through an extensive comparative study involving static and dynamic nonlinear analysis of a 7-story frame shear wall structure and a 15-story frame shear wall structure. It is shown that the new approach manages to provide much improved response predictions throughout the entire deformation range, in comparison to those obtained by force-based methods. This novel adaptive pushover method is therefore shown to constitute an appealing displacement-based tool for structural assessment, fully in line with the recently introduced deformation- and performance-oriented trends in the field of earthquake engineering.

Title: On the distribution of lateral loads for pushover analysis
Author: Colajanni, P; Potenzzone, B
Source: 14th World Conference on Earthquake Engineering: Innovation Practice Safety. 2008
Descriptors: Assessments; Dynamic response; Invariants; Mathematical analysis; Vectors (mathematics); Models; Seismic phenomena; Benchmarking; Displacement; Seismic engineering; Criteria; Safes; Stress concentration; Adaptive structures; Mathematical models; Lateral loads; Modelling

Abstract: Two new simplified adaptive load patterns for pushover analyses are proposed, able to provide an accurate and on safe side assessment of the actual non linear dynamic response, by enveloping the results provided by using the two load vectors. Initially it will be shown how the input modelling can affect the assessment

of the response parameters in Non-Linear Response History Analysis (NRHA), which will be assumed as benchmark to judge the effectiveness of the proposed load patterns. Then, the two new load patterns are presented and their effectiveness in reproducing the results provided by NRHA are compared with those of invariant and adaptive load patterns suggested by seismic codes and proposed in literature, for two structures of different typologies. To this aim, criteria for choosing target displacement in POA are shortly discussed.

Title: An innovative adaptive pushover procedure based on storey shear
Author: Shakeri, Kazem; Shayanfar, Mohsen A
Source: 2008 Seismic Engineering Conference Commemorating the 1908 Messina and Reggio Calabria Earthquake Part Two (AIP Conference Proceedings Volume 1020, Part 2). Vol. 1020, pp. 1121-1126. 2008
Descriptors: Shear; Loads (forces); Dynamic mechanical properties; Structural steels; Dynamics; Civil engineering; Dynamic tests

Abstract: Since the conventional pushover analyses are unable to consider the effect of the higher modes and progressive variation in dynamic properties, recent years have witnessed the development of some advanced adaptive pushover methods. However in these methods, using the quadratic combination rules to combine the modal forces result in a positive value in load pattern at all storeys and the reversal sign of the modes is removed; consequently these methods do not have a major advantage over their non-adaptive counterparts. Herein an innovative adaptive pushover method based on storey shear is proposed which can take into account the reversal signs in higher modes. In each storey the applied load pattern is derived from the storey shear profile; consequently, the sign of the applied loads in consecutive steps could be changed. Accuracy of the proposed procedure is examined by applying it to a 20-storey steel building. It illustrates a good estimation of the peak response in inelastic phase.

Multimode Adaptive Pushovers

Title: An incremental response spectrum analysis procedure based on inelastic spectral deformation for multi-mode seismic performance evaluation
Author: M.N. Aydinoglu
Source: *Bulletin of Earthquake Engineering*, 1(1), 3-36, 2003.

Abstract: The so-called Nonlinear Static Procedure (NSP) based on pushover analysis has been developed in the last decade as a practical engineering tool to estimate the inelastic response quantities in the framework of performance-based seismic evaluation of structures. However NSP suffers from a major drawback in that it is restricted with a single-mode response and therefore the procedure can be reliably applied only to the two-dimensional response of low-rise, regular buildings. Recognizing the continuously intensifying use of the pushover-based NSP in the engineering practice, the present paper attempts to develop a new pushover analysis

procedure to cater for the multi-mode response in a practical and theoretically consistent manner. The proposed Incremental Response Spectrum Analysis (IRSA) procedure is based on the approximate development of the so-called modal capacity diagrams, which are defined as the backbone curves of the modal hysteresis loops. Modal capacity diagrams are used for the estimation of instantaneous modal inelastic spectral displacements in a piecewise linear process called pushover-history analysis. It is illustrated through an example analysis that the proposed IRSA procedure can estimate with a reasonable accuracy the peak inelastic response quantities of interest, such as story drift ratios and plastic hinge rotations as well as the story shears and overturning moments. A practical version of the procedure is also developed which is based on the code-specified smooth response spectrum and the well-known equal displacement rule.

Title: Modeling of higher-mode effects using an optimal multi-modal pushover analysis
Author: Attard, T; Fafitis, A
Source : Earthquake Resistant Engineering Structures V , pp. 405-414. 2005
Descriptors: Optimization; Buildings; Construction; Seismic phenomena; Vibration; Dynamic structural analysis

Abstract: An accurate optimal pushover analysis is developed to predict the higher-mode influence in multi degree of freedom (DOF) buildings. Performance levels are determined and seismic demands are calculated using two different ground acceleration records. The methodology is based on elastic structural dynamics theory and retains the simplicity of standard pushover procedures that rigorous time history analyses do not provide. A variant inertial load pattern is determined by updating the building's vibration properties at each stage of yielding. Each load pattern is derived using one mode shape at every yielding stage thereby capturing the higher-mode effects (HME). Using the energy under the building's capacity curve then enables a single optimal mode shape to be determined; this defines a representative single-DOF system (R-SDOF). Towards this end, an optimization algorithm is written to minimize the target displacement error between the pushover and nonlinear time-history analyses of a few buildings for a certain ground record. Optimal capacity and demand parameters are then determined and used to combine the individual mode shapes from each stage of yielding into the single optimal mode shape. This approach enables HME and phenomena such as HME and P-Delta effects to be captured through the optimal parameter identification. These same parameters are then applied in a pushover analysis of other buildings. The results are shown to compare favorably to a separate nonlinear time-history analysis.

Title: An improved nonlinear static inelastic analysis based on displacement.
Author: Gong, Huguang; Shen, Pusheng
Source Dizhen Gongcheng yu Gongcheng Zhendong (Earthq. Eng. Eng. Vib.). Vol. 25, no. 3, pp. 18-23. May-June 2005

Descriptors: Seismic phenomena; Displacement; Mathematical models

Abstract: Summarized and evaluated herein is an improved displacement-controlled pushover analysis procedure based on the structural dynamics theory, which adopts the adaptive distribution of lateral force and combines several modal responses of pushover analysis results to account for the contributions of higher modes. A numerical example is proposed to evaluate the accuracy by comparing the structural responses of the proposed analysis procedure with the results of the nonlinear history analysis (NHA). It is demonstrated that the structural responses of the proposed pushover analysis are generally similar to the results from the NHA, especially in the story drift and the story shear, which are mostly affected by the higher modes.

Title: Structural response and damage assessment by enhanced uncoupled modal response history analysis

Author: Li, Quanwang; Ellingwood, Bruce R

Source: Journal of Earthquake Engineering, Vol. 9, no. 5, pp. 719-737. Sept. 2005

Descriptors: Frames; Beams (structural); Earthquake damage; Seismic phenomena; Nonlinear dynamics; Welded joints; Cracking (fracturing)

Abstract: The Uncoupled Modal Response History Analysis (UMRHA) method developed by Chopra et al. is modified in this paper to estimate damage to welded moment-resisting connections in a steel frame (MRSF) subjected to earthquake ground motions. The behaviour of these connections is modelled by a moment-rotation relationship that accounts for the cracking of the beam flange-to-column flange groove weld. The behaviour of the frame is approximated by a sequence of single-degree-of-freedom (SDOF) models for the first three modes to allow for the contribution of higher modes of vibration. The dynamic properties of these SDOF systems are determined by nonlinear static pushover analyses of the building frame. Because of the significant drop in connection strength caused by beam-to-column weld cracking, the pushover procedure uses a changing rather than invariant distribution of horizontal loads, while the structural responses are calculated from shapes that are based on the displaced shape of the frame after damage occurs. The accuracy of the method is demonstrated by a comparison with the results of a nonlinear time history analysis of the frame. This method can be used for rapid assessment of seismic damage or damage potential and to identify buildings requiring more detailed investigation.

Title: Nonlinear procedures in revised Turkish code for seismic performance assessment and retrofit design

Author: Aydinoglu, M Nuray

Source: First European Conference on Earthquake Engineering and Seismology. 2006

Descriptors: Seismic phenomena; Seismic engineering; Marketing; Demand; Reinforcing steels; Earthquake design; Deformation; Seismic

response; Nonlinearity; Retrofitting; Performance assessment; Ductile brittle transition; Spectrum analysis; Demand analysis; Mathematical analysis; Seismic design; Reinforced concrete; Strain; Brittleness

Abstract: Turkish seismic design code has recently undergone a major revision whereby a new chapter is added for the seismic performance assessment and retrofit of existing structures. The new chapter follows a fully performance-based approach, in which ductile deformation demands and brittle force demands are required to be estimated for multi-level earthquake actions and these demands are then evaluated against the corresponding deformation and internal force capacities to assess if the performance objectives defined in the code are met. The new chapter includes both linear and nonlinear analysis procedures for the seismic demand estimation, the latter of which involves single-mode pushover analysis through Incremental Equivalent Seismic Load Method and multi- mode pushover analyses with Incremental Response Spectrum Analysis (IRSA) Method. In reinforced concrete sections seismic demands are first estimated in terms of plastic rotations followed by the calculation of concrete and reinforcing steel strains. The corresponding deformation capacities have been specified for both unconfined and confined sections.

Title: Adaptive modal combination procedure for nonlinear static analysis of building structures

Author: Kalkan, Erol; Kunnath, Sashi K

Source: Journal of Structural Engineering (New York, N.Y.). Vol. 132, no. 11, pp. 1721-1731. Nov. 2006

Descriptors: Displacement; Seismic phenomena; Seismic engineering; Earthquake construction; Marketing; Adaptive structures; Tools; Dynamic characteristics; Demand; Drift; Nonlinearity; Demand analysis; Spectra; Performance evaluation; Graduates; Structural steels; Roofs; Approximation; Inertia

Abstract: A new pushover analysis procedure derived through adaptive modal combinations (AMC) is proposed for evaluating the seismic performance of building structures. The methodology offers a direct multimode technique to estimate seismic demands and attempts to integrate concepts built into the capacity spectrum method recommended in ATC-40 (1996), the adaptive method originally proposed by Gupta and Kunnath (2000) and the modal pushover analysis advocated by Chopra and Goel (2002). The AMC procedure accounts for higher mode effects by combining the response of individual modal pushover analyses and incorporates the effects of varying dynamic characteristics during the inelastic response via its adaptive feature. The applied lateral forces used in the progressive pushover analysis are based on instantaneous inertia force distributions across the height of the building for each mode. A novel feature of the procedure is that the target displacement is estimated and updated dynamically during the analysis by incorporating energy-based modal capacity curves in conjunction with constant-ductility capacity spectra. Hence it eliminates the need to approximate the target displacement prior to commencing the

pushover analysis. The methodology is applied to two existing steel moment-frame buildings and it is demonstrated that the AMC procedure can reasonably estimate critical demand parameters such as roof displacement and interstory drift for both far-fault and near-fault records, and consequently provides a reliable tool for performance assessment of building structures.

Title: Use of load dependent ritz vectors in modal pushover analysis
Author: Kayhani, Hossein; Ghafory-Ashtiany, Mohsen
Source: 14th World Conference on Earthquake Engineering: Innovation Practice Safety. 2008
Descriptors: Mathematical analysis; Dynamical systems; Vectors (mathematics); Dynamics; Accuracy; Spatial distribution; Loads (forces); Seismic design; Nonlinearity; Computation; Inclusions; Nonlinear dynamics; Estimating

Abstract: The performance of a structural system can be estimated using a non-linear static analysis which has found widespread use in performance based seismic design due to its simplicity in estimating inelastic structural response. Modal Pushover Analysis (MPA) has been suggested to increase the accuracy of Pushover analysis; but it fails in some cases of the irregular structural systems (i.e. stiffer lower stories). The objective of this paper is to present the use of Load Dependent Ritz vectors (LDR) which takes into account the spatial distribution of dynamic force; instead of commonly used eigen-mode shape in the MPA in order to improve the accuracy of calculated response of irregular systems when limited number of modes is to be considered, especially for stiff systems where higher mode effects cannot be ignored. The numerical results have indicated that using LDR vectors, in case of stiffer lower stories, increase the accuracy of force response significantly (because of inclusion of higher mode effects without really computing them). There are also some suggestions about choosing adequate number of required Ritz vectors for vertically regular or irregular structures considered.

Title: An improved modal pushover analysis procedure for estimating seismic demands of structures
Author: Mao, Jianmeng; Zhai, Changhai; Xie, Lili
Source: Earthquake Engineering and Engineering Vibration. Vol. 7, no. 1, pp. 25-31. Mar. 2008
Descriptors: Seismic phenomena; Earthquake construction; Seismic engineering; Marketing; Force distribution; Earthquake engineering; Inertia; Buildings; Computation; High rise buildings; Demand; Demand analysis

Abstract: The pushover analysis (POA) procedure is difficult to apply to high-rise buildings, as it cannot account for the contributions of higher modes. To overcome this limitation, a modal pushover analysis (MPA) procedure was proposed by Chopra et al. (2001). However, invariable lateral force distributions are still adopted in the MPA. In this paper, an improved MPA procedure is presented to estimate the seismic

demands of structures, considering the redistribution of inertia forces after the structure yields. This improved procedure is verified with numerical examples of 5-, 9- and 22-story buildings. It is concluded that the improved MPA procedure is more accurate than either the POA procedure or MPA procedure. In addition, the proposed procedure avoids a large computational effort by adopting a two-phase lateral force distribution.

Title: A spectra-based multi modal adaptive pushover procedure for seismic assessment of buildings
Author: Shaker, K; Shayanfar, M A; Asbmarz, M Mohebibi
Source: 14th World Conference on Earthquake Engineering: Innovation Practice Safety. 2008
Descriptors: Seismic phenomena; Seismic engineering; Marketing; Spectra; Demand; Polymethyl methacrylates; Remedies; Stiffness matrix; Assessments; Dynamic structural analysis; Adaptive structures; Earthquake construction; Dynamics; Buildings; Demand analysis

Abstract: Since the conventional pushover analyses are unable to consider the effect of the higher modes and progressive variation in dynamic attribute of structure in inelastic phase, during the recent years, some advanced multi modal and also adaptive pushover procedures have been proposed. However they are not complete and suffer from some drawbacks explained in this paper. In order to remedy these drawbacks, an advanced spectra-based multi modal adaptive (MMA) procedure is proposed. This method incorporates the adaptive method in multi modal pushover analysis while in consecutive steps the effects of the yielding in one mode are reflected in the stiffness matrix of the other modes, whereas the capacity curve and seismic demand are derived for each mode individually. The total seismic demands are estimated by combining the modal demands due to some selected number of modes.

Degradation and Reversed Cyclic Pushovers

Title: The Seismic shear of ductile cantilever wall systems in multistorey structures
Author: Rutenberg, A
Source: Earthq. Eng. Struct. Dyn. Vol. 33, no. 7, pp. 881-896. June 2004
Descriptors: Walls; Seismic engineering; Stress concentration; Earthquake construction

Abstract: The distribution of seismic base shear demand among ductile flexural cantilever walls, comprising the lateral load resisting system of a multistorey building, is studied. It is shown that the base shear force demand depends on the sequence of hinge formation at the wall bases, and this in turn depends on the relative wall lengths. Hence, the routine elastic approach in which the shear forces are allocated per relative flexural rigidity or (when some consideration is given to plastic hinge formation) to moment capacity at the wall base, may appreciably underestimate the shear force demand on the walls, particularly the shorter (usually the more

flexible) ones. A simple procedure yielding the results of 'cyclic' pushover analysis is proposed to predict the peak seismic wall forces for a given total base shear when plastification is confined to the wall base. The effects of plastic hinges developing at higher floors on (1) shear distribution among the walls and (2) the in-plane floor forces are also considered. Two numerical examples are presented to demonstrate the main points made.

Title: Optimal seismic analysis of degrading planar frames using a weighted energy method to associate inelastic mode shapes: part i optimal parameters
Author: Attard, Thomas L; Fafitis, Apostolos
Source: Engineering Structures. Vol. 29, no. 8, pp. 1977-1989. Aug. 2007
Descriptors: Optimization; Marketing; Demand; Seismic phenomena; Seismic engineering; Buildings; Energy use; Frames; Strain hardening; Acceleration; Reduction; Dissipation; Nonlinearity; Degrees of freedom; Degradation; Demand analysis; Spectra; Mathematical analysis; Energy methods

Abstract: The objective of this paper is to compute three optimal parameters that are subsequently used to formulate the pre-yielded and post-yielded portions of an equivalent single degree of freedom system (E-SDOF) that is used to predict the seismic target demands in planar frames. The procedure uses an optimal number of inelastic mode shapes from a structure's capacity (pushover) curve to account for any significant higher-mode effects (HME) and predict the inelastic demands. Using a variant inertial load pattern, weighted energy gradients under the capacity curve are used to define an optimal ductility parameter, which is in turn used to combine the inelastic (and elastic) mode shapes into a single mode shape. This is used to determine the pre-yielded portion of the E-SDOF system, where the post-yielded portion is determined using an inelastic modes parameter. The procedure also utilizes a reduction factor parameter to adjust the one-second spectral acceleration demand. The three optimal parameters are established using several buildings, whose responses are generally influenced by specific material strain hardening and plastic flow rules, and by the dissipated energy due to the yielding of the individual members. Using this methodology, the predicted target displacement demands are very reasonably predicted when compared to a nonlinear time-history analysis, which enables the parameters to later be used in the formulation of other buildings' E-SDOF systems.

Energy-based pushovers

Title: Pushover analysis: an energy based approach
Author: Albanesi, T; Biondi, S; Petrangeli, M
Source: The Twelfth European Conference on Earthquake Engineering [Proceedings] [electronic resource] , pp. 10 pages. 2002
Descriptors: Mathematical models; Displacement; Energy use; State of the art; Capacity; Dynamic tests; Resources; Nonlinear dynamics; Finite

element method; Mathematical analysis; Energy of formation; Frames; Earthquake engineering; Fibers; Equivalence

Abstract: A critical review of pushover analysis and capacity spectrum methods is presented; numerical examples carried out on two different frames, using a state-of-the-art fibre finite element model, are discussed. Results, based on different pushover analysis approaches, are compared with the results found with elastic response spectrum and nonlinear direct integration analyses. Using energy equivalence, a consistent formulation for the pushover procedure is proposed and a tentative formulation for energy-based pushover is presented. This energy-based approach can be performed either with a dynamic analysis or a quasi-static adaptive procedure. The latter is a displacement-controlled incremental analysis based on recursive formulas which modifies the imposed displacement profile according to the inertial properties and the nonlinear response of the structure.

Title: Evaluation of site-specific energy demand for building structures
Author: Chou, Chung-Che; Uang, Chia-Ming
Source: Seventh U.S. National Conference on Earthquake Engineering (7NCEE): Theme: Urban Earthquake Risk [electronic resource]; 10 pages pp. 2002
Descriptors: Multistory frames; nonlinear static pushover analysis; Office buildings; site-specific spectra; Hysteretic energy

Abstract: Based on a total of 273 ground motion records from 15 significant earthquakes in California, energy demand in the form of absorbed energy spectra was established by an attenuation relationship. The absorbed energy was proposed for evaluating the energy demand in an inelastic system because the absorbed energy is related to the pseudo-velocity in the elastic case. A procedure for evaluating the absorbed energy in a multidegree-of-freedom (MDOF) system from the energy spectra was also developed. It requires a static pushover analysis of the MDOF system to determine the modal yield force and ductility factor of an equivalent single-degree-of-freedom (SDOF) system for the first two modes. After the ductility is determined for each mode, the energy spectrum then can be used to determine the contribution of each mode. A case study shows that the summation of the absorbed energy from the first two modes compares well with that obtained from a nonlinear MDOF time history analysis.

Title: Evaluating distribution of seismic energy in multistory frames
Author: Chou, Chung-Che; Uang, Chia-Ming
Source: 13 WCEE: 13th World Conference on Earthquake Engineering Conference Proceedings. 2004
Descriptors: Energy distribution; Frames; Seismic energy; Energy spectra; Nonlinearity; Absorbance; Earthquake engineering

Abstract: A simplified procedure similar to the response spectrum method has been developed to estimate the energy absorbed in each mode from energy spectra, and the distribution of energy along frame height is evaluated based on energy shapes

established by non-linear modal pushover analysis. The statistics of the estimate of energy are presented for a variety of building frames subjected to ground motion ensembles. The study shows that (1) the proposed procedure which includes the higher mode effects can reasonably predict the total energy and the energy distribution in a structure, (2) the majority of the seismic energy is contributed by the first mode response, and (3) the second-mode energy needs to be considered to predict the damage in the upper stories.

Title: An energy-based formulation for first- and multiple-mode nonlinear static (pushover) analyses.
Author: Hernandez-Montes, E; Kwon, O-S; Aschheim, M A
Source: Journal of Earthquake Engineering. Vol. 8, no. 1, pp. 69-88. Jan. 2004
Descriptors: Displacement; Roofs; Domains; Statics; Equivalence; Yield point; Spectra; Distortion; Spectral lines; Absorbance; Earthquake engineering

Abstract: Existing nonlinear static (pushover) methods of analysis establish the capacity curve of a structure with respect to the roof displacement. Disproportionate increases in the roof displacement, and even outright reversals in the case of higher mode pushover analyses, can distort the capacity curve of the 'equivalent' SDOF system. Rather than viewing pushover analyses from the perspective of roof displacement, this paper considers the energy absorbed (or the work done) in the pushover analysis. Simple relations establish an energy-based displacement that is equivalent to the spectral displacement obtained by conventional pushover analysis methods within the linear elastic domain. Extensions to the nonlinear domain allow pushover curves to be established that resemble traditional first mode pushover curves and which correct anomalies observed in some higher mode pushover curves. An example illustrates the application of a modified Multimode Pushover Analysis procedure using Yield Point Spectra.

Title : Application of modified capacity spectrum method to performance-based rehabilitation of school buildings
Author: Chai, Juin-Fu; Teng, Tsung-Jen
Source: ICEE 2006: 4th International Conference on Earthquake Engineering. 2006
Descriptors: School buildings; Strength; Nonlinearity; Rehabilitation; Seismic phenomena; Seismic response; Instability; Reduction; Degradation; Coefficients; Damage; Seismic engineering; Hazards; Seismic design; Acceptance criteria; Confidence; Earthquake construction; Stability

Abstract: In this paper, an energy-based and normalized performance index is proposed to measure the damage state through the full range capacity curve determined from a static pushover analysis. The critical value of the proposed index to indicate the global instability was inferred by the in-situ pushover test of three full-scaled school buildings. Based on the modified capacity spectrum method, the elastic

supply strengths of a building at any performance state can be assessed from the capacity curve that can be determined either by the static pushover analysis or from the in-situ test data. In this paper, an energy-based modified capacity spectrum method which involves the effect of strength degradation is developed by modifying the strength reduction factor that is defined by the seismic design code for new buildings in Taiwan. The proposed method is compared with the coefficient method (specified by FEMA 440) and further, validated by the nonlinear time history analyses of the target building. Based on the estimated IM-DM curve, the maximum nonlinear response of a school building before or after rehabilitation under any selected seismic hazard level can be evaluated, and the acceptance criteria can be defined by the demand-capacity factor method for a certain level of confidence in the building's ability to meet the desired performance objectives.

Title: Pseudo-energy response spectra for the evaluation of the seismic response from pushover analysis
 Author: Mezzi, Marco; Comodini, Fabrizio; Lucarelli, Matteo; Parducci, Alberto; Tomassoli, Enrico
 Source: First European Conference on Earthquake Engineering and Seismology. 2006
 Descriptors: Spectra; Seismic phenomena; Seismic response; Seismic engineering; Earthquake design; Design engineering; Earthquake damage; Dissipation; Damage; Earthquake dampers; Dynamic tests; Mathematical models; Dynamics; Methodology; Evolution; Damping; Ductility; Computation; Spectral lines

Abstract: The application of non linear static analysis method through the energy approach is based on the idea that the energy of the seismic input transferred to the structure is dissipated by the controlled damage of its members. The pushover curve is computed considering that, in each step, the work of the floor forces is equal to the structure internal work and is expressed in terms of energy capacity. It can be compared with energy response spectra representative of the seismic input to find the performance point defining the structural response to the design earthquake. The use of pseudo-energy spectra is proposed, alternative to the conventional reduced design spectra. Solutions are carried out for a case of study. The results are compared with those coming from non linear static analyses based on reduced spectra with controlled damping or ductility and from non linear dynamic analyses. The potential evolutions of the methodology are outlined.

Title: Energy-based non linear static analysis
 Author: Parducci, Alberto; Comodini, Fabrizio; Lucarelli, Matteo; Mezzi, Marco; Tomassoli, Enrico
 Source: First European Conference on Earthquake Engineering and Seismology. 2006
 Descriptors: Design engineering; Energy use; Mathematical models; Nonlinearity; Equivalence; Transformations; Pushing; Earthquake

design; Seismic phenomena; Displacement; Seismic engineering;
Energy spectra; Criteria; Stress concentration; Estimates

Abstract: The seismic behaviour of a structure can be analysed using non-linear static analyses (pushover analyses). The new Italian code introduces this procedure as an alternative design method. The applications require that the complex non-linear response of a MDOF model stressed by the increasing action of an assigned distribution of lateral forces is transformed in the response of a SDOF system, in order to compare it with an assigned design spectrum. The energy approach EA proposed in this paper is a rational improvement of the pushover analysis method devised by the first author of this paper; it can be used to carry out this transformation through a simple energy equivalence, so the comparison can be directly performed. According to the energy criterion of the Performance-Based-Design a suitable virtual energy equivalent displacement is then defined. It can be used to estimate a SDOF capacity curve which reproduces the total elastic and plastic energy cumulated by the whole structure during the pushing procedure. The use of this proposed procedure is illustrated and is compared with the methods indicated by the design literature, mainly when spatial problems are examined. The possibility of a design approach based on the use of energy spectra is also discussed.

Title: Seismic analysis of reinforced concrete frame - core structures based on energy concept.

Author: Zhu, Jianhua; Shen, Pusheng

Source: Dizhen Gongcheng yu Gongcheng Zhendong (Earthquake Engineering and Engineering Vibration). Vol. 26, no. 5, pp. 109-113. Sept.-Oct. 2006

Descriptors: Hysteresis; Energy use; Seismic phenomena; Reinforced concrete; Drift; Seismic engineering; Energy distribution; Vibration; Nonlinear dynamics; Demand; Mathematical models; Civil engineering; Tall buildings; Marketing; Equivalence; Computation; Earthquake engineering; Frames

Abstract: The seismic ability analysis of reinforced concrete frame-core structures based on energy concept was performed. Equivalent single-degree-of-freedom (SDOF) systems were used to estimate the hysteretic energy demands of the frame-core structures in order to simplify the computational effort. Pushover analysis was used to get the distribution of hysteretic energy in each story as well as the energy capacity of the structure. The relationship between hysteretic energy and inelastic story drift was used to get the inelastic story drift. A numerical example of reinforced concrete frame-core tall building is proposed. The comparison with that of the nonlinear dynamic analysis proves the possibility of the methods used in this paper.

Title: Energy-based approach of static pushover analysis

Author: Kotanidis, C; Doudoumis, I N

Source: 14th World Conference on Earthquake Engineering: Innovation Practice Safety. 2008

Descriptors: Displacement; Mathematical analysis; Equivalence; Roofs; Frames; Shear; Walls; Degrees of freedom; Dissipation; Diaphragms; Concretes; Seismic energy; Methodology

Abstract: This paper presents an energy approach of Static Pushover Analysis method. It proposes the replacement of roof displacement that is used in classic 'base shear - roof displacement' pushover curve with an equivalent energy-based displacement u_{en} , calculated as a function of the work of external lateral forces acting on the structure. Consistent analytical formulas are provided for the calculation of work of lateral forces acting on the floors of an N-storey frame with rigid floor diaphragms and of the equivalent energy-based displacement. The proposed methodology is applied on characteristic multi-storey concrete frames (moment frame, wall-frame system, coupled shear walls) which are analyzed using Pushover Analysis. Results indicated that classic 'base shear - roof displacement' pushover curve could lead to incorrect estimation of the amount of seismic energy the structure is able to dissipate, whereas the proposed energy-based displacement leads to an energy consistent equivalent Single Degree of Freedom (ESDOF) system.

Title: Static pushover analysis based on an energy-equivalent sdof system

Author: Manoukas, G E; Athanatopoulou, A M; Avramidis, I E

Source: 14th World Conference on Earthquake Engineering: Innovation Practice Safety. 2008

Descriptors: Nonlinearity; Equivalence; Mathematical analysis; Degrees of freedom; Strain; Philosophy; Frames; Lateral loads; Coefficients; Methodology

Abstract: In this paper a new enhanced Nonlinear Static Procedure (NSP) is presented and evaluated. The steps of the proposed methodology are quite similar to those of the well-known Coefficient Method (FEMA 356/440). However, the determination of the characteristics of the equivalent single degree of freedom (E-SDOF) system is based on a different philosophy. Specifically, the E-SDOF system is determined by equating the external work of the lateral loads acting on the MDOF system under consideration to the strain energy of the E-SDOF system. After a brief outline of the method, a series of applications to planar regular frames is presented. Considering the results obtained by nonlinear time-history analysis as the reference solution, a comparison between the proposed and the conventional NSPs is conducted, which shows that the proposed method gives, in general, much better results.

Other methods

Title: Capacity control method for seismic assessment of low-to-medium rise reinforced concrete buildings

Author: Gunay, M Selim; Sucuoglu, Haluk

Source: First European Conference on Earthquake Engineering and Seismology. 2006

Descriptors: Seismic phenomena; Shear; Seismic engineering; Earthquake construction; Byproducts; Beams (structural); Assessments; Nonlinearity; Mathematical analysis; Buildings; Reinforced concrete; Limit states; Seismic response; Spectrum analysis; Demand; Modal response; Marketing; Flexing; Failure modes

Abstract: A practical and efficient seismic assessment method is presented in this paper for low-to-medium rise ordinary reinforced concrete buildings, which employs linear elastic modal response spectrum analysis in combination with capacity principles. The method is called the 'Capacity Control Method' (CCM). In this method, first the expected locations and failure modes (flexure, shear, etc.) of inelastic member behavior are identified, and then the member performances are determined by computing demand-to-capacity ratios (DCR) in force terms, and comparing them with the associated DCR limits. Finally, a decision is made about the building performance by combining the member performances. One important feature of the method is the calculation of axial forces in the columns by using the shear forces that can be transmitted from the beams at the ultimate limit state. As a by-product of the method, base shear capacity of the building can also be calculated. Another important feature of the method is the consideration of all modes in determining seismic demand. The method is implemented on a twelve story building, for which higher mode effects are significant. The results are compared with nonlinear response history analysis. In addition, conventional (single mode) and modal pushover analyses are conducted in order to examine the validity of CCM. It is observed that CCM predictions are in the same order, sometimes better than the predictions of conventional and modal pushover analyses when nonlinear response history analysis is accepted as the reference.

H.1.4 P-Delta Effects

Title: Evaluation of P-Delta effects in non-deteriorating MDOF structures from equivalent SDOF systems

Author: Adam, Christoph; Ibarra, Luis F; Krawinkler, Helmut

Source: 13 WCEE: 13th World Conference on Earthquake Engineering Conference Proceedings. 2004

Descriptors: Seismic engineering; Gravitation; Dynamic structural analysis; Frame structures; Earthquake construction

Abstract: This paper addresses the assessment of destabilizing effects of gravity, usually referred to as P-Delta effects, in highly inelastic structures when subjected to seismic excitations. The proposed approach is based on an equivalent single-degree-of-freedom (ESDOF) system of the actual building. Appropriate properties of the ESDOF system are defined, based on results of a corresponding global pushover analyses. P-Delta effects are incorporated via an auxiliary backbone curve, which is rotated by a uniform stability coefficient. The procedure is evaluated for several multistory generic frame structures. The collapse capacity of these structures is derived from a set of Incremental Dynamic Analysis (IDA) studies involving 40 ground motions whose intensity is increased until P-Delta instability occurs. The

results are translated from the ESDOF domain into the domain of the multi-degree-of-freedom (MDOF) system, and utilized for the estimation of P-Delta effects in MDOF structures. "Exact" results are contrasted with outcomes of the analyses utilizing ESDOF systems. Assumptions and limitations of the ESDOF system approach are discussed. The emphasis is on the level of response at which the structure approaches dynamic instability (sidesway collapse).

Title: Effect of second-order forces on seismic response
Author: Humar, J; Mahgoub, M; Ghorbanie-Asl, M
Source: Canadian Journal of Civil Engineering. Vol. 33, no. 6, pp. 692-706. June 2006
Descriptors: Stiffness; Seismic phenomena; Instability; Stability; Earthquake construction; Seismic engineering; Strength; Strain hardening; Earthquake design; Loads (forces); Seismic response; Gravitation; Shears; Resists

Abstract: In a building structure subjected to seismic forces, the gravity loads acting through the lateral displacements lead to additional shears and moments. This is generally referred to as the P-Delta effect; it tends to reduce the capacity of the structure to resist the seismic forces and may lead to instability. It has been suggested that an increase in structural strength, in stiffness, or in both would mitigate the P-Delta effect and ensure stability of the structure. It is shown here that instability results when the P-Delta effect causes the stiffness of the structure to become negative in the post-yield range, in which case increasing the strength, the stiffness, or both does not ensure stability. In a single-storey structure, stability can be ensured if there is sufficient strain hardening that the post-yield stiffness is positive even in the presence of the P-Delta effect. For a multistorey building the vulnerability of the structure to P-Delta instability can be judged by obtaining a pushover curve. It is shown that as long as the maximum displacement produced by the design earthquake lies in the region of positive slope of the pushover curve, the structure will remain stable.

H.1.5 Modeling Choices

Structural components

Title: Simple nonlinear flexural stiffness model for concrete structural walls
Author: Adebar, Perry; Ibrahim, Ahmed M. M.
Source: Earthquake Spectra. Vol. 18, no. 3, pp. 407-426. Aug. 2002
Descriptors: Reinforced concrete walls; nonlinear static pushover analysis; Coupled walls; dynamic properties; Tall buildings

Abstract: A trilinear bending moment-curvature model is proposed for the nonlinear static (pushover) analysis of concrete walls. To account for the effect of cracking on the flexural stiffness of concrete walls in a simple yet accurate way, the elastic portion of the bending moment-curvature relationship is modeled as bilinear. To

account for the influence of cyclic loading on tension stiffening of cracked concrete, the concept of upper-bound response for a previously uncracked wall and lower-bound response for a severely cracked wall is introduced. To validate the proposed model, the results of a large-scale test on a slender concrete wall are compared with predictions from the model. The application of the proposed model in a pushover analysis of a 131-m- (430-ft) high coupled-wall structure demonstrates the importance of accurately modeling the nonlinear flexural stiffness of concrete walls.

Title: Modeling of steel moment frames for seismic loads
Author: Foutch, Douglas A.; Yun, Seung-Yul
Source: Journal of Constructional Steel Research. Vol. 58, no. 5-8, pp. 529-564. 2002
Descriptors: Northridge; California earthquake; Jan. 17; 1994; steel moment-resisting frames; SAC Joint Venture; United States; U.S. Natl. Earthquake Hazards Reduction Program (NEHRP) 1997 Recommended Provisions; structural design criteria; Los Angeles; tall buildings; Southern California; multistory structures; Steel beam-column joints; fractures; Nonlinear analysis; Story drift

Abstract: Simple elastic models based on centerline dimensions of beams and columns are widely used for the design of steel moment-resisting frames. However, for the performance prediction and evaluation of these structures, different nonlinear models are being used to better simulate their true behavior. Simple nonlinear modeling methods widely used as well as those with more detailed modeling representations are investigated and compared. A 9-story building and a 20-story building were designed for this study according to the 1997 NEHRP provisions. Different models for these structures were developed and analyzed statically and dynamically. The models investigated involved the use of centerline dimensions of elements or clear length dimensions, nonlinear springs for the beam connections, and linear or nonlinear springs for the panel zones. A second group of models also incorporated the fracturing behavior of beam connections to simulate the pre-Northridge connection behavior. Two suites of ground motions were used for the dynamic analysis: typical California and near fault ground motions. The differences in structural responses among different models for both suites of motions are investigated. According to static pushover analyses with roof displacement controlled, the benefit of the increase in capacity that results from the detailed models is consistently observed for both the 9-story and 20-story buildings. When the models were excited by different ground motions from each suite, the median responses of the more detailed models showed an increase in capacity and a decrease in demand as expected. However, due to the randomness inherent in the ground motions, variations were also observed. Overall, the model which incorporates clear length dimensions between beams and columns, panel zones and an equivalent gravity bay without composite action from the slab seems to be a practical model with appropriate accuracy.

Title: The effects of R/C frame stiffness modeling on seismic performance
Author: Jankovic, Srdjan; et al.
Source: Concrete Structures in Seismic Regions: FIB 2003 Symposium [Proceedings] [electronic resource] , pp. 8 pages. 2003
Descriptors: Stiffness; Frames; Mathematical models; Reinforced concrete; Seismic engineering; Seismic phenomena; Beams (structural); Concretes; Damage; Slabs; Resources; Earthquake design; Ductility tests; Nonlinear dynamics; Drift; Structural members; Statics; Reinforcing steels; Floors

Abstract: Realistic modelling of reinforced concrete structural elements is necessary to accurately evaluate the seismic performance of reinforced concrete structures. An analysis of the consequences of using different effective stiffness (EI) models is presented in this paper using an example of an eight-story reinforced concrete frame designed according to the EC8 code. Other modelling issues, such as post-elastic stiffness, stiffness of joint zones, floor slabs, and nonstructural elements, have not been investigated. Instead, suitable values have been adopted as constants for all analyzed frames. Comparison of values of flexural stiffness obtained using nonlinear analysis of sections of a given reinforced concrete frame to two recent proposals (by Mehanny and by Priestley), as well as to proposed values from selected seismic codes, is presented first. The second part of the paper presents a comparison of frame response using nonlinear static (pushover) and nonlinear dynamic analysis methods. Frame member stiffness was modeled in three ways: 1) effective stiffnesses were adopted as 45% and 70% of gross concrete section stiffnesses for beams and columns, respectively; 2) effective stiffnesses for beams were defined using a bilinear moment-curvature relation obtained using nonlinear fiber-based analyses of sections, while Mehanny's proposal was adopted for stiffness of column sections; and 3) stiffnesses of gross concrete sections were adopted. Behavior of reinforced concrete frames was described using two parameters: interstory drift ratio (IDR), which is believed to be a relevant measure for nonstructural damage, and story ductility, which can be related to structural damage.

Title: Accounting for shear in seismic analysis of concrete structures
Author: Gerin, Marc; Adebar, Perry
Source: 13 WCEE: 13th World Conference on Earthquake Engineering Conference Proceedings. 2004
Descriptors: Reinforcement; Shear strain; Reinforced concrete; Stiffness; Seismic engineering; Plastic deformation; Concrete structures

Abstract: Techniques for modelling the seismic response of concrete structures are limited by the accuracy of the material models. Current models for reinforced concrete subjected to shear typically do not account for the effects of cracking and yielding. Diagonal cracking has a very pronounced effect on the shear stiffness of concrete structures, however, recommendations for cracked section shear stiffness are not readily available. The plastic strain of reinforcement is another important parameter that must be considered in the nonlinear seismic shear analysis of

reinforced concrete. There is a strong relationship between plastic strain of reinforcement and plastic shear strain, e.g. yielding of the reinforcement results in yielding in shear of the element. Pinching of hysteresis loops is directly linked to the plastic strain in reinforcement, as is the deviation of principal compression stress and principal compression strain angles in concrete. The authors have recently developed a general model to predict the complete load-deformation response of reinforced concrete elements subjected to reverse-cyclic shear. A unique feature of the model is that deformations at the cracks are separated from deformations of concrete between cracks, and crack deformations are assumed to be a consequence of strain compatibility between concrete and reinforcement. This paper presents simplified methods for modelling the non-linear seismic shear response of reinforced concrete based on the underlying principles of the general model. The methods include an effective cracked section shear stiffness determined from the shear strength and the shear strain at yield. The shear strain at yield is primarily a function of the yield strain of the horizontal reinforcement and strain of the vertical reinforcement. The cracked section shear stiffness can be used for linear analysis. For non-linear static analysis, a complete envelope is provided where the shear response is assumed to be elastic-plastic. The ultimate shear strain is determined from the shear strain at yield and the shear strain ductility. The latter is a function of the ratio of shear stress to concrete compression strength. Simple hysteretic rules are also provided to define the complete reverse-cyclic shear response for non-linear dynamic analysis.

Title: Nonlinear static and dynamic analyses - the influence of material modelling in reinforced concrete frame structures
Author: Lin, Ermiao; Pankaj, Pankaj
Source: 13 WCEE: 13th World Conference on Earthquake Engineering Conference Proceedings. 2004
Descriptors: Reinforced concrete; Earthquake design; Seismic phenomena; Frame structures; Reinforcing steels; Strain hardening; Strain rate; Dynamic structural analysis; Plasticity

Abstract: There has been considerable research on modelling inelastic behaviour of reinforced concrete. However, nonlinear material models used for seismic response history analyses and for nonlinear static analysis (NSA) procedures tend to be simple. It can be argued that sophisticated material models for a complex material like reinforced concrete are perhaps not essential for earthquake analysis in view of several other uncertainties associated with the seismic phenomenon. This paper examines the influence of material modelling on RHA responses for a simple reinforced concrete frame structure. Five acceleration time histories compatible to elastic design spectrum of Eurocode 8 are used for RHA. Two material models are considered: a concrete damaged plasticity model that uses the Drucker Prager criterion and in which concrete and reinforcement are modelled separately and a homogenized Drucker Prager model. In both cases the influence of strain hardening and strain rate effects are considered. The results show that the design response from

RHA analyses is significantly different for the two models. The paper then compares the NSA and RHA responses for the two material models for reinforced concrete. The NSA procedures considered are the Displacement Coefficient Method (DCM) and the Capacity Spectrum Method (CSM). A comparison of RHA and NSA procedures shows that there can be a significant difference in local response even though the target deformation values at the control node match. Moreover, the difference between the mean peak RHA response and the pushover response is not independent of the material model.

Title: Response analysis of reinforced concrete wall-frame structure considering strength deterioration
Author: Matsui, Tomoya; Kabeyasawa, Toshimi; Kuramoto, Hiroshi
Source: 100th Anniversary Earthquake Conference. 2006
Descriptors: Beams (structural); Shear walls; Reinforced concrete; Deformation; Seismic engineering; Shake table tests; Failure mechanisms

Abstract: Pushover analysis and earthquake response analysis of reinforced concrete wallframe structure of full-scale 3D shaking table test that is planed by "DaiDaiToku Research Project", was carried out, and seismic performance of the specimen was numerically examined. Shear wall model considering strength deterioration was used in modeling of the structure. From results of Analysis, the specimen formed overall yielding mechanism. However, failure mechanism of the specimen could be change to story yielding mechanism in first story by increasing the effective width of slab. Because reversed shear force effect, which was given to shear wall by beam, become large with increasing effective width of slab, shear wall in first story fail in shear at smaller level of deformation, and the deformation concentrated in first floor.

Title: Axial-Shear-Flexure Interaction (ASFI) approach for displacement-based analysis of reinforced concrete columns
Author: Mostafaei, H; Kabeyasawa, T
Source: 100th Anniversary Earthquake Conference. 2006
Descriptors: Concretes; Axial strain; Seismic phenomena; Performance evaluation; Fibers; Deterioration; Strength; Displacement

Abstract: An approach is presented in this paper in order to evaluate seismic performance of reinforced concrete columns based on axial-shear-flexure interaction concept. The total average axial strain is determined as equal to the summation of average axial strains induced by flexural, axial and shear mechanisms. In the method, fiber model in one-dimensional stress field is applied for modeling the flexural behavior. Strength deterioration is applied on the concrete fibers due to reduction of shear capacity. An integration point, representing the average strain-stress relationship of the element from one end to the inflection point, simulates the shear behavior of a reinforced concrete column. Pushover analyses were carried out to evaluate the performance of shear, shear-flexural, and flexural dominated reinforced concrete column specimens applying the proposed method. The analytical results

such as ultimate lateral forces and ultimate drift ratios as well as post-peak responses have shown consistent agreement with the test results.

Title: Simulation of damage progression in lower stories of 11-story building
Author: Bechtoula, Halam; Sakashita, Masanobu; Kono, Susumu; Watanabe, Fumio; Eberhard, Marc O
Source: 13 WCEE: 13th World Conference on Earthquake Engineering Conference Proceedings. 2004
Descriptors: Frames; Axial loads; Beams (structural); Reinforced concrete; Hinges; Earthquake design

Abstract: Seismic behavior of two reinforced concrete frames with two stories and one span were investigated in Kyoto University. These frames were scaled to 1/4 and represented the lower part of an 11-story reinforced concrete frame building prototype. They were identical and designed with the 1999 Japanese guidelines. Axial load variation was the only test parameter for this experiment. From the test results it was found that, slight difference was observed between the two frames from the experimental load-drift relationship. Both frames did not show any strength degradation even though they were loaded beyond 6 % drift. The second floor beam elongated as much as 1.50% of the total span length for both frames. Some of the beam's longitudinal reinforcements buckled near the column face due to high compression. Frame under high axial load showed more cracks than the one under moderate axial load. Analysis of the frame specimens was carried out with the nonlinear IDARC program. The analytical curvature-drift relationships for frame components matched well the experimental ones, for a plastic hinge lengths equal half of the column depth and half of the beam height. Good agreement was also found for the load-drift at the first story, second story and the entire frame. Pushover analysis carried out using the nonlinear SAP2000 predicted with a very good accuracy the envelope curves of the experimental hysterises curves. The plastic hinge region was modeled in SAP2000 using the tri-linear model suggested in the Japanese design guideline.

Title: Nonlinear seismic response analyses of existing R/C building and evaluation of system components contribution
Author: Faggella, Marco; Spacone, Enrico; Conte, Joel P; Restrepo, Jose
Source: First European Conference on Earthquake Engineering and Seismology. 2006
Descriptors: Nonlinearity; Frames; Seismic response; Computer programs; Software; Seismic phenomena; Damage; Frame structures; Foundations; Modelling; Accuracy; Earthquake construction; Soil (material); Diaphragms; Structural analysis; Earthquake damage; Models; Slabs

Abstract: A four-story existing R/C building damaged during the 2002 Molise, Italy earthquake, is modelled using the nonlinear structural analysis software framework OpenSees. The software allows modelling of different types of subsystems and

components (frames, diaphragms, infills, foundations, surrounding soil). The objective of this study is to evaluate the influence of different structural components on the nonlinear seismic response of the building. The influence of each component is assessed through nonlinear analyses carried out by adding one system component at a time. Four different structural models are analyzed and compared: A) bare frame structure; B) bare frame + linear elastic slabs; C) bare frame + linear elastic infills; D) bare frame + linear elastic infills + bare first story. The comparative study of pushover (both conventional and multi-modal) and time history analyses is expected to provide valuable information on both the accuracy of the nonlinear pushover analyses and the effects and relative importance of the different system components.

Title: Pushover analysis of masonry buildings: remarks on code provisions
Author: Guadagnuolo, Mariateresa; Faella, Giuseppe
Source: First European Conference on Earthquake Engineering and Seismology. 2006
Descriptors: Beams (structural); Masonry; Spandrels; Mathematical analysis; Seismic phenomena; Seismic engineering; Tuff; Finite element method; Frames; Mathematical models; Buildings; Walls; Displacement; Cracks; Earthquake construction; Sensitivity; Strength

Abstract: The paper deals with the non linear static procedures for tuff low-rise masonry buildings, as implemented in the recent Italian seismic code. The attention is mainly focused on the evaluation of the maximum top displacement and of the performance point. Specifically, the results obtained through masonry-type frame models are compared with the ones obtained using a refined finite element model based on smeared crack approach. Comparative pushover analyses are carried out by varying the masonry strength and the wall geometry. Different modeling and behavior types for spandrel beams are also taken into account in the analyses. The Italian seismic code procedure related to non linear static analyses is discussed. Conclusive remarks are presented on the sensibility and reliability of the upshot of the code procedure provided by masonry-type frame models and by finite element models for tuff masonry structures. The noteworthy influence of the spandrel beam behavior and the excessive dependence on masonry modeling of the results of non linear static analysis is eventually highlighted.

Title: Study of variation in seismic performance evaluation of concrete frames
Author: Takeuchi, Takashi; Sun, Yuping; Fukuhara, Taheshi
Source: First European Conference on Earthquake Engineering and Seismology. 2006
Descriptors: Beams (structural); Frames; Finite element method; Mathematical models; Horizontal; Seismic phenomena; Seismic engineering; Performance evaluation; Nonlinearity; Concretes; Gravitation; Reinforced concrete; Hinges; Axial loads; Frame structures; Columns (structural); Position (location)

Abstract: A Multi-segment beam element is proposed in this paper for nonlinear pushover analysis of reinforced concrete frames under earthquake-simulating horizontal force. This multi-segment beam element model is developed to take into account effect of the horizontal gravity on the location of yield hinge region of horizontal beams. Based on the beam element model, a nonlinear pushover analysis program is developed to investigate effects of several important structural factors on the seismic performance evaluation of concrete frame structures. These factors include the variation of the axial load in the side columns of frame, the P-Delta effect, and the flexural model of beam section. It has been indicated that the variations due to the use of different flexural model and the P-Delta effect may change the calculated performance by five to ten percent.

Title: Influence of element modeling on the predicted seismic performance of an existing RC building

Author: Vamvatsikos, D; Alexandropoulos, K; Giannitsas, P; Zeris, C

Source: 100th Anniversary Earthquake Conference. 2006

Descriptors: Seismic engineering; Reinforced concrete; Earthquake design; Beams (structural); Stiffness; Frames; Seismicity; Flexibility; Fibers

Abstract: The effect of different element modeling formulations for reinforced concrete (RC) elements on the predicted performance of an RC building under seismic excitation is examined. The building selected is a typical existing five-story RC frame designed for moderate seismicity in the late 1960s, according to the older generation of Greek seismic codes with no special provisions for ductile behavior. Fiber elements are used to model the beams and columns using both stiffness and flexibility formulations, which lead to distinctly different behaviors. To evaluate the seismic performance of each alternate model, both static pushover and incremental dynamic analysis are used. The results are compared across all models, both at the local and the global level, to reveal the differences in the predicted seismic performance resulting from such a subtle modeling choice.

Title: Inelastic modeling sensitivity of the predicted seismic performance of an existing RC building

Author: Zeris, C; Giannitsas, P; Alexandropoulos, K; Vamvatsikos, D

Source: First European Conference on Earthquake Engineering and Seismology. 2006

Descriptors: Seismic phenomena; Seismic engineering; Mathematical models; Reinforced concrete; Earthquake design; Mathematical analysis; Earthquake construction; Frames; Damage; Earthquake damage; Finite element method; Conventions; Standardization; Nonlinearity; State of the art; Criteria; Seismicity; Error analysis; Excitation

Abstract: Inelastic modeling of entire reinforced concrete (RC) buildings under seismic excitation is a complex problem that influences directly the predicted seismic performance. Modeling assumptions and conventions adopted become more important in existing RC frame response predictions, due to these structures'

structural characteristics and non conforming detailing. The problem is investigated for a typical existing five-story RC frame which has been designed for moderate seismicity according to the past generation of Greek seismic codes. Different plane frame finite element models are formulated adopting state of the art as well as state of the practice analysis codes and finite element formulations. The seismic performance of each model is estimated, following both a conventional static pushover as well as nonlinear time- history analyses under different levels of seismic intensity. The models range from the simple yet widely adopted in practice concentrated plasticity elements with axial-flexural strength interaction only, to the more complex distributed damage stiffness or flexibility-based fiber elements accounting or not for joint deformations. The results of the analyses are compared at the global and primarily the local damage prediction levels, to reveal substantial discrepancies and scatter in key performance Response Indices introduced in a Performance Based (re)Design approach by the model limitations, which are often ignored. It is concluded that, in addition to standardization of the criteria and procedures of evaluation, the analytical model for evaluating these Response Indices should also be well defined to avoid error and conflict.

Title: Multi-Scale modelling approach for the pushover analysis of existing RC shear walls-part I: model formulation

Author: Mulas, Maria Gabriella; Coronelli, Dario; Martinelli, Luca

Source: Earthquake Engineering & Structural Dynamics. Vol. 36, no. 9, pp. 1169-1187. 25 July 2007

Descriptors: Mathematical models; Reinforcing steels; Walls; Reinforced concrete; Modelling; Models; Shear; Design engineering; Finite element method; Constitutive relationships; Seismic phenomena; Philosophy; Instrumentation; Seismic engineering; Earthquake design; Mathematical analysis; Fibers; Prototypes; Concretes

Abstract: This work focuses on the modelling issues related to the adoption of the pushover analysis for the seismic assessment of existing reinforced concrete (RC) structures. To this purpose a prototype reference structure, one of the RC shear walls designed according to the multi-fuse concept and tested on shaking table for the CAMUS project, is modelled at different levels of refinement. The meso-scale of a stiffness-based fibre element and the micro-scale of the finite element (FE) method are herein adopted; in the latter separate elements are adopted for the concrete, the steel and the steel-concrete interface. This first of the two companion papers presents in detail the wall under study, illustrating the design philosophy, the geometry of the wall, the instrumentation set-up and the test programme. The two modelling approaches are then described; the most important points in terms of element formulation and constitutive relations for materials are presented and discussed for each approach, in the light of the particular design of the wall and of its experimental behaviour.

Title: Multi-scale modelling approach for the pushover analysis of existing RC shear walls-part II: experimental verification
Author: Mulas, Maria Gabriella; Coronelli, Dario; Martinelli, Luca
Source: Earthquake Engineering & Structural Dynamics. Vol. 36, no. 9, pp. 1189-1207. 25 July 2007
Descriptors: Mathematical models; Reinforced concrete; Shear; Modelling; Displacement; Finite element method; Models; Seismic phenomena; Failure; Nonlinear dynamics; Walls; Nonlinearity; Damage; Seismic engineering; Earthquake design; Mathematical analysis; Anchorages; Fibers; Accuracy

Abstract: In a companion paper two different modelling approaches have been described, operating at the meso-scale of the fibre elements and at the micro-scale of the finite element (FE) method. The aim of this paper is to explore the efficiency of these models in the pushover analysis for the seismic assessment of existing reinforced concrete (RC) structures. To this purpose a prototype reference structure, one of the RC shear walls designed according to the multi-fuse concept and tested on shaking table for the CAMUS Project, is modelled at different levels of refinement. At the micro-scale the reinforcement and anchorage details are described with increasing accuracy in separate models, whereas at the meso-scale one single model is used, where each element represents a large part of the structure. Static incremental non-linear analyses are performed with both models to derive a capacity curve enveloping the experimental results and to reproduce the damage pattern at the displacement level where failure is reached. The comparison between experimental and numerical results points out the strong and weak points of the different models inside the procedure adopted, and the utility of an integration of results from both approaches. This study confirms, even for the rather difficult case at study, the capability of the pushover in reproducing the non-linear dynamic response, both at a global and a local level, and opens the way to the use of the models within a displacement-based design and assessment procedure.

Title: Uncertainty in analytical structural response associated with high level modeling decisions
Author: Mitra, N
Source: 14th World Conference on Earthquake Engineering: Innovation Practice Safety. 2008
Descriptors: Uncertainty; Decisions; Mathematical analysis; Nonlinearity; Reinforced concrete; Design engineering; Computer simulation; Marketing; Columns (structural); Demand

Abstract: Current performance based design approach requires an improved understanding of the behavior of structural components which can be realized through nonlinear analysis of structures and structural components. A lot of research exists in characterizing the epistemic uncertainty associated with demand and capacity of a structure or a structural component. However very few researches exist on characterizing the epistemic uncertainty associated with high level analytical

modeling decisions for simulation of a structure. In this research, epistemic uncertainty in structural response of reinforced concrete structural system has been investigated through a nonlinear pushover analysis of a reinforced concrete column. While performing nonlinear analysis of the structural component with a particular analytical model, the analyst is required to make certain high level decisions such as with respect to element type, integration rules and material models, to obtain the response of a structural component subjected to a certain kind of loading. The research highlights the loss of objectivity in response associated with high level modeling decisions by an analyst.

Capacity Curve Definition and Bounds

Title: Definition of suitable bilinear pushover curves in nonlinear static analyses
Author: Faella, Giuseppe; Giordano, Aldo; Mezzi, Marco
Source: 13 WCEE: 13th World Conference on Earthquake Engineering Conference Proceedings. 2004
Descriptors: Spectra; Ductility tests; Stability; Seismic engineering; Nonlinear dynamics; Viscous damping

Abstract: Reliability of results obtained through nonlinear static analyses is strongly dependent on the assessment of the performance point, usually computed by means of the capacity spectrum method. The use of constant ductility spectra as demand spectra, in place of reduced spectra for assigned equivalent viscous damping, can provide better results and a larger stability in the evaluation method of the performance point. In this case, the capacity curve of the SDOF equivalent system has to be transformed in a bilinear curve for computing the available ductility. Such a conversion can be performed according to several criteria that significantly influence results. In this paper, results of analyses carried out in order to assess the dependence of the performance point value on parameters controlling the bilinear relationship and on conversion procedure are shown. Reliability and accuracy of procedures proposed by ATC 40, Eurocode 8 and Italian seismic code PCM 3274 as well as of procedures based on the use of constant ductility spectra is assessed by comparing results with the ones from nonlinear dynamic analyses.

Title: Influence of capacity curve approximations on seismic response
Author: Kadas, Koray; Binici, Baris; Yakut, Ahmet
Source: First European Conference on Earthquake Engineering and Seismology. 2006
Descriptors: Approximation; Displacement; Demand; Marketing; Computation; Deformation; Databases; Seismic phenomena; Seismic response; Statistics; Vibration; Nonlinearity; Grounds; Degrees of freedom; Coefficients; Seismic engineering; Mathematical analysis; Errors; Stiffness

Abstract: Performance based engineering generally relies on the approximate procedures that are based on the use of capacity curve derived from pushover

analysis. The most important parameter in the displacement-based approach is the inelastic deformation demand computed under a given seismic effect. The Capacity Spectrum Method and the Displacement Coefficient Method are the most common procedures employed for the estimation of inelastic displacement demand. Both of these procedures are based on bi-linearization of the capacity curve. Although there are some recommendations for this approximation, there is a vital need to investigate the most appropriate method of approximating the capacity curve among several alternatives. In view of this, a comprehensive research has been undertaken to study the influence of several existing alternatives used for approximating the capacity curve on the inelastic displacement demand. Single degree of freedom systems (SDOFs) associated with fundamental periods of vibration and load deformation curves (capacity curve) were analyzed under a comprehensive ground motion database. A parametric study employing the most common shapes of capacity curves was carried out. The capacity curve of the SDOF was approximated using the FEMA 356 and the Initial Stiffness approaches to determine the inelastic displacement demand. The results obtained for each case were compared with the ones computed using the actual nonlinear capacity curve. The error statistics corresponding to each method are presented along with the recommendations on the use of different approximations for the capacity curve

Title: Evaluating assumptions for seismic assessment of existing buildings
Author: Bardakis, V G; Dritsos, S E
Source: Soil Dynamics and Earthquake Engineering. Vol. 27, no. 3, pp. 223-233. Mar. 2007
Descriptors: Assessments; Seismic phenomena; Seismic engineering; Earthquake construction; Buildings; Excitation; Plastic deformation; Safety; Stiffness; Rigidity; Civil engineering; Yield point

Abstract: This paper evaluates the American FEMA 356 and the Greek GRECO (EC 8 based) procedural assumptions for the assessment of the seismic capacity of existing buildings via pushover analyses. Available experimental results from a four-storeyed building are used to compare the two different sets of assumptions. If the comparison is performed in terms of initial stiffness or plastic deformation capacities, the different partial assumptions of the procedures lead to large discrepancies, while the opposite occurs when the comparison is performed in terms of structural performance levels at target displacements. According to FEMA 356 assumptions, effective yield point rigidities are approximately four times greater than those of EC 8. Both procedures predicted that the structure would behave elastically during low-level excitation and that the structural performance level at target displacement for a high-level excitation would be between the Immediate Occupancy and Life Safety performance levels.

H.1.6 Efficacy and Limitations

Relative to analytical results

Title: State of the art review for non linear static methods
Author: Albanesi, T; Nuti, C; Vanzi, I
Source: The Twelfth European Conference on Earthquake Engineering [Proceedings] [electronic resource] , pp. 10 pages. 2002
Descriptors: Mathematical models; Dynamical systems; Nonlinear dynamics; Statics; Displacement; State of the art; Capacity; Coefficients; Resources; Reinforced concrete; Approximation; Reliability; Numerical analysis; Alluvial deposits; Degradation; Rock; Frames; Earthquake engineering; Spectrum analysis

Abstract: This paper presents a critical description of the most popular nonlinear static procedures based on pushover analysis, i.e., the capacity spectrum, the displacement coefficient and the N2 methods. Their distinctive characteristics and the differences between them are highlighted and clarified. The results of an extensive numerical analysis, performed on (i) either bilinear and degrading Takeda single degree-of-freedom systems or (ii) fibre models of reinforced concrete frames are presented. The aim is to estimate the degree of reliability of the above methods in assessing the expected response on systems subjected to both artificial and natural accelerograms recorded on rock, alluvium and soft soils. Results are compared with those found from response spectrum analysis, equal energy and equal displacement approximations and nonlinear dynamic analysis.

Title: Analysis procedures for performance-based seismic design
Author: Falcao, Sebastiao; Bento, Rita
Source: The Twelfth European Conference on Earthquake Engineering [Proceedings] [electronic resource] , pp. 10 pages. 2002
Descriptors: Marketing; Statics; Demand; Seismic engineering; Seismic phenomena; Rotation; Displacement; Deformation; Design engineering; Ductility; Capacity; Resources; Earthquake design; Demand analysis; Nonlinear dynamics; Roofs; Acceptance criteria; Earthquake engineering

Abstract: The performance of a structural system can be evaluated resorting to nonlinear static analyses. These involve the estimation of the structural strength and deformation demands and the comparison with the available capacities at desired performance levels using a so-called pushover analysis. This paper aims at evaluating and comparing the response of a building by the use of different methodologies, namely, the ones described by the ATC-40 and the FEMA 273 design codes, using nonlinear static procedures, with described acceptance criteria. Some results are also compared with the experimental results of a pseudodynamic test and nonlinear dynamic procedure for which five accelerograms were used. Comparisons among the different methods are made in terms of global deformation demands, such as maximum roof displacement and base shear, as well as local demands in the form of inter-story displacements, rotations and rotation ductility at critical sections. The

results show that the described nonlinear static procedure provides adequate information on the seismic demand imposed by the ground motion on a regular structural system.

Title: Evaluation of capacity-demand-diagram methods to predict inelastic lateral displacements
Author: Hidalgo, P. A.; Varas, S.; Jordan, R. M.
Source: Seventh U.S. National Conference on Earthquake Engineering (7NCEE): Theme: Urban Earthquake Risk [electronic resource]; 10 pages pp. 2002
Descriptors: Capacity-demand diagram methods; Reinforced concrete shear walls; nonlinear analysis; Multistory cantilever shear wall structures; displacements (structural)

Abstract: The main objective of this study is to examine the capability of Capacity-Demand-Diagram methods to predict the inelastic lateral displacements of reinforced concrete shear wall multistory buildings induced by severe earthquake ground motions. Two of these methods are evaluated: the methodology proposed by Chopra and Goel and the direct use of inelastic spectra. Both methods use ductility as the parameter to characterize the earthquake demand. The evaluation is performed by comparing the roof displacements predicted by these methods with those obtained from nonlinear time history responses of the same buildings. The study is performed on structural models, not on real buildings. Structural characteristics of models are chosen in order to simulate the behavior of typical shear wall buildings. By varying the number of stories and the thickness of the walls, different types of structural behavior may be obtained. Three earthquake records and the corresponding response spectra are used. Three lateral load patterns are used to obtain the capacity curve through a pushover analysis. The results obtained from this study indicate that these Capacity-Demand-Diagram methods yield lateral displacements that constitute a reasonable approximation of maximum displacement values obtained from inelastic time history responses. The accuracy of the prediction depends on the lateral load pattern used, on the structural characteristics of the models, and on the earthquake records used to carry out the comparison. Nevertheless, there is no direct relationship between these parameters and the quality of results. Although no definite trends can be observed, the prediction of these methods tends to fall on the conservative side.

Title: Correlating dynamic and static nonlinear analysis of frames
Author: Marsh, Jenelle N.; Browning, JoAnn
Source: Seventh U.S. National Conference on Earthquake Engineering (7NCEE): Theme: Urban Earthquake Risk [electronic resource]; 10 pages pp. 2002
Descriptors: Reinforced concrete frames; nonlinear analysis; Multistory frames; nonlinear static analysis; Tall buildings; story drift

Abstract: The evaluation of building performance in seismic events is inevitably limited by the success of the selected analysis technique for determining the building

response. Nonlinear dynamic analysis has traditionally been regarded as a preferred method for estimating the response of a structure to a particular event, but the selection of an appropriate ground motion or suite of ground motions remains a controlling variable that is difficult to predict with accuracy. A possible alternative that conveniently eliminates the selection of an earthquake motion is to use nonlinear static analysis. This type of procedure has been used in simplified analysis and design methods to estimate maximum drift, story drift ratios, element shear, and rotational demands for elements in the modeled system. The purpose of this study is to investigate the correlation between estimates provided using nonlinear static analysis and estimates calculated using nonlinear dynamic analysis for a group of reinforced concrete frames. Overall, the drift and story drift ratio calculations for the static nonlinear analyses provided a better approximation of dynamic response than shear and rotation-based calculations. Even in this context, the calculated results are only an approximation, as shown by the variability.

Title: Assessment of nonlinear static analysis procedures for seismic evaluation of building structures
Author: Yu, Kent; Heintz, Jon; Poland, Chris D.
Source: Seventh U.S. National Conference on Earthquake Engineering (7NCEE): Theme: Urban Earthquake Risk [electronic resource]; 10 pages pp. 2002
Descriptors: Steel moment-resisting frames; nonlinear static pushover analysis; Modal pushover analysis; United States; U.S. Federal Emergency Management Agency (FEMA) FEMA 356

Abstract: Nonlinear static analysis procedures, or pushover analyses with invariant lateral force patterns, have been developed for routine application in structural engineering practice due to their conceptual simplicity. However, concerns have been raised regarding limitations inherent in nonlinear static analysis procedures. In this paper, the relative accuracy of the FEMA 356 Nonlinear Static Procedure (NSP) and a new procedure, the Modal Pushover Analysis (MPA) Procedure, are evaluated through comparison with nonlinear response history analyses of an existing 13-story steel moment-resisting frame building. The building is first subjected to nonlinear response history analyses using a suite of ground motion records representing a 2%/50-year hazard level in the Los Angeles region. Seismic response parameters including the magnitude and spatial distribution of plastic hinge rotations and story drift ratios are considered, and results are used as benchmarks to compare nonlinear static procedures. Three variations on the MPA procedure are studied to observe additional trade-offs between accuracy and practicality. It is found that the MPA procedure is able to predict the building seismic deformation reliably. The FEMA 356 uniform load pattern overwhelms the prediction of the building seismic response, indicating that the FEMA 356 uniform load pattern could be abandoned.

Title: Comparison of simplified procedures for nonlinear seismic analysis of structures
Author: Zamfirescu, Dan; Fajfar, Peter
Source: The Third U.S.-Japan Workshop on Performance-Based Earthquake Engineering Methodology for Reinforced Concrete Building Structures, 16-18 August 2001, Seattle, Washington , pp. 63-76. 2002
Descriptors: Seismic engineering; Seismic phenomena; Seismic response; Earthquake construction; Reinforced concrete; Nonlinear dynamics; Frame structures; Earthquake engineering

Abstract: Six simplified procedures for nonlinear seismic analysis and/or performance evaluation of building structures, based on pushover analysis and response spectrum approach, are briefly described and employed for analysis of a regular multistory frame structure. Two simple procedures that do not require pushover analysis are also included. The results of simplified procedures are compared with the results of nonlinear dynamic analyses. The comparison indicates that the employed procedures generally yield results of adequate accuracy. However, they differ with regard to simplicity, transparency and clarity of the theoretical background.

Title: Local response evaluation in reinforced concrete frames via pushover analysis
Author: Albanesi, Tommaso; Nuti, Camillo
Source: Concrete Structures in Seismic Regions: FIB 2003 Symposium [Proceedings] [electronic resource] , pp. 12 pages. 2003
Descriptors: Mathematical models; Nonlinear dynamics; Displacement; Frames; Reinforcing steels; Dynamic tests; Reinforced concrete; Capacity; Accuracy; Seismic engineering; Seismic phenomena; Stress concentration; Forecasting; Statics; Seismic response; Fibers; State of the art; Loads (forces); Steel fibers

Abstract: Pushover analyses (POA) are currently very popular among researchers and professional engineers as simple and fast tools for assessing the seismic resistance of civil structures, but they are still prone to criticisms. In the past, the most commonly used procedures to perform POA have been studied by the authors and compared so as to clarify the difference between displacement- and force-based POA, the different definitions of the capacity curve, and its effect on the result of nonlinear static methods (NSM), e.g., the capacity spectrum method, the displacement coefficient method, and the N2 method. Since accuracy in forecasting using NSM depends both on accuracy of the maximum displacement estimation and on POA capability to catch the real force and displacement distributions, it is interesting to compare, with reference to dynamic analyses, local responses (deformations, interstorey drifts, plastic rotations, plastic hinge distributions, concrete and steel fibre demands and storey shears) computed with different POAs, imposing top displacements equal to the maximum dynamic one. Numerical examples are carried out on existing reinforced concrete frames using a nonlinear fibre finite

element model. Results obtained with different approaches which stem from the POA are compared with those found from nonlinear step-by-step analyses (using the same model) with the aim of assessing the goodness of POA in forecasting the expected "real" dynamic response. Global and local responses of two 2D real reinforced concrete frames, a lowrise and a highrise one, are determined via NSM based on different POAs and compared to "real" nonlinear dynamic responses. Static and dynamic analyses are performed with the same nonlinear fibre beam model. Both structures have been analysed with displacement- and force-based pushover techniques, also considering different state-of-the-art proposal load profiles. Roughly speaking, POAs of the lowrise frame give accurate results with respect to maximum dynamic responses, both in the elastic and plastic range, while for the highrise frame, POAs are accurate in the linear range but become less accurate with increasing excursion in the plastic range although enhanced load profiles have been considered also.

Title: Evaluation of modal pushover analysis using generic frames
Author: Chintanapakdee, Chatpan; Chopra, Anil K
Source: Earthquake Engineering & Structural Dynamics. Vol. 32, no. 3, pp. 417-442. 2003
Descriptors: Frames; Marketing; Dispersion; Ductility; Accuracy; Seismic phenomena; Demand analysis; Demand; Height; Buildings; Earthquake engineering; Variations; Earthquake design; Seismic engineering; Vibration; Ductility tests; Stress concentration; Dynamic structural analysis; Drift

Abstract: The recently developed modal pushover analysis (MPA) has been shown to be a significant improvement over the pushover analysis procedures currently used in structural engineering practice. None of the current invariant force distributions accounts for the contribution of higher modes--higher than the fundamental mode--to the response or for redistribution of inertial forces because of structural yielding. By including the contributions of a sufficient number of modes of vibration (generally two to three), the height-wise distribution of responses estimated by MPA is generally similar to the "exact" results from nonlinear response history analysis (RHA). Although the results of the previous research were extremely promising, only a few buildings were evaluated. The results presented below evaluate the accuracy of MPA for a wide range of buildings and ground motion ensembles. The selected structures are idealized frames of six different heights: 3, 6, 9, 12, 15, and 18 stories and five strength levels corresponding to SDF-system ductility factor of 1, 1.5, 2, 4, and 6; each frame is analysed for 20 ground motions. Comparing the median values of storey-drift demands determined by MPA to those obtained from nonlinear RHA shows that the MPA predicts reasonably well the changing height-wise variation of demand with building height and SDF-system ductility factor. Median and dispersion values of the ratios of storey-drift demands determined by MPA and nonlinear-RHA procedures were computed to measure the bias and dispersion of MPA estimates with the following results: (1) the bias and dispersion in the MPA procedure tend to

increase for longer-period frames and larger SDF-system ductility factors (although these trends are not perfect); (2) the bias and dispersion in MPA estimates of seismic demands for inelastic frames are usually larger than for elastic systems; (3) the well-known response spectrum analysis (RSA), which is equivalent to the MPA for elastic systems, consistently underestimates the response of elastic structures, e.g., up to 18% in the upper-storey drifts of 18-storey frames. Finally, the MPA procedure is simplified to facilitate its implementation in engineering practice--where the earthquake hazard is usually defined in terms of a median (or some other percentile) design spectrum for elastic systems--and the accuracy of this simplified procedure is documented.

Title: Feasibility of pushover analysis for estimation of strength demands
Author: Gupta, A; Krawinkler, H
Source: STESSA 2003: Proceedings of the Conference on Behaviour of Steel Structures in Seismic Areas, 9-12 June 2003, Naples, Italy , pp. 29-35. 2003

Descriptors: Deformation; Steel structures; Earthquake design; Frame structures

Abstract: The nonlinear static pushover analysis method has gained wide popularity in deformation-based design methods. Focusing only on deformation demands and capacity can often overlook unexpected patterns in strength demands, which can result in very undesirable structural behavior. This paper evaluates the effectiveness of the pushover method in estimating global and member strength demands for steel moment-resisting frame structures. Results indicate that in many cases the pushover method leads to nonconservative strength demand estimates and is unable to capture the distribution of dynamic demands over the height of the structure. In some of these cases, evaluation and sizing of members based on a simple story capacity approach provides a better solution for reducing the potential for undesirable behavior modes. This does not invalidate the value of a pushover analysis, but it puts limits on the reliance the profession should place on results obtained from such an analysis.

Title: Effects of higher modes and seismic frequency content on the accuracy of pushover analysis of steel frames
Author: Pavlidis, G; Bazeos, N; Beskos, D E
Source: STESSA 2003: Proceedings of the Conference on Behaviour of Steel Structures in Seismic Areas, 9-12 June 2003, Naples, Italy , pp. 547-550. 2003

Descriptors: Seismic phenomena; Frames; Structural steels; Dynamic tests; High frequencies

Abstract: This paper investigates the effects of the higher modes and the seismic frequency content on the accuracy of the inelastic static seismic (pushover) analysis of plane steel frames. Seven different frames designed using EC8 are analyzed for lateral static load distributions along their height and their complete inelastic response is compared against their dynamic one when subjected to 30 historic seismic records of low, moderate, and high frequency content. The effect of higher

modes is taken into account by appropriately modifying the lateral load distribution leading to very good results. It is also found that the seismic frequency content significantly affects the accuracy of pushover analysis, leading to very good results only for the cases of moderate-frequency earthquakes. A simple remedy is proposed for the treatment of this frequency content effect.

Title: Pushover analysis in the evaluation of the seismic response of steel frames
Author: Marino, E M; Muratore, M; Rossi, P P
Source: STESSA 2003: Proceedings of the Conference on Behaviour of Steel Structures in Seismic Areas, 9-12 June 2003, Naples, Italy , pp. 427-433. 2003
Descriptors: Seismic response; Frames; Dynamics; Loads (forces); Steel structures

Abstract: Nowadays pushover analysis has great importance among the methods for the evaluation of the seismic response of structures. Unfortunately, it provides results which sometimes strongly depend on the type of analysis of the generic step (static or modal) and on the load pattern. In this paper, the response of different typologies of seismic-resistant frames is analyzed by means of pushover and step-by-step dynamic analyses with the aim of highlighting differences. The results of the dynamic analyses of moment-resisting frames, eccentrically braced frames and tied eccentrically braced frames are compared with those obtained by means of pushover analyses in which different invariant and adaptive load patterns are used. The comparison of such results allows some interesting observations regarding the range in which the pushover analysis, with appropriate load patterns, provides a good estimation of dynamic seismic response.

Title: Evaluation of modal and FEMA pushover analyses: SAC buildings
Author: Goel, R.K.; Chopra, A.K.
Source: Earthquake Spectra. Vol. 20, no. 1, pp. 225-254. Feb. 2004
Descriptors: Buildings; Seismic response

Abstract: This paper comprehensively evaluates the Modal Pushover Analysis (MPA) procedure against the 'exact' nonlinear response history analysis (RHA) and investigates the accuracy of seismic demands determined by pushover analysis using FEMA-356 force distributions; the MPA procedure in this paper contains several improvements over the original version presented in Chopra and Goel (2002). Seismic demands are computed for six buildings, each analyzed for 20 ground motions. It is demonstrated that with increasing number of 'modes' included, the height-wise distribution of story drifts and plastic rotations estimated by MPA becomes generally similar to trends noted from nonlinear RHA. The additional bias and dispersion introduced by neglecting 'modal' coupling and P-*D effects due to gravity loads in MPA procedure is small unless the building is deformed far into the inelastic range with significant degradation in lateral capacity.

Title: Evaluation of seismic deformation demands using non linear procedures in multistory steel and concrete moment frames
Author: Kunnath, Sashi K; Kalkan, Erol
Source: ISET Journal of Earthquake Technology. Vol. 41, no. 1, pp. 159-181. Mar. 2004
Descriptors: Concretes; Frames; Reinforcing steels; Ductility tests; Seismic phenomena; Acceptance criteria

Abstract: A key component of performance-based seismic evaluation is the estimation of seismic demands. In FEMA-356 (FEMA, 2000b), which is now recognized as the model for future performance-based seismic codes in the US, these demands are evaluated at the component level in terms of ductility demands or plastic rotations when using non-linear procedures. Since acceptance criteria for various performance objectives are assessed in terms of local component demands, it is essential that a rational basis be established for determining such demands. Of the non-linear procedures advocated in FEMA-356, pushover procedures are becoming increasingly popular in engineering practice. However, there are still several unresolved issues in identifying appropriate lateral load patterns to be used in a pushover procedure. This paper investigates the correlation between demand estimates for various lateral load patterns used in non-linear static analysis. It also examines the rationale for using component demands over story and system demands. Results reported in the paper are based on a comprehensive set of pushover and non-linear time-history analyses carried out on eight- and twelve-story steel and concrete moment frames. Findings from this study point to inconsistencies in the demands predicted by different lateral load patterns when using pushover analysis and also highlight some issues in the current understanding of local demand estimates using FEMA-based procedures.

Title: Assessment of modal pushover analysis procedure and its application to seismic evaluation of existing buildings
Author: Yu, Qi-Song Kent; Pugliesi, Raymond; Allen, Michael; Bischoff, Carrie
Source: 13 WCEE: 13th World Conference on Earthquake Engineering Conference Proceedings. 2004
Descriptors: Buildings; Structural steels; Seismic engineering; Force distribution; Concrete construction; Benchmarking

Abstract: Nonlinear static analysis procedures (or pushover analyses with an invariant lateral force pattern) have been developed for routine application in the practice of performance-based earthquake engineering due to their conceptual simplicity and computational effectiveness. Nonlinear static procedures, however, are limited in their ability to consider higher mode effects and possible redistribution of inertial forces in a structure due to yielding. An improved static procedure termed the Modal Pushover Analysis (MPA) (Chopra and Goel, 2001) was developed to consider explicitly higher mode effects. The MPA Procedure assumes that uncoupling of modal responses for a building system is still valid in its inelastic

stage. The seismic response of each mode is determined from pushing the structure to its modal target displacement with an invariant modal lateral force distribution. Overall building peak response is obtained by combining the seismic response of each mode per the appropriate modal combination rule. In the first part of this paper, the reliability and accuracy of the MPA procedure are evaluated through nonlinear static analyses and nonlinear response-history analyses (NL-RHA) of an existing 13-story symmetrical Steel Moment Frame building. Seismic response parameters including the magnitude and spatial distribution of plastic hinge rotations and story drift ratios are considered, and results are used as benchmarks to compare nonlinear static procedures. Three variations on the MPA procedure are studied to observe additional trade-offs between accuracy and practicality. In the second part of this paper, the MPA procedure is extended to evaluate asymmetric buildings in three dimensions with lateral force patterns including both lateral forces and torsional moments. The MPA procedure is implemented to assess an existing 15-story composite steel and concrete pier-spandrel building with an irregular plan configuration.

Title: On the pushover analysis as a method for evaluating the seismic response of RC Buildings
Author: Diotallevi, P P; Landi, L
Source: Earthquake Resistant Engineering Structures V , pp. 203-217. 2005

Descriptors: Seismic phenomena; Earthquake construction; Reinforced concrete; Dynamic tests; Buildings; Load distribution (forces)

Abstract: The purpose of this work was to compare the non-linear pushover and dynamic methods of analysis. Pushover analyses of a RC building were performed considering different load distributions and incremental dynamic analyses were carried out considering a large number of earthquake motions. Then several simplified non-linear procedures based on the pushover analysis were applied in order to assess their capability in the prediction of the seismic demand.

Title: Evaluation of conventional and adaptive pushover analysis I: methodology
Author: Papanikolaou, Vassilis K; Elnashai, Amr S
Source: Journal of Earthquake Engineering. Vol. 9, no. 6, pp. 923-941. Nov. 2005
Descriptors: Reinforced concrete; Performance evaluation; Dynamic structural analysis; Seismic response; Earthquake engineering

Abstract: In this paper, a methodology is suggested and tested for evaluating the relative performance of conventional and adaptive pushover methods for seismic response assessment. The basis of the evaluation procedure is a quantitative measure for the difference in response between these methods and inelastic dynamic analysis which is deemed to be the most accurate. Various structural levels of evaluation and different incremental representations for dynamic analysis are also suggested. This

method is applied on a set of eight different reinforced concrete structural systems subjected to various strong motion records. Sample results are presented and discussed while the full results are presented alongside conclusions and recommendations, in a companion paper.

Title: An application of modal pushover analysis to medium-rise shear-wall reinforced concrete buildings

Author: Arevalo, L; Cruz, E F

Source: 100th Anniversary Earthquake Conference. 2006

Descriptors: Buildings; Seismic phenomena; Earthquake construction; Shear walls; Reinforced concrete; Structural damage

Abstract: The application of the Modal Pushover Analysis (MPA) method to real Chilean medium rise buildings based on reinforced concrete shear walls is presented. The evaluation of the results obtained is made by comparison with results from time history analysis of the nonlinear response (NLRHA). The precision of the seismic demand determined by the MPA is studied for three buildings (7, 11, and 12 stories) with a percentage of area of walls with respect to the area of the plan of the order of 3%. For the analysis of the building the analytical model considered includes failure modes for the wall in flexure and in shear. For the MPA the P-0 effects were considered and for the NLRHA the program LARZ (2D) was used. For both analyses procedures the actual records of events that in the past affected these buildings and caused some structural damage represented the earthquake excitation. The results obtained show that MPA tends to underestimate the response obtained from the NLRHA, but the quantitative description of the overall nonlinear behavior as obtained from the global responses of the buildings using MPA, is found to be quite good.

Title: Application of pushover analysis procedures for predicting the seismic response of RC structures

Author: Diotallevi, Pier Paolo; Landi, Luca

Source: First European Conference on Earthquake Engineering and Seismology. 2006

Descriptors: Invariants; Reinforced concrete; Elevation; Seismic response; Seismic phenomena; Displacement; Regularity; Frames; Mathematical models; Nonlinear dynamics; Performance enhancement

Abstract: In this work an extensive numerical investigation was carried out in order to study the effectiveness of several invariant, modal and adaptive pushover procedures. These procedures were applied considering two RC frames with nine storeys, and with different properties in terms of regularity in elevation. The results were compared with non-linear dynamic analyses, which were performed considering various earthquake records. The comparison regarded the base shear- top displacement curves as well as different storey response parameters. The results confirmed the better performance of the improved procedures, especially of the

modal pushover. However they showed also a quite good behaviour for some invariant procedures.

Title: Assessment of adaptive pushover procedures by dynamic analysis
Author: Ferracuti, Barbara; Savoia, Marco; Pinho, Rui; Francia, Roberto
Source: First European Conference on Earthquake Engineering and Seismology. 2006
Descriptors: Nonlinear dynamics; Dynamic tests; Assessments; Nonlinearity; Dynamics; Design engineering; Seismic phenomena; Seismic response; Offices; Drift; Horizontal; Seismic engineering; Spectra; Earthquake design; Mathematical analysis; Displacement; Reinforced concrete; Fibre; Finite element method

Abstract: Nonlinear dynamic analysis is the most reliable method to describe structural response under seismic action. Nevertheless, such technique can still be a very time-consuming and complex process, inadequate for general design office application. As such, recent years have witnessed an increased focus on the development of design/assessment procedures based on nonlinear static analysis (or pushover analysis). The latter can effectively describe the capacity of the structure under horizontal forces in the nonlinear range with a reduced computational effort with respect to nonlinear dynamic analysis. In the present study, different pushover procedures, applied to the case of reinforced concrete frames, are compared using a fibre finite element code. For non- adaptive analyses, two different force distributions are considered, uniform and proportional to the first modal shape. For adaptive pushover procedures, Force-based (FAP) and Displacement-based (DAP) techniques are employed instead. In order to validate these procedures, incremental dynamic analyses (IDA) are carried out using a set of artificial time-histories derived to fit the Eurocode response spectra. Comparisons of static against dynamic results for three case studies have been performed, in terms of both capacity curves as well as interstory drift profiles.

Title: Verification of an adaptive pushover technique for the 3d case
Author: Meireles, Helena; Pinho, Rui; Bento, Rita; Antoniou, Stelios
Source: First European Conference on Earthquake Engineering and Seismology. 2006
Descriptors: Three dimensional; Methodology; Displacement; Adaptive structures; Mathematical models; Asymmetry; Planar structures; Grounds; Seismic response; Algorithms; Drift; Nonlinear dynamics; Spears; Excitation; Accuracy; Bidirectional

Abstract: The displacement based adaptive pushover (DAP) technique is an improved pushover technique in which a set of laterally imposed displacements, rather than forces, are applied in adaptive fashion to the structure. The technique has been extensively tested for two dimensional planar structures with considerable improvements when compared to conventional pushover techniques. It seems paramount, then, to verify its efficiency for the 3D case, in which it is hoped that the

algorithm, will also lead to improved seismic response predictions. Herein, the DAP methodology is evaluated for a 3D asymmetric building structure (the SPEAR building). It is investigated how the pushover results of a spatial model can be best compared with the nonlinear dynamic envelopes. Bidirectional excitation is considered. Seven different ground motions were used, all fitted to the same code-defined response spectrum. Additionally, the DAP methodology has been compared with a conventional non-adaptive pushover, where lateral forces in a triangular pattern are applied. Good agreement is obtained with the time history analysis results although torsional induced interstorey drifts are slightly underestimated. The advantages of the methodology are clear when compared to its non-adaptive conventional counterpart. Further testing on more irregular and complex buildings would manage to fully evidence the benefits of the method.

Title: Evaluation of conventional and adaptive pushover analysis II: comparative results
Author: Papanikolaou, Vassilis K; Elnashai, Amr S; Pareja, Juan F
Source: Journal of Earthquake Engineering. Vol. 10, no. 1, pp. 127-151. Jan. 2006
Descriptors: Adaptive structures; Dynamic tests; Reinforced concrete; Methodology; Ductility tests; Buildings; Earthquake engineering

Abstract: In this paper, the methodology for evaluation of conventional and adaptive pushover analysis presented in a companion paper is applied to a set of eight different reinforced concrete buildings, covering various levels of irregularity in plan and elevation, structural ductility and directional effects. An extensive series of pushover analysis results, monitored on various levels is presented and compared to inelastic dynamic analysis under various strong motion records, using a new quantitative measure. It is concluded that advanced (adaptive) pushover analysis often gives results superior to those from conventional pushover. However, the consistency of the improvement is unreliable. It is also emphasised that global response parameter comparisons often give an incomplete and sometimes even misleading impression of the performance.

Title: FEA modeling and modal pushover analysis of a 14-story office building in Anchorage, Alaska
Author: Liu, H; Bai, F; Gobeli, J L
Source: Proceedings of the 2006 Structures Congress: Structural Engineering and Public Safety; St. Louis, MO; USA; 18-21 May 2006. 2006
Descriptors: Finite element method; Buildings; multistory; Alaska; Seismic phenomena; Seismic engineering; Earthquake construction; Mathematical models; Dynamics; Calibration; Earthquake damage; Loads (forces); Tools; Grounds; Mathematical analysis; Earthquake dampers; Office buildings; Invariants; Dynamical systems

Abstract: Presented is a detailed case study on structural Finite Element (FE) modeling and Modal Pushover Analysis (MPA) of a 14-story office building

instrumented for seismic response investigation. The system identification tool was used to identify the structural dynamic properties, including the natural periods of vibration of the structure and level of critical damping based on seismic data recorded during small seismic ground motions. A series of FE models were created to improve the modeling technique. The final "corrected" FE model was refined and calibrated to match the identified structural natural periods. It was found that a FE model can be calibrated to give a good prediction of earthquake response. Using the calibrated FE model, the structural seismic behavior has been examined using the MPA procedure. In the MPA procedure, an improved analysis based on structural dynamic theory with invariant force distributions was used to generate the push loads. Four recorded ground acceleration time histories were used as input data for the MPA procedure. Five sets of push forces, corresponding to the effective earthquake forces from the first five modal expansions, were applied to the FE model. The final MPA results were combined from these five push-over cases using the Square-Root-of-Sum-of-Squares (SRSS) rule and the Complete Quadratic Combination (CQC) rule to get the total response. The MPA results were also compared with the Incremental Dynamic Analysis (IDA). It is found that the MPA and IDA results are reasonably matched. The MPA procedure is an improved tool for estimating seismic demands on buildings. Using the MPA procedure, the structural behavior can be examined during seismic loading and future performance of the building during damaging earthquakes can be predicted.

Title: Static pushover methods explanation, comparison and implementation

Author: Powell, Graham H

Source: 100th Anniversary Earthquake Conference. 2006

Descriptors: Seismic phenomena; Redesign

Abstract: This paper reviews and explains a number of static push-over methods, compares them for accuracy, and identifies the most promising method. It must be emphasized in advance that the procedure used to compare the methods is neither detailed nor scientific. Rather, it represents the type of study that a practicing engineer might use to gain confidence in push-over methods. The paper also shows that push-over analysis can give useful sensitivity information for redesign.

Title: Observations on the reliability of alternative multiple-mode pushover analysis methods

Author: Tjhin, T; Aschheim, M; Hernandez-Montes, E

Source: Journal of Structural Engineering (New York, N.Y.). Vol. 132, no. 3, pp. 471-477. Mar. 2006

Descriptors: Seismic engineering; Nonlinear dynamics; Buildings; Earthquake construction; Frames; Structural engineering

Abstract: Although multiple-mode pushover analysis methods have been proposed for general use in the seismic analysis of moment resisting frames, difficulties have been encountered in their implementation with specific structures. Two alternative

multiple mode methods were developed to overcome these difficulties. Estimates of four response quantities determined with the alternative methods are compared herein for a set of five buildings subjected to suites of scaled ground motions. The uneven accuracy of the estimates, relative to the range of values determined by nonlinear dynamic analysis, suggests that results obtained by both alternative methods should be regarded with caution, until such time that the scope of applicability of the methods has been clearly established.

Title: Assessment of improved nonlinear static procedures in FEMA-440
Author: Akkar, S; Metin, A
Source: Journal of Structural Engineering , no. 9, pp. 1237-1246. Sept. 2007

Descriptors: Seismic effects; Drift; Approximation methods; Performance characteristics; Frames; Statistics; Demand; Marketing; Deformation; Nonlinearity; Displacement; Seismic phenomena; Correlation; Coefficients; Seismic engineering; Buildings; Drift estimation; Reinforced concrete; Structural engineering

Abstract: Nonlinear static procedures (NSPs) presented in the FEMA-440 document are evaluated for nondegrading three- to nine-story reinforced concrete moment-resisting frame systems. Evaluations are based on peak single-degree-of-freedom displacement, peak roof, and interstory drifts estimations. A total of 78 soil site records and 24 buildings with fundamental periods varying between 0.3 s - 1.3 s are used in 2,832 linear and nonlinear response-history analyses to derive the descriptive statistics. The moment magnitude of the ground motions varies between 5.7 and 7.6. All records are within 23 km of the causative fault representing near-fault ground motions with and without pulse signals. The statistics presented suggest that lateral loading patterns used in pushover analysis to idealize the building systems play a role in the accuracy of NSPs investigated. Both procedures yield fairly good deformation demand estimations on the median. Displacement coefficient method (DCM) tends to overestimate the global deformation demands with respect to the capacity spectrum method (CSM). The conservative deformation demand estimations of DCM are correlated with the normalized lateral strength ratio, R . The CSM tends to overestimate the deformation demands for the increasing displacement ductility, μ .

Title: Evaluation of Seismic demands for rc building frames using modal pushover analysis method
Author: El-Esnawy, N A
Source: Journal of Engineering and Applied Science. Vol. 54, no. 3, pp. 339-358. June 2007
Descriptors: Seismic phenomena; Seismic engineering; Earthquake construction; Drift; Demand analysis; Dynamics; Reinforced concrete; Marketing; Standards; Dynamic tests; Frames; Earthquake design; Egypt; Earthquake damage; Earthquakes; Failure; Shear; Dynamic structural analysis; Damage

Abstract: Performance-based seismic design of multistory buildings requires proper evaluation of story drifts as they are related to damage arising in buildings during earthquakes. Hence, this paper demonstrates the evaluation of seismic drift demands for a 12-story RC building frame meeting the design practice in Egypt by applying the modal pushover analysis method. This MPA method is gaining wide attention from the seismic engineering community because of its structural dynamics theory and its ability to overcome the failure of standard pushover analysis to account for the effects of higher modes. First, details of the MPA method are presented. Then, the MPA method is applied to evaluate the target roof drift, base shear and story drifts of the RC building frame. These seismic demands are compared with the results of inelastic dynamic analysis for Aqaba and Landers earthquake records. Also, the results of standard pushover analysis are illustrated. The comparative study shows that the seismic demands evaluated by the MPA method compare well with the dynamic results and are significantly better than those evaluated by standard pushover analysis. Thus, the MPA method provides a simpler and more practical analysis alternative than inelastic dynamic analysis for seismic evaluation of regular mid-rise RC buildings.

Title: Assessment of current nonlinear static procedures for seismic evaluation of buildings
Author: Kalkan, Erol; Kunnath, Sashi K
Source: Engineering Structures. Vol. 29, no. 3, pp. 305-316. Mar. 2007
Descriptors: Seismic phenomena; Earthquake construction; Seismic engineering; Earthquake design; Nonlinearity; Marketing; Demand; Grounds; Reinforcing steels; Buildings; Reinforced concrete; Arrays; Invariants; Recording; Drift; Demand analysis; Mathematical analysis; Hazards; Probability theory

Abstract: An essential and critical component of evolving performance-based design methodologies is the accurate estimation of seismic demand parameters. Nonlinear static procedures (NSPs) are now widely used in engineering practice to predict seismic demands in building structures. While seismic demands using NSPs can be computed directly from a site-specific hazard spectrum, nonlinear time-history (NTH) analyses require an ensemble of ground motions and an associated probabilistic assessment to account for aleatoric variability in earthquake recordings. Despite this advantage, simplified versions of NSP based on invariant load patterns such as those recommended in ATC-40 and FEMA-356 have well-documented limitations in terms of their inability to account for higher mode effects and the modal variations resulting from inelastic behavior. Consequently, a number of enhanced pushover procedures that overcome many of these drawbacks have also been proposed. This paper investigates the effectiveness of several NSPs in predicting the salient response characteristics of typical steel and reinforced concrete (RC) buildings through comparison with benchmark responses obtained from a comprehensive set of NTH analyses. More importantly, to consider diverse ground motion characteristics, an array of time-series from ordinary far-fault records to near-

fault motions having fling and forward directivity effects was employed. Results from the analytical study indicate that the Adaptive Modal Combination procedure predicted peak response measures such as inter-story drift and component plastic rotations more consistently than the other NSPs investigated in the study.

Title: Elastoplastic analysis of a tall SRC structure under major earthquakes
Author: Nie, Jianguo; Tian, Shuming
Source: Qinghua Daxue Xuebao / Journal of Tsinghua University. Vol. 47, no. 6, pp. 772-775. June 2007
Descriptors: Seismic phenomena; Elastoplasticity; Slabs; Earthquakes; Dynamic structural analysis; Collapse; Deformation effects; Vibration; Shear; Nonlinear dynamics; Drift; Resists; Nonlinearity; Grounds; Education; Seismic engineering; Reinforcing steels; Civil engineering; Error analysis

Abstract: The seismic behavior of a tall steel reinforced concrete (SRC) structure was analyzed using dynamic elastoplastic analysis. The CANNY06 (a 3-D nonlinear static and dynamic structural analysis program) was used. The internal forces and deformations, including shear forces, overturning moments, lateral displacements, and drifts, were compared with those of a static elastoplastic analysis to evaluate the effectiveness of the pushover analysis. The behavior of the composite floor slab during the earthquake was also analyzed. The results show that the pushover analysis can not accurately predict whether a structure will resist major earthquake ground motions without collapse, and the rigid floor slab assumption for the composite floor slab is suitable for the structure height-width ratio greater than 3 with larger height-width ratios resulting in smaller errors.

Title: Seismic performance evaluation of reinforced-concrete buildings by static pushover and nonlinear dynamic analyses
Author: Boonyapinyo, Virote; Choopool, Norathape; Warnitchai, Pennung
Source: 14th World Conference on Earthquake Engineering: Innovation Practice Safety. 2008
Descriptors: Seismic phenomena; Earthquake construction; Nonlinear dynamics; Seismic engineering; Dynamical systems; Earthquake design; Bangkok; Grounds; Nonlinearity; Performance evaluation; Reinforced concrete; Seismic response; Computer simulation; Buildings; Mathematical models; Ductility; Failure; Soils; Beam-columns

Abstract: The prediction of inelastic seismic responses and the evaluation of seismic performance of a building structure are very important subjects in performance-based seismic design. The seismic performances of reinforced-concrete buildings evaluated by nonlinear static analysis (pushover analysis and modal pushover analysis) and nonlinear time history analysis are compared in this research. A finite element model that can accurately simulate nonlinear behavior of building is formulated by considering several important effects such as p-delta, masonry in-fill walls, soil-

structure interaction, and beam-column joints that can be considered rigid zones with joint failure due to poor detailing of joints. Both global response such as system ductility demand and local response such as inter-story drift are investigated in this research. A numerical example is performed on a 9-story reinforced concrete building in Bangkok. Because Bangkok is located in soft to medium soils, response of studied building under a simulated earthquake ground motion at Bangkok site is compared with that under a measured earthquake ground motion of EI-Centro. Finally, the global and local responses obtained from the modal pushover analysis are compared with those obtained from the nonlinear dynamic analysis of MDOF system. The results show that the MPA is accurate enough for practical applications in seismic performance evaluation when compared with the nonlinear dynamic analysis of MDOF system. The results also show that ductility of the studied building can be estimated to 2.40, 2.02 and 1.65 by Fajfar, Chopra and Lee methods, respectively, for simulated ground motion at Bangkok site for a 500-year return period.

Title: Influence of lateral load distributions on pushover analysis effectiveness
 Author: Colajanni, P; Potenzzone, B
 Source: 2008 Seismic Engineering Conference Commemorating the 1908 Messina and Reggio Calabria Earthquake Part One (AIP Conference Proceedings Volume 1020, Part 1). Vol. 1020, pp. 880-887. 2008
 Descriptors: Seismic response; Loads (forces); Dynamics; Eccentricity; Dynamic tests; Load distribution (forces); Seismic phenomena; Seismic engineering; Stress concentration; Frames; Braced; Lateral loads

Abstract: The effectiveness of two simple load distributions for pushover analysis recently proposed by the authors is investigated through a comparative study, involving static and dynamic analyses of seismic response of eccentrically braced frames. It is shown that in the upper floors only multimodal pushover procedures provide results close to the dynamic profile, while the proposed load patterns are always conservative in the lower floors. They over-estimate the seismic response less than the uniform distribution, representing a reliable alternative to the uniform or more sophisticated adaptive procedures proposed by seismic codes.

Title: Evaluation of ASCE-41 nonlinear static procedure using recorded motions of reinforced-concrete buildings
 Author: Goel, Rakesh K; Chadwell, Charles
 Source: Proceedings of the 2008 Structures Congress: Crossing Borders; Vancouver, BC; Canada; 24-26 Apr. 2008. 2008
 Descriptors: Reinforced Concrete; Concrete structures; ASCE Publications; Buildings; Roofs; Estimates; Drift; Nonlinearity; Borders; Seismic phenomena; Seismic engineering; Marketing; Earthquake construction; Documents; Demand

Abstract: This paper evaluates the nonlinear static procedures (NSP) specified in the ASCE-41 document using strong motion records of five reinforced-concrete

buildings. For this purpose, seismic demands - peak roof displacements, floor displacements, and inter-story drifts - estimated from the NSP are compared with the values derived from recorded motions. It is shown that the ASCE-41 NSP may significantly under- or over-estimate the peak roof displacements. While the NSP may provide accurate estimates of floor displacements, it is unable to provide accurate estimates of story drifts, especially for taller buildings where higher modes may be more significant.

Title: Modal and cyclic pushover analysis for seismic performance evaluation of buckling-restrained braced steel frame
Author: Jia, Ming-Ming; Lu, Da-Gang; Zhang, Su-Mei; Jiang, Shou-Lan
Source: 14th World Conference on Earthquake Engineering: Innovation Practice Safety. 2008
Descriptors: Hysteresis; Seismic phenomena; Braced; Seismic engineering; Structural steels; Frames; Seismic response; Ultimate tensile strength; Iron and steel industry; Nonlinearity; Steel making; Compressive strength; Vibration mode; Dissipation; Performance evaluation; Yield strength; Energy dissipation; Deformation; Seismic energy

Abstract: Buckling-Restrained Braces (BRBs) are confirmed to have nearly the same yielding stress and ultimate strength under tension and compression. The BRBs can undergo fully-reversed axial yield cycles without loss of stiffness and strength, whose seismic energy dissipation ability is superior. Based on modal pushover analysis, the influence of higher vibration modes of Buckling-Restrained Braced steel frame was considered. Compared to non-linear static procedure, the results of modal pushover analysis agree better with that of nonlinear response history analyses. Based on cyclic pushover analysis, the hysteretic behavior of Buckling-Restrained Braced Steel Frame (BRBSF) was researched. After installed with BRBs, the energy dissipation of BRBSF is completed by the hysteretic deformation of BRBs, the seismic responses of the structure will be greatly reduced and seismic performance will be improved.

Title: Seismic response evaluation of irregular high rise structures by modal pushover analysis
Author: Khoshnoudian, F; Mohammadi, S A
Source: 14th World Conference on Earthquake Engineering: Innovation Practice Safety. 2008
Descriptors: Seismic phenomena; Seismic engineering; Irregularities; Earthquake construction; Estimates; Deterioration; Seismic response; Frames; Stiffness; Nonlinear dynamics; High rise buildings; Strength

Abstract: This paper investigates the accuracy of the modal pushover analysis to estimate the seismic performance of high-rise buildings. The effects of structural irregularities in stiffness, strength, mass and combination of these factors are considered. In other words, reliability of the modal pushover analysis (MPA) has been verified by defining a referenced regular structure for comparison between MPA and nonlinear dynamic analysis. Using two analysis method for vertically

irregular and regular frames leads to the following results: (1) the mass irregularity conditions were found to have a negligible impact on the seismic performance of building, (2) The accuracy of modal pushover analysis to estimate the seismic performance increases when irregularities conducted at lower half stories, (3) Additionally the accuracy does not deteriorate when irregularities provides in the middle or upper story, and (4) Time saving and accuracy besides conceptual simplicity of MPA in brief leads to reliable estimation of seismic performance.

Title: Study on lateral load patterns of pushover analysis using incremental dynamical analysis for RC frame structures
Author: Ma, Qianli; Ye, Lieping; Lu, Xinzheng; Miao, Zhiwei
Source: Jianzhu Jiegou Xuebao/Journal of Building Structures. Vol. 29, no. 2, pp. 132-140. Mar.-Apr. 2008
Descriptors: Lateral loads; Reinforced concrete; Frames; Nonlinearity; Frame structures; Mathematical models; Earthquake design; Design engineering; Seismic response; Seismic phenomena; Foundations; Safes; Drift; Numerical stability; Computation; Fibers; Shear

Abstract: In this research, the nonlinear static procedures with different lateral load patterns were compared by using incremental dynamical analysis method based on a six-storey and a ten-storey RC frame fiber model. For each story of different frames, the inter-story shear force vs. drift curves computed by pushover analysis by using different lateral load patterns and time history analysis with a series of earthquake records on the design site have been compared to give a rational lateral load pattern of pushover analysis. Finally, for a whole frame structure, the lateral load pattern choice was suggested, that is, uniform load pattern was better for the stories near foundation; load pattern with the story heights taken into consideration was suitable for the mid stories and the SRSS pattern or Chinese Code pattern was suitable for upper stories. It is also shown that the nonlinear static procedure gives a safe estimation of the inelastic seismic response statistically for regular RC frames with good numerical stability

Title: Non-linear methods for seismic assessment of existing structures: a comparative study on italian RC buildings
Author: Maddaloni, G; Magliulo, G; Martinelli, E; Monti, G; Petti, L; Saetta, A; Spacone, E
Source: 14th World Conference on Earthquake Engineering: Innovation Practice Safety. 2008
Descriptors: Nonlinearity; Reinforced concrete; Buildings; Dispersions; Earthquake design; Assessments; Seismic phenomena; Seismic engineering; Building codes; Earthquake construction; Trends; Construction

Abstract: The present paper reports on an Italian collaborative research study on the applicability of nonlinear methods of analysis to regular and irregular existing RC buildings designed and constructed according to older building codes. The mentioned methods are applied to two case studies of practical interest and the results are

compared in order to identify general trends and major unresolved issues with reference to the key properties of the considered structures. Non-linear time history analyses are carried out to obtain reference values for the expected response parameters, characterized in terms of median value and dispersion, to be compared with the results obtained through nonlinear pushover analyses.

Title: Static and dynamic non linear analysis of plan irregular existing R/C frame buildings
Author: Magliulo, Gennaro; Maddaloni, Giuseppe; Cosenza, Edoardo
Source: 14th World Conference on Earthquake Engineering: Innovation Practice Safety. 2008
Descriptors: Seismic phenomena; Planes; Earthquakes; Frames; Limit states; Nonlinearity; Seismic engineering; Buildings; Dynamic tests; Spreads; Collapse; Seismic response; Fittings; Acceleration; Nonlinear dynamics; Columns (structural); Horizontal; Amplification; Grounds

Abstract: The paper deals with the topic of seismic response of three existing structures. They are multi-storey r/c frame buildings, a very spread typology in Italy; in particular, the first has a rectangular plane shape, the second has a L plane shape and the third has a rectangular plane shape with courtyard. The second and the third are irregular in plane according to the rules proposed by the Italian seismic code OPCM n.3431 and by the Eurocode 8 (EC8). Nonlinear static (pushover) and dynamic analyses are performed considering three different seismic zones, with PGA (peak ground acceleration) equal to 0.35 g, 0.25 g and 0.15 g. These are performed using sets of seven earthquakes (each with both the horizontal components), fully satisfying the EC8 provisions. Twelve different earthquake directions are considered, rotating the direction of both the orthogonal components by 30 deg for each analysis (from 0 deg to 330 deg). The analyses have been performed at Significant Damage Limit State, with earthquakes fitting the EC8 elastic spectrum characterised by a return period of 475 years; furthermore, the Near Collapse Limit State is also considered, amplifying the previous earthquakes by a factor equal to 1.5. The results of non linear static analyses are compared to the ones obtained by nonlinear time-history analyses, in terms of demanded / available rotation ratio at the top and at the bottom of each column in the two directions and in terms of maximum frame top displacements.

Title: Controlling ability of lateral load pattern in pushover analysis on seismic responses of frame
Author: Yang, Hong; Luo, Wen-Jin; Wang, Zhi-Jun
Source: Zhejiang Daxue Xuebao (Gongxue Ban)/Journal of Zhejiang University (Engineering Science). Vol. 42, no. 9, pp. 1526-1531. Sept. 2008
Descriptors: Lateral loads; Error analysis; Frames; Seismic phenomena; Nonlinearity; Hinges; Ductility; Loads (forces); Focusing; Statistical methods; Seismic response; Samples; Statistical analysis; Seismic

engineering; Mathematical analysis; Stress concentration; Reinforced concrete; Errors; Stiffness

Abstract: A typical six-story reinforced concrete frame was chosen as an example to investigate the controlling ability of lateral load pattern in pushover analysis on the load structural responses. Base on the OpenSees framework, a series of the nonlinear time-history analyses under a large sample of thirty rare earthquake waves and Pushover analysis with three common lateral load patterns were performed, respectively. The statistical results of the nonlinear time-history analyses were taken as the benchmark for comparison research. The characteristics of the responses of three kinds of Pushover analysis were studied by focusing the investigation on the local responses of the frame, such as the plastic hinge distribution and the rotation ductility. The results indicate that the errors of the Pushover analysis with uniform lateral load pattern, namely storey forces proportional to storey masses are biggest. The errors of the adaptive lateral load pattern, which is calculated based on the instant secant stiffness at each load step are smallest, and this pattern's plastic hinge distributions and rotation ductility of yielded element ends have smallest errors with respect to the results of time-history analyses, but the errors of local response of columns should not be neglected. The errors of the inverted triangular lateral load pattern lie between the above two patterns.

Title: Efficacy of pushover analysis methodologies: A critical evaluation

Author: Dutta, Sekhar Chandra; Chakroborty, Suvonkar; Raychaudhuri, Anusrita

Source: Structural Engineering and Mechanics. Vol. 31, no. 3, pp. 265-276. 10 Feb. 2009

Descriptors: Design engineering; Marketing; Nonlinear dynamics; Demand analysis; Accuracy; Guidelines; Dynamic response; Mathematical analysis; Earthquake design; Combustion; Offices; Seismic phenomena; Seismic engineering; Computation; Pictures

Abstract: Various Pushover analysis methodologies have evolved as an easy as well as designersfriendly alternative of nonlinear dynamic analysis for estimation of the inelastic demands of structures under seismic loading for performance based design. In fact, the established nonlinear dynamic analysis to assess the same, demands considerable analytical and computational background and rigor as well as intuitive insight into inelastic behavior for judging suitability of the results and its interpretation and hence may not be used in design office for frequent practice. In this context, the simple and viable alternative of Pushover analysis methodologies can be accepted if its efficacy is thoroughly judged over all possible varieties of the problems. Though this burning issue has invited some research efforts in this direction, still a complete picture evolving very clear guidelines for use of these alternate methodologies require much more detailed studies, providing idea about how the accuracy is influenced due to various combinations of basic parameters regulating inelastic dynamic response of the structures. The limited study presented in the paper aims to achieve this end to the extent possible. The study intends to

identify the range of applicability of the technique and compares the efficacy of various alternative Pushover analysis schemes to general class of problems. Thus, the paper may prove useful in judicial use of Pushover analysis methodologies for performance based design with reasonable accuracy and relative ease.

Relative to empirical results

Title: Pseudo-dynamic test of full-scale RCS frame, Part II: analysis and design implications
Author: Cordova, Paul
Source: Proceedings of the International Workshop on Steel and Concrete Composite Construction (IWSCCC-2003), October 8-9, Taipei, Taiwan , pp. 119-131. 2003
Descriptors: Frames; Concrete construction; Reinforcing steels; Design engineering; Earthquake design

Abstract: This is the second of a two-part paper, describing an investigation of a full-scale three-story composite reinforced concrete-steel (RCS) frame that was tested in the NCREE laboratory in Taipei, Taiwan. The frame specimen was pseudodynamically loaded to represent four earthquake ground motions of varying hazard levels after which the frame was subjected to a monotonic pushover loading out to interstory drift ratios of 10 percent. This paper summarizes the analytical studies of the test frame, including comparisons with measured response and design implications. Damage indexes are investigated to help interpret the analytical results and relate the calculated engineering demand parameters to physical damage in the frame. In terms of peak displacements and overall response, the analytical and measured frame response agree fairly well up to drift ratios of about 3 percent. Beyond this, discrepancies occur, which are likely due to degradation effects (e.g., local flange buckling) that are not modeled in the analysis. Comparison between calculated damage indexes and observed damage suggest the need for further research to improve the performance simulation tools.

Title: Pseudo-dynamic testing of a 3d full-scale high ductile steel-concrete composite MR frame structure at ELSA
Author: Bursi, Oreste S; Caramelli, Stefano; Fabbrocino, Giovanni; Pinto, Artur V; Salvatore, Walter; Taucer, Fabio; Tremblay, Robert; Zandonini, Riccardo
Source: 13 WCEE: 13th World Conference on Earthquake Engineering Conference Proceedings. 2004
Descriptors: Earthquake damage; Seismic phenomena; Frame structures; Reinforced concrete; Joints; Reinforcing steels; Ductility; Computer simulation

Abstract: Composite moment resisting (MR) frame structures consisting of steel-concrete beams and reinforced concrete partially encased columns can provide efficient and economical alternatives to traditional steel or reinforced concrete constructions. In addition to economies achieved by effective use of different

materials, this research shows the feasibility of composite MR frames with partially encased columns and partial strength beam-to-column joints to provide strength and ductility exceeding that in conventional steel or reinforced concrete MR frame structures. In detail, energy dissipation is concentrated both in column web panels which are not surrounded by concrete and in composite beam-to-column connections. A full-scale two-storey composite building was used to validate the system performance of composite MR frames with partial strength joints. The frame structure was subjected to pseudo-dynamic (PsD) tests at the European Laboratory for Structural Assessment (ELSA) of Joint Research Centre (JRC), in order to simulate the structural response under ground motions corresponding to earthquake hazards for a highseismicity site with 10 % and 2 % chance of exceedence in 10 years. The ground motion for 10 % chance of exceedence in 10 years earthquake hazard caused minor damage while the one for 2 % chance of exceedence in 10 years earthquake hazard entailed column web panel yielding, connection yielding and plastic hinging at column base joints. An earthquake level chosen to approach the collapse limit state induced more damage and was accompanied by further column web panel yielding, connection yielding and inelastic phenomena at column base joints without local buckling. Successively, the structure was subjected to a final quasi-static cyclic test with interstorey drift ratios up to 4.6 %. Extensive cracks in the slabs and failure of extended end plates at weld toes were observed. Moreover, test offered additional opportunities to examine construction methods and validate the performance of simulation FE models. Exploiting inelastic static pushover and time-history analysis procedures, behaviour factors, design overstrength factors and the ductility demand of the structure was estimated. Finally, behaviour factors and overstrength factors were identified and compared to code-specified assumptions.

Title: Blind Predictions of the Seismic Response of a Woodframe House: An International Benchmark Study

Author: Folz, Bryan; Filiatrault, Andre

Source: Earthquake Spectra. Vol. 20, no. 3, pp. 825-851. Aug. 2004

Descriptors: Mathematical models; Benchmarking; Seismic response; Houses; Wooden structures

Abstract: As part of the CUREE-Caltech Woodframe Project, the international engineering community was invited to blind predict the dynamic characteristics and inelastic seismic response of a two-story woodframe house that had been extensively tested on a shake table. This research study provided a unique opportunity to assess the state of the art of numerical models in predicting the inelastic dynamic response of woodframe structures. Another objective of this study was to foster cooperation between the CUREE-Caltech Woodframe Project and other related research activities being conducted worldwide. Five international teams completed the benchmark exercise and provided blind predictions of the nonlinear time-history response of the shake-table test structure under varying levels of seismic input as well as its pushover response. The participating teams adopted a wide range of numerical models and

solution strategies. This paper provides a summary of the activities conducted under the CUREE-Caltech Woodframe Project International Benchmark Study.

Title: Dynamic response of lightly reinforced concrete walls
Author: Ghobarah, A; Galal, Khaled; Elgohary, Medhat
Source : 13 WCEE: 13th World Conference on Earthquake Engineering Conference Proceedings. 2004
Descriptors: Walls; Panels; Reinforced concrete; Seismic phenomena; Ductility; Load carrying capacity

Abstract: There are many lightly reinforced concrete walls that were constructed in buildings and even in nuclear power plant installations in various countries. It is expected that these walls will behave in a nonductile manner during severe earthquakes. In order to rehabilitate this type of wall, it is necessary to evaluate the behaviour and determine its load carry capacity during moderate and major seismic events. The objective of the investigation is to determine the response of typical lightly reinforced walls when subjected to scaled ground motion records up to failure and to establish the load carrying capacity and ductility of the walls. The wall was modeled using six node two dimensional panel elements. The panel elements have lumped Flexural/axial plasticity at their top and bottom fibre sections. Nonlinear static and dynamic time history analyses were conducted. The response of the wall was evaluated in terms of pushover, spectral, displacement-based, and time-history analyses. The analytical results indicated that the wall behaved in a nonductile manner with brittle shear failure. The model and the response data were verified against available measurements from a test program conducted using a shake table. The comparison indicated that the model closely represented the behaviour observed in the test.

Title: Accuracy of numerical analysis for prediction of inelastic cyclic behavior of full-scale steel moment frame -Test on full-scale three story frame for evaluation of seismic performance
Author: Matsumiya, Tomohiro; Nakashima, Masayoshi; Suita, Keiichiro; Liu, Dawei; Zhou, Feng; Fukumoto, Naoaki
Source: Journal of Structural and Construction Engineering , no. 585, pp. 215-222. Nov. 2004
Descriptors: Frames; Steels; Beams (structural); Fatigue (materials); Mathematical models; Error analysis; Permissible error; Yield strength; Cyclic loads; Stiffness; Strength; Seismic phenomena; Strain hardening; Numerical analysis; Iron and steel industry; Intermediate frequency; Steel making; Seismic engineering; Performance evaluation

Abstract: This paper presents a study on the calibration of numerical inelastic analyses for the capacity of estimating the elastic stiffness and yield strength of multi-story steel moment frames and of tracing inelastic cyclic behavior of such frames. To this end, a set of test results obtained from a full-scale cyclic loading test

applied to a three-story, two span by one span steel moment frame were used as the reference. Pushover analyses using nominal material strength were able to estimate the frame's elastic stiffness and yield strength very reasonably, with the degree of errors not greater than 5%. Analyses for cyclic loading to a drift angle of 1/25 rad were also very accurate (with errors - not greater than 4%) IF appropriate values were adopted for strain hardening of individual columns, column-bases, panel-zones, and beams and for increase of strength by floor composite action. The fish-bone (generic frame) model traced the experimental behavior nearly as accurately as the original frame model.

Title: Full-scale test of three-story steel moment frames for examination of extremely large deformation and collapse behavior
Author: Matsumiya, Tomohiro; Nakashima, Masayoshi; Suita, Keiichiro; Liu, Dawei
Source: 13 WCEE: 13th World Conference on Earthquake Engineering Conference Proceedings. 2004
Descriptors: Steels; Frames; Earthquake design; Seismic engineering; Numerical analysis; Beams (structural)

Abstract: This paper presents an overview of the full-scale test on a three-story, two-span by one-span steel moment frame. The test was conducted to characterize the cyclic behavior of steel moment frames beyond the deformation ranges considered in the contemporary seismic design. Stable behavior was observed up to an overall drift angle of 1/25. Pinching behavior was notable for cyclic loading with larger amplitudes primarily because of cyclic yielding and resulting slip-type hysteresis experienced at the column bases. Pushover analyses using numerical analysis codes commonly adopted in seismic design practices are very reasonable to predict the elastic stiffness and the strength. Adding strain hardening after yielding and composite action between the steel beams and RC floor slabs, numerical analyses are able to duplicate the experimental cyclic behavior very accurately. The generic frame model is also very accurate and effective in seismic design.

Title: Comparison of displacement coefficient method and capacity spectrum method with experimental results of RC columns.
Author: Lin, Y.-Y.; Chang, K.-C.; Wang, Y.-L.
Source: Earthquake Engineering & Structural Dynamics. Vol. 33, no. 1, pp. 35-48. Jan. 2004
Descriptors: Mathematical models; Errors; Displacement; Reinforced concrete; Stiffness; Degradation; Damping capacity; Earthquake design; Seismic engineering; Seismic phenomena; Cyclic loads; Marketing; Buildings; Earthquake construction; Rehabilitation; Earthquake engineering; Deformation

Abstract: For the performance-based seismic design of buildings, both the displacement coefficient method used by FEMA-273 and the capacity spectrum method adopted by ATC-40 are non-linear static procedures. The pushover curves of structures need to be established during processing of these two methods. They are

applied to evaluation and rehabilitation of existing structures. This paper is concerned with experimental studies on the accuracy of both methods. Through carrying out the pseudo-dynamic tests, cyclic loading tests and pushover tests on three reinforced concrete (RC) columns, the maximum inelastic deformation demands (target displacements) determined by the coefficient method of FEMA-273 and the capacity spectrum method of ATC-40 are compared. In addition, a modified capacity spectrum method which is based on the use of inelastic design response spectra is also included in this study. It is shown from the test specimens that the coefficient method overestimates the peak test displacements with an average error of +28% while the capacity spectrum method underestimates them with an average error of -20%. If the Kowalsky hysteretic damping model is used in the capacity spectrum method instead of the original damping model, the average errors become -11% by ignoring the effect of stiffness degrading and -1.2% by slightly including the effect of stiffness degrading. Furthermore, if the Newmark-Hall inelastic design spectrum is implemented in the capacity spectrum method instead of the elastic design spectrum, the average error decreases to -6.6% which undervalues, but is close to, the experimental results.

Title: Analyses of reinforced concrete wall-frame structural systems considering shear softening of shear wall
Author: Sanada, Yasushi; Kabeyasawa, Toshimi; Nakano, Yoshiald
Source: 13 WCEE: 13th World Conference on Earthquake Engineering Conference Proceedings. 2004
Descriptors: Shear walls; Reinforced concrete; Softening; Seismic phenomena; Earthquake construction; Simulation

Abstract: Seismic performances of reinforced concrete wall-frame structural systems were investigated through a shaking table test and three-dimensional nonlinear frame analyses. A reinforced concrete wall-frame building with soft first story was designed as a prototype structure for this study. A one-third scaled model of the prototype structure was tested on the Large-scale Earthquake Simulator, NIED, Japan. The testing methods and major findings were reported herein. The three-dimensional nonlinear dynamic analysis of the test structure was conducted using a four-node isoparametric element model, which was based on the two-dimensional constitutive law for reinforced concrete panel elements, in order to verify its reliability. This analytical model could simulate the displacement concentration, the shear failure of shear wall and the story yielding in the soft first story of the test structure, which was due to the shear softening of shear wall. Moreover, the effects of the shear softening of shear wall on responses of fifteen wall-frame buildings with different number of stories and different column and wall sections, which included regular buildings as well as vertically irregular ones, were investigated through three-dimensional nonlinear pushover analyses.

Title: Displacement based seismic assessment for retrofitting R.C. structures
Author: Siachos, G; Dritsos, S.
Source: High Performance Structures and Materials II , pp. 631-642. 2004
Descriptors: Reinforced concrete; Structural members; Seismic response; Earthquake engineering; Retrofitting; Computer simulation

Abstract: The main object of this investigation was to develop a pushover analysis procedure for an existing building in order to define the expected seismic performance and to verify a proposed mathematical equation that calculated the plastic hinge rotations in order to simulate the inelastic behaviour of the building. A series of tests have taken place in the past on the building in question. Based on the results, a critical comparison of the local and global response between the pushover analysis and the experimental data has been made. The analysis results include a clear view of the seismic behaviour, the mechanism of development of plastic hinges, the members and storeys with the maximum vulnerability and the development of the inelastic dissipation mechanism. This paper shows that, during a moderate earthquake, the pushover analysis gives satisfactory results for the global as well as the local response. This paper also shows that, during an intense earthquake, the pushover analysis result only approaches the lower level the experimental local response.

Title: Evaluation of modal and FEMA pushover procedures using strong-motion records of buildings
Author: Goel, Rakesh K
Source: Earthquake Spectra. Vol. 21, no. 3, pp. 653-684. Aug. 2005
Descriptors: Seismic phenomena; Buildings; Earthquake construction; Spectra

Abstract: The objective of this investigation is to evaluate the FEMA-356 Nonlinear Static Procedure (NSP) and a recently developed Modal Pushover Analysis (MPA) procedure using recorded motions of four buildings that were damaged during the 1994 Northridge earthquake. For this purpose, displacements and drifts from the FEMA-356 NSP and the MPA procedures are compared with the values "derived" from the recorded motions. It is found that the FEMA-356 NSP typically underestimates the drifts in upper stories and overestimates them in lower stories when compared to the recorded motions. Among the four FEMA-356 distributions considered, the "Uniform" distribution led to the most excessive underestimation or overestimation indicating that the need to carefully reevaluate the usefulness of this distribution in the FEMA-356 NSP. Furthermore, FEMA-356 distributions failed to provide accurate estimates of story drifts for a building that satisfied the FEMA-356 criterion for detecting the presence of higher mode effects indicating the need to carefully re-examine this criterion. The MPA procedure, in general, provides estimates of the response that are much closer to the values from the recorded motion compared to those from the FEMA-356 NSP. In particular, the MPA procedure, unlike the FEMA-356 NSP, is able to capture the effects of higher modes. For a

building that exhibits dominant effects of "soft" first story, however, neither the MPA procedure nor the FEMA-356 NSP led to reasonable estimate of the response.

Title: A method of estimating earthquake responses of asymmetric reinforced concrete structures based on nonlinear deformation modes
Author: Kabeyasawa, Toshikazu; Kabeyasawa, Toshimi
Source: Journal of Structural and Construction Engineering , no. 596, pp. 87-94. Oct. 2005
Descriptors: Deformation; Reinforced concrete; Seismic phenomena; Frames; Earthquake design; Nonlinear dynamics; Computer simulation,

Abstract: The paper presents a method of estimating earthquake responses of asymmetric reinforced concrete structures based on nonlinear deformation modes. Shaking table tests of one-third scale six-story eccentric reinforced concrete wall-frame specimens were conducted and analyzed with a nonlinear three-dimensional frame model. A fair correlation was observed between the test and the frame analysis. Several wall-frames were designed by varying the plan, location and stiffness of the walls from the specimen to simulate general cases of torsional responses, where the 2nd mode is dominant as well. The intensities of the earthquake motions for the simulation were also varied to simulate also wide range of structural responses from elastic to inelastic deformations. The dominant modes were derived from the nonlinear responses, in which general characteristics were discussed in terms of effective mass ratio. The value approaches a constant when the inelastic response is large. The constant could be derived from nonlinear pushover analysis considering the first mode and the second mode in the assumed load vectors. A new method of estimating nonlinear responses based on the deformation modes in the dynamic responses are proposed based on the general characteristics. The estimates are compared with the results of nonlinear dynamic frame analysis, where a better correlation was observed than those by past simple methods generally from elastic to inelastic responses.

Title: Micro-meso-macro scale modeling and analysis of the Camus I RC shear wall
Autho: Coronelli, Dario; Martinelli, Luca; Martinelli, Paolo; Mulas, Maria Gabriella
Source: First European Conference on Earthquake Engineering and Seismology. 2006
Descriptors: Walls; Modelling; Mathematical models; Models; Beams (structural); Shear; Stress-strain relationships; Reproduction; Assessments; Seismic response; Discretization; Indication; Standards; Mathematical analysis; Dynamic tests; C (programming language); Flexibility; Dynamics; Displacement

Abstract: This work describes the structural modelling of one of the two 5-story, 1/3rd scale, R/C shear walls tested on a shaking table, under a sequence of five accelerograms, for the CAMUS I Program, and the analysis issues related to the reproduction of the experimental results. The wall, designed according to the French

code PS92, is representative of large lightly reinforced walls in the Eurocode 8 standard. Three different levels of refinements have been adopted in the structural discretization of the wall, namely the micro-scale of the finite element method, the meso-scale of a fibre model, and the macro-scale of a beam spread-plasticity element. The micro and meso-scales follow the material constitutive behaviour in terms of stress-strain relations, differing for the richness of the kinematic field. The macro scale accounts for the material behaviour in terms of moment-curvature relation, and relies on a flexibility approach. Two different numerical approaches of analysis have been adopted: a push-over monotonic analysis within a displacement-based assessment, at the micro and meso scales; and a dynamic step-by-step analysis, at the meso and macro-scales. The comparison of numerical and experimental results provides useful indications about the modelling approaches to be adopted in predicting the non linear seismic response through simplified and 'exact' procedures.

Title: Nonlinear pushover analysis of infilled concrete frames
Author: Huang, Chao Hsun; Tuan, Yungting Alex; Hsu, Ruo Yun
Source: Earthquake Engineering and Engineering Vibration. Vol. 5, no. 2, pp. 245-256. Dec. 2006
Descriptors: Frames; ACI; Nonlinearity; Hoops; Failure; Shear; Fatigue (materials); Chaos theory; Carbon fiber reinforced plastics; Failure mechanisms; Masonry; Civil engineering; Specifications; Structural engineers; Construction; Concretes; Reinforced concrete; Design engineering; Cyclic loads

Abstract: Six reinforced concrete frames with or without masonry infills were constructed and tested under horizontal cyclic loads. All six frames had identical details in which the transverse reinforcement in columns was provided by rectangular hoops that did not meet current ACI specifications for ductile frames. For comparison purposes, the columns in three of these frames were jacketed by carbon-fiber-reinforced-polymer (CFRP) sheets to avoid possible shear failure. A nonlinear pushover analysis, in which the force-deformation relationships of individual elements were developed based on ACI 318, FEMA 356, and Chen's model, was carried out for these frames and compared to test results. Both the failure mechanisms and impact of infills on the behaviors of these frames were examined in the study. Conclusions from the present analysis provide structural engineers with valuable information for evaluation and design of infilled concrete frame building structures.

Title: Test and analysis on inelastic soil-structure interaction of an existing reinforced concrete school building
Author: Kabeyasawa, Toshikazu; Kabeyasawa, Toshimi; Kim, YouSok; Sanada, Yasushi
Source: 100th Anniversary Earthquake Conference. 2006
Descriptors: Pile foundations; Hysteresis; School buildings; Soil structure interactions; Reinforced concrete; Nonlinear dynamics; Earthquake construction; Deformation resistance

Abstract: The interaction between soil and structure for seismic response analysis has been idealized with simple springs in the modified Penzien model though nonlinear properties of the super-structures and the soils have been introduced into the model, the inelastic and hysteretic behavior of the neighborhood soil around the pile and the foundation have not yet been verified sufficiently with experimental investigation. Nonlinear static test of a two-story school building was conducted to identify the lateral sway property of the foundation with piles. The lateral resistance was measured with deformations mainly in sway with slight rocking mechanism. Nonlinear pushover analysis and dynamic analysis was carried out using the modified Penzien model. The response properties observed in the test are compared with those from the analytical model.

Title: Test on full-scale three-storey steel moment frame and assessment of ability of numerical simulation to trace cyclic inelastic behaviour

Author: Nakashima, Masayoshi; Matsumiya, Tomohiro; Suita, Keichiro; Liu, Dawei

Source: Earthquake Engineering & Structural Dynamics. Vol. 35, no. 1, pp. 3-19. Jan. 2006

Descriptors: Frames; Beams (structural); Structural steels; Yield strength; Computer simulation; Fracture mechanics; Fatigue (materials)

Abstract: A test on a full-scale model of a three-storey steel moment frame was conducted, with the objectives of acquiring real information about the damage and serious strength deterioration of a steel moment frame under cyclic loading, studying the interaction between the structural frame and non-structural elements, and examining the capacity of numerical analyses commonly used in seismic design to trace the real cyclic behaviour. The outline of the test structure and test program is presented, results on the overall behaviour are given, and correlation between the experimental results and the results of pre-test and posttest numerical analyses is discussed. Pushover analyses conducted prior to the test predicted the elastic stiffness and yield strength very reasonably. With proper adjustment of strain hardening after yielding and composite action, numerical analyses were able to accurately duplicate the cyclic behaviour of the test structure up to a drift angle of 1/25. The analyses could not trace the cyclic behaviour involving larger drifts in which serious strength deterioration occurred due to fracture of beams and anchor bolts and progress of column local buckling.

Title: Deflection-based method for seismic response analysis of concrete walls: Benchmarking of CAMUS experiment

Author: Basu, Prabir C; Roshan, A D

Source: Nuclear Engineering and Design. Vol. 237, no. 12-13, pp. 1288-1299. July 2007

Descriptors: Displacement; Deflection; Stresses; Mathematical models; Strain; Reinforcing steels; Concrete construction; Compressive properties; Walls; Seismic phenomena; Modulus of elasticity; Benchmarking;

Mathematical analysis; Atomic energy; Conferences; Stiffness;
Nuclear engineering; Concretes; Nuclear reactor components

Abstract: A number of shake table tests had been conducted on the scaled down model of a concrete wall as part of CAMUS experiment. The experiments were conducted between 1996 and 1998 in the CEA facilities in Saclay, France.

Benchmarking of CAMUS experiments was undertaken as a part of the coordinated research program on 'Safety Significance of Near-Field Earthquakes' organised by International Atomic Energy Agency (IAEA). Technique of deflection-based method was adopted for benchmarking exercise. Non-linear static procedure of deflection-based method has two basic steps: pushover analysis, and determination of target displacement or performance point. Pushover analysis is an analytical procedure to assess the capacity to withstand seismic loading effect that a structural system can offer considering the redundancies and inelastic deformation. Outcome of a pushover analysis is the plot of force-displacement (base shear-top/roof displacement) curve of the structure. This is obtained by step-by-step non-linear static analysis of the structure with increasing value of load. The second step is to determine target displacement, which is also known as performance point. The target displacement is the likely maximum displacement of the structure due to a specified seismic input motion. Established procedures, FEMA-273 and ATC-40, are available to determine this maximum deflection. The responses of CAMUS test specimen are determined by deflection-based method and analytically calculated values compare well with the test results.

Title: 3-D Collapse tests and analyses of the three-story reinforced concrete buildings with flexible foundation
Author: Kabeyasawa, T; Matsumori, T; Kim, Y
Source: Proceedings of the 2007 Structures Congress, Proceedings of the Research Frontiers Sessions of the 2007 Structures Congress, and Proceedings of the 2007 Forensic Engineering Track of the 2007 Structures Congress; Long Beach, CA; USA; 16-19 May 2007. 2007
Descriptors: Collapse; Buildings; multistory; Concrete; reinforced; Foundations; Shear; Shake table tests; Friction; Retrofitting; Reinforcing steels; Paper; Structural steels; Seismic phenomena; Dislocations; Failure; Nonlinear dynamics; School buildings; Nonlinearity

Abstract: Full-scale shake table tests were planned and conducted at E-Defense from September to November 2006 in the second phase of the Dai-Dai-Toku project. Two three-story specimens on flexible foundation, the bare specimen and the retrofit specimen, were tested with the following specific objectives: (1) the simulation of progressive collapse of existing school buildings, (2) verification of strengthening effect by the attached steel frames, and (3) soil-structure interaction with flexible foundation. Backgrounds of the test plan and the details of the specimens are reported in another paper, while analyses and measured responses are reported in this paper. For the planning of the test specimens, preliminary nonlinear pushover analysis and dynamic analysis were carried out. The bare specimen was supposed to fail in shear

before/after flexural yielding of the short columns. The effect of the dislocation at the flexible base and the brittle shear failure of the columns on the failure modes were considered in the analysis. An overall mechanism of rocking was to be observed in the retrofit specimen with the steel braces and seismic slits. In this paper, the preliminary analyses of the two specimens and the observed behavior of the two specimens in the shake table test are presented mainly focused on the failure mechanisms of the structure considering the base conditions. The results of the static test to identify the base friction coefficient are also reported.

Title: Assessing the 3d irregular spear building with nonlinear static procedures
Author: Pinho, R; Bento, R; Bhatt, C
Source: 14th World Conference on Earthquake Engineering: Innovation Practice Safety. 2008
Descriptors: Nonlinearity; Three dimensional; Assessments; Seismic response; Seismic phenomena; Seismic engineering; Earthquake construction; Employment; Spears; Accuracy; Constraining; Earthquake design; Design engineering; Two dimensional; Frames; Nonlinear dynamics; Estimating

Abstract: The employment of Nonlinear Static Procedures (NSP) in the seismic assessment of existing structures (or design verification of new ones) has gained considerable popularity in the recent years, backed by a large number of extensive verification studies that have demonstrated its relatively good accuracy in estimating the seismic response of buildings that are regular in plan (and hence can be analysed by means of planar 2D frame models). The extension of such use to the case of plan-irregular structures, however, has so far been the object of only restricted scrutiny, which effectively ends up by limiting significantly the employment of NSPs to assess actual existing structures, the majority of which do tend to be irregular in plan. In this work, therefore, four commonly employed nonlinear static procedures (CSM, N2, MPA, ACSM) are applied in the assessment of the well-known SPEAR building, an irregular 3D structure tested in full-scale under pseudo-dynamic conditions, and subjected to bi-direction seismic loading. Comparison with the results obtained with nonlinear dynamic analysis of a verified model of the structure then enables the evaluation of the accuracy of the different NSPs.

H.2 Dynamic Approaches

H.2.1 Incremental Dynamic Analysis and Approximations

Title: Practical estimation of the seismic demand and capacity of oscillators with multi-linear static pushovers through incremental dynamic analysis
Author: Vamvatsikos, Dimitrios; Cornell, C. Allin
Source: Seventh U.S. National Conference on Earthquake Engineering (7NCEE): Theme: Urban Earthquake Risk [electronic resource]; 10 pages pp. 2002

Descriptors: Single degree-of-freedom systems; nonlinear analysis; Oscillators; linear static pushover analysis

Abstract: The seismic behavior of numerous single-degree-of-freedom (SDOF) systems is investigated through Incremental Dynamic Analysis (IDA), a computer-intensive procedure that offers thorough (demand and capacity) prediction capability by using a series of nonlinear dynamic analyses under a suitably scaled suite of ground motion records. The oscillators are of moderate period with pinching hysteresis and feature backbones ranging from simple bilinear to complex quadrilinear with an elastic, a hardening and a negative-stiffness segment plus a final residual plateau that terminates with a drop to zero strength. The results of the analysis are summarized into their 16%, 50% and 84% fractile IDA curves which are in turn fitted by flexible parametric equations. The final product is SPO2IDA, an accurate, spreadsheet-level tool for performance-based earthquake engineering that is available on the web. It offers effectively instantaneous estimation of demands and global-collapse instability capacities in addition to conventional strength reduction R-factors and inelastic displacement ratios, for any single degree-of-freedom system whose static pushover curve can be approximated by such a quadrilinear backbone.

Title: Incremental dynamic analysis
Author: Vamvatsikos, Dimitrios; Cornell, C. Allin
Source: Earthquake Engineering & Structural Dynamics. Vol. 31, no. 3, pp. 491-514. Mar. 2002
Descriptors: Multistory steel moment-resisting frames; nonlinear analysis; Steel braced frames; limit design; Story drift

Abstract: Incremental dynamic analysis (IDA) is a parametric analysis method that has recently emerged in several different forms to estimate more thoroughly structural performance under seismic loads. It involves subjecting a structural model to one (or more) ground motion record(s), each scaled to multiple levels of intensity, thus producing one (or more) curve(s) of response parameterized versus intensity level. To establish a common frame of reference, the fundamental concepts are analysed, a unified terminology is proposed, suitable algorithms are presented, and properties of the IDA curve are looked into for both single-degree-of-freedom and multidegree-of-freedom structures. In addition, summarization techniques for multi-record IDA studies and the association of the IDA study with the conventional static pushover analysis and the yield reduction R-factor are discussed. Finally, in the framework of performance-based earthquake engineering, the assessment of demand and capacity is viewed through the lens of an IDA study.

Title: IN2 - A simple alternative for IDA
Author: Dolsek, Matjai; Fajfar, Peter
Source: 13 WCEE: 13th World Conference on Earthquake Engineering Conference Proceedings. 2004
Descriptors: Seismic engineering; Reinforced concrete; Probability theory; Dynamic tests; Risk analysis; Frames

Abstract: Simplified inelastic procedures used in seismic design and assessment combine the nonlinear static (pushover) analysis and the response spectrum approach. One of such procedures is the N2 method, which has been implemented into the Eurocode 8 standard. The N2 method can be employed also as a simple tool for the determination of the approximate summarized IDA (incremental dynamic analysis) curve. Such analysis is called the incremental N2 method (IN2). The IN2 curve can substitute the IDA curve in the probabilistic framework for seismic design and assessment of structures. In the paper, the IN2 method is summarized and applied to two test examples of infilled reinforced concrete (RC) frames, which are characterized by a substantial degradation of the strength after the infill fails. The approximate summarized IDA curves, determined by the IN2 method, and the data on dispersion due to randomness in displacement demand, determined in a previous study by the authors, were employed in the probabilistic risk analysis of test structures. The results were compared with the results obtained using the "exact" IDA curves. A fair correlation of results suggests that the IN2 method is a viable approach.

Title: Applied incremental dynamic analysis.
Author: Vamvatsikos, D.; Cornell, C.A.
Source: Earthquake Spectra. Vol. 20, no. 2, pp. 523-533. May 2004
Descriptors: Seismic phenomena; Seismic engineering; Dynamic tests; Dynamical systems; Nonlinear dynamics; Earthquake engineering; Stability; Earthquake damage; Demand analysis; Fracturing; Dynamic structural analysis; Mathematical analysis; Seismic response; Probability theory; Earthquake construction; Interpolation; Frames; Algorithms

Abstract: We are presenting a practical and detailed example of how to perform incremental dynamic analysis (IDA), interpret the results and apply them to performance-based earthquake engineering. IDA is an emerging analysis method that offers thorough seismic demand and capacity prediction capability by using a series of nonlinear dynamic analyses under a multiply scaled suite of ground motion records. Realization of its opportunities requires several steps and the use of innovative techniques at each one of them. Using a nine-story steel moment-resisting frame with fracturing connections as a test bed, the reader is guided through each step of IDA: (1) choosing suitable ground motion intensity measures and representative damage measures, (2) using appropriate algorithms to select the record scaling, (3) employing proper interpolation and (4) summarization techniques for multiple records to estimate the probability distribution of the structural demand given the seismic intensity, and (5) defining limit-states, such as the dynamic global system instability, to calculate the corresponding capacities. Finally, (6) the results can be used to gain intuition for the structural behavior, highlighting the connection between the static pushover (SPO) and the dynamic response, or (7) they can be integrated with conventional probabilistic seismic hazard analysis (PSHA) to estimate mean annual frequencies of limit-state exceedance. Building upon this detailed example

based on the nine-story structure, a complete commentary is provided, discussing the choices that are available to the user, and showing their implications for each step of the IDA.

Title: On the modal incremental dynamic analysis
Author: Mofid, Massood; Zarfam, Panam; Fard, Babak Raiesi
Source: Structural Design of Tall and Special Buildings. Vol. 14, no. 4, pp. 315-329. Dec. 2005
Descriptors: Mathematical models; Seismic phenomena; Seismic engineering; Dynamic tests; Dynamics; Earthquake construction; Design engineering; Equivalence; Approximation; Demand; Nonlinearity; Degrees of freedom; Earthquake design; Mathematical analysis; Dynamic response; Civil engineering; Accuracy; Marketing; Personal computers

Abstract: In this article a new technique for the dynamic response of structures is investigated. This applied procedure can predict the approximate seismic performance of the structures and it is fast, inexpensive and results are reasonably acceptable. In fact, this novel method logically combines two different techniques, incremental dynamic analysis (IDA) and modal pushover analysis (MPA), presented by other researchers. This method will take advantage of both methodical ideas such as equivalent single degree of freedom of multi-degree structures and the implementation of different scaled level of an earthquake record to the provided equivalent SDF structure. Using this procedure, simple approximate curves that present a realistic linear and non-linear seismic behaviour of the structure due to the applied scaled level of earthquakes can easily be extracted. In this investigation, several four-, eight- and 12-storey structures are specified as the example models and are dynamically analysed. Next, three different scaled earthquakes, El Centro, Northridge and San Fernando, are applied to each example problem. The results of the presented technique, modal incremental dynamic analysis (MIDA), are then compared with the IDA method. Comparison of the results reveals good accuracy in building seismic demands evaluation. Finally, it is also shown that the MIDA method is simple enough to be carried out on most personal computers and the authors believe this technique will serve design engineers working in real design conditions.

Title: Direct Estimation of Seismic Demand and Capacity of Multidegree-of-Freedom Systems through Incremental Dynamic Analysis of Single Degree of Freedom Approximation
Author: Vamvatsikos, Dimitrios; Cornell, C Allin
Source: Journal of Structural Engineering (New York, N.Y.). Vol. 131, no. 4, pp. 589-599. Apr. 2005
Descriptors: Seismic engineering; Approximation; Stability; Computer programs; Degrees of freedom; Dynamic structural analysis

Abstract: Introducing a fast and accurate method to estimate the seismic demand and capacity of first-mode-dominated multidegree-offreedom systems in regions ranging from near-elastic to global collapse. This is made possible by exploiting the

connection between the static pushover (SPO) and the incremental dynamic analysis (IDA). While the computer-intensive IDA would require several nonlinear dynamic analyses under multiple suitably scaled ground motion records, the simpler SPO helps approximate the multidegree-of-freedom system with a single-degree-of-freedom oscillator whose backbone matches the structure's SPO curve far beyond its peak. Similar methodologies exist but they usually employ oscillators with a bilinear backbone. In contrast, the empirical equations implemented in the static pushover 2 incremental dynamic analysis (SPO2IDA) software allow the use of a complex quadrilinear backbone shape. Thus, the entire summarized IDA curves of the resulting system are effortlessly generated, enabling an engineer-user to obtain accurate estimates of seismic demands and capacities for limit-states such as immediate occupancy or global dynamic instability. Using three multistory buildings as case studies, the methodology is favorably compared to the full IDA.

Title: Approximate incremental dynamic analysis using the modal pushover analysis procedure
Author: Han, Sang Whan; Chopra, K
Source: Earthquake Engineering & Structural Dynamics. Vol. 35, no. 15, pp. 1853-1873. Dec. 2006
Descriptors: Approximation; Dynamics; Nonlinear dynamics; Buildings; Accuracy; Computation; Dynamical systems; Limit states; Instability; Grounds; Dynamic structural analysis; Hysteresis; Stability; Seismic phenomena; Collapse; Seismic response; Vibration; Architecture; Nonlinearity

Abstract: Incremental dynamic analysis (IDA)-procedure developed for accurate estimation of seismic demand and capacity of structures-requires non-linear response history analysis of the structure for an ensemble of ground motions, each scaled to many intensity levels, selected to cover the entire range of structural response-all the way from elastic behaviour to global dynamic instability. Recognizing that IDA of practical structures is computationally extremely demanding, an approximate procedure based on the modal pushover analysis procedure is developed. Presented are the IDA curves and limit state capacities for the SAC-Los Angeles 3-, 9-, and 20-storey buildings computed by the exact and approximate procedures for an ensemble of 20 ground motions. These results demonstrate that the MPA-based approximate procedure reduces the computational effort by a factor of 30 (for the 9-storey building), at the same time providing results to a useful degree of accuracy over the entire range of responses-all the way from elastic behaviour to global dynamic instability-provided a proper hysteretic model is selected for modal SDF systems. The accuracy of the approximate procedure does not deteriorate for 9- and 20-storey buildings, although their dynamics is more complex, involving several 'modes' of vibration. For all three buildings, the accuracy of the MPA-based approximate procedure is also satisfactory for estimating the structural capacities for the limit states of immediate occupancy, collapse prevention, and global dynamic instability.

Title: Direct estimation of the seismic demand and capacity of oscillators with multi-linear static pushovers through IDA
Author: Vamvatsikos, Dimitrios; Cornell, C Allin
Source: Earthquake Engineering & Structural Dynamics. Vol. 35, no. 9, pp. 1097-1117. 25 July 2006
Descriptors: Seismic phenomena; Seismic engineering; Oscillators; Nonlinear dynamics; Dynamical systems; Earthquake engineering

Abstract: SPO2IDA is introduced, a software tool that is capable of recreating the seismic behaviour of oscillators with complex quadrilinear backbones. It provides a direct connection between the static pushover (SPO) curve and the results of incremental dynamic analysis (IDA), a computer-intensive procedure that offers thorough demand and capacity prediction capability by using a series of nonlinear dynamic analyses under a suitably scaled suite of ground motion records. To achieve this, the seismic behaviour of numerous single-degree-of-freedom (SDOF) systems is investigated through IDA. The oscillators have a wide range of periods and feature pinching hysteresis with backbones ranging from simple bilinear to complex quadrilinear with an elastic, a hardening and a negative-stiffness segment plus a final residual plateau that terminates with a drop to zero strength. An efficient method is introduced to treat the backbone shape by summarizing the analysis results into the 16, 50 and 84% fractile IDA curves, reducing them to a few shape parameters and finding simpler backbones that reproduce the IDA curves of complex ones. Thus, vast economies are realized while important intuition is gained on the role of the backbone shape to the seismic performance. The final product is SPO2IDA, an accurate, spreadsheet-level tool for performance-based earthquake engineering that can rapidly estimate demands and limit-state capacities, strength reduction R-factors and inelastic displacement ratios for any SDOF system with such a quadrilinear SPO curve.

Title: Incremental dynamic analysis with two components of motion for a 3D steel structure
Author: Vamvatsikos, D
Source: 100th Anniversary Earthquake Conference. 2006
Descriptors: Seismic engineering; Dynamic structural analysis; Space frames; Steel structures; Nonlinear dynamics

Abstract: Incremental dynamic analysis (IDA) is employed to evaluate the seismic performance of a 20-story steel space frame under biaxial seismic loading. Originally developed for planar frames and uniaxial loading, the IDA framework is now extended to 3D. This involves performing a series of nonlinear timehistory analyses under a suite of ground motion records by equally scaling both components of each record to several levels of intensity and recording the structural response. The structure is thus forced to show its complete spectrum of behavior from elasticity to final global instability for combinations of intensities in the two directions. Using proper intensity measures (e.g., spectral acceleration coordinates of the record components) and engineering demand parameters (e.g., maximum interstory drifts),

the familiar IDA curves plus novel IDA surfaces are created, representing the structural response and its statistical summary at any intensity level. These enable a rational definition of limit-states and the calculation of the resulting capacities in a manner consistent with current IDA techniques. A powerful analysis procedure is thus created that is capable of thoroughly assessing the seismic performance of 3D structures and may serve as a solid benchmark for evaluating the accuracy of simpler methods.

Title: A comparative study of the traditional performance and The Incremental Dynamic Analysis approaches (IDA)
Author: Nicknam, Ahmad; Ahmadi, Hamid Reza; Mandavi, Navideh
Source: 14th World Conference on Earthquake Engineering: Innovation Practice Safety. 2008
Descriptors: Frames; Spectra; Magnetorheological fluids; Structural steels; Dynamic tests; Mathematical analysis; Assessments; Seismic response; Standard error; Structural analysis; Compatibility; Drift; Dynamics; Shear; Estimating

Abstract: In this study, the applicability of different load patterns in traditional pushover for seismic response assessment is investigated. At first Cornell UPSHA approach is used for estimating response spectra with probability of exceedance $PE=10\%$ and a time histories compatible with those of estimated response spectra were determined to be used in IDA method. Following this, three steel MRF frames (3, 9 and 15-story) according to IBC-ASD have been selected and designed, then the frames loaded under different load patterns (inverted triangular, uniform and first mode-based) that is frequently used in traditional pushover analysis methods. The outputs of the structural analysis, in the forms of, story shear versus story drift ratios of upper, middle and lower portions of structural heights were depicted and compared with those of IDA method and standard error of selected frames were calculated.

Title: Stochastic incremental dynamic analysis considering random system properties
Author: Yu, Xiao-Hui; Lu, Da-Gang; Song, Peng-Yan; Wang, Guang-Yuan
Source: 14th World Conference on Earthquake Engineering: Innovation Practice Safety. 2008
Descriptors: Seismic phenomena; Nonlinear dynamics; Dynamical systems; Earthquake construction; Earthquake engineering; Seismic engineering; Stochasticity; Loads (forces); Tools; Sampling; Transformations; Estimates; Grounds; Dynamic structural analysis; Demand analysis; Frame structures; Dynamic tests; Strategy; Planes

Abstract: As an extension of static pushover analysis into nonlinear dynamic analysis to estimate more thoroughly structural performance under seismic loads, incremental dynamic analysis (IDA) has been widely applied in the field of Performance-Based Earthquake Engineering (PBEE). A single-record IDA cannot fully capture the behavior that a building may display in a future earthquake event. Therefore, the multi-record IDA is developed to consider the record-to-record

variations in earthquake ground motions. However, neither single-record IDA nor multi-record IDA can take into account the random system properties of structures. In this paper, a stochastic IDA method is proposed, which is a coupling of point estimation method (PEM) based on Nataf transformation for approximating the statistical moments of random functions, and single-record IDA approach. The multi-variable random IDA curve is developed from single-variable random IDA ones according to the sampling strategy in PEM, and the fractile IDA curves are also advanced. The proposed methodology is applied in R.C. frame structures. A three-bay and five-storey plane R.C. frame is taken as an example in case study. It is demonstrated by this example that the approach proposed in this paper is an efficient and accurate tool for probabilistic seismic demand and capacity analysis of structures considering the inherent random system properties.

Title: Comparison of exact IDA and approximate MPA-based IDA for reinforced concrete frames
Author: Vejdani-Noghreiyani, H R; Shooshtari, A
Source: 14th World Conference on Earthquake Engineering: Innovation Practice Safety. 2008
Descriptors: Approximation; Seismic phenomena; Reinforced concrete; Marketing; Computation; Frames; Reduction; Demand; Nonlinearity; Estimates; State of the art; Demand analysis; Seismic engineering; Dynamic tests; Planes; Simplification; Dynamics; Accuracy; Earthquake engineering

Abstract: Recent decade has witnessed the improvement of performance-based earthquake engineering (PBEE) methods. Therefore, procedures to estimate performance levels of structures have developed in accuracy as well as simplification in practice. Incremental dynamic analysis (IDA) and modal pushover analysis are probably the most important methods in this aspect. IDA was identified as the state-of-the-art method to assess the performance level of structures by FEMA-350 but is a computational demanding technique. On the other hand, modal pushover analysis - despite its inherent approximate nature- is broadly used as the simplified nonlinear static method to evaluate seismic demands of structures. Recently these two methods have combined and constituted a more advanced method called MPA-based IDA which possesses the advantages of the two methods. In this paper, a comparative study is carried out to evaluate the reliability of MPA-based approximate method for regular and irregular RC plane frames. Results show that MPA-based IDA procedure is satisfactory for structural demands with a huge reduction in computational effort for regular buildings.

H.2.2 Simplified Dynamic Analysis

Title: Efficient non-linear dynamic analysis using Ritz vectors
Author: Blakeborough, Anthony; Williams, David M; Williams, Martin S

Source: The Twelfth European Conference on Earthquake Engineering [Proceedings] [electronic resource] , pp. 9 pages. 2002

Descriptors: Finite element method; Mathematical analysis; Resources; Plastic deformation; Nonlinear dynamics; Frames; Elastic deformation; Earthquake engineering

Abstract: The derivation of an explicit time-stepping nonlinear Ritz finite element analysis is presented. The method uses elastic modes and a set of Ritz vectors derived from the plastic deformations of a pushover analysis. The results of an analysis of the response of a single bay portal frame using the method and the finite element program DRAIN-2DX are encouraging since the method reproduces the DRAIN-2DX results well.

Title: Elastic-plastic dynamic and static analysis of building structures

Author: Li, Yungui

Source: Journal of Building Structures. Vol. 23, no. 5, pp. 56-62. 2002

Descriptors: Slabs; Dynamics; Walls; Efficiency; Precision; Earthquake design; Seismic engineering; Computer programs; Seismic phenomena; Dynamical systems; Earthquake construction; Dynamic tests; Geometry; Reliability; Commercial buildings; Dynamic structural analysis; Concrete construction; Statics; Frames

Abstract: Tall buildings today have many special features, for example, the types of structural systems are numerous and varied, and the arrangement of the plan and elevation is becoming more complicated. For analysis and design of these complex tall buildings in seismic regions, rational consideration of the elastic and plastic performance of the building under the action of seismic load is very important, as it determines the precision, efficiency and reliability of the analysis results. This paper introduces the programming principles of the software EPDA. EPDA was especially developed for elastic and plastic dynamic analysis of tall buildings. It consists of 4 parts: simplified storey model, simplified 2-D frame model, 3-D model, and pushover analysis model. It can be applied to analyze not only steel buildings but also concrete buildings. The key to EPDA is to provide a helpful tool for the designer with as high precision and efficiency as possible. In order to solve the problems of the rational modeling of shear walls and floor slabs and to make the analysis model of tall buildings as reasonable as possible, two types of special elements-- an elastic and plastic wall element and an elastic slab element--are introduced. EPDA has strong pre- and post-processing functions. It is the first commercial software for the elastic and plastic analysis of tall buildings. All the information needed in EPDA is created automatically based on the structural database, including geometric information, loading information, reinforcement of concrete elements, and so forth. The elastic and plastic wall element and the elastic slab element can be further meshed automatically, too. All of the above features greatly simplify user operations.

Title: Evaluation of predictors of non-linear seismic demands using 'fishbone' models of SMRF buildings.
Author: Luco, N; Mori, Y; Funahashi, Y; Cornell, C A; Nakashima, M
Source: Earthquake Engineering & Structural Dynamics. Vol. 32, no. 14, pp. 2267-2288. 25 Nov. 2003
Descriptors: Steels; Buildings; Seismic phenomena; Elasticity; Nonlinear dynamics; Earthquake construction; Dynamic structural analysis

Abstract: Predictors (or estimates) of seismic structural demands that are less computationally time-consuming than non-linear dynamic analysis can be useful for structural performance assessment and for design. In this paper, we evaluate the bias and precision of predictors that make use of, at most, (i) elastic modal vibration properties of the given structure, (ii) the results of a non-linear static pushover analysis of the structure, and (iii) elastic and inelastic single-degree-of-freedom time-history analyses for the specified ground motion record. The main predictor of interest is an extension of first-mode elastic spectral acceleration that additionally takes into account both the second-mode contribution to (elastic) structural response and the effects of inelasticity. This predictor is evaluated with respect to non-linear dynamic analysis results for 'fishbone' models of steel moment-resisting frame (SMRF) buildings. The relatively small number of degrees of freedom for each fishbone model allows us to consider several short-to-long period buildings and numerous near- and far-field earthquake ground motions of interest in both Japan and the U.S. Before doing so, though, we verify that estimates of the bias and precision of the predictor obtained using fishbone models are effectively equivalent to those based on typical 'full-frame' models of the same buildings.

Title: Simplified non-linear dynamic response analysis on moment-resisting frames
Author: Ohi, K; Ito, T
Source: STESSA 2003: Proceedings of the Conference on Behaviour of Steel Structures in Seismic Areas, 9-12 June 2003, Naples, Italy, pp. 533-540. 2003
Descriptors: Frames; Nonlinear dynamics; Seismic response; Steel structures; Computer simulation

Abstract: To simplify the nonlinear dynamic design procedure for a moment-resisting steel frame subjected to seismic actions, a new design-friendly reduced analysis method is proposed; and its validity is checked by comparison with a detailed computer analysis on a 6-story, 2-bay frame model as well as by means of a pseudodynamic test on a steel frame specimen.

Title: Simplified dynamic inelastic analysis of tall buildings
Author: Ju, Y K
Source: Proceedings of the Institution of Civil Engineers, Structures and Buildings. Vol. 159, no. SB3, pp. 165-178. June 2006
Descriptors: Inelastic analysis; Dynamic structural analysis; Tall buildings; Seismic engineering; Earthquakes; Computer programs

Abstract: Since the Kobe and Northridge earthquakes, static inelastic analysis has become an accepted and simple method for the seismic evaluation of high-rise buildings. In this method, the lateral load is monotonically increased with the same profile to find the ultimate capacity of the structure. Pushover analysis, however, has a limitation in the evaluation of a higher-mode dominant structure: for this reason, inelastic time history is used to compensate. In engineering practice, using inelastic time history analysis to evaluate the inelastic capacity of a building is impractical for tall buildings owing to the amount of computational time required and the difficulties in interpreting results. Therefore, a simplified inelastic analysis method is required for practical application. In the present paper, a simplified dynamic inelastic analysis (SDIA) method using elastic and inelastic response spectrums is introduced as a way to perform an inelastic analysis of a structure. The relative accuracy and efficiency of SDIA are explored by comparing the results with those of time history analysis software, DRAIN-2DX. The results of SDIA and DRAIN-2DX are almost identical, while with SDIA the computational time is dramatically reduced and time-consuming efforts interpreting results are saved.

Title: An investigation on the accuracy of pushover analysis for estimating the seismic deformation of braced steel frames

Author: Moghaddam, H; Hajirasouliha, I

Source: Journal of Constructional Steel Research. Vol. 62, no. 4, pp. 343-351. Apr. 2006

Descriptors: Steel frames; Seismic phenomena; Structural steels; Earthquake design; Nonlinear dynamics; Deformation

Abstract: This paper investigates the potentialities of the pushover analysis to estimate the seismic deformation demands of concentrically braced steel frames. Reliability of the pushover analysis has been verified by conducting nonlinear dynamic analysis on 5, 10 and 15 story frames subjected to 15 synthetic earthquake records representing a design spectrum. It is shown that pushover analysis with predetermined lateral load pattern provides questionable estimates of inter-story drift. To overcome this inadequacy, a simplified analytical model for seismic response prediction of concentrically braced frames is proposed. In this approach, a multistory frame is reduced to an equivalent shear building model by performing a pushover analysis. A conventional shear-building model has been modified by introducing supplementary springs to account for flexural displacements in addition to shear displacements. It is shown that modified shear-building models have a better estimation of the nonlinear dynamic response of real framed structures compared to nonlinear static procedures.

Title: A non-linear response history model for the seismic analysis of high-rise framed buildings

Author: Wilkinson, S; Hiley, R A

Source: Computers & Structures. Vol. 84, no. 5-6, pp. 318-329. Jan. 2006

Descriptors: Mathematical models; Nonlinearity; High rise buildings; Translations; Seismic phenomena; Stiffness matrix; Mathematical analysis; Dynamics; Earthquake construction; Runge-Kutta method; Condensing; Seismic response; Redundancy; Plastic properties; Beam-columns; Inversions; Bays; Degrees of freedom; Intersections

Abstract: A materially non-linear plane-frame model is presented that is capable of analysing high-rise buildings subjected to earthquake forces. The model represents each storey of the building by an assembly of vertical and horizontal beam elements. The model introduces yield hinges with ideal plastic properties in a regular plane frame. The displacements are described by the translation (sway) of each floor and the rotation of all beam-column intersections. The mass is only associated with the translations, and thus the analysis can be carried out as a static condensation of the rotations, combined with integration of the dynamic equations for the translations. The dynamic integration is here carried out by use of the Runge-Kutta scheme. This approach allows a building to be modelled by $m(n+2)$ degrees of freedom (where m is the number of storeys and n is the number of bays). The rank of the condensed stiffness matrix is only m . Its construction, which requires the inversion of the rotational, rank $m(n+1)$, stiffness matrix, is required only at time-steps where the pattern of yielding has altered from the previous time-step. This model is particularly attractive for non-linear response history analysis of high-rise buildings as it is efficient, allows each storey to have multiple redundancies, and each connection to be modelled with any suitable moment-rotation relationship. Three verification examples are presented and the results from static push-over analysis are compared with time-history results from the simplified model. The results verify that the model is capable of performing non-linear response history analysis on regular high rise buildings.

Title: The scaled nonlinear dynamic procedure

Author: Aschheim, Mark; Tjhin, Tjen; Comartin, Craig; Hamburger, Ron; Inel, Mehmet

Source: Engineering Structures. Vol. 29, no. 7, pp. 1422-1441. July 2007

Abstract: Although nonlinear static procedures (NSPs) have become widely accepted for use in seismic design and evaluation in recent years, their accuracy is poor for response quantities that are significantly affected by the vibration of multiple degrees of freedom (termed MDOF effects). In recent work performed for the ATC-55 project, a design-oriented approach, called the scaled nonlinear dynamic procedure (Scaled NDP), was identified for determining such response quantities for nonlinear systems. The Scaled NDP provides an alternative to current code approaches for scaling ground motions for dynamic analyses and is readily used in performance-based seismic design and evaluation. The Scaled NDP appears to provide a valid basis for establishing force quantities at stated levels of confidence and provides an indication of deformation demands for use in design and evaluation. The results can be used to determine the strengths required of members in order to ensure that ductile behavior develops, and to evaluate the deformation performance of a given design.

Title: To what type of beam can be associated a building?
Author: Chesnais, C; Boutini, C; Hansl, S
Source: 14th World Conference on Earthquake Engineering: Innovation Practice Safety. 2008
Descriptors: Mathematical models; Beams (structural); Mathematical analysis; Homogenizing; Construction; Bending moments; Vibration; Dynamic tests; Boundary element method; Criteria; Frames; Dynamics; Shear; Homogenization; Media; Horizontal

Abstract: This article is devoted to the study of the dynamics of usual buildings made up of identical stories. The aim is to build analytical beam models enabling to describe the first horizontal modes of vibrations. The homogenization method of periodic discrete media is applied to a class of unbraced framed structures. Depending on the order of magnitude of the shear force and two bending moments, seven families of beam are proved to be possible. The macroscopic parameters of the homogenized model are expressed in function of the static mechanical and geometrical characteristics of the frame elements. Simple criteria are established to identify the relevant model for real structures. Lastly, the models are validated by comparison with numerical calculations and experimental data.

Title: Simplified nonlinear seismic assessment of structures using approximate SDOF-IDA curves
Author: Perug, I; Fajfar, P; Dolgek, M
Source: 14th World Conference on Earthquake Engineering: Innovation Practice Safety. 2008
Descriptors: Mathematical models; Databases; Assessments; Nonlinearity; Seismic phenomena; Seismic engineering; Displacement; Data base management systems; Approximation; Nonlinear dynamics; Envelopes; Standards; Earthquake design; Seismic design; Reinforced concrete; Methodology; Damping; Interpolation; Ductility

Abstract: Simplified inelastic procedures used in seismic design and assessment combine the nonlinear static (pushover) analysis and the response spectrum approach or nonlinear dynamic analysis of a single-degree of freedom model (SDOF). One of such procedures is the N2 method which has been developed at the University of Ljubljana and implemented into the Eurocode 8 standard. The inelastic spectrum, which is prescribed by Eurocode 8 and used for the determination of the target displacement, allows only a rough bi-linear idealization of the pushover curve and assumes an unlimited ductility. In this study an attempt has been made to predict the target displacement by four-linear idealization of the pushover curve using the approximate SDOF-IDA curves. Instead of calculating the SDOF-IDA curve for particular input parameters that describe the equivalent SDOF system, a large database of SDOF-IDA curves, which correspond to uniformly distributed input parameters (i.e. periods, damping ratios, force-displacement envelopes) and different ground-motion records, was established. The prediction of the IDA curve for a specific structure can be made by combining the database of the SDOF-IDA curves

with a simple approach, known as n-dimensional linear interpolation. The application of the proposed methodology is demonstrated using an example of a four-storey reinforced concrete structure. The results obtained by the simplified nonlinear seismic assessment method are compared with the results based on the IDA analysis.

Title: Seismic response analysis of 3D structures through simplified non-linear procedures
Author: Petti, L; Marino, I; Cuoco, L
Source: 14th World Conference on Earthquake Engineering: Innovation Practice Safety. 2008
Descriptors: Nonlinearity; Seismic phenomena; Seismic engineering; Benchmarking; Three dimensional; Nonlinear dynamics; Seismic response

Abstract: New tools for the analysis of the seismic behaviour of plan-asymmetric structures are herein presented and the concepts of 'polar spectrum' and limit domains are discussed. Both polar spectrum and limit domains allow researchers to investigate the non-linear capacities of plan-asymmetric structures. The proposed procedure has been validated by comparing the results obtained with those of non-linear dynamic analyses for two benchmark structures.

Title: DYNAMIC INELASTIC ANALYSIS OF HI-RISE BUILDINGS USING LUMPED MODEL
Author: Yoon, Taeho; Song, Younghoon; Song, Jingyu; Cheong, Myungchae; Cheong, Sungjin
Source: 13 WCEE: 13th World Conference on Earthquake Engineering Conference Proceedings. 2004
Descriptors: Seismic phenomena; Earthquake construction; Nonlinear dynamics; Deformation; Dynamic structural analysis; High rise buildings; Structural members

Abstract: The current earthquake design codes generally allow inelastic deformation in some structural members of a building subjected to severe earthquakes. Therefore the information about the post-elastic behavior of a building is very important in the evaluation of the safety against earthquake loading. However the three dimensional nonlinear dynamic analysis of high-rise building structures requires a lot of time and cost, and has difficulties for application in practice. Thus more simplified lumped model is often used for approximate results of the building behavior under earthquake loads. In this approach a building structure is idealized as a combination of masses and springs, and the behavior is predicted by analysis of the transformed system. In order to ensure the accuracy of the lumped model analysis it is important to provide appropriate values to the model parameters. In this study the parameters are determined from a nonlinear static push-over analysis, which is generally used to estimate member forces and global as well as local deformation capacity of a structure. Then the validity of the lumped model approach is investigated by comparing the results with those obtained from the three dimensional frame model.

The nonlinear static and dynamic analysis are performed using the program 'Canny' (Li, 1996).

H.2.3 Collapse Prediction

Title: Collapse behaviour of high-rise buildings - a response history approach
Author: Wilkinson, S M; Hiley, R A
Source: 13 WCEE: 13th World Conference on Earthquake Engineering Conference Proceedings. 2004
Descriptors: Collapse; Beams (structural); Ductility; Seismic phenomena; Joints; Stiffness; High rise buildings; Earthquake construction

Abstract: The results of a series of non-linear response history analyses are presented. The non-linear model includes elasto-plastic behaviour of beam connections up to a critical moment where upon the connection 'breaks' and suffers irrecoverable loss of strength and stiffness. This corresponds to an extreme, idealized form of material degradation and when coupled with P-Delta effects, allows the complete collapse of the structures to be investigated. Three generic frames are subjected to seven earthquake excitations. Results were obtained for both the plastic limit (i.e. where all beams remain within their plastic range) and the collapse limit (where all beams exceed their ultimate capacity) and are presented in terms of number of storeys and ductility. The results show that significant reserve capacity is achievable even in structures with minimal ductility. The results are very dependant on the correspondence between the frequency content of the earthquake and the natural periods of the building and also the building configuration. Simple pushover analysis is not capable of predicting the collapse load of structure.

Title: Collapse assessment of degrading MDOF structures under seismic excitations
Author: Chenouda, M; Ayoub, A
Source: Proceedings of the 2006 Structures Congress: Structural Engineering and Public Safety; St. Louis, MO; USA; 18-21 May 2006. 2006
Descriptors: Collapse; Seismic effects; Excitation; Seismic phenomena; Seismic engineering; Mathematical models; Degradation; Earthquake design; Dynamical systems; Dynamics; Hysteresis; Assessments; Public safety; Demand; Gravitation; Criteria; Dynamic structural analysis; Mathematical analysis; Displacement

Abstract: Seismic code provisions are now adopting performance-based methodologies, where structures are designed to satisfy multiple performance objectives. Most codes rely on approximate methods to predict the desired seismic demand parameters. Most of these methods are based on simple SDOF models, and do not take into account neither MDOF nor degradation effects, which are major factors influencing structural behavior under earthquake excitations. More importantly, most of these models can not predict collapse explicitly under severe seismic loads. This study presents a newly developed model that incorporates

degradation effects into seismic analysis of MDOF structures. A new energy-based approach is used to define several types of degradation effects. Collapse under severe seismic excitations, which is typically due to the formation of structures mechanisms, was modeled in this work through the degrading hysteretic structural behavior along with P-Delta effects due to gravity loads. The model was used to conduct extensive statistical dynamic analysis of different structural systems subjected to a large set of recent earthquake records. To perform this task, finite element models of a series of generic MDOF structures were developed. An ensemble of recent earthquake records was used in the work, and a variety of degrading MDOF structures that cover a wide range of periods, yield values, and levels of degradation were considered. For each MDOF structure, collapse was investigated and inelastic displacement ratios curves were developed in case collapse doesn't occur. In addition, seismic fragility curves for a collapse criterion were also developed. The findings provide necessary information for the design evaluation phase of a performance-based earthquake design process.

Title: Collapse of lightly confined reinforced concrete frames during earthquakes
Author: Ghannoum, Wassim M; Moehle, Jack P; Bozorgnia, Yousef
Source: 100th Anniversary Earthquake Conference. 2006
Descriptors: Seismic phenomena; Earthquake construction; Computer simulation; Reinforced concrete; Beam-columns; Nonlinear dynamics; Building components

Abstract: Post earthquake studies show that the primary cause of reinforced concrete building collapse during earthquakes is the loss of vertical-load-carrying capacity in critical building components leading to cascading vertical collapse. In cast-in-place beam-column frames, the most common cause of collapse is the failure of columns, beam-column joints, or both. This study emphasizes failure of "nonconforming" columns using data from laboratory studies. Failure models are incorporated in the nonlinear dynamic analysis software OpenSEES, enabling complete dynamic simulations of building response including component failure and progression of collapse. This approach enables more realistic simulation of building collapse than is possible using simplified assessment procedures, and provides insight into the conditions that cause collapse and the variability of collapse as a function of input ground motions.

Title: Collapse analysis of building structures under excitation of near-fault ground motion with consideration of large deformation and displacement
Author: Shih, Ming-Hsiang; Chen, Chang-Liang; Sung, Wen-Pei
Source: Structural Design of Tall and Special Buildings. Vol. 16, no. 2, pp. 165-180. June 2007
Descriptors: Mathematical models; Deformation; Seismic phenomena; Dynamic structural analysis; Thresholds; Dynamics; Earthquake construction; Stiffness; Nonlinearity; Mathematical analysis; Excitation;

Displacement; Collapse; Elastic deformation; Shear; Nonlinear dynamics; Grounds; Coefficients; Statistical analysis

Abstract: The dynamic analysis of structural stability with consideration of material and geometrical non-linearity is necessary for near fault-earthquake that is rich in long-period components and often induces the non-linear large displacement and deformation response of a building structure. A macro-element bilinear geometric stiffness model and simplified analytical model are proposed and developed to analyze the P- effects of structural dynamic response using a numerical approach. A structural stable threshold diagram is then proposed to evaluate the geometric stability of a building structure with large deformation under the excitation of a near-fault earthquake. The analysis results reveal: (1) the simplified geometric stiffness analytical model is useful for analyzing structural dynamic P- effects and acquire very good accurate results even though the structural geometric stiffness varies between elastic and plastic zone; (2) stable threshold diagrams, based on dynamic analysis and statistical analysis procedures, are conducted by application of this proposed model to easily evaluate structural geometric stability with larger deformation imposed by a near-fault earthquake. This method can supplement the insufficient capability for the static pushover analysis procedure to estimate the seismic proof demands for building without dynamic P- effects analysis; (3) the analysis results of stable threshold diagrams indicate that when stability coefficient of a building is greater than 1 or base shear factor (V/W) of the building is less than 0.2 , static P- effects become noticeable.

H.2.4 Sensitivity of Response to Modeling

Title: Effects of model idealization on the collapse threshold of simple systems
Author: Tarnowski, Michael; Bernal, Dionisio
Source: Seventh U.S. National Conference on Earthquake Engineering (7NCEE): Theme: Urban Earthquake Risk [electronic resource]; 10 pages pp. 2002
Descriptors: Pendulums; Vertical ground motion; Nonlinear time history analysis

Abstract: The phenomenon of collapse of structures from cyclic dynamic excitation such as that induced by earthquakes is a transitional behavior between bounded oscillations and unbounded drift. To track the response near collapse is difficult and most of the analytical research in this area has been carried out using very simple models. The work presented in this paper continues to focus on simple systems, but investigates the impact that various idealizations have on the computed collapse thresholds. In particular, the effect of large deformations, degrading strength and stiffness, vertical excitations, and bi-directional effects are examined for a hysteretic inverted pendulum system. The justification for the various simplifications commonly applied when deriving reduced models of practical building structures is examined in light of the results obtained.

Title: A comparative study of concentrated plasticity models in dynamic analysis of building structures
Author: Dides, Maurice A; De La Llera, Juan C
Source: Earthquake Engineering & Structural Dynamics. Vol. 34, no. 8, pp. 1005-1026. 10 July 2005
Descriptors: Dynamic structural analysis; Plasticity; Frames; Hinges; Steel structures; Computer programs; Commercial buildings; Earthquake construction

Abstract: Concentrated plasticity (CP) models are frequently used in static and dynamic building analysis and have been implemented in available commercial software. This investigation deals with three different CP-models, a simplified macroelement model (SEM) for a complete building story, a frame element with elasto-plastic interaction hinges (PH), and a frame element with fiber hinges (FB). The objectives of this work are to evaluate the quality of the earthquake responses predicted by these models and to identify important aspects of their implementation and limitations for their use in dynamic analysis. The three elements are tested in a single-story asymmetric plan building and in a three-story steel building. Results show that base shear and global response values are usually computed with better accuracy than interstory deformations and local responses. Besides, the main limitation of elasto-plastic CP models is to control the displacement offsets that result from perfect elasto-plastic behavior. On the other hand, calibration of the SEM-model shows that global responses in steel structures may be computed within 20% error in the mean at a computational cost two orders of magnitude smaller than that of the other CP elements considered. However, the three element models considered lead to increasing levels of accuracy in the dynamic response and their use depends on the refinement of the analysis performed.

Title: Effect of hysteresis type on drift capacity for global collapse of moment frame structures for seismic loads.
Author: Huang, Zhenhua
Source: Dissertation Abstracts International. Vol. 68, no. 2. 2006
Descriptors: Degradation; Hysteresis; Seismic phenomena; Drift; Seismic engineering; Earthquake construction; Seismic response; Stiffness; Frames; Buildings; Marketing; Strength; Collapse; Demand; Earthquake design; Estimating; Nonlinearity; Criteria; Demand analysis

Abstract: It is conjectured that different hysteresis behavior in moment frames subjected to seismic loads may lead to different levels of response because of degradation in strength and stiffness. To examine the existence and magnitude of this effect, this research aims to: (1) Determine the global collapse capacities of several classes of moment frame buildings under seismic loads. (2) Develop the basis for the seismic criteria for design and evaluation of moment frame buildings that reflect and account for the global drift capacity. (3) Evaluate the hysteresis effects on the demand level response and capacity/demand ratio of moment frame buildings under seismic

loads. (4)Develop a nonlinear cyclic pushover procedure that can be used for estimating the global drift capacity of a specific building. To achieve these objectives, seismic analyses of 3-, 9- and 20-story moment resisting frame buildings were conducted to evaluate the effects of the hysteretic behavior of beam-to-column connections, structural stiffness, and structural strength on the collapse potential and the demand level response. Five hysteresis models: basic bilinear, strength degradation, stiffness degradation, stiffness degradation + strength degradation, and pinching are evaluated. The effects of hysteresis behaviors are very significant for both global drift capacities and demand level responses. Two interesting results for the mid-rise/high-rise buildings are that (1)strength degradation significantly decreases both the global drift capacity and the Sa capacity, whereas, (2)the existence of stiffness degradation increases the global drift capacity and the Sa capacity.

Title: Comparison of different finite-element modeling approaches in terms of estimating the residual displacements of RC structures
Author: Yazgan, Ufuk; Dazio, Alessandro
Source: 100th Anniversary Earthquake Conference. 2006
Descriptors: Finite element method; Earthquake design; Reinforced concrete; Seismic phenomena; Temporal logic; Plasticity; Fiber composites

Abstract: Conventional earthquake resistant design methods are mainly set up to estimate the maximum values of response parameters, such as displacements and forces. As a result, most of the finite-element modeling approaches and tools have been verified for estimating these maximum values. However, in the last decade there has been an increasing interest in the direct consideration of post-earthquake residual displacements in the design and assessment processes. In this study, it is shown that the residual displacement estimates computed using nonlinear dynamic finite-element analyses can be strongly influenced by the adopted modeling approach and the simplifications introduced. Nonlinear response of a representative reinforced concrete column to static cyclic and dynamic loads is simulated using various implementations of lumped plasticity and fiber models. Comparative evaluation of the results shows that significantly different residual displacements are computed using different implementations of the same models. On the other hand, the maximum displacements are found to be less sensitive to the differences among implementations. Results indicate that the assumptions related to temporal and spatial discretization of the system has an important influence on the computed residual displacements.

Title: A study on seismic structural demands on frames considering variability in strength of structural components
Author: Mori, Yasuhiro; Oba, Maya
Source: 8th Pacific Conference on Earthquake Engineering Conference Proceedings. 2007
Descriptors: Mathematical models; Demand; Marketing; Strength; Seismic phenomena; Computer simulation; Seismic engineering; Earthquake

design; Accuracy; Uncertainty; IMP; Estimating; Nonlinear dynamics; Estimates; Grounds; Design engineering; Frames; Performance assessment

Abstract: Estimating seismic structural demands simply and precisely can be important for structural performance assessment and for design. Nonlinear dynamic analysis (NDA) is widely used to evaluate structural response to a given ground motion, and the result is considered to be rigorous. However, it is true only if the structural characteristics are known. There exists uncertainty in the strength of structural components, and a result of single NDA using a deterministic structural model is only a sample of the sample space of possible response of a given structure. Thus, NDA using a deterministic structural model can be considered as one of predictors (or estimates) of structural demands. The accuracy of the predictor as well as simplicity can be compared with those of the other techniques such as Inelastic Modal Predictor (IMP) proposed by one of the authors. In this paper, the influence of the uncertainty in strength of structural components on structural response is investigated via simulation-based approach with NDA. Then the accuracy of the IMP is investigated along with that of NDA using a deterministic structural model based on the results of the simulation.

Title: Sensitivity of nonlinear frames to modelling parameters and earthquake excitations
Author: Wilkinson, S M; Sivaselvan, M V
Source: 14th World Conference on Earthquake Engineering: Innovation Practice Safety. 2008
Descriptors: Mathematical models; Seismic phenomena; Earthquake design; Earthquake construction; Nonlinearity; Design engineering; Seismic response; Seismic engineering; Earthquake dampers; Modelling; Hysteresis; Models; Frames; Collapse; Initial conditions; Acceleration; Mechanical engineering; Dissipation; Buildings

Abstract: Modern seismic codes permit the use of response-history methods to assess buildings for adequate seismic resistance. However, before this procedure can be implemented, it is necessary to first develop a suitable structural model and then to subject this to a relevant earthquake acceleration. For the ultimate design earthquake, it is now usual to increase the efficiency of the design, by allowing the structure to exceed its elastic limit and hence dissipate energy in hysteretic damping. If the designer is using response-history analysis as the primary means of assessing structural adequacy, then this design strategy requires the structural model to be nonlinear. It has long been known in both mathematics and mechanical engineering that non linear dynamic models can be very sensitive to both modeling assumptions and initial conditions; however this is rarely investigated in structural engineering designs. This paper presents the results of a large number of nonlinear time history analyses that have been conducted on simple frames. The model used in the analyses considers both material and geometric non-linearities. Inelastic behavior of the structure is modeled by an extended perfectly elastic, perfectly plastic moment

rotation relationship. The extension to the moment rotation relationships enables analysis up to complete collapse of the structure by allowing the connection to fracture once its deformation has exceeded its ultimate rotation. The results of these analyses are presented as a parameter space of modelling parameters and load parameters. A number of earthquakes are investigated and the sensitivity of the results to these is discussed.

H.2.5 Efficacy and Limitations Relative to Empirical Results

Title: Pre- and post-test mathematical modeling of a plan-asymmetric reinforced concrete frame building
Author: Fajfar, Peter; Dolsek, Matjaž; Marusic, Damjan; Stratan, Aurel
Source: Earthquake Engineering & Structural Dynamics. Vol. 35, no. 11, pp. 1359-1379. Sept. 2006
Descriptors: Reinforced concrete; Earthquake engineering; Seismic response; Plasticity; Computer simulation; Dynamics; Frame structures

Abstract: Pre- and post-test analyses of the structural response of a three-storey asymmetric reinforced concrete frame building were performed, aimed at supporting test preparation and performance as well as studying mathematical modelling. The building was designed for gravity loads only. Full-scale pseudo-dynamic tests were performed in the ELSA laboratory in Ispra. In the paper the results of initial parametric studies, of the blind pre-test predictions, and of the post-test analysis are summarized. In all studies a simple mathematical model, with one-component member models with concentrated plasticity was employed. The pre-test analyses were performed using the CANNY program. After the test results became available, the mathematical model was improved using an approach based on a displacement-controlled analysis. Basically, the same mathematical model was used as in pre-test analyses, except that the values of some of the parameters were changed. The OpenSees program was employed. Fair agreement between the test and numerical results was obtained. The results prove that relatively simple mathematical models are able to adequately simulate the detailed seismic response of reinforced concrete frame structures to a known ground motion, provided that the input parameters are properly determined.

H.3 Special Configurations and Typologies

H.3.1 Torsional or Plan Irregularities

Title: EAEE Task Group (TG) 8: behaviour of irregular and complex structures asymmetric structures -- progress since 1998
Author: Rutenberg, A
Source: The Twelfth European Conference on Earthquake Engineering [Proceedings] [electronic resource] , pp. 12 pages. 2002
Descriptors: Resources; Paper; Nonlinear dynamics; Asymmetry; Seismic response; Eccentrics; Frames; Earthquake engineering

Abstract: Published research on the seismic response of horizontally irregular structures since 1998 is briefly reviewed. Studies on 1-storey monosymmetric models still predominate, but the interest in the behaviour of eccentric multistorey frames is increasing. Most of the latter studies relate to pushover analysis and its ability to simulate the nonlinear dynamic response. There are several studies on passive control aimed at reducing twist, and a surprisingly small number of papers reporting experimental results.

Title: Simplified seismic method of evaluation of asymmetric buildings
Author: Ayala, A Gustavo; Tavera, Elias A; Ayala, Mauricio
Source: Revista de Ingenieria Sismica , no. 67. July-Dec. 2002
Descriptors: Seismic engineering; Earthquake construction; Approximation; Asymmetry; Nonlinearity; Performance evaluation

Abstract: This paper presents an approximate method for the seismic performance evaluation of asymmetric building structures. The method is based on a non-linear pushover analysis, the transformation of the capacity curve into a behavior curve of an equivalent single degree of freedom system, the evaluation of its maximum response to a given seismic demand and the back transformation of the response to the original structure. In the application of the pushover analysis, the structure is pushed in two orthogonal directions with lateral forces with distributions and proportions defined as recommended by the current code. The potentiality of the proposed method to estimate seismic performance of asymmetric buildings is shown when the approximate results for two illustrative examples are compared with those obtained with "true" non-linear step by step analyses.

Title: A new approach for the evaluation of the seismic performance of asymmetric buildings
Author: Ayala, A. G.; Tavera, E. A.
Source: Seventh U.S. National Conference on Earthquake Engineering (7NCEE): Theme: Urban Earthquake Risk [electronic resource]; 10 pages pp. 2002
Descriptors: Asymmetric structures; nonlinear static pushover analysis; Multistorey reinforced concrete structures; nonlinear analysis; Story drift; Mexico City; building codes

Abstract: This paper presents a new simplified method for the seismic performance evaluation of asymmetric 3D building structures. The method is based on a nonlinear pushover analysis carried out with a distribution of forces equivalent to that produced by earthquake action and on the analysis of a single degree of freedom system equivalent to the original structure. During the application of the method, the structure is pushed in two orthogonal directions with lateral forces defined in accordance with a current seismic design code. These forces consider the contribution of all modes of vibration. From this analysis, the curve base shear vs. roof displacement in two orthogonal directions and the curve base moment vs. rotation are constructed and transformed using basic concepts of structural dynamics,

first into capacity curves considering only forces produced by the fundamental mode and then into the behavior curve of an equivalent single degree of freedom system corresponding to the fundamental mode. This equivalent system is then subjected to an earthquake or group of earthquakes to determine its absolute maximum displacement and, hence, the corresponding displacements of the center mass of the roof of the building. Finally, the seismic performance of the structure is determined from the pushover analysis corresponding to these roof displacements. The validity of the proposed method is assessed via an illustrative example comparing the results with those of a "true" nonlinear step-by-step dynamic analysis.

Title: Static vs. modal analysis of asymmetric buildings: effectiveness of dynamic eccentricity formulations
Author: Calderoni, Bruno; et al.
Source: Earthquake Spectra. Vol. 18, no. 2, pp. 219-231. May 2002
Descriptors: Multistory asymmetric structures; nonlinear analysis; Irregular structures; Europe; Eurocode 8; building codes; Catania; Univ. of; Italy; office buildings

Abstract: The use of modal analysis appears necessary in order to reduce both displacement demand under weak seismic events and ductility demand under strong earthquakes. Static analysis can be effective only if used with proper values of additional eccentricities. To overcome the inaccuracy of the code formulations, the authors propose a simple procedure that gives the exact values of these eccentricities and discuss the influence of the main parameters that govern the structural behavior. They also point out the difficulty in evaluating some parameters (stiffness radius of gyration, structural eccentricity) in the case of multistory buildings and discuss the validity of simplified formulations proposed to overcome this problem. The effectiveness of static analysis, applied to three-dimensional multistory structures with properly evaluated corrective eccentricities, is analyzed with reference both to regularly asymmetric multistory schemes and to an actual irregularly asymmetric structure (the main building of the Faculty of Engineering at the University of Catania, Italy).

Title: Capacity spectrum method for plan asymmetric multistory building structures
Author: Faella, G.; Mezzi, M.
Source: Seventh U.S. National Conference on Earthquake Engineering (7NCEE): Theme: Urban Earthquake Risk [electronic resource]; 10 pages pp. 2002
Descriptors: Multistory reinforced concrete frames; nonlinear static pushover analysis; Europe; Eurocode 8; building codes; Story drift; Asymmetric structures; dynamic properties

Abstract: The paper investigates the use of nonlinear static analyses and the capacity spectrum method for multistory reinforced concrete L-shaped buildings. For this purpose, the seismic behavior of 3-story and 6-story framed buildings designed

according to the enhanced ductility provisions of the last draft of Eurocode 8 for structures is studied. The building torsional response is analyzed in terms of base shear, floor rotation and displacement when the eccentricity of static lateral loads varies. Comparison with the dynamic response under several input ground motions shows that pushover analysis can identify the actual stiff and flexible side of buildings in the inelastic range of behavior and can capture structural deficiencies that the usual design linear analyses are unable to recognize. The numerical examples show that, differently from what is reported in some relevant papers, the capacity spectrum method leads to suitable target displacements by using only the mass center displacement as a structural landmark and the base-shear-top-displacement relationship computed by loading the structure at the mass center as the capacity curve. Furthermore, if the earthquake demand curves are represented by inelastic spectra, the procedure shows enough numerical stability and absence of convergence troubles.

Title: Simplified nonlinear seismic analysis of asymmetric multistorey R/C building

Author: Kilar, V; Fajfar, P

Source: The Twelfth European Conference on Earthquake Engineering [Proceedings] [electronic resource] , pp. 10 pages. 2002

Descriptors: Nonlinear dynamics; Asymmetry; Dynamic tests; Resources; Seismic engineering; Computer programs; Seismic phenomena; Demand analysis; Marketing; Seismic response; Earthquake construction; Walls; Earthquake engineering

Abstract: The paper examines the extension of the N2 method, which is based on pushover analysis and the response spectrum approach, to the analysis of asymmetric structures. The results obtained by the extended N2 method are compared with the results obtained by the method proposed by Moghadam and Tso and by nonlinear dynamic analyses. Several variants of an asymmetric four-storey stiffness- and strength-eccentric building, which includes also shear walls, are investigated. The original building variant was designed according to Eurocode 8. For the dynamic analysis, a set of five accelerograms, which approximately match the demand spectrum, was used. Nonlinear dynamic and pushover analyses were performed with the computer program CANNY.

Title: 3D pushover analysis: the issue of torsion

Author: Penelis, Gr G; Kappos, A J

Source: The Twelfth European Conference on Earthquake Engineering [Proceedings] [electronic resource] , pp. 10 pages. 2002

Descriptors: Nonlinear dynamics; Dynamic tests; Dynamical systems; Mathematical models; Loads (forces); Buildings; Resources; Spectra; Statics; Torsion; Earthquake engineering; Equivalence

Abstract: A methodology is presented for modelling the inelastic torsional response of buildings in nonlinear static (pushover) analysis, with the aim of reproducing to the

highest possible degree inelastic dynamic time history analysis results. The load vectors are defined using dynamic elastic spectral analysis while the dynamic characteristics of an equivalent single mass system, which incorporates both translational and torsional modes, are derived using an extension of earlier methods based on the single degree-of-freedom (SDOF) approach. The proposed method is verified for the case of single-storey monosymmetric buildings.

Title: Preliminary assessment of a simplified code method for earthquake design of asymmetric buildings
Author: Anagnostopoulos, Stavros; Demopoulos, Athanasios
Source: Concrete Structures in Seismic Regions: FIB 2003 Symposium [Proceedings] [electronic resource] , pp. 8 pages. 2003
Descriptors: Buildings; Design engineering; Dynamics; Dynamic tests; Eccentricity; Earthquake design; Seismic phenomena; Accident analysis; Amplification; Accidents; Asymmetry; Statics; Earthquake construction; Torsion; Compatibility; Resources; Optimization; Seismic engineering; Reinforced concrete

Abstract: The so-called simplified modal response spectrum analysis referred to in Eurocode 8 or the equivalent lateral force procedure referred to in the International Building Code 2000 is the traditional method of analysis for earthquake-resistant design of buildings, used long before dynamic analyses were introduced into the codes and became popular. Because the method is an approximate one, its applicability has been limited in some codes to regular buildings only. In the last edition (EAK 2000) of the Hellenic code, the simplified method that was included in the earlier edition (NEAK 1995) was modified to improve the design of asymmetric buildings through the introduction of two static eccentricities and a so-called elastic pseudo-axis or an optimum torsion axis. For ease of reference, in this paper, this method is referred to as the Torsionally Enhanced Simplified Method (TESM). The traditional, simplified method of EC8 that uses a design accidental eccentricity of 5% is referred to as the Simplified Method (SM); the simplified method of IBC and NEAK-1995, where amplified accidental eccentricities are used, is referred to as the Simplified Method with Amplified eccentricity (SM-Ae); and the multi-modal Dynamic Analysis Method is referred to as the Dynamic Analysis method (DA). While the TESM method may rationalize the static elastic design for torsion, it has complicated substantially the simplified method to the extent that practically everyone prefers to use the dynamic multi-modal method of analysis. In this paper, the effectiveness of the TESM method is evaluated through comparisons of the designs of 3-story, reinforced concrete frame-type buildings using all four methods by means of inelastic dynamic response predictions when the buildings were subjected to a set of 10 earthquake motion pairs, compatible with the design spectrum.

Title: A modal pushover analysis procedure to estimate seismic demands for unsymmetric-plan buildings : theory and preliminary evaluation
Author: Chopra, Anil K.; Goel, Rakesh K.
Source: UCB/EERC-2003/08
Descriptors: Seismic engineering; Seismic phenomena; Marketing; Earthquake construction; Dynamics; Demand; Buildings; Demand analysis; Stress concentration; Dynamical systems; Dynamic structural analysis; Spectrum analysis; Equivalence

Abstract: Based on structural dynamics theory, the modal pushover analysis procedure (MPA) retains the conceptual simplicity of current procedures with invariant force distribution. The MPA procedure for estimating seismic demands is extended to unsymmetric-plan buildings. When applied to elastic systems, the MPA procedure is equivalent to standard response spectrum analysis (RSA). The MPA estimates of seismic demand for torsionally stiff and torsionally flexible unsymmetric systems are shown to be similarly accurate as they are for the symmetric building.

Title: Design for forces induced by seismic torsion.
Author: Humar, J.; Yavari, S.; Saatcioglu, M.
Source: Canadian Journal of Civil Engineering. Vol. 30, no. 2, pp. 328-337. Apr. 2003
Descriptors: Buildings; Building codes; Design engineering; Earthquake design; Seismic phenomena; Earthquake construction; Eccentricity; Torsion; Seismic engineering; Flexibility; Inertia; Dynamic tests; Loads (forces); Constrictions; Rigidity; Mathematical analysis; Dynamics; Earthquake engineering; Equivalence

Abstract: Eccentricities between the centres of rigidity and centres of mass in a building cause torsional motion during an earthquake. Seismic torsion leads to increased displacement at the extremes of the building and may cause distress in the lateral load-resisting elements located at the edges, particularly in buildings that are torsionally flexible. For an equivalent static load method of design against torsion, the 1995 National Building Code of Canada specifies values of the eccentricity of points through which the inertia forces of an earthquake should be applied. In general, the code requirements are quite conservative. They do not place any restriction on the torsional flexibility, however. New proposals for 2005 edition of the code which simplify the design eccentricity expressions and remove some of the unnecessary conservatism are described. The new proposals will require that a dynamic analysis method of design be used when the torsional flexibility of the building is large. Results of analytical studies, which show that the new proposals would lead to satisfactory design, are presented.

Title: Inelastic static-dynamic analysis method of high-rise steel structures under earthquake action
Author: Yang, Zhiyong; He, Ruoquan
Source: Journal of Building Structures. Vol. 24, no. 3, pp. 25-32. 2003

Descriptors: Mathematical models; Vibration modes; Seismic phenomena; Earthquake construction; Structural steels; Dynamic tests; Nonlinear dynamics; Frame structures; Asymmetry; Realizability; Equivalence

Abstract: This paper presents an inelastic static-dynamic analysis method of highrise steel structures under earthquake action. This method colligates the virtues of the dynamic nonlinear time history analysis method, the equivalent inelastic storey model, and the pushover method. This method can be used in those highrise buildings in which high-order vibration modes and torsional effects should not be ignored. From the analysis of some example buildings, the rationality and security of the inelastic storey model have been validated, as well as the feasibility of applying the inelastic static-dynamic analysis method to plane frame structures considering high-order vibration modes and to 3D asymmetric structures.

Title: A modal pushover analysis procedure to estimate seismic demands for unsymmetric-plan buildings.

Author: Chopra, A K; Goel, R K

Source: Earthquake Engineering & Structural Dynamics. Vol. 33, no. 8, pp. 903-927. 10 July 2004

Descriptors: Seismic phenomena; Earthquake construction; Buildings; Elastic systems

Abstract: Based on structural dynamics theory, the modal pushover analysis (MPA) procedure retains the conceptual simplicity of current procedures with invariant force distribution, now common in structural engineering practice. The MPA procedure for estimating seismic demands is extended to unsymmetric-plan buildings. In the MPA procedure, the seismic demand due to individual terms in the modal expansion of the effective earthquake forces is determined by non-linear static analysis using the inertia force distribution for each mode, which for unsymmetric buildings includes two lateral forces and torque at each floor level. These 'modal' demands due to the first few terms of the modal expansion are then combined by the CQC rule to obtain an estimate of the total seismic demand for inelastic systems. When applied to elastic systems, the MPA procedure is equivalent to standard response spectrum analysis (RSA). The MPA estimates of seismic demand for torsionally-stiff and torsionally-flexible unsymmetric systems are shown to be similarly accurate as they are for the symmetric building; however, the results deteriorate for a torsionally-similarly-stiff unsymmetric-plan system and the ground motion considered because (a) elastic modes are strongly coupled, and (b) roof displacement is underestimated by the CQC modal combination rule (which would also limit accuracy of RSA for linearly elastic systems).

Title: Simplified nonlinear analysis procedure for single-story asymmetric buildings subjected to bi-directional ground motion.

Author: Fujii, K; Nakano, Y; Sanada, Y

Source: First International Conference on Urban Earthquake Engineering [March 8-9, 2004], pp. 97-104. 2004

Descriptors: Buildings; Nonlinear dynamics; Earthquake engineering; Ground motion; Nonlinear analysis; Asymmetric structures; Dynamic structural analysis; Performance prediction

Abstract: A simplified procedure for single-story asymmetric buildings subjected to bidirectional ground motion is proposed. In this procedure, the responses are predicted through a nonlinear static analysis of a multidegree-of-freedom model considering the effect of bidirectional excitation and a nonlinear dynamic analysis of an equivalent single degree-of-freedom model. The results are compared with those of the nonlinear dynamic analysis of multidegree-of-freedom models, and satisfactory prediction can be found in the nonlinear response of asymmetric buildings.

Title: A simplified approach to the analysis of torsional effects in eccentric systems: the Alpha method

Author: Gasparini, Giada; Silvestri, Stefano; Trombetti, Tomaso

Source: 13 WCEE: 13th World Conference on Earthquake Engineering Conference Proceedings. 2004

Descriptors: Dynamical systems; Nonlinear dynamics; Dynamic structural analysis; Joining; Excitation; Seismic phenomena; Nonlinearity

Abstract: Eccentric structures, characterized by non coincident center of mass and center of stiffness, when subjected to dynamic excitation, develop a coupled lateral-torsional response that may increase the local peak dynamic response of such a structure: this behaviour becomes particularly important for seismic isolated structures for which large displacements are developed in the isolators. The coupled lateral-torsional response can be estimated only through a three-dimensional analysis which is specifically carried out for a single structure subjected to a determined dynamic input. In this paper the authors present the analytical formulation of a simplified method which allows to understand, predict and govern the global trend of one-storey eccentric structures to develop a torsional response to dynamic inputs through the identification of a system key parameter named "alpha". This parameter can be easily used to effectively estimate the maximum rotational response of a given eccentric system under a dynamic excitation through a simple linear elastic analysis of the "equivalent" non-eccentric system. Moreover, the results of the analysis in the non-linear field show that the linear elastic value of "alpha" acts as an upper bound for the corresponding value of elastic-perfectly plastic systems. In summary, this paper proposes a physically-based general theory which frames the problem of torsional phenomena of one-storey eccentric systems subjected to dynamic inputs and immediately allows the quantification of the system torsional response and the identification of the structural parameters governing it.

Title: Predictive capabilities of the Alpha method: shaking table tests and field data verification

Author: Gasparini, Giada; Trombetti, Tomaso; Silvestri, Stefano; Ceccoli, Claudio

Source: 13 WCEE: 13th World Conference on Earthquake Engineering Conference Proceedings. 2004

Descriptors: Excitation; Seismic phenomena; Dynamical systems; Earthquake engineering

Abstract: This paper verifies the accuracy and effectiveness of the "alpha" method for maximum rotational response prediction as applied to a wide range of eccentric systems and earthquake excitations. The verification is carried out either through extensive numerical investigations, through shaking table tests and through the analysis of actual responses of two Californian base isolated structures subjected to some of the most recent earthquakes occurred in their regions. These studies showed the applicability of the proposed "alpha" method which is found to be sufficiently accurate (for engineering purposes) and robust over a wide range of eccentric system parameter values and dynamic excitations. These successful verification results also confirm that the dimensionless structural parameter "alpha" used in the proposed simplified method can alone be used to quantify the pre-disposition of a given eccentric system in developing a rotational response under earthquake excitations.

Title: Capacity spectrum for structures asymmetric in plan

Author: Prasad, B K Raghu; Ramaiah, A Seetha; Singh, A K

Source: 13 WCEE: 13th World Conference on Earthquake Engineering Conference Proceedings. 2004

Descriptors: Spectra; Acceleration; Ductility; Displacement; Equations of motion; Columns (structural); Eccentricity; Earthquake engineering

Abstract: Capacity spectra are obtained by pushover analysis. In the pushover analysis the six equations of motion are used to obtain the column forces due to incremental lateral forces at the mass centre. As the equations of motion contain the contribution due to eccentricities the column forces do exhibit the influence of rotations about the vertical axis. Plots of spectral acceleration Vs spectral displacement (ADRS format) are obtained from independent spectral acceleration and spectral displacement spectra for various levels of ductilities. Juxtaposing one on the other will confirm the ductility required for the given yield acceleration.

Title: Validation of single storey models for the evaluation of the seismic performance of multi-storey asymmetric buildings

Author: Zarate, Gonzalo; Ayala, A Gustavo

Source: 13 WCEE: 13th World Conference on Earthquake Engineering Conference Proceedings. 2004

Descriptors: Seismic engineering; Earthquake construction; Dynamics; Buildings; Dynamic mechanical properties; Degrees of freedom

Abstract: Of all the models used in the past for the development and evaluation of seismic design criteria for asymmetric structures, the most common has been the single-storey model with the same number of resisting planes as the structure it represents, same uncoupled dynamic properties and three degrees of freedom. When considering the coupled dynamic properties of these models, they are different to

those of the structure they aim to represent. The only model that allows a correspondence of results with the structures represented is the parametric model proposed by Kan and Chopra. Based on this model, and with the purpose of evaluating and transforming to real buildings the massive amount of available results generated with single-storey models and investigating new cases of interest, this paper presents an approximate procedure that allows the definition of a 3-degree of freedom simplified "structure" representing the real structure and satisfying the requisites of the parametric model of Kan and Chopra. The non-linear force-displacement relationships for this model are obtained from the capacity curves of the real structure. Once the performance point of the approximate model is obtained, the seismic performance of the real building is obtained using the correspondence relationships to transform this performance point to the response of the real structure. Finally the forces and displacements corresponding to this performance point are recovered from the results of a pushover analysis.

Title: Pushover Analysis Of Asymmetric Three-Dimensional Building Frames
Author: Barros, Rui Carneiro; Almeida, Ricardo
Source: Journal of Civil Engineering and Management. Vol. 11, no. 1, pp. 3-12. 2005
Descriptors: Vibration; Asymmetry; Frames; Seismic phenomena; Earthquake construction; Earthquake engineering; Grounds; Seismic engineering; Orientation; Nonlinearity; Stiffness; Nonlinear dynamics; Civil engineering

Abstract: The effect of higher modes of vibration on the total non-linear dynamic response of a structure is a very important and unsolved problem. To simplify the process the static non-linear pushover analysis was proposed associated with the capacity spectrum method, utilising a load pattern proportional to the shape of the fundamental mode of vibration of the structure. The results of the pushover analysis, with this load pattern, are very accurate for structures that respond primarily in the fundamental mode. But when the higher modes of vibration become important for the total response of the structure, this load pattern loses its accuracy. To minimise this problem a new multimode load pattern is proposed based on the relative participation of each mode of vibration in the elastic response of a structure subjected to an earthquake ground motion. This load pattern is applied to the analyses of symmetric frames as well as to stiffness asymmetric and mass asymmetric irregular building frames, under seismic actions of distinct orientations, permitting to draw significant conclusions.

Title: Torsional effects in the pushover-based seismic analysis of buildings
Author: Fajfar, Peter; Marusic, Damjan; Perus, Iztok
Source: Journal of Earthquake Engineering. Vol. 9, no. 6, pp. 831-854. Nov. 2005

Descriptors: Nonlinear dynamics; Buildings; Seismic engineering; Elastic limit; Earthquake construction; Approximation; Structural members

Abstract: The general trends of the inelastic behaviour of plan-asymmetric structures have been studied. Systems with structural elements in both orthogonal directions and bi-axial eccentricity were subjected to bi-directional excitation. Test examples include idealised single-storey and multi-storey models, and a three-storey building, for which test results are available. The response in terms of displacements was determined by nonlinear dynamic analyses. The main findings, limited to fairly regular and simple investigated buildings, are: (a) The amplification of displacements determined by elastic dynamic analysis can be used as a rough, and in the majority of cases conservative estimate in the inelastic range. (b) Any favourable torsional effect on the stiff side, which may arise from elastic analysis, may disappear in the inelastic range. These findings can be utilised in the approximate pushover-based seismic analysis of asymmetric buildings, e.g. in the N2 method. It is proposed that the results obtained by pushover analysis of a 3D structural model be combined with the results of a linear dynamic (spectral) analysis. The former results control the target displacements and the distribution of deformations along the height of the building, whereas the latter results define the torsional amplifications. The proposed approach is partly illustrated and evaluated by test examples.

Title: Prediction of seismic response of single-story unsymmetric buildings using equivalent SDOF model and its applicability

Author: Fujii, Kenji; Nakano, Yoshiaki; Sanada, Yasushi; Sakata, Hiroyasu; Wada, Akira

Source: Journal of Structural and Construction Engineering , no. 596, pp. 101-108. Oct. 2005

Descriptors: Excitation; Buildings; Nonlinear dynamics; Construction engineering; Seismic response

Abstract: A nonlinear static procedure for single-story unsymmetric buildings subjected to bi-directional excitation is presented and its applicability is discussed. In this procedure, their responses are predicted through a pushover analysis of MDOF model considering the effect of bi-directional excitations and a estimation of the nonlinear response of equivalent SDOF model. The predicted results are compared with the nonlinear dynamic analysis results, and it is shown that the equivalent modal mass ratios of the first and second modes are the indices to discuss the applicability of the presented procedure.

Title: Pushover analysis of 3D eccentric structures.

Author: Li, Gang; Liu, Yong

Source: Jisuan Lixue Xuebao (Chinese Journal of Computational Mechanics) (China). Vol. 22, no. 5, pp. 529-533. Oct. 2005

Descriptors: Eccentrics; Three dimensional; Earthquake engineering; Seismic phenomena; Nonlinearity; Earthquake design; Seismic design; Structural analysis; Lithium; Earthquake construction; Deformation; Irregularities

Abstract: Pushover analysis has caused much interest in the field of earthquake engineering, and it is suggested as a nonlinear analysis method of the structural deformation under severe earthquake in the new seismic design code in China. Structural irregularity is one important factor that affects the application of pushover method, and selecting an appropriate load patterns is very important in pushover analysis. In the present paper, the pushover analysis of two typical eccentric 3D building structures is studied considering 3 common load patterns suggested by FEMA 273, using ETABS program. The results by pushover analysis are compared with those by nonlinear time history analysis, and some suggestions on the selection of load patterns for eccentric structures are given.

Title: New insight into and simplified approach to seismic analysis of torsionally coupled one-story, elastic systems
Author: Trombetti, T L; Conte, J P
Source: Journal of Sound and Vibration. Vol. 286, no. 1-2, pp. 265-312. Aug. 2005
Descriptors: Mathematical models; Dynamics; Eccentrics; Dynamical systems; Seismic phenomena; Seismic engineering; Deformation; Excitation; Design engineering; Free vibration; Unity; Grounds; Constraining; Exact solutions; Stiffness; Displacement; Approximation; Gyration; Sheds

Abstract: Structures characterized by non-coincident center of mass and center of stiffness, referred to herein as eccentric structures, develop a coupled lateral-torsional response when subjected to dynamic excitation. This phenomenon is particularly important for seismic isolated structures due to the potentially large deformations imposed on the seismic isolators by the earthquake ground motion. A careful examination of the governing equations of motion of linear elastic, one-story eccentric systems sheds new light and new insight into the coupled lateral-torsional dynamic behavior of such systems and leads to the identification of a basic system parameter, the 'alpha' parameter, which controls the maximum rotational response of such systems under free and forced vibrations. The 'alpha' parameter is defined as the mass radius of gyration of the structure multiplied by the ratio of the maximum rotational to the maximum longitudinal displacement response developed by a one-story eccentric system under free vibration from a given initial deformation. Closed-form exact and approximate solutions for the 'alpha' parameter are provided for undamped and damped eccentric systems, respectively, for a wide range of system parameters. A new basic result is that the 'alpha' parameter has an upper bound of unity, thus physically limiting the maximum rotational response of an eccentric system in free vibration from an initial imposed deformation. A new physically based, simplified analysis procedure is developed, based on the 'alpha' parameter to effectively estimate the maximum rotational response of a given eccentric system under seismic excitation. The extensive numerical and experimental verification of the simplified 'alpha' method performed demonstrate that the proposed 'alpha' method is accurate enough for design purposes, is robust and is significantly more accurate

than the current International Building Code (IBC) design provisions. The experimental verification was performed through a suite of 88 shaking table tests performed on a versatile, carefully designed, one-story small-scale building model able to represent the dynamic characteristics of a wide range of eccentric systems. The dimensionless 'alpha' parameter, bounded between zero and unity, can also be used as a formal index for the inherent property of a given structure to develop a rotational response under dynamic excitation. Sensitivities of the 'alpha' parameter to various physical system characteristics are investigated and provide valuable guidance for eccentric system design.

Title: Evaluation of the modal pushover analysis procedure for unsymmetric-plan buildings
Author: Chopra, Anil K; Goel, Rakesh K
Source: 100th Anniversary Earthquake Conference. 2006
Descriptors: Seismic phenomena; Earthquake construction; Demand analysis; Buildings; Estimates; Force distribution; Roofs

Abstract: Recently, the modal pushover analysis (MPA) procedure for estimating seismic demands has been extended to unsymmetric-plan buildings. In the MPA procedure, the seismic demand due to individual terms in the modal expansion of the effective earthquake forces is determined by nonlinear static analysis using the inertia force distribution for each mode, which for unsymmetric buildings includes two lateral forces and torque at each floor level. These "modal" demands due to the first few terms of the modal expansion are then combined by the CQC rule to obtain an estimate of the total seismic demand for inelastic systems. The MPA estimates of seismic demand for torsionally-stiff and torsionally-flexible unsymmetric systems are shown to be similarly accurate as they are for the symmetric building; however, the results deteriorate for a torsionally-similarlystiff unsymmetric-plan system and the ground motion considered because (a) elastic modes are strongly coupled, and (b) roof displacement is underestimated by the CQC modal combination rule [which would also limit accuracy of response spectrum analysis (RSA) for linearly elastic systems].

Title: Simplified probabilistic performance assessment of a plan-asymmetric building
Author: Dolsek, M; Fajfar, P
Source: 100th Anniversary Earthquake Conference. 2006
Descriptors: Seismic phenomena; Nonlinear dynamics; Probability theory; Earthquake construction; Dynamic tests; Seismic engineering; Reinforced concrete

Abstract: A simplified approach, called IN2 (incremental N2 analysis), has been proposed as an alternative to Incremental Dynamic Analysis, where N2 is a simplified nonlinear method for seismic analysis, based on pushover analysis and inelastic response spectrum approach, developed at the University of Ljubljana and implemented in Eurocode 8. The IN2 can be, in combination with predetermined data

on dispersion typical for a specific structural system, employed in the PEER probabilistic framework. Using this simplified approach, the computational efforts can be substantially reduced. In the paper, the simplified approach is summarized. Its application is demonstrated by an example of a three-story planasymmetric reinforced concrete frame building. The structure was pseudodynamically tested in full-scale in the ELSA laboratory in Ispra. The mathematical model, used in analyses presented in the paper, has been validated by test results.

Title: Seismic evaluation of a 15-story composite steel-concrete hospital building

Author: Allen, Michael G; Yu, Qi-Song Kent; Mitchell, Carrie E; Pugliesi, Raymond S

Source: 100th Anniversary Earthquake Conference. 2006

Descriptors: Seismic phenomena; Earthquake construction; Concrete construction; Hospitals; Reinforcing steels; Structural members

Abstract : This paper describes the seismic assessment of a 15-story hospital building located in San Francisco. The building is a composite steel and concrete pierspandrel building built in the early 1950s. The lateral force resisting system consists of composite steel and concrete pier-spandrel frames on the perimeter with composite shear walls at the ends of the building. Due to its irregular plan configuration, a complex 3-D mathematical model made of frame elements was developed. Contribution of structural steel was considered explicitly to develop inelastic flexural and shear properties of all composite members. Then a 3D Modal Pushover Analysis (MPA) was implemented to evaluate and determine the adequacy of the existing structure. Unlike the FEMA 356 Nonlinear Static Procedure, the MPA procedure explicitly considers higher mode effects. In each direction, two modes were considered in the pushover analyses. Lateral force patterns for each mode were determined from the corresponding building mode shapes and included not only lateral forces but also torsional moments. The building was pushed to the target displacement for each mode calculated using a site-specific response spectrum. Plastic hinge rotations of each structural element for each mode were combined to evaluate and determine the building performance status. This paper discusses the use of the MPA procedure to show that the building meets the FEMA 356 Life Safety criteria for the BSE-1 earthquake.

Title: The N2 method for asymmetric buildings

Author: Fajfar, Peter; Marusi, Damjan; Perus, Iztok

Source: First European Conference on Earthquake Engineering and Seismology. 2006

Descriptors: Asymmetry; Three dimensional; Dynamics; Mathematical models; Spectral lines; Dynamic tests; Dynamic structural analysis; Amplification; Buildings; Stiffness; Nonlinear dynamics; Deformation

Abstract: The paper deals with the extension of the N2 method to asymmetric building structures, represented by a 3D structural model. The results of recent parametric studies suggest that in the majority of cases an upper limit for torsional effects can be estimated by a linear dynamic (spectral) analysis. Based on this observation, it is proposed that the results obtained by pushover analysis of a 3D structural model be combined with the results of a linear dynamic (spectral) analysis. The former results control the target displacements and the distribution of deformations along the height of the building, whereas the latter results define the torsional amplifications. In the paper, the extension of the N2 method is summarized and applied to several test examples. A variant of the bilinear idealization of the pushover curve with positive post-yield stiffness is also discussed. The results are compared with results of nonlinear dynamic

Title: Comparison of 2D and 3D pushover analysis with time history analysis in asymmetric buildings
Author: Forootan, F; Moghadam, A S
Source: First European Conference on Earthquake Engineering and Seismology. 2006
Descriptors: Displacement; Frames; Three dimensional; Coefficients; Asymmetry; Mathematical models; Two dimensional; Drift; Buildings; Seismic phenomena; Eccentricity; Eccentrics; Nonlinearity; Grounds; Center of mass; Earthquake construction; Design engineering; Structural steels; Stiffness

Abstract: In this paper the drift response of multistory asymmetric buildings are compared using 2D & 3D pushover and nonlinear time history analyses. The structure models are mass or stiffness eccentric multistory three dimensional steel moment resisting frames with bracing at the external frames. The structures are subjected to seven earthquake ground motions and the edge displacement ratio of the frames to the displacement of the center of mass is defined as a coefficient (?) to consider the effect of eccentricity and asymmetry. The target displacement of the structure and each individual frame is calculated by the displacement coefficient method and are multiplied by the (?) coefficient. 2D & 3D pushover analyses are conducted and the drift responses of the building in different frames are compared with the results of time history analyses. The result shows that the procedure of determining target displacement in pushover methods should be modified to provide conservative results, suitable for design purpose.

Title: Prediction of seismic response of multi-story unsymmetric frame buildings
Author: Fun, Kenji; Nakano, Yoshiaki
Source: Journal of Structural and Construction Engineering , no. 607, pp. 149-156. Sept. 2006
Descriptors: Mathematical models; Excitation; Buildings; Nonlinearity; Frames; Equivalence; Nonlinear dynamics; Seismic response

Abstract: A nonlinear static procedure for multi-story unsymmetric frame buildings subjected to bi-directional excitation is presented and its applicability is discussed. In this procedure, their responses are predicted through a pushover analysis of MDOF model considering the effect of bi-directional excitations and an estimation of the nonlinear response of equivalent SDOF model. The predicted results are compared with the nonlinear dynamic analysis results, and satisfactory predictions can be obtained by the proposed procedure.

Title: Displacement-based seismic assessment of torsionally irregular wall structures
Author: Ha, T H; Hong, S G
Source: First European Conference on Earthquake Engineering and Seismology. 2006
Descriptors: Displacement; Seismic phenomena; Seismic engineering; Walls; Eccentrics; Earthquake design; Marketing; Assessments; Design engineering; Stress concentration; Adaptive systems; Stiffness; Failure; Demand analysis; Demand; Stresses

Abstract: Torsional behavior of eccentric structures under seismic loading may cause the stress and/or stress concentration, which result in the failure of the structures in an unexpected manner. This study proposes how to draw capacity curves for translational displacement and rotation angle for eccentric wall systems based on mechanism-based approach. The seismic demands for displacement are assessed by so called displacement-based design approach and the maximum angle of rotation of system dependent on the elastic stiffness of system. To extend these concepts to the seismic displacement demand of multi-story eccentric wall systems effectively an adaptive pushover analysis are used to consider mode shapes of inelastic behavior.

Title: Earthquake response characteristics of equivalent sdof system reduced from one-story asymmetric buildings and prediction of higher mode responses
Author: Kuramoto, Hiroshi; Miura, Naoyuki; Hoshi, Tatsunori
Source: Journal of Structural and Construction Engineering , no. 606, pp. 123-130. Aug. 2006
Descriptors: Seismic phenomena; Earthquake construction; Dynamics; Asymmetry; Dynamical systems; Equivalence; Mathematical analysis; Buildings; Eccentricity; Dynamic tests; Degrees of freedom; Standards; Reinforced concrete; Law enforcement; Decomposition; Strength

Abstract: This paper shows two methods of reducing from a single-story asymmetric building under uni-directional earthquake motion to the equivalent single degree of freedom system (ESDOF) to improve the capacity spectrum method used in the calculation of response and limit strength provided in the Building Standard Law Enforcement Order of Japan. One is the static reducing method with mode-adaptive pushover analysis and the other is the dynamic reducing method using modal decomposition procedure together with earthquake response analysis. Applying both

methods for four types of single-story RC buildings with different eccentricity, the validity of the methods and the earthquake response characteristics of ESDOF system are examined. Based on the latter method, an evaluation method of the higher mode effect in story responses is also proposed.

Title: Seismic analysis of asymmetric building systems
Author: Lin, Jui-Liang; Tsai, Keh-Chyuan
Source: 100th Anniversary Earthquake Conference. 2006
Descriptors: Beams (structural); Seismic phenomena; Roofs; Earthquake construction; Torque; Force distribution; Eccentricity

Abstract: Under the push of modal inertia force distribution, a bifurcating characteristic of the pushover curves, representing the relationships of base shear versus roof translation and base torque versus roof rotation for asymmetric structures, is observed. A novel 2DOF modal stick with lump mass eccentrically placed at the end of the beam, connected with the column by a rotational spring, is conceived to simulate this characteristic. A two-story asymmetric building system has been analyzed by MPA procedure incorporating with the proposed 2DOF modal sticks (2DMPA) and conventional SDOF modal sticks (SDMPA), respectively. The analytical results are compared with those obtained by nonlinear RHA. It illustrates that the accuracy of rotational response time histories obtained by 2DMPA, taking the interaction of modal translation and rotation into consideration, is much better than those obtained by SDMPA.

Title: Simplified probabilistic seismic performance assessment of plan-asymmetric buildings
Author: Dolsek, Matjaz; Fajfar, Peter
Source: Earthquake Engineering & Structural Dynamics. Vol. 36, no. 13, pp. 2021-2041. 25 Oct. 2007
Descriptors: Seismic phenomena; Seismic engineering; Probability theory; Probabilistic methods; Earthquake construction; Performance assessment; Buildings; Dispersions; Dynamic tests; Three dimensional; Reinforced concrete; Reliability analysis; Frames; Dynamics; Spears; Viability

Abstract: A relatively simple approach for the probabilistic seismic performance assessment of plan-asymmetric structures has been proposed. It is based on the PEER probabilistic framework, in which the most demanding part, i.e. the incremental dynamic analysis (IDA), is replaced by the much simpler Incremental N2 (IN2) analysis. Predetermined default values for dispersion measures are needed for the practical implementation of this approach, which can be used for the analysis of plan-asymmetric buildings requiring a 3D structural model. In this paper, this simplified approach is summarized. Its application is demonstrated by means of an example of a three-storey reinforced concrete frame (SPEAR) building. The results are compared with the results of a more accurate approach, based on IDA. The test example demonstrates the viability of the proposed approach.

Title: Prediction of seismic response of multi-story unsymmetric frame buildings
Author: Fujii, K
Source: 8th Pacific Conference on Earthquake Engineering Conference Proceedings. 2007
Descriptors: Buildings; Nonlinearity; Mathematical models; Frames; Seismic response; Nonlinear dynamics; Excitation; Equivalence; Earthquake design; Grounds; Seismic design; Seismic phenomena; Seismic engineering; Earthquake construction; Uncertainty

Abstract: The estimation of nonlinear response of buildings subjected to a strong ground motion is a key issue for the rational seismic design of new buildings and the seismic evaluation of existing buildings. For this purpose, the nonlinear time-history analysis of Multi-Degree-Of-Freedom (MDOF) model might be one solution, but it is often too complicated whereas the results are not necessarily more reliable due to uncertainties involved in input data. To overcome such shortcomings, several researchers have developed Nonlinear Static Procedures (NSP). This approach is a combination of a nonlinear static (pushover) analysis of MDOF model and a nonlinear dynamic analysis of the equivalent Single-Degree-Of-Freedom (SDOF) model, and it would be a promising candidate as long as buildings oscillate predominantly in the fundamental mode. Although the simplified procedures have been more often applied to planar frame analyses, only a few investigations concerning the extension of the nonlinear static procedure for unsymmetric buildings under bi-directional excitation have been made. In this paper, a nonlinear static procedure for multi-story unsymmetric frame buildings subjected to bi-directional excitation is presented. The predicted results are compared with the nonlinear dynamic analysis results, and satisfactory predictions can be obtained by the proposed procedure.

Title: Simplified seismic analysis of asymmetric building systems
Author: Lin, Jui-Liang; Tsai, Keh-Chyuan
Source: Earthquake Engineering & Structural Dynamics. Vol. 36, no. 4, pp. 459-479. 10 Apr. 2007
Descriptors: Mathematical analysis; Asymmetry; Beams (structural); Bifurcations; Roofs; Translations; Seismic phenomena; Eccentricity; Shear; Columns (structural); Format; Nonlinearity; Seismic engineering; Modal response; Elastic constants; Civil engineering; Equations of motion; Accuracy; Springs (elastic)

Abstract: The paper reviews the uncoupled modal response history analysis (UMRHA) and modal pushover analysis (MPA) procedure in the analysis of asymmetric structures. From the pushover curves in ADRS format, showing the relationships of base shear versus roof translation and base torque versus roof rotation, a bifurcating characteristic of the pushover curves of an asymmetric structure is observed. A two-degree-of-freedom (2DOF) modal stick is constructed using lump mass eccentrically placed at the end of beam which is connected with the

column by a rotational spring. By converting the equation of motion of a whole structure into 2DOF modal equations, all of the elastic properties in the 2DOF modal sticks can be determined accurately. A mathematical proof is carried out to demonstrate that the 2DOF modal stick is consistent with the single-degree-of-freedom (SDOF) modal stick at elastic state. The bifurcating characteristic of modal pushover curves and the interaction of modal translation and rotation can be considered rationally by this 2DOF modal stick. In order to verify the effectiveness of this proposed 2DOF modal stick, a two-storey asymmetric building structure was analysed by the UMRHA procedure incorporating this novel 2DOF modal sticks (2DMPA) and conventional SDOF modal sticks (SDMPA), respectively. The analytical results are compared with those obtained by nonlinear response history analysis (RHA). It is illustrated that the accuracy of the rotational response histories obtained by 2DMPA is much better than those obtained by SDMPA. Consequently, the estimations of translational response histories on flexible side (FS) and stiff side (SS) of the building structure are also improved.

Title: An Overview Of Pushover Procedures for the Analysis of Buildings Susceptible to Torsional Behavior
Author: Baros, D K; Anagnostopoulos, S A
Source: 14th World Conference on Earthquake Engineering: Innovation Practice Safety. 2008
Descriptors: Earthquake design; Seismic phenomena; Earthquake construction; Nonlinear dynamics; Seismic engineering; Symmetry; Buildings; Dynamic tests; Asymmetry; Design engineering; Nonlinearity; Horizontal; Accuracy

Abstract: This paper compares results from pushover type static analyses of a 5-story building having one axis of symmetry with results obtained by nonlinear dynamic analyses, using semi-artificial earthquake motions generated to match the spectrum with which the building was designed. The analyses aim at evaluating the seismic capacity of the building. Results are also presented for 50% increased earthquake intensity. By considering only one-component motion along the axis of no symmetry, three non-linear static procedures are examined: the so called Modal Pushover Analysis, the N2 method as it was extended for asymmetric buildings and the FEMA recommended procedure for two variations of horizontal load pattern (modal and uniform). It was observed that all three methods, especially the Modal Pushover method, may lead to results in good agreement with those obtained by dynamic analyses for design level earthquakes. However, for increased earthquake intensities, when the behavior of the building is strongly affected by the yielding of structural components, the results differed significantly. In this case nonlinear dynamic analysis appears to be the only appropriate method for the evaluation of the seismic capacity of the building.

Title: A simple code-like formula for estimating the torsional effects on structures subjected to earthquake ground motion excitation
Author: Gasparini, G; Silvestri, S; Trombetti, T
Source: 14th World Conference on Earthquake Engineering: Innovation Practice Safety. 2008
Descriptors: Asymmetry; Mathematical models; Dynamics; Dynamical systems; Eccentricity; Excitation; Seismic phenomena; Estimating; Earthquake design; Mathematical analysis; Dynamic response; Seismic design; Exact solutions; Sensitivity analysis; Seismic response; Eccentrics; Grounds; Seismic engineering; Preliminary designs

Abstract: Plan asymmetric (eccentric) structures, characterized by non coincident centre of mass and centre of stiffness, when subjected to dynamic excitation, develop a coupled lateral-torsional response that may increase their local peak dynamic response. In order to effectively apply the performance-based design approach to seismic design, there is a growing need for code oriented methodologies aimed at predicting deformation parameter. In this respect, for plan asymmetric structures, estimating maximum displacements at different locations in plan, especially at the perimeter, requires an evaluation of the floor rotations. The ability to predict floor rotations can be also useful to extend simplified procedures of seismic design, such as push-over analyses, to plan irregular structures. In this paper, starting from a closed-form formulation identified in previous re-search works by the authors, an estimation of the maximum rotational response of one-storey asymmetric systems under seismic excitation is obtained and developed with respect to different applications. In detail: (1) a corrective eccentricity for the evaluation of the dynamic response of asymmetric systems through 'equivalent'static procedures is identified, (2) a sensitivity analysis is carried out upon the accidental eccentricity, (3) the increase in the peak local displacements due to the eccentricity is evaluated at the corner-point of the side of the system. The results provide useful insight into understanding the torsional behavior of asymmetric systems and may directly used for preliminary design and/or check of results obtained through three-dimensional finite-element modeling of the structural system.

Title: Seismic analysis of two-way asymmetric building systems under bi-directional seismic ground motions
Author: Lin, Jui-Liang; Tsai, Keh-Chyuan
Source: Earthquake Engineering & Structural Dynamics. Vol. 37, no. 2, pp. 305-328. Feb. 2008
Descriptors: Seismic phenomena; Asymmetry; Earthquake construction; Seismic engineering; Mathematical analysis; Roofs; Bifurcations; Translations; Earthquake engineering; Simulation; Modal response; Shears; Nonlinearity; Construction; Torque; Excitation

Abstract: An approximation approach of seismic analysis of two-way asymmetric building systems under bi-directional seismic ground motions is proposed. The procedures of uncoupled modal response history analysis (UMRHA) are extended to

two-way asymmetric buildings simultaneously excited by two horizontal components of ground motion. Constructing the relationships of two-way base shears versus two-way roof translations and base torque versus roof rotation in ADRS format for a two-way asymmetric building, each modal pushover curve bifurcates into three curves in an inelastic state. A three-degree-of-freedom (3DOF) modal stick is developed to simulate the modal pushover curve with the stated bifurcating characteristic. It requires the calculation of the synthetic earthquake and angle . It is confirmed that the 3DOF modal stick is consistent with single-degree-of-freedom modal stick in an elastic state. A two-way asymmetric three-story building was analyzed by UMRHA procedure incorporating the proposed 3DOF modal sticks. The analytical results are compared with those obtained from nonlinear response history analysis. It is shown that the 3DOF modal sticks are more rational and effective in dealing with the assessment of two-way asymmetric building systems under two-directional seismic ground motions.

Title: A simplified pushover method for evaluating the seismic demand in asymmetric-plan multi-storey buildings

Author: Lucchini, A; Monti, G; Kunnath, S

Source: 14th World Conference on Earthquake Engineering: Innovation Practice Safety. 2008

Descriptor: Buildings; Seismic phenomena; Seismic engineering; Earthquake construction; Asymmetry; Marketing; Demand analysis; Classification; Grounds; Joining; Stiffness; Nonlinear dynamics; Translating; Elastic constants; Excitation; Strength; Demand

Abstract: Buildings with in-plan non symmetric mass and stiffness distributions are characterized by a seismic behavior that is commonly defined as irregular. The reason for such classification is twofold. First, when excited by a lateral ground motion, such buildings instead of simply translating also exhibit torsional behavior. This is basically due to the translational-rotational coupling of the modes. The other reason is that the response of asymmetric-plan buildings usually changes when transitioning from elastic to inelastic behavior. In particular, depending on the elastic properties of the system, on the in-plan distribution of the resisting elements strengths and on the level of the seismic action intensity, the torsional effects may either increase or decrease. Consequently, the seismic demand in such buildings cannot be evaluated through simple conventional analysis procedures, commonly adopted for regular structures. The objective of the present paper is to propose a new pushover method that explicitly takes into account the torsional behavior of asymmetric-plan buildings. The effectiveness of the method is evaluated by comparing the seismic demand of selected case studies with that obtained through both nonlinear dynamic analyses and other pushover methods from literature.

Title: Extension of N2 method to plan irregular buildings considering accidental eccentricity

Author: Magliulo, Gennaro; Maddaloni, Giuseppe; Cosenza, Edoardo

Source: 14th World Conference on Earthquake Engineering: Innovation Practice Safety. 2008

Descriptors: Seismic phenomena; Eccentricity; Buildings; Dynamic tests; Dynamics; Accidents; Frames; Nonlinear dynamics; Computer programs; Demand; Horizontal; Drift; Seismic engineering; C (programming language); Linear analysis; Earthquake construction; Marketing; Earthquakes

Abstract: The paper deals with the topic of analyses performed according to modern code provisions, in particular Eurocode 8 (EC8) rules. Elastic, non linear static and non linear dynamic analyses of a plan irregular multi-storey r/c frame building designed according to Eurocode 2 (EC2) and EC8 provisions are carried out. The elastic analysis is performed by the computer program SAP2000, while the non linear analyses by CANNY99. A set of 7 earthquakes (each considering both the horizontal components), fully satisfying the EC8 provisions, are used as input of non linear dynamic analyses. The problem of extension of N2 method to plan irregular buildings, which makes up for the underestimate of seismic demand on stiff side, is focused: three methods, which take into account the accidental eccentricity provided by modern codes, are proposed. The results, in terms of pushover curves, frame top displacements and interstorey drifts, are compared with ones obtained by nonlinear dynamic time-history analyses. Non linear static analyses are carried out both applying the 'modal' and 'uniform' force pattern. The 'orthogonal effects', evaluated by SRSS rule, result to be negligible.

Title: Predicting inelastic torsional response with the inclusion of dynamic rotational stiffness

Author: Pettinga, Didier; Christopoulos, Constantin; Pampanin, Stefano

Source: 14th World Conference on Earthquake Engineering: Innovation Practice Safety. 2008

Descriptors: Rotational; Asymmetry; Inertia; Dynamics; Constraints; Diaphragms; Eccentricity; Derivation; Mathematical analysis; Assessments; Representations; Seismic design; Estimates; Buildings; Inclusions; Stiffness; Estimating

Abstract: Inherent to the development of performance-based seismic design and assessment techniques, is the need to adequately predict the inelastic displacements of structures. To date, research has provided a range of prediction approaches based on 2 and 3-dimensional representations. While the 2-D response can often be adequately assessed for design using simplified hand-predictions, the 3-D cases have tended to rely on push-over techniques that do not capture the effects of the rotational inertia on the diaphragm twist that develops in asymmetric structures. This paper presents the basis of a new approach for estimating, by hand calculation, the expected maximum torsional response of buildings with in-plan asymmetry. Fundamental to a prediction procedure is the quantification of the apparent twist restraint that is a result of the rotational mass inertia of the floor diaphragm. The derivation of this dynamic torsional restraint is presented here. For a series of simple structures subjected to

sinusoidal pulse inputs, comparative results between recorded inelastic time-history and predicted response are presented. For realistic eccentricity cases the predictions are shown to provide sufficiently accurate estimates of response for use in design.

Title: Determination of equivalent sdof characteristics of 3D dual RC structures
Author: Vuran, E; Bale, I E; Crowley, H; Pinho, R
Source: 14th World Conference on Earthquake Engineering: Innovation Practice Safety. 2008
Descriptors: Buildings; Reinforced concrete; Three dimensional; Displacement; Assessments; Representations; Mathematical models; Equivalence; Irregularities; Deformation effects; Computer programs; Nonlinear dynamics; Demand; Raw materials; Nonlinearity; Software; Mathematical analysis; Marketing; Uncertainty

Abstract: The recent drive for the use of a single-degree-of-freedom representation in displacement-based design and assessment of 3D reinforced concrete (RC) structures has significantly increased the demand for the determination of equivalent SDOF characteristics of such buildings. Nonlinear static analyses are frequently used to describe the response of a structure with reduced computational effort with respect to nonlinear dynamic analyses. The response parameters of interest include the mechanical SDOF characteristics such as yield period, deformed shape etc. However, the inherent irregularities and uncertainties of existing RC buildings render the SDOF representation rather difficult and more demanding. The main focus of this study is on existing dual (frame-wall) structures; 4 case study RC buildings from the existing Turkish building stock have been modelled in 3D using a fibre-based finite elements software. Displacement-based adaptive pushover (DAP) analyses have been conducted in both directions of the buildings. The DAP capacity curves have been used to extract the yield periods, deformed shapes, and effective heights of the case study buildings in order to define the SDOF characteristics of dual structures for use in displacement-based assessment.

Title: An alternative approach for assessing eccentricities in asymmetric multistory buildings. 2. Inelastic systems
Author: Georgoussis, George K
Source: Structural Design of Tall and Special Buildings. Vol. 18, no. 1, pp. 81-103. Feb. 2009
Descriptors: Eccentricity; Buildings; Grounds; Nonlinearity; Mathematical models; Equivalence; Seismic phenomena; Elastoplasticity; Dynamical systems; Vibration; Nonlinear dynamics; Walls; Shears; Elastic constants; Asymmetry; Excitation; Construction; Earthquake construction; Methodology

Abstract: The approximate method, presented in the companion paper, for assessing modal eccentricities of elastic multistory buildings with simple eccentricity is extended in systems composed by elastoplastic resisting bents. Following the technique of the aforementioned paper for computing modal properties of such

buildings by means of an equivalent single-story system composed of elastic elements, modal capacity curves of these systems may also be drawn when the resisting elements are defined by a bilinear force-displacement (characteristic) curve. The procedure for constructing element-characteristic curves is based on the methodology presented by the author in an earlier paper, and modal capacity curves of the equivalent single-story system may be drawn by performing a non-linear pushover analysis using the inertia force eccentricity of each mode of this system. Therefore, base shears and their eccentricities for the first two modes of vibration of multistory inelastic buildings can be determined as in real one-story non-linear systems. The method is illustrated in a 10-story partial symmetric building, having along the direction of the ground motion three identical, inelastic, coupled wall bents. The structure is analyzed for a strong ground motion, equal to 1*5 X El Centro earthquake excitation, and the results are compared with those obtained from a step-by-step non-linear time history analysis of the discrete member model.

H.3.2 Weak Stories

Title: Computing story drift demands for RC building structures during the 1999 Chi-Chi Taiwan earthquake

Author: Tsai, K C; Weng, Yuan-Tao

Source: The Third U.S.-Japan Workshop on Performance-Based Earthquake Engineering Methodology for Reinforced Concrete Building Structures, 16-18 August 2001, Seattle, Washington , pp. 119-134. 2002

Descriptors: Drift; Marketing; Demand analysis; Earthquake engineering; Reinforced concrete; Earthquake damage; Seismic phenomena; Earthquake construction; Computation; Construction specifications; Pedestrians; Stiffness; Construction; Nonlinear dynamics; Mathematical analysis; Spectra; Statics; Demand; Spectrum analysis

Abstract: The September 21, 1999, Chi-Chi, Taiwan, earthquake caused a very significant number of building collapses or damage of various degrees. Many collapsed buildings had a pedestrian corridor and an open front at the ground floor. Using a modified modal participation factor and a generalized shape function computed from a nonlinear pushover analysis, story drift demands imposed on soft first story building systems are studied in this paper. Generalized shape functions are constructed from the nonlinear static pushover analysis of shear buildings having specific distributions of story stiffness and strength. Nonlinear response spectrum analyses were performed on the ground acceleration recorded from 62 sites in the Taichung region. Analytical results indicate that soft first story buildings are likely to have story drift demands significantly greater than regular buildings of short fundamental periods. Results of the nonlinear dynamic analysis of a six-story structure indicate that the maximum story drift demand can be satisfactorily predicted by the story spectral drift constructed from the generalized shape functions.

Title: A simplified pushover analysis of existing low-rise RC buildings
Author: Lee, Hung-Jen; Hwang, Shyh-Jiann
Source: Proceedings of the International Symposium on Earthquake Engineering Commemorating Tenth Anniversary of the 1995 Kobe Earthquake (ISEE Kobe 2005). 2005
Descriptors: Seismic phenomena; Buildings; Earthquake construction; Reinforced concrete; Ultimate tensile strength; Failure modes

Abstract: Several new standards for the seismic evaluation of existing buildings have been developed around the world. Since construction practice is influenced by culture and tradition, the seismic evaluation methods vary from region to region. In the post-earthquake reconnaissance of 1999 Chi-Chi Earthquake, the majority of low-rise reinforced concrete buildings in Taiwan were damaged in a common failure mode of weak-column and strong-beam. According to the observation of shear-building behavior, a simplified nonlinear static pushover method is proposed to evaluate low-rise shear buildings in which the capacity of an existing building is estimated by superposing the load-displacement response of vertical members in the damage story. The proposed method is verified with data of laboratory testing. Observations of shaking table tests of two ductile model buildings are reviewed and compared to the proposed seismic evaluation method. Reasonable agreement is found in the prediction of ultimate strengths, displacements, and failure modes.

H.3.3 Vertical Irregularities

Title: Seismic response of steel frames with symmetric setback
Author: Osman, A. M.
Source: Seventh U.S. National Conference on Earthquake Engineering (7NCEE): Theme: Urban Earthquake Risk [electronic resource]; 10 pages pp. 2002
Descriptors: Multistory steel moment-resisting frames; nonlinear static pushover analysis; Setback structures; linear response; Office buildings; dynamic properties; Egypt; building codes; Al-Fayoum area

Abstract: An analytical study was conducted to investigate the seismic response of steel moment-resisting frames with symmetric setbacks. Ten 8-story buildings with uniform and setback profiles were designed and analysed for both static (pushover) and earthquake forces. The results of the analyses including the story shear, story displacements, overall ductility and over-strength factors were presented and discussed. Also, the implications of these findings on the design of frames with setbacks were summarized.

Title: Design of vertically irregular R/C frames
Author: Iorio, Paolo; et al.
Source: Concrete Structures in Seismic Regions: FIB 2003 Symposium [Proceedings] [electronic resource] , pp. 12 pages. 2003

Descriptors: Frames; Seismic engineering; Seismic phenomena; Stiffness; Dynamic tests; Earthquake design; Earthquake damage; Regularity; Nonlinear dynamics; Statics; Criteria; Earthquake construction; Resources; Reinforced concrete; Concrete construction; Seismic response; Buildings; Dissipation; Reinforcing steels

Abstract: The presence of irregularities in the vertical distribution of some parameters (i.e., mass, stiffness, strength) which characterise the seismic behaviour of reinforced concrete buildings can cause the concentration of the damage at a certain level and, consequently, undesirable types of dissipation mechanisms. This is already acknowledged by all the international seismic codes; they provide criteria which distinguish vertically regular from irregular structures. In the latter case, specific rules are imposed in order to mitigate the effects of vertical irregularity. In this paper, results which follow those shown in two studies by Magliulo, Ramasco and Realfonzo (2002) and concerning mass, stiffness and strength vertical irregularities in plane frames are presented. Indeed, many of the analysed frames are the same with respect to those presented in both of the studies by Magliulo, Ramasco and Realfonzo, but the analyses that are carried out are nonlinear pushover instead of dynamic. As for other studies on the same topic, the evaluation of the seismic response regularity is based on the comparison between the nonlinear response of regular frames, assumed as reference, and the nonlinear response of frames obtained by the regular ones modifying the vertical distribution either of mass or of stiffness or strength. The nonlinear static analysis results are discussed and the frame regularity judgment obtained by them is compared to the estimate gained by the vertical irregularity criteria of some international codes. Finally, some considerations based on the comparison between the results obtained by the presented nonlinear static analyses and the ones obtained by the dynamic analyses discussed in one of the 2002 studies by Magliulo, Ramasco and Realfonzo are withdrawn.

Title: Evaluation of modal and FEMA pushover analyses: vertically 'regular' and irregular generic frames.
Author: Chopra, A.K.; Chintanapakdee, C.
Source: Earthquake Spectra. Vol. 20, no. 1, pp. 255-271. Feb. 2004
Descriptors: Frames; Seismic engineering; Buildings; Earthquake construction

Abstract: The accuracy of the nonlinear static procedure (NSP) using the lateral force distributions specified in the FEMA-356 document (ASCE 2000), now standard in engineering practice, and the recently developed dynamics-based modal pushover analysis (MPA) procedure (Chopra and Goel 2002) was evaluated in the companion paper by Goel and Chopra (2003). The median seismic demands were computed by these procedures for six SAC buildings, each analyzed for 20 ground motions, and compared with 'exact' results obtained from nonlinear response history analysis (RHA). This paper complements the companion paper by investigating the higher-mode contributions to seismic demands and evaluating the two approximate procedures for a wider range of buildings and ground motions. The generic frames

considered include 30 'regular' frames covering six different heights: 3, 6, 9, 12, 15, and 18 stories, each designed for five different strength levels; and 24, 12-story-high irregular frames representing three types of irregularity - stiffness, strength, stiffness-and-strength irregularity - introduced at eight different locations/regions along the height. For an ensemble of 20 ground motions, median and dispersion values of the story-drift demands using an approximate method (FEMA-356 or MPA) and nonlinear-RHA are computed and the bias and dispersion in the approximate procedure is documented.

Title: Adaptive Modal Combination Procedure for Predicting Seismic Response of Vertically Irregular Structural Systems
Author: Kalkan, E; Kunnath, S K
Source: 100th Anniversary Earthquake Conference. 2006
Descriptors: Adaptive structures; Seismic phenomena; Earthquake construction; Reinforced concrete; Approximation; Nonlinear dynamics

Abstract: A new direct multi-modal pushover procedure called the Adaptive Modal Combination (AMC) procedure has been developed to estimate seismic demands in building structures. The proposed methodology is an attempt to synthesize concepts from three well-known nonlinear static methods. The basic ideas that are integrated into the procedure include: the concept of a performance or target point introduced in the Capacity Spectrum Method, recognition of the variation in the dynamic characteristics of the structural system as implemented in adaptive pushover schemes, and the modal decomposition of a multi-degree-of-freedom as suggested in the Modal Pushover Analysis (MPA). A novel feature of the AMC procedure is that the target displacement is updated dynamically during the analysis by incorporating energy based modal capacity curves in conjunction with inelastic response spectra. Hence it eliminates the need to approximate the target displacement prior to commencing the pushover analysis. The methodology has been validated for regular steel and RC moment frame buildings. In this paper, the proposed scheme is further validated for a range of buildings with vertical irregularities. It is demonstrated that the AMC procedure can reasonably estimate critical demand parameters such as interstory drift ratio for impulsive near-fault forward directivity records, and consequently provides a reliable tool for performance assessment of building structures.

Title: Seismic performance of R/C plane frames irregular in elevation
Author: Athanassiadou, C J
Source: Engineering Structures. Vol. 30, no. 5, pp. 1250-1261. May 2008
Descriptors: Frames; Seismic phenomena; Earthquake construction; Elevation; Seismic engineering; Buildings; Earthquake design; Ductility; Planes; Dynamic tests; Design engineering; Reinforced concrete; Dynamics; Materials selection; Irregularities; Civil engineering; Acceleration

Abstract: The paper addresses multistorey reinforced concrete (R/C) frame buildings, irregular in elevation. Two ten-storey two-dimensional plane frames with two and four large setbacks in the upper floors respectively, as well as a third one, regular in elevation, have been designed to the provisions of the 2004 Eurocode 8 (EC8) for the high (DCH) and medium (DCM) ductility classes, and the same peak ground acceleration (PGA) and material characteristics. All frames have been subjected to both inelastic static pushover analysis and inelastic dynamic time-history analysis for selected input motions. The assessment of the seismic performance is based on both global and local criteria. It is concluded that the effect of the ductility class on the cost of buildings is negligible, while the seismic performance of all irregular frames appears to be equally satisfactory, not inferior to (and in some cases superior than) that of the regular ones, even for motions twice as strong as the design earthquake. As expected, DCM frames are found to be stronger and less ductile than the corresponding DCH ones. The overstrength of the irregular frames is found to be similar to that of the regular ones, while DCH frames are found to dispose higher overstrength than DCM ones. Pushover analysis seems to underestimate the response quantities in the upper floors of the irregular frames.

Title: Evaluation of Conventional and Advanced Pushover Procedures for Regular And Irregular RC Frames
Author: Diotallevi, P P; Landis, L; Pollio, B
Source: 14th World Conference on Earthquake Engineering: Innovation Practice Safety. 2008
Descriptors: Frames; Seismic phenomena; Reinforced concrete; Elevation; Seismic engineering; Regularity; Displacement; Marketing; Estimates; Mathematical models; Nonlinear dynamics; Demand

Abstract: This paper describes an investigation on the effectiveness of several conventional, multi-modal and adaptive pushover procedures. An extensive numerical study was performed considering eight RC frames characterized by a variable number of storeys and different properties in terms of regularity in elevation. The results of pushover analyses were compared with those of non-linear dynamic analyses, which were carried out considering different earthquake records and increasing values of earthquake intensity. The study was performed with reference to base shear-top displacement curves and to different storey response parameters. The obtained results allowed a direct comparison between pushover procedures, which in general were able to give a fairly good estimate of seismic demand with a tendency to better results for lower frames. The advanced procedures, in particular the multi-modal pushover, produced an improvement of results, more evident for irregular frames.

Title: Evaluation of FEMA440 Equivalent Nonlinear Static Seismic Analysis For Irregular Steel Moment Resisting Frames
Author: Momtahn, Ali; Banan, Mahmoud-Reza; Banan, Mohammad-Reza

Source: 14th World Conference on Earthquake Engineering: Innovation Practice Safety. 2008

Descriptors: Mathematical models; Frames; Nonlinearity; Displacement; Equivalence; Seismic phenomena; Coefficients; Seismic engineering; Earthquake design; Earthquake construction; Structural steels; Roofs; Estimating; Irregularities; Nonlinear dynamics; Shear; Drift; Iron and steel industry; Grounds

Abstract: It is well established that for seismic evaluation, design, and retrofitting of building structures, a simplified design-oriented modeling procedure is more practical. One of well-established procedures is the equivalent nonlinear static procedure summarized in FEMA356 based on nonlinear static pushover analysis using the target displacement predicted by the Coefficient Method (CM). CM utilizes a displacement modification procedure in which several empirically derived factors are used to modify the response of a single-degree-of freedom model of the structure assuming that it remains elastic. FEMA440 has suggested some recommendations for improving the performance of CM leading to a Modified Coefficient Method (MCM). This paper presents a detailed investigation on performance of FEMA440 MCM for estimating frame maximum roof displacement, base shear, and median story drifts of steel moment resisting frames with irregularities in elevation. Results of nonlinear dynamic analyses of 22 irregular frames subjected to a family of 14 ground motions and nonlinear equivalent static analyses of all frames up to the target roof displacement computed by MCM are compared to evaluate the accuracy and conservatism of FEMA440 MCM.

H.3.4 Diaphragm Flexibility

Title: Seismic response of low-rise masonry buildings with flexible roof diaphragms

Author: Cohen, G. L.; et al.

Source: Seventh U.S. National Conference on Earthquake Engineering (7NCEE): Theme: Urban Earthquake Risk [electronic resource]; 10 pages pp. 2002

Descriptors: Lowrise reinforced masonry structures; displacements (structural); Shaking table tests; similitude theory; Reinforced masonry shear walls; linear analysis; Central United States; warehouses

Abstract: The study described compares the responses from shaking table testing and analytical predictions, evaluated in the context of geometric scaling, to provide a coherent description of the seismic response of lowrise masonry buildings with flexible roof diaphragms. Two half-scale lowrise reinforced masonry buildings with flexible roof diaphragms are subjected to carefully selected earthquake ground motions on the Tri-axial Earthquake and Shock Simulator at the U.S. Army Construction Engineering Research Laboratory, Engineer Research and Development Center. Geometric scaling analysis relates response and damage of the half-scale specimens to those of the full-scale prototype structures. In contrast to what is usually assumed in design, the half-scale specimens do not behave as systems with a single

degree-of-freedom associated with the in-plane response of the shear walls. Calculated responses from linear elastic finite element models are compared to measured responses. Linear elastic modeling is simplified to a generalized 2-DOF idealization. Response-spectrum analysis of such an idealization is accurate and justified for prediction of dynamic response of the half-scale specimens and the corresponding full-scale prototypes.

Title: Displacement-Based Design of Concrete Tilt-Up Frames Accounting for Flexible Diaphragms
Author: Adebar, Perry; Guan, Zhao; Elwood, Kenneth
Source: 13 WCEE: 13th World Conference on Earthquake Engineering Conference Proceedings. 2004
Descriptors: Diaphragms; Frames; Roofs; Concretes; Walls; Earthquake design; Seismic phenomena

Abstract: This paper presents a simplified procedure to estimate the amplification of inelastic drifts in concrete tiltup frames due to steel deck roof diaphragms designed to remain elastic during the design earthquake. The procedure assumes that roof diaphragm displacements relative to the ground are independent of wall strength, while roof diaphragm displacements relative to the walls are proportional to wall strength. Results obtained using this simplified procedure are in good agreement with results obtained from nonlinear dynamic analysis. A rational basis to decide when concrete tilt-up frames must meet seismic design requirements for cast-in-place frames is also presented.

Title: Pushover Analysis of Reinforced Concrete Buildings with Flexible Floor Diaphragm
Author: Deb, Sajal Kanti; Kumar, Geddam Vijaya
Source: First European Conference on Earthquake Engineering and Seismology. 2006
Descriptors: Diaphragms; Buildings; Flexibility; Grounds; Seismic phenomena; Reinforced concrete; Dynamic structural analysis; Earthquake construction; Estimates; Frames; Nonlinearity; Columns (structural); Nonlinear dynamics; Lateral loads

Abstract: The pushover analysis is a non-linear static procedure that can be used to estimate the dynamic needs imposed on a structure by earthquake ground motions. Assumption of floor diaphragm as rigid holds good for most of the buildings, but several other building configurations may exhibit significant floor flexibility. However, the pushover analysis of such buildings has not been addressed in the literature. In this paper, pushover analysis procedure for buildings with flexible floor diaphragm has been presented. The prime focus of this paper is to investigate the difference in the results of pushover analysis based on the rigid floor idealization and flexible floor idealization of a sample building with flexible floor for three different lateral load patterns. Results indicate that the frame displacements have been reduced

for flexible floor diaphragm idealization. A considerable change in profile of column moments is observed for flexible floor

Title: Interstory drift estimates for low-rise flexible diaphragm structures
Author: Lee, Ho Jung; Aschheim, Mark A; Kuchma, Daniel
Source: Engineering Structures. Vol. 29, no. 7, pp. 1375-1397. July 2007
Descriptors: Drift; Diaphragms; Mathematical analysis; Design engineering; Shear; Seismic phenomena; Principal component analysis; Modulus of rupture in bending; Walls; Demand; Gravitation; Seismic engineering; Dynamic response; Earthquake design; Framing; Flexural strength; Preliminary designs; Marketing; Safety

Abstract: Current seismic codes allow regular structures to be designed using an equivalent lateral force procedure if the interstory drifts calculated on the basis of the design lateral forces are less than the specified allowable story drifts. While this approach assures that structures have some minimum lateral stiffness, calculated interstory drifts may be significantly less than actual peak interstory drifts particularly for structures with flexible diaphragms. Consequently, the gravity framing systems in such structures may be exposed to interstory drift demands several times greater than would be expected on the basis of design calculations, calling into question their perceived safety. In this paper, a simple method to more accurately estimate peak interstory drifts that accounts for higher mode effects is described for low-rise perimeter shear wall structures having flexible diaphragms or even for stiff diaphragms. The proposed method is based on the principal modes obtained from a principal components analysis (PCA) of computed dynamic response data. The method, applicable to both elastic and inelastic response, considers the shape of the design response spectrum and gives interstory drift estimates for use for preliminary design of the structure as well as for use with the approaches proposed in the companion paper for determining the required diaphragm shear and flexural strengths.

Title: Investigation of Floor Rigidity Effect on Behavior of Steel Braced Frames
Author: Zaregarizi, Shahabodin
Source: 14th World Conference on Earthquake Engineering: Innovation Practice Safety. 2008
Descriptors: Rigidity; Diaphragms; Frames; Structural steels; Safes; Seismic phenomena; Shear; Design of buildings; Braced; Iron and steel industry; Steel making; Degrees of freedom; Seismic engineering; Earthquake design; Mathematical analysis; Dynamic tests; Stress concentration; Flexibility; Dynamics

Abstract: One of the most important assumptions for analysis and design of building against lateral force is rigidity of floor diaphragms. The rigid floor assumption distributes forces between lateral resistant elements according to the proportion of elements rigidity. In addition, this assumption decreases the degrees of freedom and makes the analysis simpler. But the application of this assumption to the seismic

analysis of building structures may be not valid in many cases and make the design not safe and economical. In this study, to investigate the effect of floor rigidity, one type of steel frame including simple frame with X-braces was considered. The linear static analysis and spectral dynamic analysis both was used to investigate the flexibility of diaphragm in each case via Variables such as thickness of diaphragm, plan dimensions ratio and number of stories. This study shows that the lower three stories of the building are sensitive to the amount of floor rigidity. So some part of structure may be subjected to increased stress due to shear force redistribution caused by the large in-plane deformation of floor diaphragms.

H.3.5 Base-Isolated Buildings

Title: Energy-based seismic design method for passively controlled structural systems
Author: Fuentes, F; Kabeyasawa, T
Source: Workshop on Smart Structural Systems organized for U.S.-Japan Cooperative Research Programs on Smart Structural Systems (Auto-adaptive Media) and Urban Earthquake Disaster Mitigation [proceedings] , pp. page 383-396. 2002
Descriptors: Seismic phenomena; Earthquake dampers; Dynamics; Energy dissipation

Abstract: A simple energy-based analysis and design method for passively controlled single-degree-of-freedom systems was developed. First, energy ratios based on the relationship between energy dissipation characteristics of passive dampers and the earthquake response spectra was derived and used to estimate the required energy dissipation capacities of dampers for a given ground motion and target ductility ratio. Second, considering frame-damper interaction between single degree-of-freedom systems with different damper types, equivalent linear system equations based on frame-damper stiffness and strength property ratios were derived. Using both the damper energy response ratios and the frame-damper property ratios, a method for estimating seismic responses and determining required parameters for damper design, applicable to various types of damper devices, was shown. Maximum deformation estimates using the equivalent linear systems show good correspondence with time-history analysis responses for the bilinear Takeda frame with hysteretic damper systems investigated. Moreover, an example of damper parameters determined for a given ground motion and ductility level show good correspondence with results of the dynamic analysis of the system.

Title: Capacity-diagram method of base-isolated structures
Author: Zhou, Yun; An, Yu; Liang, Xing-wen
Source: World Earthquake Engineering. Vol. 18, no. 1, pp. 46-50. 2002
Descriptors: Mathematical models; Dynamic tests; Indexes; Stress concentration; Marketing; Dynamics; Statics; Demand; Earthquake engineering

Abstract: The capacity-diagram method is a simple and effective nonlinear static method for evaluating the performance of structures. This paper applies the method

to the evaluation of the performance of base-isolated structures. Characteristics of the base-isolated structures are fully considered. Questions concerning a mechanical model, the distribution of lateral forces, the establishment of a demand diagram, and evaluated indexes are presented. A factual example is presented, and a dynamic analysis method is used to test it, proving that it is credible.

Title: A Comparative Study on Static Push-Over and Time-History Analysis Methods In Base Isolated Buildings
Author: Doudoumis, Nikolaos I; Kotanidis, Christos; Doudoumis, Ioannis N
Source: First European Conference on Earthquake Engineering and Seismology. 2006
Descriptors: Buildings; Mathematical analysis; Isolation systems; Superstructures; Seismic phenomena; Categories; Shear; Nonlinear dynamics; Bearings; Nonlinearity; Dynamic structural analysis; Seismic engineering; Earthquake design; Accuracy; Displacement; Earthquake construction; Design engineering; Hinges; Roofs

Abstract: For the analysis and design of seismic isolated buildings with an expected inelastic behaviour of the superstructure, two analysis methods are generally acceptable today by the Code Provisions: (a) the dynamic non-linear time-history analysis, that is permitted for all structures and (b) the static push-over analysis which can be applied to a broad category of buildings that meet certain requirements. In the current paper, a specific analytical case study is presented, where these methods are comparatively used for the calculation of certain response quantities of a multi-storey concrete building with a base isolation system consisting of Lead Rubber Bearings. The purpose of the paper is to clarify certain details which are essential for the application of these methods and to study similarities and differences in their results. The results showed that there is a very good agreement between the values of the maximum base shear of the building, its corresponding maximum roof displacement and the total number of plastic hinges formed at the superstructure during the time-history analyses, with the respective values given by the pushover analysis. All these confirm in principal the FEMA Provisions that accept the pushover method for this particular base isolation system, however there are still several open issues that must be further studied.

Title: Response Analysis Study of a Base-Isolated Building Based on Seismic Codes Worldwide
Author: Feng, Demin; Chan, Tian-Chyuan; Wang, Shuguang; Chen, Hsi-Yun; Chang, Yaw-Nan
Source: ICEE 2006: 4th International Conference on Earthquake Engineering. 2006
Descriptors: Building codes; Equivalence; Linear analysis; Earthquake design; Design engineering; Seismic response; Seismic phenomena; Seismic engineering; Earthquake construction; Superstructures; Dynamic response; Reinforced concrete; Bearings; Deformation; Shear; Reduction; Coefficients

Abstract: The procedures to do response analysis of a seismically isolated building are summarized based on the building codes of Japan, China, the USA, Italy and Taiwan. While a dynamic response analysis method is recommended in all five building codes, a simplified design procedure based on equivalent linear analysis is also permitted under limited conditions. Subsequently, a typical 14-story reinforced concrete building, isolated with lead-rubber bearings is analyzed using each of the five building codes. The average response values are taken as design values to compare with the results by the equivalent linear analysis method. The deformation of the isolation level and the base shear force coefficient of the superstructure are compared. Finally, the response reduction factor defined in the Japanese code is applied to the other four building codes to improve the accuracy of equivalent linear analysis results.

Title: Simplified methods for design of base-isolated structures in the long-period high-damping range
Author: Weitzmann, Ruediger; Ohsaki, Makoto; Nakashima, Masayoshi
Source: Earthquake Engineering & Structural Dynamics. Vol. 35, no. 4, pp. 497-515. 10 Apr. 2006
Descriptors: Mathematical models; Damping; Spectra; Equivalence; Design engineering; Adjustment; Acceleration; Statistical tests; Earthquake engineering; Seismic phenomena; Viscous damping; Transforms; Nonlinearity; Dynamics; Trends; Spectrum analysis

Abstract: A recent trend in the design of base-isolated structures is the extension of the natural period and the incorporation of high damping. This paper shows that the existing simplified methods perform less accurately in this field of application, mainly due to inappropriate use of spectral data and insufficiently adjusted equivalent models. The paper proposes new period-dependent concepts to reduce pseudo-acceleration spectra and to transform these values into total accelerations with respect to the viscous damping ratio. The model of equivalent damping is adjusted to reflect several period-dependent effects. The estimation of the accelerations in MDOF systems is based on additional period shifts. All modifications are derived for a simplified linear approach based on eigenforms, and a non-linear approach based on pushover and capacity spectrum analysis. To illustrate observed problems and to demonstrate the capabilities of the proposed concepts, example structures are studied in detail. Furthermore, intensive statistical tests prove the effectiveness of the modifications in a wide parameter range and show considerable improvements over traditional approaches.

Title : Simplified Analysis for Preliminary Design of Base-Isolated Structures
Author: Ramirez, C M; Miranda, E
Source: Proceedings of the 2007 Structures Congress, Proceedings of the Research Frontiers Sessions of the 2007 Structures Congress, and Proceedings of the 2007 Forensic Engineering Track of the 2007 Structures Congress; Long Beach, CA; USA; 16-19 May 2007. 2007

Descriptors: Isolation; Structural design; Base isolation; Mathematical models; Design engineering; Preliminary designs; Approximation; Nonlinear dynamics; Miranda; Seismic phenomena; Dynamical systems; Bearing; Earthquake construction; Marketing; Earthquake design; Acceleration; Nonlinearity; Isolators; Computation

Abstract: Current building codes require nonlinear dynamic analyses to design most base-isolated structures. This necessitates extensively detailed and well-defined structural models that require heavy computational effort. Unfortunately, many decisions regarding the building's lateral force resisting system are made during the early stages of design, when much of the structure is not fully, well-defined. The benefits of base-isolation may not be as apparent if practicing engineers are not able to effectively approximate the building's performance based on limited knowledge of its final design. Even under circumstances where the structural engineers have enough information to construct elaborate analytical models, most engineering firms reserve the time and the financial resources needed to create such models for the latter stages of design and not for proposing design alternatives that may never be implemented. Furthermore, there are different types of isolation bearing systems currently available that can perform very differently from one another. Decisions regarding the type of bearings are also usually made during preliminary design and require substantial resources and computational effort to make a comparison that would yield the best isolation alternative. A simplified method of analysis that provides reasonably accurate results, based on limited knowledge of the structure, would facilitate these types of decisions during preliminary design. The 1997 Uniform Building Code currently provides a statically equivalent method of analysis that is often used for preliminary design; however, this procedure is very limited and has many shortcomings. The static procedure does not capture the dynamic effects of structural response when subjected to seismic ground motions. It oversimplifies the response of the superstructure (the structural system above the isolators) by assuming a simplified and often unrealistic lateral force distribution. The analysis only considers the first mode response and ignores higher mode effects that contribute to acceleration demands. There is no procedure for estimating acceleration demands. The intrinsic nonlinear behavior of isolators is poorly approximated by using equivalent linear procedures. For these and other reasons, isolation experts often consider the 1997 UBC procedure overly complicated and conservative. Miranda, Miranda and Reyes, and Miranda and Taghavi have shown that a simplified method of analysis, using a continuum model that approximates the dynamic characteristics of buildings, can predict reasonably accurate displacement, drift and acceleration demands on a multistory building when subjected to seismic ground motions. The continuous model is very useful in preliminary design because it only requires a three or four structural parameters that are typically known or can be estimated during the early stages of design. The objective of this paper is to present a simplified method of analyzing base-isolated multistory buildings for preliminary design. The procedure uses the continuous model's dynamic properties to approximate a structure's response

parameters when experiencing earthquake excitation. The procedure also attempts to improve estimating the inherent nonlinear behavior of isolator bearings by deriving a nonlinear element that is based on Menegotto and Pinto's hysteretic model. The method's accuracy is assessed by comparing the results of the approximate method, to those produced by using the dynamic properties of two example structures, which have been calculated by more rigorous analytical techniques and documented in previous research literature.

Title: Usage of Simplified N2 Method for Analysis of Base Isolated Structures
Author: Kilar, V; Koren, D
Source: 14th World Conference on Earthquake Engineering: Innovation Practice Safety. 2008
Descriptors: Displacement; Nonlinearity; Rubber; Seismic phenomena; Devices; Seismic engineering; Earthquake design; Isolation systems; Superstructures; Damping; Bearing; Stiffness; Tools; Computer programs; Demand; Degrees of freedom; Intersections; Mathematical analysis; Isolators

Abstract: The paper examines the usage of a simplified nonlinear method for seismic analysis and performance evaluation (N2 method) for analysis of base isolated structures. In the paper the N2 method is applied for analysis of a fixed base and base isolated simple four-storey frame building designed according to EC8. Two different sets of base isolation devices were investigated: a simple rubber (RB) and a similar lead rubber bearing (LRB) base isolation system. For each system a Soft, Normal and Hard rubber stiffness and three different damping values were used. The paper shows how we can obtain base displacement and top (relative) displacement for different bearing stiffness and selected damping. The target base displacement was determined as an intersection of the capacity curve of single degree of freedom system with rigid behavior of the superstructure and demand spectrum curve for selected damping of isolators. In the following step the pushover analysis of the whole isolated structure was performed up to the target base displacement using constant load distribution. The results are presented in terms of base and top displacements and ductility factors for those base isolation systems which were not able to protect the superstructure. It has been shown in the paper that N2 method might be a valuable tool for design, analysis and verification of behavior of base isolated structures with different linear or nonlinear seismic devices. Nonlinear pushover analyses were performed with the computer program SAP2000.

H.3.6 Systems with High Viscous Damping

Title: Optimization of Viscous Damper Properties for Reduction of Seismic Risk in Concrete Buildings
Author: Kargahi, Mohsen; Ekwueme, Chukwuma G
Source: 13 WCEE: 13th World Conference on Earthquake Engineering Conference Proceedings. 2004

Descriptors: Earthquake dampers; Seismic phenomena; Buildings; Concrete construction; Retrofitting

Abstract: Concrete buildings designed in California before 1976 present a major earthquake risk because they do not possess the ductility required to survive the displacements induced by large earthquakes. Consequently, the seismic retrofit of these buildings typically involves the addition of new, stiff structural elements to reduce earthquake-induced displacements. This approach often requires significant strengthening of the structure and typically involves extensive and expensive foundation work that intrudes on building operations. This paper explores the use of viscous dampers as an alternative method for the seismic rehabilitation of non-ductile concrete buildings. The dampers dissipate energy in proportion to velocity and not displacement and therefore do not cause large increases in earthquake forces. The methodology presented here is based on nonlinear static analyses that are particularly suited to buildings retrofitted with viscous dampers. In such analyses, the effect of external dampers is included by an iterative procedure that modifies the overall building damping to match that from the expected response in the dampers. Once the equivalent damping has been obtained, the design response spectrum is modified to account for the increase in damping. This means that the pushover curve needs to be calculated only once for the unretrofitted building since changes to the damper properties only affect the loading used in the analysis. This approach simplifies and speeds up the optimization by reducing the number of calculations that need to be performed. The paper presents an optimization technique for selecting damper properties that incorporates the nonlinear behavior of a building. The optimization ensures that the dampers are highly effective, even at relatively small displacements, by selecting properties for dampers at different stories that result in overall minimum cost. An existing building is used as an illustration, and the impact of dampers is evaluated for several building performance levels and ground motion levels.

Title: Effect of the Position and Number of Dampers on the Seismic Response of Frame Structures

Author: Tovar, Carolina; Lopez, Oscar A

Source: 13 WCEE: 13th World Conference on Earthquake Engineering Conference Proceedings. 2004

Descriptors: Frame structures; Seismic response; Earthquake dampers

Abstract: Little attention has been paid to evaluating the influence of the number and placement of dampers on the dynamic response, although many studies have been made of these systems. The objectives of this paper are: i) to assess how the variation of placement and number of dampers affect the seismic response of a frame structure, and ii) to evaluate a simplified method to analyze frame structures that have non-classical damping, in order to study how the error in the simplified method is influenced by placement of dampers. To fulfill these objectives, five-story moment resisting frames with two values of the fundamental period subjected to two earthquake ground motions were used. Several distributions of dampers varying

number and location were considered, while maintaining the same amount of damping in each case. The results showed that the dampers placement influences significantly the structural response. A large number of dampers do not always leads to the best benefit in terms of drift reduction for all stories. Three dampers lead to the best overall benefit for all stories in this structure. If one damper is placed, this should be located at the first story in order to obtain the best overall drift reduction. The best damper placement is one damper per story; if the number of dampers is less than the number of stories, one damper per story beginning at the lowest story is the best choice. The simplified method is not recommended for a damper distribution concentrated in a few stories, because large errors in the structural response could be obtained. The analysis considering the simplified method may be used, without introducing significant errors, in the systems with a more uniform damping distribution, that is, one damper per story with the same damping constant.

Title: Equivalent Linearization to Predict Dynamic Properties and Seismic Peak Responses of a Structural System with High Viscous Damping and Hysteretic Damping
Author : Kasai, Kazuhiko; Wanabe, Yoshifumi Ka
Source: Journal of Structural and Construction Engineering , no. 591, pp. 43-52. May 2005
Descriptors: Hysteresis; Viscous damping; Dynamics; Damping; Equivalence; Earthquake dampers; Seismic phenomena; Dynamic mechanical properties; Vibration; Dynamical systems; Seismic response; Seismic engineering; Linearization; Displacement; Ductility; Stiffness; Reduction

Abstract: This paper proposes a simplified method to estimate the dynamic properties and seismic peak responses of a single-degree-of-freedom structure with high viscous damping and hysteretic damping. The dynamic properties of this structure vary according to its velocity and displacement. The method is based on equivalent linearization as well as spectrum modification and reduction, reflecting increase in equivalent vibration period, viscous damping ratio and hysteretic damping ratio. Accuracy of the method is validated through numerous time history analyses, over a wide range of viscous damping ratio, elastic vibration period, post-yield stiffness, ductility ratio, and earthquake type.

Title: Simplified design procedure for frame buildings with viscoelastic or elastomeric structural dampers
Author: Lee, Kyung-Sik; Fang, Chih-Ping; Sause, Richard; Ricles, James
Source: Earthquake Engineering & Structural Dynamics. Vol. 34, no. 10, pp. 1271-1284. Aug. 2005
Descriptors: Elastomers; Frames; Reinforced concrete; Retrofitting; Buildings; Viscoelasticity; Earthquake dampers; Nonlinear dynamics

Abstract: A simplified design procedure (SDP) for preliminary seismic design of frame buildings with structural dampers is presented. The SDP uses elastic-static

analysis and is applicable to structural dampers made from viscoelastic (VE) or high-damping elastomeric materials. The behaviour of typical VE materials and high-damping elastomeric materials is often non-linear, and the SDP idealizes these materials as linear VE materials. With this idealization, structures with VE or high-damping elastomeric dampers can be designed and analysed using methods based on linear VE theory. As an example, a retrofit design for a typical non-ductile reinforced concrete (RC) frame building using high-damping elastomeric dampers is developed using the SDP. To validate the SDP, results from non-linear dynamic time history analyses (NDTHA) are presented. Results from NDTHA demonstrate that the SDP estimates the seismic response with sufficient accuracy for design. It is shown that a non-ductile RC frame building can be retrofit with high-damping elastomeric dampers to remain essentially elastic under the design basis earthquake (DBE).

Title: Experimental Study on Displacement Based Seismic Retrofit Design of Structures with Energy Dissipation Devices
Author: Kuo-Chun, Chang; Chang-Yuo, Chen
Source: 100th Anniversary Earthquake Conference. 2006
Descriptors: Earthquake dampers; Seismic phenomena; Retrofitting; Buildings; Displacement; Energy dissipation

Abstract: This paper proposes a seismic retrofit method for existing multi-story buildings with supplemental dampers. The design procedure will result in well control of the design displacements while obtaining the roof acceleration under the design earthquake. Substitute structure and pushover approach are also used in this study. This study, however, defines the equivalent stiffness and equivalent damping ratio by considering the average stored energy and average dissipated energy, respectively. The equivalent damping ratio will take into account the nonlinear behavior of the structure and the energy dissipation devices. The proposed method is applied to the multi-story steel buildings, and the design results are verified through experimental study as well as dynamic nonlinear time history analyses.

Title: Performance-Based Seismic Design of Supplemental Dampers in Inelastic System
Author: Li, Bo; Liang, Xing-wen
Source: ICEE 2006: 4th International Conference on Earthquake Engineering. 2006
Descriptors: Damping; Dampers; Design engineering; Dynamical systems; Seismic design; Hysteresis; Nonlinear dynamics; Equivalence; Viscous damping; Marketing; Performance evaluation; Deformation; Demand

Abstract: A simplified yet effective design procedure for viscous dampers was presented based on improved capacity spectrum method in the context of performance-based seismic design. The amount of added viscous damping required to meet a given performance objective was evaluated from the difference between the total demand for effective damping and inherent damping plus equivalent damping

resulting from hysteretic deformation of system. Application of the method is illustrated by means of two examples, using Chinese design response spectrum and mean response spectrum. Nonlinear dynamic analysis results indicate that the maximum displacements of structures installed with supplemental dampers designed in accordance with the proposed method agree well with the given target displacements. The advantage of the presented procedure over the conventional iterative design method is also highlighted.

Title: Comparison of Nonlinear Static and Nonlinear Dynamic Analyses in the Estimation of the Maximum Displacement for Structures Equipped with Various Damping Devices

Author: Tehrani, Payam; Maalek, Shahrokh

Source: ICEE 2006: 4th International Conference on Earthquake Engineering. 2006

Descriptors: Nonlinear dynamics; Nonlinearity; Displacement; Dynamical systems; Seismic phenomena; Devices; Shear; Walls; Dissipation; Retrofitting; Friction; Steel structures; Reinforcing steels; Earthquake dampers; Energy use; Viscoelasticity; Dampers; Reinforced concrete; Load distribution (forces)

Abstract: In this study, the nonlinear static (pushover) and nonlinear dynamic procedures in the determination of maximum displacements of an existing steel structure retrofitted with different methods have been compared. These methods include the use of the EBF systems; RC Shear Walls and the use of Passive energy dissipators such as metallic, viscous, viscoelastic and friction dampers. In nonlinear dynamic procedure, the response of the structure to seven scaled earthquake records has been obtained and the average value of the responses is used for comparison. At the same time in nonlinear static procedure, the maximum displacements of the structure in two different load distribution patterns have been obtained. The results demonstrate that the nonlinear static procedure determines the maximum displacement of the structure conservatively.

Title: Study on the capacity-spectrum seismic design method for buildings equipped with passive energy dissipation systems.

Author: Zhang, Sihai; Liang, Xingwen; Deng, Mingke

Source: Tumu Gongcheng Xuebao (China Civil Engineering Journal). Vol. 39, no. 7, pp. 26-32. July 2006

Descriptors: Dampers; Seismic design; Drift; Energy dissipation; Seismic phenomena; Nonlinear dynamics; Architecture; Nonlinearity; Criteria; Seismic engineering; Earthquake design; Buildings; Earthquake dampers; Viscoelasticity; Reinforced concrete; Damping; Equivalence; Frames

Abstract: A seismic design procedure for energy dissipation systems is proposed by using the capacity spectrum method in combination with Chinese seismic design code. The performance level is quantified by the inter-story drift ratio, and the equivalent damping ratio is evaluated by the simplified method in the proposed

procedure. Nonlinear static analysis is conducted for the evaluation of the seismic performances of structures without supplement dampers. The size and number of dampers are selected according to the requirements of the prescribed performance objective. Pushover analysis is carried out for structures with supplement dampers to verify whether the inter-story drift satisfies the prescribed performance criterion or not. Application of the procedure is illustrated by using a regular reinforced concrete frame with visco-elastic dampers. The results from the case study indicate that the proposed method is simple, feasible, and agrees well with nonlinear dynamic analysis.

Title: Approximate establishment of pushover curve for frame with supplemental visco elastic dampers on the basis of plastic analysis.
Author: Li, Bo; Liang, Xingwen
Source: Dizhen Gongcheng yu Gongcheng Zhendong/Earthquake Engineering and Engineering Vibration. Vol. 27, no. 3, pp. 30-34. May-June 2007
Descriptors: Seismic phenomena; Seismic engineering; Earthquake design; Earthquake dampers; Performance evaluation; Dampers; Earthquake construction; Frames; Lithium; Vibration; Architecture; Nonlinearity; Civil engineering; Viscoelasticity; Construction; Energy dissipation; Structural analysis; Approximation; Earthquake engineering

Abstract: Nonlinear static procedure is used to evaluate the seismic performance of a newly designed or existing structure with passive energy dissipation systems. The pushover curve of a structure needs to be established before seismic performance evaluation. This paper presents a simplified method based on plastic analysis theory to rapidly and effectively construct the idealized bilinear pushover curve for the moment resisting frame added with viscoelastic dampers without the aid of the structural analysis program. The application of the presented method is illustrated with an example. Comparing the results determined by the proposed method using three force distribution patterns with those obtained by computer analysis, it is demonstrated that the presented simple method makes an accurate estimate of the pushover curve, provided the beam sideway mechanism develops in the primary structure.

Title: Performance Based Seismic Design of Supplemental Viscous Dampers for Inelastic Sdof Systems
Author: Li, Bo; Liang, Xing-Wen; Yang, Ke-Jia
Source: Gongcheng Lixue (Engineering Mechanics). Vol. 24, no. 6, pp. 147-152. June 2007
Descriptors: Damping; Dampers; Design engineering; Dynamical systems; Seismic design; Hysteresis; Nonlinear dynamics; Equivalence; Viscous damping; Lithium; Marketing; Performance evaluation; Deformation; Architecture; Demand; Civil engineering

Abstract: A simplified yet effective design procedure for viscous dampers was presented based on improved capacity spectrum method using the concept of performance based seismic design. The amount of added viscous damping ratio required to meet a given performance objective was evaluated from the difference between the total demand for effective damping ratio and the inherent damping ratio plus equivalent damping ratio resulting from hysteretic system deformation. Application of the method is illustrated with two examples, using Chinese design response spectrum and mean response spectrum. Nonlinear dynamic analysis results indicate that the maximum displacements of structures installed with supplemental dampers designed in accordance with the proposed method agree well with the given target displacements. The advantage of the presented procedure over the conventional iterative design method is also highlighted.

Title: Nonlinear Static Procedure for Reinforced Concrete Asymmetric Buildings with Linear Viscous Dampers

Author: Fujii, K

Source: 14th World Conference on Earthquake Engineering: Innovation Practice Safety. 2008

Descriptors: Nonlinearity; Mathematical models; Dampers; Asymmetry; Equivalence; Reinforced concrete; Buildings; Frames; Drift; Linearization

Abstract: In this paper, the Nonlinear Static Procedure (NSP) is extended for reinforced concrete single-story asymmetric building with linear viscous dampers. In this procedure, their responses are predicted through a nonlinear static analysis of MDOF model considering the contribution of linear viscous damper to the fundamental mode shape and an estimation of the nonlinear response of equivalent SDOF model using equivalent linearization technique. The peak drift of each frame predicted by the proposed procedure are compared with the results obtained by the time-history analysis. The results show that nonlinear response of single-story asymmetric buildings with viscous dampers can be satisfactory predicted by the procedure discussed in this paper.

Title: Performance-based seismic design for structures with viscoelastic dampers.

Author: Han, Jianping; Yan, Ru; Li, Hui

Source: Dizhen Gongcheng yu Gongcheng Zhendong/Earthquake Engineering and Engineering Vibration. Vol. 28, no. 1, pp. 175-181. Jan.-Feb. 2008

Descriptors: Seismic phenomena; Earthquakes; Buildings; Viscoelasticity; Dampers; Disasters; Lithium; Vibration; Demand; Damage; Seismic engineering; Spectra; Earthquake design; Earthquake dampers; Performance evaluation; Seismic design; Reinforced concrete; Marketing; Damping

Abstract: According to the characteristics of viscoelastic damper (VED) and the requirements of the seismic code, the elastic and inelastic demand spectra are

proposed respectively. The former is based on the simplified formulas of equivalent damping ratio and the response spectrum of the code. The latter is based on the modified $R(\mu)$ - μ - T relationship proposed by Vidic. Furthermore, the performance-based approach using capacity spectrum method is presented for analyzing the buildings with VED(s) and higher mode effects can be considered by virtue of modal pushover analysis. Finally, the analyses of an eight-storey reinforced concrete frame with or without VED are performed under two performance levels. The first level is that the building has no damage under moderate earthquakes and the second one is that the building is repairable under rarely occurring earthquakes. The results indicate that the proposed approach is viable and effective for performance evaluation of buildings with VED(s).

H.4 Engineering Demand Parameters

H.4.1 *Estimation of EDPs Using Different Analysis Methods and Simplified Structural Models*

Title: Peak displacements and interstory drifts of nonlinear MDOF systems using principal components analysis
Author: Cuesta, I.; Aschheim, M. A.
Source: Seventh U.S. National Conference on Earthquake Engineering (7NCEE): Theme: Urban Earthquake Risk [electronic resource]; 10 pages pp. 2002
Descriptor: Steel moment-resisting frames; nonlinear static pushover analysis; Story drift; Mode shapes

Abstract: Principal Components Analysis (PCA) is a method to extract the principal components (or modes) of response from recorded or computed response data of systems exhibiting linear and/or nonlinear response. For linear systems, the PCA mode shapes coincide with the elastic mode shapes, if the nodal mass is uniformly distributed. For nonuniform mass distributions, the PCA modes are related to the elastic modes. The PCA technique is particularly valuable when applied to systems responding nonlinearly because it identifies the "predominant mode" of response and the degree to which the response is in this mode. This paper illustrates the use of the PCA technique for estimating floor and interstory drifts for a 12-story moment-resistant steel frame responding to earthquake ground motions. Linear and nonlinear responses are considered, and the observed mode shapes and the accuracy of drift estimates are discussed. The interaction of modal amplitudes in time is considered in detail. The peak roof drift and interstory drifts are expressed as linear combinations of the PCA modes, and are represented graphically, together with the observed interaction response. A technique is described to determine peak values of these quantities by maximizing the drift functions relative to the observed modal interactions.

Title: Approximate Method for Evaluation of Seismic Damage of RC Buildings

Author: Ferraioli, Massimiliano; Avossa, Alberto Maria; Malangone, Pasquale

Source: 13 WCEE: 13th World Conference on Earthquake Engineering Conference Proceedings. 2004

Descriptors: Mathematical models; Earthquake damage; Seismic phenomena; Buildings; Nonlinear dynamics; Reinforced concrete

Abstract: An approximate method for the estimation of the seismic damage of r.c. multistory buildings is presented. The method is based on the Capacity Spectrum Method and the Inelastic Demand Response Spectra which are obtained with a reduction rule defined from a statistical data analysis. The local damage index was defined with an improved Park & Ang model starting from the pushover analysis of the building and the nonlinear dynamic analysis of the equivalent bilinear SDOF system. The approximate method was applied to r.c., multistory buildings when subjected to earthquake ground motion. The results obtained are compared with those computed using step-by-step time history analysis of the structure.

Title: Estimating Rotational Demands in High-Rise Concrete Wall Buildings

Author: White, Timothy; Adebar, Perry

Source: 13 WCEE: 13th World Conference on Earthquake Engineering Conference Proceedings. 2004

Descriptors: Walls; Earthquakes; Cantilever beams; Displacement; Concrete construction; Buildings; Nonlinear dynamics

Abstract: Results from numerous nonlinear dynamic analyses on high-rise concrete buildings, ranging in height from 120 to 480 ft, were used to develop simplified procedures for estimating maximum inelastic wall rotations and maximum coupling beam chord rotations. The results indicate that, due to higher mode effects and forces applied by coupling beams, maximum rotations in slender cantilever walls and in coupled walls usually do not occur at the same time as the maximum displacement. However, it is reasonable to estimate maximum inelastic rotation from maximum total displacement using a fictitious elastic displacement, which is proportional to actual wall strength to elastic demand ratio. Due to coupling. beams "pulling back" on the coupled walls, the "elastic displacements" of coupled walls are smaller than cantilever walls. The maximum coupling beam rotation depends on the wall slope and floor slope at the critical level. A simplified procedure that gives reasonable results is to assume that the combination of wall and floor slope at the critical level is equal to the maximum global drift.

Title: Modal Damage Index and Its Application in Structure Damage Assessment

Author: Zhu, Hong-Wu; Wang, Kong-Fan; Tang, Shou-Gao

Source: Tongji Daxue Xuebao/Journal of Tongji University (Natural Science) (China). Vol. 32, no. 12, pp. 1589-1592. Dec. 2004

Descriptors: Damage; Buildings; Accuracy; Seismic engineering; Force distribution; Earthquake damage; Seismic phenomena; Dynamic structural analysis; Effectiveness; Damage assessment; Earthquake construction; Computation

Abstract: Modal pushover analysis (MPA) is an improved pushover analysis procedure based on structural dynamics theory. It not only retains the conceptual simplicity and computational effectiveness of the procedure with invariant force distribution, but also provides superior accuracy in estimating seismic damage on buildings. On the basis of MPA procedure, combined with the approach proposed by A. Ghobarah for the assessment of the damage index for multi-story buildings by using results of twice pushover analyses, a modal damage index is proposed in this paper.

Title: Probabilistic Estimation of Seismic Story Drifts in Reinforced Concrete Buildings

Author: Dinh, Thuat V; Ichinose, Toshikatsu

Source: Journal of Structural Engineering (New York, N.Y.). Vol. 131, no. 3, pp. 416-427. Mar. 2005

Descriptors: Earthquake construction; Buildings; Reinforced concrete; Probability theory; Standard deviation; Probabilistic methods

Abstract: Probabilistic techniques are of vital use in predicting the seismic story drifts of buildings, which vary due to uncertainties in the characteristics of future earthquake motions. This paper proposes a procedure for evaluating the expected mean and standard deviation of seismic story drifts of reinforced concrete buildings by considering both total and story failure mechanisms. The estimation process consists of a pushover analysis of the structure against inverted triangular forces to evaluate the most probable mechanism during earthquakes, followed by consideration of the relative reserve strengths to evaluate the probability of other mechanisms. The relative reserve strengths against story and total mechanisms are expressed by two newly defined story-safety and total-reduction factors, respectively. In this paper, the proposed procedure is verified by conducting dynamic response analyses of 9-story wall and frame structures with various story-safety and total-reduction factors using 36 records from 14 different earthquakes. The proposed procedure well predicted the mean and standard deviation of story drifts of the structures. Application to wall-frame structures is also discussed.

Title: Approximate Floor Acceleration Demands in Multistory Buildings. I: Formulation

Author: Miranda, Eduardo; Taghavi, Shahram

Source: Journal of Structural Engineering (New York, N.Y.). Vol. 131, no. 2, pp. 203-211. Feb. 2005

Descriptors: Buildings; Acceleration; Stiffness; Seismic phenomena; Dynamic mechanical properties

Abstract: An approximate method to estimate floor acceleration demands in multistory buildings responding elastically or practically elastic when subjected to earthquake ground motion is presented. The method can be used to estimate floor acceleration demands at any floor level for a given ground motion record. The dynamic characteristics of the building are approximated by using a simplified model based on equivalent continuum structure that consists of a combination of a flexural beam and a shear beam. Closed-form solutions for mode shapes, period ratios, and modal participation factors are presented. The effect of reduction of lateral stiffness along the height is investigated. It is shown that the effect of reduction in lateral stiffness on the dynamic characteristics of the structure is small in buildings that deflect laterally like flexural beams. For other buildings, approximate correction factors to the closed-form solutions of the uniform case are presented to take into account the effects of reduction of lateral stiffness. Approximate dynamic properties of the building are then used to estimate acceleration demands in the building using modal analysis.

Title: Simple Predictor of Maximum Displacement of SMRF Buildings, Backbone curve of equivalent SDOF system and lateral load pattern for pushover analysis

Author: Mori, Yasuhiro; Yamanaka, Takashi

Source: Journal of Structural and Construction Engineering, no. 597, pp. 127-133. Nov. 2005

Descriptors: Dynamical systems; Backbone; Nonlinear dynamics; Drift; Displacement; Equivalence; Seismic phenomena; Nonlinearity; Demand analysis; Seismic engineering; Spectra; Earthquake design; Buildings; Mathematical models; Stress concentration; Accuracy; Earthquake construction; Marketing; Design engineering

Abstract: Predictors or estimates of seismic structural demands, such as inter-story drift angles, that are less time-consuming than nonlinear dynamic analysis can be useful for structural performance assessment and for design. The authors have proposed a predictor using the SRSS rule of modal composition, and taking into account a first-mode inelastic spectral displacement and a post-elastic first-mode shape approximated by the distribution of the story drifts obtained through a nonlinear static pushover analysis. This paper statistically investigates the dependence of the accuracy of the predictor on the lateral force distribution in the static pushover analysis and the backbone curve of an equivalent 500F system using frame models with various stiffness distributions.

Title: Approximate Floor Acceleration Demands in Multistory Buildings. II: Applications

Author: Taghavi, Shahram; Miranda, Eduardo

Source: Journal of Structural Engineering (New York, N.Y.). Vol. 131, no. 2, pp. 212-220. Feb. 2005

Descriptors: Approximation; Buildings; Acceleration; Dynamic characteristics; Finite element method; Earthquake construction; Structural engineering

Abstract: The accuracy of an approximate method to estimate floor acceleration demands in multistory buildings responding elastically or practically elastic when subjected to earthquake ground motion is investigated. Modal analysis is used in combination with approximate dynamic characteristics computed using a simplified continuous model that is fully defined with only four parameters. The accuracy of the method is first evaluated by comparing the response computed with the approximate method to that computed with response history analyses of complete finite element models of two generic buildings available in the literature. A comparison of exact and approximate dynamic characteristics is presented. Approximate peak floor acceleration demands and its variation along the height of the buildings are compared to exact demands when the buildings are subjected to an ensemble of 20 ground motions. The accuracy of the method is then evaluated by comparing floor acceleration demands computed with the approximate method to those recorded in four instrumented buildings in California. Results show that the approximate method produces good results with a very small computational effort.

Title: Drift Demand of Frame Structures Subjected to Vrancea Earthquake Ground Motions

Author: Albota, Emil; Demetriu, Sorin; Enache, Ruxandra

Source: First European Conference on Earthquake Engineering and Seismology. 2006

Descriptors: Drift; Seismic phenomena; Frame structures; Grounds; Spectra; Computation; Dynamic characteristics; Demand; Bucharest; Mathematical analysis; Dynamic tests; Mathematical models; Dynamics; Accuracy; Displacement; Marketing; Roofs; Stiffness; Frames

Abstract: In this paper a method for computing the maximum inter-story drift ratio (MIDR) and roof drift ratio (RDR) for 2D-frame structures is presented. This method extends the applicability of drift spectra for general multi-story frame structures. Based on modal analysis, this method was developed only for frames vibrating predominantly in the first mode. Computational relations are relatively simple and capable to evaluate with enough accuracy drift ratio. Earthquake ground motions used in this study were recorded in different site conditions in Bucharest during the 1977, 1986 and 1990 Vrancea subcrustal earthquakes. The generic multi-story frame structures used in analysis were developed having some particular dynamic characteristics. MIDR and RDR are expressed as a function of the beam-to-column stiffness ratio and spectral displacement (SD). Results obtained using presented method are compared with these obtained from a linear time- history dynamic analysis.

Title: Reducing to Equivalent SDOF System and Evaluation of Higher Mode Shear Responses for Multi-Story Wall-Frame Buildings
Author: Kuramoto, Hiroshi; Akita, Tomofusa
Source: Journal of Structural and Construction Engineering , no. 605, pp. 79-86. July 2006
Descriptors: Shear; Seismic phenomena; Earthquake construction; Walls; Equivalence; Reinforced concrete; Frames; Buildings; Mathematical analysis; Standards; Positioning; Law enforcement; Strength; Accuracy

Abstract: This paper shows two methods of evaluating earthquake responses for RC wall-frame buildings to improve the capacity spectrum method used in the Calculation of Response and Limit Strength provided in the Building Standard Law Enforcement Order of Japan. One is a method of redistributing the representative shear in an equivalent SDOF system reduced from the wall-frame building to the first mode components of the story shears contributed by the shear walls and frames, and the other is a method of evaluating the higher mode components of the story shears. Time history earthquake response analysis and pushover analysis for four types of 12 story RC wall-frame building which have the different wall arrangement are executed to examine the prediction accuracy of earthquake responses by the proposed methods. Good agreements between the results of the proposed methods and the earthquake response analysis are obtained in the story shears contributed by the shear walls and frames.

Title: Statistical Evaluation of Critical Inter-Storey Drift Concentration of RC Frames
Author: Lu, Yong; Gu, Xiaoming; Wei, Jianwu
Source: First European Conference on Earthquake Engineering and Seismology. 2006
Descriptors: Drift; Regularity; Frames; Demand; Grounds; Reinforced concrete; Marketing; Seismic phenomena; Estimating; Nonlinear dynamics; Correlation; Mathematical analysis; Frame structures; Displacement; Design engineering; Roofs; Tasks; Stiffness; Capacity factor

Abstract: In performance based design, the evaluation of displacement (drift) demand in a structure is a crucial task. Simplified methods are desired for estimating the overall drift demand in a frame structure, as well as the critical inter-storey drift and the drift distributions. In this paper, a modified approach is employed to evaluate the regularity of a frame in accordance with the distribution of the storey capacity factor, which is defined as a combination of the storey overstrength and stiffness factors. The relationship between the corresponding regularity index and the critical inter-storey drift to roof drift ratio is investigated through the nonlinear dynamic analysis of a group of multi-storey RC frames under a set of selected earthquake ground motions. It is observed that the actual drift concentration correlates well with the new regularity index. The statistical feature of the drift concentration is discussed based on the analytical results for various ground

Title: Estimating Inelastic Drift Demands of Concrete Walls
Author: White, T; Adebar, P
Source: 100th Anniversary Earthquake Conference. 2006
Descriptors: Walls; Cantilever beams; Displacement; Joining; Seismic design; Concretes

Abstract: To develop simplified procedures for estimating inelastic drift (rotation) demand, nonlinear dynamic analyses were conducted on cantilever and coupled walls ranging in height from 120 to 480 ft. The results indicate that due to higher mode effects and forces applied by coupling beams, maximum inelastic rotations in tall cantilever walls and in coupled walls usually do not result from maximum displacement demands. It is reasonable nonetheless to estimate maximum inelastic rotation from maximum total displacement and an equivalent elastic displacement. The elastic displacements are equal to the first mode yield displacements of short cantilever walls; but are much smaller in coupled walls due to the restraining action of the coupling beams. Due to the variability of top wall displacements, the most accurate method for estimating inelastic rotation of slender cantilever walls and coupled walls involves the maximum mid-height displacement, and equations are presented to facilitate this approach accounting for the initial fundamental period and degree of coupling.

Title: A Modal Combination Rule for Peak Floor Accelerations in Multistoried Buildings
Author: Kumari, Rashmi; Gupta, Vinay K
Source: ISET Journal of Earthquake Technology. Vol. 44, no. 1, pp. 213-231. Mar. 2007
Descriptors: Acceleration; Dynamics; Dynamical systems; Excitation; Seismic phenomena; Seismic engineering; Spectra; Buildings; Mathematical models; Civil engineering; Error analysis; Permissible error; Hazards; Earthquake construction; Random vibration; Damping; Dynamic mechanical properties; Safety; Approximation

Abstract: It is useful to estimate peak floor accelerations consistent with the specified seismic hazard for ensuring the safety of rigid nonstructural components in structural systems. A modal combination rule is formulated here to estimate peak floor accelerations in a multistoried building directly in terms of the dynamic properties of the building and pseudo spectral acceleration ordinates of the base excitation. The formulation is developed under the framework of stationary random vibration theory for a linear, lumped-mass, classically damped, multi-degree-of-freedom system with the help of some approximations. A numerical study shows that the proposed rule performs well with the maximum average absolute error in any combination of building and excitation being less than 20% in case of 5% damping. Two simpler SRSS-type variants of the proposed rule, one considering modal cross-correlation and another ignoring this, are also shown to perform reasonably well, particularly when the building is not flexible to the ground motion.

Title: Prediction of Higher Mode Story Drift Response for Multi-Story Buildings Under Earthquake Motions
Author: Kuramoto, Hiroshi
Source: 8th Pacific Conference on Earthquake Engineering Conference Proceedings. 2007
Descriptors: Seismic phenomena; Earthquake engineering; Earthquake construction; Drift; Buildings; Equivalence; Eigenvalues; Mathematical analysis; Degrees of freedom; Reinforced concrete; Displacement; Nonlinearity; Construction; Decomposition; Force distribution

Abstract: Two methods of reducing from a multi-story building to the equivalent single degree of freedom (ESDOF) system have been proposed by the author to improve the capacity spectrum method which is a typical evaluation procedure of the maximum earthquake response of the building in Performance Based Earthquake Engineering. One is a nonlinear modal adaptive pushover analysis method, which uses a stiffness-dependent lateral force distribution at each loading step without the eigenvalue analysis, and the other is a method using modal decomposition procedure together with earthquake response analysis. Applying both methods for 4-story and 12-story reinforced concrete buildings, the earthquake response characteristics of the ESDOF system are examined in this paper. Based on the latter method, an evaluation method of the higher mode effect in the interstory drift responses is also proposed. The higher mode component of the interstory drift can be estimated by using the representative displacement of another ESDOF system which is reduced from higher mode components subtracting the first mode component from the whole building's responses.

Title: Prediction of Shear Contribution of Walls In RC Wall-Frame Buildings Under Earthquake Motions
Author: Kuramoto, Hiroshi; Akita, Tomofusa
Source: 14th World Conference on Earthquake Engineering: Innovation Practice Safety. 2008
Descriptors: Shear; Seismic phenomena; Earthquake construction; Walls; Reinforced concrete; Frames; Buildings; Equivalence; Accuracy

Abstract: This paper shows two earthquake response evaluation methods for multi-story wall-frame buildings. One is a method of redistributing the representative shear in an equivalent SDOF system reduced from the wall-frame building to the first mode components of the story shears contributed by the shear walls and frames, and the other is a method of evaluating the higher mode components of the story shears. Time history earthquake response analysis and pushover analysis for three types of 12 story RC wall-frame building with different wall layouts are performed to examine the prediction accuracy of earthquake responses by the proposed methods. Good agreements between the results of the proposed methods and the earthquake response analysis are obtained in terms of the story shears contributed by the shear walls and frames.

H.4.2 Complexity of Response and Effect of Configuration on Accuracy of Estimation of EDPs

Title: Nonlinear Dynamic Analysis - the Only Option for Irregular Structures
Author: Chambers, Jonathan; Kelly, Trevor
Source: 13 WCEE: 13th World Conference on Earthquake Engineering Conference Proceedings. 2004
Descriptors: Nonlinear dynamics; Seismic phenomena; Buildings; Earthquake engineering; Stiffness; Irregularities

Abstract: The response of buildings to earthquakes is a complex, three dimensional, nonlinear, dynamic problem. Limitations in technology and the depth of our understanding of this problem have lead to the profession developing a number of simplified methods for representing it, most of which disregard one or more of its fundamental aspects: the Linear Dynamic Procedure (LDP) ignores nonlinearity; the Nonlinear Static Procedure (NSP) ignores dynamic effects; the Linear Static Procedure (LSP) ignores both. In contrast, the Nonlinear Dynamic Procedure (NDP) attempts to fully represent the seismic response of buildings without any of these major simplifying assumptions. This paper discusses some of the obstacles preventing the widespread adoption of NDP, and presents a number of examples where its uncompromised representation is crucial for satisfactorily predicting the seismic response of structures. Specific case studies include rocking systems, structures with significant stiffness irregularities and existing structures with inadequate seismic resistance. It is concluded that the NDP is the only universally appropriate method for verifying the performance of structures, and that the traditional reasons preventing its widespread adoption are all but invalid. The profession needs to change their collective mind set, stop resisting and start embracing what technology now enables us to do.

Title: Analysis paralysis: a 2003 state-of-the-art report on seismic analysis.
Author: Kelly, T.E.
Source: Bulletin of the New Zealand Society for Earthquake Engineering. Vol. 37, no. 1, pp. 23-34. Mar. 2004
Descriptors: Seismic phenomena; Seismic engineering; Nonlinear dynamics; Computer simulation; Dynamic structural analysis

Abstract: A 2003 state-of-the-art report on seismic analysis for structural engineers would be similar to one that could have been produced in 1993 or 1983, and in fact not much different from 1973. Development of structural engineering analysis tools has not kept pace with the rapid improvement in computer hardware. Our common analysis tools ignore either nonlinearity (response spectrum analysis), dynamic effects (pushover analysis), or both (equivalent static analysis) even though these effects are critical in evaluating the performance of a structure under earthquake loads. This paper examines the effects of nonlinearity and dynamic loads on the response of structures and illustrates cases where ignoring either of these leads to

erroneous results. Given this need for nonlinear dynamic analysis, impediments to more widespread use are discussed and areas where more research information is required are identified. The conclusion of this paper is that our profession needs to be more active in implementing software development, graduate training in analysis and the processing of research results to a format suited for analysis models. We have a wealth of research information providing detailed response of structural components but, by failing to convert this into detailed rules for nonlinear analysis, we are neglecting much of the value in this research.

Title: Approximate modal decomposition of inelastic dynamic responses of wall buildings.

Author: Sangarayakul, C; Warnitchai, P

Source: Earthq. Eng. Struct. Dyn. Vol. 33, no. 9, pp. 999-1022. 25 July 2004

Descriptors: Decomposition; Walls; Buildings; Vibration mode; Seismic engineering

Abstract: Two approximate methods for decomposing complicated inelastic dynamic responses of wall buildings into simple modal responses are presented. Both methods are based on the equivalent linear concept, where a non-linear structure is represented by a set of equivalent linear models. One linear model is used for representing only one vibration mode of the non-linear structure, and its equivalent linear parameters are identified from the inelastic response time histories by using a numerical optimizer. Several theoretical relations essential for the modal decomposition are derived under the framework of complex modal analysis. Various numerical examinations have been carried out to check the validity of the proposed modal decomposition methods, and the results are quite satisfactory in all cases. Fluctuating bending moment and shear at any location along the wall height contributed by each individual vibration mode can be obtained. Modal contributions to shear and flexural strength demands, as well as the corresponding modal properties, under various seismic loading conditions can also be identified and examined in detail.

Furthermore, the effects of higher vibration modes on seismic demands of wall buildings are investigated by using the modal decomposition methods. Several new insights into the complicated inelastic dynamics of multi-story wall buildings are presented.

Title: Effect of RC structural wall area on seismic response of open ground storey RC buildings

Author: Vijay, G; Dasgupta, K; Murty, C V R

Source: 8th Pacific Conference on Earthquake Engineering Conference Proceedings. 2007

Descriptors: Walls; Reinforced concrete; Buildings; Seismic phenomena; Grounds; Seismic engineering; Earthquake construction; Shear; Earthquake design; Stiffness; Failure; Irregularities; Seismic response; Nonlinearity; Indian; Seismic design; Construction; Displacement; Performance enhancement

Abstract: Reinforced Concrete (RC) frame buildings with open ground storey are common in urban construction of developing countries. Structural walls are used to reduce the irregularity in the ground storey. The present study investigates the influence of RC structural wall areas on seismic vulnerability of these buildings. Typical five-storied RC frame-masonry infill buildings, with varying structural wall areas, are designed as per Indian Seismic Design Codes. Both thickness and length of those walls are varied, along with their locations in the outer periphery. Seismic shear capacity and lateral stiffness characteristics of these buildings are estimated using displacement-based nonlinear pushover analyses. Shear capacity and stiffness characteristics are significantly improved and flexural failure of RC members is mobilised with increasing wall areas. Structural wall area of at least 2% of building plan area seems desirable for ensuring improved seismic performance of typical 5-storey buildings.

H.5 Probabilistic Treatments

Title: Probabilistic basis for 2000 SAC Federal Emergency Management Agency steel moment frame guidelines
Author: Cornell, C. Allin, Jalayer, F., Hamburger, R., and Foutch, D.
Source: Journal of Structural Engineering. Vol. 128, no. 4, pp. 526-533. Apr. 2002

Abstract: This paper presents a formal probabilistic framework for seismic design and assessment of structures and its application to steel moment-resisting frame buildings. This is the probabilistic basis for the 2000 SAC Federal Emergency Management Agency (FEMA) steel moment frame guidelines. The framework is based on realizing a performance objective expressed as the probability of exceeding a specified performance level. Performance levels are quantified as expressions relating generic structural variables "demand" and "capacity" that are described by nonlinear, dynamic displacements of the structure. Common probabilistic analysis tools are used to convolve both the randomness and uncertainty characteristics of ground motion intensity, structural "demand," and structural system "capacity" in order to derive an expression for the probability of achieving the specified performance level. Stemming from this probabilistic framework, a safety-checking format of the conventional "load and resistance factor" kind is developed with load and resistance terms being replaced by the more generic terms "demand" and "capacity," respectively. This framework also allows for a format based on quantitative confidence statements regarding the likelihood of the performance objective being met. This format has been adopted in the SAC/FEMA guidelines.

Title: Probabilistic seismic assessment of existing R/C buildings: static push-over versus dynamic analysis
Author: de Felice, G; Giannini, R; Pinto, P E
Source: The Twelfth European Conference on Earthquake Engineering [Proceedings] [electronic resource] , pp. 10 pages. 2002

Descriptors: Dynamic tests; Earthquake design; Seismic engineering; Seismic phenomena; Dynamics; Statics; Earthquake construction; Frames; Loads (forces); Resources; Reinforced concrete; Safety; Criteria; Buildings; Probability theory; Failure; Earthquake engineering; Probabilistic methods

Abstract: The seismic safety of a reinforced concrete frame, designed for vertical loads only, is evaluated through a probability-based assessment procedure. The procedure takes into account uncertainty in global and local failure criteria as well as in overall response of the frame. Both a dynamic procedure and a pushover-based static procedure are applied with the purpose of assessing the accuracy of pushover predictions.

Title: A Probabilistic Performance Evaluation of an Asymmetric Reinforced Concrete Frame (Spear) Building

Author: Dolsek, Matjaz

Source: First European Conference on Earthquake Engineering and Seismology. 2006

Descriptors: Mathematical models; Collapse; Limit states; Dynamics; Probability theory; Probabilistic methods; Seismic phenomena; Spears; Dynamic tests; Reinforced concrete; Frames; Dynamical systems; Dispersions; Nonlinear dynamics; Columns (structural); Amplification; Demand analysis; Seismic engineering; Asymmetry

Abstract: An important goal of performance-based earthquake engineering is the prediction of the mean annual probabilities of exceedance of a given performance level (limit state). One of the methods, which is realizing this goal, is the SAC-FEMA method developed as a part of broader probabilistic framework adopted at PEER center. The SAC-FEMA method involves the so-called Incremental Dynamic Analysis which represents the relation between the engineering demand parameter and the seismic intensity measure. As an alternative to Incremental Dynamic Analysis, a simplified approach, called IN2 (incremental N2 analysis), has been proposed. The IN2 can be, in combination with predetermined data on dispersion typical for a specific structural system, employed in the PEER probabilistic framework. Using this simplified approach, the computational efforts can be substantially reduced. In the paper, the IN2 analysis is summarized. Its application is demonstrated by an example of a three-story plan-asymmetric reinforced concrete frame building. The structure was pseudo-dynamically tested in full-scale in the ELSA laboratory in Ispra within the SPEAR project. The mathematical model, used in analyses, which were performed with OpenSees program, consists of one-component lumped plasticity elements. It has been validated by test results. The probability of exceedance of the near collapse limit state, which is assumed to be met when the near collapse chord rotation is exceeded in the first column, is calculated with the proposed simplified approach and compared with results of a more accurate analysis. The intermediate results, determined by the N2 method, like the summarized IN2 curve, torsional amplification factors and the top displacement

corresponding to the near collapse limit state, are also presented in the paper and compared with results obtained by nonlinear dynamic analysis.

Title: Convex set model-based bound pushover analysis.
Author: Jia, Lizhe; Duan, Zhongdong; Lu, Qinnian
Source: Dizhen Gongcheng yu Gongcheng Zhendong (Earthquake Engineering and Engineering Vibration). Vol. 26, no. 5, pp. 81-87. Sept.-Oct. 2006
Descriptors: Seismic phenomena; Mathematical models; Seismic engineering; Probability theory; Probabilistic methods; Vibration; Earthquake engineering; Loads (forces); Performance evaluation; Uncertainty; Shear; Civil engineering; Acceleration

Abstract: Many uncertain factors are involved in seismic performance evaluation and the probabilistic results drawn from inadequate information are suspectable. Considering the uncertainties of peak acceleration and frequency characteristics by using a bounded convex set model, the bounds of shear forces are derived from the Chinese seismic code, and then a new lateral bound load method for pushover analysis is proposed. Then the convex analysis method is integrated into pushover analysis to study the bounds of structural capacity. As a result, the convex model-based pushover analysis makes an estimation of the performance of structure with an interval, and it is more objective and robust with respect to probabilistic perspective.

Title: A static predictor of seismic demand on frames based on a post-elastic deflected shape
Author: Mori, Yasuhiro; Yamanaka, Takashi; Luco, Nicolas; Cornell, C Allin
Source: Earthquake Engineering & Structural Dynamics. Vol. 35, no. 10, pp. 1295-1318. Aug. 2006
Descriptors: Seismic phenomena; Earthquake design; Nonlinear dynamics; Approximation; Dynamic structural analysis; Buildings

Abstract: Predictors of seismic structural demands (such as inter-storey drift angles) that are less time-consuming than nonlinear dynamic analysis have proven useful for structural performance assessment and for design. Luco and Cornell previously proposed a simple predictor that extends the idea of modal superposition (of the first two modes) with the square-root-of-sum-of-squares (SRSS) rule by taking a first-mode inelastic spectral displacement into account. This predictor achieved a significant improvement over simply using the response of an elastic oscillator; however, it cannot capture well large displacements caused by local yielding. A possible improvement of Luco's predictor is discussed in this paper, where it is proposed to consider three enhancements: (i) a post-elastic first-mode shape approximated by the deflected shape from a nonlinear static pushover analysis (NSPA) at the step corresponding to the maximum drift of an equivalent inelastic single-degree-of-freedom (SDOF) system, (ii) a trilinear backbone curve for the SDOF system, and (iii) the elastic third-mode response for long-period buildings.

Numerical examples demonstrate that the proposed predictor is less biased and results in less dispersion than Luco's original predictor.

Title: Probabilistic Demand Models and Fragility Curves for Reinforced Concrete Frames
Author: Ramamoorthy, Sathish K; Gardoni, Paolo; Bracci, Joseph M
Source: Journal of Structural Engineering (New York, N.Y.). Vol. 132, no. 10, pp. 1563-1572. Oct. 2006
Descriptors: Reinforced concrete; Probability theory; Frames; Probabilistic methods; Fragility; Retrofitting; Earthquake design; Seismic engineering; Gravitation; Seismic phenomena; Construction; Marketing; Demand; Earthquake construction; Grounds; Limit states; Methodology; Uncertainty; Strengthening

Abstract: Fragility curves are constructed to assess the seismic vulnerability of a hypothetical two-story reinforced concrete frame building designed only for gravity loads. Fragility curves are also developed for the same building modestly retrofitted by means of column strengthening. A Bayesian methodology is used to construct probabilistic demand models to predict the maximum inter-story drifts, given the spectral acceleration at the fundamental period of the building. The data for the models are obtained using two-dimensional inelastic time history analyses of the building for a suite of synthetic ground motions, developed for the Memphis region. The models are developed using both equality data and lower bound data, and are developed to properly account for both aleatory and epistemic uncertainties. In the absence of probabilistic capacity models for gravity load designed structures, capacity limit states are considered based on FEMA 356 guidelines and deterministic nonlinear pushover analyses. The results quantify the vulnerability of low-rise reinforced concrete frame buildings and show the effectiveness of seismic retrofitting in reducing the probability of failure.

Title: Application of Nonlinear Static Analyses to Probabilistic Seismic Demand Analysis
Author: Tothong, P; Cornell, C A
Source: 100th Anniversary Earthquake Conference. 2006
Descriptors: Approximation; Seismic phenomena; Demand analysis; Seismic engineering; Nonlinear dynamics; Spectra; Probabilistic methods

Abstract: Many approximate methods for Nonlinear Dynamic time history Analysis (NDA) have been recently proposed to estimate inelastic responses in multi-degree-of-freedom (MDOF) structures. This paper will focus on two methods: (i) the modified modal pushover analysis (MMPA, Chopra et al. (2004)), and (ii) the method proposed by Mori (Mori et al. 2004), which incorporates inelastic shape functions into the approximation. The objective is to extend these two approximate methods to develop a structural demand hazard curve via a Probabilistic Seismic Demand Analysis. Unlike assessing the performance of structures for a given ground motion hazard level, the structural demand hazard curve provides multi-objective

structural performance information, which has been integrated from all possible ground motion hazard levels. This paper will describe a methodology to approximate incremental dynamic analysis results from nonlinear static analyses, and then further to integrate such results with an inelastic spectral displacement (S_{di}) ground motion hazard curve ($\lambda_{S_{di}}$) (Tothong and Cornell 2005a). These inelastic spectral ordinates provide an improvement over conventional elastic ones. The resulting demand hazard curves are then compared with one obtained from rigorous NDA. This comparison identifies apparent strengths and weaknesses of using these methods as estimates of NDA results.

Title: Prediction of the median IDA curve by employing a limited number of ground motion records

Author: Azarbakht, Alireza; Dolsek, Matjaz

Source: Earthquake Engineering & Structural Dynamics. Vol. 36, no. 15, pp. 2401-2421. Dec. 2007

Abstract: A methodology has been proposed which can be used to reduce the number of ground motion records needed for the reliable prediction of the median seismic response of structures by means of incremental dynamic analysis (IDA). This methodology is presently limited to predictions of the median IDA curve only. The reduction in the number of ground motion records needed to predict the median IDA curve is achieved by introducing a precedence list of ground motion records. The determination of such a list is an optimization problem, which is solved in the paper by means of (1) a genetic algorithm and (2) a proposed simple procedure. The seismic response of a simple, computationally non-demanding structural model has been used as input data for the optimization problem. The presented example is a three-storey-reinforced concrete building, subjected to two sets of ground motion records, one a free-field set and the other a near-field set. It is shown that the median IDA curves can be predicted with acceptable accuracy by employing only four ground motion records instead of the 24 or 30 records, which are the total number of ground motion records for the free-field and near-field sets, respectively.

Title: Seismic structural demands taking accuracy of response estimation into account

Author: Mori, Yasuhiro; Maruyama, Yutaka

Source: Earthquake Engineering & Structural Dynamics. Vol. 36, no. 13, pp. 1999-2020. 25 Oct. 2007

Descriptors: Seismic phenomena; Seismic engineering; Hazards; Accuracy; Marketing; Demand; Earthquake design; Seismic response; Oscillators; Drift; Design engineering; Equivalence; Frames; Performance assessment; Nonlinear dynamics; Architecture; Nonlinearity; Demand analysis; Safety factors

Abstract: Predictors of seismic structural demands (such as inter-storey drift angles) that are less time consuming than nonlinear dynamic analysis (NDA) have proven useful for structural performance assessment and for design. Several techniques have

been proposed using the results of a nonlinear static pushover analysis. These techniques often use the maximum response computed via NDA of the inelastic oscillator that is equivalent to the original frame. In practice, it is desirable to estimate the response approximately via a simpler method such as an equivalent linearization technique and uniform hazard spectra at the site. In reliability-based seismic performance assessment and design of a structure, it is necessary to consider the level of accuracy of the techniques used in the assessment. A simple technique is proposed in this paper to estimate the r-year return period value of the inter-storey drift angle of a moment-resisting steel frame using a single uniform hazard spectrum of the r-year return period displacement of an elastic oscillator. The structural demand is estimated using the safety factors evaluated taking the variability in the seismic hazard, accuracy of the techniques for estimating structural response, and the structural performance level into account. The accuracy of the technique is investigated relative to the structural demand estimated more directly from the probability distributions of the seismic hazard.

Title: Approximate Seismic Performance Uncertainty Estimation Using Static Pushover Methods
Author: Fragiadakis, M; Vamvatsikos, D
Source: 14th World Conference on Earthquake Engineering: Innovation Practice Safety. 2008
Descriptors: Seismic phenomena; Uncertainty; Seismic engineering; Backbone; Estimates; Computer simulation; Approximation; Monte Carlo methods; Tools; Hardening; Earthquake construction; Nonlinear dynamics; Earthquake engineering; Stiffness; Strength; Stopping; Methodology; Ingredients; Hysteresis

Abstract: An approximate method based on the static pushover is introduced to estimate the seismic performance uncertainty of structures having uncertain parameters. Performance uncertainty is one of the driving forces behind modern seismic guidelines (e.g. FEMA-350) and it is arguably an essential ingredient of Performance-Based Earthquake Engineering (PBEE). We propose a methodology that uses a minimum of static nonlinear analyses and is capable of accurately estimating the demand and capacity epistemic uncertainty. As a testbed, the well-known nine-story LA9 steel frame is employed using beam-hinges with uncertain backbone properties. These range from simple elastic-perfectly plastic backbones with kinematic hardening to full quadrilinear backbones with pinching hysteresis, including an elastic, a hardening, a negative stiffness and a residual plateau branch, terminating with a final drop to zero strength. The properties of the backbone can be fully described by six parameters which are considered uncertain with given mean and standard deviation values. Using latin hypercube sampling with classic Monte Carlo simulation, the pushover curve is shown to be a powerful tool that can accurately estimate the uncertainty in the seismic performance. Coupled with the SPO2IDA tool, such estimates can be applied at the level of the results of nonlinear dynamic analysis, allowing the evaluation of seismic capacity uncertainty even close

to global dynamic instability. In summary, the method presented can inexpensively supply the uncertainty in the seismic performance of first-mode dominated buildings, offering for the first time an estimator of the accuracy of typical performance calculations.

Title: Structural Seismic Performance Evaluation in Consideration of Earthquake Ground Motion Uncertainties Using Convex Set Model
Author: Jia, Lizhe; Duan, Zhongdong
Source: Advances in Structural Engineering. Vol. 11, no. 3, pp. 269-279. June 2008
Descriptors: Seismic phenomena; Seismic engineering; Earthquake construction; Performance evaluation; Mathematical models; Probability theory; Uncertainty; Probabilistic methods; Loads (forces); Reinforced concrete; Displacement; Marketing; Set theory; Shear; Demand; Acceleration

Abstract: When data is insufficient to support a probabilistic assumption, the structural seismic performance evaluation results with probabilistic approach are suspicious. In this paper, the convex set theory, which requires much less information, is employed to model the uncertainties of peak acceleration and frequency characteristics of earthquake ground motions. The bounds of shear forces are first derived with Chinese seismic code, and then a lateral bound load method for Pushover analysis is conducted. Then the convex analysis is integrated into Pushover analysis to study the bounds of structural capacity. Furthermore, the bounds of earthquake demand are deduced with the bounded convex set model and Chinese seismic code. The bounds of target displacement are obtained using capacity spectrum method. The seismic performance of structure is then evaluated with an interval. Finally, seismic performance evaluation of a three-storey RC building is given to demonstrate the benefits of the proposed method.

Title: Maximum Displacement Response of SMRF Buildings Considering Spectral Characteristics of Ground Motions and Uncertainty in Component Strength
Author: Oba, Maya; Mori, Yasuhiro
Source: Journal of Structural and Construction Engineering. Vol. 73, no. 628, pp. 859-866. June 2008
Descriptors: Mathematical models; Strength; Uncertainty; Demand; Spectra; Marketing; Seismic phenomena; Environmental studies; Nonlinear dynamics; Seismic engineering; Earthquake design; Buildings; pH; Earthquake construction; Displacement; Design engineering; Random variables; Performance assessment

Abstract: It is important to estimating seismic structural demands simply and precisely for structural performance assessment and for design. Nonlinear dynamic analysis (NDA) is generally used to evaluate structural response to a given ground motion, and the result is considered to be rigorous. However, there exists uncertainty in the strength of structural components, and structural response to the ground motion

should be considered as a random variable. In this sense, NDA using a deterministic structural model can be considered as one of predictors of structural demands. In this paper, the influence of the uncertainty in strength of structural components on structural response is investigated considering spectral characteristics of ground motions. Then the accuracy of NDA using deterministic structural models as well as simple predictors such as Calculation of Response and Limit Strength and Inelastic Modal Predictor is investigated using numerical examples.

H-6 Design Methods

Title: Seismic design based on the yield displacement
Autho: Aschheim, Mark
Source: Earthquake Spectra. Vol. 18, no. 4, pp. 581-600. Nov. 2002
Descriptors: Multistory steel moment-resisting frames; nonlinear analysis; Nonlinear static pushover analysis; Dynamic properties

Abstract: Although seismic design traditionally has focused on period as a primary design parameter, relatively simple arguments, examples, and observations discussed in this paper suggest that the yield displacement is a more stable and more useful parameter for seismic design. The stability of the yield displacement is illustrated with four detailed examples, consisting of moment-resistant frame buildings. Each frame is designed to limit roof drift for a specific ground motion using an "equivalent" single degree-of-freedom model in conjunction with Yield Point Spectra. The effectiveness of the simple design method is established by nonlinear dynamic analysis. Yield displacements were stable and consistent while the fundamental periods of vibration (and lateral stiffness) required to meet the performance objective differed substantially.

Title: Deformation-based design of shear wall buildings
Author: Ekwueme, Chukwuma G.; Kubischta, Melissa A.
Source: Seventh U.S. National Conference on Earthquake Engineering (7NCEE): Theme: Urban Earthquake Risk [electronic resource]; 10 pages pp. 2002
Descriptors: Masonry shear walls; displacement-based design; Multistory shear walls; nonlinear static pushover analysis; Limit design; United States; building codes

Abstract: Engineers have long understood that displacements are the primary result of building response to earthquakes. However, most seismic design codes still utilize force-based procedures that can sometimes produce designs that respond unfavorably when subjected to a wide range of ground motion intensity. This paper presents a deformation-based approach for the seismic design of buildings that utilize masonry or concrete shear walls as the primary lateral-load-resisting elements. The methodology is a two-phased procedure that enables the structural engineer to use displacements as the principal variables in the design process. Such an approach is particularly useful for performance-based design since displacements and the

corresponding deformations such as strains and rotations can be used to determine the acceptability of earthquake response for various structural performance goals. The first phase of the design method involves the development of a preliminary design based on properties of typical shear walls, evaluation of the structural characteristics of specific walls, and estimates of the displacement demand from response spectra. The paper presents procedures for completing this preliminary design in a manner that allows the designer to incorporate ductility into the initial phase of the design process. The second phase involves confirming, or modifying, the preliminary design with moment-curvature computations that more accurately calculate the properties of the walls and nonlinear analyses to determine their response to the design earthquakes. The deformation-based procedure is illustrated on a typical masonry shear wall building. Comparisons in performance with a design using typical code procedures are made for various levels of ground motion intensity. The results of the comparisons show that the displacement-based design methodology, in which the designer has more control over the behavior of the structure, yields more predictable response and thus provides engineers with more confidence in their designs.

Title: Non linear analysis based seismic design
Author: Romao, Xavier; Costa, Anibal; Delgado, Raimundo
Source: The Twelfth European Conference on Earthquake Engineering [Proceedings] [electronic resource] , pp. 10 pages. 2002
Descriptors: Mathematical models; Design engineering; Earthquake design; Seismic phenomena; Earthquake engineering; Resources; Computer simulation; Seismic engineering; Reinforced concrete; Cost engineering; Structural design; Nonlinear dynamics; Design factors; Linear analysis; Equivalence

Abstract: In light of the actual knowledge of the behaviour of structures subjected to earthquakes, it can be easily verified that nonlinear structural behaviour models are more accurate in predicting the expected structural performance than methods based on equivalent horizontal forces scaled by a behaviour factor associated with elastic analysis. Most of the existing nonlinear design methodologies are based on pushover analysis and are mostly considered as design verification and performance evaluation tools. Computers allow for complex calculations to be performed with ease, reducing significantly the cost engineering calculations, thus making way for direct design to be based on nonlinear structural behaviour. A direct methodology for structural design of reinforced concrete structures based on nonlinear dynamic analysis is proposed. The basic steps are explained, pointing out some code-related issues and outlining methods for future development.

Title: A seismic design method of reinforced concrete wall-frame system with soft first story
Author: Sanada, Yasushi

Source: Proceedings of the Fourth Forum on Implications of Recent Earthquakes on Seismic Risk: Tokyo Institute of Technology, May 27-29, 2002 , pp. 309-318. 2002

Descriptors: Seismic phenomena; Earthquake design; Seismic engineering; Reinforced concrete; Softening; Seismic response; Design engineering; Shaking; Walls

Abstract: Response properties of a reinforced concrete wall-frame system with a soft first story have been investigated through a shaking table test and three-dimensional nonlinear analyses. In this paper, the effects of shear softening of reinforced concrete shear walls on the responses of this system were shown from pushover analyses considering both with and without the shear softening. A rational and practical seismic design method for this system was proposed based on the results of the test and analyses.

Title: Displacement-based seismic design of reinforced concrete structural wall buildings

Author: Tjhin, T. N.; Aschheim, M. A.; Wallace, J. W.

Source: Seventh U.S. National Conference on Earthquake Engineering (7NCEE): Theme: Urban Earthquake Risk [electronic resource]; 10 pages pp. 2002

Descriptors: Multistory reinforced concrete walls; nonlinear analysis; Nonlinear static analysis; Drift; roofs

Abstract: This paper puts forward a displacement-based design method for reinforced concrete structural wall buildings using yield displacement as the primary design parameter. The method employs an "equivalent" single-degree-of-freedom (ESDOF) system representation of the structure in conjunction with Yield Point Spectra (YPS), to determine the base shear strength required to limit drift and ductility demands to satisfy multiple seismic performance objectives. Graphical and analytical procedures allow design to be done for only the governing performance objective. Each performance level is expressed in terms of roof drift and plastic hinge rotation at the base of the member having the smallest displacement capacity. The plastic hinge rotation limit is determined based on the axial force level, shear stress level, and boundary confinement provided. Once the base shear coefficient is obtained, standard procedures are used to distribute the lateral forces over the height of the structure and to determine vertical and horizontal reinforcement and details for each member. A six-story structural wall building is used to illustrate the technique; nonlinear static and dynamic analyses of the building demonstrate the simplicity and effectiveness of the design method.

Title: A Simple Proposal for Seismic Demand Evaluation of Steel Framed Structures Based on Simplified Safety Domain

Author: Ito, Takumi; Ohi, Kenichi

Source: 13 WCEE: 13th World Conference on Earthquake Engineering Conference Proceedings. 2004

Descriptors: Structural steels; Earthquake design; Seismic engineering; Frames; Nonlinear dynamics; Polyhedrons; Failure modes

Abstract: To simplify the non-linear dynamic design procedure on steel framed structures to seismic actions, a new design-friendly reduced analysis is proposed as a vibration-mode failure-mode integrated analysis. The present method is based on two kinds of simplified plastic surface model: one modeling is a yield polyhedron model with reduced number of failure modes, and another much simpler model is a yield hyper-ellipsoidal model. The validity of the simplified analyses proposed is checked by comparison with a pseudo-dynamic response test on a 2-story steel frame specimen and a detailed analysis on a 9-story 3-bay frame model.

Title: Performance-Based Seismic Design of 3D R/C Buildings Using Inelastic Static and Dynamic Analysis Procedures

Author: Kappos, Andreas J; Panagopoulos, Georgios

Source: ISET Journal of Earthquake Technology. Vol. 41, no. 1, pp. 141-158. Mar. 2004

Descriptors: Seismic phenomena; Earthquake construction; Design engineering; Reinforced concrete; Hinges; Displacement

Abstract: A performance-based design procedure for realistic 3D reinforced concrete (R/C) buildings is presented, that involves the use of advanced analytical tools. Depending on the building configuration, use of two alternative tools is suggested, i.e. either time-history analysis for appropriately scaled input motions, or inelastic static (pushover) analysis, both for two different levels of earthquake loading. The critical issues of defining appropriate input for inelastic dynamic analysis, setting up the analytical model that should account for post-yield behaviour of the plastic hinge zones, defining loading in two directions and target displacement for the pushover analysis, and detailing in a way consistent with the deformations derived from the advanced analysis, are discussed. The proposed method is then applied to a regular multistorey reinforced concrete 3D frame building and is found to lead to better seismic performance than the standard code (Eurocode 8) procedure, and in addition leads to a more economic design of transverse reinforcement in the members that develop very little inelastic behaviour even for very strong earthquakes.

Title: Preliminary Design and Inelastic Verification of Earthquake-Resistant Structural Systems

Author: Rubinstein, Marcelo; Moller, Oscar; Giuliano, Alejandro; Martinez, Marcelo

Source: 13 WCEE: 13th World Conference on Earthquake Engineering Conference Proceedings. 2004

Descriptors: Earthquake design; Seismic phenomena; Displacement; Ductility

Abstract: A displacement-based design methodology for a preliminary seismic design of structures is presented. The approach includes two ground motion input levels: occasional and rare. The occasional earthquake level design is governed by elastic structural response and controlled by limiting inter-story drifts provided by

codes for serviceability states. The limiting engineering states associated with the exceptional ground motion level have been adopted as: maximum inter-story drifts given by standards, global ductility and damage index. By using these limiting states within the conceptual design philosophy, and based on a simple hand-made calculations, structural components are sized. The seismic demand is defined by both the elastic and the inelastic displacement response spectra for the occasional and rare earthquake input level respectively. The system yield displacement is derived from the components geometry and longitudinal rebar yielding. Thus, the structural stiffness is computed as the ratio of the strength suitable provided to the mentioned yielding deformation. Preliminary design results are verified by both push-over and dynamic time history analyses, applying a 3D mathematical model with components connected by rigid slabs at each story level. Three degrees of freedom per story are assumed: two horizontal displacements and a twist around the vertical axis. Each component is discretized by nonlinear bar elements. The Newmark algorithm is applied for the step-by-step integration of the equation of motion. The equilibrium at each time-step is achieved by using the Newton-Raphson iterative scheme. Numerical example of a conventional buildings with asymmetry-plan is presented which can be suitable assessed by the proposed approach since the post-elastic torsion effects are taken into account in the evaluation

Title: Displacement-based seismic design method of RC frames.
Author: Liang, Xingwen; Huang, Yajie; Yang, Qiwei
Source: Tumu Gongcheng Xuebao (China Civil Engineering Journal). Vol. 38, no. 9, pp. 53-60. Sept. 2005
Descriptors: Reinforced concrete; Seismic design; Displacement; Drift; Frames; Columns (structural); Elastoplasticity; Stress concentration; Buildings; Spectral lines

Abstract: According to the characteristics of RC frames, its seismic performance is divided into three levels: serviceability, life-safety, and collapse protection. The three levels are quantified with storey drift ratios. Applying the inverted triangular distribution of lateral force to the cantilever column of identical section, and the displaced shape of the column is regarded as the initial mode of lateral displacement. The multi-degree-of-freedom system is transformed into an effective single-degree-of-freedom system, and the corresponding equivalent parameters are derived. The target displacement is determined according to the corresponding performance level, and the lateral displacement curve is modified by the assumed lateral displacement mode. Based on equivalent linearization, the equivalent period is determined by using the elastic displacement response spectra, and then the structural members are designed. The buildings are analyzed by using a static elastoplastic analysis method, if the calculated significantly different from drift curve is the initial assumed shape, then take the pushover drift curve as the modifying drift shape and calculate again. It is demonstrated the method is accurate enough to be employed in building evaluation and design.

Title: Dynamic Behaviour of Reinforced Concrete Frames Designed With Direct Displacement-Based Design
Author: Pettinga, J; Priestley, M J N
Source: Journal of Earthquake Engineering. Vol. 9, no. Special Issue 2, pp. 309-330. 2005
Descriptors: Frames; Displacement; Earthquake design; Seismic phenomena; Columns (structural); Force distribution; Reinforced concrete; Dynamic structural analysis; Bending moments

Abstract: The Direct Displacement-based Design methodology is applied to six reinforced concrete tube-frame structures and tested using inelastic time-history analyses. Using the established design method inter-storey drifts are found to exceed assumed drift limits, and a series of changes to the design displacement profiles and lateral force distribution are proposed to improve agreement. These changes are then applied to the six frames and further time-history analyses carried out at different earthquake intensities. The inter-storey drift behaviour is found to be significantly improved, with code-based drift limits consistently satisfied. Finally a revised form of the Modified Modal Superposition is proposed to account for higher-mode amplification of column shear forces, while a simple intensity-dependent scaling factor to be applied in the capacity design process is developed for column bending moments. The suggested equations are applied to the frame designs, and found to be in acceptable agreement with time history results at a range of earthquake intensities.

Title: Inclusion of P-Delta Effect in Displacement-Based Seismic Design of Steel Moment Resisting Frames
Author: Asimakopoulos, Aristidis; Karabalis, Dimitris; Beskos, Dimitri
Source: First European Conference on Earthquake Engineering and Seismology. 2006
Descriptors: Displacement; Frames; Coefficients; Seismic design; Steels; Beams (structural); Amplification; Design engineering; Stability; Seismic phenomena; Elastoplasticity; Dynamical systems; Seismic response; Inclusions; Bays; Iron and steel industry; Steel making; Degrees of freedom; Seismic engineering

Abstract: A procedure for treating the P-Delta effect in the direct displacement-based seismic design of elastoplastic regular steel moment resisting frames is proposed. A simple formula for the yield displacement amplification factor as a function of ductility and the stability coefficient is derived on the basis of the seismic response of an inelastic single degree of freedom system taking into account the P-Delta effect. Extensive parametric seismic inelastic analyses of plane moment resisting steel frames result in a simple formula for the dynamic stability coefficient as a function of the number of bays and stories of a frame as well as the column to beam stiffness ratio. Thus, the P-Delta effect can be easily taken into account in a displacement-based seismic design through the stability coefficient and the yield displacement amplification factor. A simple design example serves to illustrate the application of the proposed method and demonstrate the importance of P-Delta effects in design.

Title: A Simple Design Procedure for Tied Braced Frames
Author: Rossi, Pier Paolo; Bosco, Melina; Lombardo, Anna
Source: First European Conference on Earthquake Engineering and Seismology. 2006
Descriptors: Collapse; Frames; Links; Braced; Dynamic tests; Earthquake design; Optimization; Grounds; Seismic phenomena; Displacement; Seismic engineering; Dynamics; Hypotheses; Acceleration

Abstract: The paper describes a design procedure of tied braced frames aiming at an optimal collapse seismic behaviour, i.e. at a global collapse mechanism characterised by relatively uniform plastic rotations of links. In order to achieve direct and efficient control over the value of the ultimate peak ground acceleration, the procedure is founded on the displacement-based approach. Applications are carried out on different numbers of storeys and lengths of links and incremental dynamic analyses on ten artificially generated accelerograms performed with the aim of obtaining confirmation of the efficiency of the design hypotheses and methodologies.

Title: A Method to Improve Distribution of Story Drift Angle Responses in CFT Moment-Resistant Frames Under Severe Earthquakes
Author: Kawakami, Shujiro; Wano, Akihiko Ka; Okamoto, Yuuki
Source: Journal of Structural and Construction Engineering , no. 585, pp. 223-230. Nov. 2004
Descriptors: Mathematical models; Drift; Frames; Dynamic tests; Earthquakes; Mathematical analysis; Design engineering; Seismic phenomena; Nonlinearity; Dynamics; Damage; Shear strength

Abstract: As the performance-based design will be widely used, it will be more necessary for a frame to be evaluated by the responses obtained from a dynamic analysis. In this paper, we proposed a simple method to modify the story shear strength so as to make the story drift distribution smooth over the building height, being based on a pre-calculated story responses. The method is derived from the theory of damage concentration by Akiyama. The applicability of the method was confirmed by a numerical calculation of a full nonlinear analysis.

Title: Performance-based seismic design of building structures.
Author: Ghorbanie-Asl, Mohammad
Source: Dissertation Abstracts International. Vol. 68, no. 5. 2007
Descriptors: Mathematical models; Design engineering; Grounds; Compatibility; Drift; Estimates; Degrees of freedom; Mathematical analysis; Preliminary designs; Strength; Seismic phenomena; Shear; Walls; Demand; Nonlinearity; Resists; Spectra; Standards; Earthquake design

Abstract: A new method for the displacement-based design (DBD) of a variety of structures to resist the earthquake forces experienced by them is developed. The proposed method requires the determination of yield and ultimate displacements of the structure. For preliminary design these parameters are determined from approximate empirical relationships. The required strength of the structure is then

determined from the inelastic demand spectrum corresponding to the ductility capacity and the estimated yield strength. The method can be used for a multi degree of freedom system by transforming it into an equivalent single degree of freedom system. For final design, a modal analysis is carried out on a model of the structure that is based on its preliminary design. A pushover analysis of the structure for forces that are distributed according to the first mode now provides better estimates of the yield and ultimate displacements. These refined estimates are then used to obtain a more precise value of the required strength. Iterations may have to be carried out to obtain convergence between the assumed and calculated values of the design displacements. Finally, to account for the effect of higher modes in shear wall structures and high-rise moment resisting frames, the standard modal pushover analysis (MPA) method available in the published literature is used. Nonlinear time history analyses of the structures designed according to the proposed DBD method are carried out for sets of ground motions that are compatible with the design response spectra. Procedures for the selection and scaling of the spectrum compatible ground motions are studied. A set of such ground motions that is compatible with the UHS of Montreal corresponding to a probability of exceedance of 2% in 50 years is developed as a part of the present research. This set and a similar set for Vancouver, developed in another research study, are used in time history analyses, first to develop relationships between inter-story drift and roof drift, and second to validate the proposed DBD method.

Title: Preliminary design and inelastic assessment of earthquake-resistant structural systems
Author: Rubinstein, Marcelo; Moller, Oscar; Giuliano, Alejandro
Source: Structural Engineering and Mechanics. Vol. 26, no. 3, pp. 297-314. June 20 2007
Descriptors: Seismic phenomena; Asymmetry; Dynamics; Displacement; Dynamical systems; Yield point; Eccentricity; Demand; Seismic engineering; Iron; Spectra; Earthquake design; Mathematical analysis; Dynamic tests; Containers; Seismic design; Preliminary designs; Earthquake construction; Marketing

Abstract: A preliminary performance-based seismic design methodology is proposed. The top yield displacement of the system is computed from these of the components, which are assumed constant. Besides, a simple procedure to evaluate the top yield displacement of frames is developed. Seismic demands are represented in the form of yield point spectra. The methodology is general, conceptually transparent, uses simple calculations based on first principles and is applicable to asymmetric systems. To consider a specific situation two earthquake levels, occasional and rare are considered. The advantage of an arbitrary assignment of strength to the different components to reduce eccentricities and improved the torsional response of the system is addressed. The methodology is applied to an asymmetric five story building, and the results are verified by push-over analysis and non linear dynamic analysis.

Title: Yield displacement-based seismic design of RC wall buildings
Author: Tjhin, Tjen N; Aschheim, Mark A; Wallace, John W
Source: Engineering Structures. Vol. 29, no. 11, pp. 2946-2959. Nov. 2007
Descriptors: Walls; Spectra; Seismic design; Reinforced concrete; Yield point; Buildings; Displacement; Design engineering; Roofs; Shear strength; Shear; Nonlinear dynamics; Drift; Nonlinearity; Dynamic tests; Great Britain; Hazards; Hinges; Equivalence

Abstract: A simple method is presented for the performance-based seismic design of ductile RC wall buildings. The design method is based on an estimate of the roof displacement at yield. The required base shear strength is determined using Yield Point Spectra based on an 'equivalent' single-degree-of-freedom (ESDOF) system representation of the wall system. The walls are designed for a single base shear force that is established based on one or more performance objectives, where each performance level is expressed in terms of roof drift and plastic hinge rotation at the base of the wall. A six-story building is used as an example to illustrate the method, with the hazard represented by either smoothed design spectra or recorded ground motions. Nonlinear static and dynamic analyses confirm the adequacy of the method to achieve the intended performance objectives.

Title: Displacement-based seismic design of reinforced concrete shear wall buildings.
Author: Elrodesly, Amr Ahmed Salah Eldin
Source: Masters Abstracts International. Vol. 46, no. 5. 2008
Descriptors: Walls; Shear; Buildings; Marketing; Design engineering; Estimates; Ductility; Demand; Reinforced concrete; Seismic phenomena; Displacement; Yield strength; Earthquake construction; Seismic design; Demand analysis; Hazards; Seismic engineering; Nonlinearity; Collapse

Abstract: A displacement-based design method for the seismic design of symmetric and unsymmetric but torsionally stiff buildings with reinforced concrete shear walls is presented. For the preliminary design of such buildings approximate estimates of the yield displacements of individual walls are required: they are calculated from simple empirical relations that depend only on the geometry of the walls. The relative strengths of the walls are then selected, and based on these the global yield displacement is obtained. The ultimate displacement is determined so as to ensure stability under P-Delta effects, keep the ductility demand within ductility capacity, and limit the maximum storey drift to that specified by the codes in order to achieve the near collapse performance level under specified seismic hazard represented by a uniform hazard spectrum. For a multi storey building the structure is converted to an equivalent single-degree-of-freedom system using an assumed deformation shape to represent the first mode shape. The required base shear strength and the corresponding base moment of the system are determined from the inelastic demand spectrum corresponding to the ductility demand, or the ratio of ultimate to yield displacement. In subsequent iterations a pushover analysis for the force distribution

based on the first mode is used to obtain better estimates of the yield and ultimate displacements. When the process has converged, a multi-mode pushover analysis is carried out to find more accurate estimates of the shear demands. For a torsionally stiff unsymmetric building the multi-mode pushover analysis is carried out using only the lateral displacement dominant mode shapes. The contribution of the rotational or torsion dominant mode shapes to the different response parameters is negligible. The evaluation of the two design methods is performed using rigorous nonlinear response history analyses for 20 ground motion records scaled to match the seismic demand represented by the UHS of the city of Vancouver. The results of the nonlinear response history analysis show that: (1) the near collapse performance level is achieved for the symmetric buildings and for each edge of the unsymmetric buildings, (2) the roof displacements that the symmetric building and each edge of the unsymmetric building have been designed to experience are not exceeded except for very few records, (3) the square root of the sum of squares (SRSS) rule for combining the modal contributions somewhat underestimates the base shear, while the absolute sum (ABSSUM) combination rule provides a conservative estimate of the base shear. Thus the design methods developed in this work provide a safe and conservative design for the two types of buildings.

Title: Seismic Evaluation of Eccentrically Braced Steel Frames Designed by Performance-Based Plastic Design Method
 Author: Furukawa, Sachi; God, Subhash C; Chao, Shih-Ho
 Source: 14th World Conference on Earthquake Engineering: Innovation Practice Safety. 2008
 Descriptors: Frames; Eccentricity; Hysteresis; Steels; Links; Shear; Degradation; Braced; Earthquake design; Seismic response; Seismic phenomena; Seismic engineering; Steel making; Iron and steel industry; Strength; Methodology

Abstract: This paper discusses the influence of degrading hysteretic behavior of shear links and P-Delta effect on seismic response of steel Eccentrically Braced Frames (EBF). A 10-story example frame was designed by a newly developed Performance-Based Plastic Design (PBSD) methodology and current code method. The responses of the two frames under inelastic pushover and time history analyses are compared to evaluate the influence of strength degradation of shear links and the P-Delta effect.

Title: Displacement-Based Seismic Design of Regular Reinforced Concrete Shear Wall Buildings
 Author: Humar, Jagmohan
 Source: 14th World Conference on Earthquake Engineering: Innovation Practice Safety. 2008
 Descriptors: Displacement; Marketing; Shear; Demand; Estimates; Ductility; Walls; Buildings; Seismic design; Reinforced concrete; Shear strength; Drift; Demand analysis; Preliminary designs; Empirical analysis; Equivalence; Deformation; Approximation; Stability

Abstract: A displacement based method for the seismic design of reinforced concrete shear wall buildings of regular shape is presented. For preliminary design, approximate estimates of the yield and ultimate displacements are obtained, the former from simple empirical relations, and the latter to keep the ductility demand within ductility capacity and to limit the maximum storey drift to that specified by the codes. For a multi storey building the structure is converted to an equivalent single-degree-of-freedom system using an assumed deformation shape that is representative of the first mode. The required base shear strength of the system is determined from the inelastic demand spectrum corresponding to the ductility demand. In subsequent iterations a pushover analysis for the force distribution based on the first mode is used to obtain better estimates of yield and ultimate displacements taking into account stability under P-A effect. A multi-mode pushover analysis is carried out to find more accurate estimates of the shear demand.

Title: An Energy Based Method for Seismic Evaluation Of Structures
Author: Leelataviwat, Sutat; Saewon, Winai; Goel, Subhash C
Source: 14th World Conference on Earthquake Engineering: Innovation Practice Safety. 2008
Descriptors: Dynamical systems; Nonlinear dynamics; Design engineering; Earthquake design; Seismic phenomena; Seismic engineering; Direct power generation; Energy use; Displacement; Marketing; Nonlinearity; Coefficients; Demand; Hazards

Abstract: This paper presents a seismic evaluation procedure based on an energy concept that has been recently developed and successfully used for design purposes called Performance-Based Plastic Design (PBPD). The underlying theory and the framework for carrying out the analysis are first presented. The skeleton force-displacement (capacity) curve of the structure is converted into energy capacity plot which is superimposed over the corresponding energy demand plot for the given hazard level to determine the expected peak response. The method is applied to a number of example single-degree-of-freedom (SDOF) and multi-degree-of-freedom (MDOF) structural systems with excellent results. The results are compared with those obtained from nonlinear dynamic analyses as well as those from methods proposed by other investigators including the Modal Pushover Analysis Method and the FEMA Displacement Coefficient Method. For SDOF systems, the results indicate that the proposed method provides response values that are identical to those obtained from a well-established procedure using inelastic design spectrum. For MDOF systems also, the proposed method provides response values that are reliable when compared to the results from non-linear dynamic analysis and other well-established nonlinear static procedures.

Title: Rational Use of Inelastic Response in Seismic Design
Author: Mwafy, A M
Source: 14th World Conference on Earthquake Engineering: Innovation Practice Safety. 2008

Descriptors: Design engineering; Reduction; Demand analysis; Inelastic analysis; Marketing; Simulation; Seismic phenomena; Seismic response; Grounds; Exploitation; Seismic engineering; Earthquake design; Buildings; Correlation analysis; Seismic design; Preliminary designs; Earthquake construction; Reinforced concrete; Uncertainty

Abstract: Inelastic analysis procedures effectively accounts for several sources of force reduction. They are therefore more dependable means for predicting inelastic demands compared with elastic analysis procedures. Encouragement to employ the former procedures is still limited and designers tend to favor elastic procedures. The significant reduction allowed in response parameters obtained from elastic analysis procedures unlike those from inelastic analysis results in high uncertainties and discourages the effective exploitation of the latter procedure in design. The present study proposes a simple and theoretically-based approach that utilizes inelastic seismic response to refine the initial structural design. To effectively describe the proposed design approach, correlation of seismic demands obtained from different analysis procedures carried out using a comprehensive set of reinforced concrete buildings of different characteristics is investigated. Verified analysis tools and rational input ground motions are employed in the elastic and inelastic simulations. The benefits obtained from assessing the preliminary design using pushover analysis to determine the need for additional inelastic simulations are discussed. The presented approach enables engineers to arrive at a realistic and cost-effective design without compromising safety.

Title: Seismic design of irregular space steel frames using advanced methods of analysis

Author: Vasilopoulos, A A; Bazeos, N; Beskos, D E

Source: Steel & Composite Structures. Vol. 8, no. 1, pp. 53-84. Feb. 2008

Descriptors: Frames; Mathematical models; Mathematical analysis; Seismic design; Design engineering; Structural steels; Limit states; Nonlinear dynamics; Damage; Seismic phenomena; Eccentricity; Nonlinearity; Dynamic tests; Civil engineering; Containers; Time domain; Defects; Compatibility; Finite element method

Abstract: A rational and efficient seismic design methodology for irregular space steel frames using advanced methods of analysis in the framework of Eurocodes 8 and 3 is presented. This design methodology employs an advanced static or dynamic finite element method of analysis that takes into account geometrical and material non-linearities and member and frame imperfections. The inelastic static analysis (pushover) is employed with multimodal load along the height of the building combining the first few modes. The inelastic dynamic method in the time domain is employed with accelerograms taken from real earthquakes scaled so as to be compatible with the elastic design spectrum of Eurocode 8. The design procedure starts with assumed member sections, continues with the checking of the damage and ultimate limit states requirements, the serviceability requirements and ends with the

adjustment of member sizes. Thus it can sufficiently capture the limit states of displacements, rotations, strength, stability and damage of the structure and its individual members so that separate member capacity checks through the interaction equations of Eurocode 3 or the usage of the conservative and crude q-factor suggested in Eurocode 8 are not required. Two numerical examples dealing with the seismic design of irregular space steel moment resisting frames are presented to illustrate the proposed method and demonstrate its advantages. The first considers a seven storey geometrically regular frame with in-plan eccentricities, while the second a six storey frame with a setback.

Title: Equivalent Static Loads for Nonlinear Seismic Design of Spatial Structures

Author: Zhang, Jingyao; Ohsaki, Makoto; Uchida, Atsushi

Source: 14th World Conference on Earthquake Engineering: Innovation Practice Safety. 2008

Descriptors: Equivalence; Earthquake design; Seismic response; Seismic phenomena; Earthquake dampers; Seismic engineering; Mathematical models; Damping; Trusses; Elastic systems; Seismic design; Dissipation; Static loads; Linearization; Accuracy

Abstract: A new approach to determination of equivalent static seismic loads is presented for evaluating peak seismic responses. The responses are estimated by series of multi-modal pushover analysis considering possible phase differences in the dominant modes: the loads are directly applied in the elastic systems, and the damping due to plastic dissipation is modeled by equivalent linearization in inelastic systems. The accuracy of the proposed method is demonstrated in the numerical example of an arch-type long-span truss.

Resource Paper 9, "Seismic Design using Target Drift, Ductility, and Plastic Mechanisms as Performance Criteria", pp. 289-310, 2009 NEHRP Recommended Seismic Provisions for New Buildings and Other Structures, FEMA-P750, 2009.

H.7 Applications

H.7.1 Masonry

Title: Evaluation of simplified models for lateral load analysis of unreinforced masonry buildings

Author: Kappos, Andreas J.; Penelis, Gregory G.; Drakopoulos, Christos G.

Source: Journal of Structural Engineering. Vol. 128, no. 7, pp. 890-897. July 2002

Descriptors: Lowrise unreinforced stone structures; nonlinear response; Perforated unreinforced masonry walls; nonlinear static pushover analysis; Kalamata; Greece earthquake; Sept. 13; 1986; damage; Displacements (structural)

Abstract: The paper aims at evaluating the relative accuracy of different models, mainly intended for use by practicing engineers, for the analysis of unreinforced masonry buildings, and to determine whether, and under what conditions, a simple

equivalent frame model can be used for design and/or assessment purposes. Several parametric analyses involving finite element (FE) models of two-dimensional and three-dimensional structures have been performed, first in the elastic range, using both refined and coarse planar meshes. They were followed by analyses of the same structures using equivalent frames with alternative arrangements of rigid offsets. Subsequently, two-dimensional nonlinear static (pushover) analyses of both FE and equivalent frame models were performed to check the validity of the conclusions drawn from the elastic analysis. The results presented shed some further light on the feasibility of using simplified and cost-effective analytical models as a tool for practical design and/or assessment of typical masonry structures.

Title: On the Use of Pushover Analysis for Existing Masonry Buildings
Author: Galasco, Alessandro; Lagomarsino, Sergio; Penna, Andrea
Source: First European Conference on Earthquake Engineering and Seismology. 2006
Descriptors: Masonry; Walls; Buildings; Seismic phenomena; Algorithms; Horizontal; Seismic engineering; Displacement; Earthquake construction; Loads (forces); Three dimensional; Assessments; Assembling; Nonlinearity; Critical point; Modelling; Adaptive algorithms; Simplification; Models

Abstract: The application of nonlinear static (pushover) procedures for the assessment of existing masonry buildings has been introduced into seismic codes (e.g. EC8, new Italian Seismic Code OPCM 3274/03), but it still includes several critical points in the implementation to real structures. The three-dimensional model of a masonry building can be obtained by assembling frame-type macro-element models of the walls and orthotropic membrane elements in order to represent the mechanical behaviour of flexible floors. This modelling, although very effective in representing the actual behaviour, does not allow to use common simplifications such as rigid floor motion. Moreover, a 3D pushover algorithm requires a predefined pattern of horizontal forces to be applied to the structure and, keeping constant the relative force ratios, the horizontal displacement of a control node is incremented. A new displacement-based algorithm for the adaptive pushover analysis of masonry walls and buildings is presented: the load pattern, in this case, is directly derived, step-by-step, by the actual deformed shape evaluated during the pushover analysis. The proposed procedure seems to be very powerful for in-plane analyses of walls, whilst it requires some corrections in order to be applied to three-dimensional masonry buildings.

Title: The Evaluation and Retrofit of a Historic Unreinforced Masonry Building Using Nonlinear Adaptive Pushover And Dynamic Analysis Methods
Author: Hachem, Mahmoud M; Paret, Terrence F; Searer, Gary R; Freeman, Sigmund A
Source: 14th World Conference on Earthquake Engineering: Innovation Practice Safety. 2008

Descriptors: Seismic phenomena; Historic; Earthquake construction; Nonlinear dynamics; Nonlinearity; Masonry; Mathematical models; Earthquake damage; Dynamical systems; Walls; Dynamic structural analysis; Retrofitting; Dynamics; Finishes; Dynamic characteristics; Vibration; Ordinances; Damage; Structural members

Abstract: Various nonlinear analysis techniques were used to analyze a historic unreinforced masonry landmark structure in San Francisco in its original and seismically retrofitted condition. The structure is a monumental 100-year old synagogue that survived the 1906 San Francisco Earthquake. Although the building escaped the Great 1906 earthquake with relatively little damage, the building was recently threatened with closure due to non-compliance with an Unreinforced Masonry Building Ordinance. The most appropriate structural solution consistent with preserving the historic fabric takes advantage of the dynamic separation between the modes predominated by in-plane and out-of-plane wall shaking. The solution consisted of a combination of intervention techniques, each developed to minimize disturbance to the nonstructural historic finishes and retain the original dynamic characteristics. The structure was subjected to linear and nonlinear static and dynamic analyses to benchmark its behavior during the 1906 earthquake. Adaptive pushover analyses were also performed using the first natural mode of vibration of each wall. To validate the full three-dimensional response of the building and to develop design forces for the new structural elements that were added to strengthen the system, a three-dimensional model was constructed in SAP2000 and subjected to static and dynamic analyses.

Title: Seismic Performance-Based Analysis of Confined Masonry Structures

Author: Lihong, Xiong; Qiushen, Xue

Source: 14th World Conference on Earthquake Engineering: Innovation Practice Safety. 2008

Descriptors: Masonry; Earthquake design; Seismic phenomena; Earthquake construction; Nonlinearity; Buildings; Walls; Brick; Promotion; Design engineering; Seismic engineering; Concrete construction; Mathematical models; Construction; Stiffness

Abstract: Confined masonry buildings (CMBs) have been widely used in China. The field survey conducted during the recent great Wenchuan Earthquake had been proved that the CMBs well designed and constructed performed well even in severely affected areas. However, the performance-based design for the CMBs has been few reported. In this paper based on the previous work conducted by the author a four-linear skeleton curve with negative stiffness for the confined masonry walls along with the parameters characterizing the different performance levels is developed. Nonlinear time history analysis (NTHA) and nonlinear static analysis -pushover analysis (POA) for four typical 5- to 7-story confined concrete/ brick masonry buildings are performed. From comparisons of the numerical results some

conclusions are made, they could be helpful for further investigation and promotion of a wider application of the CMBs.

Title: Displacement-Based Seismic Assessment of Low-Height Confined Masonry Buildings
Author: Amador, T.-G.; Oscar, Z.-C.; Jorge, R.-G.
Source: Earthquake Spectra. Vol. 25, no. 2, pp. 439-464. May 2009
Descriptors: Buildings; Masonry; Displacement; Seismic phenomena; Earthquake construction; Assessments; Seismic engineering

Abstract: This paper presents a practical displacement-based evaluation procedure for the seismic assessment of low-height regular confined masonry buildings. First, the so-called Coefficient Method established in several FEMA documents is adapted to obtain rapid estimates of inelastic roof displacement demands for regular confined masonry buildings. For that purpose, a statistical study of constant relative strength inelastic displacement ratios of single-degree-of-freedom systems representing confined masonry buildings is carried out. Second, a nonlinear simplified model is introduced to perform pushover analysis of regular confined masonry buildings whose global and local behavior is dominated by shear deformations in the masonry walls. The model, which can be applied through the use of commercial software, can be used to establish the capacity curve of such buildings. Finally, the evaluation procedure is applied to a three-story building tested at a shaking table testing facility.

H.7.2 Wood

Title: Simplified Seismic Analysis of Woodframe Structures
Author: Folz, Bryan; Filiatrault, Andre
Source: 13 WCEE: 13th World Conference on Earthquake Engineering Conference Proceedings. 2004
Descriptors: Shear walls; Seismic response; Seismic engineering; Computer programs; Hysteresis; Diaphragms; Dynamic characteristics; Cyclic loads

Abstract: A simple numerical model to predict the dynamic characteristics, quasi-static pushover and seismic response of woodframe buildings is presented. In this model, the building structure is composed of two primary components: rigid horizontal diaphragms and nonlinear lateral load resisting shear wall elements. The actual three-dimensional building is degenerated into a two-dimensional planar model using zeroheight shear spring elements connected between adjacent diaphragms or the foundation. The hysteretic behavior of each wood shear wall in the building can be characterized using an associated numerical model that predicts the walls load-displacement response under general quasi-static cyclic loading. In turn, in this model, the hysteretic behavior of each shear wall is represented by an equivalent nonlinear shear spring element. With this simple structural model, the response of the building is defined in terms of only three-degrees-of-freedom per floor. This numerical model has been incorporated into the computer program SAWS - Seismic

Analysis of Woodframe Structures. The predictive capabilities of the SAWS model are compared with shake table tests performed on a full-scale two-storey woodframe house as part of the recently completed CUREE-Caltech Woodframe Project. It is shown in this study that the SAWS computer program provides reasonably accurate estimates of the dynamic characteristics, quasi-static pushover and seismic response of this test structure. Furthermore, the SAWS program requires a minimum amount of data input and provides a fast computational turn-around time to analyze a given structure. As a result, this simple numerical model may be a useful structural analysis tool for practicing engineers and researchers.

Title: Performance Based Pushover Analysis of Wood Framed Buildings
Author: Jain, Anurag; Hart, Gary C; Ekwueme, Chukwuma; Dumortier, Alexis P
Source: 13 WCEE: 13th World Conference on Earthquake Engineering Conference Proceedings. 2004
Descriptors: Wood; Stiffness; Buildings; Seismic engineering; Computer programs; Finite element method; Structural members

Abstract: This paper presents a nonlinear pushover analysis to evaluate the structural performance of existing lightframe wood structures subjected to earthquake-induced ground motions. The seismic evaluation of such buildings requires analysis techniques to determine lateral load resisting capacities and predict inelastic performance parameters. The initial phase of evaluation presented herein comprises of assessing the mass and stiffness characteristics of the building through available plans or on-site building investigation. The stiffness of the building lateral force resisting structural elements (walls) are obtained from experiments performed on similar elements at the University of California, Irvine as part of the City of Los Angeles and the University of California, Irvine (COLA-UCI) Light-Frame Test Program directed by the Structural Engineering Association of California (SEAOC) [1]. Utilizing this force-deflection information, a pushover curve (capacity) for a light-frame wood building can be developed with a finite element computer program such as SAP2000 [2]. FEMA-356 [3] procedures are then adopted to evaluate the performance (response) of the building to a given level of ground motion (demand). Expected levels of drift, consequent damage and any deficiencies in the lateral force resisting capacity at a given level of ground motion intensity can be identified through this process and corrective measures can be implemented.

Title: Direct Displacement-Based Design of Glulam Timber Frame Buildings
Author: Zonta, D; Piazza, M; Zanon, P; Loss, C; Sartori, T
Source: 14th World Conference on Earthquake Engineering: Innovation Practice Safety. 2008
Descriptors: Displacement; Joints; Frames; Mathematical models; Timber; Warehouses; Simplification; Equivalence; Structural members; Fasteners; Estimates; Nonlinearity; Glulam; Buildings; Commercial buildings; Damping capacity; Methodology

Abstract: The work we present here aims at defining a direct Displacement Based Design (DBD) methodology that specifically applies to warehouses or commercial buildings, based on glued laminated timber portal frames. The case study investigated is an industrial wood-framed warehouse with two-hinged frames where the post-beam connections are semi-rigid moment-resisting joints with dowel-type fasteners. A necessary condition for applying DBD is that it be possible to estimate a priori (i) the target displacement of the portal and (ii) the equivalent damping ratio of the structure at the ultimate capacity. The general assumption is that the displacement capacity of the building mainly depends on single joint behavior and only to a smaller extent on the size of structural members. This observation lets us define a practical expression for calculation of the target displacement with only the dimensions of members and connections. Using pushover non-linear analyses, we demonstrated that the expression provides prior values of target displacement that are close to those obtained a posteriori using a much more refined model that takes account of the exact geometry of members and connections. The comparison with the results of Eurocode 8 shows that the DBD method potentially can overcome some of the simplifications that a Force Based Design (FBD) method necessarily leads to.

Title: Seismic performance evaluation and full-scale shaking table test of timber frame, conventional construction
Author: Isoda, Hiroshi
Source: Journal of Structural and Construction Engineering. Vol. 74, no. 636, pp. 321-330. Feb. 2009
Descriptors: Walls; Shear; Frames; Timber; Composite structures; Columnar structure; Wood; Seismic phenomena; Houses; Shake table tests; Horizontal; Nonlinearity; Seismic engineering; Mathematical analysis; Earthquake design; Performance evaluation; Seismic design; Accuracy; Construction

Abstract: This paper describes seismic behavior of three different wood construction, timber frame with moment resisting joints, conventional wood house with shear wall and composite structure consisting moment frame with resisting joint and shear wall on the same floor. Some performance evaluation procedure such as allowable stress design, horizontal load-carrying capacity method using pushover analysis and so on. The shaking table test was conducted to evaluate the capability of seismic design method. The non-linear skeleton curve is good agreement between analysis and test result in timber frame with moment resisting joint and composite structure but it is a key point to determine the limit deformation of column and joint in bending. In conventional construction, the skeleton curve calculated from cumulation of shear wall including non-structural wall in structural design is 10 to 20% lower than that of test result as well as the past similar study.

H.7.3 Reinforced Concrete

Title: Mathematical modelling of an infilled RC frame structure based on the results of pseudo-dynamic tests
Author: Dolsek, Matjaz; Fajfar, Peter
Source: Earthquake Engineering & Structural Dynamics. Vol. 31, no. 6, pp. 1215-1230. June 2002
Descriptors: Brick-reinforced concrete infill wall-frame interaction; nonlinear static pushover analysis; Europe; Eurocode 8; building codes; Story drift; Brick infill walls; pseudodynamic tests

Abstract: A technique is presented which employs the results of pseudodynamic tests for the development of a mathematical model. This technique, described by means of the mathematical modelling of a three-storey reinforced concrete frame building with infill in the bottom two storeys, which was tested at ELSA in Ispra, proved to be effective and to lead to a fairly accurate structural model. The results of analyses suggest that the global nonlinear seismic response of reinforced concrete frames with masonry infill can be adequately simulated by a relatively simple mathematical model, which combines beam elements with concentrated plasticity, simple connection elements, and equivalent strut elements representing the infill walls (provided that the infill does not fail out of plane and that no shear sliding failure occurs).

Title: Simplified non-linear seismic analysis of infilled reinforced concrete frames
Author: Dolsek, Matja; Fajfar, Peter
Source: Earthquake Engineering & Structural Dynamics. Vol. 34, no. 1, pp. 49-66. Jan. 2005
Descriptors: Nonlinear dynamics; Seismic engineering; Reinforced concrete; Frames; Dynamic structural analysis; Buildings

Abstract: The N2 method for simplified non-linear seismic analysis has been extended in order to make it applicable to infilled reinforced concrete frames. Compared to the simple basic variant of the N2 method, two important differences apply. A multi-linear idealization of the pushover curve, which takes into account the strength degradation which occurs after the infill fails, has to be made, and specific reduction factors, developed in a companion paper, have to be used for the determination of inelastic spectra. It is shown that the N2 method can also be used for the determination of approximate summarized IDA curves. The proposed method was applied to two test buildings. The results were compared with the results obtained by non-linear dynamic analyses for three sets of ground motions, and a reasonable accuracy was demonstrated. A similar extension of the N2 method can be made to any structural system, provided that an appropriate specific R- μ -T relation is available.

Title: Seismic Evaluation of Multi-Storey RC Frame Using Modal Pushover Analysis
Author: Chandrasekaran, S; Roy, Anubhab
Source: Nonlinear Dynamics. Vol. 43, no. 4, pp. 329-342. Mar. 2006
Descriptors: Mathematical models; Shear; Reinforced concrete; Frames; Seismic phenomena; Dynamic tests; Dynamics; Design engineering; Acceleration; Aseismic buildings; Drift; Links; Seismic engineering; Spectra; Tremors; Mathematical analysis; Standards; Earthquake design; Civil engineering

Abstract: The recently developed pushover analysis procedure has led a new dimension to performance-based design in structural engineering practices. With the increase in the magnitude of monotonic loading, weak links and failure modes in the multi-storey RC frames are usually formed. The force distribution and storey displacements are evaluated using static pushover analysis based on the assumption that the response is controlled by fundamental mode and no mode shift takes place. Himalayan-Nagalushai region, Indo-Gangetic plain, Western India, Kutch and Kathiawar regions are geologically unstable parts of India and some devastating earthquakes of remarkable intensity have occurred here. In view of the intensive construction activity in India, where even a medium intensity tremor can cause a calamity, the authors feel that a completely up-to-date, versatile method of aseismic analysis and design of structures are essential. A detailed dynamic analysis of a 10-storey RC frame building is therefore performed using response spectrum method based on Indian Standard Codal Provisions and base shear, storey shear and storey drifts are computed. A modal pushover analysis (MPA) is also carried out to determine the structural response of the same model for the same acceleration spectra used in the earlier case. The major focus of study is to bring out the superiority of pushover analysis method over the conventional dynamic analysis method recommended by the code. The results obtained from the numerical studies show that the response spectrum method underestimates the response of the model in comparison with modal pushover analysis. It is also seen that modal participation of higher modes contributes to better results of the response distribution along the height of the building. Also pushover curves are plotted to illustrate the displacement as a function of base shear.

Title: Shaking Table Tests On Thin Lightly Reinforced H-Shaped Structural Wall
Author: Coelho, Ema; Fischinger, Matej; Costa, Alfredo Campos; Joao, Maria; Silva, Falcao; Kante, Peter
Source: First European Conference on Earthquake Engineering and Seismology. 2006
Descriptors: Walls; Mathematical models; Beams (structural); Three dimensional; Reinforcement; Seismic phenomena; Computer simulation; Seismic engineering; Joining; Confining; Failure; Shear; Shake table tests; Piers; Boundaries; Earthquake design; Dynamic tests; Compressing; C (programming language)

Abstract: The paper presents an experimental program on a 5 storey structural wall physical model performed in LNEC 3D shaking table, in Lisbon, within the Project ECOLEADER-LIS. The characteristics of the reduced model and the test set-up are described, as well as the analysis of the main experimental results. Furthermore the results of numerical simulations are discussed. These tests had the main purpose of studying and evaluating the seismic resistance of thin lightly reinforced structural walls representative of the Central Europe practice. Particular issues have been addressed: (a) To investigate the influence of simultaneous 3D loading conditions. (b) To study walls with T (H) cross-sections. (c) To investigate the free edge of a T (H) shaped walls in compression and different types of confinement. (d) To investigate the behaviour of coupled walls and the behaviour of diagonally reinforced coupling beams in thin walls. (e) To calibrate and further develop numerical models. Inelastic dynamic analysis was also performed using Multiple-Vertical-Line-Element-Model (MVLEM), which was extended into 3D and implemented into OpenSees. This macro model proved the ability to simulate and predict the global behavior of the wall as well as the behavior of confined boundary areas and local extensions of longitudinal reinforcement. Considerable overstrength was observed in the wall with minimum reinforcement. However, its deformation capacity was limited to less than 1% of the height. Relatively thick slab enhanced the strength of thin coupling beams considerably. Consequently, they did not perform as expected in capacity design and high axial forces as well as shear failure were induced into the wall piers. The EC8 confining reinforcement proved to be efficient. Simpler details (i.e. U-shaped stirrups) might be acceptable for low walls (5-storey) and/or in the case of low seismic intensity. Sequence of loading and pre-cracking influenced the response considerably. The influence of bi-axial loading was relatively low.

Title: Practical Modeling for Nonlinear Seismic Response Of RCc Wall Structures

Author: Lepage, A; Neuman, S L; Dragovich, J J

Source: 100th Anniversary Earthquake Conference. 2006

Descriptors: Shear walls; Reinforced concrete; Seismic phenomena; Stiffness; Strengthening; Retrofitting; Yield strength; Rubber

Abstract: A simplified analytical model is proposed for modeling the nonlinear response of flexural-yielding reinforced concrete walls using standard structural analysis software. The program SAP2000 is used to implement the proposed model for evaluating structural response by means of user-defined nonlinear response history analysis. The model is useful for performing practical nonlinear static or nonlinear dynamic procedures. The use of the model is illustrated by its application to two structures previously tested in the laboratory. The walls are modeled using a fine mesh of linear-response shell elements coupled with uniaxial line elements. The use of line elements allows one to invoke the typical nonlinear response parameters available for such elements. The axial stiffness of the shell elements is gradually transferred to and from the line elements using stiffness modifiers between 0 and 1 at

the expected plastic hinge region and its vicinity. The nonlinear model assigned to the line element corresponds to a multilinear plasticity model. In this type of model the nonlinear force-deformation relationship is given by a multilinear curve defined by a set of points that need not be symmetrical with respect to the origin. The first slope of the force-deformation curve on either side of the origin defines the range of linear elastic response. The remaining segments define plastic deformations. The experimental data used to validate the proposed analytical model show agreement with the calculated response. The model is capable of capturing with reasonable accuracy the main response parameters of the wall structures: initial stiffness, onset of yielding, and yield strength. Additionally, the measured displacement response waveforms as well as the amplitudes are reasonably matched by the calculated values during the duration of strong base motion. The development of a scheme for structural strengthening of an existing 9 storey reinforced concrete mixed frame and shear wall building is described. This strengthening is to allow the addition of an 9 storey vertical extension and upgrade of the building's ability to resist earthquake effects as required by current New Zealand Building Codes. The change of use from office to residential triggers the Building Act requirement for the building to be strengthened to comply "as nearly as reasonably practicable" with the current code. The principal features of the scheme are to strengthen the structure of the existing building and to modify the building's dynamic performance in a major earthquake event. Structural modifications include: Modify the foundations and structure up to 2nd floor slab level to carry the modified structure above. Retrofit into each floor level (2 to 8) additional shear wall capacity with enhanced damping characteristics. These units are to reduce torsional eccentricity in the existing building. Strengthen selected elements of the existing structure. Introduce lead/rubber base isolation bearings on the roof of the existing structure to support the 9 storey steel frame vertical extension. An outline description of the building is provided with details of the modifications and how they will modify the dynamic behaviour of the building.

Title: Simulation of the shaking table test of a seven-story shear wall building
Author: Martinelli, Paolo; Filippou, Filip C
Source: Earthquake Engineering & Structural Dynamics. Vol. 38, no. 5, pp. 587-607. 25 Apr. 2009
Descriptors: Mathematical models; Shear; Walls; Simulation; Shake tables; Seismic phenomena; Discretization; Portland cements; Blinds; Nonlinear dynamics; Shake table tests; Beam-columns; Bending moments; Mathematical analysis; Strategy; Excitation; Fibers; Accuracy; Earthquake construction

Abstract: This paper presents the simulation of the nonlinear dynamic response of a full-scale seven-story reinforced concrete shear wall shaking table specimen under base excitations representing four earthquake records of increasing intensity. The study was motivated by the participation in the blind prediction contest of the shaking table specimen organized by University of California at San Diego (UCSD), NEES,

and Portland Cement Association (PCA). Owing to the time constraints of the contest a relatively simple two-dimensional (2d) model was used for the shear wall specimen. In this model, the shear wall was represented by 2d beam-column elements with fiber discretization of the cross-section that account for the interaction of the axial force with the bending moment. Upon conclusion of the contest, the available experimental measurements permitted a thorough examination of the analytical results. While the measured data confirmed the excellent accuracy of the model predictions, some limitations also became apparent. The paper addresses the benefits and limitations of the selected modeling strategy and investigates the sensitivity of this type of model to parameter selection.

H.7.4 Steel Braced Frames

Title: Estimation of seismic drift and ductility demands in planar regular X-braced steel frames
Author: Karavasilis, Theodore L; Bazeos, Nikitas; Beskos, Dimitri E
Source: Earthquake Engineering & Structural Dynamics. Vol. 36, no. 15, pp. 2273-2289. Dec. 2007
Descriptors: Drift; Structural steels; Ductility; Deformation; Seismic phenomena; Reduction; Seismic engineering; Seismic design; Earthquake construction; Marketing; Strength; Frames; Seismic response; Vibration; Demand; Columns (structural); Nonlinearity; Statistical analysis; Demand analysis

Abstract: This paper summarizes the results of an extensive study on the inelastic seismic response of X-braced steel buildings. More than 100 regular multi-storey tension-compression X-braced steel frames are subjected to an ensemble of 30 ordinary (i.e. without near fault effects) ground motions. The records are scaled to different intensities in order to drive the structures to different levels of inelastic deformation. The statistical analysis of the created response databank indicates that the number of stories, period of vibration, brace slenderness ratio and column stiffness strongly influence the amplitude and heightwise distribution of inelastic deformation. Nonlinear regression analysis is employed in order to derive simple formulae which reflect the aforementioned influences and offer a direct estimation of drift and ductility demands. The uncertainty of this estimation due to the record-to-record variability is discussed in detail. More specifically, given the strength (or behaviour) reduction factor, the proposed formulae provide reliable estimates of the maximum roof displacement, the maximum interstorey drift ratio and the maximum cyclic ductility of the diagonals along the height of the structure. The strength reduction factor refers to the point of the first buckling of the diagonals in the building and thus, pushover analysis and estimation of the overstrength factor are not required. This design-oriented feature enables both the rapid seismic assessment of existing structures and the direct deformation-controlled seismic design of new ones. A comparison of the proposed method with the procedures adopted in current seismic design codes reveals the accuracy and efficiency of the former.

H.7.5 Moment Frames

Title: Seismic Evaluation of Steel Moment Resisting Frame Buildings with Different Hysteresis and Stiffness Models

Author: Shin, Jiwook; Lee, Kihak

Source: 14th World Conference on Earthquake Engineering: Innovation Practice Safety. 2008

Descriptors: Magnetorheological fluids; Seismic phenomena; Seismic engineering; Buildings; Earthquake construction; Structural steels; Earthquake design; Hysteresis; Frames; Iron and steel industry; Steel making; Seismic design; Marketing; Beam-columns; Demand; Drift; Dissipation; Nonlinearity; Estimates

Abstract: Current seismic design procedures that apply to an estimation of inelastic deformation capacity of lateral force resisting systems have been questioned since no rationality exists for determining the values of R tabulated in seismic design code. For this study, 3-, 9- and 20-story Steel Moment Resisting Frame (MRF) buildings were designed to satisfy the seismic requirements based on the IBC 2000 including the current value of 8 for the steel special moment resisting frame (MRF) buildings. Then, these analysis building models were redesigned using 6 different hysteresis models, which provide an ability to dissipate seismic input energy, for the beam-column connections. These models were also extended to account for the effects of period of the buildings. A total of 90 different building models were subjected to 20 ground motions representing a hazard level of 2% probability of being exceeded in 50 years to estimate the seismic demands. Pushover and nonlinear time history analysis were performed to calculate story drift and plastic rotation demands. The effects of hysteresis models and various periods of the steel special MRF are investigated and discussed.

References - Supporting Documentation

- ACI, 2008, *Building Code Requirements for Structural Concrete and Commentary*, ACI 318-08, ACI Committee 318, American Concrete Institute, Farmington Hills, MI.
- AISC, 2005, *Prequalified Connections for Special and Intermediate Steel Moment Frames for Seismic Applications*, AISC 358-05, American Institute of Steel Construction, Inc., Chicago, IL.
- ASCE, 2003, *Seismic Evaluation of Existing Buildings*, ASCE Standard ASCE/SEI 31-03, American Society of Civil Engineers/Structural Engineering Institute, Reston, VA.
- ASCE, 2006, *Minimum Design Loads for Buildings and Other Structures*, ASCE Standard ASCE/SEI 7-05, including Supplement No. 1, American Society of Civil Engineers, Reston, VA.
- ASCE, 2007, *Seismic Rehabilitation of Existing Buildings*, ASCE Standard ASCE/SEI 41-06, American Society of Civil Engineers, Reston, VA.
- ASCE, 2010, *Minimum Design Loads for Buildings and Other Structures*, ASCE Standard ASCE/SEI 7-10, American Society of Civil Engineers, Reston, VA.
- ATC, 1996, *Seismic Evaluation and Retrofit of Concrete Buildings*, ATC 40 Report, Volumes 1 and 2, Applied Technology Council, Redwood City, CA.
- AzARBakht, A. and Dolsek, M., 2007, "Prediction of the median IDA curve by employing a limited number of ground motion records," *Earthquake Engineering and Structural Dynamics*, Vol. 36, pp. 2401-2421.
- AzARBakht A. and Dolsek M., 2010, "Progressive incremental dynamic analysis for first-mode dominated structures," *Journal of Structural Engineering*, ASCE, in production.
- Chopra, A. K. and Goel, R. K., 2001, *A Modal Pushover Analysis Procedure to Estimate Seismic Demands for Buildings: Theory and Preliminary Evaluation*, PEER 2001/03 Report, Pacific Earthquake Engineering Research Center, University of California Berkeley.

- Chopra, A.K. and Goel, R.K., 2002, "A modal pushover analysis procedure for estimating seismic demands for buildings," *Earthquake Engineering and Structural Dynamics*, Vol. 31, No. 3, pp. 561-582.
- Chopra, A.K., 2007, *Dynamics of Structures. Theory and Applications to Earthquake Engineering*, 3rd Edition, Pearson Prentice Hall, Upper Saddle River, NJ.
- Cordova, P.P., Deierlein, G.G., Mehanny, S.S., and Cornell, C.A., 2000, "Development of a two-parameter seismic intensity measure and probabilistic assessment procedure," *Proceedings of the 2nd U.S.-Japan Workshop on Performance-based Earthquake Engineering Methodology for Reinforced Concrete Building Structures*, Sapporo, Hokkaido, pp. 187-206.
- FEMA, 2000a, *Recommended Seismic Evaluation and Upgrade Criteria for Existing Welded Steel Moment-Frame Buildings*, FEMA 351 Report, prepared by the SAC Joint Venture, a partnership of Structural Engineers Association of California (SEAOC), Applied Technology Council (ATC), and California Universities for Research in Earthquake Engineering (CUREE) for the Federal Emergency Management Agency, Washington, D.C.
- FEMA, 2000b, *Recommended Postearthquake Evaluation and Repair Criteria for Welded Steel Moment-Frame Buildings*, FEMA 352 Report, prepared by the SAC Joint Venture, a partnership of Structural Engineers Association of California (SEAOC), Applied Technology Council (ATC), and California Universities for Research in Earthquake Engineering (CUREE) for the Federal Emergency Management Agency, Washington, D.C.
- FEMA, 2005, *Improvement of Nonlinear Static Seismic Analysis Procedures*, FEMA 440 Report, prepared by the Applied Technology Council for the Federal Emergency Management Agency, Washington, D.C.
- FEMA 2009a, *Effects of Strength and Stiffness Degradation on Seismic Response*, FEMA P-440A Report, prepared by the Applied Technology Council for the Federal emergency Management Agency, Washington, D.C.
- FEMA 2009b, *Quantification of Seismic Performance Factors*, FEMA P-695 Report, prepared by the Applied Technology Council for the Federal emergency Management Agency, Washington, D.C.
- FEMA, 2009c, *NEHRP Recommended Provisions for New Buildings and Other Structures*, FEMA P-750 Report, prepared by the Building Seismic Safety Council of the National Institute of Building Sciences for the Federal Emergency Management Agency of the U.S. Department of Homeland Security.
- Fragiadakis, M. and Vamvatsikos, D., 2010, "Fast performance uncertainty estimation via pushover and approximate IDA," *Earthquake Engineering and Structural Dynamics*, Vol. 39, No. 6, pp. 683-703.

- Goel, R.K. and Chopra, A.K., 2005, "Extension of Modal Pushover Analysis to compute member forces", *Earthquake Spectra*, Vol. 21, pp. 125-140.
- Gupta, A. and Krawinkler, H., 1999, *Seismic Demands for Performance Evaluation of Steel Moment Resisting Frame Structures*, SAC Task 5.4.3, Rep. No. 132, John A. Blume Earthquake Engineering Center, Stanford University, Stanford, CA.
- Haselton C.B., 2006, *Assessing Seismic Collapse Safety of Modern Reinforced Concrete Moment Frame Buildings*, PhD Thesis, Stanford University, Stanford, CA.
- Ibarra, L.F., Medina, R.A., and Krawinkler, H., 2005, "Hysteretic models that incorporate strength and stiffness deterioration," *Earthquake Engineering and Structural Dynamics*, Vol. 34, No. 12, pp. 1489-1511.
- ICC, 2003, *International Building Code*, International Code Council, Washington, D.C.
- Krawinkler, H. and Zareian, F., 2009, "Effects of P-Delta and deterioration on pushover target displacement," in *Nonlinear Static Methods for Design/Assessment of 3D Structures*, Editors: R. Bento and R. Pinho, IST Press, pp. 59-73.
- Lignos, D.G., 2009, *Interactive Interface for Incremental Dynamic Analysis, IIIDAP: Theory and Example Applications Manual, Version 1.1.5*, Department of Civil and Environmental Engineering, Stanford University, CA.
- Lignos, D.G. and Krawinkler, H., 2007, "A database in support of modeling of component deterioration for collapse prediction of steel frame structures," *Proceedings*, ASCE Structures Congress, Long Beach, CA.
- Lignos D.G. and Krawinkler H., 2009, *Sidesway Collapse of Deteriorating Structural Systems under Seismic Excitations*, John A. Blume Earthquake Engineering Center Report No. TR 172, Department of Civil Engineering, Stanford University, CA.
- Lignos, D.G. and Krawinkler, H., 2010, "Deterioration modeling of steel components in support of collapse prediction of steel moment frames under earthquake loading," *Journal of Structural Engineering*, ASCE (under review).
- Liu, J. and Astaneh-Asl, A., 2004, "Moment-rotation parameters for composite shear tab connections," *Journal of Structural Engineering*, ASCE, Vol. 130, No. 9, pp. 1371-1380.
- Luco, N. and Cornell, C.A., 2007, "Structure-specific scalar intensity measures for near-source and ordinary earthquake ground motions," *Earthquake Spectra*, Vol. 23, No.2, pp. 357-392.

- Luco, N., Mori, Y., Funahashi, Y., Cornell, C.A., and Nakashima, M., 2003, "Evaluation of predictors of non-linear seismic demands using 'fishbone' models of SMRF buildings," *Earthquake Engineering and Structural Dynamics*, Vol. 32, No. 14, pp. 2267-2288.
- McKenna, F., 1997, *Object Oriented Finite Element Programming Frameworks for Analysis, Algorithms and Parallel Computing*, Ph.D. Dissertation, University of California Berkeley.
- NIST, 2010, *Evaluation of the FEMA P-695 Methodology for Quantification of Building Seismic Performance Factors*, NIST GCR 10-917-8, prepared by the NEHRP Consultants Joint Venture for the National Institute of Standards and Technology, Gaithersburg, MD.
- Orakcal, K. and Wallace, J. W., 2006, "Flexural modeling of reinforced concrete walls – model calibration," *ACI Structural Journal*, Vol. 103, No. 2, pp 196-206.
- Orakcal, K., Massone, L.M., Wallace, J.W., 2006, *Analytical Modeling of Reinforced Concrete Walls for Predicting Flexural and Coupled-Shear-Flexural Responses*, PEER-2006/07 Report, Pacific Earthquake Engineering Research Center, University of California Berkeley.
- PEER/ATC, 2010, *Modeling and Acceptance Criteria for Seismic Design and Analysis of Tall Buildings*, PEER/ATC-72-1 Report, prepared by the Applied Technology Council in cooperation with the Pacific Earthquake Engineering Research Center, Redwood City, CA.
- Poursha, M., Khoshnoudian, F., and Moghadam, A.S., 2009, "A consecutive modal pushover procedure for estimating the seismic demands of tall buildings," *Engineering Structures*, Vol. 31, No. 2, pp. 591-599.
- Prakash, V., Powell, G. H., and Campbell, S., 1993, *DRAIN-2DX: Basic Program Description and User Guide*, Report No. UCB/SEMM-1993/17, University of California Berkeley.
- Tothong, P. and Cornell, C.A., 2008, "Structural performance assessment under near-source pulse-like ground motions using advanced ground motion intensity measures," *Earthquake Engineering and Structural Dynamics*, Vol. 37, pp. 1013-1037.
- Vamvatsikos, D. and Cornell, C.A., 2002, "Incremental Dynamic Analysis," *Earthquake Engineering and Structural Dynamics*, Vol. 31, No. 3, pp. 491-514.
- Vamvatsikos, D. and Cornell, C.A., 2004, "Applied Incremental Dynamic Analysis," *Earthquake Spectra*, Vol. 20, No. 2, pp. 523-553.

- Vamvatsikos, D. and Cornell, C.A., 2005, "Developing efficient scalar and vector intensity measures for IDA capacity estimation by incorporating elastic spectral shape information," *Earthquake Engineering and Structural Dynamics*, Vol. 34, No. 13, pp. 1573-1600.
- Vamvatsikos, D. and Cornell, C., 2006, "Direct estimation of the seismic demand and capacity of oscillators with multi-linear static pushovers through IDA," *Earthquake Engineering and Structural Dynamics*, Vol. 35, No. 9, pp. 1097-1117.
- Vulcano, A. and Bertero, V.V., 1987, *Analytical Models for Predicting the Lateral Response of RC Shear Walls: Evaluation of Their Reliability*, EERC Report No. UCB/EERC-87/19, Earthquake Engineering Research Center, University of California, Berkeley.
- Zareian, F. and Krawinkler, H., 2009, *Simplified Performance-Based Earthquake Engineering*, Report No. TR 169, John A. Blume Earthquake Engineering Center, Department of Civil Engineering, Stanford University, CA.

Project Participants

National Institute of Standards and Technology

John (Jack) R. Hayes
Building and Fire Research Laboratory (MS8604)
National Institute of Standards and Technology
100 Bureau Drive
Gaithersburg, Maryland 20899

Kevin K.F. Wong
Building Fire and Research Laboratory (MS8603)
National Institute of Standards and Technology
100 Bureau Drive
Gaithersburg, Maryland 20899

NEHRP Consultants Joint Venture

APPLIED TECHNOLOGY COUNCIL
201 Redwood Shores Parkway, Suite 240
Redwood City, California 94065
www.ATCouncil.org

CONSORTIUM OF UNIVERSITIES FOR
RESEARCH IN EARTHQUAKE ENGINEERING
1301 S. 46th Street, Building 420
Richmond, California 94804
www.CUREE.org

Joint Venture Management Committee

James R. Harris
J.R. Harris & Company
1776 Lincoln Street, Suite 1100
Denver, Colorado 80203

Christopher Rojahn
Applied Technology Council
201 Redwood Shores Parkway, Suite 240
Redwood City, California, 94065

Robert Reitherman
Consortium of Universities for Research in
Earthquake Engineering
1301 S. 46th Street, Building 420
Richmond, California 94804

Andrew Whittaker
University at Buffalo
Dept. of Civil, Structural, and Environ. Engin.
230 Ketter Hall
Buffalo, New York 14260

Joint Venture Program Committee

Jon A. Heintz (Program Manager)
Applied Technology Council
201 Redwood Shores Parkway, Suite 240
Redwood City, California 94065

William T. Holmes
Rutherford and Chekene
55 Second Street, Suite 600
San Francisco, California 94105

C.B. Crouse
URS Corporation
1501 4th Ave. Suite 1400
Seattle, Washington 98101

Jack Moehle
University of California Berkeley
325 Davis Hall – MC 1792
Berkeley, California 94720

Michael Constantinou
University at Buffalo
Dept. of Civil, Structural and Environ. Engin.
132 Ketter Hall
Buffalo, New York 14260

James R. Harris (ex-officio)
Andrew Whittaker (ex-officio)

Project Technical Committee

Michael Valley (Technical Director)
Michael Valley – Structural Engineer
124 Columbia Heights
Brooklyn, NY 11201

Mark Aschheim
Santa Clara University
Dept. of Civil Engineering
500 El Camino Real
Santa Clara, CA 95053

Craig Comartin
CDComartin Inc.
7683 Andrea Avenue
Stockton, California 95207-1705

William T. Holmes
Rutherford and Chekene
55 Second Street, Suite 600
San Francisco, California 94105

Helmut Krawinkler
Stanford University
Dept. of Civil & Environmental Engineering
473 Via Ortega
Stanford, California 94305

Mark Sinclair
Degenkolb Engineers
235 Montgomery St. Suite 500
San Francisco, CA 94104

Project Review Panel

Michael Constantinou
University at Buffalo
Dept. of Civil, Structural and Environ. Engin.
132 Ketter Hall
Buffalo, New York 14260

Jerome F. Hajjar
Department of Civil and Environmental Engineering
400 Snell Engineering Center
360 Huntington Avenue
Northeastern University
Boston, Massachusetts 02115

Joseph Maffei
Rutherford and Chekene
55 Second Street, Suite 600
San Francisco, California 94105

Jack Moehle
University of California Berkeley
325 Davis Hall – MC 1792
Berkeley, California 94720

Farzad Naeim
John A. Martin & Associates, Inc.
1212 S. Flower Street, 4th Floor
Los Angeles, CA 90015

Michael Willford
ARUP
560 Mission St. Suite 700
San Francisco, CA 94105

Working Group Members

Michalis Fragiadakis
Dept. of Civil and Environmental Engineering
University of Cyprus

Dimitrios Lignos
Dept. of Civil Engineering and Applied Mechanics
McGill University
Macdonald Engineering Building
817 Sherbrooke West, Room 488
Montreal, Quebec, H3A 2K6

Chris Putman
Degenkolb Engineers
235 Montgomery St. Suite 500
San Francisco, CA 94104

Dimitrios Vamvatsikos
Dept. of Civil and Environmental Engineering
University of Cyprus

Workshop Participants

Gregory Deierlein
Stanford University
Dept. of Civil & Environmental Engineering
John A. Blume Earthquake Engineering
Stanford, CA 94305-3037

Subhash Goel
University of Michigan
Dept. of Civil and Environmental Engineering
2350 Hayward, 2340 G.G. Brown Building
Ann Arbor, MI 48109

Charles Kircher
Kircher & Associates Consulting Engineers
1121 San Antonio Road, Suite D-202
Palo Alto, CA 94303

Mervyn Kowalsky
North Carolina State University
Department of Civil Engineering
Box 7908
Raleigh, NC 27695

Sashi Kunnath
University of California, Davis
Dept. of Civil & Env. Engineering
One Shields Ave., 2001 Engr III
Davis, CA 95616

Michael Mehrain
URS Corporation
915 Wilshire Blvd., Suite 700
Los Angeles, CA 90017

Eduardo Miranda
Stanford University
Dept. of Civil and Environmental Engineering
Yang and Yamazaki Building Rm. 281
Stanford, CA 94305

Mark Moore
ZFA Consulting
555 Howard St. Suite 202
San Francisco, CA 94105

Robert Pekelnicky
Degenkolb Engineers
235 Montgomery St. Suite 500
San Francisco, CA 94104

Charles Roeder
University of Washington
Department of Civil Engineering
223-B More Hall Box 2700
Seattle, WA 98195

Rafael Sabelli
Walter P. Moore
595 Market St. Suite 950
San Francisco, CA 94105

